NUREG/CP-0120
SAND92-0173

Proceedings of the

# Fifth Workshop on Containment Integrity

Held in
Washington, DC
May 12–14, 1992

Edited by M. B. Parks, C. E. Hughey

**Sponsored by**
**U.S. Nuclear Regulatory Commission**

**Proceedings prepared by**
**Sandia National Laboratories**

Available from

Superintendent of Documents
U.S. Government Printing Office
P.O. Box 37082
Washington D.C. 20013-7082

and

National Technical Information Service
Springfield , VA 22161

NUREG/CP-0120
SAND92-0173
R1, RD, RM

Proceedings of the

# Fifth Workshop on Containment Integrity

Held in
Washington, DC
May 12–14, 1992

Manuscript Completed: June 1992
Date Published: July 1992

Edited by M. B. Parks, C. E. Hughey

**Sponsored by**
**Division of Engineering**
**Office of Nuclear Regulatory Research**
**U.S. Nuclear Regulatory Commission**
**Washington, DC 20555**

**Proceedings Prepared by**
**Sandia National Laboratories**
**Albuquerque, NM 87185-5800**
**NRC FIN A1401**

# PREFACE

The Fifth Workshop on Containment Integrity was held in Washington, DC, on May 12-14, 1992. The purpose of these workshops is to provide an international forum for the exchange of information on performance of containments in nuclear power plants under severe accident loadings. Severe accident investigations of existing containment designs as well as future advanced containments were presented during the workshop. There were 145 participants at the workshop from 15 countries.

Ivan Selin, Chairman of the NRC, provided the opening address for the meeting. A total of 39 papers were presented on the following topics: Containment Design Considerations for Severe Accident Conditions, Advanced Containment Designs and Related Research, Containment Behavior Under Accident Conditions, Testing/Analysis of Containment Systems, and Containment Operational Experience (Leakage, Aging, and Operation). Papers that were presented at the workshop make up the body of this report. A copy of the final program, including last minute changes, is also included in these proceedings.

The workshop was hosted by Sandia National Laboratories under the sponsorship of the U.S. Nuclear Regulatory Commission. Principal organizers for the workshop were James F. Costello of the U.S. Nuclear Regulatory Commission and Walter A. von Riesemann and M. Brad Parks of Sandia National Laboratories.

The workshop organizers would like to express their sincere appreciation to the session chairpersons, paper authors and presenters, and Workshop attendees for making this meeting possible. Special thanks are due to Mr. Cecil Hughey of Sandia for his valuable assistance in making the preparations required to conduct the Workshop. Many others from the NRC and Sandia have contributed to the planning and conducting of the Workshop. Their assistance is gratefully acknowledged.

## CONTENTS

**CONTENTS** (Cont'd)

# Fifth Workshop on Containment Integrity

## May 12-14,1992

## Washington Marriott • Washington, DC

Hosted by: Sandia National Laboratories
Sponsored by: U.S. Nuclear Regulatory Commission

Conference Organizers: James F. Costello, U.S. Nuclear Regulatory Commission
Walter A. von Riesemann, Sandia National Laboratories
M. Brad Parks, Sandia National Laboratories

## PROGRAM

### Monday, May 11

6:00 p.m. - 8:30 p.m. Registration

### Tuesday, May 12

7:00 a.m. - 8:15 a.m. Registration

9:30 a.m. - 5:00 p.m. Registration

8:15 a.m. - 9:30.a.m. **OPENING OF THE WORKSHOP**

Chairpersons: Lawrence C. Shao - Director, Division of Engineering, Office of Nuclear Regulatory Research, U.S. Nuclear Regulatory Commission
Andrew J. Murphy - Chief, Structural and Seismic Engineering Branch, Office of Nuclear Regulatory Research, U.S. Nuclear Regulatory Commission

Introductory Remarks

Eric S. Beckjord - Director, Office of Nuclear Regulatory Research, U.S. Nuclear Regulatory Commission

Opening Address *(p. 17)*

Ivan Selin - Chairman, U.S. Nuclear Regulatory Commission

*Containment Severe Accident Phenomenology (p. 21)*

Themis P. Speis - Deputy Director for Research, Office of Nuclear Regulatory Research, U.S. Nuclear Regulatory Commission
Farouk Eltawila - Chief, Accident Evaluation Branch, Office of Nuclear Regulatory Research, U.S. Nuclear Regulatory Commission

*Proposed Criteria to Accommodate Severe Accidents in Containment Design (p. 31)*

David A. Ward - Advisory Committee on Reactor Safeguards, U.S. Nuclear Regulatory Commission

9:30 a.m. - 9:45 a.m. Break

9:45 a.m. - 12:30 p.m. **SESSION 1**

CONTAINMENT DESIGN CONSIDERATIONS FOR SEVERE ACCIDENT CONDITIONS

Chairpersons: Charles Ader - U.S. Nuclear Regulatory Commission
Bernard Barbe - Commissariat a l'Energie Atomique, France

*A Review of Containment Accidents (p. 37)*

B. De Boeck - AIB-Vincotte Nuclear, Belgium

9:45 a.m. - 12:30 p.m. **SESSION 1**(cont'd)

*Deterministic Severe Accident Criteria (DSACs) as Severe Accident Design Criteria and Policy for the New Production Reactor-Heavy Water Reactor (p. 51)*

P. T. Rhoads - U.S. Department of Energy

*Proposed Deterministic Severe Accident Criteria (DSACs) for the Heavy Water New Production Reactor (p. 61)*

K. D. Bergeron, S. E. Slezak - Sandia National Laboratories;
C. E. Leach - Westinghouse Savannah River Co.

*A Generic Approach for Containment Success Criteria Under Severe Accident Loads (p. 81)*

R. F. Sammataro, W. R. Solonick - General Dynamics Corporation;
N. W. Edwards - NWE Services, Inc.

12:30 p.m. - 2:00 p.m. Lunch

2:00 p.m. - 6:00 p.m. **SESSION 2**

ADVANCED CONTAINMENT DESIGNS AND RELATED RESEARCH

Chairpersons: Zoltan Rosztoczy - U.S. Nuclear Regulatory Commission
Werner Kuntze - Gesellschaft für Anlagen-und Reaktorsicherheit (GRS), Federal Republic of Germany

*ALWR Utility Requirements Document Containment Performance Requirements (p. 111)*

D. E. Leaver, S. ... Additon - Tenera

*Study of Potential Design Margins in the Codes of Practice for Structural Design of Primary Containment (p. 135)*

S. S. Kay - Taywood Engineering Ltd., United Kingdom.

*Design Considerations for Concrete Containments Under Severe Accident Loads (p. 151)*

M. Amin, A. C. Eberhardt, B. A. Erler - Sargent & Lundy Engineers

*Design Bases and Severe Accident Considerations for the System 80+™ Containment Design (p. 163)*

R. E. Schneider, L. D. Gerdes - ABB-Combustion Engineering Inc.;
J. T. Oswald, F. Snipes - Duke Engineering & Services, Inc.

*Comparison of the Westinghouse-GOTHIC Containment Code Predictions to PCCS Test Results (p. 179)*

M. D. Kennedy, J. Woodcock - Westinghouse Electric Corp.

*SBWR Reinforced Concrete Containment Structural Performance During a Severe Accident (p. 191)*

G. Orsini, Giuseppe Pino - ENEA-DISP, Italy

*Post-Test Analysis of a 1:10-Scale Top Slab Model of ABWR/RCCV Subjected to Internal Pressure (p. 227)*

H. Saito - Tokyo Electric Power Co.;
Y. M... matsu - Toshiba Corporation;
H. H... wa - Hitachi Ltd.;
T. Ha... awa, A. Mutoh - Shimizu Corp., Japan

6:30 p.m. - 8:00 p.m. Reception/Mixer

## Wednesday, May 13

8:30 a.m. - 12:00 a.m. **SESSION 3**

ADVANCED CONTAINMENT DESIGNS AND RELATED RESEARCH (cont'd)

Chairpersons: Goutam Bagchi - U.S. Nuclear Regulatory Commission
H. T. Tang - Electric Power Research Institute

*L.I.R.A.: An Advanced Containment System to Minimize the Accidental Radioactive Releases (p. 247)*

A. Turricchia, ENEL/DCO, Italy

8:30 a.m. - 12:00 a.m. **SESSION 3**(cont'd)

*Design of the Internal Geometry of an Advanced Containment for Mitigating Deflagration Overpressures (p. 271)*

M. Carcassi, F. Fineschi - University of Pisa, Italy

*Studies on ALWR's Containment System Penetrations (p. 285)*

F. Mantega, E. Penno - CISE-Segrate (MI);
P. Vanini- ENEL/DSR/VDN, Italy

*Severe Accident Risk Minimization Studies for the Advanced Neutron Source (ANS) Reactor Plant at the Oak Ridge National Laboratory (p. 305)*

R. P. Taleyarkhan, S. H. Kim - Oak Ridge National Laboratory

*Extreme Loadings of Inner Structures of Next Generation PWR-Containments (p. 323)*

R. Krieg, H. Alsmeyer, G. Jacobs, H. Jacobs, - Kernforschungszentrum Karlsruhe (KfK);
J. Eibl, F. H. Schlüter, T. Klatte - Universität Karlsruhe,
Federal Republic of Germany

*An Improved Design Concept for Next Generation PWR-Containments (p. 337)*

J. Eibl, F. H. Schlüter, T. Klatte - Universität Karlsruhe;
W. Breitung, F. Erbacher, B. Göller, R. Krieg, W. Scholtyssek, J. Wilhelm -
Kernforschungszentrum Karlsruhe (KfK), Federal Republic of Germany

12:00 a.m. - 1:30 p.m. Lunch

1:30 p.m. - 5:30 p.m. **SESSION 4**

CONTAINMENT BEHAVIOR UNDER ACCIDENT CONDITIONS

Chairpersons: Sudhamay Basu - U.S. Nuclear Regulatory Commission
Jacques Royen - OECD Nuclear Energy Agency, France

*Overview of NUPEC Containment Integrity Project (p. 367)*

K. Takumi, A. Nonaka - Nuclear Power Engineering Corporation (NUPEC), Japan

*Plan on Test to Failure of a Prestressed Concrete Containment Vessel Model (p. 381)*

K. Takumi, A. Nonaka, K. Umeki - NUPEC;
K. Nagata, M. Soejima - Mitsubishi Heavy Industries, Ltd.;
Y. Yamaura - Mitsubishi Atomic Power Industries, Ltd., Japan;
J. F. Costello - U.S. Nuclear Regulatory Commission;
W. A. von Riesemann, M. B. Parks, D. S. Horschel - Sandia National Laboratories

*Plan on Test to Failure of a Steel Containment Vessel Model (p. 387)*

K. Takumi, A. Nonaka, K. Umeki, Y. Yoshida - NUPEC;
O. Oyamada, H. Furukawa, K. Saito - Hitachi Works, Hitachi Ltd.,Japan
J. F. Costello - U.S. Nuclear Regulatory Commission;
W. A. von Riesemann, M. B. Parks, R. A. Watson - Sandia National Laboratories

*Concerning Assessment of the Strength and Leaktightness of the Double Containment of a 1300 MWe PWR (p. 393)*

D. Dussarte, B. Barbe - IPSN/DES, France
E. Debec - CISI, France

*Eccentric $H_2$ Detonation in a Nuclear Power Plant Steel Containment (p. 407)*

G. Maresca, Giovanni Pino - ENEA-DISP, Italy

*Analysis of Containment Parameters During the Main Steam Line Break with the Failure of the Feedwater Control Valves (p. 423)*

L. Fabjan, S. Petelin, B. Mavko, O. Gortnar, I. Tiselj - "Jozef Stefan" Institute, Slovenia

## Thursday, May 14

8:30 a.m. - 12:00 a.m. **SESSION 5**

TESTING/ANALYSIS OF CONTAINMENT SYSTEMS

Chairpersons: Andrew Murphy - U.S. Nuclear Regulatory Commission
Akira Nonaka - Nuclear Power Engineering Corporation (NUPEC), Japan

*Small Scale Penetration Leak Tests in ALPHA Program (p. 439)*

N. Yamano, J. Sugimoto, Y. Maruyama, A. Hidaka, K. Soda - Japan Atomic Energy Research Institute (JAERI), Japan

*High-Temperature Leak Characteristics Test of PCV Hatch Flanges Gasket (p. 457)*

K. Hirao - Tokyo Electric Power Co.;
M. Goto, Y. Naruse - Toshiba Corp.;
K. Saito, T. Suzuki - Hitachi Ltd.;
H. Sugino - Ishikawajima-Harima Heavy Industries Co., Japan

*An Investigation of Liner Tearing in Reinforced Concrete Reactor Containment Buildings: Comparison of Experimental and Analytical Results (p. 465)*

B. L. Spletzer, L. D. Lambert, J. R. Weatherby - Sandia National Laboratories

*Numerical Simulation of the Ultimate Load Capacity of a Reactor Containment Building (p. 497)*

V. Andreoli, P. Angeloni, P. Contri - ISMES;
L. Brusa - ENEL/DSR/VDN, Italy

*Research and Development Performed at CEA/DMT in the Field of Nuclear Reactors Containments (p. 515)*

A. Millard, Ph. Jamet, B. Barbe, C. Lecomte - CEA/IPSN, France

*Creep Rupture Failure in a Mark-I Containment with a New Thermal Failure Material Model (p. 551)*

J. C. Castro, R. A. Dameron, Y. R. Rashid - ANATECH Research Corp.

12:00 a.m. - 1:30 p.m. Lunch

1:30 p.m. - 5:30 p.m. **SESSION 6**

## CONTAINMENT OPERATIONAL EXPERIENCE (LEAKAGE, AGING, OPERATION)

Chairpersons: Jocelyn Mitchell - U.S. Nuclear Regulatory Commission
Anthony Roberts - Nuclear Design Associates, United Kingdom

### Leakage

*Containment Leakage Rate Testing Requirements (p. 567)*

E. G. Arndt - U.S. Nuclear Regulatory Commission

*ANSI/ANS 56.8 Standard Status Report/NUMARC Activities (p. 573)*

J. P. Glover - Commonwealth Edison Company

*Industry Current and Future Plans for Implementation of Proposed Revision of 10 CFR Part 50, Appendix J, Containment Leak Rate Testing (p. 579)*

W. J. Smith - NUMARC

### Aging

*Containment Penetrations - Flexible Metallic Bellows Testing, Safety, Life Extension Issues (p. 583)*

J. A. Brown, G. A. Tice - NUTECH Engineers, Inc.

*Aging of Concrete Containment Structures in Nuclear Power Plants (p. 595)*

D. J. Naus, C. B. Oland - Oak Ridge National Laboratory;
B. Ellingwood, Y. Mori - The Johns Hopkins University;
E. G. Arndt - U.S. Nuclear Regulatory Commission

### Operational Experience

*Updated ASME Code Rules for Inservice Inspection of Steel and Concrete Containments (p. 625)*

R. F. Sammataro - General Dynamics Corporation

*A Review on Operating Experiences of Containment Isolation Systems in Korea (p. 651)*

I. Kim, H. J. Kim - Korea Institute of Nuclear Safety, Korea

## Fifth Workshop on Containment Integrity

List of Attendees

Stephen L. Additon
TENERA, L.P.
7272 Wisconsin Avenue, Suite 300
Bethesda, MD 20814-4836

Charles Ader
U.S. Nuclear Regulatory Commission
Washington, DC 20555

Mohammad Amin
Sargent & Lundy Engineers
55 East Monroe Street
Chicago, IL 60603

William C. Arcieri
Idaho National Engineering Laboratory
EG&G Idaho Inc.
11426 Rockville Pike, Suite 300
Rockville, MD 20852

Gunter Arndt
U.S. Nuclear Regulatory Commission
Structural and Seismic Engineering Branch
MS NL/S-217/A
Washington, DC 20555

Hans Ashar
U.S. Nuclear Regulatory Commission
MS OWFM 7H15
Washington, DC 20555

Goutam Bagchi
U.S. Nuclear Regulatory Commission
MS 8D22
Washington, DC 20555

M. B. Barbe
Commissariat a l'Energie Atomique
Institut de Protection et de Sûreté Nucléaire
Centre d'Etudes de Fontenay aus Roses BP No. 6
F-92265 Fontenay-aux-Roses Cedex
FRANCE

Sudhamay Basu
U.S. Nuclear Regulatory Commission
RES/DSR/AER, MS N/LN 344
5640 Nicholson Lane
Rockville, MD 20850

Sam Basu
Ontario Hydro
700 University Ave. H18 A05
Toronto, Ontario M5G 1X6
CANADA

James Mitchell Baughman
Duke Power Company
4800 Concord Road
York, SC 29745

Eric S. Beckjord
U.S. Nuclear Regulatory Commission
Director, Office of Nuclear Regulatory Research
Washington, DC 20555

Zahoor Beg
Ontario Hydro
700 University Ave.
Toronto, Ontario M5G 1X6
CANADA

Kenneth Bergeron
Sandia National Laboratories
Org. 6402
Albuquerque, NM 87185-5800

Vicki Bergmann
Sandia National Laboratories
Org. 1561
Albuquerque, NM 87185-5800

John M. Boyles
Duke Power Company
Oconee Nuclear Station
130 Rochester Highway
Seneca, SC 29679

## Fifth Workshop on Containment Integrity

List of Attendees

James A. Brown
Pacific Nuclear - Nutech Engineers
1111 Pasquinelli Drive, Suite 100
Westmont, IL 60559

Giamfranco Capponi
U.S. Nuclear Regulatory Commission
RES/ARB
5600 Nicholson
Rockville, MD 20852

Marco Carcassi
University of Pisa
Dept. of Mechanical & Nucl. Construction
Via Diotisalvi 2
I-56126 Pisa
ITALY

John C. Castro
ANATECH Research Corp.
5435 Oberlin Drive
San Diego, CA 92121

Angela T. Chu
U.S. Nuclear Regulatory Commission
Office of International Programs
Washington, DC 20555

Paolo Contri
ISMES S.p.A.
Viale G. Cesare, 29
I-24100 Bergamo
ITALY

James F. Costello
U.S. Nuclear Regulatory Commission
Structural & Seismic Engr. Branch
Mail Stop NL/S-217A
USNRC/RES
Washington, D. C. 20555

D. R. Davies
Nuclear Electric plc
Booths Hall, Chelford Road
Knutsford, Cheshire WA16 8QG
UNITED KINGDOM

Marwan Daye
Bechtel Power Corp.
9801 Washingtonian Blvd.
Gaithersburg, MD 20878

Benoit De Boeck
AIB-Vincotte Nucleaire
Institut de Surete Nucleaire
Avenue du Roi, 157
B-1060 Brussells
BELGIUM

Dennis Dervay
Cleveland Electric Illuminating Co.
Perry Nuclear Power Plant
P. O. Box 97
Perry, OH 44081

Moni K. Dey
U.S. Nuclear Regulatory Commission
RES/DSR/ARB
Washington, DC 20555

Ann M. Dummer
U.S. Nuclear Regulatory Commission
ORR/DSIB/SAIB
NICHOLSON LANE SOUTH
Washington, DC 20555

Arthur C. Eberhardt
Sargent & Lundy Engineers
55 East Monroe Street
Chicago, IL 60603

Norman W. Edwards
NWE Services Inc.
17469 Hoot Owl Way
Morgan Hill, CA 95037

Josef Eibl
Institut für Massivbau und Baustofftechnologie
Universität Karlsruhe
Am Fasanengarten, Pastfach 8980
D-7500 Karlsruhe 1
FEDERAL REPUBLIC OF GERMANY

## Fifth Workshop on Containment Integrity

List of Attendees

Farouk Eltawila
U.S. Nuclear Regulatory Commission
RES/DSR/AEB
MS NL/N-353
Washington, DC 20555

Brian A. Erler
Sargent & Lundy Engineers
55 East Monroe Street
Chicago, IL 60603

Ljubo Fabjan
Institut "Jozef Stefan"
Univerza v Ljubljana
Reactor Engineering Division
61111 Ljubljana, Jamova 39, POB 100
SLOVENIA

William Kirby Farrell
Cleveland Electric Illuminating Co.
Perry Nuclear Power Plant
10 Center Road
North Perry, OH 44081

Nathaniel Foster
Tennessee Valley Authority
1101 Market Street
LP4G-C
Chattanooga, TN 37408

Wiktor E. Frid
Swedish Nuclear Power Inspectorate
Box 27106
S-10252 Stockholm
SWEDEN

Hideyasu Furukawa
Hitachi Ltd., Hitachi Works
1-1, 3-chome, Saiwai-cho
Hitachi-chi, Ibaraki-ken 317
JAPAN

James Glover
Commonwealth Edison
1400 Opus Place, Suite 300
Downers Grove, IL 60515

Edward Goodwin
U.S. Nuclear Regulatory Commission
NRR
Washington, DC 20555

Masashi Goto
Toshiba Corporation
Isogo Nuclear Engineering Center
8, Shinsugita-cho, Isogo-ku
Yokohama 235
JAPAN

Herman L. Graves, III
U.S. Nuclear Regulatory Commission
Structural & Seismic Engr. Branch
Mail Stop NL/S-217A
USNRC/RES
Washington, D.C. 20555

Toshiyasu Hasegawa
Shimizu Corporation
Nuclear Power Division
SEAVANS SOUTH
No. 2-3, Shibaura 1-chome, Minato-ku
Tokyo 105-07, JAPAN

Harald Hirschmann
Paul Scherrer Institute (PSI)
CH-5302 Villengen
SWITZERLAND

Dean Houston
U.S. Nuclear Regulatory Commission
ACRS/Nuclear Reactors Branch
MS P-315
Washington, DC 20555

Ten Hsieh
U.S. Department of Energy
1000 Independence Ave. S.W.
Washington, DC 20585

Cecil E. Hughey
Sandia National Laboratories
Org. 6473
Albuquerque, NM 87185-5800

## Fifth Workshop on Containment Integrity

List of Attendees

Mark A. Hutcheson
Duke Power Company
P.O. Box 1007, MS WC23C
Charlotte, NC 28201-1007

John S. Hyslop
U.S Nuclear Regulatory Commission
RES/DSR/AEB
Nicholson Lane North
Rockville, MD 20852

Katsuyoshi Imoto
Obayashi Corporation
4-640, Shimokiyoto
Kiyose-shi, Tokyo 204
JAPAN

Deborah A. Jacksor
U.S. Nuclear Regulatory Commission
Office of Nuclear Reactor Regulation
DAR/LRPD
Washington, D.C. 20555

J. L. Jemielewski
Colenco Power Consulting Ltd.
Mellingerstrasse 207
CH-5405 Baden
SWITZERLAND

Mr. Murray Jennex
Southern California Edison
P.O. Box 128, MS P2J
San Clemente, CA 92674-0128

James W. Johnson
U.S. Nuclear Regulatory Commission
Office of the Chairman
Washington, DC 20555

Marcia D. Kennedy
Westinghouse Electric Corporation
Nuclear & Advanced Technology Division
Energy Center MS 3-08 East
P.O. Box 355
Pittsburgh, PA 15230-0355

Ingoo Kim
Korea Institute of Nuclear Safety
Safety Analysis Department
150, Dukjn-dong, Yoosung-gu
Taejon, 305-353
KOREA

Seok-Ho Kim
Martin Marietta Energy Systems, Inc.
Oak Ridge National Laboratory
Engineering Technology Division, 9104-1, Y-12
P.O. Box 2009
Oak Ridge, TN 37831-8057

Vasil Krett
International Atomic Energy Agency
Wagramerstrasse, 5
P.O. Box 100
A-1400 Vienna
AUSTRIA

Rolf Krieg
Kernforschungszentrum Karlsruhe GmbH
Institut für Reaktorsicherheit
Postfach 3640
D-7500 Karlsruhe
FEDERAL REPUBLIC OF GERMANY

Akio Kumazawa
MITI(ANRE)
1-3-1, Kasumigaseki
Chiyoda-ku
Tokyo 100
JAPAN

Werner M. Kuntze
Gesellschaft fur Anlagen-und Reaktorsicherheit (GR
Schwertnergasse 1
D-5000 Koln 1
FEDERAL REPUBLIC OF GERMANY

Takashi Kuroda
Shimizu Corporation
Director and General Manager, Nucl. Power Div.
SEAVANS SOUTH
No. 2-3, Shibaura , 1-chrome, Minato-ku,
Minato-ku, Tokyo 105-07, JAPAN

Seung J. Lee
U.S. Nuclear Regulatory Commission
NRR/DET/ESGB
OWFN 7H15
Washington, DC 20555

## Fifth Workshop on Containment Integrity

List of Attendees

Josh C. Lee
Ontario Hydro
700 University Ave H15A12
Toronto, Ontario M5G 1X6
CANADA

John Ludwigsen
Sandia National Laboratories
Org. 6473
Albuquerque, NM 87185-5800

Dan Lurie
U.S. Nuclear Regulatory Commission
OC/DBA
Washington, DC 20555

Franco M. Mantega
CISE - Technologie Innovative
Via Reggio Emilia, 39
Casella Postale 12081
1-20134 Segrate (Milano)
ITALY

Giuseppe Maresca
ENEA-DISP
Via Vitaliano Brancati 48
1-00144 Roma
ITALY

Martin Marugg
American Nuclear Insurers
29 S. Main Street
W. Hartford, CT 06107

Michael M. McIntyre
Rolls Royce & Associates Ltd
PO Box 31
Raynesway, Derby DE2 8BJ
UNITED KINGDOM

Zen T. Mendoza
SAIC
5150 El Camino Real #C-31
Los Altos, CA 94022

Steven M. Mirsky
SAIC
1710 Goodridge Drive
McLean, VA 22102

Jocelyn A. Mitchell
U.S. Nuclear Regulatory Commission
DSIR/EIB
Washington, DC 20555

Steve Morales
Omaha Public Power District
Fort Calhoun Station, MS FC-2-3
P. O. Box 399
Fort Calhoun, NE 68023

Andrew Murphy
U.S. Nuclear Regulatory Commission
MS NL/S-302
Washington, DC 20555

Atsushi Mutoh
Shimizu Corporation
Nuclear Power Division
SEAVANS SOUTH
No. 2-3, Shibaura 1-chome,Minato-ku,
Tokyo 105-07, JAPAN

Kefah Y. Naom
Nuclear Electric PLC
Berkeley Nuclear Laboratories
Berkeley, Gloucestershire GL13 9PB
UNITED KINGDOM

Dan Naus
Oak Ridge National Laboratory
PO Box 2009, Bldg. 9204-1
MS 8056
Oak Ridge, TN 37831-8056

Paul A. Nielsen
Pacific Gas & Electric
P.O. Box 56
Avila Beach, CA 93443

## Fifth Workshop on Containment Integrity

List of Attendees

Yoshihiro Nishiwaki
U.S. Nuclear Regulatory Commission
NRR/ED/ACSB
5650 Nicholson Lane MS 217B NL/S
Rockville, MD 20852

Akira Nonaka
NUPEC
Nuclear Power Engineering Test Center
Shuwa-Kamiyacho Bldg
4-3-13 Toranomon, Minato-ku
Tokyo 105, JAPAN

Yukimitsu Okano
The Kansai Electric Power Co.,Inc.
3-3-22, Nakanoshima
Kita-ku, Osaka 530
JAPAN

Timo J. Okkonen
Finnish Centre for Radiation & Nuclear Safety (STUK)
P.O. Box 268
SF-00101 Helsinki
FINLAND

C. Barry Oland
Oak Ridge National Laboratory
PO Box 2009, Bldg. 9204-1
MS 8056
Oak Ridge, TN 37831-8056

Richard S. Orr
Westinghouse Electric Corporation
Nuclear and Advanced Technology Division
MS 4-28
P.O. Box 355
Pittsburgh, PA 15230-0355

Giampiero Orsini
ENEA-DISP
via Vitaliano Brancati 48
I-00144 Roma
ITALY

Nestor Ortiz
Sandia National Laboratories
Org. 6400
Albuquerque, NM 87185-5800

J. Todd Oswald
Duke Engineering and Services, Inc.
230 South Tryon Street
P.O. Box 1004
Charlotte, NC 28201-1004

Dave Pace
Sandia National Laboratories
Org. 6473
Albuquerque, NM 87185-5800

M. Brad Parks
Sandia National Laboratories
Org. 6473
Albuquerque, NM 87185-5800

Marvin J. Parnes
Ebasco Services Inc.
Two World Trade Center
New York, NY 10048

Coilin Patchett
HM Nuclear Installations Inspectorate
St. Peter's House, Rm 421
Stanley Precinct, Balliol Road
Bootle, Merseyside L20 3LZ
UNITED KINGDOM

Enrico Penno
CISE spa - Technologie Innovative
Via Reggio Emilia, 39
Casella Postale 12081
1-20134 Segrate (Milano)
ITALY

Massimo Pezzilli
ENEA
C.R.E. CASACCIA
Via Anguillarese, 301
I-00060 S. Maria di Galeria (Roma)
ITALY

Claude Pilette
Atomic Energy Control Board
P.O. Box 1046, Station B
270 Albert Street
Ottawa, Ontario K1P 5S9
CANADA

## Fifth Workshop on Containment Integrity

List of Attendees

M. Sajid Quraishi
Atomic Energy of Canada Ltd.
Sheridan Park Research Community
2251 Speakman Drive
Mississauga, Ontario L5K 1B2
CANADA

S. S. Ray
Taywood Engineering Limited
Taywood House, 345 Ruislip Road
Southall, Middlesex UB1 2QX
UNITED KINGDOM

Patrick T. Rhoads
U.S. Department of Energy
Reactor Design Division, NP-43
Forrestal Building, Rm 1H088
1000 Independence Avenue SW
Washington, DC 20545

Jacques L. Ricard
Atomic Energy Control Board
% Ontario Hydro
P. O. Box 4000
Bowmanville, Ontario L1C 3Z8
CANADA

Anthony C. Roberts
Nuclear Design Associates
Edmundson House, Tatton Street
Knutsford, Cheshire WA16 6AF
UNITED KINGDOM

Zoltan Rosztoczy
U.S. Nuclear Regulatory Commission
MS NL-007
Washington, DC 20555

Jacques G. Royen
OECD Nuclear Energy Agency
Nuclear Safety Division
38 Boulevard Suchet
F-75016 Paris
FRANCE

Christopher P. Ryder
U.S. Nuclear Regulatory Commission
Probalistic Risk Analysis Branch
MS MS-372
Washington, DC 20555

Smanchai Sae-Ung
Bechtel Corporation
9801 Washington Blvd.
Gaithersburg, MD 20878-5356

Robert F. Sammataro
General Dynamics/Electric Boat Div.
Nuclear Engineering/Dept. 478
75 Eastern Point Road
Groton, CT 06340-4984

Ken-ichi Sato
Brookhaven National Laboratory
Nuclear Energy Dept., Bldg. 197D
Upton, NY 11973

P. Singh Sawhney
Bechtel Power Corp.
50 Beale Street
San Francisco, CA 94119

Jack C. Scarborough
U.S. Nuclear Regulatory Commission
OCMKR
One White Flint (16H3)
11555 Rockville Pike
Rockville, MD 20852

Ivan Selin
Chairman
U.S. Nuclear Regulatory Commission
Washington, DC 20555

Lawrence C. Shao
U.S. Nuclear Regulatory Commission
Director, Division of Engineering, NRR
Washington, DC 20555

W. J. M. Slegers
N.V. KEMA
Utrechtseweg 310
N-6812 AR Arnhem
THE NETHERLANDS

## Fifth Workshop on Containment Integrity

List of Attendees

Scott Slezak
Sandia National Laboratories
Org. 6402
Albuquerque, NM 87185-5800

Walter J. Smith
NUMARC
1776 Eye St. N.W., Suite 300
Washington, DC 20006-3706

J. Frank Snipes
Duke Engineering & Services, Inc.
230 South Tryon Street
P.O. Box 1004
Charlotte, NC 28201-1004

Amy J. Soderberg
Consumers Power Company
Palisades Nuclear Plant
27780 Blue Star Memorial Highway
Covert, MI 49043

William R. Solonick
General Dynamics/Electric Boat Div.
Nuclear Engineering/Dept. 478
75 Eastern Point Road
Groton, CT 06340-4989

Themis P. Speis
U.S. Nuclear Regulatory Commission
Deputy Director Research
Office of Nuclear Regulatory Research
Washington, DC 20555

Barry Spletzer
Sandia National Laboratories
Org. 6473
Albuquerque, NM 87185-5800

Peter M. Stoop
Netherlands Energy Research Foundation ECN
Westerduinweg 3
N-1755 LE, Petten
THE NETHERLANDS

Takehira Takayangi
Taisei Corporation
1-25-1, Nishi-Shinjuku
Shinjuku-ku, Tokyo 163
JAPAN

Rusi P. Taleyarkhan
Martin Marietta Energy Systems, Inc.
Oak Ridge National Laboratory
Engineering Technology Division, 9104-1
P.O. Box 2009
Oak Ridge, TN 37831-8057

Chen P. Tan
U.S. Nuclear Regulatory Commission
NRR/DET/SGB
OWFN
Washington, DC 20555

H. T. Tang
Electric Power Research Institute
3412 Hillview Avenue
PO Box 10412
Palo Alto, CA. 94303

Kannan N. Tennankore
Atomic Energy of Canada Ltd.
Whiteshell Laboratories
Pinawa, Manitoba R0E 1L0
CANADA

Greg A. Tice
Pacific Nuclear - Nutech Engineers
1111 Pasquinelli Drive, Suite 100
Westmont, IL 60559

Richard H. Toland
United Engineers & Constructors
30 S. 17th Street
Philadelphis, PA 19101

Arnaldo Turricchia
ENEL - DCO
Direction of Construction
Via G.B. Martini 3
I-00198 Roma
ITALY

## Fifth Workshop on Containment Integrity

List of Attendees

Makoto Uchida
Mitsubishi Heavy Industries, Ltd.
4-1, Shibakoen 2-chome
Minato-ku,
Tokyo 105
JAPAN

Katsuhiko Uchiki
Nuclear Power Engineering Corporation
3-13, 4-chome, Toranomon
Minato-ku
Tokyo 105
JAPAN

Walt von Riesemann
Sandia National Laboratories
Org. 6403
Albuquerque, NM 87185-5800

John G. Waldie
Ontario Hydro
P.O. Box 4000
Bowmanville, Ontario L1C 3Z8
CANADA

David A. Ward
U.S. Nuclear Regulatory Commission
ACRS
Phillips Bldg. P-315
Washington, DC 20555

Bob Watson
Sandia National Laboratories
Org. 6473
Albuquerque, NM 87185-5800

Steve Weisskoff
Phys-Chem Scientific Corp.
36 W. 20th Street
New York, NY 10011

George K. Wierzbowski
Niagara Mohawk Power Co.
Nine Mile Point Nuclear Station
P.O. Box 63
Lycoming, NY 13093

Lothar Wolf
Battelle - Europe
AM Römerhof 35
D-6000 Frankfurt/Main 90
FEDERAL REPUBLIC OF GERMANY

Dr. Peter T. Wong
CANATOM
55 Queen Street East
Totonto, Ontario M5C 1R6
CANADA

Joel Woodcock
Westinghouse Electric Corporation
Nuclear & Advanced Technology Division
Energy Center MS 3-07 East
P.O. Box 355
Pittsburgh, PA 15230-0355

Dick Wullaert
SAIC
12850 Middlebrook Rd., Suite 300
Germantown, MD 20874

Mikio Yamamoto
Obayashi Corporation
3-5, Kaji-cho, Kanda
Chiyoda-ku,
Tokyo 101
JAPAN

Norihiro Yamano
Japan Atomic Energy Research Institute
Severe Accident Research Lab.
Tokai-mura, Naka-Gun
Ibaraki-ken 319-11
JAPAN

Yoshihisa Yamaura
Mitsubishi Atomic Power Industries, Ltd.
Shuwa Shiba Park Bldg.
2-4-1 Shibakouen Chome
Minato-ku, Tokyo 105
JAPAN

Masashi Yokota
Tokyo Electric Power, DC Office
1901 L Street, N.W.
Suite 720
Washington, DC 20036

Angie P. Young
U.S. Nuclear Regulatory Commission
NRR/DST/PSE
OWFN 8-D-1
Washington, DC 20555

# INTRODUCTORY SESSION

# OPENING OF THE WORKSHOP

# OPENING REMARKS

Dr. Ivan Selin
Chairman, U.S. Nuclear Regulatory Commission

Good morning, ladies and gentlemen. I am pleased to welcome you to the Fifth Workshop on Containment Integrity. It is gratifying to see such a large turnout of representatives from the U.S. nuclear industry and the international community. This workshop provides an important opportunity for enhancing our common understanding of containment performance under severe accident conditions, both for current and advanced light water reactor designs.

As most of you know, since Three Mile Island the NRC has increasingly emphasized the need to understand the variety of containment challenges that could occur as a result of a severe core damage accident. The focus of this effort has been on those containment challenges where the resultant pressure and temperature conditions could threaten the integrity of the containment building.

Numerous containment integrity initiatives have been completed over the past several years. As a result, the NRC has concluded that the design basis criteria used to license nuclear power plants provide a considerable margin of safety. In turn, this safety margin provides reasonable assurance that the public is protected from significant radiation releases even under the core damage conditions that occurred at Three Mile Island. However, we all recognize that accident scenarios resulting in even greater core damage than that which occurred at TMI are physically possible. Thankfully, they are very unlikely.

Such scenarios could present even greater challenges to containment integrity and justify the continued interest and research in containment performance. Accidents which lead to containment failure are the major source of the residual risk to the public. Since the containment is the last barrier between fission products and the environment, its performance across a wide spectrum of potential accidents is of critical importance.

One can more fully appreciate the importance of containment performance to public safety by contrasting the TMI and Chernobyl accidents. The TMI accident showed that robust containments can protect against a variety of core damage conditions and challenges. In spite of a loss of fuel integrity, the public was not exposed to an uncontrolled release of fission products. Such was not the case at Chernobyl. While the Chernobyl accident was due to a combination of design inadequacies and human failures, the lack of a containment capability was a major factor in the devastation visited upon the surrounding populace. The contrasting experiences at Chernobyl and Three Mile Island Unit 2 showed how important containment survival is in minimizing the release of radioactivity to the environment in the event of a core melt accident.

The nuclear industry's reliance on defense-in-depth requires the integration of preventive and mitigative efforts. Containment is, primarily, mitigative in its design. It is called upon should other barriers be overcome. Evaluation of the effectiveness of containment performance, therefore, must consider plausible but low likelihood scenarios. Containment designs must also be robust and tolerant of beyond design basis events.

The NRC has a high degree of confidence that the containments of the current light water reactors can perform the functions for which they were designed. Our research is, therefore, focused largely on understanding containment capabilities and the margins in performance that go beyond design loads and severe core damage threats. The consequences of core damage accidents depend very strongly on whether and when containment failures occur in the course of the accident.

Consequently, we need to better understand what occurs in containment during the later stages of an accident. This knowledge will enhance accident management strategies and emergency planning.

The goal of the NRC Containment Integrity Program is to develop general methods to estimate containment performance. This goal is being accomplished through the combined use of analytical and experimental programs. In complex areas, where numerical solutions have not yet evolved, testing is being used to empirically predict the behavior of some components of the containment pressure boundary.

Ultimately, predicting a containment's behavior requires information in five specific areas: (1) the combinations of pressure and temperature that could lead to the failure of the containment pressure boundary, (2) the timing of containment failure (early or late) in the accident sequence, (3) the failure mode, (4) the leak area and the associated leak rate, and (5) the location of the failure.

NRC's containment integrity research focuses directly on the phenomena considered most likely to produce combinations of high pressures and temperatures that might cause the containment to fail. These include scenarios such as the high-pressure ejection from the reactor vessel of finely divided particles of molten core debris; the generation of noncondensible and flammable gases from the decomposition of concrete by hot core debris; direct thermal and chemical attack on structures and engineered safety features; and, the burning or detonation of hydrogen and other gases produced in the course of the accident. At this point, I need to acknowledge the expertise of yourselves and members of the NRC staff. My understanding of these phenomena is at best, superficial. Fortunately, Dr. Speis, Deputy Director of the Office of Nuclear Regulatory Research, will address these topics in much greater detail in his presentation.

The NRC's experimental and analytical research has included the testing of large models of actual containment structures as well as large and full-scale testing of penetration assemblies. These research results are being used to predict failure thresholds and modes, and their related leak rates. When loads anticipated from severe accidents are included, estimates of plant releases and off-site consequences can be made.

The complexity and costs of such large scale tests provide a strong incentive for engaging in jointly sponsored research programs. The NRC research program on containment integrity has been enhanced by significant international cooperation. Research organizations from the United Kingdom, France, Germany, and Italy have worked with us, particularly with respect to "testing to failure" various models of steel and reinforced concrete PWR containments. In Japan, the Ministry of International Trade and Industry (MITI) is sponsoring a research program on containment performance under severe accident conditions. Discussions between Japan and the U.S. have led to the conclusion that it would be mutually advantageous to engage in a jointly sponsored research program. This research program would use, as its principal element, tests-to-failure of various models of a prestressed concrete PWR containment and a steel BWR containment. Models of these containment types have not been tested in the NRC research effort. This joint testing program should, therefore, fill voids in our understanding of containment failure under severe accident conditions.

In the area of severe accident phenomena and containment challenges, the NRC and 16 countries have signed research agreements under the Cooperative Severe Accident Research Program. The partners in this program have a mutual interest in realizing the safety benefits that can be obtained from integrated severe accident research and a sharing of research data and results.

During the course of the severe accident research performed by the NRC over the past 13 years, significant progress has been made in the development of computer codes to analyze nuclear power plant responses to severe accidents. All of this information is available to the Co-op participants.

In return, the participants share their technical reports and experimental data. Joint programs, using facilities owned by the other parties and under specific commercial agreements are also being pursued. The severe accident research specified in the signed agreements cover a wide gamut of research areas. I do not need to detail them here today.

Several of the Co-op countries have participated for five to ten years, and have developed significant severe accident programs of their own. Thus, they now conduct insightful peer reviews and provide increasingly valuable data and reports. Finally, the program fosters a wide-scale testing of the major computer codes as participants apply them in their own programs. This has uncovered various code errors and deficiencies and has allowed the codes to be greatly improved. Moreover, the application of the codes to numerous experiments tests the various failure models. All of these interactions improve the overall quality assurance of the overall severe accident program.

## ADVANCED REACTORS

The programs I have described so far have emphasized the current generation of light water reactors. We are also devoting considerable effort to the containment issues of the next generation of reactor designs. In this regard, we expect to build as much as possible on the existing base of research.

For all advanced reactor containment designs submitted for certification, the NRC will evaluate containment performance under severe accident conditions. These evaluations will include the likelihood of, and uncertainties associated with, severe accidents involving potential containment failure, containment bypass leakage, and inadvertent containment openings. The NRC will also assess overall containment performance to ensure that systems designed to contain radioactive materials, when combined with other mitigation systems, provide an acceptably low probability of a large release of radioactive materials.

Containments for some of the advanced light water reactors are significantly different from current designs. For example, the containment for ABB's System 80+ reactor is a large volume, spherical steel shell, similar to some existing ones located in Germany. Westinghouse's AP600 containment is a return to simplicity inasmuch as it uses a largely passive heat removal system, requiring few active components. For these containments, the NRC is addressing a number of issues that have arisen from our prior LWR safety assessments. These issues include hydrogen control, core concrete interaction, high pressure core melt ejection, and debris cooling.

Other future designs are also being considered by the NRC in its pre-application interactions with prospective applicants. These reactors also have certain novel or unique containment design features. The advanced liquid metal reactor (ALMR), the modular high temperature gas reactor (MHTGR), the Swedish designed, PIUS (Process Inherent Ultimate Safety), and the Canadian heavy water reactor design (CANDU) will all generate their own specific sets of questions. The NRC will need to be assured in the adequacy and accuracy of the design assumptions and operational capabilities. Only then will certification be possible. In all of these cases, the intent is to ensure the robustness of the containment design against severe accident phenomena that could lead to early containment failure. I would also note that as a measure of containment performance and as a basis for regulatory guidance, the Commission has approved the use of a 0.1 conditional containment failure probability for the evolutionary light water reactors. The Commission, however, directed that this containment performance objective should not be imposed as a requirement. Also, the use of the conditional containment failure probability should not discourage accident prevention. To help in this matter, the staff was directed to investigate suitable alternative, deterministically-established, containment performance objectives which could be submitted by the applicants.

## SUMMARY

In summary, the NRC has made considerable progress in recent years in understanding what happens during severe accidents. Such information is essential for assessing potential safety improvements and for making decisions on whether or not particular improvements are warranted. This program is what we have to offer to our international partners in safety research.

I hope this brief overview of containment integrity issues and initiatives gives you an appreciation of the great deal of effort that has been and continues to be invested in this area. We must continue to ensure that the results of our research efforts are applied effectively, on a timely basis, where they are most needed, and that effective initiatives are not allowed to wane.

Let me close my remarks by again expressing my appreciation for your willingness to join us today and invite your active participation in this important workshop.

# Containment Severe Accident Phenomenology

Themis Speis, Farouk Eltawila
U.S. Nuclear Regulatory Commission
Washington, DC 20555

## Introduction

The role of the containment as a vital barrier to the release of fission products to the environment has been widely recognized. The public safety record of nuclear power plants has been fostered by applying the "defense-in-depth" principle, which relies on a set of independent barriers to fission product release. The containment and its supporting systems are one of these barriers. Containment design criteria are based on a set of deterministically derived challenges. Pressure and temperature challenges are usually based on the design basis loss-of-coolant accident. Also, criteria based on external events such as earthquakes, floods, and tornadoes are considered. The margins of safety provided by such practices have been the subject of considerable research and evaluation, and these studies have shown the ability of containment systems to survive pressure challenges of as much as 2.5 to 3 times design levels if identifiable weak links, such as for example inflatable seals, are eliminated. Because of these margins, the various containment types presently utilized in the western world have the capability to withstand, to varying degrees, many of the challenges presented by severe accidents. For each type of containment, however, there remain failure mechanisms which could lead to either early or late containment failure, depending on both the accident scenarios involved and the containment types.

Containment loads (i.e., higher than those considered in the design basis) that might lead to such failures can result from the thermal-hydraulic/material interaction processes which take place during core melt accidents involving a large part of the core; some of these loads manifest themselves even before the primary system is completely breached (e.g., hydrogen generation/transport and burning in the containment), while others follow the release of the core melt debris into the containment space.

The understanding of these phenomena and their range of behavior is important for taking advantage of existing reactor system and containment capabilities and exploring additional accident management strategies for the different reactor and containment types and also for developing plant performance criteria for future light water reactors (LWRs) against severe accident challenges.

These phenomena have their origin in a variety of initiating events and sequences and generally involve multiphase flow and heat transfer processes. The phenomena to be discussed here include high pressure sequences with their concomitant consequences, corium-concrete interactions and debris bed coolability including steam spikes, and hydrogen combustion related issues.

After more than 10 years of rather broadly directed research, where the focus was in understanding the underlying physical and chemical phenomena that can occur in a severe accident, the NRC issued in May 1989, its revised Severe Accident Research Program (SARP) Plan. The SARP revision documented in NUREG-1365 was motivated by the need to focus efforts and crystallize positions of value to the

regulatory mission of the agency. Early containment failure, or avoidance of it, became the focal point, and issues associated with it constituted the key elements of that plan.

Since 1989, significant progress has been made on the technical issues of concern regarding containment performance and release of fission products in the event of containment failure to warrant a further update of NUREG-1365 which is presently underway. For those cases where guesstimates were made, we now have more relevant data that enable us to characterize containment performance on more technical bases. In my remarks today, I will speak of the current understanding of the more important phenomena and the associated mechanical and thermal loads on the containment which result from an evolving severe accident both in-vessel and ex-vessel, and also summarize on-going work to further enhance our understanding and reduce residual uncertainties in a number of these areas. Therefore what I plan to summarize shortly are the conditions which containments should be evaluated against for the purpose of either understanding the margins of the existing generation of containment systems or as I said earlier to develop performance criteria for future plants against severe accident challenges.

Containment Loading in Severe Accidents

The severe accident phenomena that are capable of generating a much higher level of loading than that considered in the design basis may be summarized as follows in terms of nomenclature employed in WASH-1400 for PWRs. In general, the key phenomena are generic in nature but can affect containment performance in various ways depending on reactor type, containment size and configuration, and/or other unique design features associated with a specific system.

Alpha ($\alpha$): Large scale in-vessel molten core-water energetic interaction, usually referred to as steam explosion, with potential to cause early containment failure via energetic missile penetration of the containment.

Gamma ($\gamma$): Hydrogen deflagration or detonation; it is more or less important according to the type of reactor and containment design.

Early Delta ($\delta_e$): Rapid containment overpressurization early in the accident; it is more or less important according to the type of reactor and containment design.

Delayed Delta ($\delta_l$): Gradual overpressurization at a late stage of the accident.

Epsilon ($\varepsilon$): Basemat melt-through via [illegible] decomposition from contact with high temperature core debris.

Beta ($\beta$): Failure to isolate the containment.

V: Containment bypass (or interfacing system (LOCA).

Other severe accident phenomena that were not addressed in WASH-1400, but were recognized to challenge containment integrity in the recent past include direct containment heating (DCH) and BWR Mark I liner failure:

DCH: Involves melt release at high pressure and the potential for large-scale melt dispersal throughout the containment volume. Such dispersal could lead to direct heating of the containment atmosphere and associated pressurization. Containment geometry could play a significant role here. Conceptually similar to the early delta.

M[illegible] failure: Because the tight Mark I containment geometry relative to the large corium inventory, direct exposure of the liner in the vicinity of the drywell floor to the high temperature melt can provide an obvious potential mechanism for liner failure (melt-through or creep failure). A variant of the Epsilon failure mode.

Most of the research effort of the recent past relating to containments loads associated with severe accident phenomena has involved the performance of scaled experiments as well as the development of analytical tools for analyzing severe accident scenarios and consequences. In addition to addressing generic issues, both the experimental and analytical programs have addressed issues unique to specific containment configurations and scenarios, such as for example, the presence of water in a reactor cavity and under what conditions could the molten core debris be coolable. This is an important question not only for a number of issues relating to existing containments, but also to the mode of cooling the containment of the advanced W LWR design, the AP-600, under both design and severe accident scenarios.

Initial and Boundary Conditions

Clearly, the extent of the challenges to containment integrity, at least for a number of these phenomena, depends on the state of an LWR reactor core at the time of vessel failure (i.e., the melt mass, rate of release, composition and temperature of melt released from the core). Due to lack of relevant data, bounding analyses and experts' panels were used to address these phenomena at the time of WASH-1400, and even to some extent the more recent NUREG-1150 efforts.

Since then, a great deal of information has been obtained on the processes involved in the early phase of melt progression that extends through core degradation and metallic (but not ceramic) material melting and relocation. This information has come from integral tests in the PBF, ACRR, NRU, NSRR, and Phebus test reactors, from the LOFT FP-2 test, from tests in the CORA ex-reactor fuel-damage test facility, and from separate-effects experiments on significant phenomena. Most of the available information on late-phase melt progression has come from the post accident examination of the TMI-2 reactor. Despite the core reflooding that successfully terminated the TMI-2 accident, the general late-phase melt progression phenomenology of that accident, although not the detailed behavior, appears to be applicable to unrecovered as well as to recovered accidents and possibly to some BWR accidents as well.

We now believe that the TMI-2 configuration illustrates essentially all the general melt progression phenomenology that apply to large numbers of PWR and BWR blocked-core accident sequences. This expanded knowledge of the melt conditions has contributed significantly to the reduction in the degree of conservatisms and reduced some of the difficulties that jeopardized or detracted from the credibility of earlier studies on assessing containment performance For

example, the observation that the risk significance of DCH has decreased relative to earlier studies can be partially attributed to an improved understanding of melt progression.

A more detailed discussion of our current state of understanding the severe accident phenomena related to containment challenges, including on-going related research efforts, is provided in the remainder of this paper.

## FUEL-COOLANT INTERACTIONS (Including α-mode Containment Failure)

Significant fuel coolant interactions can occur when molten core debris drops into lower plenum water.

As the past confirms, issues associated with FCIs can be widely varying and controversial, and, as in many other cases, resulting from the often limited ability to specify the initial conditions for the interaction. To clarify this point further for LWR severe accidents, it is often unclear what is the quantity and temperature of the melt available to pour, nor is it clear what is the size of the pour opening. Other complications arise due to the inherently unstable multi-phase flow regimes and lack of experimental information at properly scaled conditions.

Since its first attempted quantification in WASH-1400, the energetics of large, coherent FCIs (in particular, those energetic enough to produce containment failure, α-mode) have dominated research activities. Significant progress has been made to the point that α-failure does not seem to be a dominant contributor to early containment failure probability in current risk analyses. However, the shift in emphasis to accident management for variety of reactor geometries and meltdown scenarios, coupled with the wide uncertainties in the NUREG-1150 expert quantifications of FCIs, the subject of FCI is again the focus of some reactor safety research. The current research effort is to provide the appropriate methodological and analytical tools for evaluating major aspects of the accident sequence, including quantification of steam and hydrogen production from FCIs, the mode and timing of vessel failure, and ex-vessel events of potential significant to debris coolability and containment loading (i.e., Mark-I melt spreading and liner attack, Mark-II, and Mark III suppression pool FCIs, AP600, and SBWR). There are fundamental aspects of FCIs that are germane, of course, to both the in-vessel and ex-vessel FCIs; however, the dominant regimes and hence major aspects of the detailed approach can be quite different.

Three experimental programs are currently addressing this topic. The one at UCSB is examining the fundamental component of an explosion e.g., premixing and fragmentation. The purpose of the second set of FCI is being done at UW to study triggering and measure explosion yield. The third program being carried out at the FARO facility in Italy is to observe the integral behavior of fuel-melt quenching at high pressure.

## DIRECT CONTAINMENT HEATING

This process is postulated to arise from an accident sequence which develops while the primary system is at high pressure. Failure of the primary system would in such circumstances be most likely to occur when the core was extensively

molten. If the breach in the primary system occurred at a part of the boundary retaining molten debris the result would be a massive expulsion of very hot liquid material driven by the primary system pressure. The consequent dispersal of finely divided debris may lead to rapid heating of the containment atmosphere and to a sudden and large rise in containment pressure. Clearly, the extent of dispersal would be geometry-dependent, and it is still not clear what is the appropriate manner to quantify such effects. Furthermore the sequence would also give rise to a highly dynamic release of hydrogen formed earlier during the core heat-up and slumping phase and during the subsequent blowdown.

Considerable research on direct containment heating has been undertaken to provide new insights and an improved data base to answer the questions, What is the nature of the DCH threat, and what mechanisms and configurations exist ex-vessel that will mitigate or eliminate it? It should be noted that some of the problem associated with DCH could potentially be eliminated if a highly reliable primary system depressurization could be achieved prior to vessel failure, however, the advantage and disadvantage of such strategies should be carefully evaluated. This paper is not addressing this issue.

In addition to predicting the dispersal of debris from the reactor cavity, DCH models are being developed that are capable of evaluating or suitably accounting for debris fragmentation, debris to gas heat transfer, debris trapping, hydrogen generation, hydrogen combustion, and water vaporization as a result of debris-water interactions in the cavity or other containment regions.

While the details of the cavity configuration, for the limited range of variations considered, have been shown to have less effect on debris dispersal at elevated pressures, it is intuitive and has long been argued that compartmentalization and structures downstream of the cavity would trap or deentrain debris from the flow stream exiting the cavity on its way to the bulk containment.

Integral testing, sponsored by NRC, was initiated to investigate the containment loadings resulting from DCH. The experimental program explores integral DCH phenomena at different scales for representative reactor designs and for representative mitigative features. In addition, separate-effects testing to confirm the validity of the assumptions employed in the scaling analysis and to validate the model discussed above was also initiated.

Interpretation of the integral tests conducted thus far using scaling evaluations based on the evaluation of conditions for a station blackout at the Zion plants indicate that the pressure rise and temperature loads generated by DCH is much less than we originally thought and within the capability of the containment.

## HYDROGEN DEFLAGRATION AND DETONATION

The safety significance of hydrogen combustion during a severe accident for non-inerted containments is that the concomitant energy release manifested as pressurization and heating of the containment atmosphere could pose a threat to containment integrity or to the survival or functioning of essential safety equipment. When hydrogen combustion alone is insufficient to threaten containment integrity, combustion may still represent a significant contribution to containment loadings when considered conjunctively with direct containment heating or steam pressurization. In the event hydrogen released into the

containment during a severe accident accumulates without igniting but mixes rapidly throughout the entire volume, the global concentrations in most instances will remain below the limits for detonation. If mixing does not occur because of stratification or pocketing in enclosed areas, those richer mixtures that occur, at least locally, present a greater likelihood for flame acceleration and detonation.

Research conducted world-wide over the past 12 years has extensively investigated a number of issues related to hydrogen combustion and transport during severe reactor accidents. Much of the work, focused on global deflagrations of premixed volumes of hydrogen, air and steam. Diffusive burning of hydrogen has also been the subject of experimental research conducted by both the NRC and the industry. Diffusion flame research has also been carried out at Sandia National Laboratories and at other research facilities, including the large scale facility at Factory Mutual Research Corporation, used to investigate hydrogen mixing and combustion in a Mark III containment.

In conjunction with hydrogen combustion research, the research community has also experimentally explored the issue of hydrogen transport and mixing.

Computer codes on hydrogen transport and combustion have been developed to evaluate the static or dynamic pressure loads from hydrogen combustion and detonation in containment.

Results of these evaluations should enable us to make regulatory decisions to assess the potential threat to containment integrity. In particular, for PWRs with large dry containments, combustible concentrations build up very slowly. Because of the large volume, detonable compositions are unlikely to develop unless significant spatial concentrations exist. Hydrogen is released into the containment from the pressure vessel through leaks or valves and also as a result of a melt-concrete interaction. The distribution into the containment results mainly from natural circulation currents, diffusion and condensation processes. In containments with many compartments these processes will take a longer time than for relatively open containments. These aspects are sequence- and plant-specific and require additional work before final conclusions can be drawn. However, an accident management strategy could be developed by which early ignitions and burning could limit the concentrations of hydrogen below the combustion-detonable limits.

To address the effects of elevated temperatures on flame acceleration and detonation transition, the NRC initiated a high-temperature, high-speed hydrogen combustion program under a joint agreement (signed in June 1991) for a cooperative program with the Ministry of International Trade and Industry of Japan and the Nuclear Power Engineering Center. Under this agreement, a high-temperature high-speed hydrogen combustion research program, extending over 5 years, has been developed.

In the low-speed hydrogen combustion research program, the aspects of diffusion flames scalability and transient high-temperature combustion will be investigated at RPI.

## CORE-CONCRETE INTERACTION AND DEBRIS COOLABILITY

Core-concrete interactions would occur during a severe accident only after penetration of the reactor vessel and flow of the core debris onto the concrete basemat. Decomposition of the concrete from this interaction results in the release of steam and carbon dioxide, which may be partially reduced to the combustible gases hydrogen and carbon monoxide. As the gases pass through the hot molten debris, they sparge small but potentially important quantities of radioactive elements from the debris. These radioactive aerosols can be released to the containment, thereby adding to the accident source term. The major areas of concern associated with the core-concrete interactions during a severe accident are the complete penetration of the basemat and the generation of radioactive aerosols and combustible gases. Another related concern is the overheating of important structures inside the containment.

An extensive program of analytic and experimental research to obtain improved understanding of core-concrete interactions was undertaken in U.S. and abroad. The analytical research focused on the development of models for studying phenomenological aspects of core-concrete interactions such as heat and mass transfer, while the experimental research focused on conducting scaled-down experiments simulating prototypic reactor accident scenarios. These studies have recognized the variety of concretes used in nuclear power plants in the U.S. and the widely diverse accident scenarios that lead to core-concrete interactions. The effort to understand core-concrete interactions was also broadened to include a reassessment of the models used to predict radionuclide release.

Arguments can be adduced that for certain designs in which there is room for debris to spread out and to be submerged in water the debris will be cooled so that gas evolution is effectively limited. The efficacy of attempts to control core-concrete interactions by applying water seems to depend significantly on the amount of water available and on the nature of solid crust formation at interfaces between water and melt. Some additional work, including experiments, is needed to assess the adequacy of that strategy in preventing concrete basemat penetration. It must also be borne in mind that if the application of water is effective in cooling the debris the heat thereby conveyed by steam has to be rejected by the systems for condensing steam in the containment or other means. If the debris is not effectively cooled the permanent gases generated would cause overpressurization but that could be countered by venting the containment.

A particular problem affecting BWR Mark I containment is risk of contact between debris and containment wall. If hot core debris penetrates through the bottom of the reactor pressure vessel, it spreads on the drywell floor and through the pedestal door and attacks the containment steel shell (liner).

NRC research over the past several years has addressed the key phenomena associated with the liner melt-though issue, such as melt conditions at the time of vessel failure; melt spreading characteristics; thermal-hydraulic characteristics of molten core-concrete interactions both with and without an overlying water pool; heat transfer characteristics at the interface of the molten core, overlying water pool, and liner; and fission product attenuation in the presence of an overlying water pool.

of the research information derived from these programs into an assessment of the conditional probability of liner failure both with and without an overlying water pool in the drywell, given a core melt accident that proceeds to vessel failure, was completed. A description of this methodology and its conclusion is provided in NUREG/CR-5423.

In order to obtain data to support the development of coolability criteria, an experimental program called MACE was developed under the sponsorship of NRC, EPRI, and several other countries. The program is intended to determine the ability of water to quench and fragment molten core debris during MCCI and to enable characterization of the resulting debris for assessment of permanent coolability.

## SUMMARY OF CONTAINMENT CHALLENGES

In summary, an early containment failure usually results in an immediate high release of radioactive fission products to the environment. Later an uncontrolled leakage cannot usually be closed by normal measures and also allows a continuing release of fission products. Loads early in the severe accident sequence may arise in various ways:

- It is generally considered - although not completely established - that a steam explosion (alpha-mode) threatening containment integrity is a low probability event.

- The loads from a hydrogen deflagration or detonation (gamma-mode) are very sequence- and plant-specific and thus no generic assessment is applicable.

- Loads from rapid steam production resulting from a core melt and water interaction are plant-specific; currently assessed as less likely to result in a threat to integrity of large dry containment.

- Loads from rapid heat addition to the containment atmosphere (direct containment heating) could, for some designs especially small volume, result in containment failure. This conclusion is sensitive to the assumptions and method of analysis employed and more research is under way to study this process. Preliminary results from tests conducted at SNL and ANL for the Zion plants indicate that DCH loads are much smaller than originally thought and is less than the containment pressure capability. Subcompartment entrapment of debris is the most significant mitigative feature.

The most likely routes to late containment failure are pressure and temperature build-up due to vaporization of water or the production of non-condensible gases from a basemat melt-through. However, the fission product release from a late failure is usually very much less than for early failure and more time is available for appropriate accident management actions.

Reactor containment structural integrity research is being conducted to assess the risk posed by pressure and temperature loads outside the design basis and estimate the effectiveness of proposed mitigative steps. Efforts include assessing the ability of the containment to withstand the loads generated in a severe accident and analyzing information on aging degradation of containments.

The major source of risk to the public from the operation of nuclear power plants stems from accidents that lead to a containment failure, especially early failures. The research results will be used to predict the threshold of failure, the mode of failure, and the related leak rates in order to estimate plant releases and offsite consequences.

## SEVERE ACCIDENT RULEMAKING

We believe that research and engineering on the significant severe accident phenomena and scenarios and cost effective methods to mitigate them, coupled with our understanding of the details of future plant designs, have sufficiently matured to allow the development of standards for plant performance for future LWRs. The NRC staff has prepared an advanced notice of proposed rulemaking which it has discussed already with the ACRS and will be presenting it to the Commission during the next few months and will be asking interested parties for advice and recommendations on the proper scope and method to incorporate these considerations into the NRC's regulations. This notice will reflect consideration of the extensive work accomplished in the severe accident area. The Commission has continued to take all reasonable steps to further reduce the risk from severe accidents at existing plants through its regulatory programs. For example, the Commission completed rulemakings on several key items of concern (e.g., station blackout, anticipated transients without scram, hydrogen generation and control), has implemented a containment performance improvement program based upon insights regarding containment performance under severe accident conditions and has initiated a program for individual plant examination (IPE) for severe accident vulnerabilities.

The staff has been reviewing proposed criteria for future light water reactors submitted by Electric Power Research Institute (EPRI) and several new LWR designs with respect to the Commission's severe accident policy and 10 CFR 52. In performing these reviews, the staff has proposed criteria to address severe accident and containment issues that go beyond the existing regulations. The staff has sought and received Commission guidance on the application of these proposed severe accident and containment criteria to the LWR designs now under review. The criteria discussed in this Advanced Notice of Proposed Rulemaking (ANPR) would serve to codify much of the Commission's guidance for general application to all future LWRs.

# PROPOSED CRITERIA TO ACCOMMODATE SEVERE ACCIDENTS IN CONTAINMENT DESIGN

by
David A. Ward, Member
Advisory Committee on Reactor Safeguards

Paper presented at
Fifth Workshop on Containment Integrity
May 12-14, 1992
Washington, D.C.

## Introduction

A year ago the ACRS sent to the Commission a letter entitled 'Proposed Criteria to Accommodate Severe Accidents in Containment Design'. This letter was our advice to the Commission on how they might go about, and have the NRC staff go about. bringing containment design into the modern world. At our own suggestion the ACRS had been tasked by the Commission, about two years earlier, to develop ideas on how containment design requirements might be developed to better account for what is now known about the nature of severe accidents and the job of mitigation for which containments are intended.

We proceeded in our task by trying to find out what experts knew and believed about containments and severe accidents. We held a long series of information-gathering meetings and did a lot of reading. We heard directly or indirectly from many experts, including many of you at this meeting. From an abundance of input, which was not, by the way, all in a single coherent stream, we formulated a proposal for the Commission. The proposal is one part safety philosophy, one part regulatory approach, and one part technical strawman.

## ACRS role

Before going on, let me take a minute to explain what the ACRS is and what it does, and to mention an important caveat related to what I am going to say. ACRS, the Advisory Committee on Reactor Safeguards, is an independent, part-time advisory body to the Commissioners of the NRC. It has existed for almost forty years. ACRS gathers information by interacting with the Commissioners, NRC staff, and experts on nuclear safety and regulation from industry, academia, laboratories, and the public. We then provide advice to the Commission or NRC staff management through formal written letter-reports on a wide variety of subjects related to reactor safety and regulation. Neither the Commission nor the staff management has any legal compunction to take our advice. They are under some constraint to listen to it. And that is probably all we can ask.

Our advice is always a consensus of what the Committee believes. ACRS speaks only through its formal letters. No individual member is authorized to speak for the Committee or even to interpret a letter in the name of the Committee. Hence, the caveat I mentioned earlier. What I say here today will represent my own views and not necessarily those of the Committee. What the Committee wanted to say on this subject is in its letter of May 1991.

## Observations about existing containment requirements

When we had completed our series of information-gathering meetings somewhat over a year ago, three general observations could be made. One was expected, a second was a pleasant surprise, and the third was a disappointment.

A first observation was that the existing regulatory requirements for containment design were seriously inadequate. The surrogate requirements which had been developed as a stop-gap measure thirty years ago were technically overly simple, and applied by rigging together pieces of several regulations and regulatory practices. I don't want to be too negative. In the 1960s, not much was known about the nature of severe accidents and something had to be done. The pragmatic, surrogate design basis for LWR containments, a large LOCA, was not all that bad. ACRS was a party to the jury-rigging, in fact. The system worked well under its limited challenge in the TMI accident in 1979. But, when we [and you] looked harder we had to admit that the next challenge might not be as conveniently limited and some of us became a little nervous about how well the system could then do its job.

The second observation, the pleasant one, was that a tremendous amount of good technical information about the nature of severe accidents and containment capabilities was available. The twin impetus for development of this information, from the late 1970s through the 1980s had been the TMI accident and the evolution of credible risk-analysis methods, PRA. TMI taught us that bad things can happen -- even to good people who have been loyal to precepts of excellence and QA. PRA gave us an intellectual means of dealing with this reality -- without wanting to jump off the nearest bridge. As a result, a much improved understanding of severe accidents and containments had been developed through research and analysis. The understanding was not perfect, it was not complete. But, nothing ever is, and the technical information was sufficient to support much more knowledgeable design choices.

The third observation, the disappointing one, was that there was in place no serious, comprehensive effort to synthesize this improved information into a new set of design requirements. There was an awareness of the new information, and containments designed to the old requirements were being "checked against" selected challenges from severe accidents. This was, however, an imprecise and inefficient process. Neither the NRC nor industry was focusing on the development of an updated set of requirements which would explicitly deal with the consequences of severe accidents.

The 1991 ACRS letter was then a proposal which reacted to these three observations:
1] Something better was needed
2] Something better was available
3] But, there was no process of synthesis underway to make effective use of this available knowledge

Conclusions about what should be done

Our proposal was that a practical and complete-enough new set of design requirements, a new surrogate for severe accident challenges should be developed. There were three key conclusions leading to our proposal:

First, the surrogate design basis should be developed by the NRC. There are several reasons for this. Tradition; NRC [actually, of course, the AEC] developed the old one. NRC staffers have the best command of the totality of information available. Finally, NRC should have a definite position on this most important aspect of reactor safety and they might just as well clearly describe that position to applicants up front.

Second, the surrogate would have to be more complex than the old one. It is clear from research and analysis of the past decade that there is not a single enveloping accident which covers all possible phenomenological challenges to a containment -- comforting as that concept might be. However, the more complex set of requirements must still, unambiguously, be a surrogate. Precise definition of severe accident challenges is not possible and the judgment of experts and authorities will be necessary. There is no reason to apologize for that.

Third, the time to move ahead with this effort is now. There is no point in waiting for more research or better analyses. There are no indications that anything more than incremental gains in knowledge are just around the corner. This is not to say that some research should not continue. If some splendid new insights do become available, that will be wonderful and we should then figure out how to take advantage. But, we cannot plan for them. We should consolidate our gains and move ahead now with what we have.

Proposed regulatory program

A possible regulatory program to effect these changes would be as follows:

First, the General Design Criteria in Part 50 would be revised to acknowledge that containments should be designed for a range of challenges that can threaten their function during severe accidents. Several different classes of challenge or containment loads would be defined. For each, the nature of the challenge would be described in general terms; specifics and bounding quantification would be relegated to an ancillary Regulatory Guide. Also, for each, a success criterion would be specified. In most cases success will be defined simply as maintenance of the containment function without excessive leakage for some appropriate period following the particular challenge.

Second, Regulatory Guides would detail an acceptable means by which the design requirements can be implemented. What we had in mind is a relationship between each GDC requirement and its companion Regulatory Guide similar to the existing relationship between GDC Criterion 35 for Emergency Core Cooling and Appendix K to Part 50 for ECCS Evaluation Models. Criterion 35 states that a system shall provide "abundant emergency core cooling." Appendix K gives, in reasonably unambiguous terms, a technical definition of the leak to be accommodated and what is meant by the terms "abundant" and "cooling."

The technical content of each Regulatory Guide should provide as complete and unambiguous a basis for containment system design as can be practically developed. It would not include probabilistic statements or requirements. For example, the criterion for capacity to accommodate hydrogen combustion might state the total amount of hydrogen to be considered, say 150% of that which could be generated by complete oxidization of cladding in contact with active fuel, and then insist that a specific analysis for mixing and stratification should be performed. The Regulatory Guide would describe acceptable mixing models, based on containment type.

An important advantage of this program would be that the NRC would thereby take responsibility for the important technical judgments necessary to transform knowledge from severe accident research and risk assessments into criteria and requirements that can be used by a designer. This would not be done in a vacuum. Review and input from the industry and the reactor safety community should be sought as the rule changes and Regulatory Guides are developed. That's part of the rulemaking process. This procedure avoids the uncertainty and opportunity for licensing instability that will result if the NRC merely passes on to applicants probabilistic goals or "white papers" on severe accident research with the expectation that, after a number of back-and-forth trials, the applicant will eventually develop something the NRC finds acceptable.

We concluded that an adequate strawman surrogate should include a description of eight challenges. Note that this list is as important for what it leaves out as for what it includes. The intent is that this list of eight is a "good enough" representation of the entire spectrum of possible phenomena and challenges. There are other possibilities. Our judgment is that these are adequate. The specific list is as follows:

a] Loss of coolant accident

b] Energetic fuel-coolant interactions, in particular

- missiles from in-vessel steam explosions
- pressure pulses from ex-vessel steam explosions

c] Hydrogen combustion and detonation

d] Direct melt attack on structure or pressure boundary

e] High pressure melt ejection
f] Corium-concrete interaction
g] Pressurization from decay heat
h] Local high temperatures at critical structures or components

Two comments on this surrogate list:
1] Given particulars of the design of a specific LWR plant, some of the challenges might be ruled out as requirements if an explicit analysis demonstrated them to be sufficiently improbable.
2] ACRS and others have gone on record as in favor of a containment design requirement which would, given a severe accident challenge, fail not more than 10% of the time. We mean, and we suspect others mean, by this that we do not expect containments to be able to manage anything anyone can think of, but only most things. As many of you know, only better than I, a generalized CCFP becomes very difficult to define with precision. To some it means, that for a string of particular severe challenges, the containment will hold together 90% of the time. To me it means that the containment will withstand 90% of the spectrum of possible severe accident challenges to which it could be exposed. I don't know how to calculate that, but I see the above list of eight challenges as an attempt to define that sort of capability. I don't believe we can be more precise at this time.

What the Commission is doing

The Commission has not yet decided whether to follow all, some, or none of the ACRS proposals. The NRC staff has a couple of programs in place which relate to the issues we have raised. One program intends to revise Part 50 of the regulations to more explicitly account for certain severe accident conditions. The staff is about to issue an Advanced Notice of Proposed Rulemaking which describes three alternatives and asks for public input. Although the ACRS letter is one of the alternatives, the staff has stated concern about our proposal to incorporate new criteria in the GDC and would prefer that another section be added to Part 50. Their concern is that inclusion in the GDC would imply the necessity for a lot of QA requirements and "bells and whistles" which would not necessarily be appropriate for advanced containment features. I don't disagree, but believe new GDC for containment features could specify a different level of redundancy and reliability requirements than is now traditional for so-called safety grade systems. I favor an explicit recognition that what we have been discussing are design bases, in the plain English sense of those words. There is, at least, a problem of semantics when we describe severe accidents as being "beyond design basis". Of course containments should be designed for severe accidents. That is, after all, their major purpose.

A second related program is inclusion of some severe accident and containment issues in lists of policy issues which the NRC staff is asking the Commission to consider. One such paper is SECY-90-016, "Evolutionary Light Water Reactor [LWR] Certification Issues and Their Relationship to Current Regulatory Requirements". At least one more similar paper is being developed. These papers raise technical issues, some of which are related to containment, but it is yet unclear what "raising an issue" means. If nothing else, applicants and potential applicants are alerted that the NRC is interested and will be asking questions about some particular item. Perhaps that is enough.

I would prefer a system of regulation in which NRC takes responsibility for making key judgments about important safety issues and then tells applicants what it expects in terms that are as practical and unambiguous as possible. I think that can be done now for containment requirements, if we set our minds to it.

---

Reference: ACRS letter to NRC Chairman Carr, May 17, 1991, "Proposed Criteria to Accommodate Severe Accidents in Containment Design"

# SESSION 1

# CONTAINMENT DESIGN CONSIDERATIONS FOR SEVERE ACCIDENT CONDITIONS

# A REVIEW OF CONTAINMENT ACCIDENTS

Benoît De Boeck
AIB-Vinçotte Nuclear

## Abstract

The consequences of severe reactor accidents depend greatly on containment safety features and containment performance in retaining radioactive material. If the containment function is maintained in a severe accident, the radiological consequences will be minor. If the containment function does fail, the timing of failure can be very important. The longer the containment remains intact relative to the time of core melting and radionuclide release from the reactor coolant system, the more time is available to remove radioactive material from the containment atmosphere by engineered safety features or natural deposition processes. Delay in containment failure or containment bypass also provides time for protective action, a very important consideration in the assessment of possible early health effects. Thus, in evaluating the performance of a containment, it is convenient to consider no failure, early failure, late failure, and containment bypass as separate categories characterizing different degrees of severity. The paper reviews the containment challenges posed by the severe accidents, on the basis of an extensive list of references. First the phenomena that could lead to early containment failure are described: direct containment heating, steam explosions, hydrogen combustion, and isolation failures. Then the late containment failure modes are treated: gradual overpressurization, basemat meltthrough, and overheating. Finally, some words are said about containment bypass.

## 1. INTRODUCTION

The consequences of severe reactor accidents depend greatly on containment safety features and containment performance in retaining radioactive material [1]. The early failure of the containment structures at the Chernobyl power plant contributed to the size of the environmental release of radioactive material in that accident. In contrast, the radiological consequences of the Three Mile Island Unit 2 accident were minor because overall containment integrity was maintained and bypass was small.

Normally three barriers (the fuel rod cladding, the reactor coolant system pressure boundary, and the containment pressure boundary) protect the public from the release of radioactive material generated in nuclear fuel. In most core meltdown scenarios, the first two barriers would be progressively breached, and the containment boundary represents the final barrier to release of radioactivity to the environment. Maintaining the integrity of the containment can affect the source term by orders of magnitude.

In most severe accident sequences, the ability of a containment boundary to maintain integrity is determined by two factors: (1) the magnitude of the loads, and (2) the response to those loads of the containment structure and the penetrations through the containment boundary. Although

there is no universally accepted definition of containment failure, it does not necessarily imply gross structural failure. For risk purposes, containment is considered to have failed to perform its function when the leak rate of radionuclides to the environment is substantial.

Thus, failure could occur as the result of a structural failure of the containment, tearing of the containment liner, or a high rate of a leakage through a penetration. The containment is also said to have failed when a failure in the containment isolation system results in an important leakage of radioactive material to a secondary building or directly to the environment. Finally, in some accidents, the containment building is completely bypassed. This is the case in interfacing-system loss of coolant accidents and in steam generator tube rupture accidents.

If the containment function is maintained in a severe accident, the radiological consequences will be minor. If the containment function does fail, the timing of failure can be very important. The longer the containment remains intact relative to the time of core melting and radionuclide release from the reactor coolant system, the more time is available to remove radioactive material from the containment atmosphere by engineered safety features or natural deposition processes. Delay in containment failure or containment bypass also provides time for protective action, a very important consideration in the assessment of possible early health effects. Thus, in evaluating the performance of a containment, it is convenient to consider no failure, early failure, late failure, and containment bypass as separate categories characterizing different degrees of severity.

It is important to realise that not all core meltdown accidents lead to containment failure. Recent studies [1] have shown that, at least for PWR's, the containment has a high probability of remaining intact during a severe accident. The average conditional probability of no containment failure is 81% for Surry, 73% for Zion, and 65% for Sequoyah. BWR containments appear to be less robust: the average conditional probability of no containment failure is 28% for Peach Bottom, and 23% for Grand Gulf.

The following sections will describe the containment challenges posed by the severe accidents. The description will mainly be related to accidents occurring in hot condition, but when needed, the peculiarities of cold shutdown states will be mentioned. Some actions which have the potential to protect the containment function, and thus increase the conditional probability of no containment failure, will also be described.

## 2. EARLY CONTAINMENT FAILURE

Early containment failure is defined as failure prior to or shortly after the core debris penetrates the reactor vessel. An early failure is important because it tends to result in shorter warning times for initiating off-site protective measures and it also reduces the time available for deposition of radioactive materials within the containment. Potential early containment failure modes include direct containment heating, steam explosions, hydrogen burns, and isolation failures.

## 2.1 Direct Containment Heating

In certain core damage accidents, such as a small LOCA or station blackout, in which the reactor system remains pressurized during core meltdown, it has been estimated that certain modes of vessel failure could lead to a high pressure ejection of molten core material. In case of a local failure of the lower head, the molten materials would initially be ejected into the cavity beneath the pressure vessel but may subsequently be swept out of the cavity into the containment atmosphere where the liberation of thermal and chemical energy (oxidation of debris) can directly heat the atmosphere. This complicated physical and chemical process is known as direct containment heating (DCH) and may be a significant source of containment pressurization [2].

The DCH loading is expected to be most important for large dry PWR containments [3]. The expulsion of corium into the containment atmosphere will occur only from a sufficiently high-pressure system. BWR's are provided with an automatic depressurization system, which is designed to depressurize the primary system following the loss of emergency cooling and prior to severe fuel damage. Many BWR containments are inerted and thereby eliminate oxidation. The ice-condenser containments for PWR's have a cavity configuration that would obstruct debris dispersal and ice beds that would cool the core debris prior to ejection into the containment atmosphere.

Calculations were performed at SNL by using the CONTAIN code [3]. Under the assumption that the complete core is ejected and that 100% oxidation of cladding occurs, a peak pressure of 1.2 MPa and a peak temperature of 1000 K are calculated. This is expected to represent an upper bound.

In 1989 a series of DCH-calculations was performed for Ringhals by the UKAEA at Winfrith, using the CORDE code [4]. The calculations gave too high values for the pressure peaks because the containment was treated as a single volume in CORDE. The peak pressure for the base case was 0.92 MPa. Sensitivity calculations showed that the most important quantities in the variation of the accident scenario were the primary system pressure and the mass of debris in the lower head before meltthrough. The maximum containment pressure is reduced to 0.46 MPa if the initial primary system pressure is reduced from 15.3 to 0.9 MPa. The modelling parameter variations which had the largest impact on the results were options for chemical reactions and the values used for the radius of debris particles in the dispersed melt.

In support of the NUREG-1150 project, BNL performed DCH parametric studies for the ZION plant [5]. A seven-cell and a single-cell nodalization of the Zion containment building were used in the analysis. The seven-cell calculations incorporate all the features of the CONTAIN-DCH model. A comparison of the seven-cell calculation results with the upper-bound single-cell results indicates that the mechanistic CONTAIN treatment of DCH (albeit parametric) leads to calculated DCH pressure rise magnitudes which are significantly lower (by about 50%) than those predicted by the single-cell upper bound calculation. This difference in the predicted results is attributable to mechanistic treatment of various (mitigating) heat and mass transfer processes involved in the seven-cell nodalization. The results for the seven-cell nodalization indicate that the DCH containment loadings predicted by the CONTAIN code are close to the

estimated Zion containment capacity for initial conditions involving high primary system pressure (>7 MPa) and large participating melt mass (>70% of core melt inventory).

Experimental investigations were also performed at SNL (SPIT/HIPS and SURTSEY-DCH tests) and at ANL (CWTI tests) using high temperature melts [2]. The simulated melt ejection in the SNL experiments was achieved by burning an iron-oxide/aluminium thermite in a small steel vessel that was pressurized with either nitrogen or carbon dioxide. The SURTSEY-DCH experiments include a large (approximately 100 m3) steel vessel representing a scaled large dry containment. Preliminary results show substantial pressurization of the SURTSEY vessel and also show the importance of debris impact onto steel surfaces.

The calculational and experimental investigations have allowed to identify the important DCH parameters. These parameters include:

- system pressure prior to vessel failure
- mass of molten material in the lower plenum
- composition and temperature of the melt
- particle size distribution
- entrainment of debris
- trapping of debris by freezing onto surfaces
- oxidation of the debris by steam
- heat transfer coefficients
- interactions with water in the cavity
- transport and burning of hydrogen

Large uncertainties still exist in the quantification of these parameters, leading to a large uncertainty in containment loading due to DCH. Nevertheless, from the studies performed up to now, it can generally be concluded that containment integrity would be threatened if a large fraction of melt is involved in the process and a hydrogen burn occurs [5]. However, containment loading is plant specific, as it strongly depends on the reactor cavity configuration and the subcompartment arrangement in the containment.

Depressurization of the primary system (by opening the pressurizer relief valves) is the only measure that has so far been identified as a possible means of preventing DCH [2]. Some countries have, or intend to introduce, procedures involving depressurization of the system [6]. Such a procedure, if carefully implemented, has the potential to offer several benefits: to prevent core melt by gaining access to low pressure water injection means; and if this is not successful, to delay core melt and to prevent high pressure melt ejection [7].

The main issues associated with this action are: (1) establishment of appropriate criteria for initiation of depressurization (if initiation is too early, there will be an additional loss of coolant inventory through the relief valves, which could result in an early heat up of the core), and (2) adequacy of the systems designed to achieve depressurization. It has to be checked for plant specific systems, that it is possible to depressurize to a level which would be effective in limiting debris dispersal. This level is sometimes called the DCH cutoff pressure. Recent calculations based on corium dispersal considerations indicate that the DCH cutoff pressure lies in the range of 1.5 to 2.5 MPa [5].

## 2.2 Steam Explosions

The term "steam explosion" refers to a phenomenon in which molten fuel rapidly fragments and transfers its energy to the coolant resulting in steam generation, shock waves, and possible mechanical damage. To result in a significant safety concern the interaction must be very rapid and must involve a large fraction of the core mass. If such events were to take place within the reactor pressure vessel, missiles could be generated which might penetrate the containment and allow early release of radioactive material. In the Reactor Safety Study [8] this mode of containment failure was denoted as the alpha-mode failure.

In a recent review of the probability of alpha-mode failure, a group of experts, the Steam Explosion Review Group (SERG), performed independent analysis and examined available experimental data. The spectrum of opinions indicated that the probability of alpha-mode failure is considered to be much less likely than was estimated in WASH-1400 [5]. The SERG divided the fundamental processes of steam explosion into three general areas:

1) Initial conditions: this involves the geometrical configuration of the reactor vessel at the time of fuel-coolant contact and the amount of fuel and coolant available for the interaction.

2) Mixing and conversion ratio: this involves the basic physics of the vapour explosion such as the fuel-coolant mixing, triggering, propagation, and the resultant conversion of fuel thermal energy to the slug kinetic energy.

3) Slug-missile dynamics: this involves the expansion characteristics of the slug within the specific reactor geometry, and the coupling to solid missile generation and containment penetration.

Steam explosion requires a triggering mechanism. Experiments indicate that high ambient pressure tends to reduce the likelihood of, although not preclude, the triggering of a steam explosion. In-vessel steam explosions, which are controlled by the triggering mechanism, are more likely to occur when the primary system is at low pressure. On the other hand, direct containment heating is associated with high pressure sequences. So there is a kind of balance between the probability of alpha-mode and DCH containment failure. Given the present evidence, experts tend to favour steps to preclude DCH.

The analyses in NUREG-1150 indicate that the potential for in-vessel steam explosions to result in early containment failure is less than 1 percent for each of the five plants which were analyzed [1]. For Surry and Zion, steam explosions represent a significant fraction of the early failure probability, but only because the overall likelihood of early failure is small.

When molten core material drops into water outside the vessel, the potential failure mechanisms are different. In the Grand Gulf plant, a shock wave could propagate through water and impact the concrete structure that provides support to the reactor vessel. Substantial motion of the vessel could then lead to the tearing of penetrations through the drywell wall. Because of the

shallow water pool at Peach Bottom, dynamic loads from steam explosions do not represent a similar mechanism for failure.

In general, the threat to containment integrity posed by ex-vessel steam explosions is plant specific, but it appears that PWR large dry containments are less vulnerable.

Accident management measures to prevent steam explosions do not seem to exist.

Core melt accidents in cold shutdown states have also the potential to trigger steam explosions because the pressures involved are low, but as far as we know this has not yet been assessed.

## 2.3 Hydrogen Combustion

During a severe accident in a LWR, oxidation of the metallic components of the reactor core will produce hydrogen. Hydrogen combustion in the containment building could produce pressure and temperature levels that may threaten the integrity of the containment boundary. The threat to containment depends on the details of the accident sequence and the containment design.

### Hydrogen Generation

The most important hydrogen source during a degraded core accident is the oxidation of zirconium by steam. This reaction becomes important when zirconium in the reactor core is heated to high temperatures as the core is partially or completely uncovered. Typically, a zirconium temperature in excess of 1000°C is required to produce a high reaction rate. In addition, steel in the reactor vessel could react with steam at high temperatures when the core is uncovered. The oxidation rate of steel can become larger than that of zirconium when the melting point of steel is approached at 1370 to 1500°C [5].

Both the Zr/steam and Fe/steam reactions are exothermic. During the heatup transient, the reaction heat is an important heat source and directly enhances the hydrogen production. The two reaction rates are dependent on the temperature and the amount of steam available at the reaction surface.

Hydrogen generation is difficult to predict. The calculation of the hydrogen generation rate requires an accurate prediction of the temperature and steam availability. Large uncertainties still exist in these computations, and different codes will predict different amounts of produced hydrogen. Nevertheless, there exist a consensus that for most core melt accidents, enough hydrogen will be produced to exceed the flammability limit.

### Hydrogen Transport and Mixing

The transport and mixing of hydrogen inside containment are critical in determining the time and nature of hydrogen combustion. Rapid mixing could result in uniform distribution of hydrogen and burns that are global in nature. Slow mixing may lead to localized burning and locally detonable mixtures. The physical processes which govern the mixing in gaseous mixtures

are forced convection, natural convection and diffusion. The mixing processes are affected by the rate of hydrogen released into the containment and the operability of the containment heat removal systems, such as water sprays and fan coolers.

Here again, large uncertainties exist in the hydrogen transport models. The calculation of the hydrogen transport and mixing requires the modelling of the heat transfer and natural convection phenomena in de containment. A recently completed International Standard Problem (ISP) showed serious shortcomings for most of the utilized analytical simulation models, and particularly, that the exchange of heat between the containment atmosphere and the surrounding structures requires improved modelling concepts, as long-lasting natural convection must be predicted more reliably [9]. The ISP-29, which is currently under way, more specifically addresses the hydrogen distribution inside the containment.

**Hydrogen Combustion**

Hydrogen combustion can cause containment and secondary building failure by static (deflagration and diffusion flame) or dynamic (detonation) overpressurization, missile generation, and equipment failure due to thermal or pressure effects.

Deflagrations are combustion waves in which unburned gases are heated by thermal conduction to temperatures high enough for chemical reaction to occur. Deflagrations normally travel subsonically and result in quasi-static (nearly steady state) loads on containment. For substantial combustion to take place, an ignition source must be present and the gaseous mixture must be flammable. In containments without deliberate ignition, the common sources of random ignition are sparks from electrical equipment and from the discharge of small static charges.

The flammability limit in gaseous mixtures such as air/hydrogen/steam, is defined as the minimum concentration of hydrogen required to propagate a flame in an environment where oxygen is present in excess. The experimentally determined low flammability limit in steam-saturated air at room temperature and pressure are given below [5]:

| | |
|---|---|
| Upward propagation | 4.1 Vol% |
| Horizontal propagation | 6.0 |
| Downward propagation | 9.0 |

Depending on the conditions under which hydrogen or a hydrogen/steam mixture is released into containment, it is possible that hydrogen may burn as a diffusion flame if the hydrogen is injected into containment in a form of a jet. A diffusion flame is one in which the burning rate is controlled by the rate of mixing of oxygen and hydrogen.

Diffusion flames and slow deflagrations are not expected to represent a serious threat for most containments. Therefore, the greatest effort has been aimed at the accelerated flames, the deflagration to detonation transition (DDT), and the detonations [10], [11], [12].

Detonations are combustion waves in which heating of the unburned gases is caused by compression from shock waves. Detonation waves travel supersonically and produce dynamic

or impulsive loads on containment in addition to quasi-steady-state loads. A hydrogen detonation can be developed by either direct initiation or flame acceleration. Direct initiation requires a high energy source such as a spark or an explosion. In a containment environment, it is unlikely that enough energy or power is available to cause a direct detonation. Thus, only flame acceleration possesses the potential to initiate a detonation. A flame acceleration can occur due to turbulence, change in geometry, obstacles and wall roughness.

The key parameters that determine the likelihood of DDT in a practical enclosure are the system geometry (obstructions, compartments, etc.) and the thermodynamic state (pressure, temperature and composition) of the mixture. With regard to containments, system geometry is complex and plant specific. The thermodynamic state of the mixture is dependent on the accident scenario. Further, the codes and models used to calculate the distribution of the mixture conditions during a scenario are not fully validated. The above would lead to a large variation and significant uncertainty in the calculated distribution of mixture conditions.

This, together with the complicated influence of geometry on flame acceleration, means that the assessment of the likelihood of DDT in reactor containments has to involve a significant amount of judgement, say in the selection of conservative mixture conditions and in arriving at simplified representation of the system geometry [12].

**Hydrogen Control**

Especially after the degraded core accident at TMI-2, during which a hydrogen deflagration took place, the reactor safety community has been aware of the potential threat to the containment integrity posed by hydrogen. As a consequence, small volume containments, equipped with a pressure suppression system, are inerted during normal operation. These are mainly BWR containments of the types Mark I and II, as well as modified versions e.g. in Sweden and Germany. For long term accident management, attention has to be paid to the sump water radiolysis, because the oxygen generation will decrease the level of inerting.

Deliberate ignition systems are installed in containments with ice condensers and of the Mark III type.

Currently no requirements have been established worldwide on hydrogen control in large dry containments. The threats to the integrity of this type of containment, posed by hydrogen burns, are valued differently in different risk investigations [1], [13]. Nevertheless, various hydrogen control measures for large dry containments are under investigation in some countries like Germany, Canada, Belgium and the Netherlands. The systems being studied are based on deliberate ignition and/or catalytic recombiners [14].

## 2.4 Isolation Failures

A containment isolation failure can be due either to an inadvertent pre-existing opening or to a failure of the containment isolation system. When an accident occurs, a number of valves must close to isolate the containment from the environment. If there is a non-isolable hole in the containment (like a spare penetration left unsealed) or if some containment isolation valves fail

to close, the containment leakage rate will be much larger than expected during the whole course of the accident.

The nuclear power plant operational record has shown several instances of failure of the containment isolation function. The probability that the containment leakage rate exceeds the allowable limit at any given time during plant life has been shown to be relatively high [15]. In most of the cases, the leakage rate was not much higher than the allowable limit, but in some cases it was such that the potential environmental consequences of an accident would have been large.

In NUREG-1150, failure to isolate the containment was not found to be a likely source of containment failure for any of the plants analyzed. Primarily because of the low frequency of early containment failure by other means, containment isolation failure is a relatively important contributor to early failure at Zion. The subatmospheric containments and the inerted containments are particularly reliable in this regard since it is highly likely that leakage would be identified during operation.

For atmospheric containments, methods exist to detect large openings in the containment during reactor operation [15]. These methods do not have the same accuracy as the pressure tests of the containment, but they can be performed continuously and are able to detect leaks in the containment that are smaller than the ones which would be a concern for accident conditions. Methods to assess the leaktightness of the containment during reactor operation are used routinely in some countries.

Accident management measures also exist to detect and isolate openings in the containment after an accident has taken place [16]. Of course priority should be given to the prevention of containment isolation failures, but, in line with the defence-in-depth concept, means should be available to the operator to take corrective actions after the onset of an accident.

## 3. LATE CONTAINMENT FAILURE

If the containment does not fail early, there are still mechanisms which may threaten the containment integrity in the longer term after the molten core has penetrated the reactor vessel. There are four potential late failure modes: late combustible gas burning, gradual overpressurization, basemat meltthrough and overheating.

Late combustible gas burning is not very different from early combustible gas burning, with one addition: carbon monoxide, which is also combustible, would be produced in the later stage of an accident involving the attack of concrete by molten core debris. The reader is therefore referred to section 2.3.

### 3.1 Gradual Overpressurization

Without containment heat removal and/or venting, the containment would fail by slow pressurization due to the addition of steam and noncondensible gases to the atmosphere. The noncondensible gases may evolve from corium/concrete interactions.

If the reactor vessel is depressurized, the core debris pouring out of the reactor vessel is likely to remain in the reactor cavity where it will interact with structural concrete. The erosion of concrete due to the thermal attack by core debris releases steam and carbon dioxide over the following temperature range [5]:

1) Release of free water at about 80 to 140°C
2) Release of chemically bound water at about 350 to 520°C
3) Release of carbon dioxide at about 550 to 1000°C

Pressurization caused by corium/concrete interactions is governed by many factors, among which are the presence of water in the cavity and the potential for debris coolability. If the cavity is flooded with water prior to vessel failure, then, as the molten core materials fall into the water, rapid cooling and fragmentation is possible. This process could result in the formation of a coolable debris bed in which all the core decay heat is removed by boiling water and concrete attack is prevented. Under these circumstances, providing water flow to the cavity would replenish water loss due to boiling and ensure that the corium remains in a coolable and stable configuration.

If the cavity is initially dry and the core debris forms a deep bed, it could remain hot for a relatively long time and extensive concrete attack would occur. Under these circumstances, pouring water on top of the core debris may have the effect of rapidly cooling and stopping the concrete attack. However, experiments have shown that a crust can form on top of the molten core debris and effectively prevent the water from mixing with and cooling the debris. The experiments were performed at small scale and the stability of the crust under the conditions of a severe accident in a power plant has not been established.

Thus, the effect of pouring water on top of the core debris is uncertain. Therefore, even though water flow is restored to the core debris, continued concrete attack with the generation of more noncondensible gases and release of radioactive material is still possible. The presence of water above the debris does have the advantage, however, of trapping a fraction of the radioactive material generated during the concrete attack, which would otherwise have reached the containment atmosphere.

Computer codes have been developed to model the corium/concrete interactions. Some of these codes were compared in an ISP [17]. The results of the codes used in this blind post-test calculations exercise of the SURC-4 experiment exhibit large discrepancies with each other and with the experimental results. All the codes used in the study failed to reproduce the trend of the melt temperatures measured in the experiment. The concrete erosion history was reproduced in some of the calculations. It was also noted that the calculated results from different participants using the same code were quite different. More work is needed before a satisfactory state of understanding of the phenomena will be reached

In severe accident studies, assessments of the time needed to reach the containment failure pressure are made [1], [13]. In case of dry interaction, the pressurization is slow, and the failure pressure is not expected to be reached before several days, depending on the containment free volume and the type of concrete (some concretes release more gases than others). If the molten

core is covered by water, the steam production accelerates the pressurization, and the failure pressure can be reached in less than one day, depending again on the free volume, but also on the containment heat removal rate.

Two strategies are possible to avoid or to delay containment failure by overpressurization: removal of heat from the containment and removal of mass from the containment (containment venting). Heat removal can be accomplished by conventional means (spray, fan coolers) if available, or by specially provided systems (alternate internal spray, external spray for steel containments). When the pressurization is mainly due to non-condensible gases, heat removal has only a minor impact on the pressure in the containment.

The other strategy is to vent the containment. Some European countries have, or intend to install, filtered vent systems. The objective is to provide the operator with means for controlling the situation, and in particular for maintaining the containment function, and this in a way that still limits the level of release into the environment [18].

### 3.2 Basemat Meltthrough

After vessel meltthrough, some potential exists for core debris to be quenched as a particulate debris bed and cooled in the reactor cavity or pedestal region if a continuous source of water is available. A significant likelihood exists, however, that, even if a replenishable water supply is available, molten core debris will attack the concrete basemat [1], (see section 3.1).

The corium/concrete interaction rate depends on many factors, such as corium mass, composition and temperature, cavity configuration, and overlying water pool. For example, the axial concrete erosion rate for the Zion plant is estimated to be in the range of 2.1 cm/hr to 5.2 cm/hr depending on whether the cavity is flooded and when it is flooded [5]. The basemat thickness for the Zion plant (a prestressed concrete containment) is 2.7 m. The complete erosion of the basemat would therefore take several days. Similar results were obtained for the Biblis plant [13].

After basemat meltthrough, the molten core reaches the underlying soil. The projected consequences are site-specific, but it is expected that they are small compared with those of aboveground failures [1]. A depressurization of the containment can also mitigate the consequences associated with the basemat meltthrough because the mixture of concrete and molten mass can be relieved from its active forces, and the release of fission products into the soil can be mitigated [13].

### 3.3 Overheating

Overheating is a potential delayed containment failure mechanism. Analyses of the thermo-mechanical response of a 1:6-scale reinforced concrete containment were performed at Argonne National Laboratory [19]. Three temperature-pressure scenarios were analyzed up to complete loss of the pressure integrity. The results showed that the global failure of the containment vessel under combined thermal and pressure loading does not appear to be significantly changed from the case with internal pressure alone. It is believed that this conclusion applies to most

containments. Although very high gas temperatures can be achieved as a result of hydrogen combustion, the structure temperatures are not predicted to reach temperatures at which the strength of the structure would be substantially reduced or sealant materials would be degraded [1].

However, some small steel containments can be more vulnerable. For example, the effect of high temperature in the drywell on containment failure probability and mode was considered for Peach Bottom (BWR Mark I containment) [1]. The Peach Bottom drywell is relatively small. Substantial convective and radiative heat transfer from hot core debris could result in very high drywell wall temperatures. Failure could result from the combination of high pressure in the drywell and decreased strength of the steel containment wall.

## 4. CONTAINMENT BYPASS

In some accidents, the containment building is completely bypassed. Containment bypass arises with a fault sequence which allows primary coolant and any fission products accompanying it to escape to the outside atmosphere without having been discharged into and mixed with the air in the containment volume. In interfacing-system loss of coolant accidents, check valves isolating low-pressure piping fail, and the piping connected to the reactor coolant system fails outside the containment. The radionuclides can escape to secondary buildings through the reactor coolant system piping without passing through the containment. A similar bypass can occur in a core meltdown sequence initiated by the rupture of a steam generator tube in which release is through relief valves on the steam line from the failed steam generator.

Interfacing-system LOCA (ISL) refers to a class of accidents in which the reactor coolant system pressure boundary interfacing with a supporting system of lower design pressure is breached. If this occurs, the low pressure system will be overpressurized and could rupture outside the containment. This failure would establish a flow path directly to the environment or, sometimes, to another building of small pressure capacity. Depending on the accident sequence, the emergency core cooling system may fail, resulting in a core melt with containment bypass. One important reason for the failure of the emergency cooling system is that the cooling water is lost outside containment and is therefore not available any more. If the accident is not terminated before the reactor water storage tanks are empty, the cooling to the core is lost.

BNL has performed a detailed study of interfacing systems LOCA for three pressurized water reactors [20]. The interfacing lines which have been identified as potential ISL pathways include lines of low pressure injection, high pressure injection, residual heat removal suction, letdown and the core flooding tank (accumulator) outlet lines. The results of the BNL study indicate that the contributors from two groups of pipe lines, namely the residual heat removal suction and low pressure injection lines, dominate the core damage frequency (CDF) due to ISLs. The total contribution of ISL events to CDF is generally less than a few percent of the overall CDF. However, they can potentially be important contributors to risk if core damage occurs because ISLs may bypass the containment and allow radioactive material release directly to the environment.

Steam generator tube rupture (SGTR), either as an initiating event or induced by high temperature, represents another containment bypass event. Analyses have indicated a potential for very high gas temperatures in the reactor coolant system during accidents involving core damage with the primary system at high pressure. The high temperature could fail the steam generator tubes long before the core begins to relocate. The rupture of steam generator tubes would depressurize the reactor vessel, and if the steam generator relief valves are open, a path would exist from the damaged core to the environment.

The two paths, SGTR and ISL, only become important in the event of multiple faults, so they are designed to be of very low probability. For example, in the case of an initiating SGTR, the consequences are perfectly acceptable when judged against a single failure criterion, that is the safety systems and the secondary steam relief valves work properly. In probabilistic safety assessments, a single failure criterion is no longer relevant, and it has been found that the SGTR combined with failure of a secondary side relief valve to reset, is a significant hazard sequence [21]. This is due to a combination of circumstances. Firstly, and most importantly, water is lost from the emergency supplies direct to atmosphere, so core melting is inevitable if all the water is used up. Secondly, core melting in this case would lead to a large source term because the release bypasses the containment.

## References


1. USNRC, "Severe Accident Risks: An Assessment for Five U.S. Nuclear Plants" NUREG-1150, Final Report, December 1990.

2. OECD, "Status of Direct Containment Heating in CSNI Member Countries", CSNI Report 153, March 1989.

3. Kerr, W., and M.K. Dey, "Containment Loads from Severe Accidents - U.S. Program", NUCLEAR SAFETY, Vol. 29, No. 1, January-March 1988, pp. 29-35.

4. Gustavson, V., and B. Morris, "Direct Containment Heating Calculations for Ringhals 3", Proceedings of the Second International Conference on Containment Design and Operation, Toronto, Canada, October 1990.

5. Yang, J.W., "PWR Dry Containment Issue Characterization" NUREG/CR-5567, Brookhaven National Laboratory, August 1990.

6. OECD, "Proceedings of the Specialist Meeting on Intentional Coolant System Depressurization", Garching, Germany, CSNI Report 158, June 1989.

7. OECD, "Note on the Outcome of the June 1989 CSNI Specialist Meeting on Intentional Coolant System Depressurization", CSNI Report 163, February 1990.

8. USNRC, "Reactor Safety Study: An assessment of Accident Risks in U.S. Commercial Nuclear Power Plants", WASH-1400 (NUREG-75/014), NTIS, October 1975.

9. OECD, "ISP-23 - Rupture of a Large Diameter Pipe in the HDR Containment", CSNI Report 160, December 1989.

10. Guirao, C.M., et al., "A Summary of Hydrogen-Air Detonation Experiments", NUREG/CR-4961, McGill University, May 1989.

11. Stamps, D.W., et al., "Hydrogen-Air-Diluent Detonation Study for Nuclear Reactor Safety Analyses", NUREG/CR-5525, Sandia National Laboratories, January 1991.

12. OECD, "State-of-the-art Report on Flame Acceleration and Transition to Detonation in Hydrogen/Air/Diluent Mixtures", CSNI Report R(92)3, January 1992.

13. GRS, "German Risk Study - Nuclear Power Plants - Phase B - A Summary", GRS-74, July 1990.

14. OECD, "Hydrogen Management Techniques in Containment", to be published.

15. OECD, "Inadequate Isolation of Containment Openings and Penetrations", CSNI Report 179, December 1990.

16. Duco, J., et al., "PWR Severe Accident Mitigation Measures - The French Point of View", Proceedings of the Second International Conference on Containment Design and Operation, Toronto, Canada, October 1990.

17. OECD, "ISP-24 - SURC-4 Experiment on Core-Concrete interactions", CSNI Report 155, December 1989.

18. OECD, "Filtered Containment Venting Systems", CSNI Report 156, November 1988.

19. Pfeiffer, P.A., J.M. Kennedy, and A.H. Marchertas, "Thermal Effects in Concrete Containment Analysis", Proceedings of the Fourth Workshop on Containment Integrity NUREG/CP-0095, Sandia National Laboratories, November 1988.

20. Bozoki, G., et al., "Interfacing Systems LOCA: Pressurized Water Reactors", NUREG/CR-5102, BNL-NUREG-2135, Brookhaven National Laboratory, February 1989.

21. CEC, "Proceedings of the CEC seminar on Studies of Severe Accidents in Light Water Reactors", Brussels, November 1986, Report EUR 11019.

# DETERMINISTIC SEVERE ACCIDENT CRITERIA (DSACs) AS SEVERE ACCIDENT DESIGN CRITERIA AND POLICY FOR THE NEW PRODUCTION REACTOR - HEAVY WATER REACTOR

Patrick T. Rhoads,
U.S. Department of Energy

## Abstract

One of the most important functions that a nuclear containment serves is to protect the public from the radiological consequences of severe accidents, i.e., those beyond design basis events which result in significant core damage. However, the design basis and design processes for light water containments have not generally been explicitly linked to accommodating these extreme events into the containment design. For light water reactors, the containment design basis has been based on considerations other than severe accidents, such as the consideration of the containment pressurization due to a loss of coolant accident. The resulting containment designs for certain pressurized light water reactors were then assessed and shown to have adequate resistance to severe accidents. The light water reactor containment design basis would not be directly applicable for the New Production Reactor-Heavy Water Reactor (NPR-HWR) because of the low stored energy of the Heavy Water Reactor. The Department of Energy's Office of New Production Reactors (NP) established as a fundamental point of policy that the NPR-HWR containment would be designed under the following requirements:

- The NPR-HWR containment would be designed to accommodate hypothetical severe accident challenges.
- A full-scope probabilistic analysis of reactor operations, including severe accidents, would be performed to complement deterministic analyses and demonstrate containment adequacy.
- The defense-in-depth philosophy would be fully integrated into the containment design.

The implementation of these and other requirements relevant to the containment design basis is being accomplished in a systematic manner for the NPR-HWR. Deterministic Severe Accident Criteria (DSACs), a significant element of the integrated strategy for design consideration of severe accidents, have been established by the Office of Heavy Water Reactor to ensure that the containment is designed to withstand a wide spectrum of severe accident challenges.

This paper traces NP's development and implementation of the DSACs with a focus on examining the underlying technical decisions embedded in the DSACs. These decisions include the following illustrative examples:

- o Degrees of conservatism required in the design specifications;
- o Ability to establish a defensible and reviewable set of design criteria;
- o Extent of accounting for mitigating factors in determining severe accident challenges;
- o Specification of the acceptable conditional containment failure probability, given the incidence of a severe accident challenge initiator;
- o Use and aggregation of expert opinion data in the decision-making process;
- o Need to accommodate unprotected (i.e., unscrammed) accident sequences for the containment design.

The net result of NP's actions and decisions in regard to the DSACs is expected to be a strong, robust containment design which is highly resistant to severe accident challenges and which has a technically defensible design basis. This approach represents a logical approach for accommodating severe accident challenges early in the NPR-HWR design process. This approach may also be applicable to future light water reactor containments and is similar in principle to approaches recently advocated by the Advisory Committee on Reactor Safeguards to the Nuclear Regulatory Commission.

## BACKGROUND

Consideration of severe accidents for reactor safety analysis and design has become increasingly important since the accidents at Three Mile Island and Chernobyl. This increased emphasis on severe accidents since 1979 is directly related to the fact that the consequences associated with severe accidents tends to dominate all other radiologically significant events from the operation of nuclear facilities. For the nation's production reactors, the need for increased emphasis on severe accidents became readily evident in 1987 when the National Academy report on the safety of defense production reactors concluded:

> "...[The] existing level of understanding of severe accident behavior for the production reactors is inadequate to permit a realistic assessment of the effectiveness of these designs in mitigating the consequences of severe accidents." [1]

At approximately the same time that the National Academy of Sciences report was released, The United States Department of Energy concluded that new production reactor capacity was required on an urgent schedule to support the nation's defense requirements for nuclear materials, especially tritium. The Department established the Office of New Production Reactors in October 1988 to satisfy the need to provide new production capacity. As a consequence of

NP's commitment to addressing severe accident concerns, NP's policy established a series of design requirements to ensure that severe accidents were explicitly covered in the earliest design phases. [2] Specifically, the policy of NP was and continues to be that severe accidents would be explicitly addressed in the design to ensure both prevention and mitigation [2] and that the New Production Reactors would meet or exceed the level of safety and safety assurance offered by modern commercial nuclear reactors.

The combined requirements of establishing severe accident criteria and satisfying an urgent schedule led the Department to undertake a new approach regarding design criteria for severe accidents. Previous approaches for severe accidents used by commercial nuclear facilities were predicated on either or both of the following conditions: availability of an existing, mature design in which to base severe accident analyses or the use of probabilistic analytic techniques. Neither of these approaches was appropriate to the case at hand because a mature design was not available and a definitized, deterministic set of requirements was required to establish design criteria on an urgent schedule. Furthermore, the existing regulatory basis for containment designs could not be implemented since the regulatory basis assumes high energy water being released from an escaping main coolant stream, an assumption that does not hold for the specific low temperature, low pressure heavy water reactor (HWR). Therefore, a new approach- Deterministic Severe Accident Criteria (DSACs)- was adopted. The fundamental objectives underlying the DSAC approach for the HWR were ensuring that a wide spectrum of severe accident challenges had been conservatively accommodated in the containment design and that the severe accident criteria were posed so as to provide guidance for a reactor designer to directly implement.

## OBJECTIVES

The foundation for the DSACs rests in a programmatic policy document entitled "Design for Normal Operation and Abnormal Events, including Severe Accidents." [3] This document describes the overall philosophical approach for the design of the new production reactors. DSACs are required by this document to ensure a conservative spectrum of challenges are considered, such as:

- Missiles
- Fires
- Explosions
- Rapid pressurization
- Slow pressurization
- High temperatures

In the case of the HWR, the DSACs have been initially restricted to the containment design. This focus was adopted early since the containment represents the final barrier to release of

fission products to the environment and is the system most clearly linked to severe accident consequence mitigation. For the HWR design, the following challenges were determined to be applicable for developing an initial set of DSACs for the HWR:

- Missile generation
- Blast
- Rapid pressurization
- Slow pressurization

The DSACs, which are combined stylized problem statements of the postulated severe accident threats and the applicable containment survival criterion, act as a design envelope for the containment. In this manner, the integrity of the containment is directly linked to a particular class of severe accident threats. This approach is a significant advancement from previous design methodologies which have not coupled the containment design with the severe accident challenges for which the containment is ultimately provided. This DSAC approach is then similar in principle to the containment design approach for commercial light water reactors advocated by the Advisory Committee on Reactor Safeguards. [4]

## OVERALL APPROACH

A detailed description of the DSAC development process can be found in one of the papers that accompanies this paper. [5] The brief overview that is provided here is for understanding the strategic implications of the implementation of the DSAC process for the HWR.

One aspect of an integrated approach to considering severe accidents in design is in mitigation of severe accident consequences. The containment design is a critical dimension of the severe accident mitigation strategy. The focus on the containment design complements other objectives of the severe accident program for the HWR, including the design objectives of minimizing the frequency of severe accident initiators and the resultant energetics of postulated severe accident sequences.

Once committed to focus the DSAC effort on the containment design, creation of a specific mechanism to specifically link the containment design to the postulated severe accident energetics was required. Two fundamental approaches were considered for this mechanism. The first method assumed specific accident sequences and initiators and followed them to their conclusions. This path in some respects parallels the path that some probabilistic analyses adopt for assessing the impact of severe accidents in Level II probabilistic risk assessments (PRAs). The second method assumed the occurrence of a specific stylized sequence which was a representative but conservative surrogate for a specific class of challenges to the containment in which the challenges might arise from any number of specific accident progression routes. This approach is described in Ref [5]. Whereas the first method represented a logical extension of traditional analytical processes, this option proved to be unacceptable for several reasons, including:

(a) Specific design detail would have been required to trace particular accident sequences. This data base did not exist.

(b) A detailed understanding of all phenomenology along the event sequence was not available.

(c) The design criteria that would arise from such an approach would be specific to a particular design and, perhaps, to particular accident sequences. This approach would not necessarily result in a consistent set of criteria which would be robust with respect to: (1) small design perturbations; (2) different analytical techniques, or (3) refinements in branch probability estimates.

Recognizing the limitations to the first approach, NP adopted the second. This second approach requires one to investigate the physical challenges to the containment and the sequences that might give rise to them. The resulting analyses showed that the significant physical challenges, which could lead to a design loading on the containment, were missile generation, blast, rapid pressurization, and slow pressurization, as already noted above.

In defining the challenges, the obvious obstacle of quantifying the challenges presented itself. Computational capability does not exist to permit directly quantifying the challenges. Modelling and understanding of phenomena are not well enough established to create a straightforward path to quantification of the challenges. Therefore, reliance on expert opinion was necessary. In this regard, the DSAC effort paralleled the NUREG-1150 process in which the mitigative capabilities of some existing commercial nuclear reactors were assessed.

Complete elicitations and integrated documentation were forwarded to NP by the prime contractors responsible for the DSAC development process, namely Sandia National Laboratories and Westinghouse Savannah River Company. This input was technically reviewed by an independent set of experts. This group provided an assessment of the technical quality of the DSAC process, the elicitations, and the recommendations as an additional input to NP.

## STRATEGIC NP DECISIONS

Several strategic NP decisions were required to generate the DSACs. Some of the significant, management-level decisions and decision-making processes are outlined below. This discussion focuses on issues which might be useful in future considerations of DSAC-like processes.

### A. Defense in depth

The traditional defense-in-depth approach assures multiple barriers to release of fission products to the environment. In the HWR, utilizing this principle required one to assume core melt even for cases in which core melt probability was essentially negligible. Core melt was assumed because the defense-in-depth approach so required this assumption. Whereas making this assumption may also be required in analyzing some light water reactor severe accident sequences, the significance of this assumption is more pronounced for the case of the HWR. This is so since the HWR design maintains a cadre of safety systems in which active systems

are backed up by passive systems. This layering results in preliminary projected frequencies of core melt one or more orders of magnitude lower than existing modern commercial reactors. Notwithstanding, the approach of the NP with respect to defense in depth was to conservatively assume core melt in an attempt to conservatively include a wide spectrum of severe accident challenges into the containment design envelope.

B. Degree of mitigation capability

In parallel with the DSAC effort, NP was separately undertaking a so-called safety-in-design program. Under this initiative, the reactor design was thoroughly reviewed to ensure that the core melt frequency was driven to as low a value as was practical, to ensure that energetic mitigation capability for core melt events was included to the extent practical, and to maximize the potential for in-vessel retention of a postulated whole-core melt. This initiative led to the addition of a number of mitigation and prevention features to the HWR design which were not included in the design considered in the expert elicitations. While it was well established that the elicited DSAC parameters would overstate the actually expected loads with the new mitigative and preventive features, no credit was taken for these features in the establishment of the accepted DSAC parameters. No credit was taken because the degree of the decrement of accident energetics attributable to these features was not readily calculable, because the attempt to revise the parameters without an established technical basis would run counter to one of the governing principles of the DSACs in maintaining scrutability of the DSAC basis, and because a degree of conservatism was inherently retained.

C. Protected and unprotected accidents

Consideration of unprotected accidents, accidents which are postulated to occur while at power with a failure to scram when demanded, is usually implemented for the light water reactors in the context of establishing criteria for the back-up reactor protection system(s). For the HWR design, there are already independent systems to meet these so-called anticipated transients without scram (ATWS) incident criteria. Notwithstanding, the HWR assumed the incidence of unprotected accidents and considered the associated energetics in the context of the containment design. This decision was based on the presumption that unprotected sequences for the HWR might result in more energetic challenges than protected sequences would. Whereas this statement is probably true for LWRs as well, it was believed that difference between the two might be more pronounced for the HWR than for the LWRs due to specific technology differences. Indeed, in all elicited cases, the DSAC energetic parameters for the unprotected cases exceeded the analogous energetic parameters for the protected case, as might be expected. Consideration of unprotected accidents in the design represents a significant departure from past, traditional approaches for light water reactors. Accepting the inclusion of the unprotected parameters into the context of the containment design envelope then begs the question as to how to integrate the unprotected and protected energetic parameters into a single set of definitized criteria, the ultimate goal of the DSAC effort. Based on inputs from the Savannah River "K" Reactor PRA document, commercial reactor PRAs, and phenomenology experts, it was estimated that the expected frequency of a protected accident, low that it was, probably exceeded the value for an unprotected accident by a factor of 10-100. It was realized that combining the unprotected and protected DSAC parameters on an expected frequency basis alone would be

tantamount to ignoring unprotected accidents because their relative contribution would be diluted out. A compromise position was accepted, based on being relatively conservative (since the expected frequency estimators are not necessarily robust estimates) and on not expressing undue precision, by adopting a weighting ratio of 5:1 of the protected to unprotected energetics.

D. Conditional Containment Failure Probability (CCFP)

The nuclear industry, with some qualified endorsement from the United States Nuclear Regulatory Commission, targets a CCFP of 0.1 as providing a robust containment when accidents are weighted over the expected frequencies of all core melt accidents. A CCFP of 0.10 means that the frequency-weighted probability that the containment will perform its intended function, given the occurrence of a core melt, is 90%. The CCFP for a particular melt sequence would, in general, be different than 90%. NP recognized a desire for consistency with the industry approach in this regard but also recognized that a CCFP of 0.1 per se does not necessarily result in a robust containment. Indeed, it was demonstrated that a CCFP is not necessarily even a figure of merit for containment performance if the calculation is performed over the frequencies of all core melt accidents. To avoid the inherent limitations associated with a CCFP=0.1, NP targeted accomplishment of a CCFP when weighted over only those core melt accidents that could result in a challenge to the integrity of the containment since many-if not most-of the core melt scenarios have benign energetics that do not represent a threat to containment integrity. This more conservative definition can be shown to result in a relatively robust containment design.

E. Aggregation methodology

In some of the elicitation cases, the variance in the values of the elicited parameters between the experts was significant. Such a spread results in an inherent difficulty in aggregating the data in a meaningful way. Based on a review of the statistical approaches available to conduct the aggregations, it was learned that no methodology currently exists which is universally accepted or mathematically rigorous. However, the two most widely utilized approaches were adopted in the context that the methodology that resulted in the more conservative value of the elicited parameter was selected. One of these methodologies involves averaging the probability of a specific value of a parameter; the other approach is to average the parameter values at given probabilities. The actual approach adopted by NP in accepting the more stringent of the two values is robust with respect to the acceptability of either of the aggregation methodologies. This NP decision was considered prudent, owing to the uncertainty involved in the acceptability of the aggregation methodology.

F. Selection of values for point estimators for parameters

Once the decision to target a CCFP of 0.1 had been reached, the path to accomplishing this target still remained undefined. The question was how to pick off point estimators from the cumulative probability distributions of the aggregated elicitations of the challenges (missile generation, blast, rapid depressurization, and slow pressurization) to provide a high confidence of achieving the CCFP goal. Three options were considered relating to the incidence of two or more challenges from a single event sequence. One can choose a constant percentile pick off

point above 90%, say, for example the 95th percentile, to be able to confidently state that the overall CCFP was less than 0.1. This pick off point would accommodate more than one challenge from a single event sequence. Another option is to "manage" the selection points from the probability distributions such that a higher percentile pick off point for a challenge type that is not as taxing to the containment is selected in conjunction with a lower percentile pick off point for a more containment-taxing challenge. For example, one could choose the 99th percentile for the slow pressurization case (a challenge type which is not overly taxing on the containment) in conjunction with the 91st percentile pick off point for the missile generation (a very containment-taxing challenge) to confidently achieve an overall CCFP of 0.1. This approach is discussed in Ref [5] along with a graphical representation of a particular cumulative probability distribution curve. The third approach is to accept a constant 90th percentile pick off point for each threat. This approach considers the coincidence of two or more threats happening in the same event sequence to have a probability to be sufficiently low that the conservatisms built elsewhere into the DSAC process would compensate for this non-conservatism.

The first approach was rejected since the actual CCFP for this case was expected to be significantly below 0.1, which implies that there existed potential for significantly overdesigning the containment. The second approach was rejected because the procedure for selecting pick off points was somewhat arbitrary and because the pick off points would have to assume a higher degree of precision than the data generation process would have warranted. The third approach was judged acceptable in light of the conservatisms built elsewhere into the process.

G. Safety approval implications

The DSACs result in specific implications for the containment design. However, neither the safety approval process for commercial reactors nor that for production reactors has specifically included severe accident energetics for the containment design basis, where this term refers to the regulatory-licensing connotation of the design basis defined by the Nuclear Regulatory Commission and the Code of Federal Regulations. The institutional acceptability of the DSACs for safety/regulatory criteria is not yet finalized. Notwithstanding the lack of safety approval in a formal safety review process for the HWR, a proactive NP engineering decision was consciously made to specifically include these criteria into the containment design envelope, where the design envelope refers to the containment performance expected on a best-estimate analytical basis. That DSACs should be an ENGINEERING approach to severe accidents rather than a SAFETY design basis approach is consistent with the Electric Power Research Institute philosophy for new advanced light water reactor plants (ALWRs). This is also consistent with the realization that severe accident criteria will inherently contain a measure of subjectivity since the underlying physical processes involved in severe accidents are not always well understood, and, therefore, not amenable to traditional regulatory purview.

## COMPARISON TO LIGHT WATER REACTOR DESIGN APPROACHES

The traditional double-ended break of a main coolant system pipe has served as a regulatory design basis for containment design basis for commercial reactors. This approach would not

result in a robust containment for the HWR. In fact, the peak pressure resulting from a pipe break in the HWR is less than 5 psig. A 5 psig containment need not be particularly robust. The containment design basis for the commercial reactors does not necessarily result in a robust containment design with respect to severe accident challenges either. The Advisory Committee on Reactor Safeguards has acknowledged this weakness when it stated that:

> "Although this primary purpose [of the containment] has been recognized from the beginning, and is perhaps obvious, existing NRC requirements do not account for many severe accident phenomena that could challenge a containment's ability to perform its function."
>
> "A containment cleverly and narrowly designed to mitigate a set of accidents that has been precisely identified may not be able to cope with the unexpected. A truly "robust" containment would have improved capability to deal with the unexpected." [4]

Notwithstanding the specific linkage of the containment design to severe accident challenges in LWRs, commercial reactor containments have been assessed against these challenges and have been found to be generally acceptable.

The DSAC approach represents a departure from previous design methodologies but is a logical extension to these methodologies. The NP approach appears to be consistent in principle with the proactive, emerging ACRS and ALWR approaches to containment design. The key element in the DSAC, ALWR, and ACRS processes is the linkage of the containment capability to severe accident challenges. The DSAC approach is described above. The ALWR approach, as described in Ref [6], is to consider all severe accident challenges early in the design phases, ensure that the pressurization capability of the containment is high enough to accommodate severe accident challenges using a surrogate loading condition, and perform detailed probabilistic analyses to demonstrate containment adequacy. Like the DSAC approach, the ALWR approach is meant to be a proactive, engineering approach to addressing severe accident challenges, not a regulatory process for meeting the "clever and narrow" design criteria alluded to by the ACRS. The ACRS proposed approach also links containment performance to severe accident challenges explicitly and in this regard is very similar to the DSAC approach although the detailed implementation actions do differ.

## Acknowledgments

The success of the DSAC process is owed to many people. Drs. Kenneth Bergeron and Scott Slezak and Mrs. Carole Leach were responsible for the tremendous technical oversight required to implement the DSAC process. Special thanks are owed also to the group of six men who demonstrated superior technical and professional capabilities as the experts who analyzed and quantified the DSAC problems: Drs. Randall Gauntt, George Greene, L. Walter Deitrich, M. Lee Hyder, Jerome Morin, and David Williams. Lastly, the DSAC technical review and the decision-making processes were indebted to the skills of Dr. John Kelly in pulling the final product together.

## References


[1] National Academy of Sciences Press, "Safety Issues at the Defense Production Reactors," National Academy of Sciences Press, Washington, D.C., 1987.

[2] U.S. Department of Energy, Office of New Production Reactors, "New Production Reactors Requirements Document, Rev. 0," Washington, D.C., November 1989.

[3] U.S. Department of Energy, Office of New Production Reactors, "NPR-STD-1000, Design for Normal Operation and Abnormal Events, including Severe Accidents," Washington, D.C., June 1991.

[4] D. A. Ward, Chairman, Advisory Committee on Reactor Safeguards, letter to Kenneth Carr, Chairman, U.S. Nuclear Regulatory Commission, "Proposed Criteria to Accommodate Severe Accidents in Containment Design," Washington D.C., May 17,1991.

[5] K.D. Bergeron, S. Slezak, C.E. Leach, "Proceedings of the Fifth Workshop on Containment Integrity: submitted paper, " Washington, D.C., May 12-14,1992.

[6] S.L. Additon, D.P. Blanchard, D.E. Leaver and D. Persinko, "Passive ALWR Requirements to Prevent Containment Failure," Tenera, L.P., San Jose, CA and Bethesda, MD, December 1991.

# PROPOSED DETERMINISTIC SEVERE ACCIDENT CRITERIA FOR THE HEAVY WATER NEW PRODUCTION REACTOR CONTAINMENT

Kenneth D. Bergeron
Scott E. Slezak
Sandia National Laboratories[1]

Carole E. Leach[2]
Westinghouse Savannah River Company

## Abstract

This paper summarizes the methodology developed by the DSAC Development Project to assist the DOE's Office of Heavy Water Reactor in formulating containment design criteria for the NPR-HWR that are a practical implementation of high-level programmatic goals. The design criteria, or Deterministic Severe Accident Criteria (DSACs), represent a new approach because they address severe accidents early in the design phase of the nuclear plant. This paper describes a process and approach that considers severe accidents in containment design by establishing practical design requirements based on calculations of stylized loads on the containment. The DSAC Development Project utilized a formal expert opinion process to provide a quantitative specification of the severity of the loads and a reviewable technical basis. The goals for the Project were to (1) generate specific proposals for quantitative criteria within the specified project schedule, (2) minimize the phenomenological uncertainty residing in the problem statements and success criteria so that the design's compliance with the criteria would not be the subject of protracted contention, (3) follow a formal plan consisting of well-defined steps, each of which was scrutable and reviewable, (4) ensure that the complete spectrum of credible severe accident threats was covered by the criteria, and (5) avoid over-constraining the design. As a result of the output of this process, the DOE's Office of Heavy Water Reactor was able to integrate the project recommendations together with numerous other inputs to promulgate design criteria that were conservative, but not excessively so, and that could be technically reviewed and defended.

---

[1] This work was supported by the United States Department of Energy under Contract DE-AC04-76DP00789.

[2] Currently at Westinghouse Hanford Company.

## INTRODUCTION

The Department of Energy's Office of Heavy Water Reactor[3] (HWR) recently issued severe accident design criteria for the containment building of the New Production Reactor-Heavy Water Reactor (NPR-HWR). These Deterministic Severe Accident Criteria (DSACs) represent a new approach to containment building design requirements because they address severe accidents in the design phase, but in other respects they are logical extensions of traditional design criteria. For example, as in traditional design criteria, each of the DSACs consists of two parts: an idealized problem statement that represents a physical challenge to the containment, and a success criterion for evaluating the containment's ability to accommodate that challenge. The technical basis of the DOE's decisions related to the DSACs was provided by the DSAC Development Project, which was carried out by a multi-laboratory team over a span of one year, with the most concentrated effort occurring from December 1990 to June 1991. This paper summarizes the Project [1] with an emphasis on the methodology developed to generate proposed DSACs for DOE consideration.

There are two other papers related to the DSACs that are part of this conference. The paper by R. F. Sammataro et al. [2] provides details about the success criteria which were developed in parallel with the DSAC problem statements.[4] The paper by P. T. Rhoads [3] explains how DOE used these inputs, and others, to finalize the DSACs for the baseline design.

The specific DSAC problem statements that were developed to apply to a particular baseline NPR-HWR conceptual design are not generically applicable to designs which differ significantly from the baseline. Recent changes in national priorities have resulted in some redirection of the NPR design effort. This will probably result in a significantly downsized NPR-HWR.

Although the DSACs were developed to be applicable over a modest range of design variations, it may be desirable to modify the initial problem statements to accommodate these major design changes. However, in the absence of details regarding the ultimate design changes, it is premature to discuss corresponding adaptations of the DSACs. The context of this paper is the original baseline design, but the emphasis is on a process that considers severe accidents in containment design. This process is of interest not only for the original and future NPR-HWR designs, but also for other possible applications for which rational design criteria are needed to accommodate extremely improbable and highly uncertain events.

---

[3] Design work is proceeding on two reactor concepts for the NPR: the HWR and a Modular High Temperature Gas Reactor (MHTGR); while a parallel DSAC development effort is taking place for the MHTGR, this paper discusses only the HWR program.

[4] The compliance process described in Reference 1 proposes a slightly different application of the success criteria than that described in Reference 2, because in the latter, the DSAC problem statements are assumed to accommodate all sources of uncertainty, while in Reference 1, analysis uncertainties and uncertainties in material properties are not accommodated by the conservatism in the problem statements. Any readers interested in this subtle but rather minor difference should read Appendix M of Reference 1.

## The Role of DSACs in the NPR Program

There are similarities between the underlying technologies of the New Production Reactor and commercial nuclear reactors, but because there will be only one production reactor, and because it will be a critical element in the nation's future defense posture, it will have quite different requirements from commercial plants. One aspect of those requirements is that the DOE's Office of New Production Reactors (DOE/NP) is taking a proactive approach to safety by requiring that the NPR meet or exceed the degree of safety achieved by existing commercial nuclear power reactors, and that severe accidents be considered in the design [4].

Quantitative design criteria are needed for engineering design to reflect these high-level requirements. The traditional Double Ended Guillotine Break (DEGB) accident, which is part of the design basis for commercial nuclear power plants, would not challenge the NPR-HWR containment because the reactor operates at low pressure and temperature. The DSACs were therefore developed to create meaningful severe accident design criteria for the NPR-HWR containment. However, they should not be viewed in isolation from other design requirements.

The DSACs are not intended to replace or be independent of traditional design requirements, but are rather intended to augment the standards, codes, and good engineering practices that are traditionally employed. In particular, the DSACs deal with only one aspect of reactor safety, which is mitigation of severe accident effects; they have no effect on the important issue of severe accident prevention, which is being addressed by other approaches. The DOE's dual approach involving severe accident prevention through highly reliable and redundant system design, and severe accident mitigation through the DSAC process, reflects a commitment to defense-in-depth for the NPR-HWR design. In recognition of the need for multiple layers of design requirements, the Office of New Production Reactors has issued a Design Standard [4] which calls for DSACs as part of a hierarchy of design requirements for a series of successively less probable classes of events.

## Key Features of the Baseline Design

The NPR-HWR is a reactor dedicated to producing defense nuclear materials, primarily tritium. This difference of function compared to commercial power reactors is responsible for many significant design differences. Table 1 summarizes a number of design features (based on the Ebasco baseline established on March 19, 1991) that are relevant to severe accident considerations for the NPR-HWR.

Figure 1 shows a cross section of the fuel assembly, through which heavy water is pumped to cool the concentric fuel and target tubes. Two features of this fuel assembly are of particular importance for the HWR: the principal core constituents during operation are aluminum and water (which can undergo energetic chemical reactions on explosive time scales under extreme conditions), and the physical separation of fuel from targets is a mechanism for reactivity

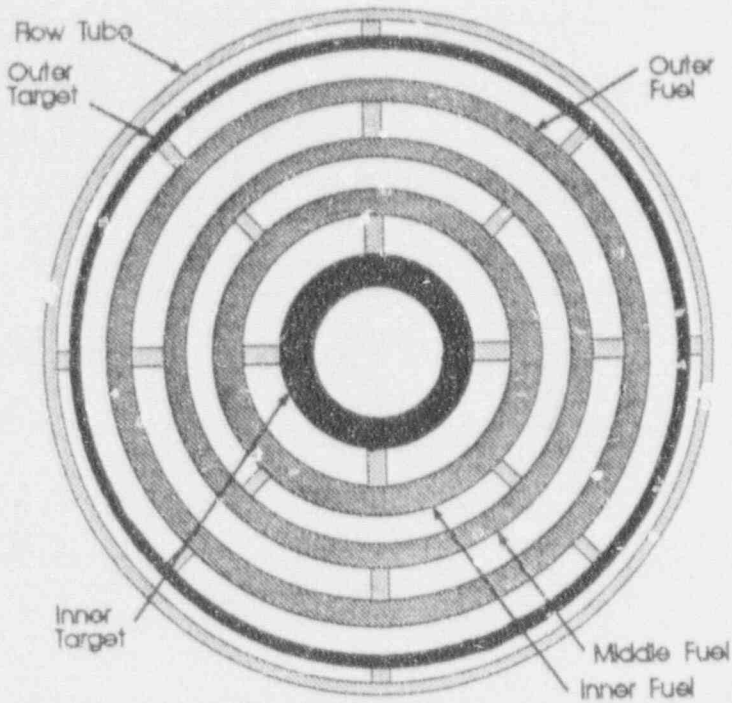


Figure 1. Cross Section of Fuel Assembly in the Baseline Design

Another important aspect of severe accidents is that the extreme conditions envisioned necessarily involve significant uncertainty. It is impossible to eliminate uncertainty regarding the nature of such highly improbable events, so the design criteria should accommodate this uncertainty. However, it is important that the reactor designer not be burdened with the full responsibility for severe accident uncertainty. It is inappropriate, for example, to leave unspecified the degree of conservatism desired in the design for highly improbable severe accident sequences. One goal of the DSAC Development Project was to accommodate the desired degree of conservatism in the problem statements so that the question of whether or not a particular design was in compliance with the design criteria could be answered unambiguously. By accommodating severe accident uncertainty in the formulation of the problem statements, the DOE removed a large portion of the burden for that uncertainty from the designer. The design process could then take place in a stable framework of requirements and specifications.

The approach to severe accident uncertainty taken in the DSAC Development Project utilized a formal expert opinion process that had the advantages of providing specific quantitative information, as well as a reviewable technical basis. The expert opinion process followed was in many respects an adaptation of the methods developed for the Nuclear Regulatory Commission's NUREG-1150 Program [5]. The shortcomings of expert opinion processes in terms of technical rigor were outweighed by the advantages--most importantly, the ability to

insertion. These features are of no concern for light-water reactors (LWRs); conversely, many severe accident concerns for LWRs are unimportant for the NPR-HWR.

Table 1. Highlights of the Baseline NPR-HWR Design (all numbers are approximate)

| Structure | Constituents | Dimensions/Quantities | Features |
|---|---|---|---|
| Coolant /Moderator | heavy water ($D_2O$) | inlet temperature: 120 F<br>outlet pressure: 90 psia | weak coupling of moderator and coolant through orifices |
| Reactor Core | 414 fuel assemblies;<br>169 blanket and control assemblies | nominal thermal power:<br>2500 MW | core and fuel assembly similar to current production HWRs |
| Fuel Assemblies | six concentric tubes:<br>two target tubes, three fuel tubes, one sleeve | 5" outer diameter<br>12.5' active length | coolant flows between concentric fuel and target tubes |
| Fuel Tubes | sandwich of U:Al alloy between aluminum layers | alloy is 27% U by weight;<br>80% enriched uranium | the three fuel tubes lie between the two target tubes |
| Target Tubes | sandwich of Li:Al alloy between aluminum layers | target alloy is approximately 2% Li by weight | targets are neutronic poisons of very high worth |
| Reactor Vessel | 316 NG stainless steel | 3" thick (nominal)<br>20.5' outer diameter<br>31.4' overall height | submerged in flooded cavity for passive cooling |
| Containment Shell | free standing steel (SA 537 Class 2) cylinder with hemispherical dome | diameter: 188'<br>height: 258'<br>free volume: 5 million cubic feet | housed in a reinforced concrete shield building which provides passive containment cooling |

## Rationale for the DSAC Development Project Approach

The DSAC Development Project began by assessing the threats most important for the NPR-HWR design. An important aspect of severe accident challenges to the containment is that there are several different mechanisms for containment failure due to severe accidents. A rational approach is therefore to establish multiple design criteria. For the NPR-HWR, four DSACs were developed, each associated with a distinct mode of containment response. (The basis for identifying just four DSACs will be explained later.)

complete the project within a finite time frame. There was a limited amount of time for developing concrete proposals for DSACs. The goal was to develop design criteria before the details of the design were completed. As a result, the DSAC Development Project took place over approximately one year, with most of the effort occurring from December 1990 to June 1991.

The experts on the panel for the DSAC project provided quantitative information about highly uncertain severe accident phenomena. It would, however, be inappropriate to ask them to make judgments about what is a reasonable degree of conservatism in design criteria. The DSAC development project thus had the responsibility to develop a methodology which could process the information from the expert opinion elicitations to produce candidate design criteria that were conservative but not excessively so. There had to be some conceptual anchor in the methodology to the notion of "reasonably conservative." The anchor chosen was a limit on the likelihood that, given a severe accident, the containment would fail. This probability is known as the Conditional Containment Failure Probability (CCFP), and 0.1 was the limit chosen as the anchor for the recommended DSACs. This is consistent with a variety of approaches to probabilistic safety goals being considered in the reactor safety community (see Reference 1). The methodology for DSAC development added conservatism to this anchor, by considering only those severe accidents that had the potential to generate a threat to the containment (e.g., disregarding accidents in which core melting terminates without breach of the reactor vessel).

Goals of the DSAC Development Project

The programmatic and technical context described above were important factors in setting these goals for the project:

- to generate specific proposals for quantitative criteria within the specified project schedule,
- to minimize the phenomenological uncertainty residing in the problem statements and success criteria so that the design's compliance with the criteria would not be the subject of protracted contention,
- to follow a formal plan consisting of well-defined steps, each of which was scrutable and reviewable,
- to ensure that the complete spectrum of credible severe accident threats was covered by the criteria, and
- to avoid over-constraining the design.

The project was successful in achieving these goals on such a tight schedule because of the extraordinary cooperation of a large number of people from many organizations including DOE, Sandia National Laboratories, Westinghouse Savannah River Company, Argonne National Laboratory (ANL), Brookhaven National Laboratory (BNL), and the Ebasco design team.

## THE DEVELOPMENT PROCESS

The DSAC development process was a large and complex technical effort. It is only possible here to summarize the highlights; it is not possible to provide details on the reasons for the numerous decisions made. The interested reader should consult the project documentation [1] for more details. For conceptual purposes, it is convenient to describe the process as a sequence of these nine steps:

Step 1--Categorize Containment Threats
Step 2--Formulate Problem Statements
Step 3--Develop Success Criteria
Step 4--Assemble Expert Panel
Step 5--Provide Technology Overview
Step 6--Formulate Representative Accident Scenarios
Step 7--Elicit Expert Opinion
Step 8--Aggregate Results
Step 9--Develop Recommendations for Quantified DSACs

In reality, there was significant overlap and important feedback among these steps, so that the products of each step evolved as a result of such interactions. A brief description of each of the nine steps is given below to convey the overall rationale of the DSAC development process.

### Step 1: Categorize Containment Threats

While a severe accident specialist might begin by categorizing types of accidents by initiators and subsequent event tree branchings, a more direct approach begins by considering the ways that containment structures respond to physical loads. (Sorting by types of accidents enters into the process in Step 6.) Five distinct categories of containment threat were initially identified for the NPR-HWR:

- Missiles (projectiles resulting from events in the reactor vessel)
- Blast (shock waves from an internal explosion such as a hydrogen detonation)
- Rapid pressurization (causing static loads which are not greatly reduced by heat transfer to containment heat sinks)

- Slow pressurization (wnen static loads are strongly affected by heat transfer from the containment atmosphere)

- Basemat penetration (due to ablation of concrete by molten core debris)

This set of threats encompassed all events that could plausibly contribute to risk measures (e.g., the probability of a large radioactive release), but not the entire spectrum of events that the imagination could generate. After considerable analysis and discussion, the last threat (basemat penetration) was dropped from the list because it was considered extremely unlikely with Ebasco's flooded reactor cavity design that significant erosion of the concrete could occur. A number of other threats to containment integrity that are not directly due to severe accident loads (such as seismic loads or containment by-pass) were considered to be beyond the scope of the DSACs. These are better addressed by other approaches. (See the section entitled "Scope and Limitations of Results" for more on this topic.)

Step 2: Formulate Problem Statements

A DSAC was developed for each of the four threat categories. The problem statement for each threat was carefully formulated prior to eliciting expert judgment so that the expert panel would know how their opinions would be used. The problem statements had to be well-posed so that all important assumptions and parameters were specified (except parameters associated with the design itself, which the designer would specify in the compliance process). Ideally, the severity of the threat to the containment would be dominated by a single parameter which was called the DSAC parameter. The expert panel would play a key role in quantifying the DSAC parameter, by following the formal process described in Steps 5 through 7, below. Other parameters, which had less effect on the severity of the threat, were called support parameters, and were established prior to the expert opinion process on the basis of engineering judgment and a variety of scoping analyses.

The most challenging aspect of developing problem statements for the DSACs was the stated goal of "calculability." The analyses and calculations required to determine whether a design was in compliance with a DSAC should be straightforward and not subject to significant uncertainty because of assumptions about severe accident phenomenology. In this way, the DOE could remove a great deal of the burden for severe accident uncertainty from the designer. Once there was reasonable assurance that the design satisfied the DSACs (as well as a broad range of other design requirements), the designer could proceed with detailed design work without assessing the entire spectrum of hypothetical severe accidents at every step of the design process. The challenge in formulating the wording of the problem statements was ensuring that the inherent nature of the threat to containment integrity was preserved while the uncertain details of severe accident phenomenology were eliminated.

Initial versions of the DSAC problem statements were developed early in the project. They were thoroughly reviewed, and as the project progressed, the forms of the statements were refined and frozen prior to the elicitation of the experts' opinions. Each of the problem statements is given below in its entirety. The DSAC parameter for each of them is identified by quotation marks (e.g., "$Q_{net}$"). Other parameters are support parameters, and these are either given as specific values or left to the designer to specify.

*Missile DSAC Problem Statement. At time zero, the top vessel head and attached structures become a single large missile with a total kinetic energy of "$KE_m$". Using the appropriate success criteria and the best estimate value for the mass of the vessel head, control rod drive mechanism, mechanism service structure, and any other structures that would remain attached to the head, demonstrate that this missile, or any resulting secondary missiles, cannot perforate the containment. All internal containment structures may be considered for missile shielding.*

*Local Blast DSAC Problem Statement. Assume a blast wave contacts all points on the containment shell at the same time. The air blast is formed by an explosive energy release of "$E_b$". Using the radius of the containment as the distance from the point of energy release, use standard compiled air blast parameters to determine the peak reflected blast wave pressure, duration, and reflected impulse. Assume that the post-blast pressure is equal to the pressure that results if the containment atmosphere absorbs all of the blast energy. Assume that the containment atmosphere at the time of the blast contains 30% steam at saturated conditions, and neglect the addition of noncondensible gases to the atmosphere. (All concentrations expressed as percentages refer to mole fractions of the gas mixture). Demonstrate with a dynamic analysis that the containment does not exceed the limits set by the success criteria for dynamic loads.*

*Rapid Pressurization DSAC Problem Statement. Determine the maximum pressure and temperature that can occur by rapid addition of energy to the containment atmosphere. Assume that an energy addition of "$Q_{net}$" occurs over 2 seconds. Neglecting noncondensible gas addition to the atmosphere, assume that the atmosphere contains 30% steam at saturated conditions at the time of the energy addition. Demonstrate that the containment response does not exceed the limits set by the success criteria for rapid pressurization.*

*Slow Pressurization DSAC Problem Statement. At time zero, the reactor is shut down and 100% of the core decay power, $Q_d(t)$, begins to directly boil water into steam that enters the containment. A severe accident adds a total energy of "$Q_{add}$", starting 24 hours after reactor shutdown. Assume that the energy "$Q_{add}$" is added uniformly over one hour, and the energy directly boils water into steam that enters the containment. The containment atmosphere is at normal operating conditions at the time of reactor shutdown, but assume 10% moles of additional noncondensible gases are added to the containment uniformly during the time of severe accident energy addition. With no active cooling and using the best estimate of the core total decay power curve, $Q_d(t)$, perform a mass-energy balance calculation on the containment to determine the maximum pressure and temperature that can*

*occur after the addition of "$Q_{add}$" (that is, after more than 25 hours). Demonstrate that the containment response does not exceed the limits set by the success criteria.*

Step 3: Develop Success Criteria

Given the problem statement and a quantitative specification of the DSAC parameter, the designer could calculate the load on the containment and its response to that load. The success criteria for each DSAC are the tests applied to the containment response calculations to determine if the design satisfies the DSAC. Generally, the success criteria are surrogates for containment failure, but they are formulated in precise mathematical terms so that compliance with the DSAC would be unambiguous. The development of success criteria for the DSACs was assigned to a team of specialists in containment structural analysis. The development of success criteria proceeded in parallel with the load quantification part of the project, but it was, by intention, quite independent of the load quantification development except for the general knowledge of the four generic threats. This independence was intentional because it helped ensure the integrity of the loads assessment by isolating it from considerations about the ability of the design to comply.

Generally speaking, each success criterion has the form:

$$m_i < M_i,$$

The quantity on the left, $m_i$, is the value of the response measure (e.g., stress in the steel shell) calculated by the designer for the conditions specified by the i'th DSAC. The quantity on the right $M_i$, is the threshold value for compliance, and it was specified by the structural analysis team as a surrogate for containment failure.

A summary of the success criteria developed for the DSACs is provided in Reference 2 and they will not be discussed in additional detail here. We focus instead on the methodology for quantifying the containment loads, where most of the uncertainty related to severe accident phenomena was accommodated.

Step 4: Assemble Expert Panel

Steps 4, 5, 6, and 7 were critical elements of the DSAC Development Project, but they may seem unorthodox for developing engineering design criteria because they utilize formal expert opinion processes. However, it should be recognized that more traditional approaches require a consensus formation process which also depends substantially on expert judgment. The two principal differences are that the formal expert opinion processes can be accomplished within a specified and short schedule, and that the approach is amenable to external review because all steps in the process are planned in advance and thoroughly documented.

An expert panel was formed by identifying the desirable attributes of the panel and then recruiting six experts with broad experience in reactor safety and design. The selection of the experts and their subsequent activities were guided by two specialists in the use of formal expert opinion methods (designated "normative specialists"). The panel of technical experts was called the DSAC Quantification Team (DQT), and consisted of six members, two from Sandia National Laboratories, two from Westinghouse Savannah River Company, one from Argonne National Laboratory, and one from Brookhaven National Laboratory. Although the individuals within the group were chosen on the basis of their expertise in severe accidents, they were not expected to be equally proficient in all topics considered. Therefore, an integral part of the DSAC quantification process was the exchange of technical views among the DQT members as technical complements of each other. Following the formation of the DQT the team would spend approximately four months studying severe accident issues for the NPR-HWR and assisting the DSAC Development Project team in refining the expert opinion process that culminated in eliciting quantitative opinions.

Step 5: Provide Technology Overview

Preparation of the DQT for DSAC parameter quantification was supported by a review of HWR severe accident technology. This review included technical presentations by WSRC, SNL, ANL, and invited consultants, as well as technical documentation compiled in "DQT Information Packages." The review exposed the DQT to the spectrum of relevant severe accident topics based on research performed for the NRC, DOE, foreign sponsors, and the US nuclear industry. Of particular importance was the progress made in ongoing DOE-sponsored efforts for the NPR and for the current production reactors at the Savannah River Site. The information packages, technical presentation materials, and transcripts of the DQT meetings constituted approximately 27,000 pages.

Step 6: Formulate Representative Accident Scenarios

If the DSAC problem statements were posed without specific limitations on the scenarios envisaged, the controlling parameters (e.g., the various specified energies) would be essentially arbitrary and might vary too much from expert to expert to be combined into a meaningful result. Consequently, the design criteria would bear no relationship to actual risk considerations. By contrast, the methodology used for DSAC quantification established quite rational bounds on the severe accident conditions that were to be considered in specifying the parameters in the problem statements. As a result, the proposed quantified DSACs provide a defensible, conservative set of severe accident design criteria for the NPR-HWR containment without dictating unreasonable measures to protect against virtually incredible events.

In the expert judgment process, specialists are asked to provide a cumulative probability distribution expressing their "degree of belief" about the numerical value of a parameter (the DSAC parameter in our case), based on assumed conditions or events. Essential to the

implementation of this process is the specification of the "assumed conditions or events" for each elicitation. Clearly, the containment design criteria should be based on the assumption that a severe accident has occurred and there is a potential for a challenge to containment integrity. However, it is necessary to be more specific to ensure that the proper conditions are being considered for each threat. To ensure this, the concept of the Representative Conservative Accident Scenario (RCAS) was developed.

The RCASs are general descriptions of the initial conditions and events in hypothetical accident sequences that are used to assess a particular containment threat. An RCAS is a *scenario* because it is only an outline of conditions and events; it is not a detailed specification of a particular accident sequence. An RCAS is *representative* in the sense that it is typical of the more plausible scenarios that can give rise to a particular containment threat; it is not necessarily the most extreme or bounding scenario. An RCAS is *conservative* because it describes a type of accident with the potential to become a severe accident that would result in a containment threat.

The RCASs represent a categorization of phenomena sorted by accident conditions, in contrast to the categorization defined by the four DSACs that is sorted by structural effects on the containment. Double-sorting by both categorization schemes created a matrix of conditions for the DQT to address. These conditions were individually much more clearly defined than they would be by simply postulating a generic threat to the containment from an uncharacterized severe accident.

An alternative approach to categorization of severe accident phenomena that was discussed extensively in the conceptual stages of the DSAC Development Project would consider specific accident sequences along the lines of Level 1 and Level 2 Probabilistic Risk Assessments (PRAs). This approach was not followed because the detailed NPR-HWR design is incomplete; this makes it impossible to estimate the relative probabilities of specific accident sequences. The design criteria for the containment are needed well in advance of the availability of specific sequence probabilities. The goal of the categorization employed in the DSAC development process was design criteria that are insensitive to significant changes in the relative probabilities of the multitude of possible accident sequences.

Draft versions of proposed RCASs were initially developed for the DQT, who then substantially revised, reordered, and condensed the set. Although it is beyond the scope of this paper to discuss the rationale for each RCAS, this example of a scenario specific to the missile DSAC may help the reader understand how an RCAS provides a coarse accident condition description (FCI is Fuel-Coolant Interaction):

> *RCAS M2b Description: FCI in lower plenum following melting of initial blockages. Assume that flow passages to the lower plenum initially plug, permitting hot molten fuel (or fuel plus target material) to accumulate in the lower part of the core region. Assume that eventually blockages remelt, or supporting structures fail, allowing the accumulated molten*

*material to interact with water in the lower plenum and lower head region, and an FCI results. Consider the potential for an FCI under these conditions to generate a large-mass missile.*

The complete set of RCASs is shown in Table 2. The DQT was not required to consider so many RCASs that every conceivable accident condition was represented by at least one of them. Rather, they were only required to consider the minimal set of conditions which would ensure that the resulting loads assessment was robust regardless of the details of severe accident sequence probabilities characteristic of the final design.

Table 2. Summary of DSACs and RCASs Used for Quantification[1]

| DSAC | RCAS | RCAS Description |
|---|---|---|
| Missile | M1a | Large-scale Core degradation causes RIA; vessel rupture |
| | M1c | Prompt criticality in lower plenum; vessel rupture |
| | M2a | FCI following lower vessel head failure |
| | M2b | FCI in lower plenum |
| Blast | B1a (air shock) | Large-scale core degradation causes RIA; vessel rupture |
| | B1c (air shock) | FCI following lower vessel head failure |
| | B1d (air shock) | FCI in lower plenum |
| | B2b (local $H_2$) | Detonation of hydrogen produced by all possible sources |
| | B2c (local $H_2$) | Detonation of hydrogen produced by all sources except CDBI |
| | B2e (global $H_2$) | Detonation of hydrogen produced by all possible sources |
| | B2f (global $H_2$) | Detonation of hydrogen produced by all sources except CDBI |
| Rapid Pressurization | R1a | Large-scale core degradation causes RIA; vessel rupture |
| | R1c | FCI following lower vessel head failure |
| | R2e | Burn of hydrogen produced by all sources |
| Slow Pressurization | S2a | High steam addition to atmosphere |

[1] (Initialisms: RIA = Reactivity Insertion Accident; FCI = Fuel Coolant Interaction; CDBI = Core Debris-Basemat Interaction; $H_2$ implicitly includes $D_2$ and HD)

Superimposed on this matrix (of RCASs x DSACs) was a third categorization related to the success of plant protection systems. It was decided early in the project that the distinction between accidents in which at least one of the scram systems succeeded (protected accidents) and those in which none succeeded (unprotected accidents) was so important that it should be

preserved throughout the methodology. In other words, it should be possible to obtain separate results for all DSAC parameters for the protected and unprotected cases. This feature was requested by DOE and the designer because unprotected accidents would probably generate the most severe containment loads, but their probabilities were expected to be extraordinarily low because of the extremely high reliability expected of the NPR-HWR scram systems.

In summary, the experts were to be asked to give their quantitative "degree of belief" about the value of the DSAC parameter for each of many "elicitation cases," representing the conditions assumed for eliciting opinions. An elicitation case consisted of a choice from one of the four DSACs, a choice from one of the several RCASs for each DSAC, and a choice of the protected or the unprotected case. Figure 2 provides a schematic illustration of the several stages of the decomposition. In Figure 2 the DSAC is decomposed into two RCASs. The result is four elicitation cases (ECs). Further optional decompositions and subsequent recompositions are represented by the boxes downstream of the ECs. The product of the process is an uncertainty distribution for each elicitation case.

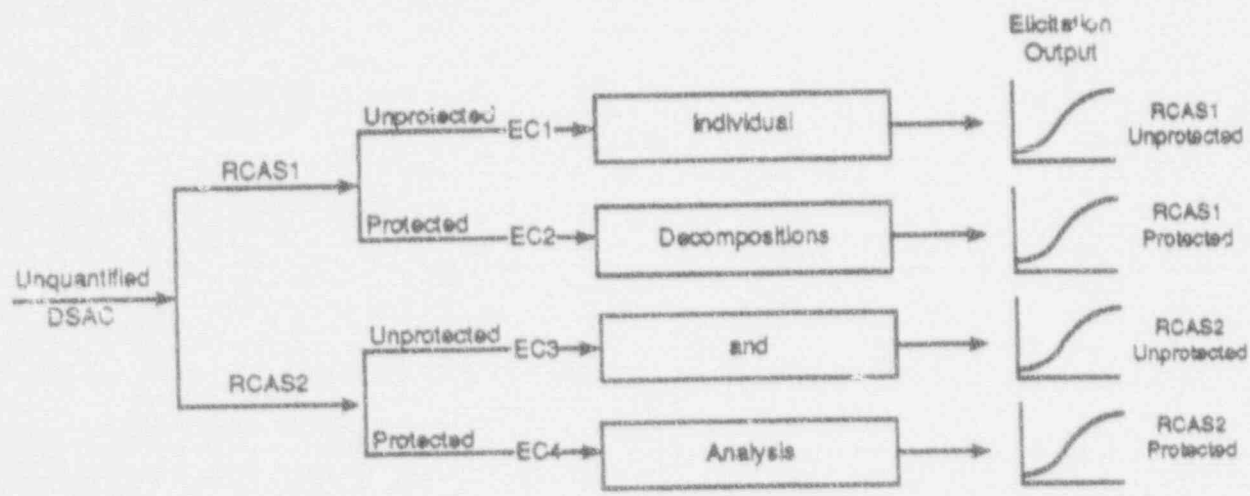


Figure 2. Simplified Depiction of DSAC Decomposition

Step 7: Elicit Expert Opinion

The culmination of the DQT activities was formal elicitation of the experts' opinions. For each Elicitation Case, the experts were individually asked to provide a response to questions of the following form:

> *Assuming the conditions described in the specified RCAS, and given the specified assumption about scram success, what is your degree of belief (expressed as a probability, P, ranging from 0 to 1.0) that the DSAC parameter would be less than the value "x"? Provide your answers in the form of a plot of P(x).*

The experts were not required to address every RCAS shown in Table 2, but they were required to consider at least one for each DSAC. If they chose not to be elicited on a particular RCAS (e.g., because they believed that the set of RCASs that they did consider was sufficiently complete) they were required to explain their reasons. In addition, each expert assigned a weight to each RCAS (summing to 1 for each DSAC) that expressed the expert's opinion about the degree to which that RCAS should contribute to quantitative design criteria for the containment.

The experts were assisted in their responses by the normative specialists, who had provided initial training to the DQT in quantitatively addressing such questions and who then acted as objective facilitators in one-on-one, private elicitation sessions. The normative specialists took notes on the experts' expressed basis for the quantitative opinions and later produced summaries of these rationales. The experts themselves were given the opportunity after the formal elicitation to review and revise their responses. They also wrote individual reports describing the rationales for their opinions. All of this information is provided in entirety in Volume 2 of the project documentation [1].

Step 8: Aggregate Results

The result of the elicitation process was a large number of curves, P(x), corresponding to each elicitation case and each expert (see right side of Figure 2). To develop a data base for quantifying each DSAC these curves had to be aggregated. The method followed had been substantially established before the elicitations and consisted of two steps:

1. For each DSAC and expert, calculate the weighted average of the probabilities among the different RCASs, using the RCAS weights provided by the DQT member.

2. Using the results of step 1, calculate the unweighted average of the probabilities among the different experts for each DSAC.

Figure 3 illustrates the general aggregation process for six experts given the unquantified DSAC depicted in Figure 2.

The result was a set of two curves for each DSAC (one for the protected case and one for the unprotected case). As an example, Figure 4 shows the results for the Rapid Pressurization DSAC. The "Energy" shown on the x axis is the quantity $Q_{net}$, described in the problem statement discussed in Step 2. The "Probability" shown on the y axis is the result of the two-step aggregation process described above as applied to the set of P(x) curves from all six experts and for each of the RCASs for the Rapid Pressurization DSAC they considered (see Table 2).

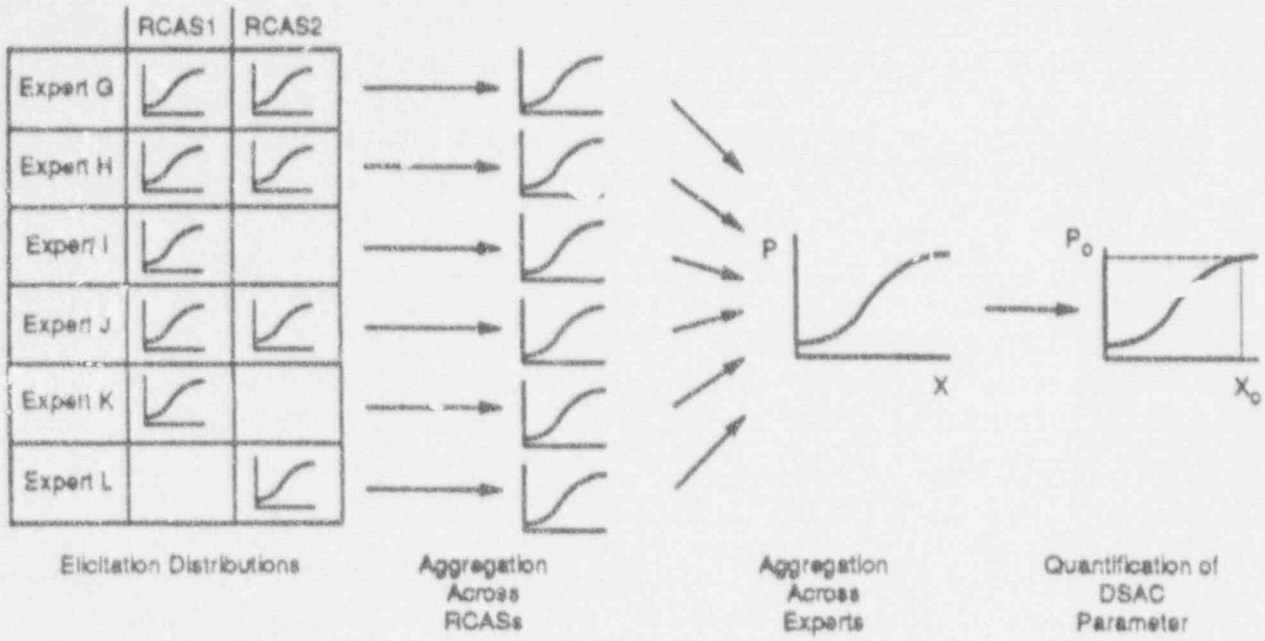


Figure 3. Aggregation Process

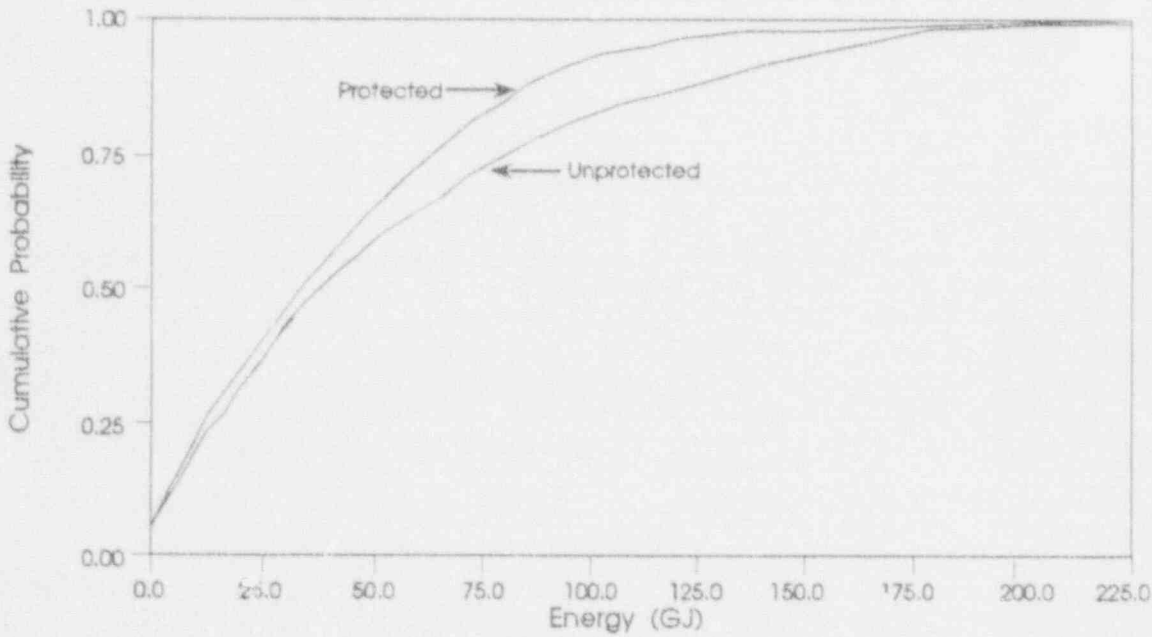


Figure 4. Aggregated Elicitation Results for Energy ($Q_{net}$) in the Rapid Pressurization DSAC

Step 9: Develop Recommendations for Quantified DSACs

The curves such as shown in Figure 4 are the processed output of the expert elicitation. Two steps remained before quantified DSACs could be formulated for DOE's consideration: (1) combining the protected and unprotected cases, and (2) selecting the final DSAC parameter from the probability curves. For each step, a significant degree of judgment was required involving more than just technical issues (e.g., safety policy, consistency with other DOE/NP initiatives, etc.). The project documentation provided recommendations and evaluations of the pros and cons of alternative options for consideration by the Review Team of DOE employees which was formed for the purpose of deciding on the final DSACs [4].

The first issue was how to treat the distinction between protected and unprotected accidents. As expected, the unprotected case generated more severe loads than the protected case (Figure 4). However, given the expected very low probability of unprotected accidents there was concern that designing the containment for such conditions would be unnecessarily conservative. The project documentation discussed various options, including, designing only for the protected case by relegating unprotected accidents to the "residual risk" category. However, the option finally recommended to the DOE was weighting the two cases equally for probability averaging. This recommendation was chosen because it would be very easy to defend as exceptionally conservative. As explained in Reference 3, the DOE Review Team decided to use a weighted average of the protected/unprotected split with a different conservative value for the weighting factor.

The second issue--how to select the final DSAC parameter from the aggregated probability distributions--was discussed in terms of the "pickoff point" for the probability curve. Simplistically, if we neglect uncertainties in material properties and in the designer's calculations, and if we furthermore assume that if there is only one DSAC (i.e., only one type of containment threat), then a CCFP goal of 0.1 can be assured by choosing a pickoff point of 0.9; in other words, to set the DSAC parameter at the value whose aggregated probability is 90%. In the case of multiple threats the situation is more complicated because of the possibility that a single accident sequence can give rise to more than one threat at different times in the sequence. The rather subtle effect of multiple threats was extensively analyzed, and the mathematical conditions which would be needed to justify various assumptions about multiple threats were derived in the project documentation [1], but these details are not reviewed here. The effects of analysis uncertainty and materials properties uncertainties are also addressed in [1], but not in this summary paper.

The recommendation finally made to DOE was to use an "unequal pickoff" approach: i.e., to use a 91% pickoff point for the Missile DSAC (the most challenging) and a 99% pickoff for the other three. It was shown that this method completely accommodates dual threats in the same sequence while neglecting triple or quadruple threats.

After review of this recommendation and receiving input from additional sources, the DOE Review Team decided that there were enough additional conservative steps in the overall DSAC development process that it was justified (and more easily explained) to use a 90% pickoff point for all DSACs [3]. After some rounding and simplification, the final set of quantified parameters for the DOE's DSACs are as shown in Table 3. Reference 1 provides more details about the DOE team's rationale. The complete specification of DSACs for the NPR-HWR therefore consists of the problem statements given in Step 2, the numbers for the DSAC parameter given in Table 3, and the success criteria discussed in Reference 2.

Table 3. Quantified DSAC Parameters in DSACs

| DSAC | Quantity | Value |
|---|---|---|
| Missile | $KE_m$ | 150 MJ |
| Local Blast | $E_b$ | 7.2 GJ |
| Rapid Pressurization | $Q_{net}$ | 100 GJ |
| Slow Pressurization | $Q_{add}$ | 190 GJ |

Since the DSACs were promulgated, the reactor designer has initiated preliminary analyses to determine whether the baseline design (which was developed prior to the issuance of the DSACs) would comply with these criteria. These preliminary analyses indicated that the last three DSACs would be adequately accommodated by the current design. However, some design changes (judged feasible by the designer) would be needed to accommodate the Missile DSAC. It is interesting to note that the degree of conservatism embodied in the DSACs was of the same order of magnitude as the degree of conservatism already incorporated by the designer into the design on the basis of qualitative interpretations of high-level programmatic goals and good engineering judgment.

## SCOPE AND LIMITATIONS OF RESULTS

It is important to view the DSAC development project in the proper context. It has already been emphasized that the quantitative results are applicable only to designs within a rather narrow envelope, and not to systems as different as commercial light-water reactors (LWRs). However, there are other limitations and clarifications of scope which should be mentioned briefly.

The DSACs deal only with the types of threats to the containment that result directly from core melting and subsequent loss of core geometry. Another important set of design criteria for the containment deal with seismic loads. Stringent criteria for resistance of the containment to large seismic loads are being developed under another program for DOE/NP. There is only one

important area of overlap between seismic threats and the DSACs: severe accidents that are initiated by seismic events which are not in themselves large enough to fail the containment. Such accidents were considered to be in the realm of conditions to be assessed by the DQT, but it is not expected that there would be any unique severe accident phenomena occurring in such seismically induced core melt accidents.

Some modes of containment failure may be important to risk, but were not covered by the DSACs because of their unique natures. For example, containment bypass events are not covered by the DSACs. Also, the DQT decided that it would probably be sufficient to consider only the large missile described in the Missile DSAC Problem Statement, although there was a possibility that some types of small missiles could be important. Finally, the topic of dynamic loading of key interior walls due to a hydrogen detonation was identified as a potential safety issue, but it was not covered by the DSACs.

For each of these concerns there were good reasons for not expecting the DSACs to be adequate surrogates. It was recommended that as the design progressed, specific attention be paid to them in the form of traditional engineering analyses or reliability goals. The fact that a number of minor safety issues were identified that were not amenable to the "umbrella" approach of the DSACs was not surprising; the success of the process should be judged by the much larger range of severe accident issues that do fall under that umbrella.

Given recent events in the NPR program, the most important limitation of the DSACs is that they are not robust with respect to significant design changes. As explained at the beginning of this paper, the DOE is currently exploring approaches for adapting the current set of DSACs to the downsized NPR-HWR design, but work in this area has not yet progressed enough to allow a discussion of these approaches.

## SUMMARY AND CONCLUSIONS

In this paper we have summarized the methodology developed to assist the DOE's Office of Heavy Water Reactor in formulating containment design criteria that are a practical implementation of high-level programmatic goals. The project was large and complex, even though the implementation of the methodology required only about six months. It is not possible to provide much quantitative detail here or to explain the reasoning behind the many decisions which went into developing and implementing the methodology. The project documentation provides extensive additional detail [1].

It is possible that other uses of this quantification methodology could be found both for the NPR and for other systems. For example, this methodology, or variations on it, could be used to establish performance criteria, under extreme conditions, for safety systems or other systems important to safety in nuclear reactors.

We have summarized the sequence of steps taken in the formal process that was devised to generate quantitative criteria concerning a subject area characterized by extensive phenomenological uncertainty. As a result of the output of this process, the DOE's Office of Heavy Water Reactor was able to integrate the project recommendations together with numerous other inputs to promulgate design criteria that were conservative, but not excessively so, and that could be technically reviewed and defended.

## Acknowledgments

This work was supported by the United States Department of Energy under contract DE-AC04-76DP00789, as part of the DOE's Office of Heavy Water Reactor Engineering Development Program.

The authors of this paper constituted the Project Management Team of the DSAC Development Project, but the overall effort involved a large number of technical personnel from many organizations, including DOE/NP, ANL, SNL, BNL, WSRC, Ebasco, and Battelle Memorial Institute. Of particular importance to the success of the project was the expertise and dedication of the members of the DSAC Quantification Team, who are identified by name and affiliation in the project documentation [1]. Special acknowledgments are owed to Dr. David C. Williams of SNL, who was not only a member of the DQT, but was also responsible for developing many of the most important conceptual elements for the DSAC development process.

## References

1. DSAC Development Project, "Heavy Water New Production Reactor Design Review Guidelines," NPRW-DSAC91-5, Sandia National Laboratories, Albuquerque, NM, to be published.

2. R. F. Sammataro, W. R. Solonick, and N. W. Edwards, "A Generic Approach for Containment Success Criteria Under Severe Accident Loads," Proceedings of the 5th Workshop on Containment Integrity, May 1992.

3. P. T. Rhoads, "Deterministic Severe Accident Criteria (DSACs) as Severe Accident Design Criteria and Policy for the New Production Reactor," Proceedings of the 5th Workshop on Containment Integrity, May 1992.

4. U.S. Department of Energy, "Design for Normal Operation and Abnormal Events, Including Severe Accidents," Office of New Production Reactors, NPR-STD-1000, Rev. 0, DOE, Washington, DC, June 1991.

5. U.S. Nuclear Regulatory Commission, "Severe Accident Risks: An Assessment of Five U.S. Nuclear Power Plants," NUREG-1150, Vol. 1, NRC, Washington, DC, December 1990.

# A GENERIC APPROACH FOR CONTAINMENT SUCCESS CRITERIA UNDER SEVERE ACCIDENT LOADS[1]

Robert F. Sammataro
General Dynamics Corp.

William R. Solonick
General Dynamics Corp.

Norman W. Edwards
NWE Services, Inc.

## Abstract

The U.S. Department of Energy (DOE), Office of New Production Reactors (NP), has identified safety as the foremost design criterion for the Heavy Water New Production Reactor (NPR-HWR). The DOE-NP has issued the Deterministic Severe Accident Criteria (DSACs) to guide the design of the NPR-HWR containment for resistance to severe accidents. The DSAC concept provides for a generic approach for success criteria to predict the threshold of containment failure under severe accident loads. This concept consists of two parts: (1) *Problem Statements* that are qualitative and quantitative bases for calculating associated loadings and containment response to those loadings, and (2) *Success Criteria* that specify acceptable containment response measures and limits for each problem statement. This paper is limited to a discussion of a generic approach for containment success criteria. The main elements of these success criteria are expressed in terms of elastic stresses and inelastic strains. Containment performance is based on the "best estimate" of failure as predicted by either stress or strain, buckling, displacements, or ability to withstand missile perforation. Since these limits are "best estimates" of failure, no conservatism exists in these success criteria. Rather, conservatism is to be provided in the problem statements, i.e., the quantified severe accident loads. These success criteria are presented on a multi-tiered basis for static pressure and temperature loadings, dynamic loadings, and missiles. Within the static pressure and temperature loadings and the dynamic loadings, the criteria are separated into elastic analysis success criteria and inelastic analysis success criteria. Each of these areas, in turn, defines limits on either the stress or strain measures as well as on measures for buckling and displacements.

## INTRODUCTION

### The DSAC Concept

The DOE-NP has identified safety as the foremost design criterion for the Heavy Water NPR-HWR. Specifically, the DOE-NP has required that the NPR-HWR designs consider severe accidents despite their extremely low likelihood of occurrence. Severe accidents are very unlikely accidents that can result in significant core damage, containment failure, and a potential release of radioactive material to the environment. Containment failure under severe accident loadings is defined as the threshold at which the containment no longer retains its structural or leak-tight integrity.

The DOE-NP has issued the Deterministic Severe Accident Criteria (DSACs) [1], [2] to guide the design of the NPR-HWR containment for resistance to severe accidents. The DSAC concept provides for a generic approach for success criteria to predict the threshold of containment failure under severe accident loads.

1 This paper is based upon work performed under Contract No. 78-5066 for Sandia National Laboratories, Albuquerque, New Mexico, operated by Sandia Corporation for the United States Department of Energy.

The DSAC concept consists of two parts:

(1) *Problem Statements* that are qualitative and quantitative bases for calculating associated loadings and containment response to those loadings.

(2) *Success Criteria* that specify acceptable containment response measures and limits for each problem statement.

## Success Criteria

Success criteria are presented in this paper for four DSACs: (1) Rapid Pressurization, (2) Slow Pressurization/Overtemperature, (3) Blast, and (4) Missiles. Success criteria for these DSACs are expressed in terms of two general measures, elastic stresses and inelastic strains. These measures best serve the need for success criteria. Additional measures are based upon considerations for buckling and displacements. Empirical equations are defined for determining the ability of the containment to withstand missile perforation.

Containment performance is based on the "best estimate" of failure as predicted by either stress or strain, buckling, displacements, or ability to withstand missile perforation. Since these limits are "best estimates" of failure, no conservatism exists in these success criteria. Rather, conservatism is provided in the problem statements, i.e., the DSACs. Introducing additional conservatism in these success criteria is therefore neither needed nor warranted because of the extremely unlikely occurrence of a severe accident. A containment design whose calculated performance is within the specified limits is considered acceptable from a severe accident perspective.

These success criteria are presented on a multi-tiered basis for static pressure and temperature loadings, dynamic loadings, and missiles. Within the static pressure and temperature loadings, these success criteria are separated into elastic analysis success criteria and inelastic analysis success criteria. Each of these, in turn, defines limits on either the stress or strain measures as well as on measures for buckling and displacements. Similar success criteria are presented for dynamic loadings.

A design that satisfies either the set of elastic analysis success criteria or the set of inelastic analysis success criteria is considered acceptable. The determination as to which of the two sets of success criteria is utilized is at the option of the designer. Neither set of success criteria is considered to be preferable over the other. It is acceptable to use the elastic analysis success criteria to qualify portions of the containment for a given DSAC and the inelastic analysis success criteria to qualify the remainder of the containment for the same DSAC. It is also acceptable to use a different set of success criteria (elastic or inelastic) for different DSAC static pressure and temperature loading conditions or dynamic loading conditions.

## Application to Severe Accident Loads

The applicability of the containment success criteria to severe accident loads is summarized in Table 1. The loadings are defined in the following paragraphs.

### Rapid Pressurization

For rapid pressurization, containment failure is defined as the threshold at which the stress or strain limits that constitute loss of vessel integrity or initiation of leakage are reached. Either the elastic analysis success criteria or the inelastic analysis success criteria may be applied. Limits for buckling and displacements must be met. The time scale for rapid pressurization is such that the dynamic loading success criteria are not applicable.

Table 1. Applicability of Containment Success Criteria to Severe Accident Loads

| SUCCESS CRITERIA | | SEVERE ACCIDENT LOADS | | | |
|---|---|---|---|---|---|
| | | Rapid Pressurization | Slow Pressurization/ Overtemperature | Blast | Missiles |
| STATIC PRESSURE & TEMPERATURE LOADING | ELASTIC ANALYSIS | X | X | | |
| | INELASTIC ANALYSIS | X | X | | |
| DYNAMIC LOADING | ELASTIC ANALYSIS | | | X | X [1] |
| | INELASTIC ANALYSIS | | | X | X [1] |
| MISSILES | PERFORATION EQUATIONS | | | | X |

Note: (1) Applicable for missiles outside the limits of perforation equations.

### Slow Pressurization/Overtemperature

For slow pressurization/overtemperature, containment failure is defined the same as for rapid pressurization. However, the effect of high temperature on the containment and the impact on material properties and ultimate performance of the containment must be addressed. Either the elastic analysis success criteria or the inelastic analysis success criteria may be applied. Containment evaluation is similar to that required for rapid pressurization. The pressure boundary metal temperature is limited to a maximum of 700°F.

### Blast

Blast imposes a dynamic load on the containment boundary (e.g., air shock). This loading must be evaluated using a time-dependent pressure (i.e., dynamic) analysis for the initial impulse of the pressure load. Analysis methods based upon an equivalent static pressure are not considered acceptable. Success criteria for the containment require that either the elastic dynamic response or inelastic dynamic response success criteria be satisfied. Containment evaluation is similar to that required for rapid pressurization. Also, the hatches and other portions of the containment must not buckle and specified displacement limits must be satisfied.

### Missiles

Internal missiles resulting from an explosion or vessel rupture are thought to have the potential to generate the most severe threats to the containment. This is because they can deliver high concentrations of energy over small areas. The success criterion for missiles is that the containment boundary not be perforated by (a) direct impact from a primary missile, (b) indirect impact from a primary missile through reflection, or (c) impact from secondary missiles formed by impact of primary missiles. This success criterion is based upon empirical energy balance equations that include the missile mass, diameter, and velocity and the containment material properties and geometrical parameters.

## Containment Success Criteria

### Elastic Analysis Success Criteria

Containment failure is defined as the threshold at which the containment no longer retains its structural or leak-tight integrity. Success criteria in this paper address qualitative severe accident loadings. However, to best represent the response of the containment when subjected to these kinds of loadings, *measures* of failure are established based upon both the nature of the loading and the method of analysis. Therefore, for both static and dynamic loadings, separate success criteria are established for elastic and inelastic analysis.

Within the elastic analysis success criteria, the measure of failure for the containment is the quantity *stress measure*. By definition, *stress measure* is the equivalent intensity of combined stress computed by the Distortion Energy Theory. Limits are expressed as a function of the actual material yield stress ($S_y$) or ultimate stress ($S_u$).

Elastic analysis success criteria limits are established for primary stress measures and primary plus secondary stress measures. The primary stress measure limits are further divided into general membrane, local membrane, and general or local membrane plus bending stress measures. Similarly, the primary plus secondary stress measures are divided into general membrane, local membrane, and local membrane plus bending stress measures. Application of each of these measures to the containment is a function of the location of the area being evaluated, the nature of the applied loading, and the type of stress.

For the elastic analysis success criteria, the measure of failure for bolting within the containment boundary is *stress intensity*. *Stress intensity* is the equivalent intensity of combined stress computed by the Maximum Shear Stress Theory. Separate elastic analysis success criteria are also established for welds, buckling, and displacements.

### Inelastic Analysis Success Criteria

Inelastic analysis success criteria limits for static pressure and temperature loadings are expressed in terms of the quantity *equivalent plastic strain*. These limits are expressed as a function of the material ultimate strain, $\varepsilon_u$. Limits unique to the success criteria in this paper are defined.

For the inelastic analysis success criteria, bolting strain is limited to an average strain computed as $S_y/E$ where E is the modulus of elasticity of the bolt material. The total surface strain for bolts is limited to $0.60\varepsilon_u$. Limits for buckling and displacements are similar to those for the elastic analysis success criteria.

## Success Criteria for Dynamic Loading

Dynamic loadings require a time-dependent dynamic analysis to account for the transient nature of the containment response. The success criteria for dynamic loadings for elastic analysis are the same as the elastic analysis success criteria for static pressure and temperature loadings. The success criteria for dynamic loading for inelastic analysis are the same as the inelastic analysis success criteria for static pressure and temperature loadings.

## Success Criteria for Missiles

Three empirical equations based upon energy balance approaches are defined as measures for missiles. These equations may be used to determine the maximum diameter, mass, and velocity of missiles that will not perforate the containment. Conversely, the equations may be used to

determine the containment thickness required to resist perforation by missiles of a given mass, diameter, and velocity. Applicability of these equations is limited in terms of missile and containment parameters. Loadings from extremely large missiles that exceed the parameters of the empirical equations must be treated as dynamic loads on the containment. When subjected to these loads, the containment must be evaluated in accordance with the success criteria established for dynamic loadings.

### Additional Information

This paper is based upon a technical report [3] by the same authors. This technical report provides additional detail regarding the development and application of and rationale for these success criteria. Reference 3 also provides recommendations for analytical methods and computer modeling, typical design curves for missiles, and a qualitative assessment of uncertainties associated with application of these criteria.

## DISCUSSION

### Containment Analysis

Present methods for containment design and analysis are not suitable for severe accident loadings. Design Basis Accident (DBA) loadings and methods of analysis for present containments are typically highly conservative. Therefore, the analyses ensure a rather low probability that the containment would fail under the most severe DBA conditions. However, severe accidents are considered to be so unlikely, and the associated phenomena so complex, that it is counterproductive to use conservative analysis methods. Rather, a "best estimate" approach based upon containment failure is appropriate.

There are fundamental qualitative differences between DBA loadings and severe accident loadings. These differences require a different approach to containment analysis. New design criteria and a new definition of containment failure are needed if the design is to include a robust containment intended to withstand the highly unlikely severe accidents without needlessly impacting the design.

### Success Criteria Considerations

Success criteria *measures* must be established to assess containment performance and ultimately containment failure. One challenge is to select the measures that best serve the need for these success criteria. Desirable attributes of these success criteria include:

(1) Zero or low margin of safety (little or no conservatism),

(2) Low design variability (different designs will fail at approximately the same value of the measure),

(3) Low calculational variability (different analysts converge quantitatively),

(4) Calculation is within broad engineering state of the art (existing analytical methods and techniques may be used), and

(5) Provide a "best estimate" of containment failure.

Generally, elastic stress and inelastic strain have these attributes and have been selected as the primary measures for containment performance (with the exception of missiles).

The success criteria on which containment failure will be based should not incorporate large safety factors because the probability of severe accidents is very low and an adequate degree of conservatism is intended to be incorporated into the quantified severe accident loadings. Introducing additional conservatism in these success criteria or in the analysis method could result in unrealistic requirements. The measures selected for these success criteria are best estimates of the elastic stress, inelastic strain, buckling or other measures for prediction of failure. In that respect, the user should be alerted that these success criteria are intended to be used in conjunction with loading definitions that contain conservatisms consistent with the intended margins of safety against failure of the pressure boundary for the severe accident loads.

The containment success criteria in this paper are intended to be satisfied after the containment design has been shown to meet all requirements of Section III, Division 1 of the ASME Boiler and Pressure Vessel Code [4]. Although similar to the ASME Code rules in some cases, these success criteria are a separate and unique set of rules for loading conditions that are not included in the traditional ASME Code design criteria for nuclear containment vessels. They differ significantly from the ASME Code rules in that the success criteria measures in this paper are intended to be best estimates of containment structural failure without any margin of safety.

The potential effects of radiation on material strength, ductility, or other material properties were not considered in the development of these success criteria and need not be considered in their application. Also, the potential effects of creep at elevated temperatures are considered insignificant up to the maximum metal temperature of 700°F allowed in these success criteria. This assumes that the elevated temperature does not continue for an extended period of time

The success criteria established in this paper were developed for ASME SA-537, Cl. 2 steel [5]. These success criteria may also be used for other materials, except for bolting materials and welding materials, that satisfy the following requirements:

$$S_u \leq 70{,}000 \text{ psi},$$
$$\varepsilon_u > 10\%, \text{ and}$$
$$\text{Elongation} > 20\%;$$

where: $S_u$ is the minimum ultimate tensile strength in the applicable material specification in Part A, Section II, of the ASME Boiler and Pressure Vessel Code [5],

$\varepsilon_u$ is the material ultimate strain, and

*Elongation* is the minimum value of the percentage increase in length at failure due to tensile loading for a 2-inch test specimen, as defined in the applicable material specification in Part A, Section II, of the ASME Code Boiler and Pressure Vessel Code [5].

Success criteria in this paper also apply to all bolting materials and welding materials that are permitted for containments in Subsection NE, Section III, Division 1, of the ASME Boiler and Pressure Vessel Code [6].

## SUCCESS CRITERIA MEASURES AND DEFINITIONS

### Containment Failure

*Containment failure* when subjected to severe accident loadings is defined as the threshold at which the containment no longer retains its structural or leak-tight integrity. Loss of structural integrity

occurs when the elastic stresses or inelastic strains reach a level that results in the inability of the containment to withstand further pressure, temperature or structural loadings or when buckling of the hatches or any other portion of the containment vessel is initiated. Loss of leak-tight integrity occurs at the initiation of leakage through any portion of the containment vessel boundary. The failure thresholds defined in this paper are best estimates of the actual point at which containment vessel structural or leak-tight integrity will be lost.

## Elastic Analysis

*Elastic analysis* refers to a method of structural analysis where the stress in the material is directly (linearly) proportional to the strain in the material. The state of stress at any point in a structure may be completely defined by giving the magnitude and direction of three principal stresses. When two or three of these stresses are different from zero, the proximity to yielding must be determined by means of a strength theory.

The strength theory to be used to define the state of combined stresses when applying these success criteria, except for bolts, is the Distortion Energy Theory [7]. This theory is also referred to as the shear energy theory or the von Mises-Hencky Theory. The Distortion Energy Theory is considered the best theory for ductile materials and results in the most accurate prediction of the onset of yielding. The term *stress measure* is used in these success criteria to define the maximum stress computed using the Distortion Energy Theory.

The strength theory to be used to define the state of combined stresses in bolts is the Maximum Shear Stress Theory [7]. The term *stress intensity* is used when computing stresses using the Maximum Shear Stress Theory. Stress intensities calculated in accordance with the Maximum Shear Stress Theory are the basis for all of the stress evaluations in Section III, Division 1, of the ASME Code [4].

The use of elastic analysis methods as a measure of containment failure is based on the ultimate stress of the vessel materials. Using elastic analysis methods with stress limits that exceed the material yield stress is not typical of most engineering criteria. However, as discussed in [8], this approach is recognized for loads that are considered extreme in nature in Appendix F, Section III, Division 1, of the ASME Code [9]. For ASME Class MC components under Service Level D loadings, the allowable primary membrane stress intensity is $0.60S_u$ and the allowable local primary membrane stress is $0.90S_u$. For ASME SA-516, Gr. 70 steel [5] at 300°F, the minimum yield strength is 33.7 ksi and the minimum ultimate tensile strength is 70 ksi. The primary membrane limit would therefore be 42 ksi and the local membrane limit would be 63 ksi, each greater than the minimum yield strength. Furthermore, no limit is established in Appendix F on primary plus secondary stresses for Service Level D conditions.

Elastic analysis success criteria are provided as an alternative to the inelastic analysis success criteria. It is recognized that when stress levels are significantly beyond yield stress, inelastic analysis methods are more exact and will produce results more closely representative of the capacity of the containment. However, stress analyses required to demonstrate compliance with the elastic analysis success criteria are analytically easier to perform, require less sophisticated analytical tools, and tend to provide more consistent results from analyst to analyst.

It is not the intent of these success criteria to establish a direct correlation or equivalency between the set of elastic analysis success criteria and the set of inelastic analysis success criteria. Each set of success criteria is essentially derived on its own basis although there may be close comparison with easily determined stress conditions, e.g., general membrane stress in the free field. A direct correlation between the two sets of success criteria would require extensive comparative analytical studies. The elastic analysis success criteria will tend to underestimate the capacity of the

containment relative to the inelastic analysis success criteria. Therefore, the elastic analysis success criteria will have an increased level of uncertainty relative to the inelastic analysis success criteria as a prediction of the capacity of the containment.

### Elastic Analysis Definitions

Definitions of some of the more important terms used in the elastic analysis success criteria are provided below. Some of the stress-related term definitions are similar to those used in NE-3213, Subsection NE, Section III, Division 1, of the ASME Code [6]. However, several of the definitions are unique to these success criteria.

*Stress measure, SM,* is the equivalent measure of combined stress. It is defined as the square root of one half of the sum of the squares of the difference between the three principal stresses, or:

$$SM = \sqrt{\frac{1}{2}\left[(\sigma_1 - \sigma_2)^2 + (\sigma_2 - \sigma_3)^2 + (\sigma_3 - \sigma_1)^2\right]} \qquad (1)$$

where:

$SM$ = Stress Measure, and
$\sigma_1, \sigma_2, \sigma_3$ = Principal Stresses.

*Stress intensity, (SI),* is the equivalent intensity of combined stress. It may also be defined as twice the maximum shear stress. Therefore, the stress intensity is the difference between the algebraically largest principal stress and the algebraically smallest principal stress at a given point. Tensile stresses are considered positive and compressive stresses are considered negative. That is:

$$SI = 2\,\tau_{max} \qquad (2)$$

where:

$SI$ = Stress Intensity,
$\sigma_1, \sigma_2, \sigma_3$ = Principal Stresses,
$\tau$ = Shear Stress,

$$\tau_{1,2} = \frac{\sigma_1 - \sigma_2}{2}, \qquad (3)$$

$$\tau_{2,3} = \frac{\sigma_2 - \sigma_3}{2}, \qquad (4)$$

$$\tau_{1,3} = \frac{\sigma_1 - \sigma_3}{2} \text{ and} \qquad (5)$$

$$\tau_{max} = \max\left\{|\tau_{1,2}|, |\tau_{2,3}|, |\tau_{1,3}|\right\}. \qquad (6)$$

*Membrane stress* is the component of normal stress or shear stress equal to the average stress across the thickness of a section under consideration. Membrane stress includes normal stress and shear stress. *Normal stress* is the component of stress perpendicular to the plane of reference. *Shear stress* is the component of stress tangent to the plane of reference.

*Local membrane stress* is a membrane stress associated with a discontinuity effect that could produce excessive distortion in the transfer of load to other portions of the structure. A local membrane stress region may not extend along the meridian of a shell of revolution element for a distance greater than $(Rt)^{1/2}$ where R is the minimum mid-surface radius of curvature and t is the minimum thickness in the region under consideration. The definition of a local membrane stress region does not apply to areas such as flat heads, extended lengths along meridional stiffeners, or along the edges of rectangular openings that are parallel to the axis of revolution of the shell element. More liberal membrane stress limits are permitted for local regions only as long as the

region is not closer along the shell's meridian than $(R_a t_a)^{1/2}$ to another local region where membrane stress limits are exceeded. The terms $R_a$ and $t_a$ are the averages of the values for the two regions under consideration. If two or more regions are closer together than $(R_a t_a)^{1/2}$, then only one of them may be classified as a local membrane stress region with stresses higher than permitted for general membrane stress. Although there are some subtle differences, this definition corresponds generally with the concept of local primary membrane stress as defined by NE-3213.10, Subsection NE, Section III, Division 1, of the ASME Code [6].

*Bending stress* is the variable component of normal stress. The variation may or may not be linear across the thickness or depth of a section.

*Primary stress* is any normal or shear stress developed by an imposed loading necessary to satisfy the laws of equilibrium of external and internal forces and moments. The basic characteristic of a primary stress is that it is not self-limiting. Primary stresses that considerably exceed the yield stress may result in gross distortion or even failure.

*Secondary stress* is a normal stress or a shear stress developed by the constraint of adjacent material or by self constraint of the structure. The basic characteristic of a secondary stress is that it is self-limiting. Local yielding and distortion can satisfy the condition that causes the stress to occur. The determination of secondary stresses is not required in typical elastic analyses performed for loadings that are applied only once and when fatigue is not a consideration. The elastic analysis success criteria impose limits on both primary and primary plus secondary stresses. Limits on primary plus secondary stresses are imposed since the allowable primary stresses are beyond the material yield stress and result in significant inelastic strains. Therefore, in order to limit the total strain in the vessel, a pseudo-elastic limit is placed on the primary plus secondary stresses. Limiting the elastically-determined values of primary plus secondary stresses effectively limits the maximum strains to values below the ultimate strain of the material even though the strains are not explicitly determined.

*Primary plus secondary general membrane stress measure, $SUM_m$*, is the average primary plus secondary (equivalent elastic) stress across a solid section. It includes stresses produced by thermal gradients. It excludes effects of discontinuities, both mechanical and thermal, and all peak stresses.

*Primary plus secondary local membrane stress measure, $SUM_l$*, is the average primary plus secondary (equivalent elastic) stress across a solid section. It includes effects of discontinuities, both mechanical and thermal, and stresses produced by thermal gradients. Peak stresses are excluded.

*Primary plus secondary membrane plus bending stress measure, $SUM_q$*, is the primary plus secondary (equivalent elastic) stress necessary to satisfy continuity of the structure. It occurs at structural discontinuities. It includes effects of discontinuities, both mechanical and thermal, and stresses produced by thermal gradients. Peak stresses are excluded.

*Peak stress* is that increment of stress that is additive to the primary plus secondary stress by reason of local discontinuities or local thermal stress including the effects, if any, of stress concentration. Peak stresses are ordinarily computed for determining the fatigue adequacy of a structure. Adequacy for fatigue is not a requirement for the containment under severe accident loadings. Therefore, peak stresses are not required to be determined in the elastic analysis success criteria.

*Thermal stress* is a self-limiting stress produced by a nonuniform distribution of temperature or by differing thermal coefficients of expansion. Thermal stress is developed in a solid body wherever a volume of material is prevented from assuming the size and shape that it normally would under a change in temperature. Thermal stresses are considered as secondary stresses only.

*Free end displacement* consists of the relative motions that would occur between a fixed attachment and connected piping (or other structure) if the two members were separated and permitted to move.

*Expansion stress* is stress resulting from restraint of free end displacement.

*Integral and continuous structure* is structure that is cast or forged together or structure that is welded together with full penetration welds.

*Non-integral and continuous structure* is structure that is attached by bolting, pins or clamps or structure that bears on other structure without being attached. It includes structure that is attached by means of partial penetration or fillet welds. The ring and bolted flange in the vicinity of a bolted cover are considered non-integral and continuous structure.

The *plastic shape factor, SF,* of a structural cross-section is defined as the ratio of the plastic moment capacity of a cross-section (based on a bending stress equal to yield stress through the depth of the section) to the elastic moment capacity of the cross-section (based on a bending stress equal to initial yield stress at the extreme fiber of the section). Thus,

$$SF = \frac{M_p}{M_e} \tag{7}$$

where:

SF = Plastic Shape Factor,
$M_p$ = Plastic Moment Capacity, and
$M_e$ = Elastic Moment Capacity.

## Inelastic Analysis

Inelastic analysis success criteria are provided as an alternate to the elastic analysis success criteria. Definitions of some of the more important terms used in the statement of the inelastic analysis success criteria and an explanation of the measures that have been selected are provided below.

*Stress* is a force divided by an undeformed cross-sectional area and *strain* is a change in length divided by the corresponding original length. These normal definitions are sometimes more formally referred to as the definitions for *engineering stress*, $\sigma$, and *engineering strain*, $\varepsilon$.

For the success criteria in this paper, *ultimate strain*, $\varepsilon_u$, is the strain, expressed as an engineering strain, corresponding to the maximum stress (i.e., ultimate stress), expressed as engineering stress. It is determined from a stress-strain test specimen of the material in question. In other words, it is the strain that corresponds to the maximum value of the stress (i.e., ultimate stress) as determined from an engineering stress versus engineering strain diagram representative of the material in question.

In contrast, *true stress*, $\sigma_T$, is defined as the load (for example, in a bar) divided by the corresponding deformed cross-sectional area. It differs from the more conventional definition of stress because of the change in area due to the loading itself. In a similarly refined manner, *true*

*strain*, $\varepsilon_T$, is the integral over the length of a finite extension of each infinitesimal elongation divided by the corresponding infinitesimal length of the integration.

For the inelastic analysis success criteria in this paper:

$$\varepsilon_T = \ln (1 + \varepsilon), \text{ and} \tag{8}$$

$$\sigma_T = \sigma (1 + \varepsilon). \tag{9}$$

These relationships are assumed valid up to the material ultimate strain, $\varepsilon_u$.

It is the intent of the containment success criteria to deal with the more traditional quantities of engineering stress and engineering strain. However, it is permissible to use computed structural responses reported in terms of true stress and true strain so long as the comparison is demonstrated to be conservative.

Inelastic analysis success criteria strain limits are established as functions of the material ultimate strain. Computed equivalent plastic strains are to be compared to these limits. *Equivalent plastic strain*, $\varepsilon^P$, is a scalar term related to the inelastic strain tensor at a given location. Specifically, using tensor notation:

$$\varepsilon^P = \sqrt{\frac{2}{3} e^P_{ij} e^P_{ij}} \tag{10}$$

where repeated indices denote tensor summation, and:

$$e^P_{ij} = e_{ij} - e^E_{ij} \tag{11}$$

where:

$\varepsilon^P$ = equivalent plastic strain,

$e_{ij}$ = total tensor strain component i,j,

$e^E_{ij}$ = elastic tensor strain component i,j, and

$e^P_{ij}$ = plastic tensor strain component i,j.

*Inelastic analysis* refers to a class of structural computational methods that account for the inelastic behavior of the structural material. That is, beyond some amount of material deformation, the stress in the material is no longer directly (linearly) proportional to the strain in the material. As used inelastic analysis success criteria, inelastic analysis need not consider time dependent effects of creep.

The additional nonlinearity represented by large displacements must be included in computational algorithms when displacements are large relative to certain characteristic dimensions of the structure. However, the term *inelastic analysis* used in these success criteria does not necessarily imply large displacement analysis.

*Membrane strain*, $\epsilon_m$, is defined as average strain through the thickness of the shell or plate. Therefore:

$$\epsilon_m = \frac{1}{t} \int_{-t/2}^{+t/2} \epsilon \, dz \qquad (12)$$

where:

$\epsilon_m$ = membrane strain,
$t$ = plate or shell thickness, and
$z$ = a coordinate perpendicular to the mid-plane of the plate or shell.

The averaging should be performed on a component level and then combined to determine the equivalent average strain.

*Surface strain*, $\epsilon_s$, is defined as the value of the corresponding strain component in the plane of the shell or plate, in the inside or outside fibers of the shell or plate. Therefore:

$$\epsilon_s = \epsilon \, (z = +t/2), \quad \text{or} \qquad (13)$$

$$\epsilon_s = \epsilon \, (z = -t/2) \qquad (14)$$

where:

$\epsilon_s$ = surface strain,
$t$ = plate or shell thickness, and
$z$ = a coordinate perpendicular to the mid-plane of the plate or shell.

For normal containment design, the difference between membrane and surface strain is generally only an issue with respect to the vessel's resistance to fatigue damage. The difference is usually characterized as self-limiting and would normally be of little concern with respect to rupture of the pressure boundary due to a one time loading. The distinction is that since membrane strains are allowed to reach values far in excess of the material's yield strain in the inelastic analysis success criteria, and since surface strains may be multiples of the membrane strain, separate limits are placed on the surface strain in order to prevent the initiation of an unstable fracture due to the higher surface strains.

*Free field strain* is strain in regions of the pressure boundary where structural response is not influenced by geometric discontinuities, attachments, penetrations, or sources of concentrated loads from displacement-induced interferences. Regions of free field strain constitute the majority of the containment vessel's surface area. Free field strain also exists in major regions that are normally identified with primary membrane stresses as defined by NE-3213.6 and NE-3213.8 in Subsection NE, Section III, Division 1, of the ASME Code [6].

*Local strain* is the strain that occurs in regions of the pressure boundary that are influenced by geometric discontinuities, attachments, penetrations, or sources of concentrated loads from displacement-induced interferences with items such as piping or other structural elements. This definition of local strain applies to regions in elements of the pressure boundary that can be characterized as shells of revolution.

By definition, a local strain region may not extend along the meridian of a shell of revolution element for a distance greater than $(Rt)^{1/2}$ where R is the minimum mid-surface radius of curvature and t is the minimum thickness in the region under consideration. The definition of a local strain region does not apply to areas such as flat heads, extended lengths along meridional stiffeners, or

along the edges of rectangular openings that are parallel to the axis of revolution of the shell element.

More liberal allowable strain limits are permitted for local strain regions only as long as the region is not closer along the shell's meridian than $(R_a t_a)^{1/2}$ to another local region where free field strain limits are exceeded. The terms $R_a$ and $t_a$ are the averages of the values for the two regions under consideration. If two or more regions are closer together than $(R_a t_a)^{1/2}$, then only one of them may be classified as a local strain region with allowable strains higher than permitted for free field strains.

Although there are some subtle differences in the definitions, local strain corresponds generally with the concept of local primary membrane stress as defined by NE-3213.10 in Subsection NE, Section III, Division 1, of the ASME Code [6]. Based upon linear elastic shell theory, it is understood that local primary membrane stresses have some of the characteristics of secondary stresses and the same holds true for local strains as computed on an inelastic basis and defined in these success criteria.

*Detail strain* refers to a category of strains that may be computed by inelastic methods that utilize finite elements capable of capturing more detailed results than can be expected from thin shell or thin plate finite elements. Examples of detail strain are those strains near the connection of a flange to a nozzle, strains in fillet or partial penetration welds, and strains in the vicinity of the transition from the basic shell plate to a much thicker insert plate (e.g., at the corner of such an insert plate).

There is no analog in the ASME Code for the term *detail strain* as used in these success criteria. *Detail strain* is introduced more as a result of the analysis tools that have been developed since the ASME Code parameters were established than for a concern that it is not currently addressed by the ASME Code. Capabilities exist today that allow the designer to more accurately compute the stresses (or, in this case, the strains) in a detail of the design. If these capabilities are exercised, the designer should not be handicapped by applying criteria that do not acknowledge the increased level of confidence in the accuracy of the computed results. With the increased level of understanding of the strains, higher allowables are logically permitted by these success criteria. This is acknowledged by the introduction of the parameter referred to as *detail strain*.

*Detail strain* accounts for the strain concentration associated with geometrically discontinuous regions, such as those defined above. These strain concentrations can only be assessed from detailed finite element modeling of the discontinuity by the use of other than plate or shell type elements. That is, continuum type elements must be used in the vicinity of the discontinuity, thus providing a geometric approximation of the actual design.

Figure 1(a) shows a detail strain example for a flanged nozzle. Figure 1(b) shows an idealized model for assessing the detailed strain in the region of a discontinuity. This model would produce an estimate of the total strain concentration at the geometric discontinuity, assuming that the mesh is sufficient for the particular problem. Consideration of additional sources of strain concentrations is incorporated into the detail strain limits.

The more liberal detail strain limits are permitted for regions of the containment so long as two of the three linear dimensions that define the region are no greater than six times t, the thickness of the thinnest pressure boundary material within the region. The third linear dimension defining the region (e.g., the dimension around the circumference of a nozzle-flange juncture) need not comply with the 6t restriction. Figure 1(a) illustrates the application of the dimensional limitation to a flanged nozzle. However, more liberal strain limits are permitted for a region of detail strain only if that region is not closer than 12t to another region where the local strain limits are exceeded.

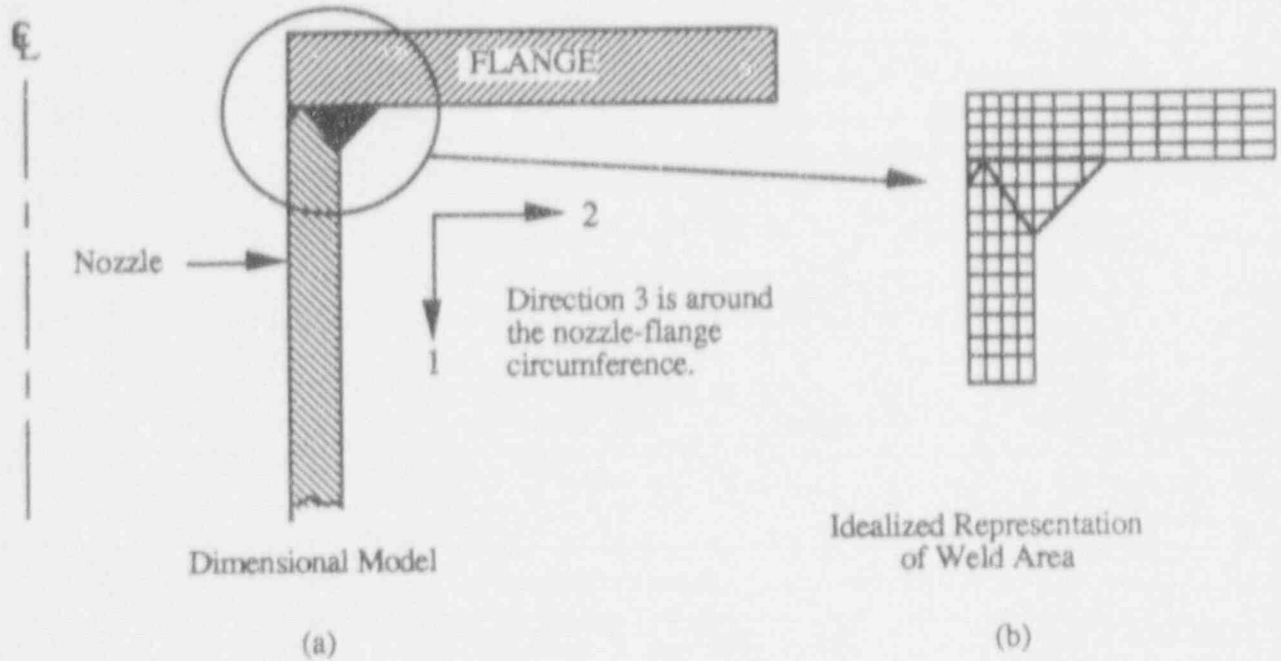


Figure 1. Detail Strain Example for Flanged Nozzle

## Buckling

*Buckling*, as used in the context of structural design and analysis, refers to a threshold of load carrying capability where branching or bifurcation into another equilibrium state is indicated. It is generally associated with membrane compressive stresses. As such, for large pressure vessels such as containments, buckling is most often associated with external pressure design loads. However, for certain geometries and in local regions, buckling can be a concern even when the overall vessel loading is dominated by internal pressure.

For thin shells of revolution, standard textbook or fundamental laboratory experiments on the subject of buckling generally focus on the topic of 'elastic instability' and the reader is left with the challenge of identifying the critical buckling mode shapes and corresponding buckling load (or stress). Under these idealized assumptions, it is possible that the compressive stresses corresponding to the buckling loads are much lower than the yield stress of the material. That is, the structure buckles within the elastic range of material response and hence the name 'elastic buckling.' Thus, it may very well be that the allowable elastic buckling stresses control the design in some regions of some vessels.

It is well understood that the values at which large as-built pressure vessels buckle are much less than the corresponding theoretical values. This is the reason that normal buckling design criteria not only apply an appropriate factor of safety to theoretical values but also require that appropriate 'correction factors' or 'knockdown factors' be applied to the theoretical values. When these factors are applied to the theoretical values, the result often is that the designer is required to work within the limits of an allowable, elastic buckling stress, i.e., buckling controls the design.

In contrast, these success criteria are intended to closely parallel actual failure thresholds. Yet, it is required that the designer account for differences between theoretical buckling values and those that are to be expected for the actual vessel material and actual as-constructed vessel geometry. These success criteria are stated in these simple terms. However, the designer is cautioned that the means

by which account is provided for the effects of geometric imperfections and nonlinearities can be controversial. A useful reference in this regard is ASME Code Case N-284 [10].

## Material Properties

Success criteria for the metallic elements of the containment vessel pressure boundary are expressed in terms of actual material properties such as the yield stress, $S_y$, and the ultimate stress, $S_u$. In order to demonstrate compliance with those elements of these success criteria that are expressed in terms of strains in the nonlinear range of material behavior, it is necessary to utilize representative material stress versus strain characterizations that extend beyond the range of linear elastic material behavior.

Success criteria measures specified in this paper are established for the materials at the corresponding service metal temperature. These success criteria do not apply for loadings that result in pressure boundary metal temperatures greater than 700°F. For temperatures equal to or less than 700°F, the effects that metal temperatures have on the material properties may be assumed to follow the same trends as provided for the corresponding properties in Appendix I, Section III, Division I, of the ASME Code [11].

The potential effects of radiation on material strength, ductility, or other material properties were not considered in the development of these success criteria and need not be considered in their application. Also, the potential effects of creep at elevated temperatures are considered insignificant up to the maximum metal temperature of 700°F allowed in these success criteria. This assumes that the elevated temperature does not continue for an extended period of time.

An estimate of actual yield stress, $S_y$, for base metal and for weld metal as a function of temperature, to be used for implementation of these success criteria, should be established by the designer. The values may be expressed as multiples (equal to or greater than 1.0) of the base metal minimum specified yield strength, at the appropriate temperatures, as provided in Table I-2.1 or Table I-2.2, Appendix I, Section III, Division 1, of the ASME Code [11]. The basis for selecting the multipliers and statistical expressions of the level of confidence associated with the selected values of the multipliers are the responsibility of the designer. When this basis is the use of historical or representative data, the values used should be subsequently qualified by comparison with actual base metal or weld metal properties.

An estimate of actual material ultimate stress, $S_u$, for base metal and for weld metal as a function of temperature, to be used for implementation of these success criteria, should be established by the designer. The values may be expressed as multiples (equal to or greater than 1.0) of the base metal minimum specified ultimate tensile strength, at the various temperatures, as specified in Table I-3.1 or Table I-3.2, Appendix I, Section III, Division 1, of the ASME Code [11]. The basis for selecting the multipliers and statistical expressions of the level of confidence associated with the selected values of the multipliers should be documented. When this basis is the use of historical or representative data, the values used should be subsequently qualified by comparison with actual base metal or weld metal properties.

If the designer elects to utilize the inelastic analysis success criteria, representative stress versus strain characterizations for base metal and weld metal that extend beyond the range of linear behavior must be established. The designer should establish such characterizations for the corresponding applicable temperatures. The basis upon which these characterizations are established and statistical expressions of the levels of confidence associated with the characterizations should be documented. When this basis is the use of historical or representative data, the values used should be subsequently qualified by comparison with actual base metal or weld metal properties.

## SUCCESS CRITERIA FOR STATIC TEMPERATURE AND PRESSURE LOADINGS

### Discussion

The following are included as static pressure and temperature loadings:

(1) The maximum value of the pressure specified for rapid pressurization.

(2) The critical combinations of pressure and temperature determined from slow pressurization/overtemperature.

A design that satisfies either the elastic analysis or inelastic analysis success criteria is considered acceptable. The determination as to which of the two sets of success criteria is utilized is at the option of the designer. Neither set of success criteria is considered to be preferable over the other.

It is acceptable to use the elastic analysis success criteria to qualify portions of the containment for a specific static pressure and temperature loading and the inelastic analysis success criteria to qualify the remainder of the containment for that loading provided that appropriate boundary conditions can be established. It is also acceptable to use different success criteria, elastic or inelastic, for separate static pressure and temperature loading conditions.

The potential for interferences resulting from deformation of the containment pressure boundary should be minimized by careful design practice. However, some displacement-induced effects are inevitable due to interactions with piping, other structures, or equipment either attached to or in close proximity to the containment. For static pressure and temperature loadings, all loads produced on the containment due to displacement-induced effects must be combined with the corresponding severe accident loadings. The resulting stresses or strains must meet the same success criteria imposed for pressure loads.

The designer should assure that accurate estimates are provided for the interactive loads from displacement-induced effects. This is particularly important when the elastic analysis success criteria are used. To the extent that interferences produce loads (possibly concentrated loads) on the pressure boundary elements (e.g., the vessel itself), those loads are considered to produce primary stresses. When resultant stresses are much greater than yield, elastically computed displacements will generally not be representative of the actual displacements that would occur under the postulated loadings.

When the elastic analysis success criteria for static pressure and temperature vessel loadings are used, the containment should be evaluated using the stresses determined from an elastic analysis. Deflections must be determined accounting for the nonlinear behavior of the material if elastically computed stresses, especially membrane stresses, are beyond the yield stress. The success criterion established to protect against failure of the containment due to buckling and the criterion for displacements must also be satisfied. Base metal and weld metal material properties should be based on actual values at temperature for each severe accident loading.

Stress measures computed in accordance with the Distortion Energy Theory should be used for comparison with the elastic analysis success criteria, except for bolting. For bolting, stress intensities computed in accordance with the Maximum Shear Stress Theory should be used.

## Elastic Analysis Stress Criteria

Elastic analysis success criteria stress measure limits for other than bolting, fillet welds, and partial penetration welds are summarized in Table 2. The primary stress measures are limited as defined below.

Table 2. Elastic Analysis Success Criteria Stress Measure Limits

| STRESS CATEGORY[1] | PRIMARY STRESS MEASURE LIMITS[2,3] (SM) | PRIMARY PLUS SECONDARY STRESS MEASURE LIMITS[2,3] (SUM) |
|---|---|---|
| GENERAL MEMBRANE | | |
| Integral and Continuous | 0.90 $S_u$ | 4.0 $S_u$ |
| Non-Integral and Continuous | 1.00 $S_y$ | 4.0 $S_u$ |
| LOCAL MEMBRANE | | |
| Integral and Continuous | 1.10 $S_u$ | 5.0 $S_u$ |
| Non-Integral and Continuous | 1.25 $S_y$ | 5.0 $S_u$ |
| GENERAL OR LOCAL MEMBRANE PLUS BENDING[4] | | |
| Integral and Continuous | 1.35 $S_u$ | 6.0 $S_u$ |
| Non-Integral and Continuous | 1.50 $S_y$ | 6.0 $S_u$ |

Notes: (1) Not applicable to bolting, fillet welds or partial penetration welds.
(2) Stress measures computed in accordance with the Distortion Energy Theory.
(3) $S_u$ is the ultimate stress of the base metal or weld metal.
(4) Primary stress measure limits for local membrane plus bending shown are based on a plastic shape factor of 1.50 for a solid rectangular cross-section.

### Primary Stress Measure Limits

The primary general membrane stress measure, $SM_m$, is derived from the average value across the thickness of a section of the general primary membrane stresses produced by pressure and other mechanical loads excluding all secondary and peak stresses. Averaging is to be applied to the stress components prior to the determination of the stress measures. The following stress measure limits apply:

(1) $SM_m$ is limited to $0.90S_u$, where $S_u$ is the ultimate stress of the base metal or weld metal, as applicable, for regions of the containment that are integral and continuous and for full penetration welds.

(2) $SM_m$ is limited to $1.00S_y$, where $S_y$ is the yield stress of the base metal, for regions of the containment that are non-integral and continuous.

The primary local membrane stress measure, $SM_l$, is derived from the average value across the thickness of a section of the local primary stresses produced by pressure and other mechanical loads excluding all secondary and peak stresses. Averaging is to be applied to the stress components prior to the determination of the stress measures. The following stress measure limits apply:

(1) $SM_l$ is limited to $1.10S_u$, where $S_u$ is the ultimate stress of the base metal or weld metal, as applicable, for regions of the containment that are integral and continuous and for full penetration welds.

(2) $SM_l$ is limited to $1.25S_y$, where $S_y$ is the yield stress of the base metal, for regions of the containment that are non-integral and continuous.

The primary general or local membrane plus bending stress measure, $SM_{lb}$, is derived from the maximum value across the thickness of a section of the general or local primary membrane stress plus maximum primary bending stress produced by pressure and other mechanical loads excluding all secondary and peak stresses. The following stress measure limits apply:

(1) $SM_{lb}$ is limited to the plastic shape factor, SF, of the structural cross-section times $0.90S_u$, where $S_u$ is the ultimate stress of the base metal or weld metal, as applicable, for regions of the containment that are integral and continuous and for full penetration welds.

(2) $SM_{lb}$ is limited to the plastic shape factor, SF, of the structural cross-section times $1.00S_y$, where $S_y$ is the yield stress of the base metal, for regions of the containment that are non-integral and continuous.

The plastic shape factor, SF, is computed on the basis of an interaction diagram of membrane versus membrane plus bending stress for a fully plastic stress distribution on a specific section. When an unsymmetric section is subject to membrane and bending stresses, the direction of the axial forces and moments must be accounted for in developing the appropriate interaction diagram. The plastic shape factor should not exceed 1.50 and can be as low as 1.00.

**Primary Plus Secondary Stress Measure Limits**

Primary plus secondary stress measures, SUM, are limited as follows. The primary plus secondary general membrane stress measure, $SUM_m$, is derived from the average value of across the thickness or depth of a section produced by the sum of all loads excluding peak stresses. Averaging is to be applied to the stress components prior to the determination of the stress measure values. The following stress measure limit applies:

$SUM_m$ is limited to $4.0S_u$, where $S_u$ is the ultimate stress of the base metal or the weld metal, as applicable. This limit applies to integral and continuous structure, full penetration welds, and non-integral and continuous structure.

The primary plus secondary local membrane stress measure, $SUM_l$, is derived from the average value across the thickness or depth of a section of the local primary and secondary stresses produced by the sum of all loads, excluding peak stresses. Averaging is to be applied to the stress components prior to the determination of the stress measure values. The following stress measure limit applies:

$SUM_l$ is limited to $5.0S_u$, where $S_u$ is the ultimate stress of the base metal or the weld metal, as applicable. This limit applies to integral and continuous structure, full penetration welds, and non-integral and continuous structure.

The primary plus secondary general or local membrane plus bending stress measure, $SUM_q$, is derived from the maximum value across the thickness or depth of a section of the membrane plus bending stresses produced by the sum of all loads, excluding peak stresses. The following stress measure limits apply:

$SUM_q$ is limited to $6.0S_u$, where $S_u$ is the ultimate stress of the base metal or the weld metal, as applicable. This limit applies to integral and continuous structure, full penetration welds, and non-integral and continuous structure.

## Bolting

Stress limits for bolting are based upon stress intensities calculated using the Maximum Shear Stress Theory. Bolting is to be evaluated for the combined effects of all credible loads. These loads include but are not limited to bolt preload, pressure-induced loads, externally applied loads, the effect of differential thermal expansion, and the effects of relative deformation between the bolted parts. All loads that produce primary and secondary stresses must be considered.

The maximum value of stress intensity computed from average stresses across the bolt cross-section and neglecting stress concentrations is limited to the yield stress of the bolt, $S_y$. The maximum value of stress intensity computed at the periphery of the bolt cross-section resulting from direct tension plus bending must not exceed the limits specified by Equation (15). Peak stresses are neglected.

$$\left(\frac{P_m}{S_y}\right)^2 + \frac{P_b}{1.7S_y} \leq 1.0 \qquad (15)$$

where: $P_m$ = membrane stress intensity in the bolt including shear and axial loads,
$P_b$ = bending stress intensity in the bolt, and
$S_y$ = yield stress of the bolt material at temperature.

Bolted flanges should be evaluated for the combined effects of mechanically induced bolt loads in combination with loads developed due to interaction between the vessel and the bolted attachment. Primary stress measures in the flange should not exceed the limits applicable to regions that are non-integral and continuous. Primary plus secondary stress measures in the flange should not exceed the limits applicable to regions that are non-integral and continuous. Interaction effects include the loads created by pressure and temperature-induced displacement as well as loads produced by the restraint of free end displacement. All loads that produce primary and secondary stresses must be considered.

## Welds

Welding electrodes should have material properties equal to or greater than the weaker of the materials being joined. Base metal and weld metal in full penetration welds must satisfy the primary stress measure and primary plus secondary stress measure limits. The average stress in fillet and partial penetration welds is computed by dividing the load per inch of the weld by the minimum effective throat dimension of the weld, $t_w$, in inches. Loads may be determined from primary plus secondary stresses obtained from the elastic containment analysis of the junction of the parts being welded, exclusive of stress concentration and peak stress effects, or directly from the analysis. The average stress in the weld is limited to $0.50S_u$, where $S_u$ is the ultimate stress of the weaker of the materials being joined.

When detailed finite element analysis of partial penetration welds is performed and stress measures are determined, the primary plus secondary membrane plus bending stress measure, $SUM_q$, exclusive of stress concentration and peak stress effects, is limited to $0.80S_u$, where $S_u$ is the ultimate stress of the weaker material being joined. This limit does not apply to fillet welds. The limits for fillet and partial penetration welds are not applicable to single sided welds.

### Buckling

The maximum buckling stress values to be used for the evaluation of instability are 1.0 times the value determined by one of the methods given below:

(1) Rigorous analysis that considers the effects of gross and local buckling, geometric imperfections, nonlinearities, large deformations and inertial forces (dynamic loads only);

(2) Classical linear analysis reduced by margins that reflect the difference between theoretical and actual load capacities; or

(3) Tests of physical models under conditions of restraint and loading the same as those to which the configuration is expected to be subjected.

### Displacements

When displacements are computed from an elastic analysis, loadings from interaction of the pressure boundary with other structure, equipment, piping, components, or other similar items should be considered in combination with the applicable loadings when computing primary and primary plus secondary stresses. The effects of containment displacement under severe accident loadings must be accounted for in the design of internal structures attached to the containment or supported by attachments to the containment.

## Inelastic Analysis Success Criteria

When qualification of the vessel pressure boundary subjected to static pressure and temperature loadings is established with results from an inelastic analysis, the strain limits for inelastic analysis success criteria must be satisfied. Criterion to protect against buckling and the limits for displacements must also be satisfied.

Strain limits, except for bolts, are limits on the equivalent plastic strain. The equivalent plastic strain at a point in the structure is a scalar quantity computed from the total strain tensor. If applicable, components of the total strain tensor may be calculated using thin plate or thin shell methods, but computation of the equivalent plastic strain must take into account the strain normal to the surface of the plate or shell.

Inelastic analysis success criteria equivalent plastic strain limits for other than bolting are summarized in Table 3 and are discussed below.

### Free Field Equivalent Plastic Strain Limits

Free field equivalent plastic strain must not exceed the limits for free field membrane and free field surface strain. Free field membrane equivalent plastic strain in base metal or full penetration welds is limited to $0.25\varepsilon_u$, where $\varepsilon_u$ is the ultimate strain in the base metal or weld metal, as applicable. Free field surface equivalent plastic strain in base metal or full penetration welds is limited to $0.40\varepsilon_u$, where $\varepsilon_u$ is the ultimate strain in the base metal or weld metal, as applicable.

### Local Equivalent Plastic Strain Limits

Local equivalent plastic strain must not exceed the limits for local membrane strain and local surface strain. Local membrane equivalent plastic strain in base metal or full penetration welds is

limited to $0.40\varepsilon_u$, where $\varepsilon_u$ is the ultimate strain in the base metal or weld metal, as applicable. Local surface equivalent plastic strain in base metal or full penetration welds is limited to $0.60\varepsilon_u$, where $\varepsilon_u$ is the ultimate strain in the base metal or weld metal, as applicable.

### Detail Equivalent Plastic Strain Limits

Detail membrane or surface equivalent plastic strain in base metal or full penetration welds is limited to $0.80\varepsilon_u$, where $\varepsilon_u$ is the ultimate strain in the base metal or weld metal, as applicable.

Table 3. Inelastic Analysis Success Criteria Equivalent Plastic Strain Limits

| STRAIN CATEGORY[1] | FREE FIELD EQUIVALENT PLASTIC STRAIN LIMITS[3] | LOCAL EQUIVALENT PLASTIC STRAIN LIMITS[3] | DETAIL EQUIVALENT PLASTIC STRAIN LIMITS[3] |
|---|---|---|---|
| MEMBRANE[2] | 0.25 $\varepsilon_u$ | 0.40 $\varepsilon_u$ | 0.80 $\varepsilon_u$ |
| SURFACE[2] | 0.40 $\varepsilon_u$ | 0.60 $\varepsilon_u$ | 0.80 $\varepsilon_u$ |
| PARTIAL PENETRATION WELDS | N/A | N/A | 0.60 $\varepsilon_u$ |
| FILLET WELDS | N/A | N/A | 0.40 $\varepsilon_u$ |

Notes: (1) Not applicable to bolting.
(2) Limits apply to base metal and weld metal in full penetration welds.
(3) $\varepsilon_u$ is the ultimate strain of the base metal or weld metal.

### Bolting

The average strain on the cross-section of a bolt is limited to the material yield stress, $S_y$, divided by the bolt material modulus of elasticity, E. That is:

$$\frac{1}{A}\int \varepsilon \, dA \leq \frac{S_y}{E} \tag{16}$$

where A is the minimum cross-sectional area of the bolt. The surface strain on a cross-section of a bolt that results from loads from all concurrent conditions is limited to $0.60\varepsilon_u$, where $\varepsilon_u$ is the material ultimate strain.

### Welds

Welding electrodes should have material properties equal to or greater than the weaker of the materials being joined. Base metal and weld metal in full penetration welds must satisfy the strain limits for free field strain, local strain, and detail strain.

When detailed finite element analysis of welds is performed consistent with the definition of detail strain, the following strain limits apply:

(1) For base metal and weld metal in full penetration welds, detail membrane and surface equivalent plastic strain is limited to $0.80\varepsilon_u$, where $\varepsilon_u$ is the ultimate strain in the base metal or weld metal, as applicable.

(2) For weld metal in partial penetration welds, detail equivalent plastic strain is limited to $0.60\varepsilon_u$, where $\varepsilon_u$ is the ultimate strain in the weld metal.

(3) For weld metal in fillet welds, detail equivalent plastic strain is limited to $0.40\varepsilon_u$, where $\varepsilon_u$ is the ultimate strain in the weld metal.

Fillet and partial penetration welds may be evaluated on the basis of allowable load. Loads on fillet and partial penetration welds may be determined from the inelastic analysis of the containment at the junction of the part being welded exclusive of peak strain effects. The average stress in fillet and partial penetration welds may be computed by dividing the load per inch of the weld by the minimum effective throat dimension of the weld, $t_w$, in inches. The average stress in the weld is limited to $0.5S_u$, where $S_u$ is the ultimate stress of the weaker of the materials being joined. The limits for fillet and partial penetration welds are not applicable to single sided welds.

### Buckling

The computed inelastic response of the containment must not exceed the response at which buckling or collapse of the containment is predicted to occur. For the application of the inelastic analysis success criteria, the predicted buckling or collapse response threshold should be based upon a rigorous analysis that considers the effects of gross and local buckling, geometric imperfections, nonlinearities, and large deformations. Inertial effects should be considered when dynamic loading is included.

### Displacements

When displacements are computed from an inelastic analysis, loadings from interaction of the pressure boundary with other structure, equipment, piping, components, or other similar items should be considered in combination with the applicable severe accident loadings when computing free field, local, and detail strains. The effects of containment displacement under severe accident loadings must be accounted for in the design of internal structures attached to the containment or supported by attachments to the containment.

## SUCCESS CRITERIA FOR DYNAMIC LOADINGS

### Discussion

Blast loadings consist of an initial airborne pressurization wave that is capable of imposing a dynamic [illegible] the containment boundary followed by a steady state pressure/temperature condition [illegible] containment. The initial airborne pressurization wave has the potential of producing a dynamic structural response of the containment. In addition, very large missiles that impact the containment can also result in dynamic structural response.

The natural vibration time characteristics of the containment (or applicable portion of the containment) must be established. Due consideration should be given to the effects that all loadings, including those that may have produced prestress (e.g., pre-blast pressure), may have on the structural vibration characteristics. The results of such evaluations are then compared with the time characteristics of dynamic loading transients and a determination made as to the level of detailed dynamic [illegible]ory analysis required to determine an accurate estimate of the true

structural response to the loading. An accurate estimate of the structural response to the dynamic loading must be used when implementing the dynamic response success criteria.

Material properties may be enhanced due to the effects of high strain rates associated with dynamic loadings. When enhanced properties are used, adequate justification should be provided.

The potential for interferences resulting from deformation of the containment pressure boundary should be minimized by careful design practice. However, some displacement-induced effects are inevitable due to interactions with piping, other structures, or equipment either attached to or in close proximity to the containment. For displacement loadings, all loads produced on the containment due to displacement-induced effects must be combined with the corresponding severe accident loadings. The resulting stresses or strains must meet the same success criteria imposed for pressure loads.

The designer should assure that accurate estimates are provided for the interactive loads from displacement-induced effects. This is particularly important when the elastic analysis success criteria are used. When resultant stresses are much greater than yield, elastically computed displacements will generally not be representative of the actual displacements that would occur under the postulated loadings.

### Dynamic Response Success Criteria

An estimate of the response of the containment, or portions of the containment, should first be established. If the response is estimated with elastic analysis methods, the requirements of the elastic dynamic response success criteria apply. If the response is estimated with inelastic analysis methods, the requirements the inelastic dynamic response success criteria apply.

For the elastic dynamic response success criteria, all requirements of the elastic analysis success criteria previously defined must be satisfied for the corresponding structural elements when dynamic loading responses are evaluated using elastic analysis methods.

For the inelastic dynamic response success criteria, all requirements of the inelastic analysis success criteria previously defined must be satisfied for the corresponding structural elements when dynamic loading responses are evaluated using inelastic analysis methods.

## SUCCESS CRITERIA FOR MISSILES

The containment pressure boundary must be shown to be capable of resisting perforation from missiles. The energy developed by the missile must be less than the energy required to perforate the containment. The effects of the missile on the containment are primarily local damage and are evaluated utilizing an empirical energy balance method. The technique for evaluating the containment boundary under missile impact consists of two parts:

(1) Determination of the energy acquired by the missile in its trajectory to the containment boundary, and

(2) Determination of the missile energy required to perforate the containment.

The adequacy of the containment is based on demonstrating the ability of the containment to resist perforation from missiles utilizing an energy balance method. Three empirical equations are used to assure resistance of the containment to missile perforation:

(1) Stanford Research Institute (SRI) Equation [12],

(2) Ballistics Research Laboratory (BRL) Equation [13], and

(3) Hershey Equation [14].

Any one these equations may be used to determine whether or not a missile of given diameter, mass, and velocity will perforate the containment. However, since the equations are based upon different parameters and tests, the equation that defines the most limiting missile diameter, mass, and velocity for any given missile threat should be used to establish acceptability of the containment for missile perforation.

The missiles success criterion is suitable for demonstrating the capacity of the containment to resist missile perforation by (1) direct impact from a primary missile, (2) indirect impact from a primary missile through reflection, or (3) impact from secondary missiles caused by impact from a primary missile. The direction of all missiles is considered to be perpendicular (normal) to the containment.

The perforation equations in this paper are limited to missiles of 20,000 lbs. or less. Extremely large missiles that do not meet the range of applicability of the empirical equations should be treated as dynamic loads on the containment.

The SRI Equation [12] is:

$$\frac{E_K}{D} = \frac{S_u}{46{,}500}\left(16{,}000\ T^2 + 1{,}500\ \frac{W_1}{W_s}\ T\right) \tag{17}$$

where:
$E_K$ = $\frac{1}{2}MV^2$ = Critical kinetic energy required for perforation (ft-lb),
$M$ = Missile mass (lb-sec$^2$/ft),
$V$ = Missile velocity at impact (ft/sec),
$D$ = Missile diameter (in.),
$S_u$ = Ultimate tensile strength of the target plate (lb/in.$^2$),
$T$ = Target plate thickness (in.),
$W_l$ = Length of a square side between rigid supports (in.), and
$W_s$ = Length of a standard width (4 in.).

The SRI Equation is applicable only within the following ranges of parameters and should not be used beyond the specified limits.

$$0.1 < T/D < 0.8,$$
$$0.002 < T/L < 0.05,$$
$$10 < L/D < 50,$$
$$5 < W_l/D < 8,$$
$$8 < W_l/T < 100,$$
$$70 < V < 400,$$

where: $L$ = Missile Length (in.).

The BRL Equation [13] is also empirically derived. It solves for the target plate thickness, T, at the threshold of perforation as a function of impact energy.

$$T^{3/2} = \frac{0.5MV^2}{17{,}400(K_B)^2D^{3/2}} \tag{18}$$

where:
- $T$ = Shell plate thickness (in.),
- $M$ = Missile mass (lb-sec$^2$/ft),
- $V$ = Missile velocity at impact (ft/sec),
- $K_B$ = Constant depending on the grade of steel (usually approximately 1.0), and
- $D$ = Missile diameter (in.).

The Hershey Equation [14] is based upon the fragments associated with a 50% probability to achieve perforation.

$$V_{50} = K_H D \sqrt{\frac{T}{W}} \tag{19}$$

where:
- $V_{50}$ = Missile velocity associated with 50% probability (ft/sec),
- $K_H$ = Empirical coefficient
- $D$ = Projectile diameter (ft),
- $T$ = Plate thickness (ft), and
- $W$ = Weight of projectile (lb).

The parameter, $K_H$ in the Hershey Equation is an empirically derived coefficient. This parameter varies with ratios of T/D; plate thickness to missile diameter. It is valid only for perpendicular strikes on steel targets. A linear approximation for $K_H$ is applies for ratios of $T/D \leq 0.35$. For $T/D > 0.35$, an exponential approximation may be used.

The coefficient $K_H$ may be determined from Equations (20) and (21):

$$K_H = 70{,}000\ (T/D) + 16{,}800 \qquad (\text{for } T/D \leq 0.35) \tag{20}$$

$$K_H = 48{,}586\ (T/D)^{0.1502} \qquad (\text{for } T/D > 0.35). \tag{21}$$

Figure 2 shows a comparison of the SRI, BRL and Hershey Equations. The plots of missile velocity versus plate thickness for perforation of plate thicknesses up to 2 inches are based upon the following parameters:

- $S_u$ = 80,000 lb/in$^2$ (minimum specified),
- $K_B$ = 1.0, and
- $K_H$ - Varies as a ratio of T/D.

The material ultimate stress, $S_u$, is used only for the Stanford Research Institute Equation The Hershey Equation was developed for material with an ultimate stress of 115,000 psi. However, it can be reasoned that the equation may be used for steels such as ASME SA-537, Cl. 2 [5] with a minimum ulumate tensile strength of 80,000 psi.

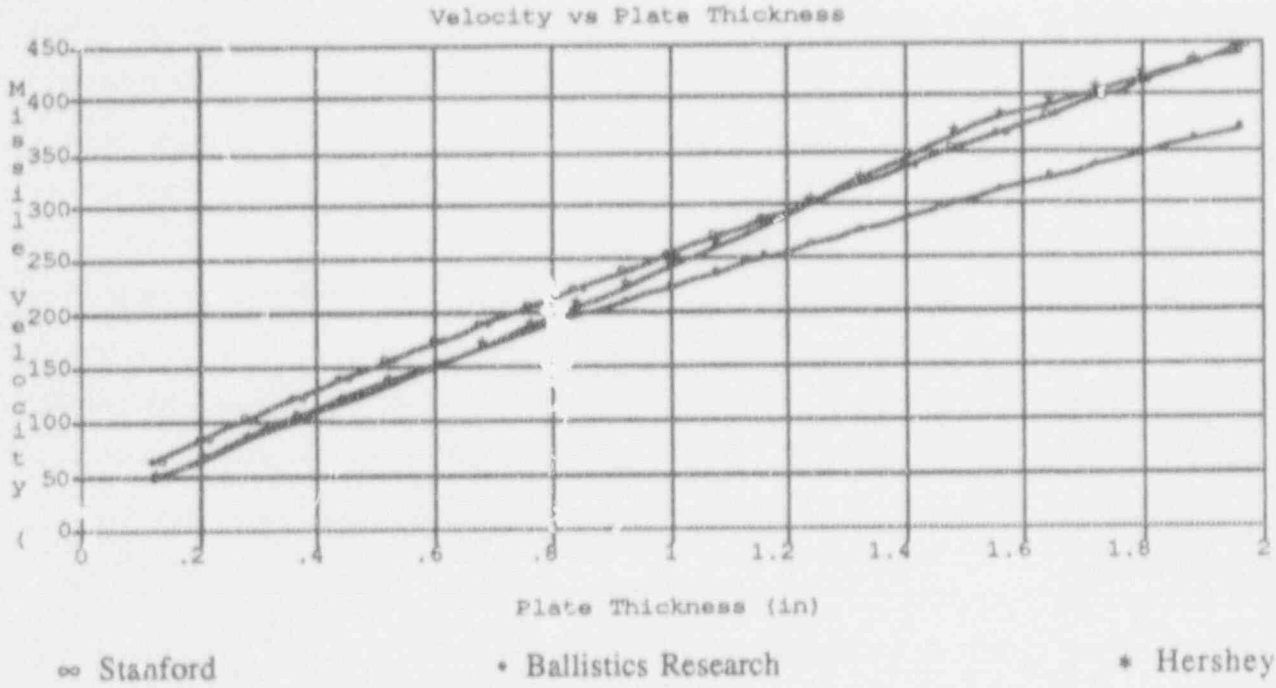


Note: W = 200 lb; D = 4.2[illegible]; A = 0.10 $ft^2$; Velocity in ft/sec.

Figure 2. Comparison of Perforation Equations

## SUMMARY

This paper provides a generic approach for containment success criteria under severe accident loads. The success criteria may be used to establish the threshold of failure for containments when subjected to severe accident loads resulting from rapid pressurization, slow pressurization/ overtemperature, blast, and missiles.

The success criteria are based upon the Deterministic Severe Accident Criteria (DSACs) proposed by the U.S. Department of Energy to guide the design of the NPR-HWR containment for resistance to severe accidents. The DSAC concept provides for a generic approach for success criteria to predict the threshold of containment failure under severe accident loads. The success criteria specify acceptable containment response measures and limits for each problem statement.

The main elements of these success criteria are expressed in terms of elastic stresses and inelastic strains. Containment performance is based on the "best estimate" of failure as predicted by either stress or strain, buckling, displacements, or ability to withstand missile perforation. Since these limits are "best estimates" of failure, no conservatism exists in these success criteria. Rather, conservatism is to be provided in the problem statements, i.e., the quantified severe accident loads. These success criteria are presented on a multi-tiered basis for static pressure and temperature loadings, dynamic loadings, and missiles. Within the static pressure and temperature loadings, the criteria are separated into elastic analysis success criteria and inelastic analysis success criteria. Each of these areas, in turn, defines limits for either the stress or strain measures as well as measures for buckling and displacements.

Failure of a containment under these loadings is defined as the threshold at which the containment no longer retains its structural or leak-tight integrity. The margins of safety or conservatism are included in quantification of the severe accident loadings and not in the containment success criteria. Consequently, the success criteria in this paper do not include any margins of safety or conservatism on the best estimate of the actual threshold of containment failure under the prescribed severe accident loadings.

## Acknowledgements

This paper is based upon work performed under Contract No. 78-5066 for Sandia National Laboratories, Albuquerque, New Mexico, operated by Sandia Corporation for the United States Department of Energy, for the Office of Heavy Water Reactor, Department of Energy, Washington, DC. Dr. Emile A. Bernard was the Sandia Project Monitor. Technical assistance was provided by Daniel S. Horschel and Dr. Robert A. Watson of Sandia National Laboratories.

The authors acknowledge the substantial technical assistance provided by the following members of the engineering staff at the Electric Boat Division of General Dynamics Corporation, Groton, Connecticut in the development of the criteria defined in this paper: Lawrence Lipkin, John A.S. Rodolico and Edward A. Rodriguez, Nuclear Engineering Analysis; David C. Church, Stephen F. Gordon, and Gerald P. Mulligan, Applied Mechanics; and Donald F. Jordan, Welding and Metallurgy.

## References

1. P.T. Rhoads, "Deterministic Severe Accident Criteria (DSACs) as Severe Accident Design Criteria and Policy for the New Production Reactor," Proceedings of the Fifth Workshop on Containment Integrity, Washington, DC, May 1992

2. K.D. Bergeron, S.E. Slezak, and C.E. Leach, "Proposed Deterministic Severe Accident Criteria for the Heavy Water New Production Reactor," Proceedings of the Fifth Workshop on Containment Integrity, Washington, DC, May 1992

3. R.F. Sammataro, W.R. Solonick, and N.W. Edwards, "HW-NPR Containment DSAC Success Criteria," NPRW-DSAC91-4, Sandia National Laboratories, To be published

4. ASME Boiler and Pressure Vessel Code, Section III, Division 1, "Rules for Construction of Nuclear Power Plant Components," American Society of Mechanical Engineers, New York, NY, 1989 Edition with 1990 Addenda

5. ASME Boiler and Pressure Vessel Code, Section II, Part A, "Material Specifications--Ferrous Materials," American Society of Mechanical Engineers, New York, NY, 1989 Edition with 1990 Addenda

6. ASME Boiler and Pressure Vessel Code, Section III, Division 1, Subsection NE, "Class MC Components," American Society of Mechanical Engineers, New York, NY, 1989 Edition with 1990 Addenda

7. J.E. Shigley and L.D. Mitchell, Mechanical Engineering Design, Fourth Edition, McGraw-Hill Book Company, New York, NY, 1983

8. G.J. Bohm and J.D. Stevenson, "External Loads and Their Evaluation with ASME Boiler and Pressure Vessel Code Limits," Pressure Vessels and Piping: Design Technology-1982-A Decade of Progress, Pressure Vessels and Piping Division, American Society of Mechanical Engineers, 1982

9. ASME Boiler and Pressure Vessel Code, Section III, Division 1, Appendix F, "Rules for Evaluation of Service Loadings With Level D Service Limits," American Society of Mechanical Engineers, New York, NY, 1989 Edition with 1990 Addenda

10. ASME Boiler and Pressure Vessel Code, Nuclear Code Case N-284, "Metal Containment Shell Buckling Design Methods, Section III, Division 1, Class MC," American Society of Mechanical Engineers, New York, NY, Approval Date: August 25, 1980

11. ASME Boiler and Pressure Vessel Code, Section III, Division 1, Appendix I, "Design Stress Intensity Values, Allowable Stresses, Material Properties, and Design Fatigue Curves," American Society of Mechanical Engineers, New York, NY, 1989 Edition with 1990 Addenda

12. R.W. White and N.B. Botsford, "Containment of Fragments from a Runaway Reactor," Report No. SRIA-113, Stanford Research Institute, Stanford, CA, September 1963

13. C.R. Russel, Reactor Safeguards, MacMillan, New York, 1962

14. V.A. Hershey, "The Construction of Plate Penetration Charts or Tables," NPG Report No. 1120, U.S. Naval Proving Grounds, Dahlgren, VA, May 1955

# SESSION 2

# ADVANCED CONTAINMENT DESIGNS AND RELATED RESEARCH

# ALWR UTILITY REQUIREMENTS DOCUMENT CONTAINMENT PERFORMANCE REQUIREMENTS

David E. Leaver
TENERA, L.P.

Stephen L. Additon
TENERA, L.P.

## Abstract

U.S. utilities, with substantial support from international utilities, are leading the industry-wide Advanced Light Water Reactor (ALWR) Program. This program is establishing a technical foundation for the next generation of LWRs through development of a comprehensive set of design requirements for the ALWR in the form of a Utility Requirements Document (URD).

The approach in the URD for severe accidents involved two main efforts: (1) accident prevention through intrinsic design characteristics to avoid accident initiation and reliable, engineered safety systems to prevent core damage, and (2) accident mitigation and containment performance. The purpose of this paper is to describe the URD containment performance requirements for severe accidents.

For containment performance, a comprehensive set of severe accident containment challenges was defined and a matrix of design features and operating characteristics specified to address the challenges. Also, the URD requires evaluation of containment response to severe accidents.

Twenty-three severe accident containment challenges were identified and a preliminary evaluation of the URD indicated that requirements are adequate for addressing each of the challenges. Further, best estimate severe accident evaluations for the ALWR containment indicate that margin exists to ASME Service Level C limits and thus containment leakage during severe accidents should be minimal. An updated accident source term was also developed by the ALWR Program to provide an improved design basis for fission product mitigation system design.

The key conclusions from this effort are as follows:

- Severe accident challenges are being systematically and explicitly addressed in the design.
- Margin exists between the loads resulting from severe accidents and the Service Level C limits.
- For a realistic source term expected to bound that from any credible severe accident sequence, the site boundary dose is less than 0.5 rem.

## INTRODUCTION

U.S. utilities, with substantial support from international utilities, are leading the industry-wide Advanced Light Water Reactor (ALWR) Program. This program, under the management of the Electric Power Research Institute, is establishing a technical foundation for the next generation of light water reactors through development of a comprehensive set of design requirements for the ALWR in the form of a Utility Requirements Document (URD). The URD defines the technical basis for improved and standardized future LWR designs; both evolutionary and passive plant designs are covered [1, 2]. The passive plant designs include more innovations in containment design [represent the most advanced LWR technology] and are the subject of this paper.

The passive plant designers, Westinghouse and General Electric, are working on designs for certification under 10CFR52[3]. Both Westinghouse and General Electric have been active participants in the URD development process and intend that their respective plant designs fully comply with the URD.

Two specific passive plant concepts are included in the URD: the passive BWR with pressure suppression containment and the passive PWR with large, dry containment. These plants employ passive safety systems for core and containment cooling, relying on phenomena such as natural circulation, gravity drain, and accumulators. These passive concepts meet the ALWR Program safety standards which reflect criteria being established by the NRC for advanced reactor designs as well as utility requirements for operational and safety improvements achieved through design simplification, refinement, and reliability assurance.

The ALWR safety policy is that there will be excellence in safety both to protect the general public and to assure personnel safety and plant investment protection. There is significant emphasis on avoiding accidents since this is considered the best way to achieve plant owner investment protection and also to achieve improved overall safety. Significant emphasis is also placed on mitigation of the consequences of potential accidents, including severe accidents, so that a balanced approach to safety is achieved.

This policy of excellence in safety is implemented through an integrated design approach to safety which includes three overlapping levels of safety protection, i.e., accident resistance, core damage prevention, and mitigation. The approach utilizes a deterministic analysis framework and design feature specification, supplemented by probabilistic risk assessment (PRA). These levels of safety protection incorporate the philosophy of defense-in-depth. Figure 1 illustrates the three defense-in-depth levels. This paper will focus on the mitigation aspect of the Passive ALWR, specifically, the assurance of containment performance for severe accident challenges.

## ALWR APPROACH TO CONTAINMENT PERFORMANCE

The ALWR Program has long recognized the critical nature of the containment issue for severe accident mitigation and has undertaken an ambitious effort to resolve this issue. This effort is directed at utilizing the substantial body of severe accident and containment

**Accident Resistant Designs**
(simplicity, design margin, other
intrinsic characteristics to minimize
frequency and severity of initiating events)

**Core Damage Prevention**
(engineered systems and features
which prevent initiating events from
progressing to core damage)

**Mitigation**
(systems to contain fission products released
from core damage and facilitate severe
accident management)

Figure 1. ALWR Defense-In-Depth

performance information developed since the TMI-2 accident to support more explicit consideration of severe accidents in the design process. The framework for this more explicit consideration is an ALWR design basis comprising two distinct parts as shown on Figure 2. One, the Licensing Design Basis (LDB), is the set of ALWR design features and analyses necessary to satisfy NRC licensing requirements, including LDB transients and accidents, in the Code of Federal Regulations and associated regulatory guidance. The second, the ALWR Safety Margin Basis (SMB), contains requirements which provide margin beyond the LDB. The SMB provides a means of incorporating severe accident features and realistic, best estimate evaluations in the plant design while maintaining a distinction between these features and evaluations and the LDB.

This distinction between the LDB and SMB is being maintained in part since severe accidents involve extremely complex phenomena for which detailed, verified design basis methods are not available in the same sense as for LDB transients and accidents. On the other hand, as a result of broad international research and development support, a substantial amount is now known about severe accidents which is sufficient to allow addressing them in plant design. This has lead to the ALWR SMB approach, i.e., more explicit consideration of severe accidents in the design process including specification of plant features and best estimate, confirmatory severe accidents evaluations. This SMB treatment of severe accidents (vs. an LDB treatment) is justified based on the margin which exists in the LDB design, the features provided which reduce the uncertainty associated with severe accident phenomena, and the extremely low likelihood of core damage in the first place in a Passive ALWR.

## URD PROVISIONS FOR SEVERE ACCIDENT CHALLENGES

As discussed above, the ALWR SMB considers accidents which go beyond the traditional licensing events. To address these severe accident challenges, the ALWR URD containment performance provisions consist of a set of deterministic requirements with PRA used in a confirmatory manner. The deterministic requirements are as follows:

- Provide a matrix of design features and plant operating characteristics which address a comprehensive set of severe accident containment challenges.

- Evaluate containment response for loads due to peak LOCA plus pressure from hydrogen generation (and burning if not inerted) and show that ASME Service Level C limits are not exceeded. Service Level C limits are selected based on 10CFR50.34(f) requirements together with the fact that low containment leak rate should be maintained if loads do not cause stress to exceed Service Level C limits.

- Evaluate containment response for loads from probabilistically important severe accident types and show that ASME Service Level C limits are not exceeded. URD evaluations indicate that the only such sequence type would be a low pressure core melt into an intact containment with containment systems functioning as designed.

| | Licensing Design Basis (LDB)[1] | | Safety Margin Basis (SMB)[2] | |
|---|---|---|---|---|
| | Event | Applicable Limit | Event | Applicable Limit |
| Containment Load | LOCA | Service Level A | LOCA plus Hydrogen (75%) with global burn | Service Level C |
| | LOCA plus Hydrogen (100%) with Control System | Service Level C | Loads from Important Severe Accidents | Load from LOCA plus Hydrogen (or Service Level C) |
| Source Term | Physically Based | Part 100 | Physically Based | PAGs |
| | | | Source Terms from Important Severe Accidents | Release from Physically Based (or PAGs) |

Notes:
1. LDB evaluation methodology uses conservative, established design methods and credit for safety grade systems (and selected nonsafety grade systems).
2. SMB evaluation methodology uses best estimate methods and credit for safety grade and nonsafety grade systems.

**Figure 2. ALWR Mitigation**
**Licensing Design Basis vs. Safety Margin Basis**

- Determine containment ultimate capacity and identify the associated failure mode on pressurization of the containment to its ultimate capacity.

The PRA requirement is to confirm that there are no probabilistically important accident sequence types, other than the low pressure core melt described above. Also, the URD specifies guidance for the use of PRA to demonstrate a $10^{-5}$ core damage frequency goal and an offsite release limit of 25 rem for cumulative frequency greater than $10^{-6}$ per year.

Each of the above requirements is further discussed below.

Matrix of Design Features

To provide confidence that ALWR containment performance is complete, a comprehensive list of severe accident challenges were considered based upon past PRAs, operating experience, and the large body of worldwide severe accident research [4,5,6,7,8,9,10]. Unique aspects of the ALWR were also considered. As a check, a comparison with the containment challenges identified in a recent Advisory Committee on Reactor Safeguards (ACRS) letter [11] was made. All of the challenges in the ACRS letter were addressed.

Table 1 lists the challenges. The upper half covers those challenges not directly related to severe accidents, i.e., challenges which precede or are coincident with core damage, are postulated to occur independent of core damage, or are traditionally evaluated apart from severe accident considerations. The lower half covers those challenges which could potentially result from the effects of a core damage accident. For each challenge, a set of design requirements (e.g., plant features, operating characteristics, evaluations) has been specified to either preclude the challenge or to accommodate those which are considered credible. The basis for resolving each challenge is discussed in detail in Reference 12.

Tables 2 and 2a summarize plant features which address the challenges including interfacing system LOCA, steam generator tube rupture, high pressure melt ejection, hydrogen combustion, core debris coolability, and decay heat generation. The list of challenges and associated requirements is preliminary and is under discussion with NRC, and will be updated as additional information becomes available.

Loads From LOCA Plus Hydrogen

This requirement specifies that the containment system pressure boundary satisfies the intended minimum requirements of 10CFR50.34(f)(3)(v) when subjected to the pressure and temperature loads associated with a LOCA combined with 75% of the active cladding oxidation, accompanied by hydrogen burning (if not precluded by inerting) and combined with the appropriate dead loads. The structural criteria are selected so that any gross distortions and subsequent large strains in pressure boundary material due to potential shell buckling modes are precluded.

Table 1. List of Severe Accident Challenges

| | Challenges/Failure Modes that are Independent of or Coincident With a Severe Accident |
|---|---|
| 1. | Containment Isolation |
| 2. | Interfacing System Loss of Coolant Accident (LOCA) |
| 3. | Blowdown Forces |
| 4. | Pipe Whip and Steam Jet Impingement |
| 5. | Steam Generator Tube Rupture (PWR) |
| 6. | Anticipated Transient Without Scram |
| 7. | Suppression Pool Bypass (BWR) |
| 8. | Catastrophic Reactor Pressure Vessel Failure |
| 9. | Internal Vacuum |
| 10. | Internal (Plant) Missiles |
| 11. | Tornado and Tornado Missiles |
| 12. | Man-Made Site Proximity Hazards |
| 13. | Seismic |
| | **Challenges/Failure Modes Potentially Resulting From a Severe Accident** |
| 14. | High Pressure Melt Ejection |
| 15. | Hydrogen Detonation/Deflagration |
| 16. | In-vessel Debris-Water Interaction |
| 17. | Ex-vessel Debris-Water Interaction |
| 18. | Noncondensable Gas Generation During Core-Concrete Interaction |
| 19. | Reactor Pressure Vessel Support Degradation or Containment Basemat Erosion During Core-Concrete Interaction |
| 20. | Core Debris in Containment Sump |
| 21. | Core Debris Contact with Containment Shell Liner |
| 22. | Decay Heat Generation |
| 23. | Steam Generator Tube Rupture from Natural Circulation of Hot Gases (PWR) |

Table 2*

## SUMMARY OF REQUIREMENTS TO ADDRESS CONTAINMENT CHALLENGES THAT ARE INDEPENDENT OF OR COINCIDENT WITH CORE DAMAGE

| CHALLENGE | AFFECTED SAFETY FUNCTION | PLANT TYPE | ALWR BASIS# | KEY PASSIVE ALWR REQUIREMENTS: LIMIT POTENTIAL FOR CHALLENGE* | KEY PASSIVE ALWR REQUIREMENTS: ACCOMMODATE CHALLENGES* |
|---|---|---|---|---|---|
| 1. Containment Isolation | Isolation | PWR/BWR | 2 | A Reduced fluid line penetrations. Isolation provisions and leakage rate testing per standards. Valves capable of closure with possible flow and full containment pressure. Control room position indication for automatic and remote manual valves.<br>A Manual valve configuration permits locking only in closed position.<br>A Closed systems penetrating containment evaluated for ex-vessel severe accidents. Fail closed or DC powered isolation valves.<br>A Capability for periodic gross check of containment integrity. | P Passive Residual Heat Removal minimizes core damage risk given isolation failure (with RHR on-line even without DC power). |
| 2. Interfacing System LOCA | Bypass | PWR/BWR | 2 | A Reduced interfaces between the Reactor Coolant System (RCS) and low pressure systems.<br>A High to low pressure interfaces provided with isolation valves leak testing capability, isolation valve position indicator in control room, and high pressure alarm. Interlocks prevent isolation valve opening when RCS pressure exceeds RSDC system design pressure (PWR).<br>A RSDC designed for full reactor pressure (BWR). Double isolation. | Pressure Relief<br>A Design pressure such that full RCS pressure is below rupture pressure and no leaks will occur which exceed RCS makeup capacity. |

# The acceptability of ALWR requirements to address containment challenges was based on the following criteria:
1. Current LWR resistance to challenge acceptable for ALWR.
2. Sufficient ALWR design features added to increase resistance to challenge by reducing the severity and/or ensuring containment.

* Passive plant design features which exceed requirements for current LWRs are identified with A (common to all ALWRs) or P (passive ALWRs only).

* NOTE: Reproduced from Reference 12.

Table 2* (continued)

## SUMMARY OF REQUIREMENTS TO ADDRESS CONTAINMENT CHALLENGES THAT ARE INDEPENDENT OF OR COINCIDENT WITH CORE DAMAGE

| CHALLENGE | AFFECTED SAFETY FUNCTION | PLANT TYPE | ALWR BASIS# | KEY PASSIVE ALWR REQUIREMENTS | |
|---|---|---|---|---|---|
| | | | | LIMIT POTENTIAL FOR CHALLENGE* | ACCOMMODATE CHALLENGES* |
| 3. Blowdown Forces | Containment Pressure Control | PWR/BWR | 1 | Design and ISI in accordance with ASME BPV Code.<br>Leak Before Break. | Design containment for double-ended guillotine break of largest pipe. |
| 4. Pipe Whip and Jet Impingement | Bypass | PWR/BWR | 1 | Design and ISI in accordance with ASME BPV Code.<br>Leak Before Break.<br>Use of only proven materials and fabrication processes.<br>Use of EPRI water chemistry guidelines. | Protection from jet/pipe whip where leak before break is not demonstrated. |
| 5. Steam Generator Tube Rupture | Bypass | PWR | 2 | Improved water chemistry.<br>Proven materials.<br>A Mechanical design of tubes, tube supports, and tube sheets reduce likelihood of SGTR.<br>A Improved design features facilitate SG cleaning and replacement. | P Operator actions can terminate leakage prior to ADS actuation for design basis leak.<br>P Automatic Depressurization System (ADS) operation terminates tube leakage automatically.<br>P Passive RHR plus additional features prevent secondary side relief following SGTR. |
| 6. ATWS | Reactivity Control | BWR | 2 | A Diverse Reactor Protection System (RPS).<br>A Diverse means of rod insertion. | Standby Liquid Control (SLC).<br>A Checkerboard pattern of scram group rods maximizes group worth. |
| | | PWR | 2 | A Diverse RPS (or capability to ride out ATWS). | Borated Safety Injection (SI).<br>A Negative moderator temperature coefficient over entire fuel cycle improves ATWS response. |

# The acceptability of ALWR requirements to address containment challenges was based on the following criteria:
1. Current LWR resistance to challenge acceptable for ALWR.
2. Sufficient ALWR design features added to increase resistance to challenge by reducing the severity and/or ensuring containment.

* Passive plant design features which exceed requirements for current LWRs are identified with A (common to all ALWRs) or P (passive ALWRs only).

* NOTE: Reproduced from Reference 12.

Table 2* (continued)

## SUMMARY OF REQUIREMENTS TO ADDRESS CONTAINMENT CHALLENGES THAT ARE INDEPENDENT OF OR COINCIDENT WITH CORE DAMAGE

| CHALLENGE | AFFECTED SAFETY FUNCTION | PLANT TYPE | ALWR BASIS# | KEY PASSIVE ALWR REQUIREMENTS: LIMIT POTENTIAL FOR CHALLENGE* | KEY PASSIVE ALWR REQUIREMENTS: ACCOMMODATE CHALLENGES* |
|---|---|---|---|---|---|
| 7. Suppression Pool Bypass | Containment Pressure Control | BWR | 2 | Vacuum Breakers: potential loads accounted for, position indication, minimal leakage.<br>P No high energy lines in wetwell airspace. | ADS use of SRVs which discharge to suppression pool and thus ensure vapor suppression despite leakage.<br>P Passive RHR (including PCCS). |
| 8. Catastrophic RPV Failure | Internal Containment Loading | PWR/BWR | 2 | A $RT_{NDT} \leq 10^{\circ}F$; initial $RT_{NDT} \leq -20^{\circ}F$ for PWR core beltline; low fluence at vessel wall.<br>A No welds in beltline region.<br>A Relief valves prevent overpressure, backed up by depressurization system and low-head injection.<br>Design in accordance with ASME code.<br>Design features to avoid relief valve opening for expected plant transients. | |
| 9. Internal Vacuum | Containment Pressure Control | PWR/BWR | 1 | | Vacuum Breakers.<br>Design for external pressure loads. |
| 10. Internal (Plant) Missiles | External Containment Loading | PWR/BWR | 2 | Turbine overspeed protection.<br>A Improved turbine integrity/one-piece rotors. | Turbine orientation avoids missile contact with containment.<br>Missile protection for any safety related components in missile path (SRP 3.5.1.3). |
| 11. Tornado and Tornado Missiles | External Containment Loading | PWR/BWR | 2 | Conformance with ANSI 2.12 and ANSI 51.5. | P Passive core cooling systems located within containment. |

# The acceptability of ALWR requirements to address containment challenges was based on the following criteria:
1. Current LWR resistance to challenge acceptable for ALWR.
2. Sufficient ALWR design features added to increase resistance to challenge by reducing the severity and/or ensuring containment.

* Passive plant design features which exceed requirements for current LWRs are identified with A (common to all ALWRs) or P (passive ALWRs only).

* NOTE: Reproduced from Reference 12.

Table 2* (continued)

## SUMMARY OF REQUIREMENTS TO ADDRESS CONTAINMENT CHALLENGES THAT ARE INDEPENDENT OF OR COINCIDENT WITH CORE DAMAGE

| CHALLENGE | AFFECTED SAFETY FUNCTION | PLANT TYPE | ALWR BASIS# | KEY PASSIVE ALWR REQUIREMENTS: LIMIT POTENTIAL FOR CHALLENGE* | KEY PASSIVE ALWR REQUIREMENTS: ACCOMMODATE CHALLENGES* |
|---|---|---|---|---|---|
| 12. Man-Made Site Proximity Hazards | External Containment Loading | PWR/BWR | 2 | Conformance with ANSI 2.12. | P Passive core cooling systems located within containment. |
| 13. Seismic | External Containment Loading | PWR/BWR | 2 | Siting requirements exclude the most vulnerable sites. | A SSE at 0.3g.<br>A Evaluation at > SSE with PRA or margins assessment as part of design process.<br>A Address vulnerabilities from past experiences, e.g., provide common basemat. |



# The acceptability of ALWR requirements to address containment challenges was based on the following criteria:
1. Current LWR resistance to challenge acceptable for ALWR.
2. Sufficient ALWR design features added to increase resistance to challenge by reducing the severity and/or ensuring containment.

* Passive plant design features which exceed requirements for current LWRs are identified with A (common to all ALWRs) or P (passive ALWRs only).

* NOTE: Reproduced from Reference 12.

Table 2a*

## SUMMARY OF REQUIREMENTS TO ADDRESS CONTAINMENT CHALLENGES RESULTING FROM CORE DAMAGE

| CHALLENGE | AFFECTED SAFETY FUNCTION | PLANT TYPE | ALWR BASIS# | KEY PASSIVE ALWR REQUIREMENTS: LIMIT POTENTIAL FOR CHALLENGE* | KEY PASSIVE ALWR REQUIREMENTS: ACCOMMODATE CHALLENGES* |
|---|---|---|---|---|---|
| 14. High Pressure Melt Ejection (HPME) | Reactor Pressure Control | BWR | 2 | P Diverse depressurization systems.<br>P Passive RHR can aid depressurization. | Suppression pool cools heated gases. Inerted containment (no combustion heat addition). |
| | | PWR | ? | P Diverse depressurization systems.<br>P Passive RHR can aid depressurization. | A Cavity configuration to limit transport of fragmented core debris. |
| 15. Hydrogen Generation to Detontable Limits | Combustible Gas Control | BWR | 1 | Inerted. | A Evaluation required if local detonation is possible. |
| | | PWR | 2 | A Limit $H_2$ generation with design features, such as ADS and cavity flooding<br>A Hydrogen control system (e.g., non-safety related igniters) designed to keep hydrogen concentration below 10% for 100% active clad equivalent reaction.<br>A Containment size prevents global detonable $H_2$ concentration (< 13%) for generation up to 75% active clad equivalent reaction.<br>A Design ensures convective mixing and minimizes DDT-prone geometry. | A Evaluation required if local detonation is possible. |

# The acceptability of ALWR requirements to address containment challenges was based on the following criteria:
1. Current LWR resistance to challenge acceptable for ALWR.
2. Sufficient ALWR design features added to increase resistance to challenge by reducing the severity and/or ensuring containment.

* Passive plant design features which exceed requirements for current LWRs are identified with A (common to all ALWRs) or P (passive ALWRs only).

* NOTE: Reproduced from Reference 12.

Table 2a* (continued)

## SUMMARY OF REQUIREMENTS TO ADDRESS CONTAINMENT CHALLENGES RESULTING FROM CORE DAMAGE

| CHALLENGE | AFFECTED SAFETY FUNCTION | PLANT TYPE | ALWR BASIS# | KEY PASSIVE ALWR REQUIREMENTS: LIMIT POTENTIAL FOR CHALLENGE* | KEY PASSIVE ALWR REQUIREMENTS: ACCOMMODATE CHALLENGES* |
|---|---|---|---|---|---|
| Hydrogen Deflagration | Combustible Gas Control | BWR | 1 | Inerted. | A Demonstrated accommodation of generation equivalent to 100% active clad reaction.<br>A Structural evaluation for LOCA plus hydrogen loads (75% active clad reaction). |
| | | PWR | 2 | A Deflagration likely at low concentrations (< 10%) given hydrogen control system (IRWST and PCCS limit steam inerting potential). | A Demonstrated accommodation of generation equivalent to 100% active clad reaction with multiple burns.<br>A Structural evaluation for LOCA plus hydrogen loads, including global burn of hydrogen equivalent to 75% active clad reaction. |
| 16. In-Vessel Debris-Water Interaction | Internal Containment Loading | BWR/PWR | 1 | Large-scale phenomena limited in probability. In-vessel geometry limits interacting quantities and size of any interaction. | Rugged reactor vessel contains forces; as backup, rugged lower drywell/reactor cavity contains lower head failure. |
| 17. Ex-Vessel Debris-Water Interaction | Internal Containment Loading | BWR/PWR | 2 | Large-scale phenomena limited in probability. Ex-vessel geometry limits interacting quantities and size of any interaction. | A Rugged lower drywell/reactor cavity confirmed by evaluation.<br>Containment design accommodates steam generation. |

# The acceptability of ALWR requirements to address containment challenges was based on the following criteria:
1. Current LWR resistance to challenge acceptable for ALWR.
2. Sufficient ALWR design features added to increase resistance to challenge by reducing the severity and/or ensuring containment.

* Passive plant design features which exceed requirements for current LWRs are identified with A (common to all ALWRs) or P (passive ALWRs only).

* NOTE: Reproduced from Reference 12.

Table 2a* (continued)

## SUMMARY OF REQUIREMENTS TO ADDRESS CONTAINMENT CHALLENGES RESULTING FROM CORE DAMAGE

| CHALLENGE | AFFECTED SAFETY FUNCTION | PLANT TYPE | ALWR BASIS# | KEY PASSIVE ALWR REQUIREMENTS: LIMIT POTENTIAL FOR CHALLENGE* | KEY PASSIVE ALWR REQUIREMENTS: ACCOMMODATE CHALLENGES* |
|---|---|---|---|---|---|
| 18. Noncondensible Gas Generation | Fuel/Debris Cooling | BWR/PWR | 2 | A Features limiting concrete erosion (see item 19) limit noncondensible gas generation as well.<br>A Sacrificial concrete specified as low gas generation type.<br>A Overlying pool cools gases from core-concrete interaction. | Containment size and pressure retention capability. |
| 19. Basemat Erosion and Vessel Support Degradation | Fuel-Debris Cooling | BWR/PWR | 2 | A Reactor cavity/lower drywell spreading area of 0.02$m^2$/MWt promotes core debris cooling.<br>A Lower drywell/cavity flooding.<br>A Lower drywell flooding thermally actuated direct from BWR gravity drain tank or suppression pool.<br>A Overflow from containment reflux via PWR IRWST prefloods reactor cavity.<br>A Backup capability for water addition from sources external to containment. | A Sacrificial concrete where debris on floor contacts boundary structures (which are the passive BWR vessel support). |
| 20. Core Debris in Sump | Fuel/Debris Cooling | BWR/PWR | 2 | A Special cavity sump design prevents localized unterminated core-concrete interaction.<br>A Sump drainline configuration precludes gravity transport of debris ex-containment.<br>A Reactor cavity/lower drywell flooding. | |

# The acceptability of ALWR requirements to address containment challenges was based on the following criteria:
1. Current LWR resistance to challenge acceptable for ALWR.
2. Sufficient ALWR design features added to increase resistance to challenge by reducing the severity and/or ensuring containment.

* Passive plant design features which exceed requirements for current LWRs are identified with A (common to all ALWRs) or P (passive ALWRs only).

* NOTE: Reproduced from Reference 12.

Table 2a* (continued)

## SUMMARY OF REQUIREMENTS TO ADDRESS CONTAINMENT CHALLENGES RESULTING FROM CORE DAMAGE

| CHALLENGE | AFFECTED SAFETY FUNCTION | PLANT TYPE | ALWR BASIS# | KEY PASSIVE ALWR REQUIREMENTS | |
|---|---|---|---|---|---|
| | | | | LIMIT POTENTIAL FOR CHALLENGE* | ACCOMMODATE CHALLENGES* |
| 21. Core Debris Contact With Liner | Fuel/Debris Cooling | BWR/PWR | 2 | A Liner protected by concrete.<br>A Lower drywell/cavity flooding.<br>A Design features to limit debris dispersal including ADS. | |
| 22. Decay Heat Generation | Containment Pressure Control | BWR | 2 | Main Condenser.<br>A Reactor Water Cleanup System.<br>P Passive RHR (RCS heat removal mode). | P Passive Containment Cooling. |
| | | PWR | 2 | Steam Generators/Main Feedwater (MFW)/Backup Feedwater.<br>Reactor Shutdown Cooling. | P Passive Containment Cooling.<br>P Passive Heat Removal through containment shell without PCCS water limits containment pressure. |
| 23. Tube Rupture from Hot Gases | Bypass | PWR | 2 | Steam Generators/MFW/Backup feedwater.<br>A Depressurization System. | |

# The acceptability of ALWR requirements to address containment challenges was based on the following criteria:
1. Current LWR resistance to challenge acceptable for ALWR.
2. Sufficient ALWR design features added to increase resistance to challenge by reducing the severity and/or ensuring containment.

* Passive plant design features which exceed requirements for current LWRs are identified with A (common to all ALWRs) or P (passive ALWRs only).

* NOTE: Reproduced from Reference 12.

The Plant Designers supported a requirement for the hydrogen plus LOCA load to augment the traditional large break LOCA in ensuring a robust containment, because it provided an objective criterion early in the design process based on existing regulations for severe accidents.

The LOCA plus hydrogen load is an SMB requirement that in practice applies principally to advanced PWRs. As shown on Figure 2, a parallel LDB requirement specifies that containment integrity be maintained during an accident that releases hydrogen generated from 100% metal water reaction of the active fuel cladding (this requirement governs advanced BWR capability).

An evaluation was performed in Reference 13 to confirm the feasibility of the passive plants meeting this requirement. For the passive PWR, assumptions were as follows:

- Hydrogen release from 75% oxidation of active fuel clad concurrent with peak LOCA pressure.
- No credit for igniter system or for spontaneous ignition prior to full hydrogen release.
- Uniform hydrogen mixing in containment.

For a design-basis LOCA, the maximum containment pressure is in the range of 50-55 psia. At this pressure, the steam partial pressure is sufficiently high that combustion of hydrogen is not possible, i.e., the containment is steam-inerted. As the containment and steam pressure decrease with time (as heat is removed from the containment by the primary containment cooling system), the relative hydrogen concentration increases until combustion is possible. The analysis in Reference 13 shows that the maximum post-combustion containment pressure is 98.5 psia which results from the assumed adiabatic combustion of all available hydrogen with containment pressure initially at 40.6 psia.

The Service Level C pressure capability of the passive PWR containment is estimated to be 121 psia. Based on these calculations, it is apparent that there is significant margin between the LOCA plus hydrogen (98.5 psia) and the Service Level C (121 psia) containment pressures.

Since the passive BWR containment is inerted with a nitrogen atmosphere, hydrogen combustion is not considered and the greater LDB specified total hydrogen generation quantity controls the BWR design. The hydrogen generation associated with the oxidation of 100% of the active fuel cladding is calculated in Reference 13 to increase the containment pressure from a LOCA pressure of 50.8 psia to a final pressure of 106.4 psia.

The Service Level C containment pressure capability is estimated to be 110.4 psia which is greater than the LOCA plus hydrogen pressure of 106.4 psia.

Loads From Low Pressure Core Melt

This requirement specifies that the loads from low pressure core melt accident sequences not exceed Service Level C limits. Reference 13 defines the characteristics of the low pressure sequences in detail. Based on Reference 13, the best estimate containment pressure profiles are shown in Figures 3 and 4 for the passive PWR and BWR, respectively. While these calculations and the limits are preliminary since the design is still evolving, it is evident that significant margin exists between the severe accident loads and the Service Level C limit.

Containment Ultimate Capacity Analysis

This requirement specifies that the Plant Designer estimate and report the ultimate pressure and temperature capability of the containment pressure boundary, and identify the associated containment failure mode. This provides information required following the TMI accident and expected by the NRC in Standard Review Plan Sections 3.8.1 and 3.8.2. While the passive plant containment designs have not been developed to a point where an accurate relationship between the ultimate capacity of containment and other structural capacities such as design pressure can be established, conclusions can be drawn based on typical ASME Code Allowables analyses and scale model test results, as presented in Reference 13.

Based on a 1:8 scale containment model test and analysis (by Sandia) [14] and a Japan Atomic Energy Institute containment analysis for a 40 psig design pressure containment, the PWR containment pressure at collapse load is expected to be approximately 3 to 4.5 times the design pressure. In addition, there is a margin of approximately 1.1 to 1.25 between the collapse load and the ultimate (failure) containment pressure. Accordingly, it is expected that the ultimate failure pressure for the passive PWR containment would be in the range of 170 to 250 psia.

Evaluation indicates that the BWR drywell head will be the limiting component of the containment vessel and the same margins as those estimated for the PWR containment would be expected. Evaluations of the drywell head plastic capability indicate that the ultimate capacity would be a pressure of approximately 1.6 times the Service Level C pressure, or about 170 psia.

The ultimate pressure capability is depicted in Figure 3 and 4 and shows significant margin beyond Service Level C limits.

PRA Confirmation

While detailed PRAs are not yet complete for the passive plants, preliminary results indicate that core damage frequency is well below the $10^{-5}$ per year ALWR goal. Significant margin to the $10^{-6}$, 25 rem goal also exists. Sequence types other than low pressure core melt are expected to yield calculated frequencies lower than $\sim 10^{-7}$ per year.

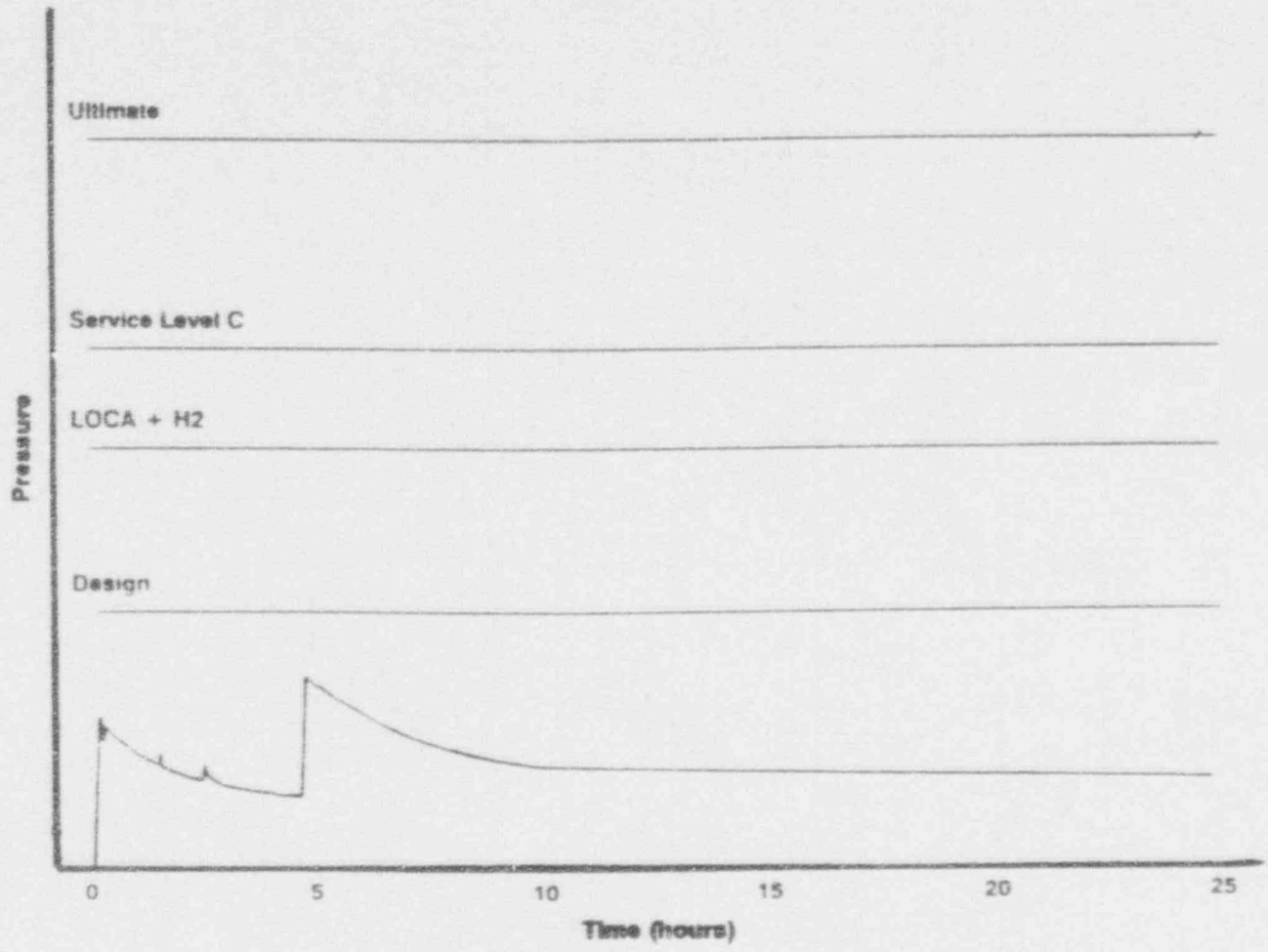


Figure 3. Containment Pressure Profile for Passive PWR
LOCA Low Pressure Core Damage Sequence

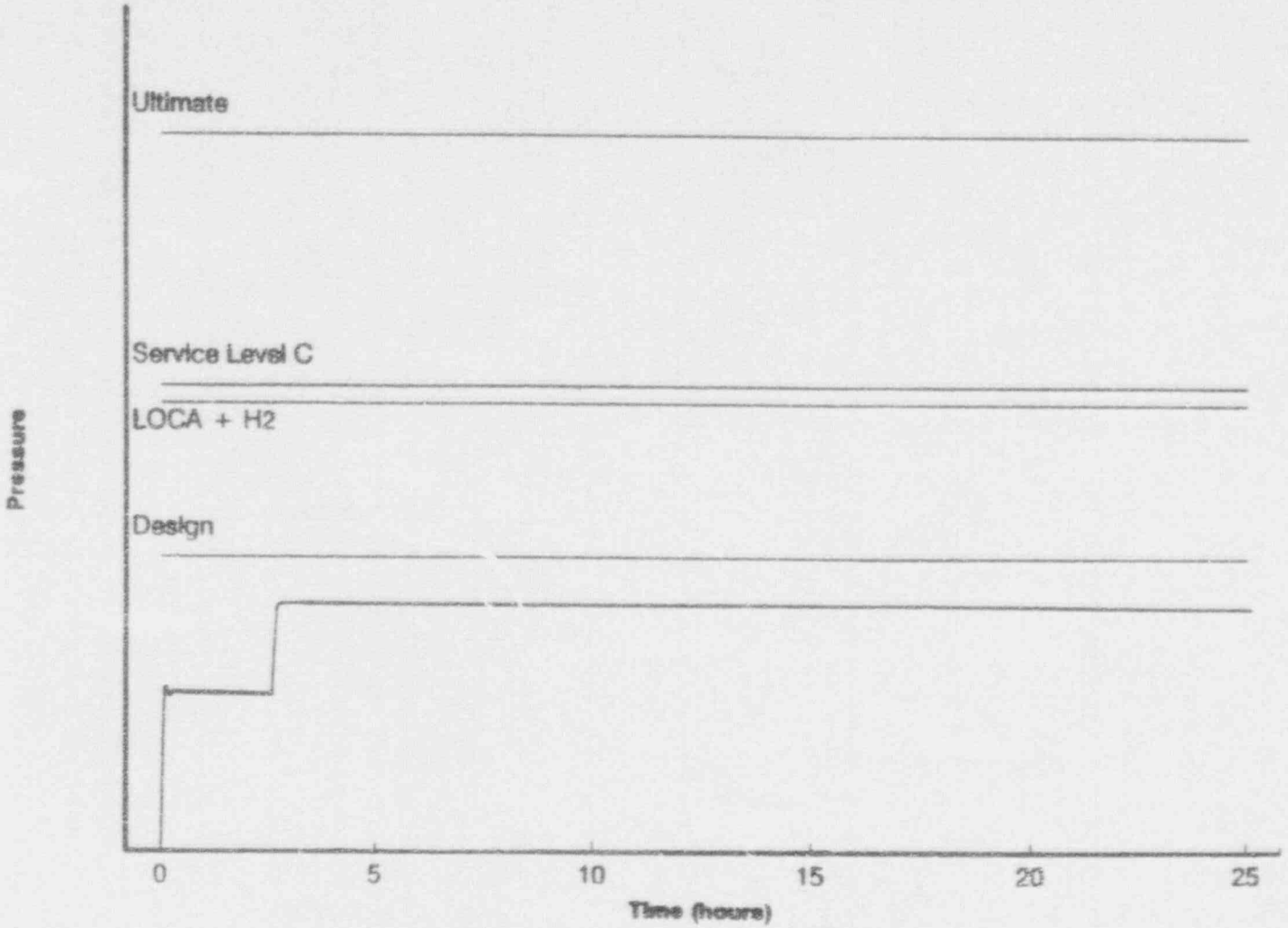


Figure 4. Containment Pressure Profile for Passive BWR
LOCA Low Pressure Core Damage Sequence

## PHYSICALLY-BASED SOURCE TERM AND DOSE EVALUATIONS

In addition to explicit consideration of severe accidents in the design, the ALWR program has developed a revised design basis fission product source term to replace the old TID 14844. This revised source term is based on the physical phenomena which occur during a core damage event thereby providing a much more physically correct representation of the source term and thus a more rational design basis for mitigation systems. Reference 15 provides details on the ALWR work.

Table 3 shows a comparison of the physically-based source term and a revised NRC source term which is being developed for the ALWR. Differences are not major and work to resolve the differences is underway.

It is an ALWR Program objective to obtain redefinition of emergency planning commensurate with the passive plant design. A necessary plant capability in this regard is to maintain best-estimate site boundary dose below 1 rem. Using the physically-based source term and taking into account URD requirements and preliminary mitigation system design capabilities, site boundary doses are estimated at less than 0.5 rem for 24 hours after the accident.

## CONCLUSIONS

The main conclusions from the Passive ALWR URD effort in the containment performance area are as follows:

- Severe accident containment challenges are being systematically and explicitly addressed in the design and the deterministic requirements coupled with PRA confirmation provide high confidence that plants designed to meet the ALWR requirements provide effective severe accident containment performance.

- Design requirements address a comprehensive list of potential containment challenges through such means as plant features, operating characteristics, and evaluations. Assessments of the effectiveness of these requirements indicate that either the challenges are effectively precluded or the containment can accommodate the challenge.

- Margin exists between the loads resulting from severe accidents and the Service Level C limits.

- Significant margin exists between the pressure corresponding to Service Level C and that pressure at which containment ultimate capacity would be expected to be exceeded.

- For a realistic source term which is expected to bound that from any credible core damage sequence, the site boundary dose is less than 0.5 rem.

Table 3. PWR Source Term Comparison

| | Requirements Document | | NRC Preliminary | |
|---|---|---|---|---|
| | In-Vessel | Ex-Vessel (Dry) | In-Vessel | Ex-Vessel (Dry) |
| Nobles | 1.0 | 0 | 1.0 | 0 |
| Iodine | .55 | .1 | .47 | .29 |
| Cesium | .48 | .1 | .36 | .39 |
| Tellurium | .11 | .35 | .175 | .29 |
| Strontium | .004 | .002 | .03 | .12 |
| Ruthenium | .004 | .01 | .008 | .004 |
| Ce | .00004 | .001 | .01 | .02 |
| La | .00004 | .001 | .002 | .015 |
| Timing | 1-5 hrs. for most of release | | 1-2 hrs. for in-vessel<br>2-4 hrs. for ex-vessel | |
| Chemical Form | 97% - CsI<br>2.85% - I<br>.15% - Organic | | 95% - CsI<br>5% - I+HI | |

## References


1. Advanced Light Water Reactor Program, Electric Power Research Institute (EPRI), "ALWR Requirements Document," Volume II.

2. Advanced Light Water Reactor Program, Electric Power Research Institute (EPRI), "ALWR Requirements Document," Volume III.

3. Code of Federal Regulations, Part 52, "Early Site Permits; Standard Design Certifications; and Combined Licenses for Nuclear Power Plants," January 1, 1991.

4. IDCOR Technical Summary Report, "Nuclear Plant Response to Severe Accidents," November 1984.

5. USNRC, "Reactor Risk Reference Document, NUREG-1150 (Draft)," January 1987.

6. USNRC, "Severe Accident Risks: An Assessment for Five Nuclear Power Plants, NUREG 1150," December 1990.

7. USNRC, "Reactor Safety Study, WASH-1400," October 1975.

8. Philadelphia Electric Company, "Probabilistic Risk Assessment, Limerick Generating Station," March 1981.

9. Long Island Lighting Company, "Probabilistic Risk Assessment, Shoreham Nuclear Power Station," June 24, 1983.

10. American Nuclear Society and the Institute of Electrical and Electronics Engineers, "PRA Procedures Guide," NUREG/CR-2300, January 1983.

11. Advisory Committee on Reactor Safeguards, "Proposed Criteria to Accommodate Severe Accidents in Containment Design," letter to the Chairman, Nuclear Regulatory Commission, May 17, 1991.

12. S.L. Additon et al, "Passive ALWR Requirements to Prevent Containment Failure," TENERA, L.P., Bethesda MD, December, 1991.

13. D.P. Blanchard et al, "Passive ALWR Severe Accident Containment Performance," TENERA, L.P., San Jose, CA, January, 1992.

14. R.T. Reese and D.S. Horshel, "Design and Fabrication of a 1/8 Scale Steel Containment Model," NUREG/CR-3647, SAND84-0048, Sandia National Laboratories, Albuquerque, NM, February 1985.

15. D.E. Leaver et al., "Passive ALWR Source Term," DOE/ID-10321, Idaho National Engineering Laboratory, Idaho Falls, ID, February, 1991.

THIS PAGE INTENTIONALLY LEFT BLANK

# Study of Potential Design Margins in the Codes of Practice for Structural Design of Primary Containment

S S Ray
Taywood Engineering Ltd

## Abstract

The structural designs of nuclear power stations all over the world have been carried out using a variety of codes of practice with hardly any uniformity. This may have given rise to primary containment structures with varying degrees of margin against failure. It is fruitless to argue about the appropriateness of the various provisions in codes of practice for design and analyses formulated by different committees in different countries. In this paper a method to find the available margin against collapse is defined without making any reference to the codes of practice used in the original design of the containment structure. A structured step-by-step method is suggested which can be universally applied irrespective of the location, condition, age or type of primary containment. The three key factors in a containment structure are the geometry, the material properties and the loading. Coupled with these there are two further aspects namely, the condition of the structure and the efficiency of the analytical method. Objective judgement of the elements influencing these factors is suggested in the method of finding the available margin. The whole process is based on the broad philosophy of assessment of existing structures where the geometric and material variabilities assumed at the design stage have been considerably narrowed down and most of the analytical conservatisms removed by the application of state-of-the-art computer software and parametric studies.

## Introduction

Nuclear power plants require a large initial capital outlay due to the high level of safety features incorporated in the design. They are also expensive to decommission. In a number of countries the first generation of nuclear power plants are reaching the end of their design life. Because of the high cost of replacing old plants there are a number of programmes underway to extend the operating licence beyond the design life of the plants. An existing primary containment for a nuclear power station would have been designed using the "state-of-the-art" analytical tools and design codes available at the time it was designed. This paper discusses a method of determining the available margin against failure of the existing structure when assessed against an understanding of the actual load effects and actual structural resistance. The margin is defined as the number which is obtained when the calculated resistance of the structure is divided by the load effects. In calculating resistance and the load effects the code of practice need not be consulted at all. The margin against collapse of a primary containment can be estimated by considering the geometry and stiffness of the existing structure and the likely effects of probable loads. The method described here can be applied irrespective of the code of practice that was followed in the design of the structure. The margin thus found gives a measure of conservatism in the Codes of Practice that was used to design the structure.[1]

## Structural Survey

Assessment of existing structures should start by carrying out a structural survey which should be as comprehensive as possible. The purpose of the survey is to determine the actual geometry and the material properties of the structures along with the existing condition of the structure. A series of destructive and non-destructive tests should be carried out to determine the actual material properties. The actual geometry should be determined measurement. In an operating power station it may not be possible to directly measure all significant dimensions of the primary containment, so existing drawings may be used to find the dimensions which cannot be measured.

Non-destructive tests or insitu tests should be carried out at regular intervals on the accessible areas of the primary containment on a square grid basis. The number of tests areas should be numerous enough to give a statistically significant material property and geometric parameter. The non-destructive tests would typically include the following:

a) Depth of cover using a cover meter survey.

b) Concrete strengths using a rebound hammer properly calibrated by cylinder test results on samples obtained from the primary containment.

c) Electropotential measurements using a half cell combined with resistivity measurements.

d) Permeability testing using initial surface absorption equipment.

e) Carbonation depth using chemical indicators.

f) Thickness of steelwork using ultrasonic equipment.

g) The ultrasonic Pulse Velocity (Pundit) technique to measure concrete quality.

Destructive testing which should be carried out at regular intervals would typically include the following:

a) Concrete cores at regular intervals.

b) Chloride content tests on samples from cores.

c) Alkali content tests on samples from cores.

d) Sulphate content tests on samples from cores.

e) Depth of carbonation in core samples.

f) Cement content in concrete core samples.

g) Aggregate grading in concrete core samples.

h) Compressive strength of concrete in cores.

i) Petrographic examination of hardened concrete as per ASTM C856-088
section analysis.

j) Endoscopic examination of grouted ducts in post-tensioned concrete.

k) Stress-strain relationship of existing materials on samples obtained from cores.

l) Stress-strain relationship of samples of reinforcing and prestressing steel.

The visual assessment should determine the extent of cracking, sealing, spalling, rust staining, leaching etc.

## Condition Factor - $F_c$

The concept of "Condition Factor" is important and its determination is dependent on the experience of the assessment engineer. This factor has a subjective element in it but when it is judged against all the factors governing it, a scientific determination of this factor can be achieved. It depends mainly on the following aspects:

**a) Quality Assurance During Construction: $F_{c1}$**

This factor plays a most vital part in the estimation of margin against failure. A strict regime of Quality Assurance system when implemented during construction assures a high degree of uniformity in the finished structure thereby reducing the need for a large factor to cover the variations in material properties. The Q.A. system when practised rigorously would also assure that the best construction methods have been adopted ensuring the highest achievable quality.

A fully recorded case history during construction should be part of the Q.A. system which in turn will record all the authorised variations from the construction specification. This system will also record the frequency and nature of all construction material sampling and testing including all test results. The factor $F_{c1}$ may vary between 1 to 0.5 depending on the evidence of the nature of Quality System adopted during construction. An excellent Q.A. system with recorded evidence of all internal and external audits and control will command a factor $F_{c1}$ equal to 1.

**b) Inspection and Maintenance History: $F_{c2}$**

It is important to have a fully recorded history of all inspection and maintenance work carried out on the primary containment together with records of all accidents and repair works thereafter. The condition factor $F_{c2}$ depends on the rigorous application of inspection routines. All changes should also be available in recorded form on drawings. This will give a level of confidence on the performance of the primary containment under operating loads. This factor may vary between 1 to 0.9 depending on the recorded performance and maintenance history.

**c) Visual Assessment of Primary Containment $F_{c3}$**

Following the structural survey and the visual assessment it should be possible to determine this factor $F_{c3}$ depending on the extent of cracking, scaling, spalling, laminations, rust staining, leaching, etc. An estimation of this factor can be made on the basis of percentage degradation of the cross sectional area of the concrete of the primary containment or loss of area of steel by corrosion. In an operating Nuclear Power Station this factor is not likely to be below 0.95 and it will generally vary between 1 and 0.95.

**d) Management Factor $F_{c4}$**

This important factor is of a very subjective nature. It depends on the overall control that the management exercises in the operation of the nuclear power plant. It also depends on the interest and regular audit of procedures by the licensing or regulatory bodies. It may be dependent on the attitude of owners, profitability of the operating company, changes in management structure, general staff morale etc. Due to bad management routine maintenance may suffer badly resulting in degradation of strength of safety related items. This factor is usually equal to 1 in a highly safety conscious environment.

$$F_c = F_{c1} \times F_{c2} \times F_{c3} \times F_{c4} \leq 1.0 \qquad (1)$$

## Material Factor $\gamma_m$

This factor represents the material strengths as actually exist in the structure and not the postulated characteristic strengths adopted at the design stage. Following the structural survey and sampling and testing the variability of the existing material properties should be clearly known, which should give a greater degree of confidence in determining the ultimate structural resistance. There are many factors which cumulatively govern this factor and they are enumerated below.

**a) Statistical Material Property Factor - $\gamma_{m1}$**

In the design phase uncertainties exist regarding the actual strength of materials when compared with postulated design strength. A large factor $\gamma_{m1}$ is usually allowed to cover this uncertainty at the design phase. From an assessor's point of view this may be unduly conservative because the strength of materials will be judged statistically from the test results on samples taken from the actual structure. If this is not possible, then the material strength test results recorded during the construction phase should be used to determine this material factor, and it should include an allowance for the likely difference in properties between laboratory and the actual insitu environment.[34]

When the characteristic material strengths and other properties are obtained statistically from test results on samples obtained from existing structure, then the material property factor $\gamma_{m1}$ should be taken equal to 1.0. Where the material strengths and other properties are only obtainable by reference to records during construction, then this factor may be between 1.0 and 1.2 depending on the consistency of the test results.

The material strengths in question here are for the ultimate limit state provided the strains and deformations of the structure remain within failure limits. A non-linear analysis may be carried out with the failure criterion decided by strain rather than stress and this may be the "ideal manner" in which a true margin against failure can be found. To illustrate the margin available against failure in materials normally used in construction namely, cold worked Deformed Bars (Type 2) as per BS 4449 the following typical test results are reproduced below.[35]

| Size | No. of Tests | Mean U.T.S. | S.D. | Actual Character-istic U.T.S. | Specified Character-istic Yield | Mean Margin Available | Margin for Yield |
|---|---|---|---|---|---|---|---|
| | | $N/mm^2$ | N/mm2 | N/mm2 | N/mm2 | N/mm2 | % |
| 16 | 144 | 569 | 19.6 | 536 | 460 | 76 | 16 |
| 20 | 40 | 564 | 12.3 | 543 | 460 | 83 | 18 |
| 25 | 72 | 562 | 24.3 | 522 | 460 | 62 | 13 |
| 32 | 47 | 557 | 16.2 | 530 | 460 | 70 | 15 |
| 40 | 28 | 605 | 26.7 | 561 | 460 | 101 | 21 |

The design of containment structures is usually based on characteristic yield strength for most codes of practice.

**b) Material Fatigue Factor $\gamma_{m2}$**

In steel containment structures fatigue can be a problem due to operational transients such as start-up, shutdown, etc. Fatigue at containment penetrations and bellows should be considered depending on the number of stress cycles over its operating life. Fatigue in containment concrete, prestress and reinforcement is not considered to be significant. This factor may be taken as 1.0 except for elements where large stress variations occur over numerous cycles. References [2], [3], [4], [5], [6], [7], [8], [26].

**c) Material Thermal Cycling Factor $\gamma_{m3}$**

Material strength degradation may happen due to large variations of temperature over many cycles during the operating life. The degradation will depend on the chemical composition of the materials in question and this factor may vary considerably depending on the temperature range and the number of cycles. Specialist literature should be consulted to determine this factor. References [9], [10], [11].

**d) Material Radiation Exposure Factor $\gamma_{m4}$**

The effects of radiation on concrete has been studied at several research institutions. Depending on the type of aggregate and cement matrix the effect of radiation may not be severe and is limited to discrete zones close to the source of radiation. The degradation of strength over a long period of intense exposure may be estimated by reference to specialist literature. This factor may be considered equal to 1.0 under normal reactor operating regimes. References [12], [13], [14] & [15].

**e) Material Chemical Degradation Factor $\gamma_{m5}$**

Concrete suffers from attacks by chlorides and sulphates. Alkali-aggregate reaction, if present, can substantially reduce the strength. The sampling and testing routines of existing concrete will establish whether any chemical degradation of concrete has taken place or is likely to take place. Likely loss of strength due to various chemical attacks is reported in many specialist literatures and based on these findings this factor may be determined. References [2], [16], [17], [18], [19], [20], [21], [22], [23], [24].

Corrosion is a major problem in steel structures, prestressing tendons and steel reinforcement. Normally in reinforced concrete the reinforcement is protected against corrosion by a number of physical and chemical processes. Firstly the highly alkaline environment within concrete encourages the formation of protective oxide films on steel surface. Secondly it provides a physical and chemical barrier to the penetration of moisture containing dissolved salts, carbon dioxide, oxygen and sulphur dioxide. The passage of electrolytic corrosion currents is also restricted by the high resistivity of the concrete. The insitu non-destructive and destructive tests should show the steel to be depassivated and the half cell potentiometer may demonstrate the presence of electolytic corrosion currents. Based on visual inspection and test results a determination of this degradation factor is possible. Reference [25].

Hydrogen embrittlement could be a serious problem for prestressing tendons exposed to the gas. Tests should be carried out on samples of prestressing tendons to evaluate the effect of hydrogen absorption [25, 33].

**f) Material Age Induced Factors $\gamma_{m6}$**

When strength is determined by actual tests on samples obtained from the existing structure, the age induced factor for concrete and steel may be taken equal to 1.0. When sampling and testing is not possible, then the increased strength of mature concrete may be assessed by determination of concrete age and the average temperature experienced during ageing. A widely accepted strength gain equation is given by:

$$[A + B \log_{10} (M * 10^{-3})]\% \qquad (2)$$

where, $A = 21$ and $B = 61$ for $f_{cu} = 17$ -35 N/mm$^2$

$M$ = Age of concrete in hours * Temperature in $^{o}$C.

Modern finely ground cements do not gain strength with age as much as older OPC. However, there is still sufficient gain if minimum cement content for durability is used in practice. Moreover it is known that partial cement replacement by Pulverised Fuel Ash (PFA) or Ground Granulated Blast Furnace Slag (GGBFS) considerably increases the rate of strength gain during maturation. The material age induced factor will be less than 1.0 in this case. Reference [2].

Age-induced stress relaxation in prestressing tendons is a known phenomenon and various specialist literatures give values of this rate of relaxation depending on the manufacture and composition of the tendons. The material age induced factor can be determined by reference to these documents. Reference [29], [30]. Though this is a material property factor, but the effect is on the permanent prestressing load as stated in the section on loading.

**g) Material Rate of Strain Factor $\gamma_{m7}$**

This factor allows an increase in strength of materials due to high rates of strain and may only be applicable to loads which cause very rapid increase of strain. An increase in yield strength of low and intermediate-grade structural and reinforcing steel with increasing rate of strain has been reported by many. There is also a dynamic increase of shear strength and ultimate tensile strength. Similarly, in concrete marked increases in both 'E' values and strength have been observed at higher rates of strain. Earthquake loading results in a rate of strain in the structure which is much higher than that used to determine the concrete crushing strength or the steel ultimate strength. This factor obtainable from specialist literature may be applied when loads causing high rates of strain are considered in the combination. References [27], [28]. This factor, if applicable, will be less than 1.0.

$$\gamma_m = \gamma_{m1} \times \gamma_{m2} \times \gamma_{m3} \times \gamma_{m4} \times \gamma_{m5} \times \gamma_{m6} \times \gamma_{m7} \geq 1.0 \qquad (3)$$

The stress-strain relationship obtained by test should be divided by this $\gamma_m$ factor for input in the

analytical model. Each material type will have a different $\gamma_m$ which is also dependent on the types of loading in the combination. It should be noted that different parts of the structure may have a different $\gamma_m$ for the same material depending on the distribution of the various components of this material factor.

## Loading

The object is to find the "worst credible load" on the primary containment during its service life. The loads will be reassessed and the load factors will apply to individual types of loads depending on the degree of uncertainty. This is not code checking and hence, the load factors suggested by the codes of practice for universal application will be unsuitable for this exercise. Each type of loading will be judged individually on the basis of structural survey and a plant "walkabout", the level of uncertainty will be judged, and a load factor applied to cover the imponderables. The following types of loading are normally encountered for global analysis and design of the primary containment. Accidental local loads from missile or aircraft impact have been left out from this exercise because the code margin under investigation refers to global collapse resulting in uncontrolled release of radioactivity. These local effects are excluded from the analysis.

### a) Dead Load Factor $\gamma_d$

The sampling and site survey carried out should be sufficient to find the Dead Load with a degree of accuracy which should not require any additional factor of uncertainty. If the dead load is determined with reference to drawings only, then a factor between 0.90 to 1.10 may be considered depending on which produces the most adverse effect. This is to account for the variation in geometry and the variation in material density. This factor could be taken as 1.0 when the calculation of dead load is based on actual geometry and material densities. The dead load in this context should include weights of all permanent structural and non-structural components including all fixed plant and equipment.

The dead load should also include other permanent loads such as prestress. The prestressing load must take into account time dependent relaxation of steel and creep and shrinkage of concrete.

### b) Operating Live Load Factor $\gamma_l$

This live load is due to the occupancy of the building and due to the loads from plant and equipment which are not fixed to the structure. The design is normally carried out with postulated uniformly distributed occupancy loads on floors. This may be considered unacceptable when an assessment for the global failure load is being carried out. A more exact determination of the global live loads during operation will be necessary. A well planned survey of floor areas over a period of time will give a fair indication of the amount of live load normally present. The factor $\gamma_l$ will depend on the degree of uncertainty and may be as high as 1.2. It may be quite acceptable to find from the operation routines of the station the total weight of all occupancy and movable plant, equipment, tools and tackles, and then distribute this load onto various areas of occupancy. Likely storage of components for routine maintenance should also be taken into consideration.

### c) Operating Temperature and Pressure Loading Factor $\gamma_0$

The operating pressures and temperatures on a primary containment structure are not usually severe but they have to be included in the analysis of load effects. The values of these presssures and

temperatures which are kept within strict operating limits can be obtained from the plant operating history. The overall factor $\gamma_{f0}$ must reflect any uncertainty of these thermal and pressure loadings. $\gamma_{f0}$ should normally be equal to 1.0.

**d) Accident Pressure Load Factor $\gamma_{fp}$**

The object is to find the "worst credible pressure load" which depends on the maximum mass and energy releases in the containment. Depending on the size and configuration of the containment and the other structures within it the pressures can be computed using the maximum releases. If these calculations prove without doubt that for accidental releases due to breaks in the primary and secondary piping the postulated pressures will not be exceeded then the load factor $\gamma_{fp}$ may be taken as 1.0.

**e) Accident Temperature Load Factor $\gamma_{ft}$**

Again the object is to find the "worst credible temperature" which in turn depends on the maximum energy releases into the containment. If the calculations prove that the maximum postulated temperatures of releases will not be exceeded, then the load factor $\gamma_{ft}$ may be taken as 1.0.

**f) Seismic Margin Earthquake Factor $\gamma_{fe}$**

This earthquake excitation may not be the design basis earthquake which could have a higher probability of occurrence. This earthquake is the worst credible at the site of the nuclear power station considering all the geotechnical and tectonic features of the surroundings. For example the geotechnical studies have demonstrated at a particular nuclear power station site in UK that the soil subgrade is incapable of transmitting an earthquake with peak ground acceleration greater than 0.27g. So, in this instance the Seismic Margin Earthquake is 0.27g. Similarly for other sites the worst credible intensity and magnitude of earthquake can be determined by considering the available geotechnical evidence. If the credibility of the earthquake acceleration is in doubt then a factor $\gamma_{fe}$ greater than 1.0 may be allowed. The ground liquefaction potential should be investigated and the Seismic Margin Earthquake may be limited by the failure of subgrade.

**g) Seismic Aftershock Earthquake Factor $\gamma_{fa}$**

This additional seismic load may be introduced because the Seismic Margin Earthquake could induce a mass and energy release due to a pipe break. The postulated worst credible pressure and temperature loads will not act simultaneously with the Seismic Margin Earthquake of short duration, but is likely to be present when an aftershock of less intensity occurs. The level of acceleration of the aftershock requires a probabilistic study involving geotechnical and tectonic considerations. The level of uncertainty in the determination of peak acceleration, for the aftershock may be covered by the factor $\gamma_{fa}$.

**h) Other Loads**

In the design of a containment structure many other loads are considered viz snow loads, equipment/piping reaction loads, tornado loads, hurricane loads, missile loads, etc. These loads do not form part of this assessment because their effect will create either a local failure or, there is statistically an extremely low probability for these loads to occur simultaneously with a seismic margin earthquake.

## Combination of Loads

In order to find the available margin against global collapse only two combinations of loads may be relevant, and they are described below.

$$LC1 = \gamma_{fd} \times D + \gamma_{fl} \times L + \gamma_{fo} \times 0 + \gamma_{fe} \times E_m \quad (4)$$

$$LC2 = \gamma_{fd} \times D + \gamma_{fl} \times L + \gamma_{fp} \times P + \gamma_{ft} \times T + \gamma_{fa} \times E_a \quad (5)$$

D = Dead load

L = Live load

O = Operating Temperature and Pressure Loads

$E_m$ = Seismic Margin Earthquake

P = Accident Pressure Load

T = Accident Temperature Load

$E_a$ = After-shock Earthquake

## Analysis Factor $\gamma_a$

This factor is introduced to account for the uncertainty in the analytical procedure adopted. $\gamma_a$ may have a value from 0.8 to 1.5 depending on the degree of accuracy in the modelling of structure and materials and the use of the analytical computer code. The limitations of the computing techniques including available hardware and software will affect the level of conservatism, which in turn will determine the value of $\gamma_a$. This factor has a subjective element in it but may be objectively determined by parametric studies of analytical methods on simple models, or by comparison of results of analysis with those obtained from tests on models or prototypes.

## Load Factor Evaluation Procedure

In an ideal situation with limitless computer power a full 3-D non-linear model of the primary containment may be created. This model should incorporate full material non-linearity and should include all items of structure contributing to strength. The steel liner for the primary containment is not normally included in the structural strength calculations but it can act compositely with the concrete containment to provide additional margin against collapse. Difficulty may arise in trying to model the soil with a view to including soil-structure interaction. The strain-dependent soil shear modulii and damping values may be obtained for different soil layers by reference to available site investigation data. Some additional geotechnical investigation may be necessary to remove any doubts. Soil may be modelled by 3-D solid elements with strain-dependent non-linear properties. The boundary of the soil structure, may be assumed well away from the structure based on Boussinesq pressure influence surface. Parametric studies on simpler models could help determine non-linear soil properties which produce the worst effects. The soil, if modelled using non-linear solid elements, could effectively predict basemat uplift.

The earthquake may be applied to the model as an acceleration time history obtained artificially from a design basis response spectrum for the appropriate level of damping anticipated. For a non-linear collapse load analysis the damping level may be as high as 10% of critical. A parametric study on a simplified model may be required to justify the use of one of the many possible time histories that can be artificially generated within the envelope of a design basis response spectrum. Site specific time histories are very difficult to obtain and hence an FRS and a postulated duration may be used to obtain these time histories.

For non-linear analysis the load combination $LC_1$ will be applied in increments. $\gamma_{fd} \times D$ in increments will be applied first, followed by $\gamma_{fl} \times L$ and $\gamma_{fo} \times O$. The deformed structure will then be subjected incrementally to $\gamma_{fe} \times E_m$ where the acceleration level will be gradually brought up to the level of the postulated $E_m$. The failure criterion is strain based with stiffness approaching zero at points where the limits of strain are reached. A global failure will be signalled when the stiffness of the whole structure approaches zero. The loading as per $LC_1$ when completed in incremental fashion may show sufficient reserve of strength. A multiple of $LC_1$ will then be applied incrementally till a global failure occurs. In other words, at the end of the process of incremental loading starting with $M_1' \times \gamma_{fD} \times D$ followed by other loads will be applied. Similar loading application procedure will be followed for the loadcase $LC_2$ and a different $M_2'$ will be found. The dynamic analysis for the earthquake will be carried out using non-linear material properties. Based on this analytical procedure the analysis factor $\gamma_a$ may be 1.1 to cover the uncertainties still remaining.

The final loadings incrementally applied which result in predicted failure of the primary containment are as follows:

$$LC_1 = M_1' \times \gamma_{fd} \times D + M_1' \times \gamma_{fl} \times L + M_1' \times \gamma_{fo} \times O$$

$$+ M_1' \times \gamma_{fe} \times E_m \qquad (6)$$

$$LC_2 = M_2' \times \gamma_{fd} \times D + M_2' \times \gamma_{fl} \times L + M_2' \times \gamma_{fp} \times P$$

$$+ M_2' \times \gamma_{ft} \times T + M_2' \times \gamma_{fa} \times E_a \qquad (7)$$

$M'$ is the lower of $M_1'$ and $M_2'$ thus found.

**The code margin** $$M = \frac{M' \times F_c}{\gamma_a} \qquad (8)$$

It should be noted that $M_1'$ and $M_2'$ could be less than 1.0 signalling that the predicted worst possible loads in combination cannot be resisted by the containment structure.

## Determination of Analysis Factor $\gamma_a$

The analysis factor, as defined previously, is dependent on the computational method applied to find the combination of loading which may cause structural collapse of the primary containment. The traditional method of analysis in elastic range with full superimposition of loads and no ductility incorporated may give rise to an analysis factor which is only 0.5. Whereas, a full 3D Non-linear analysis with a proper concrete model (Fig. 1) and reinforcement modelled as truss elements may increase the analysis factor close to 1 or more depending on the level of uncertainty. It should be noted that the concrete model illustrated is a simple uniaxial stress-strain relationship. Actual triaxial stress-strain relationship available as part of ADINA package is much more complex and is considered to be outside the scope of this paper. The following options may be looked into before deciding on the analysis factor to be applied to find the code margin.

**a) Scale Model Studies**

These studies including dynamic shake table testing may be used to calibrate the non-linear finite element programme. For static mechanical loads the non-linear F.E. analytical techniques (computer code ADINA) have been validated in the case of 1/10 scale model studies of Sizewell 'B' Containment [31, 32]. It may be necessary to carry out small scale model studies on shake tables to calibrate an F.E. package which is to be used for non-linear dynamic analysis. These studies increase the confidence level and bring the analysis factor close to 1.0. Scale model studies are ideal but expensive.

**b) Parametric studies on a Linear Elastic F.E. Model of Containment**

A less expensive option may be to carry out a full range of parametric studies on a linear elastic F.E. model created for the analysis of the containment structure. The variations in material properties are already covered by the factor $\gamma_m$ and the uncertainties of the loadings are covered adequately by $\gamma_f$. The variables which are not adequately covered are the soil properties and the earthquake time history. Parametric studies may be carried out with the full range of possible soil parameters and the probable earthquake time histories. The worst credible stress results from these parametric studies may help select the soil model and the earthquake time-history. [Fig. 2] [36]

## Conclusion

The method described in the paper can be used to compute the available margin against collapse for any primary containment - new or old. The margin thus found may be used by licensing authorities for considering extension of operating life or renewing licences. The application of this philosophy can be particularly suitable for the assessment of ageing nuclear power stations where adherence to modern safety related design principles cannot be guaranteed or in situations where access to original design documents may not be available.

## Acknowledgement

The author wishes to acknowledge the help and encouragement received from Mr R.C. Crowder, Mr D. Carlton and Dr R.D. Browne of Taywood Engineering Ltd (U.K.) in the preparation of this paper.

## References


1. M. AMIN et al, Seismic Capacity of Containments. Proceedings of the Workshop on Containment Integrity (4th), NUREG, Washington, pp. 163-178.
2. A.M. NEVILLE, Properties of Concrete, Pitman Publishing Ltd, London. Second metric edition 1973.
3. E.W. BENETT and N.K. RAJU, Cumulative fatigue damage of plain concrete in compression, Proc. Int. Conf. on Structure, Solid Mechanics and Engineering Design, Part 2, pp. 1089-1102 Southampton, April 1969; New York, Wiley-Interscience, 1971).
4. J.P. LLOYD, J.L. LOTT and C.E. KESLER, Final summary report: fatigue of concrete, T. & A.M. Report No. 675, Department of Theoretical and Applied Mechanics, University of Illinois, pp. 33 (Sept. 1967).
5. F.S. OPLE, JR. and C.L. HULSBOS, Probable fatigue life of plain concrete with stress gradient, J. Amer. Concr. Inst., 63, pp. 59-81 (Jan. 1966).
6. J.W. MURDOCK, The mechanism of fatigue failure in concrete, Thesis submitted to the University of Illinois for the degree of Ph.D., pp. 131 (1960)
7. J.A. NEAL and C.E. KESLER, The fatigue of plain concrete, pp. 226-37, Proc. Int. Conf. on the Structure of Concrete, (London, Cement and Concrete Assoc., 1968).
8. B.M. ASSIMACOPOULOS, R.F. WARNER and C.E. EKBERG, JR., High speed fatigue tests on small specimens of plain concrete, J. Prestressed Concr. Inst., 4, pp. 53-70 (Sept. 1959).
9. R.D. BROWNE, Current practice sheets - thermal movement, The Journal of the Concrete Society, November 1972, Volume 6, Number 11 - pp. 51-54.
10. Effect of high temperature on the crushing strength of concrete - Report of Fire Research Board and Report of the Director of Fire Research, H.M.S.O., London, 1964.
11. D.J. HANNANT, Strain behaviour of concrete up to 95°C under compressive stresses, Proc. Conf. PCPV - Institution of Civil Engineers, London, 1967
12. A. PEDERSEN, Radiation damage in concrete - measurements on miniature specimens of cement mortar. Paper 1, Proceedings of an EEC Information Exchange Meeting on Results of Concrete Irradiation Programmes, Brussels, Apr. 1971, p. 5.
13. B.T. KELLY, I. DAVIDSON, J.E. BROCKLEHURST, D MOTTERSHEAD and S. McNERNEY. The effects of reactor radiation on concrete. TRG Report 2136(C), 1971.
14. B.S. GRAY, The effects of reactor radiation on cements and concrete. Paper 2, Proceedings of an EEC Information Exchange Meeting on Results of Concrete Irradiation Programmes, Brussels, Apr. 1971, p. 17.
15. M.F. ELLEUCH et al. Effects of neutron radiation on special concretes and their components. American Concrete Institute, Seminar on Concrete for Nuclear Reactors, Berlin, 1970.
16. R.D. BROWNE, Properties of concrete in reactor vessels, Prestressed Concrete Pressure Vessels Conference. Institution of Civil Engineers, Paper 13, Group C, 1968.

17. T.C. POWERS and H.H. STEINOUR, An interpretation of published researches on the alkali-aggregate reaction, J. Amer. Concr. Inst., 51, pp. 497-516 (Feb. 1955) and pp. 785-811 (April 1955).

18. W.C. HANNA, Additional information on inhibiting alkali-aggregate expansion, J. Amer. Concr. Inst., 48, p. 513 (Feb. 1952).

19. HIGHWAY RESEARCH BOARD, The alkali-aggregate reaction in concrete, Research Report 18-C (Washington D.C., 1958).

20. R.C. MIELENZ and L.P. WITTE, Tests used by Bureau of Reclamation for identifying reactive concrete aggregates, Proc. A.S.T.M., 48, pp. 1071-103 (1948).

21. W. LERCH, Concrete aggregates - chemical reactions, A.S.T.M. Sp. Tech. Publicn. No. 169, pp. 334-45 (1956).

22. T.C. WATERS, Reinforced concrete as a material for containment, Proc. of Symp. on Nuclear Reactor Containment Buildings and Pressure Vessels. pp. 50-60 (Butterworths, London, 1960).

23. A.M. NEVILLE, Behaviour of concrete in saturated and weak solutions of magnesium sulphate and calcium chloride, J. Mat. A.S.T.M., 4, No. 4, pp. 781-816 (Dec. 1969).

24. G.L. KALOUSEK, L.C. PORTER and E.J. BENTON, Concrete for long-time service in sulphate environment, Cement and Concrete Research, 2, No. 1, pp. 79-89 (1972).

25. C.L. PAGE, K.W.J. TREADAWAY, P.B. BAMFORTH, Corrosion of Reinforcement in Concrete, Elsevier Applied Science, London.

26. Fatigue of Concrete - Abeles Symposium - American Concrete Insitute, Publication SP-41.

27. Structural Analysis and Design of Nuclear Plant Facilities. American Society of Civil Engineers - Manual No. 18 - 1980, pp. 316-317.

28. Structures to Resist the Effects of Accidental Explosions - Volume IV Reinforced Concrete Design - U.S. Army Armament Research, Development and Engineering Center - New Jersey, SP 84001, pp. 23.

29. K.W. LONGBOTTOM - Steel for Prestressed Concrete - Concrete Society Digest No. 4, The Concrete Society, England.

30. T. CAHILL, G.D. BRANCH, Long-term relaxation behaviour of stabilized prestressing wires and strands, Prestressed Concrete Pressure Vessels, The Institution of Civil Engineers, Group D - Paper 19, 1968.

31. C. LOMAS, Proposals for a one-tenth scale model test of the Sizewell 'B' containment, Proceedings of the Fourth Workshop on Containment Integrity, Arlington, Virgina, 1988, pp. 291.

32. J.C.W. SMITH, The design of a one-tenth scale model of a Sizewell 'B' Primary Containment, Proceedings of the Fourth Workshop on Containment Integrity, Arlington, Virginia, 1988, pp. 307.

33. B. MARANDET, Stress Corrosion Cracking and Hydrogen Embrittlement of Iron Base Alloys, Natl. Assn. Corrosion Engineers, Houston, 1977.

34. Assessment of Concrete Strength in Existing Structures, British Standards Institution, BS 6089: 1981.
35. Carbon Steel Bars for the Reinforced Concrete, British Standards Institution, BS 4449: 1988.
36. Finite Element Analysis of Reinforced Concrete, American Society of Civil Engineers, 1982, Chapter 7, pp. 401-447.

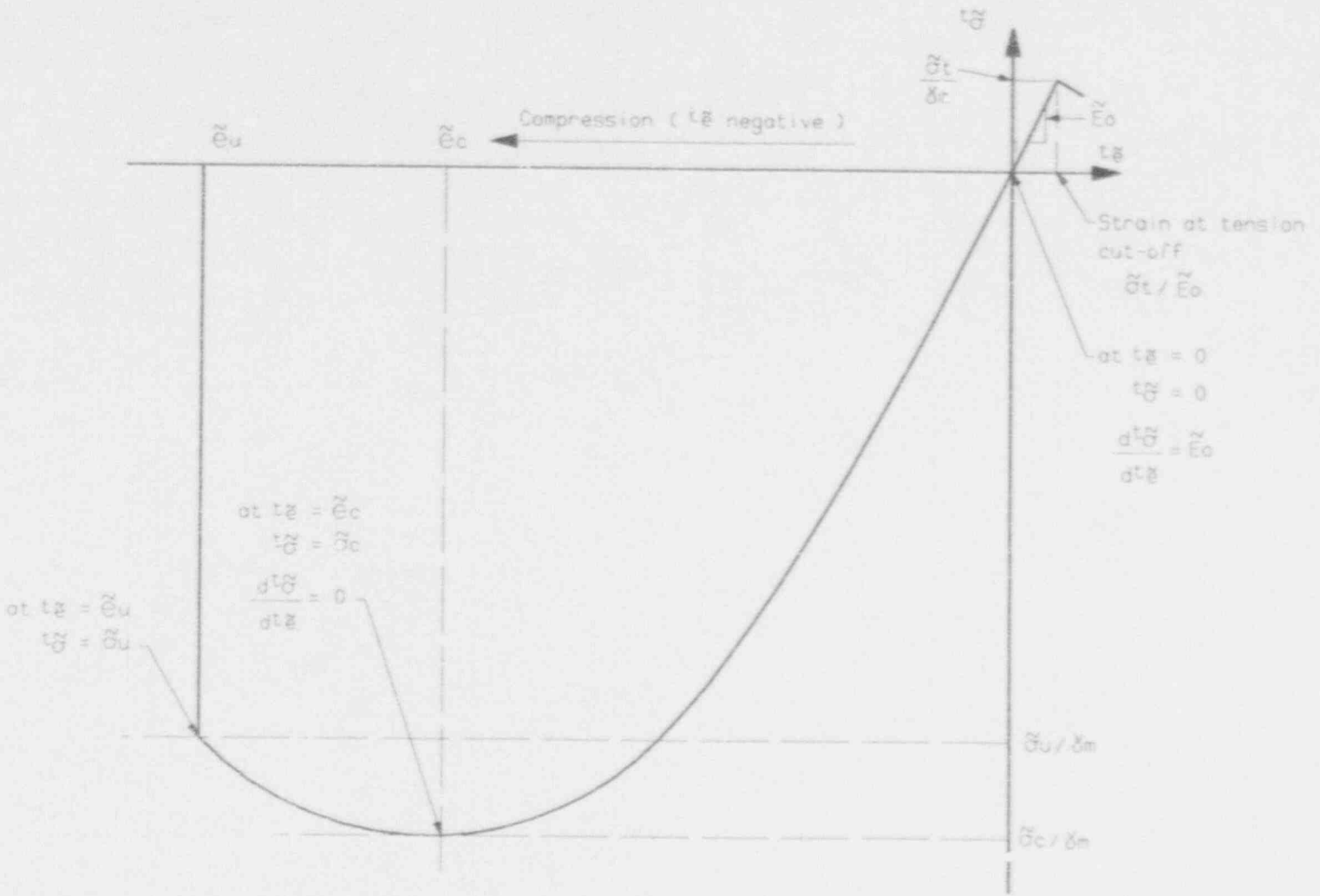


Figure 1. Typical stress-strain relation in concrete model

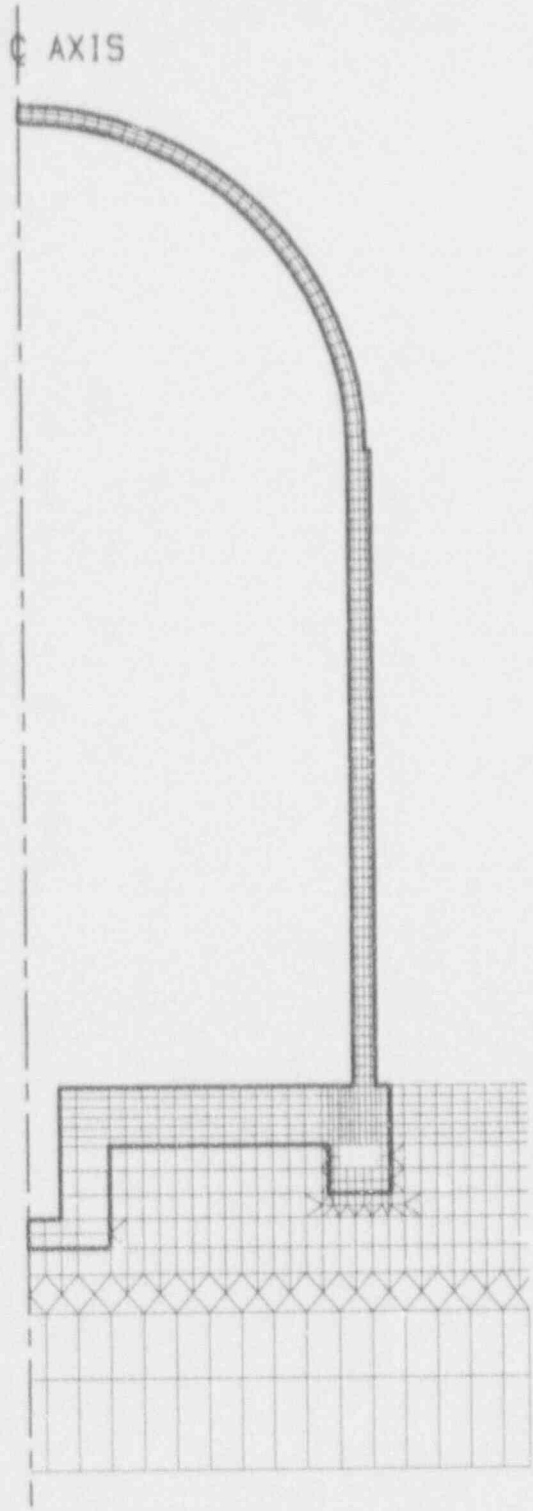


Figure 2. Parametric Studies -
Model of Containment Structure

# DESIGN CONSIDERATIONS FOR CONCRETE CONTAINMENTS UNDER SEVERE ACCIDENT LOADS

Mohammad Amin[a]
Sargent & Lundy

A. Curt Eberhardt[a]
Sargent & Lundy

Bryan A. Erler[b]
Sargent & Lundy

## Abstract

Current containments have been shown to accommodate credible severe accident loads. Future containments should be explicitly designed for severe accident loads to address the uncertainty associated with the response of containments to these low-probability events. This paper examines the experiences from the application of current structural design codes for concrete containments, ultimate pressure capacity evaluation of existing containments, and pressure fragility testing of scale model concrete containments to arrive at the directions for modification of national codes. Recommendations are provided to consider the severe accidents directly in the concrete containment design.

## INTRODUCTION

Steel-lined concrete containment structures are currently designed to the requirements of codes as follows:

- American Society of Mechanical Engineers (ASME), Section III, Division 2, Subsection CC for parts of pressure boundary that are backed by concrete
- ASME, Section III, Division 1, Subsection NE for parts of pressure boundary that are not backed by concrete

Containment internal structures are designed to the requirements of ACI Standard 349 and the American Institute of Steel Construction (AISC) Specification, as applicable. Effects of impulsive and impactive loads on internal structures are evaluated using inelastic response and ductility limits.

The containment design procedures and requirements were basically developed in the 1960s and 1970s. At that time, a sudden large-break loss-of-coolant accident (LOCA) was used as the design-basis accident (DBA). Current experience shows that existing containments can accommodate severe accidents.

In the 1990s more is known about severe accidents and containment structural response to severe accidents. This information has become available through severe accident research, structural evaluation of existing containments, testing of full-scale containment elements, and testing of

---

[a]Engineering Supervisor in Structural Department
[b]Partner and Assistant Manager, Structural Department

scale models of various containments. Because of this increased information and to reduce the risk and uncertainty of future containments to severe accidents, future containments should also be explicitly designed for severe accident loads.

Design for severe accidents implies explicit definition of severe accident loads that affect the containment. Although these loads are yet to be quantified for different reactor types and system designs, it is now clear that the following four types of challenges to the containment should be addressed (see Reference 1):

- static overpressurization combined with temperature,
- dynamic pressurization,
- internal missiles, and
- melt attack on concrete internal structures.

Additional provisions in the containment design codes are necessary to directly consider the severe accident loads in the design of future containments. This paper examines the experience from three sources to arrive at the directions for code modification. The three sources examined are:

- containment design experience including those design experiences obtained from using current requirements of ASME Code, Section III, Division 2,
- experience gained from calculating the ultimate pressure capacity of existing containments, and
- observations made on pressure fragility tests conducted on containment scale models.

Through this examination, directions for changes in the ASME Code, Section III, Division 2 are suggested. Recommendations are also made for other organizations and committees in the containment design/research community to provide additional guidance for considering severe accident loading in containment design.

## DESIGN EXPERIENCE

Figure 1 shows the cross-section through a post-tensioned containment. The nuclear steam supply system (NSSS) has a significant influence on the containment design. The example of Figure 1, chosen to summarize current design experience, is for a 1000-MW, two-loop, pressurized water reactor (PWR).

The equipment and radiation shielding requirements imposed the following minimum requirements for the containment configuration:

- The internal diameter of the cylindrical wall (144 feet) was dictated by the space required to accommodate all necessary equipment in a functional manner.
- The minimum height to spring line was dictated by the required elevation for the crane hook. The crane hook elevation is determined to ensure that major

equipment can be erected, moved during refueling, and removed from the containment.

- The radiation shielding requirement sets minimum thickness for the containment wall and dome.

The loads and load combinations for the design of containment shell and basemat are provided in ASME Code, Section III, Division 2. Table CC-3230-1 lists 15 load combinations to be considered. Table 1 indicates the 4 load combinations out of 15 that have usually been found to govern PWR, prestressed containment design. The Combinations 3, 8, and 11 usually control the design of the shell. The Combinations 11 and 15 control the design of the basemat.

Table 1. Load Combinations Usually Governing Design of Shell or Basemat (Shell: Post-Tensioned; Basemat: conventionally reinforced)

| Load Category | Combination No. ASME Code Table CC-3230-1 | Factor on | | Part of Containment Affected |
|---|---|---|---|---|
| | | $P_a$ | Seismic* | |
| Normal | 3 | 0 | 0 | Wall and dome |
| Abnormal | 8 | 1.5 | 0 | Wall and dome |
| Abnormal/Severe environmental | 11 | 1.25 | 1.25 $E_o$ | Wall, dome, and basemat |
| Abnormal/Extreme environmental | 15 | 1.0 | 1.0 $E_{ss}$ | Basemat |

*$E_o$, $E_{ss}$ = Effect of operating and safe shutdown earthquakes, respectively.

The LOCA pressure, $P_a$, is the most significant load for design of the containment wall and dome. Experience shows that usually earthquake loads are of such intensity that they do not necessitate a change in containment concrete outline. The earthquake loads can be accommodated by adding reinforcement in the areas of the shell that are optimally sized for the LOCA pressure.

Although $P_a$ does not appear in Load Combination 3 in Table 1, its effect is reflected by the prestressing load in this combination. Reference 2 discusses the optimal selection of the design prestress level. It is more economical to select the design prestress to fully counteract any membrane tension that occurs due to 1.25 $P_a$ in Load Combination 11 rather than counteracting 1.5 $P_a$ in Load Combination 8; bonded reinforcement is provided to carry the additional tension demand of Load Combination 8. Since $P_a$ determines prestressing level, the pressure effect is reflected in Load Combination 3.

The LOCA pressure, $P_a$, and temperature, $T_a$, depend on containment free volume. Figure 2 shows typical variation of $P_a$ with volume for a PWR containment. The design of containment

elements is not affected by $T_s$; however, $T_s$ affects displacements somewhat. Economic studies using preliminary designs, material take-offs, and unit costs are necessary to establish the optimal range for $P_s$. Such studies, reported in Reference 2, show the optimal range for $P_s$ is from 50 to 60 psig.

Reference 2 also considered economic configuration for the shape of the dome. Of the two alternatives, (a) hemispherical dome with inverted U vertical tendons and (b) ellipsoidal dome with ring girder for anchorage of dome and wall tendons, the hemispherical dome was found to be more economical.

For the example in Figure 1, the design pressure, $P_s$, is 54 psig. The elevation of the spring line was determined by using a hemispherical dome, with a 144-foot internal wall diameter, and the limitation for the crane girder location to provide for the volume corresponding to 54 psig. The wall thickness of 4 feet-0 inch and dome thickness of 3 feet-6 inches satisfy the radiation shielding requirement, the Service Level allowables for concrete compression in Load Combination 3 (specified $f'_c$ = 5500 psi), and the space required for the tendon and bonded steel placement.

The basemat is conventionally reinforced. The basemat thickness is principally controlled by foundation material characteristics. For the rock site in this example, the 12-foot mat thickness satisfies the Load Combinations 11 and 15 with three or four layers of bottom reinforcement, two layers of top reinforcement, and shear ties throughout the basemat.

Currently, ASME Code, Section III, Division 2 permits considering the effects of concrete cracking in determining internal shell forces. Steel stresses in bonded reinforcement are always limited to the elastic range for Service Loads. For primary Factored Loads, some yielding in the bonded reinforcement is permitted; however, no yielding can occur in the membrane zone of the shell. For membrane plus bending, bonded steel strains are limited to 2 x yield strain. Tendon stresses are limited to the elastic range for both load categories. The liner plate allowable strain limits in Table CC-3720-1 exceed plate yield strain for Service and Factored Load categories.

Two features in the internal structures of Figure 1 should be noted because of their relevance for severe accident design: (a) the primary and secondary shield walls, in addition to supporting the NSSS components, provide missile shield function against internally generated missiles; (b) the 3-foot-thick concrete fill slab protects the basemat liner. Design for potential melt attack and missile effects of severe accidents should utilize design arrangements, material selection, and impactive load design techniques to accommodate the demands on containment internal structures. A committee of ACI 349 should formulate appropriate approaches for these aspects.

## CALCULATED PRESSURE CAPABILITY OF DESIGNED CONTAINMENTS

Since the incident at Three-Mile Island nuclear plant, it has become necessary to calculate the ultimate pressure capability of containment structures. This is required by Standard Review Plan 3.8.1, although no specific acceptance criteria for the calculated capacity is specified. The

calculated capacities are also used in probabilistic risk assessment studies, including the on-going individual plant examination (IPE) in response to Generic Letter 88-20.

Table 2 summarizes the results and acceptance criteria used for pressure capacity evaluation for the PWR, prestressed containment discussed in the previous section. The containment has been designed to the current requirements of ASME Section III, Divisions 1 and 2. A simplified global shell analysis using axisymmetric elements was used to determine the shell response to pressure , prestressing, and dead loads. Nonlinearities due to concrete cracking, yielding of bonded reinforcement and liner, and basemat uplift were considered in the analysis. The minimum specified material properties were used in the response evaluation.

Table 2. Capacity Factors[a] for Major Elements in Pressure Boundary of Example Containment (Pressure = 155 psig)

| Parameter | Acceptance Criteria | Capacity Factor[a] |
|---|---|---|
| Strain: | | |
| • Hoop tendon | Yield strain = 0.01 | 1.00 |
| • Meridional tendon | Yield strain = 0.01 | 1.20 |
| • Liner | 12 x yield strain = 0.02 | 1.40 |
| • Hoop reinforcement | 5 x yield strain = 0.01 | 2.86 |
| • Meridional reinforcement | 5 x yield strain = 0.01 | 2.00 |
| Radial Shear: | | |
| • Basemat near containment wall junction | ASME, Section III, Division 2, Subsection CC, Factored Load allowables | 1.19 |
| • Containment wall near basemat junction | | 2.90 |
| • Containment wall away from basemat junction | | Greater than 18 |
| • Dome | | Greater than 30 |
| Parts not backed by concrete: | | |
| • Buckling of spherically dished head in 25' diameter equipment hatch | ASME, Section III, Division 1, Subsection NE and Appendix F, Service Level D allowables | 1.06 |
| • Highly stressed part of emergency exit airlock (elastic analysis, surface stress intensity). | | 1.02 |

[a] Capacity Factor = Response due to Pressure ÷ Criterion Limit

Table 2 also summarizes the acceptance criteria used for various elements. These are strain limits for tendons, liner, and bonded reinforcement exclusive of shear ties. For radial shear, the Factored Load allowable of ASME, Section III, Division 2 is used. For parts of pressure

boundary, not backed by concrete, the Service Level D allowables of the ASME Code, Appendix F are used.

The following observations are made from the results in Table 2:

- The pressure capacity of the containment is governed by the hoop tendon yielding in the membrane zone of the wall. The ultimate capacity, $P_u$, is 155 psig. This capacity is 2.87 times the design pressure, $P_a$, of 54 psig.
- At 155 psig, liner and bonded reinforcing bars yield; however, a margin exists against the strain acceptance limits used. These limits were set based on the 1:6-scale model reinforced concrete containment test. (This model is further discussed in the next section). The calculated liner strain at $P_u$ is 0.014. This strain exceeds the corresponding strain limit of 0.003 in Table CC-3720-1 of ASME, Section III, Division 2.
- In this containment, shear ties are provided in the basemat, dome, and wall except for the wall elevations from 40 feet above the basemat to 19 feet below the spring line. Considering the provided shear reinforcement, the calculated margin factors are comfortably high.
- For parts of pressure boundary not backed by concrete, elastic analysis and the Service Level D allowables used here show these elements do not govern. Current ASME Code permits using the Service Level D allowables for dynamic loading, such as jet impingement, but not for pressure loading. The use of Service Level D allowables for ultimate capacity evaluation is considered conservative. Code guidance is needed to have more realistic allowables for ultimate pressure evaluation.

Although not reflected in Table 2, it was also necessary to resolve certain displacement-related issues to show acceptability of 155 psig for $P_u$. These issues involved potential interactions with the polar crane bridge, piping, and adjacent buildings.

Table 3 summarizes the calculated $P_u$ for six containments. The design time- frame for these containments spans from the 1960s to the 1980s. Three different groups of engineers were involved in these evaluations. Although there is a difference in the selection of material properties used in analysis (i.e., minimum specified or actual), the calculated $P_u$ values are 2.5 or more times the corresponding design pressure, $P_a$. In all cases, the wall membrane capacity has been found to be the controlling element.

## PRESSURE CAPABILITY FROM TESTS

Testing of scale-model containments to failure and interpreting results using analytical models with increasing degrees of sophistication provides useful basic information. For design purposes, however, simplified global models are needed because the intent of the design is to estimate a pressure capacity at which a containment reaches a limit but does not fail.

Table 3. Calculated Ultimate Pressure Capacity, $P_u$, of Several Concrete Containments

| Case | Containment (Source of Data) | Design Time Frame | $P_s$ (psig) | Criteria and Material Properties for $P_u$ | $P_u$ (psig) | $P_u/P_s$ |
|---|---|---|---|---|---|---|
| 1 | PWR, post-tensioned (Reference 3) | Late 1960s | 47 | • Hoop tendon yielding<br>• Average actual properties | 134 | 2.85 |
| 2 | PWR post-tensioned (Reference 4) | 1970s | 50 | • Hoop tendon yielding<br>• Minimum specified properties | 125 | 2.50 |
| 3 | PWR, post-tensioned (This paper) | Late 1980s | 54 | • Hoop tendon yielding<br>• Minimum specified properties | 155 | 2.87 |
| 4 | BWR, Mark II, post-tensioned (Reference 5) | Mid 1970s | 45 | • Hoop tendon yielding<br>• Average actual properties | 228 | 5.07 |
| 5a | BWR, Mark III, reinforced (Reference 6) | Late 1970s | 15 | • Yielding of all reinforcement at critical section near spring line, hoop direction<br>• Average actual properties | 67 | 4.50 |
| 5b | Same as 5a | Same as 5a | Same as 5a | • Same as 5a<br>• Minimum specified properties | 56 | 3.73 |
| 6 | BWR, Mark III, reinforced (Reference 5) | Late 1970s | 15 | • Yielding of all reinforcement at critical section, mid-height of wall, hoop direction<br>• Average actual properties | 95 | 6.3 |

The following information items from the fragility test, on the 1:6-scale model reinforced concrete containment are considered important for implementing design procedures (see Reference 7):

- Except for minor modifications necessitated by the scaled down fabrication and construction requirement, the design reflected the ASME, Section III, Division 1 and Division 2 requirements. The design accident pressure was 46 psig.
- Failure occurred due to a liner tear near a cluster of piping penetrations. Although the model was pressurized up to 145 psig, the discussion in Section 3 of Reference 7 indicates this liner tear initiated at a pressure of 140 psig. This test result yields a ratio, $P_u/P_a$, of 140 ÷ 46 = 3.04
- The wall-to-basemat junction did not show any indication of shear distress at the maximum test pressure. The discussion in Section 5.9 of Reference 7 projects a shear capability corresponding to internal pressure of 175 psig.
- At maximum test pressure, the peak strains measured in the liner and reinforcing bars at locations that were not subject to strain raisers (i.e., the far-field strains) can be used to develop strain-based acceptance criteria. The values used in Table 2 were developed from this consideration and measured strains from the 1:6-scale model test. When such limits are used with global containment analysis, additional refined analytical models are not necessary for design purposes.

## DESIGN CODE AND REGULATORY IMPLICATIONS

Based on our experience in past containment evaluations for severe accidents, it is clear that existing containments have the capability to handle severe accidents because of the margin between the design basis condition and the actual ultimate capacity. However, future containment designs need to explicitly address the containment capability to handle severe accidents in order to reduce uncertainties associated with the response of containments to these low-probability events. The containment structural design requirements, defined in the national codes, should be independent of the mechanistic evaluation of the containment system to determine severe accident loads. Guidelines for making deterministic evaluations to obtain containment severe accident loads considering different reactor types and system designs should be provided by the U.S. Nuclear Regulatory Commission (USNRC) with input from industry (i.e., owners, NSSS vendors, engineering firms, and research laboratories).

Although the quantification of severe accident design loads for different system designs and reactor types remains to be made, the types of load challenges are known. The containment structural design code committees should now formulate code modifications for directly considering severe accidents. It is with this sentiment in mind that recommendations for future code changes are made based on information summarized in this paper. Suggestions for ASME, Section III, Division 2, Subsection CC; ASME, Section III, Division 1, Subsection NE; and ACI 349 follow.

**ASME, Section III, Division 2, Subsection CC**

The structural design of the concrete containment pressure boundary is within the scope of this standard. The review of design experience shows that the LOCA pressure, $P_a$, most significantly influences the containment arrangement and design. In view of the acceptability of previous designs, the design concept considering LOCA loads should be maintained; additional checks should be provided to consider ultimate pressure capability. The code currently has two categories: Service Loads and Factor Loads. It is proposed that a third category, "Ultimate Loads," should be developed. This category would include one load combination defining the load factors and allowables for the static severe accident pressurization combined with temperature. As a minimum, guidance should be provided for the following items:

- The code should provide guidance for making a global, axisymmetric, static, nonlinear analysis for the ultimate pressure condition combining the effects of concrete cracking; yielding of liner, reinforcing steel, and post-tensioning tendons; and basemat uplift.
- The code should define strain-based acceptance criteria for liner, reinforcing steel, and tendons for global far-field strains, which would ensure that local strains remain within their ultimate limit. These limits may be based on far-field test strains in scale containment models. Values used in Table 2 were obtained from the 1:6-scale reinforced containment model test (see Reference 7).
- The code requirements for the Ultimate Load category should consider realistic criteria for flexural shear. The conservatism in current flexural shear requirements of the code for Factored Load category should be reexamined for use in the Ultimate Load category. Pursuing containment model test results discussed in References 8 and 9 may be one approach to arrive at more realistic shear criteria.
- Rules should be developed to ensure that the capacity at penetrations exceeds the shell failure mode capacity.

The addition of the Ultimate Loads category to the code will factor in the displacement-related issues into the design process. The availability of code procedures for static overpressurization will also be useful for a first-order assessment of dynamic pressurization if such a severe accident condition needs to be addressed.

**ASME, Section III, Division 1, Subsection NE**

The design of pressure boundary not backed by concrete is within the scope of this code. Code guidance should be provided for reviewing components for static overpressurization considering existing test and analysis results on containments and penetrations. Criteria for shell elements subject to buckling are particularly important because buckling by itself does not imply a failure of the pressure boundary.

## ACI Standard 349

The severe accident challenges of melt attack and missiles will require design actions related to layout arrangement, material selection for boundaries that can be potentially in contact with the molten core, and impactive load design. A committee consisting of representatives from ACI 349 and organizations with expertise in the containment severe accident events should be formed to prepare recommendations for addressing severe accidents in ACI Standard 349.

## REFERENCES


1. D. A. Ward, Chairman ACRS, to Honorable K. M. Carr, Chairman, USNRC, "Proposed Criteria to Accommodate Severe Accidents in Containment Design," May 17, 1991.

2. S. Putman and A. Walser, "Containment Structure Optimization," Proceedings American Power Conference, April 23-25, 1979, Chicago IL.

3. A. Walser, "Analyses of Zion Containment," Proceedings of the Workshop on Containment Integrity, Vol. II, NUREG/CP-0033, SAND 82-1659, October 1982.

4. Commonwealth Edison Company, "Updated Final Safety Analysis Report: Byron/Braidwood Stations," Section 3.8.1.8.

5. C. N. Krishnaswamy, R. Namperumal, and A. Al-Dabbagh, "Ultimate Internal Pressure Capacity of Concrete Containment Structures," Paper J3/6, SMiRT 7, August 22-26, 1983, Chicago IL.

6. J. P. McGaughy, Jr., F. T. Lin, and S. K. Sen, "Ultimate Internal Pressure Capacity of a Reinforced Concrete Mark III Containment, Paper J3/9, SMiRT 7, August 22-26, 1983, Chicago IL.

7. D. B. Clauss, "Round-Robin Analysis of the Behavior of a 1:6 - Scale Reinforced Concrete Containment Model Pressurized to Failure: Post-test Evaluations," NUREG/CR-5341, SAND89-0349, October 1989.

8. Y. Aoyagi, O. Isobat, and N. Tanaka, "Design Method of Shell Wall End of Reinforced Concrete Containment Vessel (RCCV) Against Radial Shear," Paper J4/6, SMiRT 5, August 13-17, 1979, Berlin.

9. H. P. Walther, "Evaluation of Behavior and the Radial Shear Strength of a Reinforced Concrete Containment Structure,", NUREG/CR-5674, SAND91-7058, January 1992.

**Figure 1. Cross-Section Through a Typical PWR Prestressed Concrete Containment**

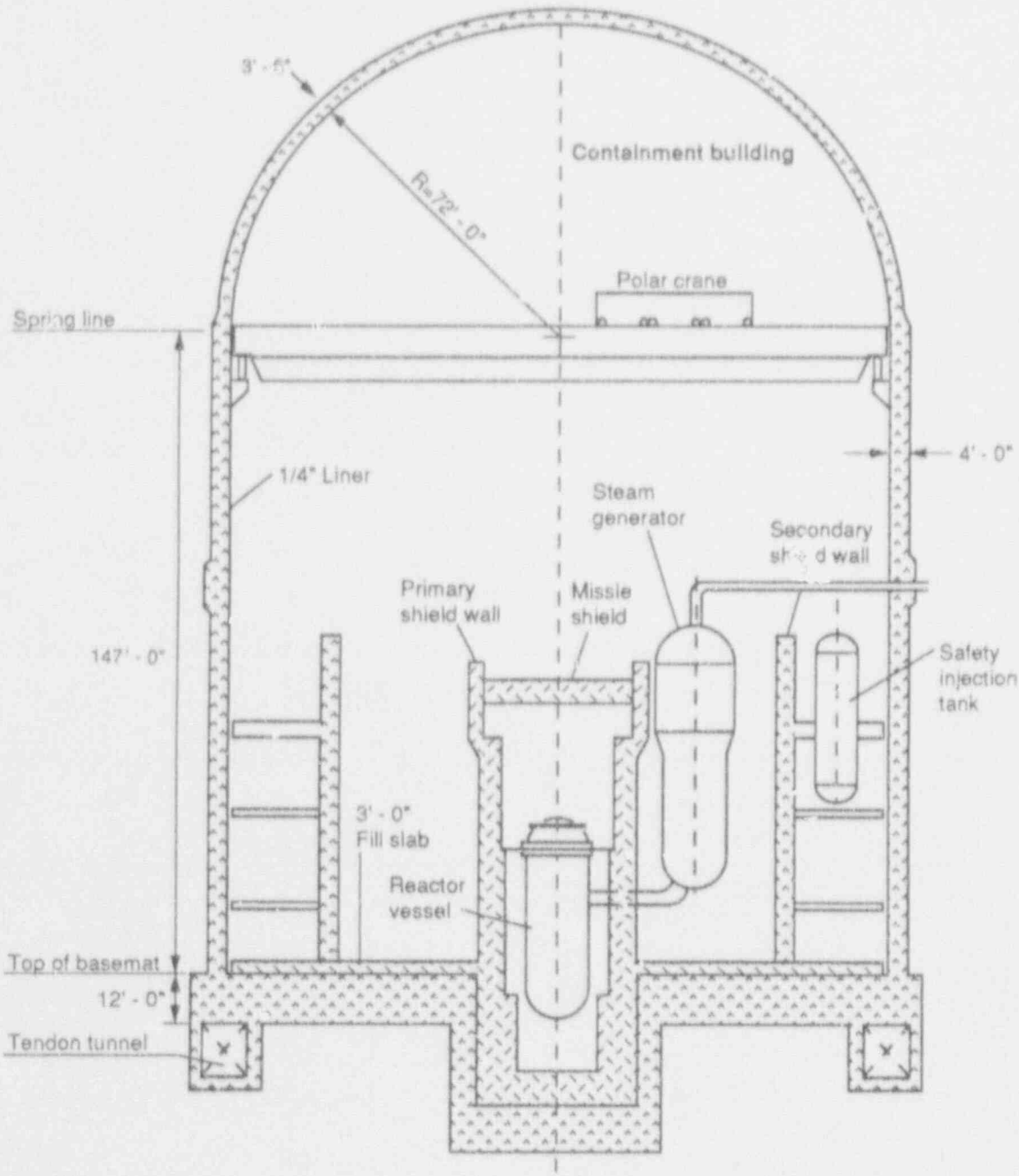


M5286.002

Figure 2. Variation of LOCA Design Pressure with Containment Volume (Typical for PWR)

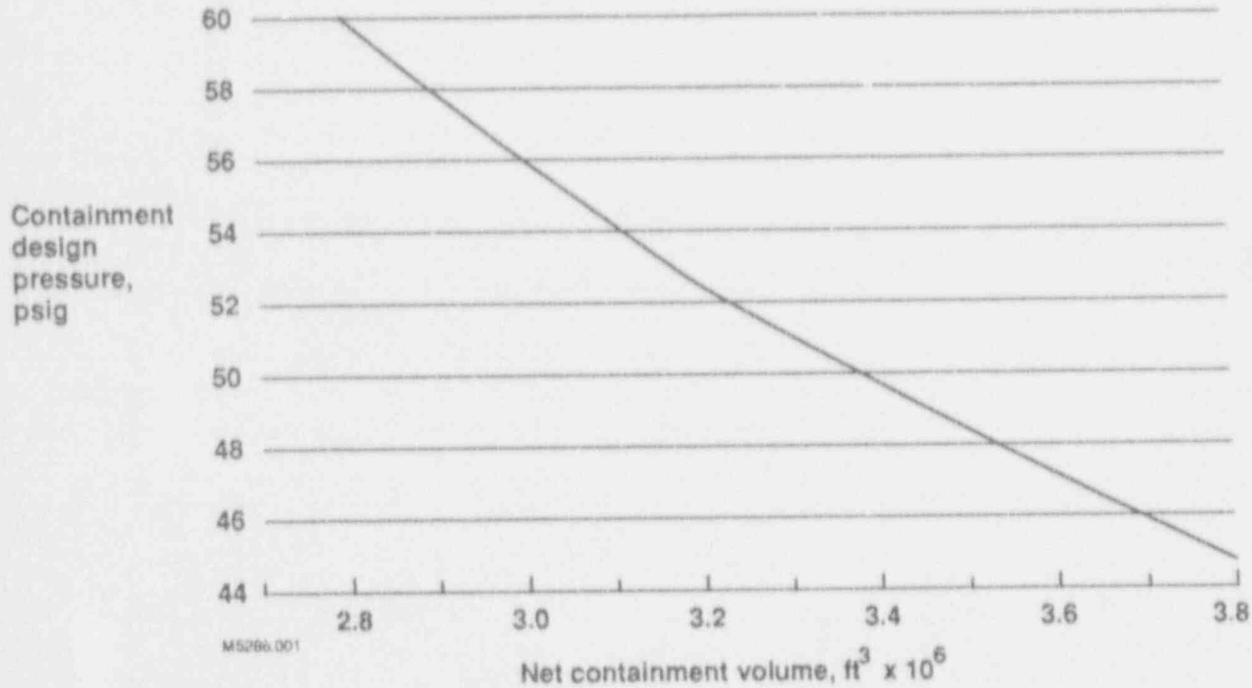

# DESIGN BASES AND SEVERE ACCIDENT CONSIDERATIONS FOR THE SYSTEM 80+™ CONTAINMENT DESIGN

Raymond E. Schneider and Lyle D. Gerdes
ABB-Combustion Engineering, Inc.

J. Todd Oswald and J. Frank Snipes, Jr.
Duke Engineering & Services, Inc.

## Abstract

Containments for Advanced Light Water Reactors (ALWRs) must not only be designed for design bases conditions but also be evaluated for postulated severe accident concerns. This paper presents the containment design description for the System 80+ ALWR, the conservative design bases specified and the System 80+ ALWR design features to prevent and mitigate the challenges considered in postulated severe accident scenarios. Included in the containment design bases are postulated primary and secondary pipe break conditions and seismic requirements for an envelope of site conditions with a control motion having much higher energy content than those used for existing reactor designs. Severe accident considerations addressed include prevention and mitigation design features incorporated into the System 80+ ALWR.

## 1.0 INTRODUCTION

The controlling design basis events for the System 80+ reactor containment consist of postulated large breaks in the primary and secondary piping and the Safe Shutdown Earthquake (SSE). The use of conservative design bases, design and analysis methods, and acceptance criteria provide a robust System 80+ containment design which is also capable of withstanding the very low-probability beyond design basis events (severe accidents). All credible challenges to the containment have been evaluated and, in addition, design features have been included to prevent and mitigate postulated severe accidents.

## 2.0 CONTAINMENT DESIGN

### 2.1 Description

The System 80+ Standard Plant design includes a two hundred foot diameter, 1-3/4 inch thick, free standing spherical steel containment vessel enclosed in a cylindrically shaped concrete shield building with a hemispherical dome (see Figure 1). The lower portion of the steel sphere is encased in concrete. Major accesses include a large equipment hatch and two personnel airlocks. The design provides a large dry containment with a free volume of approximately 3.3 x $10^6$ cubic feet (see Figure 2). The spherical shape provides maximum operating and laydown area for construction, maintenance, and refueling.

## 2.2 Codes and Standards

The containment is designed to the requirements set forth in the ASME Boiler and Pressure Vessel Code [1]. Analysis is performed for service loads, stability, ultimate capacity (including hydrogen burn), and construction loads. Design bases loads and combinations are per NUREG-0800 [2], and Regulatory Guide 1.57 [3].

## 3.0 DESIGN BASES

The safety design basis for the System 80+ containment is the requirement that the release of radioactive materials subsequent to an accident does not result in doses in excess of the values specified in 10CFR100 [4]. The containment must withstand the pressure and temperatures of the design basis accident without exceeding a design leakage rate of 0.34% volume for the first 24 hours and one percent volume thereafter is based on a leak rate associated with half of the peak pressure assuming a 0.34% volume leak rate at peak pressure.

The controlling service level design basis events for the System 80+ containment consist of postulated large breaks in the primary and secondary piping and seismic excitation. These events produce the maximum temperatures and pressures in containment and the maximum dynamic inertial loads. The maximum compressive stresses for the stability analyses are produced from a vacuum pressure due to inadvertent spray initiation and seismic excitation.

## 3.1 Postulated Design Basis Pipe Breaks

The postulated pipe breaks which are limiting for the System 80+ containment design are the double ended guillotine breaks in the primary system piping, referred to as the large Loss of Coolant Accident (LOCA), and the double ended guillotine break in the secondary piping, referred to as the Main Steam Line Break (MSLB). The containment pressure and temperature design requirements resulting from these postulated breaks are 49 psig and 290°F, respectively. All other postulated breaks are also evaluated for plant and system design; however, the large LOCA and MSLB are controlling for containment design.

## 3.2 Seismic Design Bases

The System 80+ seismic design parameters were chosen to envelope the majority of potential nuclear reactor plant sites in the United States and abroad. Both current and anticipated Nuclear Regulatory guidance were considered in selection of both ground motion and soil profile parameters.

### 3.2.1 Soil Profiles

To cover a maximum range of possible site conditions where the System 80+ design may be constructed, a range of generic site conditions was selected. A total of 13 cases were developed corresponding to 12 soil cases and one rock case. Since each potential site has unique seismic response characteristics, the investigation and selection of multiple generic sites for design purposes required the consideration of resonance between the building structures and the site soil strata. The sites selected for the Soil Structure Interaction (SSI) analyses have free-field amplifications that cover a broad range of frequencies with which fundamental structural frequencies may coincide. Hence, the envelope of the results provide the maximum seismic response to the SSE and Operating Basis Earthquake (OBE) motions when the plant is founded on soil sites that are bounded by the selected soil profiles.

Generic soil sites were selected by first choosing four generic site categories designated A, B, C and D. These categories were chosen to represent appropriate total thickness of soil overlying bedrock. Site Category A consists of 52 feet of soil overlying bedrock. The soils in Category B extend to a depth of 100 feet and those in Categories C and D extend to depths of 200 and 300 feet, respectively.

One case was selected for Category A and one case for Category D; these were designated Case A-1 and Case D-1. Four cases were initially selected for site Category B; these were designated Cases B-1, B-2, B-3, and B-4. Three cases were initially selected for site Category C; these were designated Cases C-1, C-2, and C-3. Upon examination of the results of the response analyses for these cases, three additional cases were added. The additional cases were designated Cases B-1.5, B-3.5, and C-1.5. The latter cases were selected to properly and conservatively cover the response at frequencies that did not seem to be adequately covered by the other analysis cases. A shear wave velocity distribution with depth was selected to provide a reasonably wide range and also to provide significant contrast in velocities at certain depths for a selected number of cases.

### 3.2.2 Earthquake Ground Motion

The control motion design response spectra are anchored to a 0.3g peak ground acceleration. They were developed with the objective of being in full compliance with NUREG-0800 [2] guidance as well as the EPRI ALWR Utility Requirements Document (URD) [5]. Again, to cover a maximum range of possible sites where the System 80+ standard design may be constructed, three separate control motion spectra were developed:

a. Control Motion Spectrum 1 (CMS1): This spectrum is a soil spectrum identical to Regulatory Guide 1.60 (R.G. 1.60) [6] spectrum. It is considered in order to cover sites with deep soil deposits.

b. Control Motion Spectrum 2 (CMS2): This is a rock outcrop spectrum and is developed to cover sites typical of Eastern North America which could be subjected to earthquakes with high frequency content.

c. Control Motion Spectrum 3 (CMS3): This is a rock outcrop spectrum and is developed based on recommendations of NUREG/CR-0098 [7] primarily to cover lower frequency motions which may not be covered by CMS2. In addition, it is in full compliance with NUREG-0800 [2] Section 2.5.2.6, Item 3, for "scaling the acceleration, velocity and displacement values by appropriate amplification factors." It is also enhanced with respect to NUREG/CR-0098 [7] in the high frequency range to cover earthquakes with high frequency content. The maximum spectral acceleration range is extended to 15 Hz, as opposed to 8 Hz which is used in NUREG/CR-0098 [7] motions.

All of the above Control Motion Spectra are shown in Figure 3. CMS2 and CMS3 are applied at the rock outcrop, and CMS1 is applied at the free-field ground surface. All three motions are applied to each of the 13 sites to conservatively cover all combinations. Figures 4 and 5 provide schematic representations of how the control motions are applied in the System 80+ Soil Structure Interaction (SSI) analyses.

### 3.2.3 Seismic Margin in Containment

The System 80+ containment has a large seismic margin beyond the design basis earthquake. As stated in Section 3.2.2, the control motion design response spectra are anchored at 0.3g peak ground acceleration. The containment structure would not be expected to yield until peak ground accelerations of 0.6g at the rock outcrop or 1.2g at the free field surface are experienced.

## 4.0 SEVERE ACCIDENT CONSIDERATIONS

Severe accident considerations were included in the design of the System 80+ containment by focusing on the truly risk significant concerns. The underlying philosophy in developing System 80+ severe accident design features is to emphasize accident prevention while simultaneously providing design features to mitigate any severe accident. The design process utilizes probabilistic risk assessment (PRA) methods to identify events and sequences which contribute measurably to plant risk. Deterministic analyses, in support of the PRA, were used to identify the best available courses of action for dealing with severe accident concerns. By doing this early in the plant design process, it was possible to provide timely feedback to the designer on the performance of critical systems and containment structures during severe accidents.

The following sections provide information regarding the severe accident prevention and mitigation characteristics of the System 80+ design, and an assessment of the relevent severe accident phenomenology as it applies to System 80+.

## 4.1 SYSTEM 80+ DESIGN FEATURES INTENDED FOR SEVERE ACCIDENT PREVENTION

A primary goal in designing System 80+ was to ensure that the probability of an initiating event becoming a severe accident was for all practical purposes negligible. To accomplish this goal, PRA was closely factored into the design process. This close coupling of design and PRA provided an effective means for focusing on areas in the present PWR design which could be improved and selecting effective design changes to both improve plant reliability and reduce public risk.

A partial list of System 80+ design enhancements include:

1. Use of a four train Emergency Feedwater System (EFWS) with two turbine driven pumps and two motor driven pumps to provide a highly reliable emergency feedwater supply.

2. Use of a non-safety grade Startup Feedwater System for normal startup and shutdown operations. This reduces the demands on the EFWS.

3. Use of a four train Safety Injection System (SIS) with Direct Vessel Injection (DVI) to enhance the reliability of the inventory control function.

4. Use of an In-containment Refueling Water Storage Tank (IRWST) to eliminate the need for a Recirculation Actuation Signal (RAS).

5. Use of a larger pressurizer and larger steam generators to make the system response to transients slower and more resilient.

6. Use of a Safety Depressurization System (SDS) to provide the capability to depressurize the Reactor Coolant System (RCS) allowing the capability for once through core cooling.

7. Use of dedicated batteries, independent of the station batteries, to start the diesel generators.

8. Use of a combustion turbine as an alternate backup AC source to the diesel generators.

As a result of increased system reliability and enhanced capabilities, the frequency of core damage caused by internal events was reduced to $6.7 \times 10^{-7}$ events/year. This is well below the typical $10^{-4}$ internal event core damage frequency commonly found in PRAs of operating plants. Also, the total core damage frequency including external events is $1.87 \times 10^{-6}$ which is well below the EPRI ALWR URD [5] goal of $1.0 \times 10^{-5}$.

## 4.2 SYSTEM 80+ DESIGN ENHANCEMENTS FOR USE IN SEVERE ACCIDENT MITIGATION

In addition to systems designed to prevent accidents, System 80+ also contains many unique design features to enhance severe accident mitigation and management. The overall goal of the severe accident mitigation features of the System 80+ were to reduce the risk of a core damage containment failure given a core melt to 0.1 and to minimize the contribution of early containment failure events.

### 4.2.1 Mitigation Features to Prevent Early Containment Failure

Existing PRAs note that early containment failures can arise as a result of various severe accident phenomena. Mechanisms contributing to early containment failure include:

1. Hydrogen Detonation
2. Direct Containment Heating
3. Steam Explosions (In-Vessel and Ex-Vessel)
4. Rapid Steam Generation
5. Direct Corium Attack/Missile Generation

The following sections discuss these phenomena and the role of System 80+ design features in mitigating severe accident consequences.

#### 4.2.1.1 Hydrogen Deflagration/Detonation

The production of hydrogen within the RCS and subsequent release to the containment following an assumed core melt has been noted to be a potential contributor to early containment failure for existing PWRs. Hydrogen combustion can challenge containment either statically, as a deflagration (slow hydrogen burn) or, dynamically, as a detonation. In light of this concern, System 80+ has been designed with several features to both mitigate and respond to this containment challenge. These features are discussed below.

##### 4.2.1.1.1 System 80+ Containment Design

The System 80+ design includes a large, spherical, open, steel containment. The containment structures have been designed to enhance mixing, and the containment has been sized to ensure that detonatable concentrations of hydrogen would not accumulate. Stress evaluations of this design indicated that the System 80+ containment is a very robust containment design with an ultimate failure pressure of between 185 to 208 psia (4 inch maximim radial strain) and ASME Boiler and Pressure Vessel Service Level C limit of 155 psia for a temperature of 350°F. Analyses of the ALWR designs of similar size to System 80+ (Reference 8) clearly show that the worst credible deflagration would result in containment shell loadings that are below the Service Level C stress limits (see Figure 6). These evaluations were confirmed for the System 80+.

#### 4.2.1.1.2 Hydrogen Mitigation System (HMS)

In an attempt to overwhelm the hydrogen combustion concerns, System 80+ is also equipped with an operator-actuated hydrogen mitigation (igniter) system. The purpose of this system is to minimize further the potential hydrogen challenge. Use of the HMS early in a severe accident scenario would ensure containment hydrogen challenges would be easily manageable.

### 4.2.1.2 Direct Containment Heating (DCH)

In the context of the System 80+ PRA, direct containment heating refers to a collection of assumed severe accident processes that occur upon lower head breach to pressurize an LWR containment. Processes included in DCH are (1) the blowdown of reactor coolant system steam, and hydrogen inventory into the containment, (2) the dispersal of corium into the upper containment, (3) direct heating of the containment atmosphere, (4) combustion of hydrogen released prior to and during the high pressure melt ejection process and (5) vaporization of available water. Several of these processes are not independent and the presence of certain processes in the DCH sequence may preclude others. However, all serious DCH threats are associated with depositing large quantities of energy directly into the containment atmosphere and thereby rapidly pressurizing the containment. In the design of System 80+, this issue is addressed by providing independent means of preventing any significant corium dispersal to the upper containment and by designing a strong, robust containment structure.

As discussed above, debris dispersal into the upper compartment is necessary for a DCH threat to containment. In fact, EPRI supported analyses show that by using typical System 80+ design parameters almost 60% of the total core inventory must be finely fragmented and entrained in the upper containment for a significant threat to develop (see Figure 7 and Reference 9). To minimize the potential containment threat due to DCH, ABB-CE has incorporated active (Safety Depressurization System) and passive ("debris retentive cavity with a convoluted vent") means for ensuring that most, if not all, the corium debris is retained within the reactor cavity. These systems/design features are discussed below.

#### 4.2.1.2.1 Safety Depressurization System (SDS)

The Safety Depressurization System consists of 2 trains of operator actuated relief valves located on the top of the pressurizer. The SDS serves several roles in the System 80+ design. In the context of severe accident mitigation, the SDS will allow a timely depressurization of the RCS to below the debris entrainment threshold pressure. Reactor Vessel (RV) failure at RCS pressures below the entrainment threshold pressure (approximately 250 psia for System 80+) will preclude entrainment of corium debris into the upper cavity. Successful actuation of this system will change an otherwise High Pressure Melt Ejection (HPME) scenario, with considerable entrainment potential, to a low pressure core ejection with no or very little expected corium debris entrainment. This limits DCH pressure spikes to pressures that only modestly exceed design basis limits.

#### 4.2.1.2.2 Debris Retentive Cavity

System 80+ includes a debris retentive reactor cavity configuration with sharp turns, overhangs, flowpath offsets, and a "debris trap" for the specific purposes of de-entrainment and retention of corium debris. Assessments of this ALWR design concept concluded that these design features should enable the reactor cavity to trap 90% of the ejected corium debris even during HPME scenarios.

### 4.2.1.3 Steam Explosions

A fuel induced steam explosion refers to the rapid steam generation and concomitant hydrodynamic loadings that occur when molten metal (such as corium) discharged into a water pool rapidly fragments and transfers its energy to the surrounding fluid. Steam explosions have been hypothesized to occur both interior and exterior to the RV.

#### 4.2.1.3.1 In-Vessel Steam Explosions (IVSE)

An IVSE consists of fuel coolant interaction which can hypothetically lift the RV upper head or generate a control rod missile of sufficient energy to breach the containment steel shell. Based on conclusions of the Steam Explosion Review Group (SERG), it can be expected that the potential containment failure probability due to In-Vessel Steam Explosions (IVSE) will be on the order of 0.001 (Reference 10). While this probability is very low, several members of the SERG believed this event to be even lower. In the System 80+ design the containment is protected from the consequences of an upper head or control rod missile by a missile shield located above the RV. Should any material bypass the missile shield, it would have to travel another 100 feet vertically, while still maintaining a sufficiently high velocity before the ejected material could pose a credible threat to containment.

#### 4.2.1.3.2 Ex-Vessel Steam Explosions (EVSE)

An EVSE occurs when corium ejected from the RV lower head falls into a water pool. EVSE loads are a potential concern for LWRs in that they can induce failure of RV supporting structures which may, in turn, cause failure of piping penetrating the containment. EVSEs have not been considered to be a significant threat to operating PWRs considered in the NUREG-1150 risk assessments (see Reference 11). This conclusion is also valid for System 80+. System 80+ is equipped with a Cavity Flood System (CFS). Thus, EVSE can occur in the System 80+ design when the CFS is actuated in advance of RV failure. However, the consequences of an EVSE are not expected to be significant since the loadings associated with the EVSE will not directly act upon the containment wall or any major RV or RCS supporting structure.

#### 4.2.1.4 Rapid Steam Generation

Rapid steam generation refers to the containment pressurization following RV breach associated with the RV vessel blowdown and non-explosive steam generation due to the rapid quenching of the corium debris. Assessments of containment pressure loads associated from assumed rapid steam generation indicate peak containment loadings will be below 70 psia. These loadings are well below the containment Service Level C stress limits and, consequently, do not pose a significant threat to containment integrity.

#### 4.2.1.5 Direct Shell Attack via Corium Impingement

The System 80+ containment is constructed to provide protection against missiles and hot gases that may be generated during severe accident scenarios. This protection is provided by 5 feet of concrete directly below the reactor vessel (3 feet at the edges of the reactor cavity) and containing the full RCS within a 4 foot thick crane wall. The uppermost portion of the containment shell is protected from missile impingement by the RV upper head missile shield. Thus, the System 80+ containment is invulnerable to direct corium attack below the top of the crane wall and marginally exposed to only those most energetic and very low probability corium missiles at the uppermost containment surface.

### 4.2.2 Containment Design Features to Prevent or Prolong Late Containment Failure

Mechanisms for late containment failure include:

1. Containment Overpressurization,
2. Basemat Melt-Through,
3. Temperature Induced Failure of Containment Penetration Sealant,
4. Delayed Hydrogen Burn.

Several design features of the System 80+ PWR are intended to prevent and/or mitigate the consequences of a containment failure by prolonging the containment failure. It has been a goal of the System 80+ design to deterministically demonstrate containment integrity for 48 hours after the severe accident initiating event and to probabilistically demonstrate that the conditional probability of containment failure following a core melt scenario is less than 0.1.

#### 4.2.2.1 Containment Overpressure Failure

Containment overpressure failure will result from steaming of the cooled corium debris (or, for that matter, an intact core) in the absence of containment heat removal. Such sequences are of low probability due to the high reliability of the System 80+ Containment Heat Removal (CHR) system. Severe accident analyses have demonstrated that even a partially functioning CHR system would remove sufficient energy from the containment atmosphere to maintain containment pressures well below failure limits.

In the unlikely event of a total and extended loss of CHR, MAAP [12] analyses of the System 80+ plant demonstrates that even for an unrecoverable station blackout scenario containment pressures can be maintained below the ASME Service Level C stress limits for more than 48 hours (see Figure 8). It should be noted that the analysis presented does not include any mitigative effects of station batteries. This long time to containment overpressure is a passive feature of the System 80+ plant which is a combined effect of the availability of large quantities of in-containment concrete (approximately 9% of the containment by volume) and a 500,000 gallon CFS coupled with a high strength containment structure.

#### 4.2.2.2 Basemat Melt-Through

Basemat melt-through refers to the process of concrete decomposition and destruction associated with an assumed corium melt interacting with the reactor cavity basemat. The basemat melt-through scenario is relatively benign. The accident progression is slow (taking from several days onward to penetrate the reactor cavity basemat) and the corium release to the environment is negligible since most of the corium will vitrify into a relatively impermeable substance within the containment's extended foundation.

To minimize the overall risk of containment melt-through System 80+ has been equipped with a manually actuated continuous Cavity Flood System and the cavity has been arranged with a floor area consistent with the EPRI debris coolability guidance of 0.02 $m^2$ of cavity floor area per thermal MW of core power. The intent of this design is to ensure a continuous water supply to the corium debris and to provide sufficient area so that corium accumulations will be relatively shallow (below 25 cm in depth) and coolable.

The System 80+ PRA assumes that, as a consequence of the cavity design, the availability and actuation of the CFS is sufficient to prevent a basemat melt-through scenario. While there is general agreement that water will retard the corium progression into the concrete basemat, there is not yet conclusive proof that a wetted corium debris bed with a depth greater than 25 cm will be fully coolable. It is expected that the ongoing Melt/Debris and Coolability Experiments (MACE program) will provide information to confirm the existing PRA position.

#### 4.2.2.3 Temperature Induced Failure of Containment Penetration Sealant

During an assumed dry cavity corium attack sequences, the containment atmosphere has the potential to undergo a gradual, but significant, temperature transient. Analyses of typical System 80+ accident scenarios suggest that sustained temperatures in excess of 450° F can develop throughout the containment within 48 hours after accident initiation. At these temperature levels several common penetration sealants (e.g., Nitril, Neoprene) will begin to degrade and potentially result in a localized containment failure. On the other hand, several other penetration sealants less prone to temperature failure are available on the market. By specifying an appropriate sealant, this containment failure mechanism will be averted.

#### 4.2.2.4 Delayed Hydrogen Burn

A delayed hydrogen burn can occur anytime in a postulated severe accident once a large quantity of hydrogen is generated and the containment atmosphere is not inerted. The most common scenario where a delayed hydrogen burn can occur is when a hydrogen rich, steam inerted containment is sprayed with water. This process is typically operator initiated and can result in a hydrogen combustion event at pressures just below the steam inerting limit. Because of the large amount of steam initially available, the combustion event is far more likely to be a deflagration than a detonation. Furthermore, pressures generated during this event will generally be below the containment ASME Service Level C pressure and should be well below the ultimate containment failure pressure.

As discussed in Section 4.2.1, System 80+ is equipped with igniters to burn off hydrogen at low concentrations. These igniters have been demonstrated effective in steam environments and, therefore, when actuated sufficiently early, should serve to fully eliminate any significant hydrogen induced containment threat.

## 4.3 SEVERE ACCIDENT CONSEQUENCES

The severe accident consequences for advanced reactors have been established such that the probability of exceeding radiological doses greater than 25 rem at distances beyond one-half mile from the reactor will be less than $1 \times 10^{-6}$ per reactor-year. PRA analyses for System 80+ indicate this probability to be less than $3 \times 10^{-7}$ per reactor-year.

## 5.0 CONCLUSION

The System 80+ containment is based on conservative design bases, design and analysis methods, and acceptance criteria. In addition, the System 80+ ALWR design represents a balanced approach to severe accident mitigation and prevention. Consequently, System 80+ is adequately designed with respect to severe accidents and represents a significant improvement in overall plant safety compared to existing reactor plant designs.

## REFERENCES


1. 1989 American Society of Mechanical Engineers (ASME) Boiler and Pressure Vessel Code, Section III, Division I, Subsection NE, "Class MC Components", New York, NY.

2. NUREG-0800 "Standard Review Plan for the Review of Safety Analysis Reports for Nuclear Power Plants", U.S. Nuclear Regulatory Commission, Office of Nuclear Reactor Regulation, June 1987.

3. Regulatory Guide 1.57, "Design Limits and Loading Combinations for Metal Primary Reactor Containment System Components", U.S. Atomic Energy Commission, June 1973.

4. 10CFR100, U.S. Code of Federal Regulations - Title 10, Part 100, "Energy", Office of the Federal Register National Archives and Records Administration, Washington, D.C.

5. Advanced Light Water Reactor Utility Requirements Document, Volume II, "ALWR Evolutionary Plant", Electric Power Research Institute, Palo Alto, California, 1990.

6. Regulatory Guide 1.60, "Design Response Spectra for Seismic Design of Nuclear Power Plants", U.S. Nuclear Regulatory Commission, December 1973.

7. Newmark, N.M., Hall, W.J., "Development of Criteria for Seismic Review of Selected Nuclear Power Plants", NUREG/CR-0098, May 1978.

8. ARSAP Report, "Prevention of Early Containment Failure Due to High Pressure Melt Ejection and Direct Containment Heating for ALWRs", J. Carter, et. al., March 1990.

9. "Technical Support for the Hydrogen Control Requirements for the EPRI Advanced LWR Requirements Document", FAI, January 1990.

10. NUREG/CR-5567, "PWR Dry Containment Issue Characterization", Wang, Y., August 1990.

11. NUREG-1150, Volume 2, Appendix C, "Severe Accident Risks: An Assessment for Five Nuclear Power Plants: Appendicies", USNRC, June 1989.

12. Fauske & Associates, Inc., "Modular Accident Analysis Program (MAAP)", Atomic Industrial Forum, IDCOR Program Technical Report 16.2-3, February 1987.

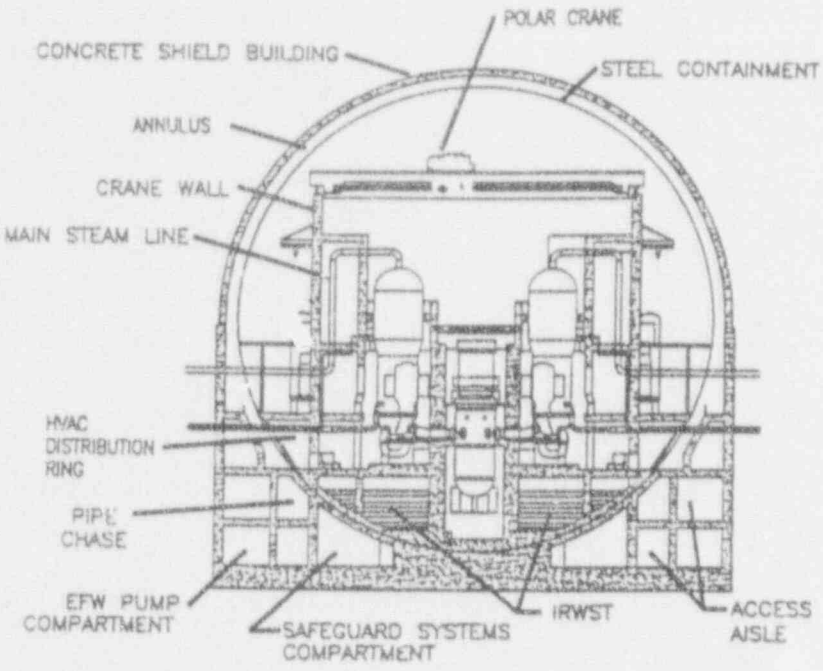


Figure 1. System 80+ Reactor Building

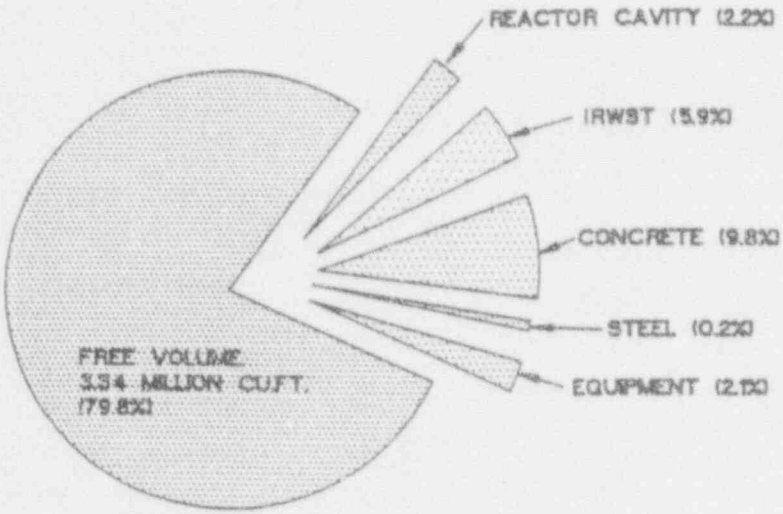


TOTAL VOLUME = 4.2 MILLION CUBIC FEET

Figure 2. System 80+ Containment Volume

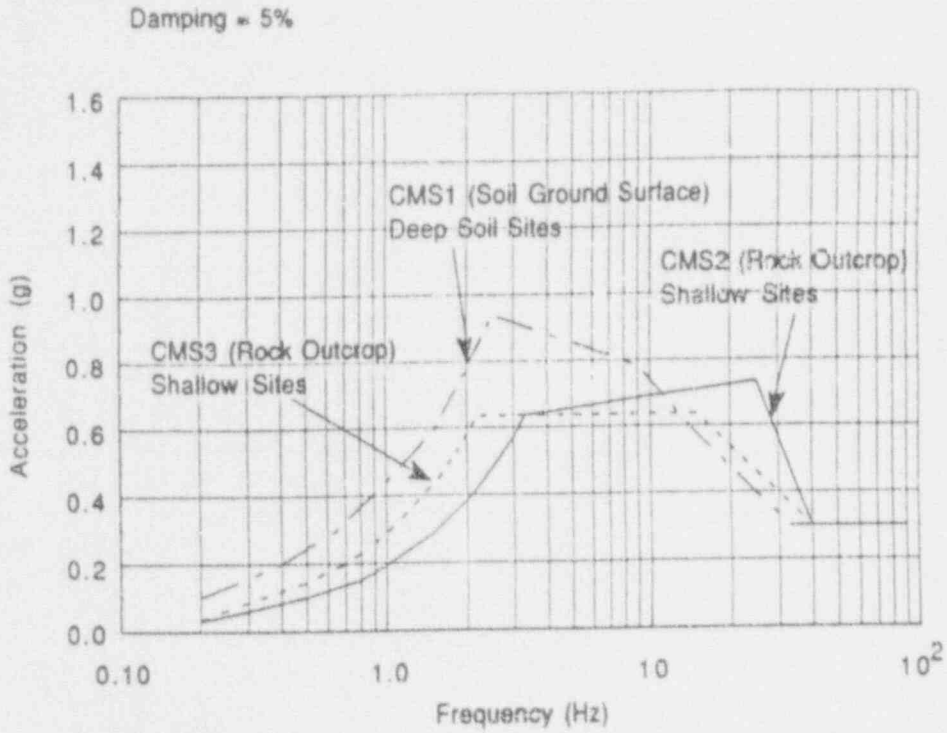


Figure 3. System 80+ Control Motion Spectra

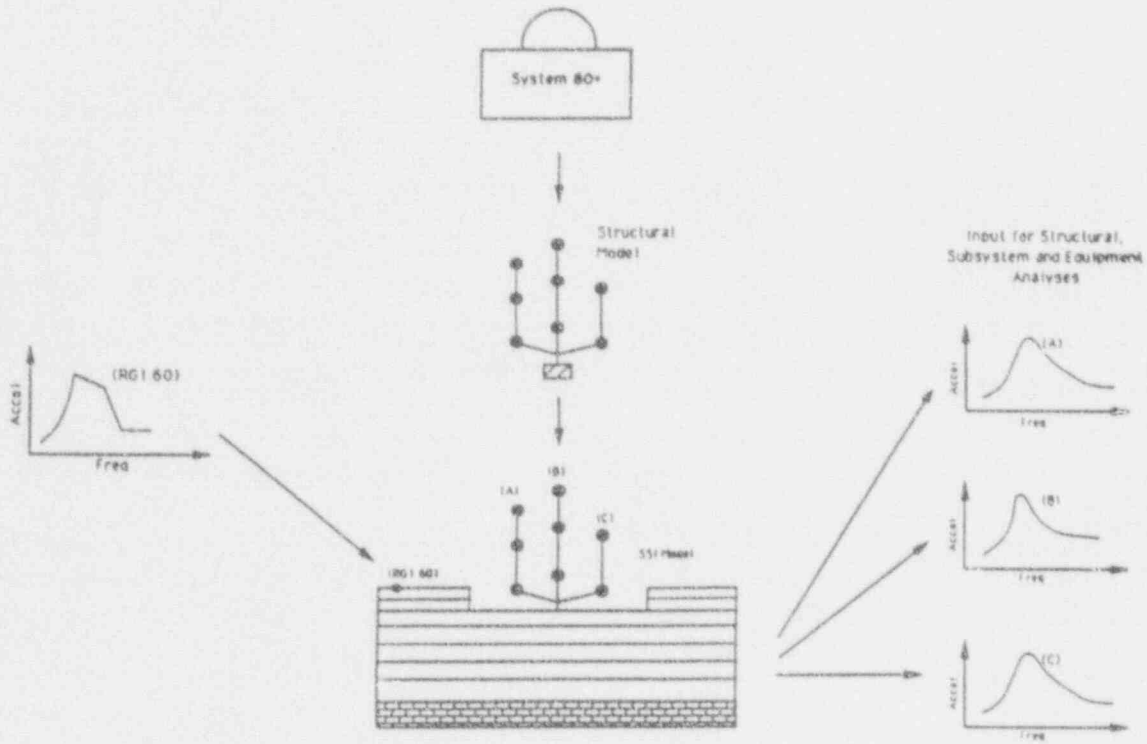


Figure 4. Application of Control Motion Spectra CMS1 in SSI Analysis

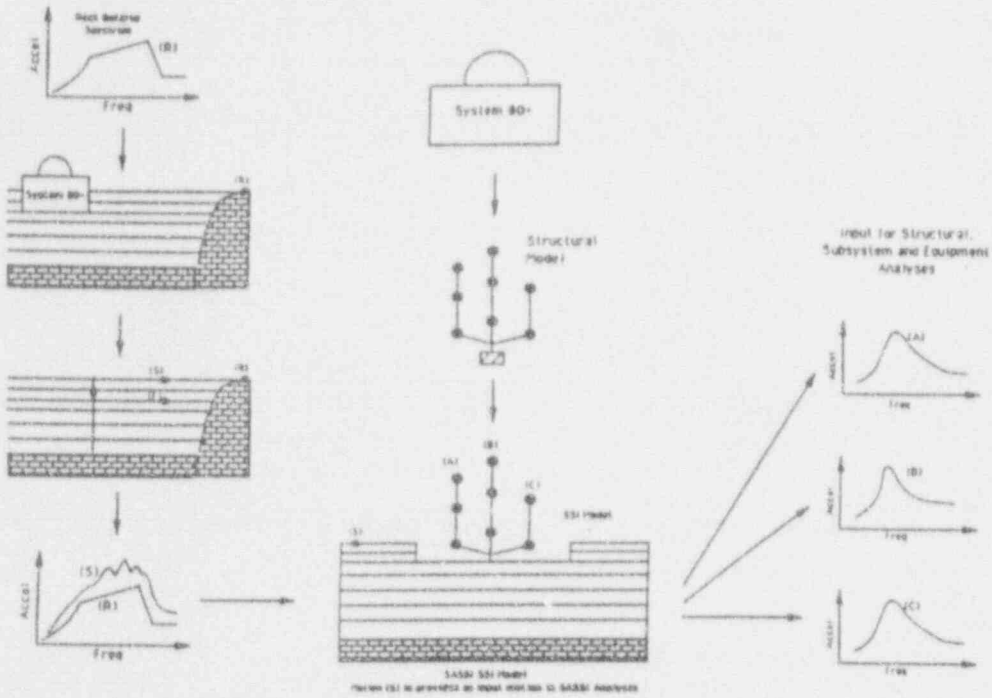


Figure 5. Application of Control Motion Spectra CMS2 and CMS3 in SSI Analysis

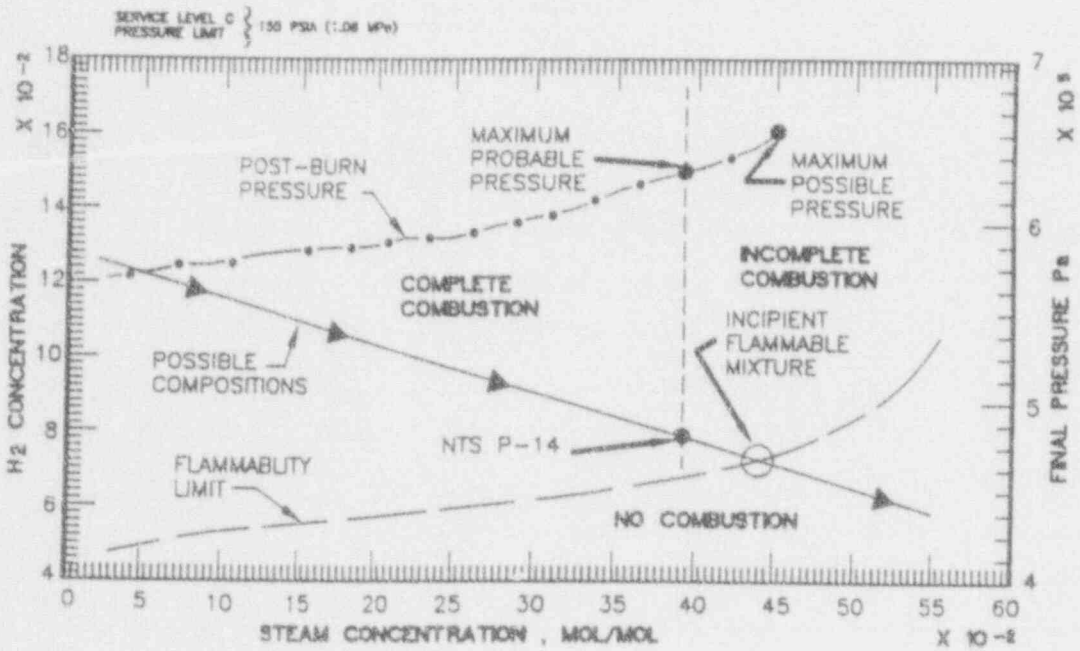


Figure 6. Combustion Potential for System 80+

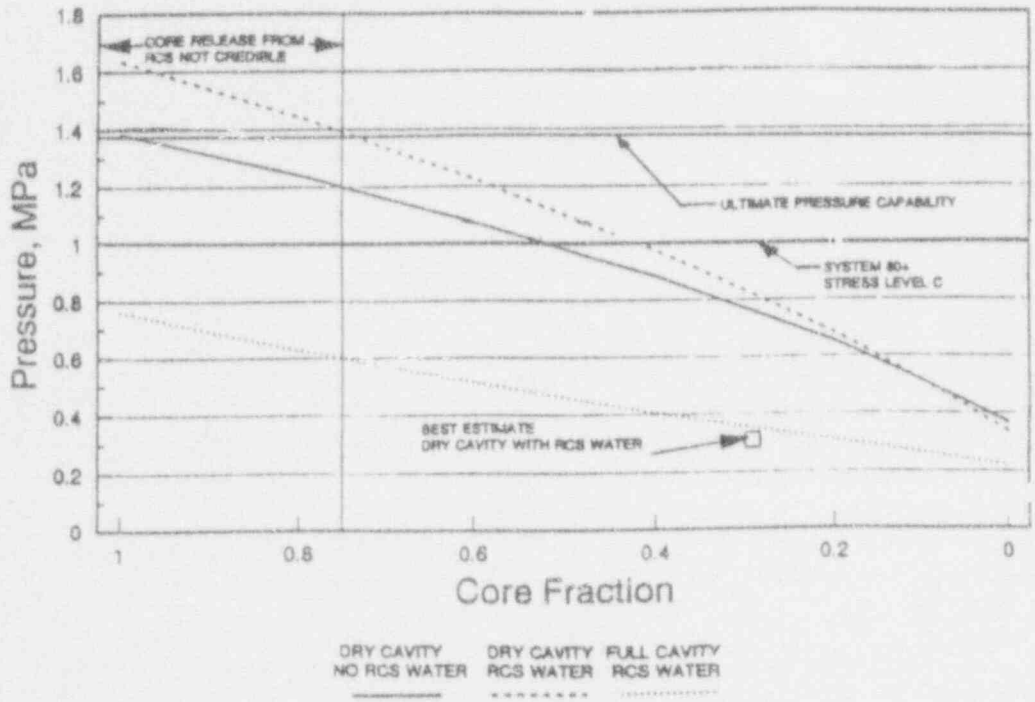


Figure 7. Bounding Estimates of ALWR Containment Responses to DCH

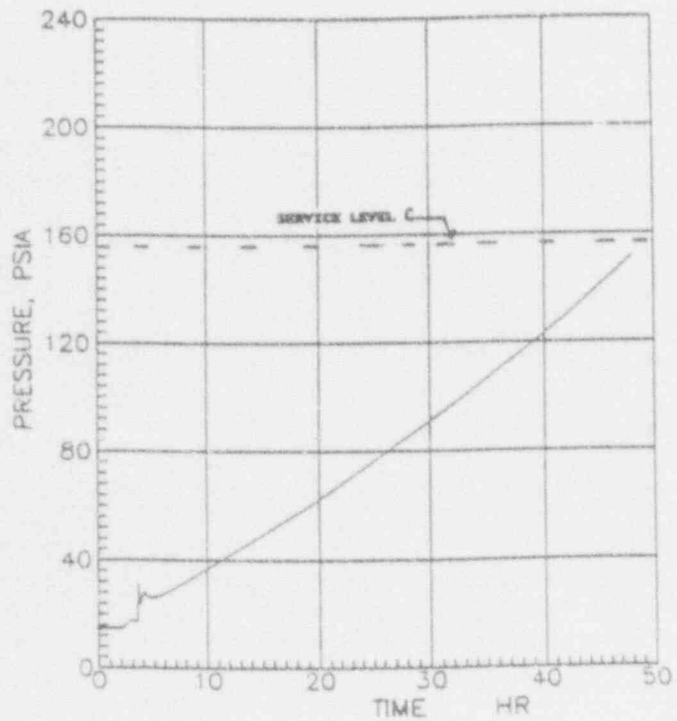


Figure 8. Response of System 80+ to a Station Blackout

# COMPARISON OF THE WESTINGHOUSE-GOTHIC CONTAINMENT CODE PREDICTIONS TO PCCS TEST RESULTS

Marcia D. Kennedy
Joel Woodcock
Westinghouse, NATD

## Abstract

The computer code calculations which are reported herein examine integral tests of a steel vessel with internal steam condensation and external heat removal by natural convection from a dry surface. Several of the advanced nuclear plant concepts utilize a passive containment cooling system (PCCS) to remove the heat released to containment following postulated events such as a Loss of Coolant Accident. Such a system employs passive or natural draft air cooling to transfer heat from the steel containment vessel to the environment. This process is simulated in the tests with a steel vessel and natural convection annular air flow. Heat is delivered to the vessel using superheated steam. Results of test simulations with a computer code are shown. A methodology is presented which includes mechanistic heat and mass transfer correlations, including wall-to-wall radiant heat transfer. A dynamic stratification of internal non-condensable gases is shown to explain the axial wall temperature distributions.

## INTRODUCTION

Several of the advanced nuclear plant concepts utilize a passive containment cooling system to remove heat released to containment following postulated events such as a Loss of Coolant Accident. Such a system employs passive or natural draft air cooling to transfer heat from the steel containment vessel to the environment. Air enters an annular space between the steel containment vessel and the concrete shield building through inlets in the shield building wall. The air then rises in the annulus as a result of the natural draft developed as the air is heated by the containment surface. The heated air exits the shield building through an outlet (chimney) located above the containment shell. Heat is transferred from the containment vessel and the shield building surfaces by natural convection and radiation. Heat is also transferred from the containment vessel to the shield building inner surface by radiation. This process is simulated in an integral Small Scale Test facility using a steel vessel and natural convection annular air flow. Heat is delivered to the vessel using superheated steam, and the tests are allowed to reach steady state. Although the facility has the capability to deliver cooling water to the outer surface and to provide forced convection with a fan in the chimney, the test results which are examined herein have pressure vessel heat removal by natural convection without water being applied to the vessel outer surface and with the fan off.

A methodology is presented based on a modified version of the GOTHIC (Reference 1) containment analysis code, referred to as Westinghouse-GOTHIC, which contains mechanistic heat and mass transfer correlations including wall-to-wall radiant heat transfer. The methodology

includes the use of both the computer code to predict flow fields and mechanistic correlations based on local fluid conditions to predict heat transfer. In the buoyancy dominated tests, it is shown that good agreement with the total vessel pressure and the axial wall temperature distribution can be achieved by modeling the buoyancy of the delivered steam and the effects of internal distributions of non-condensable gases.

A discussion of the analytical methodology is followed by a description of the tests and the computer code. Some modeling requirements found to be important are summarized, and a comparison of the code predictions to the tests is shown.

## ANALYTICAL METHODS SUMMARY

The use of correlations to model heat transfer in containments is inseparable from the formulation of the computer code in which they are used. The historical correlations used by containment pressurization transient analysis codes, such as Tagami's correlation (Reference 2) for internal condensation, have a reasonable test basis. However, the correlations had been intended for use in containment analysis codes based on conservation equations written for a single large control volume representing the entire containment. The use of a single containment control volume requires that any correlations inherently include the effects of forced and/or free convection flow fields within the containment. Computations with such an approach are fairly straightforward. However, such an approach raises questions when finer detail is required for internal containment modeling. For example, it is not clear whether Tagami applies equally to compartments containing a break and the inner surfaces of walls in a passively cooled containment, nor what should be used for the Tagami parameters, volume and total energy. Another difficulty in using total heat transfer coefficients is how to apportion the total heat transfer between convective and condensing heat transfer.

Current requirements for containment analyses, arising from hydrogen issues and reliance on passive cooling, have led to computer models that can calculate fluid distributions within a containment volume as well as within external annuli. Steam and non-condensables within the containment volume can be separately tracked. With such computer models, fluid conditions in the regions near structures are available. Since heat and mass transferred to structures (internal heat sinks and the containment shell) are governed by conditions locally within the given boundary layer, it makes sense to correlate heat transfer to known conditions as near the boundary layer as possible. Therefore, a methodology is being proposed that includes a more completely formulated set of thermal-hydraulic equations linked with correlations based on bulk fluid conditions relatively near a surface.

Justification for the proposed methodology then requires demonstrating that the computer code adequately determines the fluid flow field, and thus localized bulk fluid conditions, as well as the heat transfer based on those bulk fluid conditions. With the installation of mechanistic heat and mass transfer correlations and a film tracking model into GOTHIC (discussed in more detail later), the Westinghouse-GOTHIC code can be used to assess the validity of the proposed methods.

## TEST FACILITY AND DATA

### Description of Test Facility

The integral Small Scale Test (SST) facility, shown in Figure 1, is a 24 foot tall, 3 foot diameter steel pressure vessel. The vessel can initially contain air or nitrogen at one atmosphere and is supplied with steam at pressures up to 80 psig. A transparent acrylic cylinder around the vessel forms the air cooling annulus. Convection to the air flowing in the annulus and radiation from the vessel surface cools the vessel, resulting in condensation of steam inside the vessel.

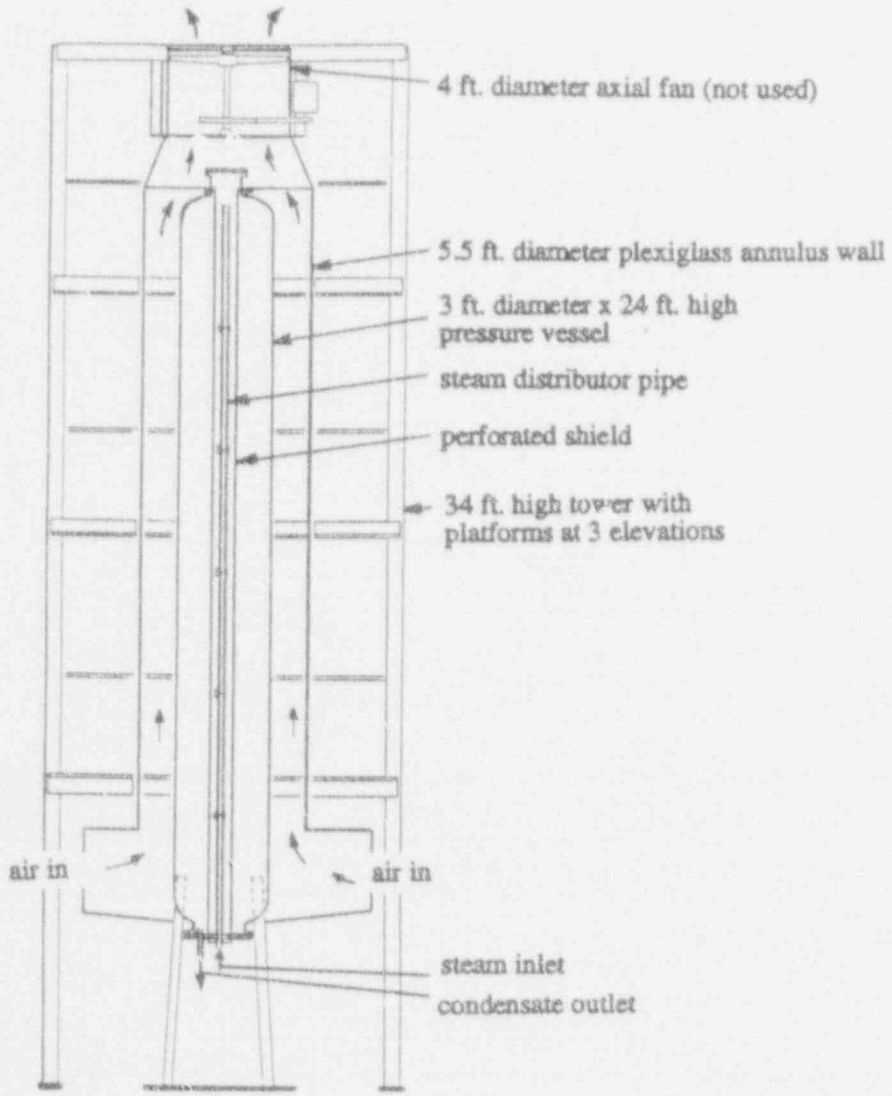


Figure 1. Section View of Small Scale Containment Cooling Test

Saturated steam from a boiler is throttled to superheated conditions at a variable but controlled pressure and supplied to the bottom of the vessel which for these tests initially contained air at atmospheric conditions. A full length distributor was developed for the first series of tests. The steam is distributed inside the vessel by a pair of steam distribution pipes. The inner steam supply pipe delivers steam uniformly along the vessel length and is surrounded by a shield pipe designed to mitigate lateral steam jets.

An axial fan, which was used to control the cooling air velocity in previous tests, is located in the chimney region above the test vessel. Although the fan was disconnected for natural draft testing presented, the fan, a component of the upper chimney, was left in place for the natural draft tests and adds only nominal flow resistance.

## Test Results Summary

The relevant test conditions are presented in Table 1. A more detailed description of the test facility and test results can be found in Reference 3. The annulus velocities (shown in Table 2) are low, indicating that the annulus heat transfer is governed by a boundary layer in the expected free convection regime. Based on the Grashof number, the flow is also turbulent.

Table 1. Small Scale Test Facility Test Data Summary

| Test Number | S101 | S102 | S103 | S104 | S105 |
|---|---|---|---|---|---|
| Run Number | 33 | 29 | 29 | 35 | 34 |
| Ambient Conditions | | | | | |
| Ambient Temperature (F) | 70 | 59 | 71 | 85 | 78 |
| Ambient Pressure (inches Hg) | 29.2 | 28.9 | 28.9 | 28.8 | 29.1 |
| Ambient Relative Humidity (%) | 68 | 61 | 61 | 87 | 96 |
| Nominal Test Conditions | | | | | |
| Vessel Internal Pressure (psia) | 30 | 45 | 60 | 75 | 90 |
| Measured Average Test Conditions | | | | | |
| Steam Inlet Temperature (F) | 252 | 278 | 293 | 308 | 321 |
| Condensate Temperature (F) | 124 | 157 | 168 | 214 | 213 |
| Condensate Flow Rate (lbm/hr) | 49 | 84 | 96 | 120 | 121 |

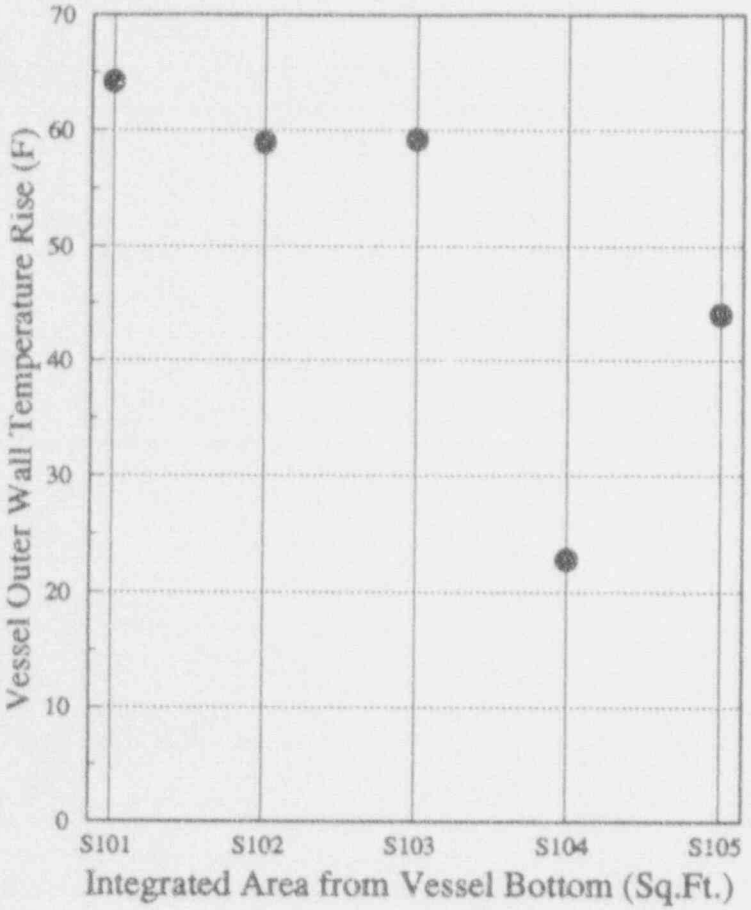


**Figure 2. Vessel Outer Wall Temperature Versus Integrated Area**

In Figure 2, the axial vessel wall temperature distribution is represented by the ΔT from top to bottom. The trend is relatively consistent for four of the tests. However, Test S104 demonstrates a decreased axial ΔT of less than half that of the other tests. Investigations showed that Test S104 had been vented during part of the test, thus expelling an undetermined portion of the non-condensable inventory. This indicates that the presence of non-condensable gases inside the vessel has a strong influence on the axial temperature distributions. Code calculations presented later show that a dynamic equilibrium with axial stratification of the non-condensables exists inside the vessel.

## COMPUTER CODE CONSERVATION EQUATIONS

The GOTHIC computer code is a containment analysis package which has been selected by Electric Power Research Institute (EPRI) and a national users group for development as a

reference containment analysis code. GOTHIC is a state-of-the art program for modeling multiphase flow. It solves the conservation equations in integral form for mass, energy, and momentum for multicomponent flow. The momentum conservation equations are written separately for each phase in the flow field (drops, liquid pools, and atmosphere vapor). The following terms are included in the momentum equation: storage, convection, surface stress, body force, boundary source, phase interface source, and equipment source.

For computational efficiency, an option exists to simplify the momentum equations by eliminating the convective terms and stress terms when the flow field is not dominated by their effects. It should be noted that the gravity terms are retained so that buoyancy dominated flows may be determined. At the same time the mass and energy conservation diffusion terms are eliminated because there are no velocity gradients available for their calculation. That option has been exercised for these test comparisons. The tests presented are those with lower injected steam flow rates, and thus are more likely to have an internal flow field dominated by buoyant forces. This allows the calculation of the distribution of hot gases with flows that are induced by buoyancy.

## HEAT TRANSFER CORRELATIONS

The GOTHIC code has been tailored by the addition of mechanistic heat and mass transfer correlations for heat transferred from the vessel internal atmosphere, through the walls, and out to the ultimate heat sink, the environment. The correlations include wall-to-wall radiant heat transfer in the annulus, as well as radiant heat transferred from a wall (heat sink) to volume gases. The tailored code is referred to as Westinghouse-GOTHIC and retains the conservation equation formulations discussed above. Although the boundary layer is not explicitly modeled, the nodal approach used with Westinghouse-GOTHIC provides bulk conditions much nearer the surface of interest for use with the correlations. The computer code provides a coarse representation of the velocity fields within the vessel and the annulus.

In the Small Scale Tests, heat is transferred to the pressure vessel wall by convection and steam condensation. Heat is conducted through the vessel wall and is then transferred to the air annulus by convection and to the baffle wall by radiation. Most of the heat removed from the vessel is removed by the buoyant air flow through the annulus. A significant amount of heat is also conducted through the baffle wall and transferred by convection and radiation to the environment from the outside surface of the baffle wall.

A solution technique which includes wall-to-wall radiation necessitates a close coupling between the vessel shell and the adjacent baffle wall. This coupling is accomplished by defining a pair of boundaries through the vessel and baffle walls, such that there is corresponding vessel and baffle portions that radiate to each other and border against the adjacent volume nodes. The wall heat source terms that are represented are the heat and mass transfer to a volume node from its bordering walls. Convective heat transfer and steam condensation on the inside of the vessel, conduction through the vessel wall, vessel wall-to-baffle wall radiation, convection from the outer vessel and inner baffle, conduction through the baffle, and convection and radiation from the baffle outer surface are modeled.

The convective heat transfer correlation applied to inner and outer surfaces of the vessel is the McAdams correlation for turbulent free convection. For the inner surface condensation, the analogy between heat and mass transfer (Reference 4) is used. That is, the form of the convective heat transfer correlation is retained, and the Nusselt number is replaced by the Sherwood number, and the Prandtl number is replaced by the Schmidt number.

On the inside, the condensate film mass flow is determined as a function of elevation. The film temperature is determined such that the overall heat transfer from the adjacent volume to the film and through the film to the wall are balanced at any given elevation. The Nusselt condensation heat transfer correlation as modified by Chun and Seban (Reference 5) to account for wavy laminar flow is used to determine the heat transfer rate through the film.

For both internal and external heat transfer, the application of these equations in Westinghouse-GOTHIC is based on average fluid conditions within the volume adjacent to the portion of the wall being evaluated. The use of those conditions varies from the traditional use of heat and mass transfer correlations in which the driving force is taken relative to some environment parameter much farther away from the surface of interest. The traditional approach is much easier to apply in design situations and does not require significant computing power. The approach in this paper has the potential to provide more accurate calculations for a wider range of geometries, but which also requires much more computation. The current approach is also consistent with the theoretical basis of correlating boundary layer heat and mass transfer phenomena to a bulk condition which is still well away from the boundary layer. When dealing with complex flow geometries, it is preferable to apply correlations based on bulk local conditions near a wall along with an appropriate calculation tool, allowing the flow field to be explicitly calculated. Such a method is consistent with the fact that the heat and mass transfer are governed by conditions near the boundary layer rather than by ambient, or environment, conditions. The traditional approach leads to a large degree of uncertainty and is difficult to justify when dealing with geometries not similar to those tested (Reference 6).

## WESTINGHOUSE-GOTHIC INPUT MODEL OF TEST FACILITY

### Input Model Description

The small scale test is modeled by dividing the 24 foot vessel and baffle sections into twelve nodes axially. Early studies showed that buoyancy driving forces of the heavier air-steam mixture outside the shield pipe can cause the lighter, pure hot steam to rise near the center of the vessel, resulting in higher steam concentrations near the top. To sufficiently describe the flow and non-condensable fields inside the vessel, the internal volume is also divided radially.

The steam flow rate and enthalpy are specified as input conditions to the bottom supply pipe volume. The steam flow rate at steady state is equal to the condensate flow, and the condensate is allowed to drain. The system air content within the vessel is set based on the measured initial atmospheric conditions. The calculation is allowed to reach a steady state pressure for a given steam flow rate, at which time the heat removed from the vessel is equal to the heat input to the vessel.

The external flow annulus is modeled with a pressure boundary condition that represents the environmental density gradient, the appropriate flow area, and a total unrecoverable loss coefficient. The annulus is divided axially into a number of nodes equivalent to those inside the vessel. The computer code explicitly calculates the flow rate through the annulus that balances the internal and external density gradients with the unrecoverable losses through the annulus. In this way, the conditions within the annulus are calculated and used with the heat transfer correlations. Such conditions, although still well away from the boundary layer, are much closer to the boundary layer conditions compared to calculations based on the environment ambient temperature.

## RESULTS

### Westinghouse-GOTHIC Comparisons to Tests

The containment pressure and axial wall temperature distributions are considered to be the primary measures of code success. Table 2 shows the steady state vessel pressure predicted and measured values for the two Series 1 tests, S101 and S102, that have internal flow fields dominated by buoyant forces. The test results are very well predicted for the complex situation of combined internal and external heat transfer. Both vessel pressure and annulus ΔT are predicted within -5/+8 % which indicates that the heat transfer methods are reasonable. The annulus velocity shows excellent agreement which supports the use of the code to calculate the natural convection flows and the resulting conditions within the annulus.

Table 2. Measured and Predicted Pressures for Integral Small Scale Tests Without External Water Flow

| Test Parameter | M/P Ratio |
|---|---|
| S101 | |
| Pressure (psia) | 1.06 |
| Annulus ΔT (F) | 1.08 |
| Annulus Velocity (ft/sec) | 1.00 |
| S102 | |
| Pressure (psia) | 1.01 |
| Annulus ΔT (F) | 0.95 |
| Annulus Velocity (ft/sec) | 0.96 |

Figures 3 and 4 show the measured and predicted axial wall temperatures, divided by the inlet temperature for each test. The abscissa is given as the integrated vessel area from the bottom of the vessel, since that represents the area over which a thermocouple reading is assumed to apply; this also separates the readings of the dome thermocouples which are not significantly different in elevation. Both measured and predicted values show a significant axial temperature gradient. Although comparisons have not been completed yet for the remaining three tests in this series, the data from Test S104 (Figure 2) support the hypothesis that a dynamic stratification of non-condensables within the test vessel occurs. Since an increase in air concentration of only a few percent can have an order of magnitude effect on the condensation

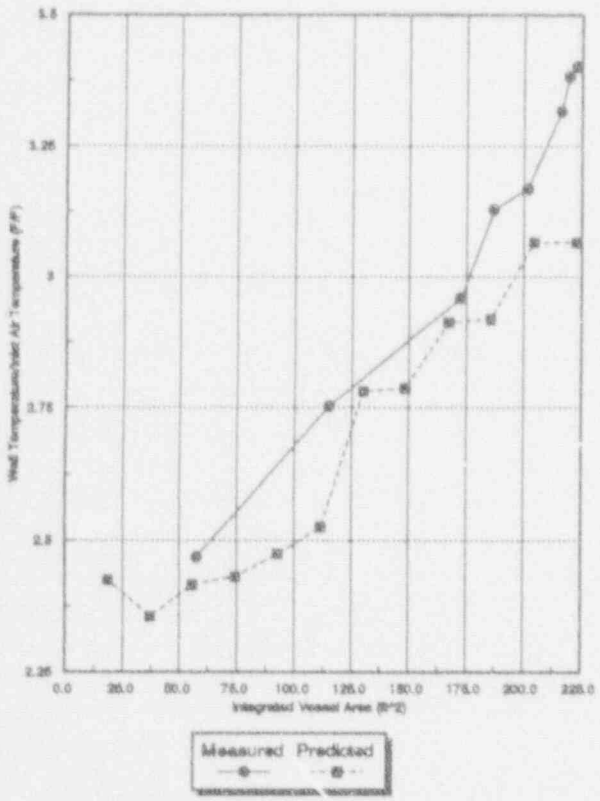


Figure 3. Test S101 - Vessel Outer Surface Temperature Ratio vs. Height

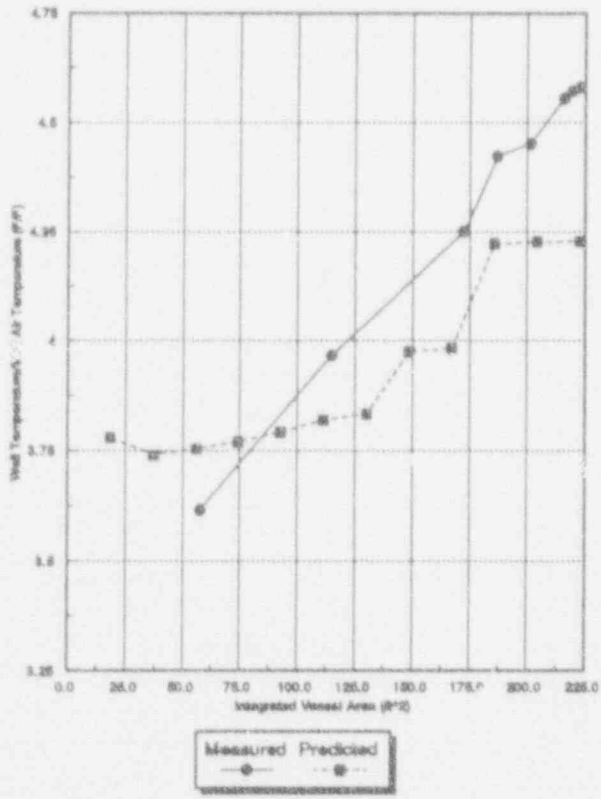


Figure 4. Test S102 - Vessel Outer Surface Temperature Ratio vs. Height

rate, the observed axial wall temperature variations can be attributed to a higher concentration of non-condensables at the bottom of the vessel, effectively insulating the wall from the central hot column of steam. Figure 5 shows the axial distribution of steam pressure ratios (partial pressure of steam / vessel total pressure) predicted by Westinghouse-GOTHIC in the nodes near the vessel wall for Tests S101 and S102.

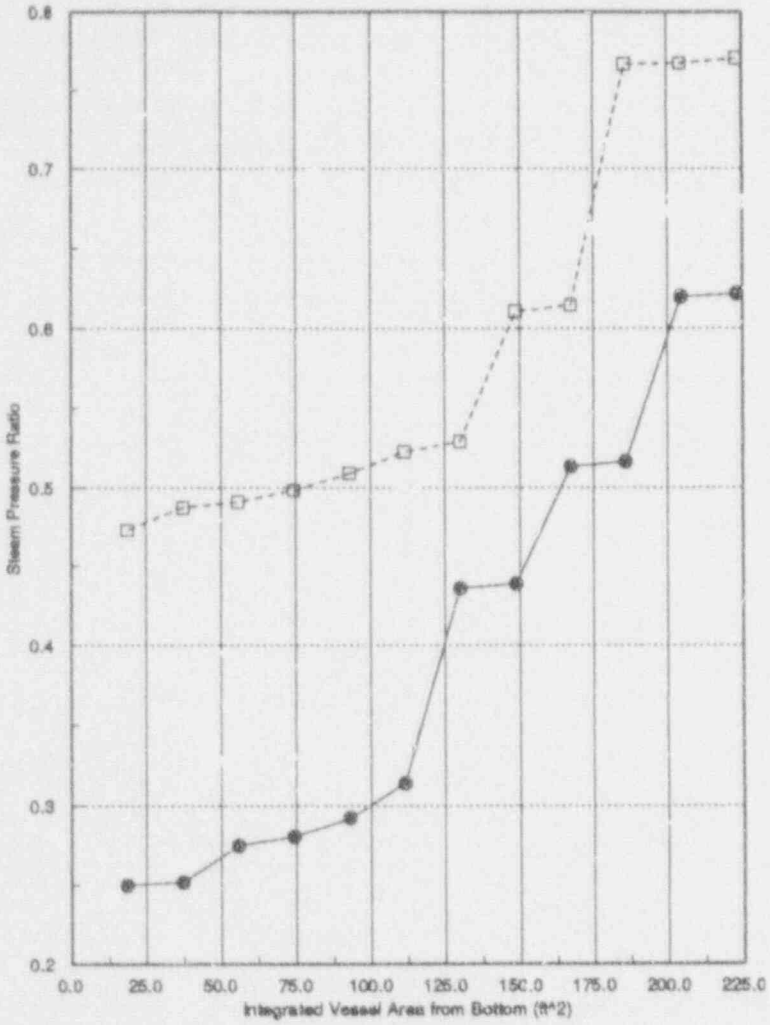


**Figure 5. Axial Distribution of Steam Pressure Ratios in Nodes Near the Vessel Wall**

## CONCLUSIONS

There is good agreement with vessel pressures which is a measure of the total heat removal rate, and with the vessel wall axial temperature variation which indicates that Westinghouse-GOTHIC is simulating the buoyancy driven flow fields, including steam and non-condensables, within the vessel and through the annulus. The postulated dynamic stratification of non-condensables is also reasonably predicted. The predicted flow field also indicated that for these tests, the lateral velocities exiting the shield pipe are redirected upward by the buoyancy driven vertical flows near the pipe.

Efforts are ongoing to develop similar models for other Small Scale Tests as well as for other PCCS tests with different vessel width-to-height ratios.

Extensive Westinghouse-GOTHIC code development work has been completed and progress has been made in developing an analytical methodology that provides good agreement with an integral Small Scale Test facility. A model of wall-to-wall radiation heat transfer permits an explicit calculation between the containment surface and the baffle wall, and from the baffle to the environment. Models are also in place for the convective heat and mass transfer on internal and external surfaces.

The multi-component, multi-dimensional capabilities of the code allow for the tracking of non-condensables, including hydrogen, which will affect the condensation rates inside containment, heat transfer coefficients, containment shell temperature distributions, as well as accounting for dynamic stratification that may occur. Such multidimensional capability to address stratification will be important for performing safety analyses for severe accidents.

## Acknowledgements

The work presented in this report was funded as part of the EBASCO team to support the design of a passive containment cooling system for the Heavy Water Reactor Facility under contract to the US Department of Energy.

The authors also gratefully acknowledge significant contributions from the following people: L.E. Conway and W.A. Stewart for ground breaking development of the methodology applied; Dr. L.E. Hochreiter for program direction; K.S. Howe for programming the heat and mass transfer correlations; and D.L. Paulsen and D.A. Kester for thorough development and verification activities.

## References

1. T.L. George, et al., "Containment Analysis with GOTHIC," Proceedings of 27th National Heat Transfer Conference, July, 1991.

2. Tagami, Takasi, Interim Report on Safety Assessments and Facilities Establishment Project in Japan for Period Ending June, 1965 (No. 1).

3. E.R.G. Eckert and R.M. Drake, Analysis of Heat and Mass Transfer, McGraw-Hill, 1972.

4. K.R. Chun and R.A. Seban, "Heat Transfer to Evaporating Liquid Films," J. Heat Transfer, Vol. 93C, pp. 391-396, 1971.

5. R.F. Wright, D.R. Spencer, F. Delose, "Reactor Passive Containment Cooling System Small Scale Containment Cooling Tests," (to be published), ANS/ASME Nuclear Energy Conference, San Diego, August 23-26, 1992.

6. G. Hugo, "Study of the Natural Convection Between Two Plane, Vertical, Parallel and Isothermal Plates:, Derived from Doctoral Dissertation University of Paris, 1972, Translated by D.R. deBoisblanc, EBASCo Services Incorporated, June, 1991.

# SBWR REINFORCED CONCRETE CONTAINMENT STRUCTURAL PERFORMANCE DURING SEVERE ACCIDENT

Giampiero Orsini
ENEA-Disp
Rome, Italy

Giuseppe Pino
ENEA-Disp
Rome, Italy

## Abstract

The Simplified Boiling Water Reactor (SBWR) reinforced concrete containment structure is analysed for its ultimate internal pressure capability under slow pressurization and the associated temperature loads in case of severe accident.
In the first phase of the analysis an axisymmetric Finite Element model has been considered with an increasing internal pressure without temperature effects; in the second phase a temperature transient load has been applied to the structure before pressurization.
Major topics of the performed analysis have been addressed, with emphasis on the failere criteria applicable to reinforced concrete structure.

## 1. INTRODUCTION.

In the frame of more intrinsecally safe Nuclear Power Plants development, a cooperation is in progress between ENEA-DISP and GENERAL ELECTRIC Co. aimed to study safety aspects of the SBWR plant in case of severe accidents.
One of the objectives of these studies is to investigate about the upper limit of strength and tightness of the reinforced concrete containment structure (Fig. 1), internally lined with a thin steel membrane, subject to a slow internal overpressurization and high temperature.
In the first work phase, the analysis of the non-linear structural behaviour of an axialsymmetric finite element model has been performed (Fig. 2); in the next phase a more refined 3-D non-linear model of a 90° sector of the containment upper part will be analyzed, in order to take into account the stiffening and strengthening action of the upper pool girders.
The complete working plan comprises also the analysis of local strain amplification in the liner surrounding a large typical penetration and the study of a protective steel structure withstanding steam explosion induced loads, following the corium falling into the water accumulated in the lower drywell.
In this report the first phase of the study and the results obtained from the non-linear analysis of the axialsymmetric model are discussed. Steel rebars arrangement as well as thickness of some membres have been assumed from preliminary evaluations and do not reflect the final design solution.

## 2 CONTAINMENT LOADS DURING SEVERE ACCIDENT

A severe accident consists of a failures and malfunctionings sequence leading to the reactor core melting. The consequences in terms of containment loads consist of rising of the internal pressure and temperature, attaining very high values, and risk of explosion (steam explosion, H2+O2).
In this case we want to know the ultimate capability of the concrete structure before loss of the containment integrity under the rising of internal pressure and temperature. The definition of the worst loading time history as consequence of a definite event sequence is affected by high uncertainties, then it was decided to apply the loads following a simple and conservative way: first the total range of temperature and after the internal overpressurization until the structural collapse.
Two reference levels of maximum temperature values have been selected; 260 °C (500 °F) and 540 °C (1000 °F), as consequences of the hypothesized accident scenarios.
The maximum value of temperature considered in this first case is 260 °C (500°F), reached in 72 hours, applied directly to the steel liner. The applied temperature time function is shown in Fig. 3. In the upper pools, the maximum temperature of 100°C (212°F) comes up from the water boiling in atmospheric environment.
Dead and permanent loads were applied in the first steps of calculation. In order to make a comparison two analyses have been performed: the first one with internal pressure alone and the second one with the temperature rising added.

## 3. AXIALSYMMETRIC FINITE ELEMENT MODEL

The finite element computer model was obtained from the drawings of the plant. In comparison with the real containment structure, approximations were introduced, to the purpose of limiting the dimension and complexity of the finite element model to a reasonable level.
The main simplification has been the transformation of the three-dimensional real structure into an axisymmetric computer model, which implied disregarding penetration holes and the girders of the upper pools.
The containment structure is connected to the reactor building by the floor slabs at the elevations -5400, 8064, 15714 and 22714 (ground level 0,00).
A limited portion of the outer floor slabs, restraining the containment in radial direction, have been represented in the analytical model.
The foundation slab was not included in the analytical model because it is not a critical element for the containment integrity and, owing to its great stiffness, the fixed restraint at the junction with the cylindrical wall is adequate.

Also the drywell steel head has not been included in the model, because the purpose of the analysis is the structural behaviour of the reinforced concrete structure until loss of containment

integrity. The drywell steel head does not work as an important restraint for the concrete structure, therefore can be studied more easily by considering it separated and subject to internal pressure and displacement of its edge.
Looking at concrete structure analysis, the overpressure acting on the steel shell is transferred to the edge restraint as a vertical increasing force.

The load resistant members of the analytical model consist of reinforced concrete walls and slabs and steel liner jointed to the containment wall through anchoring studs.
The anchoring studs were not represented in the model and liner-concrete joints are set at the finite element nodes.

Also the interaction between rebars and concrete is simply modelled by fix connections at suitable concrete elements nodes.

The finite element model consists of 993 four-noded isoparametric concrete elements and 111 four-noded isoparametric elasto-plastic steel elements for the liner.
Vertical reinforcing steel bars were modelled by truss elements and hoop rebars by ring elements, placed at nodes close to the surface. Fig.s 4 and 5 show vertical, meridional and hoop reinforcing steel bars. The total number of nodes is 1304 with 2582 degrees of freedom.

## 4. MATERIAL MODEL FOR CONCRETE

The concrete behaviour has been represented by the model implemented in the ADINA code [1]. The basic principle is to treat the general multiaxial stress-strain behaviour as an equivalent uniaxial relation. To this purpose twenty-four input points are required, covering all the expected principal stress values, to model the triaxial concrete compressive failure envelope.

The basic features of this model include (1) a nonlinear stress-strain relation allowing for the weakening of the material, (2) stress induced orthotropy, (3) failure envelopes defining tension and compression failures, (4) post-cracking and crushing modeling ability, including strain softening, and (5) loading and unloading conditions. The concrete uniaxial parameters, used in the analysis, are:

- initial tangent module = 530.000 kg/cm$^2$ (200000),
- Poisson's ratio = 0.15,
- uniaxial cut-off tensile strength = 30 kg/cm$^2$ (21),
- uniaxial maximum compressive stress (SIGMAC) = -350 kg/cm$^2$ (-210),
- compressive strain at SIGMAC = -0.002
- uniaxial ultimate compressive stress = -290 kg/cm$^2$ (-168),
- uniaxial ultimate compressive strain = -0.0035 (-0.0045).

The values between brackets have been adopted for the analysis

with pressure + temperature until 500 °F (260°C). Unfortunately, the ADINA concrete model parameters can not change throghout the computer calculation following temperature variation. Then, average values considering the temperature range of interest, have been assumed from technical literature data.

## 5. MATERIAL MODEL FOR STEEL

A thermo-elastic-plastic and creep model, with isotropic hardening, has been used to represent the behaviour of the vertical, radial rebars and liner [1,2]. It was impossible to use the same material model for the hoop rebars because not accepted by the code, then the thermo-elastic model was adopted for ring rebars when the temperature was considered.
The mechanical parameters for vertical and meridional rebars are [3,4]:

| T °C | ry (kg/sqcm) | Ey(kg/sqcm) | Eh | ALFA (1/°C) |
|---|---|---|---|---|
| 20° | 4200 | 2.1E6 | 7.0E5 | 1.E-5 |
| 200° | 3600 | 1.75E6 | 7.0E5 | 1.E-5 |
| 300° | 3150 | 1.57E6 | 6.0E5 | 1.E-5 |
| 650° | 1680 | 0.99E6 | 5.0E5 | 1.E-5 |

for hoop rebars

| | | | |
|---|---|---|---|
| 20° | 2.1E6 | | 1.E-5 |
| 200° | 1.75E6 | | 1.E-5 |
| 300° | 1.57E6 | | 1.E-5 |
| 600° | 0.99E6 | | 1.E-5 |

for the liner:

| | | | | |
|---|---|---|---|---|
| 20° | 1680 | 2.1E6 | 7.0E5 | 1.E-5 |
| 200° | 1440 | 1.90E6 | 7.0E5 | 1.E-5 |
| 300° | 1220 | 1.87E6 | 6.0E5 | 1.E-5 |
| 600° | 900 | 1.10E6 | 5.0E5 | 1.E-5 |

The values of the previous table have been selected with the aim to perform a thermal stress analysis of the structure reaching a temperature of 540 °C (1000 °F). For this level of thermal load creep fenomena on steel elements begin to be not negligible [5].
The ADINA creep law n. 3 has been used [1]:

$$e_{creep} = a_0 \, r^{a_1} \, t^{a_2} \, e^{-a_7 / T\,(^\circ K)} \qquad (1)$$

with, for "t" in hours and "r?" in tons/sqm, a0=1.17E-4, a=4.8, a2=0.7 and a7=34000,selected from data reported in the CEB Model Code [ ].
In the analysis performed with the maximum value of temperature of 260 °C (500°C), the creep strain is generally negligible. However, this material model has been used in order to load the structure until 540 °C (1000 °F) in next analyses.

The analysis without thermal loading has been performed with an elasto-plastic material model, with isotropic hardening. The material characteristics reported in the previous table in corrispondence of 20 °C have been assigned to steel elements.

## 6. METHOD OF ANALYTICAL SOLUTION

Information on this subject are reported in the ADINA code Manuals [1,2] and only a brief description is given here. The finite element system has been evaluated using an incremental solution of the equilibrium equations:

$$ {}^{t}K_{U} = {}^{t+dt}R - {}^{t}F \qquad (2) $$

where ${}^{t}K$ = tangent stiffness matrix corresponding to the configuration of the system at time t, U= vector of nodal point incremental displacements (i.e., $U = {}^{t+dt}U - {}^{t}U$), ${}^{t+dt}R$ = vector of externally applied nodal point loads corresponding to time t+dt, and ${}^{t}F$ vector of nodal point forces corresponding to the internal stresses at time t.

The solution of the previous equation yields, in general, an approximate displacement increment U. To improve the solution accuracy and in some cases to prevent the development of instabilities it may be necessary to use equilibrium iterations in each or preselected time steps.

The main features of the first analysis without thermal load are reported in the following table:

**Table 1. Analysis without thermal load**

| LOAD PATH | LOAD STEP | EQUILIBRIUM | NOTES |
|---|---|---|---|
| 0 _ 15 | 0.1 | ENERGY (E)<br>FORCES (F) | |
| 1.5 _ 3.65 | 0.05 | E - F | |
| 3.65 _ 3.67 | 0.01 | E - F | |
| 3.67 _ 3.68 | 0.001 | F | |
| 3.68 _ 3.80 | 0.01 | F | |
| 3.80 _ 4.65 | 0.05 | F | Starting of extensive cracking in concrete |
| 4.65 _ 20.4 | 0.01 | NO | |

Stiffness was reformed at every step throughout the analysis and equilibrium iterations had to be abandoned when extensive

cracking of concrete started.

For the evaluation of the stress and strain state due to temperature loads, a transient thermal analysis of the axisymmetric model has been previously performed. The temperature time histories for each nodal point have been calculated and then applied to the structural model.
Thermal analysis of concrete structure, subject to severe accident conditions, implies several problems related to mesh and time step selection, due to the low value of the thermal diffusivity of the material. In this case, the assumed temperature time history is shown in Fig. 3.
To check the effectiveness of the F. E. mesh, previous studies on simplified meshes having the same characteristics have been performed and the obtained results in term of temperature distribution and heat flux directions were satisfactory.

A typical temperature distribution through the wall thickness is shown in Fig. 6.

The structural behaviour under the previous calculated thermal loads has been evaluated by means of a non-linear F. E. analysis whose main features are reported in the following table:

Table 2. Analysis with thermal load

| Load path °C;(hours) | Load step hours | Equilibrium iterations | Notes |
|---|---|---|---|
| - ;(0. - 5.) | 5. | Energy (E) Forces (F) | dead & perm. load |
| 0 - 43;(5 - 21.5) | 5.<br>1.<br>0.5 | E + F | concrete cracks behind the cover |
| 43.-61;(21.5-24) | 0.05 | E + F | hoop concrete cracks and, near struct. joints, meridional cracks |
| 61-142;(24-49.6) | 0.2 | E + F | concrete meridional cracks |
| 142-260;(49.6-77.7) | 1.5<br>0.5 | E + F | max internal temperature reached; beginning of pressurization. |
| 260-260;(77.7-81.5) | 0.1<br>0.02 | E + F | pressure=1.8 bar |

## 7. FAILURE CRITERIA

To set reference failure criteria for the analysis of the ultimate structural behaviour until rupture is a complicated and hard task. The design codes usually used for structure dimensioning are inadequate in this case because they are limited to the linear field. It is necessary to introduce into the calculation the real stress-strain behaviour of materials until rupture, paying attention to the specific conditions of stress and deformation of the considered structure. The objective is to infer reasonable failure criteria, attempting to exploit the reserve of strength above the elastic limit of the structure. In the case of a containment structure, the potential failure mechanisms, causing the loss of containment integrity, must be first recognized in order to characterize better the related failure criteria. In this case, not considering the leakage through penetrations and the drywell head, the principal failure modes are:

- liner tearing due to local excessive strain amplification before actual structural collapse,

- sudden structural collapse occurring when liner strains are still small.

The first type of rupture, tearing of the liner, can not be detected directly from the results of the axisymmetric global model calculations, because the zones of discontinuity of the liner and the real interaction between anchors and concrete are not correctly represented in the model. Particularly, near penetrations where the liner is welded to a thicker steel plate and the anchor studs are generally arranged closer each other, large strain amplification can take place until reaching the local tearing. This happened in the test performed at the SANDIA Laboratories on a 1:6-scale r.c. containment model where the liner tearing near an electrical penetration occurred when the free field maximum principal strain was about 0.011 [6].

The liner is usually made up with a very ductile steel, able to sustain elongation greater than 20% in the stantard monoaxial tension test. Also in biaxial tension stress state, as usual in pressurized containment, it keeps a great capacity to sustain plastic deformation. In the Sandia 1:6-scale model post-test evaluations [7], it was demonstrated that also the use of an empirically-based criterion alone, the Davis Triaxiality Factor, could not explain the liner tearing and a decisive role must be ascribed to the interaction with the anchoring studs (mainly) and to local discontinuities such as thicker penetration plates, which causes large amplifications of the strain. In conclusion, great uncertainties arise for stating a deterministic strain limit value in this condition and, after assuming that accurate verifications are performed in discontinuities areas and of the interaction with the anchors, only an engineering judgement can

be expressed. Of course, from a safety point of view, conservatism must be introduced and the exploitation of the material plastic resources must be limited. On these bases, the limit for the principal plastic strain is assumed at 2%, taking into account the possibility of local strain amplifications.

The second type of [illegible] of containment integrity involves a large structural failure of reinforced concrete members.
Where membrane traction forces are prevalent, the concrete gets cracked and the rebar net sustains the load. In this case the structural failure occurs when the ultimate strength of the rebars material or splices is attained. Due to the closeness of liner and rebars, their strains are similar, therefore the failure limit of the liner strain, which was assumed taking into account the probability of local large amplifications, is reached first. In structural zones where large bending moments occur, high compression stresses give rise to concrete crushing, while tensile strains can be lower than the liner limit strain. The ADINA code accounts for concrete crushing transferring the stresses to the surrounding concrete elements and to the rebars placed in the compression region.

The concrete failure criterion is the one implemented in the ADINA code. Starting from the uniaxial compression and tension strength, a failure surface is defined in the principal stresses space, both for compression and tension zones. Crushing or cracking in the integration points of the concrete elements can happen under stresses grater or lower than the uniaxial strength, depending on the triaxial stress state in that point. Cracking of concrete does not mean failure of the structural reinforced member, whereas extensive crushing, other than the reinforcement cover, shall trigger the structural collapse.

Another failure mode which must be considered in reinforced concrete member is the shear failure. Specific shear failure mode depends on section tipology, amount of shear reinforcement and shear span value. In our case, with short shear spans, assuming that the amount of transverse reinforcement is enough to prevent yielding, the shear failure could take place as crushing of the concrete compression flange. Then, this failure mode is directly detected from the results provided by the non-linear f. e. analisys with the ADINA code, whereas the behaviour of the shear reinforcement and its yielding can not be represented satisfactorily in the non-linear model [8]. At any rate, with the aim to have a further comparison and check, the Aoyagi et alt. formula [9] will be used to verify the ultimate shear strength.

$$t_u = \frac{(P_v f_y - r_0)\cos\theta\sin^2(70-\theta) + P_w f_y \sin\theta\sin^2(\theta+20) + 0{,}75\nu F_c}{\cos^{20}+\sin\theta\cos\theta} \qquad (3)$$

where:
$t_u$ = ultimate shear strain
$P_v$ = axial rebar ratio (on one side)

$f_y$ = yield stress of rebars ($kg/cm^2$)
$r_0$ = axial stress on uncracked section ($kg/cm^2$)
$\theta$ = angle of shear cracking plane
$P_w$ = shear reinforcement ratio

## 8. ANALYSIS RESULTS WITHOUT TEMPERATURE LOAD

### 8.1 General Structural Behaviour and Displacements

The containment structure subject to internal overpressure, exhibits a behaviour different from that of the current free-standing cylindrical containment. In our case, high bending moments and shear forces arise along the structure other than membrane forces. In this particular axisymmetric model the interaction of these forces lead to select the location of the most critical section for the structural stability at the junction of the top-slab with the cylindrical wall (elev.29,60 m).

Global displacements of the containment structure vs. internal overpressure are shown in Fig.s 7- 8.

In Fig. 9, structure deformation is shown when the internal overpressure attains the design value, equal to 3.84 bar. It is clearly noticed the restrain action of the floor slabs, which contrast the swelling of the cylindrical wall.
The upper pool structure is much less stiff than the other parts of the containment. Nevertheless, the maximum displacement computed is low, about 3 mm, and that implies that the concrete structure has not undergone extensive cracking yet.

When the internal overpressure goes up to about 6 bar, the structure stiffness is greatly and sharply reduced, due to extensive concrete cracking, and displacements increase faster (Fig. 10).

The maximum absolute displacement is observed in the point A (Fig. 9) and it is caused by the flexural deformation of the upper pool. The maximum horizontal displacement takes place in the point B, caused by the membrane force in the cylindrical wall.

The displacement of the points A and B vs. the internal pressure will be discussed in more detail to point out the meaningful aspects of the structural behaviour.

- Maximum vertical displacement
In the point A, lower central corner of the upper pool (R = 5.00 m elev. 29,60 m) the maximum value of the vertical displacement. is observed.
Its increasing with the overpressure is shown in Fig. 7. In the initial load steps, its value is negative, due to dead and permanent loads while the internal pressure is low .

When the internal overpressure is 3.85 bar (design pressure), the displacement is about 3 mm. Until this point no loss of the structure stiffness is displayed due to concrete cracking.

Extensive cracking in the top-slab appears when the overpressure attains the value of 4.5 bar. From this point on the displacement curve is no more linear and when the pressure reaches the value of about 6.5 bar, a sharp and great loss of stiffness takes place which is related to the hoop cracks due to membrane tension stresses. At the end of this jump, the displacement is about 6 cm. Afterward, the curve goes up with increasing slope.

- Maximum horizontal displacement

The maximum value of the horizontal displacement is observed in the cylindrical wall at the elevation 10.70 m (point B).
In Fig. 8 is shown the variation of the displacement during containment pressurization. Until 6 bar its slope is constant at which hoop stresses reach the tension strength of concrete and general cracking of concrete in the hoop direction takes place. Consequently, the displacement jumps from less of 2 mm to about 11 mm.
After this sharp loss of stiffness, the displacement growth is nearly linear up to 15 bar. Afterward, the curve slope increases, displaying further losses of stiffness.
Horizontal displacements of the SBWR Containment are quite small comparing with the ones of current free-standing cylinder containment, due to the structural continuity of the intermediate floor slabs with the containment wall.

## 8.2 Concrete failure

The most critical location for the stress magnitude in concrete is the junction between the top-slab and the cylinder wall at elev. 29.60 m.
Both the structural members are subject to tensile force and bending moment. The progression of cracking and crashing in concrete is shown in fig.s 11-12.
When the internal overpressure is equal to the design pressure (3.85 bar), concrete cracking is limited to the bottom of the node, the most stressed zone by tension.

At 10.7 bar cracking spreads all over the concrete elements and in many points cracks occur in all the three principal directions. Also crushing of concrete in a few points of the rebars cover, in the upper part of the node, takes place, due to the high compression stress reached (360 $kg/cm^2$).

At 11.9 bar, a whole concrete element representing the reinforcement cover is crushed, at the junction with the cylindrical wall.

Increasing the internal overpressure, at 13,1 bar the nearby inner concrete element in the top-slab gets crashed and at 15,5 bar also a crushed concrete zone is detected in the outer surface

of the cylindrical wall.

The shear resistance capacity is checked using the formula given in chaper 7, where:

Pv (axial rebar ratio in one side) = 0,0043
fy (yield stress of rebars) = 4200 kg/cm$^2$
Pw (shear reinforcement ratio) = 0,01
Fc (compressive strength of concrete) = 350 kg/cm$^2$

To the purpose of obtaining the axial stress in the top-slab, the time of verification is assumed at p= 12 bar. The tensile force in the top slab is calculated using the rebars strain computed by the code and placing the neutral axis at the half height of the concrete finite element below the compression reinforcement, after having observed the cracks disposition in Fig. 12.

Stress in compression reinforcement:

$r_{s,s}$= -0.0015*2.1*106= -3231 kg/cm2 (4)

in tensile reinforcement

$r_{s,i}$= (8.3-2.09)*1/1000*2.1*10$^5$+4400= 5704 kg/cm$^2$ (5)

in the liner

$r_l$= (8.76-1.7)1/1000*2.1*10$^5$+3600= 5083 kg/cm$^2$ (6)

compression force in the concrete

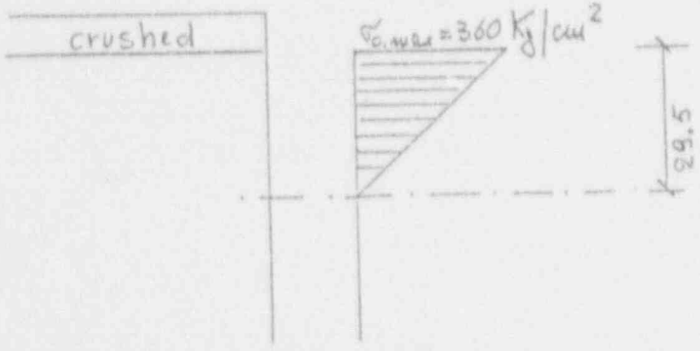


$F_c$=1/2*29,5*100*360= 531000 kg/m (7)

making the forces balance in the section, the tensile force and stress are:

$F_0$= (5704-3231)*188+5083*(100*0.9)-531000= 391000 kg/m (8)

$r_0$= 391000/(100*220))= 18 kg/cm$^2$ (9)

The angle of shear cracking plane is obtained by averaging the values computed by the computer code and it is assumed equal to 28°.

The ultimate shear capacity at p= 12 bar is

$$t_u = [(0.0043*4400-18)*\cos 28^\circ*\sin^2(70^\circ-28^\circ)+0.01*4400*\sin 28^\circ* *\sin^2(28^\circ+20^\circ)+0.75*\_350]/(\cos^2 28^\circ+\sin 28^\circ*\cos 28^\circ)= 22 \text{ kg/cm}^2 \quad (10)$$

The shear force in the top-slab is computed by hand calculation, by distributing the total vertical reaction force due to internal pressure and permanent load between the top-slab and pool upper slab.

Permanent load

$$g= (2.20+1.60)*2.5+2.5*1.00= 12 \text{ t/m}^2 = 1.2 \text{ kg/cm}^2 \quad (11)$$

Resultant load (upward)

$$Peff= p-g= 12-1.2= 10.8 \text{ kg/cm}^2 \quad (12)$$

$$R= Peff*r/2= 108*15.75/2= 850 \text{ t/m} \quad (13)$$

$$T_{ts}= 850*2.20/(2.20+1.60)= 492 \text{ t/m} \quad (14)$$

$$\tau_{ts}= 492/(2.00*1.00)= 246 \text{ t/m}^2= 24.6 \text{ kg/cm}^2 \quad (15)$$

The resultant shear stress is slightly higher than the calculated ultimate shear capacity, thus confirming that the structural collapse of the top-slab is likely to happen at the internal overpressure of 12 bar.

8.3 Rebars Strain

Results regarding the most stressed reinforcing steel bars will be examined.

A) Vertical rebars in the inner side of the cylindrical containment wall at elev. 29.60 and R= 15.94 m.

The reinforcement consists of 1 # 18/25 cm + 1 # 18/50 cm. Its strain Vs. internal pressure is shown in Fig. 13. Until the overpressure is below the design value, the strain is low. Beyond 4 bar, the rebar deformation increases more quickly and between 6 and 7 bar a little jump points out that concrete elements are extensively cracked as already noted.
The calculated strain at 12 bar is about 0.006, much smaller than the ultimate strain coming out from tests which is greater than 0,12 on the gauge length of 5 diameters.
Increasing the pressure, computed strains at 10 and 15 bar are, respectively, 0.0038 and 0.012.

B) Radial rebars in the bottom of the top-slab at the junction with the cylindrical wall.

The reinforcement consists of 2 # 9/15 cm. The rebars strain Vs.

internal pressure is shown in Fig. 14. At 12 bar of overpressure, the calculated rebars strain is 0.0083, quite far from the ultimate strain.

C) Radial rebars in the upper zone of the top-slab at the junction with the cylindrical wall.

The reinforcement consists of 2 # 9/15 cm. The rebars strain Vs. internal pressure is shown in Fig. 15. The most noticeable information gained from this curve is the overpressure value when concrete surrounding the rebars begins to crush. This fact is inferred by the sharp increase of the rebars strain when the overpressure exceeds 12 bar. At that moment, compression stresses in the crushed concrete are replaced by the sharp increase of stress in the reinforcement which, consequently, undergoes large strains.

D) Hoop rebars in the cylindrical wall at the point B of maximum radial displacement.

The reinforcement consists of 2 # 18/30 cm. The rebars strain Vs. internal pressure is shown in Fig. 16.
Calculated strains are lower than that of the previous rebars. When the internal pressure is at 12 bar, the rebars are still elastic; they yields at about 14 bar.

## 8.4 Liner strain

Liner strains Vs. internal pressure are examined in the location where the maximum value is reached and at the same elevation of point B.

The maximum liner strain occurs at the bottom of the top-slab, at the junction with the cylindrical wall. The strain Vs. pressure curve is displayed in Fig. 17. When the overpressure is 12 bar, the maximum strain reaches is about 0.009, much lower than the evaluated ultimate strain equal to 2 %. Computed strains are average values which do not account for the interaction effects with the anchors in cracked concrete and nearby discontinuities.

However, using the failure criterion established in chaper 7 it should be said that the liner is able to sustain further increases of the internal pressure over 12 bar.

In the structure section (point B) where the maximum radial displacement occurs, the liner is still elastic at 12 bar (Fig. 18).

# 9. ANALYSIS WITH THERMAL LOAD

A correct evaluation of the temperature effects on reinforced concrete structures is a very hard task, which involves the use of sofisticated analytical material model whose actual behaviour at high temperature shows numerical difficulties and, in the

case of concrete, a large spread in experimental results.
Specific content of water and its migration, pressure of pore water and age at loading time are some of the major topics to be considered in the analysis of concrete structure, as well as temperature distribution and its influence on the rate of hydratation.
The aim of the present work is the evaluation of the SBWR containment behaviour under increasing internal pressure, previously subjected to an heavy thermal load.
With respect to problems involved in thermal-stress analysis of concrete structure, this work should be considered an attempt to gather general information on the behaviour of a complex structure using an advanced commercial computer code that in past experiences, without temperature load, provided results in good agreement with test results [7].
Average values of the concrete characteristics have been used as previously shown, because the available version of the computer code does not allow variations vs. temperature, and assuming that in this case the other parameters does not significantly influence the analysis.
The internal temperature has been increased up to 260 °C (500 °F) in 72 hours, and an extensive concrete cracking in the overall structure has been detected. No concrete crushing occurred.
The stress-strain state of the steel rebars remain within the elastic range, also taking into account the mechanical properties degradation with increasing temperature.
The liner, as expected, reachs the plastic state with compression stresses in general.
The subsequent application of the internal pressure has reached 1.8 bar to date. During pressure loading, the structural behaviour is quite different from the case whitout temperature load. In some zones, temperature and pressure cause opposite stress state, so the initial phase of the pressurization acts as unloading, causing previous concrete cracks to close. This, in turn, causes numerical difficulties in computer calculation which require very small loading steps.
In the Fig.s 19,20,21,22,23,24,25 and 26 results obtained in the same points of the model whitout temperature and already illustrated are shown. Pictures with concrete cracking states are shown in Fig.s 27,28,29.
To date no precise predictions can be made on the limit pressure for this case, being the computer calculation still going on with a very small step, but extrapolating the strain values reached by the liner and rebars it could be expected not a great reduction of the previous estimated value of 12 bar.

## 10. CONCLUSIONS

The structural analysis of the simplified axisymmetric model displays that the most highly stressed zone occurs in the top-slab at the junction with the cylindrical wall. In the load case with pressure alone, when the internal pressure is 12 bar, the maximum compression stress in concrete reaches the value of about 380 kg/cm$^2$ and crushing takes place in the reinforcement cover.

The shear capacity of this section has been checked by an experimental formula which reveals that the limit state has been reached with that internal pressure.
The other resistant components, horizontal reinforcement and liner, do not experience excessive strains until the overpressure of 12 bar.
Particularly, the liner strain reaches the value of 0,009 which is deemed not to cause tearing due to local amplification.
In the load case with pressure + temperature up to 260 °C (500 °F) no definitive predictions can be done because the computer calculation is still in progress, but the results obtained to date, with the maximum temperature value applied and the internal pressure at 1.8 bar, show that the temperature load acts as a "preloading" of the structure and only the degradation of the mechanical properties of materials will probably cause the reduction of the ultimate strength.
About displacements, an extensive cracking of concrete kahes place during thermal loading and, as results, the stiffness of the structure is quite smaller during overpressurization
Moreover, considering that the real containment structure presents, in the upper part, massive girders stiffening the top-slab and not represented in the axialsymmetric model, it is reasonable to expect a higher ultimate strength capacity. In order to demonstrate that, the analysis of a more refined non-linear 3-D model, 90° sector, of the upper part of the containment structure is in progress.

## References


1. ADINA Users' Manual, Adina R&D, Inc., Watertown, MA (1987).

2. K.J. Bathe, "Finite Elemet Procedures in Engineering Analysis", Prentice-Hall, Inc., Englewood Cliffs, NJ 07632 U.S.A., (1982).

3. Bechtel Corporation, "Reactor building preliminary structural design", prepared for General Electric Company, Report #1000-COR-004, Rev.0.

4. ASME Code, Sec. III, Div. 1.

5. CEB-FIP Model Code 1990, Final Draft, July 1991, Case Postale 88, CH-1015 LAUSANNE

6. D.S. Horschel, "Design, Construction, and Instrumentation of a 1/6-Scale Reinforced-Concrete Containment Building", NUREG/CR-5083,SAND88-0030, Sandia National Laboratories, Albuquerque, NM, March 1988.

7. D. B. CLAUSS, "Round-Robin Analysis of the Behaviour of a 1:6-Scale Reinforced Concrete Containment Model Pressurized to failure: Posttest Evaluations", NUREG/CR-5341,SAND 89-0349*, Sandia National laboratories, Albuquerque, NM, October 1989.

8. G. Cross, " Ultimate Shear Design from Non-Linear Finite Element Analysis", IABSE Colloquium - Delft 1987.

9. H. Saito at alt.,"Experimental Study on RCCV of ABWR Plant, Part 2: Transverse Shear Experiments on RC Beam Element", 10th SMIRT, 1989.

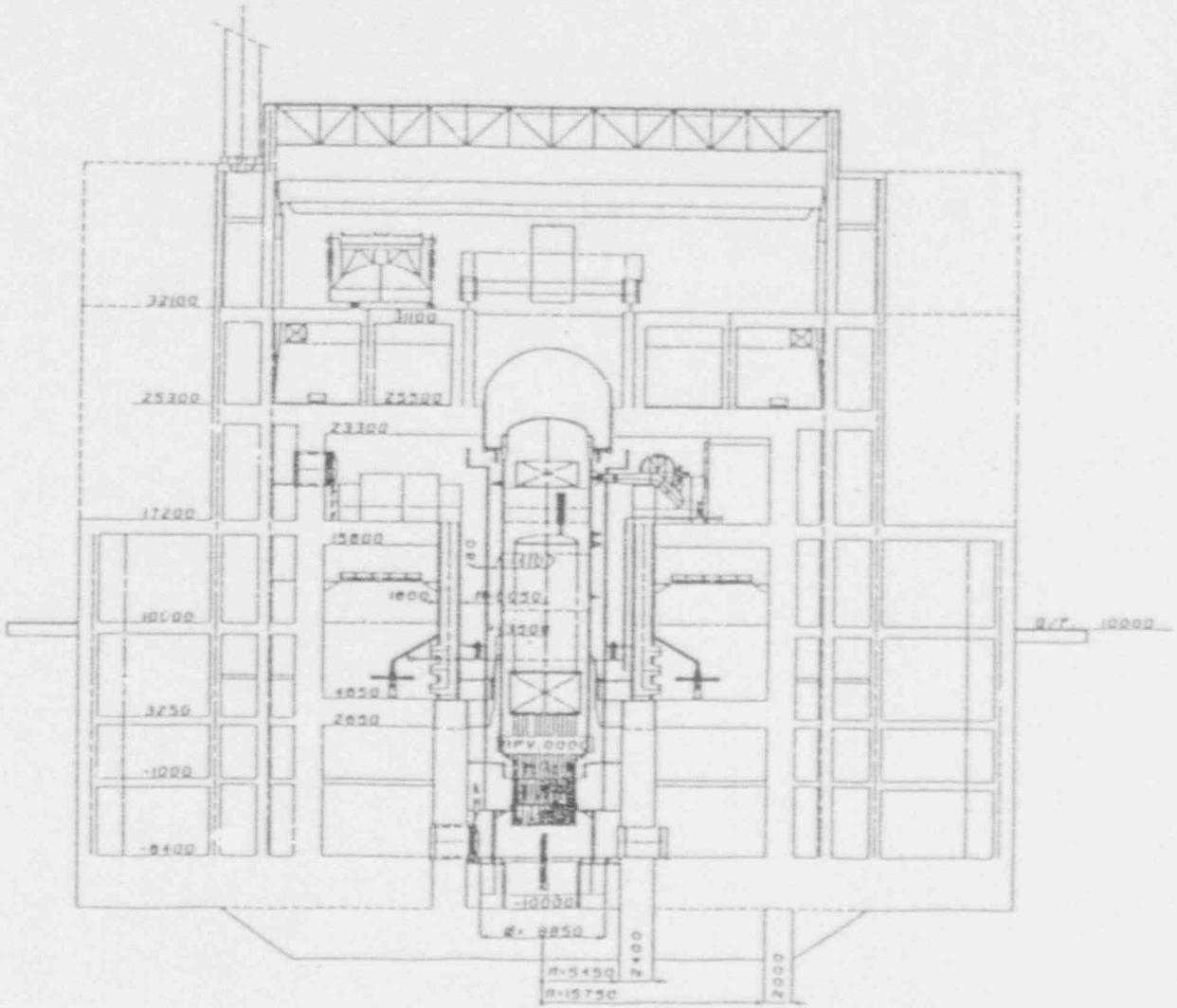


Fig. 1. SBWR Containment Structure

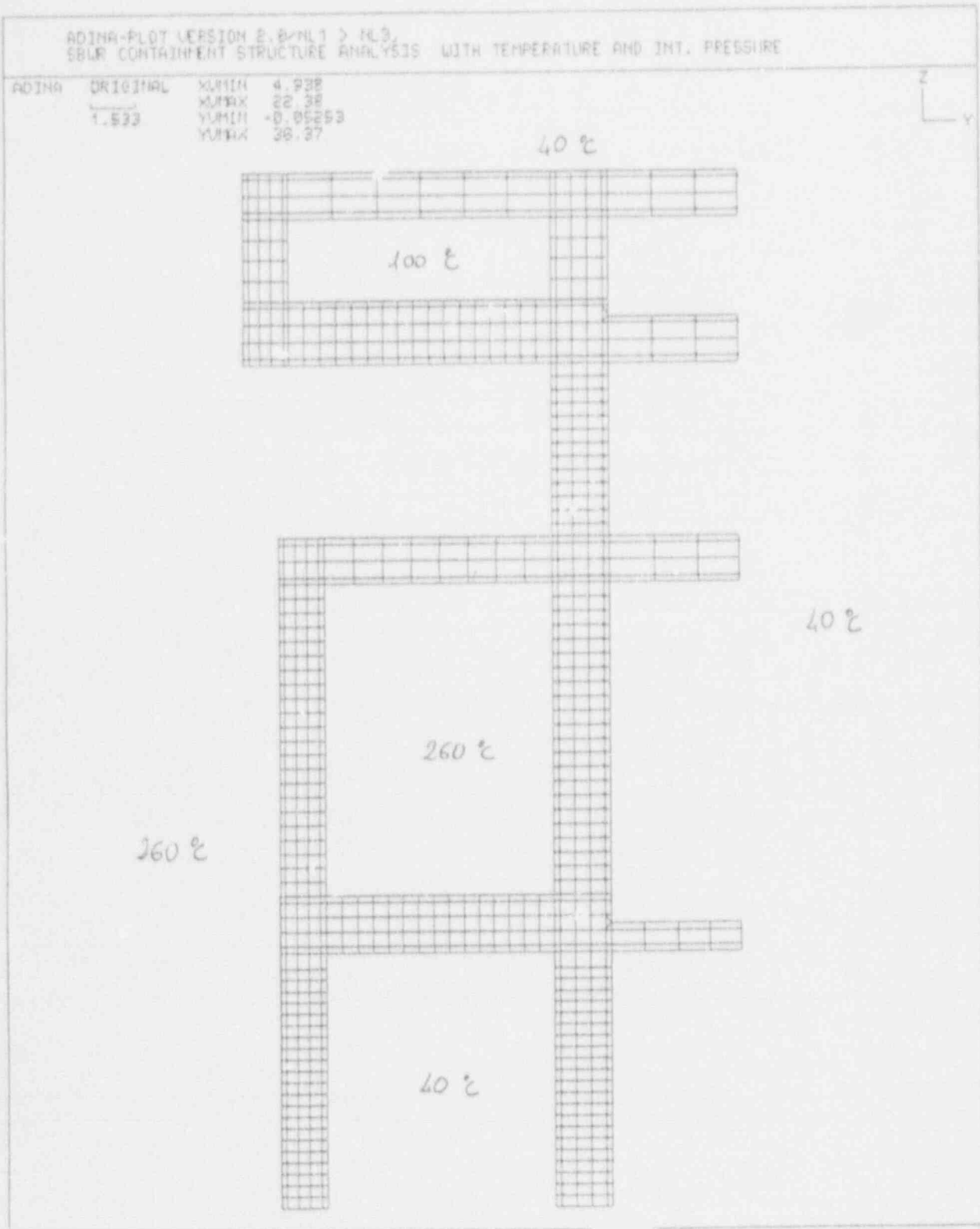


Fig. 2. F.E. model and temperature load

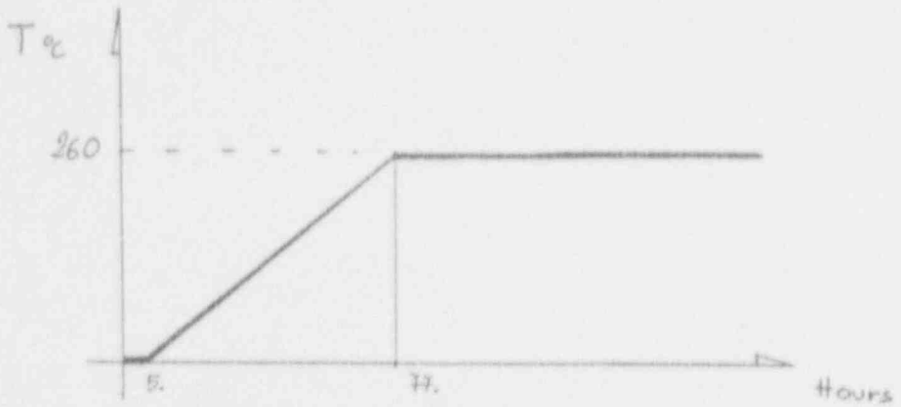


Fig. 3. Temperature time history

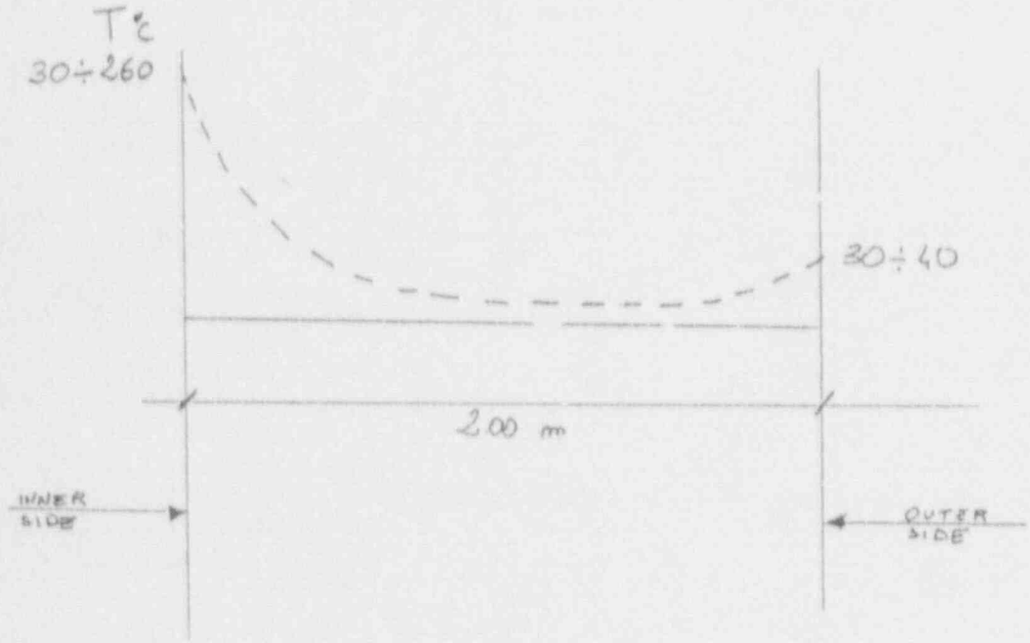


Fi 6. Temperature distribution through the wall

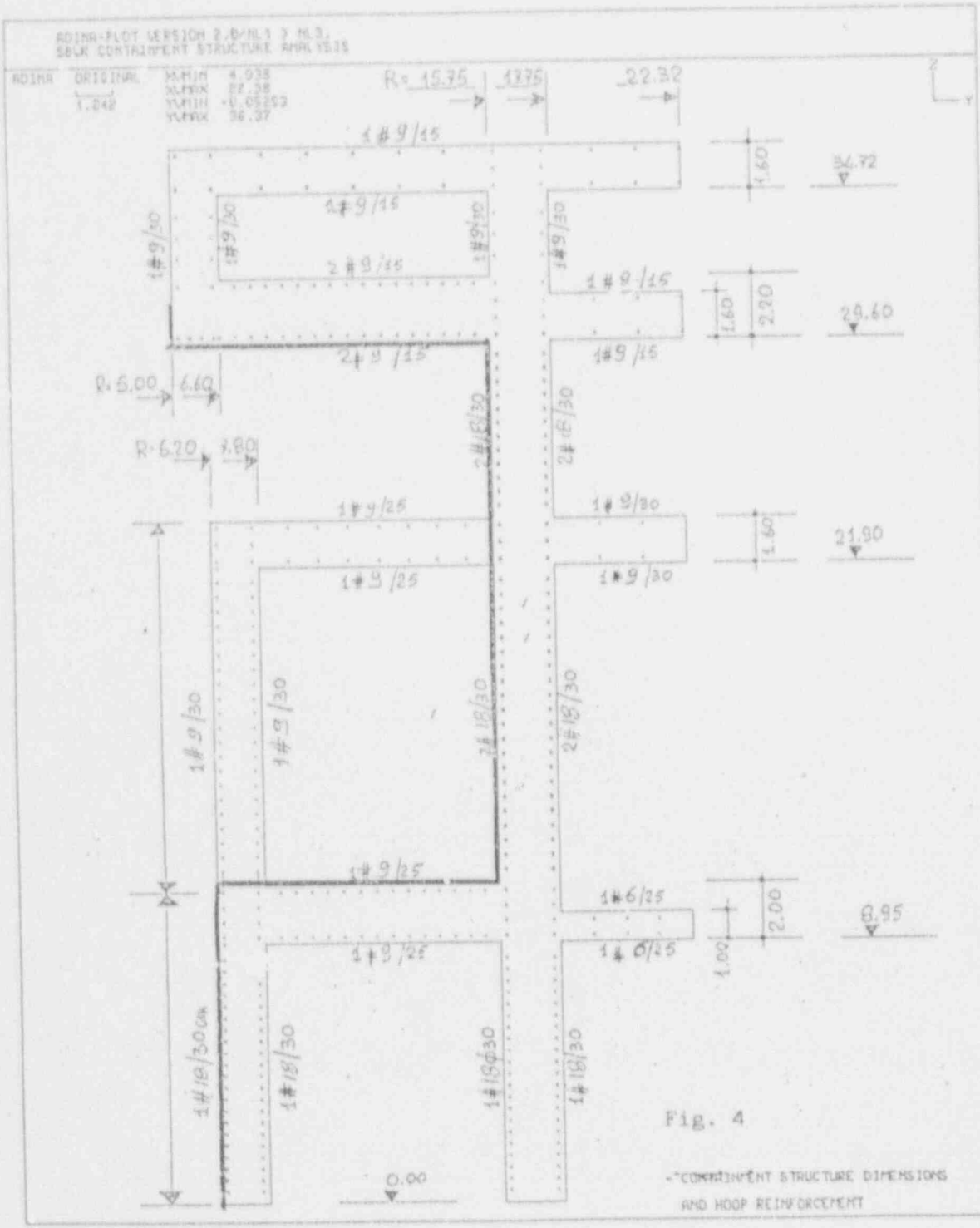


Fig. 4

-"CONTAINMENT STRUCTURE DIMENSIONS AND HOOP REINFORCEMENT

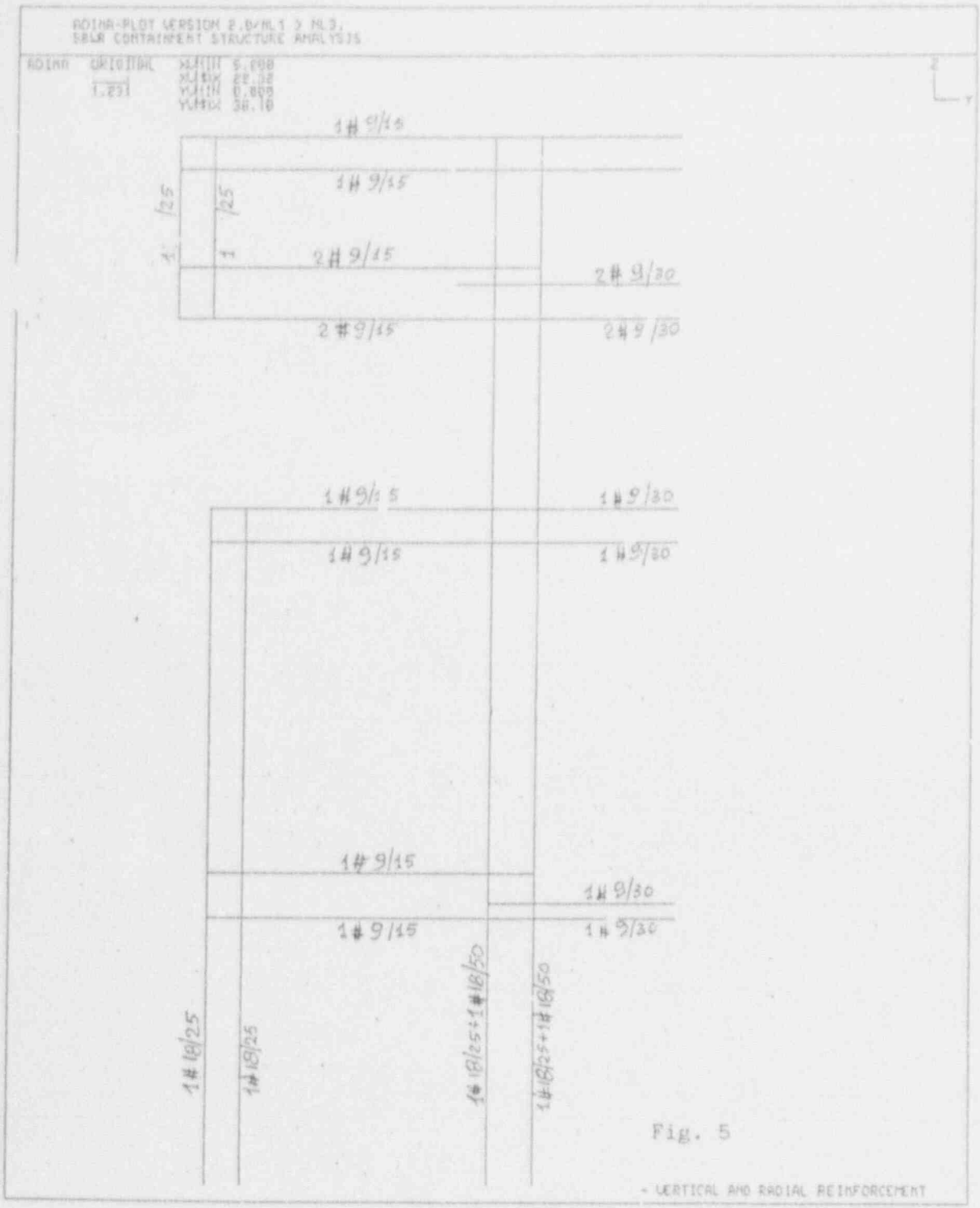


Fig. 5

- VERTICAL AND RADIAL REINFORCEMENT

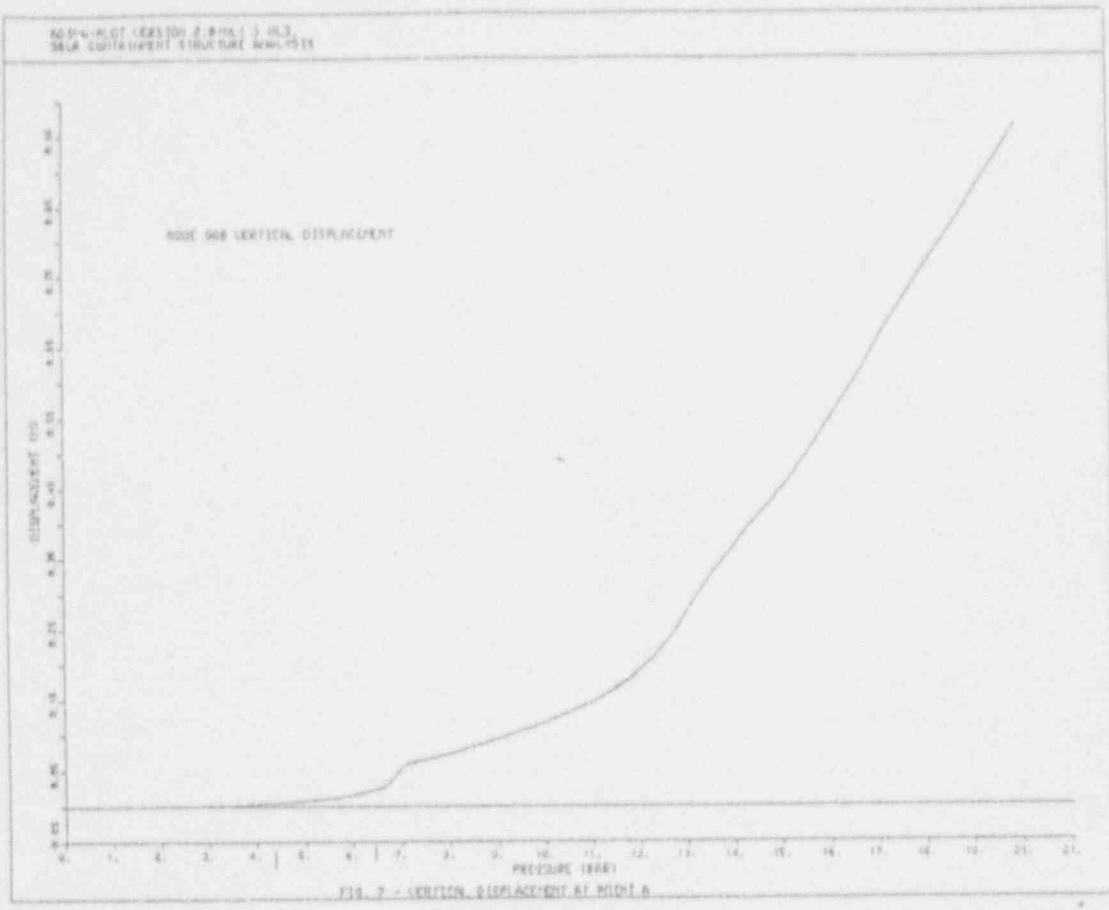


FIG. 7 - VERTICAL DISPLACEMENT AT POINT A

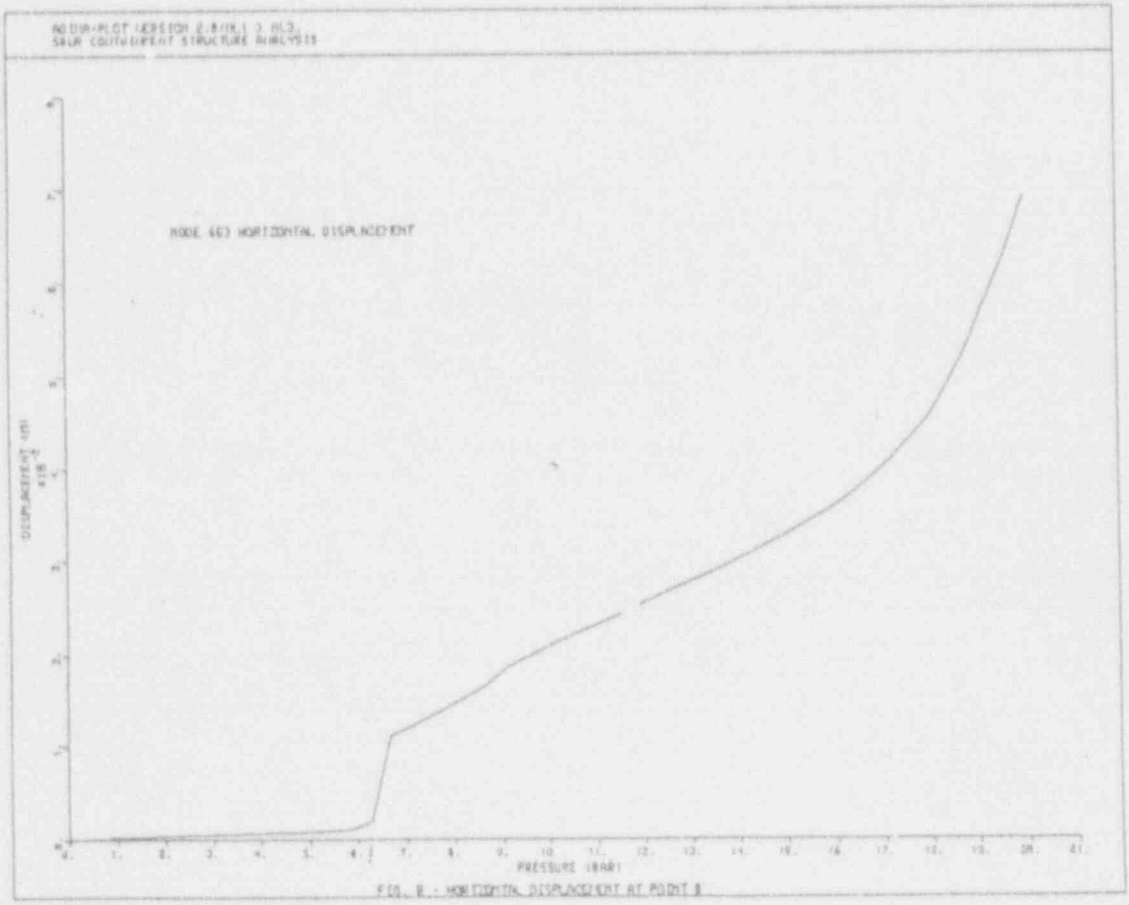


FIG. 8 - HORIZONTAL DISPLACEMENT AT POINT B

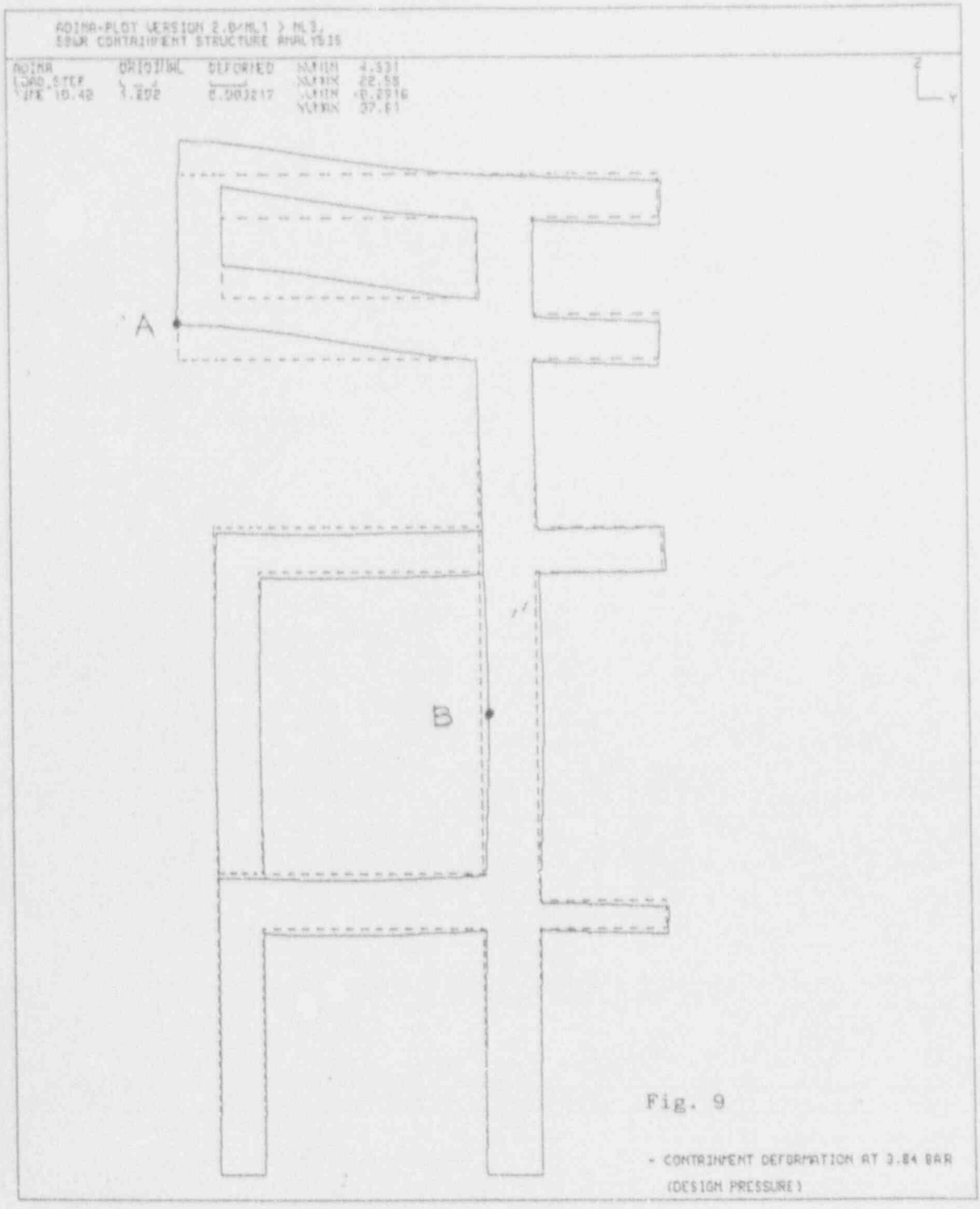


Fig. 9

- CONTAINMENT DEFORMATION AT 3.84 BAR (DESIGN PRESSURE)

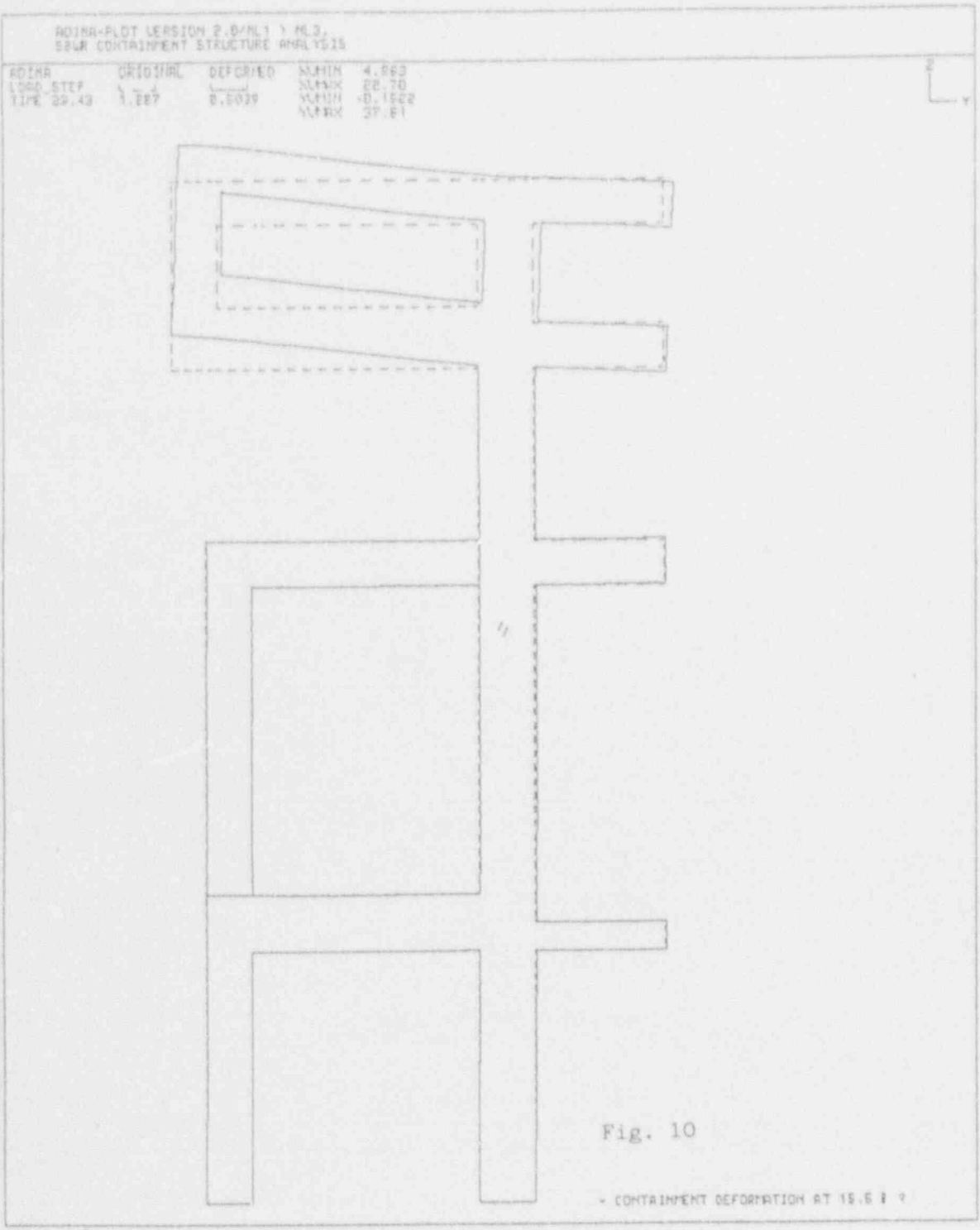


Fig. 10

- CONTAINMENT DEFORMATION AT 15.6 P ?

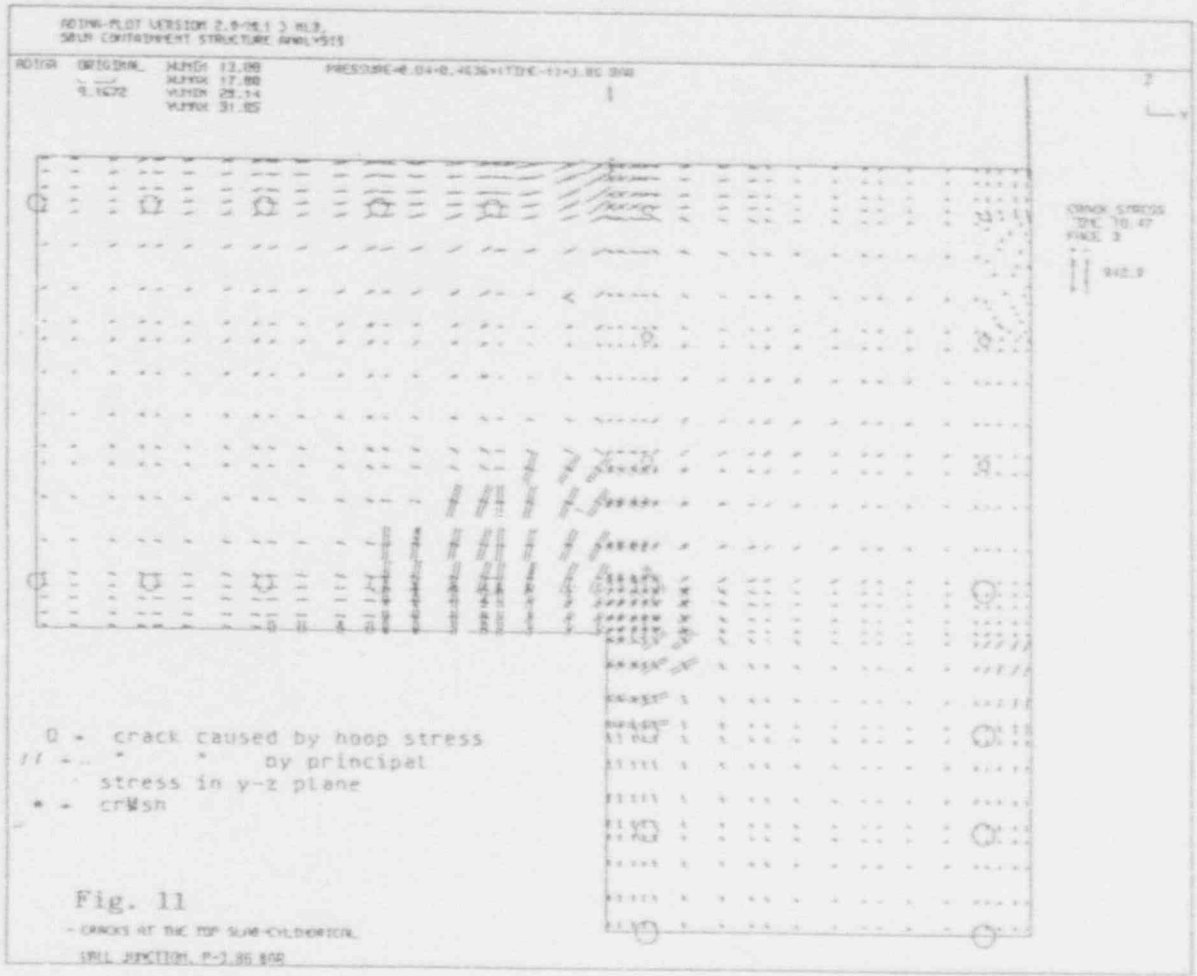


Fig. 11

- CRACKS AT THE TOP SLAB-CYLINDER JUNCTION, P=3.86 BAR

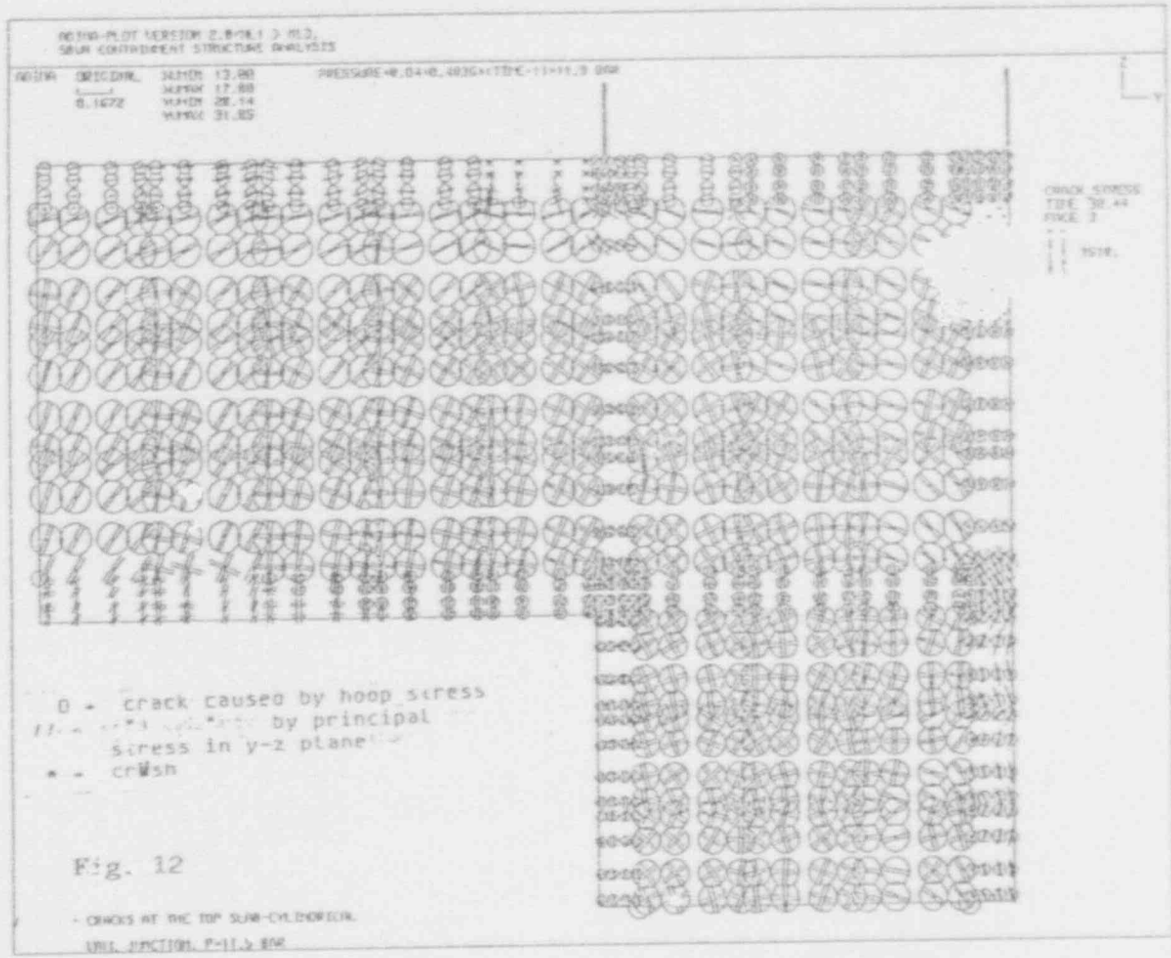
0 - crack caused by hoop stress
- crack caused by principal
stress in y-z plane
* - crush

Fig. 12

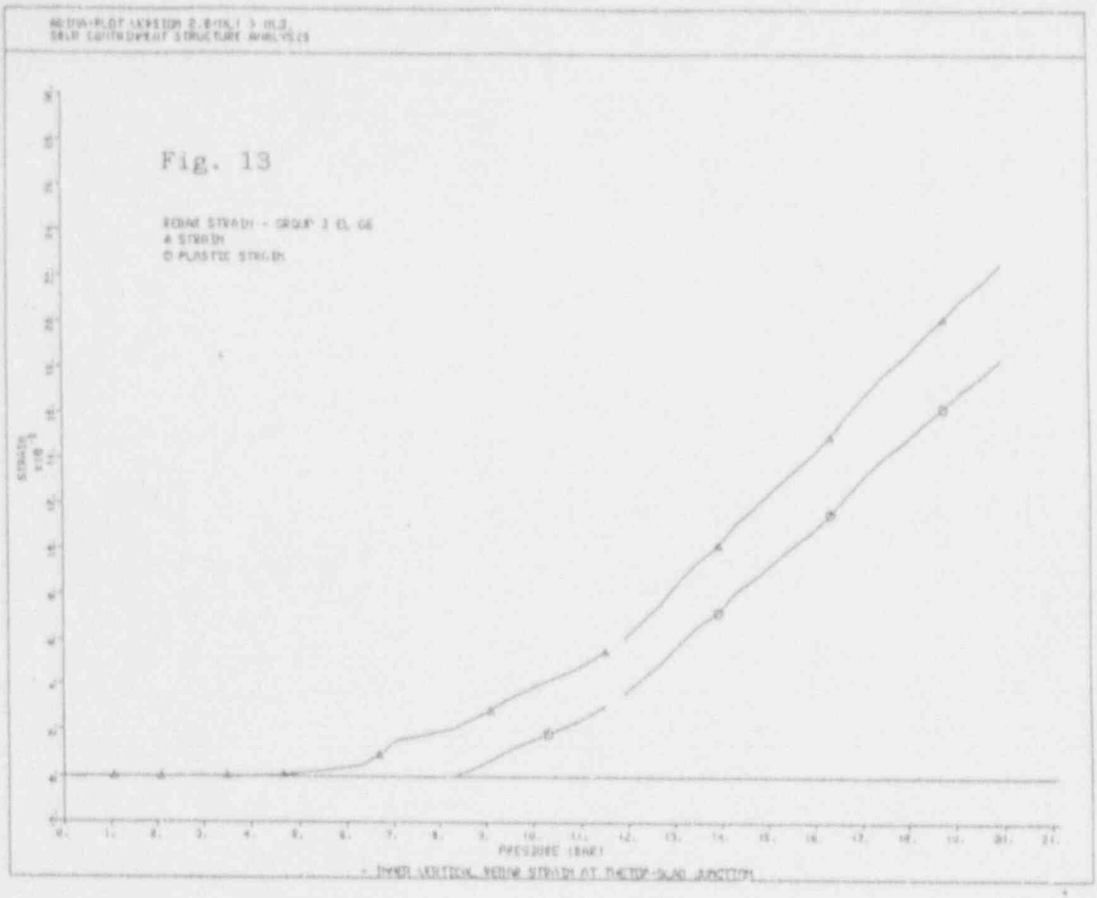

Fig. 13

REBAR STRAIN - GROUP 3 EL 66
A STRAIN
O PLASTIC STRAIN

STRAIN x10^-3

PRESSURE (BAR)

- INNER VERTICAL REBAR STRAIN AT THE TOP-SLAB JUNCTION

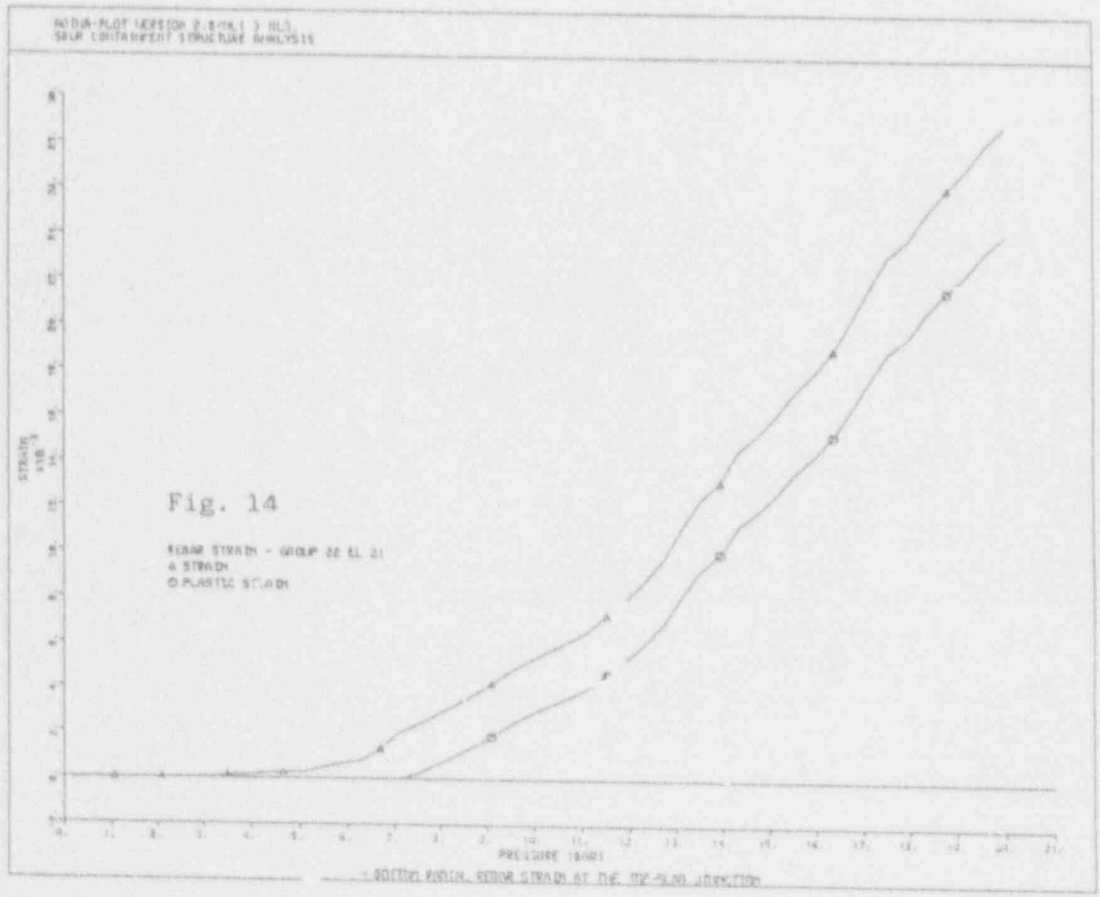

Fig. 14

REBAR STRAIN - GROUP 22 EL 21
A STRAIN
O PLASTIC STRAIN

STRAIN x10^-3

PRESSURE (BAR)

- BOTTOM RADIAL REBAR STRAIN AT THE TOP-SLAB JUNCTION

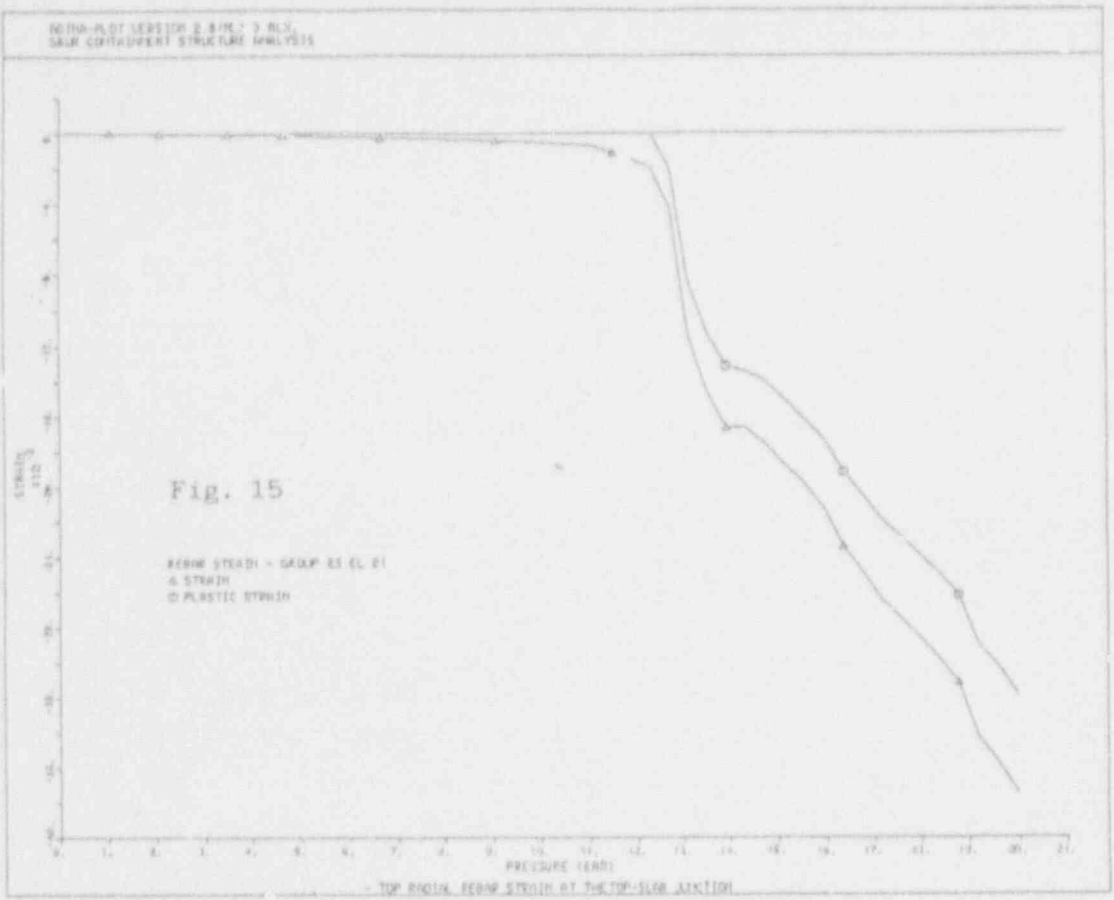
Fig. 15
REBAR STRAIN - GROUP 83 EL 21
Δ STRAIN
○ PLASTIC STRAIN
PRESSURE (PSIG)
- TOP RADIAL REBAR STRAIN AT THE TOP-SLAB JUNCTION

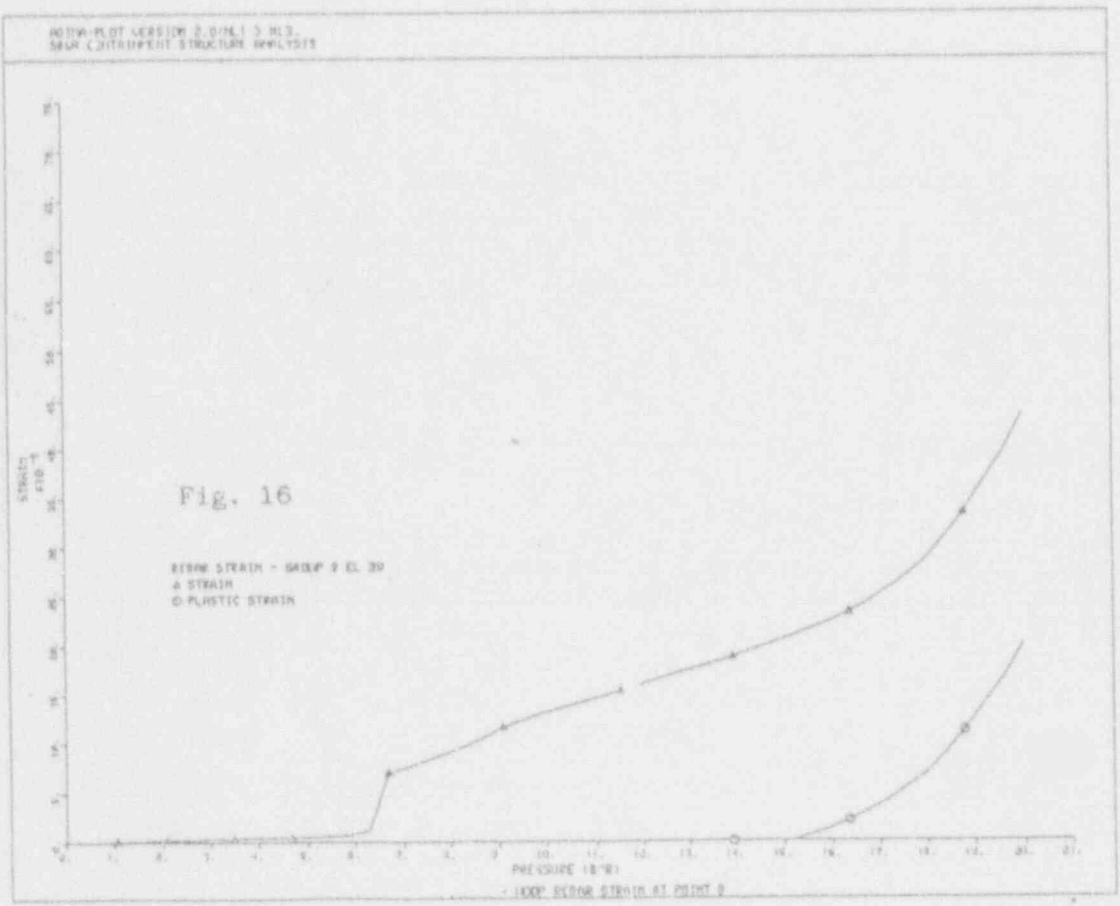
Fig. 16
REBAR STRAIN - GROUP 9 EL 39
Δ STRAIN
○ PLASTIC STRAIN
PRESSURE (PSIG)
- HOOP REBAR STRAIN AT POINT 9

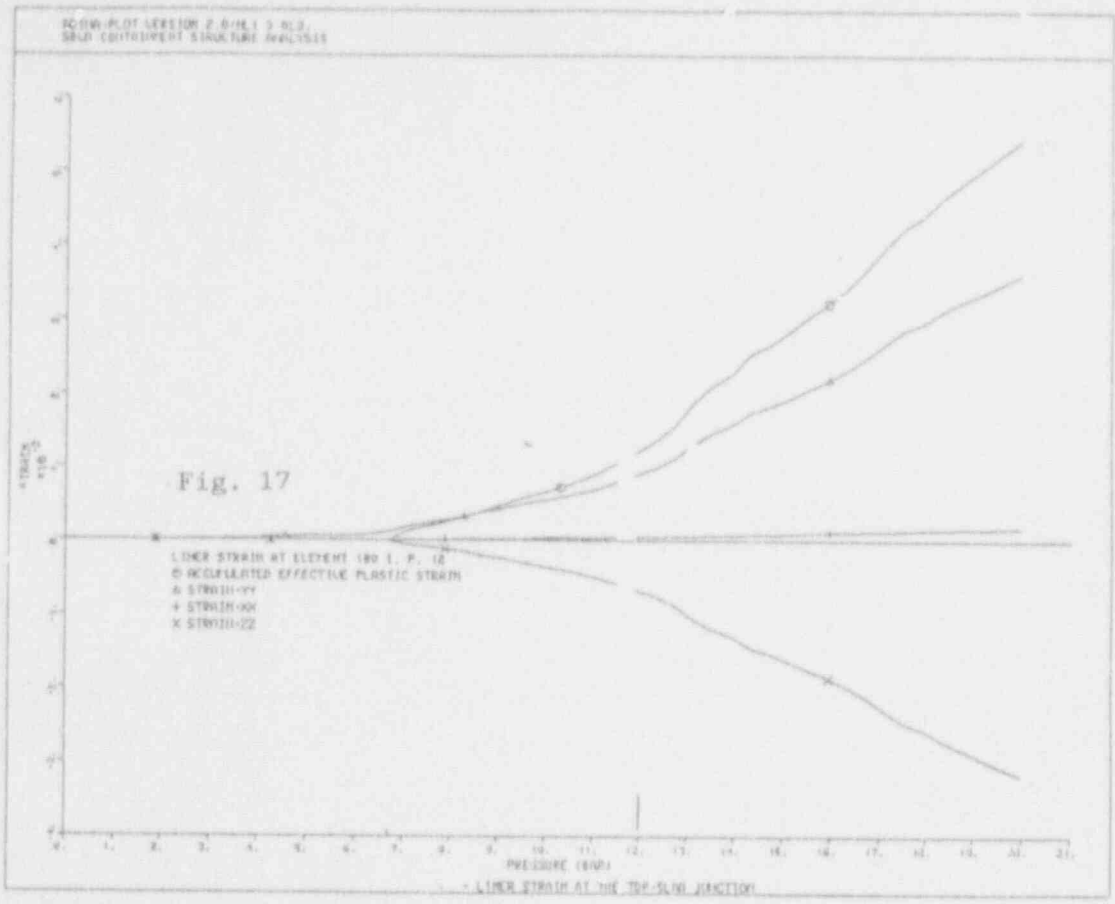
LINER STRAIN AT ELEMENT (80 I, P, 12
⊙ ACCUMULATED EFFECTIVE PLASTIC STRAIN
Δ STRAIN-YY
+ STRAIN-XX
X STRAIN-ZZ
PRESSURE (BAR)
- LINER STRAIN AT THE TOP-SLAB JUNCTION

Fig. 17

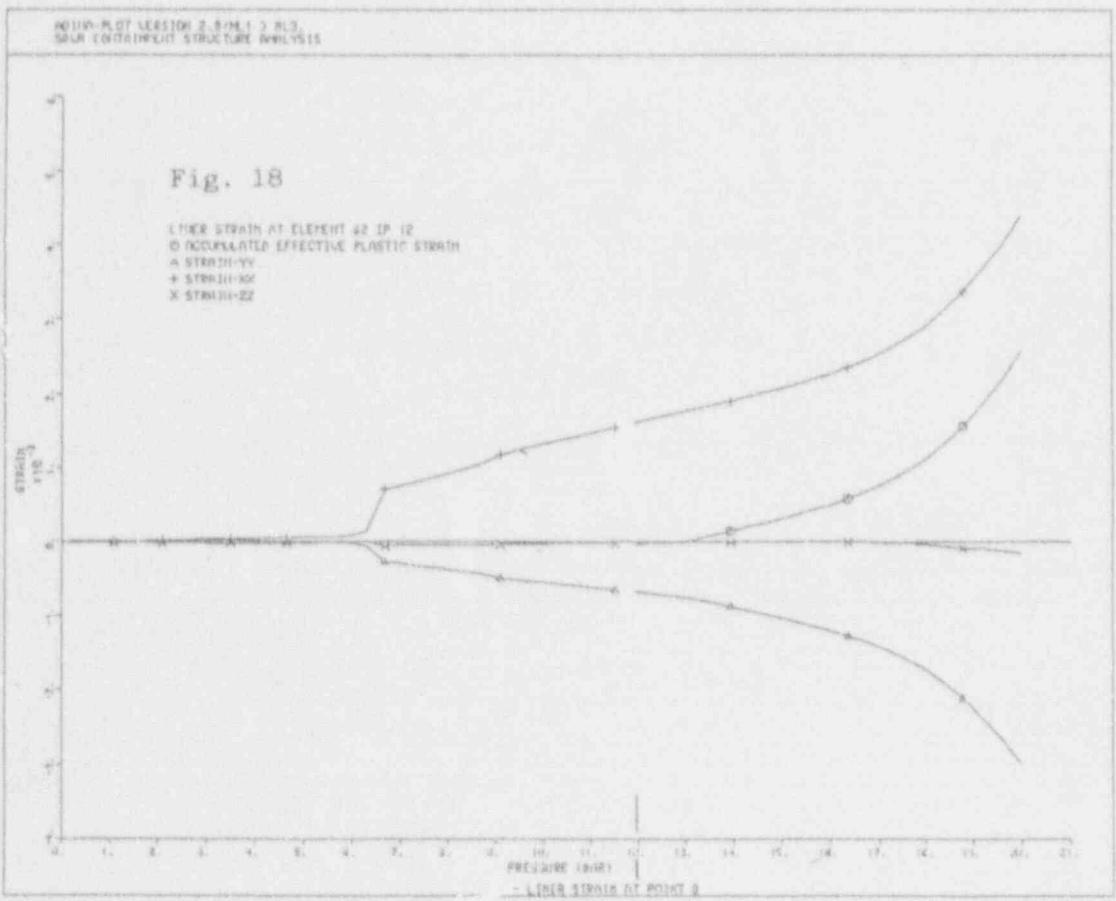
LINER STRAIN AT ELEMENT 62 IP 12
⊙ ACCUMULATED EFFECTIVE PLASTIC STRAIN
Δ STRAIN-YY
+ STRAIN-XX
X STRAIN-ZZ
PRESSURE (BAR)
- LINER STRAIN AT POINT B

Fig. 18

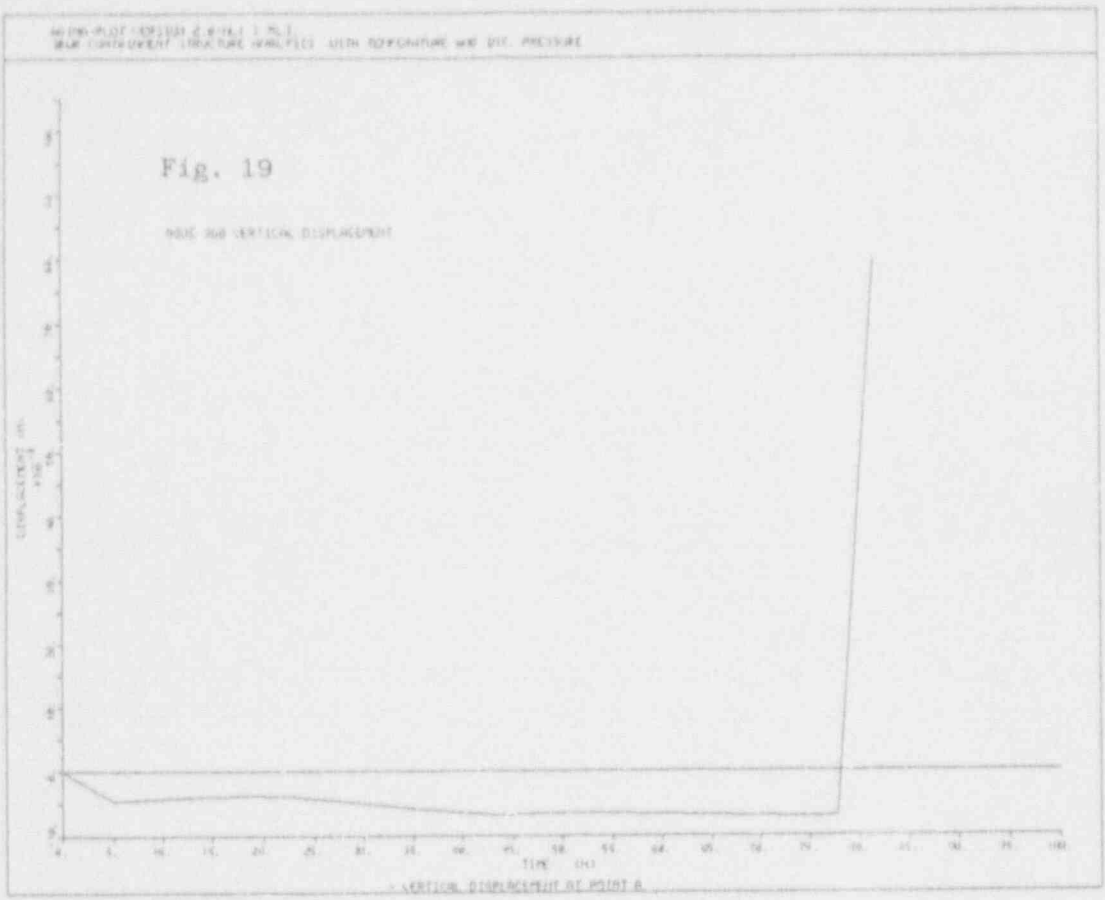
Fig. 19
NODE 368 VERTICAL DISPLACEMENT
TIME (H)

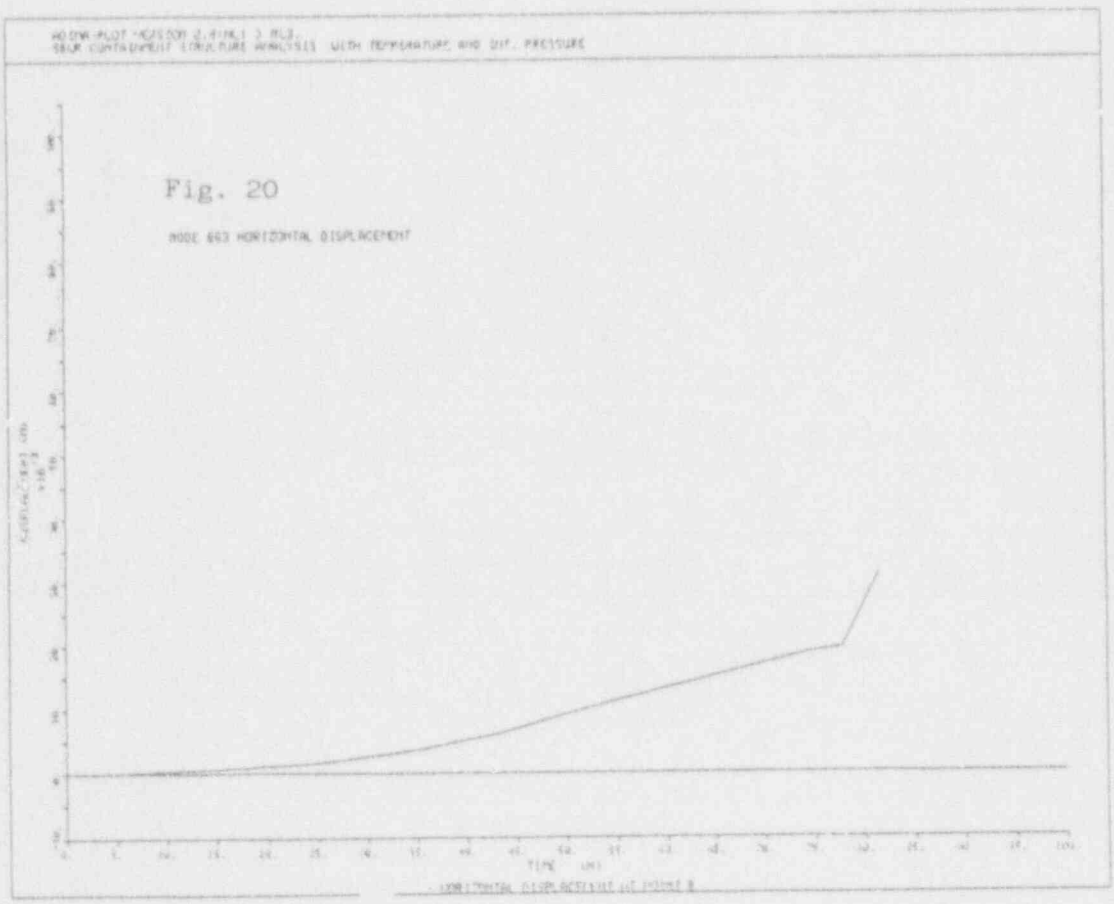
Fig. 20
NODE 663 HORIZONTAL DISPLACEMENT
TIME (H)

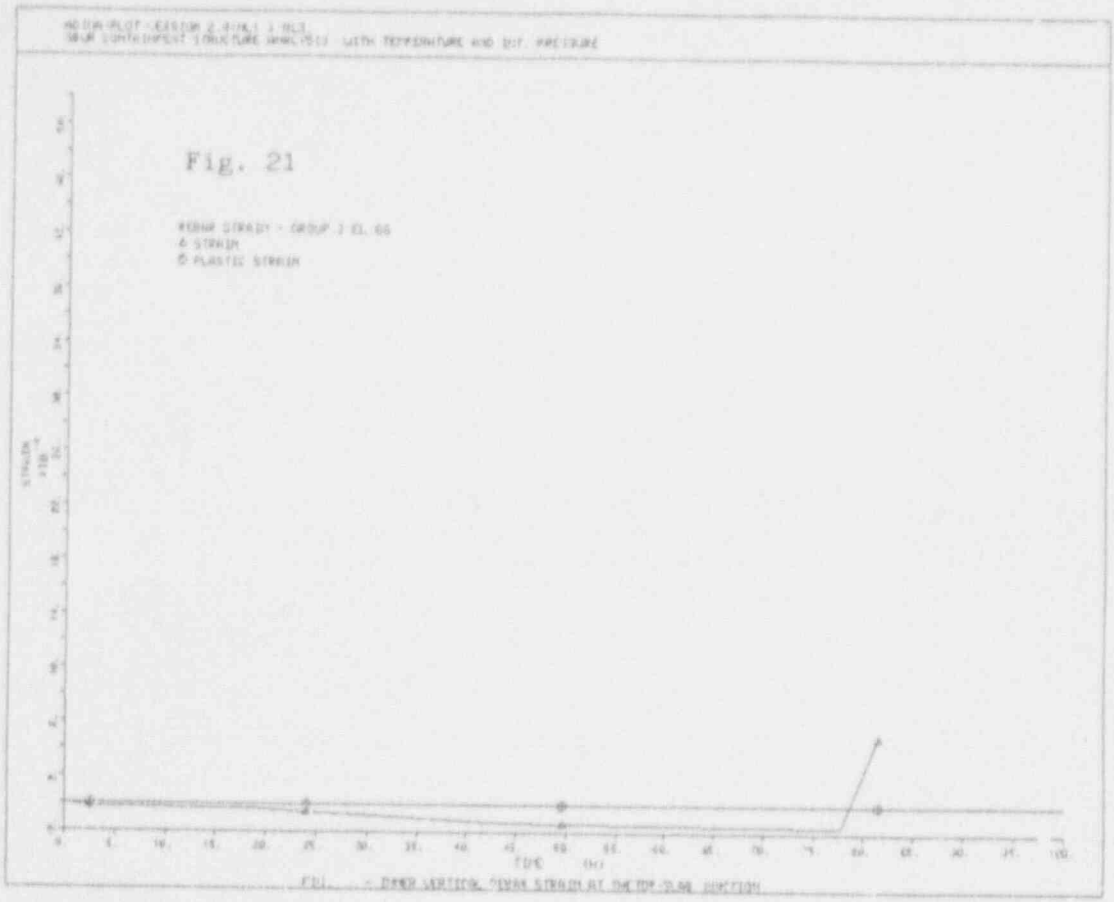

Fig. 21

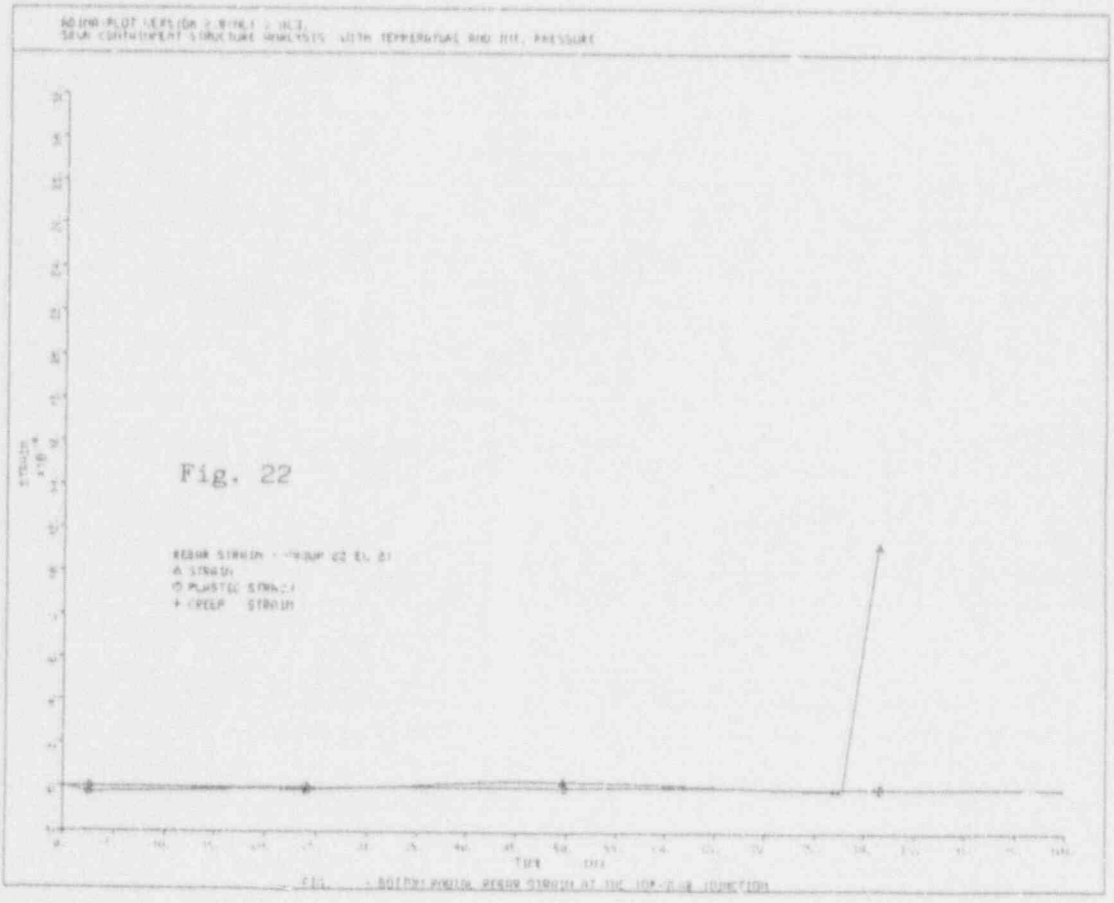

Fig. 22

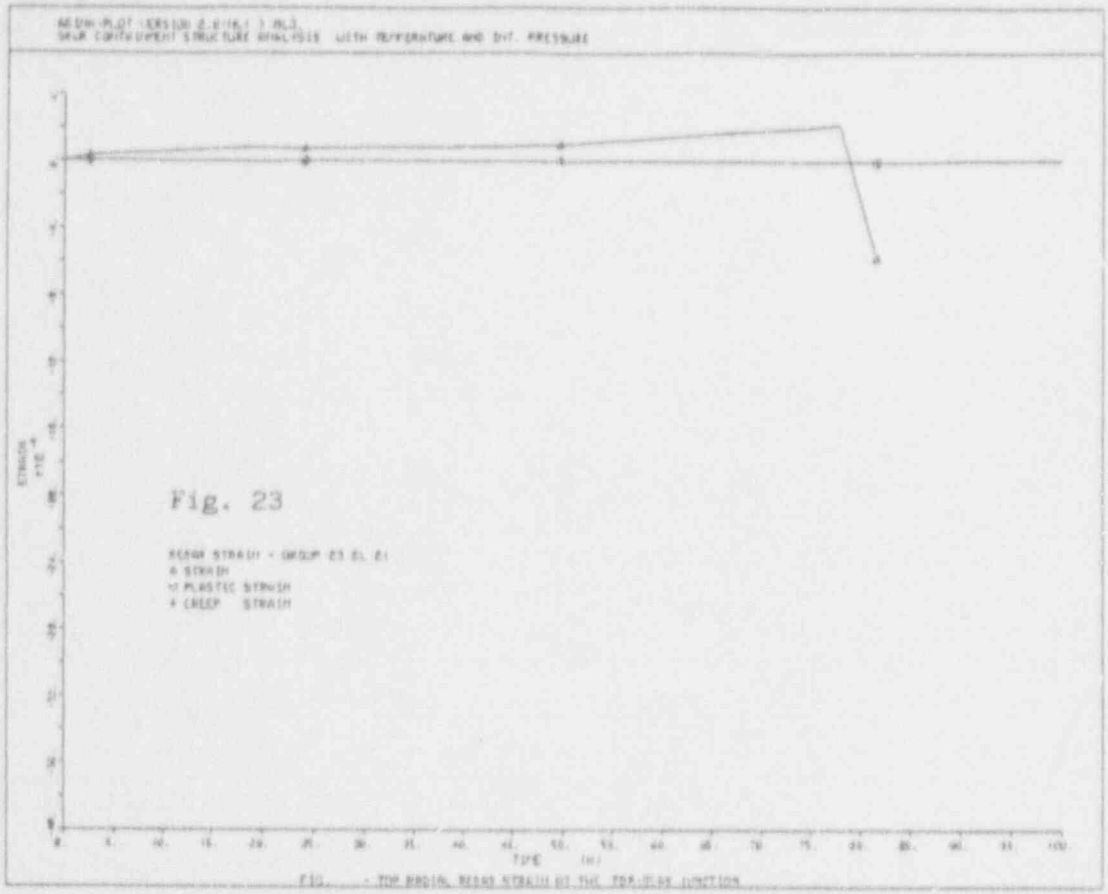


Fig. 23

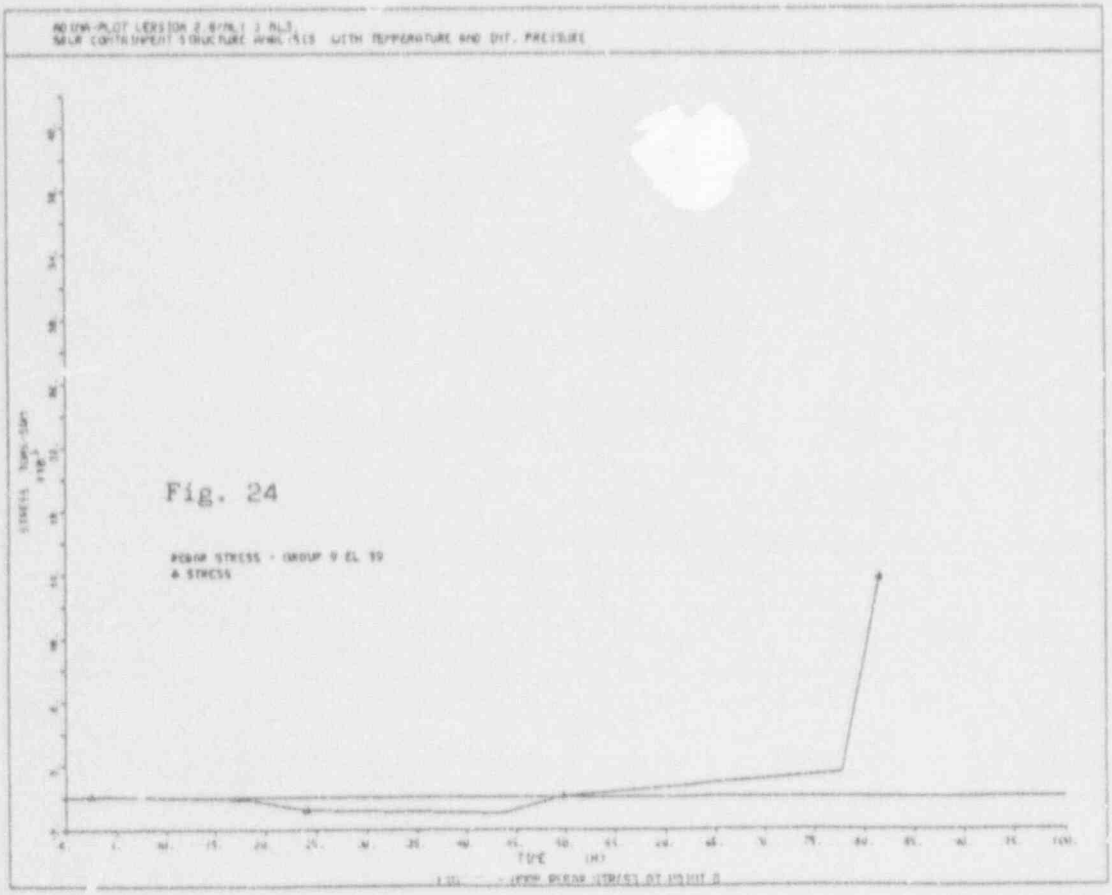


Fig. 24

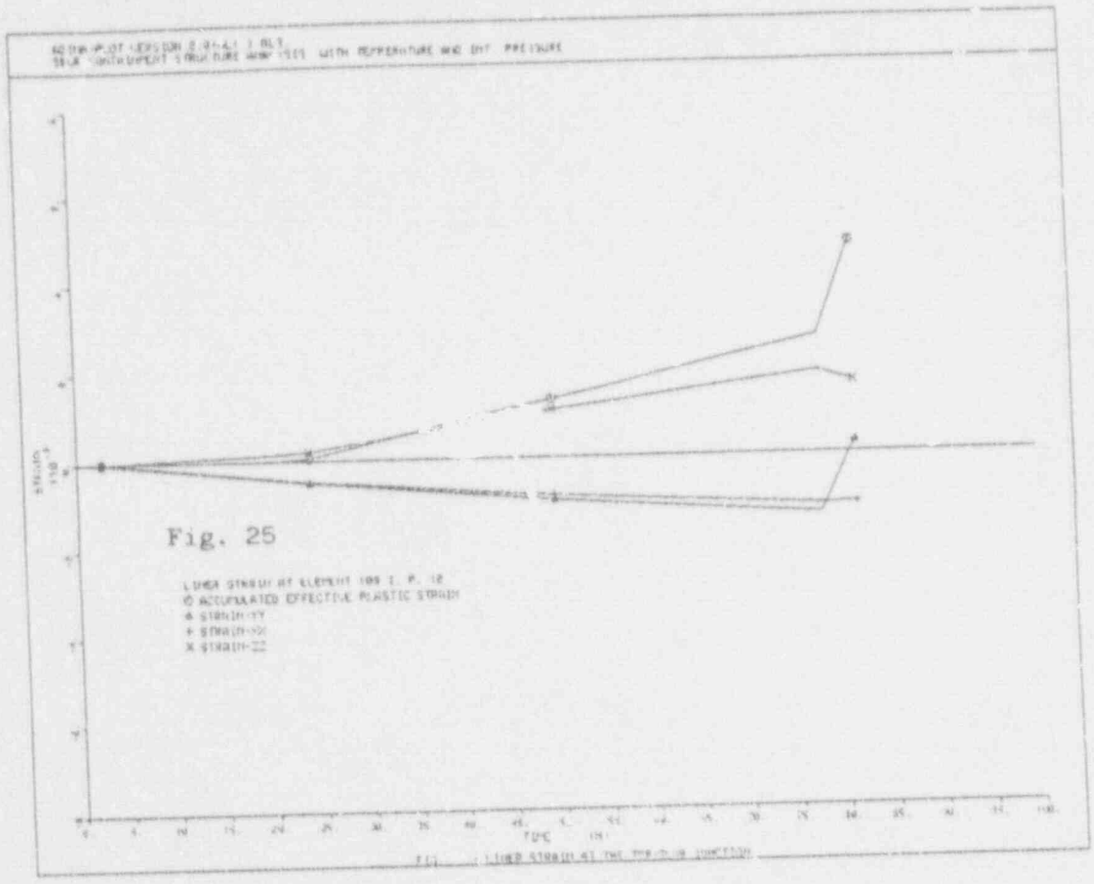

Fig. 25

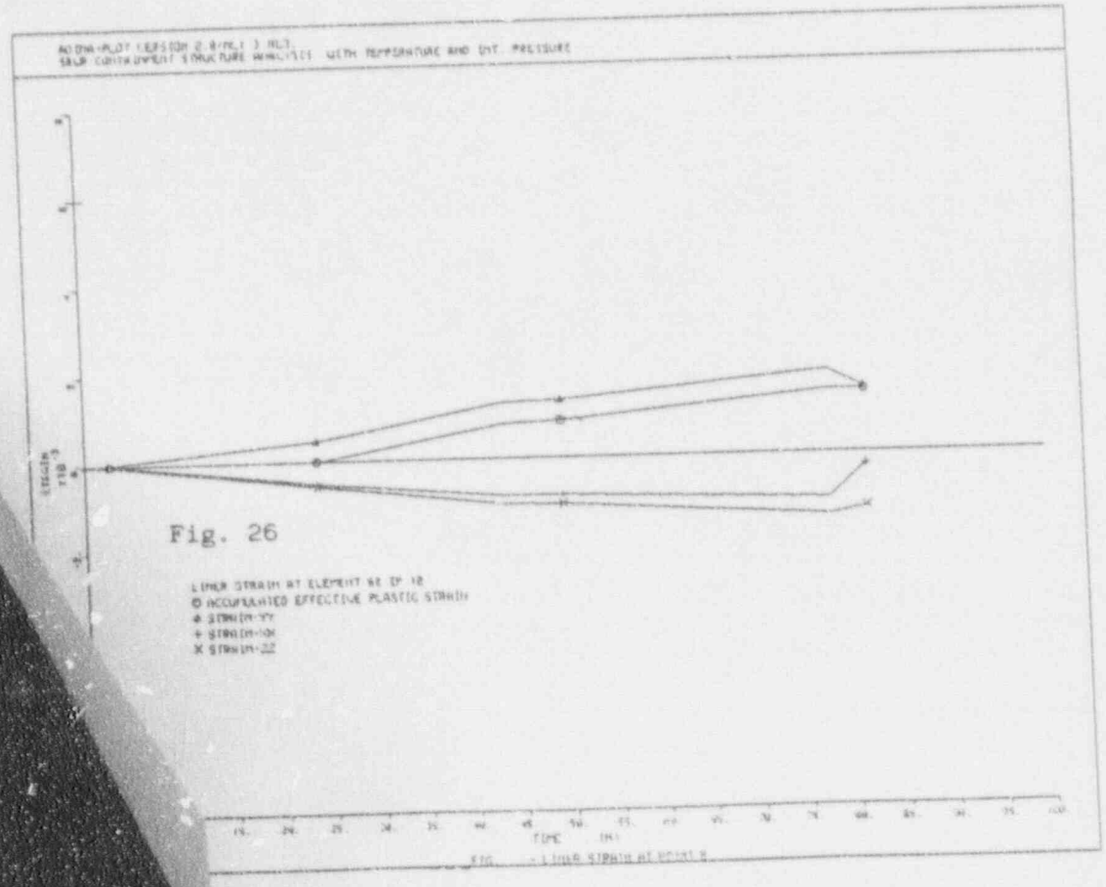

Fig. 26

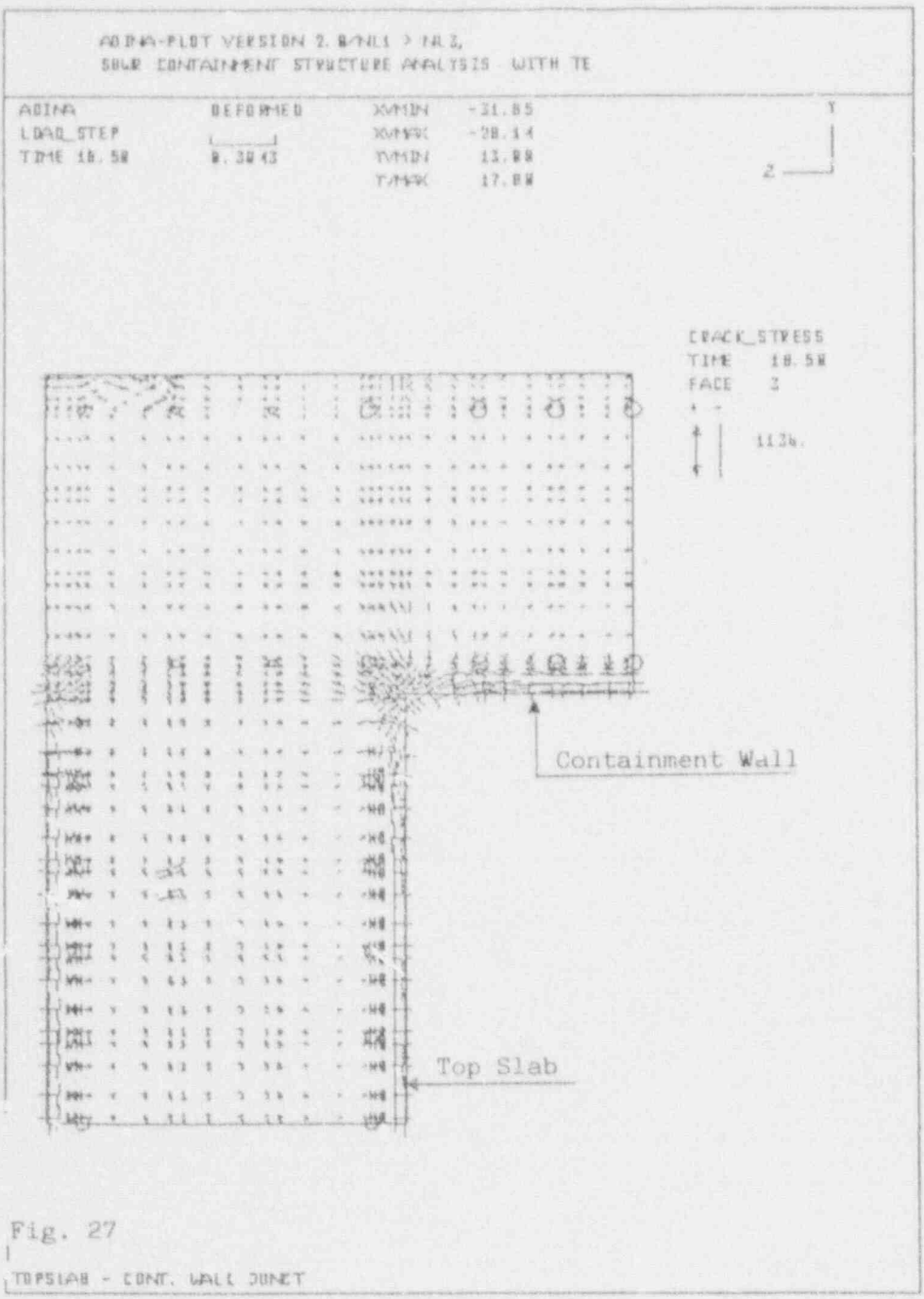


Fig. 27

TOPSLAB - CONT. WALL JUNCT

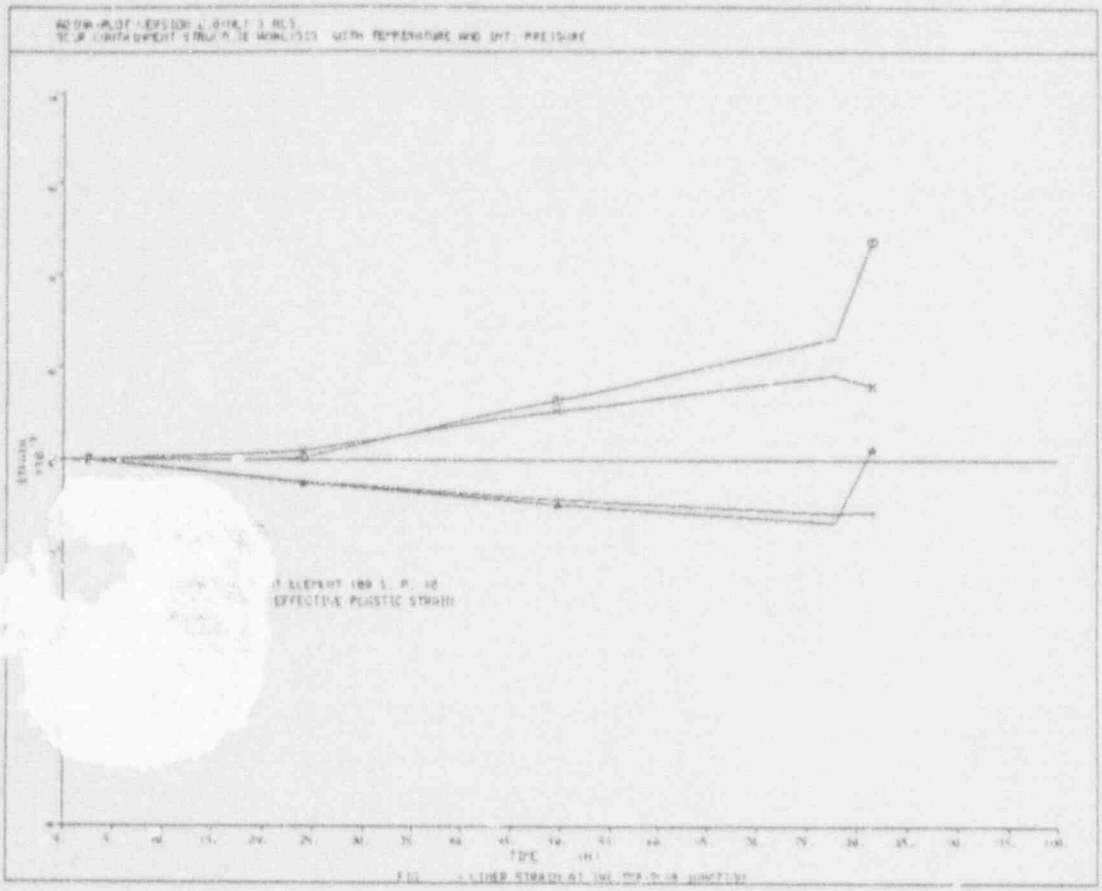

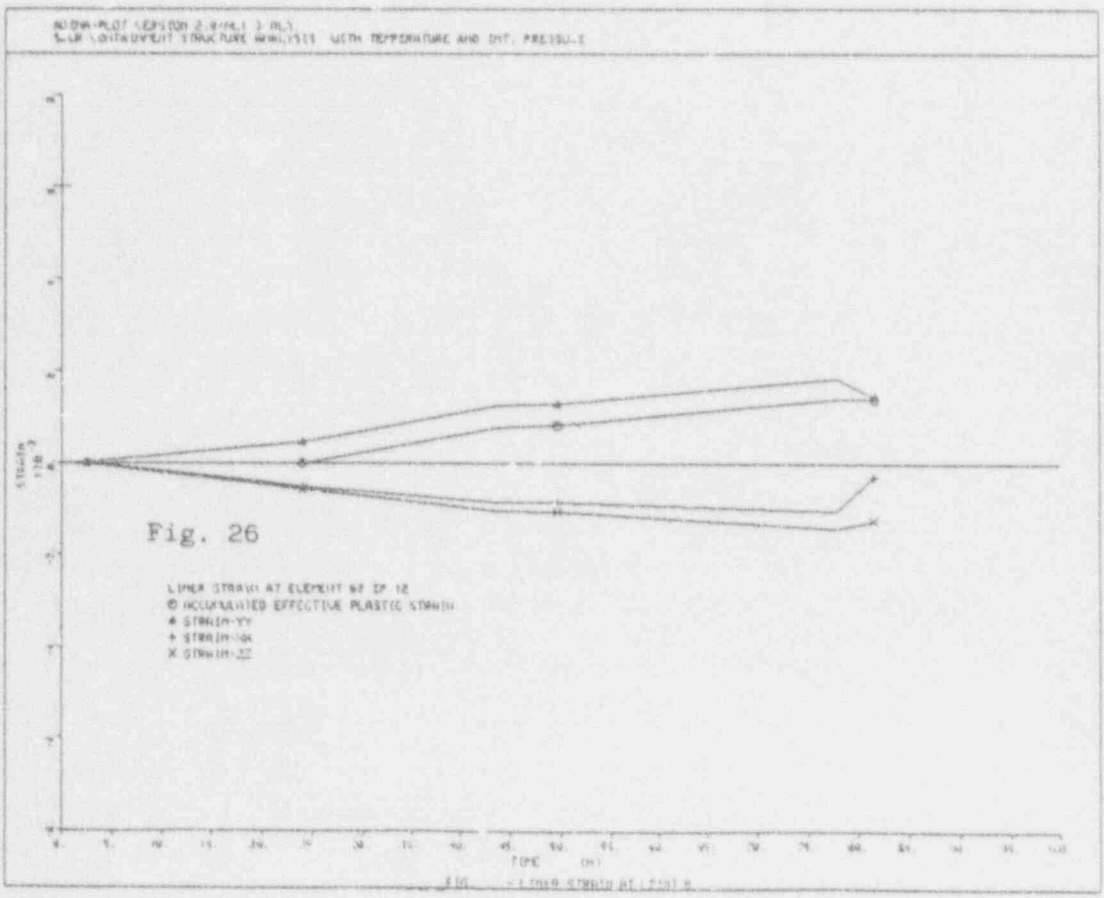
Fig. 26
LINER STRAIN AT ELEMENT NO IP 12
© ACCUMULATED EFFECTIVE PLASTIC STRAIN
♦ STRAIN-YY
+ STRAIN-XX
X STRAIN-ZZ

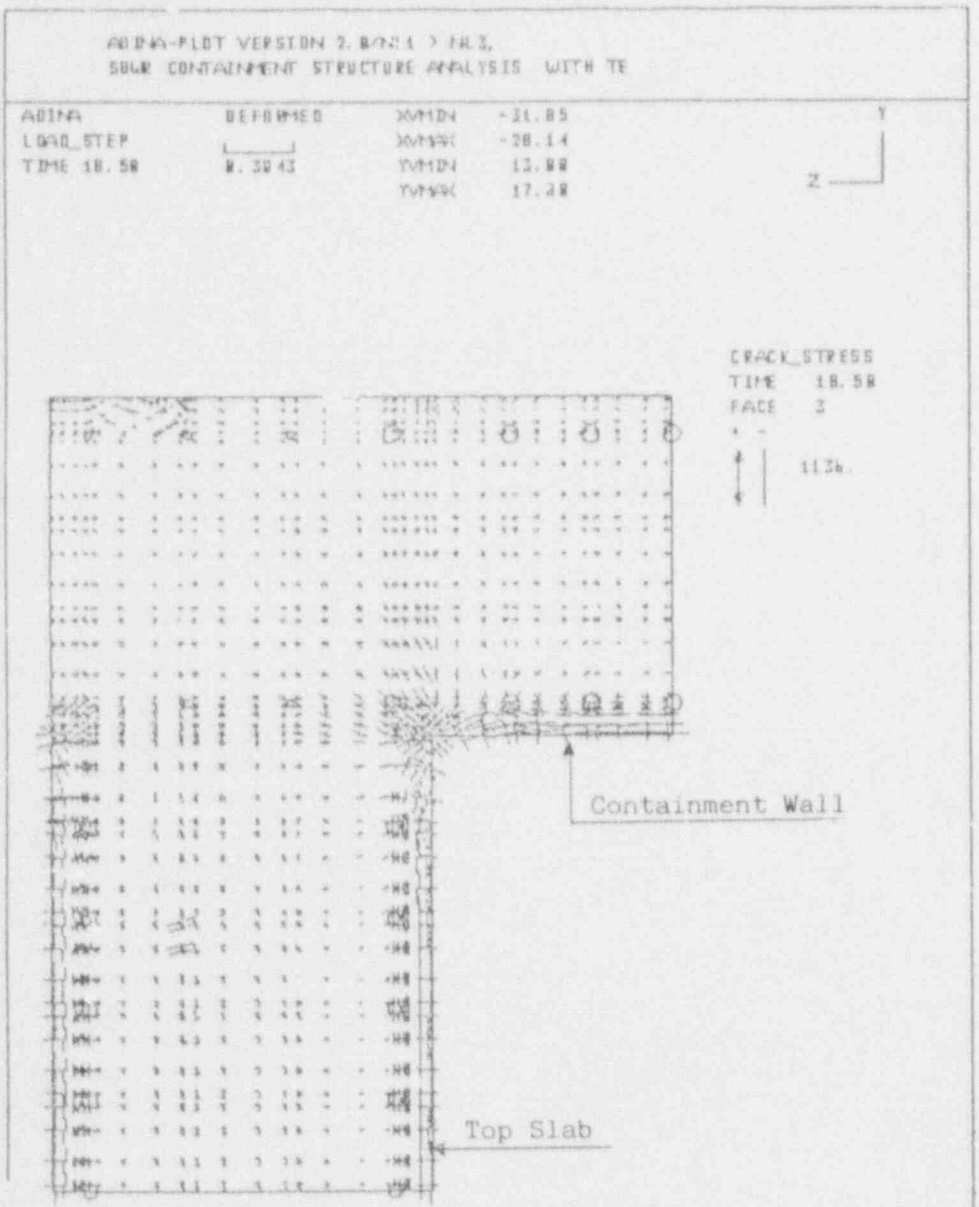


Fig. 27

TOPSLAB - CONT. WALL JUNCT

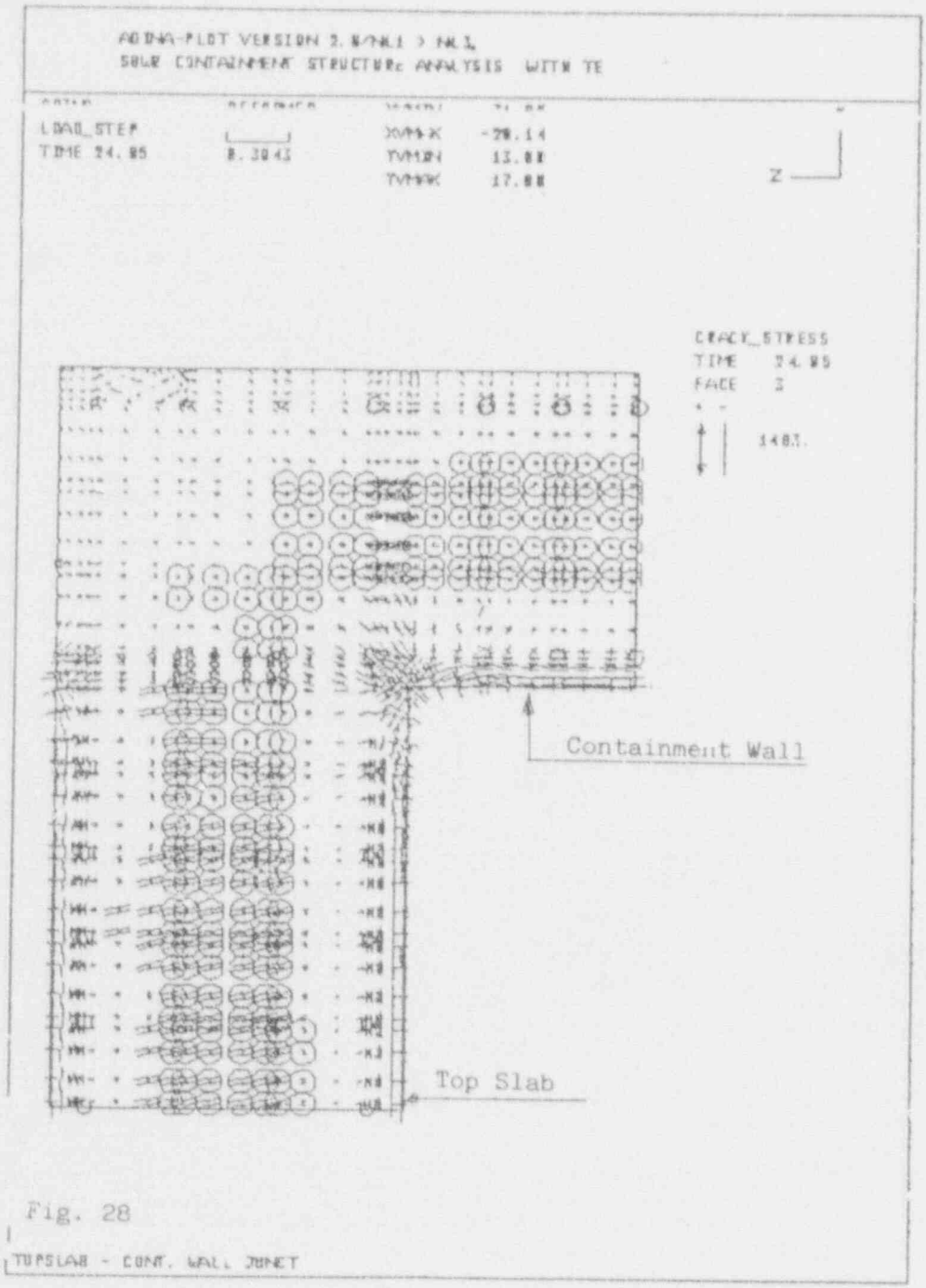
ADINA-PLOT VERSION
SOLR CONTAINMENT STRUCTURE ANALYSIS WITH TE
LOAD_STEP
TIME 24.85
XMAX -28.14
YMIN 13.88
YMAX 17.88
Z
CRACK_STRESS
TIME 24.85
FACE 2
140%
Containment Wall
Top Slab
TOPSLAB - CONT. WALL JUNCT

Fig. 28

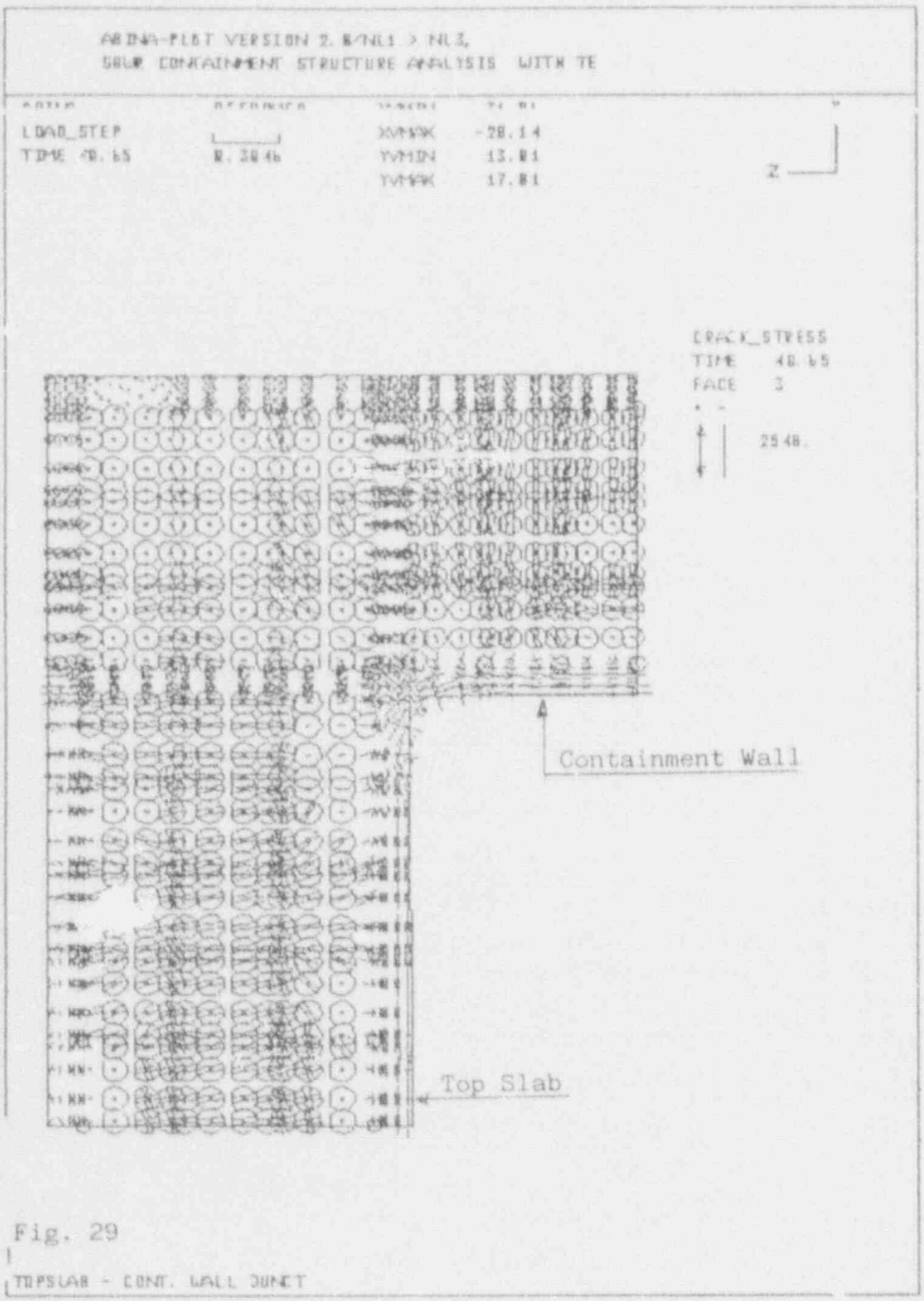
ABINA-PLOT VERSION 2.8/NL1 > NL2,
LOAD_STEP
TIME 48.65
XMAX -28.14
YMIN 13.81
YMAX 17.81
Z
CRACK_STRESS
TIME 48.65
FACE 3
2548.
Containment Wall
Top Slab
TOPSLAB - CONT. WALL JUNCT

Fig. 29

# POST-TEST ANALYSIS OF A 1:10-SCALE TOP SLAB MODEL OF ABWR/RCCV SUBJECTED TO INTERNAL PRESSURE

Hideaki Saito
Tokyo Electric Power Co , Inc.

Yutaka Muramatsu
Toshiba Corp.

Hideyasu Furukawa
Hitachi Ltd.

Toshiyasu Hasegawa
Shimizu Corp.

Atsushi Mutoh
Shimizu Corp.

## Abstract

The first Advanced Boiling Water Reactor (ABWR) employing a reinforced concrete containment vessel (RCCV) has started its construction in 1991 in Japan. As RCCV itself is the first structure of its kind in Japan, thorough verification tests have been performed. This paper presents the results of simulation analysis of the Top Slab partial model of the RCCV subjected to internal pressure beyond design load. Top Slab portion is so complicated, composed of flat Top Slab, cylindrical wall and fuel pool girders, that its simulation analysis requires the evaluation of nonlinear structural behavior of reinforced concrete members due to membrane, bending and shear forces. This paper reports that Finite Element analysis with 3-D solid approach has given a good agreement quantitatively between experimental and analysis results with respect to deformation, failure load and each nonlinear behaviors.

## INTRODUCTION

A cross section of the ABWR plant is shown in Figure 1. The RCCV cylindrical wall is integrated with the floor slab of reactor building, and the Top Slab is integrated with fuel-pool girders which are connected with the reactor building walls and floors[1].

In this paper, the post-test analysis results for the "Top Slab Experiment" are presented. This test is one of the series of verification tests performed for the trial designed RCCV. An outline of the tests was already presented in the paper of the 4th Workshop[2].

Top Slab experimental model is a 1:10-scale partial model which simulated the Top Slab portion as accurately as possible, and ultimate strength was experimentally examined by applying internal pressure up to failure. The connection between the Top Slab and cylindrical wall is a portion of discontinuity where the shape changes abruptly and stress concentration occurs. As mentioned earlier, the Top Slab is integrated with the fuel-pool girders in order to resist internal pressure (design internal pressure level : 3.16 kgf/cm$^2$). In the test, it was proven that the failure pressure is around four times the design pressure.

The analysis was performed with a 3-D FE-model using solid elements because of the asymmetric shape of the RCCV model.

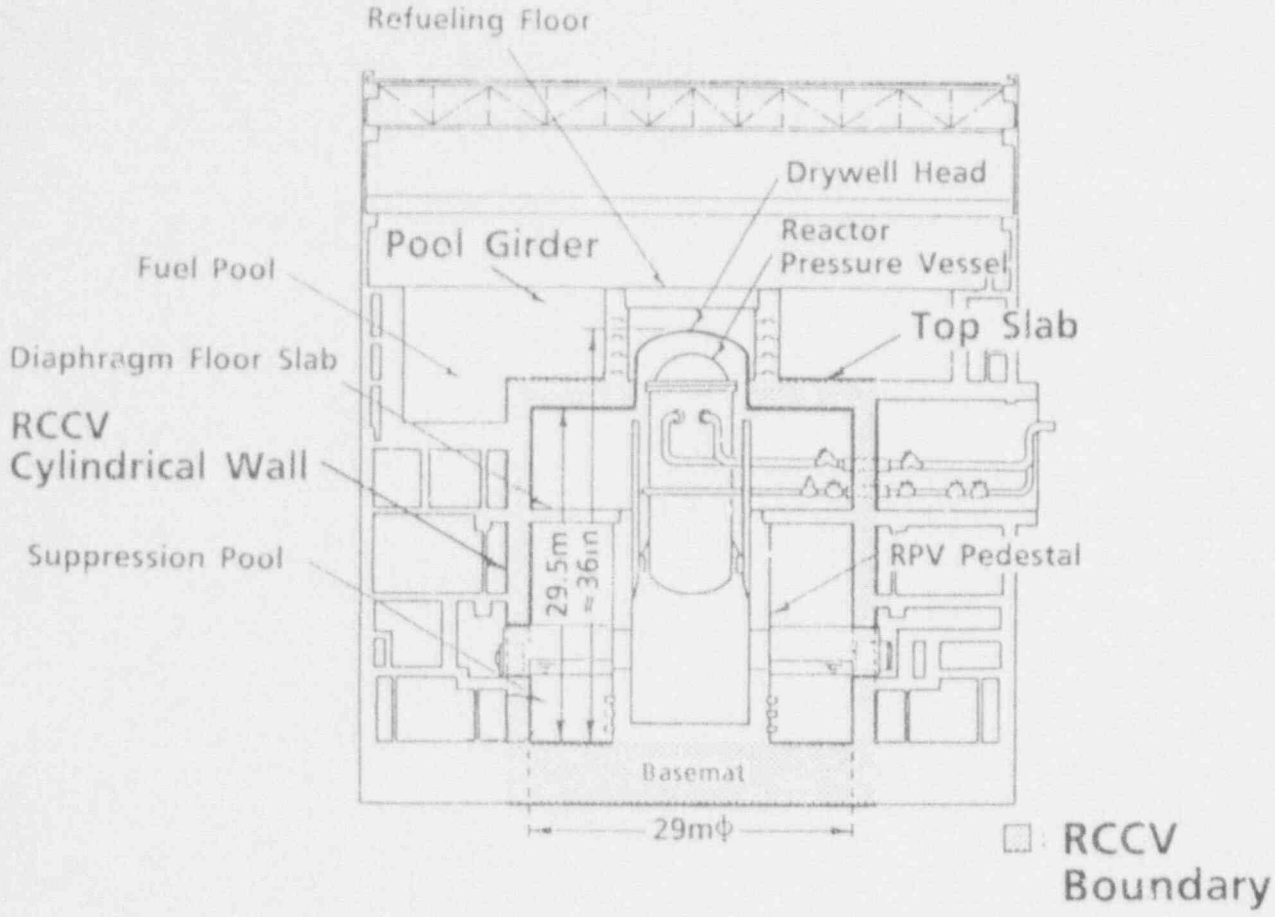


Figure 1. Section of ABWR Plant

## OUTLINE OF THE TOP SLAB EXPERIMENT

The objective of "Top Slab Test" was to examine the structural behaviors of Top Slab portion under internal pressure load. Major items for the examination were stress distributions, deformation and cracking.

### Test Model

The Top Slab portion consists of flat Top Slab with a large opening, cylindrical wall, and fuel pool girders connecting to the top surface of the Top Slab. Fuel pool girders are also connected with the exterior walls of reactor building. These structural elements exert great influences on the structural behavior of the Top Slab portion.

The configuration of the test model is shown in Figure 2, while the dimensions are given in Figure 3. The reinforcing bars of the test model simulated the rebar ratio of the trial-designed RCCV and the reinforcing bars arrangement was made considering distances between stress centers, adequate spacing of reinforcing bars, anchorage of bars and pouring of concrete. An outline of the reinforcing bar arrangement is shown in Figure 4. Concrete used in the test model had aggregate of 10mm in maximum size and the target compressive strength at test was 300 kgf/cm$^2$. Reinforcing bars used were of diameters 4 mm, 6 mm and 10 mm and of strengths equivalent to SD35. The test results of the materials used are given in Table 1 and 2.

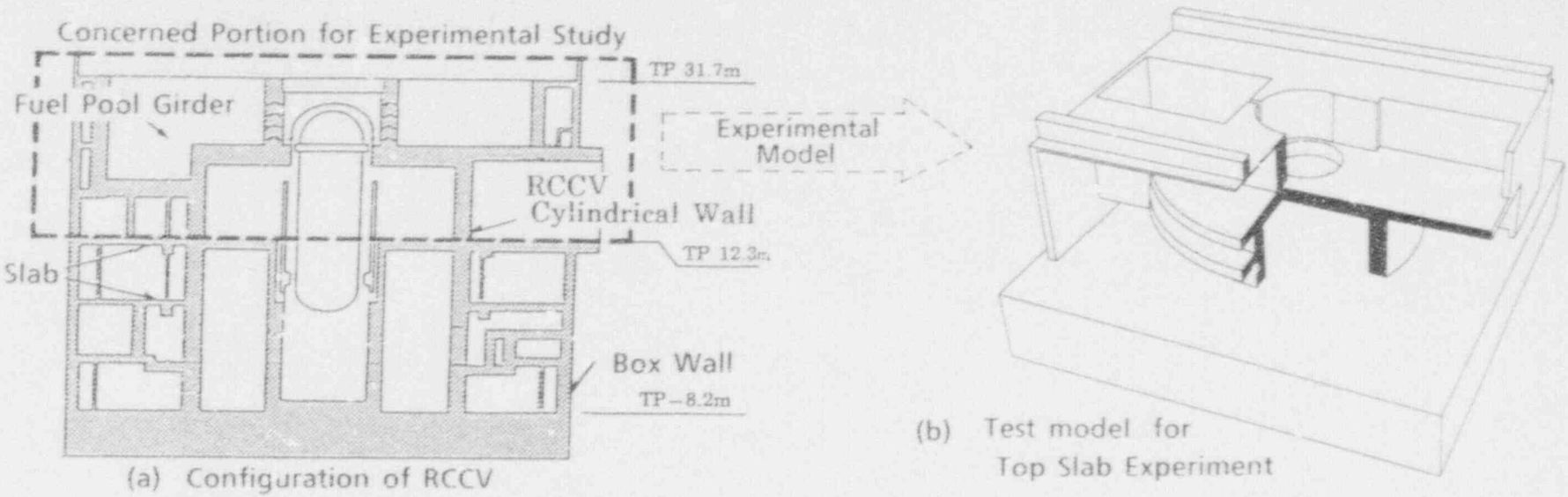


**Figure 2 Configuration of Test Model**



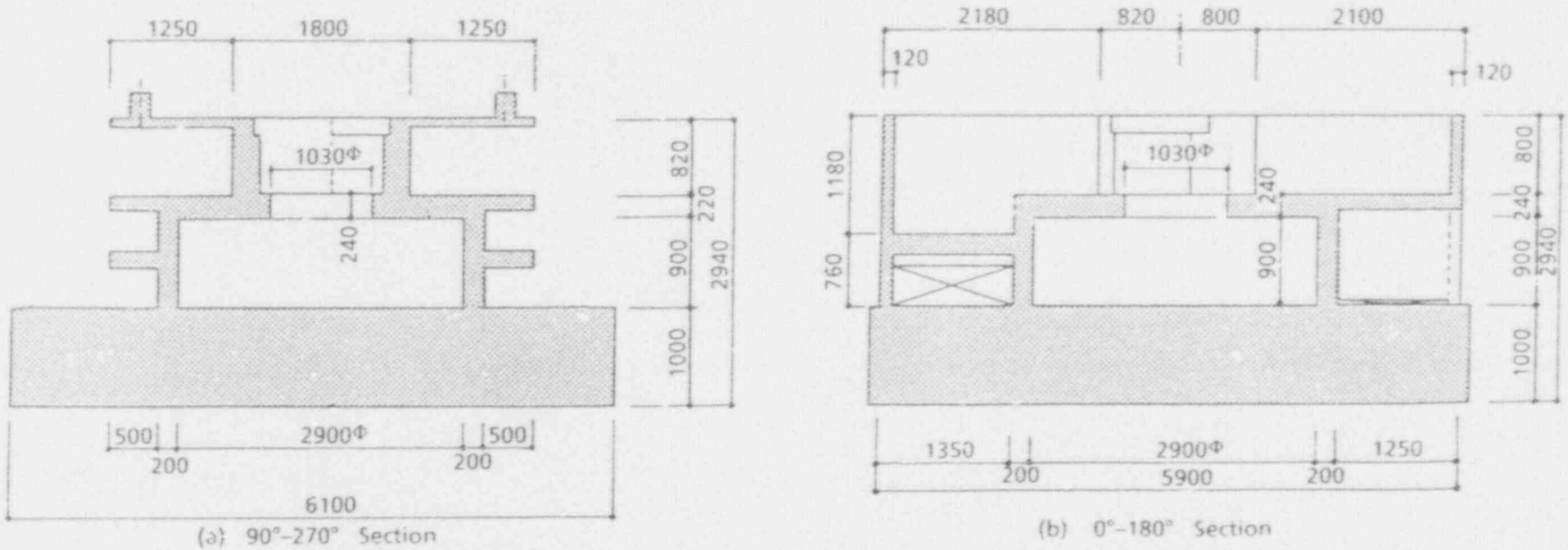


**Figure 3 Dimensions of Test Model for Top Slab Experiment**

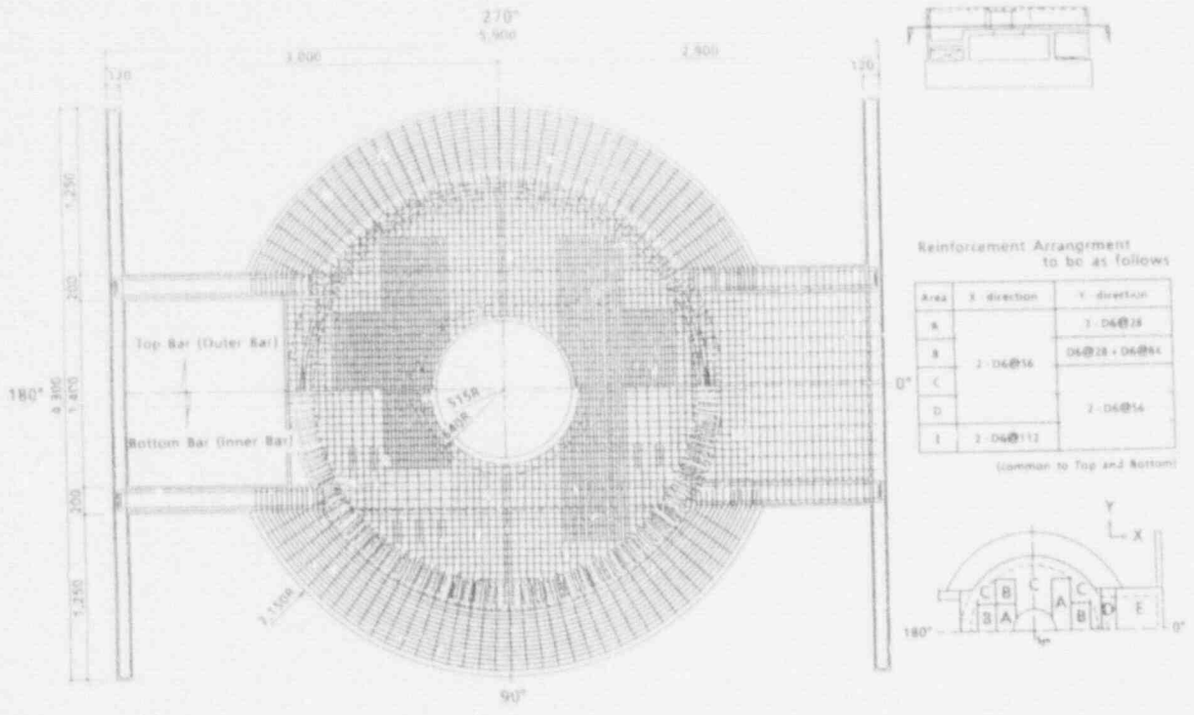


(a) Top Slab

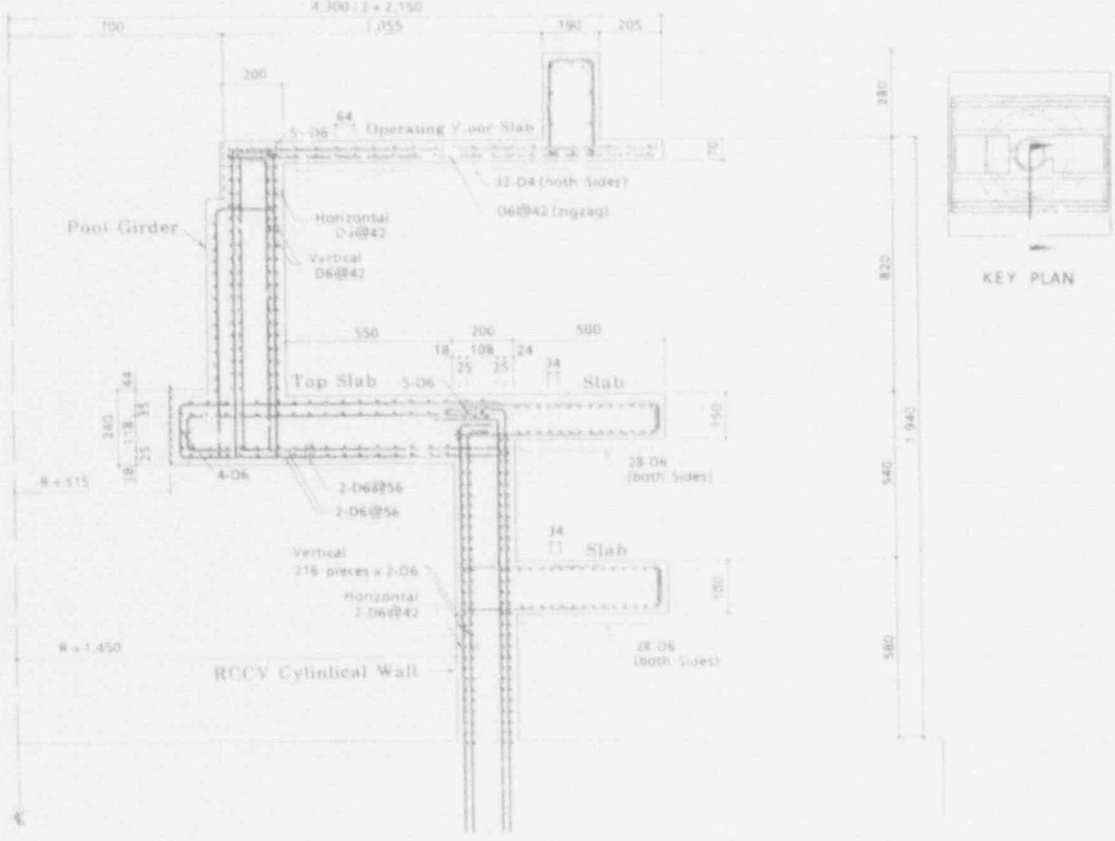


(b) 90° – 270° Section

**Fig. 4 Rebar Arrangement for Test Model**

Liner used in the test model was of rubber instead of steel in the actual RCCV.

The anchor-ring of drywell head in the test model was more strengthened than exactly reduced one to prevent it from failure before the failure of reinforced concrete structure, because the purpose of this experiment is to evaluate the strength of reinforced concrete structure.

**Table 1 Mechanical Properties of Reinforcement**

| Re-bar (sectional area) | Yield point ($kg/cm^2$) | Yielding strain ($\times 10^{-6}$) | Young's modulus ($\times 10^6 kg/cm^2$) | Tensile strength ($kg/cm^2$) | Elongation (%) |
|---|---|---|---|---|---|
| D4 (0.13 $cm^2$) | 3590 | 1840 | 1.95 | 5090 | 24 |
| D6 (0.32 $cm^2$) | 3900 | 2220 | 1.76 | 5520 | 15 |
| D10 (0.71 $cm^2$) | 4150 | 2140 | 1.94 | 5500 | 19 |

**Table 2 Mechanical Properties of Concrete**

| Portion | Age (date) | Standard curing | | | Field curing | | | |
|---|---|---|---|---|---|---|---|---|
| | | Density ($t/m^3$) | Compressive strength ($kg/cm^2$) | Tensile strength ($kg/cm^2$) | Density ($t/m^3$) | Compressive strength ($kg/cm^2$) | Young's 1) modulus ($10^5 kg/cm^2$) | Tensile strength ($kg/cm^2$) |
| RCCV Cylindrical Wall, Top Slab, Pool Girder | 7 | 2.30 | 237 | — | 2.25 | 173 | — | — |
| | 28 | 2.27 | 331 | 26.7 | 2.25 | 270 | — | 20.8 |
| | 36 beginning of experiment | — | — | — | 2.25 | 293 | 2.30 | 24.9 |
| | 56 end of experiment | — | — | — | 2.25 | 316 | 2.36 | 25.2 |
| Operating Floor Slab | 7 | 2.29 | 326 | — | 2.25 | 202 | — | — |
| | 28 beginning of experiment | 2.30 | 383 | 30.2 | 2.25 | 309 | 2.22 | 27.0 |
| | 48 end of experiment | — | — | — | 2.25 | 134 | 2.55 | 28.1 |

1) Secant modulus of elasticity at the stress equivalent to 1/3 of compressive strength

## Loadings

The loads applied were thermal load, vertical load and internal pressure load. The loading steps in the experiment are shown in figure 5. Internal pressure load was applied by injecting water from outside and the vertical load is to simulate the stress state of the trial-designed RCCV due to dead load.

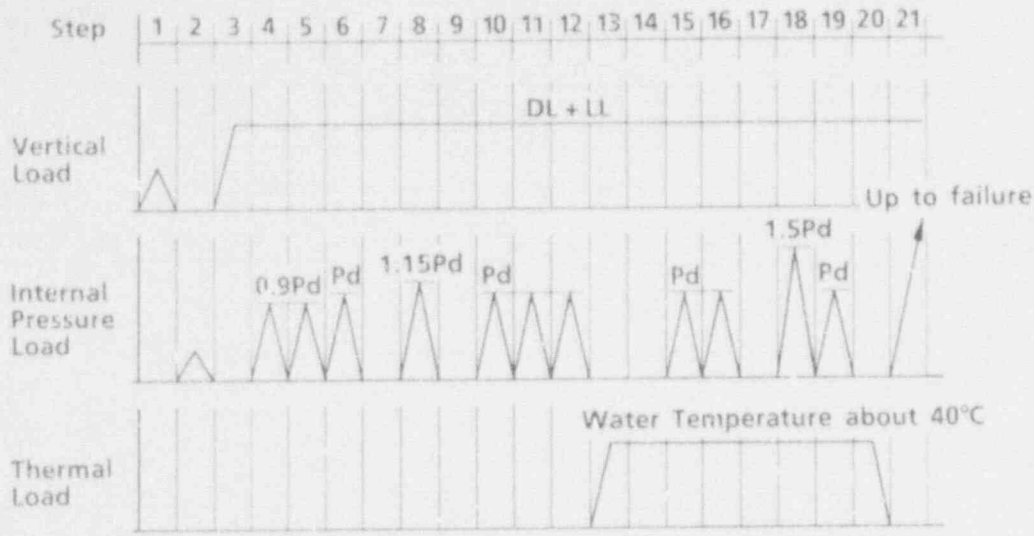


**Figure 5 Loading Steps (design pressure Pd= 3.16 kgf/cm²)**

## Summary of the Test Results

Major items in the test are described below.

* Internal Pressure Load p=1.8 kgf/cm² (=0.57Pd)

  The first cracks were observed at the top surface of the middles of the fuel pool girders and the vicinity of the Top Slab opening.

* Internal Pressure Load p=3.64 kgf/cm² (=1.15Pd: almost the same pressure as the Structural Integrity Test (SIT) )

  Cracks were observed at the Top Slab, fuel pool girder, exterior walls of reactor building and refueling floor slab.

* Internal Pressure Load p=7.0 kgf/cm² (=2.2Pd)

  The first rebar yielding occured at the Top Slab near their connection to the cylindrical wall (p=6.8kgf/cm²)

  From rebar-strain, it was estimated that shear crack plane was formed at the connection between Top Slab and cylindrical wall.

* Around the Failure Loads p=12.7 kgf/cm² (=4.0Pd)

  Shear failure with the entire Top Slab being torn out occured at the connection between Top Slab and cylindrical wall. Large horizontal cracks were observed at the connection between fuel pool girder and cylindrical wall, and finally rupture of vertical rebars and concrete of this portion terminated the test. Maximum internal pressure load was 12.7 kgf/cm².

The deformation mode of the test model are shown in Figure 6. The relationships between internal pressure loads and displacements at principal locations of the Top Slab and fuel pool girders are shown in Figure 7. It can be seen that the vertical displacement at the connection between Top Slab and cylindrical wall began to increase rapidly at internal pressure load of about 7.0 kgf/cm².

Residual cracks in Top Slab and fuel pool girder failure are shown in Figure 8. Residual cracks in cross section are shown in Figure 9. Large diagonal cracks were confirmed at the connection between Top Slab and cylindrical wall.

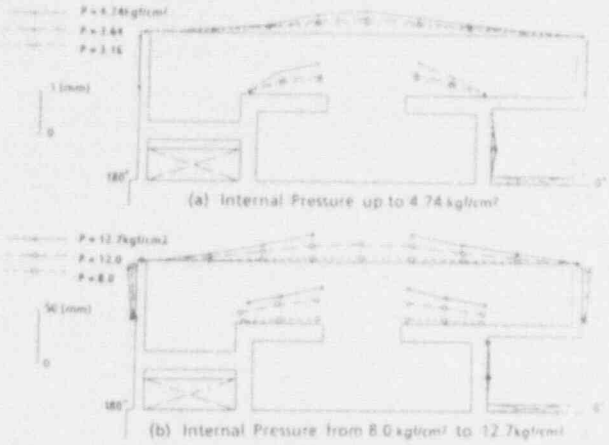


Figure 6 Deformation Mode (0° - 180° Section)

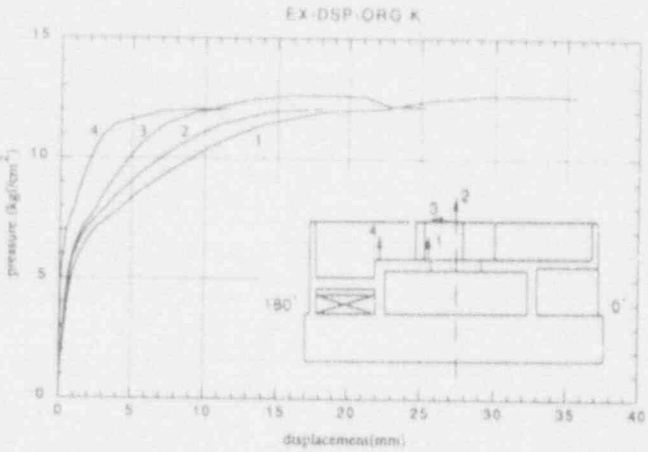


Figure 7 Pressure Load-Displacement Curve (Final step)

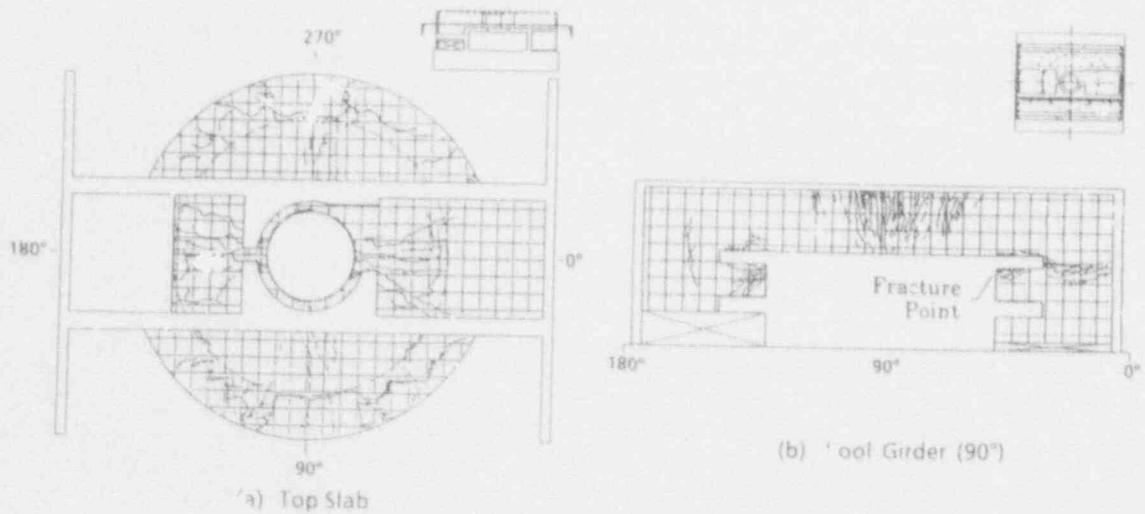


Figure 8 Crack Distribution at Final Stage (residual crack width more than 1 mm)

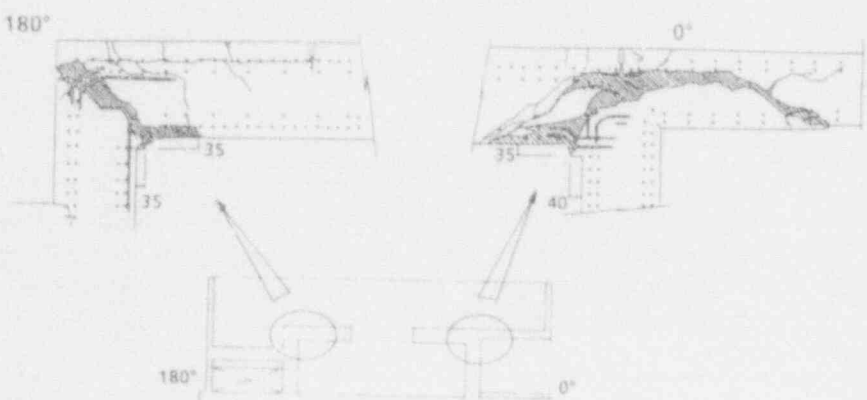


Figure 9 Crack Pattern after Failure (vertical section)

## 3-D HALF MODEL ANALYSIS

### Computer Code

In this study, DIANA (release 4.1) code was used in the analysis for a model of solid elements. DIANA code was developed by TNO Building Construction Research[3]. An outline of the assumption in the analysis is summarized in Table 3.

**Table 3 Assumption in the Analysis**

| | |
|---|---|
| element | 20-noded isoparametric quadratic solid elements<br>reduced integration (2 × 2 × 2) |
| reinforcement | smeared reinforcement<br>considered as embedded reinforcement (Figure 10)<br>orthogonal reinforcement |
| cracking of concrete | smeared crack model<br>multi-directional crack (threshold angle = 60 deg.) |
| bond | perfect bond<br>linear tension-stiffening for cracked concrete |
| constitutive law | elasto-plastic model (plasticity theory) |
| criterion | Drucker-Prager for concrete, Von-Mises for reinforcing bar |
| shear transfer | constant shear retention after cracking |

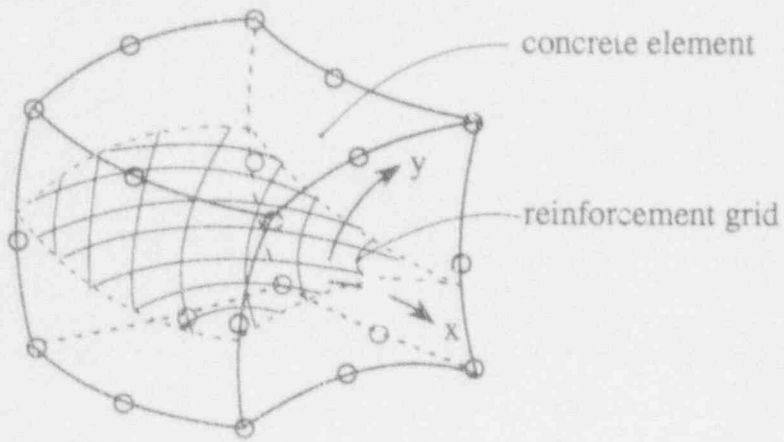


**Figure 10 Reinforcing-bars in the Element**

**Table 4 Assumed Material Properties**

| | | |
|---|---|---|
| concrete | Young's Modulus[a] | ; 236000 kgf/cm$^2$ |
| | Poisson's Ratio | ; 0.167 |
| | Density | ; 0.00000245 kgf/cm$^3$/G |
| | Uniaxial Compressive Strength[a] | ; 316.0 kgf/cm$^2$ |
| | Uniaxial Tensile Strength[a] | ; 25.2 kgf/cm$^2$ |
| | Tension-Stiffening | ; linear (zero stress with strain = 0.002216) |
| | Shear Retention Factor | ; 0.3 |
| rebar | Young's Modulus[a] | ; 1760000 kgf/cm$^2$ |
| | Density | ; 0.00000801 kgf/cm$^3$/G |
| | Yield Stress[a] | ; 3900 kgf/cm$^2$ |
| | 2nd Modulus[a] | ; 17600 kgf/cm$^2$ |

[a]given by material test

## ANALYSIS RESULTS

Load-incremental method with Newton-Raphson iteration scheme was adopted and the final step of the computation was determined by the rapid reduction of incremental tangential stiffness into nearby zero around 12.0 kgf/cm$^2$ and divergence occured over 12.2 kgf/cm$^2$.

The relationships between internal pressure loads and displacements at principal location of the structure are shown in Figure 12 along with the test results. Deformed shapes around 3,6,8 and 10 kgf/cm$^2$ are given in Figure 13. The calculated load-displacement relationships show relatively good agreement with the experimental results. More precisely, calculated displacements are smaller than observed value from around 5 kgf/cm$^2$ to maximum pressure. It is considered that the assumed tension-stiffening in the computation was a little larger than that of real phenomena and there is a delay in the stress transfer from concrete to rebars after cracking. Concerning the horizontal displacement at the center of the pool girder, calculated value exceeded the observed value beyond about 9 kgf/cm$^2$. One of the reasons seems to be attributed to the use of not so fine mesh in the refueling floor slab part. Transverse shear failure of the Top Slab/cylindrical wall connection was observed in the experiment and those corresponded to the observed vertical displacement at that connection, and the calculated load-displacement relation of this location shows good agreement with the experimental results up to failure load.

Therefore, it can be said that a 3 D solid model can simulate the behavior of the Top Slab/cylindrical wall connection dominated by the stress transfer from concrete to rebars after development of shear crack plane. It is not easy to simulate this kind of behavior by a FE-model using shell elements. In this calculation, maximum load and deformations around maximum load can be estimated with adequate accuracy.

The initial cracks occured at the Top Slab/cylindrical wall connection and vicinity of the Top Slab opening around 1.7 kgf/cm$^2$. After that, cracks increased gradually. Cracks occured at the center of the fuel pool girder around 4 kgf/cm$^2$ , at the refueling floor slab and bottom of the cylindrical

## Analysis Model

In the calculation, a half of the specimen was modelled considering the symmetric nature of the test model. The base mat was rigid enough to be idealized that a model is fixed with it at the foot in the analysis. The finite element grids are illustrated in Figure 11. Nonlinear analysis using 3-D solid elements allows precise modeling of structures. In the analysis, a total of 724 solid elements(4715 nodes) for concrete and a total of 1291 reinforcement elements(4714 nodes) were used. In the model, reinforcements are carefully modelled in the FE-mesh. Material properties used in the analysis are listed in Table 4, which are obtained by the material test except tension-stiffening and shear transfer characteristics. Linear tension-stiffening model is adopted because of the computational limitation. At present, it is not clear how much influence the shear transfer effect has on actual structures, and shear retention factor is not evaluated properly. In this analysis, constant shear retention factor of 0.3 is adopted which is considered reasonable from the previous works [4].

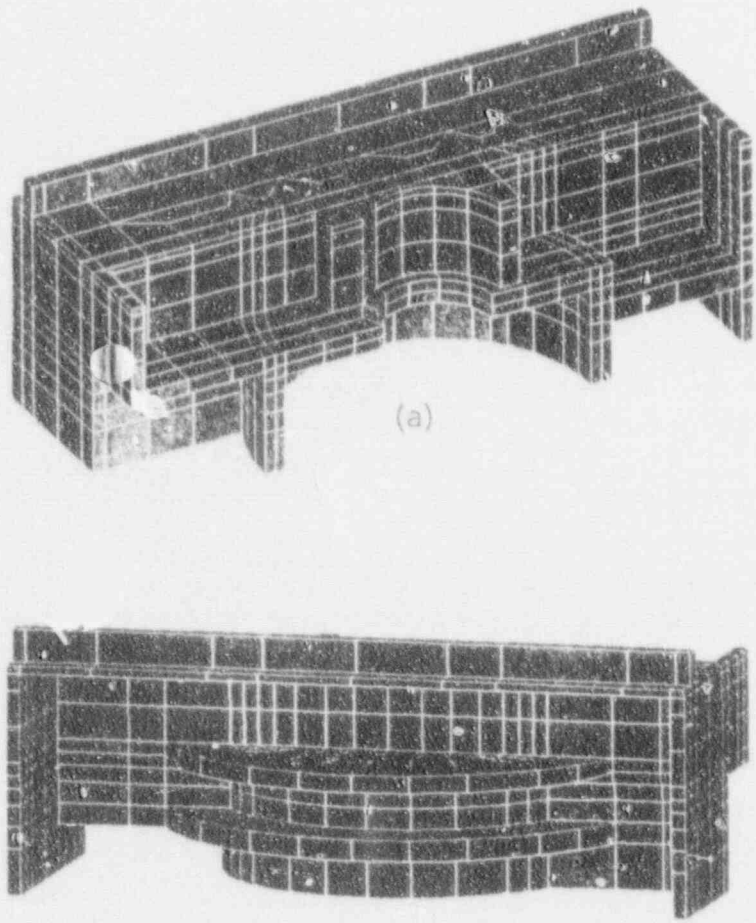


Figure 11 Mesh for Calculation

wall around 5 kgf/cm$^2$ and at the exterior wall, most of the cylindrical wall and Top Slab connection around 6 kgf/cm$^2$. In Figure 14, integration points with opening cracks are marked. Pressure level of initial crack observed at the vicinity of the Top Slab opening(1.8 kgf/cm$^2$) corresponds to the calculated results (1.7 kgf/cm$^2$). Cracking spread into almost all of the Top slab/cylindrical wall connection around 4 kgf/cm$^2$ and into the cylinder and the center the girder around 6 kgf/cm$^2$. From the analysis results, shear crack planes were found to penetrate at the Top Slab/cylindrical wall connection around 7 kgf/cm$^2$. It corresponds to the experimental results induced from the rebar strain in the experiment.

Rebar yielding started at the upper surface of Top Slab opening, at the Top Slab/cylindrical wall connection and at the refueling floor slab around 8 kgf/cm$^2$. Around 10 kgf/cm$^2$, yielding spread into the cylindrical wall. Experimental results of rebar yielding are shown in Figure 16 with the analysis results. Estimated pressure levels at which yielding started are a little higher than the experimental results in some principal portions but generally there was good agreement between test and analysis in the whole structure.

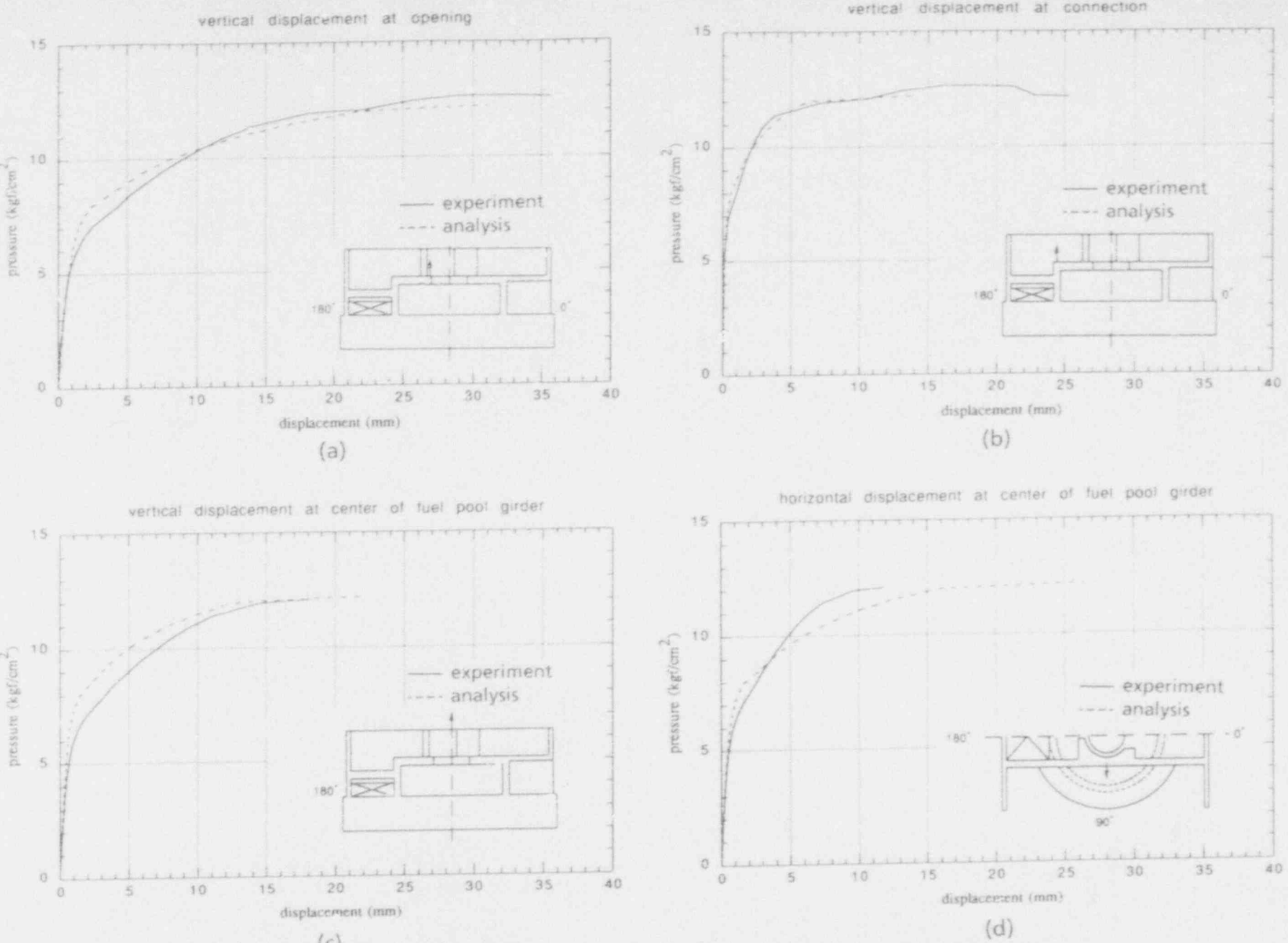


**Figure 12 Relationships between In. ernal Pressure and Displacement**

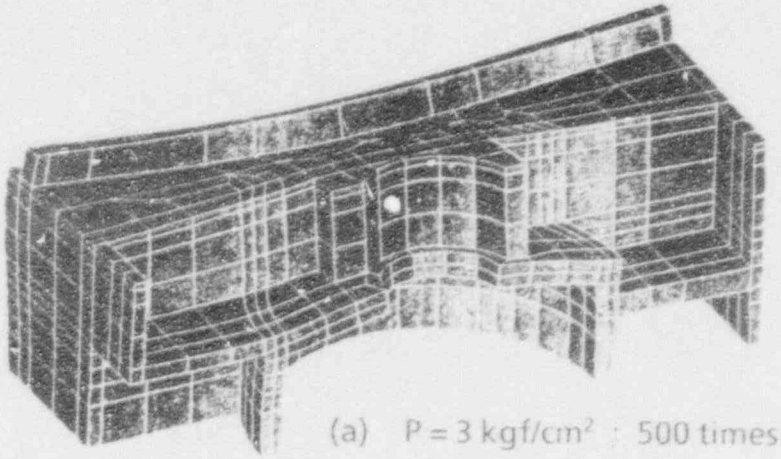

(a) $P = 3\ kgf/cm^2$ ; 500 times

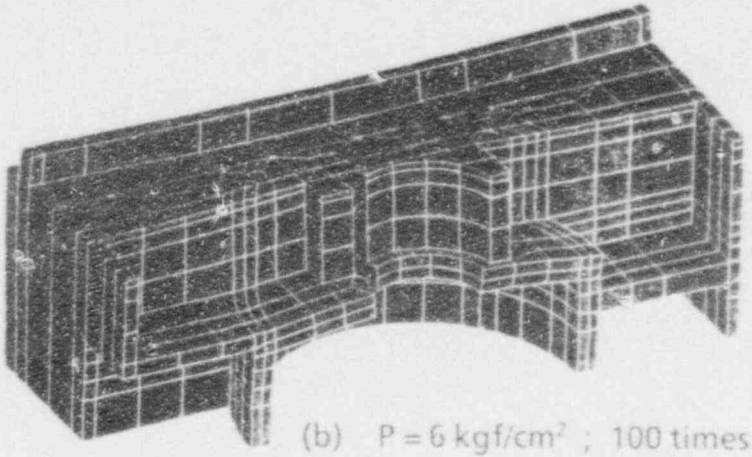

(b) $P = 6\ kgf/cm^2$ ; 100 times

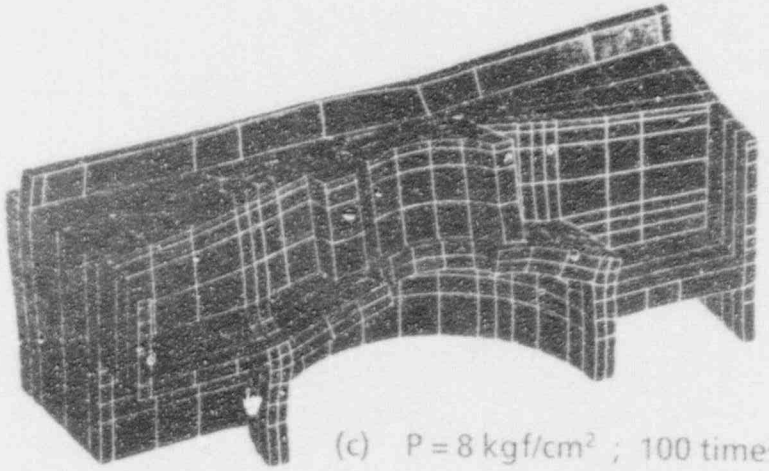

(c) $P = 8\ kgf/cm^2$ ; 100 times

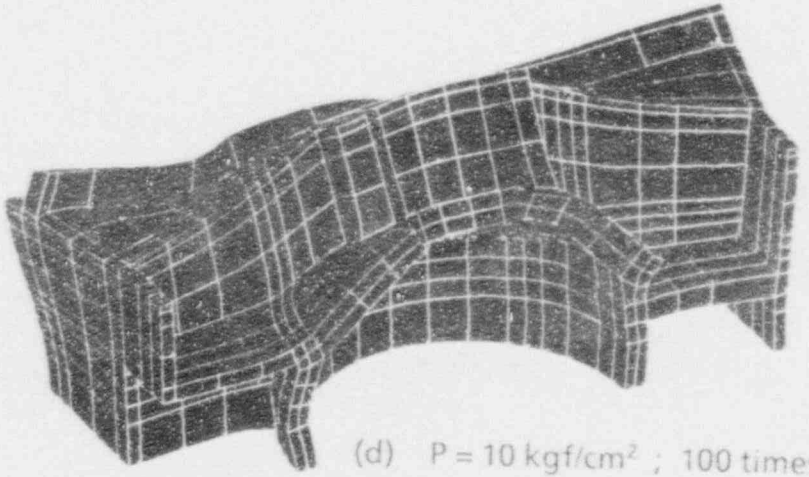

(d) $P = 10\ kgf/cm^2$ ; 100 times

**Figure 13 Deformed Shapes**

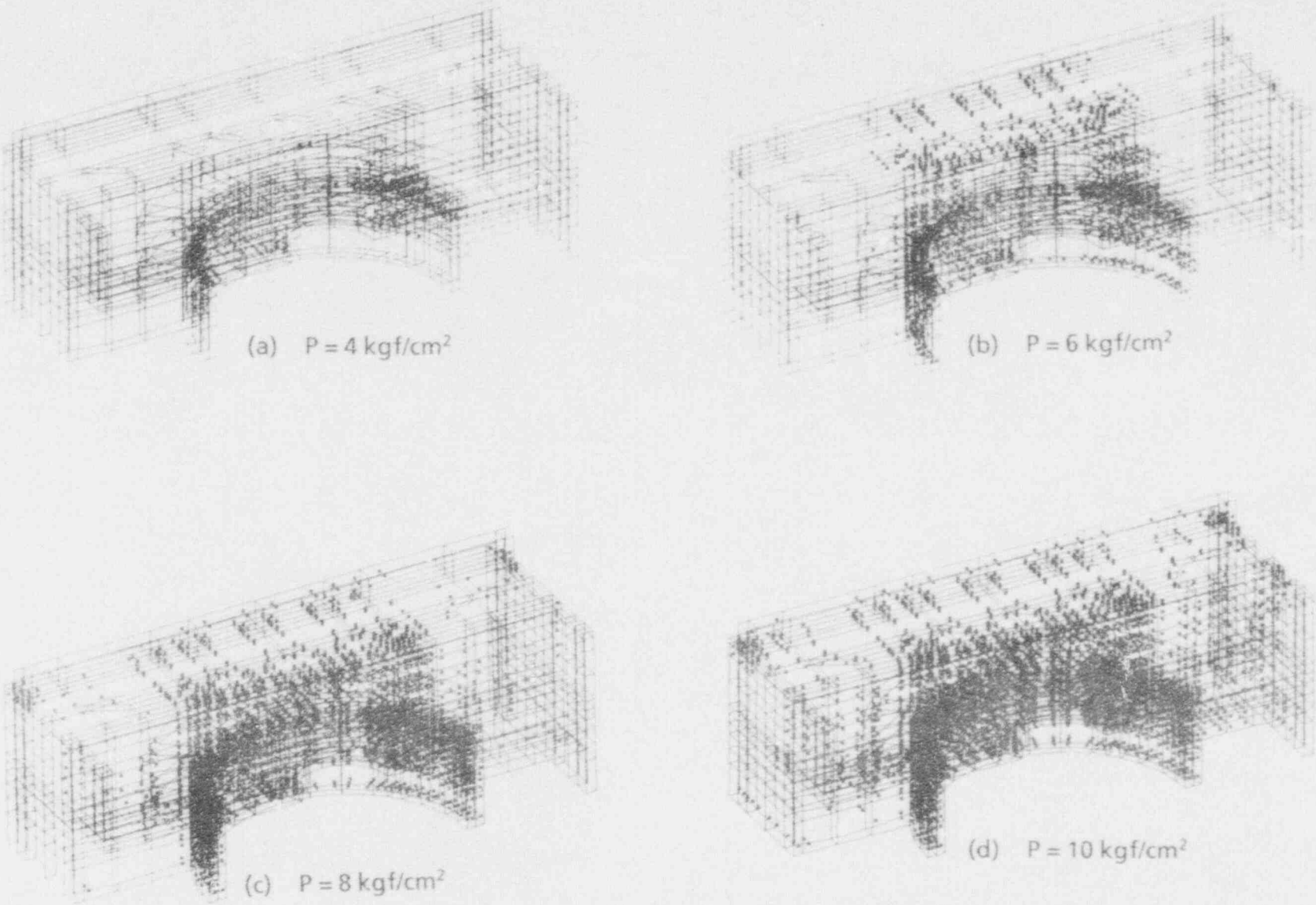


**Figure 14 Cracking Integration Points of Concrete**

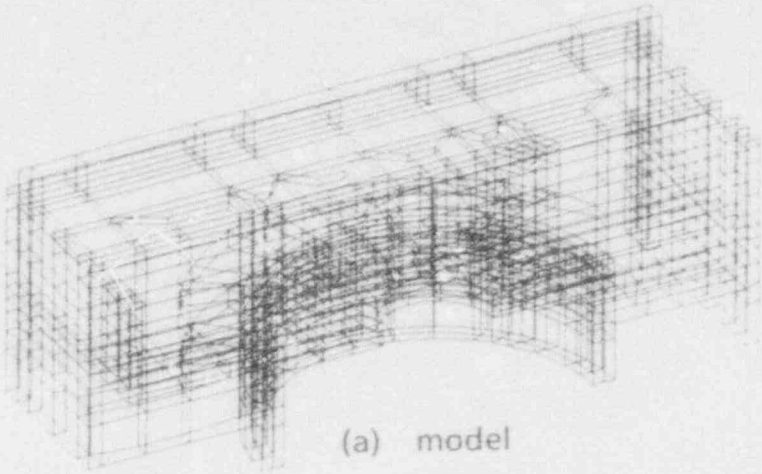

(a) model

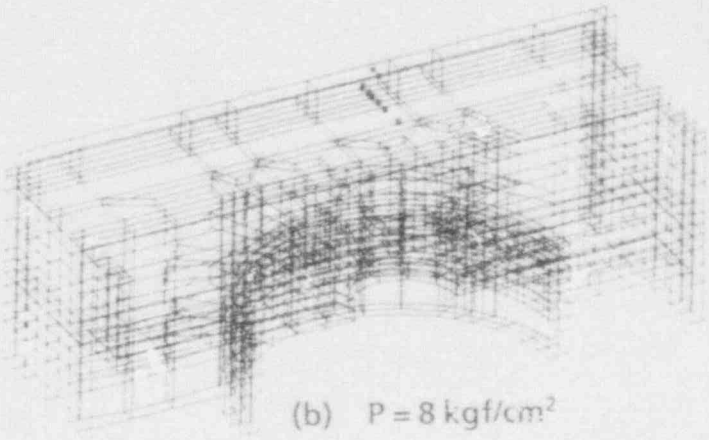

(b) P = 8 kgf/cm²

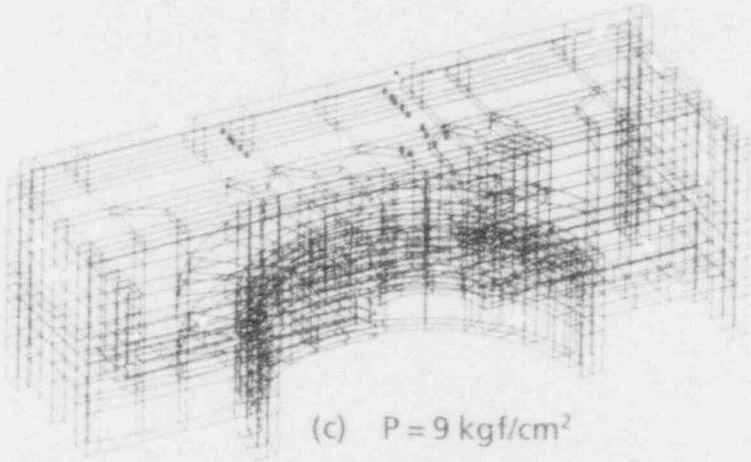

(c) P = 9 kgf/cm²

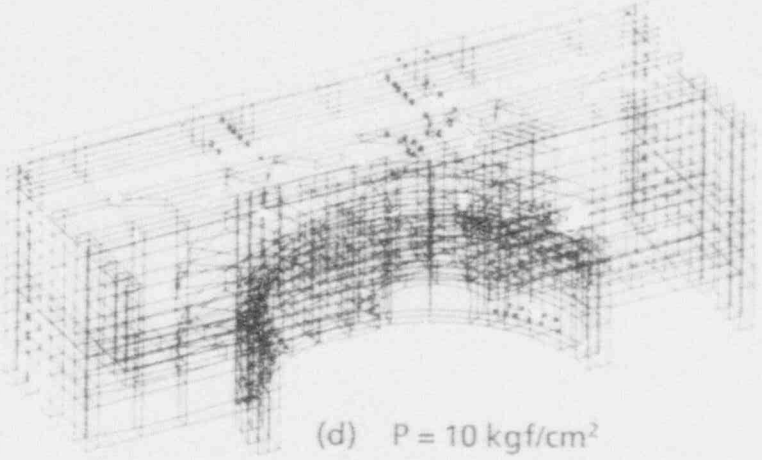

(d) P = 10 kgf/cm²

**Figure 15 Yielding Integration Points of Rebars**

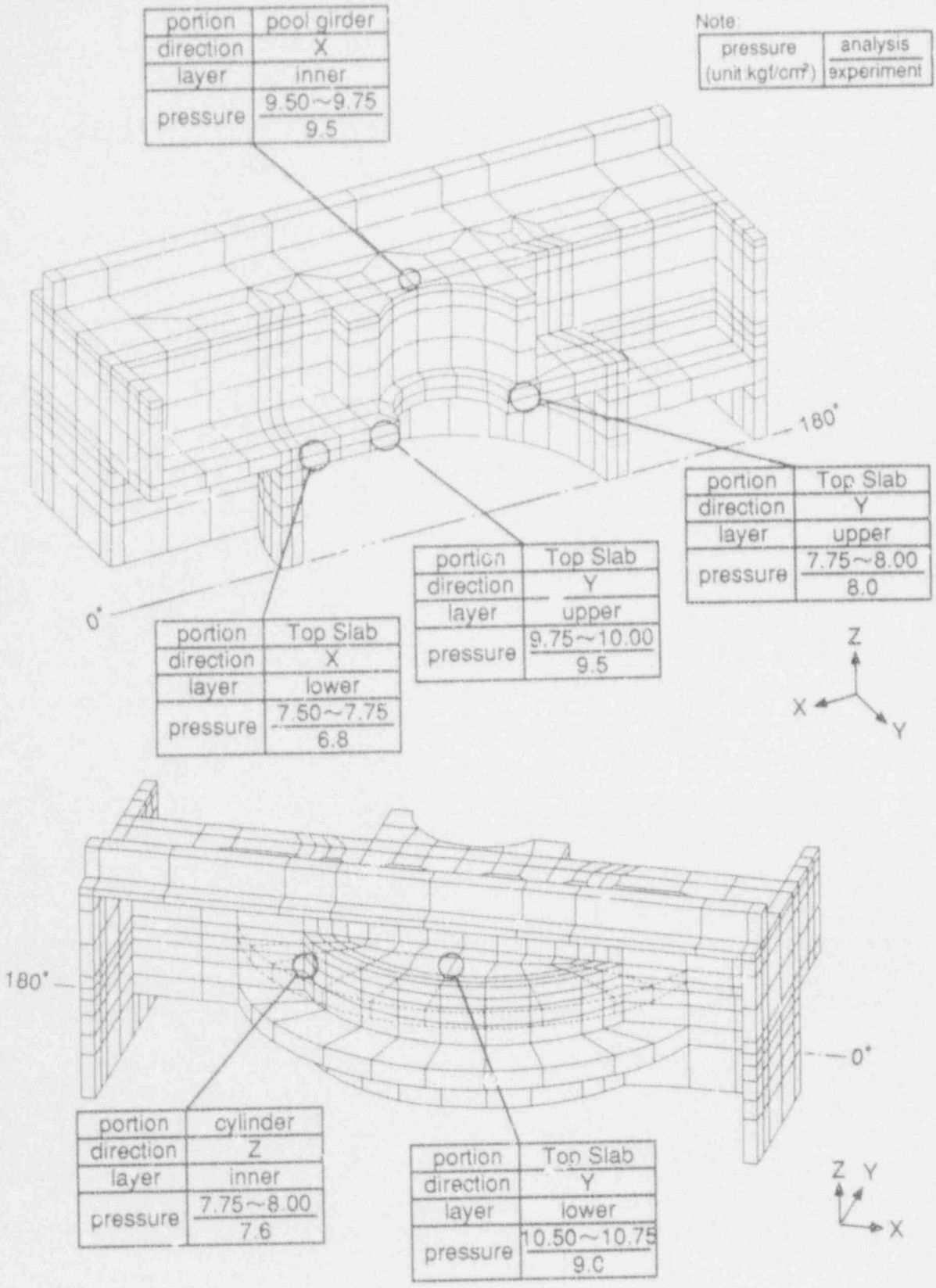


**Figure 16 Yielding of Rebars in the Experiment**

## CONCLUSIONS

Presented in this paper were results of the post-test analysis of the Top Slab partial model of the reinforced concrete containment vessel subjected to internal pressure beyond design pressure. Top Slab part of the specimen has a complicated structure that consists of cylindrical wall, flat Top Slab plate and wall girders. From the experimental results, nonlinear behaviors due to concrete cracking(caused by membrane, bending and shear stresses), yielding of rebars and transverse shear failure were confirmed. Post-test analysis was performed to simulate the behaviors with 3-D FE nonlinear analysis with solid elements. From the results obtained, not only qualitative but also quantitative agreements were found between the test results and computed results by a 3-D solid approach in the sense of maximum load, deformation and each nonlinearities.

In this case, the validity of non-linear analysis by 3-D FE Analysis using 3-D solid elements was proven but there remain some unsolved items as follows: (a)many uncertainties(compressive characteristics of cracked concrete, effect of bond, 3-D constitutive law of concrete, etc), (b)difficulty in estimating which uncertainty has an important effect in case of the complicated structure.

## Acknowledgements

The experiment presented in this paper was performed as one of the series of the joint study titled "Evaluation on RCCV Configuration and Confirmatory Test to Establish Code",which was carried out by six Japanese electric power companies and two manufactures with the technical cooperation of three construction companies. These companies were The Tokyo Electric Power Co., Inc.,(secretariat company), The Tohoku Electric Power Co., Inc., The Chubu Electric Power Co., Inc., The Hokuriku Electric Power Co., Inc., The Chugoku Electric Power Co., Inc., The Japan Atomic Power Company, Hitachi Ltd., Toshiba Corporation, Kajima Corporation, Shimizu Corporation and Takenaka Corporation.

## References

1. D.R.Wilkins, T.Seko, et al., " Advanced BWR: design improvements build on proven technology, "Nuclear Engineering International, June 1986.
2. O.Oyamada, H.Saito, et al., "Experimental Study for Structural Behavior of Reinforced Concrete Containment Vessel beyond Design Pressure,"Forth Workshop on Containment Integrity, 1988.
3. Users Manual of "DIANA Finite Element Analysis Release 4.1", TNO Building and Construction Research, The Netherlands, 1991.
4. Al-Mahaidi, R.S.H., "Nonlinear Finite Element Analysis of Reinforced Concrete Deep Members, "Report No.79-1, Dept. of Struct. Engin., Cornell Univ., Jan. 1979.

# SESSION 3

# ADVANCED CONTAINMENT DESIGNS AND RELATED RESEARCH
(CONTINUED)

# L.I.R.A.: AN ADVANCED CONTAINMENT SYSTEM TO MINIMIZE THE ACCIDENTAL RADIOACTIVITY RELEASES.

Arnaldo Turricchia
ENEL-DCO, VIA G.B. Martini 3, I-00198 ROMA

## Abstract

A containment system named L.I.R.A. has been studied for advanced PWRs with the general design objective of limiting the accidental radioactivity release to the environment to less than one millionth of core inventory (of Cesium, Iodine and other aerosols), by using substantially passive features.
The intent is to avoid, even in case of severe accident, the evacuation of the population living near the nuclear power plant and to limit the contamination of the surrounding territory to such low values as to permit its continued and unrestricted use after the accident.
The design objective has been achieved by adopting the vapour suppression principle, with a drywell concentric with the wetwell, but still retaining a large and strong containment.
The integrity and leaktightness of the containment is preserved against all the challenges posed by severe accidents by:
- making the suppression pool large enough to be able to absorb, without boling, all the heat inputs generated in the first 24 hours;
- burning the hydrogen as it emerges without steam above the suppression pool, by means of D.C. powered spark ignitors backed up by passive catalytic recombiners located near the top of the containment dome;
- locating, in the dry cavity below the pressure vessel, a stack of staggered graphite beams which causes the dispersion and solidification of the molten core in thin layers. After corium solidification, water from the suppression pool is allowed to flood gradually the cavity.

## INTRODUCTION

The fear of a large accidental release of radioactivity to the environment, such as that which took place at Chernobyl, is one of the main concerns of the general public and one of the causes of uneasiness and opposition toward the installation of new nuclear power plants (at least in some countries).

The existence of an emergency plan covering many miles of territory around a nuclear plant, and the related drilling exercises, even if dictated by the commendable intent to protect the population also in the remote event of a severe accident, far from satisfying the persons involved, contributes enormously to the perception of the nuclear station as a dangerous plant.

The large and lasting contamination of the territory experienced around Chernobyl and the forced and permanent evacuation of many people from their homes has probably had a more negative impact than the potential (and not yet fully assessed) health consequences of the accident, since the contamination is there and can be measured whereas the health effects are stochastic in nature, are difficult to predict and to verify and they appear, if ever they do, many years after the accident.

To allay the fears of the concerned citizens and make nuclear power more acceptable to the affected people, it is then evident that the factors which contribute most to the risk perception must be addressed. As a consequence, it seems important to design and construct the new nuclear power plants in such a way as to rule out the need of evacuation and the possibility of significant land contamination even in the case of a severe accident.
This goal could probably be achieved if the plant were designed according to the following safety criteria:

a) dangerous nuclear excursions must be made impossible by design, so as to avoid immediate consequential rupture of the containment; this is possible and is already so in present LWRs, thanks to the negative power coefficient;

b) the core melt-down associated to a prolonged mismatch between heat production and heat removal must have a probability as low as possible: extremely low values (of the order of $10^{-5}$ - $10^{-6}$ per year) are possible with presently envisaged reactor designs ("advanced" and "passive" types). A design which permits to exclude the core melt-down is not yet commercially available;

c) a containment system capable of withstanding the adverse effects of severe accidents without loosing its integrity and design leak-tightness , neither in the short nor in the long term, must be provided. But, in addition to that, efforts should be made to come out with a containment design which really **minimizes** the radioactivity releases, even in the worst conceivable circumstances. From this point of view there is a need to modify not only the existing containment designs (which were not conceived with severe accidents in mind) but also to modify the design of the more advanced types so far proposed.

d) the probability of containment bypass sequences must also be minimized by design, otherwise the good containment system adopted would not substantially reduce the overall risk.

In TMI-2, even if a core melt-down took place, the existence of a containment system which performed its function, the recovery of core cooling before pressure vessel melt-through and the availability of active containment cooling systems which maintained the containment pressure at very low values, permitted to have a negligible release of radioactivity to the environment. But the situation could have been worst.
In Chernobyl the accident (a nuclear excursion) caused also the failure of the existing partial confinement system. However, even if the confinement structure had withstood the accident stresses, the release of radioactivity would not have been much lower because of the poor leak tightness of the confinement system.

With the above considerations in mind a study was performed at ENEL's Direction of Construction, to see whether the general design goal of "no evacuation and no land contamination" could be achieved with a new containment design using presently available technology and without incurring into excessive costs.
An effort has been made to address all the issues associated to severe accidents in an **integrated** manner since sometimes the isolated solution to one of the problems may worsens or make difficult the solutions to the others.

This paper presents the results of this investigation. The following discussion pertains to PWRs because this type of reactor is the most widespread in the world and also because the preferences of many countries still interested in the nuclear option seem in favour this type of reactor. However, with some modifications, the proposed solution could be adapted to BWRs and HWRs.

## 1. THE GENERAL DESIGN OBJECTIVE

If the accidental release of radioactivity to the environment could be held six order of magnitude below the core inventory (for Cesium, Iodine and other fission products except noble gases) the goal of avoiding significant land contamination and people evacuation also in case of a severe accident with core melt-down would certainly be met. This has been the ambitious general design target set for the proposed containment system. And it has to be met, for the first 3 days, with substantially passive features.

## 2. PROPOSED CONTAINMENT DESIGN (L.I.R.A.)

To obtain the desired overall decontamination factor of $10^6$, the containment schematically shown in Figures 1 and 2 is proposed for adoption in the nuclear power plants of next generation. It has been named L.I.R.A., with reference to its intrinsic limitation of radioactive releases (Limitazione Intrinseca dei Rilasci Accidentali, in Italian) [1].

The volume and design pressure of the primary containment are similar to that of present large dry containment (e.g. 70 000- 80 000 $m^3$ and 0.3-0.4 MPa for a 1000 MWe plant), but, nevertheless, the containment principle adopted is that of vapour suppression, with the primary circuit inside a drywell concentric with the wetwell (Chinese box arrangement). The primary containment is a steel-lined reinforced or prestressed concrete structure and its leakage rate is about that of the best present-day containments, namely around 0.2%- 0.5% per day at design pressure.

Conceptually the system is similar to the BWR Mark-III containment but is larger, stronger and adapted to PWRs. One may also think of it as a larger and stronger ice condenser containment where the ice has been substituted by water and the water has been moved downwards so that the discharge pipes coming from the drywell plunge down into it. ( The discharge pipes may also be horizontal, with a weir wall inside the drywell, in an arrangement identical to that of the Mark-III containment.)

It should be noted that the full pressure capacity of the containment would be needed only in case of:

- gross suppression pool bypass, namely in case of large drywell leakage or rupture;
- or in case of protracted unavailability of the suppression pool cooling system.

The proposed arrangement makes it possible not to push the design pressure of the containment at or beyond the technological limits (as in the so-called super strong containments). It is well known that too large a design pressure in a reinforced or prestressed concrete containment causes civil engineering problems especially around the large penetrations.

In this context one should remember that, in the past, the vapour suppression concepts were introduced mainly for economic reasons, namely to reduce the cost of the containment system by putting, inside it, a heat sink capable of absorbing the internal energy of the primary coolant and consequently reduce (as a trade-off) the volume and the design pressure of the containment.
The main purpose of the introduction of the vapour suppression concept in the proposed containment design is the **minimization of radioactivity release** to the environment (with passive features), for all accidents including the "severe" ones.
This goal is achieved by the following specific measures:

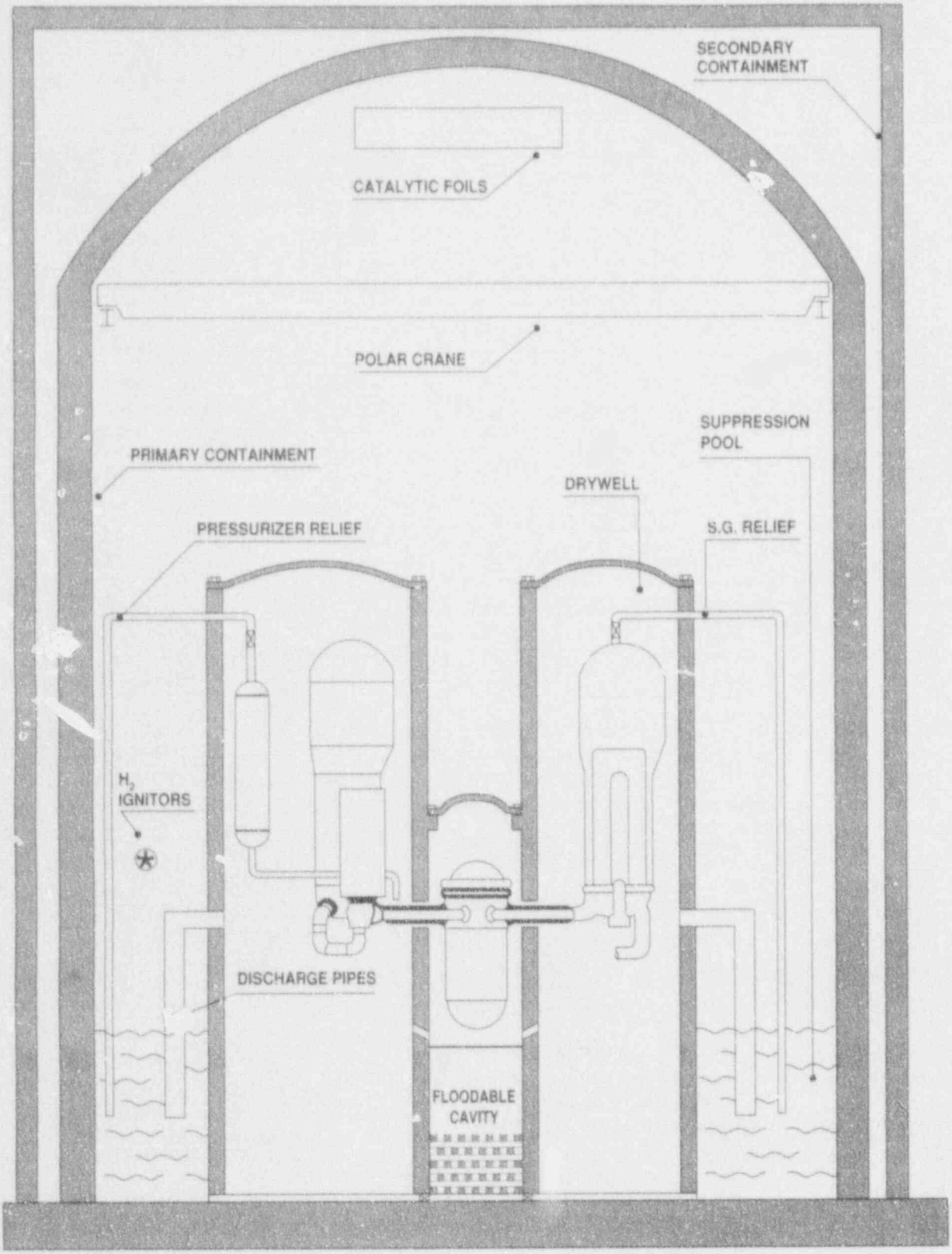


FIG. 1 - SCHEMATIC ARRANGEMENT OF THE L.I.R.A. CONTAINMENT

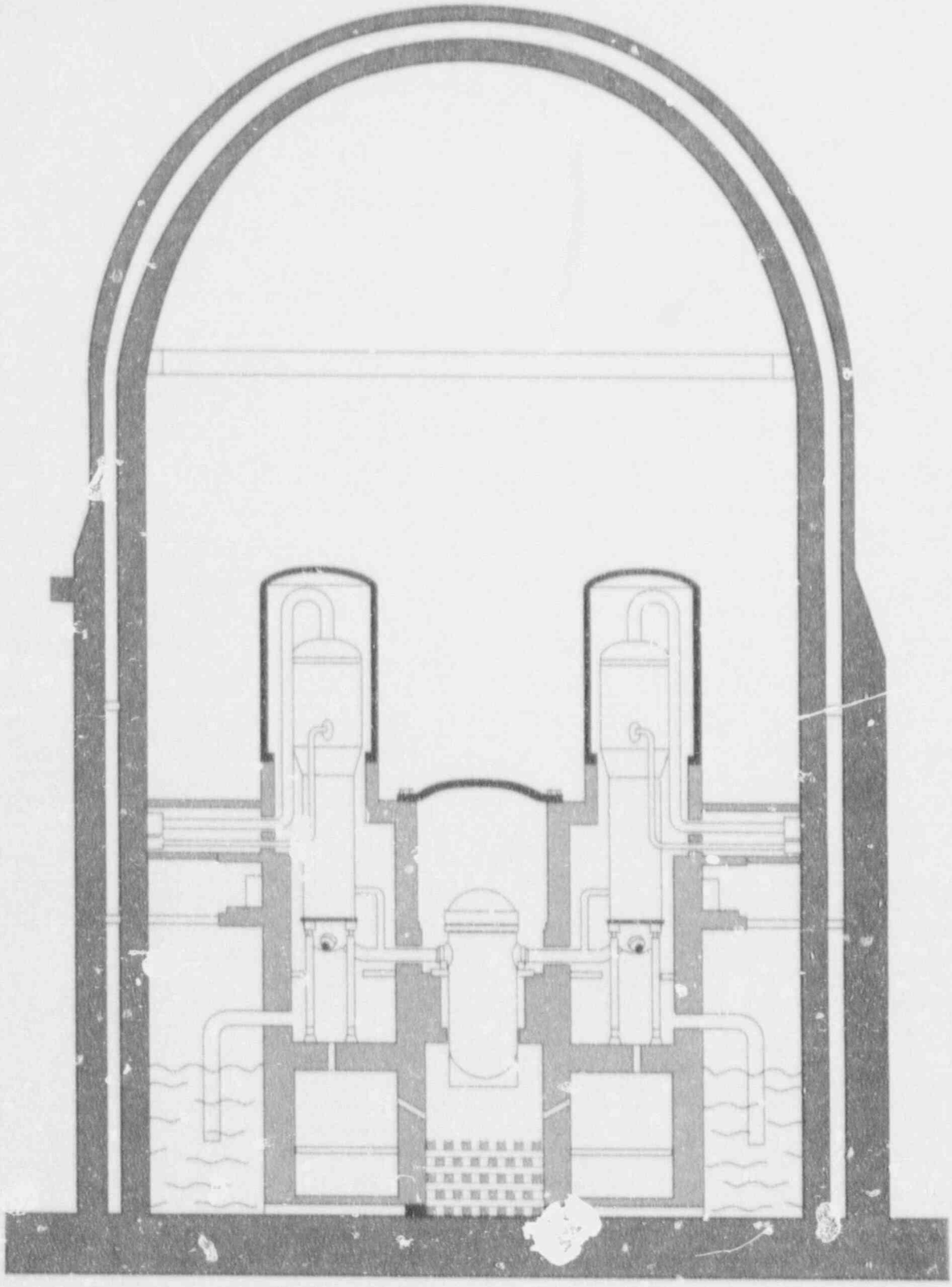

FIG. 2 - L.I.R.A. CONTAINMENT SYSTEM GENERAL LAYOUT

i) Introduction of a **large heat sink** (about 8000 cubic meter of borated water for a 1000 MWe reactor), so as to be capable of absorbing, before boiling:

- the internal energy of the primary coolant;
- the initial energy stored in the core;
- the energy released by zircalloy oxidation
- the decay power for 24 hours.

ii) Use of the suppression pool not only as a heat sink but also as a passive and reliable **radioactivity scrubber** capable of performing its function in all design-basis and severe accidents, and therefore capable of reducing the airborne radioactivity concentration in the volume in contact with the primary containment barrier. With a careful design of the downcomers extremities (quenchers/spargers) and a suitable choice of the water head and temperature, it would be possible to obtain a D.F. of the order of 100.

iii) Location of the **drywell inside the wetwell**, so that the concentration of the radioactive products liable to leakage is minimized.

iv) Exploitation of the steam quenching afforded by the suppression pool to **deliberately burn the hydrogen** emerging above it, and so avoid the hydrogen accumulation and explosion.

v) Use of the large water supply of the suppression pool to **flood the reactor cavity** and avoid the containment basemat erosion.

With reference to the large heat sink provided the containment pressure, and hence its leakage, remain extremely low for a long period of time (considerably more than 24 hours). (Refer to Table 1 for heat balance assessments).
If the suppression pool cooling system is started before the water starts boiling, the containment pressure would continue to remain very low.
If pool cooling is not recovered in time, the pool would start boiling but at least 24 more hours would have to elapse before the containment pressure reaches the design value. A grace period of more than 48 hours can be consiuered more than adequate for the recovery of active emergency cooling systems. If, however, a longer grace period were desired, the containment ought to be fitted with a filtered venting system.
After opening of the venting valves, many days would have to pass before the water volume of the suppression pool is substantially reduced (about 5% water loss per day).

The large water pool provided can also perform other useful functions:

- source of coolant for active ECCS, without the need to switch from the injection to the recirculation mode (like in the Combustion Engineering C.E. 80+ system);
- enlarged pressurizer relief tank;
- relief tank for the secondary side of the steam generators;
- source of water for reactor cavity flooding.

With these features the proposed containment system can achieve the design target of a radioactivity release less than one millionth of core inventory, as shown in Table 2. As a matter of fact, the secondary containment system might not even be needed to achieve the stated target.

TABLE 1

HEAT SOURCES AND HEAT SINKS IN THE L.I.R.A. CONTAINMENT

| | |
|---|---|
| - INTERNAL ENERGY OF PRIMARY COOLANT | 320 GJ |
| - SENSIBLE HEAT OF MOLTEN CORE | 140 GJ |
| - ONE HOUR OF DECAY HEAT ($4^{th}$ HOUR) | 110 GJ |
| - HEAT ABSORBED BY GRAPHITE STACK ($\Delta T = 800°C$) | 300 GJ |
| - DECAY HEAT OF $1^{st}$ DAY (FROM $4^{th}$ to $24^{th}$ HOUR) | 1600 GJ |
| - HEAT ABSORBED BY SUPPRESSION POOL ($\Delta T = 65°C$) | 2200 GJ |
| - DECAY HEAT IN 3 DAYS AFTER THE $1^{st}$ | 3300 GJ |
| - HEAT ABSORBED BY VAPORIZATION OF 20% OF SUPPRESSION POOL WATER | 3400 GJ |

TABLE 2

RADIOACTIVITY RELEASE FACTORS (FIRST DAY) FOR THE "LARGE DRY" AND L.I.R.A. CONTAINMENT SYSTEMS, IN CASE OF SEVERE ACCIDENT

| | LARGE DRY | L.I.R.A. |
|---|---|---|
| - PLATEOUT FACTOR IN PRIMARY CIRCUIT | 2 | 2 |
| - PLATEOUT FACTOR IN DRYWELL | - | 2 |
| - LEAKAGE FROM DRYWELL TO CONTAINMENT | - | 1% |
| - SCRUBBING FACTOR IN SUPPRESSION POOL | - | 100 |
| - PLATEOUT FACTOR IN CONTAINMENT | 10 | 5 |
| - LEAKAGE FROM PRIMARY CONTAINMENT | $5*10^{-3}$ | $1*10^{-3}$ |
| - PLATEOUT FACTOR IN SECONDARY CONTAINMENT | 2.5 | 2.5 |
| - OVERALL RELEASE (FRACTION OF CORE INVENT.) | $1*10^{-4}$ | $4*10^{-7}$ |

(NOTE: The above quoted values are to be intended as orders of magnitude, not precise values).

Up to now, the limited resources available have not permitted the adaptation of existing codes to the L.I.R.A. containment system and the performance of the safety analyses necessary to accurately evaluate the radioactivity releases for the various severe accidents. However, by comparison with and extrapolation of the results of calculations performed for other containments systems, the capabilities and merits of the L.I.R.A. containment should be clear.

The proposed containment system has one technical drawback with respect to other containments: since, from a utility point of view, it is desirable to be able to remove and substitute the steam generators during the plant lifetime, the fact that they are enveloped by the drywell structure might make it necessary:

- either to have a taller containment, to be able to extract the entire steam generators from the drywell, or
- accept the cutting and removal of the steam generators in two pieces - the dryer section and the tube bundle section.

This is an issue on which the designer must work to find an acceptable and economic solution. For example, the upper part of the structure enveloping each steam generator could be a bell-shaped removable metallic cap.

## 3. SPECIFIC DESIGN FEATURES TO MEET THE CHALLENGES OF THE SEVERE ACCIDENTS

The proposed containment must be designed to withstand all the challenges associated with severe accidents. In particular, in order to maintain its structural integrity and its design leak tightness, in all circumstances, the containment must be designed to cope with these phenomena (unless specific design features prevent them from appearing):

- Overpressurization;
- Direct Containment Heating;
- Hydrogen accumulation and explosion;
- Interaction of the molten core with the containment basemat.

One way of meeting these objectives is described hereafter.

### 3.1 Protection against Containment Overpressurization

The large internal heat sink provided and the large containment volume of the containment avoid overpressurization for well over 48 hours. After this time, if active cooling systems are not recovered, it shall be necessary to perform a **filtered containment venting.**
This feature is already state of the art and many operating reactors have been equipped with a filtered venting system.
For future reactors a design filtration efficiency of 99.9% should be the goal for both aerosols and iodine.
In this manner even a prolonged containment venting operation would lead to a negligible increase of the radioactivity release (apart from noble gases).

### 3.2 Direct Containment Heating

To avoid DCH and its associated pressure spike in the dryell, it is prudent to provide for automatic **primary circuit depressurization** before pressure vessel melt-through. This is also the trend in many PWRs currently being designed.

However, even in the unlikely event that the deliberate primary circuit depressurization does not take place, the situation, in the L.I.R.A. containment, would still look better than in a large dry containment. The worst thing that can happen is the breach of the drywell barrier with consequent suppression pool bypass. However at this point the suppression pool has nearly performed one of its tasks, namely the absorbtion of a large part of the internal energy of the primary coolant blown down through the pressurizer relief valves: as a consequence the pressure inside the primary containment is close to atmospheric and the containment is in the best conditions to face the challenge of DCH. Furthermore the suppression pool can still perform the task of cavity flooding.

### 3.3 Protection against Hydrogen Accumulation and Explosion

The hydrogen problem is a complex one. With a large and strong containment, the deflagration of the hydrogen which may accumulate in the containment atmosphere as a consequence of oxidation of the fuel cladding might be absorbed by the containment structures. Some concerns, however, might remain if, in addition to the hydrogen produced by the zirconium oxidation, there were a large contribution of hydrogen from the oxidation of other metals ( e.g. the steel of the pressure vessel bottom, of the vessel internal structures and of the reinforcing bars of the containment basemat).
For a large hydrogen accumulation the transition from deflagration to detonation (DDT) could not be ruled out and the dynamic loads associated to a detonation would constitute a more severe challenge to the containment integrity.
Because of this situation, the goal of the design must be that of preventing large hydrogen accumulation in the containment. In the proposed design this objective is met by **deliberately burning**, by means of suitable ignitors, the hydrogen as it emerges, deprived of steam, above the suppression pool, as is presently envisaged in the Mark-3 pressure suppression containment of BWRs or in the ice condenser containment of PWRs (LOVIISA, SEQUOYAH, etc.). The ignitors located above the suppression pool can be fed by a reliable DC power supply.

As a **back-up** to the ignitors or in place of them, it is possible to place, in the containment dome, **catalytic foils** [2] which are capable of inducing the hydrogen recombination in a smooth manner, starting even at low hydrogen concentration. The clean atmosphere existing in the L.I.R.A. containment, thanks to the scrubbing action of the suppression pool which is effective also against possible catalyst poisons, is a guarantee for the correct and reliable operation of the catalytic foils.

### 3.4 Protection of the Integrity of the Containment Basemat

To avoid the erosion of the containment basemat by a molten core it is necessary to develop a reactor cavity design which permits the spreading of the molten corium over a large surface area, so that the thickness of the layer is thin enough (few centimetre) to permit a quick resolidification and cooldown of the melt.
In particular, the solution proposed by the author (Fig.3 and 4) [5][6] consists in locating in the reactor cavity, below the pressure vessel, a stack of staggered graphite beams of square cross section, each with an upper channel for corium collection and distribution. This structure permits to have a **three-dimensional redistribution** of the molten core and prevents the direct contact of the corium with the containment basemat.

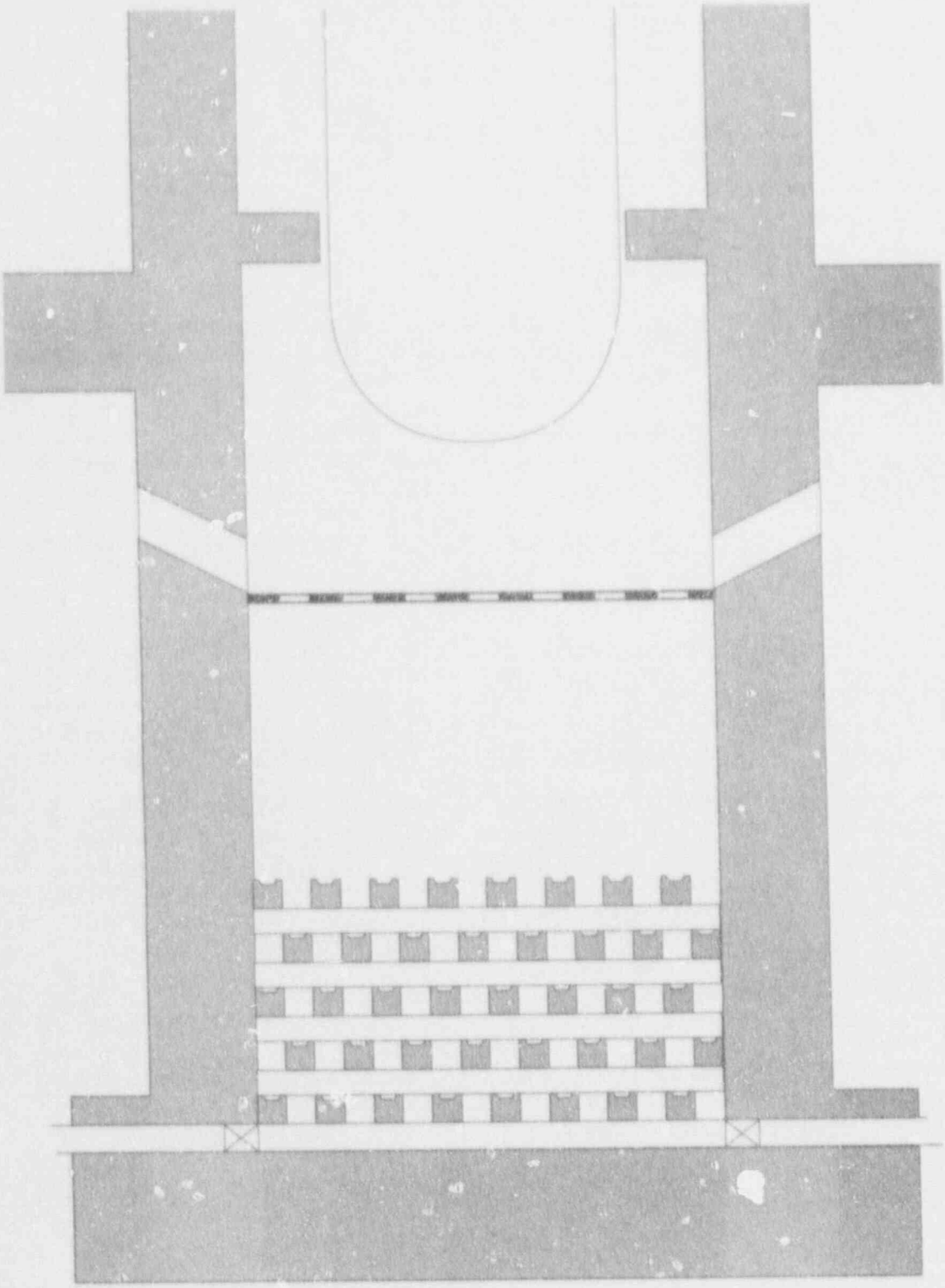

FIG.3 - FLOODABLE REACTOR CAVITY FILLED WITH A STACK OF STAGGERED GRAPHITE BEAMS FOR CORE DISPERSION AND COOLING

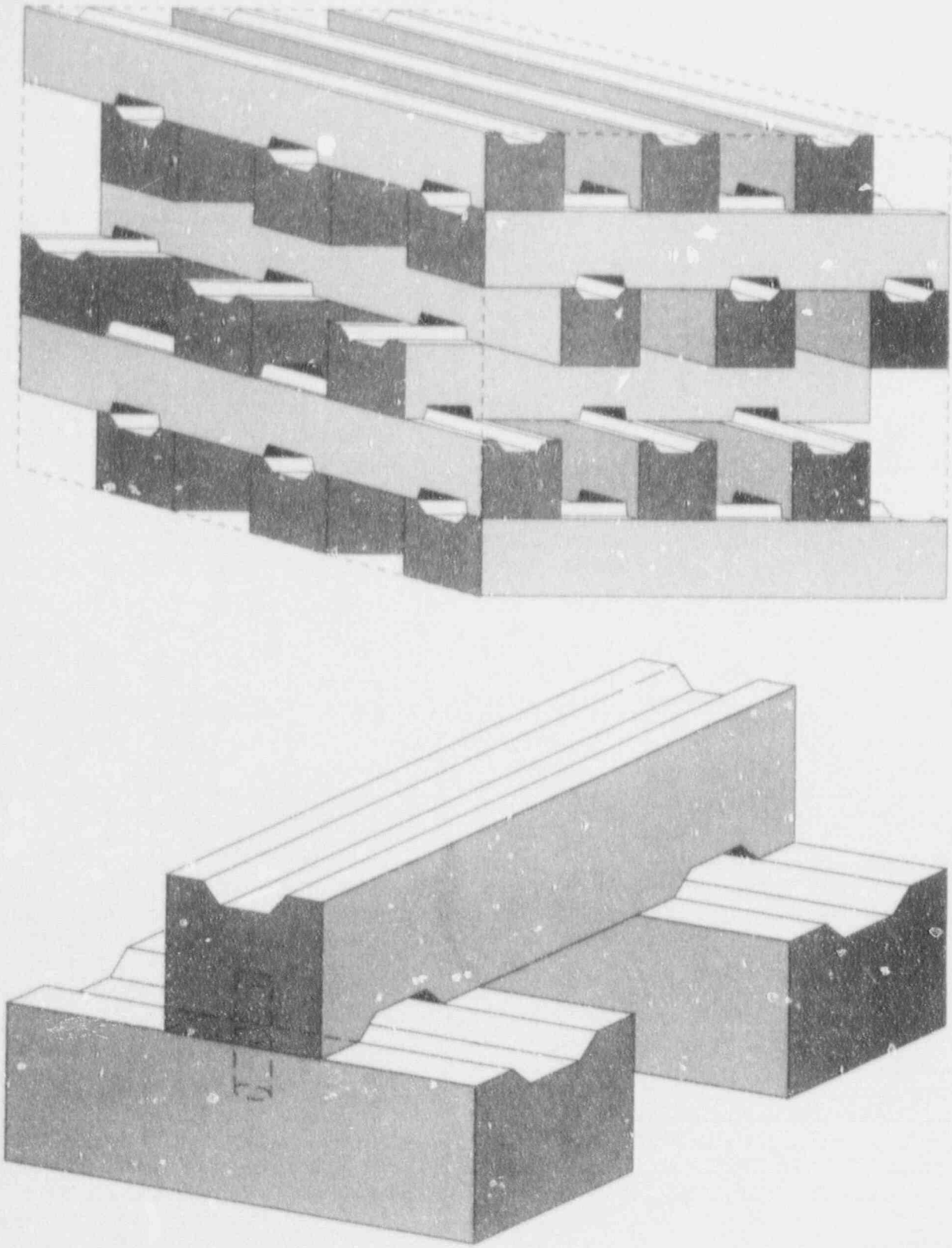

FIG. 4 - ASSONOMETRIC VIEW OF THE STACK OF GRAPHITE BEAMS TO BE LOCATED INSIDE THE REACTOR CAVITY

It is useful to remember that the core of a 1000 MWe PWR has a volume of about 10 $m^3$ and a S/V ratio of 400 $m^2/m^3$. If this core melts down and falls into a cavity of limited cross section (40-50 $m^2$), such as that of many present containment buildings, the S/V ratio is reduced by 2 orders of magnitude: this is the main reason why most of the various core catchers so far proposed have failed to give a satisfactory solution to the heat removal problem.

With the solution proposed in this report, the thin molten core layers resting on the graphite beams become easily amenable to solidification and cooling, in the first phase thanks to the **heat capacity of the stack** itself and, later on, by **flooding** the cavity with water.
The heat capacity of the stack should be large enough to absorb all the latent heat of the melt (120-140 GJ) and at least one hour of decay heat (100-120 GJ) and yet remain at a relatively low temperature (to minimize chemical reactions both in the dry phase and in the flooding phase). In other words the heat capacity of the stack should be an order of magnitude higher than that of the corium.

If **graphite** is chosen for the beam material, about 240 t of graphite (150 $m^3$) would be sufficient: with a uniform distribution of the sensible and decay heat (1 h) of corium into the graphite, the equilibrium temperature would be about 700 °C.

If one considers a typical cavity of 50 $m^2$ cross section, putting a graphite slab (3 m thick) on the bottom of the cavity would not permit the corium solidification because the rate of heat transfer to the graphite is intrinsecally limited by:

- the small heat transfer area:
- the large thickness of the corium layer (20 cm);
- the low thermal diffusivity of the corium itself.

In other words, with such a geometry, the graphite slab cannot provide its full **heat sink potential**.

On the contrary, a stack of staggered graphite beams, with the same graphite volume, would be able to give the S/V ratio necessary to solidify and cool the molten core.

### 3.4.1 Material for the Beams

The material of the beams must have, to the maximum extent possible, the following characteristics:

- a high thermal conductivity, to allow a quick corium cooldown and to facilitate the distribution of the heat removed from the corium into the whole graphite mass;
- a high melting point and chemical stability, both in dry and wet conditions, to preserve the initial geometry and limit the undesirable chemical reactions at high temperature.
- low cost.

At the moment, the preferred material for the beams of the structure is **graphite**, but other materials can be taken into consideration (and also composite materials).
The choice of graphite is a source of concern to somebody because this material is instinctively associated to the Chernobyl accident (criticality accident, graphite fire, hydrogen generation upon contact of overheated graphite with water, etc). These concerns, however, are groundless:

- if criticality were a real danger, a neutron poison could be distributed into the graphite;
- the reaction of graphite with the air present in the cavity is limited because the

graphite temperature is not allowed to reach dangerous levels and the amount of air available in the cavity for the reaction is limited;
- the reaction of graphite with water is limited by flooding the cavity within half an hour from the fall of the molten core into the cavity, i.e. before the graphite temperature reaches temperatures above 1000°C.

### 3.4.2 Reference Design Geometry

Stacks of graphite beams characterized by different geometries and different S/V ratios can be taken into consideration for the dispersing structure to be located in the bottom of the reactor cavity. To demonstrate the feasibility of the proposed concept the design shown in Fig. 5 has been chosen as a reference. Of course it shall have to be optimized on the basis of experimental tests.
This design consists of 7 layers of staggered graphite beams of square cross section, 60 cm side and 90 cm pitch. A channel, 30 cm wide and 5 cm deep, is grooved on the top side of each beam to facilitate corium collection and distribution.
The sides of the cavity, up to the level of the vessel, are lined with graphite bricks (also 60 cm thick) backed by refractory bricks (15 cm thick). In this way, a useful heat sink is provided for heat transfer by radiation from the corium deposited on the uppermost layers of the stack.
For a molten core spread uniformly on the reference stack of beams, the S/V ratio would be 5 times that associated to a single slab, even if one considers only the upper side of the beams; it is actually much larger, if one takes into consideration the vertical sides of the beams, on which a fraction of the corium is bound to stick.
With the uniform distribution of the molten core on the beams, a corium cross section of 240 $cm^2$ would be associated to the 3600 $cm^2$ of the cross section of the graphite beam. In other words, in addition to the filling up of the top channel (150 $cm^2$), there would be an equivalent layer of 1.5 cm thickness (90 $cm^2$) resting over the top.

### 3.4.3 Mechanical Impact of the Melt

As stated in Section 3.2, at the time of pressure vessel melt-through the primary circuit is depressurized.
The impact of 100 tons of molten material falling from a height of 4 meter on the underlying structure could produce the displacement or overturning of the beams of the upper layer(s).
This, however, is not a serious challenge to the structure as a whole and to the underlying layers which could still perform their function. At any rate, to better preserve the whole geometry of the stack, it is advisable to modify somewhat the two upper layers of beams by giving them also lateral stability or protect them with a slab receiving the direct impact of the falling melt.

### 3.4.4 Uniformity of the Melt Redistribution

This is a very important issue and should be carefully investigated.
In effect, it is difficult to precisely predict the degree of uniformity of corium distribution without some experimental tests. However, the following considerations can be made:

- Upon falling from a height of 4 meters (even with the primary circuit depressurized), the horizontal spread of the melt on the stack is inevitable upon impact, because of the conversion of a substantial fraction of its potential energy into kinetic energy. The corium spreading is enhanced if, at the time of pressure vessel melt-through, there is a slight overpressure inside the primary circuit.

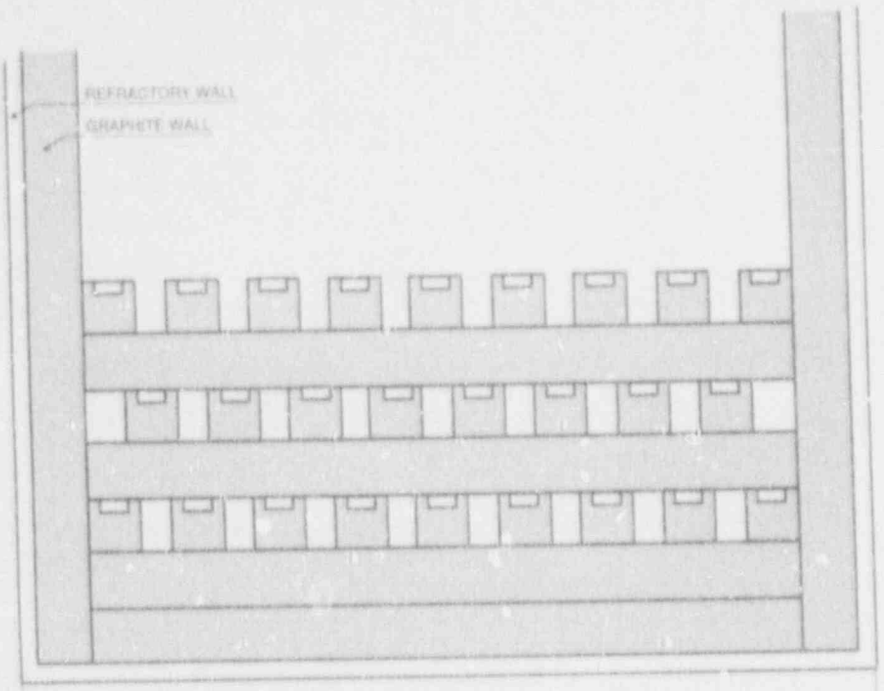


(b) VERTICAL CROSS SECTION OF THE REACTOR CAVITY

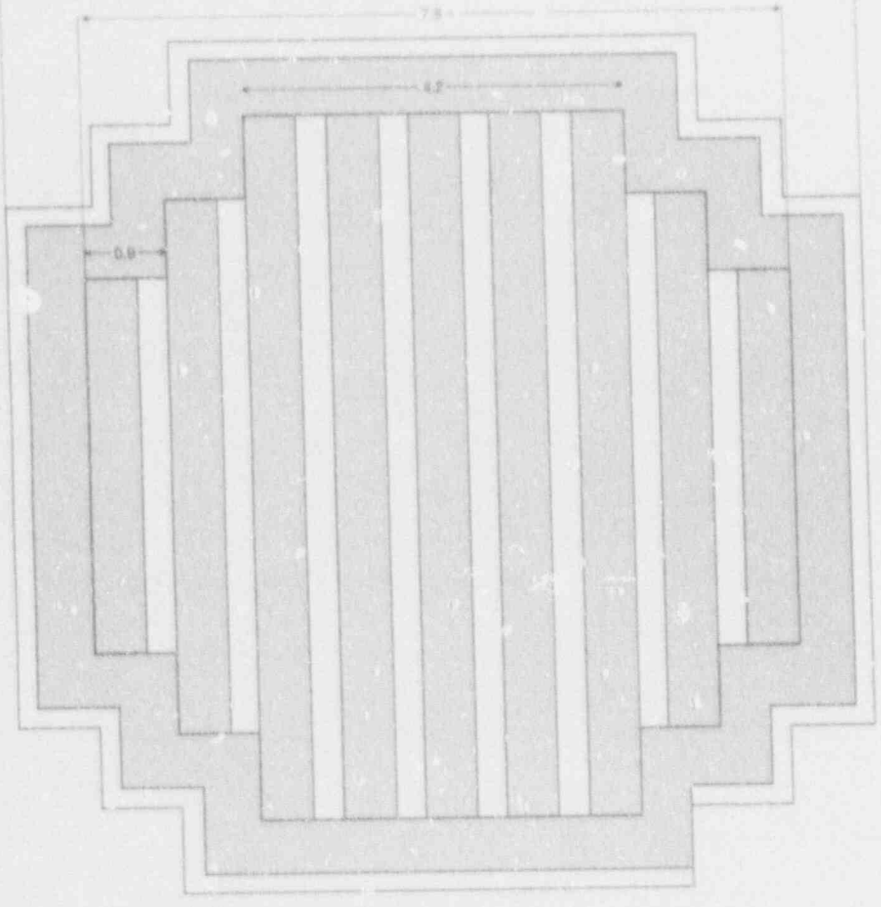


(a) HORIZONTAL CROSS SECTION OF THE REACTOR CAVITY

FIG. 5 - STACK OF BEAMS TAKEN AS RFFERENCE

- The heat capacity of the air present in the cavity is so small compared to the internal energy of the molten core that it can absorb only less than 1% of it. So its cooling effect can be neglected, even if there were an instantaneous transfer of heat to the surrounding atmosphere. Therefore, heat would be removed from the melt mainly by conduction and radiation to the graphite beams and to the cavity walls.
- Corium is a molten material with a high latent heat of fusion (280 kJ/kg) and internal heat generation (0.2-0.3 kW/kg): both these characteristics tend to maintain it in the liquid phase and to favor the uniformity of its spreading.
- A very thick layer of corium **cannot** accumulate on the upper side of the beams because it takes time for the melt to solidify: the thicker the corium layer, the longer its solidification time. As a consequence the material which is not quickly solidified tends to squirt or ooze out of the horizontal side of the beam.

Apart from these considerations, the uniformity of the melt distribution, even if desirable, needs not be rigorous, because there are margins for a certain degree of non-uniformity in the distribution. The degree of disuniformity which can be tolerated without adverse effects, can be determined by heat transfer calculations.

### 3.4.5 Temperature Transients

#### a) Mathematical Model

With a three-dimensional distribution of the melt on the stack of beams, three-dimensional heat transfer calculations would be necessary.
However, to prove the soundness of the proposed solution these complex calculations are not strictly necessary. In this preliminary phase only a simplified one-dimensional heat transfer model has been considered. Therefore a uniform thickness of corium on top of the graphite beam has been assumed.
The heat loss by radiation from the top of the beam (when considered) has been arbitrarily compensated by a similar heat input into the bottom of the beam.
The decay heat has been uniformely distributed, part in the corium and part in the graphite, the ratio between the two parts being a function of the thickness of the corium layer.
The decay power has been reduced by 20% to account for the loss of volatile fission products.
The pressure vessel melt-through has been assumed three hours after the beginning of the accident.

#### b) Variable Parameters

The temperature transients in the corium and in the graphite have been calculated by for different values of the following parameters:

- thickness of corium layer (from 0.5 to 20 cm);
- thermal diffusivity (from that of pure $UO_2$ to that 5 times larger, to encompass types of corium with a very large metallic fraction);
- heat removal by conduction only and by both conduction and radiation.

#### c) Temperature Profiles

In this section the **main** results obtained with the computer runs performed are presented. The interested reader is referred to References [5] and [6] for the entire set of parametric studies performed.

Fig. 6 shows the temperature profiles in the corium and in the graphite, in the case of a single graphite slab, 3 m thick and 50 $m^2$ cross section, over which a corium layer of 20 cm is distributed. Heat is assumed to be removed by both conduction (at the corium-graphite interface) and radiation (from the top of the corium layer) .
As expected, in this geometry the corium cannot be solidified: its internal temperature rises to extremely high values because the heat transfer area is too limited and cannot dissipate the internally generated decay power. The mathematical model adopted is not strictly correct in this situation (there could be crust break-ups) but, nevertheless, the coolability of the corium is not guaranteed.
Even doubling the cavity cross section from 50 to 100 $m^2$ would not be sufficient to obtain the corium solidification and cooldown.

Figure 7 (a,b,c,d) shows the temperature profiles in the corium and in the graphite, at various times after the fall of the melt, for the reference case (molten corium layer 4 cm thick deposited on the top of a graphite beam of 60 cm side). These results, of course, would be valid also for a single graphite slab at the bottom of a cavity of 250 $m^2$ horizontal cross section. These are the main conclusions of the calculations performed:

- the corium is always solidified and cooled down in a relatively short time. This conclusion holds irrespective of the thermal conductivity of the corium and of the heat removal scenario;

- in case of pure $UO_2$, whatever the heat removal scenario, the graphite temperature remains everywhere lower than 800 °C for at least one hour after the fall of the melt;

- in the case of corium of high thermal conductivity, and combined heat removal scenario, the corium-graphite interface temperature exceeds the 800 °C for the first 10-15 min; thereafter, it drops below 800 °C, as in the rest of the graphite and remains below said temperature for at least one hour;

- in case of corium of high thermal conductivity and heat removal by conduction only, the corium-graphite interface temperature remains between 900 and 1200 °C for the first hour after the fall of the melt; the bulk of the graphite, however, stays below 800 °C also in this case.

Calculations have been performed also for the case in which the equivalent corium thickness on the top of the graphite beam is 7 cm. This case is representative of a non uniform corium distribution on the stack of beams. The results of the calculations [5][6] indicate that the graphite surface temperature in the affected beams reaches, in the same time interval, values higher than in the average beams so that, to avoid undesirable chemical effects with water, it is necessary to perform the cavity flooding earlier, say before half an hour from the fall of the melt.
Corium layers of larger thickness are practically impossible to exist since the molten fraction of corium would tend to slip out of the top of the beam. The slipping out of the molten fraction can also be facilitated by suitable geometric features of the beam itself.

In conclusion, by spreading the corium in layers of limited thickness over a stack of graphite beams and by flooding the cavity within half an hour from the fall of the molten core, the solidification and cooldown of the molten core can be ensured and the integrity of the containment basemat preserved, without adverse effects (no steam explosion, limited hydrogen generation if any).

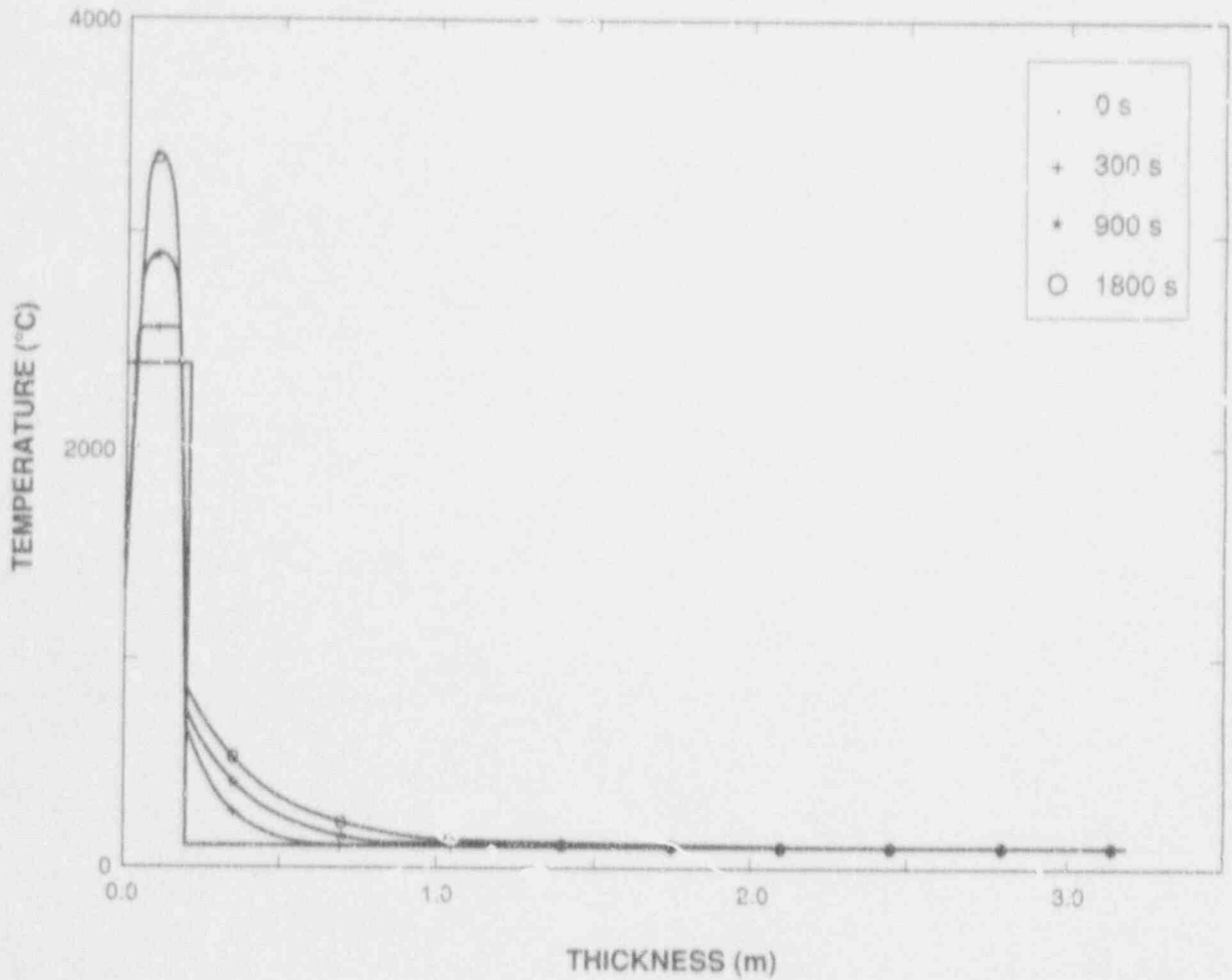


FIG. 6 - TEMPERATURE PROFILES IN CORIUM AND GRAPHITE
($UO_2$ layer 20 cm thick on single graphite slab 3 m thick -
Heat removal by conduction and radiation)

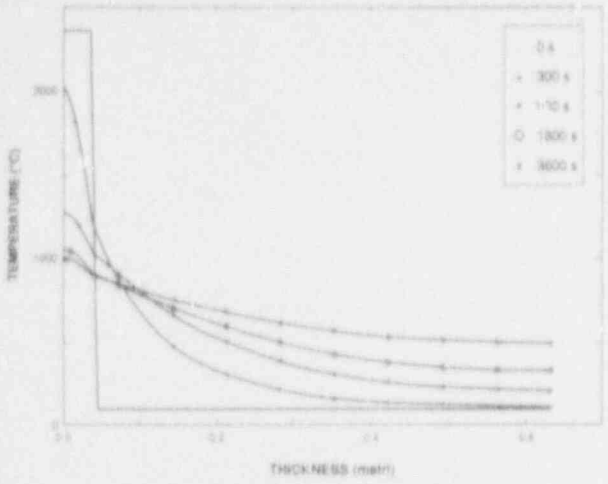


a - (Metallic corium layer 4 cm thick on graphite beam of 60 cm side - Heat removal by conduction)

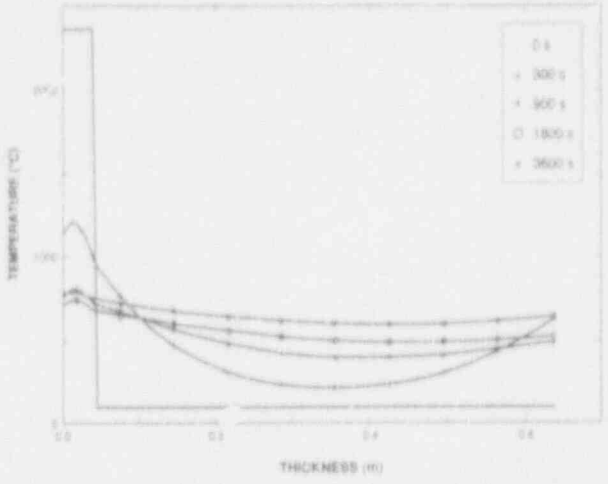


b - (Metallic corium layer 4 cm thick on graphite beam of 60 cm side - Heat removal by conduction and radiation)

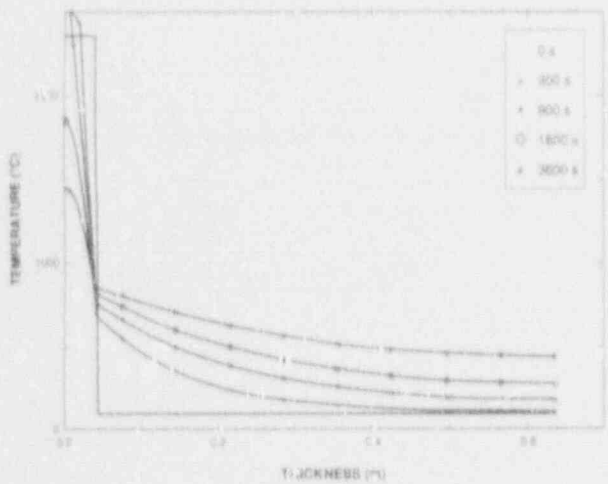


c - ($UO_2$ layer 4 cm thick on graphite beam of 60 cm side - Heat removal by conduction)

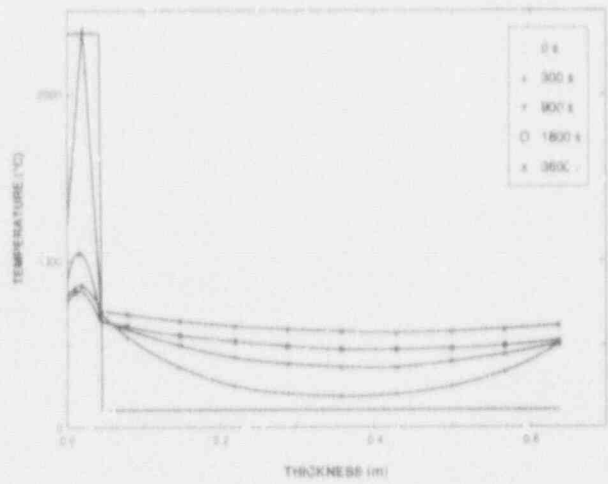


d - ($UO_2$ layer 4 cm thick on graphite beam of 60 cm side Heat removal by conduction and radiation)

## FIG. 7 - TEMPERATURE PROFILES IN CORIUM AND GRAPHITE

### 3.4.6 The Cavity Flooding

In the I.I.R.A. containment, the reactor cavity is in communication with the suppression pool through pipes located close to the bottom of the pool; these pipes are normally closed either by isolating valves or by melting plugs. The opening of the valves or the melting of the plugs causes the flooding of the cavity and the gradual quenching, starting from the bottom, of the molten corium distributed in the dispersing structure. In this manner **damaging steam explosions are avoided.**
The flooding should take place whithin half an hour from the fall of the melt to avoid graphite overheating and subsequent extensive graphite-water reactions.
As long as the graphite surface temperature stays below 1000 °C, the reaction rate with water is limited and the extent of the reaction is also limited because the time required to cool down the walls of the graphite beams to safe levels (below 700 °C) is of the order of 15 minutes or less.

(In Reference [3] the fall of molten corium directly in a flooded cavity was considered but, for the time being, that solution has been set aside untill more is known on molten core/coolant interaction and associated potential steam explosions).

### 3.4.7 Applicability

The cavity design described in the previous paragraphs can be adopted in all types of containment, even in those which do not expouse the pressure suppression concept.

## 4. SOURCE TERM AND PROBABILISTIC SAFETY ASSESSMENT

The "source term" is the reference release to the environment which is assumed to evaluate the worst possible consequences of a severe accident.

In most of the operating reactors the adoption of a source term orders of magnitude smaller than the core inventory is difficult to be justified, if one takes into consideration the results of the PRAs performed.
In fact, examining Fig. 8 which shows the so-called "Cumulative Complementary Distribution Function" (namely, the probability of having a release larger than the value chosen on the abscissa) for five typical operating reactors [4], it is evident that the probability of a release does not decrease appreciably as the release itself increases. Only the curve related to a BWR equipped with a Mark III containment shows an encouraging, albeit not very strong, downward trend. This trend is mainly due to the features of the Mark III containment and in particular to the passive scrubbing action of the suppression pool which limits the radioactivity release to the environment.

Unfortunately the design limitations of the Mark III containment (for severe accidents) do not allow to take full advantage of the potential of the system. For example, in the plant taken as a reference (Grand Gulf), the hydrogen ignitors located above the suppression pool are fed by A.C. power and therefore if power is not available the hydrogen would accumulate in the containment and its deflagration could cause the failure of the containment itself, because of its small volume and design pressure.

In the proposed containment system, hydrogen accumulation is prevented by D.C. powered ignitors and by the (passive) catalytic foils in the containment; furthermore the containment volume and design pressure are so large that even a hydrogen deflagration would probably not fail the containment.

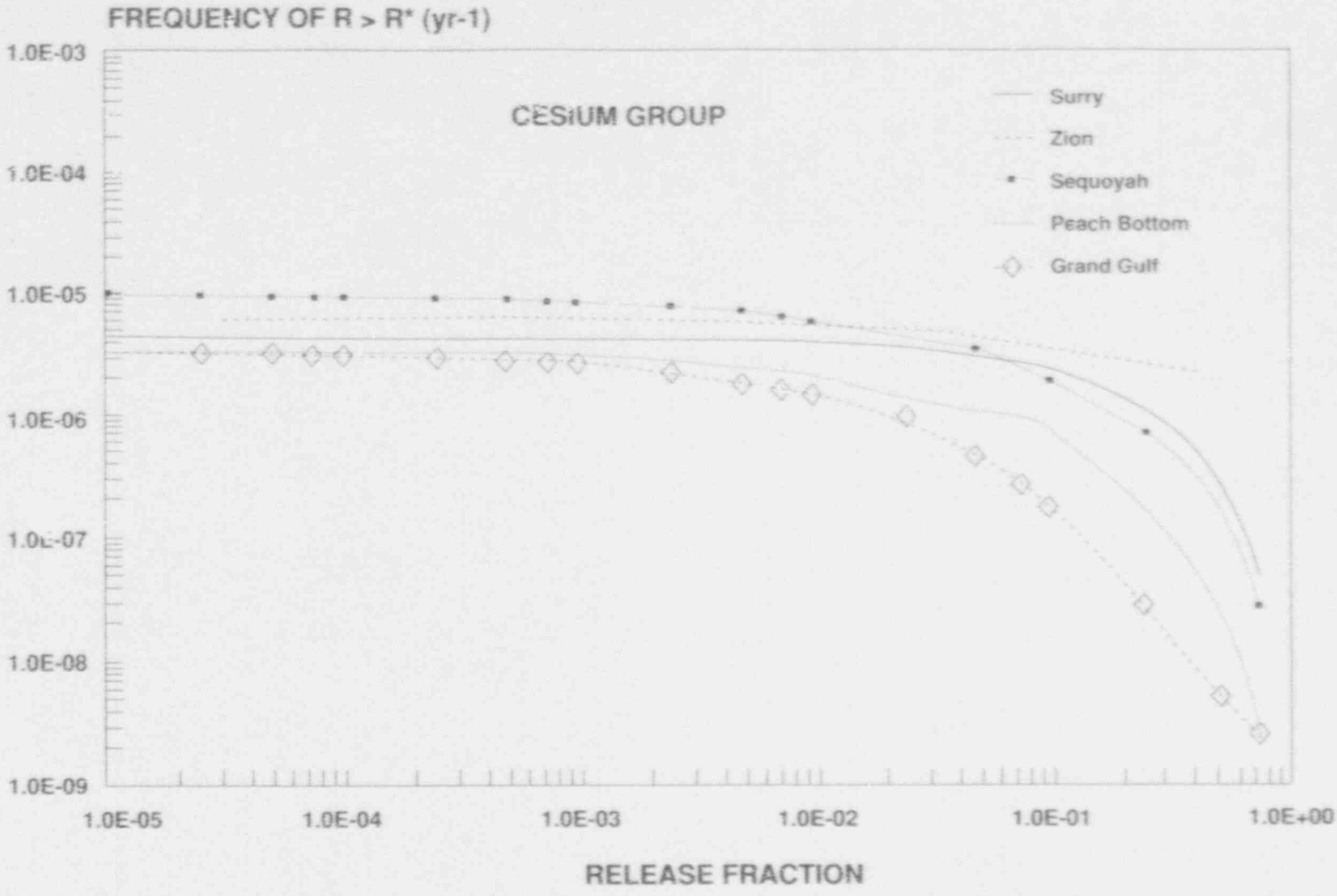


FIG. 8 - CCDF (Cumulative Complementary Distribution Function) FOR FIVE TYPICAL OPERATING NUCLEAR POWER PLANTS. (From NUREG 1150)

An other reason why the potential merits of the Mark III containment are not strikingly evident in the PRA performed is the fact that a steam explosion in the drywell is possible and has a certain probability of causing a suppression pool by-pass, with consequent failure of the containment structure. By avoiding the interaction between the molten core and the water untill the former is fully solidified the corresponding risk of containment failure could be made negligible.

If the mentioned shortcomings of the Mark III containment were eliminated as in the proposed L.I.R.A. design, a PRA level 2 would probably show a corresponding CCDF with a very clear downward trend of probability vs. release, thereby confirming the applicability of a very low source term for a reactor equipped with the proposed containment.

## 5. COSTS

Of course a containment system such as the L.I.R.A. is not cheap. One might argue that a large and strong containment with a pressure suppression pool, such as that proposed, is unnecessary and that such an expensive containment tends to make the nuclear power plants less competitive with other existing alternatives. Even if an accurate evaluation of the cost of the proposed containment cannot be made without a detailed design, an approximate and preliminary estimate can be tried.
Keeping in mind the desire to maintain a large and strong containment ( say 70 000 cubic meter of volume and 0.4 MPa of design pressure for a 1000 MWe reactor) the addition of:

- the suppression pool (of say 8000 cubic meter);
- the structure enveloping the whole primary circuit (drywell) and the associated penetrations;
- the new reactor cavity design, below the vessel;
- the hydrogen recombination devices (ignitors and catalytic foils)

might lead to an increase in the cost of the containment perhaps around 20-30% above that of a large dry containment of the present generation. Since the cost of the containment is about 4% of the total plant cost, the cost increase associated with the proposed L.I.R.A. containment is about 0.8-1.2%. And since the capital cost accounts for approximately 60-65% of the unit cost of electricity, the increase in cost of electricity associated with the L.I.R.A. containment amounts to 0.5-0.8%, i.e. not very much considering the enormous increase in safety afforded by the L.I.R.A. containment.

Furthermore, some savings might also be made since all the expenses related to the preparation of the emergency plan can be avoided; in addition, since the proposed containment system is based on well known principles and does not require knowledge in unknown scientific domains, limited costs are envisaged in related R & D.

In the opinion of the author, if the superior radioactivity retention capabilities of the proposed containment are recognized and credit is given for them by the regulatory authorities, by the scientific community and by the affected population, the proposed containment has a chance of being adopted, even in countries where there is, at present, a strong opposition against nuclear power.

In conclusion the limited cost increase associated with the L.I.R.A. containment cannot be considered an obstacle to the competitiveness of nuclear energy.

## 6. COMMERCIAL ASPECTS

The L.I.R.A. containment system described in this report requires know-how both in the field of PWR technology and in the field of vapour suppression technology.
In the West, the vapour suppression technology (in its suppression pool variety) has been developed by General Electric, the main BWR vendor; the main leader in PWR technology has been Westinghouse: since these two companies have always been traditional competitors, the blending of these two technologies does not appear easy. But it should be remembered that in the world there are at least three vendors who have both technologies:

- **ABB**, now incorporating Combustion Engineering, has experience in the design and construction of both PWRs (with large dry containments) and BWRs (with vapour suppression containments) in Sweden;
- **Siemens**, now incorporating A.E.G., has similar experience; in addition to that, it also has acquired know-how in the field of hydrogen recombination with catalytic foils;
- **Atomenergoprojekt,** the Russian reactor designer, has experience in both PWR technology and vapour suppression technology.

So, even without a G.E./Westinghouse joint venture, there is in the world the capability of designing and constructing PWRs with L.I.R.A. containment systems.

## 7. CONCLUSIONS AND RECOMMENDATIONS

The L.I.R.A. containment system proposed in this paper for adoption in future nuclear power plants affords a major increase in the safety of nuclear power plants in so far as it is capable of limiting the release of radioactivity to the environment to less than one millionth of the core inventory, also in case of a severe accident with core melt and pressure vessel melt-through. With such a small release no evacuation plan would be necessary for the surrounding population and the contamination of the surrounding territory would be negligible. Since the proposed containment is based on well proven concepts little additional experimental research is necessary to prove its feasibility and to optimize its design.
Its cost is expected to increase the cost of electricity by less than 1% with respect to the current systems.
If the containment concept proposed in this report meets, on one side, the interest and the appreciation of Utilities, Reactor Vendors, Architect-Engineers a.. ' of the Scientific Community, and , on the other, gets credit for its superior safety characteristics by the Regulatory Authorities, some experimental tests and more detailed analyses might be funded to dissipate residual doubts and confirm the feasibility and economic validity of the proposal.

## References


1) Turricchia, A. NO EVACUATION AND NO LAND CONTAMINATION: A POSSIBLE GOAL FOR FUTURE REACTOR CONTAINMENT SYSTEMS, ENEL Report 9N0 TNIU 0009, September 1991.

2) Rohde, J., HYDROGEN MITIGATION CONCEPTS AND EFFICIENCY TESTS, Report presented at the Accident Management Information Exchange USNRC-BMU/GRS, in Rockville, MD., April 15-17, 1991.

3) Turricchia, A., CONTAINMENT DESIGN FOR SEVERE ACCIDENTS: DEFENSE OF CONTAINMENT BASEMAT INTEGRITY AGAINST CORIUM ATTACK, Enel Report 9N0 2110 TNIU 0001, February 16, 1989.

4) NUREG 1150- SEVERE ACCIDENT RISKS: AN ASSESSMENT FOR FIVE U.S. NUCLEAR POWER PLANTS.- Final Summary Report- VOL.1. Dec. 1990.

5) Turricchia, A. " HOW TO AVOID MOLTEN CORE/CONCRETE INTERACTIONS (AND STEAM EXPLOSIONS)", Paper presented at the 2nd CSNI Specialist Meeting on Molten Core/Concrete Interaction, Karlsruhe, 1-3 April, 1992.

6) Turricchia, A., PROTECTION OF THE CONTAINMENT BASEMAT AGAINST CORIUM ATTACK, ENEL Report 9N0 2110 TNIU 0005, To be publisned in May 1992.

# DESIGN OF THE INTERNAL GEOMETRY OF AN ADVANCED CONTAINMENT FOR MITIGATING DEFLAGRATION OVERPRESSURES

Marco Nicola Carcassi Fabio Fineschi
Dipartimento di costruzioni meccaniche e nucleari
University of Pisa, ITALY

## Abstract

During a severe accident at a nuclear power plant, there is the potential for the generation, accumulation and combustion of hydrogen. Various models and computer codes have been developed to predict the containment loading that may result from the maximum overpressures generated from the combustion of hydrogen during a severe accident. In the first phase of our research, the DEVENT code was developed as an analytical tool to provide a more realistic evaluation of the maximum overpressures reached in the compartments as a result of a deflagration. DEVENT simulates the deflagration transient in a compartment with venting towards a constant pressure environment. Deflagration tests where carried out in a partially contained volume in the HYDRO apparatus (0.5 $m^3$ steel vessel) and in the VIEW (0.4 $m^3$ glass vessel) apparatus, where the flame front can be seen with the addition of a NaCl aerosol. The preliminary data that has been generated from our theoretical and experimental result, on the optimum collocation of venting apertures and igniters, can be used to develop of igniters or other systems, which address hydrogen mitigation in advance type containments.

## INTRODUCTION

In the case of severe accidents in a water cooled nuclear power plant, hydrogen may be present in the containment and form a flammable mixture with the atmosphere. Mixtures are considered flammable when enough fuel and comburent concentrations are present to let the combustion propagate as a wave front in the gas, after being triggered in a small volume by an external source, like a spark, quickly releasing enough energy (ignition). The process causes the rapid release of a large quantity of energy (explosion). There are various modes of propagation of the combustion wave, which may be divided into two categories:

1) slow deflagrations, which are dangerous in closed or partially confined environments, because they provoke a nearly uniform increase in pressure and loads, almost static upon the containment structures. The overpressure increases along with the degree of confinement and with the reactive state of the mixture until it reaches the stoichiometric conditions.

2) rapid deflagrations and detonations, whose probability and danger increases with the reactivity of the mixture. This combustion forms shock waves and, therefore, dynamic loads on the structure, independent of the degree of confinement since the rarefaction wave causing the burnt gas vent (this is the only pressurised gas since the fuel wave and the shock wave coincide) cannot catch up and attenuate the faster shock and fuel wave.

An explosive accident can therefore damage the safety containment and result in the release of radioactive substances into the atmosphere.

For the purpose of this investigation, we will focus on slow deflagrations.

The slow deflagration is the most probable in a nuclear plant. In order to evaluate the risks and design the safeguards to be installed to reduce the consequences of combustion, we must predict the pressure transient that a slow deflagration would propagate between the various compartments, since the safety containment is subdivided into communicating compartments. In partially confined volumes, the deflagration overpressure depends on the combustion rate, and this on the geometric and thermofluid dynamic conditions of the system affected by the propagation of the flame. The complexity of the chemophysical mechanisms responsible for the deflagration phenomenon has not yet allowed us to develop a theory complete enough to describe quantitatively the influence of each parameter on the deflagration process. The overpressures generate gas flows (venting) between communicating compartments, such that the distribution of temperature, pressure, speed and chemical composition of the gas change while the combustion transient affects the containment. This change generates retractions in the combustion rate. Since the "vented" deflagration depends on the geometry of the compartments, the overpressures caused by the deflagration can be mitigated by properly designing these compartments and the apertures which put them in communication.

At the Department of Mechanical and Nuclear Engineering at the University of Pisa (DCMN) we started a theoretical and experimental research program on vented deflagration. Initially, cases of venting towards a pressure constant environment were considered. These are not only important as a first stage for further study on deflagration vented toward variable pressure environments (typical of containments with compartments), they are also important for their direct application in the conventional field, where venting towards the atmosphere is used as a method for mitigating overpressure due to accidental deflagrations in containments or buildings where flammable gases are generated, released, stored or manipulated. The computer code, DEVENT, was developed to simulate this phenomenology and, at the same time, experiments on the apparatus called HYDRO were conducted. To visualise the evolution of the flame front during combustion and its passage between compartments, the VIEW apparatus was then designed and constructed. These first phases of our research have already provided some interesting information for optimising the design of the internal geometry of the containments of new generation nuclear reactors.

## THE DEVENT CODE

The computer codes, like MAAP, CONTAIN, RALOC, FUMO, etc, that are currently available to simulate the phenomena which may occur in the safety containment of a nuclear power plant during a postulated severe accident, operate on "concentration parameters" and do not characterise very well the containment volume that includes regions of burnt and unburnt gas, created by the combustion wave. For example, the HECTR 1.8 containment code [1] with concentrated parameter, has a deflagration model that takes into account regions of different chemical composition (burnt and unburnt states) within the compartment. However, these containment volumes within HECTR are determined in a totally unrealistic way in that the temperature and molar density are considered to be uniform throughout the compartment. This implies an incorrect assumption on the temporal evaluation of the venting characteristics and, therefore, on its effects on the pressure transient since the balances on mass and energy change as vented gas is assumed to be burnt or unburnt.

DEVENT [2], instead, takes into account the marked difference in temperature between the expanding volume occupied by the burnt gas and the decreasing volume occupied by the unburnt

gas, with characteristics of the vented gas equal to those present in the volume which face the venting apertures. The system is adiabatic, under the assumption that the energy loss due to the transfer of heat towards the walls is negligible compared to the energy released by the combustion and lost through venting. The pressure in the compartment is assumed as always uniform, as in HECTR 1.8 since the speed of the flame front is much slower than the speed of sound (slow deflagrations). An infinitesimal element undergoes an isoentalpic transformation while crossing the combustion wave, assumed to be of zero thickness. The combustion of the infinitesimal element is, therefore, instantaneous and complete because the dissociation of the reaction products is neglected. The overall increase in pressure is caused by the subsequent combustion of various mass elements and is in part counterbalanced by venting towards an external environment at constant pressure, lower than or equal to the internal pressure. Since the gas cannot enter the compartment, the chemical composition of burnt and unburnt gas is constant and, obviously, different. The unburnt gas undergoes an isoentropic compression because there is no gas input in the unburnt zone and all output gas (due to the venting or to the combustion) has the same characteristics as the gas in the region. The flame temperature, i.e. the temperature of the gas which enters the burnt zone, varies in time along with the variations in the pressure and the temperature of the unburnt gas.

In order to simplify the thermodynamic treatment, the deflagration models similar to DEVENT [3,4,5] generally assume that no individual mass element undergoes any matter or heat exchange with the other elements after it is burnt. It is isoentropically compressed from the combustion pressure to the final pressure. In essence, unlike the unburnt gas, the burnt gas is considered anisotropy. In most cases this hypothesis is unrealistic. DEVENT also considers a perfect mixing of the burn phase. This difference from the other models entails a more complex thermodynamic analysis, because the burnt gas is not isoentropically compressed. On the other hand, the model makes it much easier to determine the characteristics of a possible venting of burnt gases, because the temperature is also uniform in the unburnt gas. The gases are assumed to be ideal, with different specific heats depending on their chemical composition, evaluated as a function of temperature by means of classical empirical relationships [6].

The required input to the code is given by:
- the initial conditions of the mixture (the venting flow rate is initially zero either because the pressure is equal to the external pressure or because the venting apertures are closed);
- the law with which the volumetric combustion rate varies in time from an initial nil value (ignition); the volumetric combustion rate is calculated as a product of the burning velocity (the relative speed component of the unburnt gas with respect to the perpendicular of the flame) multiplied by the flame front. The code must therefore be provided with both the law of variation of the burning velocity due to the thermofluid dynamic variables of the system, and the law of variation of the flame front with the burnt volume;
- the pressure value at which venting begins through an aperture and the value, lower than the former, at which it may stop after having begun;
- the values of the burnt volume when the aperture is reached by the flame front (at this point the chemical composition of the vented gas changes from unburnt to burnt); these values are determined a priori by the user with geometrical considerations based upon the dimension and form of the compartment and on the venting apertures, on the position of the venting, on the position of

the ignition point and on the hypothesised geometry for the flame front while the combustion wave propagates.

## MATHEMATICAL FORMULATION OF THE DEVENT CODE

The thermodynamic analysis is based on the following balances:
- mass and energy balances in the unburnt gas;
- mass and energy balances in the flame;
- mass and energy balances in the burnt gas;
- momentum balance implicit under the assumption of pressure uniformity.

The accuracy of the code result is verified through a global mass balance. The quantities used as reference for the non-dimensional formulation of the equations are:

| | |
|---|---|
| - length | V/A |
| - surface | A |
| - volume | V |
| - temperature | Ts |
| - molar energy | RTs |
| - pressure | Pe |
| - energy | PeV |
| - mass | $\frac{P_e V M_u}{R T_s}$ |
| - speed | $c_{us} = \sqrt{\frac{\gamma_{u_s} R T_s}{M_u}}$ |
| - time | $\frac{V}{A c_{us}}$ |

The non-dimensional variables are underlined.

### Mass Balances

The molar flow rate of venting is obtained by adding unburnt to burnt flow rate:

$$\frac{d\overline{n}_v}{dt} = \overline{P}\left(\frac{C_{du}\overline{A}_{vu}\overline{c}_u\,\overline{\eta}_u}{\overline{T}_u} + \frac{C_{db}\overline{A}_{vb}\overline{c}_b\,\overline{\eta}_b}{\overline{T}_b}\right) \qquad (1)$$

where

$$\overline{\eta} = \left(\frac{2}{\gamma+1}\right)^{\frac{1}{2}\frac{\gamma+1}{\gamma-1}} \qquad \text{for } \overline{P} \geq \overline{P}_{cr} = \left(\frac{2}{\gamma+1}\right)^{\frac{\gamma}{1-\gamma}}$$

or

$$\overline{\eta} = \left(\frac{1}{\overline{P}}\right)^{\frac{1}{\gamma}}\left\{\frac{2}{\gamma-1}\left[1-\left(\frac{1}{\overline{P}}\right)^{\frac{\gamma-1}{\gamma}}\right]\right\}^{\frac{1}{2}} \qquad \text{for } \overline{P} < \overline{P}_{cr}$$

*unburnt gas*

The moles of unburnt gas decrease in time because of the combustion reaction and the beginning of venting. In differential terms the expression is:

$$dn_u = - dn_{uv} - dn_{ur}$$

with

$$n_u = \frac{PV(1-x)}{RT_u}$$

and

$$dn_{ur} = \frac{P}{RT_u} B_r \, dt$$

from which, by non-dimensional rendering:

$$(1-x)\left(\frac{d\bar{P}}{\bar{P}} - \frac{d\bar{T}_u}{\bar{T}_u}\right) - dx = -\left(C_{du} \bar{A}_{Vu} \bar{c}_u \bar{\eta}_u + \bar{B}_r\right) d\bar{t} \qquad (2)$$

*flame*

The flame is of zero dimension, hence:

$$dn_{br} = (1 + \varepsilon v)\, dn_{ur} = \frac{M_u}{M_b} dn_{ur}$$

*burnt gas*

The moles of burnt gas vary according to the balance between the positive contribution given by the combustion reaction and the negative one given by venting:

$$dn_b = dn_{br} - dn_{bv}$$

where

$$n_b = \frac{PVx}{RT_b}$$

from which, by considering the mass balance in the flame and adimensionalising:

$$x\left(\frac{d\bar{P}}{\bar{P}} - \frac{d\bar{T}_b}{\bar{T}_b}\right) + dx = \left(-C_{db} \bar{A}_{Vb} \bar{c}_b \bar{\eta}_b + \frac{M_u}{M_b} \frac{\bar{T}_b}{\bar{T}_u} \bar{B}_r\right) d\bar{t} \qquad (3)$$

## Energy Balances

*unburnt gas*

The assumption is that the unburnt gas undergoes an isoentropic compression:

$$\frac{d\bar{P}}{\bar{P}} = \frac{\gamma_u}{\gamma_u - 1} \frac{d\bar{T}_u}{\bar{T}_u} \qquad (4)$$

*flame*

The uniform pressure in the system and its adiabaticity, entail the isoentalpic combustion of the infinitesimal gas element. The gas enters the flame at the temperature of the unburnt gas and leaves it at the flame temperature:

$$\frac{M_u}{M_b}\left(\bar{h}_{bT_f} - \bar{h}_{bT_s}\right) - \left(\bar{h}_{uT_u} - \bar{h}_{uT_s}\right) + \varepsilon \Delta\bar{h}_s = 0 \qquad (5)$$

*burnt gas*

$$d(n\, u_{T_b})_b + h_{bT_b}\, dn_{bv} - h_{bT_f}\, dn_{br} = -P\, dV_b$$

from which, by using the mass balances and adimensionalising:

$$x\left(\frac{d\bar{P}}{\bar{P}} - \frac{\gamma_b}{\gamma_b - 1}\frac{d\bar{T}_b}{\bar{T}_b}\right) = \frac{M_u}{M_b}\frac{\bar{h}_{bT_b} - \bar{h}_{bT_f}}{\bar{T}_u}\,\bar{B}_f\,dt \qquad (6)$$

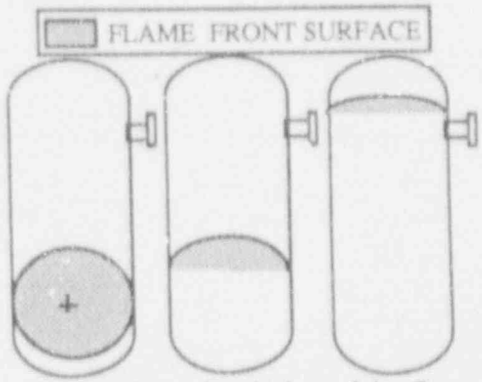


Figure 1 Evolution of the flame in a cylinder

## Solution of the mathematical problem

By using Equation (5) to find T, the differential Equations (1), (2), (3), (4), (6), can be rearranged and integrated to obtain $P$, $T_u$, $T_b$, $x$ e $n_v$ as a function of time with a standard library subroutine for the solution of ordinary differential equation systems.

DEVENT had previously been applied to the three elementary geometries (planar, cylindrical, spherical). Current application has been extended to include cylinders with bottom ignition and the flame evolution (Figure 1) [2].

## USE OF THE DEVENT CODE

The main difficulty in the use of DEVENT comes from the need to know, as input, the variation laws of the combustion speed and of the flame front. These are determined by many parameters, which include:

1) the turbulence of the unburnt gas which is due to the expansion of burnt gases and to the presence of obstacles, in relation to the geometry of the compartment . The greater the volumetric combustion rate, the greater the turbulence which, in its turn, tends to increase both the combustion speed and the flame front by distorting it;

2) the heat losses towards the walls, especially when they come in contact with the burnt gas;

3) the relative movement between hotter burnt gases and colder unburnt gases, due to buoyancy forces;

4) the distortions of the flame front due to instabilities similar to the Taylor one [7,8,9], which are caused by impulsive accelerations from the unburnt toward the burnt gas. This occurs when the flame slows down by touching the walls or when burnt gas venting begins;

5) the number and the position of the ignition sources;

6) the "jet-ignition," (the simultaneous ignition of almost all the gas present in a compartment), caused by the close mixing of burnt and unburnt gases which is provoked by the sudden burst of a flame, from an adjacent compartment in the highly turbulent fluid dynamic field which originated in the compartment. This was caused by the violent entrance of unburnt gas which precedes the arrival of the flame [10,11].

The complexity of these phenomena and the possibility of their combining in various modes makes it almost impossible to find laws of variation for the combustion rate other than those empirically derived. Today experimentally studied cases are insufficient with regard to the enormous spectrum of possible situations that may be found in practice.

DEVENT may be used in an inverse sense to derive semi-empirical laws of variation for the combustion rate, starting with the observation of experimental transients [12,13].

## EXPERIMENTS WITH THE HYDRO APPARATUS

### Experiments

Since the beginning of the 1980's, the Scalbatraio Laboratory of the Department of Mechanical and Nuclear Engineering of the University of Pisa has been conducting experiments on the deflagration of hydrogen mixtures.
Along with the theoretical work, tests have been made on the deflagration in containment with venting in a free atmosphere as the first phase of experimental studies on the effects of compartimentalization. The results allowed for a phenomenological analysis propaedeutic to the study of more complex situations. These results are of immediate interest for an understanding of the evolution of deflagration in the compartment, where ignition takes place and there is communication with compartments where the pressure remains almost constant. This is because they are larger than the vented gas volume or because the venting towards other environments is intense. The pressure also remains constant, independent of the unload pressure, when there is a critical flow conditions.

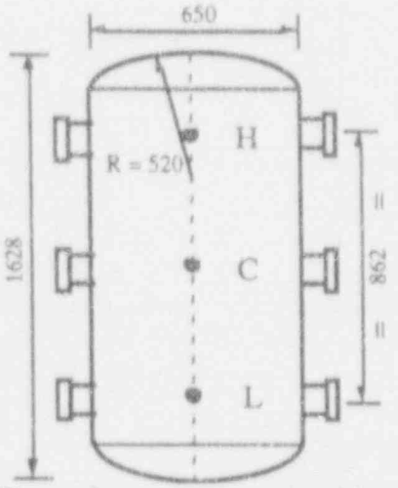

Figure 2. HYDRO vessel with vent and igniter positions.

The initial conditions and results of selected tests [14] conducted in the HYDRO apparatus [15] are found in Table 1. The test apparatus is essentially a vertical steel cylinder, 0.5 $m^3$ (Fig. 2). The composition of the hydrogen-air mixture was 14% by volume of hydrogen in all the tests in order to show the effects brought about by varying the follows parameters:

Table 1. Initial conditions and results of some HYDRO tests.

| Test number | 4 | 10 | 11 | 12 | 15 | 19 | 22 | 25 | 26 |
|---|---|---|---|---|---|---|---|---|---|
| Conc. vol. H2 (%) | 14,3 | 13,9 | 14,0 | 14,0 | 13,9 | 14 | 14 | 14,0 | 14 |
| Igniter position | L | L | L | L | L | L | L | H | H |
| Venting position | H | H | H | H | TC | C | L | L | TC |
| Φ venting (mm) | 30 | 100 | 70 | 50 | TC | 70 | 70 | 70 | TC |
| t init. vent comb. (s) | 0,125 | 0,074 | 0,092 | 0,115 | | 0,066 | 0,01 | 0,154 | |
| number of peaks of P | 1 | 2 | 1 | 1 | 1 | 1 | 1 | 2 | 1 |
| t of 1° peak of P (s) | 0,28 | 0,086 | 0,05 | 0,265 | 0,285 | 0,267 | 0,218 | 0,124 | 0,38 |
| 1° peak of P (kPa) | 297 | 139 * | 170 | 238 | 356 | 173 | 192 | 141 | 364 |
| t of 2° peak of P (s) | | 0,139 | | | | | | 0,238 | |
| 2° peak of P (kPa) | | 121 | | | | | | 142 * | |
| t end c. (from P) (s) | 0,28 | 0,139 | 0,203 | 0,270 | | 0,267 | 0,245 | 0,238 | |
| t end c. (from T) (s) | >0,28 | >0,167 | 0,190 | >0,276 | 0,285 | >0,240 | 0,225 | >0,198 | 0,38 |
| P end c. (kPa) | <297 | 120/<75 | 150 | <210 | 356 | 173 | <185 | 142 | 364 |
| t end transient (s) | 4,435 | 0,992 | 0,690 | 0,862 | NR | 0,567 | 0,76 | 0,52 | NR |

* = Max value; NR = Not recorder; TC = Test Closed; c. = combustion.
H=high, C=central, L=low (see Figure 2)

- the position of the igniter: high, low (H, L see Figure 2)
- the position of the venting: high, central, low (H, C,L see Figure 2)
- the diameter of the venting area: 30, 50, 70, 100 mm.

Based on previous experimental data [16], we assume that the volumetric concentration of the hydrogen is high enough at 14% to guarantee that the combustion wave will propagate in the entire volume of the vessel. The dimensions of the venting area are small enough, with respect to the volume of the vessel, to enable us to easily measure the overpressure.

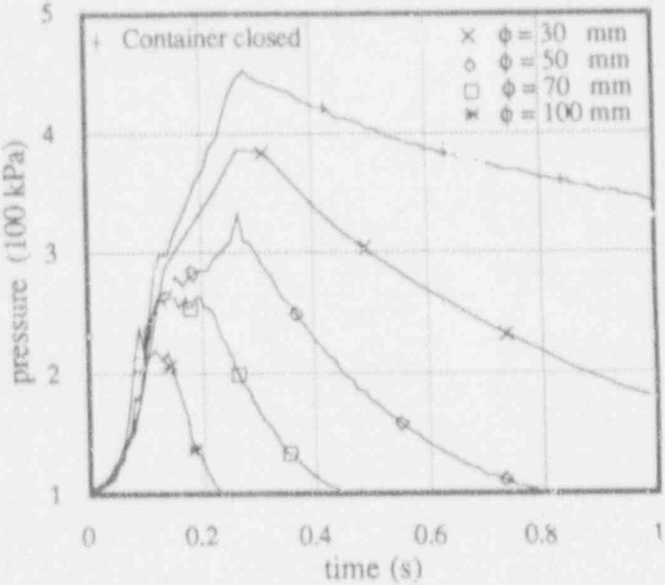


Figure 3. Pressure transients with ignition in L position and venting in H position.

The initial pressure was the same as the external pressure and the venting opened as soon as the pressure went up. For those tests not reported in Table 1, the main interest was for an application of venting in the containment of conventional plants. For these tests the overpressure of the venting aperture was varied using: 20, 40, 60, 160 kPa.

Pressure and temperature were measured at certain points inside the vessel and in the venting aperture. The thermocouples were not able to estimate the real temperature of the gas because their response times were too long with respect to the speed of the transients. They are, however, useful to evaluate when the flame front has arrived at the thermocouples since it quickly increases the exit signal.

## Analysis of the results

1) The effect of an increase in the venting aperture dimension, which diminishes the maximum overpressure, was studied in tests with the igniter at L position and the venting at H position. An increase in the venting flow rate diminishes the quantity of overall burnt gas (even during unburnt gas venting) and increases, during burnt gas venting, the energy lost towards the outside compared to the energy generated by the combustion of unburnt gases trapped in the vessel (Figure 3).

2) The experimental curves of the pressure in two tests are shown in Figure 4. The igniter was first placed in H position and

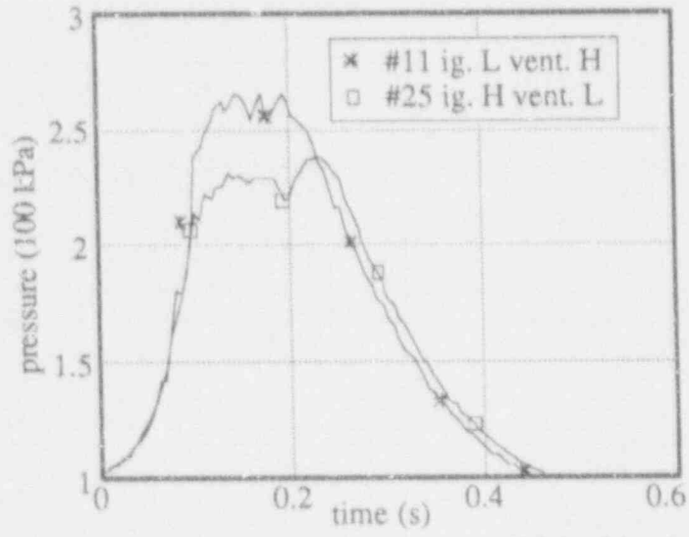


Figure 4. Pressure transients in tests with ignition in L/H position and venting in H/L position.

then in L position while venting, with an aperture diameter of 70 mm, was placed in L position and then in H position. The figure clearly shows that when the igniter is placed above the venting aperture, the maximum pressure in the compartment is lower than when the igniter is low and the venting high. In the first case, we have a $P_{max}$ value of 41 kPa and in the second 69 kPa, an overpressure 40% greater than in the first. This is probably due to the effect of the buoyancy force on the hot, burnt gases. In the test with low igniter, the advancement of the flame front is initially fostered by the buoyancy force. The induced turbulence is marked and the combustion is fast, so only when the venting of burnt gases (after 0.092 s) begins does the lost energy counterbalance the energy generated by the combustion. In the test with high igniter location, the initial combustion is less rapid because the buoyancy forces oppose the advancement of the flame front. The lost energy increases along with the pressure and is able to counterbalance the energy that was generated during the last phase of the unburnt gas venting, which ends at 0.154 s. The geometric characteristics of the system should only affect the phenomenon quantitatively and not qualitatively.

3) Figure 5 shows the experimental pressure curves registered during three tests where the igniter was placed in L position and the venting area (with an aperture of 70 mm diameter)was first close (L position), then at an intermediate distance (C position) and, finally, at the maximum possible distance in the apparatus (H position). In the test where the distance of the igniter and the venting area was maximum or minimum the initial pressurisations were faster. This could be due to a more turbulent flame. In the first case, this is due to a longer duration of the venting of the unburnt gas (ended at 0.092 s) and in the second, to a longer duration of burnt gas venting (begun at 0.010 s). In the test with the venting aperture at an intermediate distance, neither unburnt nor burnt gas venting had enough (the type of venting switches at 0.066) time to generate very high turbulence levels. The mechanisms with which the two types of venting provoke turbulent flames are essentially different and, to a certain extent, antithetical. Unburnt gas venting increases the turbulence of the flame since it tends to increase that of the unburnt gases in which the flame propagates. Venting increases the unburnt gas outflow speed, while burnt gas venting tends to make the flame turbulent due to the triggering of the Taylor instability. The maximum overpressure was greater in the test with a minimum distance between the igniter and the venting aperture because the mass of gas entirely burnt is certainly greater since the unburnt gas venting is lower. This result could have been different if the dimensions of the venting aperture had been varied.

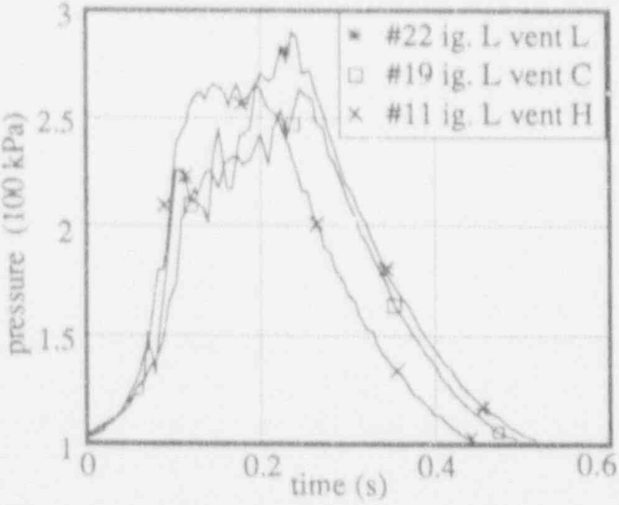

Figure 5. Pressure transients with ignition in L position and different venting positions.

## EXPERIMENTS WITH THE VIEW APPARATUS

With the HYDRO apparatus relatively high pressures can be reached, but the evolution of the flame front cannot be observed (the surfaces of the flame and the volume of the burnt gas). The VIEW

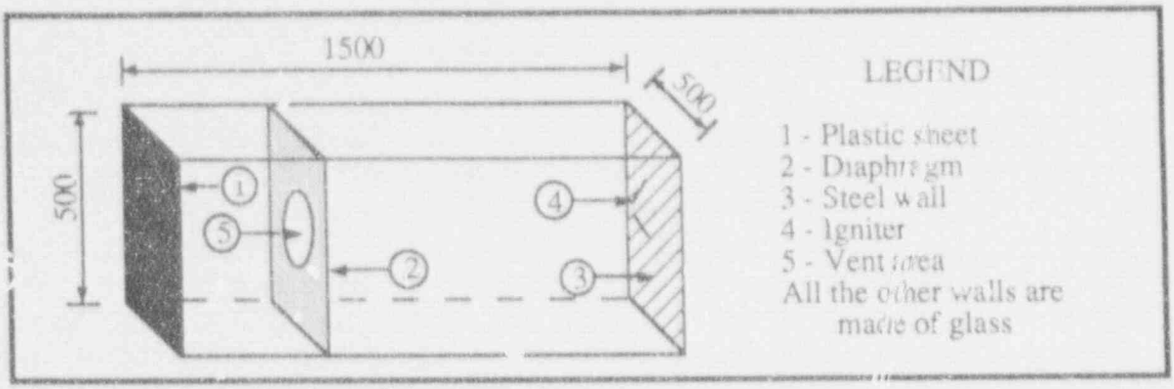


Figure 6. Schematic view of VIEW apparatus.

apparatus was designed for this purpose. Its vessel is a 0.4 $m^3$ paralielepiped with four of its walls made out of glass (Fig. 6). Since the hydrogen flame is not visible to the human eye, an aerosol is added to the gas mixture. The aerosol consists of an aqueous NaCl solution with 10 µm drops which makes the flame surface visible so that it may be videotaped. During one of the preliminary tests, a diaphragm with a 200 mm diameter circular opening was inserted in the vessel one meter from the spark igniter, in order to divide it into two compartments. Hydrogen concentration was about 10% in volume. Figure 7 shows four photographs taken during the tests. When the flame reaches the second chamber, the entire mixture catches fire almost immediately due to jet ignition. Although this research has only just begun, preliminary results suggest that this phenomenon may play a role in the pressurisation of the second chamber depending on the distance between the igniter and the aperture. For this reason, other tests have been planned which a larger apparatus (2 m long, squared base length 0.6 m) fitted with pressure and thermocouple transducers. The positions of the igniter and the diaphragm, the dimension of the diaphragm hole and the composition of the mixture will be varied inside the apparatus. To better evaluate the shape of the flame front and the volume occupied by the burnt gas, the transient will be videotape from above as well as from the front.

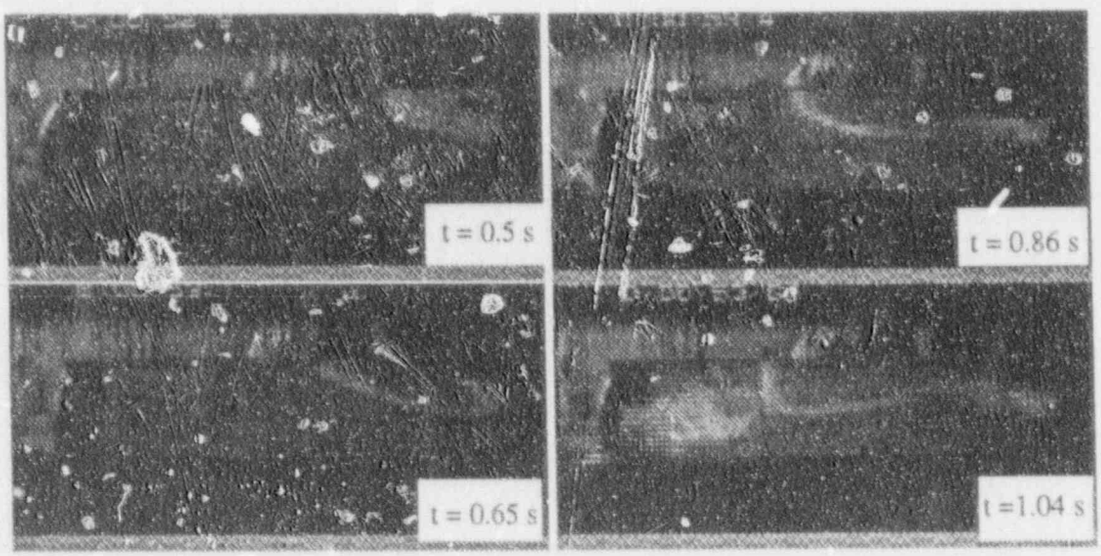


Figure 7. Test in the VIEW apparatus with diaphragm and hole of 200 mm.

## USEFUL CONCLUSIONS FOR PLACING THE IGNITERS IN THE SAFETY CONTAINMENT OF NUCLEAR PLANTS

Igniters were installed in some safety containment types of nuclear power plants. Igniters increase the potential for slow deflagrations since they are intended to induce combustion at low hydrogen concentrations. This would decrease the probability of fast deflagrations or detonations occurring at higher hydrogen concentrations. Igniters are also considered for installation in the advance type containments. The analysis of the experimental results from the preliminary phase of our research on compartimental containers carried out at DCMN Pisa, shows that overpressure in the compartments affected by the propagation of the flame depends on both the dimensions of the apertures and the relative position of igniters and apertures.
Overpressure is lower when igniters are placed above the venting apertures. An optimum distance was found between the igniter and the venting aperture. This probably depends on the ratio between the venting area and compartment volume and is related to the jet ignition phenomenon.

The DEVENT code is currently being upgraded in order to simulate the deflagration transient in communicating compartments with environments at variable pressures, which may be higher than that in the compartment where start the combustion. Future experiments planned in the HYDRO and VIEW apparatus should provide data and adequate basis to find some empirical relationships to be implemented in the code. This new work should describe the principal phenomenon and provide acceptable values for the combustion rate of the deflagration. The comparison with the experimental findings from other laboratories will be very useful to check for possible scale effects. When the code is validated we will be able to determine the optimum placement of igniters and compartment apertures of the safety containment in every possible case. Such a validated code can be used to identify, in each case, the optimum position of the igniters and the compartment apertures of the safety containments.


## Acknowledgements

While working on their theses, Pasquale Console and Fabio Del Giudice collaborated on experimental work with the HYDRO apparatus, and Giacomo Mezzetti collaborated on the drawing up the DEVENT code. We would particularly like to tank Giancarlo Giusti who helped us with the technical aspects of all the experimental research.

## Symbols

A characteristic surface of the vessel.
$A_v$ venting area.
$B_r$ volumetric combustion rate of burnt gas.
$C_d$ coefficient of venting resistance.
c speed of sound = $\sqrt{\frac{\gamma R T}{M}}$
$h_T$ molar enthalpy at temperature T.
M molecular weight.
n number of moles.
P pressure.
R constant of gases.
t time.
T temperature.
u internal molar energy.
V compartment volume.
x volume fraction occupied by burnt gas.
$\Delta h$ enthalpy variation in a constant temperature combustion when reactant and product moles are equal to the reaction's stoichiometric coefficients.
$\varepsilon$ ratio between the molar fraction of deficiency reactants in the unburnt gas and the corresponding reaction's stoichiometric coefficient.
$\eta$ pressure factor in the correlation of the venting flow rate.
$\gamma$ ratio between specific molar heat and pressure and constant volume of gas mixture.
$\nu$ difference between sums of product and reactant stoichiometric reaction coefficients.

## index

b burnt gas.
cr critical condition of venting.
e external environment.
f flame.
0 initial conditions.
r combustion reaction.
s standard conditions.
u unburnt gas.
v venting.

## References


[1] A.S.Geller , C.C.Wrong , A One Dimensional Material Transfer Model for HECTR version 1.8, SAND 88-0974, (August 1991).

[2] M. Carcassi, F. Fineschi, DEVENT, un codice per la valutazione dei transitori generati da deflagrazioni lente in ambienti parzialmente confinati, Dipartimento di costruzioni meccaniche e nucleari dell'Università di Pisa, RL 415 (1989).

[3] D. Bradley, A. Mitchetson, The Venting of Gaseous Explosions in Spherical Vessels. Theory, *Combustion and Flame*, 32 (1978).

[4] C. Chan, I.O. Moen, J.H.S. Lee, Influence of Confinement on Flame Acceleration Due to Repeated Obstacles, *Combustion and Flame*, 49 (1983).

[5] S. Chippett, Modeling of Vented Deflagrations, *Combustion and Flame*, 55 (1984).

[6] G.J. Van Wylen, R.E. Sonntag, *Fundamentals of Classical Thermodynamics*, John Wiley and sons, inc., New York (1976).

[7] S.G.I. Taylor, The Instability of Liquid Surfaces when Accelerated in a Direction Perpendicular to Their Planes, Proceedings of the Royal Society, vol. CCI (1950).

[8] G.H. Markstein, *Non-steady Flame Propagations*, Pergamon Press (1964).

[9] D.M. Solberg, J.A. Pappas, E. Skramstad, Observations of Flame Instabilities in Large Scale Vented Gas Explosion, Eighteenth Symposium (International) on Combustion (1981).

[10] J.H.S. Lee, Explosion in Vessels: Recent Results, *Plant/Operations Progress*, vol 2, n. 2, pp 84-89 (1983).

[11] T.F. Kanzleiter, K. Fischer, D. Wennerberg, Experimental Results and Modelling Strategies for Multi-compartment Hydrogen Deflagration, in *Hydrogen Behaviour and Mitigation in Water-cooled Nuclear Power reactor*, Ed. E. Della Loggia, EUR 14039 en, ISSN 1018-5593, pp. 141-150 (1992)

[12] M. Carcassi, Semi-Empirical Correlations for the Burning Velocity of Hydrogen-Air Vented Deflagrations, Proceedings of the 2nd Int. Conference on Containment Design and Operation, Toronto, Canada, October 14-17 (1990).

[13] M. Carcassi, S. Lanza, Velocità di bruciamento turbolenta. Confronto tra i risultati in grande, media e piccola scala, Atti del IX Congresso UIT, Pisa, Italy, 13-14 giugno, 1991, pp 223-234 (1991).

[14] M. Carcassi, F. Fineschi, 1ª e 2ª serie di deflagrazioni di idrogeno-aria nel contenitore HYDRO-SH con intervento di un sistema di sfiato, Dipartimento di costruzioni meccaniche e nucleari dell'Università di Pisa, RL 512 (1991).

[15] M. Carcassi, F. Carnasciali, F. Fineschi, P.L. Ficara, G. Lombardi, L'apparecchiatura HYDRO per lo studio delle deflagrazioni di gas infiammabili in contenitori chiusi, *Notiziario dell'ENEA Energia e Innovazione*, pp. 54-70 (Maggio 1989).

[16] M. Carcassi, F. Fineschi, G. Lombardi, Air-Hydrogen Deflagration Tests at University of Pisa, *Nuclear Engineering and Design*, vol. 104 , pp. 241-247 (1987).

# STUDIES ON ALWR's CONTAINMENT SYSTEM PENETRATION

Franco Mantega
CISE-Segrate(MI)-Italy

Enrico Penno
CISE-Segrate(MI)-Italy

Paolo Vanini
ENEL/DSR/VDN-Roma-Italy

## ABSTRACT

The reduction of the radioactive release during the Severe Accident can be achieved by improving some precise plant requirements, among which the Containment leaktightness to the environment. One of the critical points of this matter is due to the Containment penetrations.
The SANDIA/NUREG experience on the Callaway-2 Personnel Airlock showed good behaviour of the whole component as for pressure and, in some way, temperature. Starting from this experience studies are in progress in order to explore the possibility of realizing a mitigation of the thermal load of the elastomered sealing area of both Personnel Airlocks and Equipment Hatches during a long-term Severe Accident.
These studies, performed on one of the ALWR design concept, also regard the mechanical and thermal stress behaviours of these components as integrate (consequences of Containment deformations and radiation damages of the elastomers). On the basis of the currently used elastomers, the paper deals with new arrangements to passively improve the component performances in case of Severe Accident conditions. Calculations performed on a Personnel Airlock show that it can be possible to assure less than 170 °C of the outer door temperature and 355 °C at the inner door while the Containment temperature would be more than 450 °C by passively improving heat dissipation and thermal insulation . About the Equipment Hatch which, because of its position, represents the weak point of the whole Containment barrier it is worth noticing that the double-seal arrangement does not represent a redundant feature due to the closeness of the two gaskets. Modifications of this component are being studied to give rise to an independent sealing area far enough from the main one to assure milder radiation and thermal conditions for the elastomer even in a Severe Accident scenario. An experimental campaign is expeted to be performed in the future on a Personnel Airlock in a cancelled Power Station.

## PURPOSE OF THE WORK

A significant discussion has taken place in the scientific community in the last years on the subject of Containment performance for the nuclear plants of the new generation.
It is growing opinion that the new Containment performance shall be based upon the definite target of environmental impact limitation. The Italian design target is to reduce the environmental impact in case of any reasonably conceivable accidental event including Severe Accidents and related phenomenologies, so as to require no reliance on the success of the off-site emergency response procedures for the protection of the population health.
To attain this target it is necessary to improve the current plant design in order to comply with the technical requirements and with the "what if" beyond the plant design performances.
To do this it is necessary, about Containment, to provide a design able to:

- assure a stringent design leak-rate for any conceivable accidents, long term Severe

Accident included,

- solve Containment bypass issues (interfacing system LOCA, multiple tube rupture, isolation function improvements, etc.),
- improve the plant system design in order to be sure about the Containment leak-rate in any moment in which an accident may occur (e.g., by means of a continuous leakage monitoring system).

About the first item, due to the ALWR design philosophy allows a considerably reduction of mechanical and electrical penetrations and the current technology provides zero-leakage electrical penetrations, the most critical issue regarding the isolation device involves the Personnel Airlock and the Equipment Hatch (this paper does not report a study carried out on isolation valves of Heating Ventilation and Air Conditioning HVAC systems).

These are critical components because they are [1,2,3]:

- potential main contributors to the total Containment leak-rate in Severe Accident conditions,
- a potential direct path between the Containment atmosphere and the environment,
- a weak point because their tightness is trusted to organic materials that are susceptible of aging, thermal and radiation damages.

The purpose of ENEL/CISE studies is to develop the criteria and conceptual design for Personnel Airlocks, Equipment Hatches in order to solve the problem according to the new target for the future nuclear plants.

## APPROACH TO THE PROBLEM

The studies (started in 1990) considered events slightly beyond the current Severe Accident [4,5,6] in order to avoid unrealistic situations involving too heavy design requirements.

This approach was modified, as described below, after reading the SANDIA/NUREG report that describes the test carried out on a Personnel Airlock of the cancelled Callaway-2 Plant (that was originally designed for a .41 MPa pressure and 170 °C temperature) [7].

The conclusions of this test program were:

- although the gaskets were degraded by an accelerated aging process, simulating both heat and radiation damages, no leakage in the inner airlock door occurred during all tests at quite a high temperature and a very high pressure,
- failures in the gasket seal was related to temperature beyond the degradation temperature of EPDM E603 (approximately 330 °C),
- the gasket expanded while increasing temperature causing significant upward deflection of the door and resulting in larger gaps between the inner door and bulkhead,
- the Personnel Airlock survived 2.07 MPa internal pressurization at 427°C; in spite of these heavy conditions the structure remained in the elastic range,
- the outer door at 2.07 MPa did not leak because of its low temperature (below 100 °C).

The examination of the above results leads to these following remarks:

- the failure of the inner door gaskets must not cause temperature increase at the outer door owing to the metal-to-metal contact between the inner door and its bulkhead; even if the gaskets were completely destroyed, the metal-to-metal contact would provide a strong resistance to the gas circulation,
- heat transfer conditions of the structure have an important effect on the temperature distribution. The outer door temperature and consequently the Airlock isolation function

depend on this heat transfer.

These considerations led to a change in the approach: instead of assuming as input data the Severe Accident temperature values (whose validity is often under updating) the Personnel Airlock design value was taken as the maximum acceptable temperature value of the outer door. Starting from this point, calculations are underway to verify the gain in term of thermal mitigation produced by the improvements, such as thermal insulations and passive heat dissipation (whose passivity ranges in the No.2 Category [8]). The same approach was adopted for the Equipment Hatch. In this case it was necessary to design a modification of the component in order to realize a second (or back-up) seal area at a temperature not far from the design one even if in long-term Severe Accident conditions. As for the Personnel Airlock these results were achieved by means of thermal insulation panels and a passive heat dissipation system.

## DESCRIPTION OF THE IMPROVEMENTS

### Personnel Airlock

The improvements studied for this component have to fulfil the following requirements in order to :

- avoid any structural modification of the component
- realize both insulation shielding and dissipation featuring for a life of 60 years
- perform the heat dissipation in a strictly passive way
- perform the heat dissipation system for all kinds of layouts.

Fig. 1 shows a scheme of an improved Airlock in the hypothesis of a lay-out allowing good natural air circulation outside of Containment (the last generation French PWRs,for instance). The finned surface may help increasing the dissipation.

Fig. 2 shows the same improved component realized by a floodable annulus welded on the cylindrical surface outside the containment. Two suitable pipes link the annulus to a storage tank arranged outside the containment and filled with water. The heat dissipation of this loop can be obtained, in a passive way, by natural air exchange or evaporation or both of them.

The portion of component inside the containment (cylindrical part, bulkhead and door surfaces) is insulated by means of suitable panels that fill any free space, as for instance the space between the stiffenings. These panels must be realized in such a way as to avoid their contaminations and performances losses especially in case of shocks, during the plant life. In the same way the inner surfaces (door and bulkhead) of the portion outside the containment is to be covered with insulating and reflecting panels.

### Equipment Hatch

The improvements to apply to this component were studied in order to :

- realize both the insulation shields and the dissipation area for a life of 60 years
- perform the heat dissipation system in a strictly passive way
- perform the heat dissipation for all kinds of layouts
- minimize the structural modifications of the component.

Fig. 3 shows a scheme of a modified Hatch thus extending the component toward the environment,involving a modification of its handling operations (sometimes there is no room to

allow this movement), in the hypothesis of a good natural air convection layout (as in the French last generation PWRs).
Fig. 4 shows the same improved component realized by means of a floodable annulus welded to the flange between the two seal areas. This annulus must be linked to a suitable tank as for the personnel airlock.
Fig. 5 shows the component with an extension toward its centerline that allows a Hatch handling quite similar to the current ones but with a consequent increase in the component diameter.
Fig. 6 shows the same Hatch as fig. 5 with the floodable annulus.
The portions of the component inside the containment of both the solutions,i.e., Hatch, flange (welded to the containment wall) and a suitable part of the wall around the flange should be thermally insulated by means of proper panels, as for the Personnel Airlock.

## RESULTS OF CALCULATIONS

### Personnel Airlock

The first improvement studied was a passive heat dissipation system to be installed on the portion of the Airlock outside the Containment. Some calculations were made on the Airlock as designed and built in order to verify the rate of heat dissipated by this outer portion of the component under the assumption of a good natural air replacement. The temperature inside the Containment was supposed at 350°C with a dissipation rate outside the Containment of 10.5 kJ/m$^2$ h°C from the cylindrical surface which is some tens of m$^2$ wide and 13.8 kj/m$^2$ h°C from the bulkhead and door surface which is more than 7 m$^2$ wide.
The calculations show a temperature distribution as reported in Fig. 7 in which the inner door is supposed at 350°C, as the Containment atmosphere, and the outer door turns out to be 201°C.
Although the assumed dissipation rate is not very high, the plant layout does not, in some cases, allow such an exchange rate because of the configuration of the room where the outside portion of the Airlock is housed.
For this reason a dissipation system based on a completely passive water loop under the assumption of a boiling mode heat transfer was studied, while neglecting any possibility of air and radiation exchanges.
A second run of calculations takes into account the above mentioned water system and the thermal insulation of the bulkhead area and the cylindrical portion of the Airlock inside the Containment. The insulation of the cylindrical portion is a quite an easy problem, whereas the bulkhead area and the door involve more difficulties because of the presence of stiffenings and some other electrical and mechanical components.
The insulation panels were supposed made of a poor material, 50 mm thick (0.4 kj/m h °C), canned by suitable antishock and anticontamination liners. Studies are in progress with the goal of representing a true situation, at the present stage of the study it was supposed that the insulated portion of the bulkhead surface would be no more than 80 %.
In this condition, with a temperature of the Containment atmosphere of 350 °C,the inner door would be at 277 °C and the outer door at 175 °C, see fig. 8.
A third run of calculations is based again on the water dissipation system and the thermal shielding of the inner surface of the outer door only. At this stage, the calculations take into account only a roughly reflection contribution of these inner shielding panels.
In this condition, with a temperature of the inner door at the same value as the Containment

atmosphere, i.e. 350°C, the outer door turns out to be 167 °C see fig. 9.
A fourth run of calculations take into account the above mentioned three solutions all together and are based on the same heat transfer outside the Containment and the same Containment temperature (350°C).
By means of this configuration the temperature of the inner door is 277 °C while the outer door temperature would be no more than 145 °C, see fig. 10.
The last run of calculations are practically the same as the fourth one but with an important difference about temperature inputs. As a matter of fact, the design temperature of the outer door (outside the Containment), i.e. 170 °C, was assumed instead of the containment temperature at the inner door.
In this conditions the inner door would be at 355 °C but with the Containment atmosphere temperature at about 450 °C, see fig. 11.
Some simple calculations were made to know the volume of the tank linked to the floodable annulus around the outside portion of the Airlock when the Containment temperature is 350 °C and the Airlock is equipped with the above mentioned solutions. Even in case of evaporation only, less than 6 $m^3$ of water would be necessary for the "72 hours grace period" imposed by EPRI.
Structural calculations, although important, were not made on this component, because the conclusion of the program is expected in the spring 1993. It is worth to note that all the solutions do not imply structural modifications and the SANDIA/NUREG tests give encouraging results about the mechanical behaviour.

Equipment Hatch

A structural modification of the component is necessary to obtain a back-up seal area. For this reason calculations were made both on the thermal and structural behaviours. Some runs of calculations were performed in the aim of getting a reasonable compromise among thermal mitigation, dimensions of the modified component and acceptable stresses on materials.
The first run of calculations deal with the two proposed solutions, see figs. 3 and 5 again, without any insulating material inside the Containment and with natural air exchange with the environment according to the IAEA passive category No 1 [8].
In these conditions the temperature of the backup seal area is 220 and 225 °C, respectively, for the two proposed solutions while the temperature inside the Containment is 350 °C, see Figs. 12 and 13.
The air temperature outside the Containment is supposed to be 50 °C because of the hot air rising from the lower surfaces of the Containment. The heat transfer convection coefficient is assumed to be 6.3 kj/ $m^2$ h °C.
Figs. 14 and 15 show the temperature distributions of the two different design solutions with the inner area of the flange protected by an insulating ring and air cooled. The Containment temperature is 350 °C. The backup seal area temperature is 140 and 180 °C for the solutions described in Figs. 3 and 5, respectively.
As for the Airlock, a dissipation system based on a completely passive water loop under the assumption of a boiling mode heat transfer was studied. The insulation protection around the backup seal area, while preventing any possibility of dissipation by air, realizes an effective protection against the heat radiation flow coming from the Containment surfaces.
Figs. 16 and 17 show the behaviours of the two different design solutions with the flange inside

the Containment protected by the insulating ring, the annulus flooded by boiling water and the external surface of the backup seal area properly insulated. The Containment temperature is 350 °C. The backup seal area temperature is 106 and 120 °C for the solutions described in Figs. 2 and 4 respectively.
In the last two configurations the water evaporated during the "72 hours grace period" would be about 10 and 31 $m^3$ for solutions described in Figs. 2 and 4 respectively.
Calculations on the Containment temperature value, in the assumption of the backup sealing area at 170 °C (design value), were not performed because the closeness between the seal area and the floodable annulus does not involve important temperature increases even in the case of Containment temperatures largely beyond the Severe Accident ones. The higher heat flow through the structure obviously needs a greater rate of evaporated water. Calculations dealing with the mechanical behaviour of the Hatch under a value arbitrarily assumed as Severe Accident conditions are in progress.
Fig. 18 shows the deformations of the Equipment Hatch flange in these conditions.
Fig. 19 shows the Finite Element Model of a Large Dry Containment; the load conditions are supposed to be at 350 °C wall temperature and 0.5 MPa pressure.
Fig. 20 shows the Finite Element Model of the toward outside solution (see Fig. 4). The maximum local stress is 360 MPa, see Fig. 21.
Fig. 22 shows the Finite Element Model of the toward centerline solution (see Fig. 6). The maximum local stress is 290 MPa, see Fig 23.

## RADIATION DAMAGE OF GASKETS

Calculations are in progress. A rough evaluation by means of the Origen-2, on the assumption of 100% noble gases, 100% volatile fission products, 50% non-volatile fission products released from the core, has given encouraging results. As a matter of fact, the gaskets of the outer door of the Airlock would integrate $1x10^8$ rad in some months in case the gaskets of the inner door would fail, thanks to the metal-to-metal contact between door and bulkhead, see Fig 24.
The backup seal gaskets of the Equipment Hatch would integrate the same value in a longer time (in this case, the failure of the main seal gaskets is less important).

## CONCLUSIONS

Starting from the considerations that the next generation of nuclear power plants must have a higher Safety level in comparison with the present generation, the concept of the "Defence in Depth" has to be taken into account where possible, namely for all the critical points of the Containment.
Although the elastomer behaviours have been deeply improved and many other Penetrations have now good performances, the geometries of both Airlocks and Hatches have had little variations during the last decades.
For this reason it seems to be necessary to increase the level of the "Defence in Depth" of the Equipment Hatches as the Airlocks in which a second (or backup) seal area is present.
A second seal (or backup) area must have milder accident conditions to be effective.
The realization of all the described mitigation solutions seems to be simple, effective and safe for both Airlocks and Hatches.
The on going calculations show that it is possible to give quite a longer life to the second (or

backup) seal areas and a higher possibility to the first (or main) seal areas of surviving in conditions even beyond the Severe Accident ones and for a long time. A test programme is planning for 1993 on an actual Personnel Airlock in a cancelled ENEL Power Station and might be considered as the ideal continuation of the SANDIA/NUREG experience.

REFERENCES


1. L.N. Koenig, C.V. Subramanian, Leakage Potential of LWR Containment Penetrations under Severe Accident Conditions", Nuclear Engineering and Design 100, 1987.

2. T.L.Bridges, " Determination of Containment Large Opening Penetration Leakage During Severe Accident Conditions", NUREG/CP-0056, November 1984

3. T.L.Bridges, " Containment Penetration Elastomer Seal Leak Rate Tests",NUREG/CR-4944, July 1987.

4. "Utility Requirement Document" Vol. 3, EPRI.

5. D.E. Leaver et al. "Passive ALWR Source Term", EPRI; February 1991.

6. "Severe Accident Risks: An Assessment for Five U.S. Nuclear Power Plants", NUREG-1150, June 1989.

7. J.T.Julien, S.W.Peters,"Leak and Structural Test of Personnel Airlock for LWR Containments Subjected to Pressures and Temperatures Beyond Design Limits",NUREG/SANDIA-5118,SAND 88-7155, May 1989.

8. "Working Paper on Safety Related Terms", IAEA, Wien, October 1988.

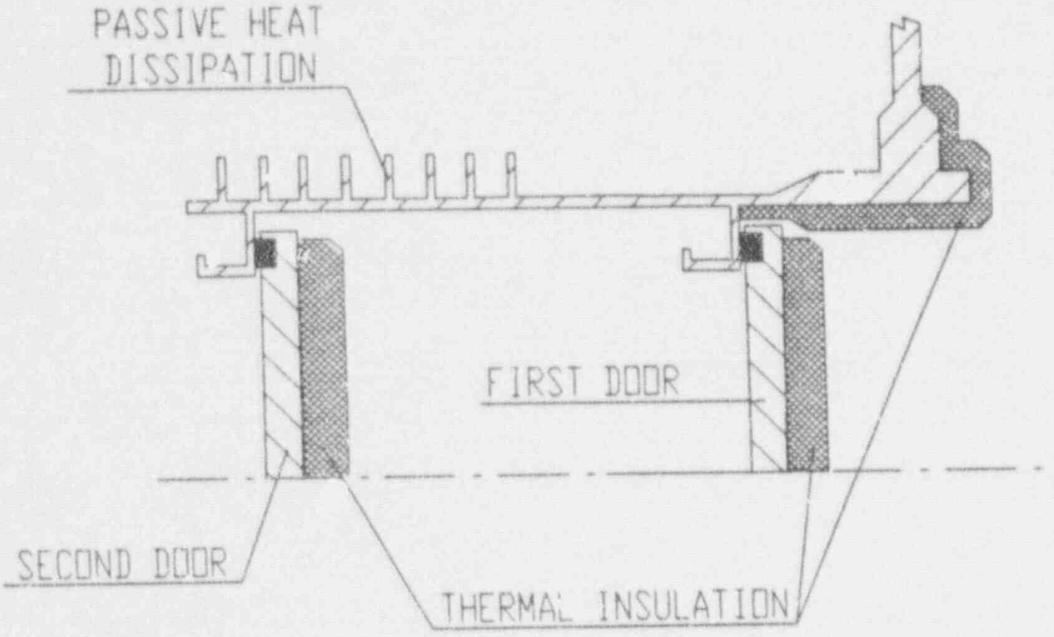


Figure 1. Air Exchange (Finned) Airlock

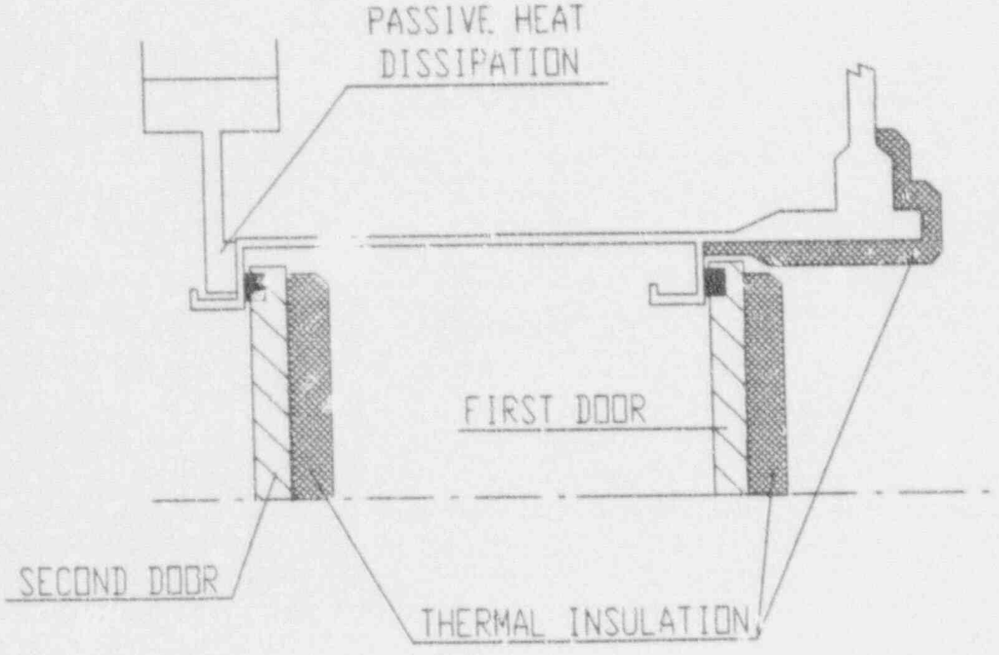


Figure 2. Floodable Annulus Airlock

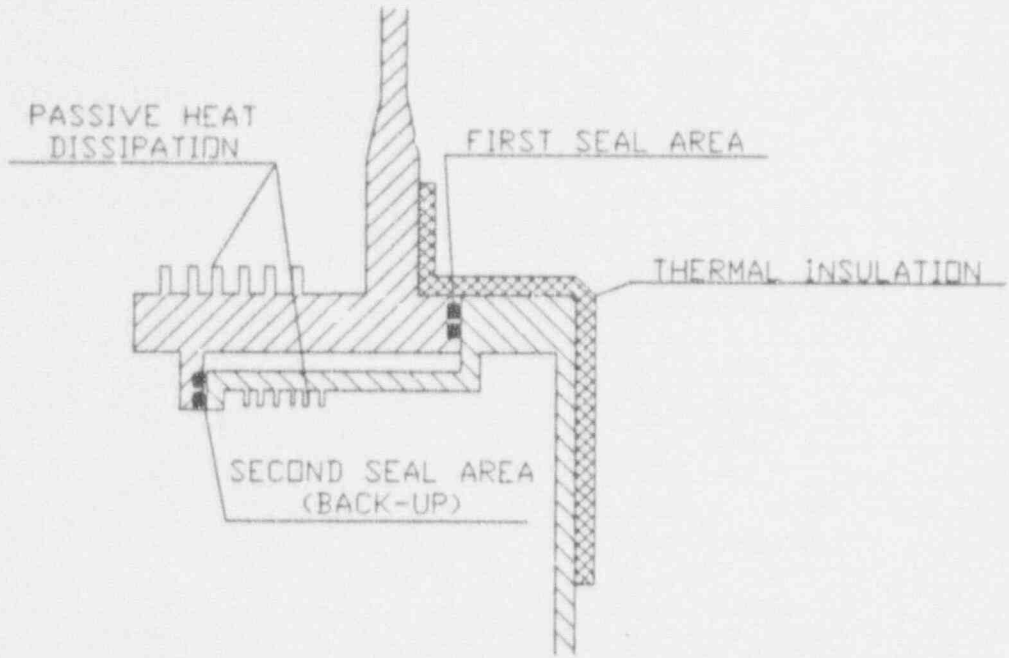


Figure 3. Toward Outside Double Seal Hatch, Air Exchange

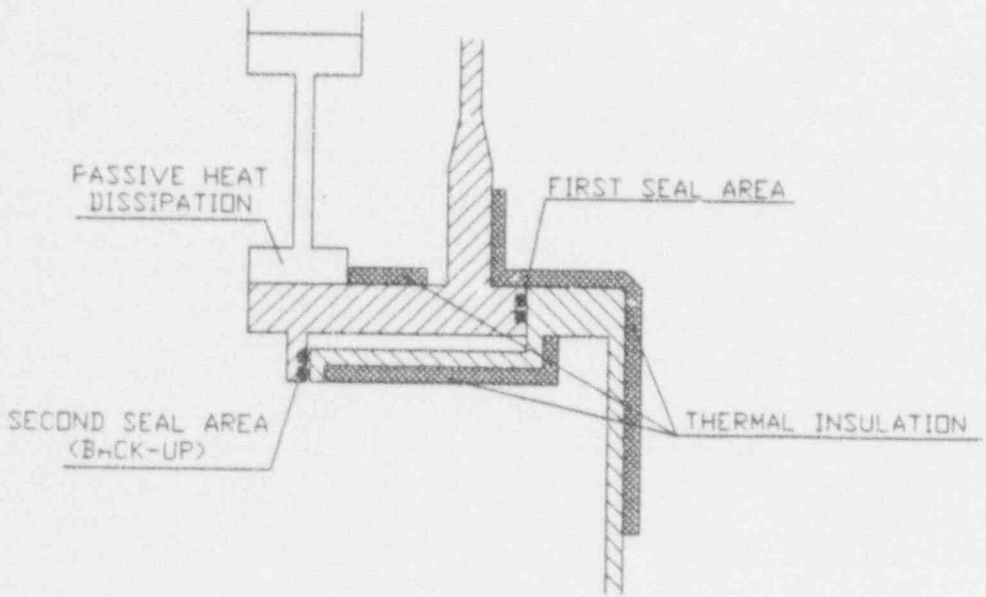


Figure 4. Toward Outside Double Seal Hatch, Floodable Annulus

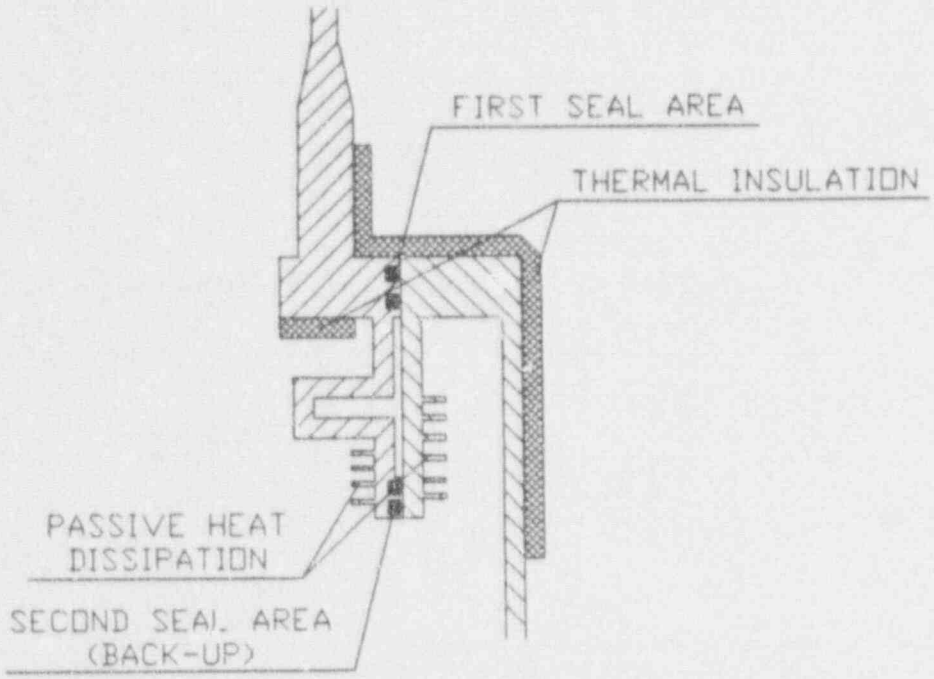


Figure 5. Toward Centerline Double seal Hatch, Air Exchange

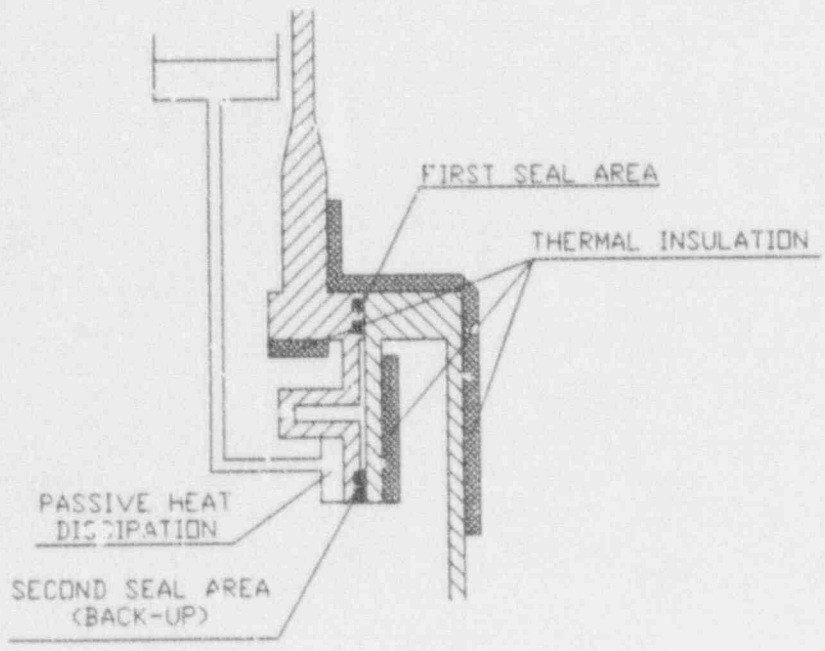


Figure 6. Toward Centerline Double Seal Hatch, floodable Annulus

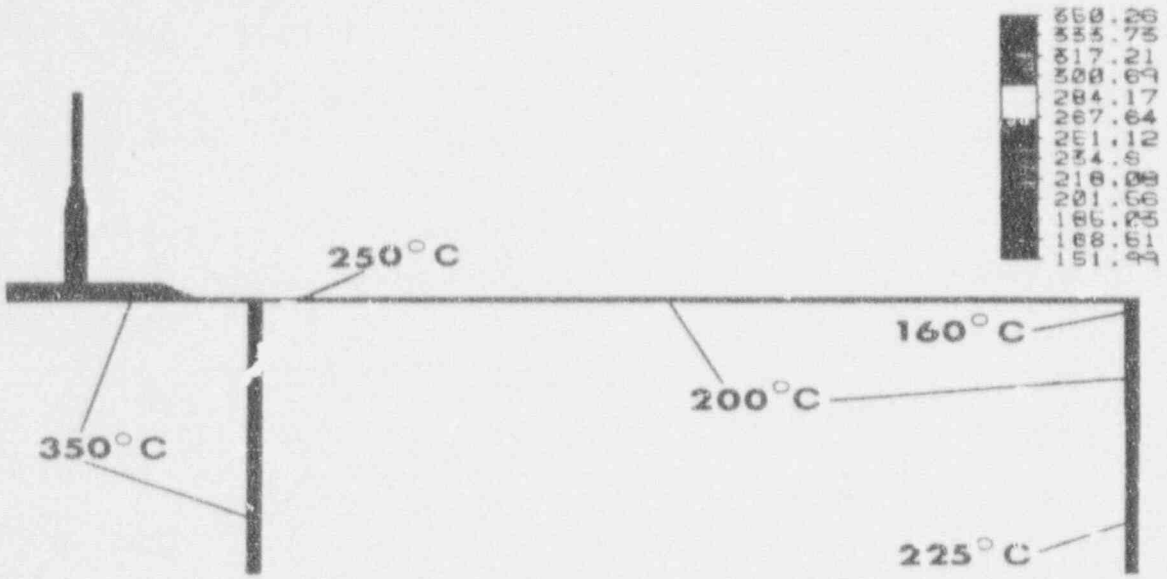


Figure 7. Airlock at 350 °C, no Insulation, Air Cooled

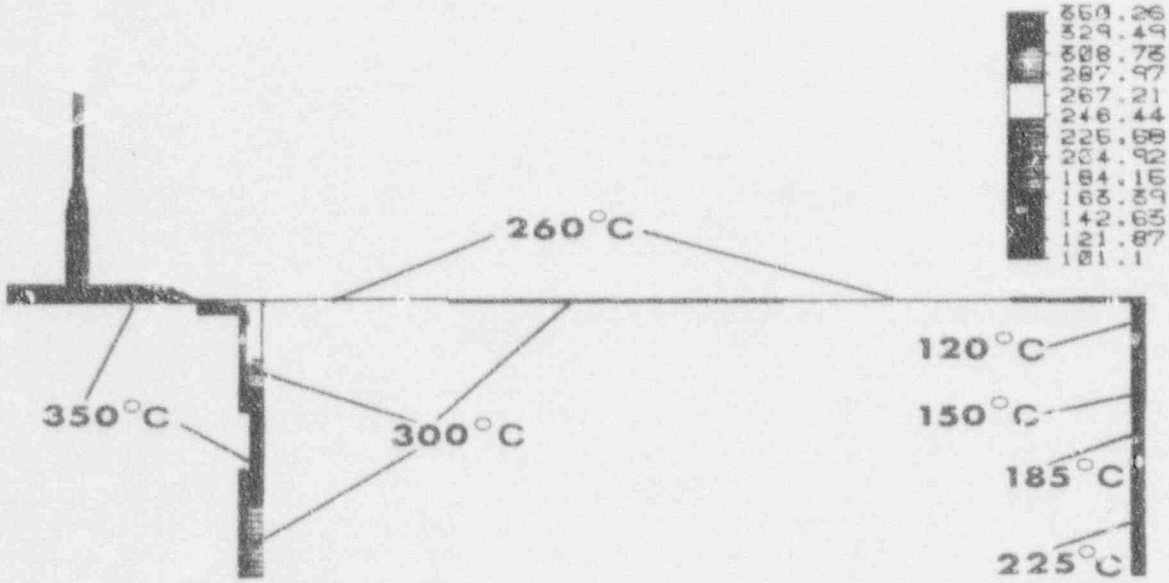


Figure 8. Airlock at 350 °C, Inner Surface Insulated Flooded Annulus

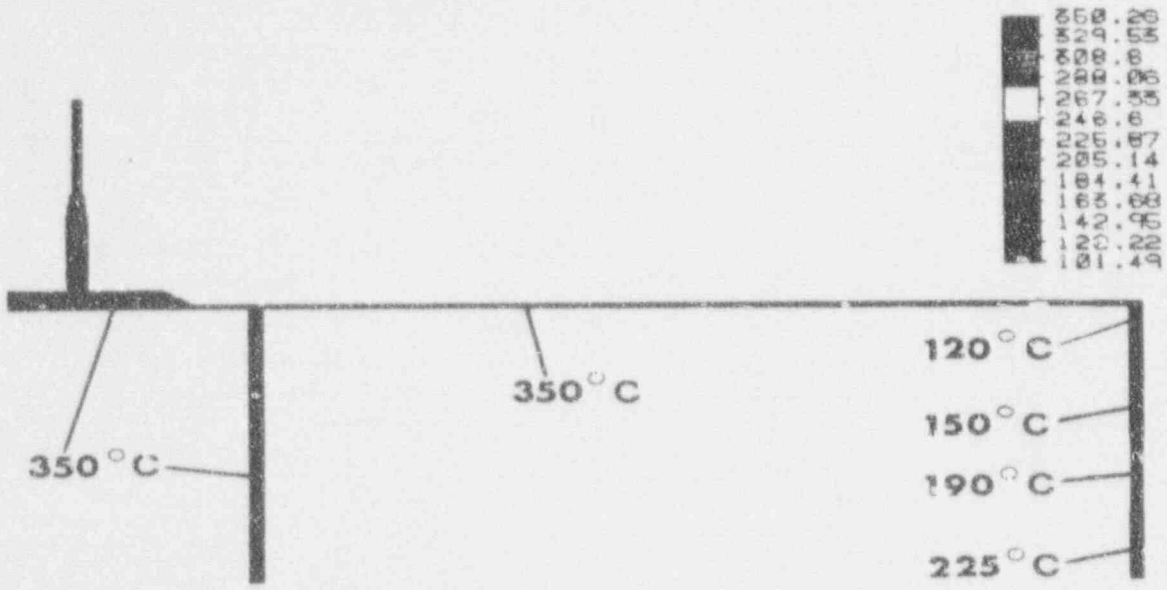


Figure 9. Airlock at 350 °C, Outer Door Thermally Shielded, Flooded Annulus

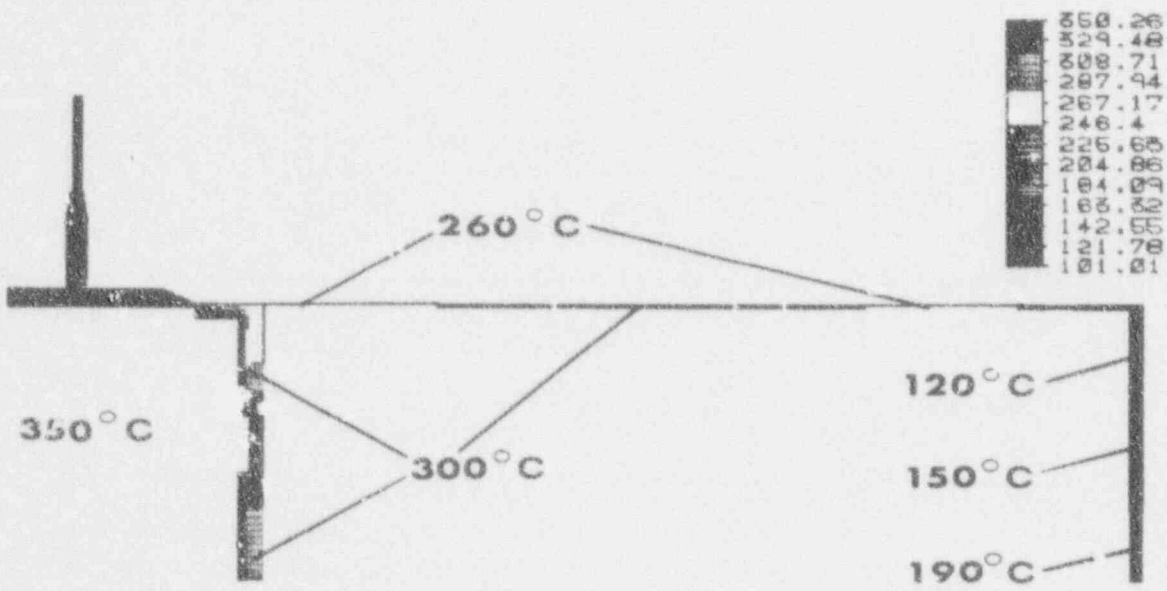


Figure 10. Airlock at 350 °C, Insulated and Shielded, Flooded Annulus

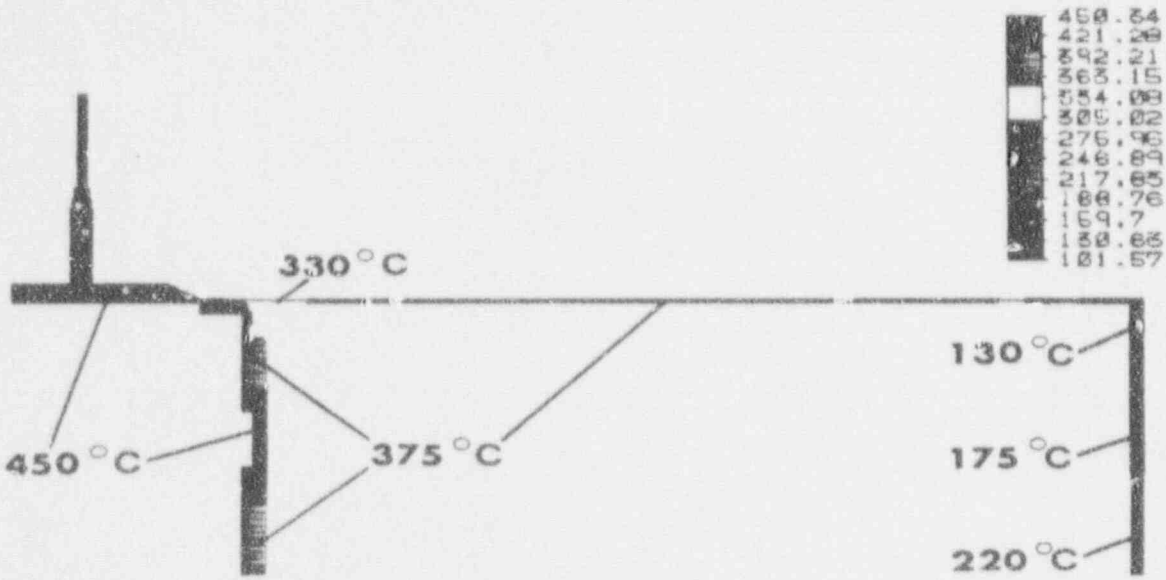


Figure 11. Outer Airlock Door at 170 °C, Insulated and Shielded, Flooded Annulus

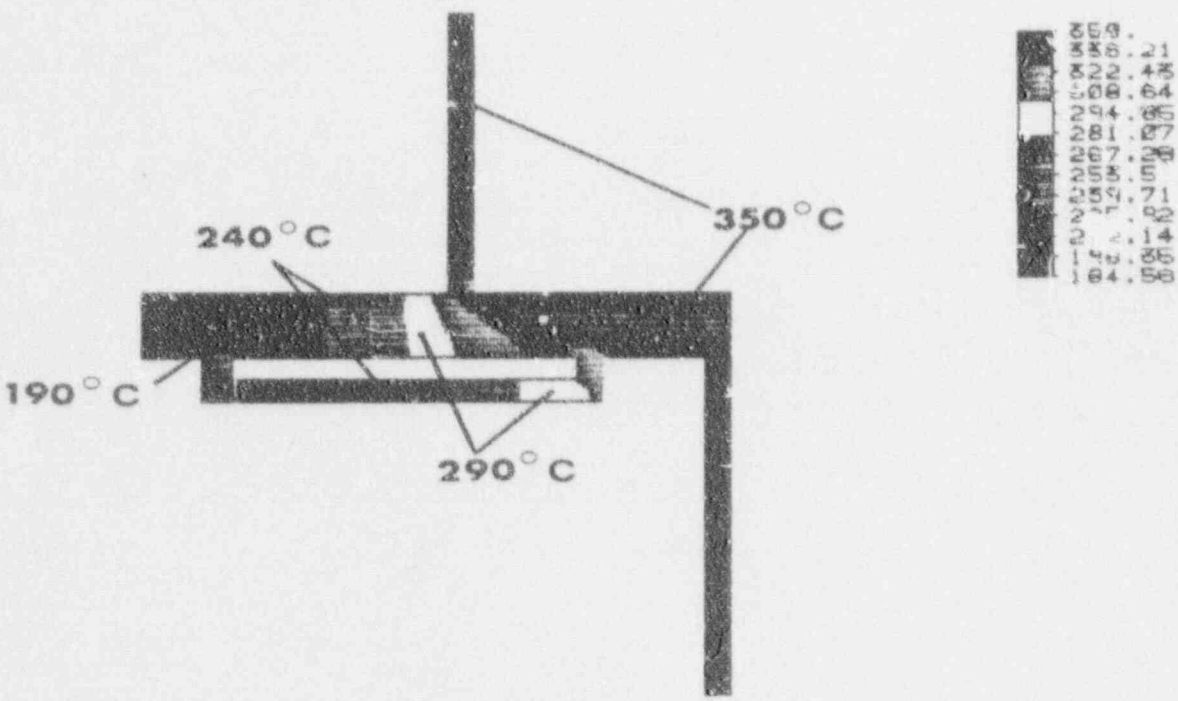


Figure 12. Temperature Distribution of the Toward-Outside Modified Hatch at 350 °C, no Insulation, Air Cooled

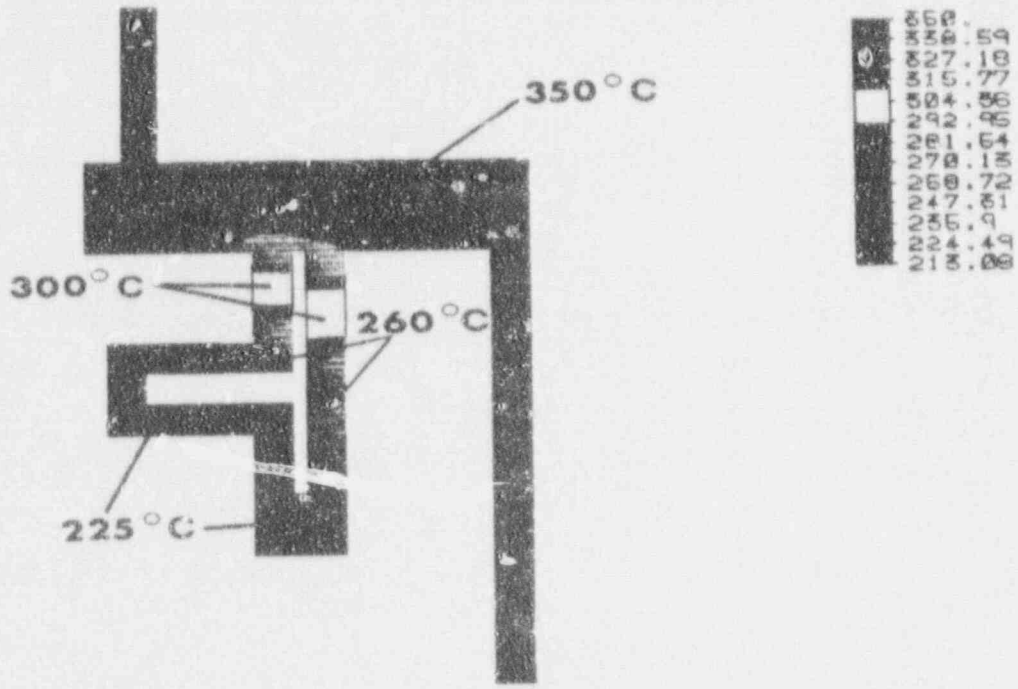


Figure 13. Temperature Distribution of the Toward-Centerline Modified Hatch at 350 °C, no Insulation, Air Cooled

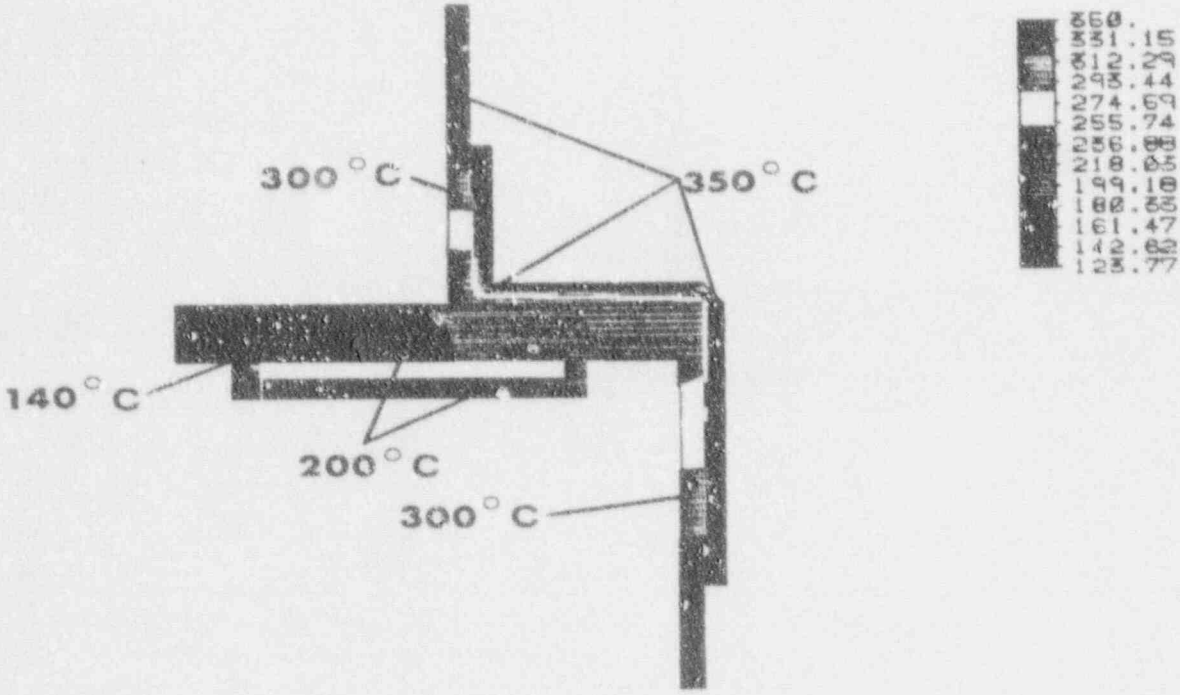


Figure 14. Temperature Distribution of the Toward-Outside Modified Hatch at 350 °C, Insulated, Air Cooled

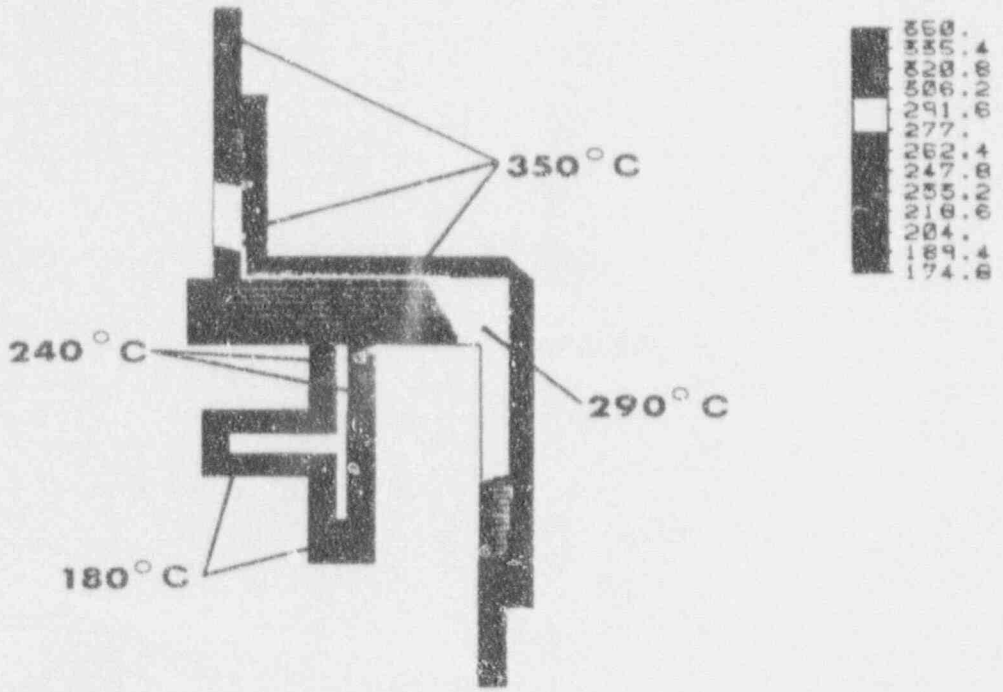


Figure 15. Temperature Distribution of the Toward-Centerline Modified Hatch at 350 °C, Insulated, Air Cooled

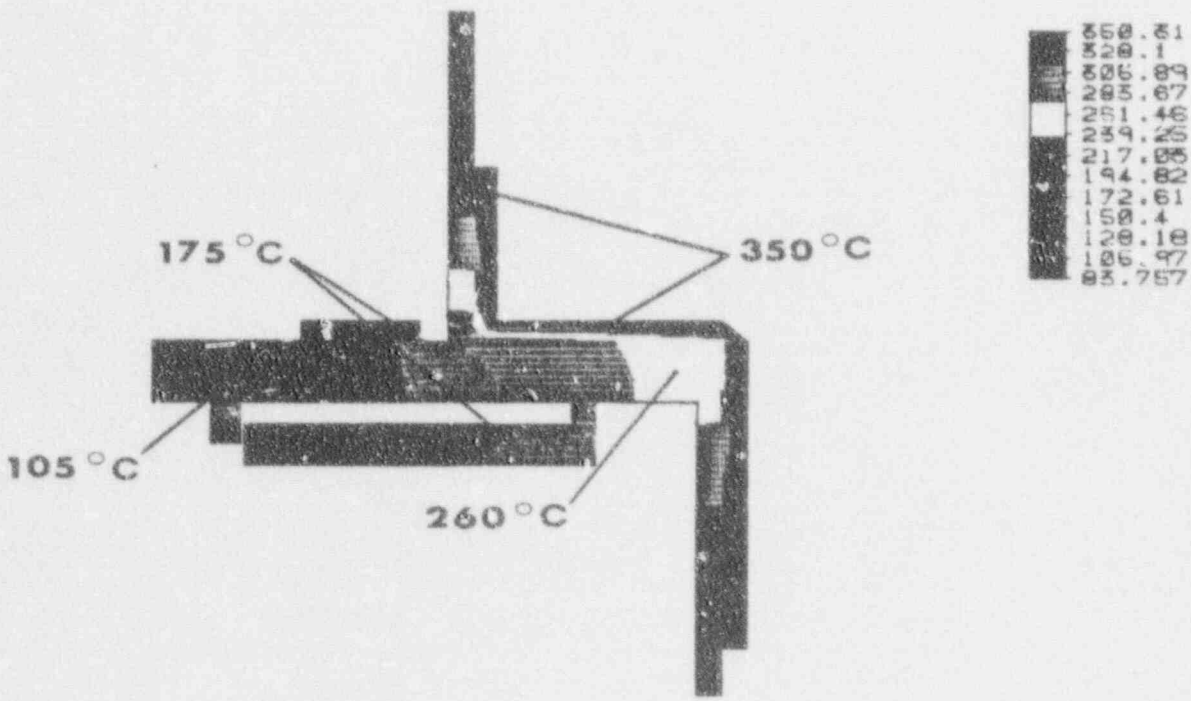


Figure 16. Temperature Distribution of the Toward-Outside Modified Hatch at 350 °C, Insulated, Flooded Annulus

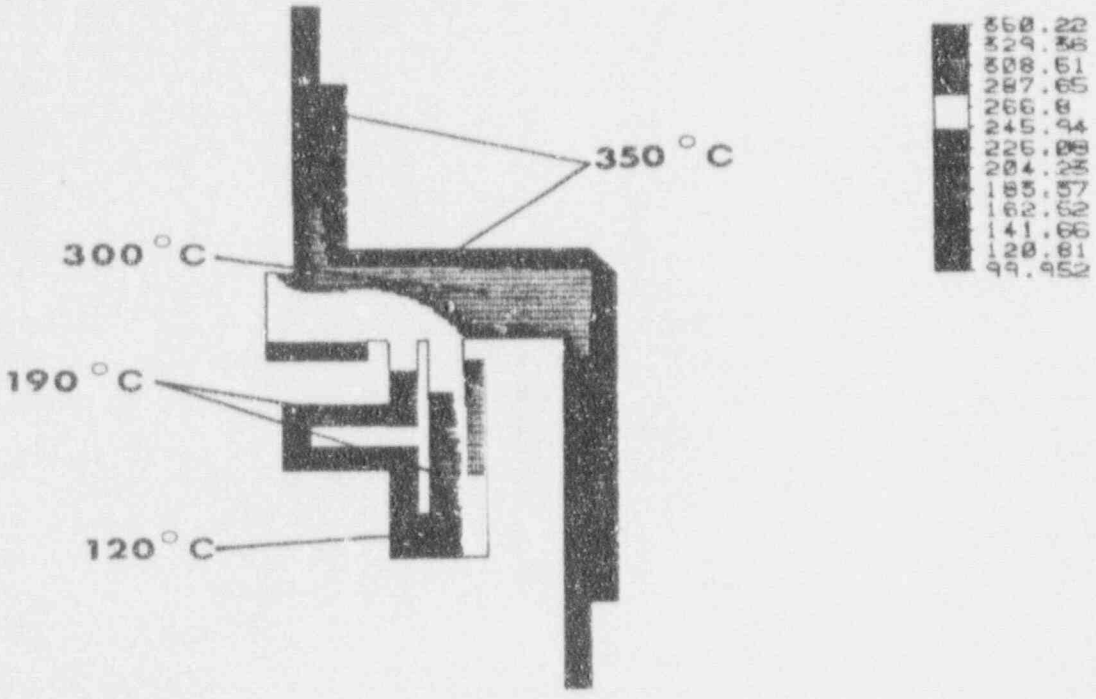


Figure 17. Temperature Distribution of the Toward-Centerline Modified Hatch at 350 °C,Insulated, Flooded Annulus

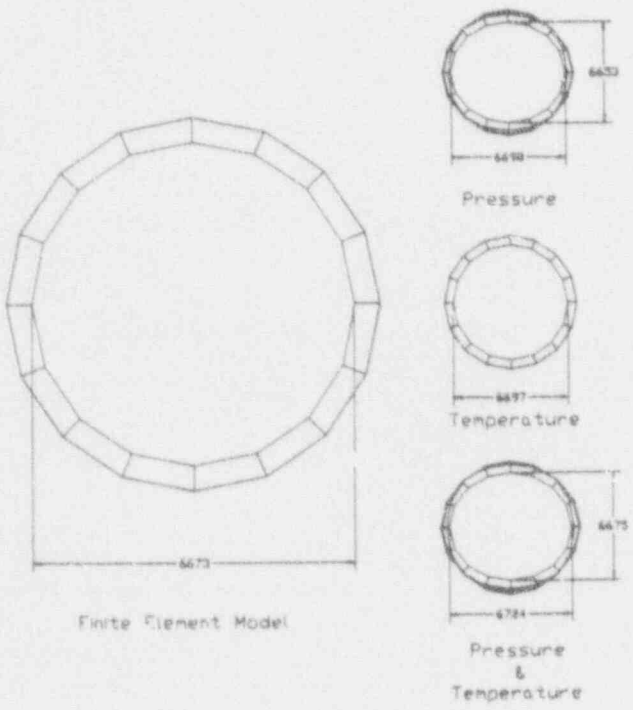


Figure 18. Deformations at 0.5 MPa and 300 °C of ΔT of a Large Dry Containment

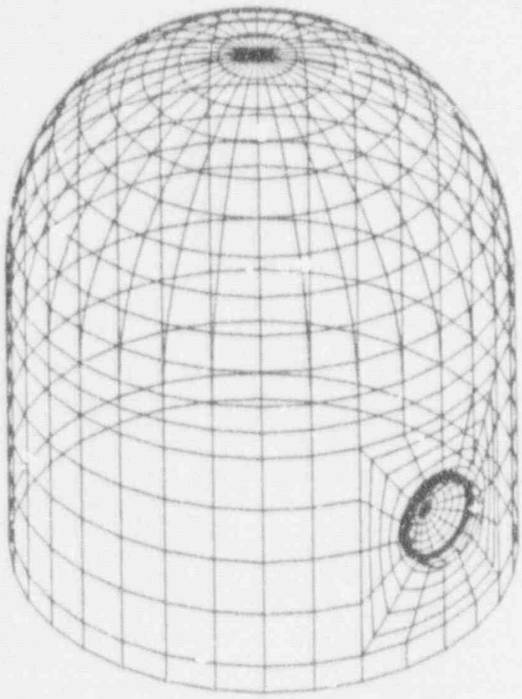

Figure 19. Finite-Element Model of a Large Dry Containment

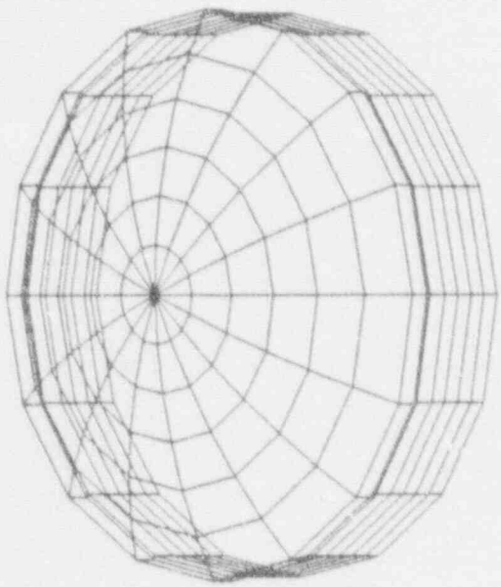

Figure 20. Toward-Outside Modified Hatch Finite Element Model

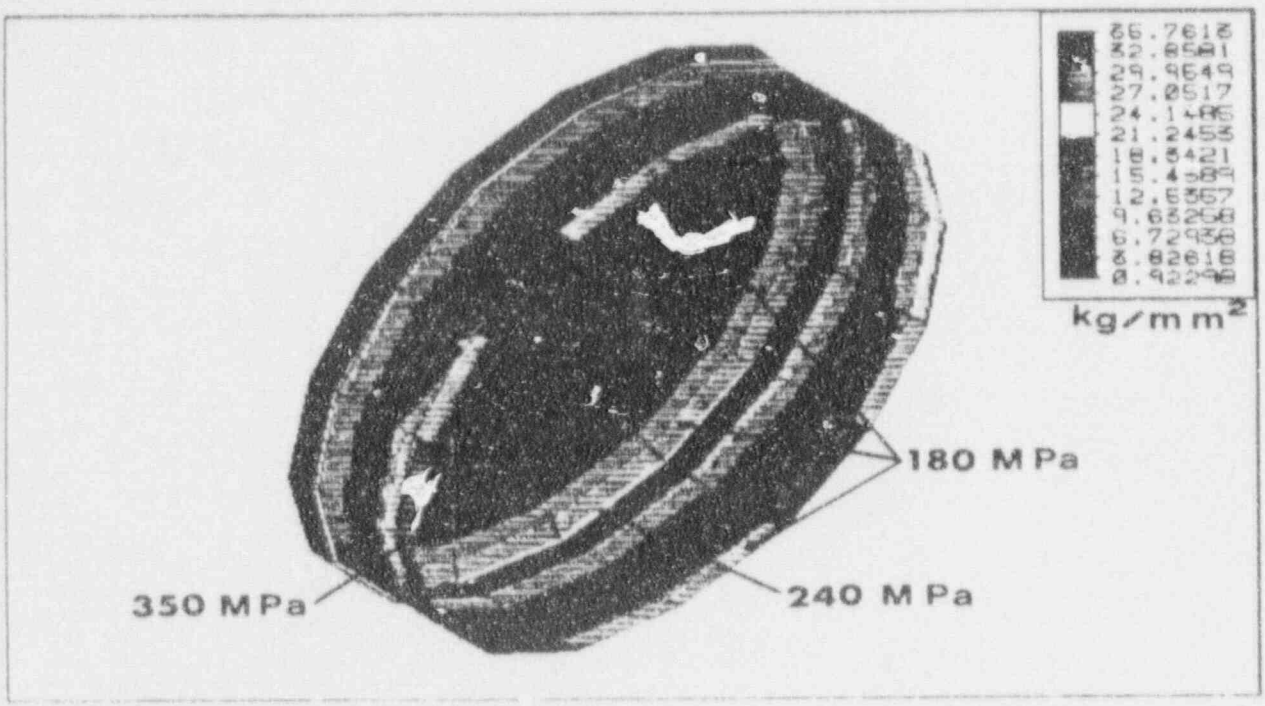


Figure 21. Stress Distribution on the Toward-Outside Modified Hatch

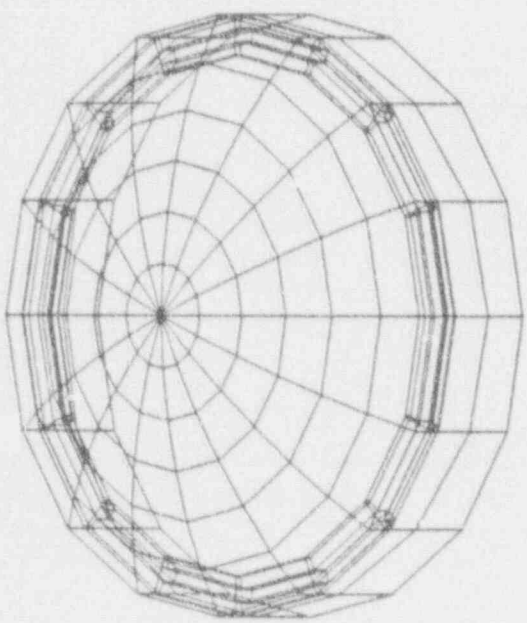

Figure 22. Toward-Centerline Modified Hatch Finite-Element model

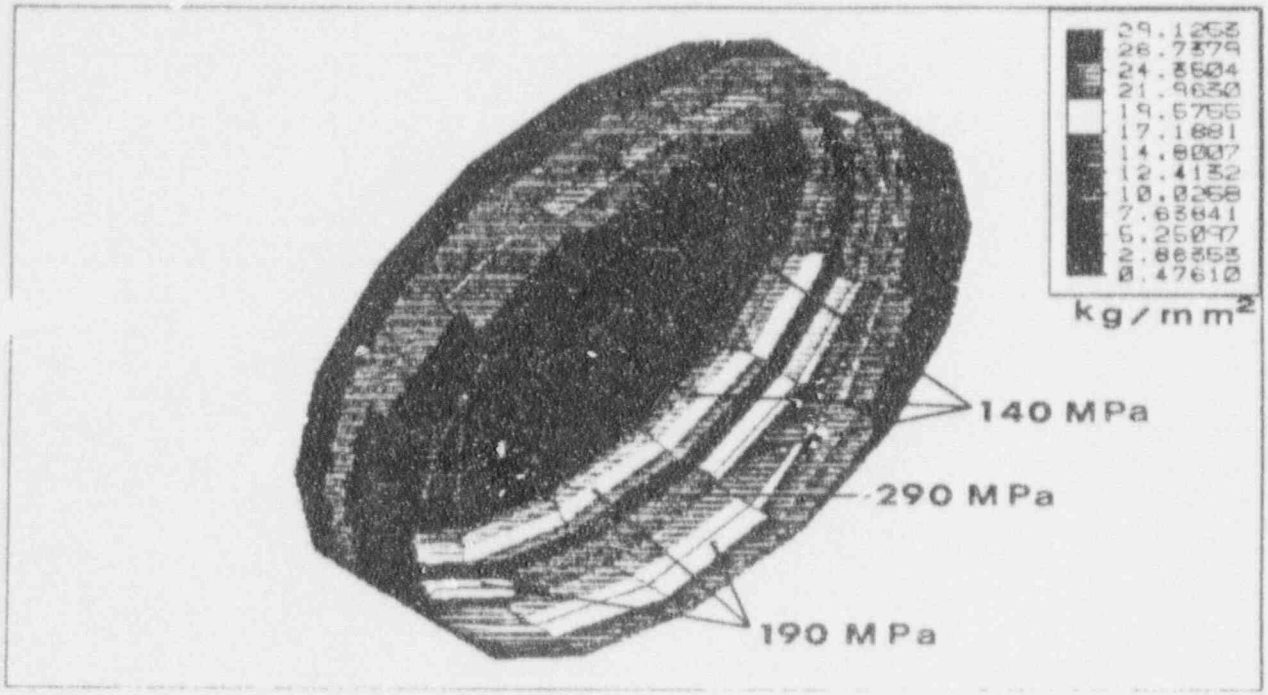


Figure 23. Stress Distribution on the Toward-Centerline Modified Hatch

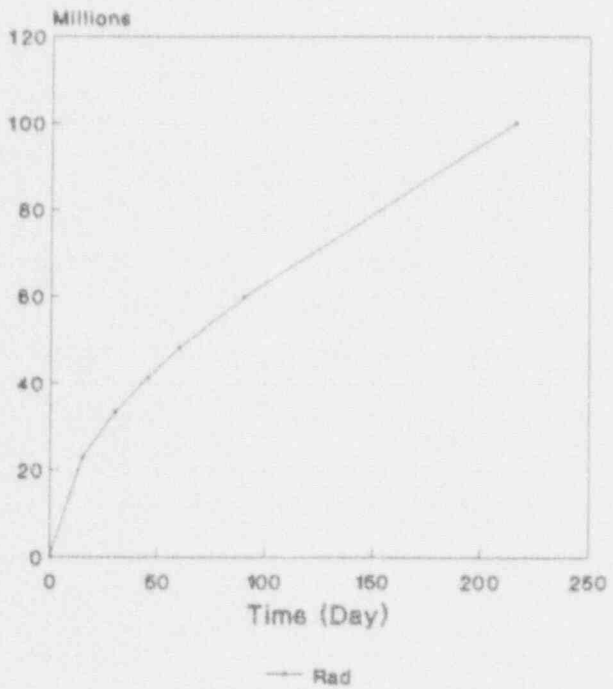


Figure 24. Integrated dose on the Airlock outer door gaskets

# SEVERE ACCIDENT RISK MINIMIZATION STUDIES FOR THE ADVANCED NEUTRON SOURCE (ANS) REACTOR PLANT AT THE OAK RIDGE NATIONAL LABORATORY

Rusi P. Taleyarkhan Seok-Ho Kim

Martin Marietta Energy Systems
Engineering Technology Division
Oak Ridge National Laboratory
Oak Ridge, Tennessee 37831-8057

## Abstract

This paper discusses salient aspects of severe accident related phenomenological considerations, scoping studies, and mitigative design features being studied for incorporation into a high-power research reactor plant. Key results of scoping studies on steam explosions, recriticality, core-concrete interactions, and containment transport are highlighted. Evolving design features of the containment are described. Containment response calculations for a site-suitability basis transient are presented that demonstrate acceptable source term values and superior containment performance.

## INTRODUCTION

Oak Ridge National Laboratory's (ORNL's) Advanced Neutron Source (ANS) will be a new user facility[1,2] for all kinds of neutron research, centered around a research reactor of unprecedented (~$10^{20}$ neutrons/$m^2$-s) neutron beam flux. A defense-in-depth philosophy has been adopted. In response to this commitment, ANS Project management initiated severe accident analysis and related technology development early-on in the design phase itself. This was done to aid in designing a sufficiently robust containment for retention and controlled release of radionuclides in the event of such an accident. It also provides a means for satisfying on- and off-site regulatory requirements, accident-related dose exposures, and containment response and source-term best-estimate analyses for level-2 and -3 Probabilistic Risk Analyses (PRAs) that will be produced. Moreover, it will provide the best possible understanding of the ANS under severe accident conditions and consequently provide insights for the development of strategies and design philosophies for accident mitigation, management, and emergency preparedness efforts.

This paper describes salient aspects of the ANS system design, results of focused severe accident scoping studies, efforts to identify mitigative design features, and strategies for reduction of the consequences of severe accidents in the ANS. Thereafter, the results of containment response calculations for a licensing basis transient are presented.

## ANS SYSTEM DESIGN

The ANS is currently in the conceptual design stage. As such, design features of the containment and reactor system are evolving based upon insights from ongoing studies. Table 1 summarizes the current principal design features of the ANS from a severe accident perspective, in comparison with ORNL's High Flux Isotope Reactor[3] (HFIR) and a commercial Light-Water Reactor (LWR). As seen in Table 1, high-power-density research reactors can give rise to significantly different severe accident issues. Specifically, the ANS reactor will use about 15 kg of highly enriched (~ 93 m/o U-235) uranium silicide fuel in an aluminum matrix with a plate-type geometry, and a total core mass of 100 kg. The power density of the ANS will be about 2 to 3 times higher than

that of the HFIR, and about 50 to 100 times higher than that of a large LWR. Such features have led to increased attention being given to phenomenological considerations dealing with steam explosions, recriticality, core-concrete interactions, core melt progression, and fission-product release. However, as opposed to power reactors scenarios, overall containment loads from hydrogen generation and deflagration are relatively unimportant for the ANS.

A schematic representation of the reactor and containment is given in Figure 1. The reactor core is enclosed within a so-called core pressure boundary tube (CPBT) and enveloped in a reflector vessel. As seen in the figure, this reactor system is immersed in a large pool of water. Experiment and beam rooms for researchers are located on the first and second floors, which are connected to the third floor high-bay region via rupture disk. The subpile room housing the control rod drive mechanisms is also connected to the third floor via lines with a rupture disk in between. The approximately 95,000-$m^3$ primary containment of the ANS consists of a 25-mm steel shell housed in a 0.8-m-thick reinforced concrete secondary containment wall with a 1.5-m gap in between. The targeted design leak rate for the primary containment is 0.5 vol %/day (to the annulus), whereas, for the secondary containment the design leak rate is 10 vol %/day. Annulus flow is exhausted through vapor and aerosol filters. The containment isolation system is designed to automatically initiate closure of isolation valves on lines that penetrate the primary containment wall.

## ANS SEVERE ACCIDENT RISK MINIMIZATION STUDIES

Based upon the salient features of the ANS identified in Table 1, relevant severe accident issues that have been identified are:

- Fuel-Coolant-Interactions (FCIs) (e.g., steam explosions),
- Recriticality,
- Debris noncoolability and ablation of structural boundaries,
- Core-Concrete-Interactions (CCI),
- Gas detonation, and
- Containment overpressurization failure.

Results from focused studies on the issues listed above are summarized in the following sections.

### Study and Prevention of Steam Explosion Loads in ANS

The study of FCIs is of particular interest to ANS safety due to well-known propensity for molten aluminum to interact explosively with water.[4,5] Such reactions can cause large amounts of mechanical energy to be generated within a very short time frame, creating missiles and shock waves that may damage the containment. Results of a recently completed scoping study[5] for the ANS have indicated that the CPBT and reflector vessel (made of aluminum) very likely would rupture under predicted FCI loads generated for a variety of severe accidents. Severe accidents considered in this focussed study included anticipated transients without scram (ATWS), reactivity excursions, and debris melting under decay heating conditions. This study clearly indicated the need for incorporation of a well-characterized set of mitigative features. Merely increasing the thickness or changing the materials of the CPBT are in conflict with the main mission of the ANS (i.e., high thermal neutron flux) and were thus not options. Considerations are being given towards the material of choice for the reflector vessel, in conjunction with the strategic introduction of a void volume for reduction of pressurization loads. More sophisticated evaluations are being made to give indications on the relative merits of the energy absorption capabilities of various system structures, including the reactor coolant system (RCS). Based on results of these studies, judiciously positioned missile shields or pressure relief valving will be considered to minimize the risk for containment failure or damaging blowdown loads.

For the ex-vessel phase of steam explosions (especially in the subpile room), evaluations are being made for the introduction of strategic flooding. As a basic recommendation, system operation is being prescribed to minimize situations in which large quantities of molten debris and water come into contact. If, for example, the core debris must be cooled with water, a flooding strategy is recommended that employs a pulsed injection mode so that if an explosive FCI does occur, the amount of water present will be limited. Another strategic flooding method would employ sprays with appropriately timed injection that causes sufficient quenching but significant steam blanketing at the water-fuel interface to prevent triggering of explosions.

As is well-known, the appropriate use of additives[4] to the water can suppress the steam explosion triggering potential to a negligibly low value. Therefore, the use of additives to the water used for flooding strategies is also under consideration in ex-vessel situations. Another mitigative feature is the use of surfactants which may assist in inhibiting steam explosion occurrence. Presently, severe accident researchers in conjunction with ANS designers are considering the feasibility of using particular preventive mechanisms in the overall context of plant design. Thereafter, a focussed experimental-cum-analytical effort will be undertaken as needed to quantify, qualify, and validate such a mitigative design feature.

## Prevention and Mitigation of Debris Recriticality Loads in ANS

As shown in Table 1, the ANS will use about 15 kg of highly enriched U-235 fuel encased in an aluminum matrix. Under certain accident scenarios the fuel material can relocate out of the control region and under the appropriate configuration, may undergo a prompt recriticality transient (an aspect that is usually considered a non-issue for power reactors). A scoping study has been conducted to evaluate such a potential for the ANS using the KENO5-SCALE neutronic code system[6] at ORNL. This preliminary recriticality study for the ANS core debris in various postulated post-accident configurations within the RCS has indicated that it might theoretically be possible to insert significant excess reactivity (i.e., 10 dollars worth). This was found to be the case only for dispersed configurations where all of the fuel (i.e., 15 kg of U-235) was involved. An alternate calculation with about 4 kg of fuel dispersed in a $D_2O$ medium resulted in a $k_{eff}$ of only 0.85. The amount of fuel which needs to be dispersed to give a $k_{eff}$ value of 1.0 has yet to be evaluated for various thermal-hydraulic conditions. All lumped fuel configurations remained significantly subcritical for the conditions studied. These evaluations demonstrated, to the extent they were representative of expected conditions, that a mechanism should be found to prevent dispersion of a large enough portion of core debris during severe accidents. If fuel dispersion is inevitable, it is clearly preferable to introduce design features that allow only small portions to disperse. Other options considered relate to the introduction of neutron poisons (e.g., borated pipes) in selected RCS regions.

This is a clear case where a design-fix, that "will" prevent recriticality, is far more preferable to an extensive research program that "may" solve the problem. This is because not much is known on modeling and analysis of "transient" debris recriticality events.

As mentioned above, a principal aspect dealing with debris recriticality in the ANS during severe accidents requiring investigation deals with debris dispersion. Research efforts are thus to be focused toward analytically quantifying melt progression aspects with the potential for leading to recriticality, possibly coupled with qualification via scaled experimentation.

## Prevention and Mitigation of CCI and Combustible Gas Detonation Loads

As mentioned previously, the potential generation of combustible $H_2$ in the ANS from oxidation of the aluminum in the fuel plates is significantly lower than for power reactors. However, additional

CO and $H_2$ gases can also be generated during the CCI stage. Fortunately, our scoping studies show that even if all the generated gases were to uniformly fill the primary containment, the concentration level would still be less than 1% by volume. This is significantly lower than the level necessary for deflagration (8 vol %) or detonation (13 vol %). However, the possibility exists for generating high concentrations (i.e., greater than the detonation limits) of combustible gases in selected containment regions. Specifically, this becomes a real possibility in the subpile room during CCI if the basemat is made with limestone-common sand concrete. For such conditions, the use of an inert atmosphere combined with igniters in selected volumes most susceptible to the buildup of detonation quantities of combustible gases has been strongly recommended. This will be considered for feasibility of introduction within the overall context of plant design.

Another means for preventing detonation loads in critical regions was studied in conjunction with minimizing concrete ablation and gas generation during CCI. For the ANS conditions, our scoping studies have shown that the threat to containment integrity from CCI loads can be prevented or mitigated if the surface lining of the basemat were made with alumina concrete coupled with the flooding strategy described above. Details of the study can be found in Reference 7. Another means considered for minimizing CCI would be to design the subpile room cavity to spread the core debris sufficiently for maintaining coolability (i.e., interface temperature below the concrete ablation temperature). This was not considered feasible from operational considerations and also because the amount of debris spreading on a level surface is limited by surface tension.

The most promising approach toward eliminating threats from CCI-generated loads for the ANS would rely on lining the basemat of the subpile room with alumina concrete. The depth of this lining (for a conservatively scoped debris-concrete configuration) should be greater than the thermal boundary layer thickness as a minimum, combined with an appropriate flooding strategy. Strategic flooding would achieve the purposes of preventing steam explosions, quenching the debris to prevent CCI, and finally to also assist in scrubbing fission products. It is recognized that the qualification and validation of this mitigative feature would require focused analytical and experimental efforts. In conjunction with this prescription, we have introduced strategically positioned igniters to burn off the greatly reduced (albeit potentially damaging) amounts of combustible gases in confined volumes.

## Measures for Minimization of Source Term, Debris Noncoolabiltiy and Structural Ablation

From an obvious perspective, for severe accidents with significant fuel melting, the best way to minimize the source term is clearly to keep the fission products bottled up in the RCS itself. This requires maintaining the debris in a coolable state. For the purposes of this discussion, we define coolability to represent a thermal condition where the interface temperature between the debris and structure under attack is lower than the structure's melting temperature. Scoping calculations have shown that in order to achieve this for ANS debris with its high-power density (viz., more than 50 to 100 times that of power reactor debris), the debris would need to be sufficiently dispersed, and covered with water. Details will be discussed in a report[8] to be published later. Dispersion would effectively increase heat transfer surface area. The precise degree of dispersion necessary is clearly a function of several parameters (viz., debris decay power level, structural material and geometry under attack, coolant thermal-hydraulic conditions, etc.). In any case, it is evident that a means should be engineered in the system to ensure that the debris does not relocate to regions in a lumped geometry if noncoolability is to be avoided. However, this approach is in conflict with design needs for minimizing recriticality loads, which can be initiated in dispersed geometries. An iterative approach is being followed toward identifying an optimized set of design features.

As is well-known, a simple but highly effective technique for reducing the source term utilizes the natural tendency of water to provide fission-product scrubbing. Every effort is being made to make sure that wherever possible, fission products are released only through a water pool. For this and other reasons, the ANS reactor vessel is located in the bottom of a large pool. Most of the RCS piping also passes through water-filled pools. It should be noted however, that the scrubbing function is dependent on and, in some cases, very sensitive to key parameters such as pool subcooling, depth, and pH, as well as the fission-product form. Therefore, the design attributes of such water pools will take into account these parameters to provide the needed scrubbing capability.

### Measures for Minimization of Overpressurization Failure

It is recognized that no amount of filtration or containment capability can help if the containment boundary fails catastrophically via overpressurization. Several possible means by which this may occur involve loads generated either due to explosions or from events such as steaming or combustible gas deflagration. Prevention of containment failure from explosive events was discussed earlier in the sections dealing with FCI and recriticality prevention. Here we discuss aspects dealing with minimization of risks from overpressurization failure due to relatively static loads.

Due to the large size of the ANS containment (> 95,000 $m^3$), containment transport calculations show that pressurization from nonexplosive conditions will not cause overall primary containment shell failure. However, for smaller compartments, such as the subpile room where a CCI event can quickly cause overpressurization failure of containment walls, pressure-relief mechanisms have been selected. Specifically, a rupture disk is allowed to open up a flow path from the subpile room to the high bay volume if the subpile room pressure goes above 115 kPa (2 psig). Another similar rupture disk allows pressure relief for the large high bay volume if the pressure exceeds 115 kPa (2 psig); that is, if the pressure in the high bay volume exceeds 115 kPa (2 psig), a rupture disk opens up to allow expansion into the first and second floor volumes. Such a zoning arrangement also serves the important purpose of facilitating personnel evacuation from the first and second floor volumes in the event of a severe accident. The effects of such a designed pressure-relief mechanism will be evident from results presented in the next section, displaying containment response characteristics for a site-suitability basis transient.

The large containment volume of the ANS coupled with the relatively smaller quantities of heat-generating fission products (about 10% of that for large power reactors) and the designed pressure-relief mechanisms make engineered safety features such as sprays unnecessary. However, fan coolers will be considered for volumes such as the subpile room where even if appropriate pressure relief is provided, the atmosphere may reach high temperatures during deflagration events.

## ANS CONTAINMENT RESPONSE DURING A SITE-SUITABILITY BASIS TRANSIENT

This section describes the thermal-hydraulic and radionuclide transport modeling aspects along with analyses conducted for evaluating the ANS containment response for a site-suitability basis transient. The scenario to be modeled follows the prescriptions given by the 10 CFR 100 guidelines outlined in Reference 9. It is hereafter referred to as the CFR100 scenario.

The MELCOR severe accident analysis code[10] was used to develop an overall representation of the ANS containment. The model, consisting of 11 control volumes, 15 flow paths, and 21 heat structures (representing walls, ceilings, shells, and miscellaneous materials) of various shapes, is shown in Figure 2. A fan model has also been included to account for flow through the large

annulus gap between the steel shell and outer containment. Aerosol and vapor filtration processes are also modeled, as are various complex aerosol and vapor transport phenomena associated with the severe accident scenario being evaluated.

The CFR100 scenario was analyzed assuming an intact primary and secondary containment. Iodine and aerosol filter trains have been incorporated to provide retention (of halogens and particulates) with decontamination factors of 100 and 200, respectively. Leakage rates of 0.5 vol %/day from the primary containment to the annulus (under design pressure difference), and 10 vol %/day from the annulus to the environment were modeled. The modeling of annulus leak rate of 10 vol %/day was performed by conducting an inverse calculation. That is, the exhaust rate of 10 vol %/day was specified as a boundary condition, and resulting pressure distributions in the annulus were back calculated. At the start of the calculation, 100% of the noble gases and 25% of the halogen inventory were sourced into the high-bay volume atmosphere as vapors. In addition, 1% of the remaining radionuclides were sourced into the high-bay atmosphere as aerosols. The remainder of the radionuclides were assumed to "stay" in the reactor pool volume of 100 $m^3$ without volatilization. Such a prescription provides for the maximum possible heat generation for steaming purposes.

Salient results of MELCOR calculations are shown in Figures 3 through 7. Pressurization traces for various regions of the containment are shown in Figure 3. As seen therein, high-bay volume pressure rises quickly after pool steaming begins in about 4 hours. Thereafter, rupture disks provide pressure relief when a pressure difference of 112 kPa (2 psig) is reached. Eventually, the entire containment volume pressure levels off at about 121 kPa (2.75 psig).

Figure 4 provides results of temperature rise in various containment regions. As the figure shows, the atmospheric temperatures in the high-bay and annulus regions can get quite high due primarily to steam condensation and radionuclide settling on various heat structures. Figure 5 shows the transient variation of total radionuclide mass deposition onto heat structures in the containment. As can be seen, more than 0.5 kg of the radionuclides that were originally deposited in the high-bay-area are deposited onto heat structures within the first 15 hours of the transient.

Figures 6 and 7 show the variation of the radionuclide source term (after passing through filter banks). As seen from Figure 6, only about 1% of the noble gases, and less than 0.0007% of the halogen inventory is released over 70 hours. Figure 7 shows that a negligible amount (i.e., less than $10^{-7}$%) of nonvolatile elements escape to the environment over 70 hours. Most of the nonvolatile release occurs soon after the high bay area volume pressure exceeds 112 kPa (2 psig).

The results presented above indicate that the negligible amounts of radionuclide releases will allow the ANS to meet site suitability criteria by a good margin. The low releases are essentially due to the leak-tight nature of the containment, coupled with halogen and aerosol removal by the filter banks.

## SUMMARY and CONCLUSIONS

To summarize, this paper has discussed salient aspects of severe accident related phenomenological considerations that have been considered for developing designed risk minimization features in the ANS. Key results from scoping and other studies on steam explosions, recriticality, CCI, containment transport, and pressurization have been described along with evolving design features of the one-of-a-kind ANS containment. Table 2 summarizes several recommendations that have been made in this paper for mitigating and/or managing containment loads from severe accidents in various phenomenological areas. As noted in Table 2, a comprehensive series of design features

are being researched for incorporation into the design of the ANS for risk minimization from severe accidents.

The results from the CFR100 scenario with an intact containment indicate that selective overpressurization in the ANS will be avoided by judicious use of pressure-relief mechanisms. Negligibly low values of radionuclides are shown to be released to the environment, indicating the effectiveness of natural heat sinks and structural deposition (in addition to filtration).

It is recognized that the overall risk will have to consider several severe accidents in various release categories. However, it is expected that when the designed mitigative features summarized in Table 2 are accounted for in the overall context of plant design, the ANS will demonstrate overall safety by a wide margin. That is, it will be shown to be safe from both probabilistic and deterministic standpoints (viz., negligibly low values of risk and no fatalities or injuries if a severe accident did occur).

## References


1. C. D. West, "The Advanced Neutron Source: A New Reactor Based Facility for Neutron Research," *Transactions of the American Nuclear Society*, 61, p. 375, June 1990.

2. F. J. Peretz, "Advanced Neutron Source Plant Design Requirements," ORNL/TM-11625, Oak Ridge National Laboratory, Oak Ridge, TN, 1991.

3. F. T. Binford and E. N. Cramer, "The High Flux Isotope Reactor, A Functional Description," ORNL-3572 (Rev. 2), Oak Ridge National Laboratory, Oak Ridge, TN. June 1968.

4. M. L. Corradini, "Vapor Explosions: A Review of Experiments for Accident Analysis," *Nuclear Safety Journal* 32(3), July–September 1991.

5. R. P. Taleyarkhan, "Steam Explosion Safety Considerations for the Advanced Neutron Source at ORNL," ORNL/TM-11324, Oak Ridge National Laboratory, Oak Ridge, TN, March 1990.

6. L. M. Petrie and N. F. Landers, "KENO5A—An Improved Monte Carlo Criticality Program with Supergrouping," Vol. 2, Section F11 from "SCALE: A Modular Code System for Performing Standardized Computer Analyses for Licensing Evaluation," NUREG/CR-0200 Rev. 2, ORNL/NUREG/CSD-2/R2, Oak Ridge National Laboratory, Oak Ridge, TN, December 1984.

7. C. R. Hyman and R. P. Taleyarkhan, "Characterization of Core Debris/Concrete Interactions for the Advanced Neutron Source," ORNL/TM-11761, Oak Ridge National Laboratory, Oak Ridge, TN, February 1992.

8. R. P. Taleyarkhan, "Core Melt Progression and Fission Product Release Considerations for the Advanced Neutron Source Reactor at ORNL," ORNL/TM-12022, Oak Ridge National Laboratory, to be published.

9. J. J. DiNunno et al., "Calculation of Distance Factors for Power and Test Reactor Sites," Atomic Energy Commission Technical Information Document TID-14844, March 1963.

10. R. M. Summers et al., "MELCOR 1.8.0: A Computer Code for Nuclear Reactor Severe Accident Source Terms and Risk Assessment Analyses," NUREG/CR-5531, Nuclear Regulatory Commission, January 1991.

**Table 1. Severe Accident Characteristics of the ANS and other Reactor Systems**

| Parameter | Commercial LWR | HFIR | ANS |
|---|---|---|---|
| Power [MW(t)] | 2600 | 85 | 300 |
| Fuel | $UO_2$ | $U_3O_8$-Al | $U_3Si_2$-Al |
| Enrichment (m/o) | 2-5 | 93 | 93 |
| Fuel Cladding | Zircaloy | Al | Al |
| Coolant/Moderator | $H_2O$ | $H_2O$ | $D_2O$ |
| Coolant Outlet Temperature (°C) | 318 | 69 | 92 |
| Average Power Density (MW/$\ell$) | <0.1 | 1.7 | 4.5 |
| Clad Melting Temperature (°C) | 1850 | 580 | 580 |
| Hydrogen Generation Potential (kg) | 850 | 10 | 12 |

**Table 2. Summary of Recommendations for Design Fixes and Mitigative Mechanisms**

| Recommendation | Notes on Recommendation |
|---|---|
| Employ an ANS design that retards or traps fission product vapors and aerosols for minimization of the source term | Fundamental safety prescription |
| Design against selective overpressurization in containment compartments | Carefully engineered venting paths with selective compartmentalization without overpressurization is desirable to provide more time for evacuation as well |
| Carefully consider a more robust reflector tank material than aluminum | Containment of steam explosion pressure pulses, and also radionuclide dispersion |
| Consider incorporation of a missile shield or other energy-absorbing mechanism | If evaluations indicate a high probability of energetic missile generation from explosive events |
| Alter the design and operation to minimize possibilities for molten core debris coming in contact with large amounts of water in the subpile room, employ strategic flooding or timed-sprays for subpile room | Improves quenching, prevents explosive fuel-coolant-interactions, and prevents core-concrete-interactions |
| Consider use of additives to sufficiently increase viscosity of water used for flooding strategies | Minimizes triggering potential; can be used in conjunction with an appropriate surfactant |
| Find a mechanism that prevents uniform dispersion of core debris in reactor coolant system to prevent recriticality. Another consideration would use borated-water-injection system as in power reactors, or borated structures | Recriticality prevention via design and operation |
| Adopt in-depth measures to prevent and mitigate combustible gas detonation | This includes igniters (e.g., in subpile room) to burn combustible gases as they evolve and before detonation concentrations are reached |
| Consider either confining debris (using a core catcher) or dispersing it to avoid noncoolability and unacceptable structural ablation | Iterate with severe accident researchers to determine location and validity of the installed mechanism |
| Line the subpile room floor with alumina concrete and provide for strategic flooding to minimize structural ablation and production of combustible gases | Unless operational considerations dictate otherwise |

**Table 2. Summary of Recommendations for Design Fixes and Mitigative Mechanisms (cont.)**

| Recommendation | Notes on Recommendation |
|---|---|
| Make every effort to design flow paths to ensure that released fission products are transported only via passage through a water pool | Iterate between designers and severe accident researchers to optimize the scrubbing potential of the water pool |
| Design to ensure that the radionuclides in the production target rods do not escape from the reactor cooling system | Work needs to be done iteratively between designers and severe accident researchers |
| Address phenomena such as combustible gas stratification via mixing mechanisms | For prevention of detonable gas formation |

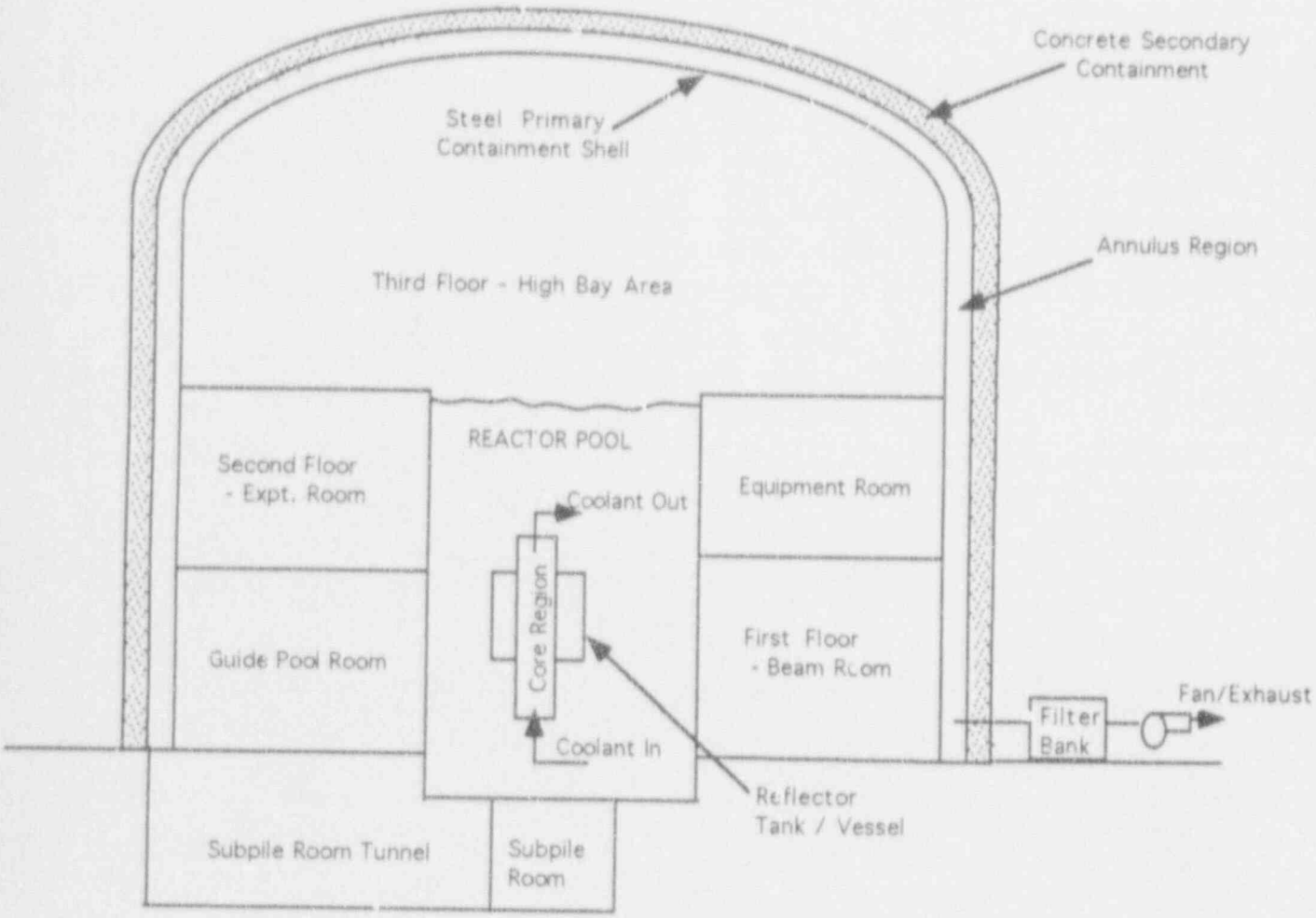


Figure 1. Schematic Representation of ANS Containment

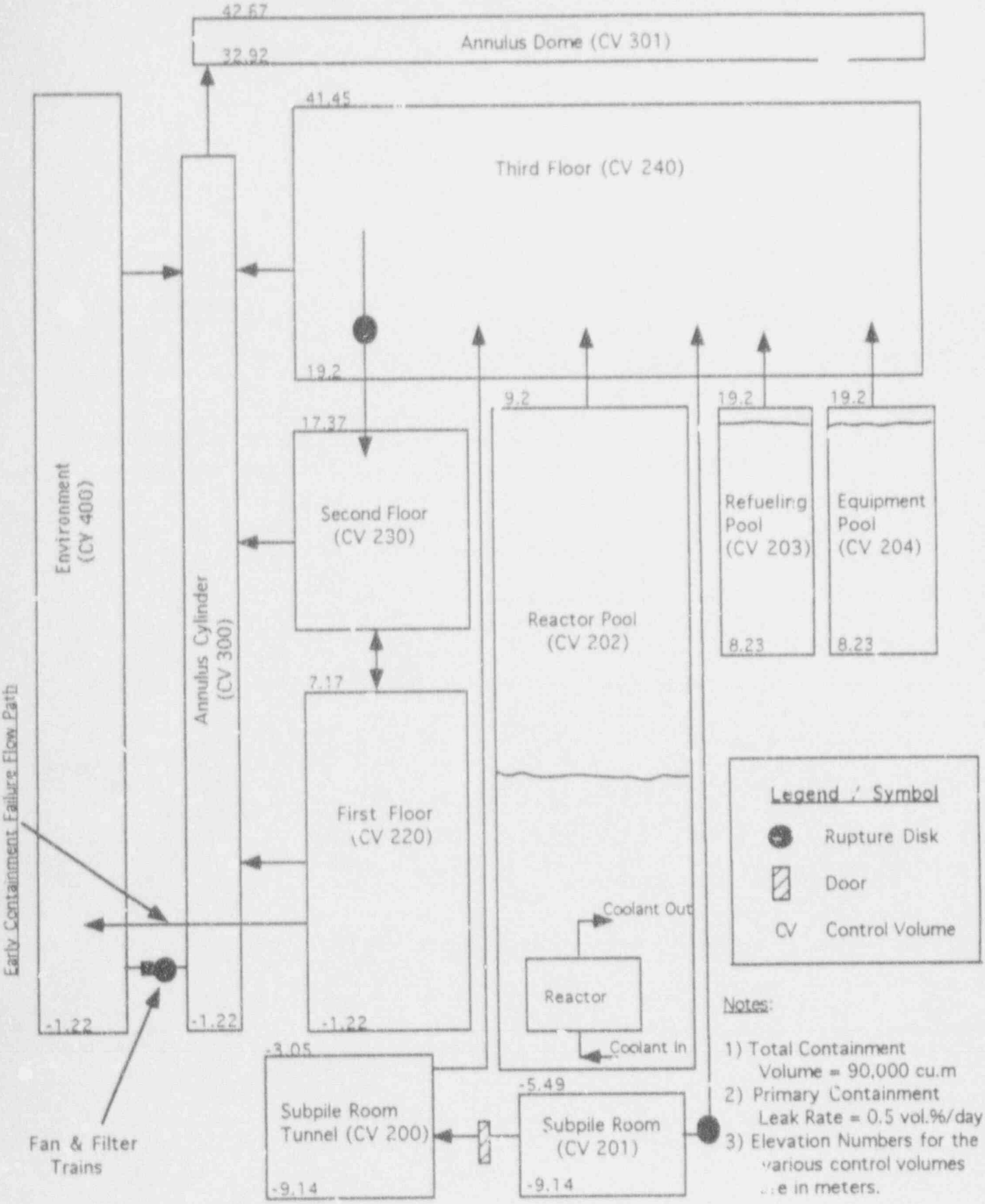


Figure 2. ANS Containment (MELCOR) Representation for Environmental Report

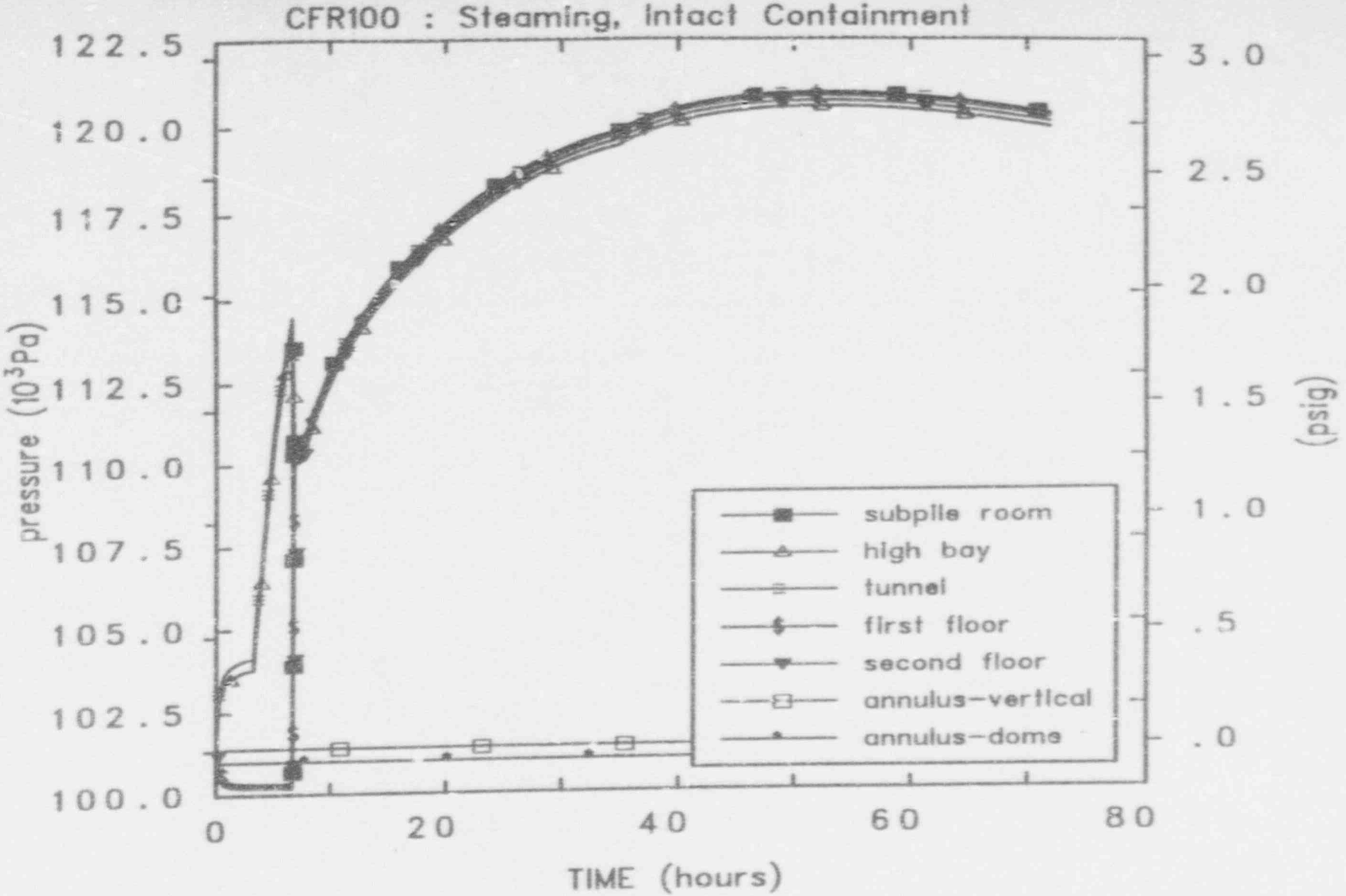


Figure 3 Variation of Containment Pressure vs Time for CFR100 Scenario

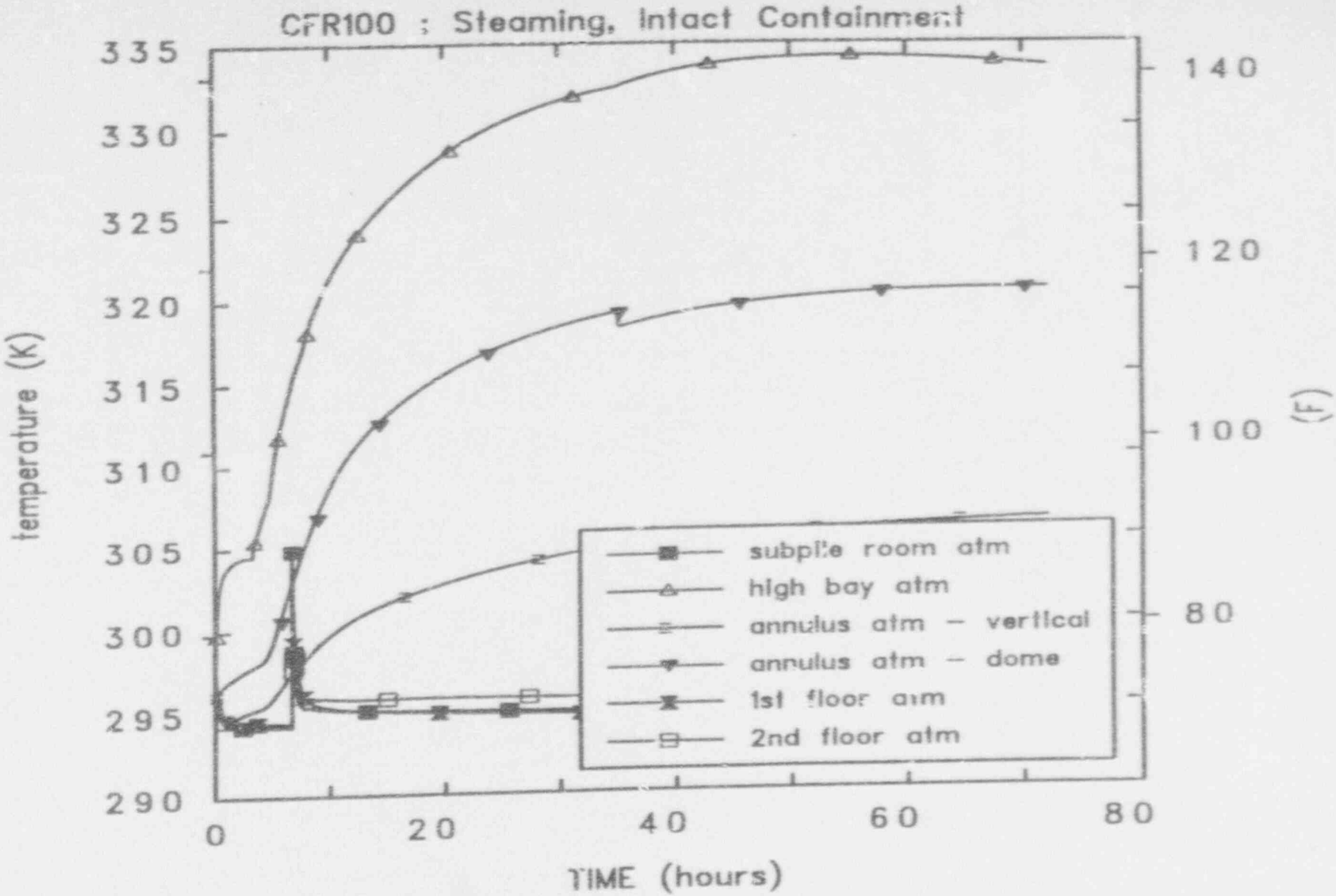


Figure 4 Variation of Containment Temperatures vs Time for CFR100 Scenario

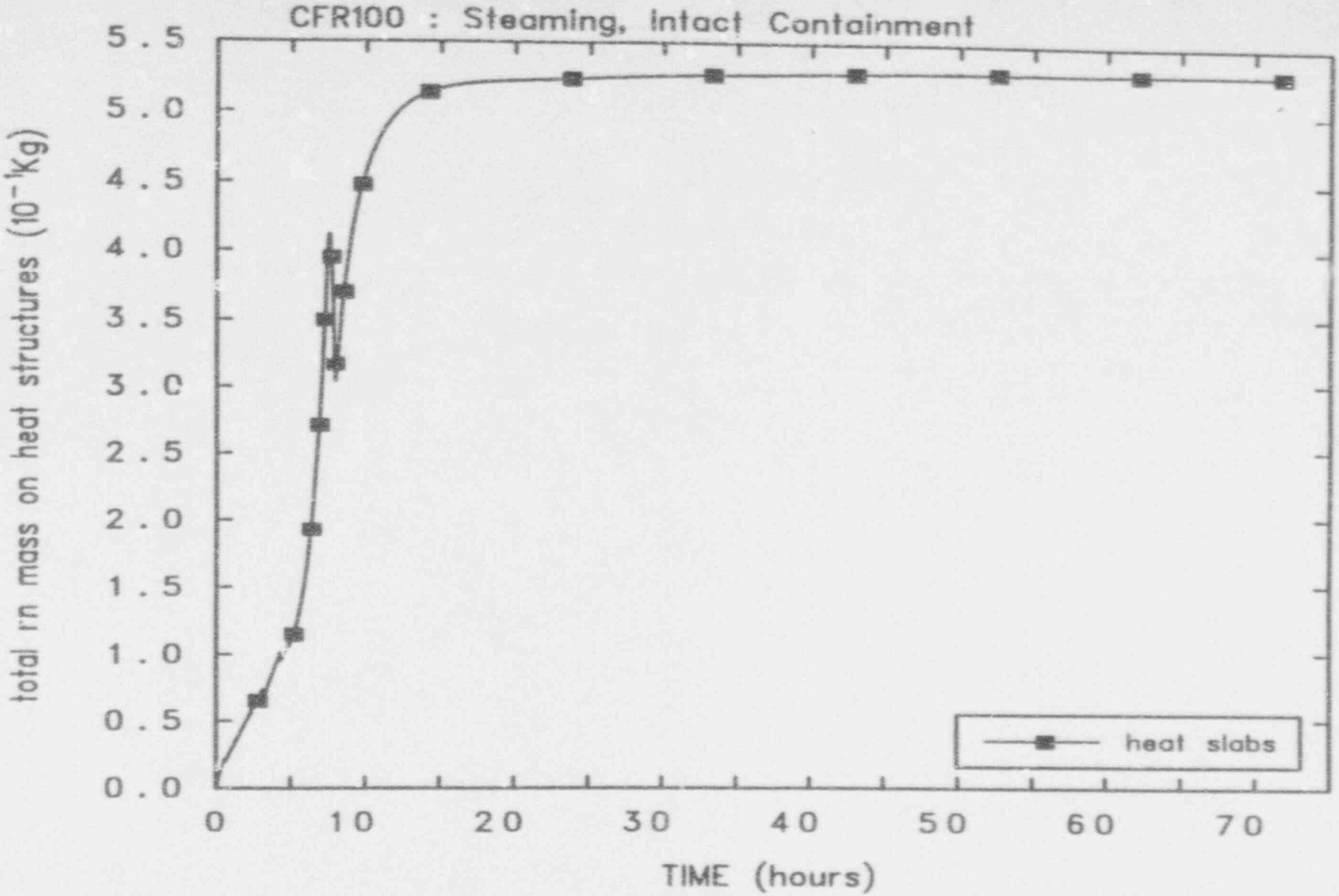


Figure 5 Variation of Total Deposited Radionuclide Masses on Containment Heat Structures vs Time for CFR100 Scenario

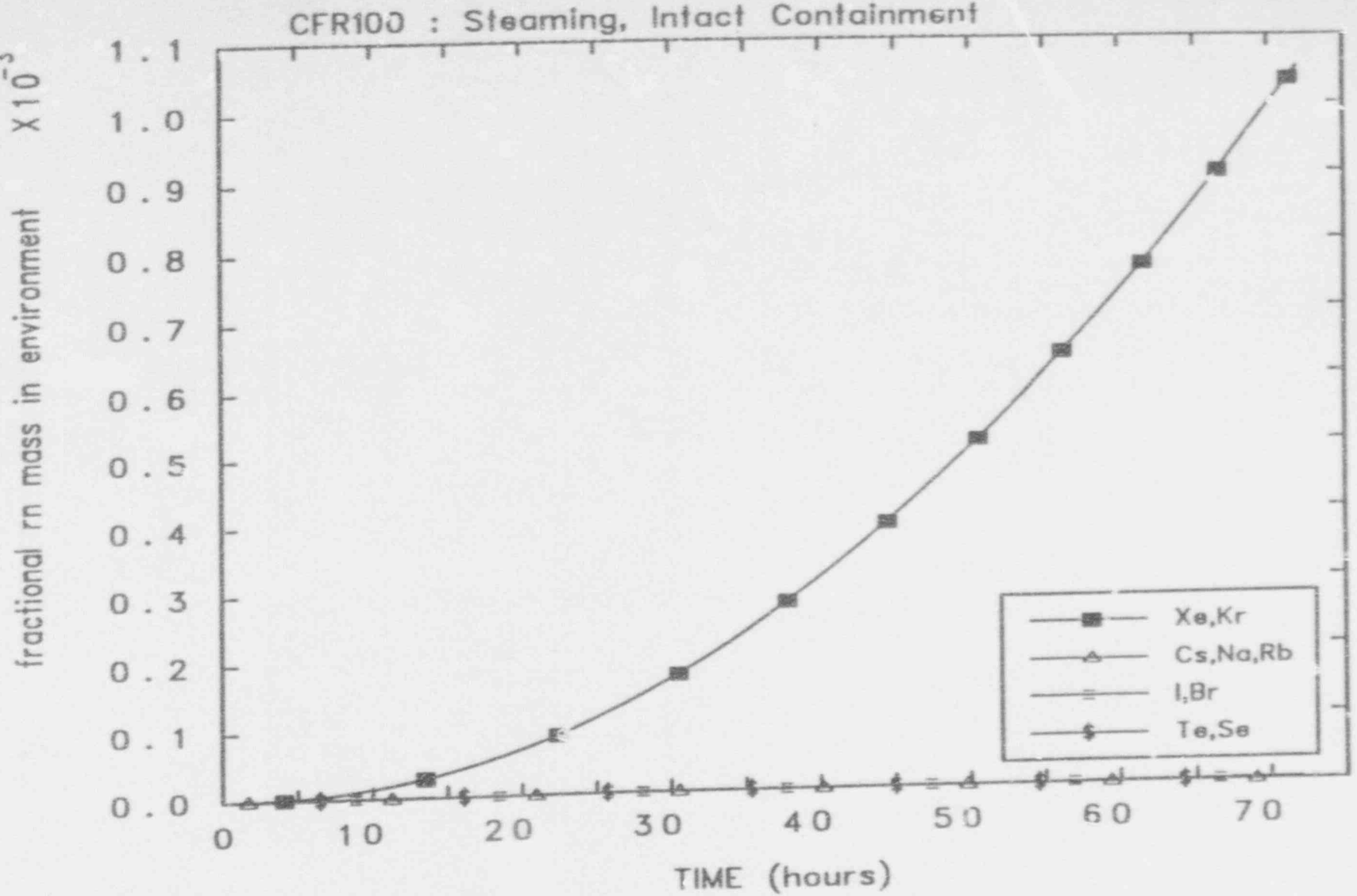


Figure 6 Variation of Volatile Fission Product Releases to Environment from Containment vs Time for CFR100 Scenario

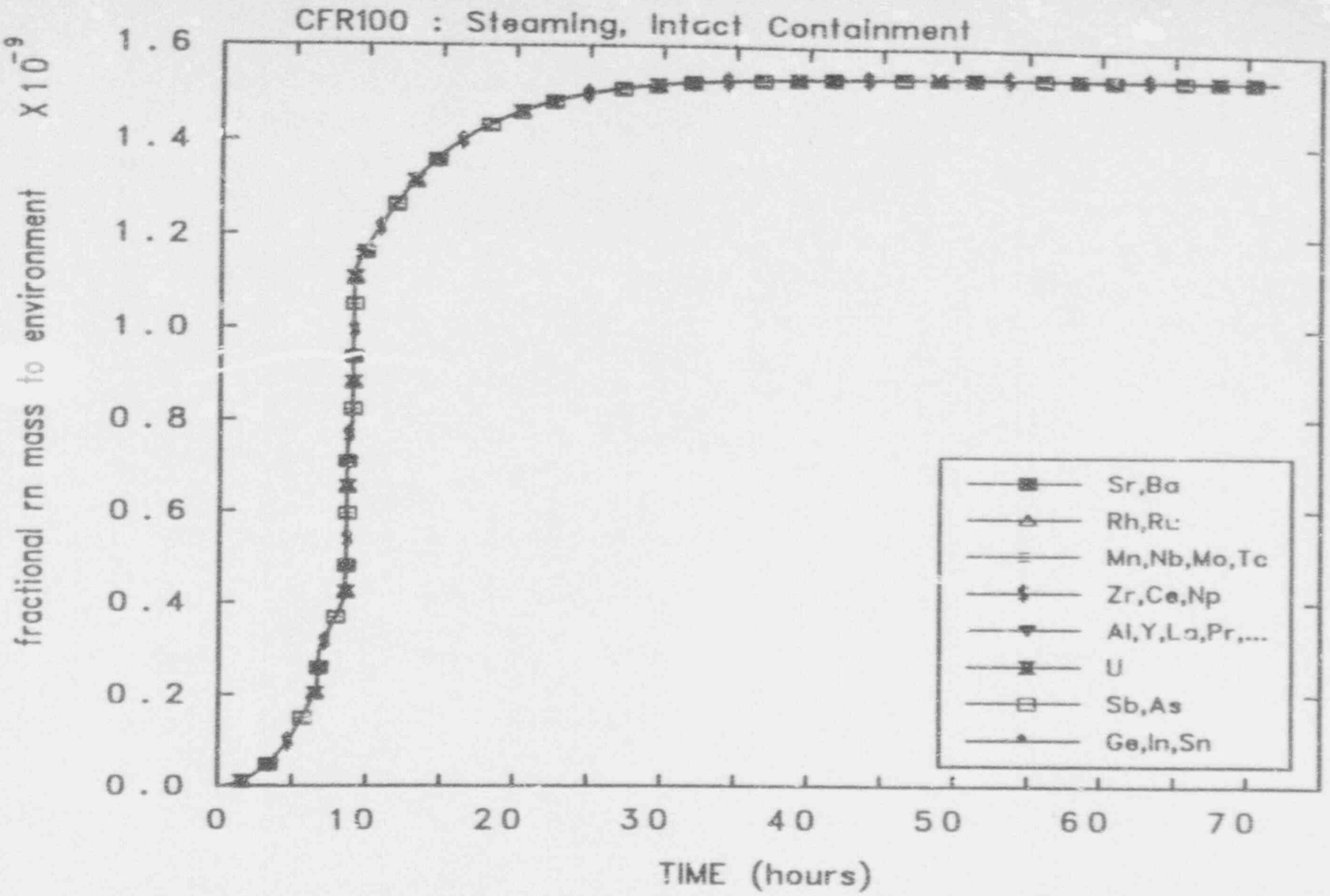


Figure 7 Variation of Non-Volatile Fission Product Releases to Environment from Containment vs Time for CFR100 Scenario

# EXTREME LOADINGS OF INNER STRUCTURES OF NEXT GENERATION PWR-CONTAINMENTS

R. Krieg, H. Alsmeyer, G. Jacobs, H. Jacobs
Kernforschungszentrum Karlsruhe GmbH
Postfach 3640, D-7500 Karlsruhe, Germany

J. Eibl, F.H. Schlüter, T. Klatte
Institut für Massivbau und Baustofftechnologie
Universität Karlsruhe
Postfach 6380, D-7500 Karlsruhe, Germany

## Abstract

Advanced safety demands call for reactor containments which are able to withstand any conceivable accident including the different types of core melt down accidents. The necessary improvements for the inner structures of the containments are discussed. Extreme loadings of these structures such as an in-vessel steam explosion and a melt-through-failure of the reactor vessel under high pressure must not endanger the containment. The ongoing research work to show this is described.

## 1. THE SAFETY PHILOSOPHY LEADING TO IMPROVED CONTAINMENTS

For technical facilities or other human activities the risk of an accident is usually quantified by the extent of the expected damage and the probability of its occurrence. From the fact that some facilities or activities are widely accepted one can conclude that their risks are accepted, too.

It turns out that for accidents causing small damage relatively high probabilities of occurrence are allowed. However, for an accident causing severe damage including the loss of lifes the probability has to be quite low.

In most countries nuclear power plants are designed in accordance with this rule. Severe accidents occur only with the same or even with lower probabilities as corresponding accidents in other power plants (Fig. 1a).

Nevertheless, in many countries the risk of nuclear power is highly questioned by the public; and this tendency is increasing. Accidents with severe consequences for the environment are felt to be unacceptable, no matter how low their probability might be. Furthermore, people want to be able to see and understand what is going on; and when this is not possible, they are against that technology.

Therefore, research has been started to design power plants taking into account these requirements. In this paper and the following paper [1] a new plant concept is proposed,

- based on the successful pressurized water reactor under operation in many countries,
- however, with an improved containment able to cope with any conceivable accident, including the different types of core melt down accidents.

  The improved containment is designed to provide a clearly defined barrier preventing any radioactive releases,

its function follows simple physical principles and can be easily understood,

its existence and readiness can be easily seen (since the containment is a huge component requiring only minor active measure),

its reliability is based on the long time experience in buildings and civil engineering.

This new plant concept with an improved containment has already been discussed in previous papers [2 - 5].

It is clear that from a theoretical point of view absolut safety can never be reached. But with the improved containment

- the risk for the environment of the plant will be additionally reduced such that it is no longer reasonable and possible to characterize it by probability numbers (Fig. 1b)

and

- the transparency of the safety measures will be strongly increased such that concerned people who cannot check all the details of a nuclear system will nevertheless have a chance to get a realistic impression about the high level of safety.

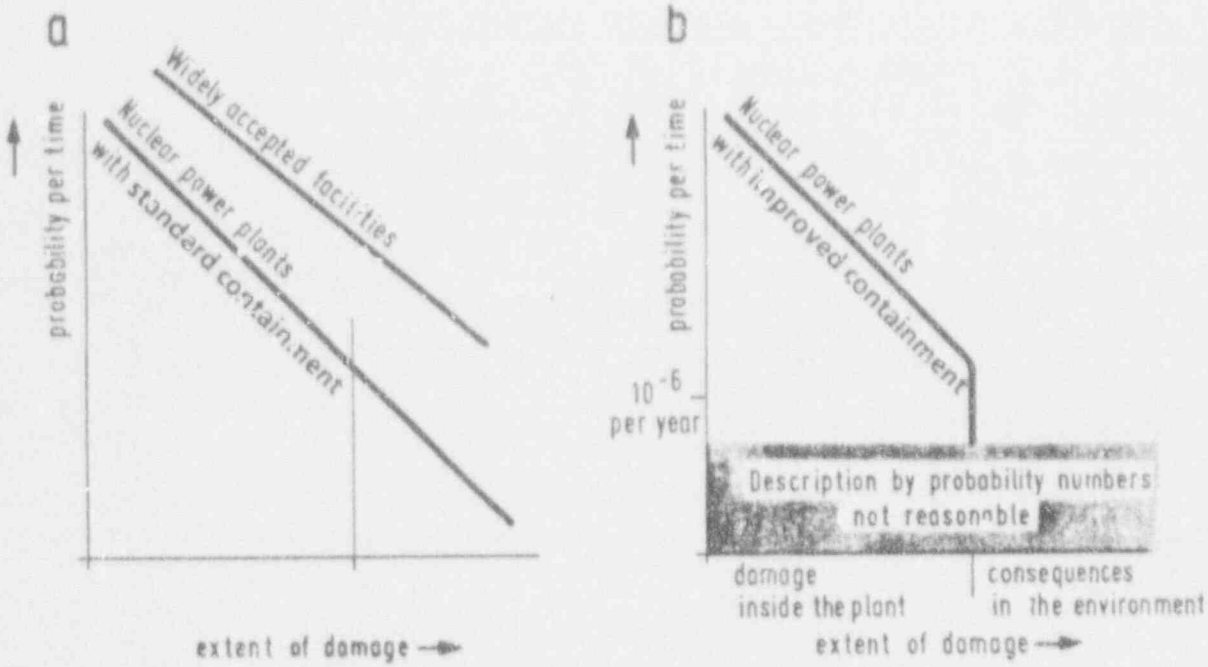


Fig. 1: Description of the risks of nuclear power plants
a) with standard containment; b) with improved containment

The impact of the new plant concept on the safety philosophy and especially the important role of transparency in our society has been discussed in [6], considering many sociological investigations about the acceptance of different technologies.

In order to prove the effectivness of the new containment a comprehensive investigation program has been started at the Nuclear Research Center Karlsruhe. Core melt down accidents with the most extreme loadings and the resulting most unfavorable failure mechanisms of the inner structures are considered.

In this paper an energetic in-vessel steam explosion and a melt-through-failure of the reactor vessel under high pressure are dealt with. The goal is to show that parts of the failed pressure vessel will not become missiles endangering the containment and that expelled core melt will be safely enclosed by a core catcher.

In the following paper [1] design concepts for the new containment are discussed. The ongoing research work will show that the new containment will be able to cope with the decay heat, the resulting pressure build up and a postulated hydrogen explosion.

## 2. ENERGETIC IN-VESSEL STEAM EXPLOSION

After a core melt down accident, the molten core masses could come in contact with water remaining below the core support structures and cause an in-vessel steam explosion [7 - 9]. It could destroy the reactor pressure vessel and resulting missiles (e.g. the pressure vessel head) could pierce the reactor containment (a mode failure).

In the recent German risk study [10] it was concluded that steam explosions with a mechanical energy release of 1.5 GJ and a pressure peak of 75 MPa would not endanger the integrity of the reactor vessel and that more violent steam explosions have a sufficiently low probability of occurrence for not to contribute significantly to the overall risk.

However, following the requirements of chapter 1 for the next generation PWR containments, the most severe steam explosion has to be considered which can be postulated on physical grounds. Furthermore, if a subsequent failure of the reactor vessel cannot be ruled out, provisions against any missiles have to be taken.

A first attempt to estimate the expenditure required to control possible missiles has been based on the data provided by Theofanous et al. [7]. Using always the most pessimistic data it was found that a steam explosion releasing 3 GJ of mechanical energy finally might cause the pressure vessel head to be catapulted away with a kinetic energy below 200 MJ. Design studies have shown that such missiles can be intercepted by reinforced internal containment structures [2, 3].

The above figures are, of course, only an illustration of what might be expected and should serve mainly to identify research needs. An equivalent set of figures, which however has to be proved to be reasonably conservative, must ensue from the research that has been initiated at the Nuclear Research Center Karlsruhe.

In the first place an upper limit of the explosion energy and corresponding pressure-time histories are required. Here we concentrate on two phenomena. The first is the autocatalytic separation of molten core masses and liquid water during premixing which is due to the high vapor production rate and which prevents the interaction of excessively large masses. The second is an upper limit to the conversion of thermal into mechanical energy that is clearly lower than the theoretically estimated thermodynamic upper bounds (e.g. half as high). Undoubtedly both effects require further experimental verification. Therefore, appropriate large-scale (field type) simulations are being prepared.

Analysis of the experiments and transfer of the results to the reactor case shall be performed using the three-dimensional multiphase computer code IVA3 [11] which describes the motions of melt, water, and steam by three separate velocity fields. For further development of this code and for its verification by a representative but somewhat simplified problem, laboratory experiments are forthcoming in which the premixing phase is simulated using large quantities of hot solid spheres. In the experimental as well as in the numerical simulations of premixing, different modes of discharge of the melt from the original core area will be investigated in order to identify the most pessimistic mode. For completeness, the melt down of the reactor core which sets the initial conditions for the outflow of the melt into the lower plenum and also for the mechanical effects of the steam explosion is studied theoretically.

It is likely that the integrity of the lower head of the reactor pressure vessel cannot be guaranteed under the extreme condition of a release of 3 GJ mechanical energy. Thus measures have to be taken to protect the core catcher located below the reactor pressure vessel against the impact caused by a failure of its lower head. These measures include a heavy bottom grid shown in Fig. 2. With a construction height of approximately 5 m, a kinetic energy of about 300 MJ could be absorbed. Steel grids can be inserted into the rectangular openings of this concrete grid to avoid the passing of smaller fragments. This could be important because small fragments might travel with high velocities and cause some impact damage.

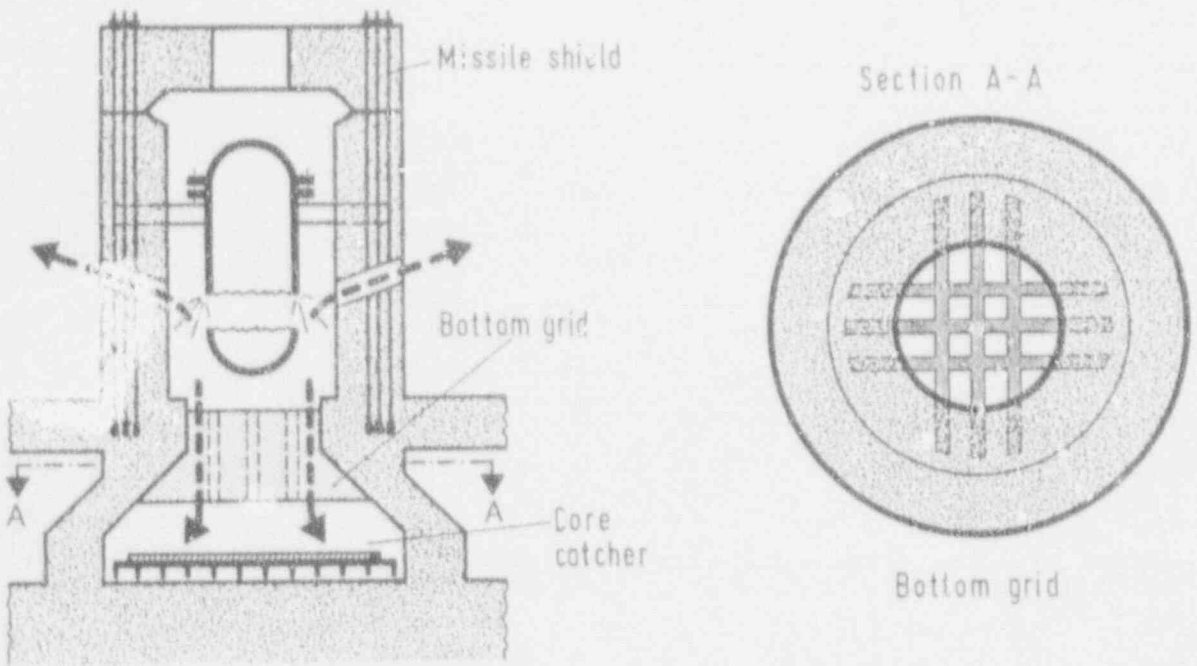


Fig. 2: Reactor vessel cavern with missile shield, bottom grid and core catcher

But on the other hand, it is quite difficult to show that the failure of the lower head will occur for sure. Fig. 3, for instance, reveals that the distribution of the plastic deformations in the lower head depends strongly on the type of loading. Under a static overpressure the lower head deforms similar to a clamped bulge with plastic strains mainly concentrated in the lower central part, but under an impulsive pressure the lower head deforms nearly spherical symmetric with plastic strains

distributed nearly uniformly. Thus, under the impulsive pressure of a steam explosion a considerable amount of energy could be dissipated in the pressure vessel head before failure occurs. Right now it is not clear whether this condition will really be reached.

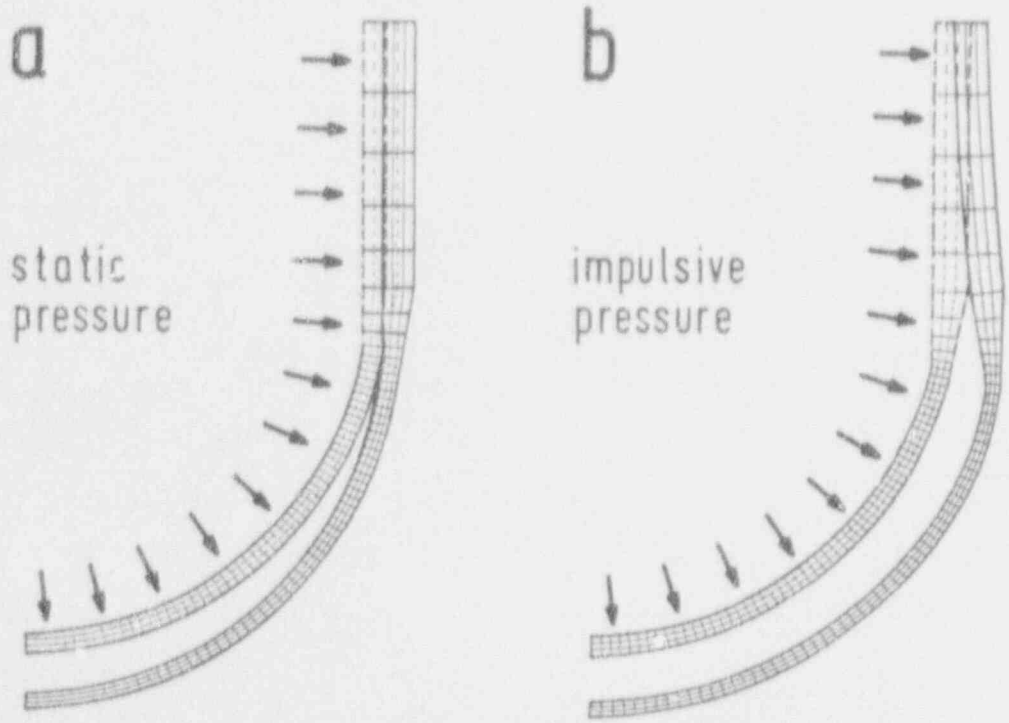


Fig. 3: Calculated plastic deformations of the lower head of the reactor pressure vessel

Therefore, as far as upper structures are concerned, that mechanical behavior of the lower head has to be assumed which causes a maximum of kinetic energy being transfered to materials which move upwards towards the upper head of the reactor pressure vessel. Furthermore, in order to have simple pessimistic conditions, it will be assumed that this material will form a coherent slug.

It appears, however, to be quite clear that much of the kinetic energy of the slug is dissipated during the interaction with the remaining internal structures above the reactor core. Here the main problem is to provide a sufficiently reliable proof of the magnitude of this effect. The same is also true for the forces on the vessel head resulting from the impact of the slug. First estimates [12] have shown that the expected forces are smaller than the strength of the bolts of the vessel head, which is in contrast to the statement in [7]. However, a reliable proof is not available yet.

To clear up this problem a model experiment is under way as shown in Fig. 4. It simulates the interactions of the upwards moving materials with the remaining internal structures and it also simulates the final impact on the vessel head. Both, the loads and the resulting strains will be measured. The experimental findings can be easily transferred to the reactor case due to the similarity between the model and the real problem.

In order to demonstrate this, additional experiments are carried out studying impact processes between liquid masses and deformable structures in different scales. First results show that indeed similarity exists under certain conditions.

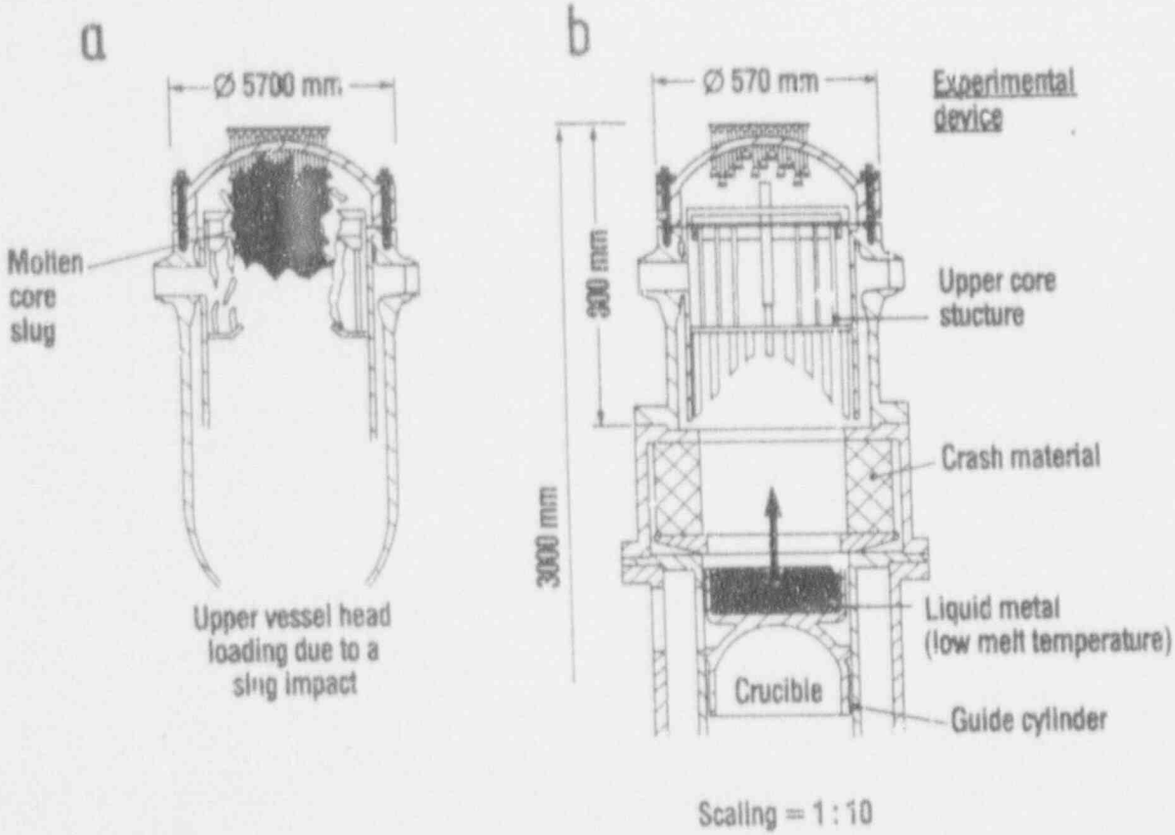


Fig. 4: Loading of the reactor vessel head by a postulated steam explosion
a) full size problem; b) model experiment

If it would turn out that the integrity of the upper head of the reactor pressure vessel cannot be guaranteed, a missile shield could be located above the pressure vessel in order to protect the containment as indicated in Fig. 2. Then the kinetic energy of the upward moving vessel head can be absorbed by unbonded prestressing cables which are anchored into the very stiff hollow box type structure that is formed by the integrated core catcher and the concrete structure at the ground floor.

Missile shields with smaller load carrying capacity sufficient to intercept a control rod drive mechanism ejected from the upper head are already used in some French PWR.

Calculations have shown that the weakest parts are the bolts connecting the head to the vessel. Their limited load carrying capacity will not allow for strains in the upper head higher than about 10 %, as indicated in Fig. 5. According to material tests these strains will not be able to initiate breaks. Consequently, the upper head will not break apart, even under excessive loadings and therefore, the missile shield could have an open central section which would facilitate the reactor operation.

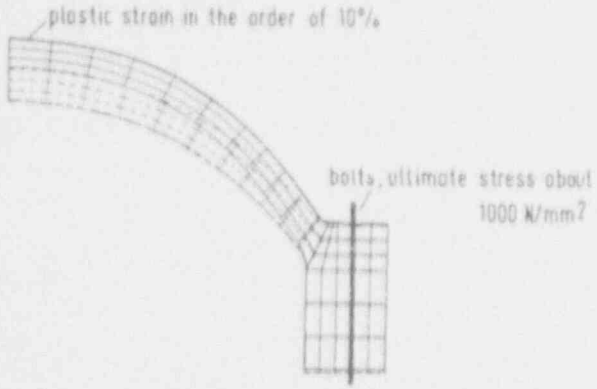


Fig. 5: Plastic deformation of the vessel head under the maximum (static) loading which can be carried by the bolts

## 3. MELT-THROUGH-FAILURE OF THE REACTOR VESSEL UNDER HIGH PRESSURE

During a core melt down accident the pressure in the primary system may assume the discharge pressure of its safety valves which is slightly above the operational pressure. In the worst case also accident management measures to depressurize the primary system may fail. Now the molten core which finally forms a pool in the lower head of the reactor vessel will heat up this lower head and thereby reduce its ultimate stresses until it is no longer able to carry the high pressure of the system. During the failure of the lower head the discharge of a two-phase mixture of steam and water under high pressure causes a strong dynamic force acting at the reactor vessel in upward direction. It must be shown that this force can be carried by the supporting structure of the reactor vessel. Otherwise, the reactor vessel would become a missile which could destroy the containment.

An equivalent dynamic force is acting at the bottom grid underneath the reactor vessel in downward direction. A quite similar loading which could be caused by a steam explosion has been discussed before. The bottom grid must be able to withstand these loadings and thereby to protect the core catcher which is needed for a reliable decay heat removal

Another consequence of a melt-through-failure of the reactor vessel under high pressure will be a strong pressure built up in the reactor vessel cavern. It must be shown that also this loading can be carried without endangering the integrity of the containment.

It is evident that reliable descriptions of the time histories of the dynamic loadings discussed above are inevitable. If the break opening caused by the failure of the lower head is given, adequate knowledge and computational models are available to solve this problem. So, successful analyses have been carried out at the Nuclear Research Center Karlsruhe recently, using the one-dimensional, two-phase thermal-hydraulics code RELAP5/MOD3, [13].

The analysis was simplified by the assumption of an instant circumferential rupture and a complete separation of the lower head from the reactor vessel near the melt pool level. The assumption leads to rather high loadings, but it seems to be not unrealistic since the maximum wall temperature is expected to occur close to the melt pool level. The lower head, which then is accelerated downward, is assumed to be filled with core melt. The ejection of melt and core debris have been neglected in this analysis.

The RELAP nodalization scheme for the analysis reflects the currently discussed design of the reactor vessel surroundings, as shown in Fig. 6. The upper part of the reactor cavern is connected to the big containment volume via large pressure relief openings. The nodalization uses 26 nodes (control volumes) for the representation of the vessel, 54 nodes for the piping of the primary system, and 3 nodes for the reactor vessel environment and the containment. The four loops of the primary system are put together to one loop in the representation. The fluid reservoir of the accumulators has not been considered since it becomes active only when the system pressure falls below a certain threshold. But then the most severe phase of the process is over.

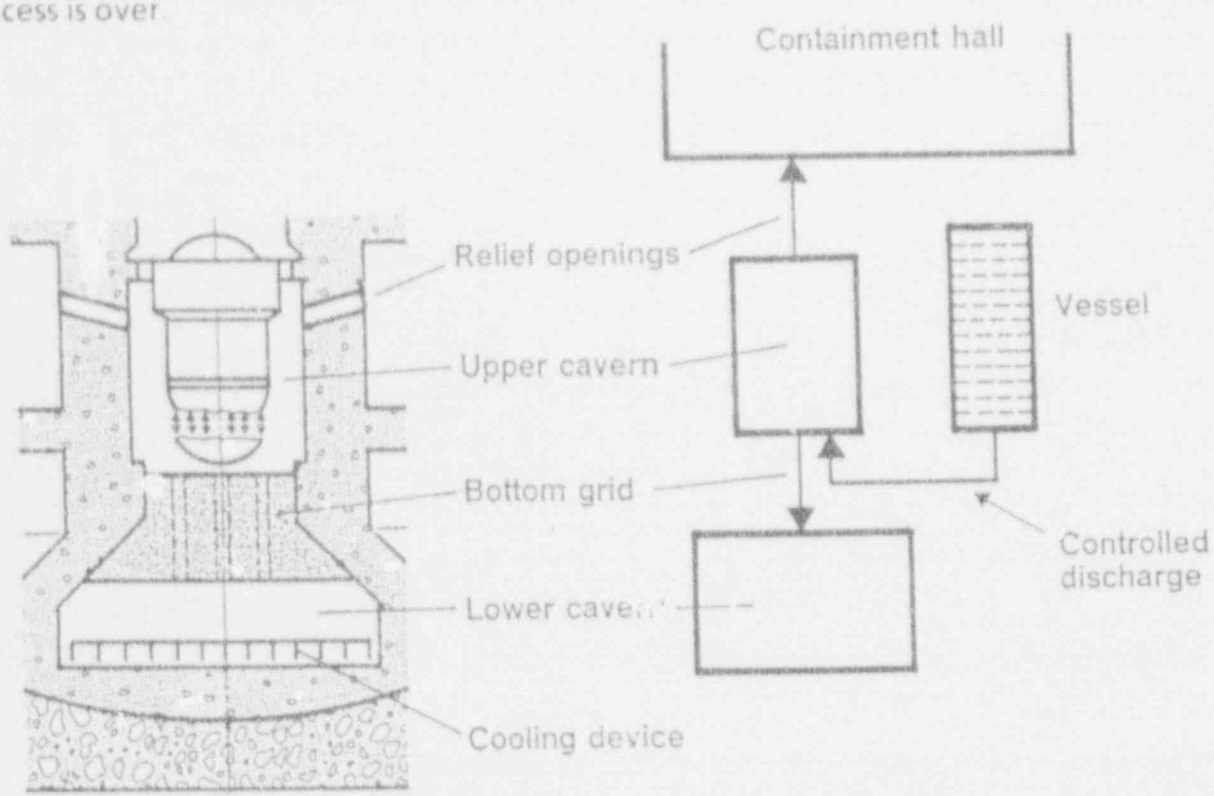


Fig. 6: Nodalization scheme to analyze the dynamic loading caused by a melt-through-failure of the reactor vessel under high pressure

The effective discharge flow area, defined as the cylindrical area between the edge of the ruptured vessel and the lower head is controlled by the strong downward acceleration of the lower head. The effective flow area reaches its maximum when the lower head hits the bottom grid.

The calculation of the force F acting on the reactor vessel is based on the following equation:

$$F = \sum_i V_i \frac{d}{dt} \rho_i v_i + (p - p_\infty) A_0 + \rho v^2 A$$

where

- $A_0$ is the circular area opened by the vessel rupture (break opening),
- $p$ is the pressure at this circular area,
- $\rho$ is the fluid density at this circular area,
- $v$ is the fluid velocity at this circular area,
- $A$ is the effective discharge flow area (defined above),
- $p_\infty$ is the pressure in the upper cavern,
- $V_i$ are the control volumes inside the reactor vessel,
- $\rho_i$ are the densities in these control volumes,
- $v_i$ are the velocities in these control volumes

RELAP5/MOD3 allows to consider the increasing effective flow area by solving the equation of motion for the accelerating lower head as well as the computation of the reaction force, along with the main thermal hydraulics computation by using the control system of the program.

The base case of the analysis is characterized by a lower head having a height of 1.5 m and a mass of 150 Mg, a circular area opened by the vessel rupture of 17.8 m², a maximum effective flow area of 8.7 m² and a relief opening area between the vessel cavern and the containment volume of 4 m².

The results for the base case are shown in Fig. 7 and 8. The main contribution to the force acting on the reactor vessel is due to the pressure exerted at the circular area opened by the vessel rupture. It is represented by the second term in the above equation. A moderate contribution is caused by the wave force, represented by the first term in the equation. The influence of the momentum described by the right most term is very small. The total force F is about 300 MN at the beginning of the blowdown and decreases rapidly to a value of 50 MN within 0.2 s (Fig. 7).

After a rapid equalization phase a pressure load of about 3.0 MPa is lasting for more than 1 s in the reactor cavern (Fig. 8). It causes an additional load of about 70 MN on the reactor vessel annular supporting frame, assuming 25 m² of exposed area of the supporting frame. However, when this load occurs the maximum of the force F is already over. Another result for the base case shows that 25 ms after the rupture the lower head hits the bottom grid with a kinetic energy of nearly 150 MJ.

Several parameter variations have been studied concerning break opening area, relief opening area, lower head distance to the bottom grid, and the initial conditions of the fluid [14]. Summarizing the results, the maximum force is nearly proportional to the break opening area, whereas the subsequent force is sensitive to the lower head distance to the bottom grid and the initial fluid conditions. The relief opening area is of minor influence. Since the assumed break opening area is almost identical with the cross section of the reactor vessel, the calculated maximum force represents roughly an upper limit. Checks based on simpler calculations which can be carried out by hand confirm this statement.

Right now research activities are under way to check, whether realistic break openings might be smaller. However, it is highly questionable whether the results will allow to rely on smaller maximum forces.

To prevent an upward movement of the reactor vessel, its supporting structure must be reinforced. Assessments show, there are no apparent reasons which would negate the technical feasibility of such improvements [2, 3].

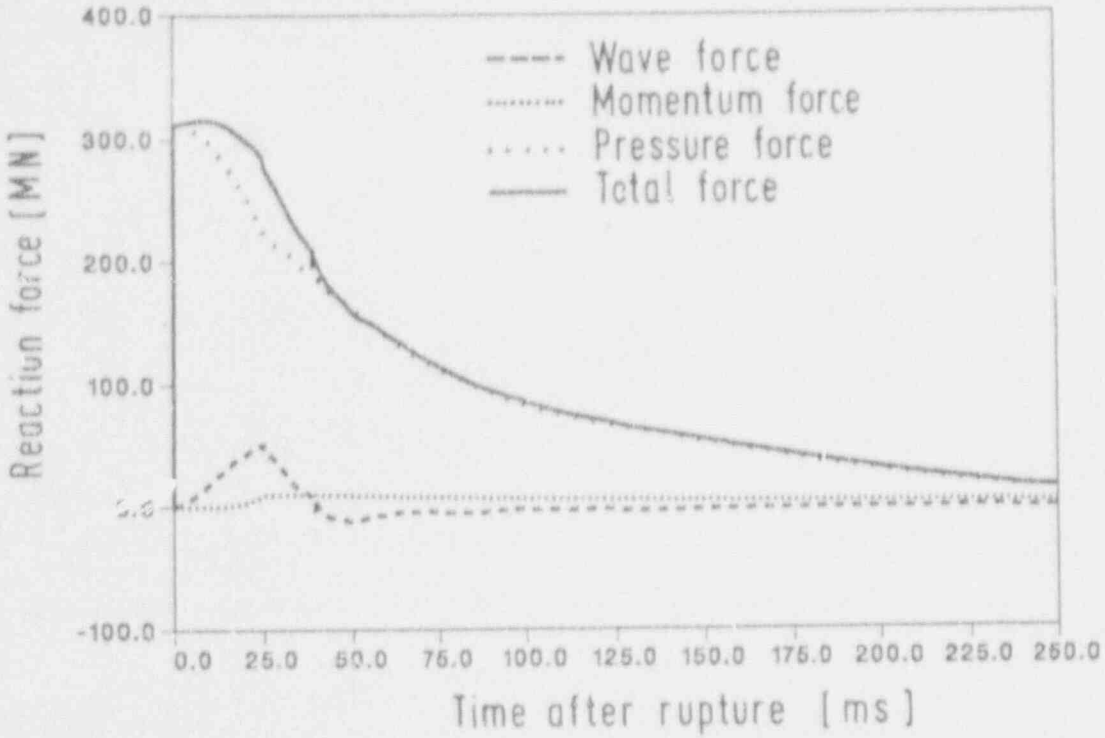


Fig. 7: Reaction force on the reactor vessel during blowdown

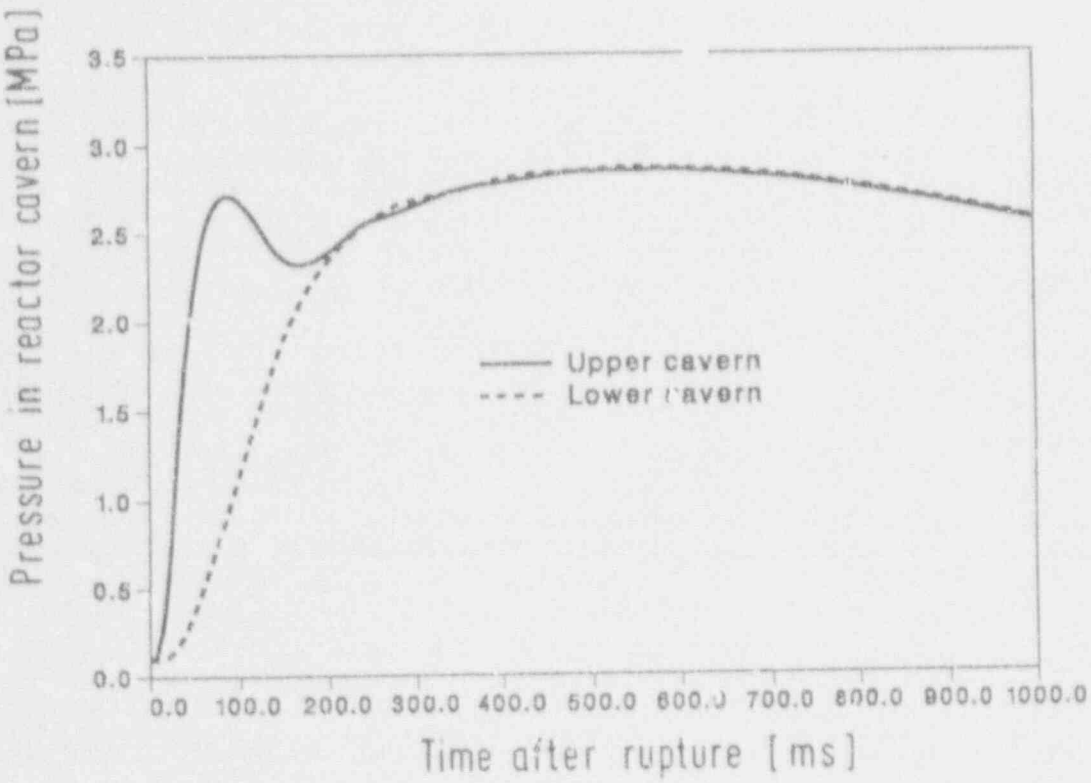


Fig. 8: Pressure build up in the reactor cavern during blowdown

## 4. CORE CATCHER CONCEPT

The core catcher is an inevitable part of the new containment concept [15] and has to cope with the core material after penetration of the lower head of the reactor vessel under all conceivable severe accident conditions. The core catcher must allow for

- the safe enclosure of the ex-vessel corium in a predefined location in order to exclude penetration of the basemat and attack of important structures and
- the removal of decay heat which corresponds to a level of 25 MW initially and 10 MW in the long term for a 1300 $MW_{el}$ reactor.

In this context it is important to consider the behavior of the less volatile fission products which are still dissolved in the melt after the accident. They only will remain in the core material if the long-term temperature of the corium is low enough, i.e. considerably below 2000 K, to exclude vaporization release over a long period of time. This imposes a more specific cooling condition on the heat extraction from the core material: besides the necessary decay heat removal the highest temperatures in the bulk of the material must remain below the vaporization temperatures of the fission products. Therefore, complete solidification of the core material is a goal to be achieved in this design.

The core catcher shown in Fig. 9 is designed to cope with both high pressure and low pressure core melt scenarios. The geometric dimensions are determined by the amount of surface needed for the cooling device and by the space needed for the reduction of the pressure in case of a reactor vessel failure under high pressure. Coolability is achieved by spreading and fragmentation of the molten masses in order to create large surfaces for sufficient heat transfer. Direct contact with water supply from the bottom produces steam which flows through the pressure release openings located in the walls of the reactor vessel cavern into the containment hall. The reflux of the steam condensate from the inner containment shell establishes a self-circulating steam/water flow.

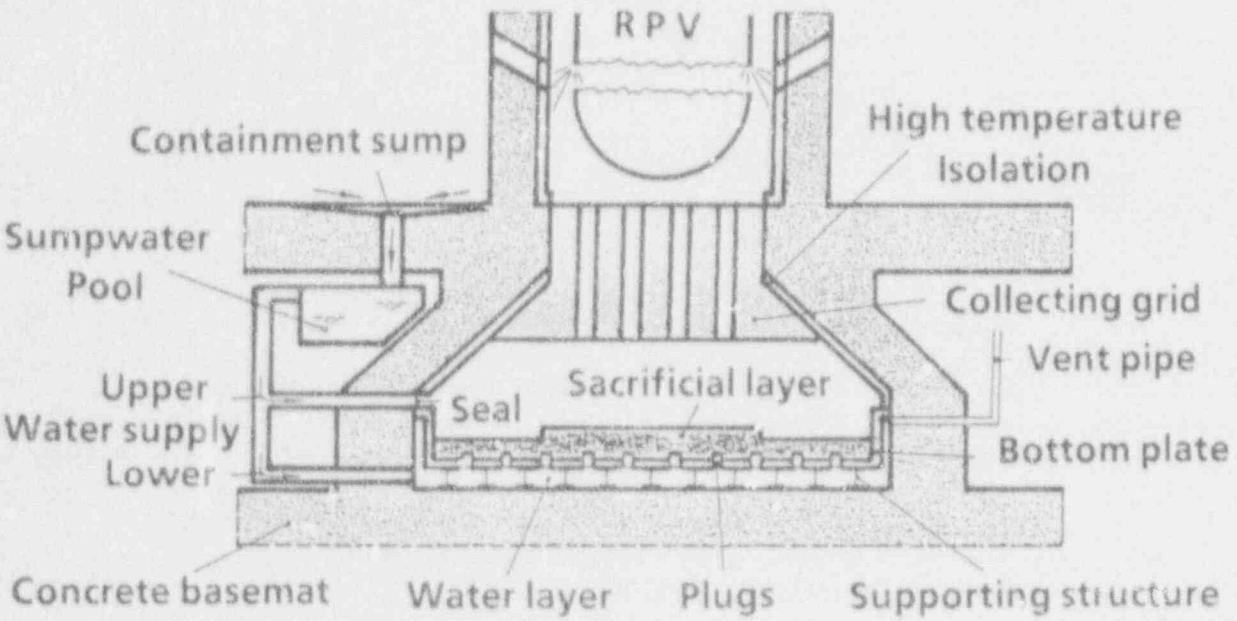


Fig. 9: Design principle of the core catcher

The key phenomenon for the safe operation of the core catcher is the process of flooding the melt from the bottom through melt plugs which are located in the sacrificial surface layer.

Prototype experiments in laboratory scale have been carried out with high temperature two component melts for a small segment of the core catcher. Complete flooding of the melt and early coolability within less than two to five minutes have been observed where the water supply rate exceeds the rate needed for the decay heat removal, by more than an order of magnitude. The melt formed a porous structure in the solidified oxidic and metallic layers, allowing continuous coolant supply and long term heat removal by evaporation.

Further experiments are presently on the way to visualize and optimize the fragmentation and safe coolability of the core melt. Future experiments will simulate the long term behavior in a scale large enough to allow extrapolation to the reactor scale.

## 5. CONCLUSIONS

The research work already carried out or under way will be sufficient to prove that the extreme loadings of the inner structures discussed above will not endanger the integrity of the containment. The most severe problem represents the in-vessel steam explosion. Here, the described experimental work is necessary. In contrast to this the investigations of the melt-through-failure of the reactor vessel under high pressure has already reached a satisfactory state. Open problems may be due to (smaller) missiles caused by other types of explosions and collapsing inner structures. Here adequate investigations are still required.

## Acknowledgement

The authors would like to thank B. Dolensky and Y.S. Hoang of the 'Institut für Reaktorsicherheit des Kernforschungszentrums Karlsruhe' and H. Cüppers and M. Ebner of the 'Institut für Massivbau und Baustofftechnologie der Universität Karlsruhe' for their substantial support.

## References

[1] J. Eibl et al., "An Improved Design Concept for Next Generation PWR-Containments", Proc. 4th Workshop on Containment Integrity, Washington, DC, May 12-14, 1992

[2] J. Eibl, "A New Containment Design for PWR's", Proc. 3rd Int. Sem. on Containment of Nuclear Reactors, Los Angeles, CA, Aug. 10-11, 1989, pp. 88-98

[3] H.H. Hennies, G. Kessler, J. Eibl, "Improved Containment Concept for Future PWR", Int. Workshop on 'Safety of Nuclear Installations of the Next Generation and Beyond', Chicago, IL, USA, Aug. 28 31, 1989

[4] B. Kuczera, "Investigations Relating to Improved Containment Concepts for Next Generation PWR Plants", ANS Int. Topical Meeting on Safety of Thermal Reactors, Portland, Oregon, USA, July 21-25, 1991

[5] H. Alsmeyer et al., "Improved Containment Concept for Future Large LWR's", IEA Int. Conf. on Technology Responses to Global Environmental Challenges, Kyoto, Japan, Nov. 6-8, 1991

[6] R. Krieg, "Can the Acceptance of Nuclear Reactors be Raised by a Simpler, More Transparent Safety Concept Employing Improved Containments?", Proc. 4th Int. Sem. on Containment of Nuclear Reactors, Shanghai, China, Aug. 14-16, 1991, pp. 51-73

[7] T.G. Theofanous et al., "An Assessment of Steam-Explosion-Induced Containment Failure". Part I - IV, Nucl. Sci. Eng. 97 (1987) 259-326

[8] H. Jacobs, "Steam Explosions during Light Water Reactor Meltdown Accidents", Proc. 3rd Int. Sem. on Containment of Nuclear Reactors, Los Angeles, CA, Aug. 10-11, 1989, pp. 302-320

[9] W.R. Bohl, "An Investigation of Steam-Explosion Loadings with SIMMER-II", Los Alamos National Laboratory Report LA-10639-MS, March 1990

[10] Gesellschaft für Reaktorsicherheit, Deutsche Risikostudie Kernkraftwerke, Phase B, Verlag TÜV Rheinland, Köln 1990

[11] N.I. Kolev, "IVA3: A transient 3D, Three-Phase, Three-Component Flow Analyzer", Proc. Int. Topical Meeting on Safety of Thermal Reactors, Portland, Oregon, July 21-25, 1991, pp. 171-180

[12] H. Jacobs and R. Krieg, "Discussion of Steam Explosion Structural Consequences in German Pressurized Water Reactors", Proc. 3rd Int. Sem. on Containment of Nuclear Reactors, Los Angeles, CA, Aug. 10-11, 1989, pp. 321-331

[13] K.E. Carlson, C.M. Allison et al., RELAP5/MOD3 Code Manual, NUREG/CR-5535, EG&G Idaho, Inc. (1990)

[14] G.J. Jacobs, "Load Behavior During Reactor Pressure Vessel Blowdown at High Pressure', ANS Winter Meeting, San Francisco, Trans. of ANS, Vol. 64, 1991, p. 670

[15] H. Alsmeyer, W. Tromm, "A Core Catcher Concept and Basic Experimental Results", Proc. Int. Topical Meeting on Safety of Thermal Reactors, Portland, Oregon, July 21-25, 1991

# AN IMPROVED DESIGN CONCEPT FOR NEXT GENERATION PWR CONTAINMENTS

J. Eibl, F.H. Schlüter, T. Klatte
( Consulting Engineers Karlsruhe )

W. Breitung, F. Erbacher, B. Göller, R. Krieg, W. Scholtyssek, J. Wilhelm
( Kernforschungszentrum Karlsruhe )

## Abstract

Considering the tremendous energy demand of a fast growing world population nuclear energy generation cannot be avoided. The safety of nuclear power plants can be increased by building strengthened containments, which will be able to withstand even severe core-melt accidents. Consequently, for a new containment design high static and dynamic internal overpressures must be taken into account. The design concept includes installation of a core catcher system and the removal of decay heat in a passive manner. Furthermore, several failure mechanisms of the reactor pressure vessel must be considered in the concept. Three design alternatives with different wall structures and cooling systems are demonstrated. The analysis of the long term thermo-hydraulic behaviour and the determination of the loads resulting from hydrogen combustion are important factors for the containment design.

## 1. IMPROVED DESIGN CONCEPT *

### 1.1 Why new PWR-Containments ?

The following table shows the expected growth of the world population for the year 2060 which can be estimated rather correct as parts of this population are already borne.

**Table 1.1 World Population**

| | 1990 | 2060 |
|---|---|---|
| Developed Countries | $1.2 \times 10^9$ | $2.0 \times 10^9$ |
| Undeveloped Countries | $3.8 \times 10^9$ | $6.0 \times 10^9$ |
| Total | $5.0 \times 10^9$ | $8.0 \times 10^9$ |

Today the energy consumption in [ kW x Years / Year ] is ( see also [1.6],[1.7] ) :

| | | | | | |
|---|---|---|---|---|---|
| US | 11 | kW | CHINA | 0.6 | kW |
| EUROPE | 4 | kW | REST | 0.45 | kW |

* J. Eibl, F.-H. Schlüter, T. Klatte, J. Wilhelm

This figures allow the prognosis, that within a very short period of time a tremendous amount of additional energy will be needed to give anybody a value of about 0.7 kW, which to experts opinion is necessary, to allow a low, but acceptable standard of living. Without the latter, social security of most human beings is only guaranteed by membership in a big family without any chance for birth control. Because this energy demand cannot be gained by wind energy and probably not by solar energy at a cheap price within the available time, we have to live with nuclear energy, if big environmental and social problems are to be avoided.

Now, is the risk connected with nuclear power acceptable? Risk is usually defined as the product of the ocurence of an unfavourable event times the resulting damage consequences. According to German Risk Studies severe core melt accidents have a probability of occurence of about $10^{-6}$ / Year for an assumed low pressure failure of the reactor pressure vessel and $10^{-7}$ / Year resp. $10^{-8}$ / Year for a high pressure failure. This are more or less the limiting probabilities of all severe accidents, which in general are very low. The appropriate resulting damage however is very large (see e.g. a recently done investigation by Keßler/Ehrhardt [1.8]) and the risk defined above as the product of the two factors is even increasing with failure scenarios adjoined to decreasing probabilities of occurence. The reason is that the consequences of failure rise faster then the probability of failure reduces with more serious scenarios. This is probably the reason why the public in many cases does not accept the risk connected with nuclear power plants. The public has a sound feeling for this here analytically discussed risk problem beyond practical experience.

To the authors opinion the only solution of this problem is to cut off, i.e to limit the consequences of failure. A further reduction of the probability of failure occurrence without a definite limitation of the failure consequences is neither economically justified nor will it lead to public acceptance. We have to convince people that in spite of a severe core melt accident, even if it happens with only a low probability of occurrence, there will be no severe harm to them due to a nearly deterministic "safe" containment. In probabilistic terms one can argue that containments as civil engineering structures have in principle a probability of failure in the range of $10^{-5}$ to $10^{-7}$ / Year so that according to the relation

$$p_f = p_{fcont} \times ( p_{fsys1} + p_{fsys2} + \ldots . ) \qquad ( 1.1 )$$

also the probabilistic safety is dramatically raised by a reasonable designed containment.

## 1.2 Design Proposals for Containments

### 1.2.1 Governing Parameters for Design

The aim of our design is to keep away any severe harm from the public and the environment even in case of a severe core melt accident in the above discussed sense. In a cooperation between the authors and the Nuclear Research Center at Karlsruhe (KfK) the following problems and actions have been identified as decisive and will be discussed partly in the following chapters (see also [1.1]--[1.5] and [1.9]) :

- Static internal overpressure mainly due to hydrogen deflagration ( 2.0 Mpa )

- Dyna[illegible] internal overpressure due to hydrogen detonation ( 10 Mpa / 12 ms )
- Failure of the reactor pressure [illegible]ssel ( see Figures 1.6 and 1.7 ) due to
  - High system pressure
  - Ste[illegible]xplosion
- Insta[illegible] of a core catcher system
- Passive [illegible]oval of decay heat
- [illegible] tig[illegible]sure of all penetrations
- [illegible]d dis[illegible]embly and removal of the power plant

[illegible]ned in detail all given values are intended to be upper boundary values exceeding [illegible]y further discussion.

### 1.2.2 [illegible]ternatives

At the time be[illegible] and regarding the authors professional status it cannot be their task to design reactor[illegible] reactor containments finally. There intention is just to investigate the feasibility of conta[illegible] structures fulfilling the abov[illegible]ulated conditions. Details have only been investigat[illegible] with regard to this aim[illegible]es being completely open for final design by competent engineers.

Figures 1.1 to 1.5 show the pri[illegible]al relevant alternatives C1, C2 and C3 in historical order. They all have i[illegible] common

- a core catcher sys[illegible] loc[illegible] underneath the reactor pressure vessel, and connected with the bo[illegible]m plate [illegible] the above arranged pressure vessel enclosure also against uplif[illegible],
- a strong outer concrete shell designed against external events as explosions, aircraft impact etc. as well as internal events.

In case of C1 the contaminated steam resulting from core catcher cooling remains within an internal loop between core catcher and steel shell, while the contained decay heat is transferred to the surrounding steel shell and will be removed from there by passive air cooling from the outside. The same is true for alternative C3, while in alternative C2 water inside the core catcher system will be used to transport the decay heat by natural convection via a steel wall into an outer water pool, a cooling tower or a similar device. The latter system C2 is therefore called water cooled to distinguish it from the air cooled systems C1 and C3.

**Alternative C1**

According to Figure 1 the internal static pressure of 2 MPa is taken by a composite wall structure consisting of an inner steel shell with 40 mm thickness and an outer concrete shell of about 2.0 m. The acting pressure is covered to about one third by the steel shell and to about two thirds by the outer concrete shell. The dynamic pressure resulting from a postulated hydrogen detonation is initially taken by the inner steel shell in tension. When the increasing radial displacement due to internal pressure or temperature rise will close the small gap between steel shell and supporting steel elements (which are anchored into the outer concrete shell), the

main part of the dynamic loading will be carried by the outer concrete shell. Internally generated impacting missiles have to be retained by the steel shell.

The circular gap between both shells is divided by radial elements, in short distances to limit bending of the steel shell. These are forming a number of vertical chimneys which are able to passively remove the decay heat from the steel shell by natural draft. Furthermore every chimney is divided in two compartments, the inner of which is filtered via the plants central chimney (about 150 m high) to achieve reasonable air stream velocities on top of the concrete shell. The natural pressure gradient between both compartments guarantees leakage tightness under normal operation. By a reasonable device single chimneys may be closed if — in spite of the design aims — the steel shell and also the filter membrane in the compartments might be violated. According to thermodynamic calculations a cooling air stream seems to be necessary only over the height of the cylindrical part of the containment, while the filtered air stream has to be led also along the upper spherical part. Discussions came up wether it is not reasonable just to filter the chimneys in areas where pipes penetrate the shell.

**Alternative C2**

As in this case (Figure 1.2) the decay heat is removed by water cooling of the core catcher environment, the upper containment may consist of a concrete shell including a tightening liner. The latter needs a missile shielding respectively a detonation protection in form of a additional inner concrete shell, as already discussed. A third outer thin concrete shell allows filtering of leakage through the lined concrete under normal operation.

Still under discussion is the question wether a solution can be found to avoid liner straining due to temperature. Such a mean could help to save the expensive liner fixing by studs which from safety considerations is questionable. Prestressing of the main shell is connected with several problems, e.g. longtime corrosion, and is therefore not preferable.

**Alternative C3**

Design alternative C3 (Figure 1.3), still under investigation, consists of an outer concrete shell which carries the static internal pressure. On its inner surface air cooled steel elements are attached (Figure 1.4). With their inner side they form a liner which is in contact with steam in case of an accident. They are designed to carry also the acting static pressure. Every cooling cell is again divided in two compartments, the inner of which is filtered as in Case C1. Nevertheless each cell may be redundantly closed at the top to avoid environment pollution in case of leakage.

With regard to its function as a leak tight liner these cooling cells may be fixed to the concrete shell in rather large vertical distances. As they are very stiff, buckling due to vertical temperature restraint is not a major problem. In horizonal direction folds in the steel decks avoid temperature stresses. Stud connections between liner and concrete, which are expensive and sometimes disadvantageous, are avoided to a high extent.

The air ducts are designed to remove the whole decay heat passively. Nevertheless water spraying from above into these ducts, if available after a few days to decrease the internal

pressure in a simple manner with regard to leakage under long time internal pressure.

The complete cooling arrangement including the liner are protected against missile impact and hydrogen detonation by a second inner concrete shell. Openings inside this shell will allow a comparatively slow gas flow, thereby enabling the steam to contact the cooling elements. However, the detonation pressure will be reflected to the containment's interior without a significant pressure rise behind the protecting walls. Similar structures are used for military structures designed against fast travelling shock waves. The advantage in comparision to the steel shell in case C1 is, that now a concrete mass is activated from the beginning loading to resist the impulse, while in the other case a steel shell with only little mass is used.

### 1.3. Reactor pressure Vessel Failure

Basing upon the German SIEMENS\KWU Convoy type PWR-reactor the acting loads in the reactor pressure vessel environment are labelled in Figure 1.6 and 1.7 as evaluated and estimated by KfK.

With respect to the so called "High Pressure Path" the following failure modes have been discussed:

- A circumferential separation of the upper spherical cap
- A circumferential separation of the lower spherical cap
- A longitudinal rupture of the cylindrical part along a straight generatrix

Until now these failure modes have been investigated only in a rather rough manner trying to decide on the principle feasibility; more detailed studies are under investigation.

It could be shown that the upper spherical cap can be kept in place by a retaining device which is designed for 300 MN. This device and the surrounding prestressed concrete cylinder are also capable of taking the pressure resulting from a steam explosion. This relevant force has to be transmitted from the pressure vessel to the supports at the surrounding concrete cylinder. The reaction forces inside the concrete wall are taken by unbonded prestressing cables connected with mild reinforcement at their lower end carrying the anchor forces to the core catcher and the bottom slab below.

The horizontal rocket forces resulting from vessel rupture along a vertical generatrix can be taken by the concrete cylinder using either prestressed or mild reinforcement in circumferrential direction.

Immedeately below the bottom of reactor pressure vessel a strong reinforced concrete grid is arranged which allows the core melt to pass through into the core catcher device and which is necessary to stop the downward moving end cap in case of separation due to high pressure failure or due to an in-vessel steam explosion.

## 2.PASSIVE DECAY HEAT REMOVAL SYSTEM *

The long term task of the containment is to evacuate the decay heat while maintaining its barrier function against radioactivity release into the environment. For this purpose, the containment must be designed to survive essentially unharmed the mechanical, chemical and thermo-hydraulic loads which may result from events occuring during the early transient post-accident phase. Moreover, its design must be capable of converting the transient situation into a quasi-stable one which can be controlled over a very long period and during which maximum thermo-hydraulic loads may not exceed critical values.

A quasi-stable configuration is reached when, after primary system failure, the core melt is quantitatively collected in the core catcher and quenched by sump water. The core catcher concept aims at a high retention of radionuclides in the debris bed. Consequently, the decay heat will be released mainly into the sump. It is transferred into the containment atmosphere by evaporation and will be distributed onto surfaces of internal structures and the containment hull by condensation. The condensate is recirculated into the sump, thus a continuous cooling system of the debris bed is maintained.

Heat removal from the building is achieved by cooling of the containment hull with an air flow operating in the gap space in a passive, natural convection mode. An important condition for the new containment concept is that, also in a severe accident case, any leak flow from the containment should be filtered before reaching the environment. This condition lead to various gap designs, of which two solutions are roughly depicted in Figure 2.1. In a first version, the complete coolant flow passes through a filter. Very large filter areas, in the order of several hundred square meters, would be needed in order to keep the flow resistance reasonably low. In version B (Figure 2.1, right) all penetrations, which are assumed to be the principal sources for leakage, are grouped into a lower section of the gap which is sealed from the remaining gap space. Leakages are collected in the lower gap section and relieved to the environment through a filter. The cooling air flows along the penetration free section of the hull which can be considered as leaktight. Without filtering, mass flow rates in the gap space are increased by about one order of magnitude as compared to the filtered case. This decreases, for a given cooling power, the heat up span in the air flow and it improves the heat transfer from the hull into the gap.

### 2.1 Analysis of long term containment thermo-hydraulic behaviour

In order to estimate upper bounds for pressure and temperature development, the long term thermo-hydraulic behaviour of the containment was analysed based on geometrical and operational reactor data which are typical for a German KONVOI PWR (see also Table 2.1). The physical processes considered in the analysis are sump water boiling, vapour condensation on structures, heat transfer by convection and radiation between hull and shield, gravitation induced air flow inside the gap, heat conduction within the internal structures and the containment shield, and leakage from the containment.

---

* F. Erbacher, W. Scholtyssek

Figure 2.2 shows the principal heat flows in the containment for the two gap designs as a function of time after accident initiation. In the early phase, the internal structures provide the principal heat sink. The KONVOI PWR profits from an important internal concrete volume, about 13000 $m^3$, which efficiently delays temperature and pressure built-up. The maximum heat transfer rates through the hull are about 7 and 9 MW for the filtered and unfiltered flow respectively, being reached at about 15 and 7 days after beginning of the accident. The corresponding containment pressure curves are shown in Figure 2.3. Peak values of about 1.0 MPa and 0.48 MPa respectively, are reached. Corresponding temperature developments of the air inside the containment and in the gap are shown in Figure 2.4.

Extensive parameter studies have shown that the thermal-hydraulic evolution is rather sensitive to various system data, e.g. heat transfer characteristics and flow data in the hull-gap system, heat capacity of internal structures, nominal power of the reactor etc.. Since precise design data of future PWR containments are not yet available, the results of the analysis presented here must be considered as preliminary. However, with respect to the long term pressure evolution it may be concluded that a failure pressure of 2.0 MPa static as specified for future containments can be safely considered as an upper bound.

**Table 2.1. Input Data for Thermo-Hydraulic Analysis**

| Parameter | Value |
|---|---|
| free containment volume | 71200 $m^3$ |
| internal concrete volume | 13200 $m^3$ |
| sump water volume | 1600 $m^3$ |
| effective hull area | 6500 $m^2$ |
| gap flow area | 120 $m^2$ |
| gap height | 40 m |
| reactor thermal power | 3670 MW |
| full power days | 585 d |
| leak rate | 1.0 Vol % / day |
| environment temperature | 20 °C |
| heat transfer coefficient<br>inner hull face<br>outer hull face | <br>$h_{c,i} = 11 + 280\ X\ W / m^2$ a)<br>$h_{c,o} = 5.6 + 4\ v\ W / m^2$ b) |
| emissivity of hull and shield | 0.5 |

a) X = mass ratio steam-to-air

b) v = air velocity in gap ( m/s )

## 3. LOADS FRO[illegible] HYDROGEN COMBUSTION *

Hydrogen is generated in severe accidents anytime hot reactive metals (Zr, Cr, Fe) contact steam. Various processes can contribute to hydrogen generation as the accident progresses. These include slow in-vessel oxidation of metals, in-vessel steam explosions, direct containment heating, ex-vessel steam explosions, quenching of a degraded or molten core by water and core-concrete interactions.

Calculations and experiments have shown that large amounts of hydrogen can be produced rapidly in direct containment heating scenarios (400 - 680 kg in 5 seconds, [3.1]), in steam explosions (20-30 % of metal oxidized [3.2]), in flooding a degraded bundle (up to 80 % of total $H_2$ [3.3], [3.4]) or in quenching a metallic melt [3.5].

Slow processes like in-vessel Zr-oxidation may lead to high hydrogen concentrations if no ignition source is available, as e.g. in station black-out scenarios. Examples for the development of detonable mixtures are given in [3.6] and [3.7]. While igniters will definitely reduce the risk for some accidents, they cannot safely cover core-melt accidents with periods of fast hydrogen generation.

In order to be able to exclude containment failure from hydrogen combustions mechanistically, conservative limits for combustions loads must be found. The work described below considers any physically possible accident scenario, independent of its (anyway uncertain) probability. Because the response of a structure depends on the load duration, static and dynamic loads are distinguished.

### 3.1 Static loads

Deflagrations result in quasi-static loads because the load time is much greater than the response time of the containment structure. The static pressure is conservatively described by the adiabatic, isochoric, complete combustion (AICC) pressure.

To identify worst-cases the parameter space of hydrogen-steam-air mixtures must be investigated. Such (homogeneous) mixtures require four intensive variables to define the initial state. Two of them may be fixed by the following reactor-typical initial conditions:

- the air density is equal to the pre-accident air density ( ≈ 1 atm, 20 °C ), and
- the containment atmosphere is steam saturated.

This leaves as two free variables a measure for the hydrogen and the steam concentration, e.g. the equivalence ratio $\varphi$ (= $1/2\ p_{H_2} / p_{O_2}$), and the steam mole fraction $x_{H_2O}$ (= $p_{H_2O} / p_{total}$). The AICC-pressure was calculated for the complete composition space of flammable $H_2$-steam-air mixtures as a function of $\varphi$ and $x_{H_2O}$ [3.8], using the code CET89 [3.9].

---

* W. Breitung

Figure 3.1 shows that the AICC-pressure increases significantly with the hydrogen concentration and weakly with the steam content. The latter effect is due to the increasing initial pressure as $x_{H2O}$ raises. For a fixed equivalence ratio the highest burn pressure results from the mixture with the highest steam content which is still flammable. For near stoichiometric mixtures this limiting steam mole fraction is about 65 % (for T ≤ 410 K).

Upper limits for hydrogen generation were discussed in [3.10]. In a German PWR of the 1300 MWe class the assumption of 100 % zircalloy oxidation leads to about 1500 kg of hydrogen production. If some credit is given to possible stainless steel and $UO_2$ oxidation, as e.g. in the case of a high pressure vessel failure, total amounts of about 2000 kg $H_2$ can be envisioned. Systematic calculations exploring worst-case accident progression paths are needed for mechanistic estimates of the maximum possible hydrogen generation. A clearly defined upper limit is given by the available oxygen. In a free volume of 70 000 m³ NPT air not more than 2400 kg $H_2$ can be oxidized. So despite the current (and future) uncertainties in the accident progression phenomena, the maximum possible hydrogen mass is limited to the quite narrow region of 2000 to 2400 kg.

Assuming globally well mixed conditions the hydrogen limit (2000 kg in 70000 m³) gives $\phi$ = 0.82 and the oxygen limit gives $\phi$ = 1.00. The corresponding worst-case AICC-pressures are about 1.5 and 1.7 MPa respectively (see also Figure 3.1).

Locally any equivalence ratio is possible. Figure 3.1 shows that the highest AICC-pressure in the complete flammability range results from a hydrogen-rich ( $\phi \approx 6.5$ ), relatively dry ( $x_{H_2O} \approx 0.10$ ) mixture. Such mixtures can be generated locally under in-vessel steam starvation or reflood conditions. The corresponding AICC-pressure is about 1.9 MPa. This value represents a conservative upper limit because the local deflagration will not proceed isochorically, as assumed in the data of Figure 3.1. In a reactor-typical multiroom structure always some pressure venting into neighbouring compartments will occur.

The above assumptions lead to a static design requirement of 2 MPa for future core-melt resistant containments. A containment designed for this static load will withstand any slow hydrogen combustion.

## 3.2 Dynamic loads

Worst-case dynamic loads result from large scale detonations. Detonations must be included in the design requirements for strong containments because it is not possible to prove that detonations will not occur.

To identify limiting detonation loads the relevant parameter space must first be identified and then explored in a systematic way. Two different approaches are currently being pursued : a) single effect studies to better understand the phenomena and the significance of a given parameter, and b) construction and investigation of conservative, self consistent accident scenarios. A detonation event tree methodology was used in approach b).

Figure 3.2 shows the relevant parameter space. Conservative parameter values were identified

in single-effect studies [3.8] and combined to an accident sequence which results in apparently limiting global detonation loads [3.10]. The assumed sequence is the release of 2000 kg of hydrogen, stratification according to HDR test T31.5, 30 % steam content in the atmosphere ( 95 °C ), burn of 800 kg in lower compartments, compression of the unburned gas in the dome by expanding combustion products, detonation of the $H_2$ enriched dome gas, triggered by jet ignition when the flame front reaches the upper containment. The calculated normally reflected peak pressure reached 10.5 MPa (Figure 3.3), the detonation impulse was about 60 kPas (in 30 ms), applied over 1385 $m^2$. The one-dimensional model still contains a high degree of conservatism, which should be reduced by more realistic 3-D modeling.

An existing 3-D detonation code [3.11], originally developed for detonation cell size investigations, was recently modified and implemented at KfK to analyze confined large scale hydrogen detonations in complex geometries. The code solves the equations of inviscid, compressible gas flow with a chemical reaction in a 3-D Eulerian cartesian grid. The $H_2$ / $O_2$ reaction kinetics are described by a one-step mechnism with an Arrhenius expression. The kinetic parameters were benchmarked by comparing calculated and measured detonation cell sizes. A two-$\gamma$-model is used to describe the thermodynamic state of reactants and products.

Figure 3.4 shows some first test results for a detonation in a half-sphere of 25 m radius, containing some arbitrary obstacles. Shown is the pressure distribution in the vertical plane [ p ( x, y = 0, z ) ] and a horizontal plane [ p ( x, y, z = 5.6 m ) ]. Cross sections of the obstacles are visible in both planes. The grid depicts the used mesh size. Ignition occured underneath the hollow cylinder. The detonation propagates towards the right, the highest pressures occuring in the primary detonation front, at the reflecting sphere surface and in the wave intersection caused by the cylindrical obstacle.

This and other calculations with more realistic geometries have shown that the point of ignition and details of the geometry can strongly influence the magnitude and timing of local pressures. However, when averaged over several 100 $m^2$ the (global) loads seem not to be very sensitive towards these parameters. It appears that global loads mainly depend on the average combustion energy released per unit area of containment surface (MJ / $m^2$). The code is currently being used to evaluate upper bounds for global detonation loads in realistic 3-D geometries. The first results with a homogeneous mixture indicate impulses which are roughly a factor of 2 below the 1-D results described above.

## 4. STATIC AND DYNAMIC CONTAINMENT RESPONSE *

### 4.1 Static internal pressure

Under normal operating conditions a gap separates the steel shell from the outer concrete shell with the attached ribs. As the internal pressure increases, the steel shell is designed to contact the ribs. Now the structure behaves as a composite shell, i.e., the reinforced concrete shell also carries a part of the internal pressure.

---

* R. Krieg, B. Göller

In the first design the gap width between shell and ribs is chosen to be about 40 mm. Finite element calculations have shown that under the loss of coolant accident primary stresses in the steel shell remain in the elastic range, whereas secondary stresses due to thermal expansion can reach values beyond the elastic limit. As the latter stresses are not required for the equilibrium between the internal pressure and the resistance of the structure this is allowed according to present German KTA-rules. However, buckling of the steel shell under thermal expansion must be analysed carefully.

For pressures increasing beyond [illegible] where contact between shell and ribs occurs, the external concrete shell participates in carrying the loading. In combination with a mild reinforcement of 3% BSt 1100 the ultimate bearing capacity of this composite containment reaches values more than 2.0 MPa of static pressure.

## 4.2 Dynamic internal pressure

In the case of a hydrogen detonation a dynamic pressure pulse with a peak value of about 10.0 MPa is expected to occur. Figure 4.1 shows a typical pressure-time-history [4.1]. It is composed of a first spike due to the detonation having a pulse content of 28 kPas and of a nearly quasistatic pressure of 1.85 MPa due to heating up the containment atmosphere by the thermal energy of the chemical reaction. One has to assure that global effects as well as local effects due to this loading do not endanger the integrity of the containment.

Assuming that this loading is axisymmetric the deformation of the cylindrical part of the concrete shell has been calculated. Material non-linearities of concrete and reinforcement were taken into account. The resulting time history is shown in Figure 4.2. The maximum radial displacement is about 20 cm, the duration of one oscillation period about 120 ms. The comparison with the short duration pressure pulse of the loading shows that due to the large mass of the concrete shell the deformation does not depend on details of the time history of the loading but rather on the amount of the pulse, i.e. the resulting impulse.

In reality, for the first few milliseconds the loading is expected to occur only in a certain region of the shell. Consequently, the axisymmetric response will be smaller but the local response may be even higher. In any case it has to be discussed whether these deformations are acceptable. The dynamic response is expected to be smaller for the spherical part of the shell where the load carrying capacity is more favorable.

The dynamic response of the steel shell is quite different. Only a pressure of about 0.5 to 1.0 MPa is carried by the shell itself while the exceeding part of the pressure pulse is accelerating the steel shell until it impacts on the ribs. The deformation state of the shell primarily does not depend on the gloabal shape of the containment but rather on the distance between steel shell and ribs and on the stiffness of the ribs themselves.

The local behaviour of the steel shell and the supporting ribs has been analysed using nonlinear finite element calculations. Only one rib with the corresponding section of the shell was modeled and the concrete shell was assumed to be rigid. Two different gap widths between steel shell and ribs were considered.

For a gap width of 40 mm and very stiff ribs, the maximum strain in the steel shell after hydrogen detonation reaches values of about 4 %. Due to the thickness of the ribs with 40 mm buckling effects will not occur.

With respect to detonation loading a containment design with a small gap between shell and ribs is advantageous. But also for a gap width of 150 mm acceptable maximum strains in the containment shell can be achieved by softening the impact. This can be reached e.g. by ribs undergoing large plastic deformations under the impact of the shell. Figure 4.3 shows a corresponding computational result. A triangular pressure pulse of 10.0 MPa with 5 ms total duration, which describes approximately the first spike of the loading in Figure 4.1, accelerates the shell to an impact velocity of 69 m/s. Under the impact the ribs with only 10 mm thickness are compressed plastically by about 50 mm. The maximum strains in the shell are about 4 %.

This concept of ribs deforming plastically under the impact of the shell will be developed further aiming to limit the maximum strains in the shell to 2 %. Parameters for modification are the distance of the ribs to each other and their mechanical stiffnesses. Of course for thin ribs buckling effects may occur. This problem can be overcome by an appropriate corrugation of the ribs as shown in Figure 4.4.

In order to demonstrate that the ribs in the final design will indeed deform under the impact as calculated and that the maximum strains in the containment shell will indeed remain acceptably low, appropriate experiments are planned. A section of the shell covering some 4 or 5 ribs will be loaded by a high-explosive charge, thus simulating the pulse of the hydrogen detonation.

## 4.3 Leak-Tightness

Another problem is the proof of the containment tightness under the different accident conditions. Here well considered manufactoring and control conditions and well predictable stress and strain distributions are essential preconditions. But also constructive measures can contribute to ensure the containment tightness.

Therefore in Figure 4.8 containment penetrations having a potential for leakages from the containment into the annular space are concentrated in the lower region of the containment shell. Here the annular space is separated and any gas flow into the environment has to pass filters. The annular space in the upper region of the containment shell which covers most of the area of the containment surface is available for heat removal by natural circulation of the surrounding atmosphere as described above.

In the upper region the only reason for leakages could be cracks going through the whole wall thickness of the shell. However, taking in mind that currently applied crack detection methods are able to detect cracks having a depth of just a few millimeters, the existence of penetrating cracks can be ruled out.

The considerations mentioned above show that the loads due to a hydrogen detonation cannot be carried without plastic deformations in the steel shell. In the final containment design a reduction of the maximum strain from 4 to 2 % seems to be possible. As outside the shell unfiltered

environmental air might be flowing for decay heat removal, occurring of any leakage due to such deformations must be avoided. Therefore it has to be discussed, if leak-tightness of the steel shell can be guaranteed even under small plastic deformations.

In [4.2] some bulge tests with the containment steel 15MnNi63 are described, in which initially plane membranes were inflated up to failure. Figure 4.5 shows the experimental set-up, Figure 4.6 a specimen membrane after failure. In Figure 4.7 a comparison of measured and computed strains is depicted. The membrane finally had failed due to plastic instability at equivalent strains of about 50 %.

In order to study the behaviour of weldings under plastic strain uniaxial tensile tests with the containment steel were performed using large specimens having a thickness of 38 mm and a width of 500 mm [4.2]. The specimens included weldings in longitudinal and transversal direction as well. Uni-axial strains of up to 19 % occured in the specimens prior to failure. Additionally, bending tests of specimens including weldings were performed. Surface strains of 50 % were reached, without any surface crack detected.

These investigations show that leakages through the containment shell will not be caused by small plastic deformations. This statement should be confirmed by the planned experiments mentioned above. The sections of the shell used will contain some weldings done under reactor specifications.

## 4.4 External events

Considering the dimension and the reinforcement of the outer concrete shell it could be shown that a typical airplane crash of a phantom military aircraft or a gas cloud explosion, as required by German regulations, can be sustained by the presented design. Also an earthquake does not endanger the structure. The maximum relative displacement between steel and concrete shell is less than 4 cm for an earthquake with a ground acceleration of 2 $m/s^2$.

## References


[1.1] J. Eibl, H.-H. Cüppers, " Core-Melt-Proof Nuclear Reactor Containments - A New Generation - ", FIP-Symposium '92, Budapest, Hungary, May 11-14, 1992.

[1.2] J. Eibl, G. Kessler, W. Breitung, " A New Generation of Pressurized Water Reactors ", IAPSE Congress, New Dehli, India, March 1-6 1992.

[1.3] J. Eibl, F.-H. Schlüter, H. Cüppers, H.H. Hennies, G. Kessler, W. Breitung, " Containments for Future PWR-Reactors ", 11th Int. Conference on Structural Mechanics in Reactor Technology, SMIRT 11, Tokyo, Japan, August 18-23, 1991.

[1.4] B. Kuczera, H. Alsmeyer, R. Krieg, J. Eibl, " Considerations on Alternative Containment Concepts for Future PWR's ", 2nd Int. Conference on Containment Design and Operation, Toronto, Canada, October 14-17, 1990.

[1.5] H.H. Hennies, G. Kessler, J. Eibl, " Improved Containment Concept for Future PWR's ", Int. Workshop on Safety of Nuclear Installations of the Next Generation and Beyond, Chicago, IL, USA, August 28-31, 1989.

[1.6] K. Knizia, " Energie - Ordnung - Menschlichkeit ", Econ Verlag, Düsseldorf-Wien 1981.

[1.7] J. Schlaich, " How much desert does a coal need ? ", IABSE Proceedings, IABSE Periodica 2/1990.

[1.8] G. Keßler, J. Ehrhardt Private Comunications, Publication under Preparation, Karlsruhe, 1992.

[1.9] R. Krieg, H. Alsmeyer, G. Jacobs, H. Jacobs, " Extreme Loadings of Inner Structures of Next Generation PWR-Containments ", Kernforschungszentrum Karlsruhe, Report Fifth Workshop on Containment Integrity, Washington, May 12-14, 1992.

[3.1] D.C. Williams, K.D. Bergeron, D.E. Carroll, R.D. Gasser, J.L. Tills, K.E. Washington, " Containment Loads Due to Direct Containment Heating and Associated Hydrogen Behaviour: Analysis and Calculations with the CONTAIN Code ", Report NUREG/CR-4896, SAND 87-0633, (May 1987) p. 39.

[3.2] M.F. Young, M. Berman, L.T. Pong, " Hydrogen Generation During Fuel / Coolant Interactions ", Nucl. Science and Engineering 98 (1988) p. 1.

[3.3] A.W. Cronenberg, " Hydrogen Generation Behaviour in the LOFT FP-2 and Other Experiments : Comparative Assessment for Mitigated Severe Accident Conditions ", Nuclear Technology 97 (1992) p. 97.

[3.4] S. Hagen, P. Hofmann, G. Schanz, G. Schumacher , F. Seibert, L. Sepold, " Effects of Quenching on LWR Fuel Rod Behaviour Observed in the CORA Severe Fuel Damage Experiments ", ANS Int. Topical Meeting on Safety of Thermal Reactors, Portland, Oregon, USA, July 21 - 25, 1991.

[3.5] G. Schumacher, Test BETA V6.1, Personal communication, Kernforschungszentrum Karlsruhe, 1991.

[3.6] J.W. Yang, Z. Musicki, S. Nimnual, " Hydrogen Combustion, Control, and Value-Impact Analysis for PWR Dry Containments ", Report NUREG/CR-5662 (June 1991), p. 71, 113.

[3.7] Gesellschaft für Reaktorsicherheit, " Deutsche Risikostudie Kernkraftwerke - Phase B ", Verlag TÜV Rheinland (1990), p. 64.

[3.8] S.R. Tieszen, " Effect of Initial Conditions on Combustion Generated Loads ", Proc. 4th Intern. Seminar on Containment of Nuclear Reactors, August 14 - 16, 1991, Shanghai, China, p. 187, Held in conjunction with the 11th Conf. on Structural Mechanics in Reactor Technology (SMiRT-11), Tokyo, Japan, August 18 - 23, 1991.

[3.9] CET89-Chemical equilibrium with transport properties, 1989 ( NASA Lewis Research Center ), Program Nr. LEW-15113 Computer Software Management and Information Center (COSMIC) University of Georgia, 30602 Georgia, USA.

[3.10] W. Breitung, Conservative Estimates for Dynamic Containment Loads from Hydrogen Combustions", Proceedings as in [4.8], p. 219.

[3.11] A. Efimenko, A. Kochurko, S Dorofeev, A. Chugunov, " 3ET and TWOL. Code Description and User Guide ", Report IRIS 91/6, Scientific Research and Development Org. " Industrial Risk ", Kurchatov Institute, Moscow, Russia ( Jan. 1992 ).

[4.1] B. Göller, R. Krieg, G. Messemer, E. Wolf, " On the failure of spherical steel containments under excessive internal pressure ", Nuclear Engineering and Design, Vol 100, (1987), pp. 205-219.

[4.2] Staatliche Materialprufungsanstalt an der Universität Stuttgart, " Zugversuche mit geschweißten Großplatten ", December 1978, Internal Report.

[4.3] H. Alsmeyer, W. Breitung, H. Cüppers, J. Eibl, F.J. Erbacher, B. Göller, H.H. Hennies, H. Jacobs, G. Jacobs, G. Kessler, R. Krieg, W. Scholtyssek, " Improved containment concept for future large LWR's ". IAEA International Conference on Technology Responses to Global Environmental Challenges, Kyoto, Japan, November 6-8, 1991.

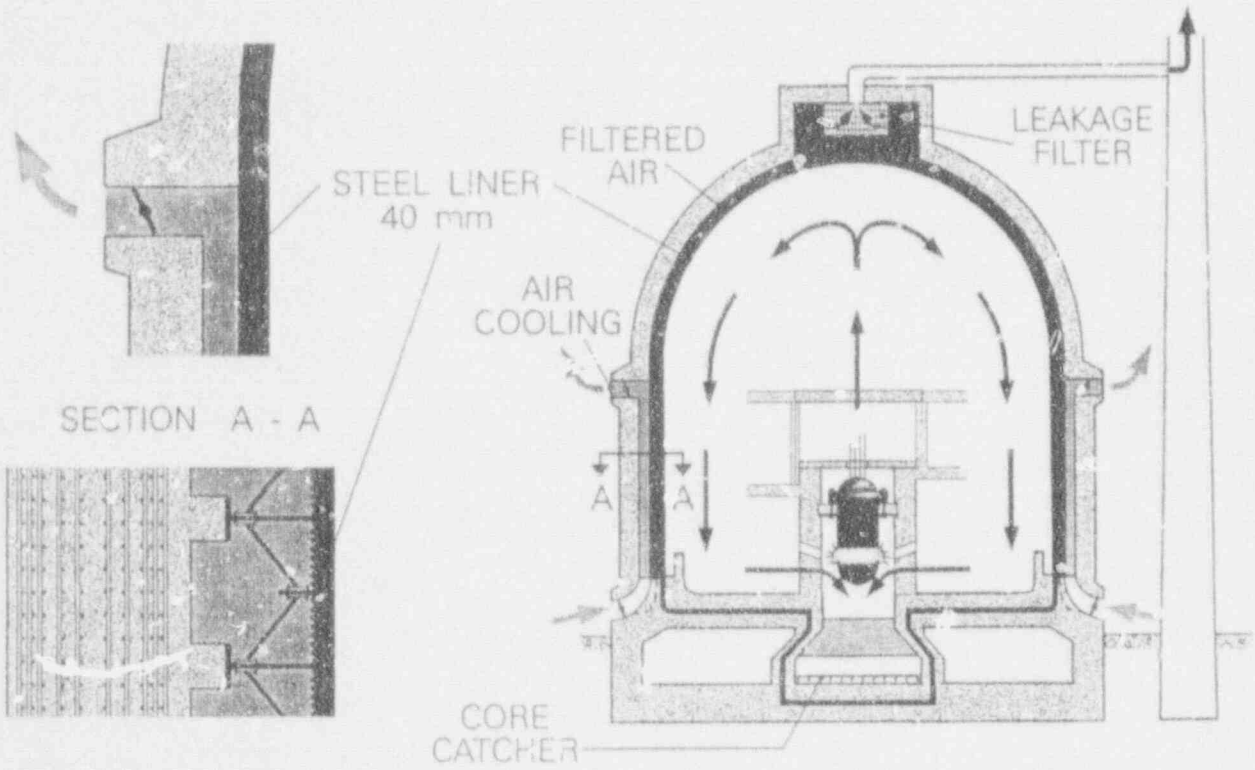


**Figure 1.1** Proposed Containment Design - Alternative C1

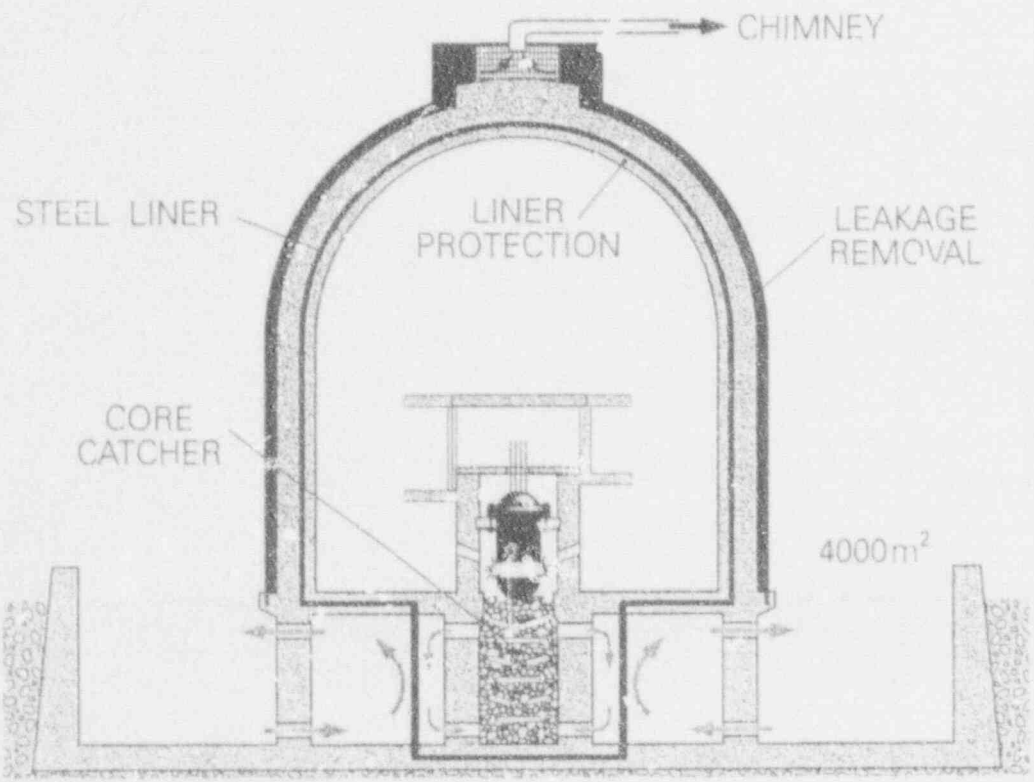


**Figure 1.2** Proposed Containment Design - Alternative C2

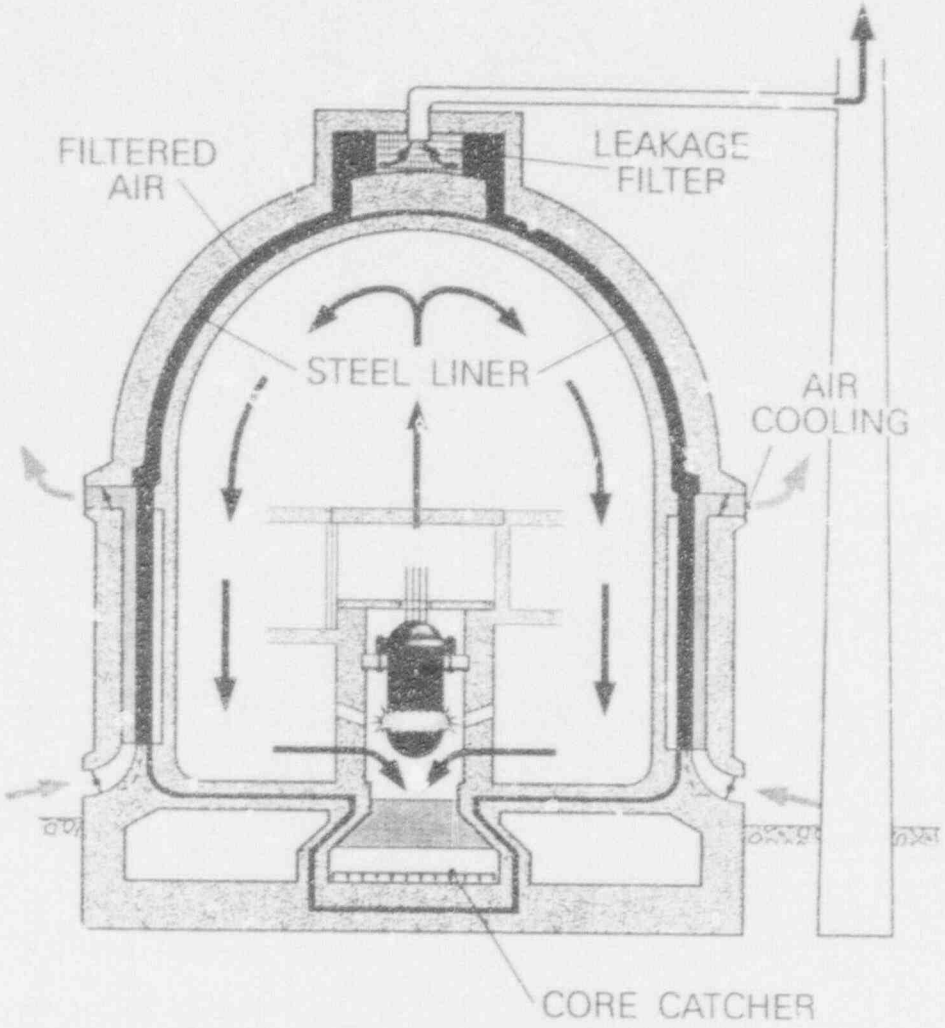


**Figure 1.3** Proposed Containment Design - Alternative C3

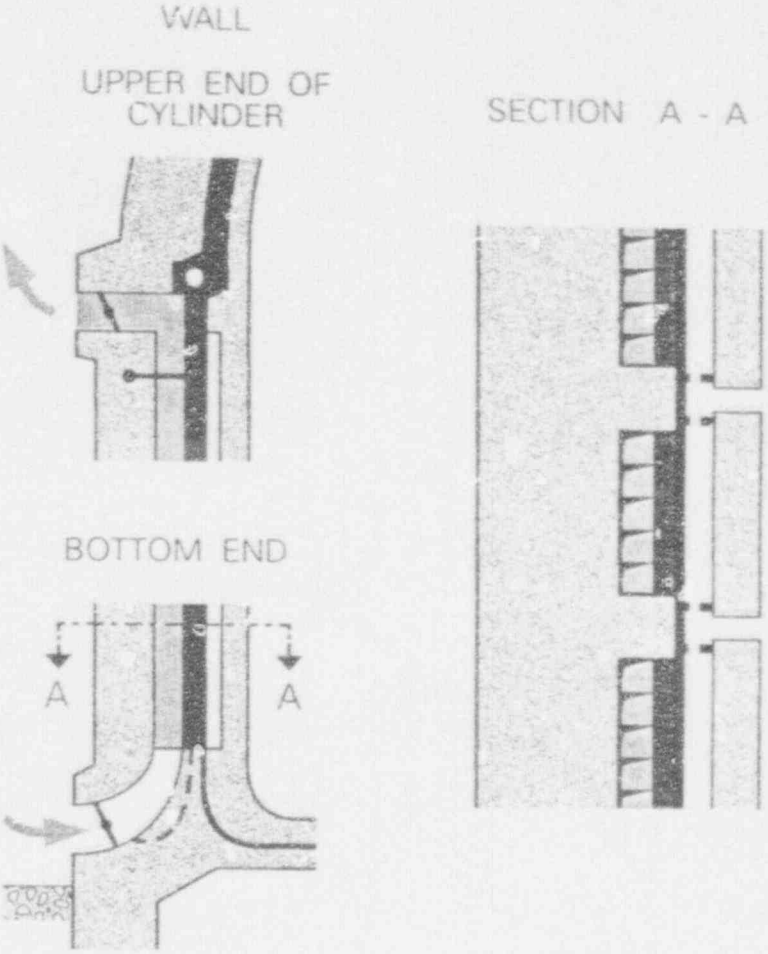


**Figure 1.4** Alternative C3 - Details of Wali Structure

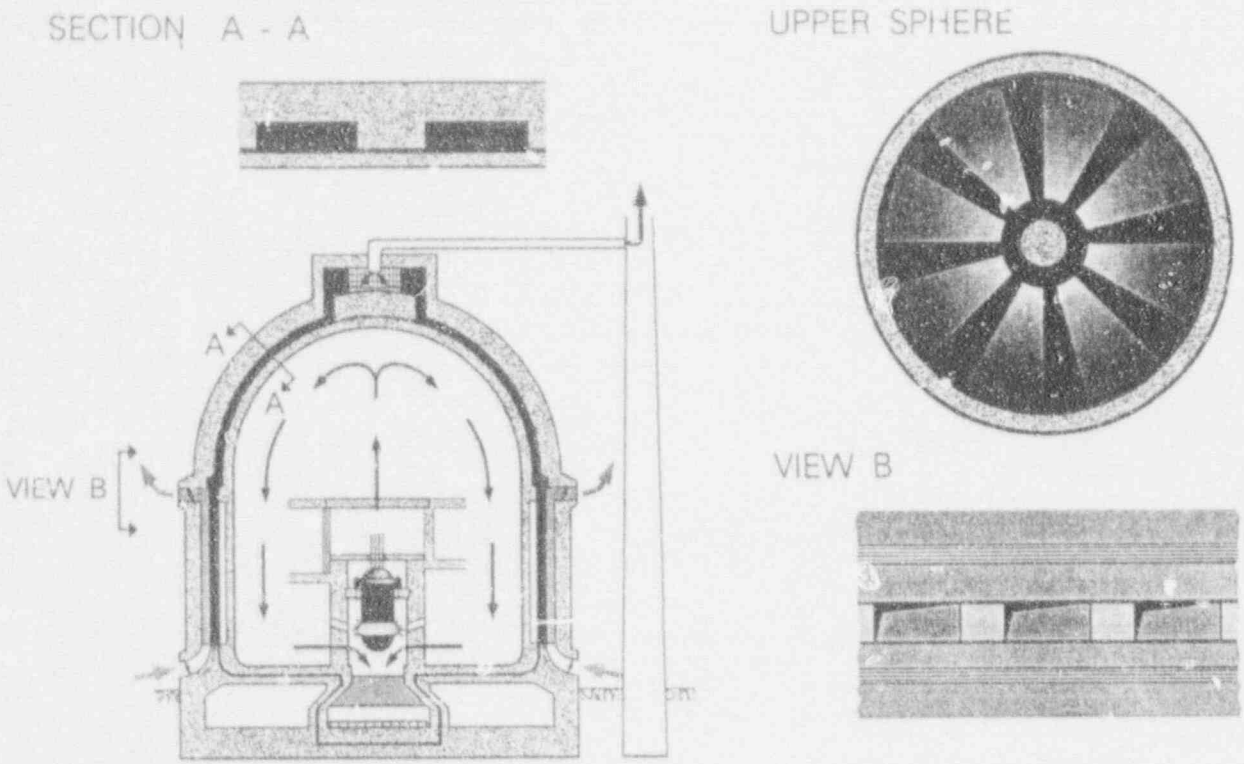


**Figure 1.5** Decay Heat Removal

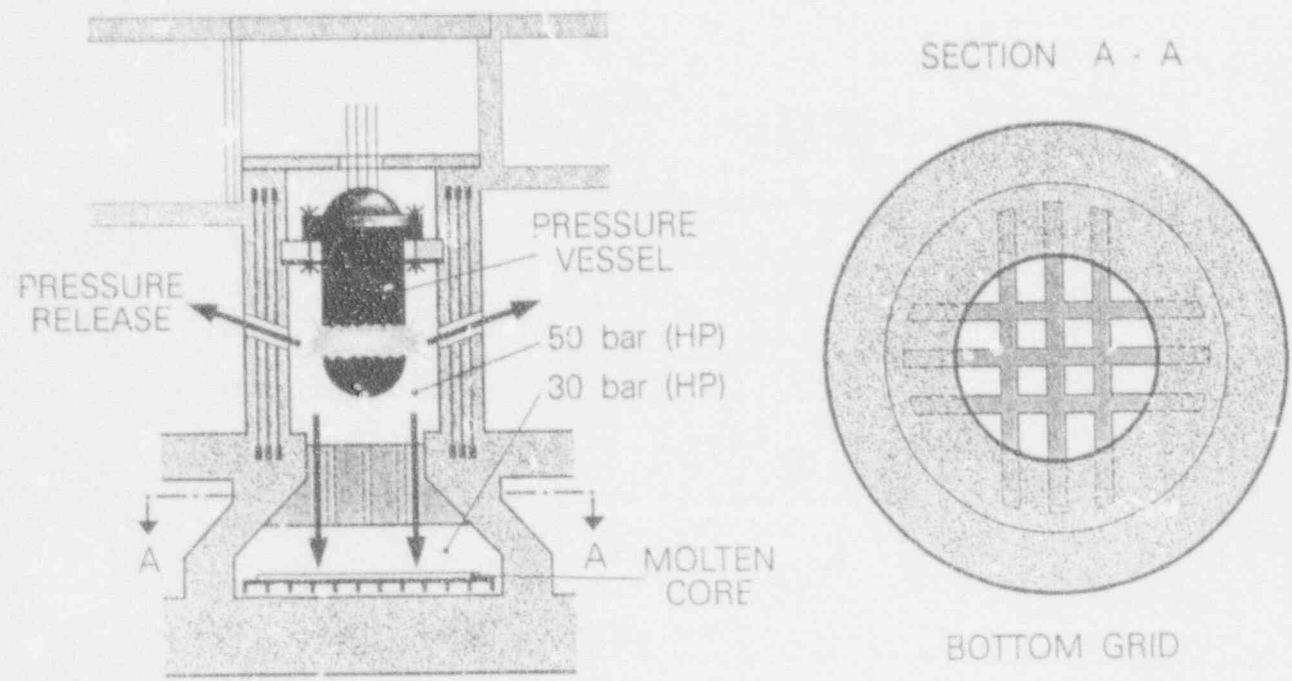


**Figure 1.6** Reactor Pressure Vessel Environment - Assumed Pressure Loadings

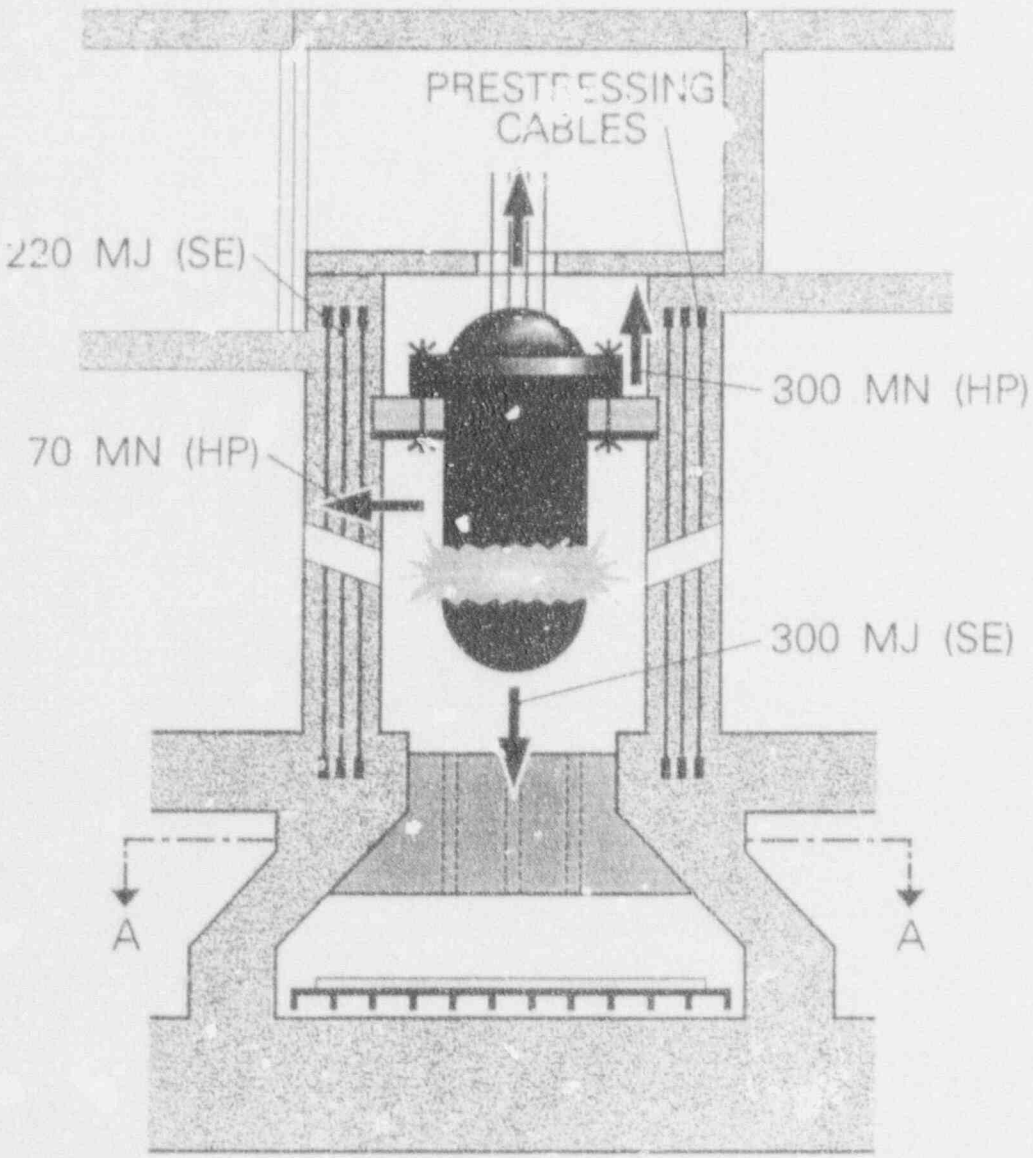


**Figure 1.7** Reactor Pressure Vessel Environment - Assumed Impact Loadings

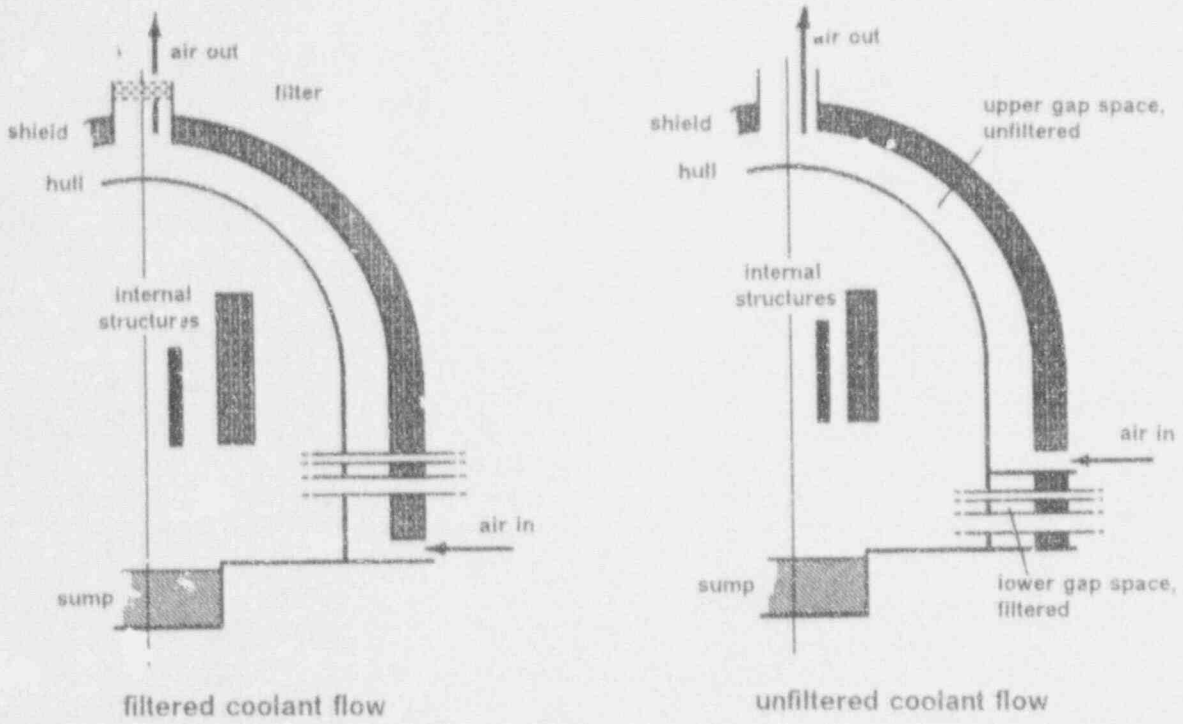


Figure 2.1 Gap Designs for Natural Convection Air Flow

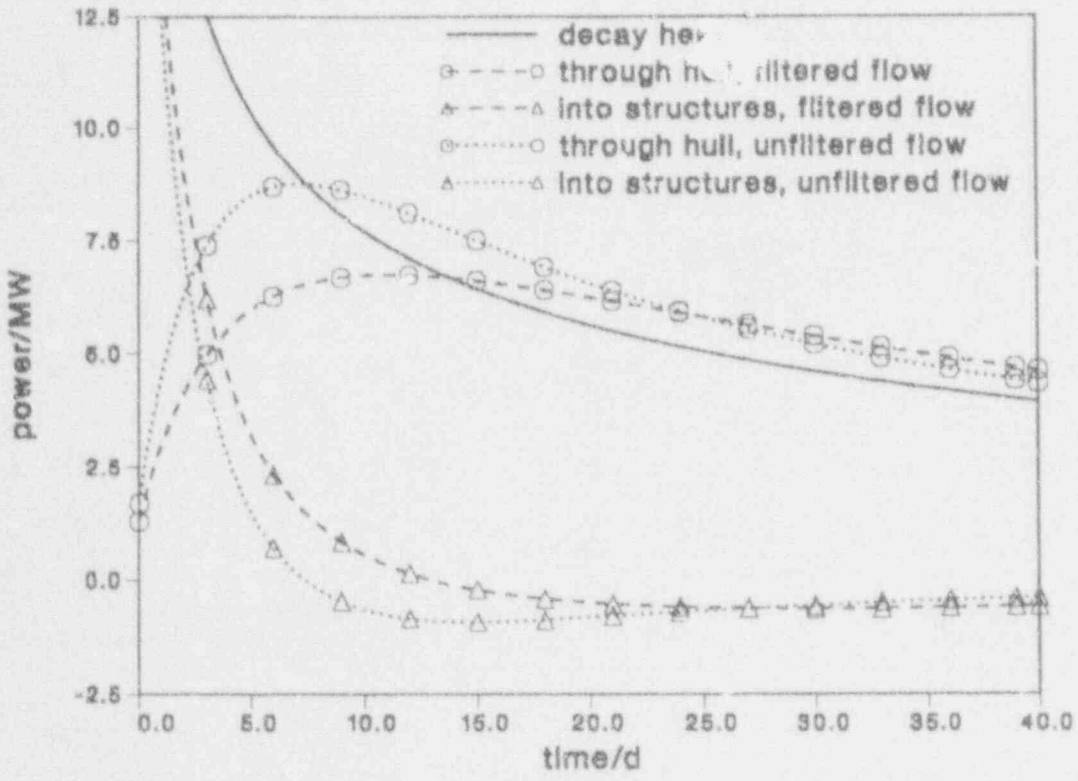


Figure 2.2 Heat Flow Rates with Passive Containment Cooling

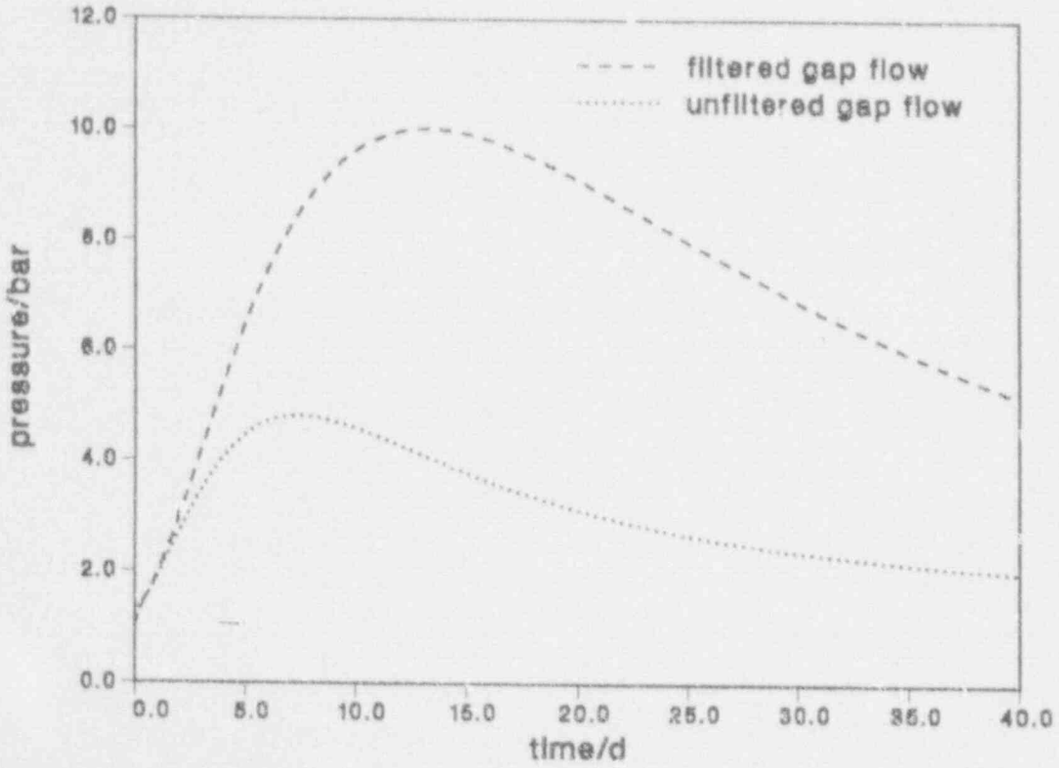


Figure 2.3 Pressure Evolution in a Containment with Gap Cooling

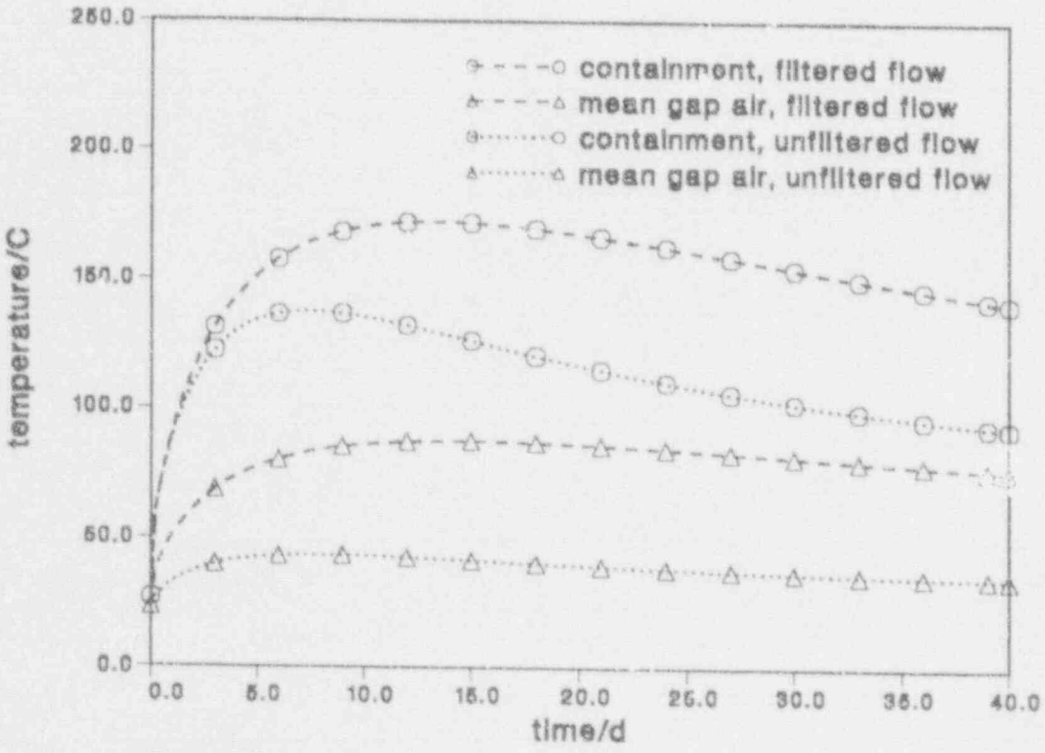


Figure 2.4 Temperature Evolution in a Containment with Gap Cooling

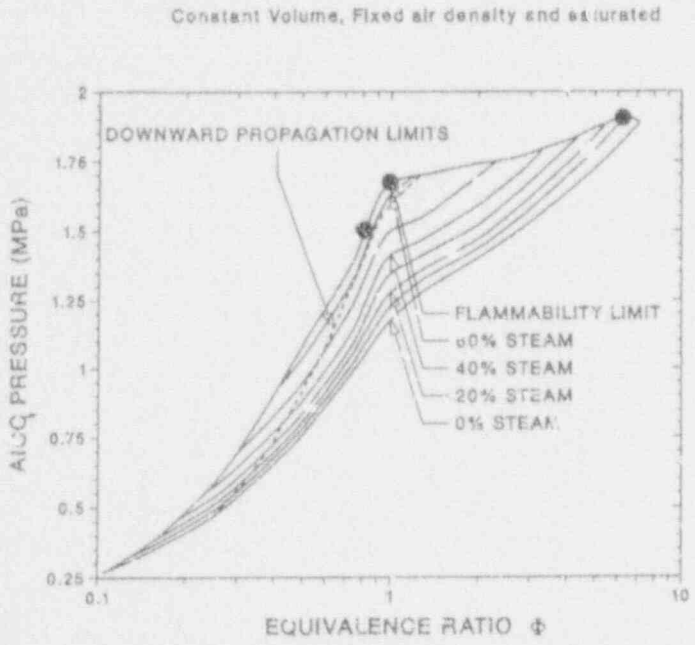


**Figure 3.1** Calculated Peak Pressures from Slow Deflagration of Hydrogen-Steam-Air Mixtures. Left Point: 2000 kg $H_2$ well mixed in 70000 $m^3$ ( $H_2$ Limit ), 1.5 MPa. Center Point: 2400 kg $H_2$ well mixed in 70000 $m^3$ ( $O_2$ Limit ), 1.7 MPa. Right Point: Local Enrichment with Highest Possible Pressure ( Fammability Limit ), 1.9 MPa.

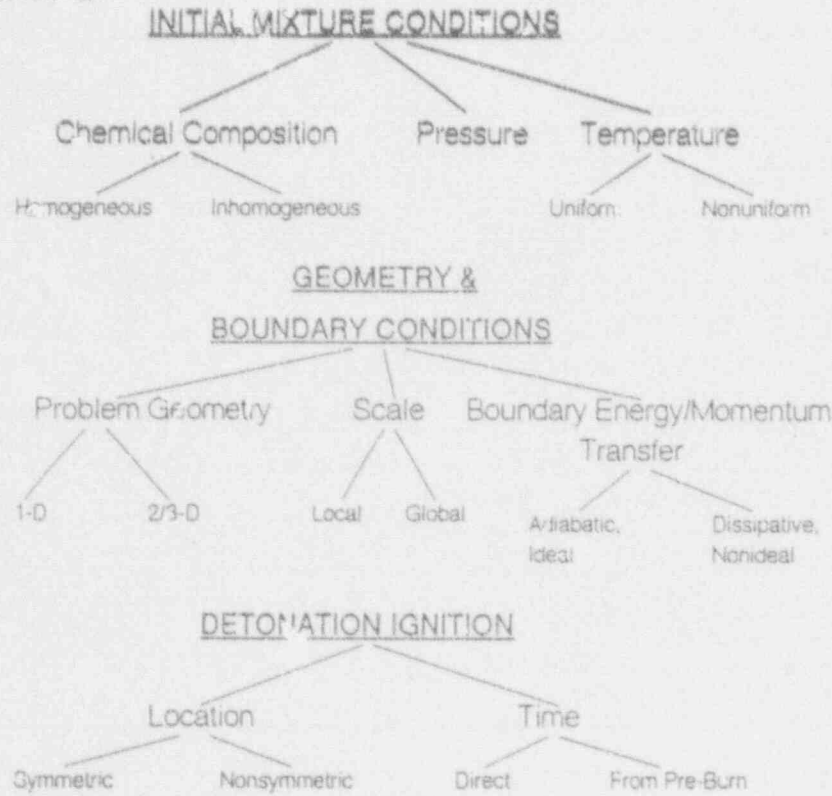


**Figure 3.2** Parameter Space for Determination of Worst-Case Detonation Loads.

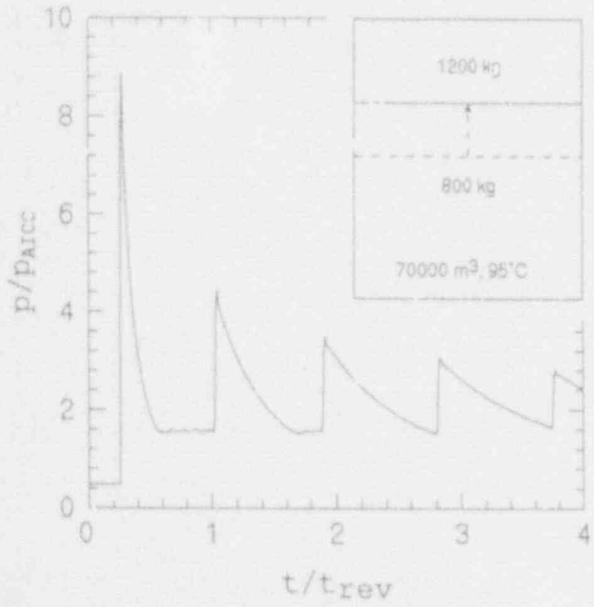


**Figure 3.3** Calculated 1-D Detonation Load for Conservative Accident Scenario Involving Hydrogen Enrichment in Dome and burn prior to Detonation. Detonation Peak Pressure is 10.5 MPa, Detonation Impulse is 60 kPas ( up to t/trev = 1 ), Loaded Area is 1285 $m^2$. ( pAICC = 1.18 MPa, trev = 29.1 ms ).

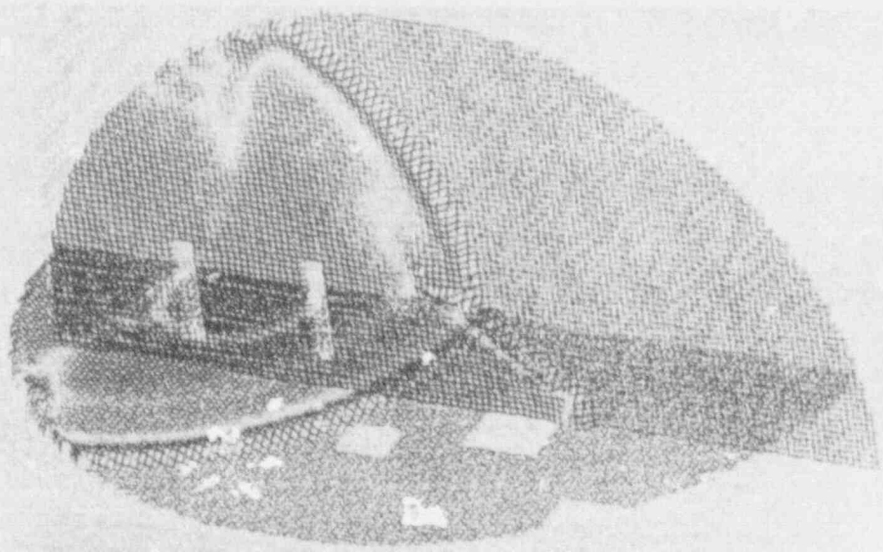

**Figure 3.4** Detonation wave in hemispherical dome ( radius = 25 m ) containing some obstacles. Shown are pressure distribution and obstacle cross sections in two orthogonal planes. Ignition was on left hand, below a hollow cylinder.

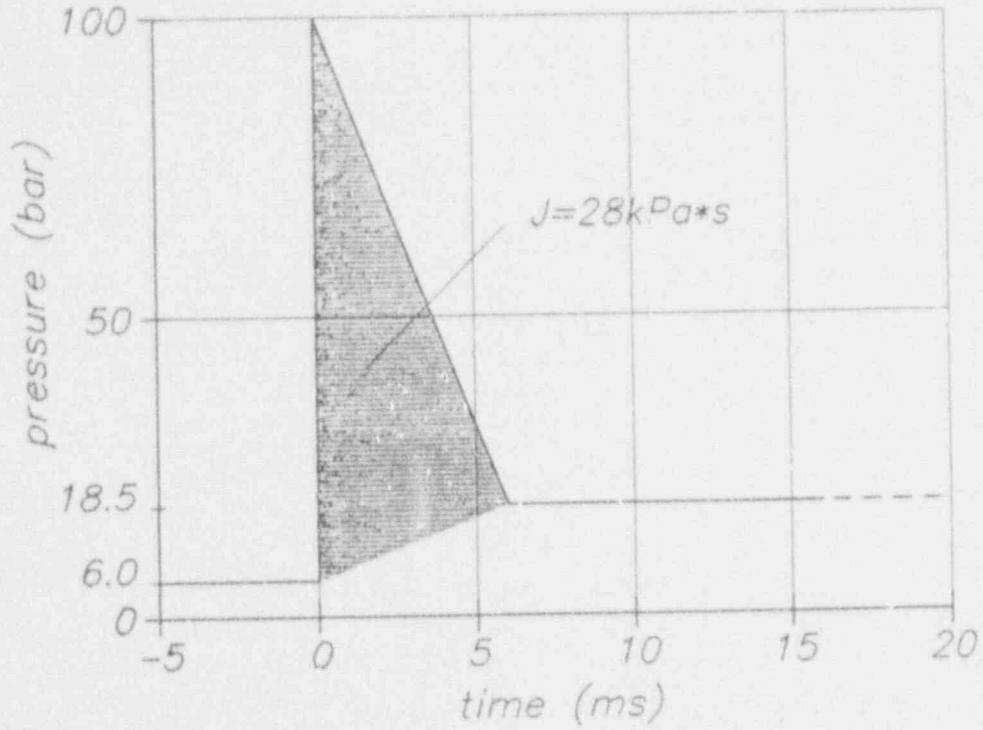


**Figure 4.1** Typical Pressure Time History due to a Hydrogen Detonation [3.11]

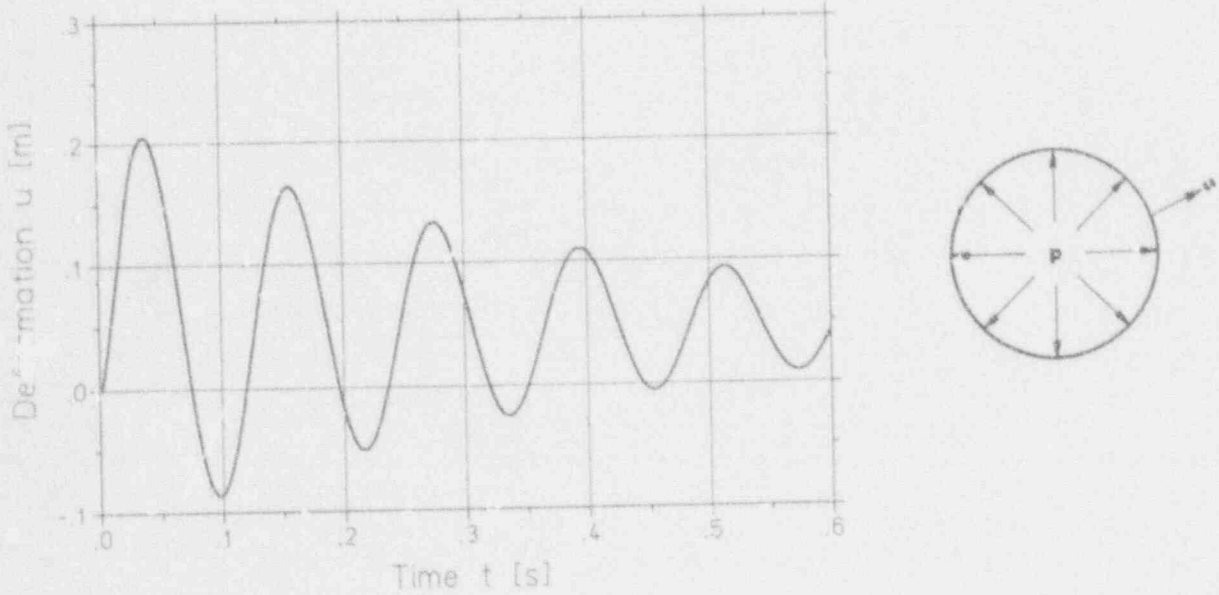


**Figure 4.2** Time History of the Radial Displacement of the Cylindrical Part of the Concrete Shell ( Global Response )

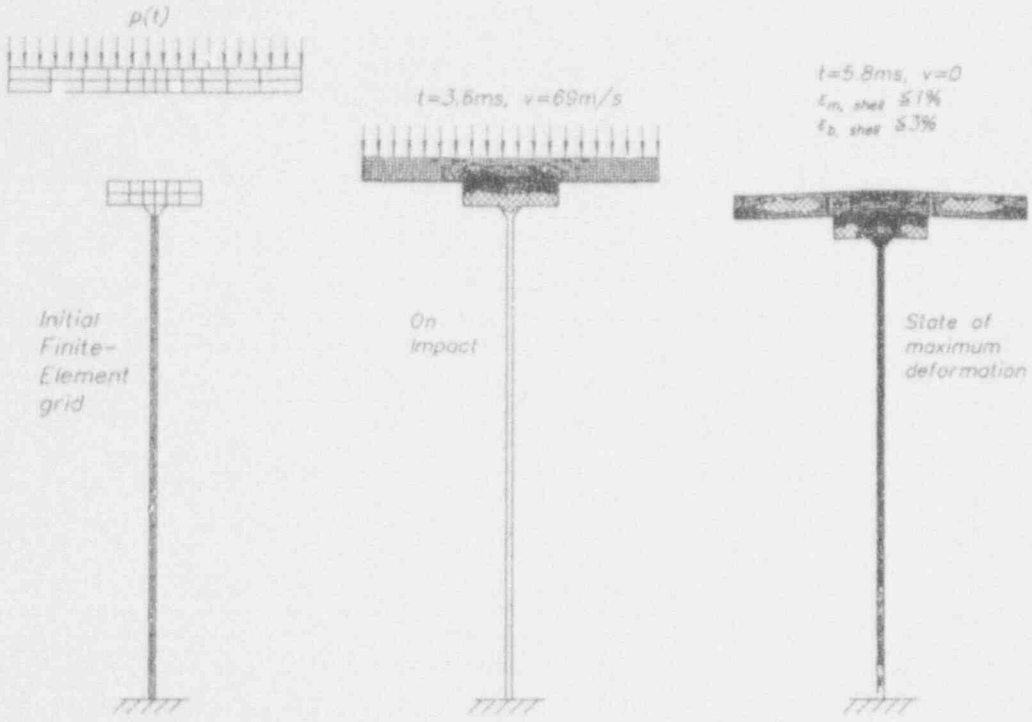


**Figure 4.3** Composite Containment with a Gap Width of 150 mm under a postulated Hydrogen Detonation

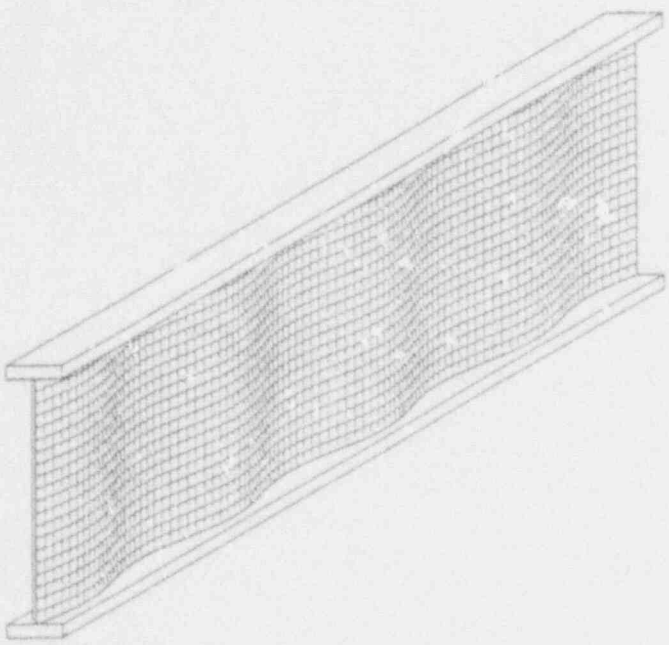

**Figure 4.4** Corrugated Rib for the Increase of the Bucklingstiffness

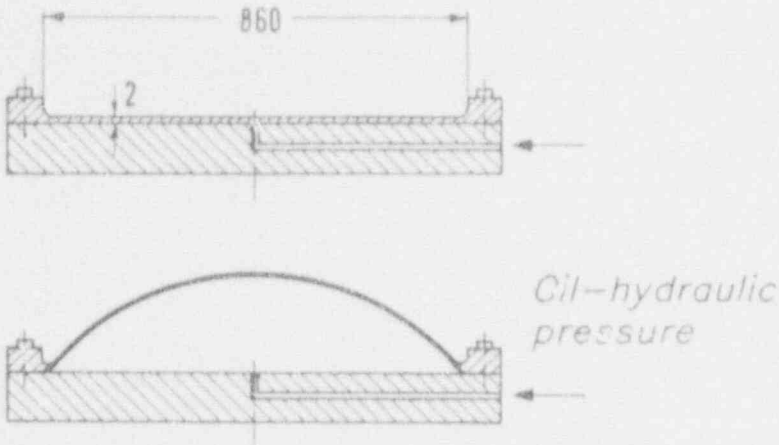


**Figure 4.5** Experimental Set-up for the Membrane Tests ( Dimensions in mm )

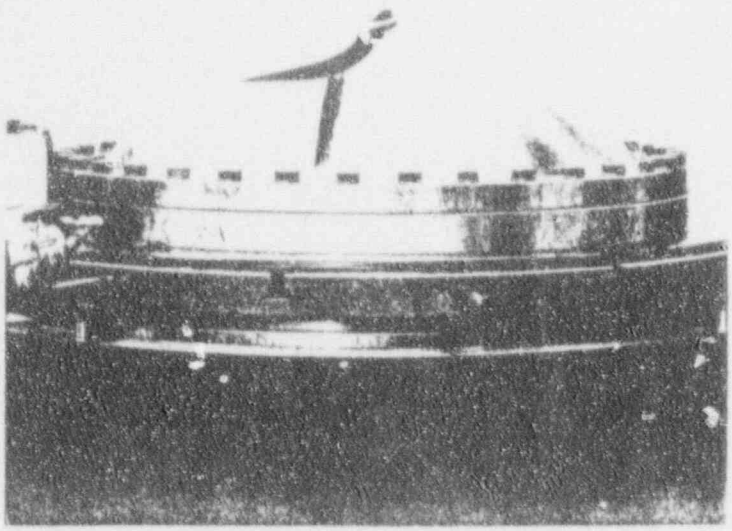

**Figure 4.6** Specimen after Failure at a Pressure of 4.3 MPa

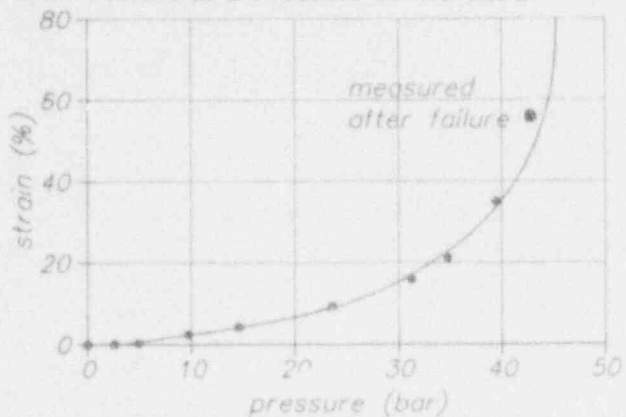


**Figure 4.7** Equivalent Strain at the Center of the Membrane.
■ Measurement by an Ultrasonic Transducer — Computation

# 1

## IMAGE EVALUATION TEST TARGET (MT-3)

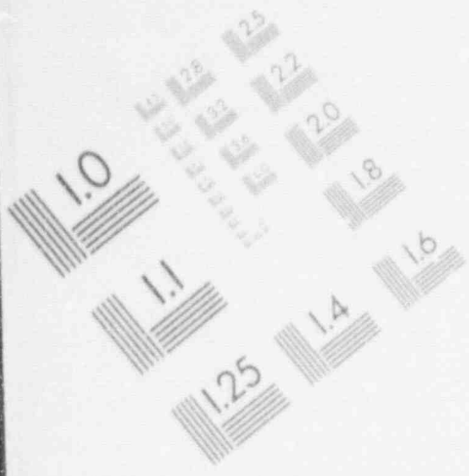


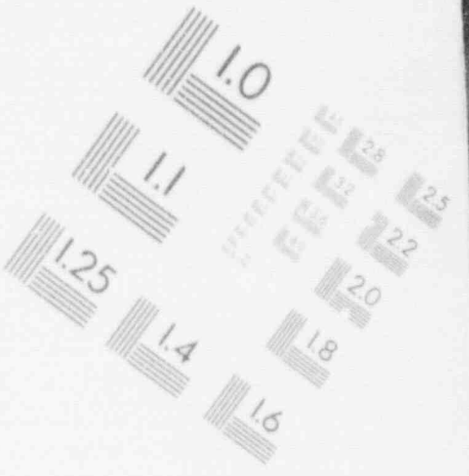



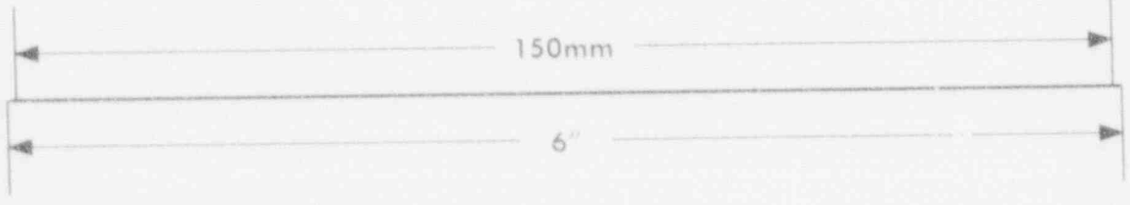




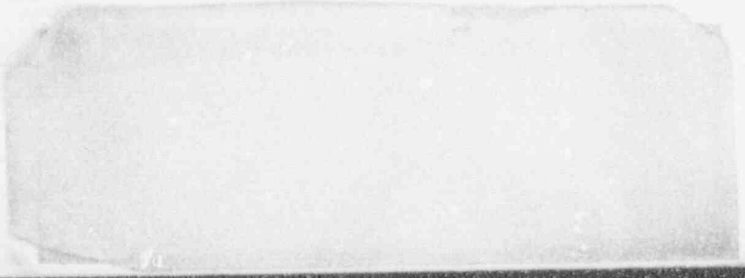

# 1

IMAGE EVALUATION
TEST TARGET (MT-3)

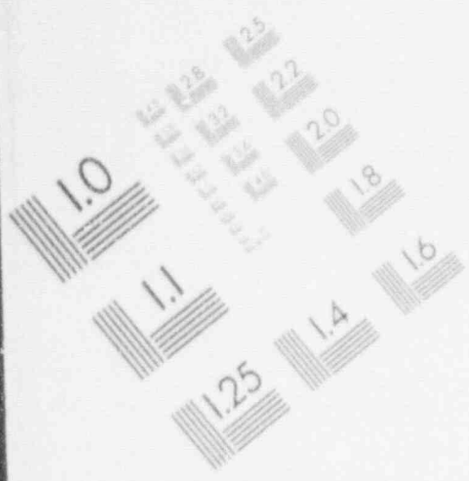


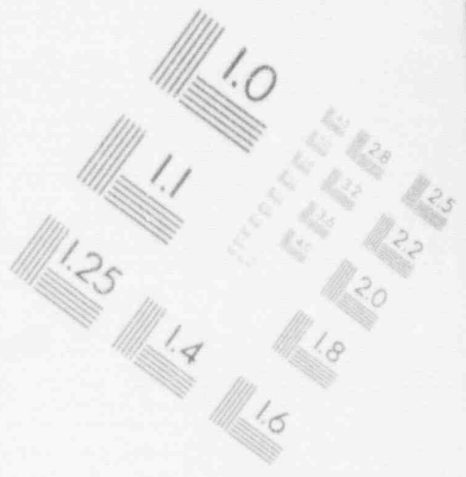



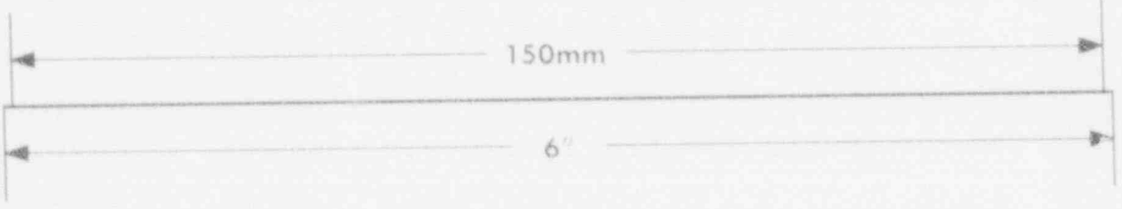


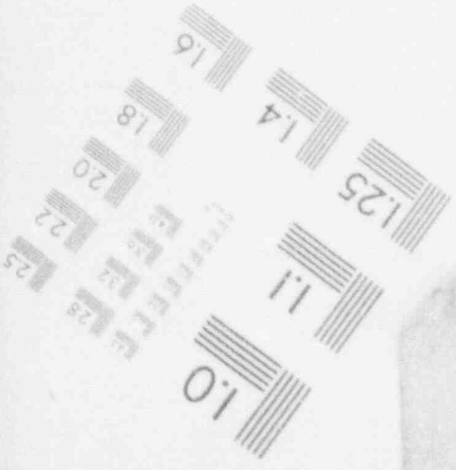


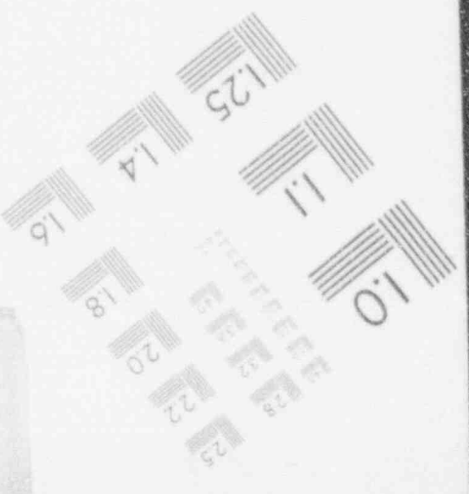


# 1

IMAGE EVALUATION
TEST TARGET (MT-3)

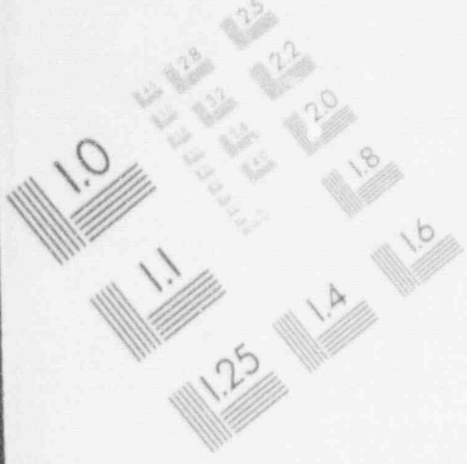


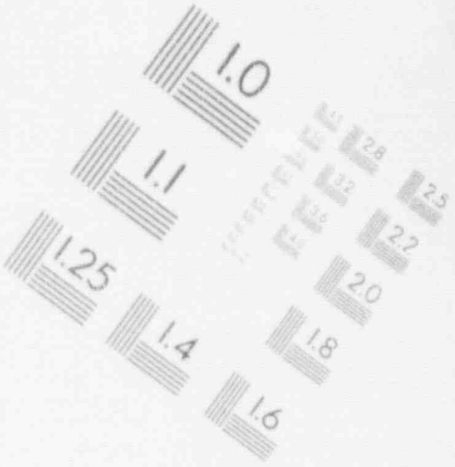



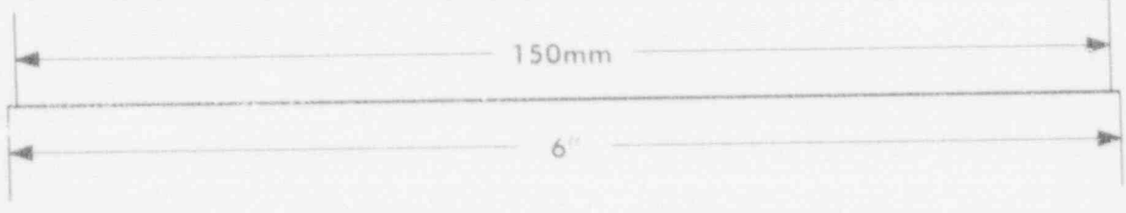



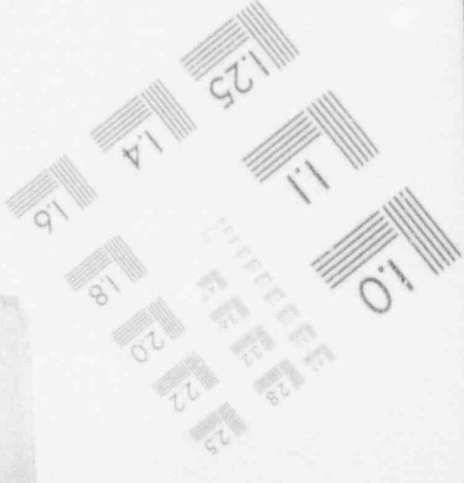


# 1

IMAGE EVALUATION
TEST TARGET (MT-3)

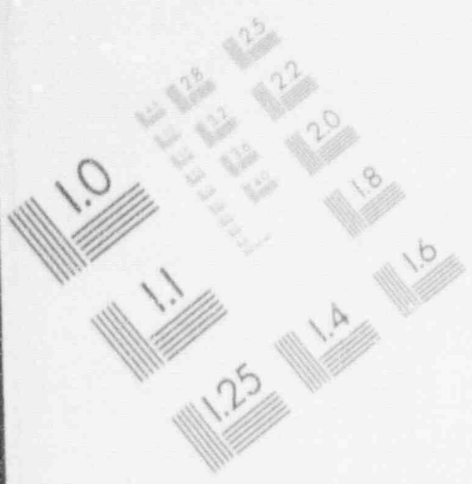


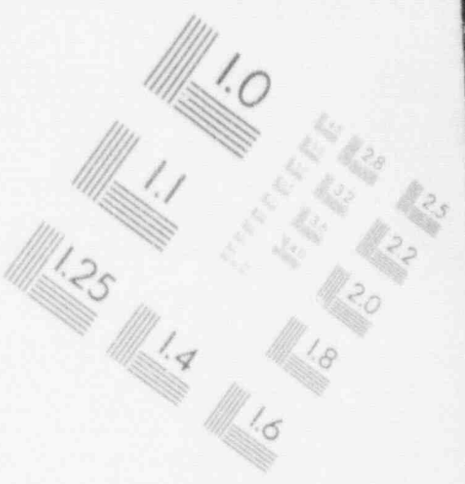



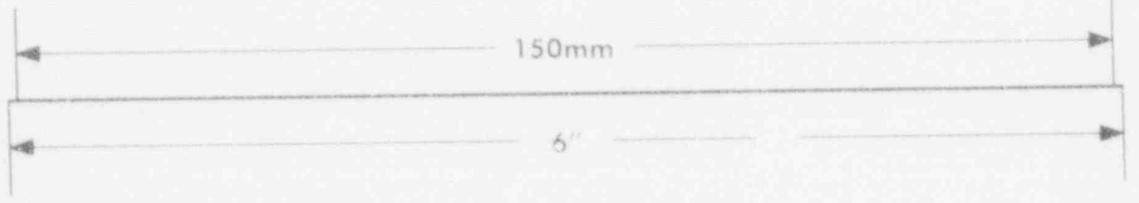



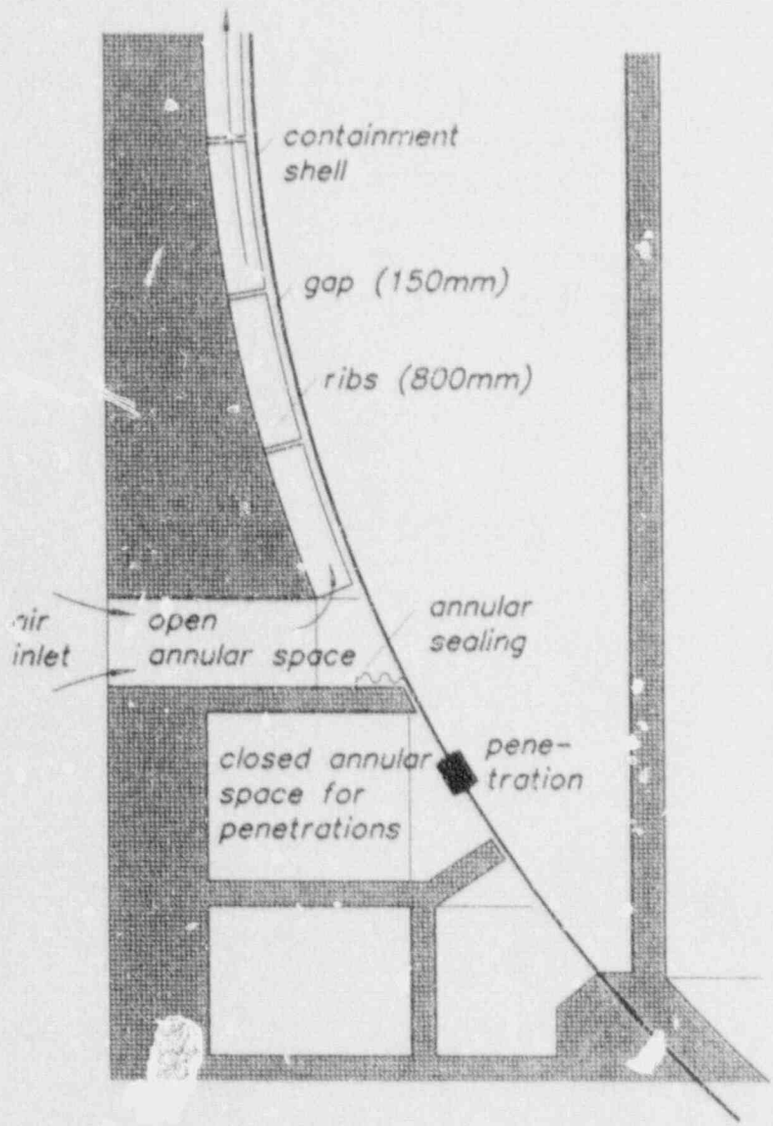


Containment for high internal pressures and with passive cooling by environmental air for decay-heat removal. Annular gap devided into a sealed one with controled atmosphere and into an open one for cooling air flow in natural circulation without filtering.

**Figure 4.8** Location of Containment Penetrations

# SESSION 4

# CONTAINMENT BEHAVIOR UNDER ACCIDENT CONDITIONS

# OVERVIEW OF NUPEC CONTAINMENT INTEGRITY PROJECT

K.Takumi and A.Nonaka
Nuclear Power Engineering Corporation , Japan

## Abstract

NUPEC has started NUPEC Containment Integrity Project entitled "Proving Test on the Reliability for Reactor Containment Vessel" since June, 1987. This is the project for the term of twelve years.

The objective of this project is to confirm the integrity of containment vessels under accident conditions.

This paper shows the outline of this project.

## 1. INTRODUCTION

In order to confirm the integrity of containment vessels, the proving tests are conducted.

The test items are (1) Hydrogen mixing and distribution test, (2) Hydrogen burning test, (3) FP behavior test and (4) Structural behavior test .

Based on the test results, computer codes are verified and as a result of analysis and evaluation by the computer codes, containment integrity is to be confirmed.

Figure 1 shows test schedule of this project.

## 2. HYDROGEN MIXING AND DISTRIBUTION TEST

The objective of this test is to investigate hydrogen distribution and mixing behavior in the containment with large volume and many compartments for the case of the relatively large amounts of hydrogen production.

Figure 2 and 3 show hydrogen mixing and distribution test facility.

This test vessel has the volume of 1600 $m^3$ that is about 1/4 th scale of actual PWR containment vessel. The diameter and height of the test vessel are 10 m and 20 m respectively.

This test vessel has 25 compartments.

The compartment number is almost the same as that of actual plants.

Having similar characteristics to hydrogen, helium is used for this test instead of hydrogen in order to prevent hydrogen explosion. Helium concentration of this test is less than 18%. The test facility has three supply systems that are helium supply system, cooling water supply system and stream supply system for simulating the burst of piping and blow down.

Table 1 shows PWR mixing and distribution test conditions. For BWR only analysis is performed.

Example of the test results is shown in Figure 4 where the pretest prediction of concentration of helium in the compartments is compared with experimental data.
The NUPEC tests conducted so far suggest that hydrogen will be well mixed in a containment vessel and the prediction by the computer code is in excellent agreement with the data.
According to the recent NUPEC tests with injection at higher position, the stratification phenomena were found.

## 3. HYDROGEN BURNING TEST

The objective of this test is to research hydrogen burning phenomena including mitigation effects of steam, spray, nitrogen inerting etc. in the containment vessel and to confirm containment integrity for hydrogen burning. This test is composed of small scale test in 5 $m^3$ cylindrical vessel and large scale test in 270 $m^3$ spherical vessel.

Figure 5 and 6 show test vessel and test facility of small scale hydrogen burning test. The diameter of the test vessel is 1.5 m and its height is approximately 3.5 m. The vessel design pressure 30 $kg/cm^2$ was decided taking account of the postulated detonation. Figure 7 shows test vessel of large scale hydrogen burning test. The diameter of spherical test vessel is 8 m. Test facility of large scale hydrogen burning test is now under construction at Takasago Engineering Laboratory of NUPEC.

The content of the small scale tests is as follows:

a) Before large scale tests are conducted, basic data pertaining to the transitional areas among combustion, deflagration and detonation is accumulated to decide the scope of the large scale tests.

b) Before large scale tests are conducted, the appropriateness of the measurement and data processing system is confirmed.

c) Comparisons are made with data from the United States to make sure that the data conforms.

d) In order to confirm the effectiveness of hydrogen combustion control, characteristic data is obtained.

e) The flammable limit under nitrogen inerting condition is confirmed.

The content of the large scale tests is as follows:

a) The effectiveness of compartments for hydrogen combustion is confirmed.

b) Small scale and large scale tests are conducted to confirm the effects of scale.
c) The effectiveness of hydrogen combustion controls using blowdown steam, nitrogen and other diluents is confirmed.

d) The flammable limit unde nitrogen inerting condition is confirmed.

Table 2 and 3 show burning test conditions.

Main test items are effect of temperature, effect of pressure, turbulence effect, spray effect, distribution effect, concentration effect of gases, etc. Figure 8 shows Iso-arrival time contour. NUPEC data has good accordance with FITS data (1) and some new data were provided in the higher concentration.
High temperature hydrogen combustion research has been started at BNL(Brookhaven National Laboratory) as joint research with NRC (U.S. Nuclear Regulatory Commission).

## 4. FP BEHAVIOR TEST

This test is composed of (1) Radioactive Material Trapping Characteristics Test, (2) FP Removal Test and (3) PHEBUS FP Program.

The objective of radioactive material trapping characteristics tests is to confirm iodine trapping effect in the leakage path of penetration assembly after reactor accident.

Organic seal materials such as epoxy resin and silicone resin are used in these penetrations as an insulator or a gasket, therefore the test is conducted on the assumption that the leakage path owing to temperature and pressure rising under accident condition grows at the organic seal.

This test program consists of following tests. One is bench scale test for surveying parameter's effect and get data to discuss iodine trapping mechanism. The other is large scale test for confirming and evaluating iodine trapping effect, and it is conducted with test assembly simulating those of actual plants.

Figure 9 shows radioactive material trapping characteristics test facility.

The objective of FP removal test is to confirm FP removal effects by natural removal or pool scrubbing.

Figure 10 and 11 show natural removal test vessel and pool scrubbing test vessel respectively.

PHEBUS FP program is being performed by CEA and CEC. The objective of this program is to study in an in-pile test facility, under sufficient prototypical conditions, phenomena governing the transport, retention and chemistry of fission products under Light Water Reactor (LWR) severe accident conditions.

NUPEC has participated in its preparation phase and is now planning to participate in its experimental phase.

## 5. STRUCTURAL BEHAVIOR TEST

The objective of this test is to confirm containment integrity structurally by analytical evaluation based on tests to failure of SCV ( Steel Containment Vessel ), PCCV ( Prestressed Concrete Containment Vessel ), and RCCV (Reinforced Concrete Containment Vessel ) in addition to flange leak test.

Figure 12 shows (1) SCV model vessel ( scale 1/10th ) , (2) PCCV model vessel ( scale 1/6th ), (3) RCCV model vessel ( scale 1/6th) and (4) vessel for flange leak test (full scale ) respectively.
Tests to failure of SCV and PCCV have been started as joint research with NRC (U.S. Nuclear Regulatory Commission ) / SNL (Sandia National Laboratories ).

## 6. CONCLUSION

Both hydrogen mixing and distribution test and hydrogen burning test (small scale) have been completed. A part of these test results has been reported. Some of other tests are being performed and the others are under design. Test results of these tests will be introduced in the near future.

REFERENCES

(1)MARSHALL Jr., B.W., "Hydrogen:Air:Steam Flammability Limits and Co ,bustion Characteristics in the FITS Vessel",NUREG/CR-3468, Dec. 1984.

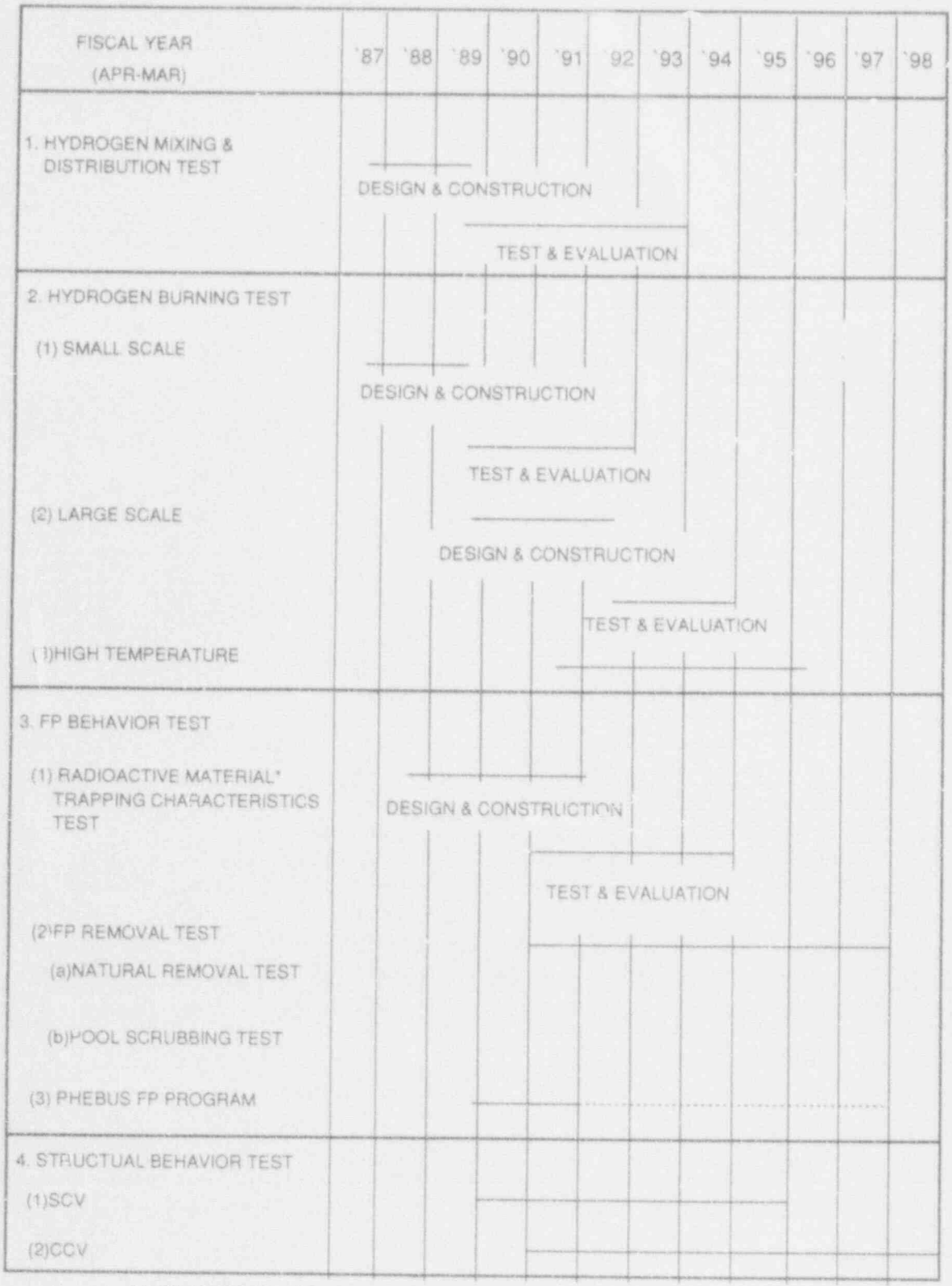


* IODINE, SCV:Steel Containment Vessel, CCV: Concrete Containment Vessel

Figure 1 Test Schedule

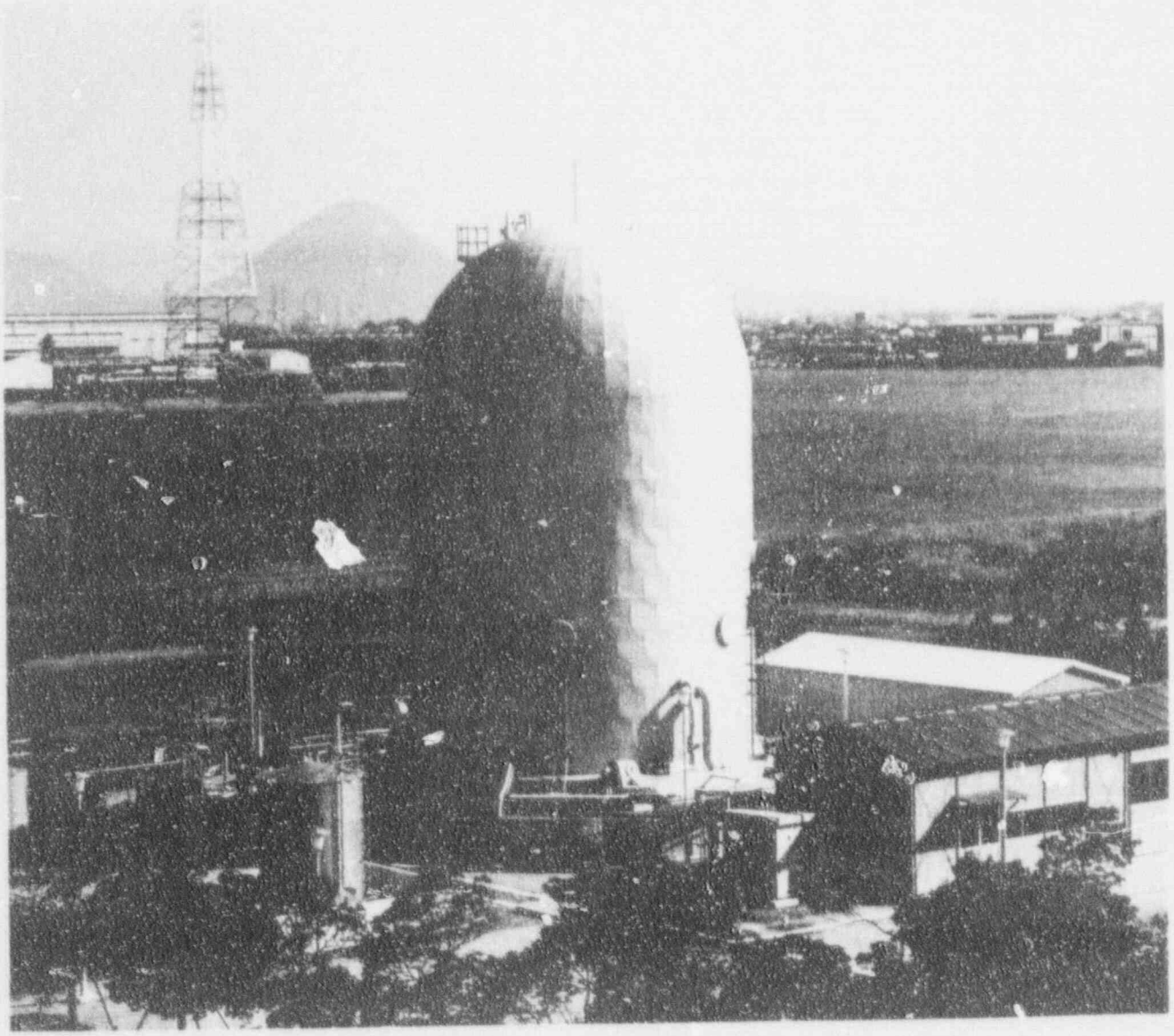

Figure 2 Hydrogen Mixing and Distribution Test Facility
(Test Site:Tadotsu Engineering Laboratory)

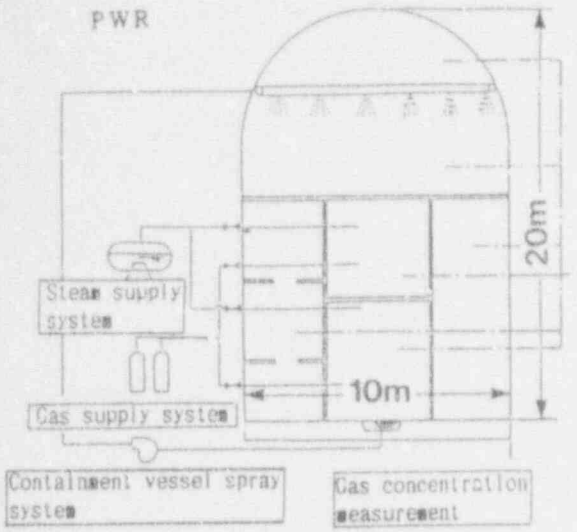


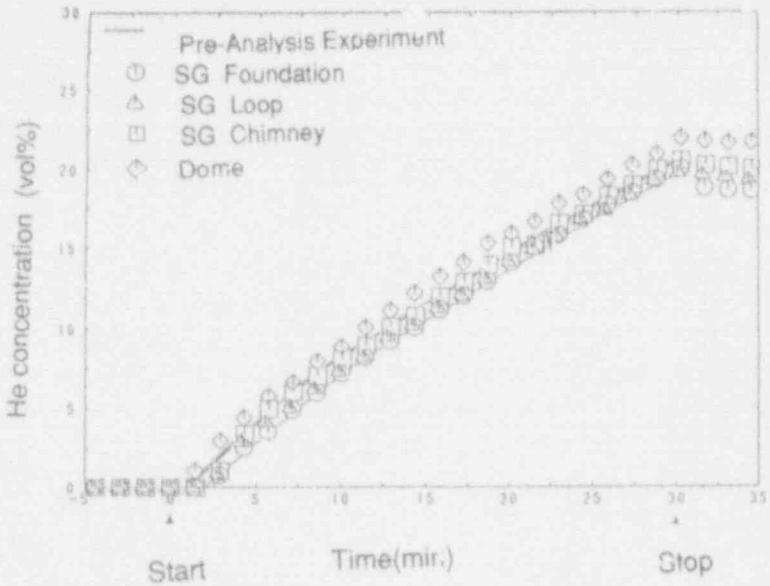


Figure 3 Hydrogen Mixing and Distribution Test Facility

Figure 4 Heium Concentration Distribution

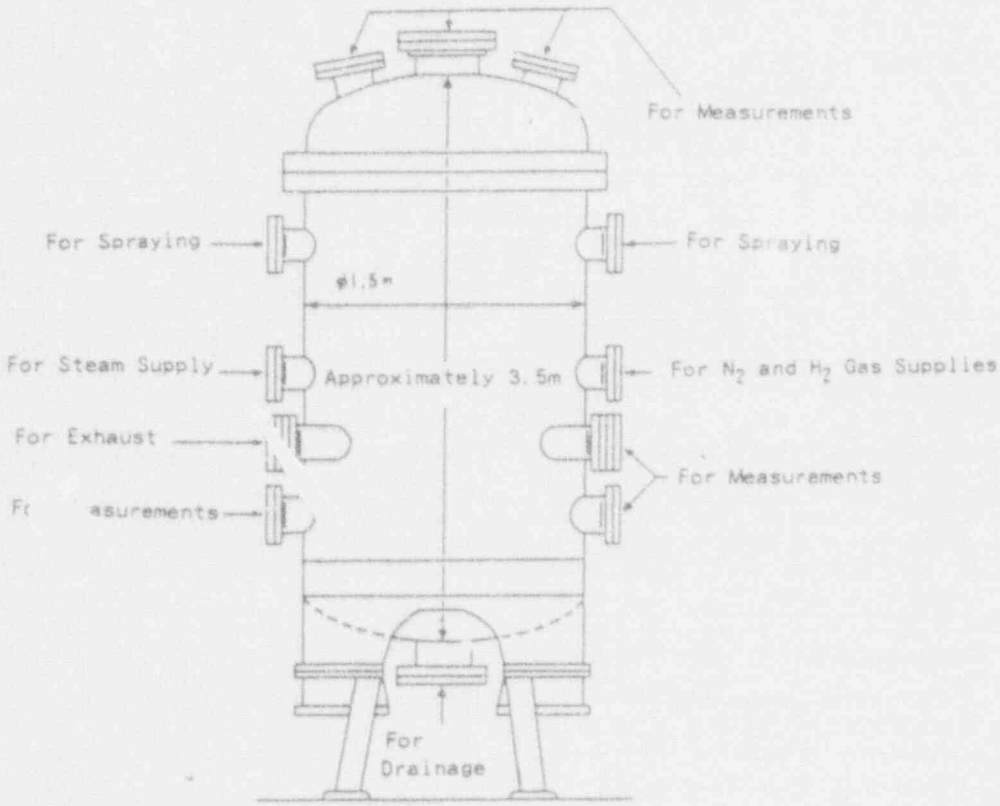


Figure 5 Test Vessel of Small Scale Hydrogen Burning Test

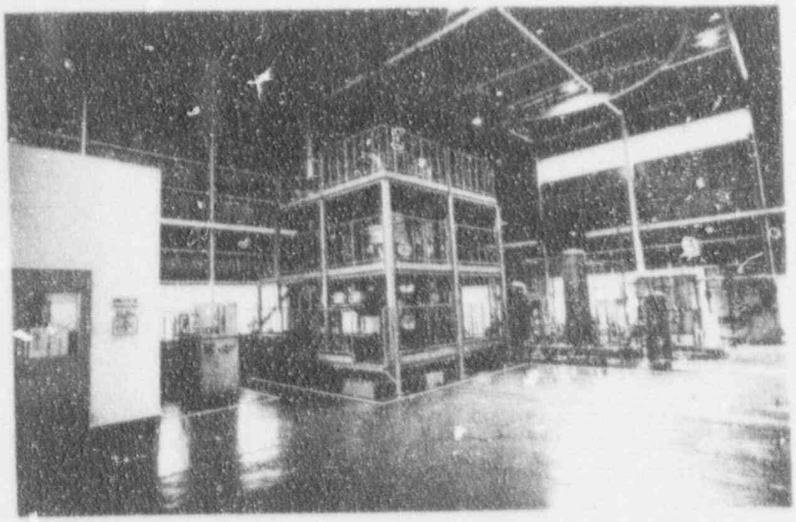

Figure 6 Small Scale Hydrogen Burning Test Facility
(Test Site:Katsuta Engineering Laboratory)

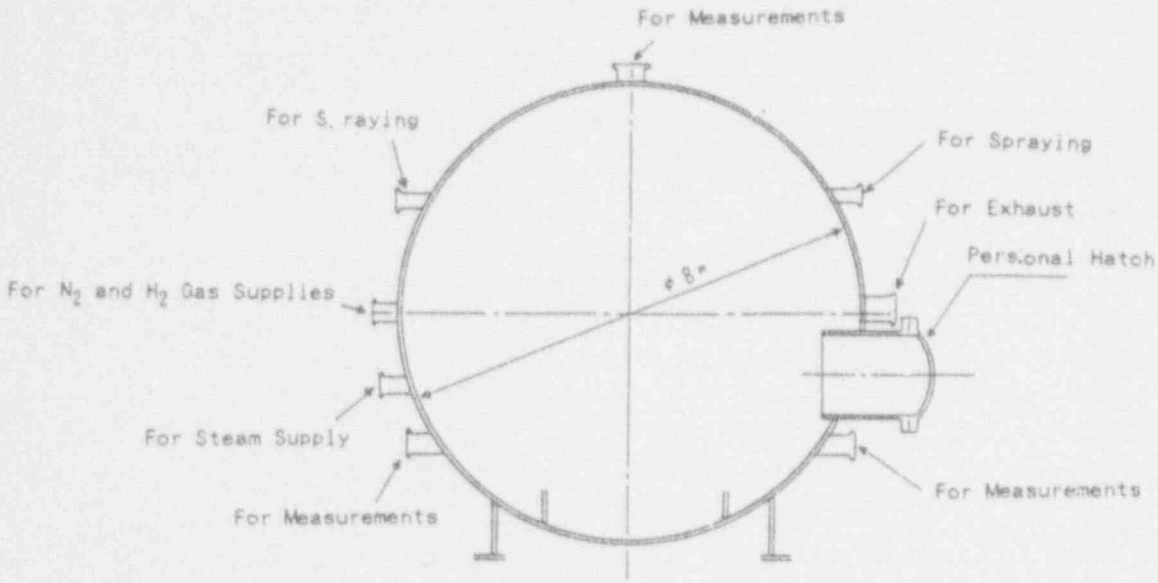


Figure 7 Test Vessel of Large Scale Hydrogen Burning Test
(Test Site:Takasago Engineering Laboratory)

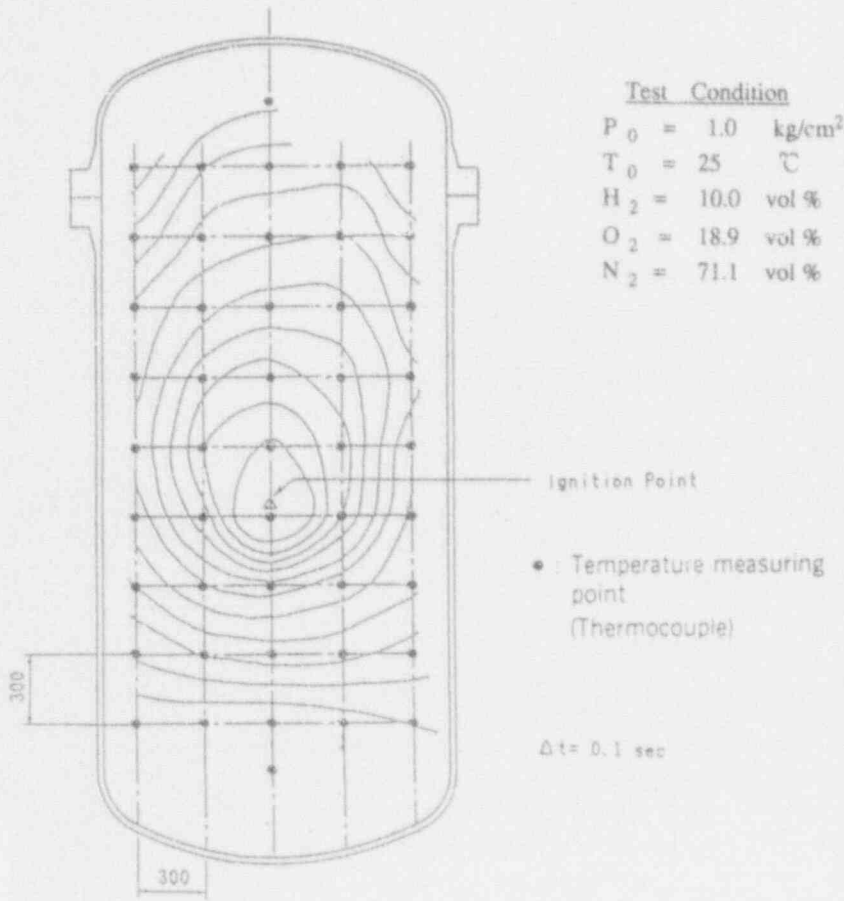


Figure 8 Iso-Arrival Time Contour

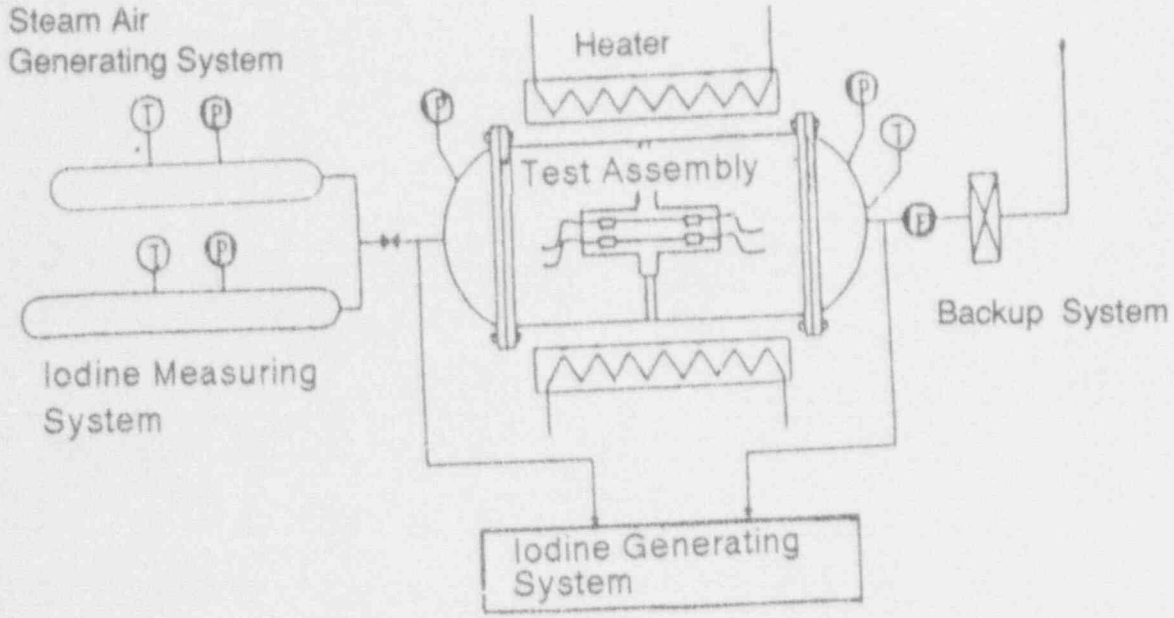


Figure 9 Radioactive Material Trapping Characteristics Test Facility
(Test Site:Isogo Engineering Laboratory)

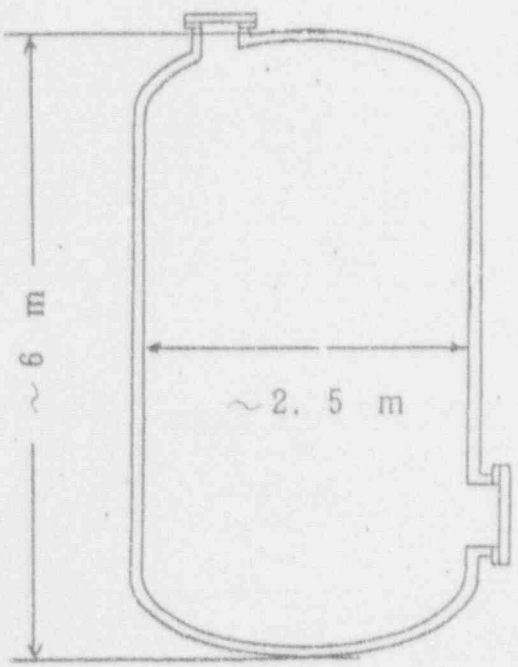


Figure 10 Natural Removal Test Vessel

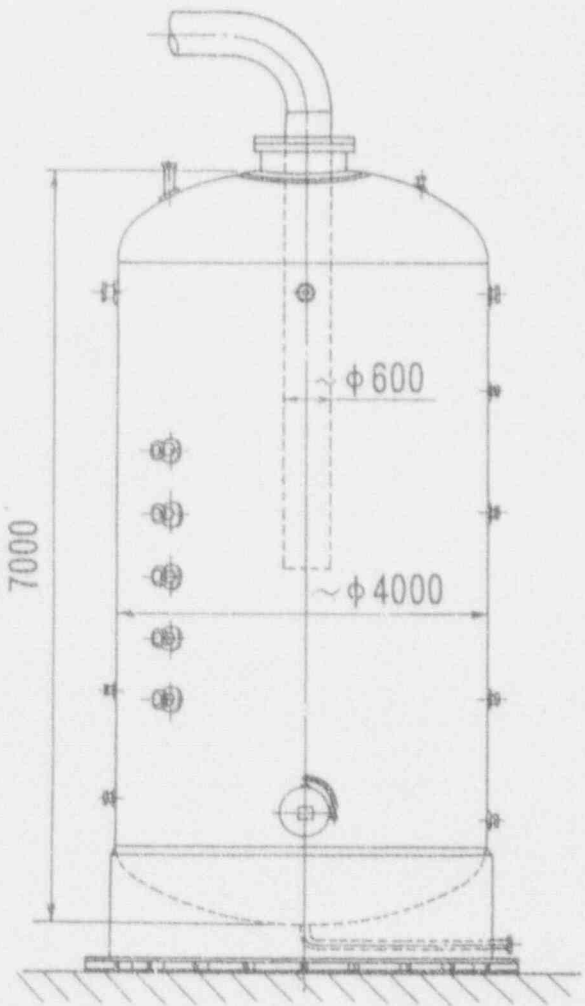


Figure 11 Pool Scrubbing Test Vessel

(1)SCV TEST TO FAILURE

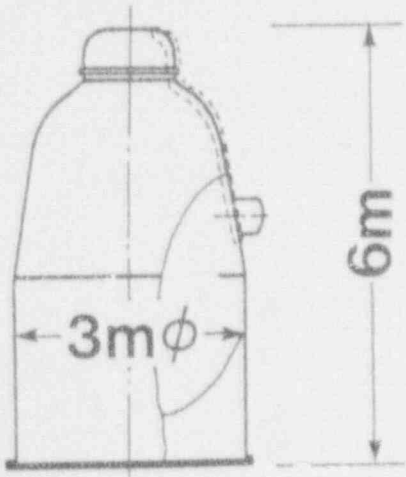


(2)PCCV TEST TO FAILURE

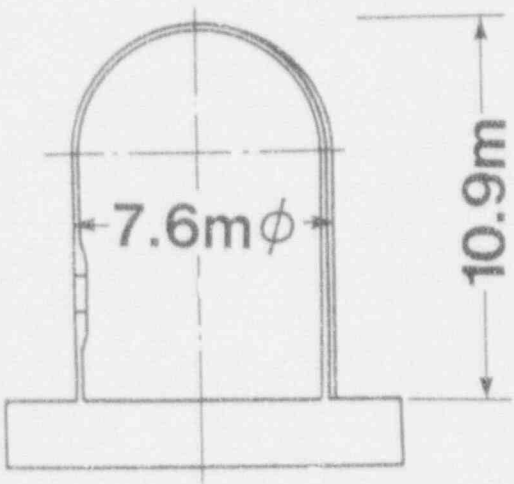


(3)RCCV TEST TO FILURE

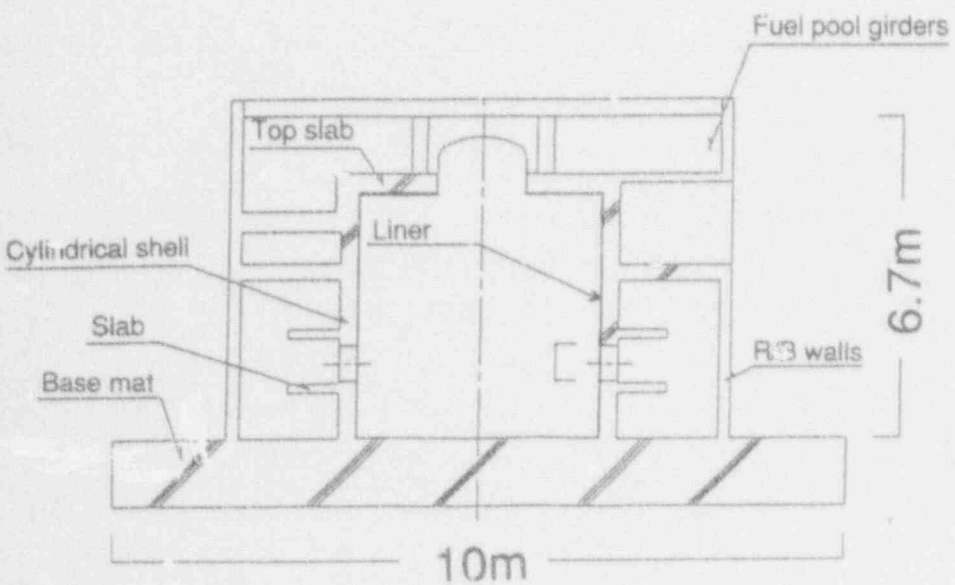


(4)FLANGE LEAK TEST

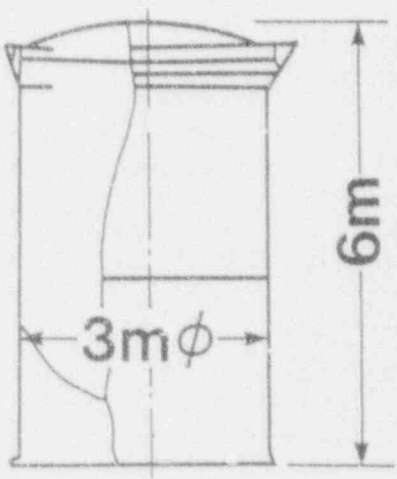


Figure 12 Test Vessels for Stractural Behavior Test

Table 1 PWR Mixing and Distribution Test Conditions

| | ITEMS | ACTUAL PLANT CONDITIONS | MIXING TEST CONDITIONS |
|---|---|---|---|
| 1 | HYDROGEN(HELIUM) CONCENTRATION | < 15 VOL % | ≦ 18 VOL % |
| 2 | STEAM CONCENTRATION | 0 - 100 VOL % | ≦ 60 VOL % |
| 3 | WATER SPRAY FLOW | 1200 $m^3$ /h | 70 $m^3$ /h |
| 4 | HYDROGEN (HELIUM) FLOW | max. 3 kg/s | max. 0.12kg/s |
| 5 | STEAM FLOW | max. 40 kg/s | max. 0.74kg/s |
| 6 | COMPARTMENT | 20 - 30 | 25 |
| 7 | IMAGINARY BREAK DOWN LOCATION | SG LOOP ROOM PRESSURIZER RELIEF TANK | |
| 8 | INITIAL NITROGEN CONCENTRATION | ATOMOSPHERIC | |
| 9 | INITIAL OXYGEN CONCENTRATION | ATOMOSPHERIC | |
| 10 | INITIAL PRESSURE | ATOMOSPHERIC | |

Table 2 Small scale burning test conditions

| | ITEMS | BWR | PWR |
|---|---|---|---|
| 1 | HYDROGEN CONCENTRATION | ≦ 70 VOL % | ≦ 20 VOL % |
| 2 | STEAM CONCENTRATION | ≦ 60 VOL % | ≦ 60 VOL % |
| 3 | NITROGEN CONCENTRATION | ≧ 97 VOL% | ATOMOSPHERIC |
| 4 | OXIGEN CONCENTRATION | ≦10 VOL % | ATOMOSPHERIC |
| 5 | SPRAY FLOW RATE | ≦ 15 $m^3$/h | ≦ 3 $m^3$/h |
| 6 | INITIAL PRESSURE | ATOMOSPHERIC | ATOMOSPHERIC |
| 7 | COMPARTMENTS | ——— | ——— |

Table 3 Large scale burning test conditions

| | ITEMS | BWR | PWR |
|---|---|---|---|
| 1 | HYDROGEN CONCENTRATION | ≦ 70 VOL % | ≦ 18VOL % |
| 2 | STEAM CONCENTRATION | ≦ 60 VOL % | ≦ 60 VOL % |
| 3 | NITROGEN CONCENTRATION | ≧ 97 VOL% | ATOMOSPHERIC |
| 4 | OXIGEN CONCENTRATION | ≦10 VOL % | ATOMOSPHERIC |
| 5 | SPRAY FLOW RATE | ≦ 350 $m^3$/h | ≦ 45$m^3$/h |
| 6 | INITIAL PRESSURE | ATOMOSPHERIC | ATOMOSPHERIC |
| 7 | COMPARTMENTS | ——— | ≦ 8 |

# PLAN ON TEST TO FAILURE OF A PRESTRESSED CONCRETE CONTAINMENT VESSEL MODEL

K. Takumi, A. Nonaka, K. Umeki
Nuclear Power Engineering Corporation, Japan

K. Nagata, M. Soejima
Mitsubishi Heavy Industries, Ltd., Japan

Y. Yamaura
Mitsubishi Atomic Power Industries, Inc., Japan

J. F. Costello
United States Nuclear Regulatory Commission, USA

W. A. von Riesemann, M. B. Parks, D. S. Horschel
Sandia National Laboratories,[1] USA

## Abstract

A summary of the plans to test a prestressed concrete containment vessel (PCCV) model to failure is provided in this paper. The test will be conducted as a part of a joint research program between the Nuclear Power Engineering Corporation (NUPEC), the United States Nuclear Regulatory Commission (NRC), and Sandia National Laboratories (SNL).

The containment model will be a scaled representation of a PCCV for a pressurized water reactor (PWR). During the test, the model will be slowly pressurized internally until failure of the containment pressure boundary occurs. The objectives of the test are to measure the failure pressure, to observe the mode of failure, and to record the containment structural response up to failure.

Pre- and posttest analyses will be conducted to forecast and evaluate the test results. Based on these results, a validated method for evaluating the structural behavior of an actual PWR PCCV will be developed.

The concepts to design the PCCV model are also described in the paper.

## 1. INTRODUCTION

A containment vessel is designed to contain the energy and radioactive material that would result from a design basis accident (DBA). However, since the Three Mile Island accident, the ability of containments to withstand loadings in excess of the design basis has been questioned. Therefore, there has been considerable research focused on studying the behavior of containments during a severe accident.

SNL has conducted static overpressure tests on a steel containment vessel (SCV) and a PWR reinforced concrete containment vessel (RCCV). The work has been conducted under the sponsorship of the NRC. Prestressed concrete containment vessels are also commonly used in

---

[1] Sandia National Laboratories is operated by the U.S. Department of Energy under contract number DE-AC04-76DP00789.

PWR plants. However, a model of a PCCV with a carbon steel liner has not yet been investigated experimentally.

NUPEC has conducted a series of programs, known as the "Proving Tests On The Reliability For Reactor Containment Vessel," for several years. As a part of this overall program, NUPEC is planning to conduct an overpressurization test to investigate the structural behavior of a containment vessel using a scale model of an existing PCCV in Japan. This paper summarizes the plan for the PCCV model test.

The test will be conducted as a part of a cooperative program on containment integrity with the joint participation of NUPEC and NRC/SNL. NUPEC has the lead role in design of the model with review and input by NRC/SNL. The model will be constructed and tested at SNL.

## 2. OBJECTIVES

The primary objectives of this program are:

1. to develop a validated analytical method that can be used to assess the behavior of an actual PCCV during a reactor accident,

2. to assess the likely failure mode of an actual liner plate system and the likely structural failure mode of an actual PCCV, and

3. to assess the ultimate capacity for leak tightness and structural integrity of an actual PCCV.

## 3. TEST MODEL

### 3.1 Design Rules

The test model will be a scaled representation of an actual PCCV in Japan, which was designed in accordance with the Japanese Concrete Containment Vessel Design Code. The actual PCCV consists of a hemispherical dome, a cylindrical wall, and a basemat. The general arrangement of the actual containment is shown in Figure 1.

Two buttresses are used to anchor the horizontal or 'hoop' tendons. In the vertical direction, a 'hairpin' tendon layout is employed. The vertical tendons extend from the basemat up through the cylinder wall, over the dome, and back to the basemat on the opposite side of the containment. They are anchored in a tendon gallery that is inside the basemat.

As shown in Figure 1, a steel liner plate is placed on the inner surface of the concrete wall, dome, and basemat and forms the containment pressure boundary in these areas. T-sections are welded to the liner in the vertical direction and flat 'rings' in the horizontal direction. The T-sections and flat rings are then embedded in the concrete, thus anchoring the liner to the concrete wall.

The test model will be designed in accordance with the following rules:

1. The test model will have the same general configuration as the actual containment. In other words, it will consist of the dome, cylinder, basemat, two buttresses, a steel liner, the larger penetration openings (such as an equipment hatch and personnel airlocks), and several penetration sleeves.

2. The liner plate shall be attached to the concrete using the same type of liner anchorage system as used in the actual containment.

3. The reinforcement ratios for reinforcing bars and prestressing tendons, which primarily determine the structural behavior of the containment, shall be equivalent to those in the actual containment.

4. There will be a 'one-to-one' replacement of tendons in the model. That is, for every tendon in the actual containment, there will be a tendon at the same relative location in the model. The area of the model tendons will be scaled.

5. The material characteristics of the steel elements and the concrete shall be the same, or as close as possible, to the respective materials in the actual structure.

### 3.2 Scale of the Model

The scaling method to be used for the model has not yet been decided. An option that is being considered would use a geometric scale of 1:6 for all dimensions except those associated with the liner, liner insert plates, and the liner anchorage system. There is some concern that the liner thickness at 1:6 scale would be too small to allow proper fabrication of the liner system. Therefore, a larger scale of 1:3 is being considered for the liner system. The configuration and dimensions of the model, based on this scaling method, are shown in Figure 2. The distorted scaling method mentioned above is still being investigated.

Smaller scales for the overall model geometry, such as 1:10 and 1:8, were considered. However, they were not acceptable because they were not large enough to allow a one-to-one modeling of the actual tendon layout.

### 3.3 Dimensions of the Proposed Test Model

A comparison of the dimensions of the current test model design and the actual containment is provided in Table 1.

Table 1. Dimensions of the Test Model* and the Actual Containment

| | Test Model | Actual Containment |
|---|---|---|
| Total Height | 10933 mm | 65600 mm |
| Inside Diameter | 7166 mm | 43000 mm |
| Wall Thickness | | |
| Cylinder | 217 mm | 1300 mm |
| Dome | 184 mm | 1100 mm |
| Design Pressure | 4.0 kg/cm$^2$ (0.392 MPa) | 4.0 kg/cm$^2$ (0.392 MPa) |

*Dimensions of the test model are based on the 1/6 scale which has not yet been finalized.

## 4. SCHEDULE

The PCCV model test is expected to be conducted in 1996.

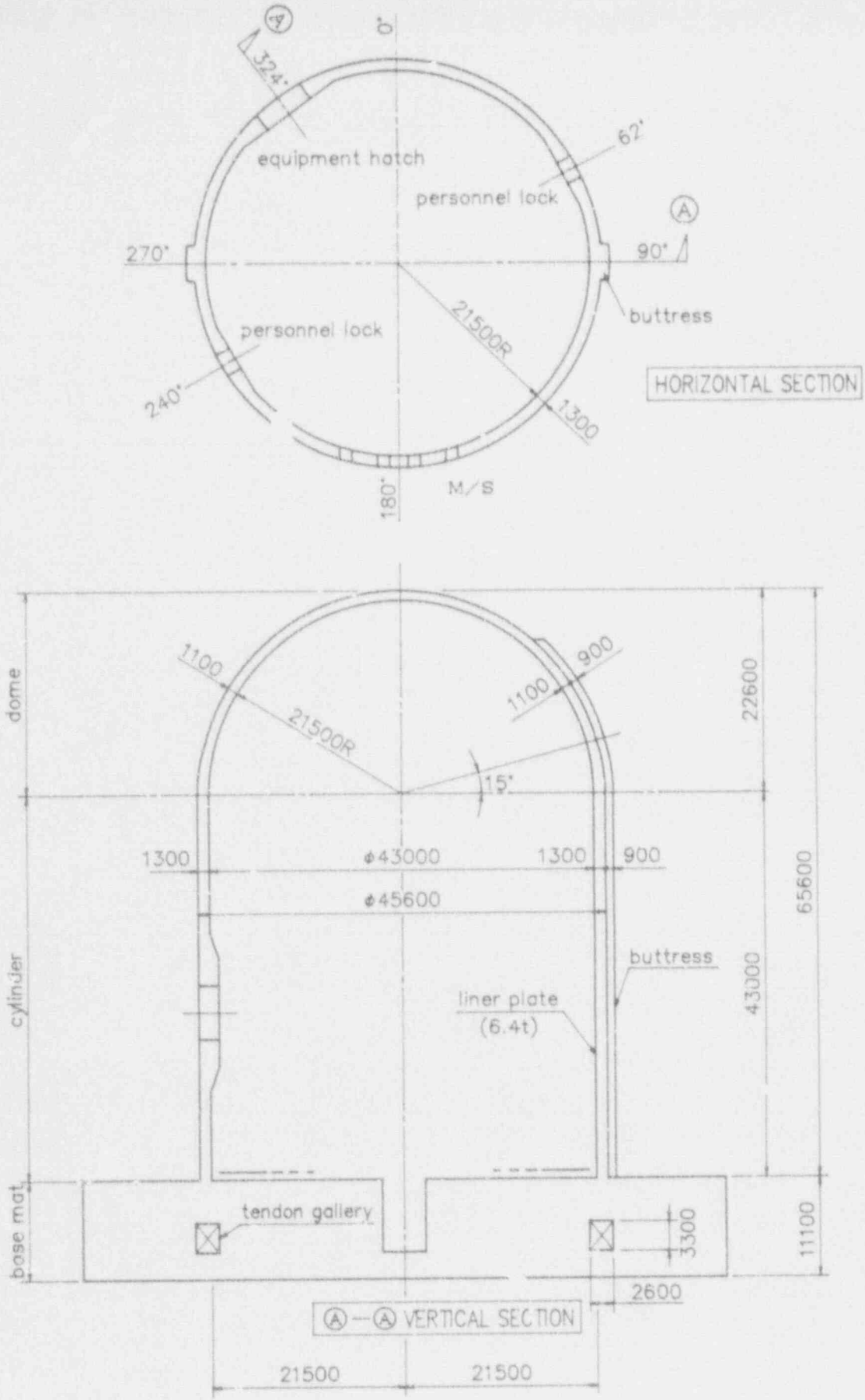


Figure 1. General Arrangement of the Actual Containment Vessel

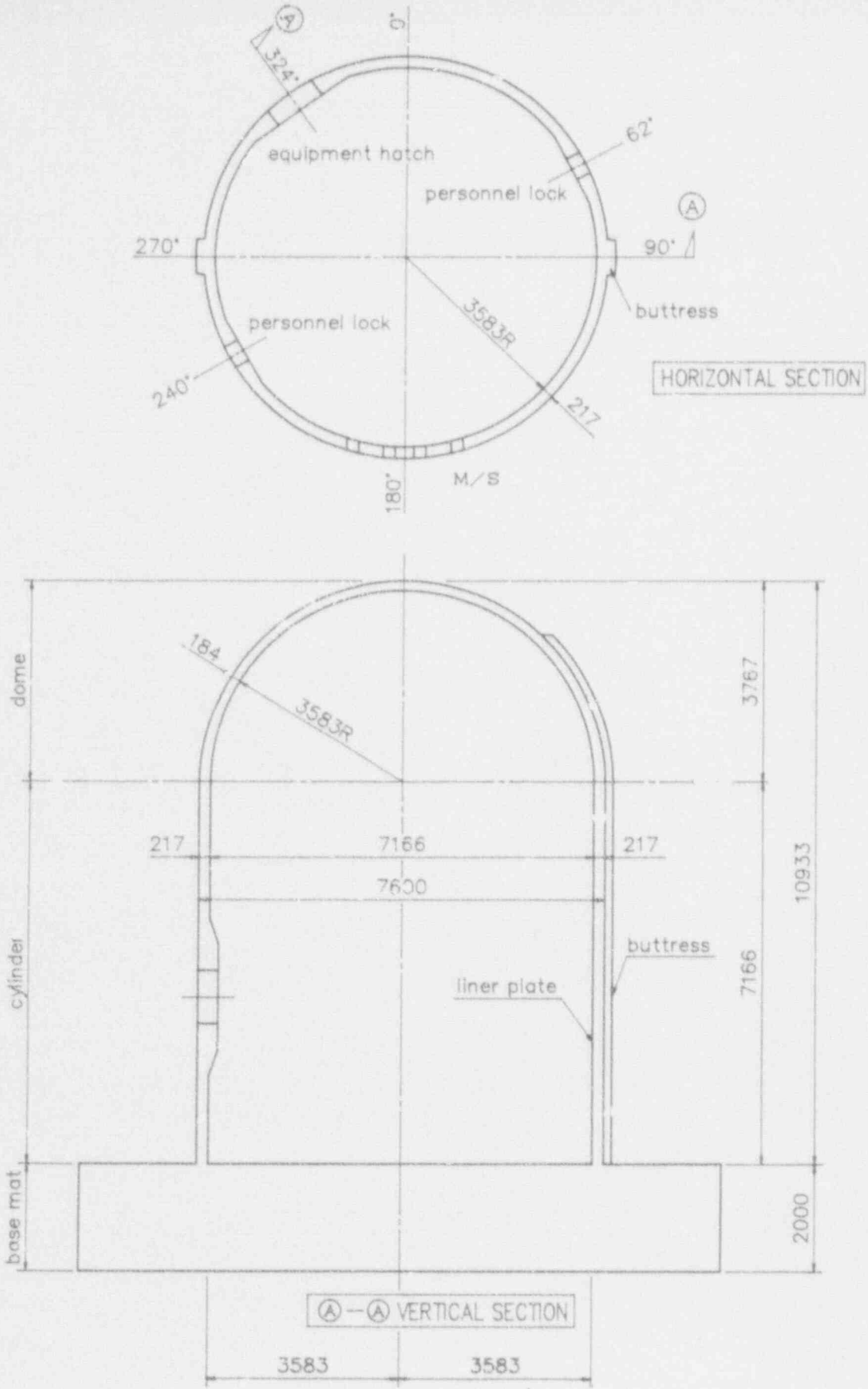


Figure 2. General Arrangement of the Test Model

# PLAN ON TEST TO FAILURE OF A STEEL CONTAINMENT VESSEL MODEL

Kenji Takumi, Akira Nonaka, Katsuhiko Umeki, Yasushi Yoshida
Nuclear Power Engineering Corporation, Japan

Osamu Oyamada, Hideyasu Furukawa, Koichi Saito
Hitachi Works, Hitachi Ltd., Japan

James F. Costello
United States Nuclear Regulatory Commission, USA

Walter A. von Riesemann, M. Bradley Parks, Robert A. Watson
Sandia National Laboratories, USA†

## Abstract

This paper describes the plan for a test to failure of a steel containment vessel model. The test specimen proposed for this test is a scale model representing certain features of an improved BWR MARK-II containment vessel. The objective of this test is to investigate the ultimate structural behavior of the model by incrementally increasing the internal pressure, at ambient temperature, until failure occurs. Pre- and posttest analyses will be conducted to predict and evaluate the results of this test. The main objective of these analyses is to validate, by comparisons with the experimental data, the analytical methods used to evaluate the structural behavior of an actual containment vessel under severe accident conditions. This experiment is part of a cooperative program between the Nuclear Power Engineering Corporation (NUPEC), the United States Nuclear Regulatory Commission (NRC), and Sandia National Laboratories (SNL).

## INTRODUCTION

The containment vessel in nuclear power plants prevents the release of fission products to the environment in the unlikely event that a severe accident occurs. Because of the importance of the containment in reducing public risk, an experiment is being conducted to investigate the ultimate structural behavior of a steel containment vessel representative of the improved MARK-II containment. This type of containment is utilized in numerous boiling water reactors (BWRs) in Japan and is designed according to Japanese regulations. The experimental data base developed from this test will be used to qualify the analytical methods used in predicting containment behavior during a hypothetical severe accident. This paper describes the conceptual plan for the test.

---

† Sandia National Laboratories is operated by the U.S. Department of Energy under contract number DE-AC04-76DP00789.

## TEST MODEL DESIGN

In BWR plants operated in Japan, only free-standing steel containment vessels (SCVs) have been utilized. The configuration of these SCVs is different from the numerous steel containment models that have been tested previously at Sandia National Laboratories. The shell of the improved BWR MARK-II containment consists of numerous geometric features such as a torispherical head with flange connection, a reverse-curvature knuckle, and spherical, conical and cylindrical sections, as shown in Figure 1. The improved BWR MARK-II containment has been used on 1100 MWe power plants. The overall size of the shell is 48 m in height, with a maximum diameter of 29 m. Except for the thickened knuckle region, the nominal thickness of the shell is less than 38 mm.

Components of the actual containment that were chosen to be represented in the SCV model are shown in Table 1. Figure 2 illustrates the configuration and dimensions of the test model. Table 2 lists the dimensions of the test model. The geometric dimensions are scaled by 1:10, while the wall thicknesses are nominally scaled by 1:5 (except for the drywell head region where the wall thickness is scaled by 1:4). These scales were selected so that the overall model size is small enough for shipping from Japan to SNL and the wall thicknesses are thick enough to maintain representative fabrication quality.

The focus of this test is the ultimate structural behavior of the drywell portion of the containment; therefore, the complete wetwell is not included in the model. A large equipment hatch is the only non-axisymmetric feature included in the model. Additionally, the bolted flange connections for the equipment hatch and drywell head are not modeled. This is because full-scale separate-effect models are more effective for characterizing the behavior and improving the evaluation methods of these connections. To investigate the leakage behavior of a bolted flange with gasket, a "hatch model test" using a full-scale model is scheduled to be conducted in Japan, as a separate NUPEC test program.

Finite element analyses were conducted to confirm the adequacy of utilizing nonuniform scaling in the SCV model. In these analyses, a large displacement formulation was utilized and nonlinear material properties were taken into account. Figure 3 and Figure 4 show the membrane strain distributions and deformations, at the same maximum strain level due to internal pressurization, for the actual containment and the SCV model, respectively. The similarity in these results suggests that the structural response of the SCV model will be comparable to that of an actual containment prior to contact with the surrounding concrete shield building. In the evaluation of an actual containment, the pressure scale factor of approximately two, which is the nominal ratio of scales for thickness and geometry, must be taken into account.

## TESTING CONDITIONS

The model will be fabricated in Japan and instrumented and tested in the US at SNL. In this test, the model will be pressurized quasi-statically with nitrogen gas at ambient temperature. A large number of data channels (strain gages, displacement transducers, pressure and temperature transducers, video cameras, etc.) will be used to measure the structural behavior of the model.

## EVALUATION

Axisymmetric and three-dimensional nonlinear finite element analyses will be performed to predict the behavior of the SCV model before the test is conducted and to compare with its response after the test has been completed. By comparisons with the experimental data, the analytical methods used to evaluate the structural behavior of an actual steel containment vessel subject to severe accident conditions will be validated.

## SUMMARY

A brief test plan has been presented for the pressurization to failure of a steel containment vessel. This experiment is part of a cooperative program between NUPEC and NRC/SNL. Details of the proposed test are currently under discussion and may be changed in the future. The test is expected to be conducted in 1995.

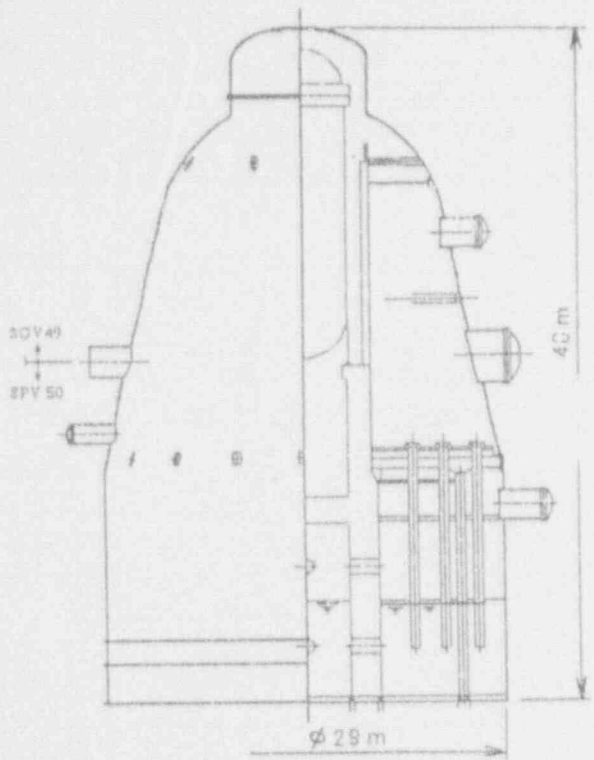


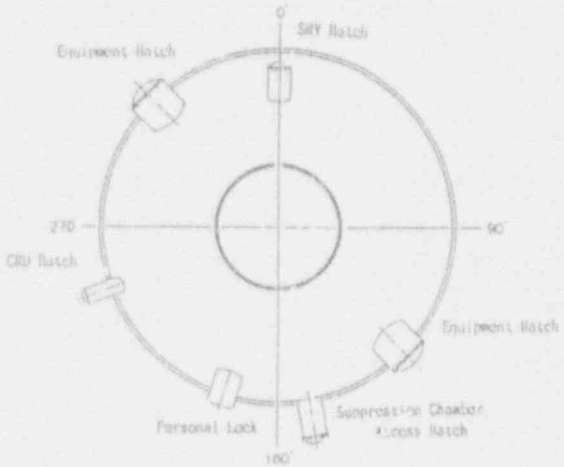


Top View

Figure 1 Actual containment vessel
(Typical BWR improved Mark-I)

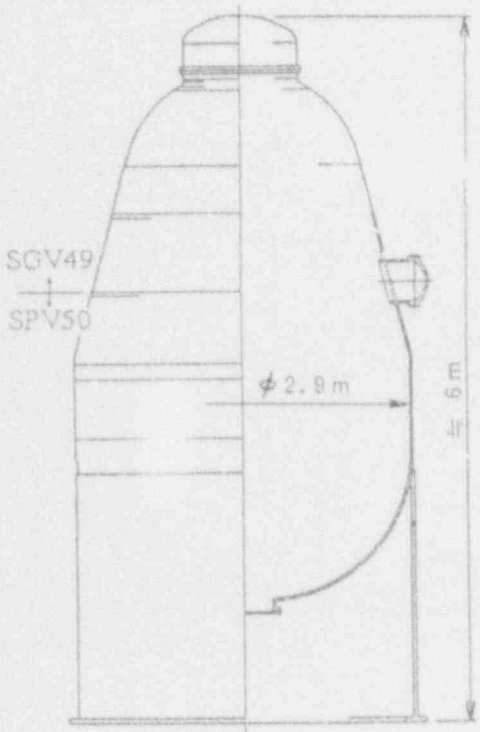


Figure 2 Configuration of test model

Table 1 Scope of modeling

| Structures | Model | Remarks |
|---|---|---|
| Top head | ○ | |
| Top flange | ^ | Only stiffeness (Without bolted connection) |
| Drywell shell | ○ | |
| Suppression chamber shell | △ | Only top portion |
| Hatches | △ | Equipment hatch |
| Penetrations | – | |
| Reinforcing ring (include spray lines) | ○ | Only stiffeness |
| Pool water | – | |
| Bottom liner & anchor | – | |
| Internal structures | – | |

○ : Modeled
△ : Partially Modeled
– : Not Modeled

Table 2 Dimensions of the test model

| Items | Test model | Actual PCV |
|---|---|---|
| Overall height | ≒ 6m | ≒ 48m |
| Max. inside diameter | 2.9m | 29m |
| Max. Wall thickness (Excluding local area) | 7.9mm (8mm) | 38mm |
| Material | SGV49 SPV50 | SGV49 SPV50 |

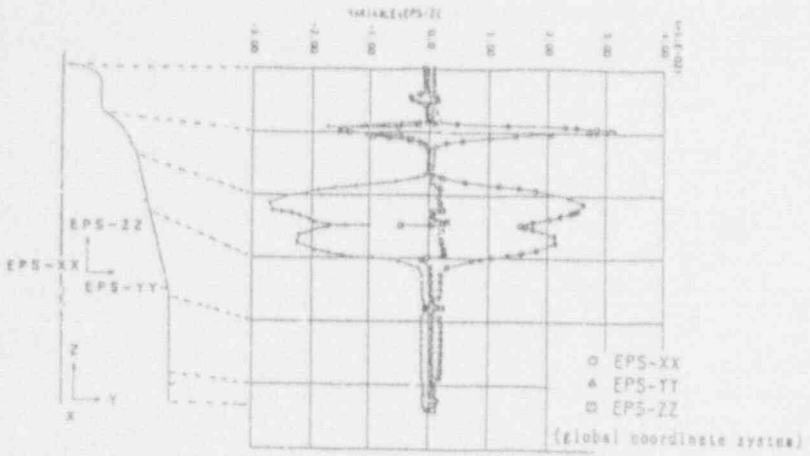


Figure 3.1 Membrane strain distribution for actual containment

Figure 4.1 Amplified Deformation for actual containment
( ~ 3% maximum strain )

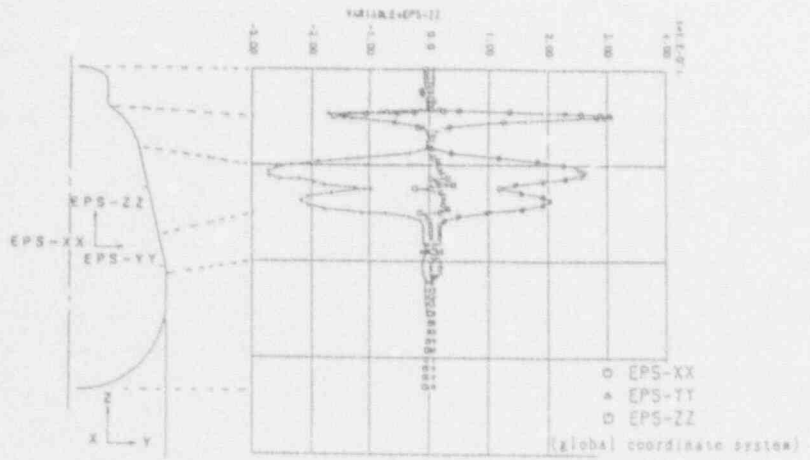


Figure 3.2 Membrane strain distribution for test model

Figure 4.2 Amplified Deformation for test model
( ~ 3% maximum strain )

# CONCERNING ASSESSMENT OF THE STRENGTH AND LEAKTIGHTNESS OF THE DOUBLE-SHELL CONTAINMENT OF A 1300 MWe PWR

D. Dussarte
IPSN/DES

B. Barbé
IPSN/DES

E. Debec
CISI

**Abstract**

The containment of a 1300 MWe PWR consists of two concentric shells (Figure 1). The inner shell is of pre-stressed concrete while the outer shell is of reinforced concrete. Leakage from the inner shell is collected in the gap between the two shells which is maintained at a negative pressure by a pumping system.

This study is concerned with two situations:

- a slow rise in pressure resulting from the presence of a source of gas, the flow rate of which is considered to be a parameter,
- a sudden pressure rise which is taken to correspond to that which would be the result from a hydrogen deflagration.

The numerical approach used in this study describes cracking of the inner shell under the effect of pressure and gives, at any given moment, the flow rate per unit mass entering the gap between the shells as well as the outflow from the containment until steady-state conditions are obtained.

## INTRODUCTION

The numerical approach used in this study describes both cracking of the inner shell under the effect of pressure and, at any given moment, the flow rate per unit mass entering the gap between the shells as well as the outflow from the containment. This calculation is carried through until steady-state conditions are reached for both of the following situations.

In the first situation, it is assumed that, in an initial state without overpressure in the inner shell, core meltdown causes a slow pressure rise arbitrarily modelled by the presence of a dry air source with a flow rate of $Q_s$, which is constant with time, taken as a parameter. The calculation is remade assuming that there was originally an overpressure of the order of its design basis pressure in the inner shell. From this state, a slow modelled pressure rise is postulated, as in the preceding case, by a dry air source of flow rate $Q_s$.

In the second situation, it is assumed that a substantial quantity of hydrogen is formed and its combustion is taken into consideration.

Hereafter, for simplicity, the term LOCA is used to designate the first situation and the term hydrogen deflagration is used to designate the second.

## THE DIFFERENT TYPES OF CRACKS

### Inner shell

Three different types of cracks can be identified in a pre-stressed concrete inner shell subjected to an increasing internal pressure:

#### Thermal contraction cracks

Such cracks allow fluid to flow from the inner shell to the inter-shell gap as soon as the pressure differential rises above zero bar. The results of leak tests indicate that the average width (e) and length (l) of such cracks remain stable while the pressure is below the test pressure. The measurements taken make it possible to obtain a clear picture of the distribution of such cracks, which are characterized by a width of $25 \times 10^{-6}$ m and an accumulated length of around 600 m.

#### Cracks between penetration sleeves and concrete

At a penetration, loss of adhesion between the sleeve and the concrete, resulting in separation at this interface, arises as soon as the compression due to the pre-stressing is overcome, which occurs at a differential pressure of 5.1 bar. Radial separation at the edges of the hole can be assessed by Kirsch's relationships derived from support theory.

#### Cracks of mechanical origin

Cracks of mechanical origin appear when tensile stresses in the concrete reach its ultimate strength, i.e. at an internal pressure of around 6.7 bar gage.

For the type of containment in question, the accumulated length l of these vertical cracks, which appear at intervals of approximately one metre, over the entire height of the cylinder, is of the order of 10,000 m.

The results of observations made with a 1/10 scale model indicate that variation of the width of such cracks with pressure P is correctly represented by a fit law corresponding to the following equation (1):

$$e = \frac{9}{100} P^2 + \frac{27}{100} P \qquad (1)$$

## Outer shell

### Permeability of concrete (microcracks)

The outer shell is not pre stressed and it is assumed that leaks through the permeable concrete and microcracks will appear as soon as the inter-shell gap and the outside environment are not in a state of pressure equilibrium. Flow is possible in either direction.

### Cracks of mechanical origin

Failure of the outer shell resulting from the appearance of cracks of mechanical origin is assumed to occur as soon as the overpressure in the inter shell gap reaches around 0.4 bars

## LAWS AND RATES OF FLOW

In the two types of problems studied, i.e. LOCA and hydrogen deflagration, the gases and gas mixtures (dry air or a mixture of dry air and steam) which can flow through the different crack systems are equated with perfect fluids with isothermal flow.

Leak rate estimates are made on the basis of the following standard equations.

### Calculation of leaks through a porous or microcracked medium

In a porous medium of geometric permeability K the type of flow is laminar and the rate of flow per unit mass Q is given by equation (2):

$$Q = \frac{K}{\eta} \frac{S}{h} \rho \frac{P_i^2 - P_e^2}{2 P_e} \qquad (2)$$

where
- K = geometric permeability (m²)
- $\eta$ = dynamic viscosity (Poiseuilles)
- s = surface of wall (m²)
- h = thickness of wall (m)
- $\rho$ = density (kg/m³)
- $P_i$ = internal pressure (bar)
- $P_e$ = external pressure (bar)

## Calculation of leakage through a crack

Calculation of leakage through a crack is carried out using flow equations for a compressible fluid between two fixed parallel flat surfaces of length l separated by a distance e.

Depending on the Reynolds' number value, the leak rate is calculated for laminar or turbulent conditions.

### Laminar conditions ($R_e$ < 2000)

Leak rate per unit mass Q is calculated using equation (3):

$$Q = \frac{P_i^2 - P_e^2}{24\, P_i\, \eta\, h}\, \rho\, e^3\, l \qquad (3)$$

The fluid may consist of a mixture of perfect gases and the equivalent dynamic viscosity of the medium is estimated using the mixture law (linear combination).

### Turbulent conditions ($R_e$ < 2000)

Leak rate per unit mass Q under turbulent conditions can be written in the form of equation (4):

$$Q = \left[ e\, P_i\, \rho \frac{1 - \left(\frac{P_e}{P_i}\right)^{1/y}}{f.h} \right]^{1/2} S \qquad (4)$$

where $y = \frac{C_p}{C_v}$

f = pressure loss coefficient

The value of f is obtained by solving the transcendental equation (5):

$$\frac{1}{f^{1/2}} = 2 \log_{10}(R_e f^{1/2}) - 1.16 \qquad (5)$$

## SOLVING

For the two types of accident (LOCA and hydrogen deflagration), use is made in solving the numeric problem of the principle of conservation of mass, of the fluid state equation and the appropriate aforementioned flow laws.

## LOCA

In the case of a LOCA followed by a slow pressure rise, the fluid is modelled by a dry air supply of which the flow rate per unit mass $Q_s$ is assumed to be constant. Solving the problem consists in solving the following equation (6):

$$\frac{dP_1}{dt} = \frac{RT_1}{V_1}\frac{Q_s + Q_1}{m_a} \qquad (6)$$

where $V_1$ = the volume of the inner shell

$Q_1$ = the outflow from the inner shell (see formula 2, 3 or 4)

$T_1$ = inner shell temperature

$m_a$ = mass of one mole of air

$P_1$ = inner shell pressure

## Hydrogen deflagration

In the case of hydrogen deflagration, it is assumed that:

- just before initiation of the combustion (t = 0), the properties of the fluid are as follows: $P_1$ = 3 bar absolute and $T_1$ = 100°C,
- the atmosphere of the containment consists (molar fractions) of 10% hydrogen, 43% air and 47% steam,
- during progressive combustion of a duration $t_c$ of the order of 20 s, no condensation phenomenon is taken into consideration.

Solving the problem consists in solving equation (7):

$$\frac{dP_1}{dt} = \frac{P_1}{T}\frac{dT_1}{dt} + \frac{RT_1}{V_1}\frac{Q_1}{m_{a,v}} \qquad (7)$$

with the following equations (8) and (9):

$$T_1(t) = T_{min} + \left[\frac{T_{max} - T_{min}}{t_c}\right] t; \text{ for } t \leq t_c \qquad (8)$$

$$T_1(t) = T_{max} \exp\left[-\lambda(t - t_c)\right] + T_{min}\left[1 - \exp\left[-\lambda(T - t_c)\right]\right] \text{ for } t > t_c \qquad (9)$$

it being known that:

$T_{min}$ = 100°C

$T_{max}$ = 900°C

$\lambda$ = 0.0125 $s^{-1}$

$T_c$ = combustion time (20 s)

## CALCULATION CONDITIONS AND RESULTS

### LOCA situation

#### Calculation conditions

Two extreme cases are considered.

Without initial overpressure in the inner shell, the slow pressure rise is modelled by the action of a constant air supply of flow rate $Q_s$ taken to be a parameter.

Furthermore, the phenomenon of condensation is not taken into consideration and the temperatures between the two shells are constant at all moments in time. The initial pressure in the inner shell is 1 bar absolute whereas that in the outer shell is 0.985 bar or 1 bar depending on whether the containment annulus ventilation system is active or inactive.

With an initial overpressure in the inner shell, it is assumed that the pressure in the inner shell is 4.8 bar absolute. From this moment in time, the increase in the pressure is modelled, as in the previous case, by the action of a dry air supply of flow rate $Q_s$.

Three values per unit mass are studied: $Q_s$ = 2, 4 and 6 kg/s. These bracket the value corresponding to that of the WASH 1400 report (3.5 kg/s).

#### Principal results

The containment annulus ventilation system ensures, whatever the size of the break and its flow rate $Q_s$, negative pressure conditions in the inter-shell gap and hence no releases to the exterior as long as internal pressure $P_1$ is less than 6.1 bar absolute. It is to be remembered that this value corresponds to total decompression of the concrete and the onset of separation of the penetration liners and the concrete. This situation is guaranteed for time and periods which are inversely proportional to flow rate $Q_s$ (Figures 2 to 5). These characteristic type periods are shown in Table 1 below.

Table 1 - Time periods

| Flow rate $Q_s$ (kg/s) | 6 | 4 | 2 |
|---|---|---|---|
| Without initial overpressure (hours) | 24 | 35 | 70 |
| With initial overpressure (hours) | 6 | 9 | 12 |

In a case where a break gives rise to an overpressure in the inner shell which is less than the design basis pressure, the characteristic time periods are

between the extreme time periods of the two cases studied. They can easily be determined by transposing the curves.

For time periods greater than these characteristic time periods, the curves for inner shell outflow to the inter-shell gap and from the gap to the exterior tend, whatever the case studied, towards the maximum equilibrium flow rate $Q_s$ (Figure 6).

The maximum equilibrium pressure reached in the inner shell (Figures 3 and 5) is around 8.4 bar absolute and the pressure in the inter-shell gap is less than the failure pressure of the outer containment for flow rates $Q_s$ of 2 and 4 kg/s. It is to be noted that the differential pressure between the inner shell and the inter-shell gap is around 7 bars (8.4 to 1.4); this value is slightly higher than the transverse cracking pressure of the inner shell which is 6.7 bar (Figure 7).

The equivalent crack areas of the inner shell which give rise to flow rates to the atmosphere equal to those of source terms $Q_s$ are 0.03 $m^2$ when $Q_s$ = 2 kg/s, 0.08 $m^2$ when $Q_s$ = 4 kg/s and 0.25 $m^2$ when $Q_s$ = 6 kg/s (Figures 7 and 8).

## Hydrogen deflagration

### Conditions of calculation

The different cases studied are show in Table 2 below.

Table 2

| CASE | CONDENSATION | | CONTAINMENT ANNULUS VENTILATION SECTION | | OUTER SHELL | |
|---|---|---|---|---|---|---|
| | YES | NO | YES | NO | LEAKTIGHT | NOT LEAKTIGHT |
| 1 | | + | + | | | + |
| 2 | + | | + | | | + |
| 3 | + | | | + | | + |
| 4 | + | | + | | + | |

### Principal results

Salient points of this study are the following.

The results do not vary greatly with the value of the combustion time $t_c$, which remains of the order of a few tenths of a second. Whatever the set of parameters utilized, the pressure peak $P_1$ reached in the inner shell is around

5 bar absolute (Figure 9). This pressure can be associated with a maximum equivalent leak area of around 5 $m^2$ (Figure 10).

Whatever the set of parameters utilized, the maximum pressure reached in the inter-shell gap is well below the outer shell failure pressure. For instance, this pressure reached 270 mbar in the case where the containment annulus ventilation system does not operate.

Allowance for the phenomenon of condensation in the inter-shell gap has little effect on this pressure level in the inter-shell gap.

## CONCLUSIONS

The purpose of this analysis was to obtain an understanding of the mechanical strength and the leaktightness of the double-shell containment of a type P4 1300 MWe PWR in the event of either a slow pressure increase or a hydrogen deflagration.

In the slow pressure rise case, it is to be noted that:

- the containment annulus ventilation system ensures that there is a negative pressure in the inter-shell gap as long as the pressure in the inner shell does not exceed 6.1 bar absolute,
- failure of the outer shell, which is assumed to occur when the overpressure in the inter-shell gap reaches around 400 mbar, can be eliminated as long as the source flow rate per unit mass is less than 6 kg/s, i.e. a value higher than that adopted in the WASH 1400 report.

In the hydrogen deflagration case, it is to be noted that:

- the maximum pressure reached in the inner shell is around 9 bar absolute, i.e. a pressure lower than its failure pressure. This result is practically independent of allowance for condensation in the inter-shell gap, the action of the containment annulus ventilation system and the leaktightness of the outer shell,
- the pressure reached in the inter-shell gap does not exceed 270 mbar, a value which remains lower than the failure pressure of the outer shell.

Finally, this simplified study only gives likely orders of magnitude as regards the mechanical strength of the containment. Further consideration is necessary as regards the phenomena of condensation and the retention of fission products in or on the concrete walls of the containment.

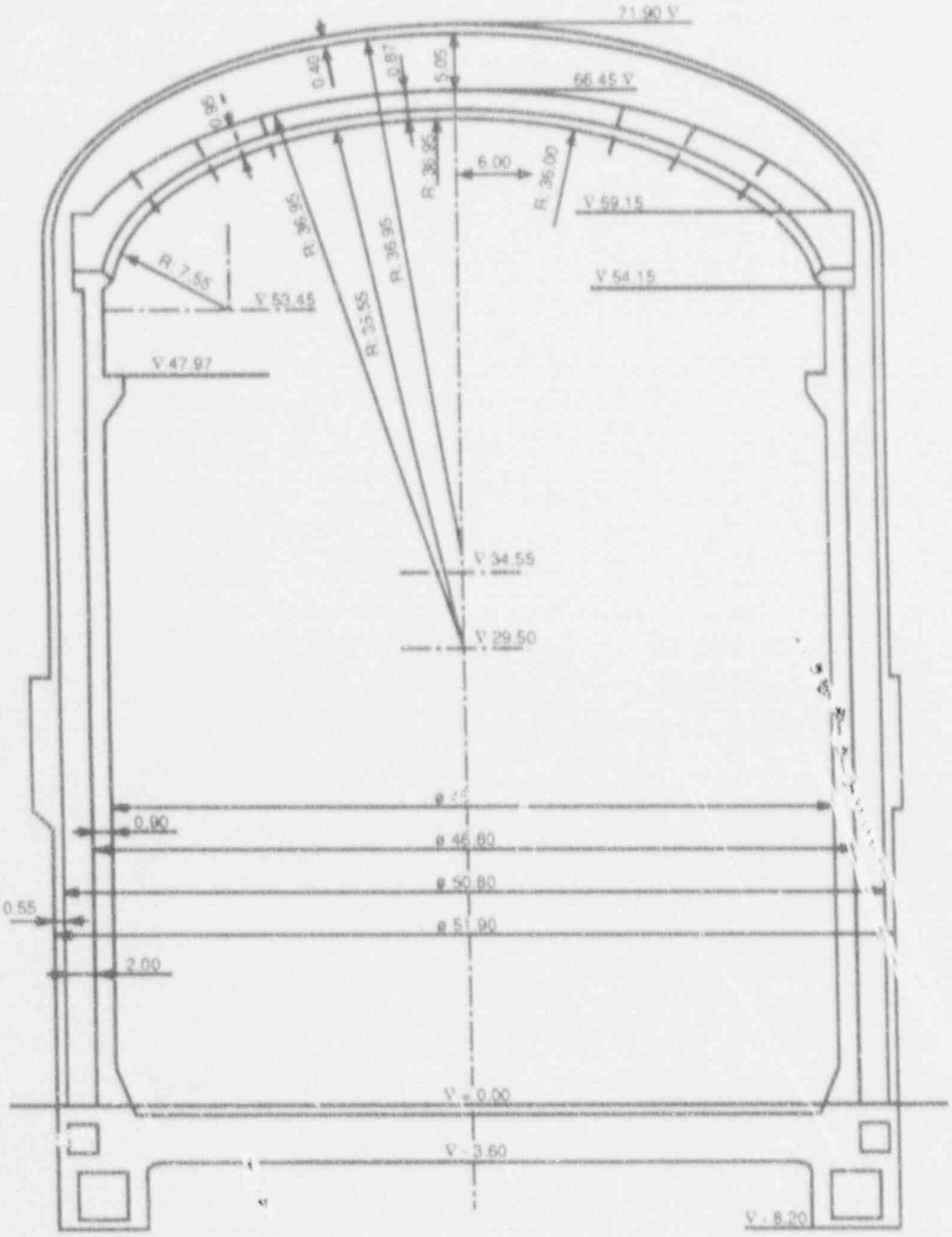


Figure 1 - P4 CONTAINMENT

WITHOUT INTERNAL OVERPRESSURE

Case of LOCA followed by a pressure rise — Curve A Q = 2 kg/s
Hypotheses: flow rate per unit mass (air) of source — Curve B Q = 4 kg/s
= Q kg/s, containment annulus ventilation system active — Curve C Q = 6 kg/s

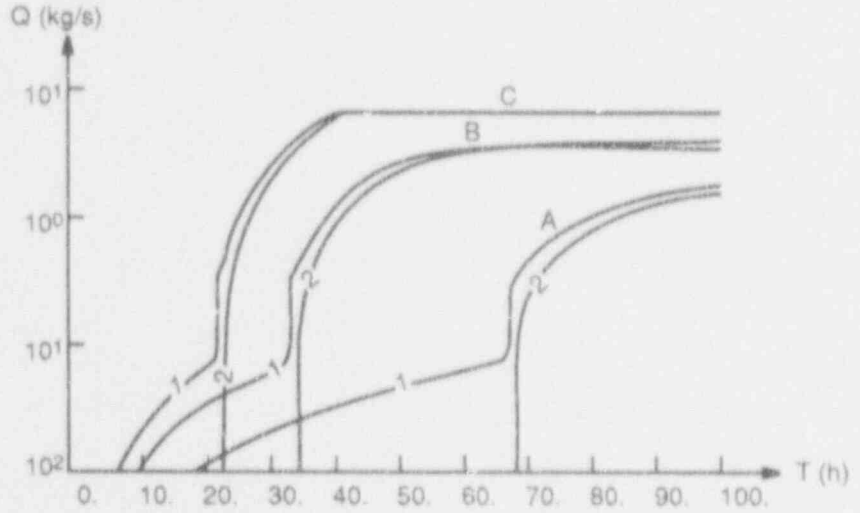


Figure 2 - VARIATION OF FLOW RATES AS A FUNCTION OF TIME

Index 1: containment to inter-shell gap
Index 2: inter-shell gap to exterior

WITHOUT INTERNAL OVERPRESSURE

Case of LOCA followed by a pressure rise — Curve A Q = 2 kg/s
Hypotheses: flow rate per unit mass (air) of source — Curve B Q = 4 kg/s
= Q kg/s, containment annulus ventilation system active — Curve C Q = 6 kg/s

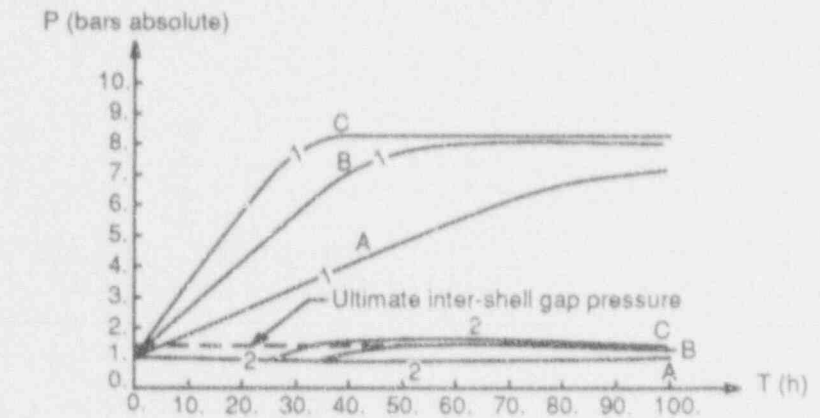


Figure 3 - VARIATION OF PRESSURE AS A FUNCTION OF TIME

Index 1: inner shell
Index 2: inter-shell gap

WITH INTERNAL PRESSURE

Case of LOCA followed by a pressure rise
Hypotheses: flow rate per unit mass (air) of source = Q kg/s, containment annulus ventilation system active

Curve A Q = 2 kg/s
Curve B Q = 4 kg/s
Curve C Q = 6 kg/s

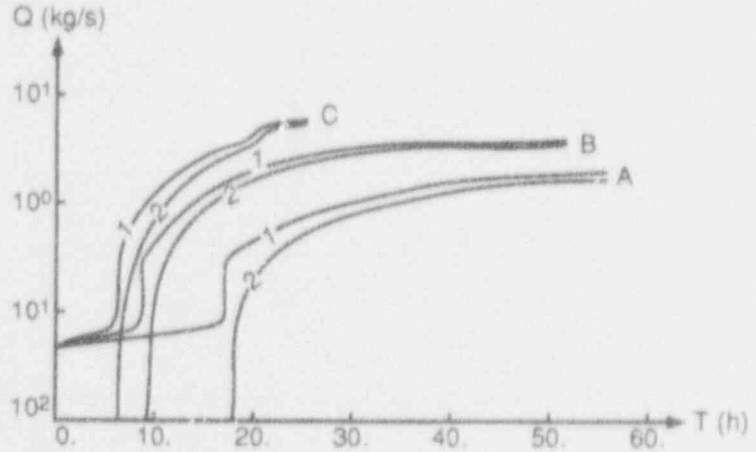


Figure 4 - VARIATION OF FLOW RATES AS A FUNCTION OF TIME

Index 1: containment to inter-shell gap
Index 2: inter-shell gap to exterior

WITH INTERNAL PRESSURE

Case of LOCA followed by a pressure rise
Hypotheses: flow rate per unit mass (air) of source = Q kg/s, containment annulus ventilation system active

Curve A Q = 2 kg/s
Curve B Q = 4 kg/s
Curve C Q = 6 kg/s

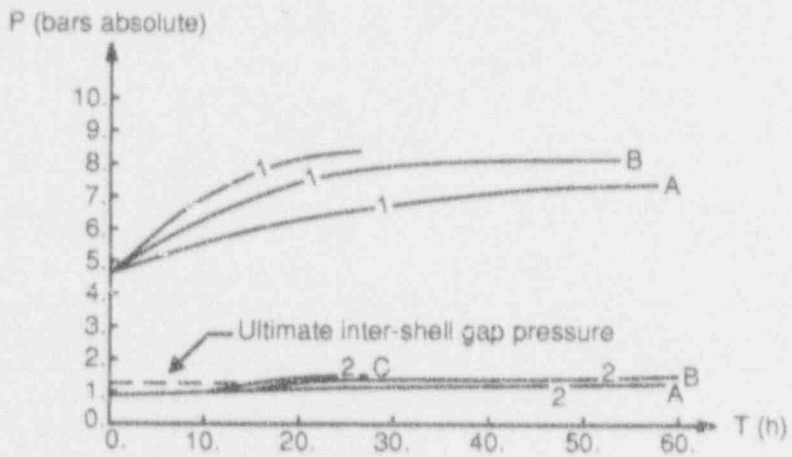


Figure 5 - VARIATION OF PRESSURE AS A FUNCTION OF TIME

Index 1: inner shell
Index 2: inter-shell gap

WITHOUT INTERNAL PRESSURE

Case of LOCA followed by a pressure rise
Hypotheses: flow rate per unit mass (air) of source = Q kg/s, containment annulus ventilation system active

Curve A Q = 2 kg/s
Curve B Q = 4 kg/s
Curve C Q = 6 kg/s

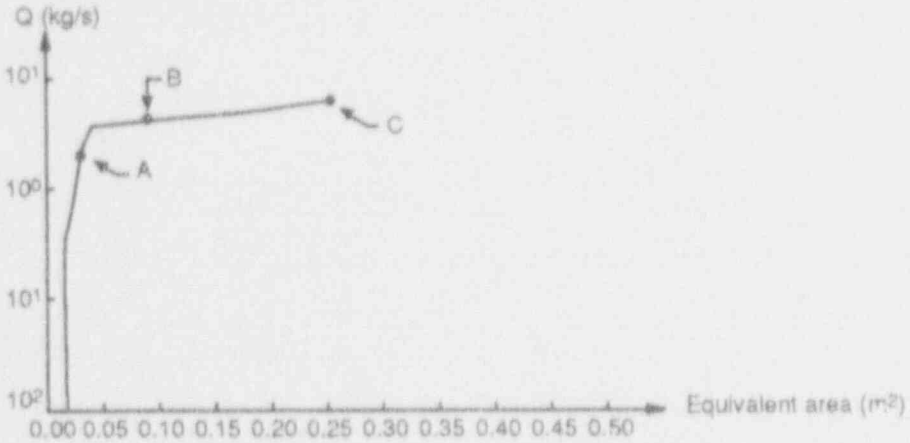


Figure 6 - FLOW RATE FROM REACTOR BUILDING TO CONTAINMENT ISOLATION SYSTEM AS A FUNCTION OF THE EQUIVALENT AREA OF LEAKAGE

WITHOUT INTERNAL PRESSURE

Case of LOCA followed by a pressure rise
Hypotheses: flow rate per unit mass (air) of source = Q kg/s, containment annulus ventilation system active

Curve A Q = 2 kg/s
Curve B Q = 4 kg/s
Curve C Q = 6 kg/s

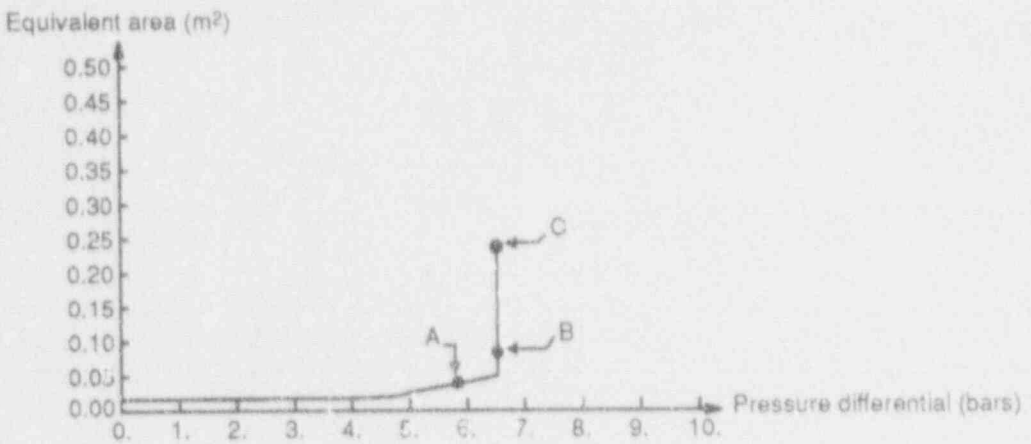


Figure 7 - CHANGE IN EQUIVALENT AREA OF LEAKAGE AS A FUNCTION OF THE PRESSURE DIFFERENTIAL BETWEEN THE REACTOR BUILDING AND THE INTER-SHELL GAP ISOLATION SYSTEM

WITHOUT INTERNAL PRESSURE

Case of LOCA followed by a pressure rise — Curve A Q = 2 kg/s
Hypotheses: flow rate per unit mass (air) of source — Curve B Q = 4 kg/s
= Q kg/s, containment annulus ventilation system active — Curve C Q = 6 kg/s

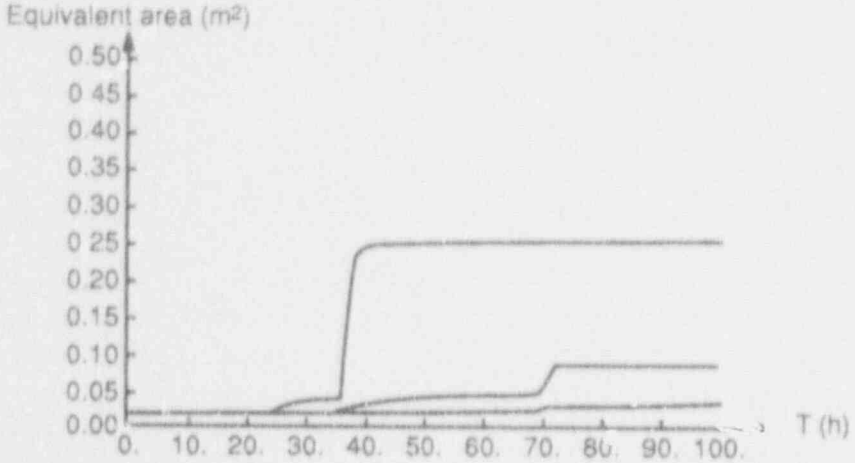


Figure 8 - CHANGE IN EQUIVALENT AREA OF LEAKAGE BETWEEN REACTOR BUILDING AND INTER-SHELL GAP AS A FUNCTION OF TIME

Case 1 - A hydrogen deflagration
Hypotheses: phenomenon of condensation in inter-shell gap not allowed for and containment annulus ventilation system active.

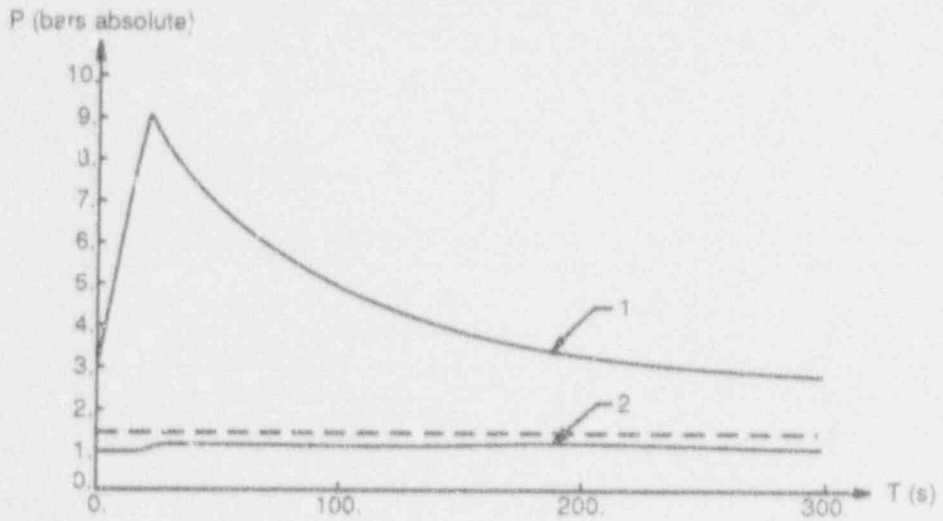


Figure 9 - CHANGE IN PRESSURE AS A FUNCTION OF TIME

Index 1: Inner shell
Index 2: Inter-shell gap

Case 4 - A hydrogen deflagration
Hypotheses: phenomenon of condensation in inter-shell gap allowed for and containment annulus ventilation system active. Outer shell assumed to be perfectly leaktight

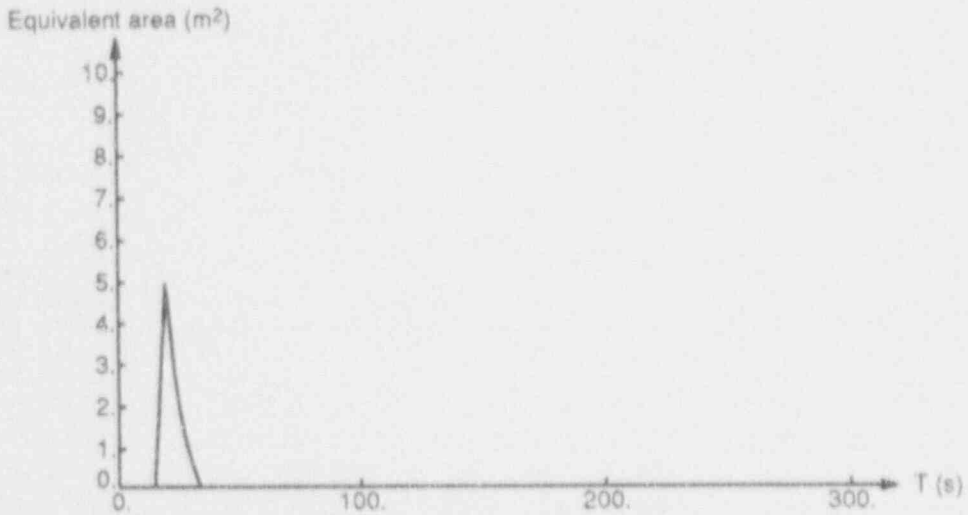


Figure 10 - CHANGE IN EQUIVALENT AREA OF LEAKAGE BETWEEN REACTOR BUILDING AND INTER-SHELL GAP AS A FUNCTION OF TIME

# ECCENTRIC $H_2$ DETONATION IN A NUCLEAR POWER PLANT STEEL CONTAINMENT

Giuseppe Maresca, Giovanni Pino
ENEA-DISP

## Abstract

At present studies are in progress at ENEA-DISP to assess the performance of a steel containment under hydrogen detonation. Although considered unprobable to occur, this event is studied as a load on the safe side challenging the containment. A complete model to simulate the shock wave behaviour and the fluid structure interaction between the containment atmosphere and the containment wall has been set up at ENEA-DISP and a monodimensional axisymmetric case already studied . In the model the Chapman-Jouguet theory of detonation is applied in order to assess the wave front conditions and the Von Neumann-Richtmyer method is used as a reference to deal with the shock discontinuity.
In the present paper the two-dimensional extension of the numerical model has been used. A plane slice of the wall and of the atmosphere filling the containment is considered. A cylindrical detonation wave is supposed to start from a source located eccentrically with respect to the containment axis. Because of the exploratory nature of the numerical model, a period of only 20 msec has been considered, although 100 msec should be considered as a minimum in a large metal containment to exclude further growing of plastic strains produced by consecutive reflections. At variance with the axisymmetric case bending stresses are developed now . The use of the model in order to assess a strain failure criterium to be applied at the dynamic portion of the $H_2$ detonation load is considered. In the paper t' influence of different initial values of the relevan parameters (pressure, temperature, hydrogen concentration and source location) is examined in order to assess a range of equivalent conditions.

## INTRODUCTION

Although considered very unlikely to occur, $H_2$ detonation following a core melt-down accident could be taken into account as a load on the safe side challenging the containment. Adopting this defence in depth strategy the question arises on tools available to investigate the structural behaviour of the containment and on their reliability. At ENEA-DISP an activity has been started at the end of 1990 in order to assess the integrity of a large metal containment under $H_2$ bursting. A first step has been the writing down of a computer code able to manage explosion gasdynamics in a simple monodimensio nal case [1]. Obviously this phase was very

useful in order to gain confidence with the matter and as a guide for subsequent investigations. The computer code used the Chapman-Jouguet theory [2], [3] to assess the initial shock front conditions, together with the Taylor's treatment of the back-front wave profile [4], [5] . The formulation is Lagrangian, with a mesh consisting in a number of gas layers located along the containment radius moving to simulate gas behaviour under detonation. The interaction of the containment atmosphere with the steel wall was also introduced, to obtain correct balance of impulse and energy at the boundary. The main result, besides general information about the numerical behaviour of this kind of models, concerned the relevance of consecutive reflections of the wave producing in some cases progressive deformation of the wall. This effect is illustrated in fig. 1, where the shock wave is showed traveling outwards, impacting the wall, reversing towards the containment axis, here reflecting again and so on producing successive impacts. Obviously only shocks strong enough to drive steel into the plastic region are effective for strain cumulation but this appears to be possible when the complete dynamics of the phenomena is considered. Actually, during the impact, some amount of impulse and kinetic energy is transferred to the wall. Because of the high velocity of the shock front, the second impact takes place when the outwards velocity of the wall has not disappeared, making a shock lesser than the first one able to contribute to plastic deformation (Fig. 2). Strain rates have been also provided by the monodimensional analysis. They range between 1 and 10 (m/sec)/m and should not modify the material behaviour with respect to the static conditions. To clarify this subject an experimental campaign is presently promoted by ENEA-DISP in the context of a general program directed to fully characterize containment wall materials. The monodimensional model appears to be a convenient tool for a first approach to the explosion problems. Nevertheless it can be charged of a number of deficiencies requiring to be eliminated in order to get a better understaning of the structural phenomena. First of all, axial stresses are neglected while their effect can be relevant especially if the plastic region is entered. Moreover, the monodimensional model is an axisymmetric one while the location of the explosion source in corrispondence of the containment axis is considered to be an ecceptional case.
These reasons leaded us to the second step: to set up a two-dimensional version of the model able to represent the axial development of an axisymmetric explosion taking place inside the containment, as well as the effect of an explosion starting from an eccentric position (fig. 3).

## THE TWO-DIMENSIONAL AXISYMMETRIC MODEL

In the two-dimensional axisymmetric model an emispherical wave is supposed to start from the bottom of the containment dome, where hydrogen released from a break in the primary circuit or, in a

most severe scenarius, produced by core-concrete interaction, is supposed to diffuse and concentrate. While details of this model will not be discussed in this paper, its importance, in order to get a realistic stress state of the containment wall, must be pointed out. In fact, only this model can determine a combined history of axial and circumferential stresses in the wall, allowing to applicate, if the case, biaxial stresses or biaxial strains failure criteria. Moreover this model provided loads on special regions of the whole structure, as the upper head or the dome floor, whose strength also should be verified.

## THE TWO-DIMENSIONAL PLANE SLICE MODEL

In the plane slice model a slice of the wall and of the atmosphere filling the containment is considered. The explosion could be started by any location on the radius, the only limit being the necessity to have a circular region (the starting wave), not intersecting the wall, around the explosion axis to put the initial conditions. In fact, in this model, as well as in the others, initial conditions are imposed providing a suitable velocity, density and pressure field in a circular region (or emispherical in the two-dimensional axisymmetric case) and cannot be well reproduced when this region is too small. For this reason a minimum distance from the wall must be assured in the plane slice model and maximum eccentricity cases cannot be managed. Outside this region the containment atmosphere is in an unperturbed state: pressure and density are the initial ones and velocity is zero everywhere. The energy located in the starting wave is computed taking into account the energy released by the combustion of all the hidrogen inside the perturbed region and therefore it is proportional to the corresponding area. Cases starting with ditferent perturbed regions actually starts with different energy. Anyway, a bursting mechanism is represented in the present model, and combustion energy of all the hydrogen in the containment should be released within the time the wave take to impact all the points located on the containment circumference. Therefore, the total energy released by combustion should be the same whatever the eccentricity is. To really simulate a detonation the bursting mechanism must be controlled by the passing of the shock front. This problem has not been completely solved in the present model and strongly affected the obtained results.

## FLUID MOTION

No special problem comes from the equations governing fluid motion. A Lagrangian of the discretized system can be easily written down and coupled with thermodynamic relations to obtain the full set of equation determining system motion. Also in the case of no heat generation thermodynamic must be involved because of the non conservation of entropy in the fluid near the shock front. For this reason in the two-dimensional model a finite

element treatment of temperature has been chosen, adopting a linear shape fu·-tionto manage heat exchange and production. To deal with shock discontinuity a bulk viscosity is introduced. While numerical in nature and related to the variable cell dimension of the mesh,the form of this term is derived from Navier Stokes equationsand should converge to physical bulk viscosity as the cell dimension goes to zero. The introduction of an artificial viscosity to deal with shock discontinuity is discussed in [6].

SHELL ELEMENTS

Although both the two-dimensional models are programmed to be used as an user subroutine of the st-uctural code MARC, in the present model the containment wall has been treated by finite differences, using shell equations for small displacement [7]. This make the shell model unreliable if too large displacements are obtained. Rotary inertia has been neglected too.

INITIAL CONDITIONS AND GEOMETRY

A cylindrical steel containment with an internal radius of 20 m is considered and carbon steel SA 516 Gr 70 is adopted as reference material. The material has been supposed elastic perfectly plastic and the yield stress of 390 MPa has been used on the basis of the static stress-strain curve at room temperature. The thickness of the wall was supposed to be .03 m. The computation starts from an initial pressure of 0.163 MPa at a temperatureof 368 k. Therefore differential pressure acting on the containment wall is 0.063 MPa before detonation. The atmosphere composition (molar fractions) is

$H_2$ = 20.0%
$O_2$ = 16.8%
$N_2$ = 63.2%

The hydrogen concentration we adopted is typical to get a full detonation condition; the absence of steam is alsc in this spirit. The gas mixture density is 1.25 Kg/m3. From these data the reaction energy per unit mass can be computed knowing the heat released when 1 Kg of hydrogen has completely reacted (121 MJ/Kg). A value of 2.06 MJ/Kg is obtained.
The adopted mesh is shown in Fig. 4 and the inital cell dimension has been chosen to be 1. 5 m.
As far as it concerns the initial condition in the perturbed region, data from Fig. 5 have been adopted. In fact these data , determined for the study of the monodimensional model, are the same (cylindrical wave).

## PRESENT RESULTS

Three different values of the eccentricity e will be considered: e=0.2, e=0.5 and e=0.8. An axisymmetric case (e=0.0) was also considered, in order to compare the results with the ones provided by the monodimensional model. The motion of the system and the containment wall loading are illustrated in Fig.s 6 and 7. The main results are summarized in Tab. 1. where the greatest strains in the outermost fiber and in the innermost one of the containment wall are reported for times ranging from 5 msec to 20 msec. It is apparent that the worst condition for the containment is provided by the axisymmetric case. Actually the maximum strain diminishes increasing the eccentricity. However, considering the quantity of hydrogen burned in different cases, it is possible to see that also this quantity diminishes increasing the eccentricity and no conclusion about the worst condition can be drawn. Anyway, the cases performed are interesting as far as it concerns the effectivenes of the bending mechanism to produce a failure in the containment. Curvatures in the wall are shown in Fig. 8, together with the stretch in the midplane of the shell and it is apparent that strectch is the most effective in order to put the containment into collapse.

## INFLUENCE OF THE INITIAL PRESSURE

The initial pressure, before the detonanation occurs, can affect the evolution of the dynamic phenomena as well as the final static pressure in the containment. Static pressure provides a primary load acting on the wall and to assure containment integrity the ultimate stress does not have to be passed. In author's opinion this means that ASME III criteria for this load should be met. Anyway as far as it concerns the dynmamic load it should be observed that severe accident can affect the containment only one time in the life and the possibility to adopt for this case a strain criterium shoul be explored. In this context the question arises on what is the worst dynamic load consistent with a given final static pressure. In order to examine this question two other plane slice cases have been studied starting from a greater initial pressure. Obviously, to preserve the same final static pressure, the hidrogen molar fraction must be diminished and it can be easily done looking at the curve in Fig. 9. In fact this curve provides for different values of the hidrogen molar fraction the initial pressure giving the final pressure of 0.8 MPa following an isochoric transformation produced by the hydrogen combustion. To compare with 0.163 MPa and 20% H2 adopted in the foregoing calculation a pressure value of 0.3 MPa has been considered together with 15% $H_2$. The value of 0.8 MPa (absolute pressure) has been considered adopting 0.7 MPa (differential pressure) as a conservative value for the ultimate strength of a large metal containment [8]. Two eccentricities have been considered: e=0.2 and e=0.5. The obtained results (Tab. 2) do not

show relevant differences with results obtained for the same eccentricty but for different initial pressures.

## CONCLUSIONS

Because of the limit of the present model, no conclusion can be drawn now as far as it concerns the worst condition for the containment integrity. In any case the possible use of the model to asses a strain failure criterium, to be limited at the dynamic portion of $H_2$ detonation load, has been shown. As a future goal, complete agreement should be obtained between the monodimensional model and the plane slice one. Also some other consistency conditions should be met, providing a reliable verification of all the three models, from the mathematical point of view at least.

## REFERENCES


[1] G. Maresca, P. P. Milella , G. Pino, "Impulsive Load and Structural Response of a Nuclear Power plant Steel Containment Under $H_2$ Bursting". SMIRT 11, J11/2 ,Tokio, August 91.

[2] Zel'dovich Ia. B., Kompaneets A. S., "Theory of Detonation". Academic Press, New York and London , 1960.

[3] Tieszen S. R., Sherman P. M., Benedick W. B., Berman M, "Detonability of $H_2$-Air Diluent Mixtures". Nureg/CR-4905, 1987.

[4] Grandry M. R., "Hydrogen Detonation Model using the Random Choice Model". M.I.T. Master's Thesis, Boston 1981.

[5] Courant R., Friedrichs K.O., "Supersonic flows and shock waves". Interscience, New York, 1948.

[6] Von Neumann J., Richtmyer R. D.,"A method for the Numerical Calculation of Hydrodynamic Shocks", Journal of Applied Physics, Vol.21, 232, March 1950.

[7] Flugge W.,"Stresses in Shells"Springer-Verlag,1960.

[8] Maresca G., Milella P.P., Pino G., "Ultimate Strength and Rupture Modes of the Metal Containment of a BWR NPP in case of Severe Accident". Nuclear Engineering and Design, Vol. 130, 147, 1991.

Table 1. Maximum deformations in the containment wall. (Pi=0.163 MPa, $X(H_2)$=0.2)

| Time from the first impact : | | 5 msec | 10 msec | 15 msec | 20 msec |
|---|---|---|---|---|---|
| eccent. : | | | | | |
| e=0.0 | εo= | 0.0057 | 0.0158 | 0.0275 | 0.0406 |
| | εi= | 0.0057 | 0.0161 | 0.0281 | 0.0416 |
| e=0.2 | εo= | 0.0051 | 0.0147 | 0.0265 | 0.0433 |
| | εi= | 0.0051 | 0.0145 | 0.0280 | 0.0457 |
| e=0.5 | εo= | 0.0036 | 0.0091 | 0.0148 | 0.0200 |
| | εi= | 0.0036 | 0.0094 | 0.0154 | 0.0208 |
| e=0.8 | εo= | 0.0013 | 0.0017 | 0.0011 | 0.0006 |
| | εi= | 0.0013 | 0.0015 | 0.0011 | 0.0008 |

Table 2. Maximum deformations in the containment wall. (Pi=0.300 MPa, $X(H_2)$=0.15)

| Time from the first impact : | | 5 msec | 10 msec | 15 msec | 20 msec |
|---|---|---|---|---|---|
| eccent. : | | | | | |
| e=0.2 | εo= | 0.0045 | 0.0124 | 0.0223 | 0.0327 |
| | εi= | 0.0045 | 0.0122 | 0.0221 | 0.0330 |
| e=0.5 | εo= | 0.0034 | 0.0081 | 0.0134 | 0.0200 |
| | εi= | 0.0034 | 0.0082 | 0.0137 | 0.0207 |

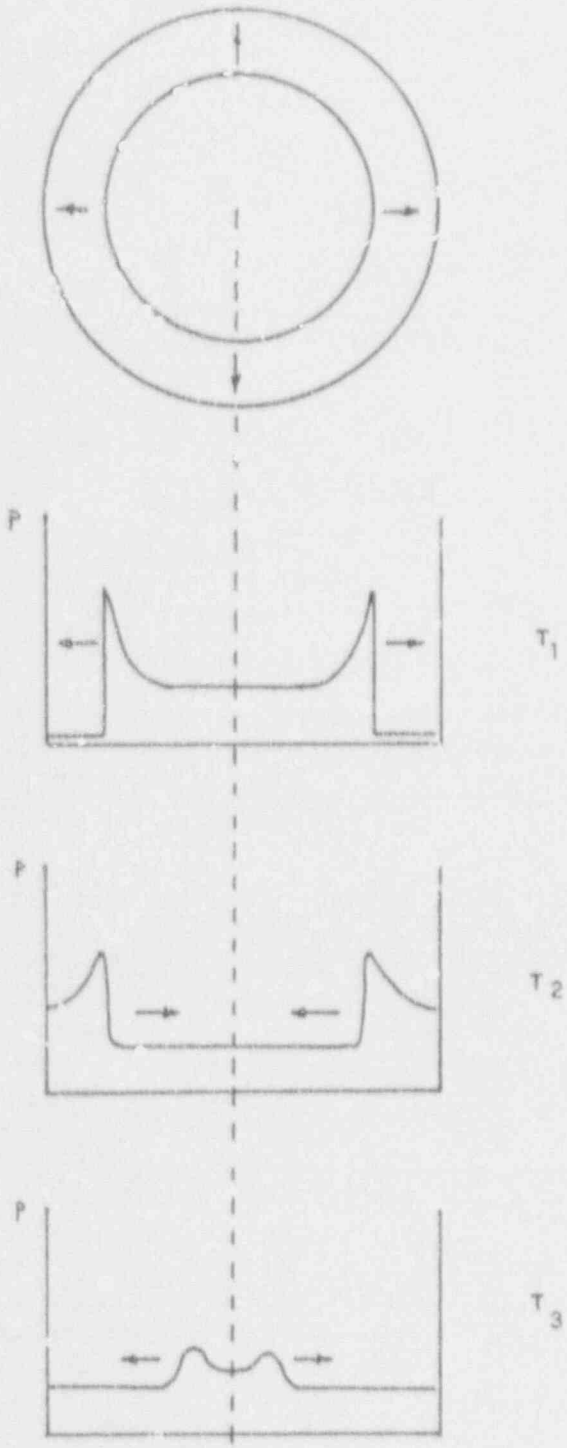


Figure 1. Multiple reflection of an axisyimmetric cylindrical detonation wave.

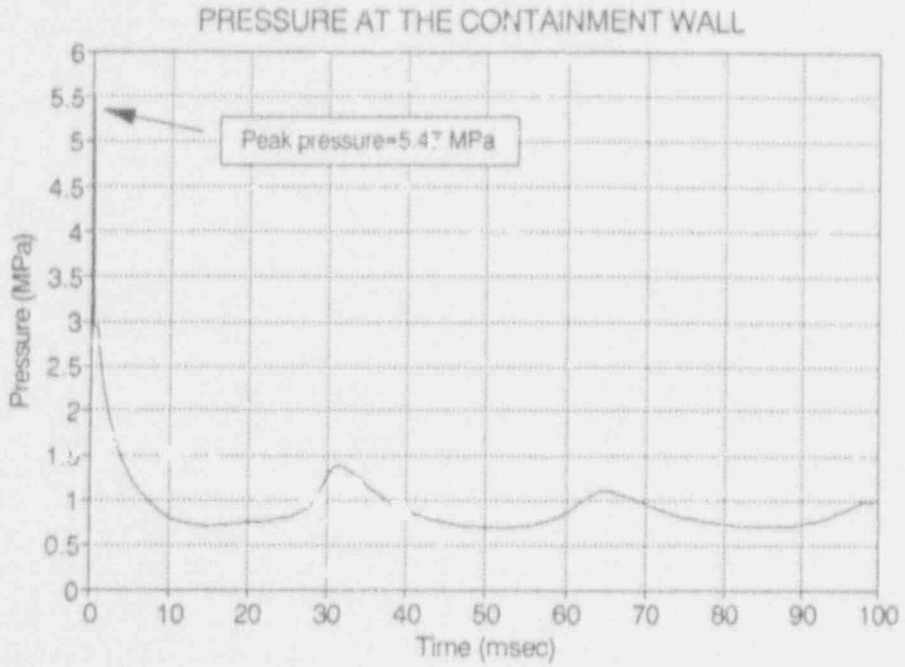


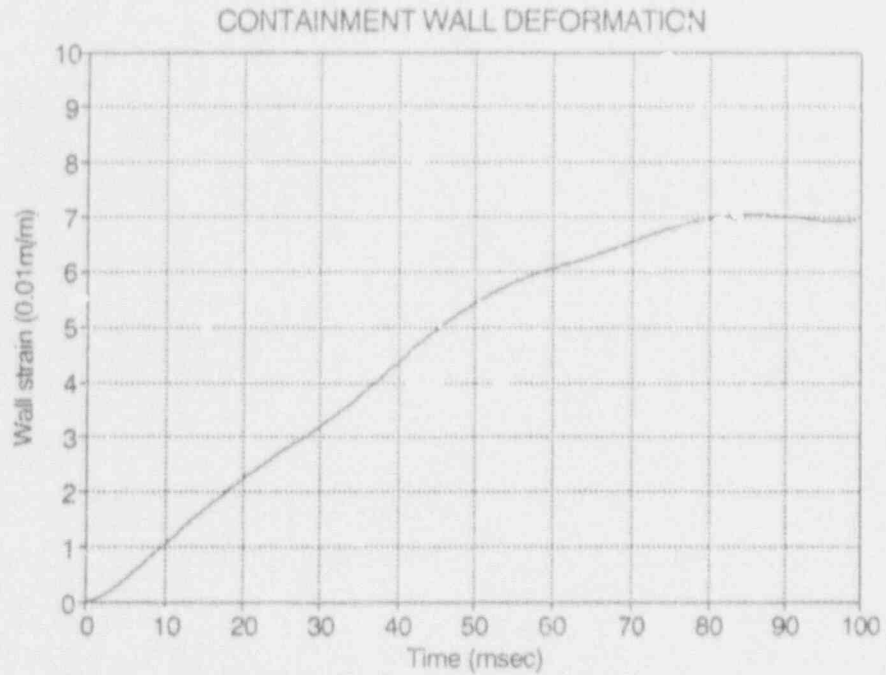


Figure 2. Multiple reflection effects from the monodimensional model [1].

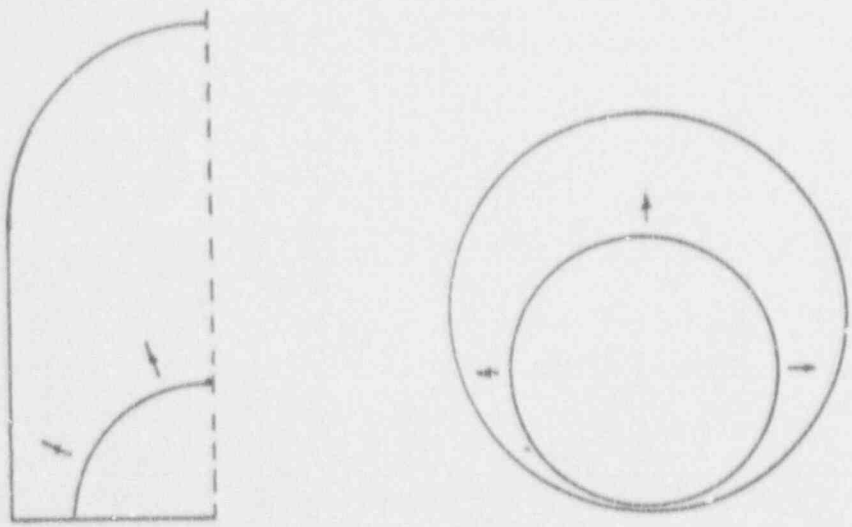


Figure 3. Axisymmetric and plane slice model.

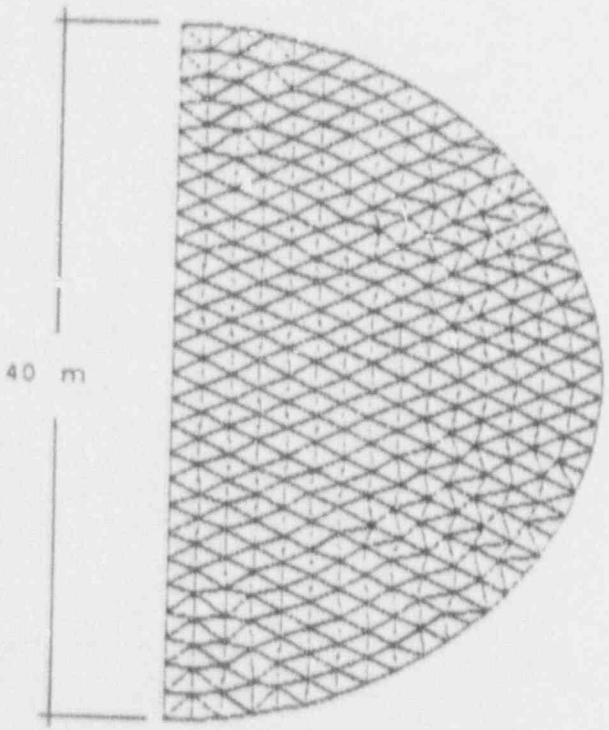


Figure 4. Triangular mesh in the plane slice model.

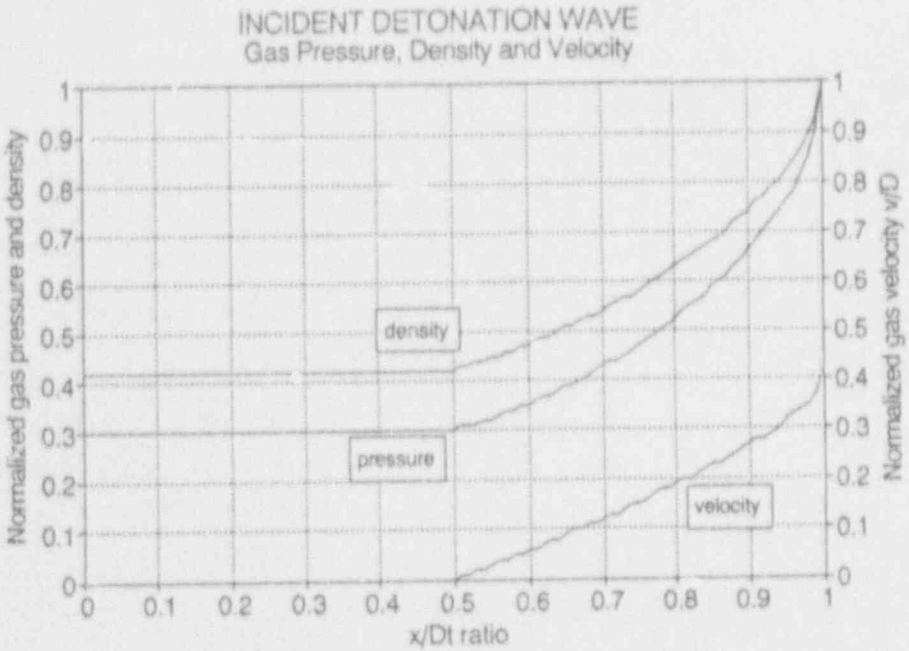


Figure 5. Incident detonation wave in the cylindrical case [1].

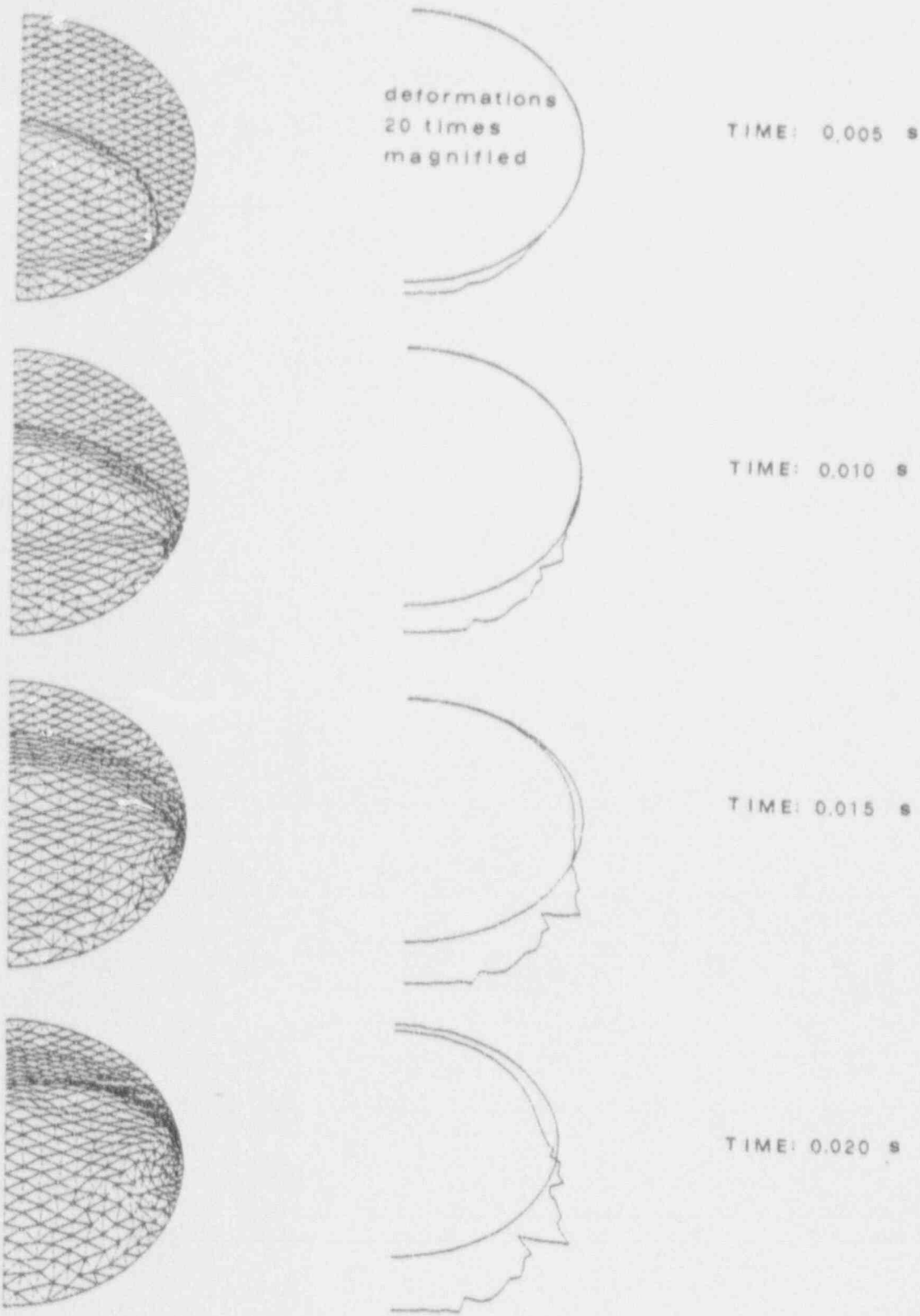


Figure 6. Shock wave and deformations untill 20 msec from the first impact (e=0.5, Pi=0.163 MPa, $X(H_2)$=20%).

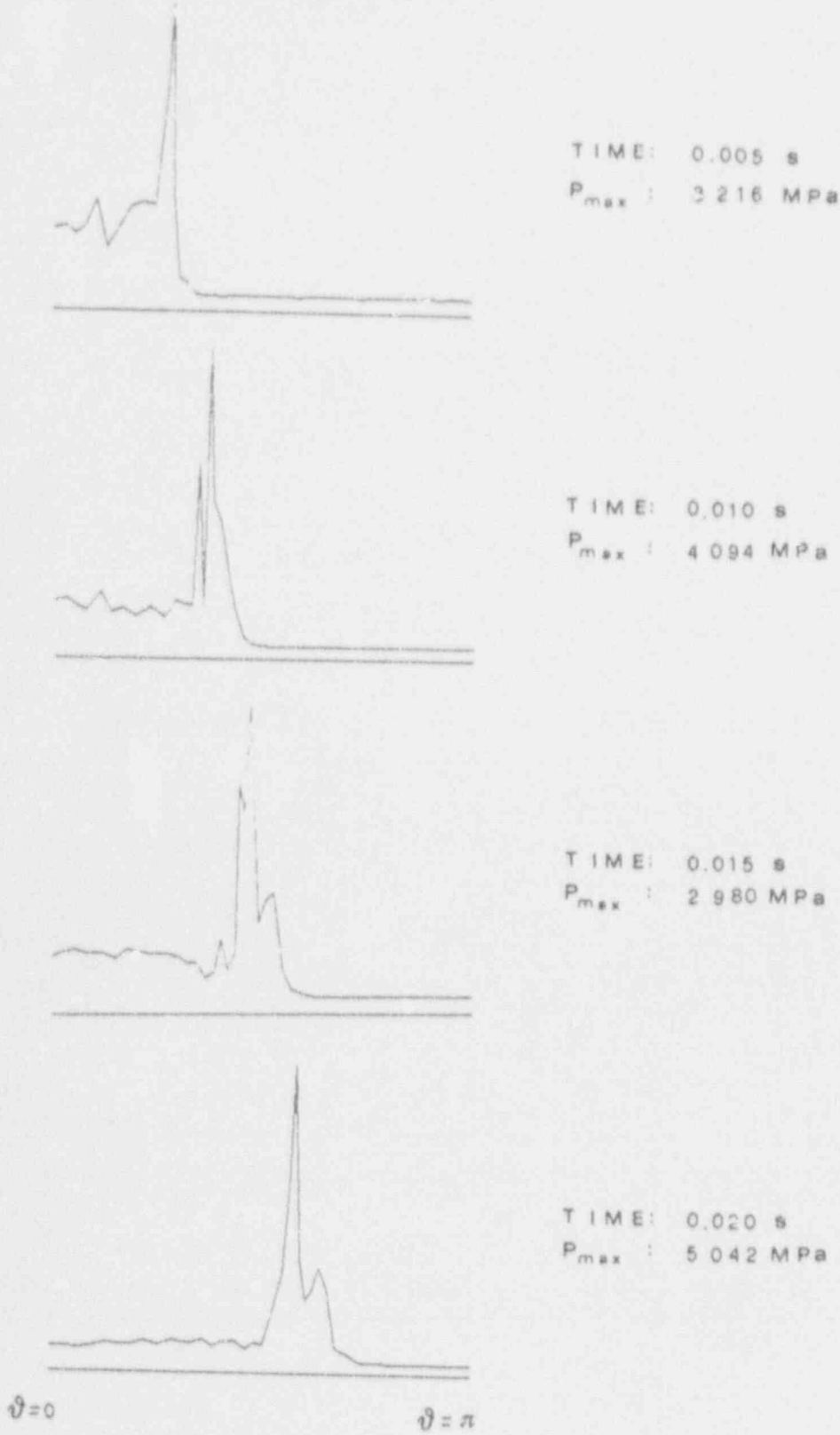


Figure 7. Pressure distribution on the containment wall untill 20 msec from the first impact.

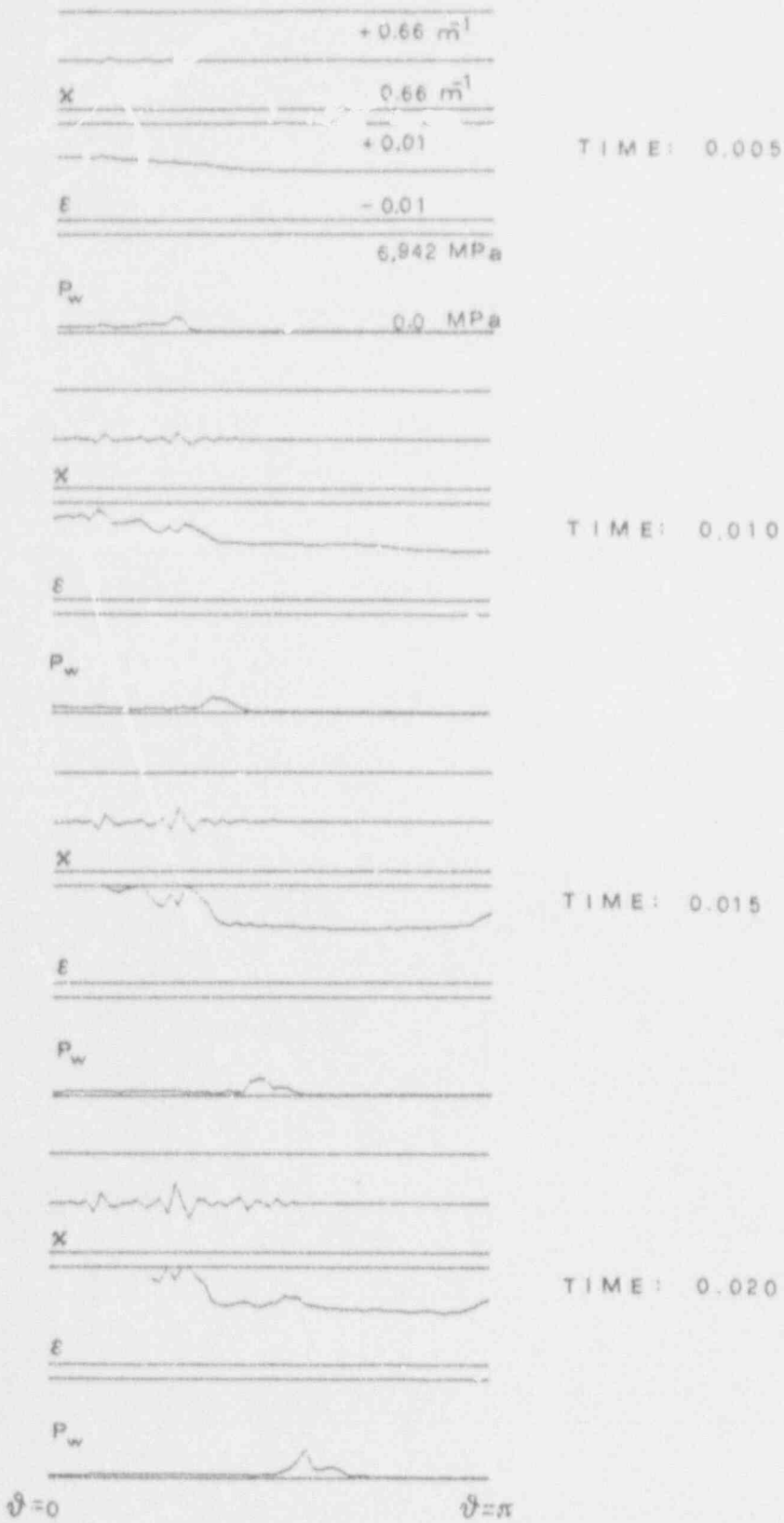


Figure 8. Curvature, midplane stretch and loading distribution on the containment wall untill 20 msec from the first impact.

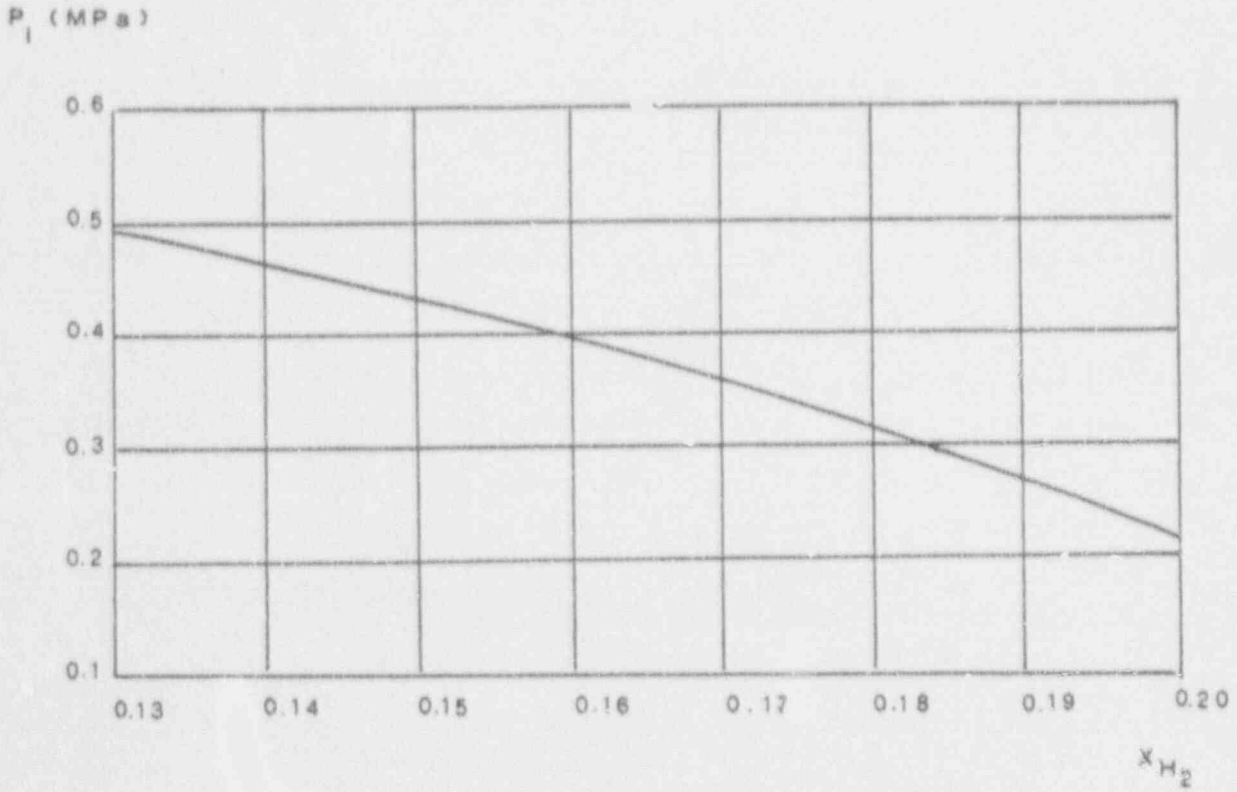


Figure 9. Initial pressure providing a final pressure of 0.8 MPa against $H_2$ molar fraction ($X(H_2O)=0$).

# ANALYSIS OF CONTAINMENT PARAMETERS DURING THE MAIN STEAM LINE BREAK WITH THE FAILURE OF THE FEEDWATER CONTROL VALVES

**Ljubo Fabjan, Stojan Petelin, Borut Mavko, Oton Gortnar, Iztok Tiselj**
"Jožef Stefan" Institute
Reactor Engineering Division
Jamova 39, P.O.Box 100
61111 Ljubljana, Slovenia

## ABSTRACT

NRC information notice 91-69: "Errors in Main Steam Line Break Analyses for Determining Containment Parameters" shows the possibility of an accident which could lead to beyond design containment pressure and temperature. Such accident would be caused by the continuation of feedwater flow following a main steam line break (MSLB) inside the containment.

NPP Krško has already experienced problems with main feedwater control valves. For that reason, analysis of MSLB has ben performed taking into account continuous feedwater addition scenario and different containment safety systems capabilities availability.

Steam and water released into the containment during MSLB was calculated using RELAP5/MOD2 computer code. The containment response to MSLB was calculated using CONTEMPT-LT/028 computer code.

The results indicated that the continuous feedwater flow following a MSLB could lead to beyond design containment pressure. The peak pressure and temperature depend on isolation time for main- and auxiliary-feedwater supply. In the case of low boron concentration injection, the core recriticality is characteristic for this type of accidents.

It was concluded that the presented analysis of MSLB with continuous feedwater addition scenario is the worst case for containment design. Based on indicated results we suggest the following:

- auxiliary feedwater should be isolated immediately on the side of the faulted steam generator
- boron injection tank boron concentration reduction may not be recommended
- appropriate feedwater valves surveillance program is recommended.

## INTRODUCTION

NPP Krško is a two-loop 660 MW(e) Westinghouse type PWR power plant. It started to operate in 1981. Containment design overpressure is 3.2 bar and temperature 128°C. The containment parameters during the design basis accidents, which could be found in Reference 1, have been estimated by Westinghouse and were later recalculated by "Jožef Stefan" Institute, Reactor Engineering Division using CONTEMPT-LT/028 computer code.

As stated in the NRC information notice 91-69, Reference 2, there exists the possibility that the feedwater systems could continue to supply water following MSLB. In this case similar failure during the MSLB could lead to beyond design containment pressure and temperature.

This issue could be even more important for NPP Krško than for the other plants, because of the special design of the steam generator feedwater systems. To avoid U-tube vibrations, the feedwater flow was split into two parts; 70% of water is entering the steam generator through the main feedwater nozzle and the other 30% through the auxiliary nozzle. Thus the number of the control valves is doubled and the possibility, that one of them could fail, is increased.

NPP Krško has already experienced difficulties with the main feedwater control valve. It started with the loss of the main generator stator cooling which caused an automatic turbine runback. During the transient the main control valve in the feedwater line remained in a half closed position. Water level in steam generator reached high-high level setpoint and caused turbine and reactor trip.

Based on the state of fact we performed containment systems capabilities verification with new scenario related to the continuous feedwater flow following MSLB inside containment. The scenario of MSLB was based on high-high steam generator water level and different isolation time for main- and auxiliary-feedwater flow.

The analysis was divided into two parts, as follows:

- the thermo-hydraulic analysis of reactor coolant system and steam generator to obtain mass and energy release rates vs. time, and
- the investigation of containment pressure and temperature response.

Steam and water releases into the containment during the MSLB were calculated using RELAP5/MOD2 code. The containment pressure and temperature response were predicted using CONTEMPT-LT/28 code. Calculations were based on conservative design and transient input models and realistic computer code.

## MSLB ACCIDENT DESCRIPTION

The MSLB is a V category event, according to ANS classification, Reference 6. The MSLB occurrence probability is assessed as very low, less than $10^{-6}$ per reactor-year.

The main steam lines are provided with isolation valves in both lines just outside the containment. Beside steam generator flow restrictor main steam line isolation valves are necessary to limit the uncontrolled steam release from steam generators even in the case of MSLB. The main steam lines up to these valves and the structure enclosing the valves are safety class equipment (seismic category 1).

High steam and water releases through the break, include the forward flow from the faulted steam generator and the reverse flow from the intact steam generator until the steam line isolation occurs.

The forward mass and energy release depends on the initial steam generator water inventory and main- and auxiliary-feedwater isolation delays. The reverse mass and energy releases depend on main steam isolation valve closing time.

The probability of feedwater control valve failure in open position coincident with feedwater isolation failure is very low. But, feedwater control valve failure coincident with delayed main- and auxiliary-feedwater isolation can be attributed higher probability. The present analysis includes complete feedwater valves failure in open position and delayed feedwater isolation.

High steam and water release and intensive vaporization process in the faulted steam generator following the secondary pressure and temperature decrease lead consequently into reactor coolant system cooldown. Under power operation reactor protection system prevents unsafe operation of the reactor which could lead to accident conditions. A different situation is established under hot-standby operating conditions (zero reactor power) when the reactor coolant cooldown causes a shutdown margin reduction and positive reactivity insertion. The positive reactivity insertion and reactor return to power could be compensated only by appropriate boron injection.

## THERMO-HYDRAULIC MODEL OF NPP KRŠKO

Thermo-hydraulic behaviour prediction is based on nuclear steam supply system model and dual containment model.

### *Nuclear Steam Supply System*

Nuclear Steam Supply System has been modelled using RELAP5/MOD2 computer code to generate the time history of mass and energy release following the break. The RELAP5/MOD2 plant model, which could be found in Reference 3, consists of the primary system with safety injection system and the important parts of the secondary system - from the main- and auxiliary- feedwater pumps to the turbine control valves. All essential control systems are simulated (rod control system, pressurizer pressure and level control system, main- and auxiliary- feedwater control system, etc). Reactor point kinetics, considering the influence of primary coolant boron concentration and heat losses to the surroundings, were also modeled.

The RELAP5 analysis involves the non-realistic conservative model of forced liquid fallback from the steam generator outlet to the steam generator bottom with an intention

to maximize the secondary vaporization process and therefore to increase the reactor coolant system cooldown and the steam release into the containment.

Such a restraint liquid release and maximized secondary vaporization coupled with assumed low boron concentration of safety injection flow result in the largest positive reactivity insertion and reactor return to power.

*Dual Containment*

Dual Containment was modelled using CONTEMPT-LT/28 computer code. CONTEMPT-LT/28 code calculates the time variation of containment pressure, temperatures, mass inventories, energy and heat structure temperature distributions. The model is capable of describing fan coolers and containment spray engineered safety systems. An annular fan model is provided for pressure control in the annular region of the dual containment.

The dual containment model is schematically presented on Figure 1. Two volumes representing the drywell and the annulus have been modeled.

Legend:

| | | |
|---|---|---|
| RCS | - | reactor coolant system |
| RHR | - | residual heat removal system |
| RWST | - | refuelling water storage tank |
| 1,2,3...- 13 | | heat structures |

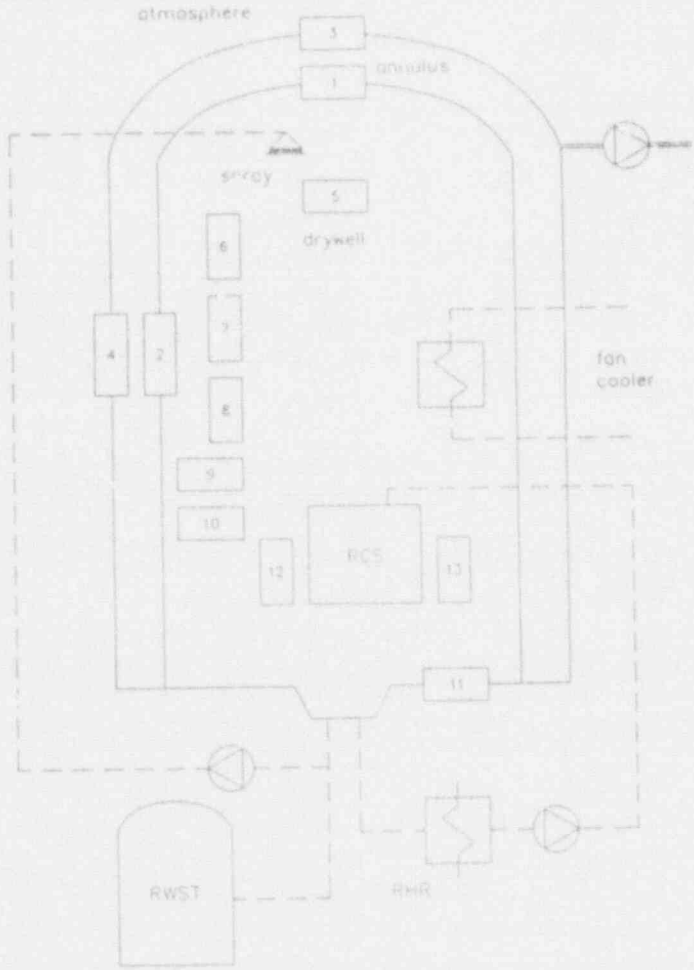


**Figure 1** NPP Krško dual containment model

The containment steam-air-water mixture in each volume was separated into two phases. The first phase consists of the steam and air, while the second phase is the liquid water. The thermo-hydrodynamic state of the liquid and vapor phases in the drywell is

dependent on assumptions made regarding the mixing and distribution of mass and energy resulting from break release.

Accordingly to CONTEMPT-LT/28 user options, we have used the temperature flash model. It means, that the mass and energy release from the main steam line is uniformly and instantaneously mixed throughout the drywell vapor region. It is supposed, that the air-steam mixture is forced into thermal equilibrium with the released water droplets which entered the vapor region.

The containment building is divided into 13 heat - conduction structures, some of which are used to describe building internals.

Prior to the MSLB initiation, the containment system parameters are assumed to be in a steady state condition.

## INPUT DATA

### *Initial Conditions*

Initial condition in nuclear steam supply system as well as in the containment drywell and annulus were based on conservative design and stated transient data.

### *Mass and Energy Release Data*

The initial steam generator water mass inventory represents the mass for the high-high steam generator water level turbine trip setpoint (82% N.R.Level). The 100 percent main feed flow was assumed before main feedwater isolation which occurred at 50 or at 170 seconds.

Auxiliary feedwater system delivers flow to the faulted and intact steam generators, actuated on low-low steam generator level signal (35%). The full auxiliary system mass flow is assumed until faulted steam generator is manually isolated.

The heat load from the primary system is estimated from hot-standby operating conditions (zero reactor power). The core reactivity feedback was calculated considering following conservative assumptions:

- minimum shutdown margin
- max. negative moderator temperature coefficient
- minimum high pressure safety injection capability (capacity of one high-pressure safety injection pump)
- low boron concentration in boron injection tank.

### *Containment - drywell and - annulus*

The containment - drywell and - annulus pressure as well as the temperature history have been calculated using results of the above described mass and energy releases prediction in addition to the main containment parameters as follows.

* Heat Conduction Structures (Passive heat sinks)

The slabs 1,2,3 and 4 on Figure 1, which represent the containment vessel cylinder, containment vessel dome, shield building cylinder and shield building dome, were modeled accounting full thickness. Both sides of these heat slabs are exposed to the drywell, annulus or environment.

One side of heat slabs 5 to 13 is exposed to the containment vapor space so they are modeled accounting the full thickness. The other side is insulated.

* Heat Transfer Coefficient

During the accident natural convection was supposed. Thus for both types of structures, concrete and steel, the Uchida correlation was used, Reference 7.

* Surfaces Exposed to the Liquid Region

The sump and the floor slabs were not modeled. These slabs were conservatively excluded, therefore there are no heat transfer coefficient values required.

* Active heat removal system

In the analysis single active failures were taken into account. A fan cooler in the active safety train was assumed to be out of operation for extended maintenance. The minimum safeguard train was assumed (a failure of one safety train), therefore, one spray train and one fan cooler train with one fan cooler were assumed to be available.

Following MSLB, the annulus negative pressure system was not initiated.

## MSLB CALCULATIONS AND RESULTS

### *Mass-Energy Releases*

A sudden increase in steam flow and vaporization process in faulted steam generator lead to larger energy removal from the primary coolant system and therefore the primary coolant temperature decrease. Faulted steam generator pressure and corresponding saturation temperature decrease rapidly following the break.

Figure 2 presents break mass flow vs. time and Figure 3 corresponding break energy flow vs. time for the Case 2 in Table 1. The feedwater isolation time delay was 50 sec. and manual isolation of auxiliary feedwater system occurred at 900 seconds.

The steam and energy release was timely stopped at approx. time 4 seconds. The reverse flow from intact steam generator had increased till the main steam line isolation valve was open. Main steam isolation valve closing was initiated at approx. time 5 sec. The valve closing time is 5 seconds. After approx. 10 seconds after the transient initiation the mass and energy release is decreasing monotonicaly up to the time when the faulted steam generator reached equilibrium.

The break mass flow in Figure 2 is two-phase. The main part of water is separated and returned to the steam generator bottom to maximize secondary side heat demand. Mass and energy release diagrams for the presented cases in Table 1 are very similar.

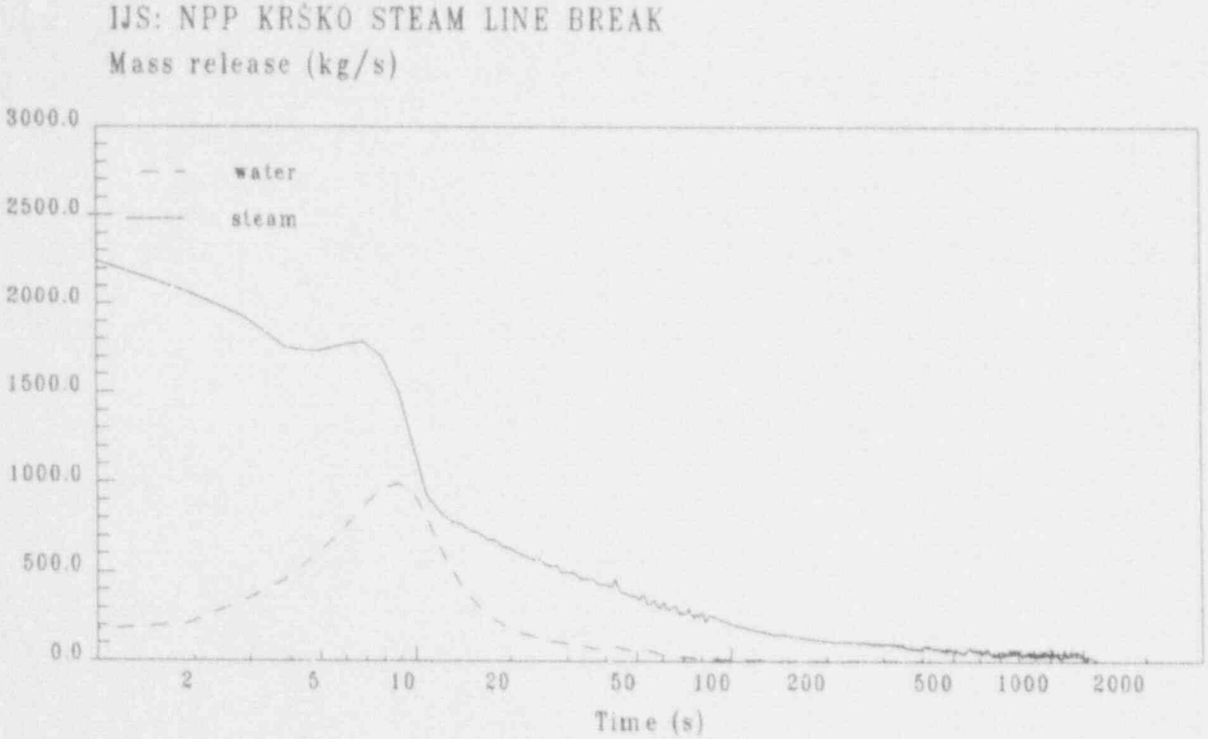


**Figure 2** MSLB mass flow vs. time regarding to Case 2 in Table 1

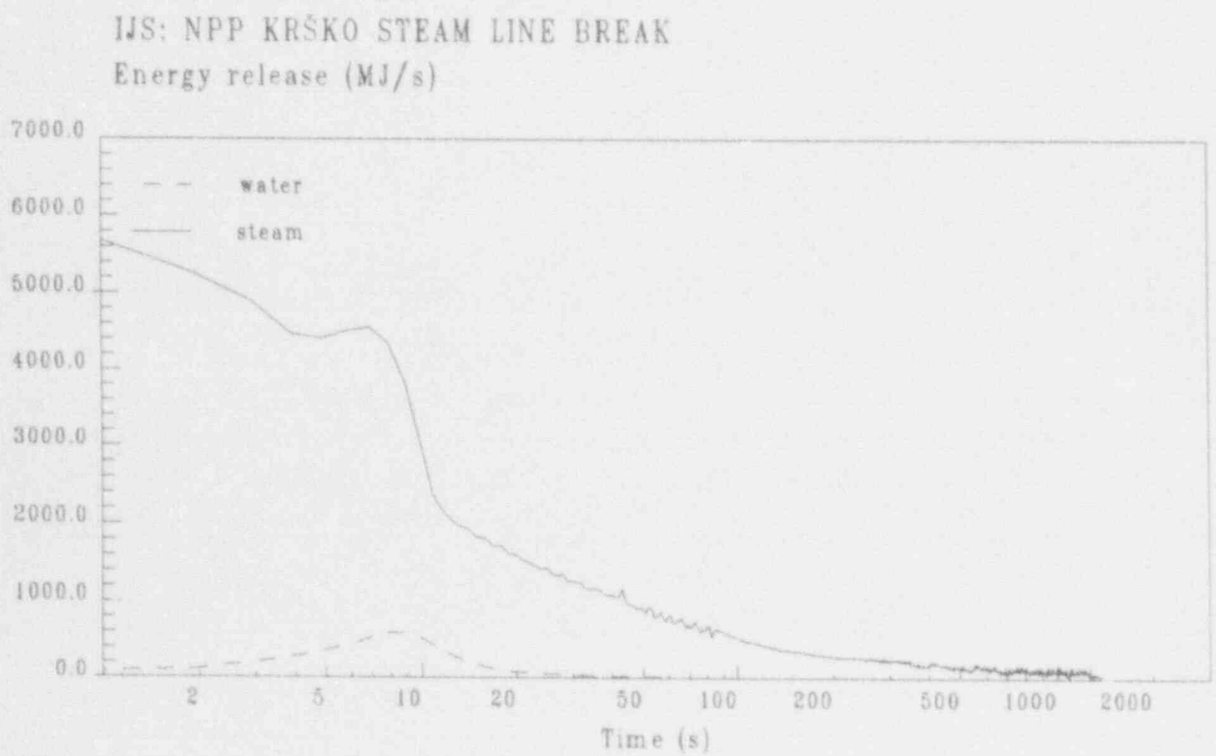


**Figure 3** MSLB energy release vs. time regarding to Case 2 in Table 1

Cooldown of the primary system caused a positive reactivity insertion. A low boron concentration of 2450 ppm was supposed for the boron injection tank which equals to the refuelling water storage tank boron concentration.

Low boron concentration in boron injection tank was supposed to assess the current proposal to remove boron injection tank from safety injection system. Presently the plant is operating with boron injection tank concentration of 20000 ppm.

Figure 4 shows sharp reactor power increase at approx. 40 sec. The reactor power reached its maximum at approx. 280 MW. The safety injection system was activated on low steam line pressure signal. The amount of injected borated water depended on primary coolant system pressure.

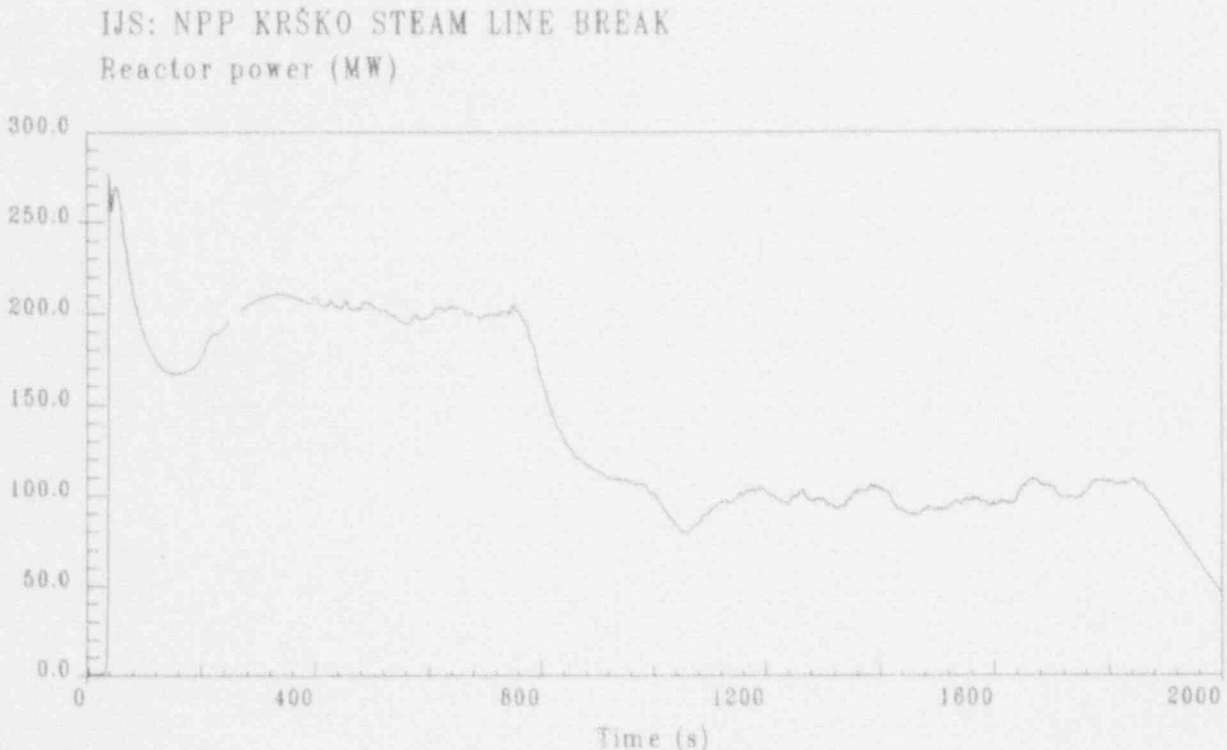


**Figure 4** MSLB reactor return to power vs.time regarding to Case 3 in Table 1

The primary coolant system pressure varied with non-balance of heat generation in the core and heat sink in the faulted steam generator. The first power peak, observed at approx. 40 sec., results from the core reactivity feedback. The amount of injected borated water at low reactor coolant pressure and Doppler coefficient partially compensated the positive reactivity. The core power increase caused reactor coolant pressure increase. The amount of injected borated water was reduced and along with the continued heat sink in the faulted steam generator again caused reactor power increase at approx. 220sec. The reactor power started to decrease after steam generator had approached the dry out. After that the reactor power changes in equilibrium with heat sink provided by auxiliary feedwater flow.

The main parameters used in analyses are presented in Table 1.

TABLE 1: Summary of MSLB initial conditions for input model and results

| System | | case 1 | case 2 | case 3 | case 4 |
|---|---|---|---|---|---|
| NSSS | | | | | |
| Steam generator level NR | (%) | 83 | 83 | 83 | 83 |
| Feedwater isolation start | (s) | 170 | 50 | 50 | 50 |
| Aux.feedwater isol. start | (s) | 0 | 900 | 1800 | 1800 |
| Main steam isol. start | (s) | 5 | 5 | 5 | 5 |
| CONTAINMENT | | | | | |
| Net free volume | ($m^3$) | 36700 | 36700 | 36700 | 40800 |
| surface area | (%) | 90 | 90 | 90 | 100 |
| spray | (No.of units) | 1 | 1 | 1 | 2 |
| fan coolers | (No.of units) | 1 | 1 | 1 | 4 |
| spray start | (s) | 95 | 95 | 95 | 95 |
| fan start | (s) | 45 | 45 | 45 | 45 |
| max. pressure | (bar) | 4,46 | 3,92 | 4,28 | 2,97 |
| max. temperature | (K) | 409 | 403 | 407 | 389 |
| time | (s) | 1380 | 910 | 1880 | 770 |

*Containment response*

The containment pressure response for different cases, as stated in Table 1, is presented in Figures 5 and 6.

The fan cooler activation at 45 sec. and spray activation at 95 sec. is indicated in Figures 5 and 6 as pressure increase rates change at approx. 3 bar. After the active heat sinks activation the containment pressure increase as long as appropriate energy release exist.

The containment temperature response during MSLB is analog to the pressure response and is indicated in Figures 7 and 8.

The maximum containment pressure of 4.46 bar and temperature of 409 K were reached for the Case 1 in Figures 5 and 7. The Case 1 is based on a very conservative scenario assuming that all water inventory in the condenser, 88000 kg, was delivered into the steam generators. The condenser was emptied at 170 seconds.

The Cases 2 and 3 in Figure 6 present more or less realistic accident scenario. The main feedwater isolation occurred at 50 sec. The peak pressure is in coincidence with auxiliary feedwater isolation. The containment peak pressure and temperature increase with increasing time delay of auxiliary feedwater isolation. Case 2 indicates that an earlier auxiliary feedwater isolation, which occurred at 900 sec., prevents containment pressure increase above the design limit.

Case 4, on Figure 6, indicates containment heat sink capabilities. In response to the Case 3, maximum containment spray and fan coolers operable with nominal containment net free volume and surfaces was supposed. The comparison of pressure response for the Cases 3 and 4 in Figure 6 shows, that the containment heat sinks are very effective. The vapor generation by auxiliary feedwater supply in last phase of accident was compensated by additional heat sinks compared to the Case 3. The peak pressure in Case 4 is lowered for 1,31 bar regarding to the Case 3.

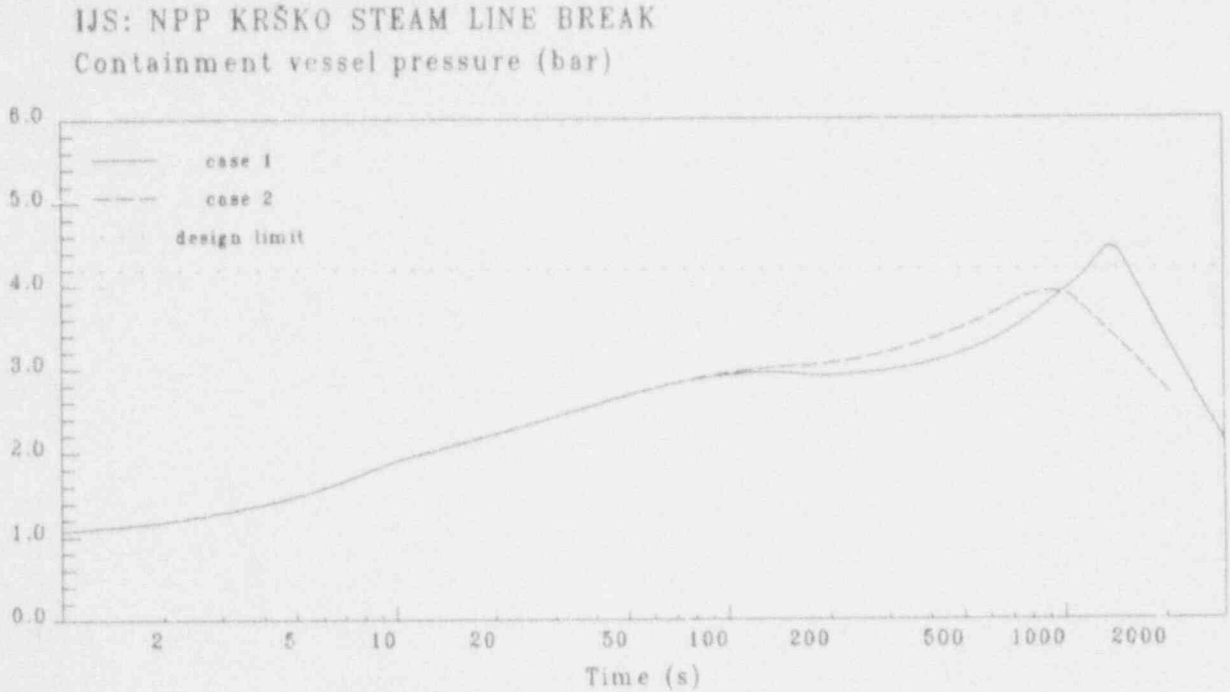


**Figure 5** MSLB containment pressure response vs. time regarding to Cases 1 and 2

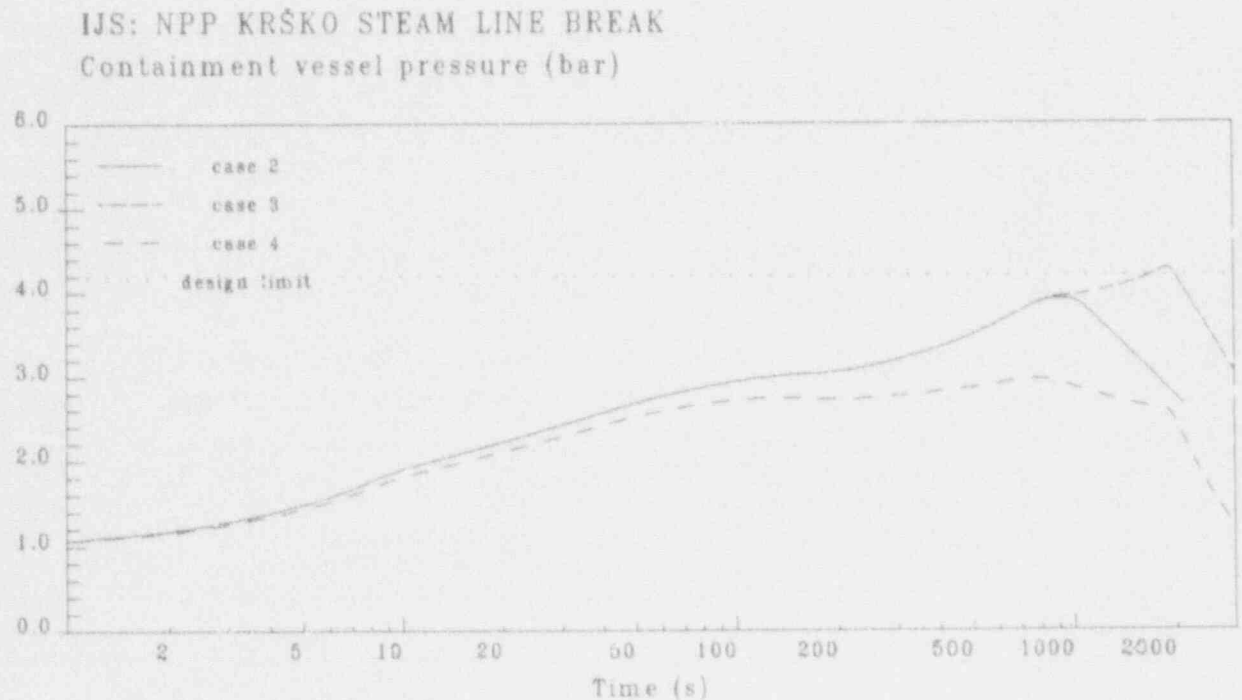


**Figure 6** MSLB containment pressure response vs. time regarding to Cases 2, 3 and 4 in Table 1

It is interesting that the containment temperature for the Case 2 in Figure 7 exceeded the design limit. The difference between design and calculated value is 2 K. The peak pressure in this case stayed below design value.

The analysis results indicated that the containment annulus pressure and temperature response is not questionable.

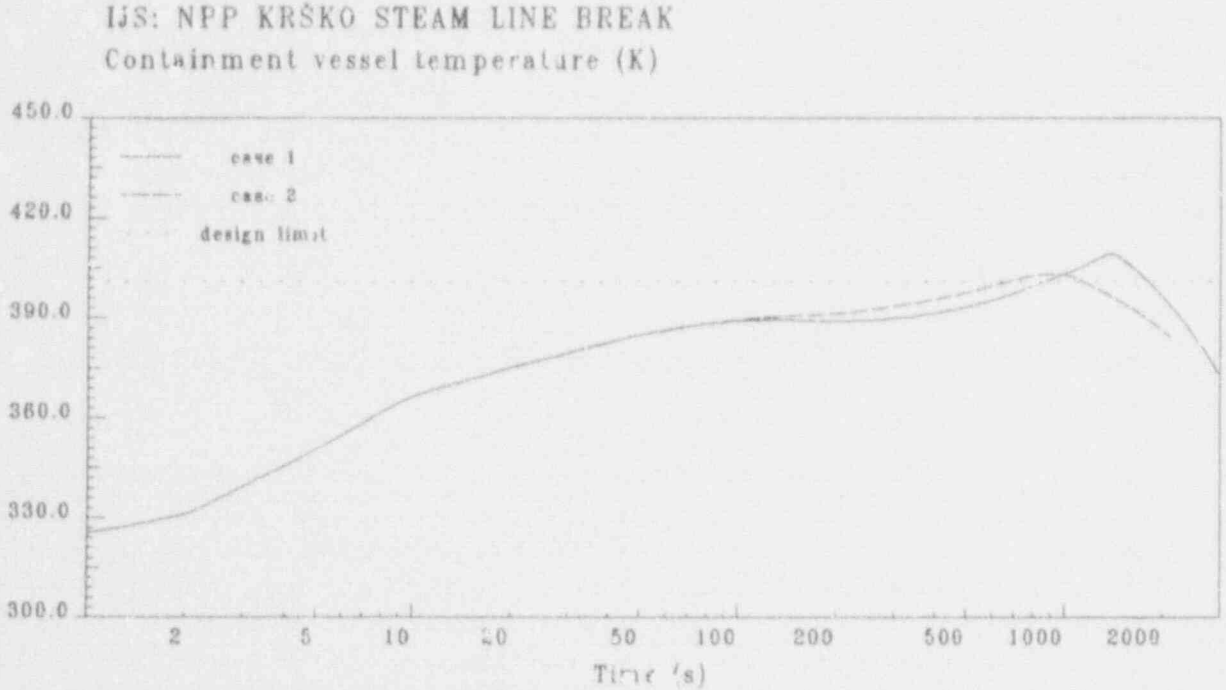


**Figure 7** MSLB containment temperature response vs. time regarding to Cases 1 and 2 in Table 1

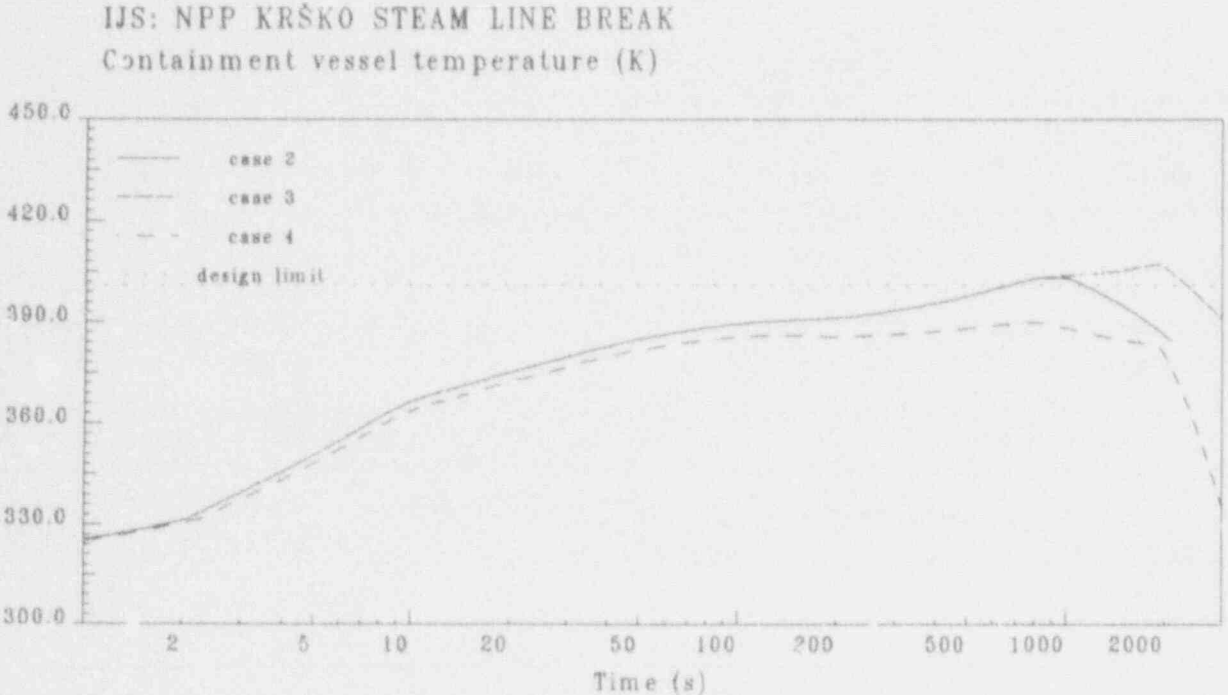


**Figure 8** MSLB containment temperature response vs. time regarding to Cases 2, 3 and 4 in Table 1

## CONCLUSION

MSLB is one of the most important PWR design accidents. The MSLB results in FSAR, Reference 1, presented three active failures where none of them was main feedwater system failure. Operating experiences with feedwater valves and NRC Information Notice 91-69, were the reason for containment analysis in the case of continuous main feedwater flow following the MSLB.

The calculations were based on Krško NPP plant specific parameters. The mass and energy break flow was predicted using realistic RELAP5/MOD2 computer code assuming conservative input model and scenario. The containment response to MSLB was modeled using CONTEMPT-LT/28 computer code.

The analyses showed that the continuous feedwater flow following a MSLB inside containment could result in peak containment pressure and temperature higher then the design limits.

The containment pressure and temperature response depends on main- and auxiliary-feedwater isolation time delay. Four cases have been calculated with different suppositions which are more or less probable. The probability for feedwater control valve failure in open position coincident with feedwater isolation failure in open position is very low (Case 1 in Table 1). While the probability for feedwater control valve failure in open position coincident with delayed main- and auxiliary-feedwater isolation is higher.

The containment pressure increases above the design pressure in the most conservative Case No. 1, when all available water in the condenser was delivered to the steam generators. In this case pressure and temperature are slightly above design limits.

In the cases with 50 sec. delayed main feedwater isolation, (Case 2 and 3), the calculations indicated that the time of manual auxiliary feedwater isolation is very important. After the steam generator empties the amount of injected auxiliary feedwater determines the containment peak pressure and temperature. Auxiliary feedwater isolation after 900 sec. could lead to beyond design containment pressure and temperature.

In the Case 2, which is more or less a realistic case, the resulting containment temperature is slightly higher than the design limit and the peak pressure slightly lower than the design limit.

Low boron concentration (2450 ppm) in boron injection tank was not sufficient to compensate core positive reactivity feedback and reactor return to power. The reactor power sharply increased to approximately 280 MW power. So the boron injection tank removal is not recommended regarding the accident with continuous feedwater flow following MSLB.

The strict surveillance of main feedwater control valve is suggested. Appropriate surveillance program should be implemented on main feedwater isolation valves.

## REFERENCES


1. Final Safety Analysis Report, NPP Krško.

2. U.S.Nuclear Regulatory Commission information notice 91-69: "Errors in Main Steam Line Break Analyses for Determining Containment Parameters, November 1, 1991.

3. S.Petelin, O.Gortnar, B.Mavko: RELAP5/MOD2 Split Reactor Vessel Model, 1991 Winter Meeting, San Francisco, California, November 10-14, 1991, American Nuclear Society, Volume 64.

4. Petelin, S.; Gortnar, O.; Mavko, B.: Steam Generator Model for Design Accident Calculations, ZAMM; Z.angew.Math.Mech., 72 (1992)6, T607-T611.

5. U.S. Nuclear Regulatory Commission, Standard Review Plan, NUREG-0800, LWR edition, Rev. 1-July 1981.

6. American Nuclear Society, Nuclear Safety Criteria for the Design of Stationary Pressurized Water Reactor Plants, ANSI/ANS-51.1-1983.

7. NUREG/CR-0255, CONTEMPT-LT/28, A Computer Program for Predicting Containment Pressure - Temperature Response to Loss-of-Coolant Accident, Date Published: March 1979.

# SESSION 5

# TESTING/ANALYSIS OF CONTAINMENT SYSTEMS

# SMALL-SCALE PENETRATION LEAK TEST IN ALPHA PROGRAM

Norihiro Yamano, Jun Sugimoto, Yu Maruyama,
Akihide Hidaka and Kunihisa Soda

Japan Atomic Energy Research Institute

## Abstract

Small scale penetration leak test has been performed as a part of ALPHA program at JAERI since 1990. Two series of experiments were performed in the test using test sections which simulate important parts of an Electrical Penetration Assembly(EPA) in a Japanese PWR. One of the test sections simulates an alumina module and the other includes silicone resin portion of the EPA. The test section was installed in a leak test vessel in which one region simulated inside of the containment and the other region simulated outside of the containment. Four experiments were performed using the alumina module test section. The test section was heated up to 720 K at maximum 1.8 MPa. No leakage was detected in the experiments. Two experiments were performed using the silicone resin test section at near atmospheric pressure. Initial leak path formation was detected at about 420 K. It was found that heat conduction along metal portion had strong influence on melt progression of the resin. It was also found from the strain measurement that the thermal loads were predominant over the pressure loads. From the results of the experiments, it is considered that the alumina module will keep integrity in severe accident conditions, although the silicone resin is estimated to melt at high temperature. Therefore, the EPA as a whole is estimated to maintain leak-tightness during the severe accident.

## INTRODUCTION

A containment of a nuclear reactor is the last physical barrier for preventing the release of radioactive materials to the environment. Therefore maintaining containment integrity is crucial to the safety of a nuclear reactor in an accident[1]. In order to investigate the phenomena which would threaten the containment integrity and containment response to severe accidents, ALPHA (Assessment of Loads and Performance of a containment in a Hypothetical Accident) Program was initiated at JAERI in 1990.

Penetration leak characterization test is one of the four test items of the ALPHA program[2]. The purpose of the test is to investigate behavior of penetrations at the containment boundary during severe accidents. Among several penetrations, present efforts are focused on the behavior of electrical penetration assemblies (EPAs).

Similar experiments to investigate EPAs' behavior under severe accident circumstances in a containment were performed at Sandia National Laboratories(SNL) in 1985 to 1986[3]. Three types of EPAs of US nuclear power plants were tested in their experiments. Their experimental results showed all of the EPAs kept leak-tight throughout the test but one which showed slight

leakage during cooling down period.

However, in order to quantify safety margin of EPAs to a severe accident, an analytical model is needed based on the detailed thermal/mechanical behaviors of EPAs. Also the types of EPAs are different in some of Japanese plants.

Objectives of the penetration leak characterization test are;
1)To obtain database on thermal/mechanical behavior of the Japanese EPAs under severe thermal-hydraulic conditions,
2)To identify leak path, if leakage occurs,
3)To quantify leak area and leak rates,
4)To obtain database on fission product aerosol behavior in the leak path, and
5)To develop an analytical model to estimate EPAs' behavior, leak rate and fission product aerosol release to the environment through a leak path.

The penetration leak characterization test consists of small-scale component experiments, full-scale integral experiment and model development for each experiments. The small-scale component experiments are performed using small-scale test sections which simulate essential portions of EPAs from the viewpoint of leak-tightness. The full-scale integral experiment is performed using a full-scale EPA test assembly. Partial models will be developed from the small-scale component experiments and incorporated into an integrated model to predict behavior of a whole EPA. The integrated model will be verified against the full scale integral experiment. It will then be finally applied for evaluating EPAs' behavior in severe accidents of LWRs.

The present paper describes the results of the small scale component experiments.

## GENERAL DESCRIPTION OF THE SMALL-SCALE COMPONENT EXPERIMENTS

### Experimental Series

Figure 1 shows concept of an EPA for instrumentation cables used in Japanese PWR plants. This EPA has symmetrical structure for inside and outside of a containment wall. A header plate of 22 mm thick inside containment is supposed to support pressure load in an accident period. Alumina modules are employed where cables penetrate header plates. An alumina module is attached to a header plate with silver brazing. Silicone resin seals alumina modules and header plates.

Two kinds of small-scale test sections were designed. Integrity of alumina modules and strength of connections with silver brazing under severe thermal-hydraulic conditions are of primary importance to keep containment boundary. Therefore one of the test sections was designed to include an alumina module and a surrounding part of header plate and named "alumina module test section." The other test section includes silicone resin with a cable and the shroud, and named "silicone resin test section". Silicone resin is estimated to decompose and/or melt in high temperature circumstances, and molten resin will be replaced by high temperature containment atmosphere. Therefore melt progression of the resin will give a thermal boundary condition to the alumina modules and the header plate.

Two series of experiments have been performed in the small-scale component experiments using each test section. Purpose of the experiments with the alumina module test section (hereafter referred to as "alumina module experiments") is to obtain database on thermal/mechanical behavior of the alumina module under high-temperature and high-pressure conditions. Melt progression of the silicone resin and effects of the cable and the shroud on the resin's behavior are studied in the experiments using silicone resin test section (referred to as "silicone resin experiments.")

Other kinds of resin plays an essential role to keep containment boundary in EPAs used in Japanese BWRs where alumina modules are not employed. Therefore experimental data of the silicone resin experiments will be also helpful for estimating behavior of those BWR EPAs by taking account of physical properties of the resin.

## Test Apparatus

The test section is installed in a small-scale leak test vessel as shown in Figure 2. A large flange of the test section called "partition plate" divides the test vessel into two regions. One region simulates inside the containment during a severe accident and is named "high-temperature and high-pressure (HTHP) region." The other region referred to as "low-temperature and low-pressure (LTLP) region" simulates outside of the containment. The HTHP region was pressurized with superheated steam and heated by a mantle heater surrounding the HTHP region of the test vessel. Dry nitrogen gas at near atmospheric pressure is supplied to the LTLP region. Table 1 summarizes the dimensions and capabilities of the small-scale leak test vessel.

In case leak path is formed in the test section, steam in the HTHP region flows into the LTLP region. The steam is mixed with dry nitrogen in the LTLP region and carried away. Therefore leak initiation can be detected by continuously monitoring the dew point of the nitrogen gas by a hygrometer. Amount of the small leakage is evaluated from the increase of the dew point. When the dew point of the nitrogen exceeds the upper limit of the measurable range of the hygrometer, a rotormeter is used to measure the total flow rate of steam and nitrogen mixture

## DETAILED DESCRIPTION OF THE EXPERIMENTS

## Alumina Module Experiments

### Test Section

Figure 3 shows a schematic diagram of the alumina module test section. Construction of the module used in the test section is illustrated in Figure 4. It should be noted that the module was designed by JAERI to simulate an alumina module used in a commercial EPA. The alumina module consists of an alumina porcelain pipe, a copper conductor and two metal coupling rings. The copper conductor which passes inside the alumina porcelain pipe is fixed to the pipe using a Fe-Ni-Co alloy coupling ring called "end coupling". The alumina pipe is connected to the header plate with a similar coupling ring named "middle coupling". The middle coupling is made of the same material as the end coupling. The silver brazing whose melting point is 1053 K was used to attach the couplings to the alumina pipe, and the end coupling to the conductor. The

silver brazing of lower melting point(923 K) was used to connect the middle coupling to the header plate. It was supposed that integrity of the coupling rings and strength of the silver brazing connections would be key issues for leak initiation of the whole EPA shown in Figure 1

Six strain gauges and seven thermocouples were located in the test section as shown in Figure 3. Circumferential and axial strains on the surface of the couplings were measured at the locations where the couplings were attached to the alumina porcelain pipe or the conductor. As shown in Figure 4, the axial strain gauges were mounted bridging both the coupling and small pad of Fe-Ni-Co alloy which is attached to the alumina porcelain pipe or the conductor due to insufficient space available on the couplings. Therefore axial strain gauges do not exactly measure the strain at the surface of the couplings, but measure the compound effect of strain and variance of distance between the coupling and the pad. It should be noted the axial strain gauges were mainly expected to detect movement of the couplings.

When the test section is installed in the test vessel, pressure boundary is along the partition plate, the shroud and the header plate. There are two holes of 24 mm in diameter on the partition plate inside the shroud. The volume surrounded by the shroud, the header plate and the partition plate which is referred to as "the inner volume" is connected to the LTLP region of the test vessel through the holes. In case leak path is formed along the alumina module, steam in the HTHP region flows into the LTLP region through the inner volume.

**Test Procedures**

The test section was mounted in the test vessel and the HTHP region of the test vessel was pressurized by nitrogen. After it was confirmed that there was no pre-existing leak path and instrumentation properly functioned, dry nitrogen was supplied to the LTLP region to remove water contents in the region and nitrogen flow path. After the dew point of nitrogen measured by the hygrometer reached below 243 K, the mantle heater was turned on and the temperature in the HTHP region was increased at a constant rate. When the temperature was increased high enough to prevent steam condensation (usually about 390 K), steam supply to the HTHP region started. Pressure and temperature in the HTHP region were increased up to the maximum pressure at the experiment and its steam saturation temperature. The condition in the HTHP region was maintained until temperatures and strains of the test section reached steady state conditions. The temperature was then elevated at the constant increasing rate while pressure was maintained at the constant value. The maximum temperature was maintained for several hours after all the temperatures and strains of the test section reached steady state. Finally steam injection was terminated and pressure in the HTHP region was decreased. The heater was turned off and the test section was naturally cooled down. The HTHP region was pressurized by nitrogen and leak-tightness was checked at the room temperature.

All the instrumentation outputs and physical properties at various locations of the test facility for operation were recorded by an automatic data logging system. Sampling frequency of the system was 1 Hz during experiments and 0.1 Hz for natural cooling periods after termination of the experiment.

### Test Conditions

Four experiments were performed in the alumina module experiments. Conditions for the experiments are summarized in Table 2. SLA001 was performed at relatively low pressure. Since this was the first experiment of all small-scale component experiments, to check the functions of the test apparatus was also one of the purposes of the experiment. The rest of the experiments were performed at similar high pressure conditions, to ensure the reproducibility of results and to obtain better strain measurement by improved instrumentation. It should be noted that the maximum temperature and pressure in the HTHP region were much higher than those predicted by analytical codes for PWR containment atmosphere during a severe accident[3],[4]. This is to ensure several margins to be included in the present experiments.

## Silicone Resin Experiments

### Test Section

Figure 5 shows a schematic diagram of the silicone resin test section. The test section was separated into two parts by the header plate, and one side of the test section was sealed with the silicone resin. The alumina module was fixed at the center of the header plate. One half of the alumina module was embedded in the resin and connected to the cable, while the other half was exposed to gaseous atmosphere in the volume surrounded by the header plate, the shroud and the partition plate. This volume is also referred to as "inner volume" as well as that of the alumina module test section. As shown in Figure 5, four series of five thermocouples in every 50 mm intervals were mounted along inside the shroud, along the cable and in the resin. The header plate had eight holes of 16mm in diameter, and the partition plate had two holes of 24mm in diameter. When a path from the HTHP region atmosphere to the header plate is formed in the resin, steam flows to the LTLP region through these holes.

Laminated epoxy resin was not included in the test section, because it was considered to have little influence on the behavior of the silicone resin. The laminated epoxy resin of the EPA has many holes for cables and it is estimated that the epoxy resin begins to decompose at lower temperature than the silicone resin. Therefore it will not prevent the steam from contacting the silicone resin.

### Test Procedures

After air in the HTHP region was replaced by nitrogen, the mantle heater was turned on. The LTLP region was continuously dried by nitrogen as in the alumina module experiments. When the temperature in the HTHP region exceeds 383 K, steam injection to the HTHP region started. The temperature in the HTHP region was increased at a constant rate while dry nitrogen gas at 290 K flew the LTLP region. The dew point of the gas flowing out of the LTLP region was continuously monitored. It was originally planned to hold the condition and to measure the increase of the dew point to quantify the leak rate when leakage initiation was detected. However the dew point exceeded so rapidly the upper limit of the measurable range of the hygrometer after the leakage initiation was detected. Therefore the hygrometer was isolated and the temperature in the HTHP region was continuously increased to the maximum temperature as

planned in the experiment. After the hygrometer was isolated, the flow rate of mixture of nitrogen and steam was measured by the rotormeter.

### Test Conditions

Two experiments were performed in the silicone resin experiments as shown in Table 3. Pressurization of the HTHP region could mechanically damage the silicon resin due to the pre-existing holes in the header plate. Therefore, the pressure of the HTHP region was kept at near atmospheric pressure in the experiments. The pressure of the HTHP region was maintained at about 0.01 MPa higher than that of the LTLP region through the experiments to ensure the steam flow between the two regions when the leak path was formed. A thermo-gravimetric analysis of a small sample of the silicone resin showed decomposition of the resin was accelerated at about 623 K. Therefore the maximum temperature in the HTHP region was defined to be 640 K in the first experiment (SLB001.) In the second experiment (SLB002), heating of the test section was terminated at 515 K to identify the initial leak path.

## RESULTS AND DISCUSSIONS

### Alumina Module Experiments

The increase of the dew point was not detected for all the experiments. Therefore, it is considered there was no leakage in the experiments. Temperature and strain were measured at several locations in the test section for the experiments. Since it is considered that the measurement is most reliable in SLA005 due to improved instrumentation for the strains, experimental results of SLA005 are presented in the following.

Figure 6 shows the temperature and the pressure histories in the HTHP region. The temperature decrease from 8,000 to 10,000 sec was caused by the initiation of the steam supply to the HTHP region which had been heated by the mantle heater. The temperature plateau between 16,000 sec and 20,000 sec corresponds to the period when the maximum pressure and its saturation temperature were maintained.

Circumferential strains at three locations on the surface of the coupling rings are shown in Figure 7 with the temperature of the test section in the inner volume. Difference between the temperatures at the locations of the strain gauges and the temperature in the figure is estimated to be within 20 K. As shown in the figure, the strains follow the temperature history. The strains measured at 290 K and 1.79 Mpa were less than 0.01 % for all of CS1, CS2 and CS3. The fact maximum strains at 723 K and 1.76 MPa were much larger than these values indicates that strains were predominantly caused by the temperature increase not by pressure load. It is considered that the thermal strains are attributed to the difference of thermal expansion rate between two contacting materials. This estimation is supported by the fact that the strain was much larger at CS1 where the coupling ring (thermal expansion rate is $6 \times 10^{-6}$ / K) was connected to the copper conductor($1.8 \times 10^{-5}$ / K) than CS2 and CS3 where the coupling ring was connected to the alumina porcelain pipe($7.5 \times 10^{-6}$ / K).

Since the experiments were performed at the pressure and the temperature much higher than

those estimated in a PWR containment during a severe accident, the present results indicate that the alumina module has large safety margin. There may be several factors which could influence the behavior of the alumina modules in the severe accident but not considered in the experiments. For example, some of the gas generated by the decomposition of the resin are burnable and chemical reaction heat might give additional thermal load. Effect of radiation was not taken into account in the experiments either. However, considering the large safety margin of the alumina module, the EPA would keep leak-tightness through the severe accident. Since the module was not destructed in the experiments, it was not succeeded to quantify the safety margin of the module. Separate effect experiment to mechanically destroy the module will be needed. Development of a model to predict the alumina module behavior has been performed. Such analytical effort will also be helpful to estimate the safety margin of the module. Functions of EPAs such as electrical continuity and insulation are also important from the viewpoint of accident management even if the geometrical integrity is maintained. Although integrity of the function was out of the scope in the small-scale component experiments, it will be investigated in the full-scale integral experiment.

**Silicone Resin Experiments**

Leak initiation was detected in SLB001 by the hygrometer when the temperature in the HTHP region was 430 K. Since the dew point exceeded rapidly the upper limit of the measurable range of the hygrometer, the hygrometer was isolated and the experiment was continued. When the temperature in the HTHP region reached 640 K, the condition was maintained. At thirty minutes after the steady state was established, the pressure in the HTHP region rapidly decreased and it was difficult to keep the pressure of the HTHP region higher than that of the LTLP region. This indicated that the large leak path was formed and the experiment was terminated.

Figure 8 shows temperatures measured by four thermocouples located in the HTHP region atmosphere in SLB001. The temperature difference in the atmosphere was 50 K at maximum.

The variance of temperature distribution along the inside of the shroud with time was presented in Figure 9. Temperature gradient from the boundary of the silicone resin and the atmosphere (near point A) toward the header plate(point E) is seen in the figure, which indicates the heat conduction along the shroud. It is found that the temperatures along the inside of the shroud were slightly lower but followed rather well the temperatures in the HTHP region.
Figure 10 presents variance of temperature distribution in the resin with time. They were much lower than the atmospheric temperature until 23,000 seconds. Temperature at point A was highest and temperature at point E was second highest for most of the period of the experiment except between 18,000 to 23,000 seconds when the temperature at point E was the highest. This indicates that the heat conduction along the shroud and the header plate was much larger than the heat conduction in the resin. Rapid temperature increase was found for point A at 23,000 sec and later for points B,C,D successively. This rapid temperature increase was not observed for point E. Since the temperatures after the rapid increase were close to the temperature in the HTHP region atmosphere, this rapid increase is considered to be caused by the exposure of the thermocouples to the steam due to melt relocation of the resin. The time of the rapid temperature increase at each thermocouple location indicates that the melt of the resin progressed from the surface of the resin to the atmosphere toward the header plate, and that the thermocouple at the

point E was still covered with the resin.

Temperatures measured with thermocouples located along the cable and the alumina porcelain module are shown in Figure 11. Temperature gradient along the cable was much smaller than that in the resin, although the average temperature along the cable was close to the average temperature of the five thermocouples in the resin. The rapid increase in the temperature similar to that in Figure 10 was found at points A and B but not found for other points. The initiation of this temperature increase at points A and B occurred later than those in the resin. This delay is considered to be caused by the heat conduction along the cable to the inner volume, resulting in the cooling of the resin around the cable.

It was found that most of the resin melted and relocated in the posttest observation of the test section in SLB001. Therefore it was impossible to identify the initial leak path in the test section. Foamy solid and highly viscous liquid were found in the shroud and the bottom of the test vessel.

In SLB002, the leak initiation was detected when the temperature in the HTHP region was 410 K. After the isolation of the hygrometer, the temperature in the HTHP region was continuously increased at a fixed rate. The experiment was terminated when the temperature in the HTHP region reached at 515 K. Since the pressure in the HTHP region could be maintained 0.01 MPa higher than that of the LTLP region throughout the experiment, it was estimated that there was no large leakage. Residue of the foamed resin was found in the neighborhood of the cable in the test section after the experiment. From the posttest observation of the test section and the measured temperature distribution, it is considered that the initial leak path was formed along the shroud and the header plate.

In the SLB001 of the silicone resin experiments, most of the resin was melted and relocated, although the experimental temperature was not so much higher than the temperature where decomposition of the resin was accelerated in the thermo-gravimetric analysis. This discrepancy is explained by the fact that the decomposition of the resin depends on the temperature increasing rate; it was 10 K/min in the thermo-gravimetric analysis but it was about 1.2 K/min in the experiment.

If the alumina modules keep integrity during an accident, the decomposition of the resin will have little influence on the leak behavior of the whole PWR EPA. However, the silicone resin works as an electrical insulator, and the melting of the resin may influence the function of the EPA. Data of the silicone resin experiments are used to verify and modify an analytical model to predict the melt progression of the silicone resin behavior. The model can be applied to evaluate behavior of the BWR EPAs in which other kind of resin plays an essential role by varying material properties and geometric configurations.

## CONCLUSIONS

Two series of small-scale component experiments were performed using test sections which simulate the alumina module and the silicone resin of EPAs used in Japanese PWR. Considering the results of the experiments, the following conclusions were obtained:

(1)The silicone resin of the EPA located inside of the containment is estimated to melt and relocate in thermal-hydraulic conditions of the containment during a severe accident. Metal parts of the EPA is supposed to have strong influence on the melt behavior of the resin by their high thermal conductivities.

(2)It is considered that the alumina modules have large safety margin and will maintain the integrity during the severe accident. Therefore, the whole EPA is supposed to maintain leak-tightness in the severe accident.

(3)Strain of the module was predominantly caused by the elevated temperature. This indicates that the thermal loads would be more threat to the integrity of the EPA than the pressure loads.

## References


1. NEA Group of Experts, "The Role of Nuclear Reactor Containment in Severe Accidents", Nuclear Energy Agency/Organisation for Economic Co-operation and Development, Paris, April 1989.

2. K.Soda et al., "Recent Development and Results from Severe Accident Research in Japan", Proceedings of 19th Water Reactor Safety Information Meeting, U.S.Nuclear Regulatory Commission. (to be published in NUREG/CP Report)

3. D.B.Clauss, "Severe Accident Testing of Electrical Penetration Assemblies," NUREG/CR-5334, SAND89-0327, Sandia National Laboratories, Albuquerque, NM, November 1989.

4. R.S.Denning et al.,"Radionuclide Release Calculations for Selected Severe Accident Scenarios," NUREG/CR-4624, BMI-2139, Battelle Columbus Division, Columbus, OH, August 1990.


## Acknowledgements


We would like to gratefully acknowledge the excellent work in preparation of the experiments and operation of the test facilities by the staffs of the Safety Facility Engineering Services Division in JAERI leaded by Mr. Hideo Itoh.

Table 1. Dimensions and Capabilities of the Small-Scale Leak Test Vessel

| Item | Quantity |
|---|---|
| Inner Diameter (m) | 0.254 |
| Volume ($m^3$) | 0.036 |
| Design Temperature (K) | 823 |
| Design Pressure (MPa) | 2.0 |
| Heater Power (kW) | 4.0 |

Table 2. Experimental Conditions of the Alumina Module Experiments

| | Experiment | | | |
|---|---|---|---|---|
| | SLA001 | SLA003 | SLA004 | SLA005 |
| Maximum Temperature (K) | 676 | 720 | 660 | 725 |
| Pressure (MPa) | 0.50 | 1.77 | 1.75 | 1.76 |
| Temperature Increasing Rate (K / s) | 0.0116 | 0.0137 | 0.0082 | 0.0123 |

Table 3. Experimental Conditions of the Silicone Resin Experiments

| | Experiment | |
|---|---|---|
| | SLB001 | SLB002 |
| HTHP Region | | |
| Initial Temperature (K) | 285 | 287 |
| Temperature Increasing Rate (K/s) | 0.0214 | 0.0064 |
| Maximum Temperature (K) | 640 | 515 |
| Pressure (MPa) | 0.15 | 0.13 |
| LTLP Region | | |
| Nitrogen Temperature (K) | 290 | 290 |
| Pressure (MPa) | 0.14 | 0.12 |

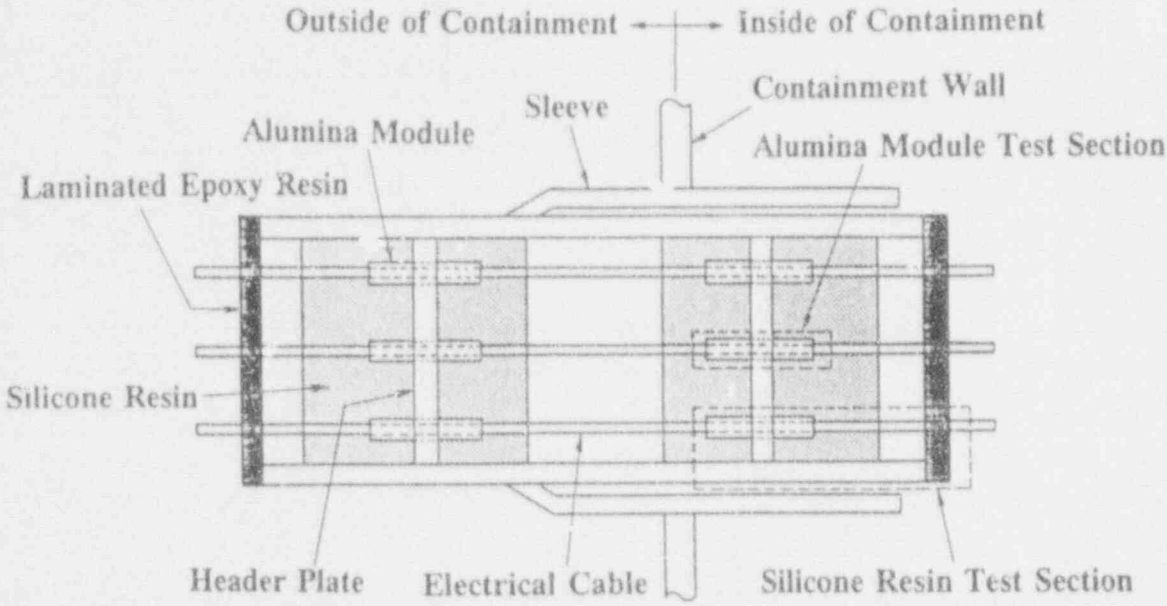


Figure 1. Schematic Diagram of an EPA used in Japanese PWRs

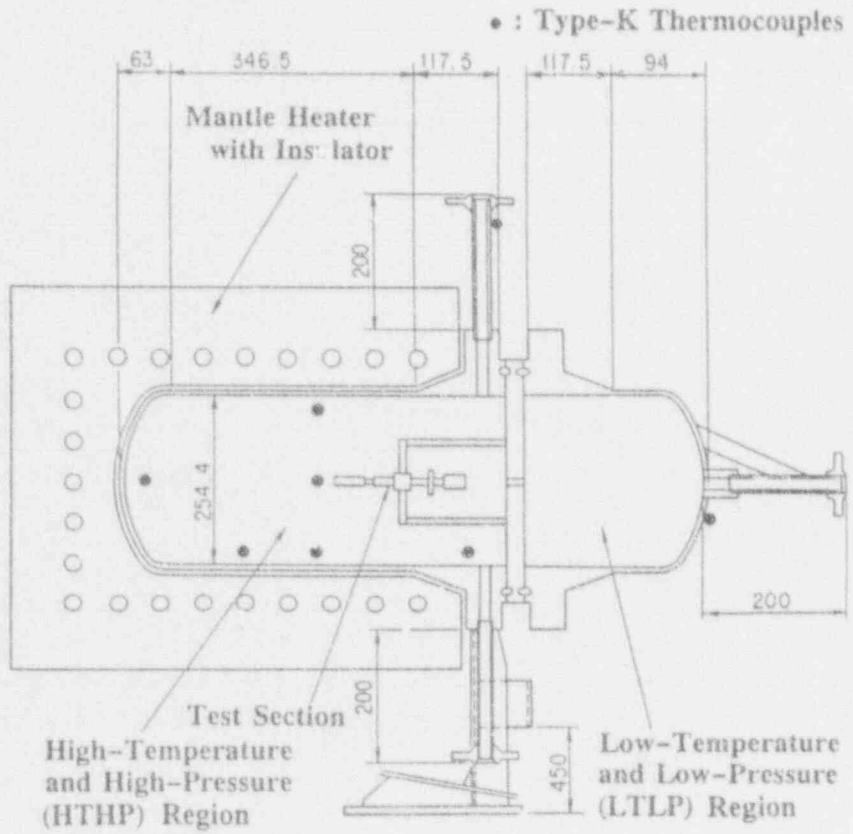


Figure 2. Small-scale Leak Test Vessel with a Test Section

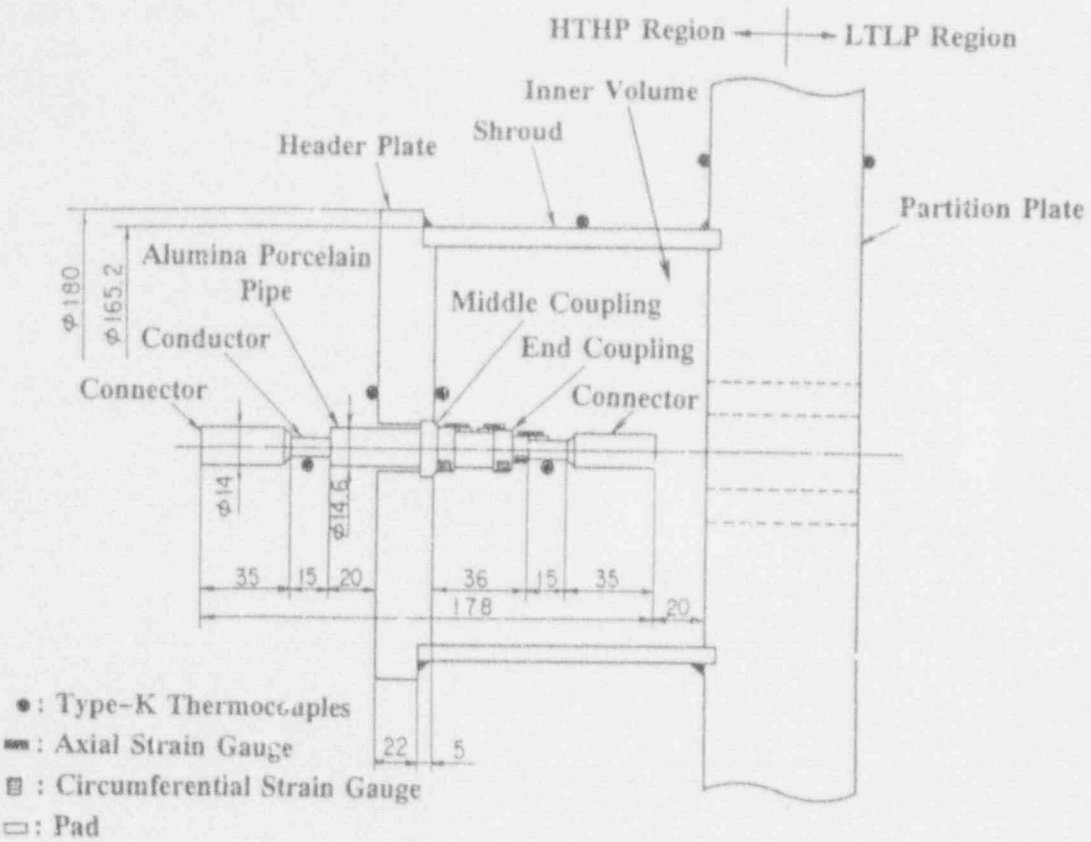


Figure 3. Schematic Diagram of the Alumina Module Test Section

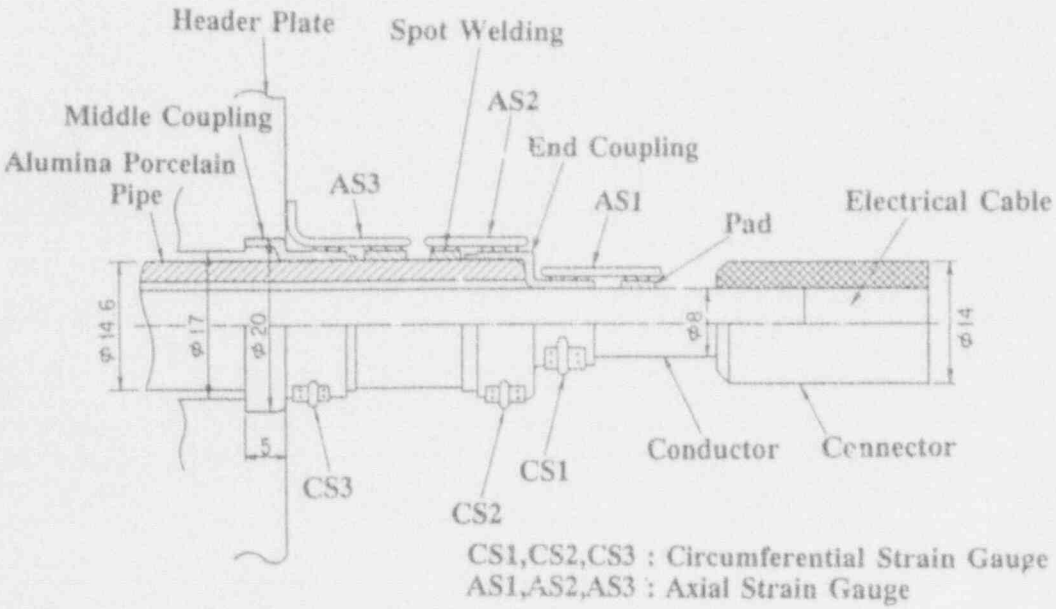


Figure 4. Structure of the Alumina Module in the Test Section

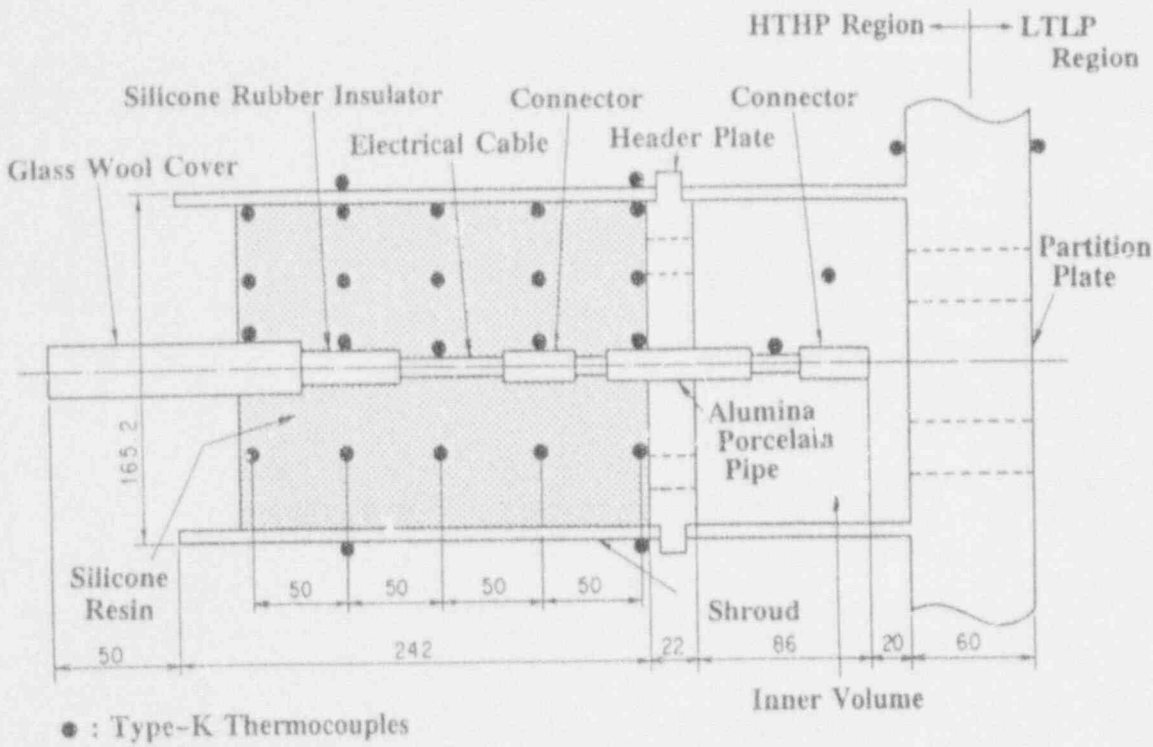


Figure 5. Schematic Diagram of the Silicone Resin Test Section

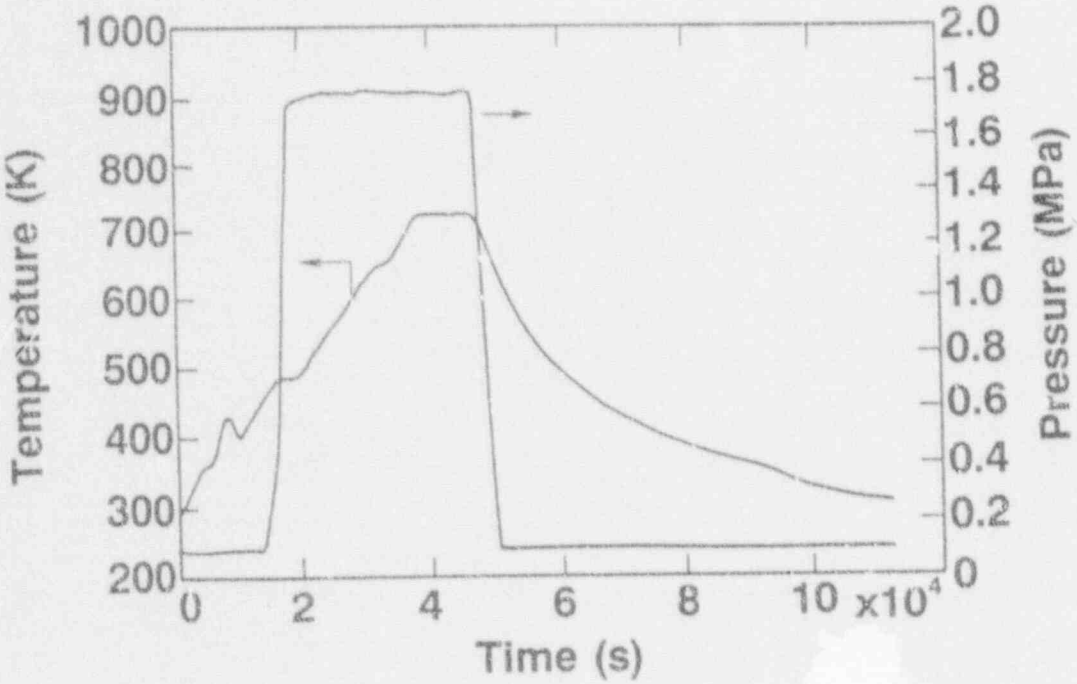


Figure 6. Temperature and Pressure History of the HTHP Region in SLA005

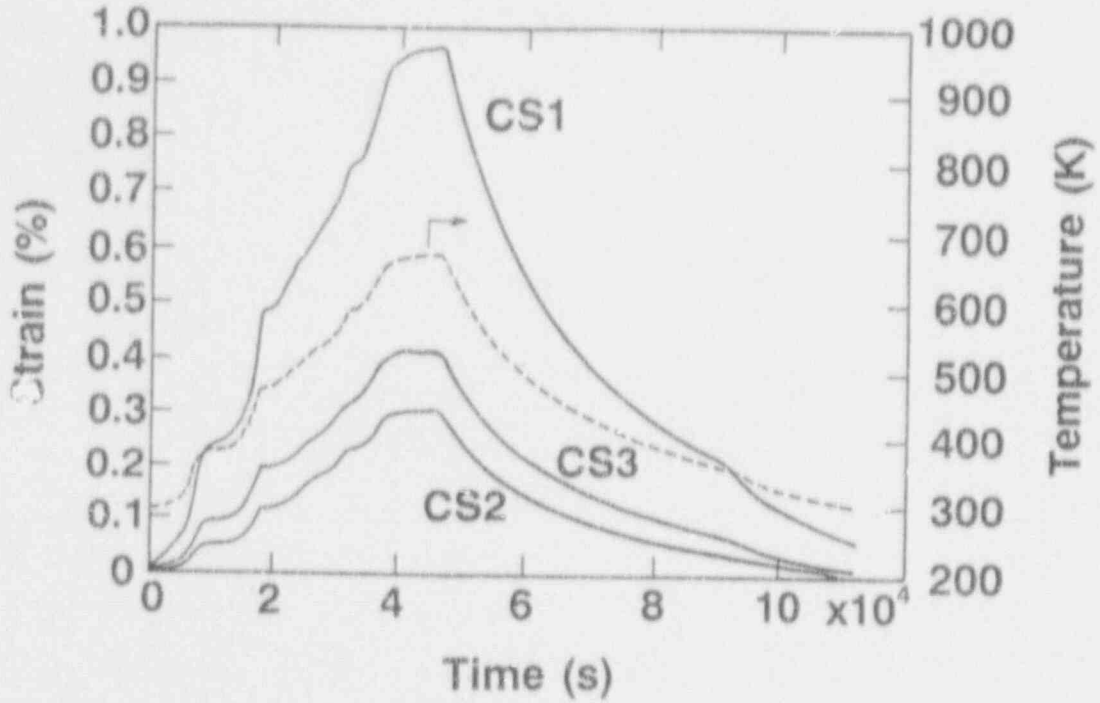


Figure 7. Circumferential Strains on the Surface of the Couplings Compared with Temperature in SLA005

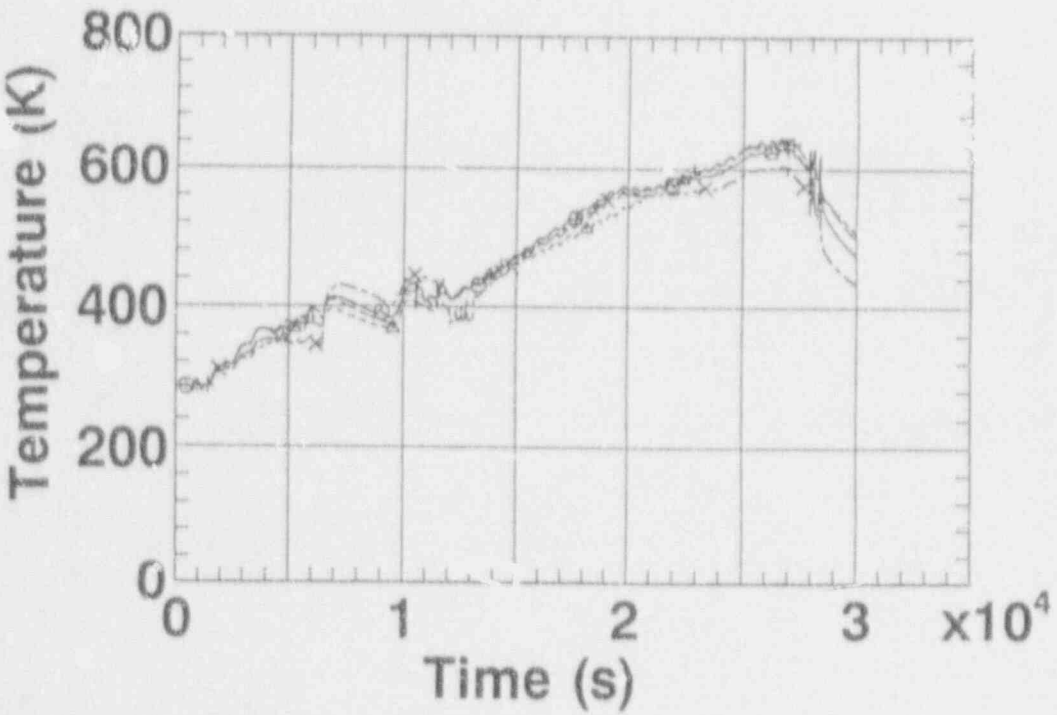


Figure 8. Temperature of the HTHP Region in SLB001

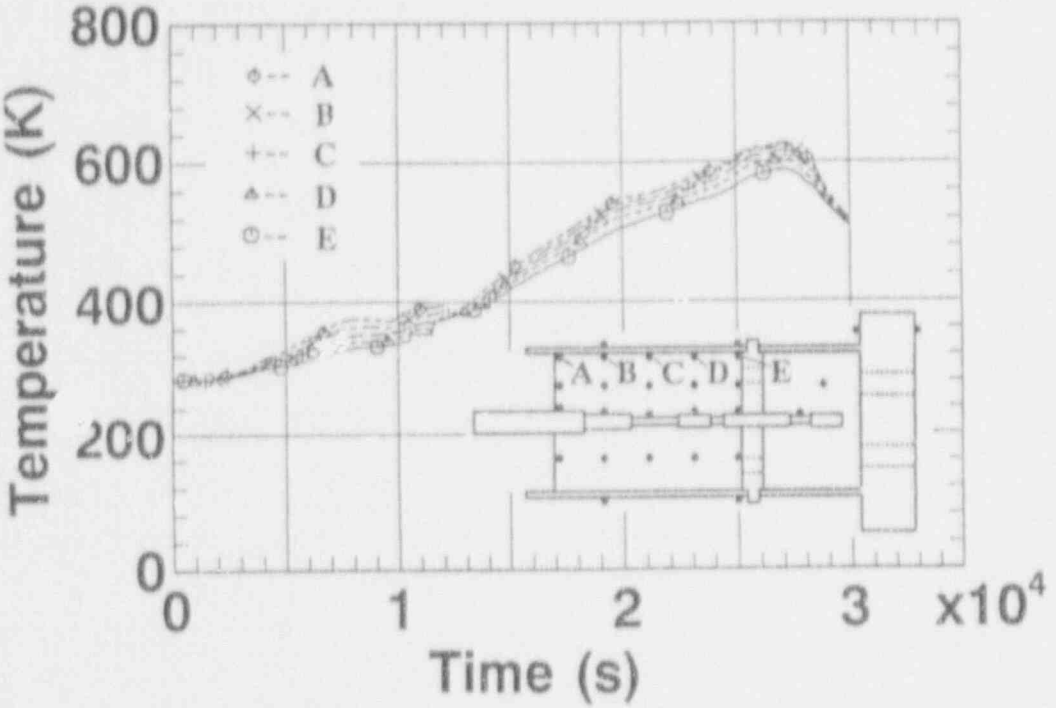


Figure 9. Temperature Distribution along the Inside of the Shroud in SLB001

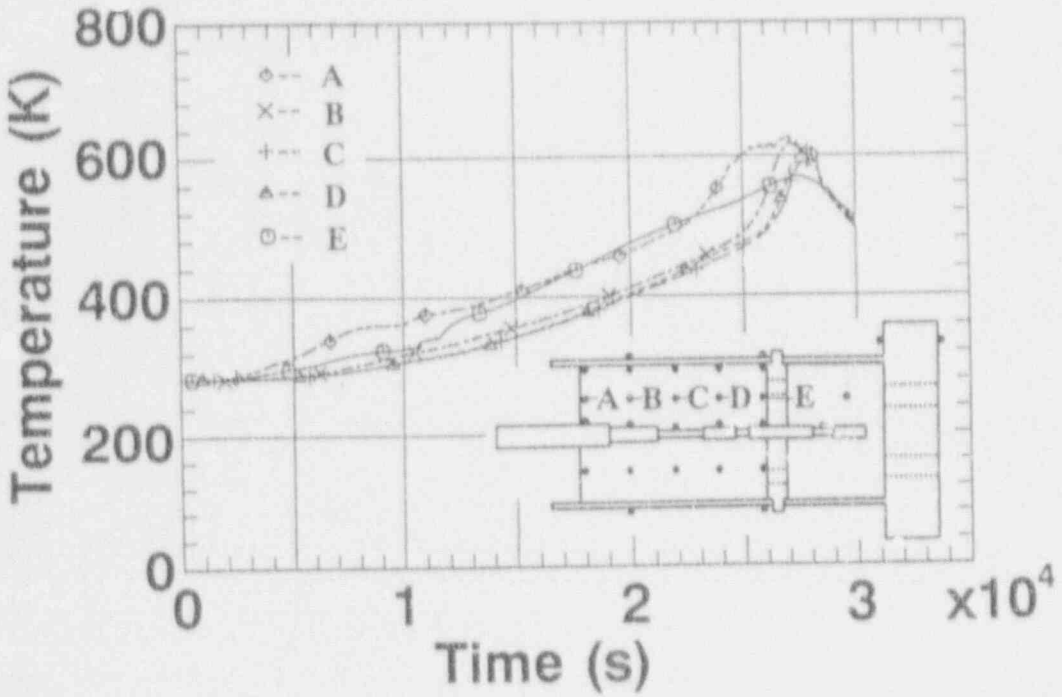


Figure 10. Temperature Distribution in the Resin in SLB001

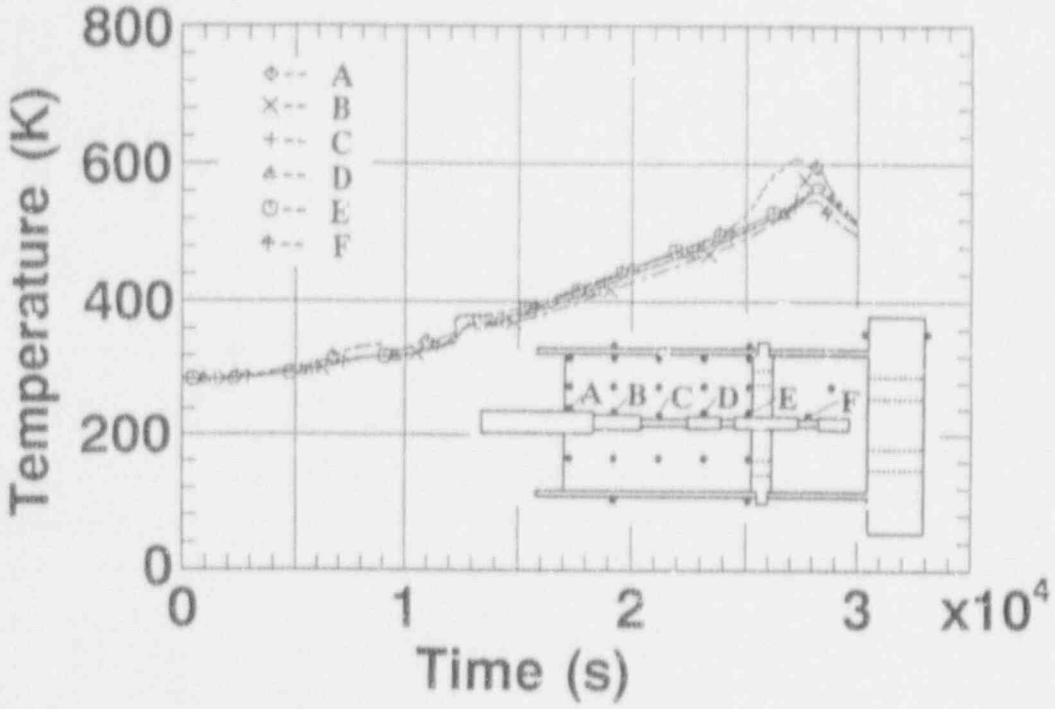


Figure 11. Temperature Distribution along the Cable in SLB001

# HIGH-TEMPERATURE LEAK CHARACTERISTICS TEST OF PCV HATCH FLANGES GASKET

KATUMI HIRAO
Tokyo Electric Power Company, Tokyo, Japan
MASASHI GOTO, YOSHIHIRO NARUSE
Toshiba Corporation, Yokohama, Japan
KOUICHI SAITO
Hitachi Ltd., Hitachi, Japan
TAKURO SUZUKI
Hitachi Engineering Co., Ltd., Hitachi, Japan
HIROYUKI SUGINO
Ishikawajima-Harima Heavy Industries Co., Yokohama, Japan

## Abstract

This paper describes the leak characteristics of the sealing materials being used at PCV hatch flanges at BWR plants in Japan at temperatures exceeding the design conditions in anticipation of severe accidents.
It was found that there was no noticeable leakage regardless of the bolt tightness at temperatures of 250℃ and below, but the mechanical characteristics of the silicon rubber were lost and the sealability was impaired at temperatures of approx. 275℃ ~ 300℃.

## 1. INTRODUCTION

It was confirmed that the PCV integrity depends on the pressure resistance and leakage resistance of each part of the PCV boundary, and it was confirmed that each part has sufficient margin for the design base accident (DBA).
A study has been made on the behavior of the internal pressure of the top-head and hatch-flange sections at the 11th SMiRT. However, the test was conducted at room temperature and did not consider the temperature effect of elevated temperature.
If the PCV temperature exceeds the design temperature, it is presumed that organic seals such as gaskets possibly reach their heatresistance limit and leak before the PCV steel section fails.
From this aspect, we believe that it is essential to anticipate a severe accident by examining to what extent the PCV function is maintained under condistions exceeding the design temperature. Therefore, we determined the maximum temperature and pressure at which flange gaskets start to leak by implementing a test of the high-temperature leak characteristics of seals now being used at plants.

## 2. TESTS

### 2.1 Purpose

The test aimed to examine the sealability of the gasket by exerting pressure at the silicon gasket and checking for any leaks.

### 2.2 Test Procedures

(1) Testpiece

Two different silicon rubber gaskets with the same specifications as those of gaskets now in use at plants were used as shown in Figure 1.

(2) Test Device

Figures 2 shows the test device. It has two different flange structures the same as those now being used at plants.
The upper and lower parts of the testpiece were placed between steel plates simulating the flange.

(3) Test Method

A testpiece was set in the flange so that the preset tightness could be obtained, and pressure was gradually exerted by $N_2$ or steam at a fixed temperature after increasing the temperature. After confirming the leakage at the seal, the pressure and temperature at that instant were recorded. The maximum internal pressure exerted on the testpiece was about 20kgf/cm² which was about five times the PCV design pressure.

(4) Test Parameters

The test parameters are given in Table 1.

Table 1 Test Parameters

| | | |
|---|---|---|
| (a) Temperature | Room temperature, 175℃ ~ 350℃ | |
| (b) Radiation | No, Yes ($8.0 \times 10^7$ rad) | |
| (c) Sealing structure | Semi-round, tongue-and-groove | |
| (d) Pressure medium | $N_2$ and steam | |
| (e) Tightness ($\delta$) (See Fig. 3) | Semi-round<br>$\delta_1 = 0.0$mm<br>$\delta_2 = 0.8$mm<br>$\delta_3 = 1.7$mm<br>$\delta_4 = 2.5$mm | Tongue-&-Groove<br>$\delta_1 = 0.75$mm<br>$\delta_2 = 1.5$ mm<br>$\delta_3 = 2.25$mm<br>$\delta_4 = 3.0$ mm |

(5) Test Method

When a leak occurred with pressure exerted on the testpiece, the pressurization medium flows into the outside groove (leakline). Leaks from the gasket could be detected by this flow from the leakline. To detect the leak, any one of the following methods which best met the test conditions was used:

- Bubbling at leakline container
- Pressure reduction in pressure line
- Sound
- External observation

## 2.3 Test Results

The following results were obtained.

- Leaks were found more easily with steam than with $N_2$.

- Silicon gasket sealability was lost at the temperature of approx. 275℃ ~ 300℃ in the $N_2$ atmosphere and at temperatures of approx. 225 ℃ ~ 300℃ in the steam atmosphere.

- After 80 Mrad of $\gamma$-irradiation, leaks from the irradiated gasket were less common compared to the non-irradiated gasket. This is thought to be because the silicon gasket was hardened by the $\gamma$-irradiation.

- At temperatures of approx. 225℃ and above, leaks occurred at pressures of 20kgf/cm² and below, but the leak pressure increased with tightness.

- There was very little defference in performance between the semi-round and tongue-and-groove gaskets. The tongue-and-groove type withstood slightly higher temperatures than the semi-round gasket. This is probably due to the difference in the structure between the two gaskets.

Based on these results, the relationship between the pressure when a leak occurred and the temperature for the type of pressure medium and structure of each seal section are shown in Figures 4~7.

## 3. Conclusion

From these results, the flange tightness created no serious problems and the pressure medium and temperature were the major governing factors. The silicon gasket can maintain its sealing function up to approx. 225℃ ~ 275℃ at a pressure of 20kgf/cm² which is about five times the PCV design pressure which defers depending on atmospheric conditions. The results of this test are almost similar to those of other tests such as SNL.

## References


1. D.A. Brinson and G.H.Graves
"Evaluation of Seals for Mechanical Penetrations of Containment Buildings"
NUREG / CR-5096(1988)

2. K.Hirao, M. Goto, Y. Naruse, H.Sugino, K. Saito, and K. Hasegawa
"Pressure Test of the Typical Vessels Flange under Pressure Loading"
SMiRT 11 J02/4 P.25 ~30 (1991)


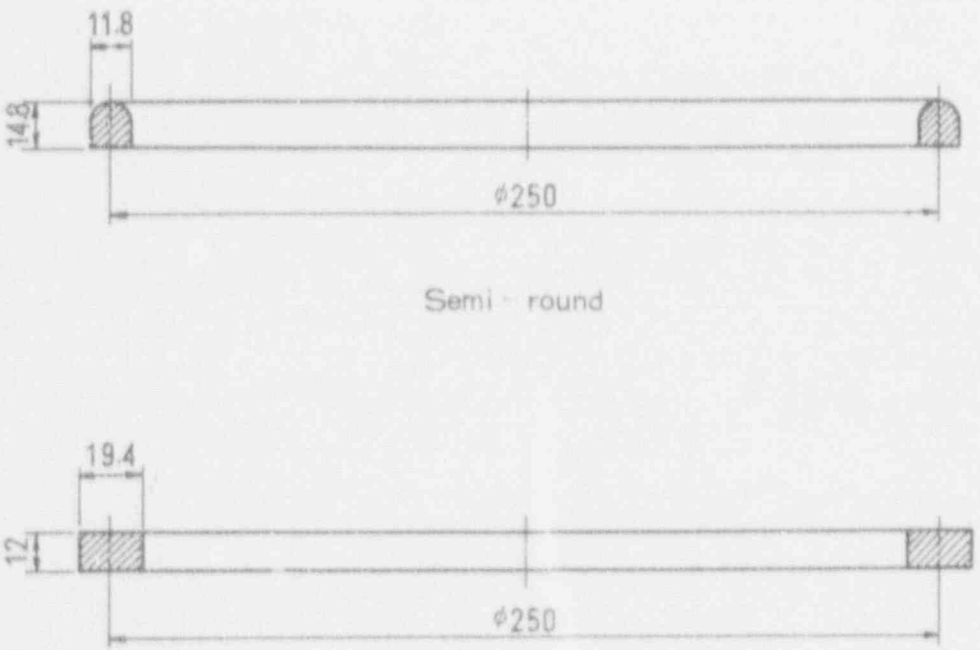


Figure 1. Test Piece Type

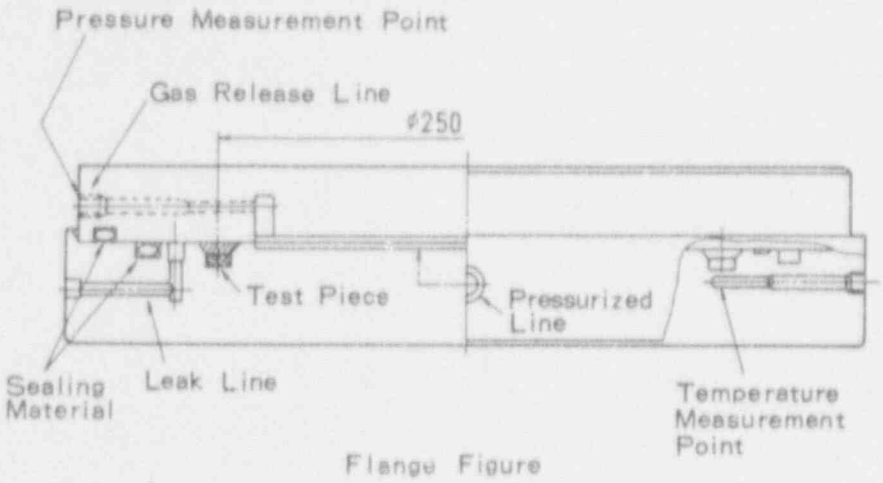


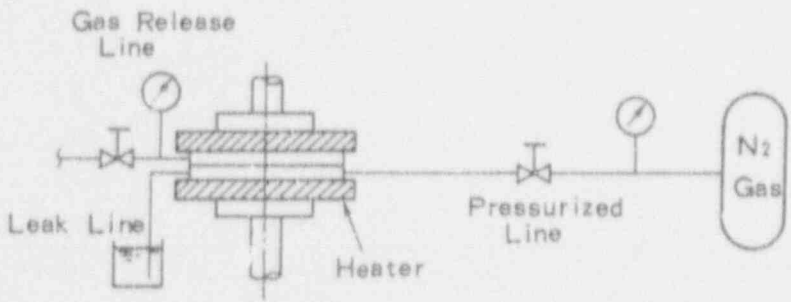


**Figure 2. Test Device**

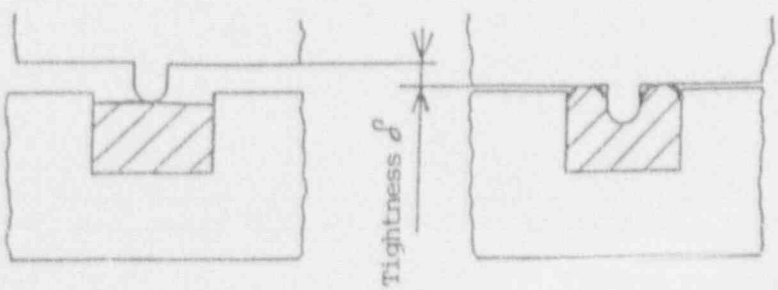


Figure 3 Definition after Tightening

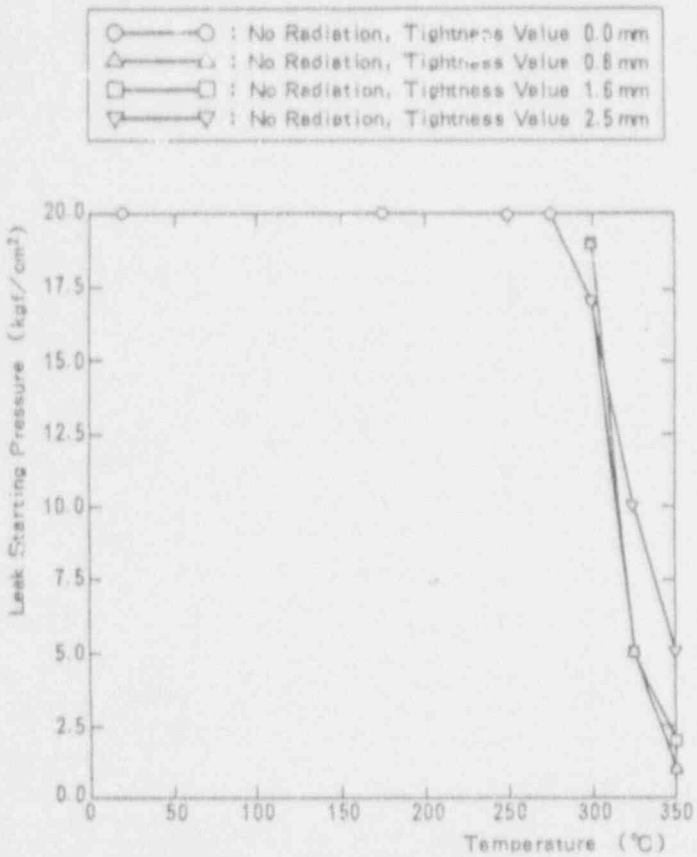


Figure 4. Test Result (Semi-Round Type, $N_2$ Gas)

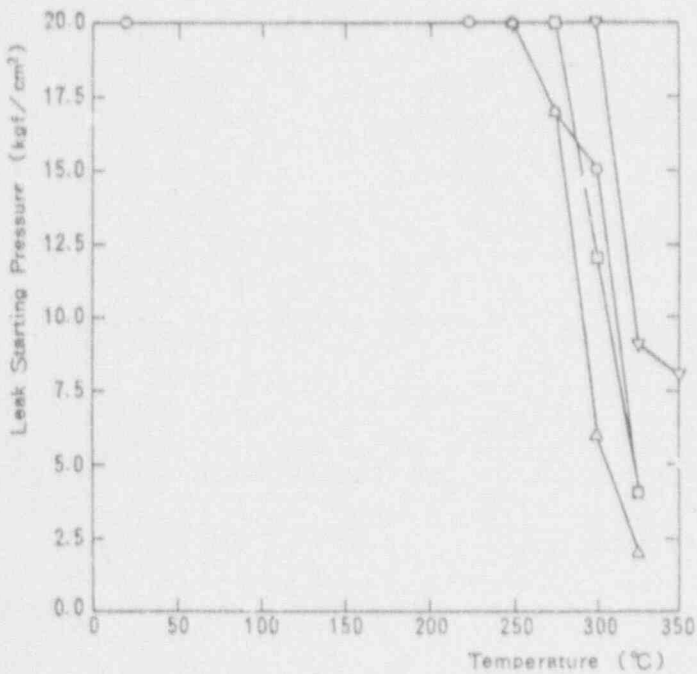


Figure 5. Test Result (Semi-Round Type, Steam)

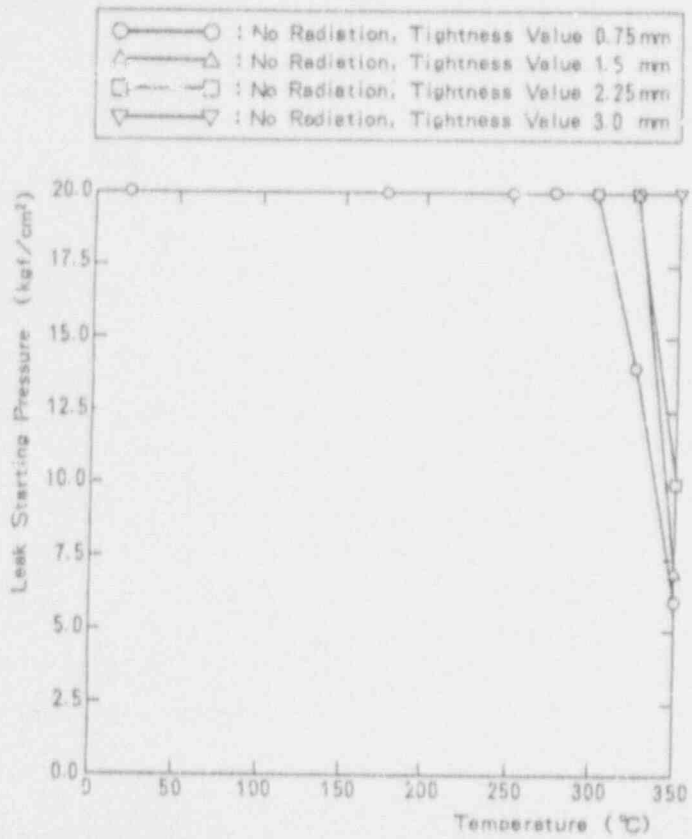


Figure 6. Test Result (Groove-and-Tongue, $N_2$ Gas)

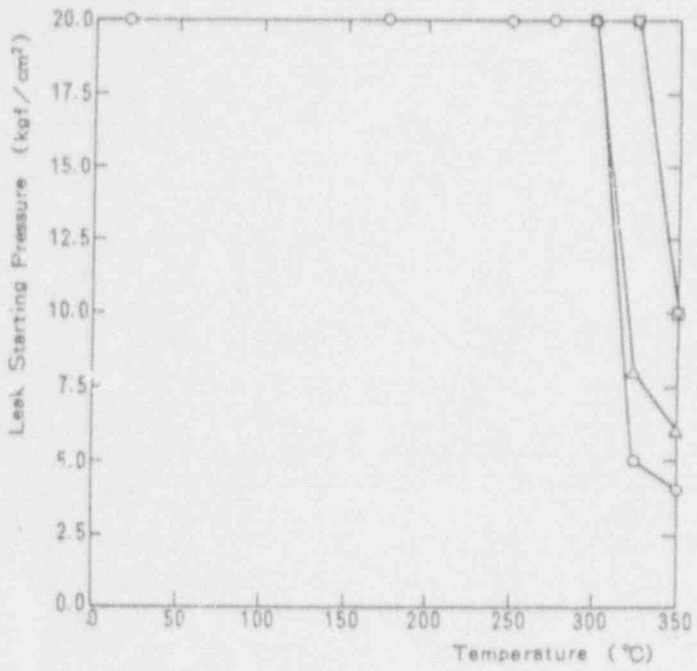


Figure 7. Test Result (Groove-and-Tongue, Steam)

# AN INVESTIGATION OF LINER TEARING IN REINFORCED CONCRETE REACTOR CONTAINMENT BUILDINGS: COMPARISON OF EXPERIMENTAL AND ANALYTICAL RESULTS

Barry L. Spletzer, L. Dwight Lambert, and J. Randall Weatherby
Sandia National Laboratories
Albuquerque, New Mexico

## Abstract

The overpressurization of a 1:6 scale reinforced concrete containment building demonstrated that liner tearing is a plausible failure mode in such structures under severe accident conditions. A combined experimental and analytical program was developed to determine the important parameters that affect liner tearing and to develop reasonably simple analytical methods for predicting when tearing will occur. Three sets of test specimens were designed to allow individual control over and investigation of the mechanisms believed to be important in causing failure of the liner plate. The series of tests investigated the effect on liner tearing produced by the anchorage system, the loading conditions, and the transition in thickness of the liner. Before testing, the specimens were analyzed using two- and three-dimensional finite element models. Based on the analysis, the failure mode and corresponding load conditions were predicted for each specimen. Test data and posttest examination of test specimens shows mixed agreement with the analytical predictions with regard to failure mode and specimen response for most tests. Many similarities were also observed between the response of the liner in the 1:6 scale reinforced concrete containment model and the response of the test specimens. This work illustrates the fact that the failure mechanism of a reinforced concrete containment building can be greatly influenced by details of liner and anchorage system design. Furthermore, it significantly increases the understanding of containment building response under severe accident conditions.

## INTRODUCTION

The U.S. Nuclear Regulatory Commission (NRC) is investigating the performance of light water reactor (LWR) containments subject to severe accidents. This work is being performed by the Containment Technology Department at Sandia National Laboratories (SNL) under NRC sponsorship. In 1987, a 1:6-scale reinforced concrete containment model (RCC) was pressurized to failure. The failure mode was a 22-inch tear in the liner plate. As a result of this test, the Separate Effects Test Program was initiated and has been conducted to investigate various parameters that could affect liner tearing. The program consisted of a two-phase effort -- one analytical and one experimental -- aimed at developing analytical and experimental modelling techniques for simulating the response of liners in RCCs loaded by internal pressure.

The basis for the analytical model to predict liner tearing and the results of the pretest analyses will be presented. The design, instrumentation, and testing of specimens to compare with the model predictions and the RCC response will also be discussed. Finally, the analytical predictions will be compared to the test results.

In addition to increasing understanding of the 1:6 scale RCC failure, the objective of this separate effects test series is to increase the understanding of potential failure modes of LWR containment buildings under severe accident conditions and to reveal factors in containment design which affect containment failure.

## BACKGROUND

Figure 1 shows a cross-section of the 1:6-scale RCC model. This model was tested in July of 1987 to failure at a pressure of 145 psig [1]. At this pressure, a large leak developed. Posttest examination revealed that the leakage was through a 22-inch long tear in the liner adjacent to a penetration insert plate. Figure 2 is a photograph of this tear. Upon closer examination, a large number of small tears and distressed areas in the liner were found. In general, the direction of the tears were vertical and were located near the corners of penetrations near the mid-height of the model cylinder. Figure 3 is a stretchout showing the location of tears and distressed areas in the liner.

The posttest examination of the model revealed several important facts. First, the large tear was not an isolated event caused by some imperfection. This is evidenced by the fact that numerous other tears in similar locations were developing at the same time. In addition, all the tears occurred in regions near the insert plate/liner plate welds, and always very close to a row of stud anchors. In addition, all the tears were propagating in a vertical direction, which appears to be in response to the liner hoop strain. Finally, the tears tended to occur near the mid-height of the cylinder where the liner strain was the largest.

The evidence of these multiple tears in the liner points to a failure mechanism which could possibly involve the liner-to-insert plate weld, the liner anchorage, or the material properties of the liner plate. In order to investigate the interactions between these items and to develop a fuller understanding of the failure mechanism of the 1:6-scale RCC model, the Separate Effects Tests (SET) Program was initiated.

## FAILURE THEORIES FOR THE 1:6 SCALE RCC

The existence of multiple, vertical tears in the liner plate near the insert plate boundary at the model mid-height leads directly to two possible failure theories for the model. These theories are of primary importance to the SET because the analysis of the model behavior and the design of specimens must be directed towards investigating the various mechanisms that could cause liner tearing. For the SET, a specimen and corresponding analytical model was developed to address each postulated failure theory.

All of the tears occurred at the most highly strained section of the liner, and always near an insert-to-liner plate weld. This suggests a possible failure mechanism that concerns the weld or the thickness transition between the two plates. The insert plate is three times the liner plate thickness and is tapered at 1:4.

Careful examination of the 1:6-scale RCC failure and consideration of a number of the model design features led to the hypothesis of a much more complicated failure mechanism. This mechanism is illustrated in Figure 4. The top half of the figure shows a schematic cross section of the 1:6-scale model in the region near the liner plate/insert-plate weld. This section is designed to represent a portion of the model wall section in the hoop direction. The lower part of the figure shows this same schematic after a uniform 3% strain has been applied to the section. It is assumed that, in regions far from the weld and thickness transition, there is uniform strain throughout the wall thickness. This means that there is no shear displacement between the liner and the reinforcing steel. Several labelled regions in the lower part of the figure explain the mechanism leading to liner tearing. Since the reinforcing steel carries the bulk of the tensile load during the test (the reinforcing steel cross section is about three times the liner cross section), it tends to dominate the strain response and exhibits uniform strain along its length. This uniform strain causes the concrete to crack regularly along the length

of the steel. The regularly fractured concrete is still attached to the relatively closely spaced studs.

The liner and insert plate to which the studs are attached do not undergo the same uniform strain. Again, since the wall strains uniformly far from the weld, the overall elongation of the liner and insert plate combination is the same as that of the reinforcing steel. However, the insert plate is three times the thickness of the liner plate; therefore, as tension is applied to the combination, the insert plate remains elastic, exhibiting very small strains, while the liner plate undergoes plastic strain. In the figure, the active portion of the liner and insert plate are approximately equal and, therefore, since the liner plate must absorb the entire elongation of the combination, the liner plate strain is twice that of the uniformly strained rebar or 6%.

This potential difference in displacement of the liner plate, insert plate and reinforcing steel creates a potential for shear load transfer. As mentioned previously, the heads of the studs are embedded in the concrete which is traveling with the uniformly strained reinforcing steel. However, the base of the stud is welded to the liner and insert plate and must experience the same displacement as the liner and insert plate. This potential mismatch in displacement causes a shear load to be transmitted from the reinforcing steel to the liner and insert plate through the studs. In the figure, both the reinforcing steel and liner/insert plate have been strained to the configuration which they would assume if no shear transfer were present. This potential mismatch in deflection causes the studs to bend. The angle at which a stud bends is directly related to the amount of shear load that it can transmit from the reinforcing steel into the liner and insert plate region.

Notice in the figure that the studs with the largest angle are those nearest the weld and thickness transition. This leads to the conclusion that, once the liner undergoes plastic strain, the load transfer caused by the studs adds additional stress to the liner. This means that the maximum stress in the liner should be immediately adjacent to the row of studs located closest to the weld. Finally, notice that the shear (angular) deformation of the first row of studs in the insert plate is the same as the first row in the liner plate. However, since the insert plate was three times thicker than the liner plate, the additional stress induced by this shear transfer is only one-third as great in the insert as in the liner. Further, since the insert plate remains elastic, the additional stress produces a much smaller additional strain than the same stress change would produce in the yielded liner plate.

Simulating the mechanisms described in this scenario is an important part of the analysis and testing efforts in the SET program.

## SPECIMEN CONCEPTS AND DESIGN

The postulated failure mechanisms described above led to the development of three SET concepts. This section presents the design and rationale of each of the test specimen types.

The first specimen investigates the effect of the liner-to-insert plate weld and thickness transition on the elongation of the liner plate at failure. This specimen is referred to as the Weld Transition Specimen. Figure 5 is a perspective drawing of the specimen as configured and a two-view assembly drawing of the specimen with the major dimensions included.

The specimen consists of a 10 inch (0.25 m) wide segment of liner plate that is 18 inches (0.46 m) long. Both ends of the liner plate are welded to sections of thicker insert plate. The insert plates are in turn attached to a pull fixture to allow the specimen to be placed in uniaxial tension.

The failure mechanisms discussed in the previous section point to an important interaction between preload in the liner material and additional stress induced by stud shear loading. The next specimen was designed to allow the effects of linear preload and stud shear to be investigated separately. The postulated failure mechanism predicts that the combination of stud shear and pre-existing liner load combine to produce a liner tear when either mechanism separately would fall far short of tearing the liner. A simplified model of this mechanism can be envisioned using the idea of net section stress in the liner. If the liner is preloaded to a stress that is beyond the yield stress of the material, plastic deformation will occurred. Since the material has not reached its ultimate strength, the liner does not tear. However, since the post-yield stress-strain curve is relatively flat, a small change in the net section stress will produce a large change in strain and could induce liner tearing. This small change is provided by the stud shear load. The increase in net section stress caused by stud shear is the average stud load divided by the average cross section a stud represents (stud pitch multiplied by liner thickness). This increase, if large enough, could cause liner failure. This second specimen is designed to investigate the effects and interactions between liner preload and stud shear.

Figure 6 shows a perspective drawing and a two-view assembly drawing of the Separately Controlled Loading Specimen. This specimen consists of two large dog-bone-shaped pieces of liner material with four anchorage studs attached across the neck of each dog bone. The dog-bone shape assures that the maximum strain induced by liner load will occur near the studs. A block of concrete is formed around the studs in the central region of the specimen and is attached to the specimen only by means of the studs. This allows stud shear to be applied separately from axial tension in the liner material. The radius of the dog bone is large to ensure that the predominant strain concentrations are those produced by the studs.

During testing, two separately controlled systems are used to apply the load. The first system applies direct tension to the liner by fixing the upper pull block and applying a downward load to the lower block. This load is increased to a predetermined net section stress at the narrowest part of the specimen. Once this load is achieved, it is maintained through a load-control device, and the second loading system provides a downward load to the concrete block. This second system operates under displacement control and slowly displaces the concrete block while measuring the force required to cause the displacement and allowing the load-controlled portion of the experiment to maintain the net section stress in the liner throughout the experiment.

By varying the initial liner preload and then displacing the concrete block until failure occurs, the interaction between liner preload and stud shear can be studied. From the postulated failure mechanism of the 1:6-scale model, it would be predicted that, at low liner preloads, motion of the concrete block will simply shear the studs from the liner while, at higher preloads, the condition exists where motion of the block will initiate a tear in the liner.

The final specimen in the SET series comes closest to a full simulation of the wall section of the 1:6-scale reinforced concrete containment. A perspective drawing of this Full Simulation Specimen is shown in Figure 7 along with a two-view assembly drawing with limited dimensions. To ensure that the load could be properly distributed on the specimen, the liner plate and insert plate are placed on both the front and back of the specimen. Ten #6 reinforcing steel bars are installed axially in each specimen. The width of the plate is 10 inches and the depth is 15 inches. The reinforcing steel used here is somewhat larger than that used in the 1:6-scale model. However, the ratio of the reinforcing steel to liner steel is the same as in the RCC model. This specimen is designed to directly investigate the complex failure mechanism discussed earlier. The end blocks on the specimen ensure that the overall elongation of the liner insert plate combination and the reinforcing steel is identical. According to the postulated failure mechanism, this will develop stud shear through load transfer between the reinforcing steel and the nonuniformly strained liner/insert plate region.

In all the above specimens, the specifications and procedures for construction were identical to those used in the 1:6-scale model whenever possible. However, in the case of the liner and insert plate, the original 1:6 scale model steel, A414 Grade D, was not available. Instead, specifically tested heats of A516 Grade 60 and A516 Grade 70 were located with properties that closely matched the A414 Grade D.

## SPECIMEN FINITE ELEMENT MODELS

The primary purpose of the finite element modelling effort was to identify a set of modelling techniques, modelling assumptions, and failure criteria which can be used in finite element simulations to accurately predict failure of the liner and liner anchorage system of the test specimens. In developing these models, two general model types were sufficient to model the three specimen types. The separately controlled loading specimen and full simulation specimens each required a specific model. However, the weld transition specimen is identical to the liner/insert plate region of the full simulation specimen without the studs attached so the model could be modified slightly to cover both specimen types.

A two-dimensional finite element model of the separately controlled loading specimen is shown in Figure 8. ABAQUS, a commercial finite element code, was used to run these simulations. In the two-dimensional model, the liner plate is represented with plane stress continuum elements (CPS4), and the studs are represented with nonlinear spring elements (SPRINGA). One end of the spring is fixed, and the other end is attached to the liner. Initially, the two nodes which define each spring element are coincident. As the specimen deforms under load, these two nodes separate and a force develops in the spring.

In the numerical simulations of the separately controlled loading experiments, loads were applied to the upper and lower edges of the model as shown in Figure 8. Several different simulations were run to determine the response of the specimen under different load histories. The loads on the upper and lower edges of the specimen were initially increased at the same rate. This is referred to as the preloading phase. Following the preloading phase, the load on the upper edge was increased while the load on the lower edge was held constant. During the preloading phase, lateral forces developed in the studs due to the Poisson contraction of the specimen. Following the preloading phase, the forces in the studs increased as they balanced the difference between the loads applied to the upper and lower edges of the specimen.

The constitutive response of the liner plate was represented by a standard metal plasticity model with a von Mises yield surface, associated plastic flow, and isotropic hardening. The relationship between the von Mises stress and the equivalent plastic strain is defined in Figure 9 (this represents the relationship between true stress and true strain). This curve was obtained from uniaxial tension tests. Stress and strain values beyond the point of necking were determined by measuring the thickness of the specimen in the necked-down region.

The load-displacement relationship for the stud anchors was determined from the stud-shear experiments described in References 1 and 2. In order to investigate the effect of the stud strength on the predicted failure mode of the specimens, three different functions describing the shear load-displacement relationship were used in simulations of the separately controlled loading specimens. These functions are plotted in Figure 10.

To predict the mode of failure in the test and the loading conditions necessary to cause failure, it is necessary to adopt appropriate failure criteria. A stud is assumed to fail when the elongation of the corresponding spring in the finite element model exceeds a specified

value. The elongation at fracture is marked in the plots shown in Figure 10. Although there is no generally accepted failure criterion applicable to the liner plate, we have adopted an empirical criterion of failure proposed by Manjoine [3]. The variables which appear in this criterion are the mean stress, the equivalent plastic strain, and the elongation at failure in uniaxial tension. Details on how Manjoine's criterion is applied can be found in Reference 1.

In addition to the uncertainty in the failure criterion for the liner plate, the stresses and strains computed in the liner elements that are attached to the studs are strongly dependent on the size of the elements. The extreme mesh sensitivity results from the transfer of load from the spring to the liner through a single point. To account for the fact that the load is actually transferred over a finite area, the continuum elements connected to the studs were given a square shape with the side length equal to the radius of the stud. Numerical experiments [1] indicate that, with this choice of element size, the stress and strain invariants computed in the liner elements adjacent to the stud anchor in a two-dimensional simulation are in reasonable agreement with the invariants computed in a three-dimensional simulation.

A total of fifteen finite element simulations were conducted for the separately controlled loading specimen. Five different loading conditions were considered for each of the three anchorage load-displacement functions shown in Figure 10. The two-dimensional finite element model used for the full simulation specimens is shown in Figure 11. As before, the liner plate was modelled with plane stress elements, and the studs were modeled with nonlinear spring elements. The steel reinforcement was represented by three rows of truss elements (CID2). The cross-sectional area of the truss elements was selected to provide the correct amount of total steel reinforcement. One end of each spring was attached to the liner plate, while the opposite end was attached a rebar element. As in the separately controlled loading model, the two nodes which define each spring element were initially coincident, but separated as the specimen deformed under load. The springs provided a path for load transfer between the liner and the reinforcement.

The relationship between the von Mises stress and the equivalent plastic strain for the liner plate and the steel reinforcement is defined in Figure 12. The tensile elongation at failure was 44% for the liner plate and 13% for the reinforcing steel.

The middle curve in Figure 10 defines the load-displacement relationship for the studs in the full simulation model reported in this paper. This corresponds to a stud strength of 1450 lb.

## SPECIMEN INSTRUMENTATION AND TESTING

In all, 13 specimens of the three types were tested. The specimens were instrumented with resistance strain gages to monitor free-field strains and strain gradients at stud and weld locations. About 800 strain gages were used in the test series. Load and displacement transducers were used to monitor the overall specimen response. In the case of the separately controlled loading specimens, a separate set of transducers was used for each loading system.

On all specimens tested, a sheet of photoelastic material was applied to the surface of the specimen to obtain a whole-field strain indication. The photoelastic material exhibits birefringent properties such that it develops characteristic fringe patterns with the fringe lines corresponding to lines of constant difference in the in-plane principal strains on the specimen surface. The value of the strain is determined by the wavelength of light used for observation, the thickness of the photoelastic coating, and the stress optic coefficient of the photoelastic coating. Typically, for these experiments, a resolution of 0.1% to 0.2% strain is readily achievable. Since the difference in principal strains is equal to the maximum shearing strain, it is a very useful measure of the material strain state.

The very large number of data channels and the use of photoelastic materials allows the response of the various specimens to be monitored with a detail not available during the 1:6-scale model test. This in turn leads to much greater insights into material behavior and, more generally, into the behavior of an anchorage system under severe accident loadings.

Figure 13 shows a typical test setup for the separately controlled loading experiments. The specimen is in the load frame. The polariscope for use in recording the photoelastic fringes is directly in front of the specimen.

Three of the weld transition specimens were tested to failure. The test consists of recording the increasing uniaxial specimen deformation with load and scanning the available strain gages. In addition to this data acquisition, a sheet of photoelastic polymer was placed in the lower half of one side of each specimen.

Six separately controlled loading specimens were tested. The change in failure mode resulting from a variation in the specimen preloading condition was the primary parameter being investigated. Liner preloads for the six specimens tested were: no liner preload; 60 ksi, 63 ksi, 65 ksi, and 70 ksi liner preload; and test to failure using liner loading alone. The various preload values were selected to study the transition in failure mode from stud shearing to liner tearing. Pretest predictions indicated that a preload range of 60 to 70 ksi would encompass the transition.

In the four tests where a liner preload was specified, the load was gradually increased under load control until the desired value was reached. Once the desired liner preload was reached, a controlled displacement was applied to the concrete block causing stud shear loads to develop. The shear displacement was increased until a failure occurred, with the failure being either the shearing of the studs from the liner or tearing of the liner.

The full simulation specimen tests were conducted under displacement control with an initial displacement rate of approximately .002 inches elongation per minute to allow data to be gathered during the elastic range of the test. As the test progressed, the ram rate was increased. The available strain gages were scanned at periodic intervals based primarily on load during the early portion of the test and on specimen elongation during the latter parts of the test after general yielding had occurred. Three specimens were tested using this method. Photoelastic data is available for all three specimens.

One additional full simulation specimen was tested. This specimen was configured to allow external pressure to be applied to the liner plate. The external pressure was applied by means of a bladder box bolted around the specimen and pressurized with dry air. During testing, the pressure in the box was controlled and set to be proportional to the total load applied to the specimen. This configuration simulated the pressure effects in the 1:6-scale model. The elongation rate under displacement control was constant during the test and the pressure loading was controlled automatically. This test has less recorded data than any other test since all surface strain gages had to be removed due to the presence of the bladder box, and photoelastic methods could not be used since the surface could not be viewed. The data for this test consists of the load and deflection as well as the response of the six reinforcing steel gages.

## EXPERIMENTAL AND FINITE ELEMENT RESULTS

Both the specimen experiments and the finite element simulation separately provide a number of insights and conclusions regarding the response of the 1:6 scale liner and anchorage systems. Comparison between the two sets of results helps to evaluate the assumptions and analytical

modelling techniques used here by providing graphic indication of similarities and differences. The comparison is most readily made for the load-deflection results and the whole-field surface maximum shearing strain. The load-deflection data gives a good measure of the overall specimen response. Whole- field strain information is available from the photoelastic data in the form of maximum shearing strain. The finite element simulation results can also be expressed as maximum in-plane shearing strain. This allows two direct comparisons between experiment and simulation to be made.

## Weld Transition Specimen Results

The weld transition specimen was originally designed to investigate the effects of the weld and thickness transition region on the failure mode of the 1:6 RCC liner. Three of these specimens were tested. A finite element model of this specimen was analyzed by using the model of the full simulation specimens with a very small value for the stud strength. Under these conditions, the resulting strain field should look like that seen in the weld transition specimens. A contour plot of this maximum shear strain field from the finite element analysis is shown in Figure 14. The overall elongation of the specimen is 1.5%. Figure 14 also shows a contour plot derived from photoelastic data taken from a weld transition specimen. In general, the two plots are very similar. Both exhibit uniform and equal strain in the free field region far from the weld and thickness transition. A marked reduction in strain near at the centerline and similar strain concentrations along the edges exist at the weld transition. The one notable difference between the two specimens is that the maximum strain point is about 1 inch from the weld in the photoelastic data and is at the weld in the finite element model. A concentration of shearing strain is expected here since, along the edge, there is a transition from Poisson restraint of the insert plate to a free edge condition. The difference in the location of the concentration on the two plots is caused by thickness effects. In the actual specimen, the liner plate thickness prevents the maximum shearing strain from developing until several plate thicknesses from the weld transition. For the finite element model, the two dimensional analysis does not include thickness effects. A three-dimensional model should predict a maximum shear strain location in better agreement with the experimental observations. However, these calculations have not yet been performed.

It should be noted that the existence of this concentration is not typical of the 1:6 scale model response. In the RCC model, the continuous liner plate provides edge restraint everywhere. For comparison to the RCC model, only the central region of the specimen, far from the edges is considered valid. The central region of the specimen contains a band, about one third the specimen width where the strain level is independent of horizontal position. This area can be considered to be most like the RCC model without studs. However, the lack of edge restraint results in significantly higher free field strains even along the specimen centerline.

The weld transition specimens adequately address the issue of a weld and thickness transition induced strain concentration. From the data, the concentration, if any, must be quite small. These test results were also very useful when considered in conjunction with the full simulation specimens. This aspect of the weld transition data will be discussed later.

## Separately Controlled Loading Specimen Results

The primary purpose of the separately controlled loading specimen was to investigate the interaction between liner loading and anchored shear on the failure mechanisms of the liner and anchored systems. As mentioned before, the specimens consisted of a section of liner plate loaded such that unifo n uniaxial stress coulo be developed along a row of studs. Then a separate loading syste.. was used to vary the shear load to the studs. As explained before, posttest examination of the one-sixth scale model indicated that a combination of liner preload and stud shear may have led to the liner tear which was experienced when neither loading

and stud shear may have led to the liner tear which was experienced when neither loading mechanism alone was capable of producing such a tear.

A total of fifteen finite element simulations were conducted for the separately controlled loading specimen. Five different loading conditions were considered for each of the three anchorage load-displacement functions shown in Figure 10. Six specimens were tested in this series (only five had applied shear load). Table 1 shows the predicted failure mode of the specimen for each load case along with the response observed in the experiment. As expected, the predicted failure mode of the specimen depends on both the assumed strength of the stud and the applied preload. The observed failure modes are most consistent with a stud strength between 1450 lb and 1600 lb. For low values of prestress, the predicted failure mode was by fracture of the studs, while for high values of prestress the predicted mode of failure was by liner tearing. Table 2 provides a comparison of the measured and predicted failure loads for each set of loading conditions.

For specimens that failed by stud shear, the analytical and experimental stud load values correspond well (about 10% discrepancy). However, for the liner tearing mode of failure, there is a greater discrepancy. For liner tearing, the difference between analysis and experiment is about 400 lb/stud which corresponds to a difference in net section stress of about 3 ksi. This is a relatively narrow band when compared to the liner failure stress of 73 ksi. A larger discrepancy may therefore be expected for a liner tearing failure mode.

Photoelastic data recorded during the separately controlled loading tests provided images of the maximum shear strain field in the plane of the liner plate. Contour plots of analytical results and photoelastic results for the maximum shear strain are shown in Figure 15 for a separately controlled loading specimen with a liner prestress of 65 ksi. The photoelastic results show the strain state immediately before the specimen failed by liner tearing. The analytical results from the pretest simulation correspond to a slightly higher level of stud force than was present when the photoelastic measurements were recorded. In general, the agreement between the photoelastic results and the finite element results is good both quantitatively and qualitatively.

Several features of the response are apparent in both the analytical and experimental results. The change in free-field strain from below the stud line to above it is dramatic and very similar, graphically showing the influence, in terms of strain, of the relatively small (~10%) increase in stress produced by the stud shear load. The highly strained regions exist outward of the outer studs due to the Poisson contraction of the liner and the restraint of the concrete. The overall shape and magnitude of the strain profiles around the stud region is very similar.

There is, however, a large discrepancy between the peak value of the maximum strain at the edge of the outer stud anchors. The analytical results show a maximum shear strain of 30% in one of the four elements connected to the outer stud anchors, while the largest shear strain seen in the photoelastic data is approximately 15%. There are a number of possible explanations for this discrepancy. At best, the strain in this element represents the strain averaged through the thickness of the liner at this point. Bending of the liner could significantly reduce the surface strains below the average value. Another possible explanation is that the strains in the element next to the stud anchor are simply a poor indicator of the average strains in the liner at this location.

By observing the photoelastic data from other separately controlled loading specimens, the combined effect of liner preload and stud shear can be compared to the individual effects. Figure 16 shows the photoelastic data from the specimens where liner load only and stud load only were applied. In both cases the figure represents the strain state immediately before failure of the specimen. Notice that, for the liner load, the strain concentration caused by the studs is not very apparent. This means that the Poisson contribution of the studs is not

significant without additional stud shear. Further, a preferential tear near a stud row, as was experienced in the 1:6 scale model, would not be expected here. The plot of the specimen with stud load only shows some concentration at the four stud locations. However, the absolute strain and strain concentration levels show that stud shear alone cannot significantly damage the liner. The difference between Figures 15 and 16 is dramatic. It shows conclusively that the combination of liner and stud load has a profound effect on the strain state and failure mode of the liner/anchorage system.

The overall load-deflection data of the separately controlled loading specimens, shows a consistent behavior in terms of the net section stress. Figure 17 shows the overall net section stress versus deflection response of the separately controlled loading specimens. Net section stress is the total load, liner plus stud, divided by the liner cross-sectional area. Deflection is the overall elongation of the specimen. The specimens show very similar behavior in terms of the stress at yield and the ultimate strength. The three specimens for which liner tearing is the mode of failure tend to have overall specimen displacement at failure which is approximately equal within 10%. On the other hand, the two specimens which exhibited stud shear failure, have an overall displacement which is significantly less and is a function of liner preload. It should be expected that the specimens which exhibited liner failure showed somewhat similar overall displacements since this represents the overall strain in the liner up to failure. The two specimens exhibiting stud failure did not reach the ultimate liner strain since liner failure did not occur. Therefore, it should be expected that the overall specimen displacement should be somewhat less than those specimens for which liner failure occurred.
From the results of the separately controlled loading specimens an important conclusion can be drawn. Very small changes in parameters of the liner and anchorage system can have a great effect on the failure mode of the system. As is shown here, an increase in initial preloading of only three percent was sufficient to produce a transition from a stud shearing failure to a full liner tear. From the concept of net section stress compared to ultimate strength of the material, it can be theorized that similarly small changes in material ultimate strength and stud shearing strength could also alter the failure mode. It was discussed earlier that posttest examination of the 1:6 scale model points to a liner failure mode where a combination of liner preload and stud shearing load generated by differential strains led to the liner tear. The results of these separately controlled loading tests strongly support this as a potential mechanism for producing failure. Further, these tests point to the fact that relatively small changes in liner and anchorage geometry and material properties could change the failure mode of the entire containment model.

## Full Simulation Specimen Results

The full simulation specimens provided a method by which a full scale simulated mock-up of a section of the wall of the 1:6 scale reinforced concrete model could be tested in the laboratory. The tests for this specimen consisted of continuously increasing the specimen elongation. As discussed before, the stud shear load was developed by differential strain between the reinforcing steel and the liner and insert plates. Internally, the response of the specimen was expected to be very similar to the schematic cross-sectional drawing of the 1:6 scale model in Figure 4. Of the four specimens tested, extensive data is available for three of them. For the fourth specimen, where external pressure was also applied, only very limited data is available. In all four cases, these specimens failed by liner tearing where the tear was adjacent to a row of studs nearest the insert plate. This failure mode matches the failure observed in the 1:6 scale RCC. Further, posttest examination of the specimens revealed stud bending very similar in direction and magnitude to that shown in the schematic of the postulated failure mode presented in Figure 4.

Important events from the finite element analysis of the full simulation specimen are marked in the load-elongation curve shown in Figure 17. The first two events in the numerical simulation

take place at an overall elongation of approximately 1.2%. At this elongation, the first row of studs on the thicker insert plate (Row 2 in Figure 17) fail. The computed stress and strain state combined with Manjoine's failure criterion indicate that the liner plate would also begin to tear at 1.2% elongation. Liner tearing would initiate next to the studs located closest to the weld (Row 1 in Figure 17). In the numerical simulation, the liner material was assumed to carry load beyond the point at which the tearing criterion was satisfied. Results from the numerical simulation at higher elongations indicate that several more rows of studs would fail before 2% elongation.

The overall force-elongation curves for the four full simulation specimens are compared to the finite element results in Figure 19. The dashed curve appearing in Figure 19 represents the calculated response when the anchorage is assumed to have no stiffness. The solid line represents the analysis with anchorage stiffness. The results from the analysis with anchorage match the experimental results very well up to the predicted failure point of 1.2% elongation. In addition, the results from the anchorage analysis lie closer to the data than do the results from without anchorage. This suggests that the anchorage transfers load between the liner and reinforcement as has been assumed in the analysis. The elongations required to fail the specimens fell between 3% and 4.5%, considerably more than the 1.2% elongation at failure predicted by the analysis. Also contrary to the analytical predictions, no stud failures were observed in any of the full simulation specimens.

The photoelastic data from the full simulation experiments provides a valuable source of information for understanding where the finite element results differ from reality. Figure 20 contains a contour plot of the maximum shear strain in the liner plate as calculated from the finite element simulation at an overall elongation of 1.5%. The location of the studs are clearly marked by high strain levels in the liner plate. Strain levels on average are much higher between the weld line and the first row of studs on the thinner liner plate. This is to be expected since load is transferred out of the liner plate and into the reinforcement with each subsequent row of studs on the thinner liner plate. The figure also contains a contour plot of the maximum shear strain as determined from the photoelastic technique at an overall elongation of 1.5%. The trends are quite different from those seen in the finite element results. Here, the strains on average tend to be lower near the weld transition than they are toward the center of the specimen. This suggests that the stud anchors near the weld line transmit far less load in the actual experiment as compared to the finite element simulation.

Referring back to Figure 14, the strain field of the weld transition specimen, the similarity between the experimental strain fields in Figures 14 and 20 indicates that the stud anchors are less effective in transferring load than was initially assumed. This seems to contradict the previous observations made with regard to the analytical and experimental load-elongation relationships.

One of the basic assumptions implicit in the analysis is that neither bending of the liner plate nor bending of the stud anchors are important in controlling failure of the liner or stud. This assumption has been made primarily for the purpose of simplifying the analytical problem. Strain measurements from the full simulation specimens and post-test inspections of the specimens suggest that bending may be an important mechanism controlling the failure mode of the liner and anchorage system.

To capture the effects of liner and stud bending requires a three-dimensional finite element analysis. Such a three-dimensional finite element analyses of the separately controlled loading specimen was run and showed that bending of the stud anchor and liner plate are strongly controlled by the response of the surrounding concrete. In the full simulation experiments, the concrete adjacent to the studs was severely fractured as the specimen was stretched to high strains. Modeling the mechanical response of such a complex material behavior presents an

enormous challenge. As a result, it is unlikely that more complex finite element models which include the effect of stud and liner bending will be more successful in predicting the failure mode of the liner or anchorage.

## CONCLUSIONS

The purpose of the Separate Effects Test program was specifically to investigate the contributing factors in the failure of the 1:6 scale reinforced concrete containment model and, more generally, to increase understanding of the response of liner and anchorage systems to severe accident loads. The tests have only recently been completed, and analysis of the data gathered is not yet complete. However, to a large extent, the goals of the program have been accomplished.

The combined effect of liner plate stress and anchorage shear has been demonstrated to have dramatic impact on the mode of liner failure. Finite element modelling of the effect of a known stud load on the liner response has been shown to compare very favorably with experimental data. The overall mechanism of stud shear has been shown to be a very likely contributor to the liner failure of the 1:6 scale RCC. The full simulation specimens exhibited a failure mode virtually identical to that seen in the 1:6 scale model. Finally, the experimental program has shown that separate effects testing is a viable technique for investigating the response of containment liner and anchorage systems.

However, in some areas, large discrepancies exist between experimental data and analytical results. The most obvious of these is in the full simulation specimens where the large load transfer predicted for the studs apparently did not take place.

## Acknowledgements

This work was supported by the U.S. Nuclear Regulatory Commission and performed at Sandia National Laboratories, which is operated by the U.S. Department of Energy under contract number DE-AC04-76DP00789.

## References

1. J. R. Weatherby, "Posttest Analysis of a 1:6-Scale Reinforced Concrete Reactor Containment Building," NUREG/CR-5476, SAND89-2603, Sandia National Laboratories, Albuquerque, NM, February 1990.

2. D. S. Horschel, "Design, Construction, and Instrumentation of a 1/6-Scale Reinforced Concrete Containment Building," NUREG/CR-5083, SAND88-0030, Sandia National Laboratories, Albuquerque, NM, August 1988.

3. M. [illegible], "Creep Rupture Behavior of Weldments," Welding Journal, Vol. 61, N0. 2, February [illegible] 50.

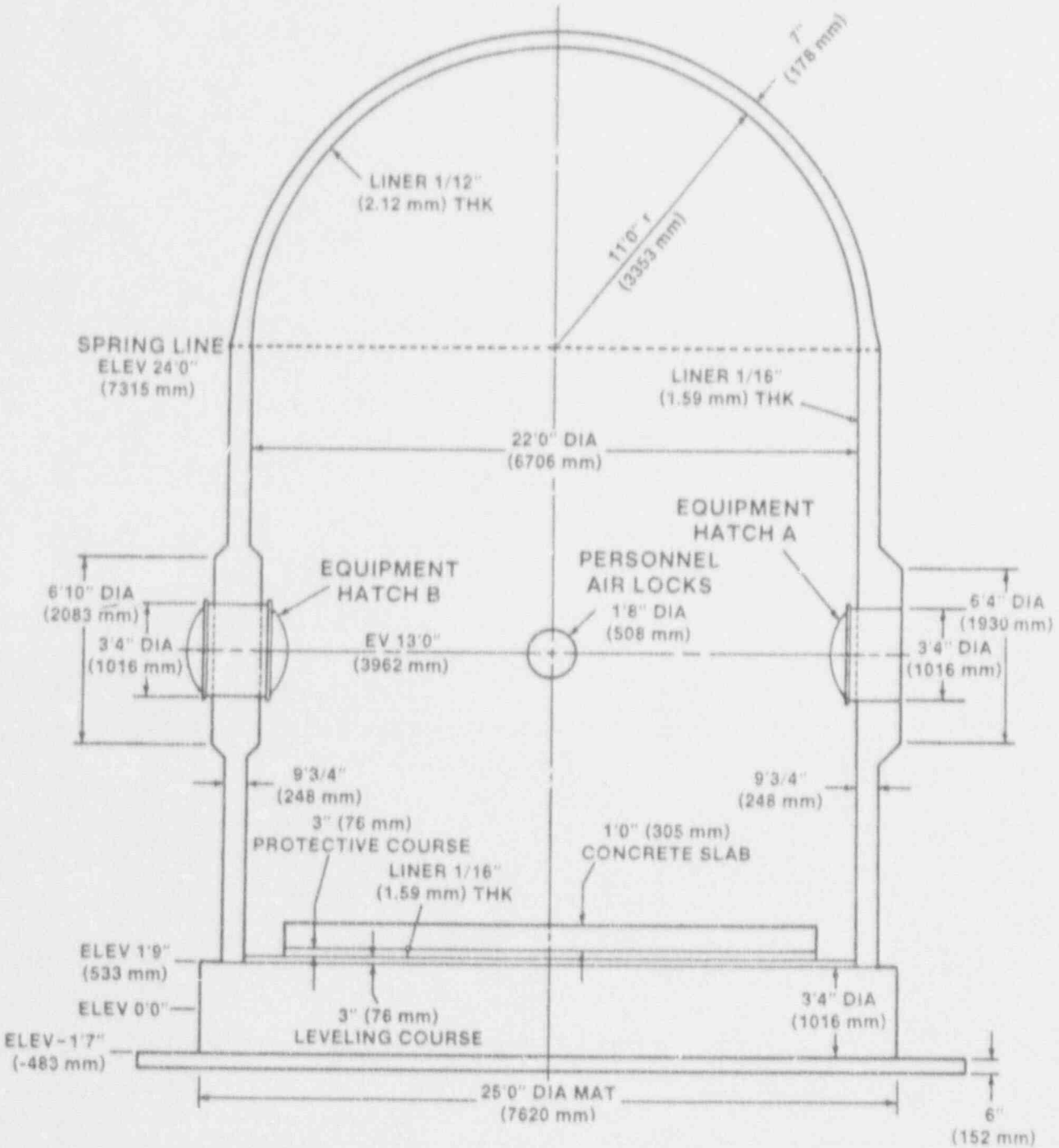


Figure 1: Cross Section of 1:6 Scale Reinforced Concrete Containment

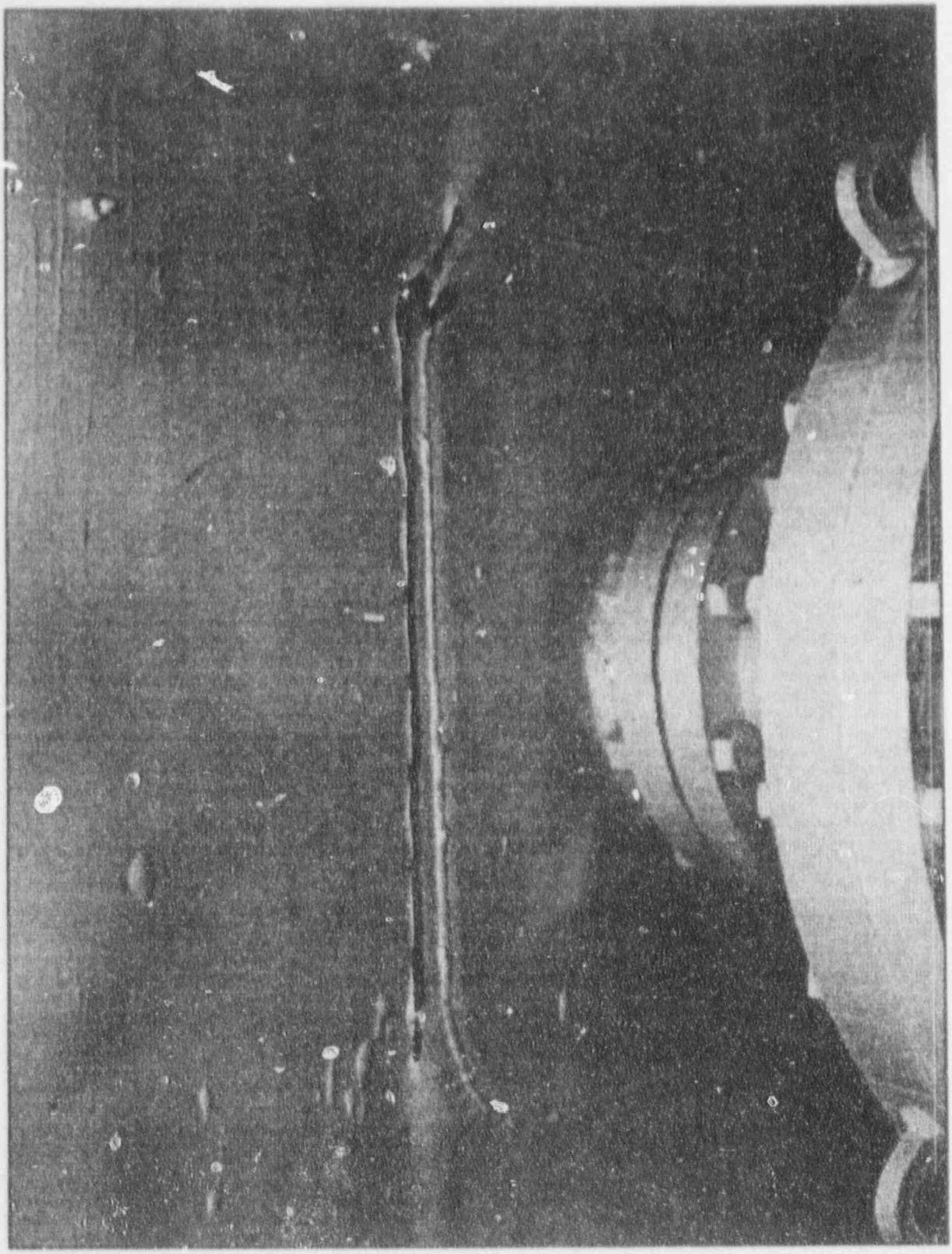

Figure 2: Liner Tear in 1:6 Scale Reinforced Concrete Containment

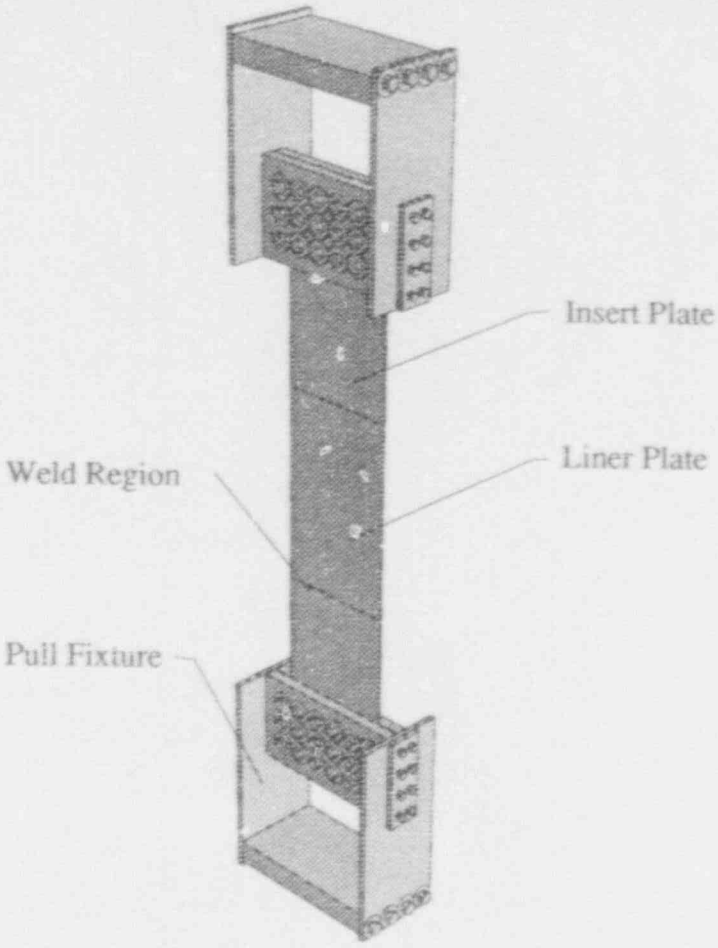


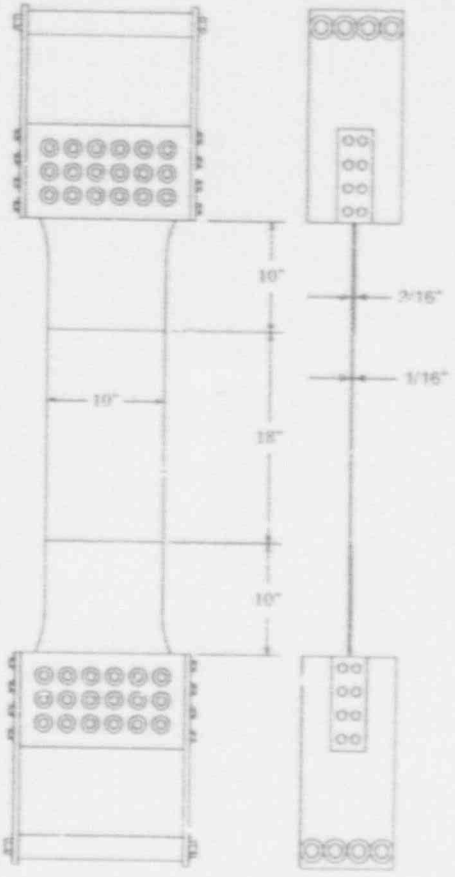


Figure 5: Weld Transition Specimen

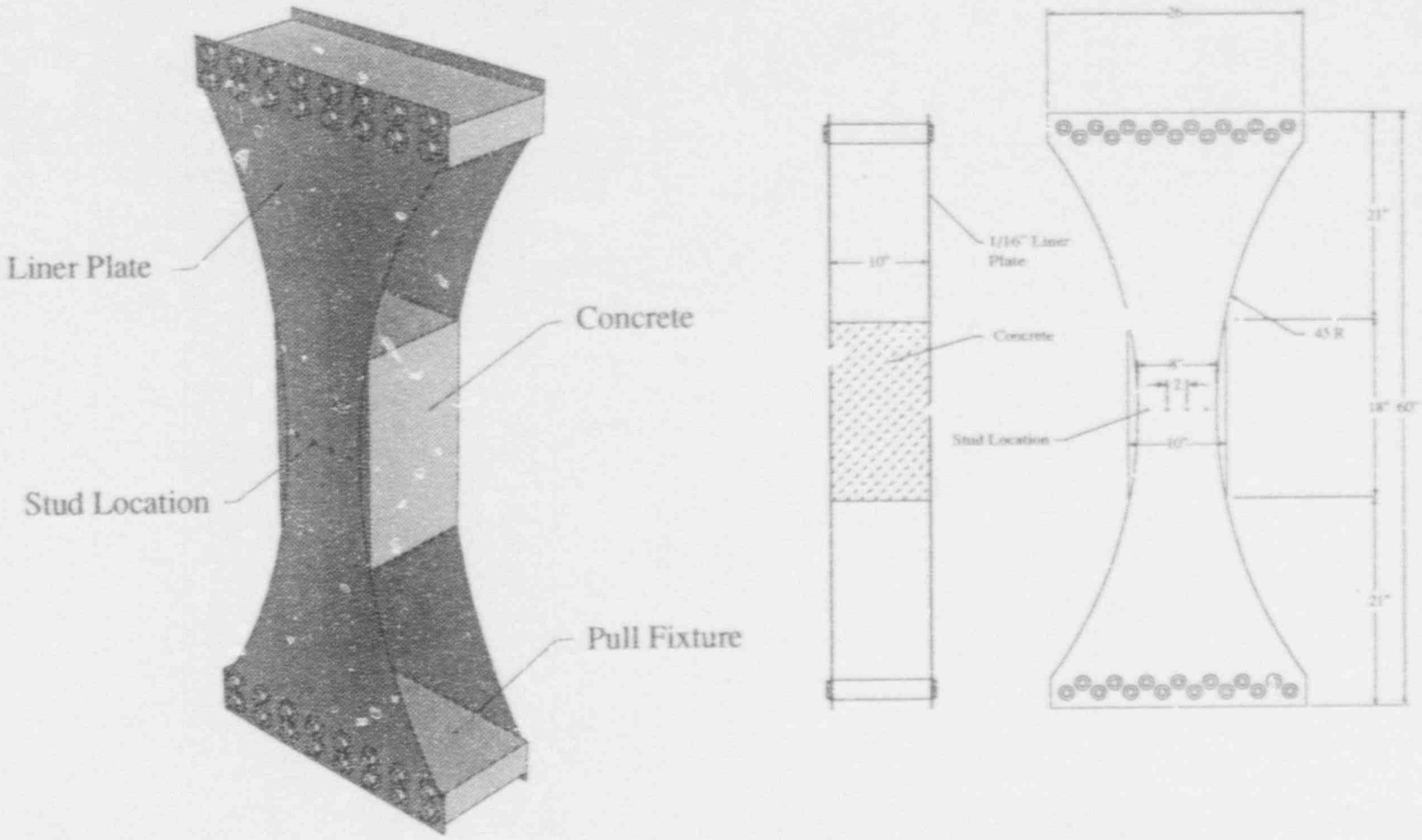


Figure 6: Separately Controlled Loading Specimen

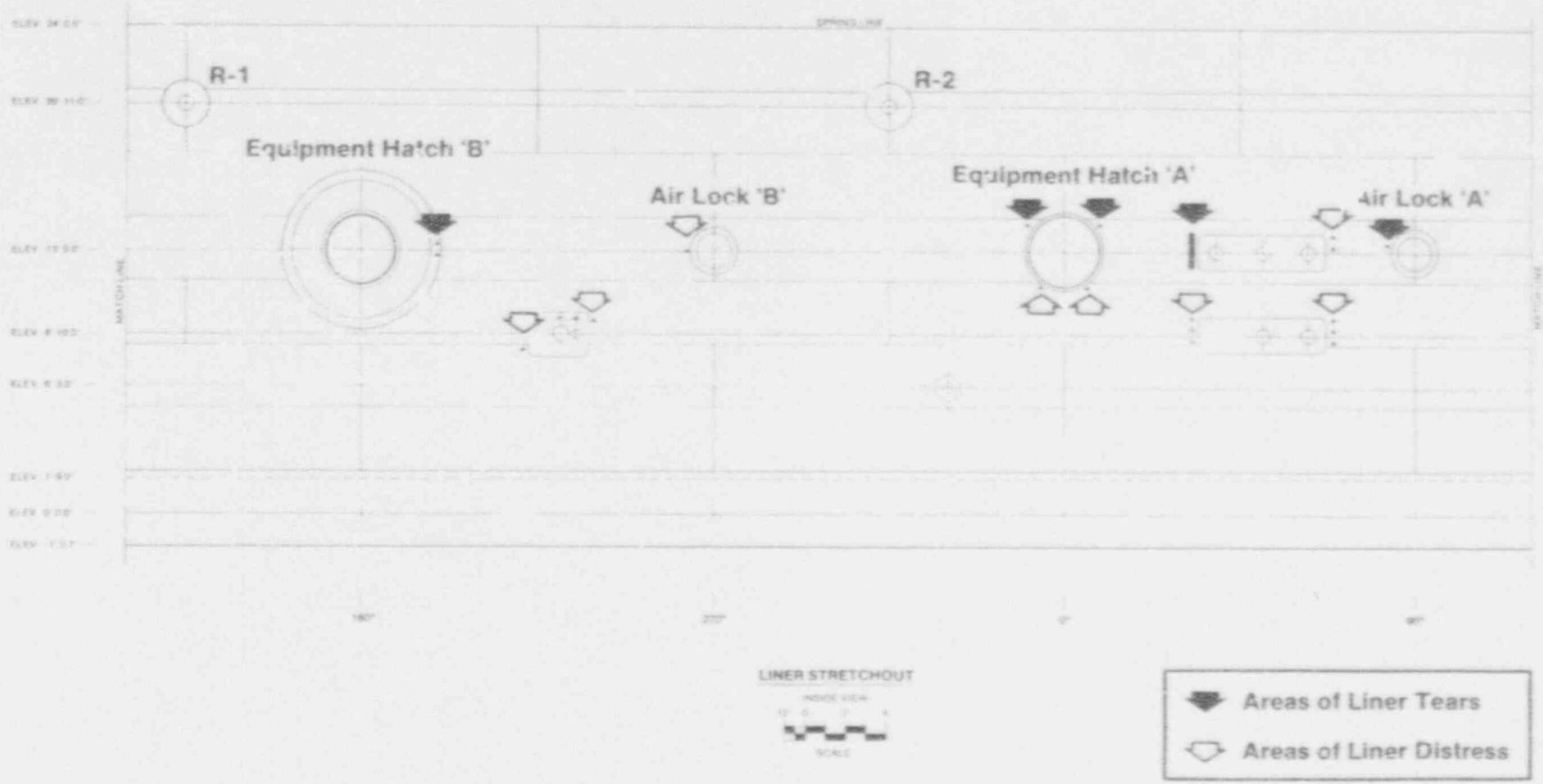


Figure 3: Stretchout of 1:6 Scale Reinforced Concrete Containment Showing Liner Tears

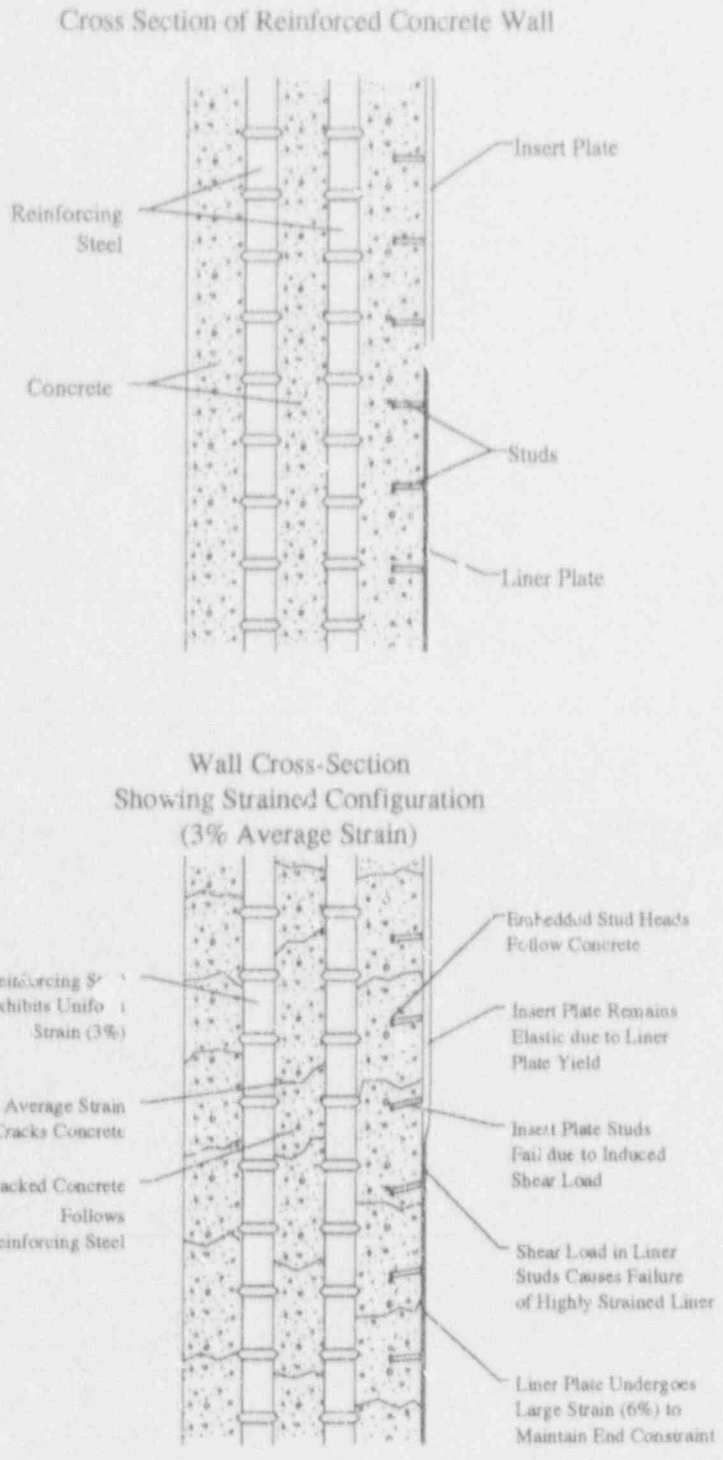


Figure 4: Postulated 1:6 Scale Model Failure Mechanism

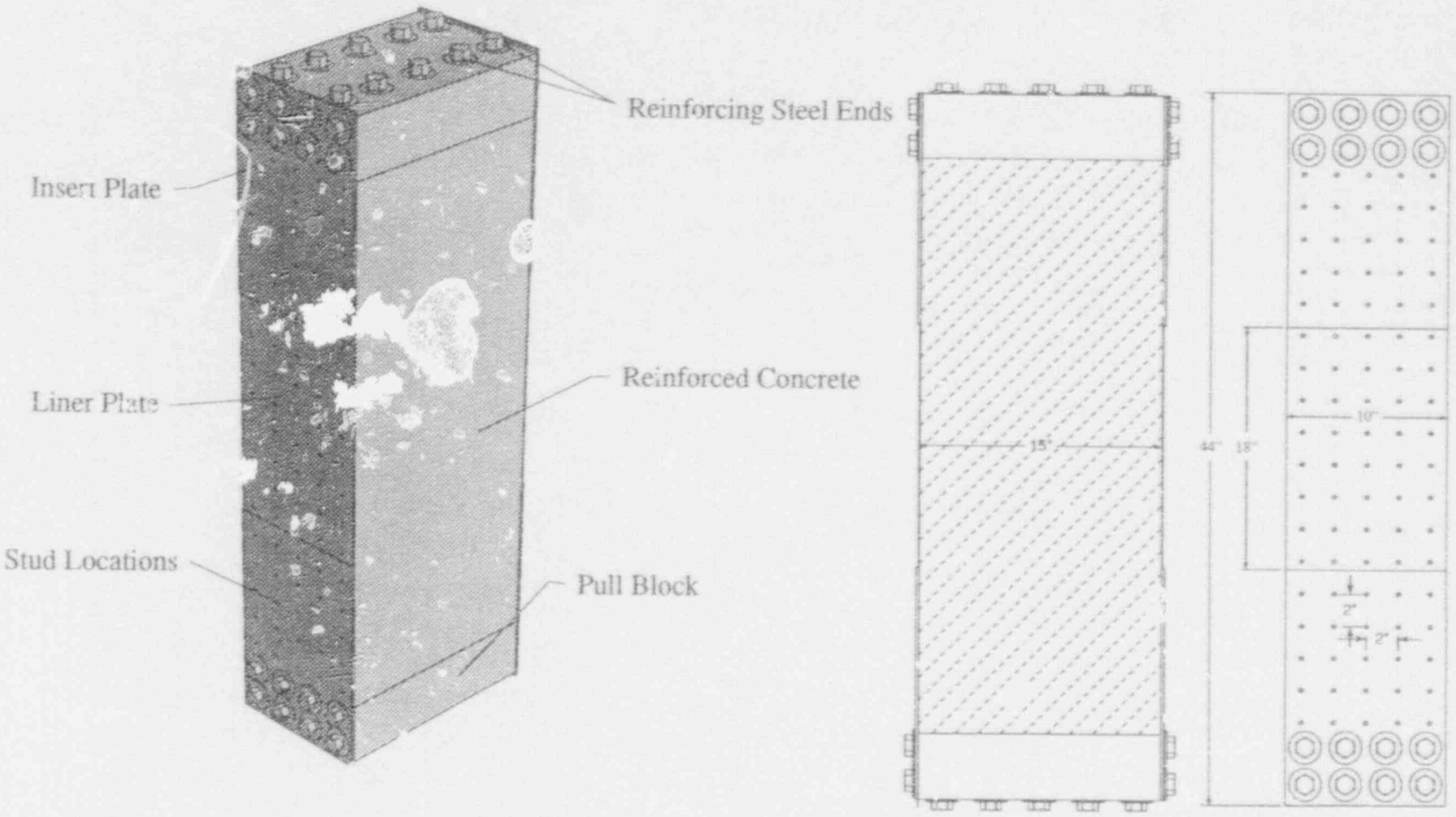


Figure 7: Full Simulation Specimen

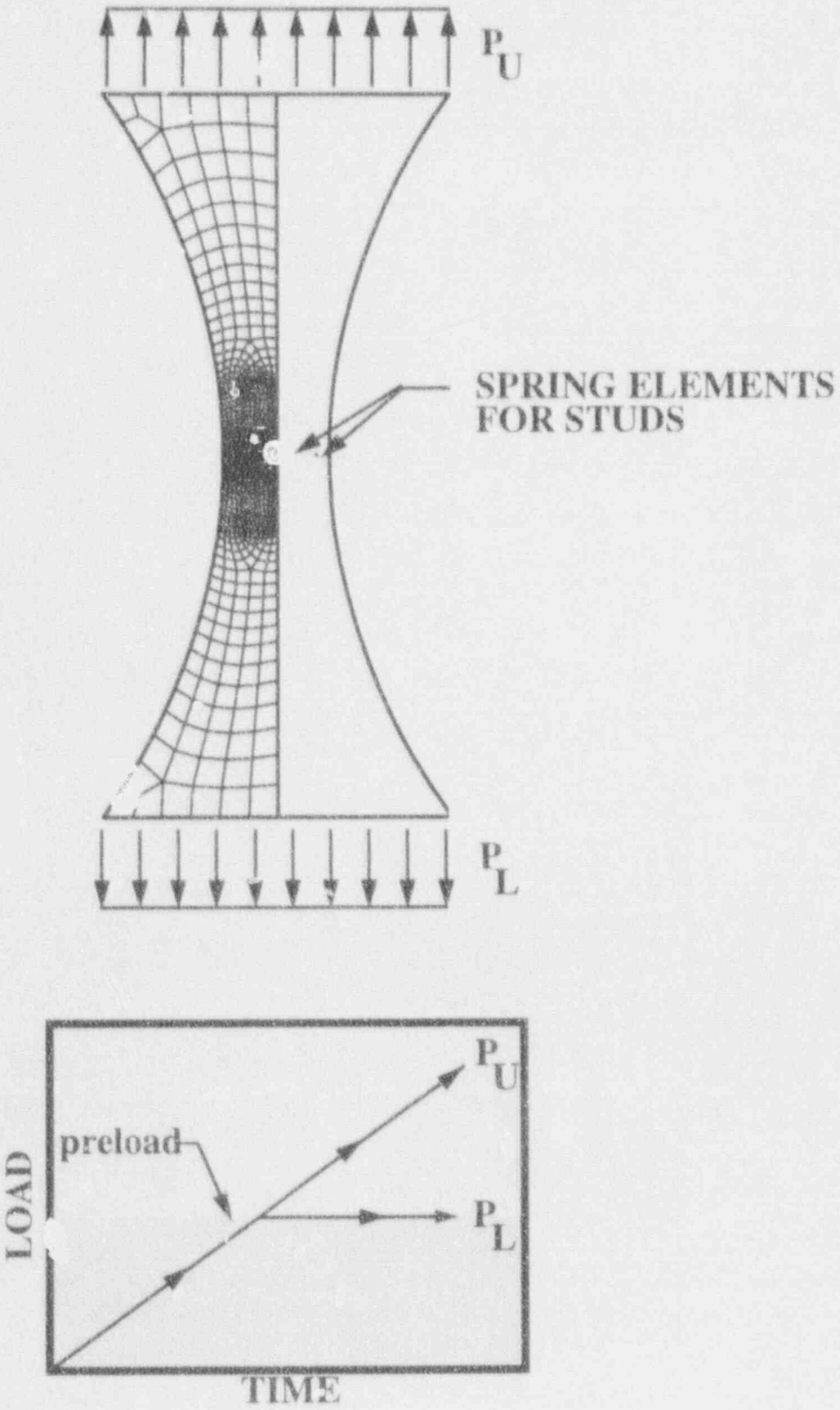


Figure 8: Finite element model and loading of the separately controlled loading specimen.

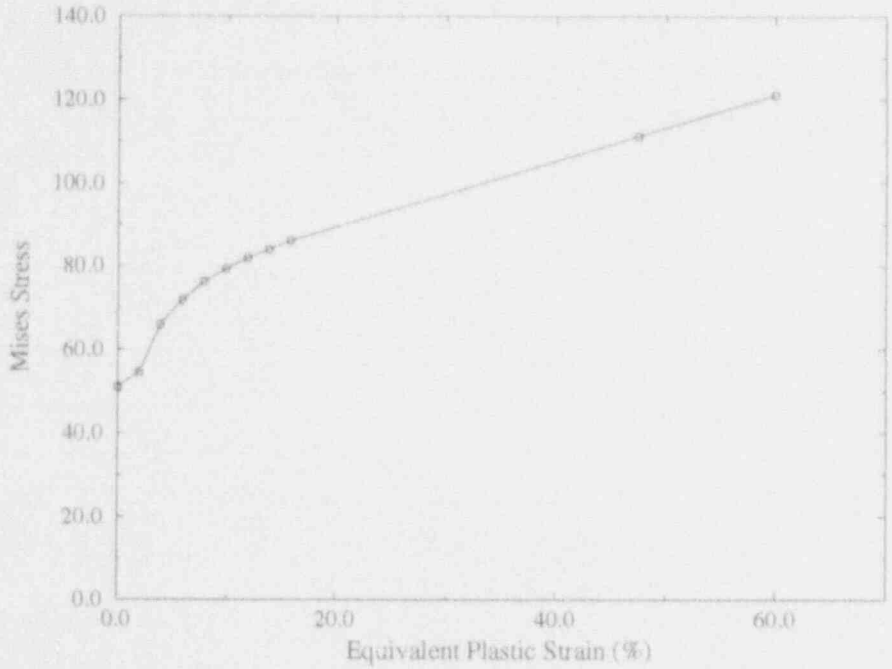


Figure 9: Relationship between the Mises stress and the equivalent plastic strain for the liner in the separately controlled loading specimens.

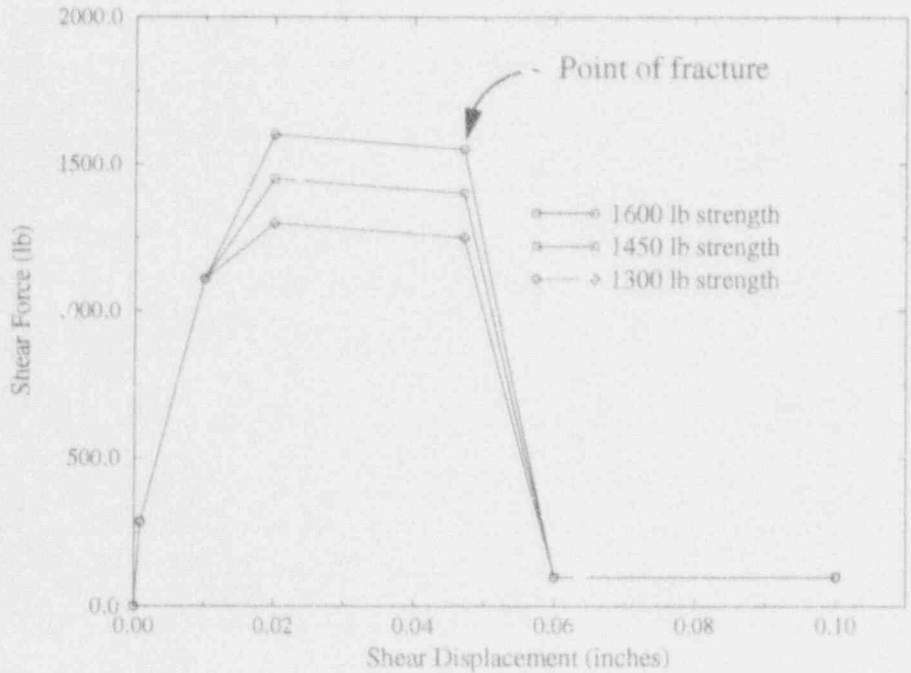


Figure 10: Three functions defining the relationship between shear force and shear displacement for the stud anchors.

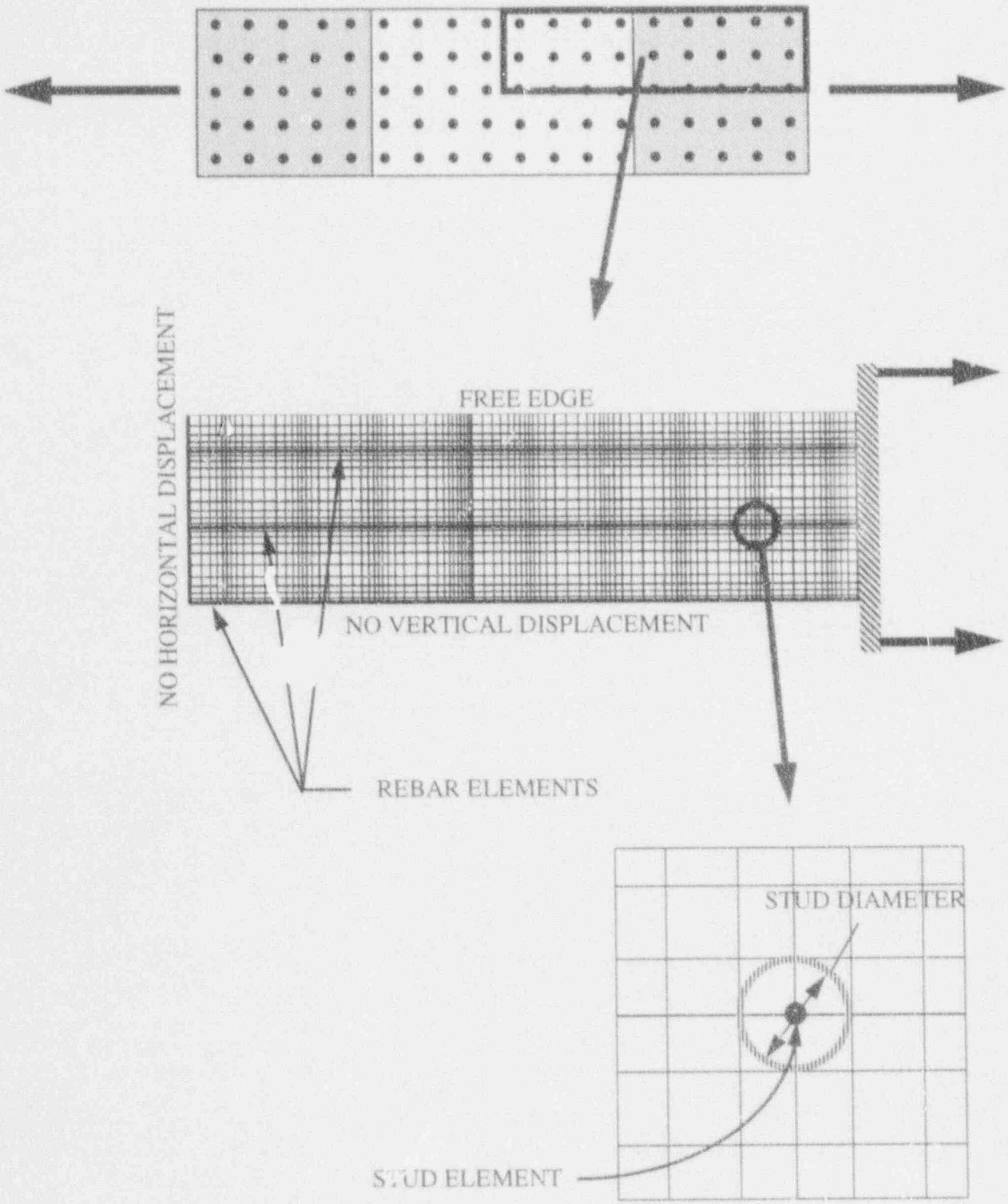


Figure 11: Finite element model and boundary conditions for the full simulation specimen.

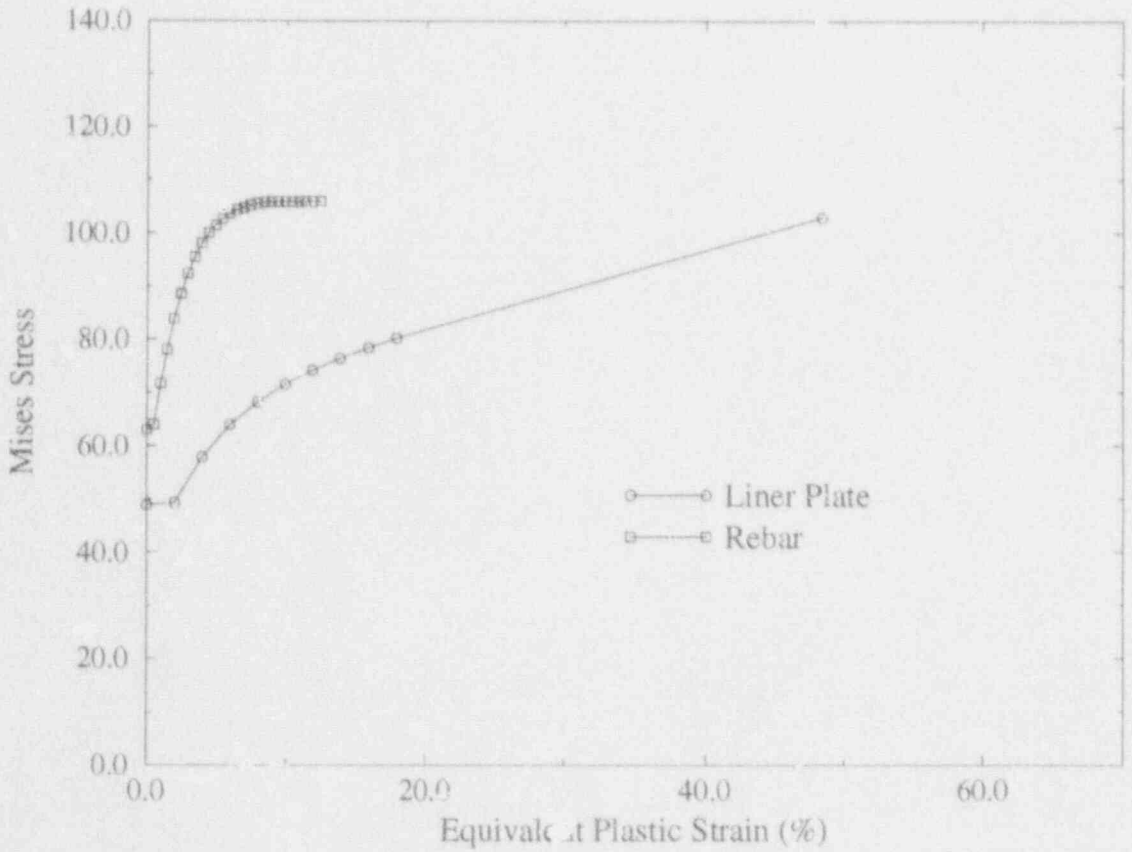


Figure 12: Relationship between the Mises stress and the equivalent plastic strain for the liner plate and rebar in the full simulation specimen.

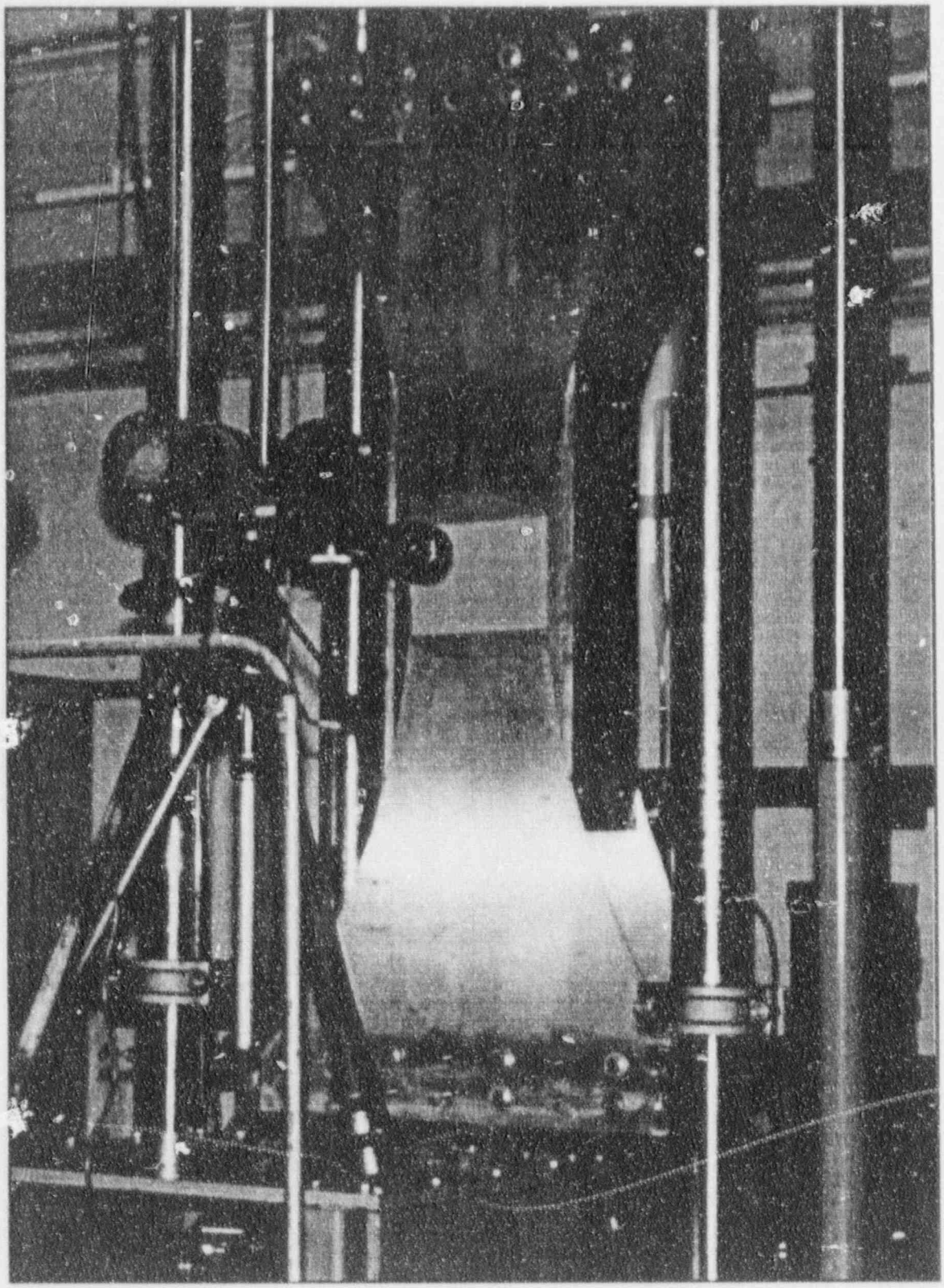

Figure 13: Typical Experimental Setup

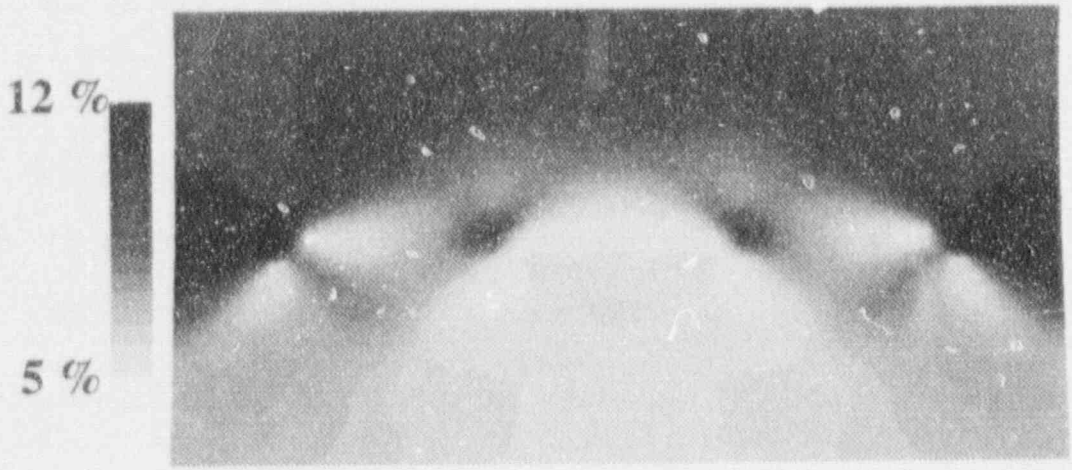


Finite Element Results With Stud Force = 850 lb/stud

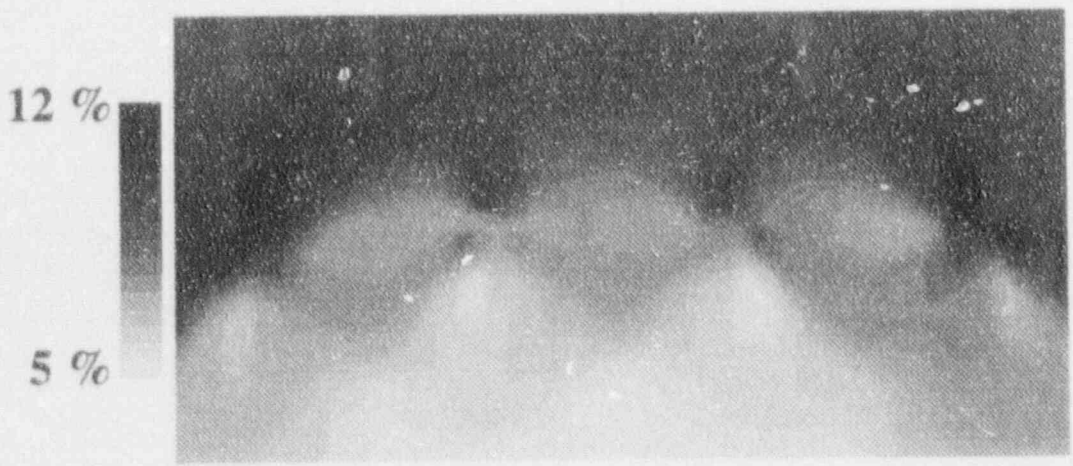


Experimental Results With Stud Force = 780 lb/stud

Figure 15: Maximum In-Plane Shear Strain in a Separately Controlled Loading Specimen With a Prestress of 65 ksi.

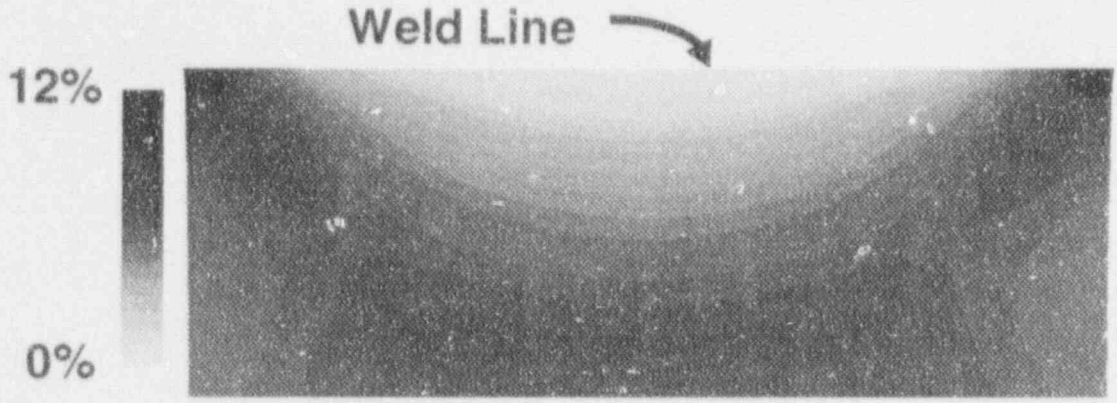


Finite Element Results

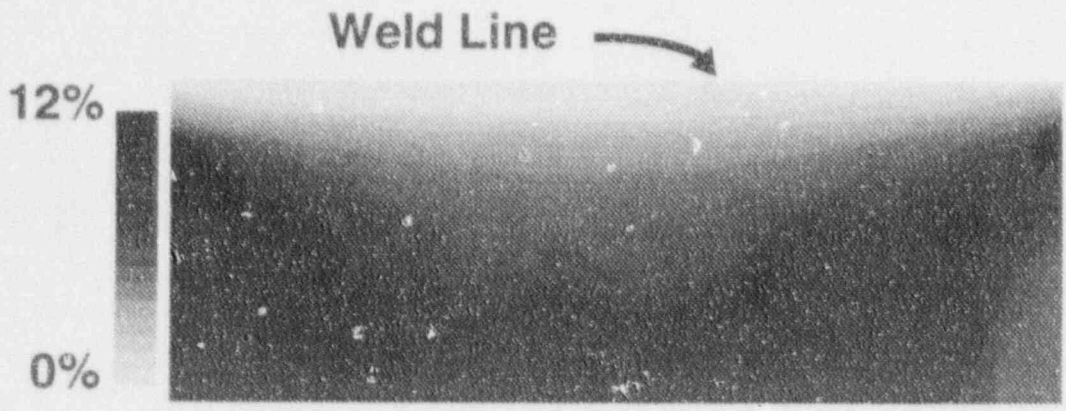


Experimental Results

Figure 14: Maximum In-Plane Shear Strain in a Weld Transition Specimen at an Overall Elongation of 1.5%.

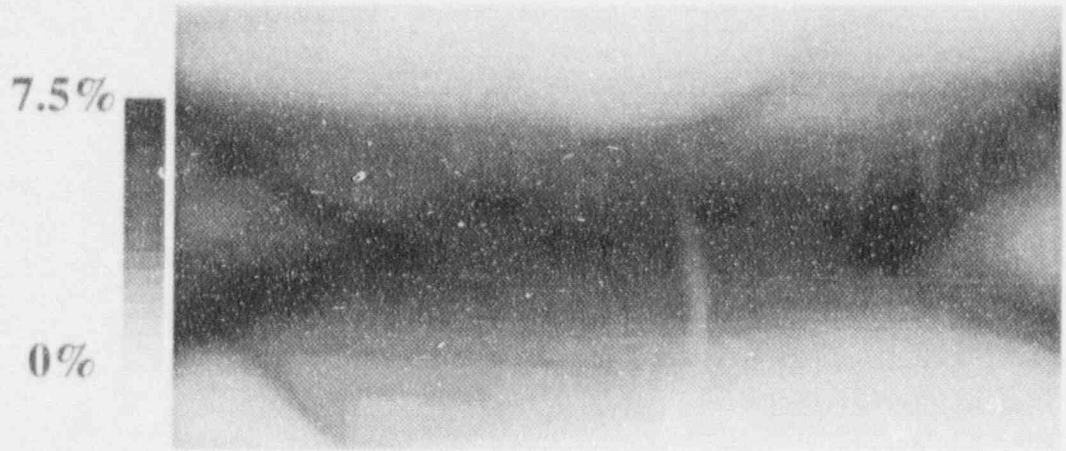


Liner Load Only


Stud Load Only

Figure 16: Photoelastic Data for Stud Load and Liner Load Separately.

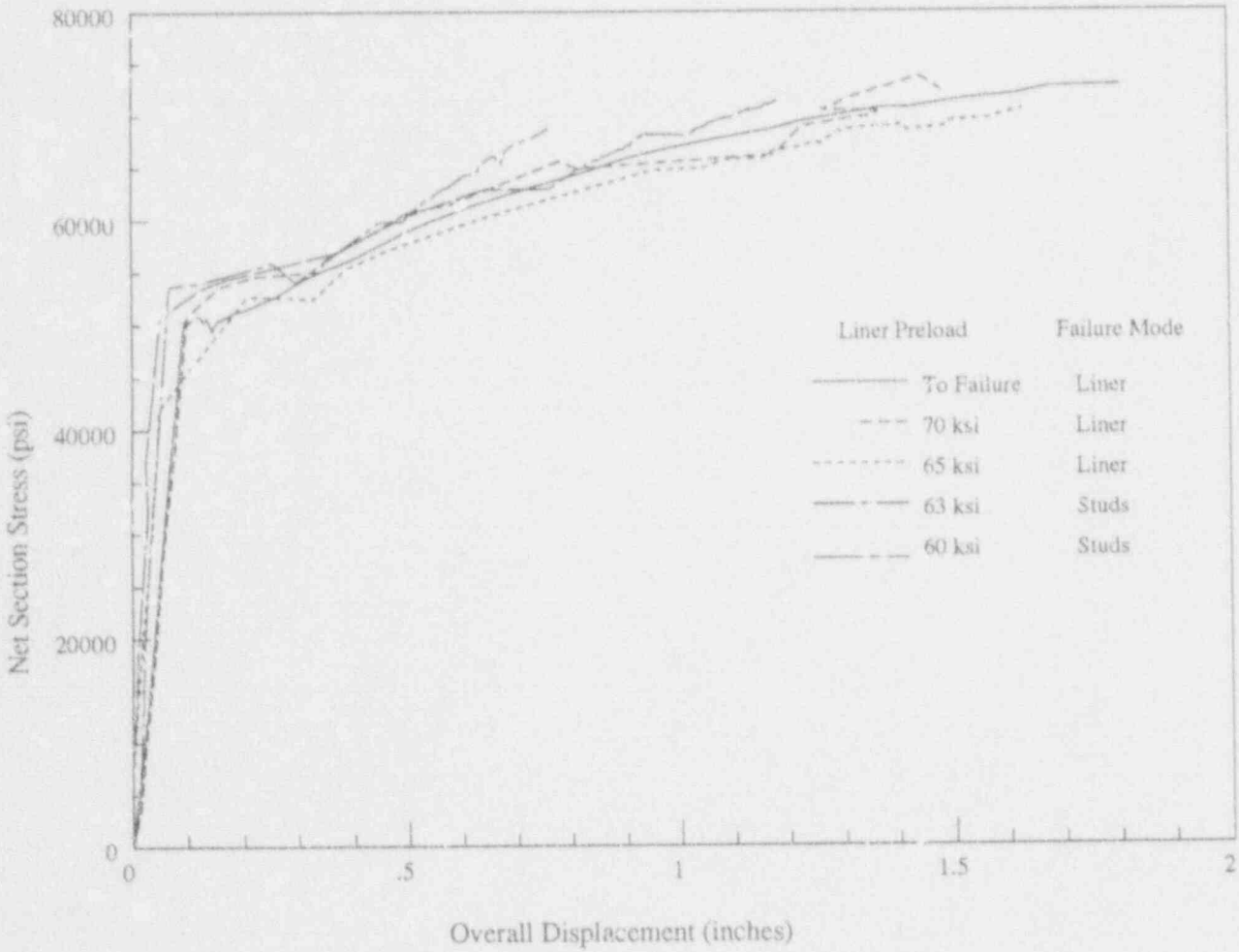


Figure 17: Overall Response of Separately Controlled Loading Specimens

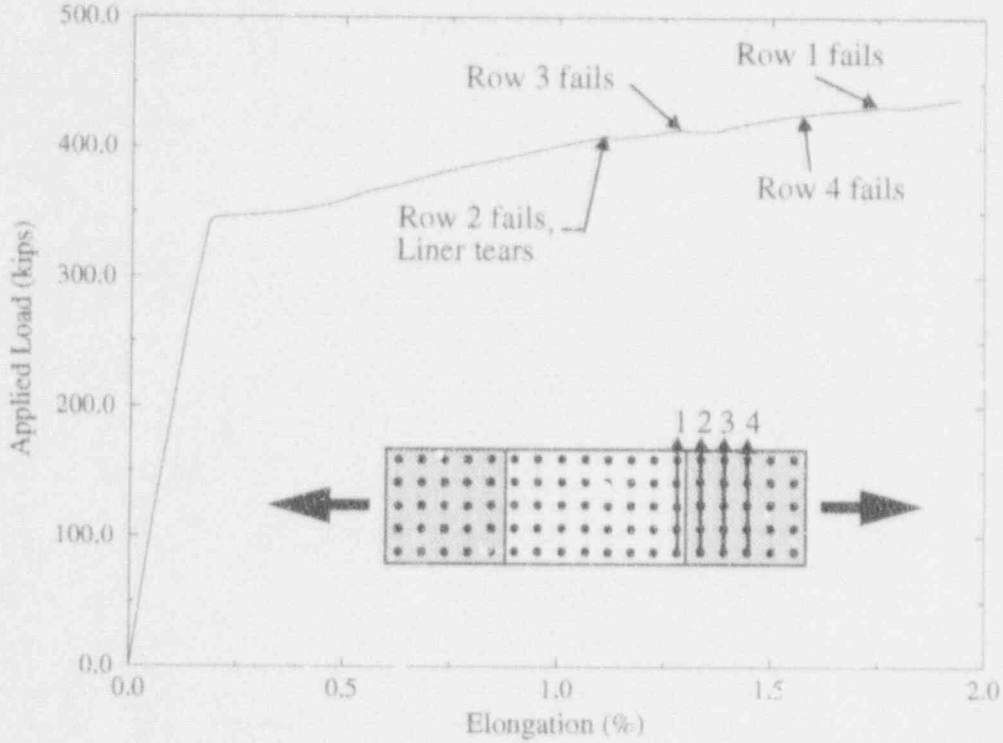


Figure 18: Overall force-elongation curve from the finite element analysis of the full simulation specimen. The predicted sequence of failure events is shown.

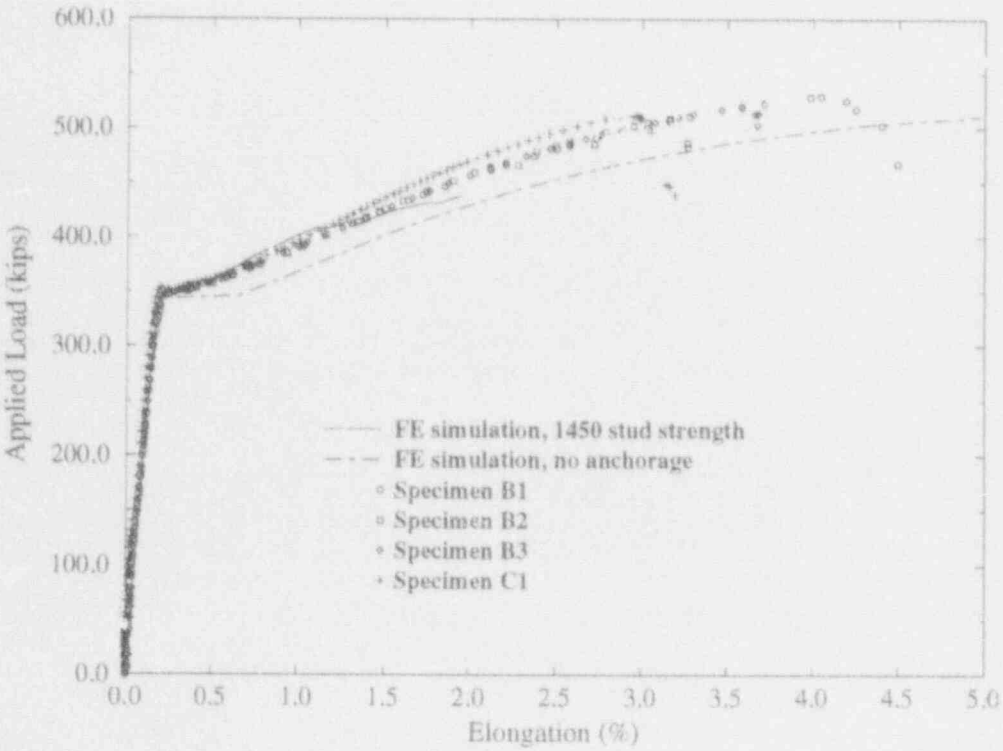


Figure 19: Comparison of experimental and analytical results for the force-elongation relationship in the tests of the full simulation specimens.

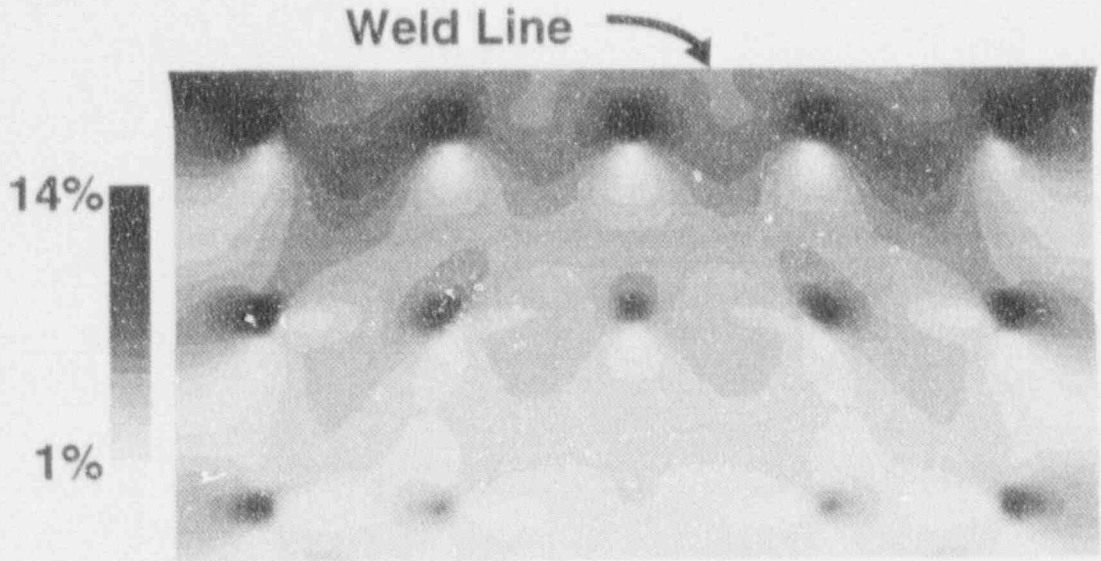


Finite Element Results

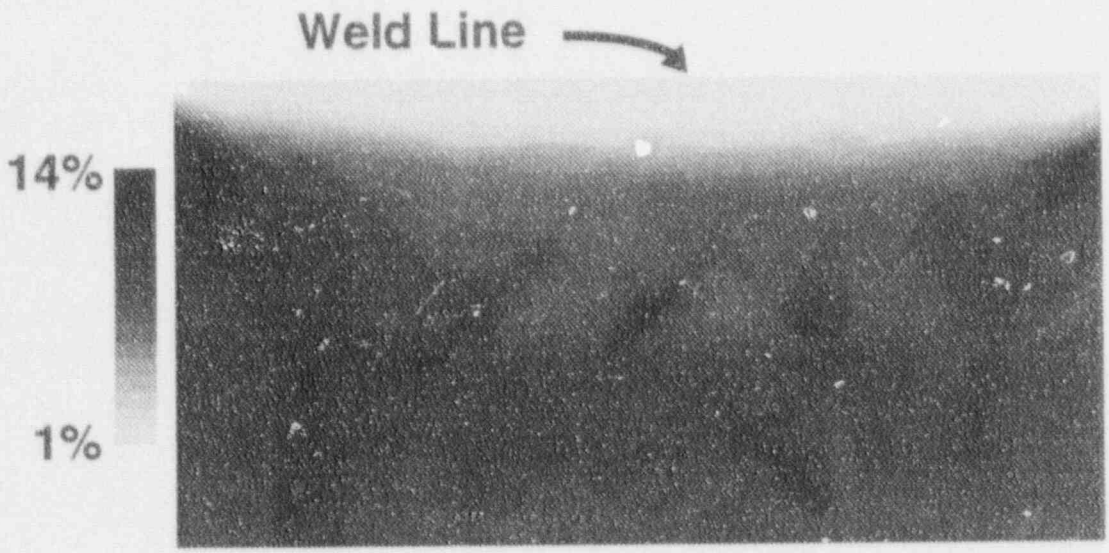


Experimental Results

Figure 20: Maximum In-Plane Shear Strain in a Full Simulation Specimen at an Overall Elongation of 1.5%.

| | Assumed Stud Strength (lbs) | Liner Preload (ksi) None | 60 | 63 | 65 | 70 |
|---|---|---|---|---|---|---|
| Predicted Failure | 1300 | Stud | Stud | -- | Stud | Stud |
| | 1450 | Stud | Stud | -- | Stud | Liner |
| | 1600 | Stud | Stud | -- | Liner | Liner |
| Observed Failure | --- | Stud | Stud | Stud | Liner | Liner |

Table 1: Predicted and Observed Failure Modes
for Separately Controlled Loading Specimens

| Prestress (ksi) | Measured (lb/stud) | Predicted * (lb/stud) | Net Stress (lb/stud) |
|---|---|---|---|
| 50 | --- | 1392 | N/A |
| 60 | 1208 | 1313 | N/A |
| 63 | 1171 | --- | 1250 |
| 65 | 780 | 1173 | 1000 |
| 70 | 510 | 107 | 375 |

Table 2: Measured, Predicted, and Net Section Stress Failure Loads
for Separately Controlled Loading Specimens

# NUMERICAL SIMULATION OF THE ULTIMATE LOAD CAPACITY OF A REACTOR CONTAINMENT BUILDING

Valter Andreoli
Paolo Angeloni
Paolo Contri
Ismes - Bergamo (Italy)

Luigi Brusa
ENEL/DSR/VDN Roma (Italy)

Abstract

From the 1980's onwards specific requirements of standard guidelines related to failure analysis have made necessary an extensive application of non linear numerical models for containment safety assessment. On the same period new structure types have been proposed which reveal high sensitivities to loadcases reproducing accident conditions. The paper present the results of preliminary non linear calculations on simplified models. The results point out how using different load incrementing schemes significantly different failure mechanisms and limit load factors can be calculated. This fact stresses the need for seeking for a general agreement on simulation criteria to be used in safety evaluations in order to obtain fully understandable and comparable results.

## CHARACHTERISTICS OF NEW CONTAINMENT DESIGN

To follow the new international developments in the field of innovative nuclear reactors, the Italian National Power Board (ENEL) is currently running several studies and research activities. The topics of interest concern the adapting of the design of a new generation of power plants for the construction in Italy.

Italian targets, and more in general European and American codes, are looking for very strict requirements in terms of maximum release of radioactivity. Some of the new safety concepts have suggested different plants arrangements and large changes to traditional structure layouts of nuclear containments, like in GE-APWR, GE-SBWR or ABB-PIUS. Instead of a simple layout composed of basemat, cylindrical wall and dome, the reactor vessel is inserted in a stiffened structure where a cylindrical body is surrounded by rooms containing pools and devices typical of new safety technology. The global stiffness of the structure is the sum of complicated contributions from a lot of members, and the response under accident loadings requires advanced numerical analyses.

In fig.1 a typical r.c. containment extensively used in the past is compared with a preliminary version of a SBWR containment, as proposed by GE in 1991. This latter structure has been used a reference configuration for above mentioned preliminary computations and is extensively referenced in the paper. The non linear effects, directly affecting the limit state evaluation of this type of structures, have shown to be highly influenced by accident scenarios. In particular, load distribution and sequence play an important role on failure mechanism and limit load because of the presence of strong stiffness redistributions and path dependencies.

Furthermore, past design experience, both numerical and experimental [1], has supported general conclusions on the dominant role in failure analyses of

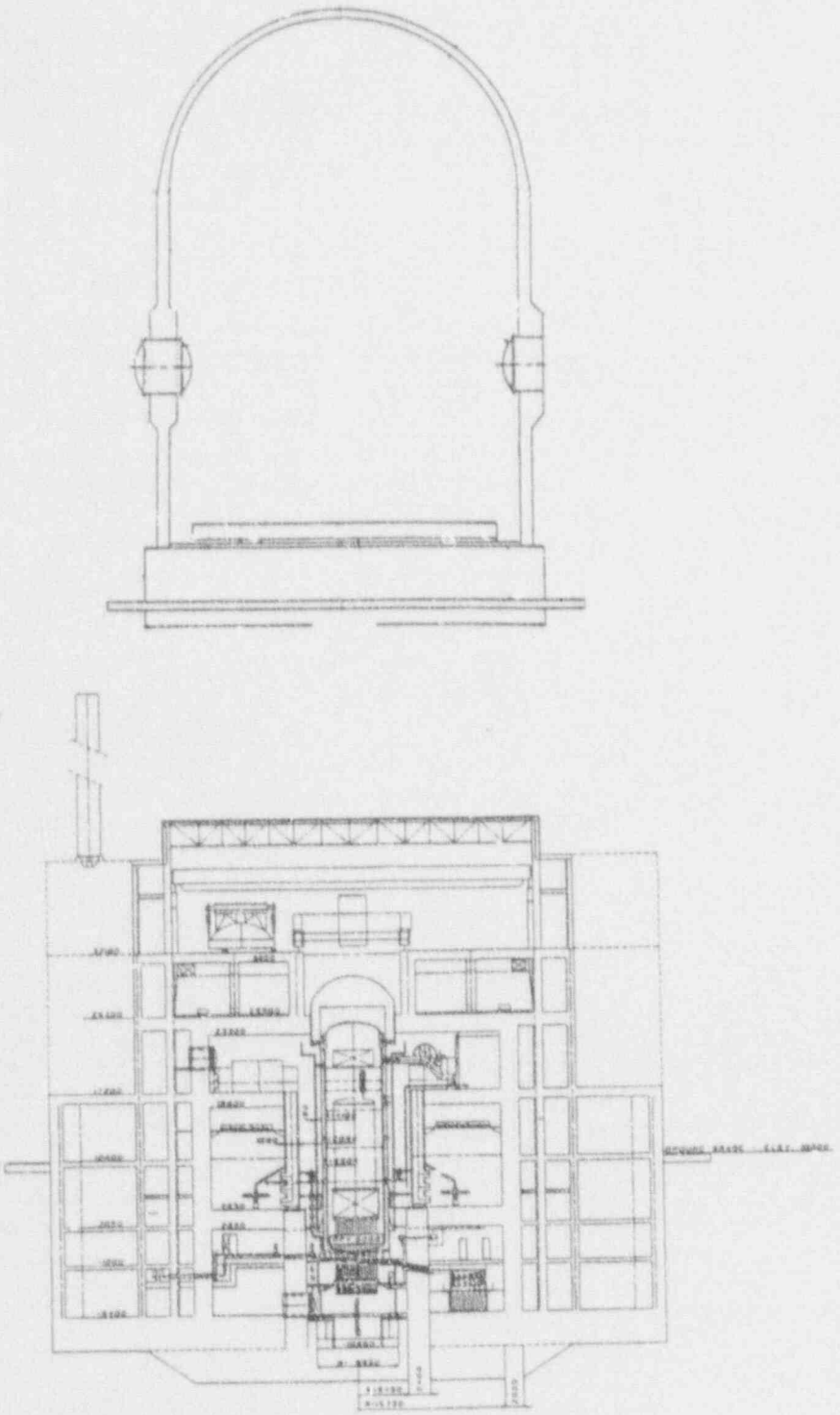

Figure 1. Different Containment Layouts in Traditional and SBWR Projects [1]

pressure internal loads, giving little importance to temperature effects and to liner-concrete interaction. After IDCOR program [2] in 1983, which relied on the margin to global structural failure, in 1984 EPRI [3] sponsored specific research on containment integrity evaluation, developing useful criteria and guidelines for predicting containment leakage, assumed as the new limit state for containment evaluation.

The traditional design reference loads relied in fact considered in fact LOCA accident as reference load accident condition. After the accident at Three Miles Island, a new accident scenario has been considered (LOCA+hydrogen burning). Finally the most updated approach includes severe accidents mainly based upon probability evaluations and corresponding to pressure and temperature combinations that could be greatly in excess of the design conditions (LOCA). However Epri assumes that LOCA+Hydrogen burning load condition bounds all the possible accident scenarios, being the reference for failure analysis.
In table 1 accident load levels are shown for a typical SBWR containment [4].

Table 1. Pressure and Temperature Values inside the Reactor Building during Severe Accidents[a]

| Accident | Ambient | Pressure (MPa) | Temperature (C) |
|---|---|---|---|
| LOCA | Drywell | 0.34 | 130 |
| (MS Pipe Break) | IC Pool | atm. | 105 |
| | Suppr. Pool | 0.34 | 60 |
| Hydr. Burning | Drywell | 0.68 | 145 |
| | IC Pool | atm | 105 |
| | Suppr. Pool | 0.68 | 80 |
| Melt ejection | Drywell | 0.90 | 160 |
| | IC Pool | atm | 105 |
| | Suppr. Pool | 0.90 | 160 |

[a]Peak values of the transients are referenced. The values has to be intended as order of magnitude for typical transients. More precise values has to be derived from the final design stage and could have large modifications.

The above mentioned considerations have suggested an initial phase of study of the most important aspects affecting containment failure behaviour. In the present study the sensitivity of the project to two load histories is highlighted, showing how they can lead to different failure modes and factors, just changing load combination rule.

## GENERAL APPROACH TO FAILURE ANALYSIS

As a general approach to non linear failure analysis, two models of the above cited typical containment structure have been used: the first oriented towards SDB design, the second addressed to assess different global failure modes and liner tearing under limit load conditions.

The first model is oriented to preliminary sizing of wall thicknesses and rebar densities, but it also clarifies a typical response to various design

loadcases. In fact, after the first analysis, a comparison of the influence of the loads on the structure response indicated the combinations to be monitored in the non linear analysis.

The subsequent non linear model, more detailed in liner, rebar and soil simulation, is based on refined models of the materials, taking into account concrete rebar interaction and cracking behaviour.

The F.E. model has been checked in detail with benchmark tests on material models before running failure analysis. The sources of nonlinearity that have to be captured are described in the following:

- the liner concrete interaction induced by cracking, which is dominated by punching shear local effects;

- the strain concentrations which occurs next to discontinuities where liner tearing appears prior to the occurrence of global structural failure;

- the stress-strain law for concrete, rebar and liner which are strongly influenced by a temperature level above 200 C;

- the large stiffness redistribution effects, subsequent to plastic hinges formation, which determine stress migrations among structure components.

The last two aspects are strictly connected to SBWR containment geometry and introduce new uncertainty sources in safety margin evaluation. In the analysis the first two aspects have been faced by means of the application of special analysis techniques assessed by ANATECH on traditional containments [3], even if the detailed 3D models required for the tuning of the formulas are not yet available.
Appropriate stress-strain laws, the third aspect, have been modelled in detail.
The fourth aspect has been modelled by means of accurate cracking criteria and convergence procedures able to reproduce stress migration effects from concrete to rebars and stiffness redistributions.

Two load histories have been applied, with different contents of thermal loadings, generally referring to two different sample accident scenarios. As the calculations are not focussed on failure limit evaluation, but only on a preliminary inspection on methods, the reference scenarios are considered sufficient for comparison purposes.
The application of two different load histories have led to quite different responses, not only at structural failure limit, but also in a load range where leakage appears due to liner tearing.

FIRST SIMPLIFIED MODEL, SIZE ORIENTED

The first phase of analysis has dealt with a simple axysimmetric model, oriented towards preliminary sizing of wall thicknesses and rebar densities.
The F.E. model shown in fig. 2 employs 90 axysymmetric shell elements and 23 springs to ground. In the same figure the secondary containment volume is enclosed in the dashed line, where the steel liner prevents leakage, and the pressure vessel bearing shelves are indicated with arrows.

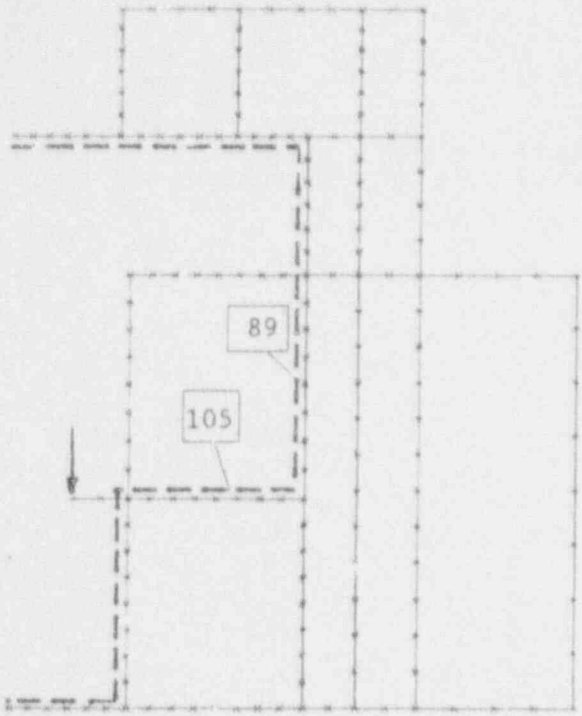


Figure 2. Simplified Axysimmetric F.E. Model

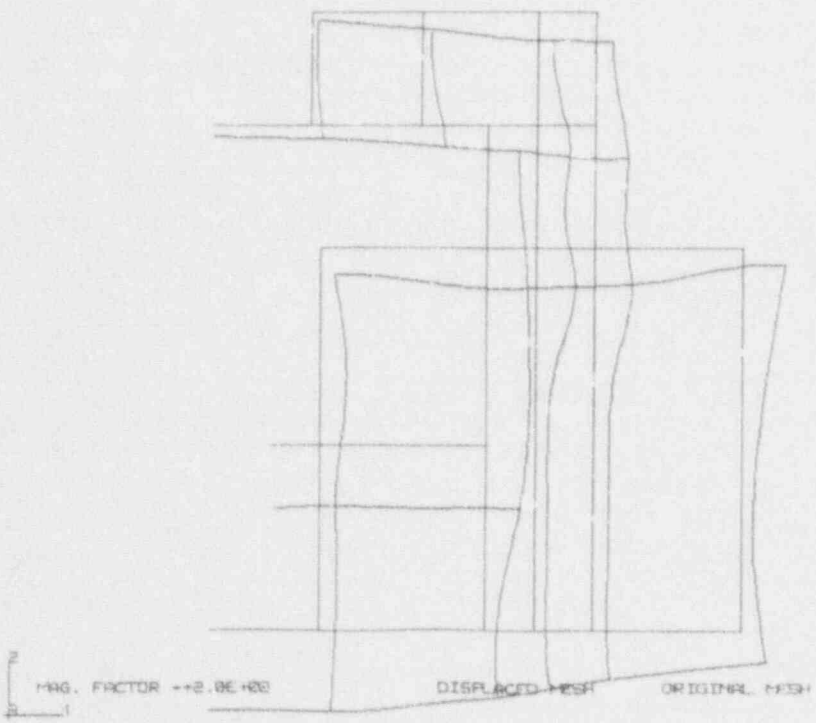


Figure 3. Simplified Linear Analysis - Deformed Shape under the most Severe Load Combination

The geometric assumptions related to the symmetry as well as the hypothesis on the homogeneity of linear material properties, have been considered not only reasonable, because of being recommended by the standards, but also sufficient for comparison purposes on different load effects.
Table 2 contains load case specifications according to standard design requirements [4].

Table 2. Reference Load Cases Intensities for Design Analysis

| Load Case | Value | Location |
|---|---|---|
| Dead Load (N/mc) | 24.525E3 | Whole structure |
| Dead Load (N) | 16.676E6 | Vessel bearings |
| Service (MPa) | 9.810E-3 | Floors |
| Hydrostatic (MPa) | 4.9E-2 1.25E-1 | Pools Bottom and Sides |
| Hydrostatic (MPa) | 1.785E-1 | Ext. with soil contact |
| Geostatic (MPa) | 1.190E-1 | Ext. with soil contact |
| Accident (MPa) | 0.371E0 | Int. Sec. Containment |
| Accident (C) | 110 | Int. Sec. Containment |
| SSE (g) | 0.3 | Whole structure |

In the design analysis pressure and temperature load intensities have been chosen with respect to plant accident simulations (LOCA) and assumed uniform and steady with the maximum values on the inner part of the liner. As thermal condition, a gradient 110-20 C have been applied across the containment wall. Seismic loads related to a SSE have been added in a simplified way after recovering the stress resultants on each floor from a stick model previously run.

In fig.3 a deformed shape related to the most sever load combination gives a global overview of the areas of most concern. The influence diagrams of fig.4 refer to the areas marked off with a label, showing the percentage contribution of the single load conditions to the stress resultants on the sections.

Temperature and earthquake loads give the major contributions to stress resultants and they suggest an extensive application of sensitivity analysis based on their values to assess the influence of their intrinsic uncertainty on the bearing capacity of the structure. However, in the following reference is made only to the temperature load, with discussions of its value and distribution.

To check the sensitivity of the system, a new global load condition has been applied: it corresponds to a gradient 110-50 C across the containment walls and to 20 C uniformly applied to the external structural components.

In fig. 4 a direct comparison between stress resultants in two specific sections under two temperature distributions are drawn in a graph, showing the average difference to be 30%. The higher average temperature of the inner part is mainly responsible of the stress peak resulting from the contact with the

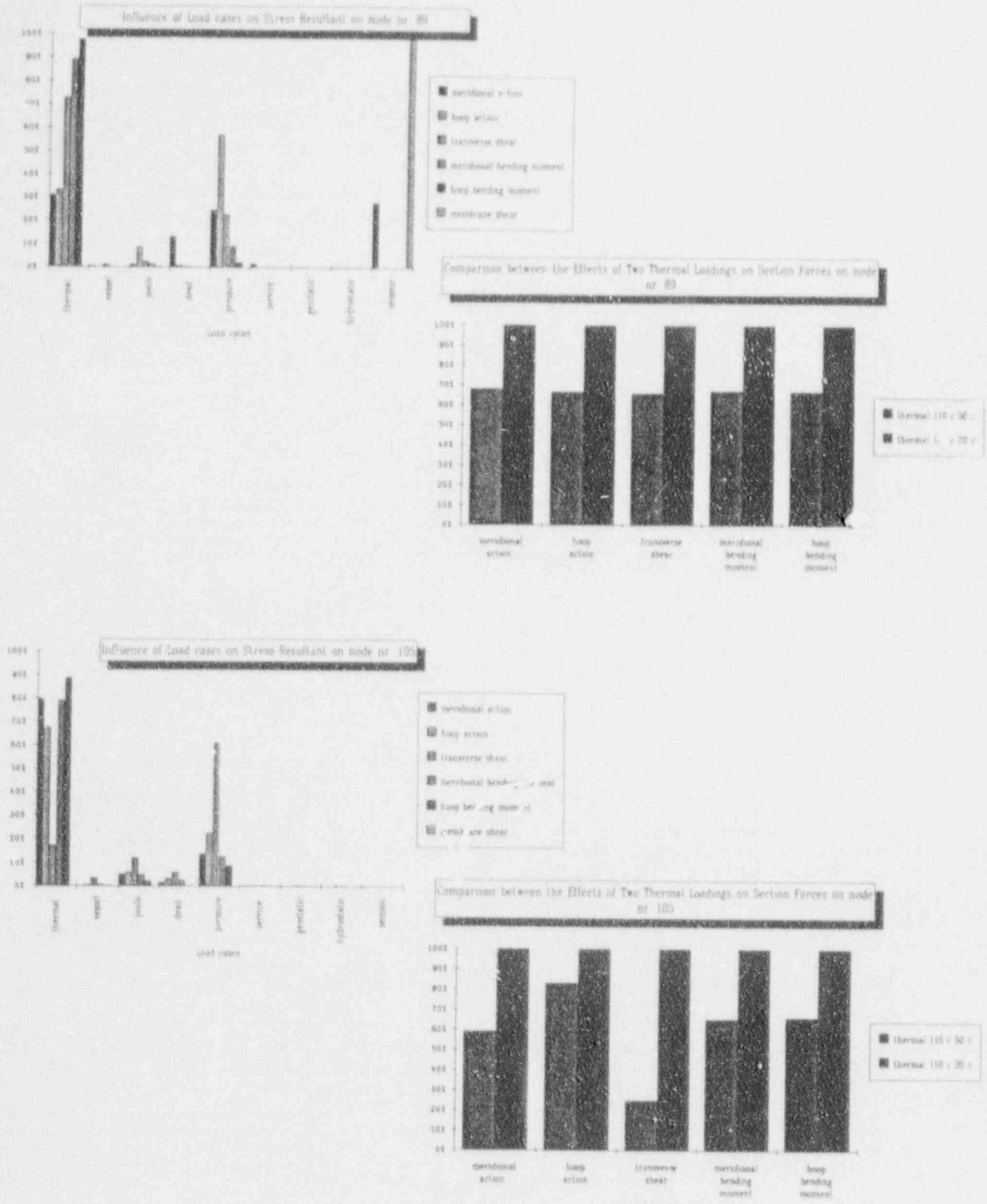


Figure 4. Diagram of Influence of Load Cases on Stress Resultant in two Critical Section - Comparison between the Effects of Two Thermal Loadings on Section Forces

external cold cylinder. On the other side, bending effect on the containment walls have diminished.

Such a high discrepancy in the results was expected and confirms, generally speaking, the need for a precise definition of temperature loads for these containment configurations. In the traditional context a temperature level below 200 C is not able to affect significantly either stress-strain behaviour or stress distribution, because of the unconstrained behaviour of the cylinder-dome structure, justifying the reasonable assumption to consider only pressure loads in failure analysis.

In this framework a more refined temperature map was not considered necessary to improve the reliability of the model: the steady state assumption of this analysis, which disregards the phase effects between the different rooms, justifies only simplified conditions, useful for global comparison with the other standard loadcases.

## NON LINEAR FAILURE ANALYSIS

Based on the results of the design analysis, a reinforcement pattern has been decided, respect to 110-50 thermal condition, and modelled in a continuous axysymmetric model (fig.5) as embedded rebar. Non linear materials have been introduced: the reference property values have been extracted from [2,4] and collected in table 3.

Table 3. Materials Reference Properties

| Material | Temp (C) | E (MPa) | Coh (Mpa) Yeld(MPa) | Fr.angle K | Plasticity law |
|---|---|---|---|---|---|
| Concrete (C30) | 20 | 3.35E4 | 8.66 | 30 | Mohr-Coulomb |
| | 200 | 2.87E4 | 8.66 | 30 | (linear soft.) |
| Rebars (MPa) | 20 | 2.00E5 | 430.0 | 0.0020 | Von Mises |
| | 200 | 1.81E5 | 430.0 | 0.0024 | (strain hard.) |
| Liner (SA537) | 20 | 2.03E5 | 414.0 | 0.0020 | Von Mises |
| | 200 | 1.90E5 | 346.0 | 0.0020 | (strain hard.) |

Due to the sensitivity of the structure to limit load combinations, two analyses have been carried out on the same geometry with different load sequences (LH), defined as in the following:

LH 1): dead loads, live loads, accident temperature and pressure at design level, then pressure and temperature progressively increased up to 170 C, finally only pressure increased up to failure;

LH 2): as LH 1), but with both pressure and temperature increased from the design level up to failure.

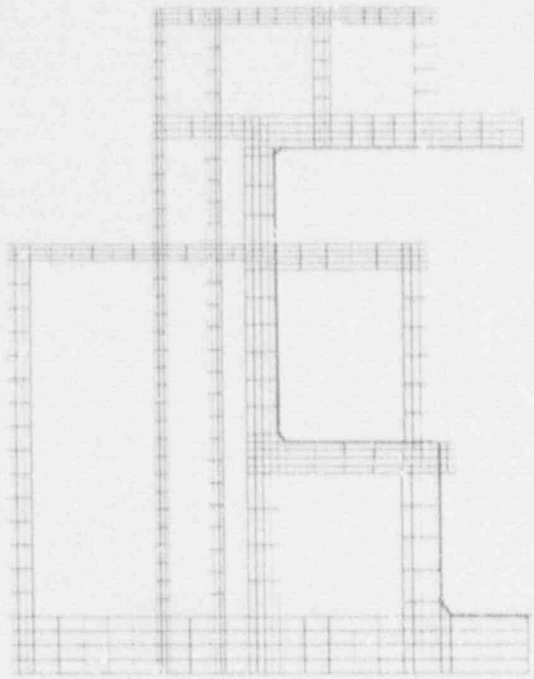

Figure 5. Continuous Axysimmetric Model - Geometry

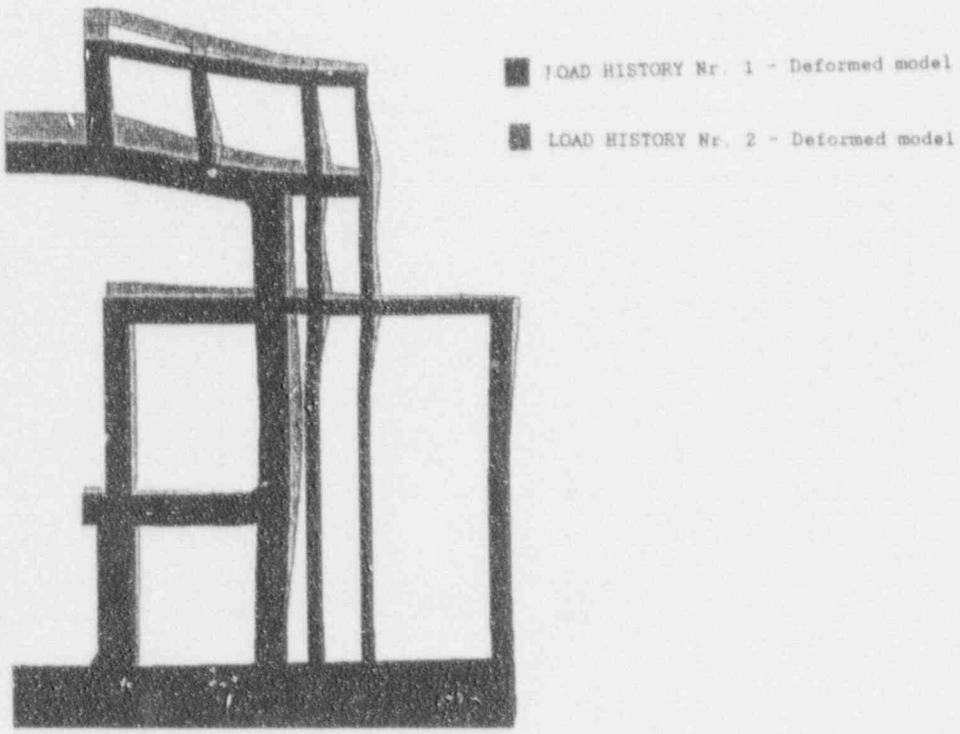


Figure 6. Load History n.1 and 2 - Deformed Shapes at LF=5.0

While the first load sequence may be considered as representative of the worst accident scenario (main steam pipe break), the second condition points to the safety factor evaluation, without any reference to a specific scenario. The latter load sequence enables the examination of the sensitivity of the system to load history choices.

The structural behaviour in the two analyses has been assumed as characterised by means of limit states, chosen as follows:

- first initiation of plastic flux either in concrete or in rebar (reversibility limit);

- liner tearing, respect to wall-top slab junction, given by [3]:

$$e_{max} = e_{merid} * K * a * b \qquad (1)$$

  where b is the inverse of the ductility ratio, a the strain localisation factor, K the strain concentration factor;

- structural failure, wich occurs when a mechanism forms at the occurrence of lability within force controlled load histories.

For load sequence 1), a deformed shape of the structure at level 5.0 of the pressure magnification factor is shown in fig.6, where the failure mechanism is evident. The principal strain plot of fig.7 confirms the position of plastic hinges on the top slab attachment which produce the non linear displacement curves, as shown in fig.8.

The development of state of cracking of fig. 9 indicates the failure history.
In fig.10 liner meridional and hoop strain are plotted along the meridional section, representing the area of concentration at the edeges.
Fig. 11 shows energy norm trend versus the load factor (LF), and load iteration numbers required to achieve convergence at each step. Structural instability load has been fixed where the analysis stopped due to numerical singularities, confirmed by load displacement curve trends.
With the application of the strain intensity factors at the highest edge, and assuming an extension of the functions validate on traditional containments, the leakage load factor corresponds to 6.0, significantly below the failure limit.

Such a high value of the load factor (LF) relative to structural failure (7.5) is mainly due to the particular way chosen to increment load conditions. After LF=1.66 in fact only pressure loads, which give a low contribution to the design load combination, are magnified. Furthermore, it has to be remembered that structural design refers to load combinations which include seismic effects. On the contrary, the failure analysis has been carried out only with respect to pressure and temperature loads, excluding any superposition of seismic actions which, in any case, would have required different approaches from axysymmetric models.

The results relevant to LH 2) are presented, in the above cited figures related to LH 1), in terms of deformed shape (superimposed to the previous one), principal strain contour plots, crack maps (fig.12), liner strain diagrams. The failure mode, which in this case corresponds to LF=5.0, now is

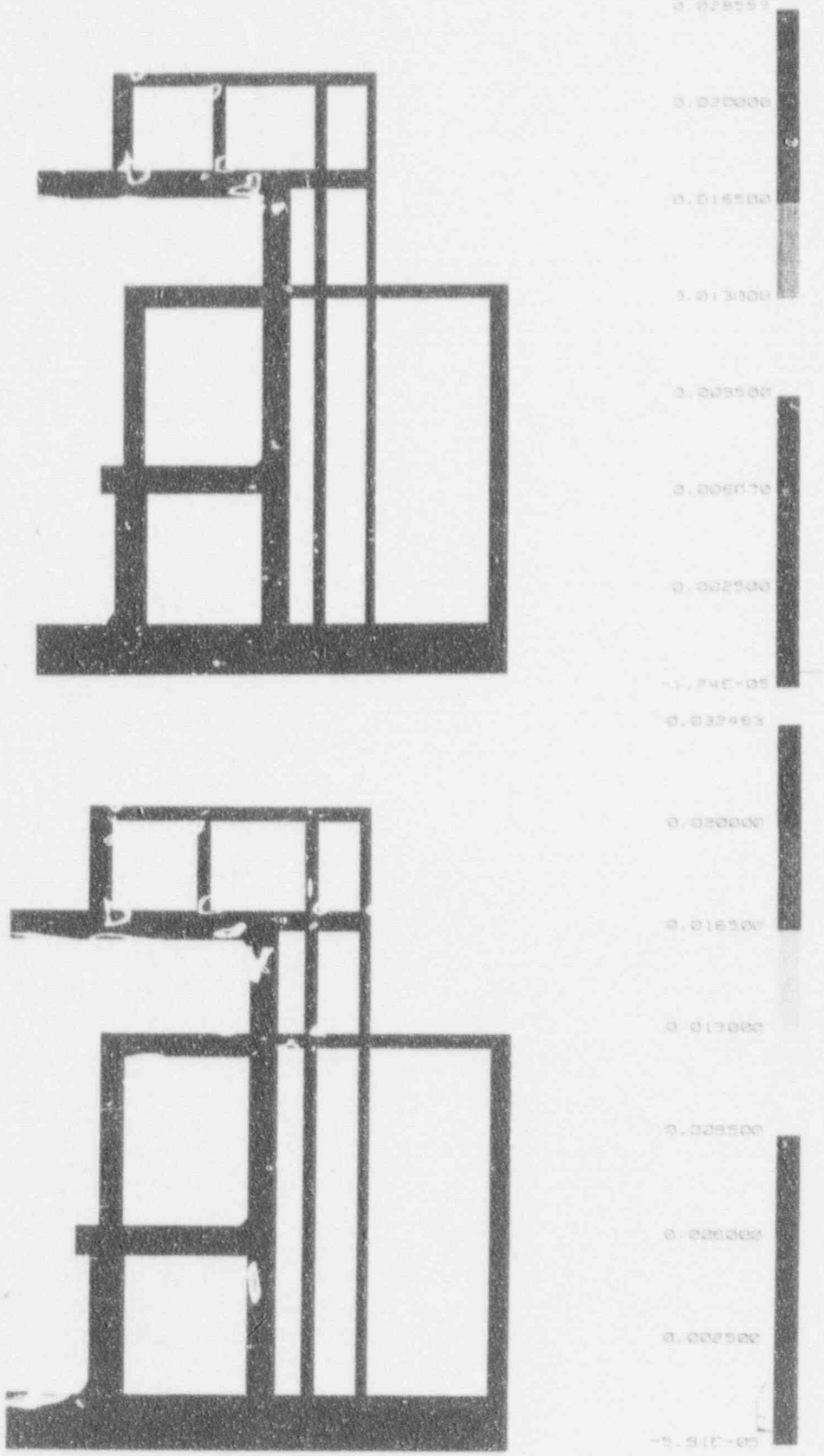


Figure 7. Load History n.1 and 2 - Principal Strain Contours

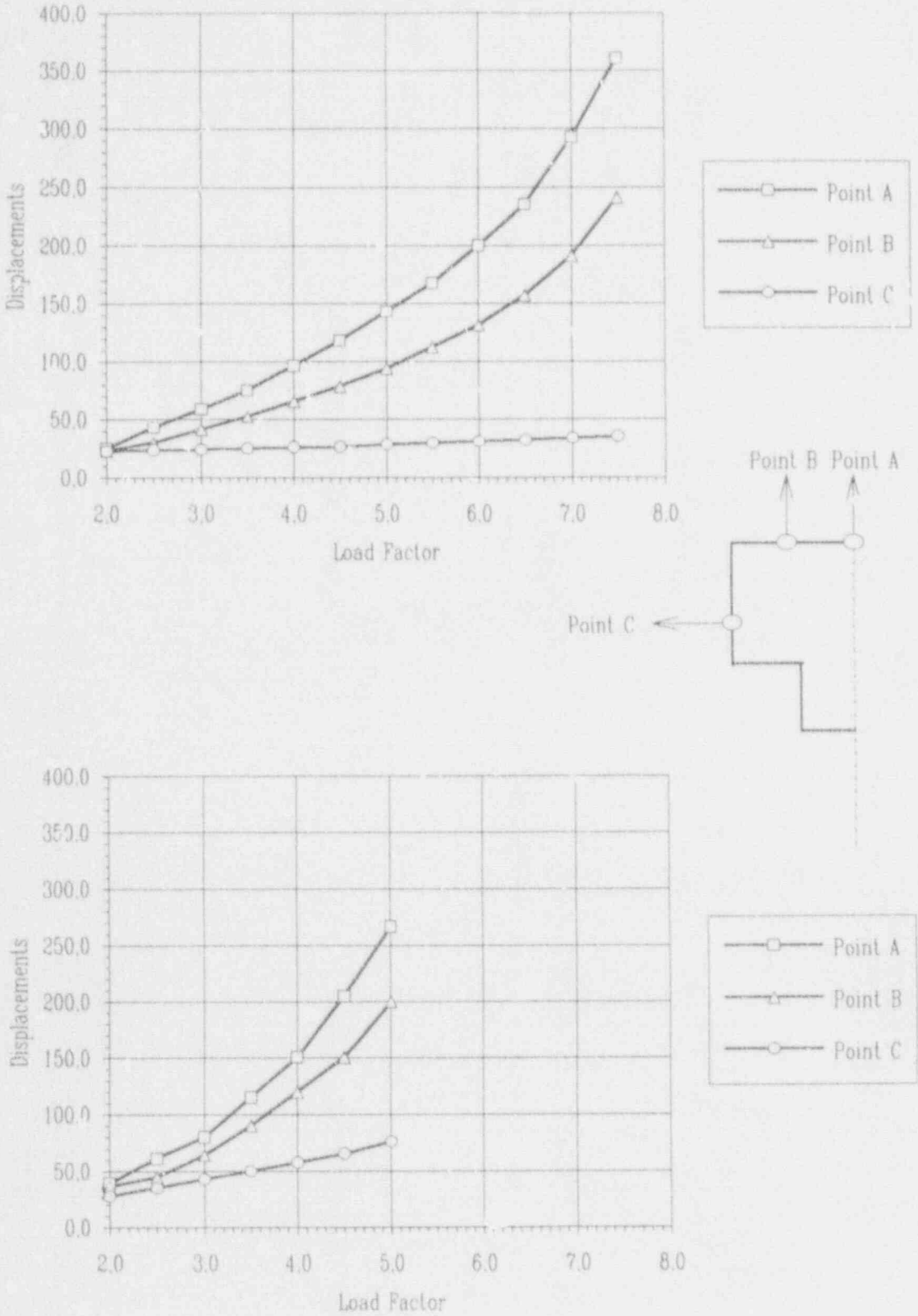


Figure 8. Load History n.1 and 2 - Load Displacement Curves for Selected Points on the Top Slab

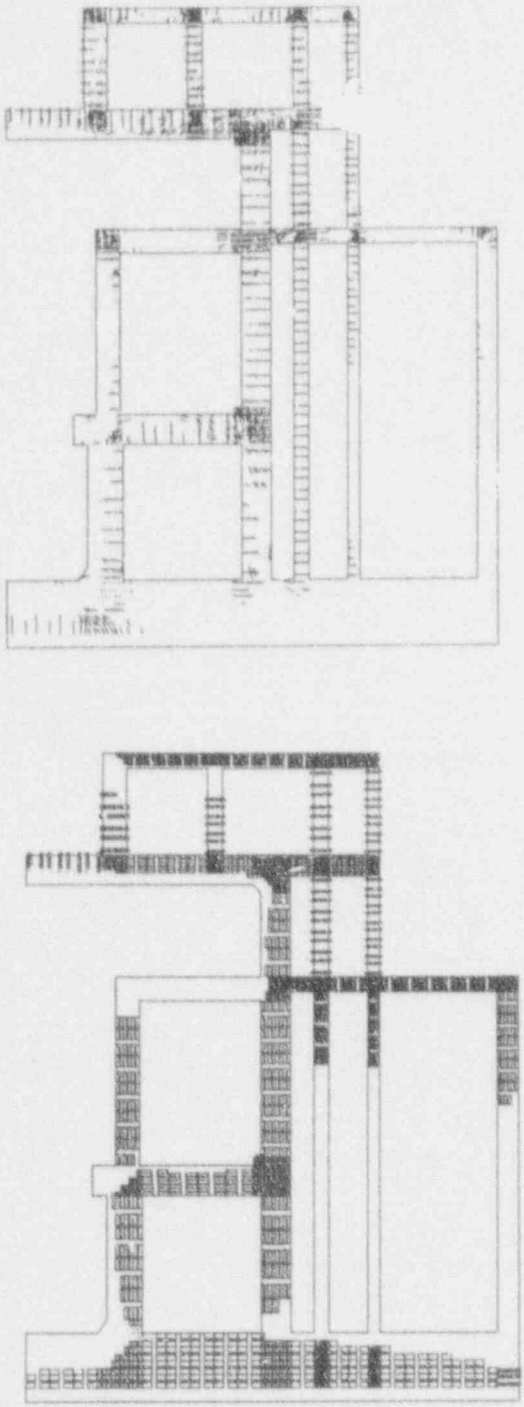

Figure 9. Load History n.1 - In Plane and Hoop Crack Status

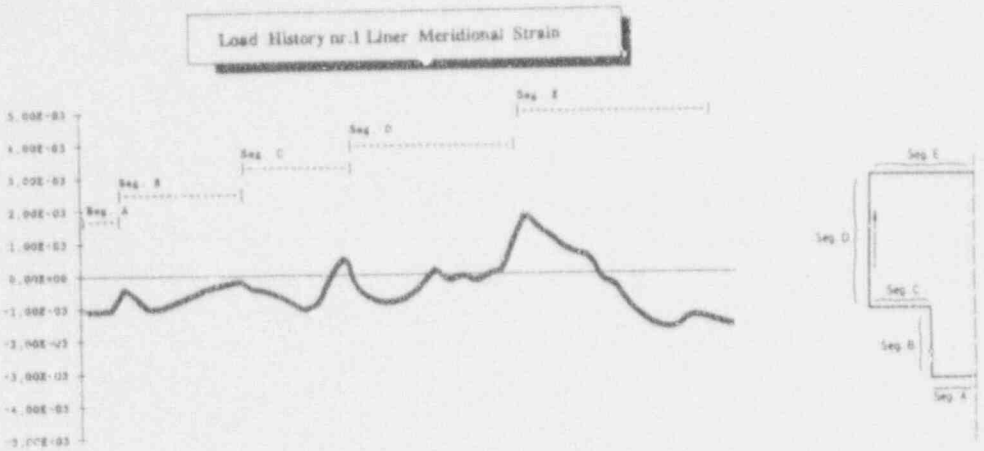


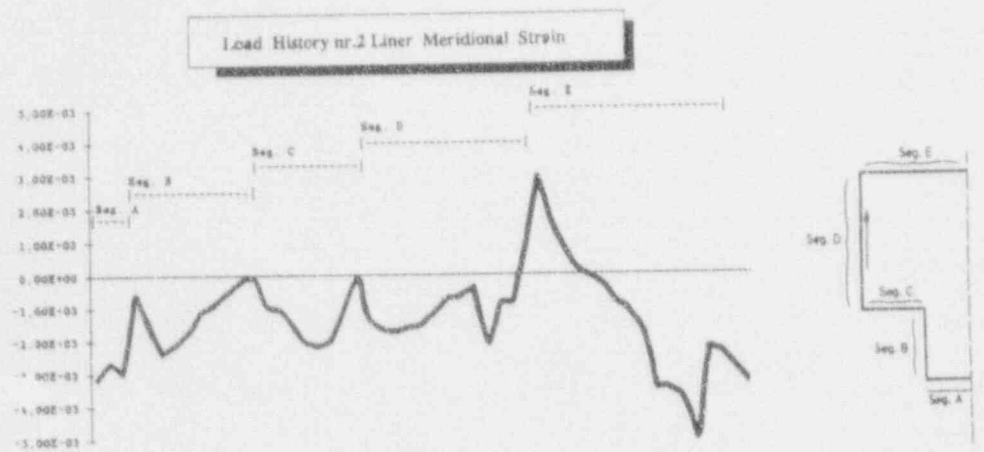


Figure 10. Load History n.1 and 2 - Liner Meridional Strain

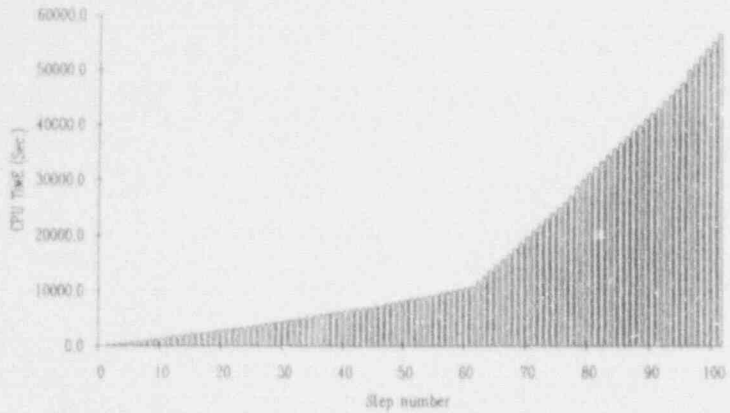


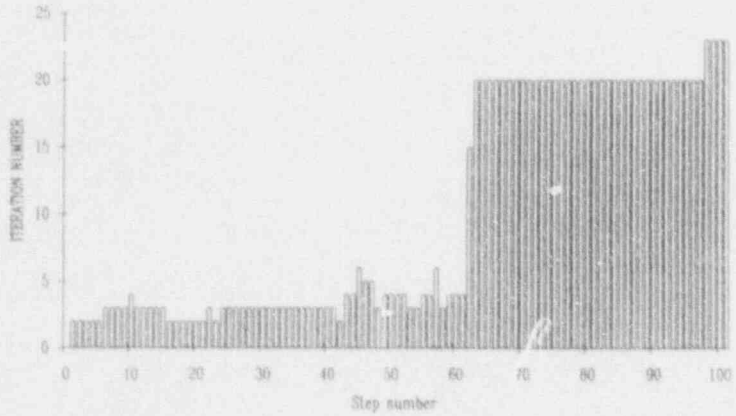


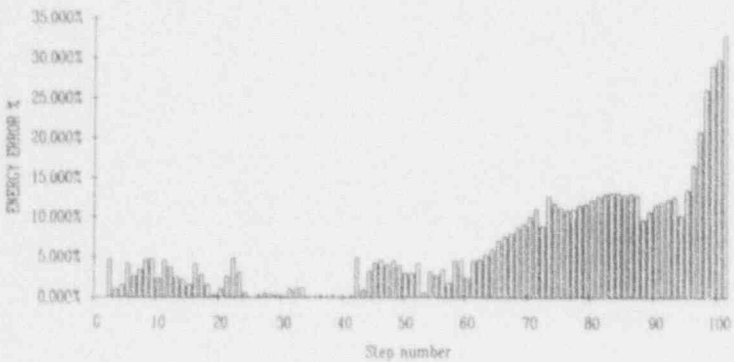


Figure 11. Load History n.1 - Energy Norm and Iteration Number versus LF

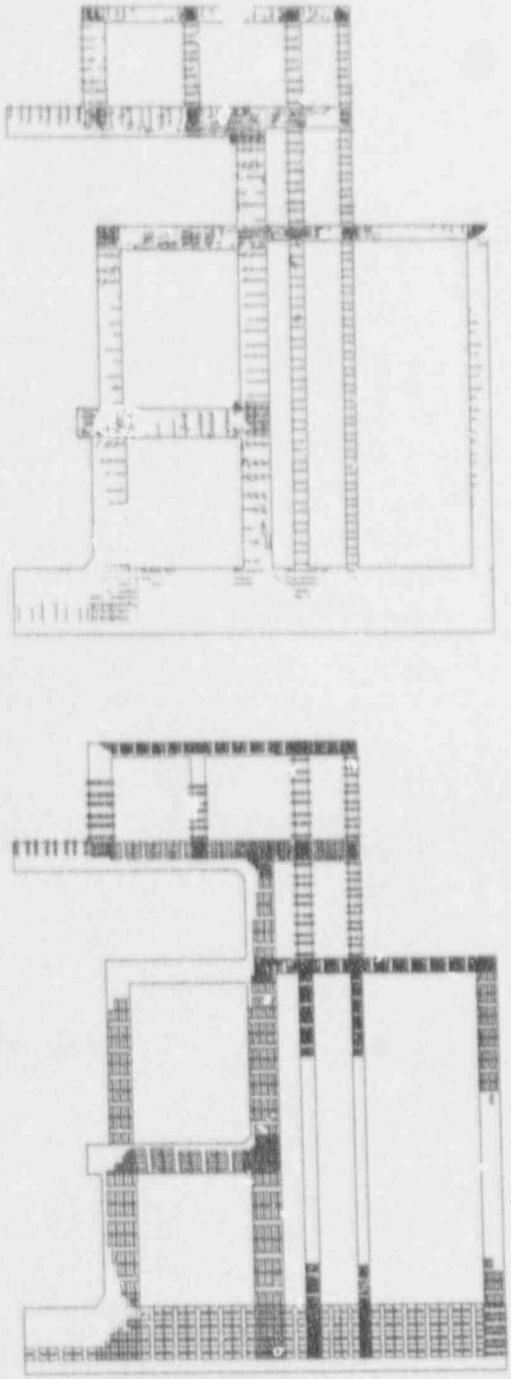

Figure 12. Load History n.2 - In Plane and Hoop Crack Status

dominated by temperature effects, that are magnified together with pressure, which cause strong bending deformations on the cylindrical wall constrained by the external horizontal floor. In this case stiffness is degraded uniformly and the whole structure is involved in the resistance to accident loads, whereas, in the previous case, only the roof slab was affected by plastic rotations.

Here again the critical point for liner integrity is located at the highest edge where a LF=5.0 is calculated. Detailed analyses would be required in the areas of most concern to evaluate more accurate strain factors, but they are beyond the scope of this study, more focussed on the comparison of limit state definition than on their absolute evaluation.

## GENERAL DISCUSSION

Two models of the same containment structure have been used to evaluate the sensitivity to limit load specification. For the non linear analysis two different load histories have been applied to check the influence on the failure mode itself.

The first load history corresponds to a simplified accident scenario; the second should represent an upper bound for a lot of scenarios and aims to evaluate the safety margin of design calculations.
The precise requirements in terms of maximum admissible leakage rates have oriented the evaluations of the different failure modes toward liner tearing estimates, based on global axysymmetric strain calculations.

The final results are summarised in table 4 where the influence of temperature load specification is outlined.

Table 4. Load factors at different limit states for the two load histories.

| Load History n. | Limit State | LF |
|---|---|---|
| 1 | Reversibility | 1.5 |
| 1 | Structural Failure | 7.5 |
| 1 | Liner Tearing | 6.0 |
| 2 | Reversibility | 1.5 |
| 2 | Structural Failure | 5.0 |
| 2 | Liner Tearing | 5.0 |

Conclusions are twofold:

a) non linear analyses are mandatory due to highly non linear effects responsible for limit state determination, like liner-concrete interaction, temperature dependency of material behaviour, stiffness redistribution after first cracking. Axysymmetric 2D global models have to be integrated with 3D detailed models which must demonstrate high reliability levels taking into account that the experimental reproduction of complex thermal phenomena is almost unfeasible;

b) structural complexity of the new generation of reactor buildings requires detailed analyses of accident scenarios because of the high level of sensitivity to temperature load distribution.

In this framework the need for new guidelines widely accepted by the design community is clear. The updating of design configurations in fact has to rely on precise limit load analyses which have to select the most critical failure mode respect to all possible accident scenarios and to evaluate the global safety margin of the structure.

As a general conclusion, there is a great deal to reach a worldwide consensus toward a precise and unique definition of the load case and load history to be used to assess the ultimate structural capacity of a containment structure. Without this specification it is in fact almost impossible to guarantee the required safety margin respect to all the possible accident scenarios.

## Acknowledgments

The calulations presented in this paper have been carried out at Ismes s.p.a. in Bergamo (Italy) on behalf of ENEL/DSR, within the cooperation in nuclear containment research.

## References

1. D. S. Horschel et al., "Insights Into the Behavior of Nuclear Power Plant Containments During Severe Accidents", SAND90-0119, Sandia National Laboratories, Albuquerque, NM, March 1990.

2. IDCOR, Technical Report 10.1, "Containment Structural Capability of Light Water Nuclear Power Plants", July 1983.

3. ANATECH RESEARCH CORP., "Criteria and Guidelines for Predicting Concrete Containment Leakage", NP-6260-SD, RP 2172-1, April 1989.

4. GE-Hitachi-Toshiba, "SBWR Study Team Final Report", NEDC-31679P, June 1989.

5. CEB-FIB, Model code, March 1990.

# Research and Development performed at CEA/DMT in the Field of Nuclear Reactors Containments

*A. MILLARD (CEA/DRN/DMT)*
*Ph. JAMET (CEA/DRN/DMT)*
*B. BARBE (CEA/IPSN/DES)*
*C. LECOMTE (CEA/IPSN/DPEI)*

## 1. INTRODUCTION

The behavior of containment is a key issue with respect to the safety of nuclear power plants. Extensive work has been performed for many years at CEA/DMT (Department of Mechanics and Technology) on this subject particularly on the behaviour of containment under severe accidents.

Large Research and Development programs have been carried out and are still under progress to handle the following problems :

- Thermo-mechanical response on the containment under increasing pressure and temperature up to the ultimate behavior of the structure.

- Behavior of the containment in case of hydrogen detonation or steam explosion.

- Modelization and evaluation of containment leaking after a severe accident inducing cracks in the structure.

- Response of the containment to seismic loads.

These studies have been carried out by means of finite element computations. The computer codes have been developed and validated using either analytical solutions or experimental results. Specific developments have been made in order to be able to solve the above mentioned problems :

- Material models for reinforced concrete,

- Fast dynamic algorithms for impacts.

- Seismic analysis techniques and soil-structure interaction.

- Gas dynamics, shock waves and fluid-structure interaction.

More recently, new programs have also been undertaken, concerning the behavior of containment after core melt and vessel break through. These programs are motivated by the recent safety requirement to take this accident into account at the design level for future reactors. Work is in progress at CEA/DMT in the two following areas :

- Conceptual studies concerning core catcher and residual power evacuation.

- Design method development for core catcher, including numerical code development.

The work performed by CEA/DMT is described in more details in the following paragraphs.

## 2. GEOMETRICAL AND MATERIAL MODELLING OF THE CONTAINMENT

According to the kind of analysis and required results, it is possible to model the whole containment using either shell finite elements or 3D continuum finite elements.

For the former case, a special material model, called the global model has been developed, which will be presented here for sake of clarity in the simple case of a reinforced concrete beam.

### 2.1 The global model for reinforced concrete ([1] to [4])

Let us consider a reinforced concrete beam loaded by a normal force and an in-plane bending moment. The basic idea of the method which is classically used in a strength of materials approach, is to derive and elasto-plastic formulation in terms of generalized stresses (N, M) and strains (membrane strain $\epsilon$ and curvature variation $\chi$).

In order to obtain the corresponding laws an homogenization technic is used : The beam is decomposed into a set of layers each layer following a given uniaxial stress-strain curve (see figure 1).

Assuming that the cross-section remain straight and normal to the mean fiber, one finds a global M-curve, for a given normal load. (see figure 2). Such a model can be generalized to plates (see [2]), as well as to reversed and dynamic loadings (see [3] and [4]). It has been implemented in various computer codes of the CASTEM system [5] for static and dynamic problems as well as in the PLEXUS code [6] for fast dynamic problems.

We illustrate the possibilities of the global model on two exemples :

- The first one is a validation of the model by comparison between experimental and calculated results [7] [8]. Static and dynamic tests have been performed on reinforced concrete slabs, simply supported on their edges and loaded in their center, in order to evaluate the ultimate behavior, and characterize the ruin of the slab (by bending, punching or both).
  The geometry and reinforcement of the slab are shown on figure 3 together with the stress-strain curves used for the steel and the concrete.
  The BILBO code of the CEASEMT System was used for the analysis of the slab subjected to quasi static loading. Two different equivalent homogeneous materials had to be defined, in order to represent the current part of the slab, and the outer walls. Unilateral constraints were necessary, in order to modelize the lift up of the corners, which results into a progressive loss of contact between the slab and its outer support. Figures 4 and 5 show the deformed shape of the slab at maximum load, and the comparison between numerical and experimental force-displacement curves at the center of the slab, before final punching. These results validate the global method for this configuration. On the other hand, the good agreement between numerical and experimental results

confirms that punching, or shear processes, do not play any significant role before the maximum load is reached, since they are not taken into account in the analysis.

- The second one is a calculation of the impact of a lear jet on a typical concrete containment [9]. Two impact locations have been studied, one at the apex of the dome and the other in the current part of the cylinder. The containment is modelled using quadrilateral shell elements. The impact is treated as a given force versus time (see figure 6). Again, an equivalent global model has been derived from steel and concrete properties.
The figures 7 and 8 show the deformed structure for the two cases.

## 2.2 Local model for concrete [10]

In order to be able to calculate the perforation of a containment by a rigid missile, which is not possible using global model, a local model has been developed accounting for the various modes of damage, which are illustrated on figure 9 :

. In region 1, the reflection of the compressive wa[illegible] leads to tensile stresses exceeding the concrete strength. Tensile failure is [illegible] to predict the scabbing phenomenon.

- In region 2, the material is subjected to very important hydrostatic compressive stresses. Concrete which contains forces is then subjected to crushing, which has to be taken into account in the analysis.

- In region 3, very high stresses appear in the vicinity of the lateral boundary of the missile, while all the principal stresses are compressive. These stresses lead to shear failure, which should also be incorporated into the model.

Concerning the damage by traction, the chosen criterion consists in limiting the maximum principal stress :

$$\text{Max}\,(\sigma_i) < \sigma_t$$
$$i = 1,3$$

were $\sigma_t$ is the tensile strength of the material. In the principal stresses space, this corresponds to a pyramid with three orthogonal faces. During the loading, if one of the principal stresses occurs to overstep the $\sigma_t$ limit, this limit is set to zero as well as the corresponding principal stress.

In the axisymmetric case, the model accounts for two different cracking modes :
- radial cracks,
- cracks in diametral plane.

This enables a description of the orthotropic behavior of cracked concrete, by keeping the memory of the direction of the first cracks.

Concerning the damage by shear stresses, two domains are distinguished, according to the confining pressure :

- a brittle domain, corresponding to low confining pressures, which is limited by a Drucker-Prager criterion, characterized by strain-softening ; this criterion may move down to another fixed Drucker-Prager criterion representative of a perfectly plastic behavior.
  This modelization enables a full unloading in the simple compression case where there is no confining pressure.
- a ductile domain, corresponding to high confining pressures, which is limited by a Von-Mises criterion and characterized by strain-hardening ; this criterion may move up to a fixed Drucker-Prager criterion representative of a perfectly plastic behavior.

Concerning the damage by hydrostatic pressure the relation between the volume variation and the hydrostatic pressure has been approximated by a bilinear diagram. The first part (elastic) corresponds to the deformation of the skeleton, the second (inelastic) corresponds to the pores crushing. In the principal stresses space, the yield surface is a plane perpendicular to the trisectrice ; it undergoes strain hardening as the material is deformed.

For all cases, the normality principle has been assumed for plastic flow. The various damage modes can be coupled, on the basis of Koiter's rule stating that the plastic flow vector lies in the cone defined by the external normal to the criteria.

This model has been validated in the frame of the SANDIA benchmark : ([12][13]) : A 1/6th scale concrete containment model has been tested in Albuquerque (New Mexico) by the SANDIA NATIONAL LABORATORIES, under an increasing internal pressure load.

Participants to the exercise were asked to predict the ultimate capacity load of the containment. The computed results were compared with the test results and some additional calculations were performed after the test.

An axisymmetric model, shown on figure 10 was used. The concrete and the rebars were modelled separately, and a perfect bond was assumed. The results obtained are as follows.

- First some meridional cracks develop at the junction between the basemat and the cylinder, for 0.2 MPa pressure.
- Then some hoop cracks develop in the cylinder for a 0.3 MPa pressure, causing a sudden increase of the radial displacement (see figure 12).
- The half-lower part of the basemat is completely cracked in the hook direction for a 0.55 MPa pressure which results in a uplift movement of the basemat.
- After a 0.64 MPa pressure the cylinder and the dome are completely cracked.

Finally, for a 0.98 MPa pressure, the displacements increase rapidly, which corresponds to the ultimate load capacity of the containment (Figure 11 shows the final meridional crack pattern). This ultimate pressure is in good agreement with the experimental value for which an important leakage of the containment was obtained.

## 3. HYDROGEN DETONATION [14]

In order to be able to compute the shock waves due to hydrogen detonation, and their consequences on the containments, some specific developments have been made in the PLEXUS Code :

The EULER equations for fluid dynamics are solved using an explicit time integration scheme. A pure Lagrangian formulation is adopted for simplicity of coupling with the structures.

The hydrogen detonation is considered as a shock front associated with a chemical reaction, which is supposed to be adiabatic and exothermic :

$$2H_2 + (H_2O)\text{steam} + \underbrace{(O_2 + 4N_2)}_{\text{air}} \qquad 3(H_2O)\text{steam} + 4N_2 + O$$

The reaction is initiated at a threshold temperature $T_1$, and is supposed to be complete and instantaneous. In order to validate this method, one-dimensional detonation calculations have been performed in plane geometry and compared to predictions by the Chapman-Jouguet theory [15].

A similar calculation in an axisymmetrical geometry, modelling a 1 m long tube, showed the focusing effects of the shock waves :

On figure 13, the evolution of pressure versus time has been plotted at various locations :
x = 0, 0.01, 0.5, 0.8 and 1 m.
One can notice the two sweeps way and back of the shock wave, the over-pressure at the first reflection and the residual pressure.

The second step of validation was a two dimensional analysis of a SANDIA containment which showed that focusing effects and multiple reflections can lead to important over-pressure in the containments [15]. Moreover, the location of the initiation point has a strong influence on the results (see Figure 14).

Some additional calculations have been performed in order to investigate the influence of obstacles like cranes, in the containment, on the pressure distribution, and also the influence of the initial concentrations of the various gas in the mixture.

## 4. STEAM EXPLOSION

In case of sudden contact between melted corium and water, important quantities of steam may be generated, which can damage the containment. This can again be modelled using the PLEXUS code. A preliminary approach used the following assumptions :

- The Corium is not modelled but a constant Corium injection in a given water volume is assumed during a certain time which results in an energy supply.

- The water is considered as an homogeneous bi-phasic material, with a variable ratio between the steam volume and the total volume, following the water and steam tables.

As illustration of the PLEXUS possibilities, a calculation of the consequences of a melted core on the bottom of a reactor vessel has been performed ; the supporting plate is assumed to be extremely rigid and fixed to the vessel bottom.

The core and supporting plate are treated as an equivalent porous medium. Moreover, a central hole due to the core fusion has been considered.

The initial conditions of the water are a 10 bars pressure and a 180°C temperature. The results are presented on figures 15 to 18. Using this simplified approach, very high pressures (more than 500 bars) are found in the water and on the vessel. The temperature of the water increases regularly. The stresses in the vessel reach values which are for beyond the elastic limit, for very short time (t = 3.5 ms) (the vessel has been considered elastic). Some additional developments are being done in particular for the treatment of materials at high temperature and the energy release by the corium injection into water.

## 5. CONTAINMENT LEAKAGE

In case of double containment without any liner, as in French 1300 MW PWR, the increase of pressure and temperature beyond design conditions would lead to through-cracks in the containment. The air and steam flow in the cracks associated with the temperature increase of the concrete would cause a certain amount of leakage which must be evaluated.

For this purpose, the diphasic flows in very thin but long cracks have been studied using the TRIO-EF Finite Element Code [16]. Figures 19 and 20 show the pressure and temperature profiles in case of a uniform thickness (200 µm) crack.

Experimental validation of the model are in progress : the cracks are simulated by a given distance between two parallel plates. Firstly, the plates are made of a non-previous material, with thermal properties as close as possible to the concrete ones. An air-steam mixture is injected under constant given pressure and temperature conditions. Various quantities are measured along the crack : pressure, air and steam flows, etc...

Some new tests will be performed in view of these first results, in order to be closer to the real case.

## 6. SOIL-STRUCTURE INTERACTION

The seismic analysis of a reactor containment requires a good modelling of the soil-structure interaction. In many cases, the simple description of the soil by means of local springs and dash-pots is no longer sufficient. The first method consists in using both finite elements and boundary elements techniques : the soil is accounted for by means of Green functions, calculated for a stratified soil. However, this approach is restricted to a linear elastic soil.

A second improvement can be obtained by a finite element representation of the soil [17]. The soil is divided into two parts : a limited region $\Omega_1$ around the structure, and an infinite region $\Omega_2$ in which the behavior is supposed to be linear.

For the region $\Omega_2$, dampers are introduced at the boundary. The forces on the boundary between $\Omega_1$ and $\Omega_2$ are determined from the impedance of $\Omega_2$ and from the free field forces and displacements. This method has been used to study the response of a containment to a San Francisco earthquake. The mesh is shown on figure 21. A linear and a non-linear Drucker model have been used for the soil. Fissure 22 shows a comparison between both predictions of vertical displacements of the basemat.

## 7. CONCEPTUAL STUDIES CONCERNING CORE CATCHER AND RESIDUAL POWER EVACUATION

At the present time, the studies performed by CEA/DMT are focused on the two following problems :

- After break-through of the vessel, the Corium has to be collected into the core catcher. Depending upon the pressure at break-through, the failure mode of the vessel as well as the design of the bottom part of reactor, different patterns can be assessed for Corium transfer from the vessel to the core catcher. At the present stage, the formation of a Corium jet with a certain velocity cannot be excluded. It is therefore necessary to study this configuration and to assess the possible deterioration of the core catcher due to a Corium jet impingment.

- Once Corium is supposed to be collected in the core catcher, it is necessary to evacuate the residual power in order to reach a steady-state thermal situation preserving integrity of the containment. Conceptual studies are underway to achieve this goal.

### 7.1 Jet Impingment studies.

A model was developed to show that the TRIO Code [16] is a suitable numerical tool to study the impingment of Corium jets on structures. The case of a steel plate was considered. The model is illustrated by Figure 23, it includes the following features :

- Energy generation by the Corium,

- Radiation heat transfer from the Corium.

- Water cooling of the steel plate.

- Possibility for the different materials to change phase.

- Special model at the steel-Corium interface including the possibility to have various phases in contact.

Typical results of the study are illustrated by Figures 24 and 25. It is assumed that the inlet temperature of Corium is 3000°C.

When the jet velocity is high (1 m/s) the steel is progressively molten and the Corium finally flows through.

When the jet velocity is low (1 cm/s), crusts form at the interface between steel and Corium and at the outer boundary of the Corium jet, while the integrity of the steel plate is preserved.

These results essentially show the applicability of the TRIO Code to these problems.

### 7.2 Conceptual studies concerning residual power evacuation

Conceptual studies have now been initiated at CEA/DMT to insure the evacuation of the residual power of the Corium, once it is supposed to ly in the core catcher. Different options are considered such as Corium fragmentation which has the advantage of increasing the surface of exchange or spread out of Corium in a single layer. Heat transfer inside and outside the containment is also studied.

## 8. DEVELOPMENT OF CORE CATCHER COMPUTATIONAL TOOL TRIREM

The development of the core catcher computational tool TRIREM has been undertaken. This project is carried out through a collaboration between CEA/DMT and CEA/DTP (Department of Thermo-hydraulics and Physics).

The problem to solve is illustrated by Figure 26.

The TRIREM Code will incorporate the description of the following phenomena :

- Natural convection in liquid Corium.

- Evolution of the crust of solid Corium.

- Thermal behavior of core catcher (Melt of sacrificial layer and steel).

- Boundary conditions (water cooling and radiation).

- Thermo-mecanical behavior.

At the present time, preliminary computations with the TRIO Code [16] have shown that the present numerical technics at CEA allow to successfully handle models with conduction, radiation in non participating media, phase change, and natural convection in incompressible, turbulent viscous flow.

## 9. CONCLUSION

The work already performed by CEA/DMT on the behavior of reactor containments under extreme conditions has lead to significant results. Analytical tools were developed and validated to assess the safety of structures and quantify the margins of current design methods with respect to ultimate behavior. However, the recent safety requirement to take extremely severe accidents into account at the design level implies further work. Therefore, conceptual studies as well as development of new analysis methods will have to be undertaken.

## REFERENCES


[1] Roche, R., Hoffmann, A., Global plastic model for computerized structural analysis, Paper L 5/5, SMiRT N° 4, San Francisco, 1977.

[2] Combescure, A., and al, Global methods for reinforced concrete slabs, Proc. Conf. on Inelastic Behavior of Plates and Shells, Rio de Janeiro, 1985.

[3] Gauvain, J., and al, Tests and calculation of the seismic behavior of concrete structures, Paper K13/1, SMiRT N° 5, Berlin, 1979.

[4] Bairrao, R., and al, A global model for reinforced concrete beams under alternate loading, SMiRT N° 9, Lausanne, 1987.

[5] Jeanpierre, F., and al, Système CEASEMT - Ensemble de programmes de calcul de structure à usage industriel, Note CEA-N-1938, 1976.

[6] Lepareux, M., and al, PLEXUS - A general computer Program for fast dynamic analysis, SMiRT N° 8, Brussels, 1985.

[7] Hoffmann, A., and al, Ultimate flexural behavior of reinforced concrete shells under static and dynamic loadings, Paper J1/8, SMiRT N° 8, Brussels, 1985.

[8] Lepareux, M., and al, Ultimate behavior of reinforced concrete shells under static and dynamic loading, Paper J4/4, SMiRT N° 9, Lausanne, 1987

[9] Lepareux, M., Bung, H., Matheron, P., Comportement des structures sous impacts, "Calcul des structures et Intelligence Artificielle", PLURALIS, Vol. 3, 1989.

[10] Jamet, P, and al, Concrete model for finite element analysis of structures subjected to severe damages, Proc. Conf. Structural Analysis and Design of Nuclear Power Plants, Porto-Alegre, 1984.

[11] Jamet, P., and al, Perforation of a concrete slab by a missile - A finite element approach, Paper J7/6, SMiRT N° 7, Chicago, 1983.

[12] Millard, A., and al, Pre-test analysis of the Sandia reinforced concrete containment model, CEA/DMT Report 87/053, 1987.

[13] Millard, A., and al, Analysis of the Sandia 1/6th scale concrete containment model using the CASTEM Finite Element System., SMiRT N° 9, Lausanne, 1987.

[14] Forestier, A., Goldstein, S., On two aspects of hydrogen risk, CEA/DMT Report 87/224, 1987.

[15] Forestier, A., Goldstein, S., Calculations of blast loading on a containment due to an internal air-hydrogen detonation, SMiRT N° 8, Brussels, 1985.

[16] Magnaud, J-P., Goldstein, S., The Finite Element version of the TRIO Code, 7th International Conference on Numerical Methods in Fluids Mechanics, Huntsville, 1989.

[17] Ni, X.M., Gantenbein, F., Petit, M., A finite element method for soil structure interaction time history calculations, SMiRT 10, Los Angeles, 1989.

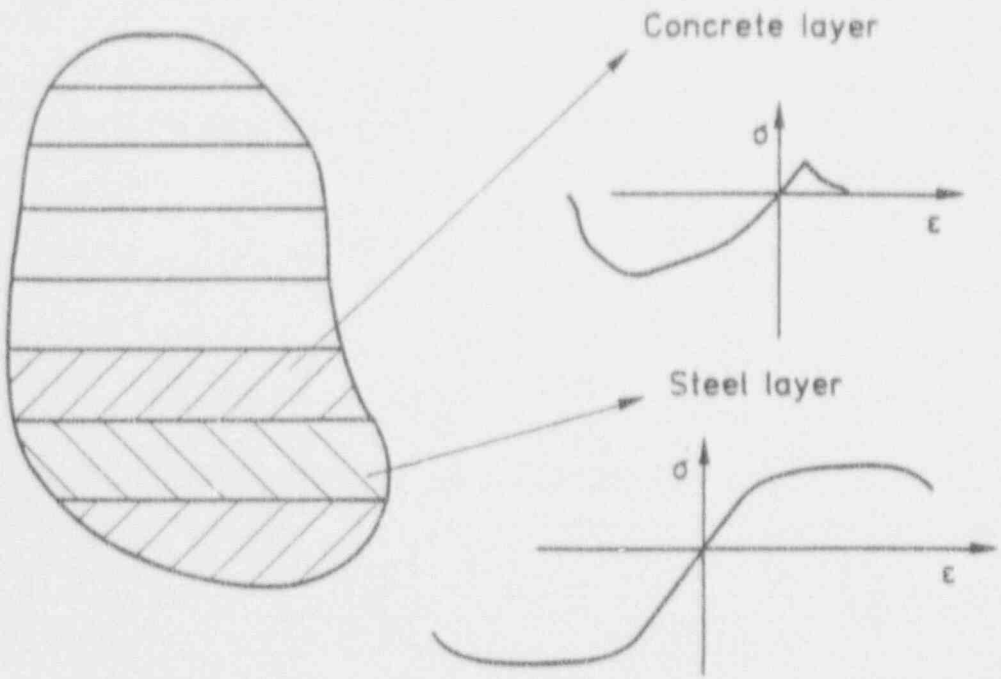


Fig. 1 - DISCRETIZATION OF A BEAM CROSS SECTION

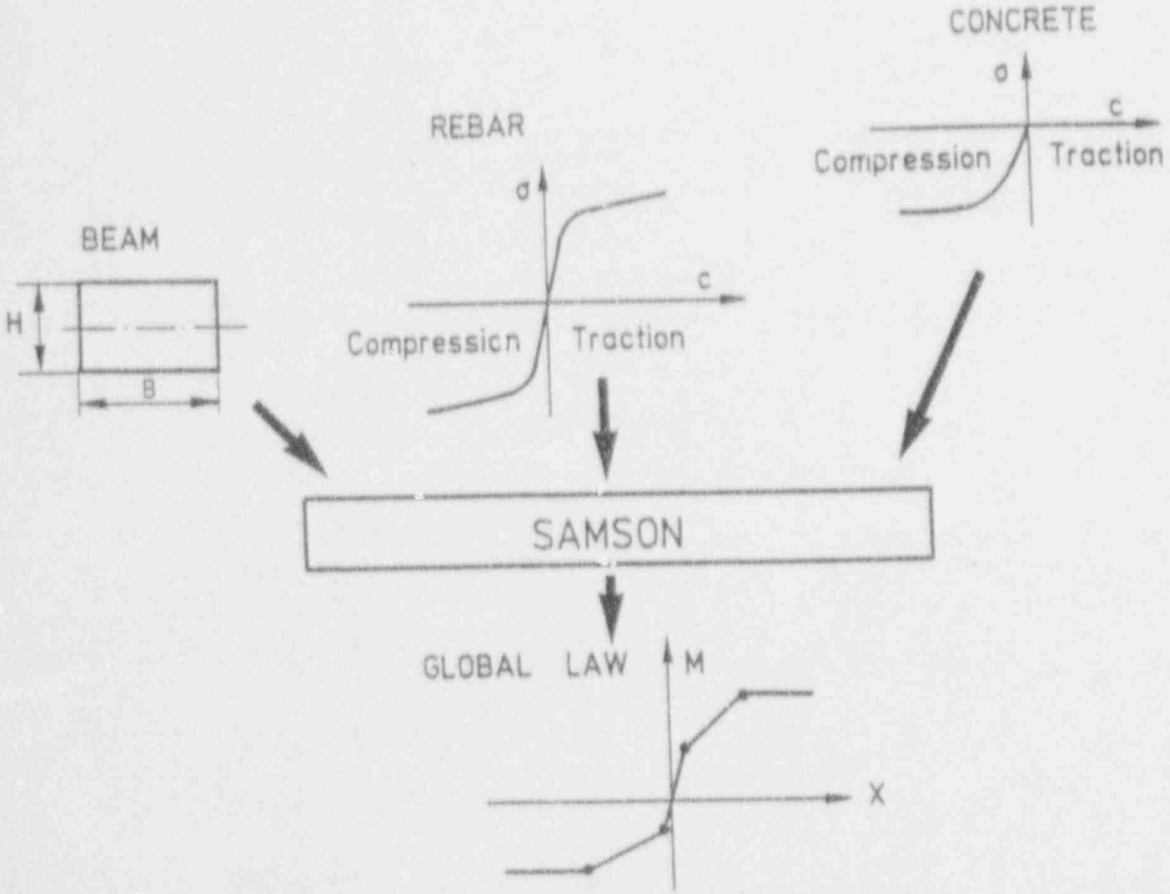


Fig. 2 - HOMOGENEIZATION TECHNIC

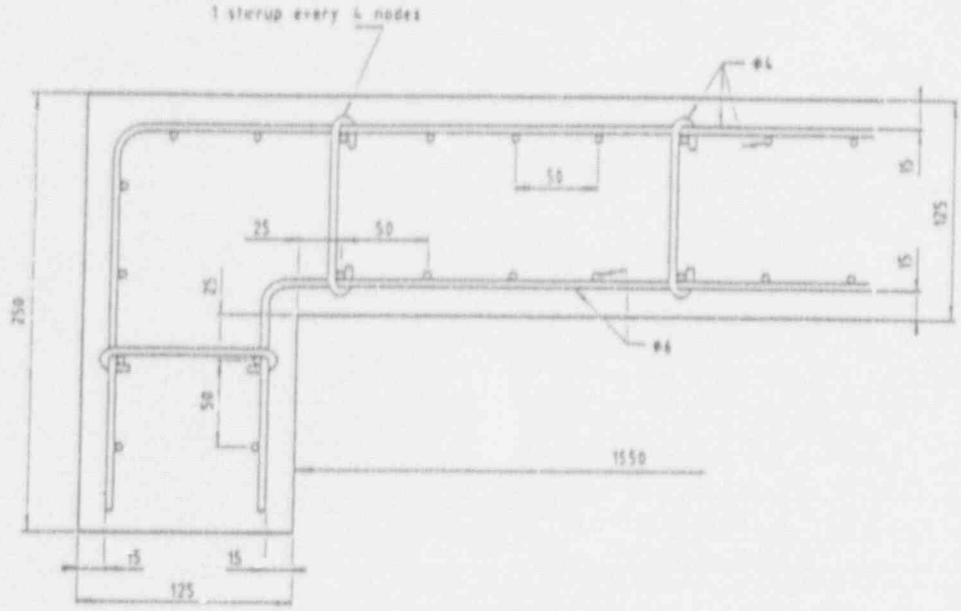


GEOMETRY AND REINFORCEMENT OF
THE EXPERIMENTAL SLABS

Fig. 3

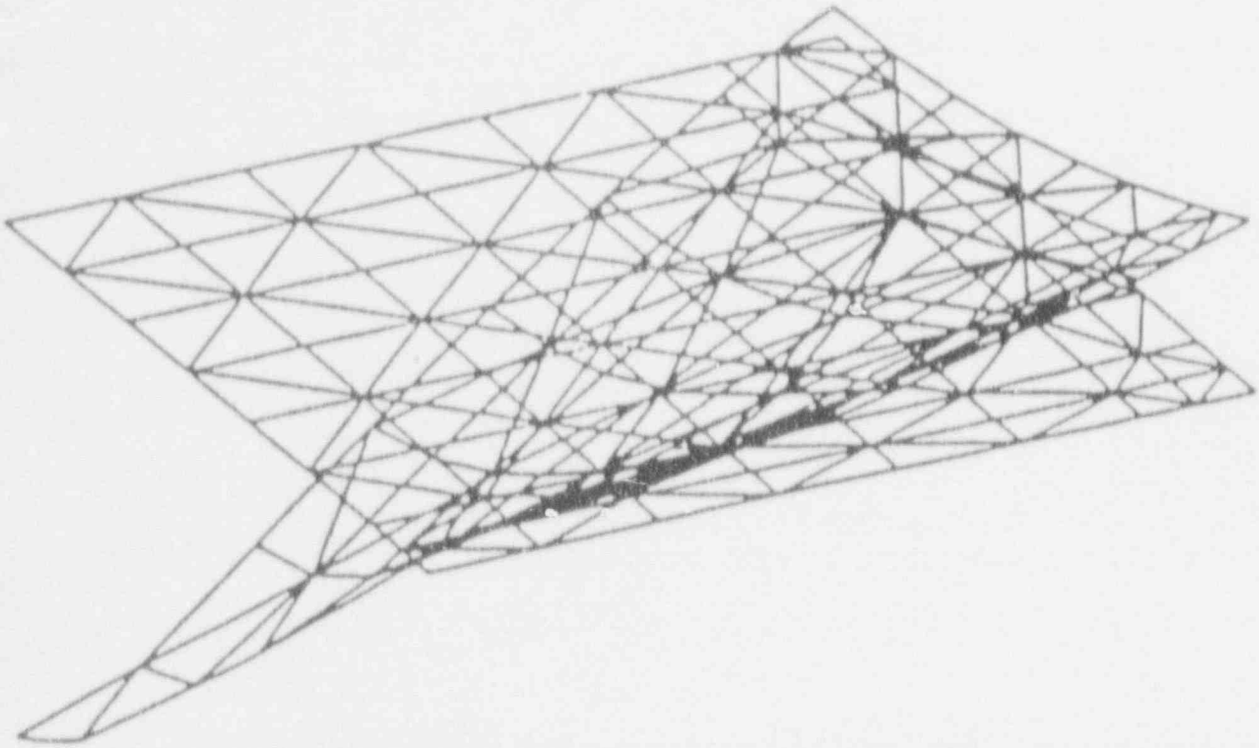

MAGNIFIED DEFORMED SHAPE OF THE
SLAB AT MAXIMUM LOAD

Fig. 4

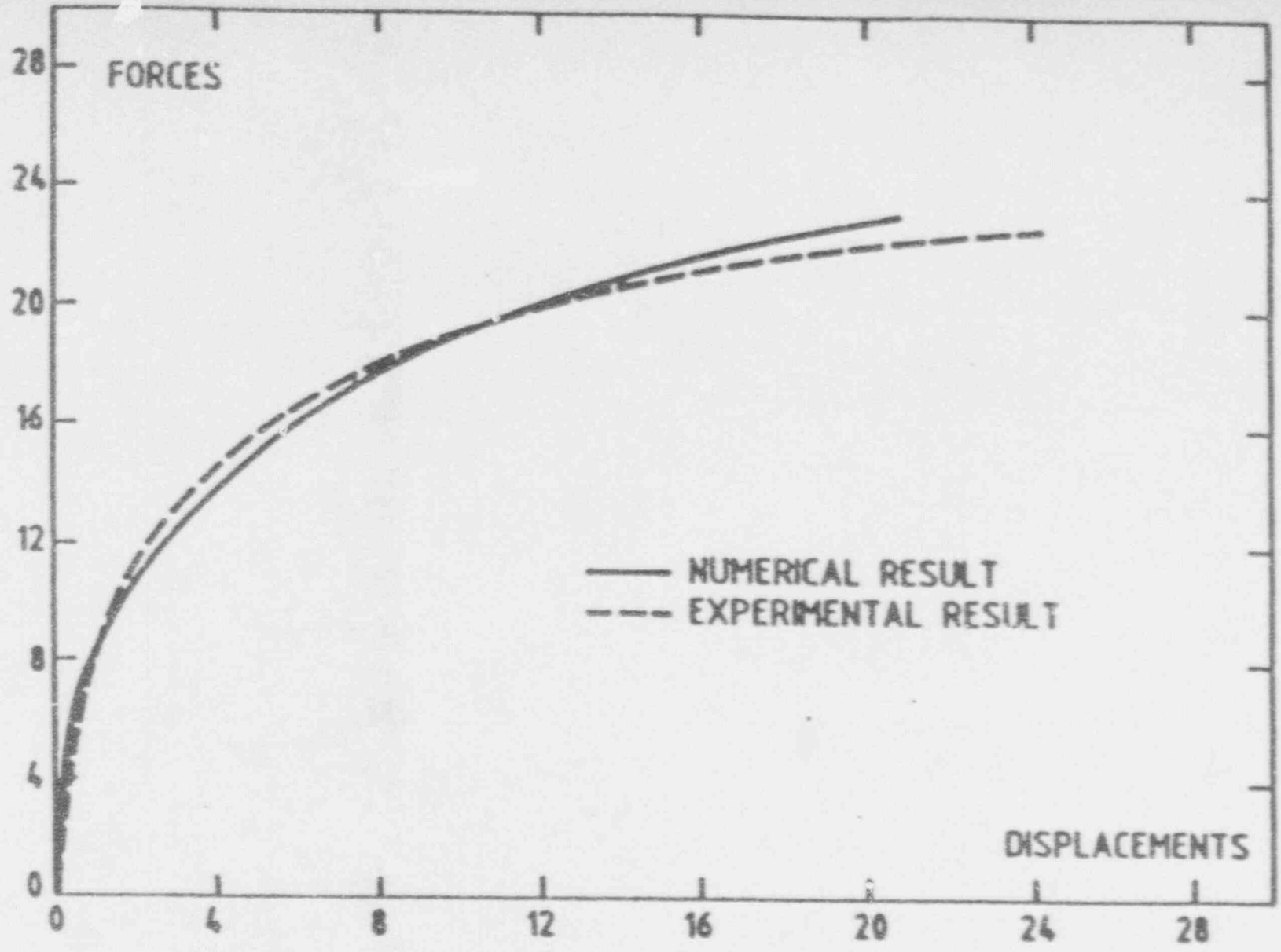


NUMERICAL AND EXPERIMENTAL FORCE-DISPLACEMENT CURVES AT THE CENTER OF THE SLAB

Fig. 5

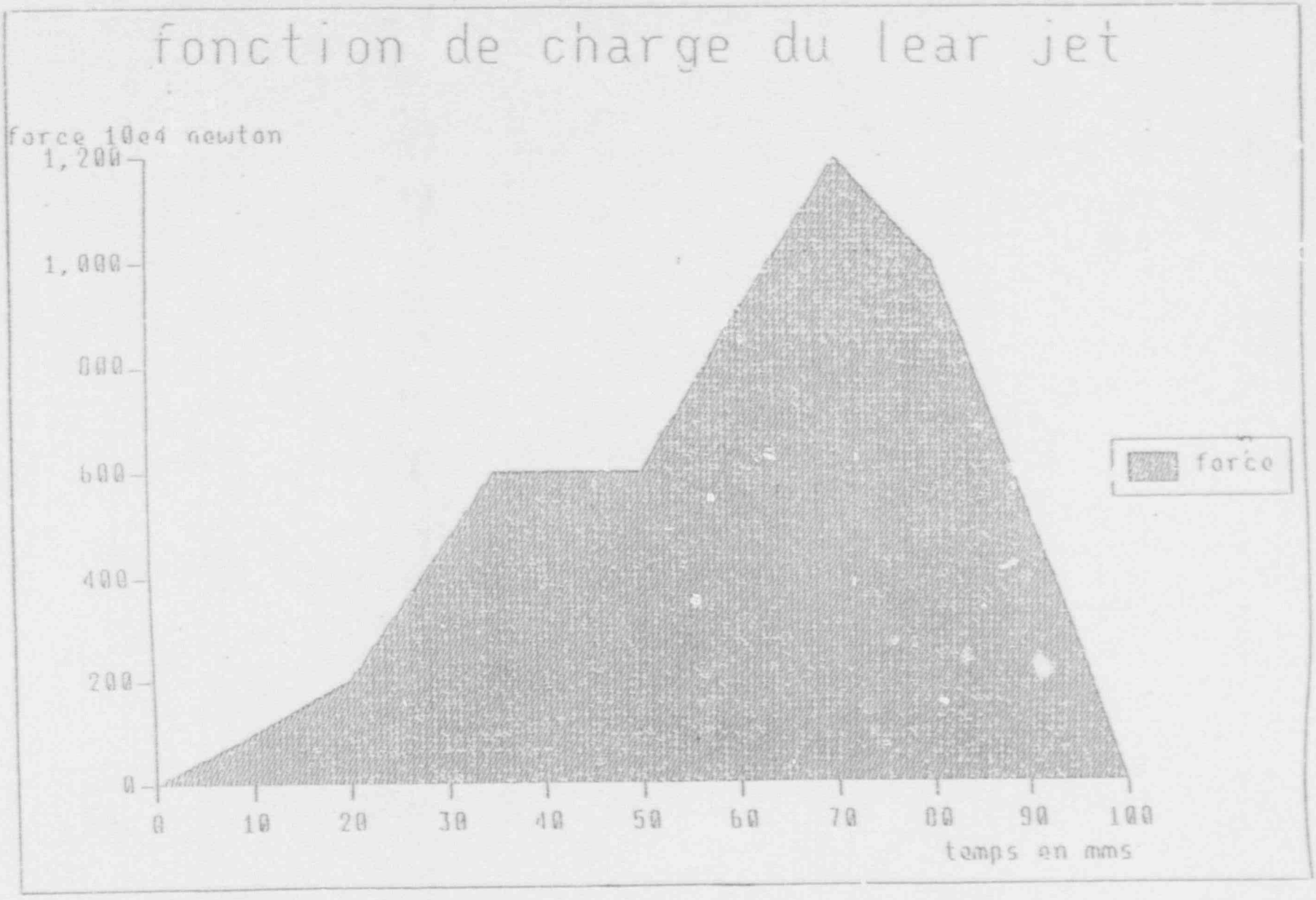
fonction de charge du lear jet
force 10e4 newton
1,200
1,000
800
600
400
200
0
0
10
20
30
40
50
60
70
80
90
100
temps en mms
force

Fig. 6

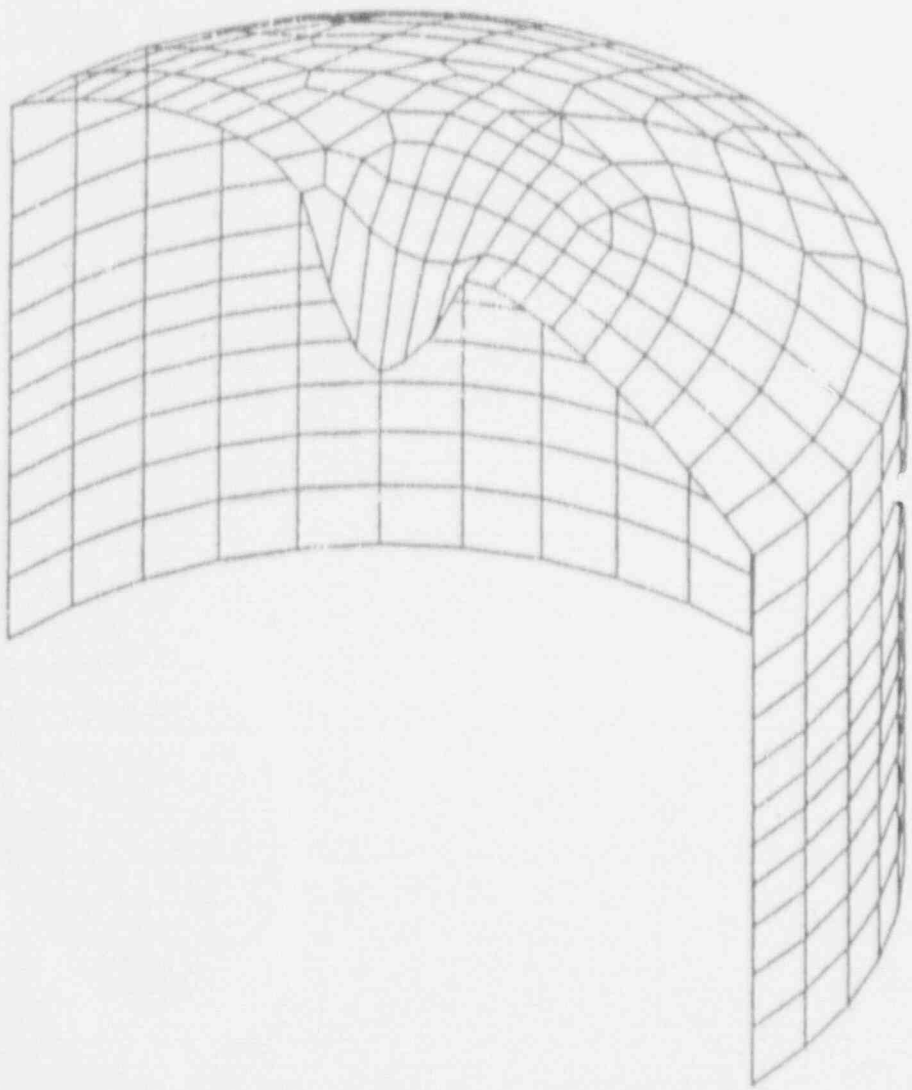

Fig. 7
Top impact of [illegible] Jet on a containment

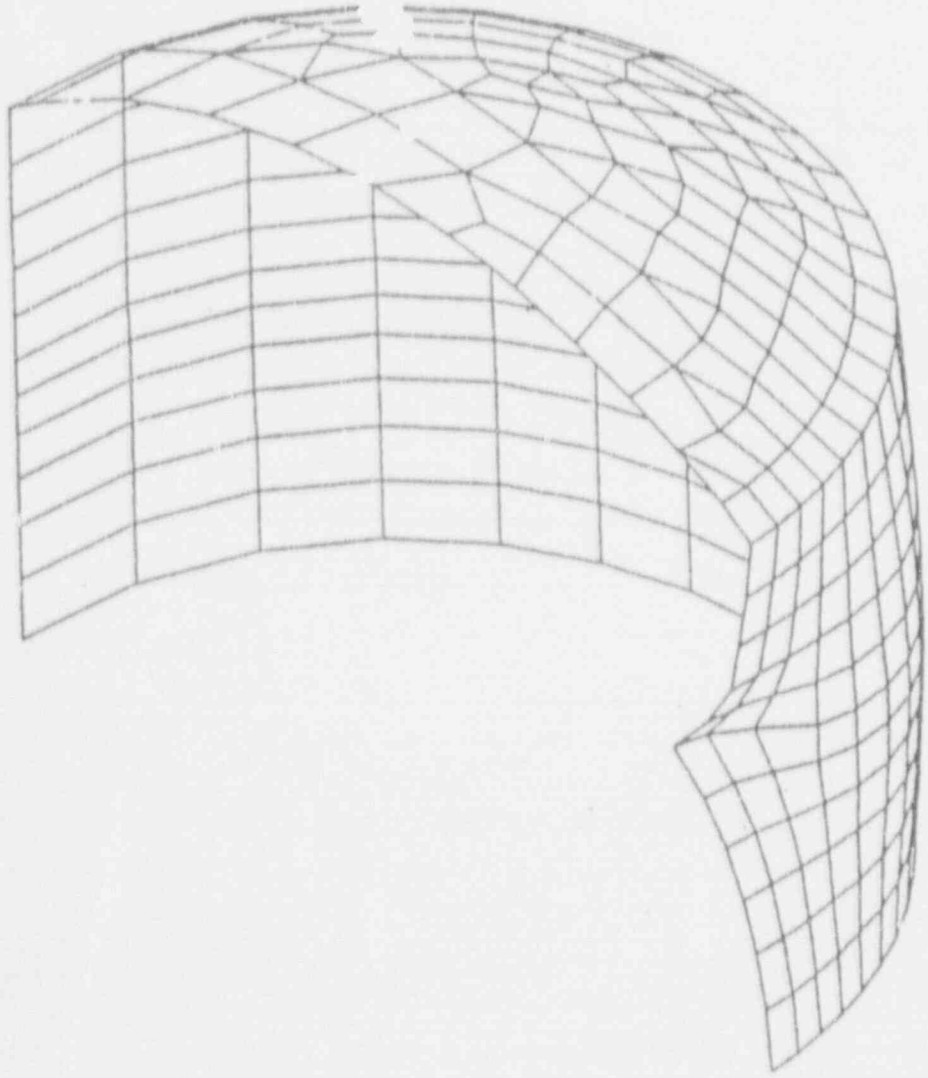

Fig. 8
Lateral impact of a Lear Jet on a containment

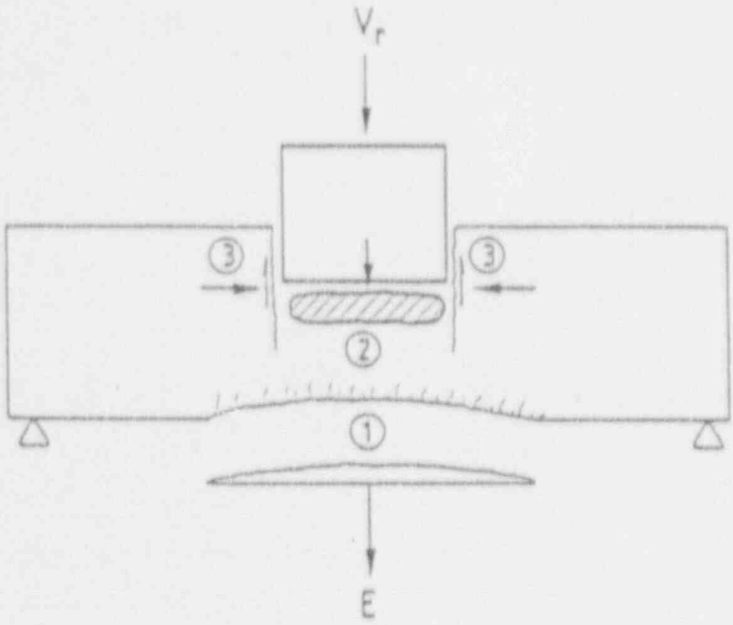


3 DAMAGE PROCESSES

- TENSION (1)
- CRUSHING (2)
- SHEAR (3)

Fig. 9
Perforation of a plain concrete stal by a rigid missile

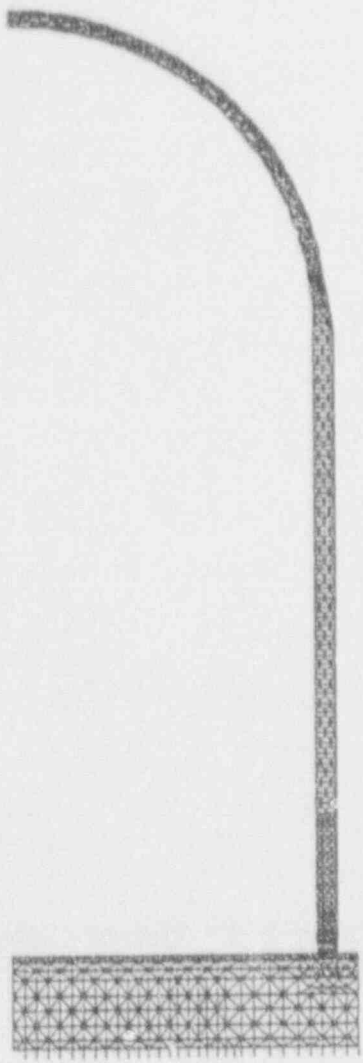

Fig. 10
Mesh of the containment

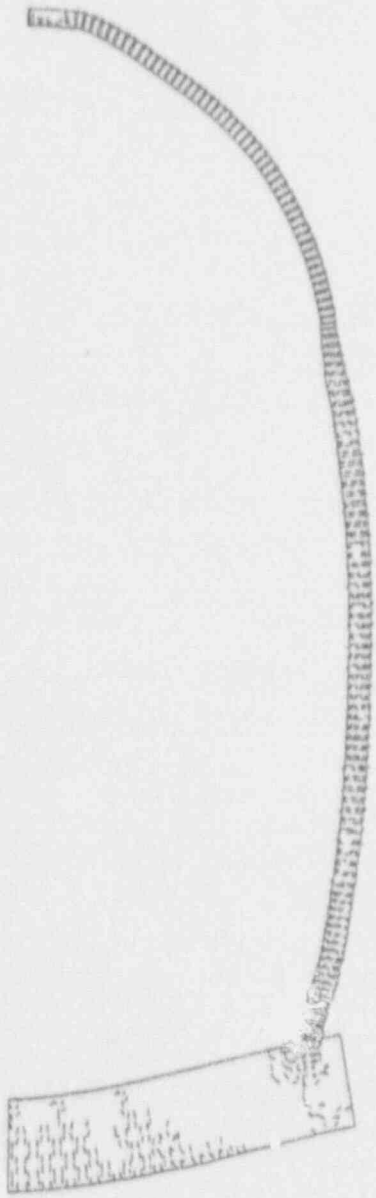

Fig. 11
Cracks pattern for 0.98 MPa pressure

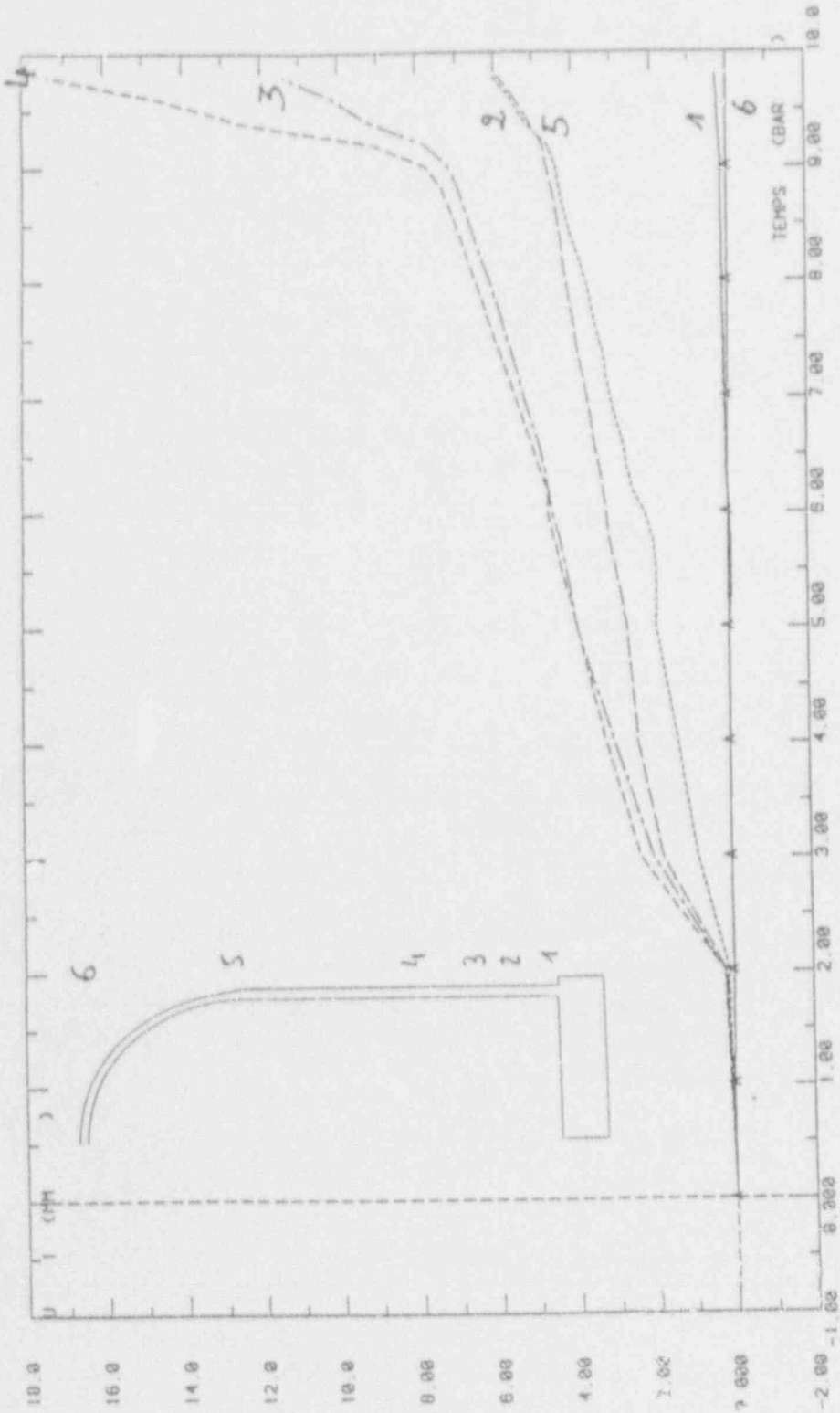


Fig. 12
Radial displacements versus pressure

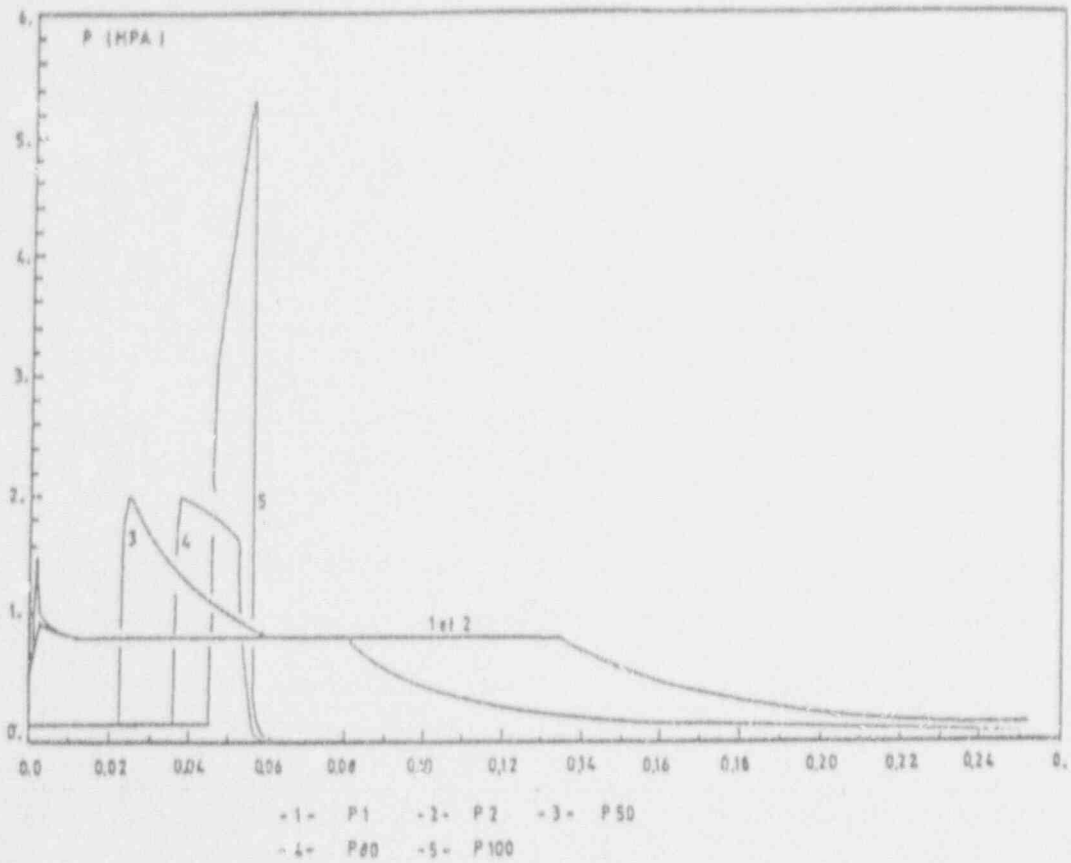


Fig. 13
Pressure versus time at various locations

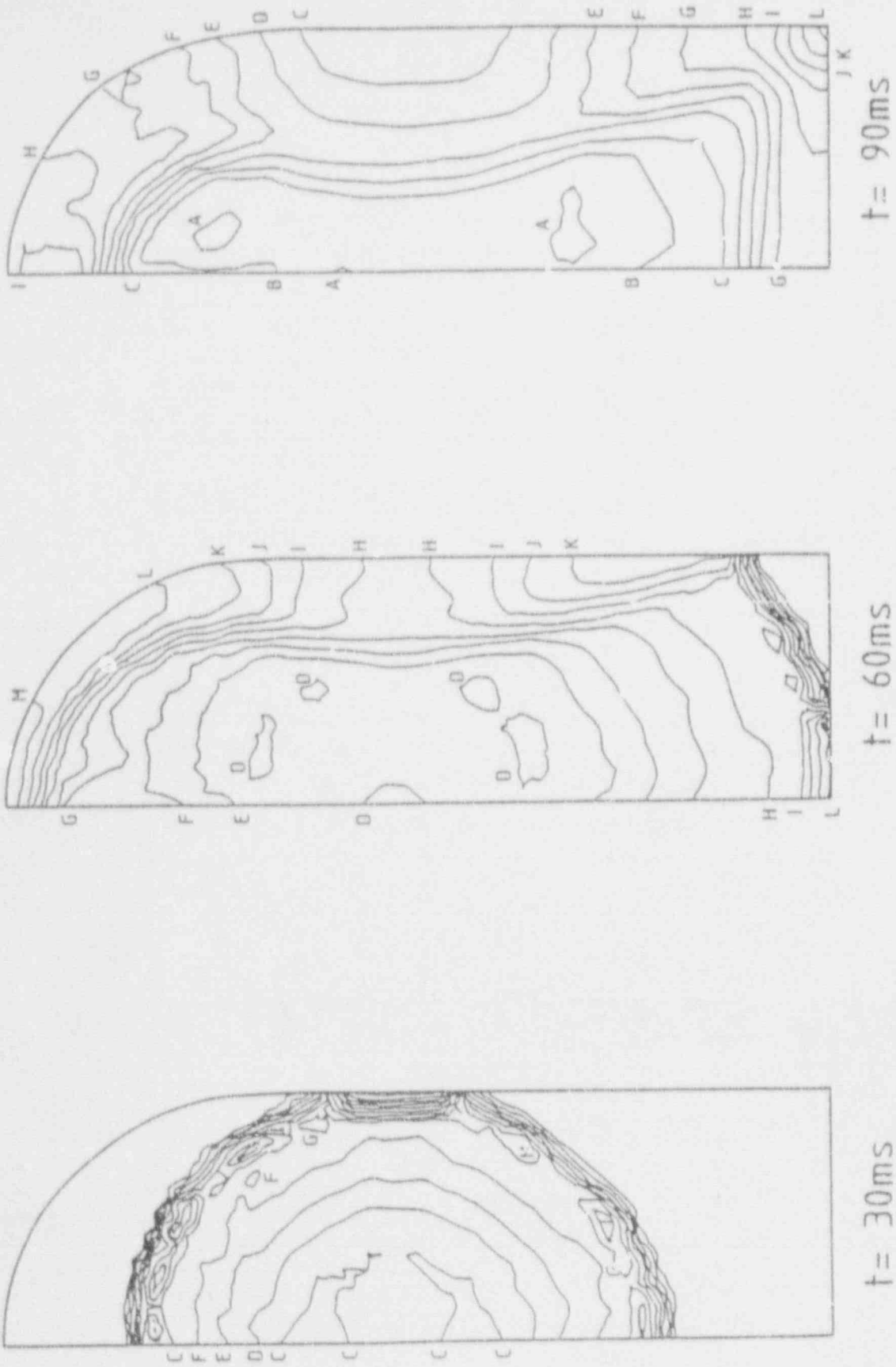


Fig. 14
Detonation of an air--hydrogen mixture inside a containment

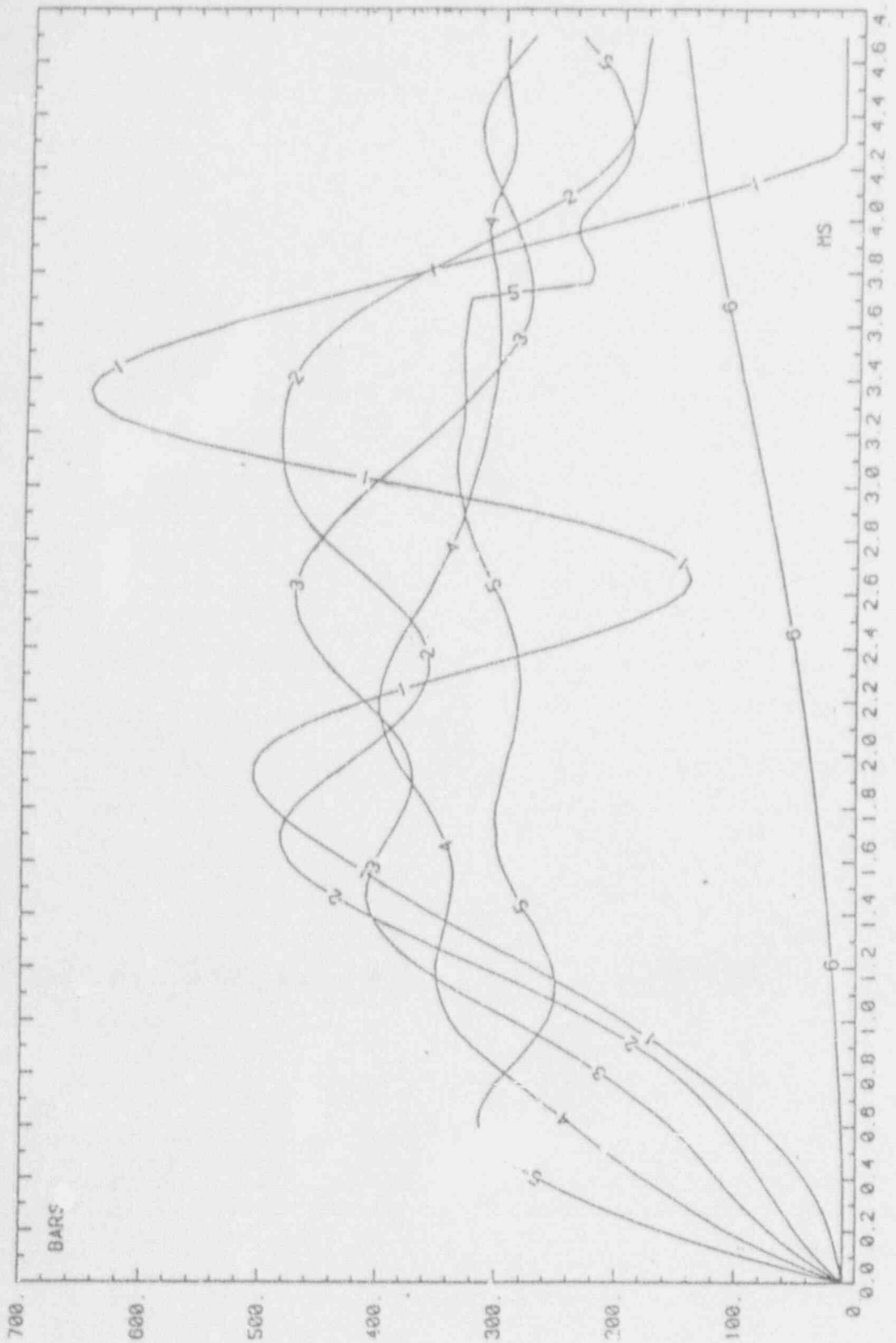


Fig. 15
Evolution of pressure on the bottom of the vessel

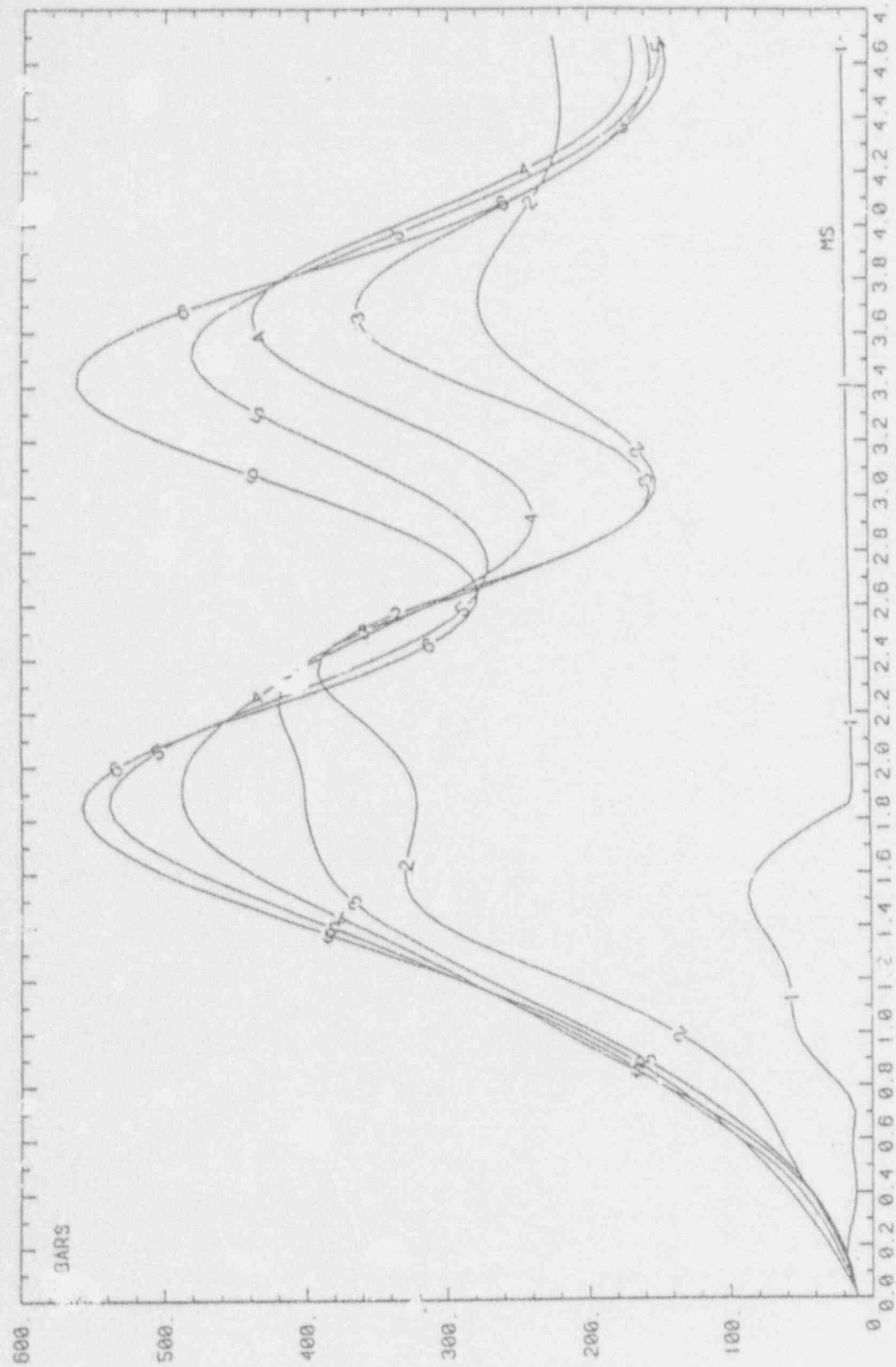


Fig. 16
Evolution of pressure in water

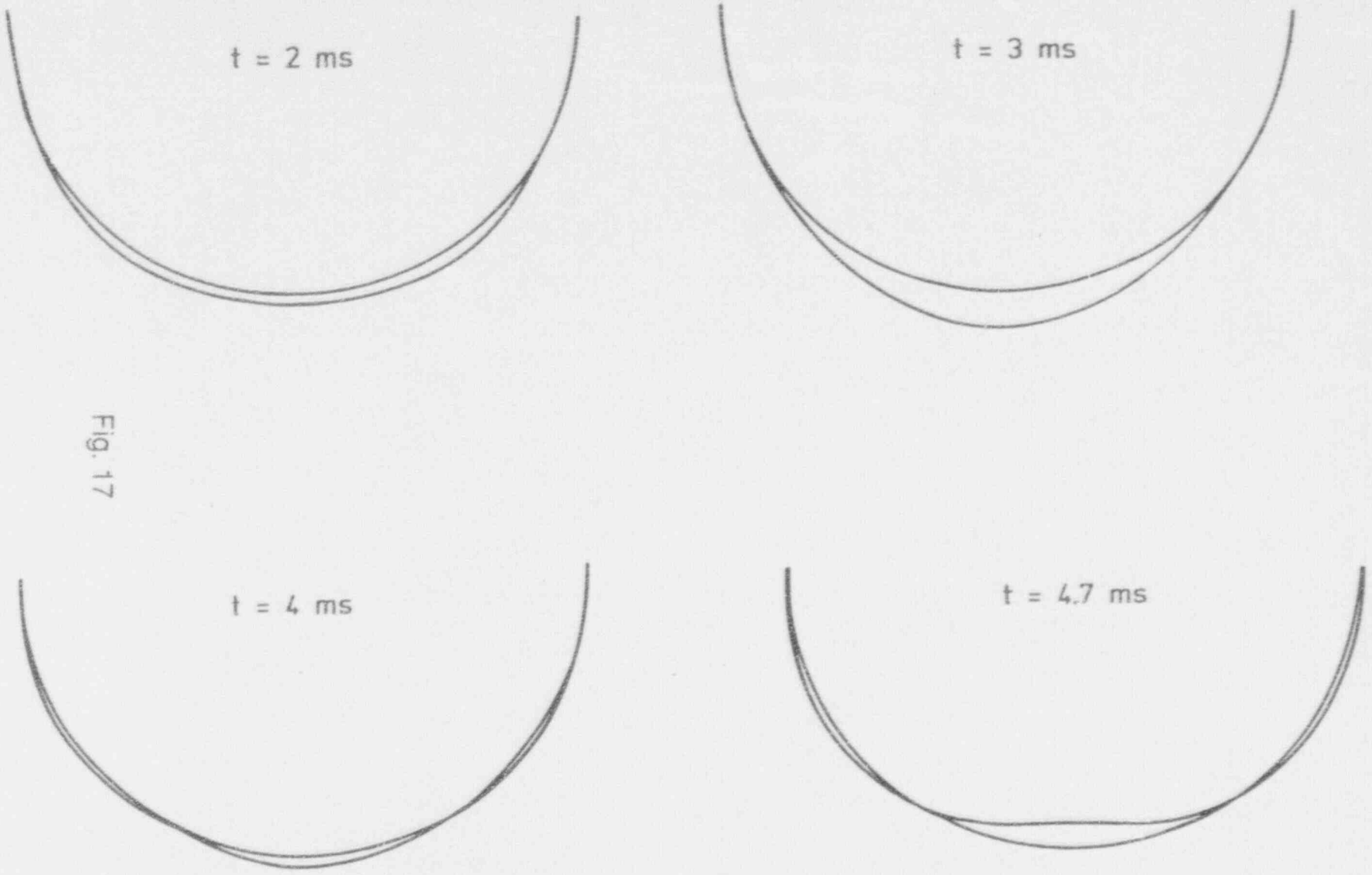


AMPLIFIED DEFORMED SHAPE (× 20)

Fig. 17

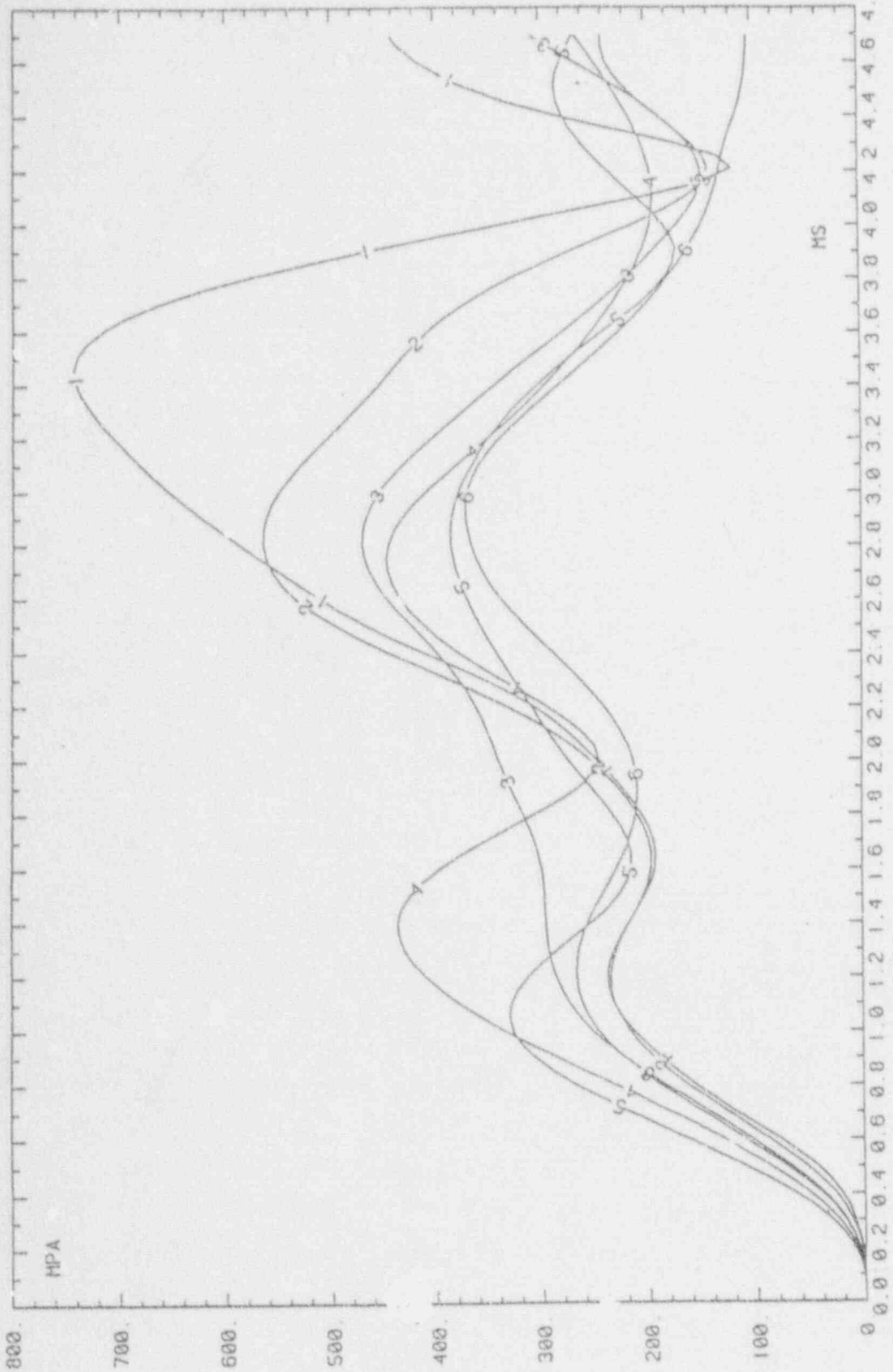


Fig. 18
Evolution of equivalent Von Mises stress in the vessel

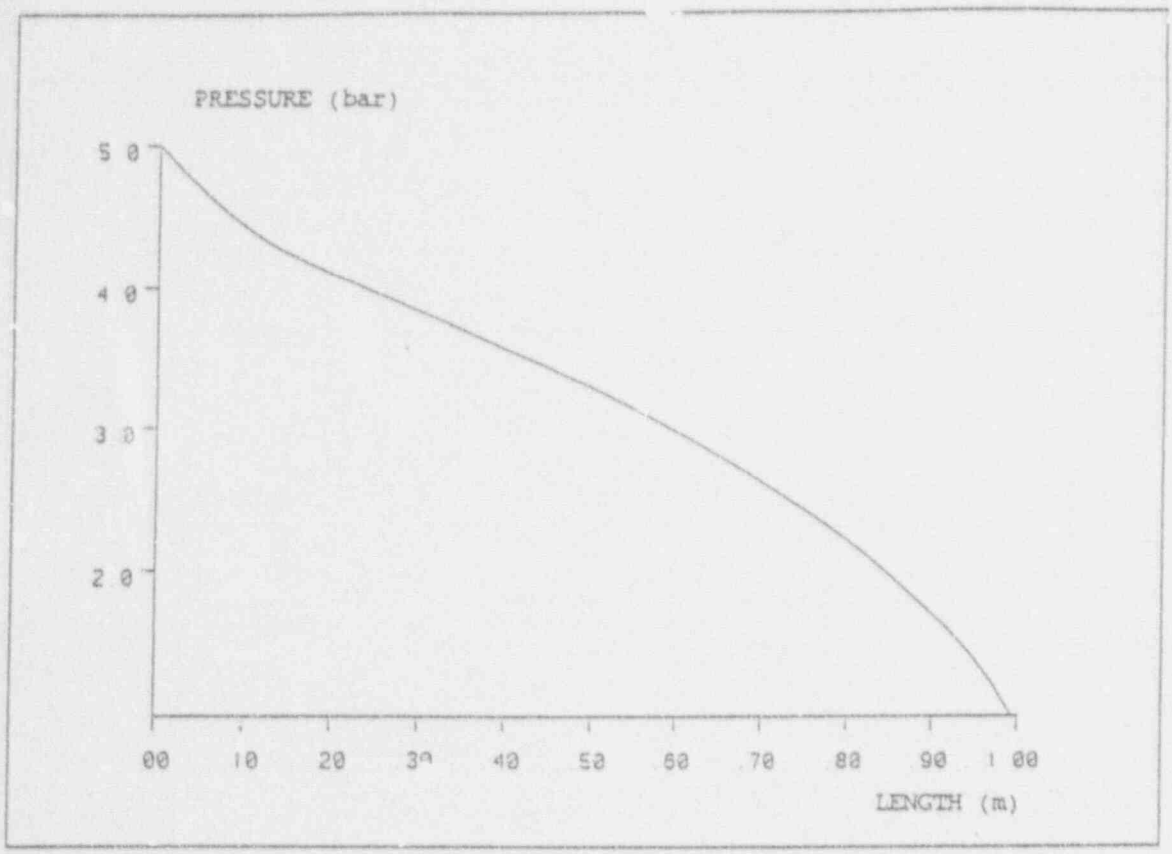


Fig. 19
Pressure profile along the crack

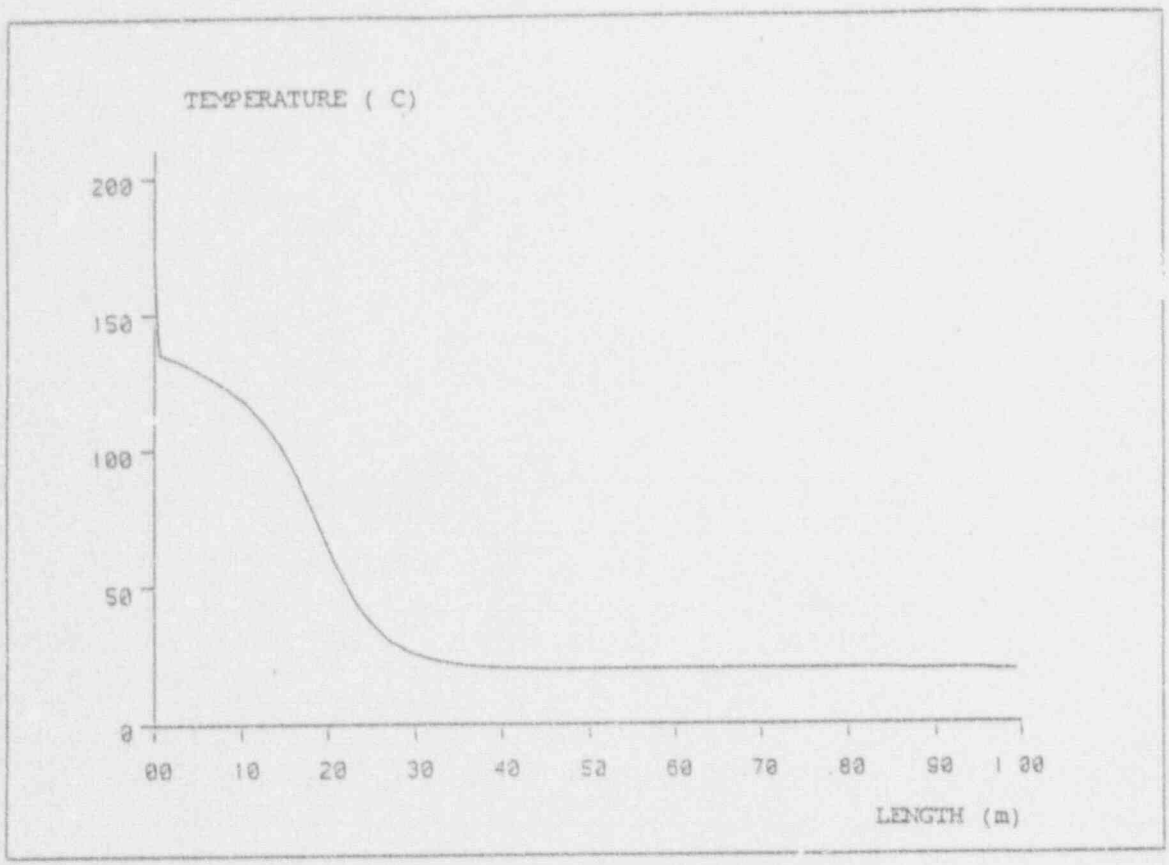


Fig. 20
Temperature profile along the crack

Fig. 21

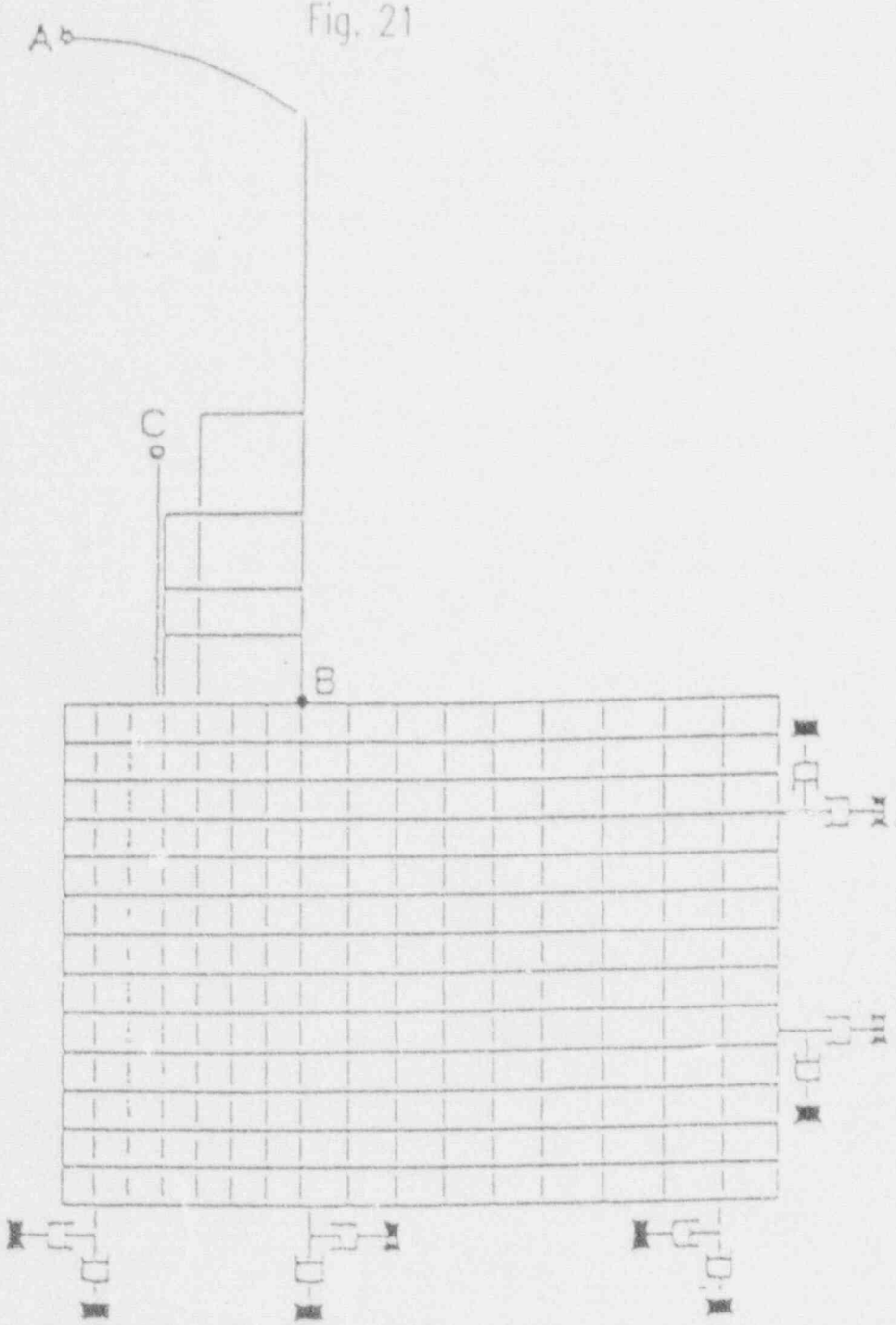


Building and soil model

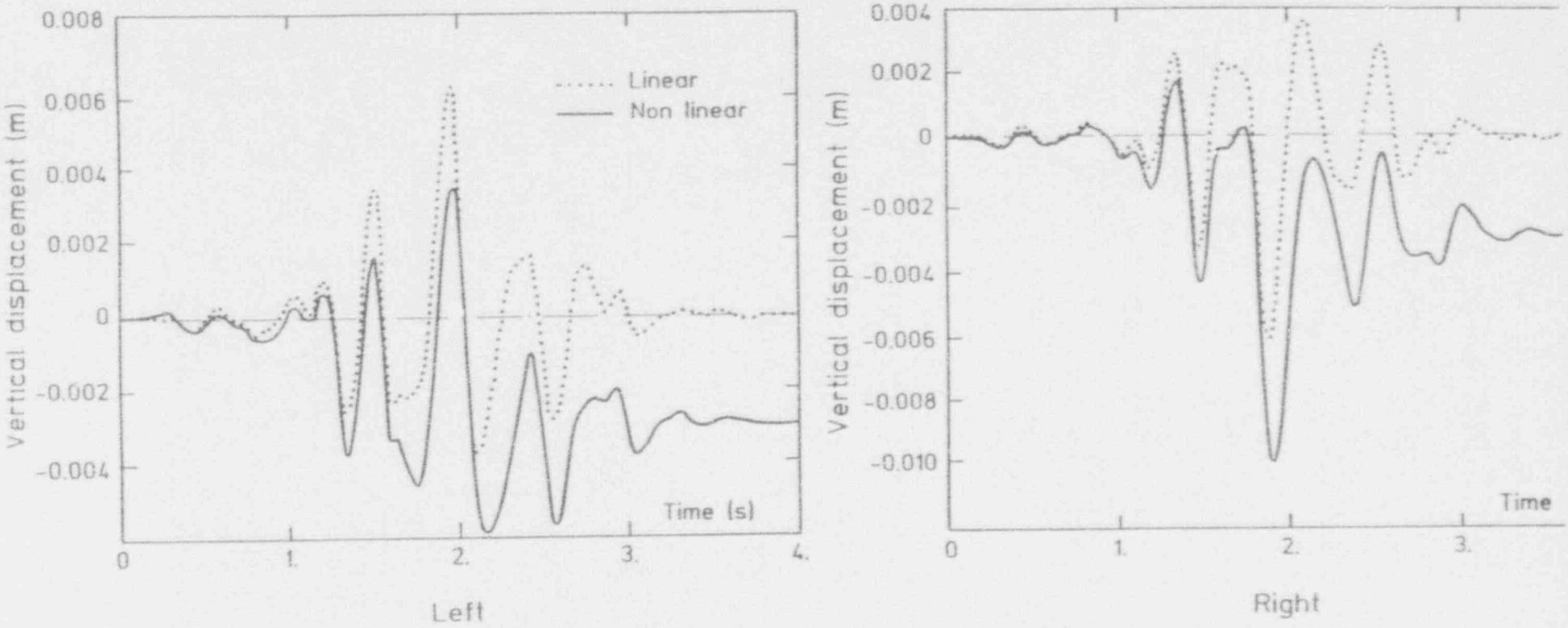


NON-LINEARITY EFFECT ON THE BASEMAT
VERTICAL DISPLACEMENT

Fig. 22

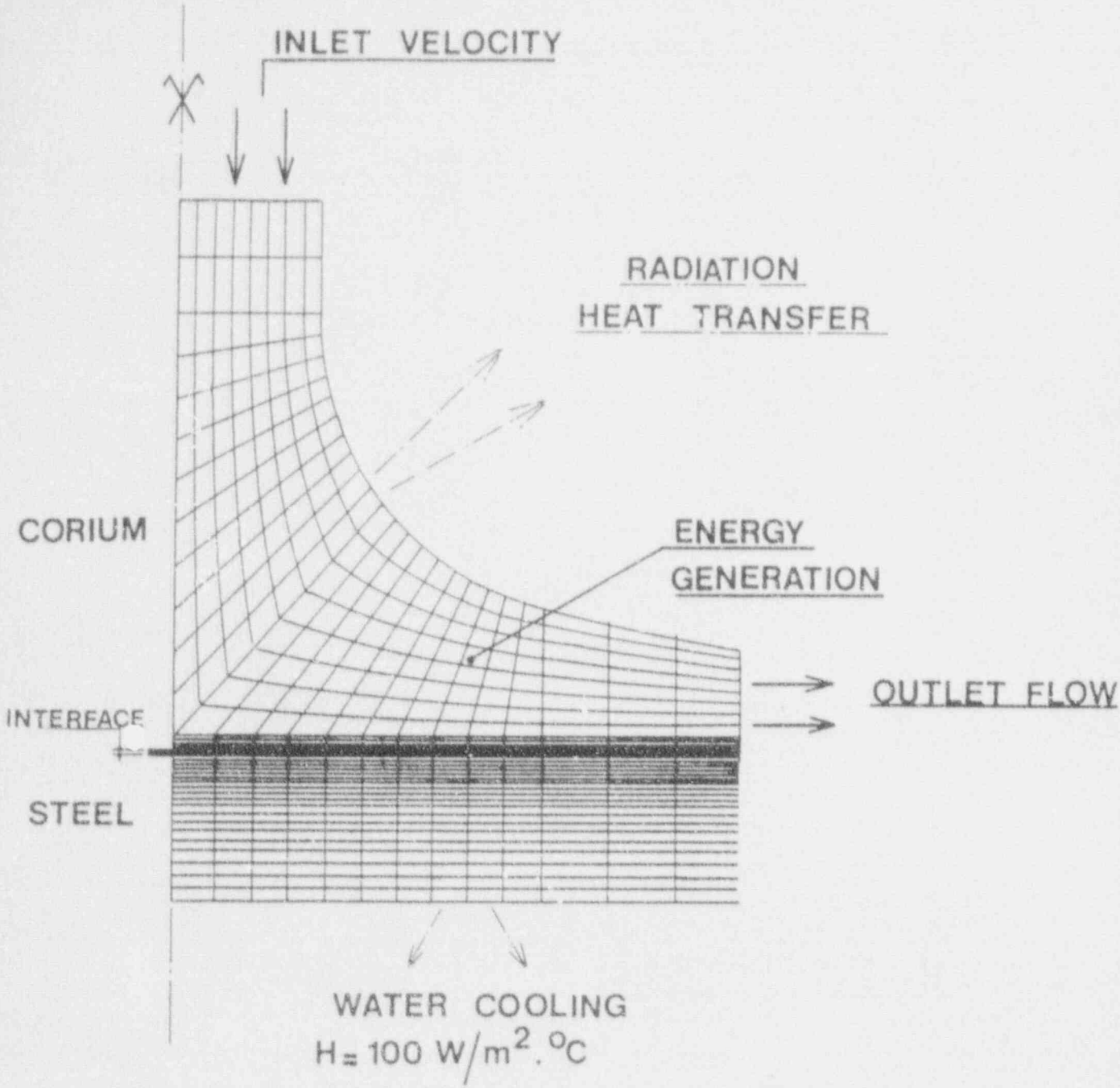


FIGURE 23 - MODEL USED TO STUDY CORIUM JET IMPINGEMENT ON STEEL PLATE

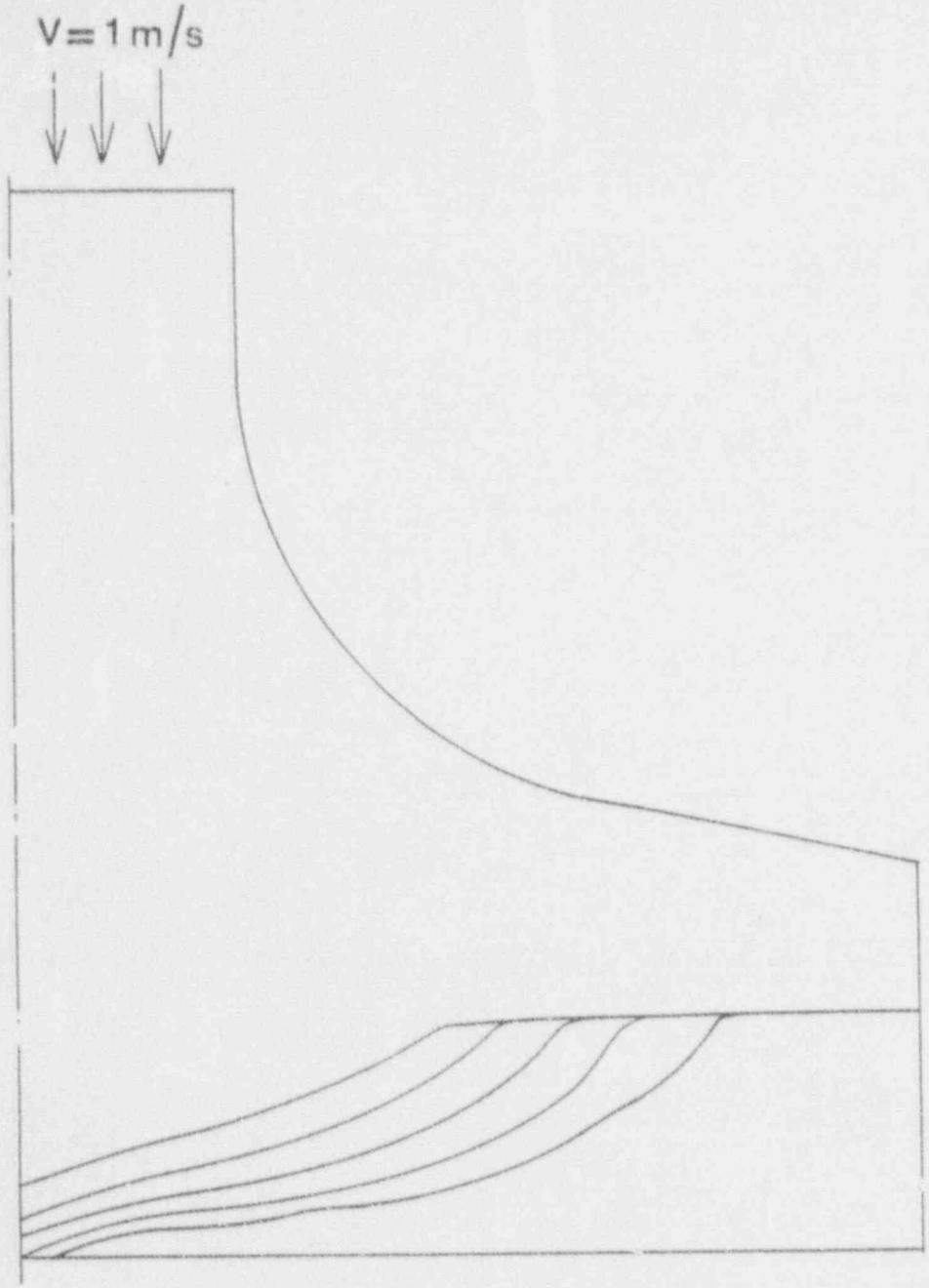


FIGURE 24 – PROGRESSION OF PLATE MELTING

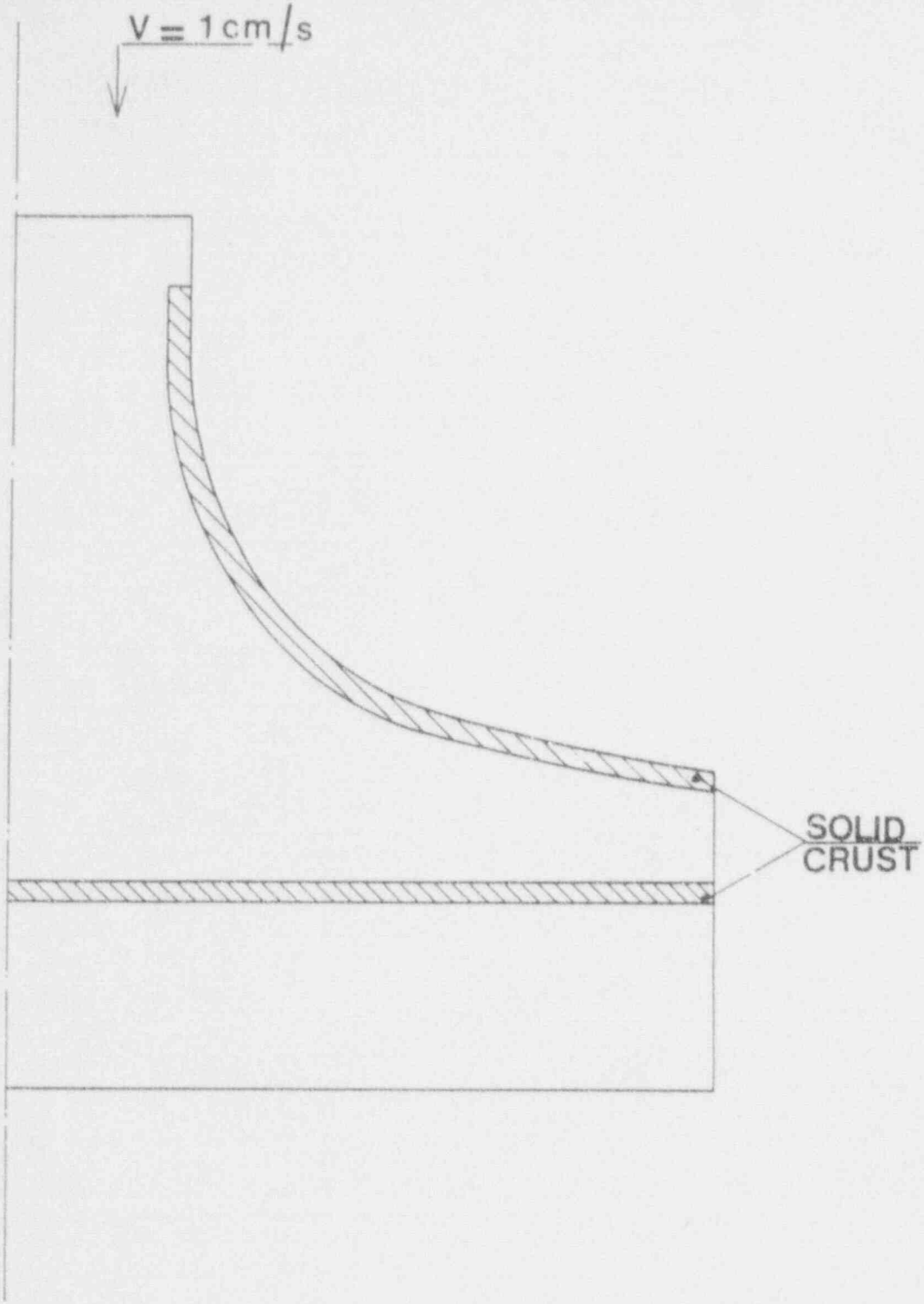


FIGURE 25 – FORMATION OF CRUST AT INTERFACES

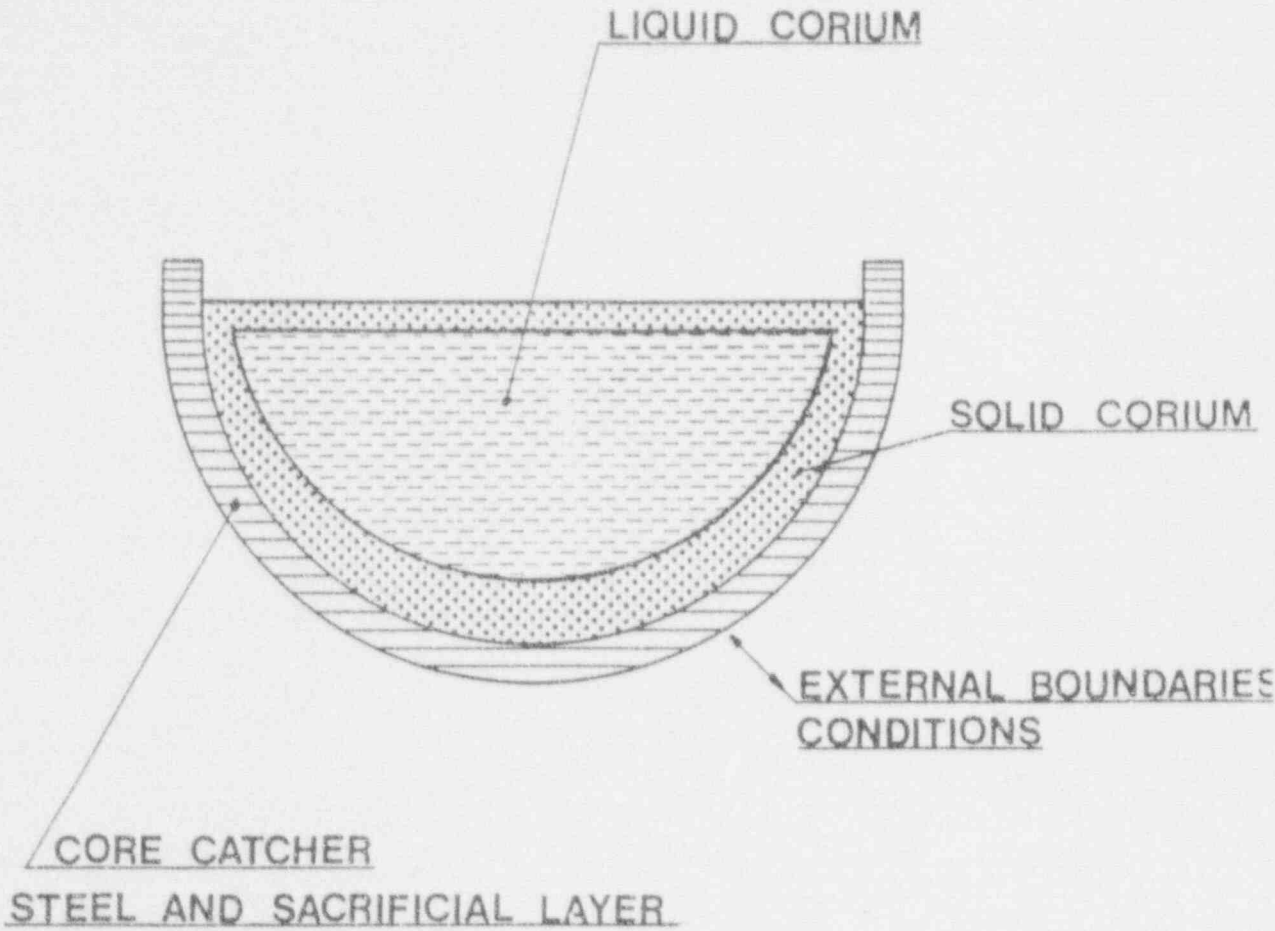


FIGURE 26 - TYPICAL CORE CATCHER SITUATION

# CREEP RUPTURE FAILURE IN A MARK I CONTAINMENT WITH A NEW THERMAL FAILURE MATERIAL MODEL

John C. Castro
Robert A. Dameron
Joe R. Rashid

ANATECH Research Corp

## Abstract

Recent failure probability studies of Mark I containments use the steel melting temperature as the failure criterion. However the possibility of creep rupture could lead to failure at lower temperatures. The present analysis uses a thermo-mechanical failure criterion that takes creep rupture into account. The analysis considers the local interaction of the shell with the surrounding concrete floor and shield building. Applied temperature and pressure boundary conditions for the liner are determined from previous studies by the University of California at Santa Barbara. The analysis focuses on the potential failure of the containment shell near the shell-concrete base juncture when the shell is subject to contact with corium during a severe accident. Material data for the response analysis and failure evaluation were obtained from INEL and EPRI. A rate-dependent viscoplastic constitutive model was developed which uses data for both the response analysis and creep rupture evaluation. The model is capable of tracking the material response throughout its history from the low temperature, purely elastic regime to the very high temperature, low strength, large strain rate regime. The 2D results indicate that creep rupture could occur at temperatures close to 1100°C. A more realistic 3D analysis could result in higher creep rupture temperatures depending on the size and distribution of the shell-corium contact surface. This analysis, however, has not yet been completed.

## INTRODUCTION

This paper presents results of an investigation of Mark I Containment failure behavior under a postulated severe accident scenario in which the molten corium contacts the containment shell near the shell-concrete base juncture. NUREG/CR-5423 [1] investigates the thermal problem in detail and provides the pressure and temperature histories used as input in the present work.

The general arrangement of Mark I containments is shown in Figure 1 with a schematic of an assumed corium-shell contact configuration. Such a condition, even with water present, can potentially lead to liner melt-through. Previous investigations of the Melt Through Issue have focused mainly on heat transfer and chemical processes. These processes include calculation of shell temperature distributions, the quantification of corium/crust volume and distribution, boundary conditions consistent with corium attack of the concrete and primary shell, and thermal and chemical reaction calculations of corium concrete interaction. The present work focuses on structural analysis and creep rupture evaluation.

To accurately model the high temperature structural response of the Mark I containment liner, a physically descriptive constitutive model is required which accounts for the rate-dependent deformations of the shell. Furthermore, local effects induce strain concentrations and can thus govern the shell's failure time. These effects demand very detailed finite element computational grids, well-posed thermal and mechanical boundary conditions

and proper accounting for the interaction of the steel shell with the concrete floor and the shield wall. The analysis addresses these requirements to the extent allowed by the availability of material data.

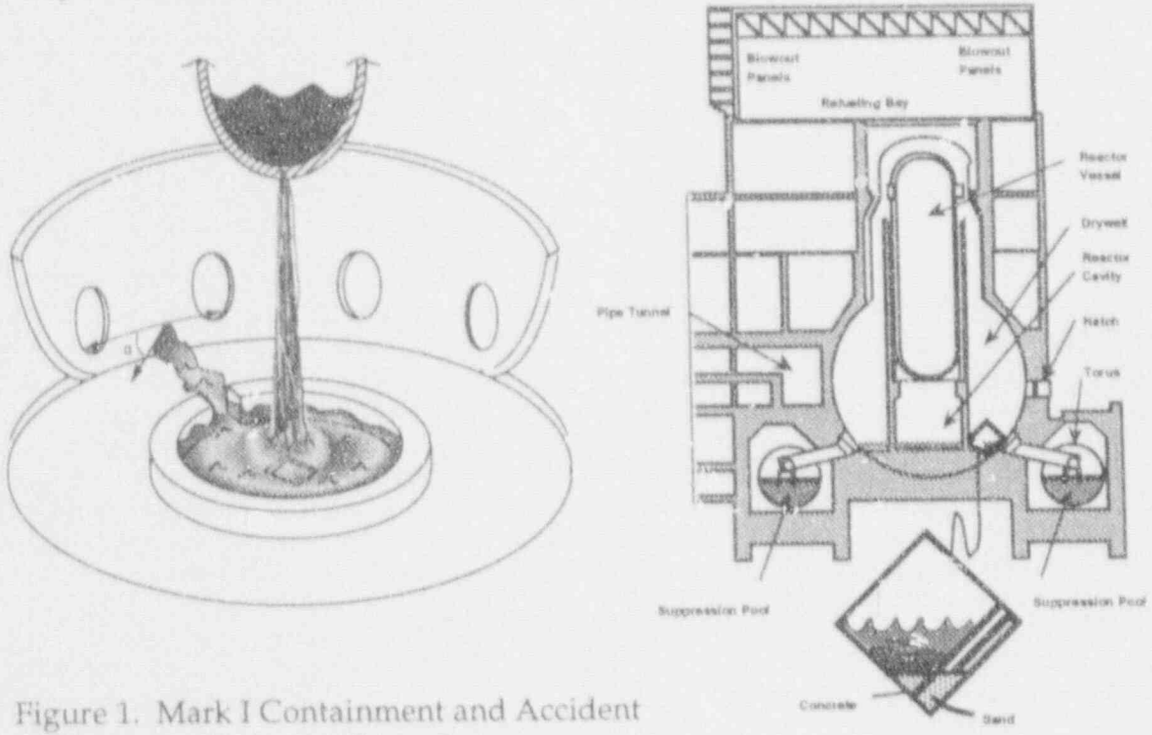


Figure 1. Mark I Containment and Accident Scenario Configuration

The present investigation makes use of high temperature properties data, including yield strength, elastic modulus, creep rates and creep rupture times. Two sets of data were utilized: one is from the INEL test program for reactor vessel lower head failure evaluation [2], the other is from an EPRI sponsored research program on high-temperature properties of reactor vessel steels [3]. These two sets of data were analyzed and mathematically fit consistently with the constitutive model parameter requirements. The data and curve fitting procedures are described in Reference 4.

A high-temperature failure model that predicts shell rupture as function of time and temperature was developed based on the cumulative damage concept. This damage model uses the Larson-Miller parameter as the failure criterion. One should note, however, that the experimental Larson-Miller parameter, determined under constant stress and temperature conditions, cannot be used directly in a time history analysis for failure prediction. The developed failure model makes it possible to use the Larson-Miller parameter to quantify failure in the form of a damage index; a value of unity for the damage index implies failure. The damage index is computed incrementally and it can be plotted along with other quantities such as stress and strain. This failure model is described in detail in Reference 4.

The constitutive model that was developed for the steel shell is a rate-dependent plasticity model that makes use of high temperature creep and yield strength data developed for reactor vessel steel. This model is coded in a subroutine for use with the ABAQUS code, a widely used general purpose finite element program [5].

The present analysis considers the local interaction of the shell with the surrounding concrete floor and shield building. It applies temperature and pressure boundary conditions for the liner determined from Reference 1. The structure is modeled in two dimensions with axisymmetric geometry and loading. This assumes an axisymmetric corium-shell contact configuration although the actual shape is three-dimensional. This approximation provides lower-bound estimates for the creep-rupture temperatures that, depending upon the three-dimensional extent of the heated section, could be significantly lower than the failure temperatures predicted in a three-dimensional analysis. In the second phase of the analysis program, a three-dimensional analysis is performed. The present results are based on the two-dimensional analysis only.

## MATERIAL DATA

The Mark I containment liner is made of SA516-70 steel, and high temperature constitutive characterization of this steel is required for creep-rupture analyses. However, interest in high temperature creep rupture has focused on the reactor vessel, and thus, the data available for the present study are derived from literature characterizing reactor vessel steel, namely, SA533-B1. Besides the fact that high temperature creep data for SA516-70 steel were not available, the use of the SA533-B1 creep data can be justified on the basis that fine-grained steels behave similarly at high temperatures. Temperature dependence of the yield stress for SA516-55 steel was examined by Gowda, B.C. [6], and these data, compared with the CEI, INEL, and ASME Boiler and Pressure Vessel Code [7] data, suggest that SA516 and SA533 steels behave similarly after the phase change at 1340 °F. Since the focus of this study is on the high temperature creep rupture modes, the SA533 data are deemed adequate for the formulation of a valid creep law.

Creep data were obtained from two sources: a Combustion Engineering Inc. (CEI) report prepared for the Electric Power Research Institute (EPRI) [3], and an Idaho National Engineering Laboratory (INEL) report prepared for the U.S. Nuclear Regulatory Commission (NRC) [2]. Both reports describe high temperature creep experiments for SA533-B1 steel.

### Creep Law

Combustion Engineering performed creep experiments at moderately high temperatures ranging from 750° to 1200° F. INEL performed experiments at high temperatures ranging from 1160° to 2012° F. At each temperature, several constant stress creep tests were reported. A creep power law, shown in Equation (1), was used to fit the data: $\varepsilon_c$ is the creep strain, $\sigma$ is the applied (constant) stress in ksi, and t is the time in hours. The parameters A, r, and s are dependent on temperature but independent of stress.

$$\varepsilon_c = A\,\sigma^r\,t^s \qquad (1)$$

The parameters A, r and S were determined by applying a least squares fit to the digitized data. They were held constant with stress and strain rate and allowed to vary only with temperature. The resulting expressions for A, r and s were incorporated into the elastic-viscoplastic constitutive model. Separate fits were performed for the primary/secondary creep portion from the tertiary creep portion. Figure 2 shows the predicted curves and experimental creep data for the temperatures 1430° and 1610° F. The valid portions of the curves are the primary/secondary curve up to the intersection point with the tertiary part and then the tertiary curve.

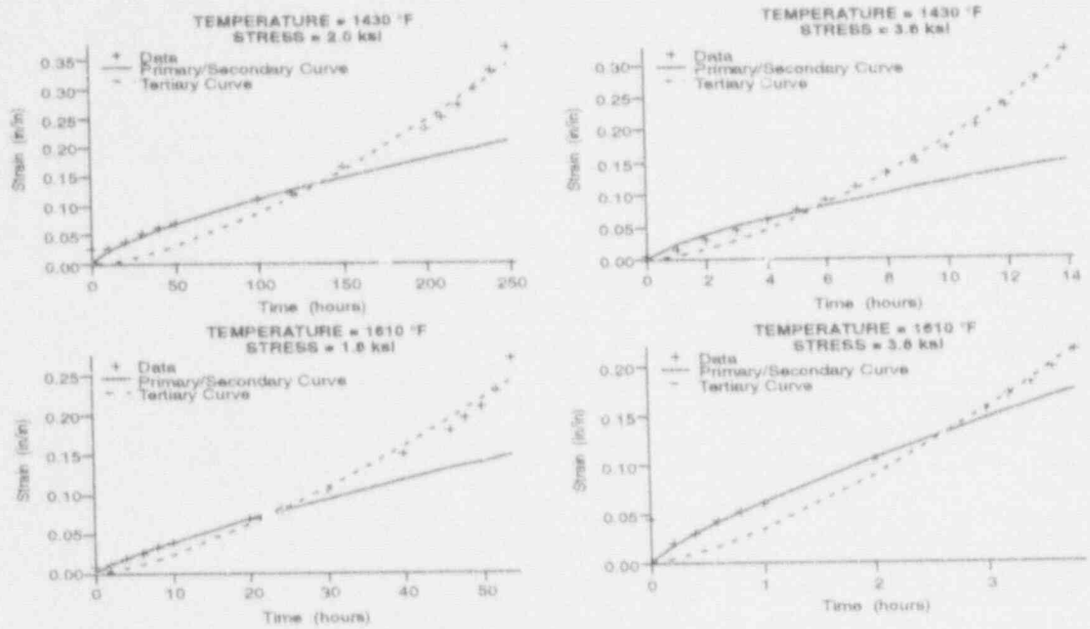


Figure 2. Creep Data For Temperatures 1430° and 1610° F

## Yield Stress and Modulus Data

The dependence on the yield strength and elastic modulus or temperature are shown in Figure 3. The yield strength fit used in the analysis is shown with a solid line in the figure. The low-temperature (CE) data and the high-temperature (INEL) data were fit separately, and the two curves were joined by interpolation. Similarly, the elastic modulus data were fit separately for the low-temperature and the high-temperature regimes and then joined by interpolation.

## Creep Rupture Failure Model

The creep-rupture failure model developed in the present program is based on the cumulative damage concept. The damage formulation maintains that under a given stress and temperature, the material sustains an amount of damage that is equal to the ratio of the time duration of the current load increment to the creep rupture (failure) time associated with the current

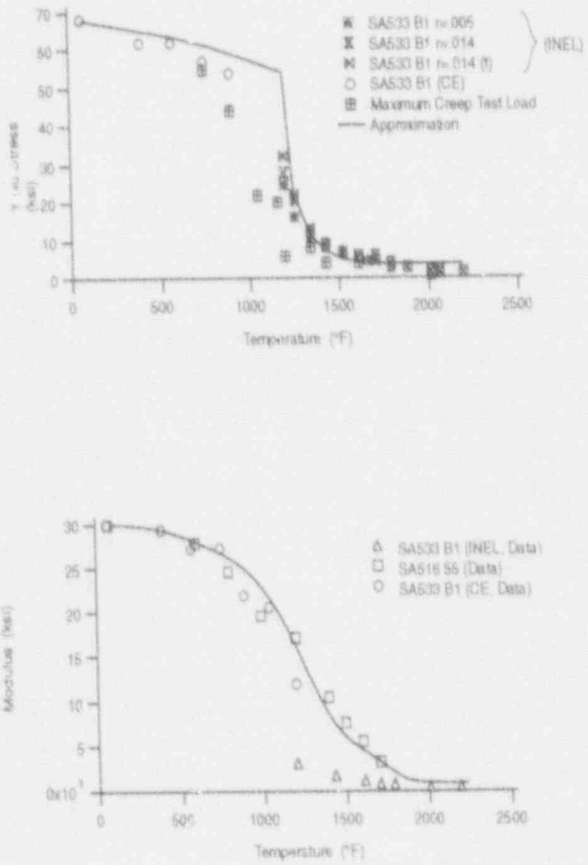


Figure 3. Yield Stress and Modulus Dependence on Temperature

temperature and stress state. This ratio, referred to here as the Damage Index, is unity in a creep-rupture test where both the load and the temperature remain constant with time. The test temperature and time-to-rupture are related through the Larson-Miller Parameter (LMP) which is constant for a given initial stress level [8]. Data from INEL [2] were used to develop a relationship between the LMP and the applied stress. From this relationship, the time to failure is determined. Creep rupture times were reported for the SA533 steel at temperatures ranging from 1160° to 2012° F. LMP values were calculated using Equation (2), where $t_r$ is the time to rupture in hours and T is the temperature in Rankine.

$$LMP = .001(20.0 + \log_{10} t_r)T \tag{2}$$

The SA533 creep rupture tests conducted by INEL are reported in Reference 2. Figure 4 shows the relationship between the applied stress and the LMP with the data points from the experiments. This data was fit with Equation (3) using a standard automated least squares fit utility, where σ is the stress (ksi), LMP is the Larson-Miller Parameter, and a and b are constants to be determined. From a least squares fit, a is determined to be 5272, and b is determined to be -0.1747. Figure 4 also displays this applied stress/LMP fit.

$$\sigma = a\, e^{b\,(LMP)} \tag{3}$$

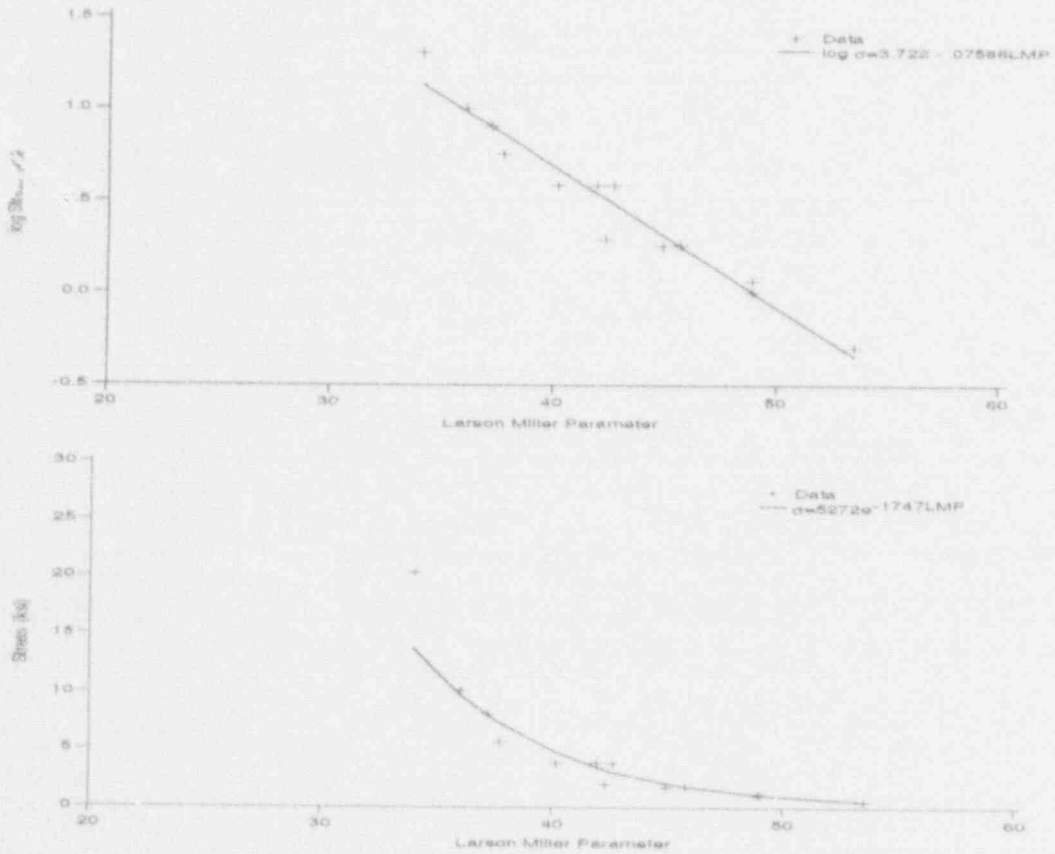


Figure 4. Stress Dependence on Larson Miller Parameter

Let a stress σ and a temperature T be applied for a time duration Δt. Then incremental damage is defined as follows:

$$\Delta D = \Delta t / t_r\,(\sigma, T) \tag{4}$$

where $t_r$ is the rupture time determined from a creep-rupture test conducted for the initial stress $\sigma$ and the temperature T. By re-arranging Equation (2), the time-to-rupture $t_r$ can be determined by equation (5), where T is the temperature in Rankine and LMP is the Larson-Miller Parameter. By rearranging Equation (3), the LMP is determined by Equation (6), where $\sigma$ is the stress (ksi), a = 5272, and b = -0.1747. The total damage at any given time is given by the sum of the incremental damages as shown in Equation (7). Thus, failure by creep rupture is indicated when $D \geq 1.0$.

$$t_r = e^{2.303[(LMP/.001T) - 20.0]} \tag{5}$$

$$LMP = b^{-1} \ln (\sigma / a) \tag{6}$$

$$D = \int_0^t \frac{d\tau}{t_r} \tag{7}$$

## DETAILED 2D STRUCTURAL ANALYSIS

### Finite Element Model

An axisymmetric finite element model was developed with relatively fine grid in the critical areas of the shell. Temperature and pressure conditions were those recommended by Professor Theofanous at UCSB. All computations were performed using ABAQUS Version 4.8-5 and the material model subroutines described above. A schematic representation of the axisymmetric model is shown in Figure 5. The steel shell thickness is exaggerated to show the element discretization. Eight-node axisymmetric continuum elements with reduced 2x2 integration were used throughout the grid. The gap between the steel shell and the concrete shield wall was modeled with gap elements that provide no resistance to radial motion of the shell until the outer shell surface comes in contact with the concrete shield wall.

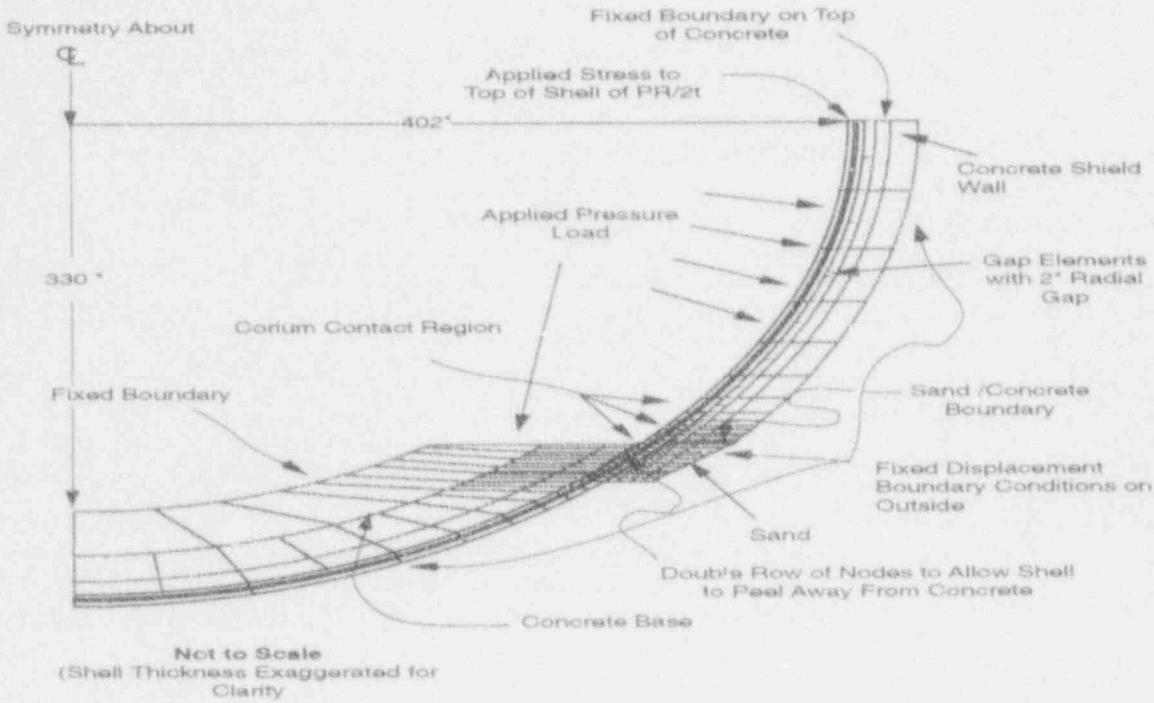


Figure 5. Schematic Representation of Mark I Containment Axisymmetric Grid

There are three materials in the model: steel shell, unreinforced concrete, and sand. The steel properties are defined in the special material model developed for this project. At lower temperatures the constitutive model uses the standard ASTM 533 elastic-plastic properties, namely, yield stress ($\sigma_y$) = 67 ksi, Young's modulus (E) = 30 x $10^6$ psi and Poisson's Ratio v = 0.3. Referring to Figure 3, these properties remain roughly unchanged below 800°F. Between 800 and 1500°F there is a precipitous drop in both yield strength and modulus, but Poisson's Ratio remains unchanged.

For the concrete material, the ANACAP model [9] was used with ultimate strength of $f_c'$ = 5000 psi, Young's Modulus of 4 x $10^6$ psi, and Poisson's Ratio of 0.15. The cracking strain for the concrete was estimated to be 100 x $10^{-6}$ in/in. For detailed discussion of the concrete constitutive model, the reader is referred to Reference 9.

The sand material below the base between the shell and the shield wall was modeled as a weak elastic material with a Young's Modulus = 1,000,000 psi, which represents highly compacted confined sand. This simple model for the sand was retrospectively justified by the analysis results.

The boundary conditions for the analysis also are illustrated in Figure 5. Horizontal constraint is imposed at the centerline and vertical and horizontal constraints are applied at the outer edges of the concrete shield wall and as otherwise noted in the figure. The roller supports around the outer grid edges represent assumption of a very stiff shield building relative to the steel shell. At elevated temperatures and once plastic flow occurs in the shell, this assumption is judged to be very good.

A key boundary condition was the treatment of the equator boundary of the steel shell which was given a stress condition equal to the membrane stress in a perfect sphere (pr/2t). It is important to apply stress rather than displacement constraint here because of the thermal conditions in the shell. With thermal expansion, this point will move up relative to the adjacent point on the shield wall. The stress boundary condition also provides the driving force for creep in the meridional direction.

The pressure recommended by UCSB is a constant pressure of two atmospheres or 29.4 psi applied at all inner surfaces including the exposed surface of the interior concrete base. This pressure represents the approximate steady state pressure that is expected during the severe accident sequence. The lower portion of the primary shell is assumed to be full of water and this water is in the free-boiling condition, that is the ambient pressure in the containment is not high enough to support substantially higher water temperatures than 212°F. The weight of the water also has been considered.

The temperature conditions away from corium contact with the shell are the same as the water, 212°F. Temperatures other than STP conditions are applied only to the shell. This includes the first 4 elements down into the concrete layer. The rest of the materials in the model are assumed to be largely unaffected by the shell temperatures. Indeed, the concrete is a relatively poor heat conductor compared to the steel and would require a long time to heat up to a significant depth even with blackbody radiation or direct shell contact. The temperature distribution associated with corium contact was taken from recommendations made by UCSB and published in NUREG/CR-5423. This distribution as it was input in ABAQUS is shown with the temperature contours in Figure 6. Note that the highest temperature applied is 2372°F (1300°C).

In the present analyses, two heating scenarios were chosen: one roughly corresponding to the NUREG Scenario I with a ten-minute rise time and another, chosen at UCSB's suggestion and to maximize conservatively creep effects, with a two-hour rise time. Both temperature histories were applied as a simple linear ramp up of the temperature distribution. In both cases, pressure was applied first to 29.4 psi over five load increments, then temperature was applied over a hundred or more increments with up to ten equilibrium iterations in each increment. Both analyses completed with convergence up to and including the point of rupture failure prediction.

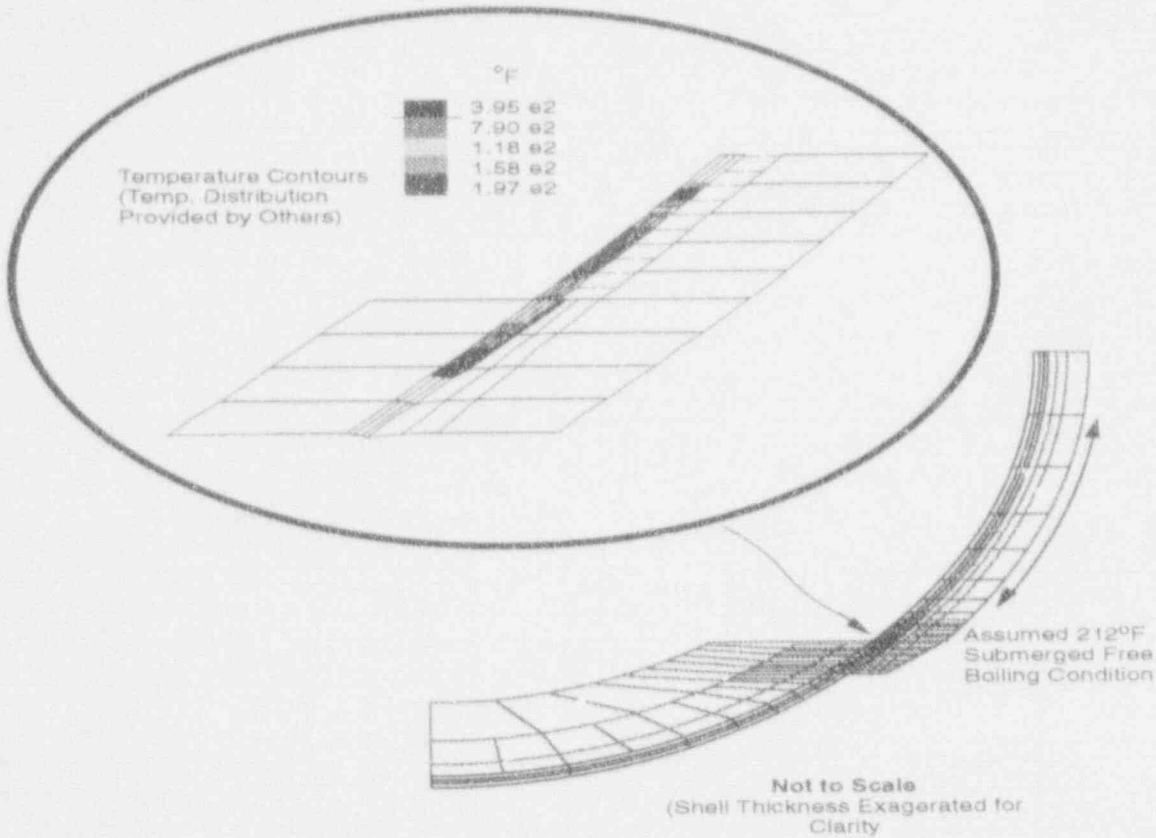


Figure 6. Computational Grid and Temperature Application

## Analysis Results

The analysis results show that for the 10-minute transient, the liner is predicted to fail by creep rupture at temperatures in the range of 1800°F (982°C) to 2012°F (1100°C). The lower limit indicates failure initiation at the inner surface of the shell, and the upper limit indicates a complete through-wall failure. The corresponding failure temperatures for the slower two-hour transient are 1670°F (910°C) to 1900°F (1040°C). As can be seen from these results, creep rupture precedes liner melting (1500°C) by several hundred degrees depending upon the heating rate. These failure temperatures, as mentioned earlier, are lower-bound limits because of the highly conservative assumption inherent in the axisymmetric representation of the corium-shell contact configuration.

A more detailed look at the response is obtained by examining the deformed shapes and strain contour and damage index contour plots. These are provided in Figures 7 through 12. Finally, the shape of the liner strain concentration near the liner-concrete juncture is shown in the strain profiles of Figures 13 and 14.

The deformed shapes for both scenarios indicate that creep rupture occurs before the shell contacts the shield wall as shown in Figures 7 and 8. [In Figure 8, for the ten-minute scenario, a kink has formed in the shell, but the shell still does not contact the shield wall.] In the 2 hour ramp up scenario, the shell moves out approximately 1.5 inches but does not quite meet the shield wall as shown in Figure 7. This deformed configuration could be significantly different in a 3D analysis.

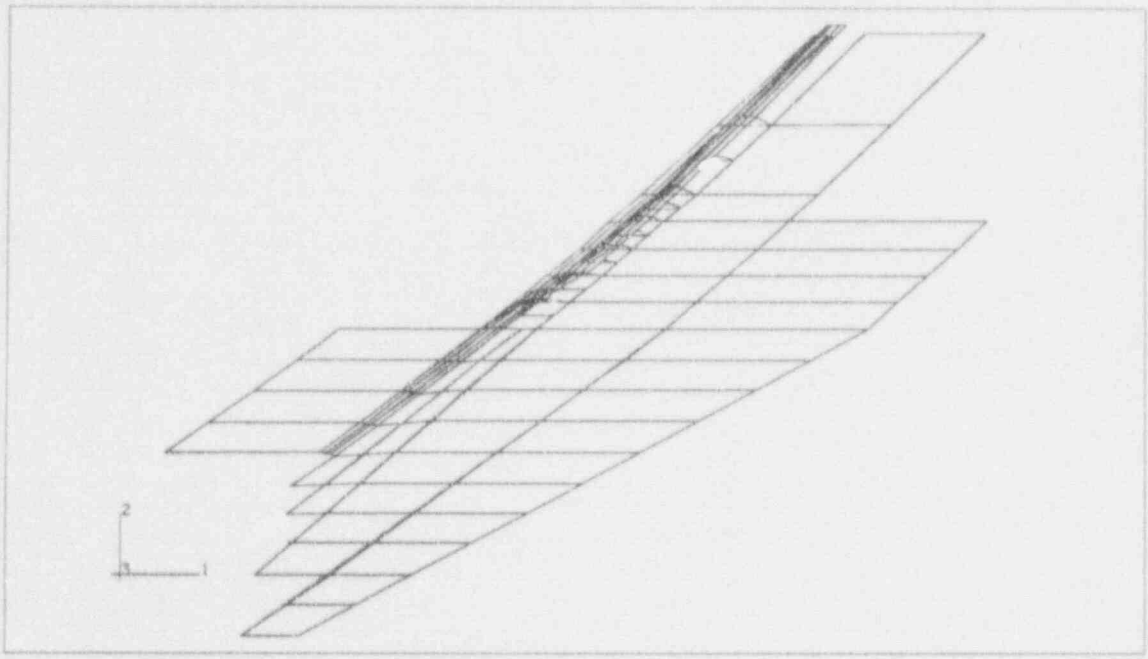

Figure 7. Deformed Grid for 2 Hour Ramp up Scenario, Temperature = 1670°F

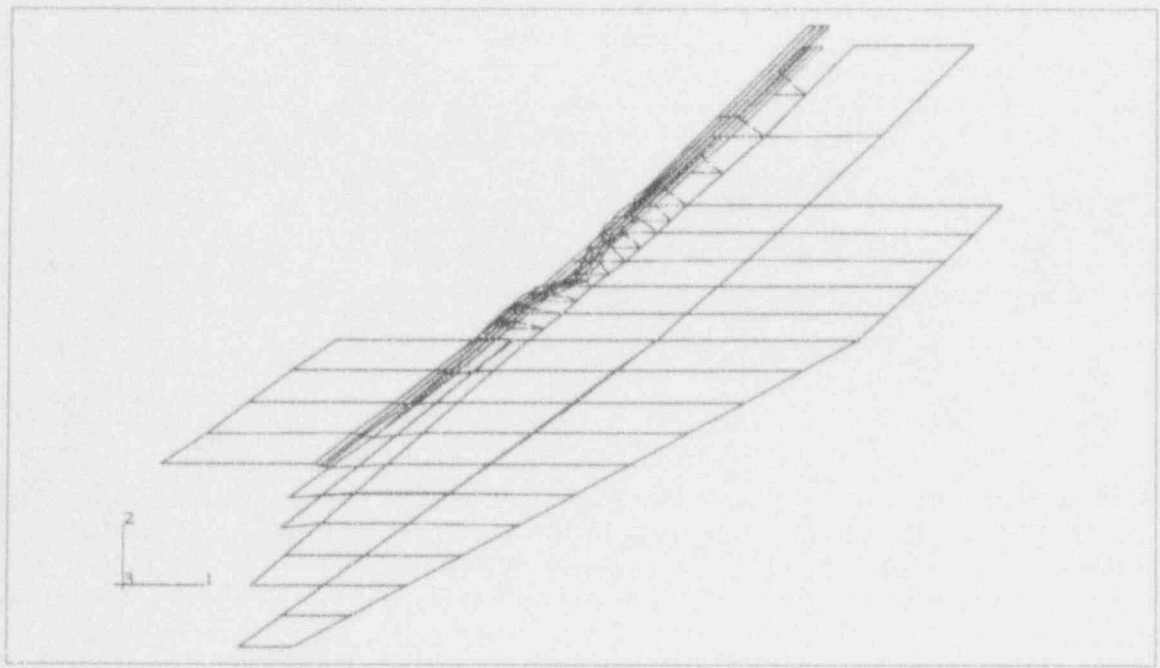

Figure 8. Deformed Grid for 10 Minute Ramp up Scenario, Temperature = 2135°F

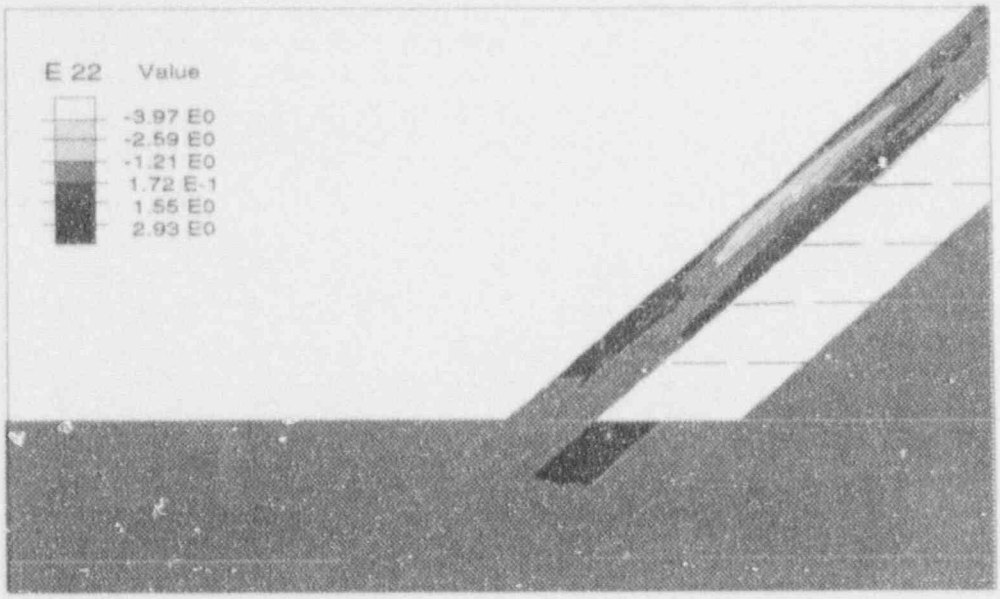


Figure 9. E22 Strain Contours at Peak Temperature of 1872 $^{O}$F, 2 Hour Ramp Up

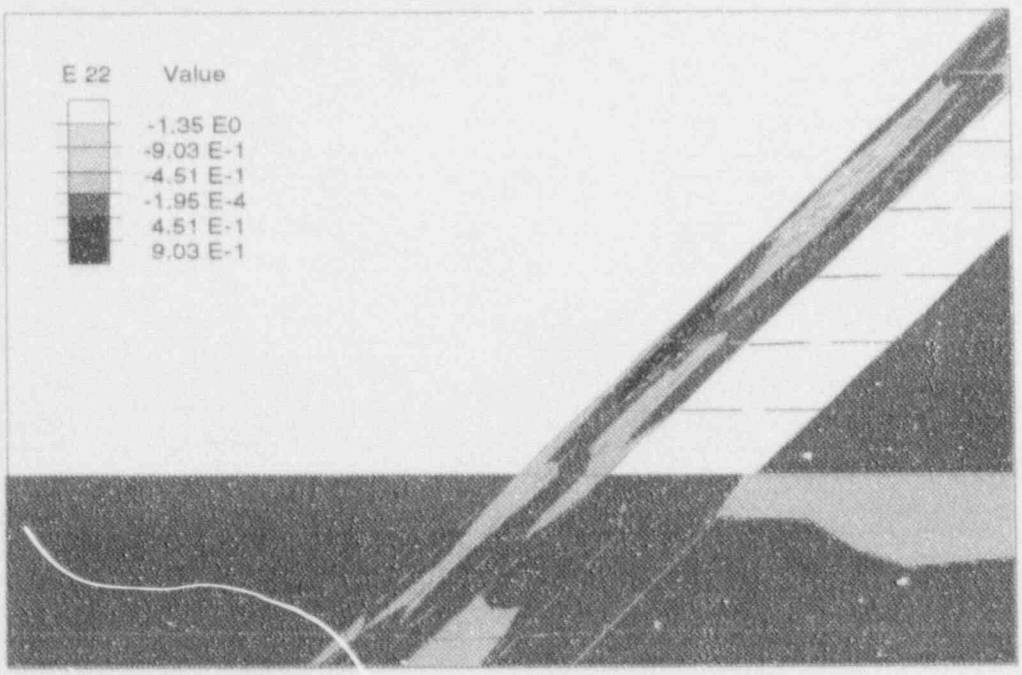


Figure 10. E22 Strain Contours at Peak Temperature of 2135 $^{O}$F, 10 Minute Ramp Up

The vertical strain $\varepsilon_{22}$ is plotted in Figures 9 and 10. In general, $\varepsilon_{22}$ is somewhat larger than $\varepsilon_{11}$, but neither are the true tangential strain due to the curved geometry. The damage index contours are shown in Figures 11 and 12, and these figures show maximum values in the second element up from the shell-concrete juncture. With a separate post-processing program, the $\varepsilon_{11}$, $\varepsilon_{22}$, and $\varepsilon_{12}$ strains were combined to plot the true tangential strain as a function of position. These are shown in the strain profiles of Figures 13 and 14. All the strain plots indicate the greatly elevated strain at the corium contact zone and the severe bending that occurs just above the shell-concrete junctures.

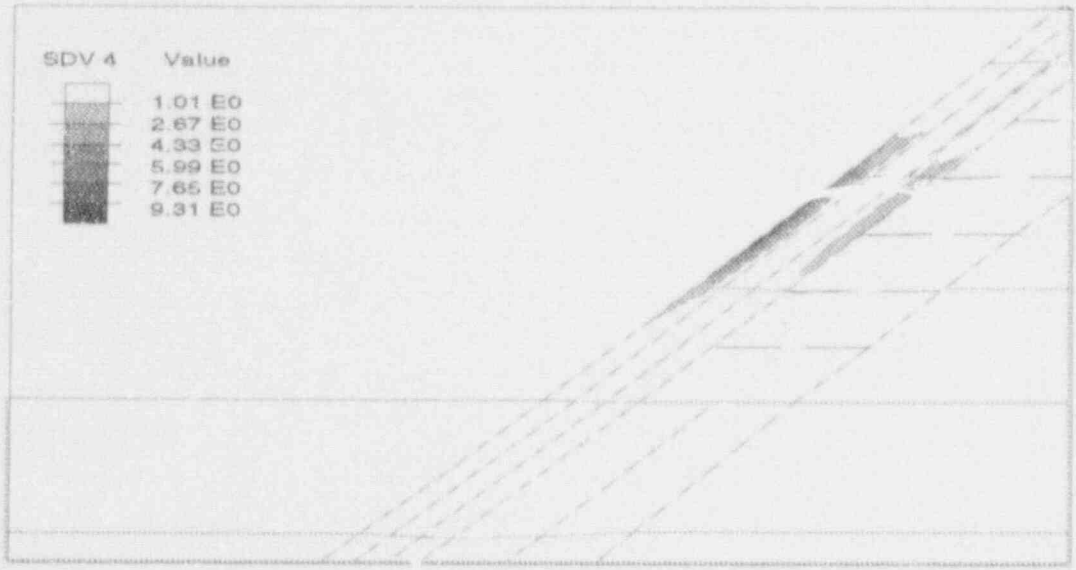


Figure 11. E22 Strain Contours at Peak Temperature of 2135°F, 10 Minute Ramp Up

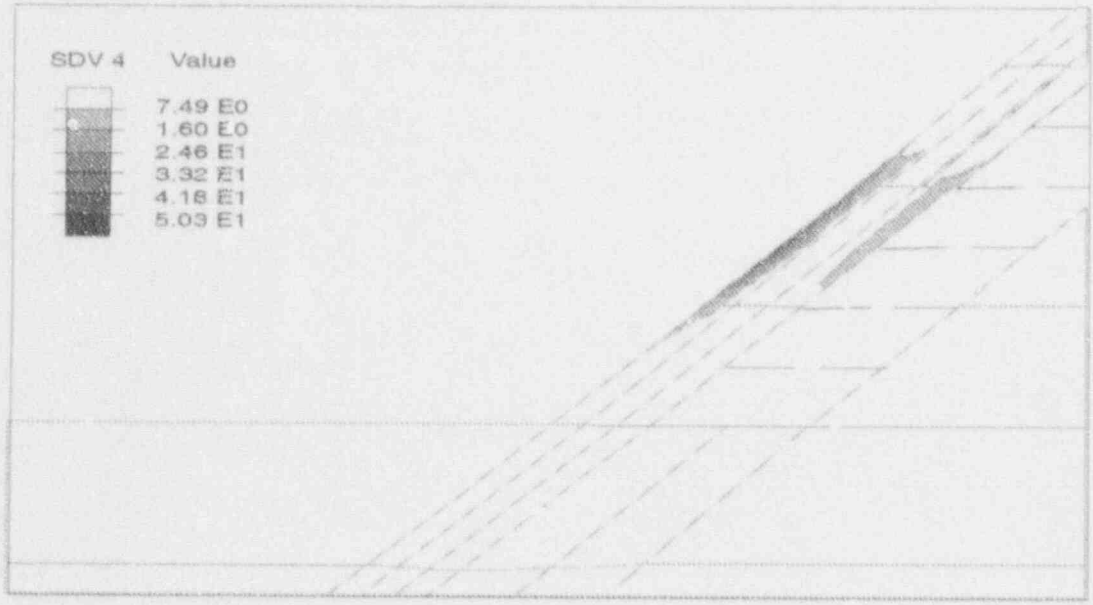


Figure 12. "D" Contours at Peak Temperature of 1872°F, 2 Hour Ramp Up

## CONCLUSIONS

The primary conclusion of this two-dimensional analysis is that liner failure by creep rupture precedes melting by several hundred degrees and is dependent on the characteristics of the temperature transient. A three-dimensional analysis will reduce the uncertainties in the 2D based failure temperatures, but it still is expe[illegible] to show lower failure temperatures than the melting temperature of 1500°C.

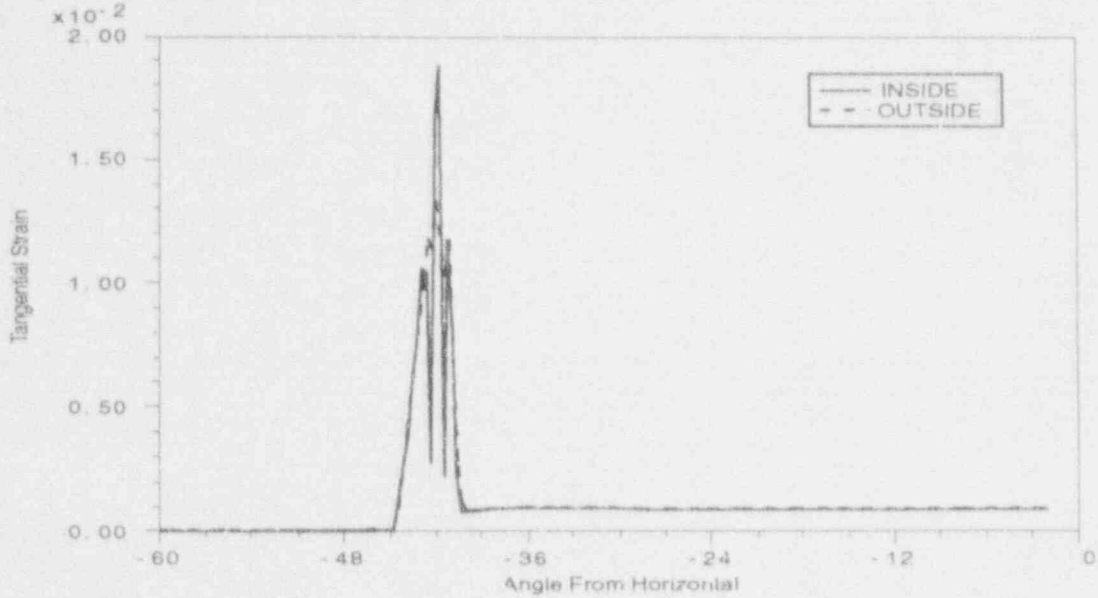


Figure 13. Profile of Tangential Strain at Peak Temperature of 1872 $^{O}$F, 2 Hour Ramp Up

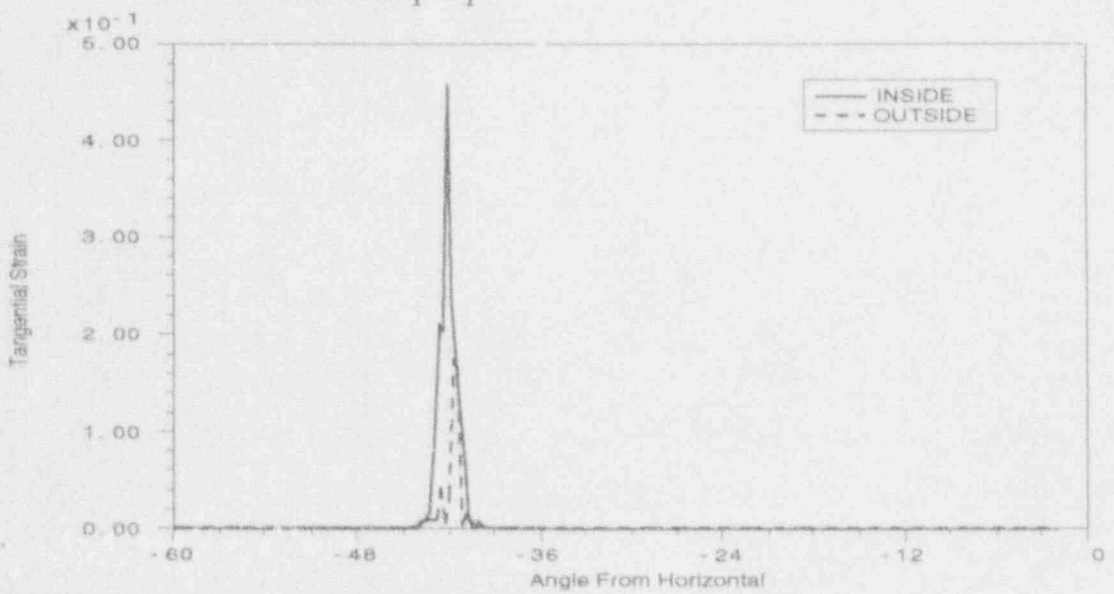


Figure 14. Profile of Tangential Strain at Peak Temperature of 2135 $^{O}$F, 10 Minute Ramp Up

## ACKNOWLEDGMENTS

The U.S. NRC financially supported this work under contract 67-3350 with Sandia National Laboratories. The authors also are indebted to Dana Powers with Sandia, Professor Theo Theofanous with UCSB, Dr. Joy Rempe with INEL, and Farouk Eltawila with the NRC for their technical assistance during the performance of this work.

## REFERENCES


1. Theofanous, T.G., Amarasooriya, W.H., Yan, H., and Ratnam, U., "The Probability of Liner Failure in a Mark-I Containment," U.S. Nuclear Regulatory Commission, NUREG/CR-5423, 1989.

2. Rempe, J.L., Thinnes, G.L., Allison, C.M., "Light Water Reactor Lower Head Failure Analysis," U.S. Nuclear Regulatory Commission, NUREG/CR-5642, 1990.

3. Reddy, G.B., Ayers, D.J., "High-Temperature Elastic-Plastic and Creep Properties for SA533 Grade B Class 1 and SA508 Materials," Electric Power Research Institute, NP-2763, 1982.

4. Rashid, Y.R., Castro, J.C., Dameron, R.A., "Creep Rupture in a Mark I Containment, " ANATECH Report for Sandia/NRC, November 1991.

5. Hibbitt, Karlsson, and Sorenson, Inc., "ABAQUS Users Manual Version 4.8," Providence, RI, 1989.

6 Gowda, B.C., "Tensile Properties of SA516, Grade 55, Steel in the temperature range of 25°-927°C and Strain Rate Range of $10^{-4}$ to $10^{-1}$ $Sec^{-1}$," Characterization of Materials for Service at Elevated Temperatures, Edited by Smith, G.V., ASME, 1978, pp. 145-158.

7. ASME Boiler and Pressure Vessel Code, Section III, Appendices I, pp 36-38.

8. Larson, F.R., and Miller, J., "A Time-Temperature Relationship for Rupture and Creep Stresses," Transaction of the ASME, July 1952, pp. 756-775.

9. ANACAP (ANATECH Concrete Analysis Package) Theory and User's Manual, Version 90-2.0, ANATECH Research Corp., San Diego CA, February 1991.

# SESSION 6

# CONTAINMENT OPERATIONAL EXPERIENCE (LEAKAGE, AGING, OPERATION)

# CONTAINMENT LEAKAGE RATE TESTING REQUIREMENTS

E. Gunter Arndt
Structural & Seismic Engineering Branch
Division of Engineering
Office of Nuclear Regulatory Research
U.S. Nuclear Regulatory Commission

## Abstract

This report presents the status of several documents under revision or development that provide requirements and guidance for testing nuclear power plant containment systems for leakage rates. These documents include the general revision to 10 CFR Part 50, Appendix J; the regulatory guide affiliated with the revision to Appendix J; the national standard that the regulatory guide endorses, ANSI/ANS-56.8, "Containment System Leakage Rate Testing Requirements"; and the draft industry Licensing Topical Report, "Standardized Program for Primary Containment Integrity Testing." The actual or potential relationships between these documents are also explored.

## CURRENT STATUS - SUMMARY

1. General revision to the rule, Appendix J: Under review by the Commission for issue as a final rule [Ref. 1].

2. Companion regulatory guide endorsing ANS-56.8: Part of general revision package; will only be issued as part of the general revision of Appendix J [Ref. 2].

3. ANSI/ANS-56.8, "Containment System Leakage Testing Requirements": The 1987 issue is being revised [Ref. 3].

4. BWROG Licensing Topical Report (LTR): On hold until #1, 2, and 3 are final [Ref. 4].

## BACKGROUND

### Rule

Appendix J of 10 CFR Part 50 was issued as a proposed rule on August 27, 1971, published as a final rule on February 14, 1973, and became effective on March 16, 1973. Since 1973, the NRC has issued two limited amendments to this Appendix. The first amendment modified the Type B (penetration) test requirements, particularly the frequency of testing during periods of heavy air lock usage. It conformed the rule to what had become accepted practice through the granting of exemptions, that is, testing of airlocks every third day instead of after each use during periods of frequent use. This amendment was published for comment January 11, 1980, published as a final rule September 22, 1980, and became effective October 22, 1980. The second amendment incorporated the Mass Point statistical analysis technique into the NRC's regulations as a permissible alternative to the "Total Time" and "Point-to-Point" techniques specified in Appendix J. The Mass Point technique had already come into widespread use for reducing leakage rate test data to a leakage rate. This second amendment was

published for comment February 29, 1988, and published as an immediately effective rule on November 15, 1988 [Ref. 5].

The current general revision of Appendix J will provide greater flexibility in applying alternative leakage rate test requirements necessitated by variations in plant design and will reflect acceptable changes in regulatory requirements resulting from:

- Experience in applying the existing requirements,
- Advances in containment leakage rate testing methods,
- Interpretive questions,
- Simplifying the text,
- Various external/internal comments since 1973, and
- Exemption requests received and approved.

Related Regulatory Guide

A regulatory guide entitled, "Containment System Leakage Testing" also will be issued. It contains specific guidance on acceptable leakage rate test methods, procedures, and analyses that may be used to implement the requirements and criteria of 10 CFR Part 50, Appendix J.

This guide is based on the 1987 ANSI National Standard ANS-56.8, "Containment System Leakage Testing Requirements," that details a consensus state of the art in containment leakage rate testing procedures and data reduction and analysis. The ANS standard is being endorsed in the guide rather than the rule. This approach limits the rule to test criteria and leaves endorsement of test procedures and statistical data reduction techniques to a guide that can be revised as the testing technology changes. The guide and the ANS standard it endorses only become requirements when a licensee commits to its use.

Public Comments on the Proposed Rule and Regulatory Guide

The proposed rule was published for comment in the Federal Register on October 29, 1986. Regulatory Guide MS 021-5 was published for comment on October 28, 1986.

During the 6-month public comment period, 45 letters were received addressing either the rule or both the rule and the regulatory guide. An additional 8 letters were received addressing only the regulatory guide, for a total of 53 comment letters.

The final rule and regulatory guide differ from the proposed rule and guide. A comparative text for comparing the proposed and final rules will be available to aid in rapidly identifying the differences. A Comment Resolution Memo will be available for each document that explains the NRC staff's disposition of the comments received. Supporting documents, which sort and describe the comments received, will also be provided. Copies of these documents will be sent to all who mailed in comments. A copy of each of these documents will be placed in the NRC Public Document Room.

The following discussion highlights the more significant comments on the proposed rule and also presents a summary of major modifications to the proposed rule.

Containment isolation valve definition. Because of concerns expressed for older, pre-General Design Criteria plants, this definition was revised to distinguish between plants that are or are not required to conform to Appendix A, "General Design Criteria," to 10 CFR Part 50.

Maximum/minimum pathway leakage definition. The maximum and minimum pathway definitions have been explicitly incorporated and used in this revision. It is expected, however, that applying these definitions to complex piping systems will continue to require clarifying discussions. It will not be possible to cover all permutations of piping and valve configurations that exist at containment boundaries.

Reduced-pressure test option. Numerous comments recommended retaining this option largely for economic reasons. However, there is universal agreement that one cannot extrapolate a leakage rate from a reduced-pressure test to a leakage rate under full pressure. Therefore, this option is being discontinued as not technically viable.

Pneumatic testing of valves. Allowing testing of valves with fluids other than air or nitrogen was requested. The NRC believes that this approach is not conservative and has not expanded the test mediums beyond air or nitrogen.

Type A, B, and C test frequency. Based on comments received and a potential trend from 18-month toward 24-month refueling cycles, the wording in the rule has been revised to provide greater flexibility in this area. Essentially, the principle of testing frequencies is as follows: For Type A tests, every other refueling outage; for Type B and C tests, every refueling outage. However, because of variations in refueling cycles (including some that are still annual), a time limitation is being used in the final rule.

Type A test duration. Although the final rule still reflects a minimum 8-hour duration, based on prior statistical evaluations and past discussions on ANS-56.8, several commenters believe that 6 hours is sufficient and will save money.

Existing exemptions. Addressing concerns expressed by utilities during the rule revision process, wording has been included in the final rule that "Specific exemptions to previous versions of this rule that have been formally approved by the NRC, according to 10 CFR 50.12, are still applicable unless specifically revoked by the NRC."

"As found" acceptance criteria. In 1987, there was considerable resistance to determining how badly a component leaked before its leakage was reduced to an acceptable "as left" value. Now, however, based on an ongoing dialogue between the NRC staff and plant owners, a better understanding has developed of the value of the concept as well as the need for practical limits on the application of the concept. This dialogue continues in order to refine details of applying the concept in a rational manner.

A number of comments were received expressing concern over how the "as found" leakage rate testing is intended to be applied under this revision. Some commenters erroneously believed that every single modification, repair, or replacement of a penetration or valve, regardless of relevance to containment integrity, would require an "as found" test. Paragraphs IV.A and B have been reworded to clarify that the intent of the regulation is to require both "as

found" and "as left" testing only when the work has a potential effect on the containment system leakage rate. The NRC staff has stated its philosophy on the existing rule with regard to as found leakage rate testing to be that as found testing is broadly required for all actions that have a potential impact on containment leakage rate. Exceptions to this are being defined for those instances where obtaining further leakage performance information on a component has no practical value, or where the cost, in financial or radiological exposure terms, of obtaining the information is demonstrably out of proportion to the safety value obtained from such information. These exceptions, however, will continue to be reviewed by the NRC staff and agreed upon on a case-by-case basis as they are identified.

Technical specification references. A number of comments recommended that documentation of bases and alternatives not be "...in the Technical Specifications..," but "...in the licensee's Appendix J Program...." The reason was that efforts have been under way to remove excess material from the Technical Specifications. However, acceptance of this recommendation would significantly diminish NRC control over critical elements of this safety-related testing program, and this recommendation was not adopted.

Reporting. Comments have been received on duplication in reporting of failed Type B and C tests with reporting of the events under the Licensee Event Report (LER) system. Paragraph VI.A. has been revised to address this issue. Type B and C tests summaries continue to be reported in the next Type A test report filed with the NRC. However, failed Type B and C tests must also be reported in a more timely manner.

Backfit Conclusion. This is currently under review by the Commission.

## ANSI/ANS-56.8

American National Standard ANSI/ANS-56.8-1987, "Containment System Leakage Testing Requirements," is currently being reviewed by the ANS-56.8 Committee for updating and revision. The NRC draft regulatory guide on this rule revision endorses the 1987 issue of ANS-56.8. It is the intent of the Commission that, if and when this national standard is revised and reissued, the NRC regulatory guide endorsing the standard will also be revised to reflect the Commission's position with regard to the acceptability for use in the licensing process of the most current published issue of that standard.

## Licensing Topical Report

The draft Licensing Topical Report (LTR), "Standardized Program for Primary Containment Integrity Testing," [Ref. 4] was developed in draft form by the Boiling Water Reactor Owner's Group (BWROG), and was also discussed with the NRC staff during its development. The Nuclear Management and Resources Council (NUMARC) is understood to be planning to make this an industry-wide guidance document. Since it was drafted to be consistent with the general revision to Appendix J and ANS-56.8, it has been on hold until both documents have been completed.

The BWROG did a fine job in developing this LTR, and is to be commended for the effort put into it. The NRC staff has encouraged, and continues to encourage, the development of standardized containment leakage testing practices throughout

the industry. This document can be a very useful aid in achieving this goal. However, it is also important to look closely at the number and relationships of the various documents with which people conducting such tests must deal. With a regulation, regulatory guide, and ANSI National Standard providing requirements and guidance, what would be an .ppropriate role for this LTR?

One possibility would be to consider its use as a standard, in-house utility procedures manual that implements the requirements and guidance of the other three documents. While conforming to them, it would also provide additional detailed procedural guidance at a level that would not be routinely reviewed by the NRC. It would be presumed to be in accord with Appendix J and the NRC's endorsement of ANS-56.8. The LTR would not then be viewed as a regulatory document, eliminating the resources both sides would need to have it reviewed, approved, and maintained. The NRC would focus its regulatory attention on the requirements of Appendix J and on the commitments to use of ANS-56.8 as endorsed by the NRC. This would fulfill safety needs and minimize regulatory involvement in procedural details. It would also keep the testing program standardized so that it would be generically useful to the industry as a whole, and to the NRC, keeping the testing program from disintegrating into myriad, unique, site-specific containment leakage rate tests.

## CONCLUSION

### Status

At the time of writing, the Commission has not concluded its review of the final rule revision and the associated regulatory guide, the ANS-56.8-1987 standard is undergoing revision, and the BWROG LTR is being held until Appendix J and ANS-56.8 are revised.

### Relationship

Appendix J to 10 CFR Part 50 is the principal regulatory document and it is mandatory. Its requirements take precedence over all the other documents discussed here. The revised Appendix J will identify additional guidance to be used by a licensee in implementing Appendix J's requirements.

ANSI/ANS-56.8, to the degree endorsed by the NRC's regulatory guide, is an acceptable means of implementing the requirements of Appendix J, but it becomes mandatory only when committed to by a licensee. The Standard provides useful, more detailed guidance than Appendix J on how to conduct a containment leakage rate test.

The BWROG draft LTR is an even more detailed procedural document on how to conduct containment leakage rate tests. It should provide consistent procedural guidance from test to test, when the test intervals (2-5 years) may be long enough for testing personnel to change or long enough for the remaining test personnel to need reinstruction.

All three documents have their own complementary roles to play in ensuring a consistent, useful, and efficient check on the proper leakage performance of the containment system boundary.

## References


1. Proposed general revision to 10 CFR Part 50, Appendix J.
2. Draft Regulatory Guide 1.xxx, "Containment System Leakage Testing."
3. ANSI/ANS-56.8-1987, "Containment System Leakage Testing Requirements."
4. BWROG Draft Licensing Topical Report (LTR), "Standardized Program for Primary Containment Integrity Testing," NEDO-31722, Class I, August 8, 1989.
5. Title 10 of the Code of Federal Regulations, Part 50, Appendix J, "Primary Reactor Containment Leakage Testing for Water-Cooled Power Reactors."

# ANSI/ANS 56.8 STANDARD COMMITTEE STATUS REPORT

James P. Glover
Commonwealth Edison Company

## Abstract

This report discusses the major changes being made to the 1987 version of ANSI/ANS-56.8, "Containment System Leakage Rate Testing Requirements". A brief history and current status of a related document NEDO-31722, "Standardization Program for Primary Containment Integrity Testing" is also presented. The possible relationship between these two documents and the draft revision of 10 CFR 50 Appendix J are outlined.

## BACKGROUND

The requirements for testing the primary reactor containment system are specified in 10CFR 50 Appendix J, "Leakage Rate Testing of Containments of Light-Water Cooled Nuclear Power Plants". Appendix J references ANSI 45.4-1972[1]. The regulation specifies that all Type A testing must be conducted in accordance with the provisions of that standard.

ANSI 45.4-1972 is for all practical purposes an obsolete standard. It specifies use of the Total Time, Point to Point and even the Reference Vessel Methods for Type A testing. These methods are almost never used for currents tests. Since Appendix J directly references ANSI 45.4-1972, the industry is required to follow that version of the standard.

The proposed revision to Appendix J[2] does not reference any ANSI standard. Instead, it is intended to be used with a companion technical document. Regulatory Guide MS 021-5[3] was written for this purpose. This guide, with specified exceptions and additions, endorses ANS/ANSI 56.8-1987[4].

By not referencing a specific technical document in the regulation, the NRC gave itself the flexibility to more easily update and keep the technical guidance document current. Although, an additional effect of not referencing a specific document was to leave open the possibility for a licensee to reference documents other than the Regulatory Guide and ANSI Standards in their Appendix J program submittals.

## THE DRAFT INDUSTRY TOPICAL REPORT

In 1986, a revised version of Appendix J and the Regulatory Guide were issued for public comments. The Boiling Water Reactor Owners Group,(BWROG) formed a Subcommittee for the purpose of formulating and submitting a joint BWR response to the proposed regulations. Overall, the group's(and the industry's) comments on the regulation and the Regulatory Guide were very negative.

The most common objections to the Reg Guide and the standard were that these documents required costly actions with no appreciable payback in terms of safety. The ANSI standard specified techniques which were good practices, although were not tasks that should be requirements.

The BWROG subcommittee expanded its original charter to include the writing of a Topical Report on containment leakage rate testing. This document was intended to be used in place of the Regulatory Guide/ANSI Standard combination.

The philosophy taken in writing this document was to take an objective engineering approach to the standardization and clarification of the containment system leakage rate testing program. This report was written by station personnel who administer containment leakage rate programs and perform the testing. The result of a that effort is BWROG report NEDO-31722[5]. This document was reviewed and endorsed by 20 BWR utilities.

While NEDO-31722 was written by and for BWR type plants, it is with minor modifications also applicable to PWRs. In order to increase the scope of applicability of this document, it was given to NUMARC for modification and subsequent release as a containment system testing document applicable to both BWR and PWR plants.

NUMARC established an Ad Hoc Advisory Committee (AHAC) to modify the BWR Owners Group Document and also to address the pending revision to Appendix J. The AHAC is intended to provide support for the development of industry positions and to provide an interface with the NRC to identify and resolve issues of concern.

## DRAFT CHANGES TO ANSI/ANS 56.8-1987

In June of 1990, the 56.8 committee reconvened and determined that a major update of the 1987 standard was required. This update would make the Standard a document more suitable for use as a requirement, be in general compliance with the proposed Appendix J, and address as many Reg Guide issues as possible so as to minimize or eliminate exceptions and additions to the standard.

As of April 1992, the major changes in the draft ANSI Standard relative to the existing 1987 version are as specified below.

### Instrumentation Selection Guide,(ISG) For The Type A Test Instrumentation System Was Eliminated

The ISG formulation was defined in the 1987 ANSI Standard as a means of determining the ability of a Type A test instrumentation system to measure the integrated leakage rate of a primary reactor containment system. This rather long formulation is labor intensive to calculate either by hand or by computer. It was noticed that if all of the Type A test instrumentation specifications and requirements already contained in the standard were met, then the ISG criteria was automatically satisfied. For this reason, the requirement to calculate this parameter was eliminated.

### The Extended ANSI Method Was Added To The Standard

The 1987 version of ANSI/ANS 56.8 allowed for the performance of an eight hour Type A test utilizing the Mass Point method. The Regulatory Guide took exception to the standard on this issue and required that for a Type A test to be successful, two additional criteria be met. These criteria place restrictions upon the magnitude of leakage rate curvature and dry air mass scatter. The application of these two acceptance criteria to the Mass Point Method is referred to as the

Extended ANSI/ANS Method.

A widely held view was that these additional criteria did nothing to improve the quality of Type A testing and added the burden of complex computer code and procedure modifications. There exist numerous alternative methodologies which have been documented to yield comparable or even superior results.

For the sake of simplifying the regulations by reducing the number of exceptions in the Regulatory Guide to the Standard, and because these addition criteria are thought to not pose any significant difficulty in passing an Integrated Leakage Rate Test,(ILRT), it was voted to include the Extended ANSI/ANS Method.

The Standard's formulation for calculation of the acceptance criteria is presented in a much simplified form. These new equations have been verified to yield the same results as those specified in the Regulatory Guide.

**The Correction Of LLRT Results For Instrument Error Was Dropped**
The 1987 version of the ANSI Standard requires that all measured Type B and C test results be corrected for instrument error. The statistical method prescribed was technically correct and good engineering practice. Although, if all of the instrumentation specifications and requirements for Type B and C testing equipment in the standard are followed, the magnitude of this error is very small.

The value of a plant's allowable leakage is based upon Part 100 Post-LOCA offsite dose calculations. These in turn are based upon many broad assumptions which have a high degree of uncertainty built-in to them. Weather conditions, filter efficiency, source terms etc are very difficult parameters to accurately quantify. Due to this uncertainty, estimates of their values are made in a very conservative manner. The elimination of the small correction for LLRT instrument error, and the station labor required to perform these calculations was determined to be prudent.

**Definitions**
Additional definitions associated with local leakage rate testing were added. All definitions were reviewed for compatibility with those contained in the proposed Appendix J.

**Increased Amount of Information On LLRTs**
The concepts and methodology for calculating Maximum and Minimum Pathway leakage rates were added to the standard. The concept of As Found and As-Left leakage rates were also added. More specific guidance is given on the performance of LLRTs and the addition of LLRTs as penalties to the Type A test results.

**Major Changes To The Section On Instrumentation**
The section of the Standard on instrumentation was extensively modified. ILRT and Local Leakage Rate Tests,(LLRTs) instrumentation has in the past been very specialized equipment. The rewrite intended to modify the Standard so that this equipment is specified and instrument parameters defined in a manner consistent with the mainstream instrumentation industry.

Due to the recent use of relative humidity sensors to measure humidity, specifications for these sensors were added.

The calibration interval specifications were dropped, leaving it up to the licencee's Instrument Quality Assurance Program to properly determine those intervals.

In-Situ checks were replaced with pretest checks. This requires the licencee to check sensors shortly before the ILRT, after the final connections have been made. This change eliminates the impractical task of checking the sensor in the actual location in containment where it is to be used. In large PWR type containment with 150' domes, in-situ checks were especially difficult.

The instrumentation accuracy, resolution and sensitivity specifications were relaxed. This allowed them to be measured and defined in a way standard to the instrumentation industry and to be met by existing instrumentation on both an As Found and As Left basis. The ability to accurately measure the desired magnitudes of containment leakage rate were not significantly affected by these changes.

**Type A Test Data Rejection Criteria Clarified And Improved**

The 1987 standard allowed for a maximum of 60 containment dry air mass points to be reviewed for outliers. The new revision allows for up to 100 points to be examined. This is more typical of the number of points actually expected in a Type A test. The text discussing data rejection philosophy was added to and improved.

**Calculation Of Total Containment Dry Air Mass**

The calculation of total containment dry air mass and intermediate parameters were shown in more detail. New features include a dew temperature/vapor pressure correlation and a RH, temperature/ dew temperature correlation for use with RH sensors. Also, a method of correcting the total containment dry air mass for changes in total containment free air volume due to water level changes is given.

**Modifications To The Standard To Make It Compatible With The Proposed Revision To Appendix J**

- The interval between the preoperational and the first periodic Type A test is now required to not exceed three years.

- The Type A test schedule was decoupled from the 10 year ISI schedule. The interval between periodic tests may be as long as four years, with a 25% margin subject to a 3.25 times limiter on any three consecutive tests.

- The requirement to perform to a reduced pressure preoperational Type A test was eliminated. Also, the option to perform reduced pressure periodic Type A tests was dropped.

- The acceptance criteria for the As Found Maximum Pathway leakage was changed from 0.75La to La.

- The maximum Type A retest interval was changed from 18 months to 30 months for units on accelerated schedules.

- The Type A test pressure was allowed to drop by up to 4% below Pa during the Type A test.

It is significant to note that the proposed Appendix J prescribes that the total As Found Maximum Pathway leakage rate be used for comparison against the 0.6La criteria. The 56.8 committee felt strongly enough against this position so as to retain their view in the standard that this leakage should be calculated on a Minimum Pathway basis.

## CURRENT STATUS

Following completion of this revision to the Standard, it is currently planned to modify and issue the NUMARC document. This would now serve as a detailed technical supplement to the Standard, rather than an alternative to it.

It is believed the major changes to 56.8 have been completed, and a final draft will soon be sent though the ANSI review process. After the final draft of the standard is completed, work on the NUMARC document may begin, so as to assure compatibility.

All of the above actions are based upon the proposed Appendix J being approved. If this were to not occur, then both the ANSI standard and the NUMARC report would require considerable rework.

## References


1. ANSI 45.4-1972, "American National Standard Leakage-Rate Testing of Containment Structures for Nuclear Reactors".

2. September, 1991 Draft Revision to 10 CFR Part 50, Appendix J.

3. Draft Regulatory Guide,"Containment System Leakage Rate Testing", MS 021-5, October 28, 1986.

4. ANSI/ANS-56.8, 1987, "Containment System Leakage Testing Requirements".

5. BWROG Draft Licensing Topical Report (LTR), "Standardization Program for Primary Containment Integrity Testing", NEDO-31722, Class I, August 8, 1989.

# INDUSTRY CURRENT AND FUTURE PLANS FOR IMPLEMENTATION OF PROPOSED REVISION OF 10 CFR PART 50, APPENDIX J, CONTAINMENT LEAK RATE TESTING

## BACKGROUND

The NRC has proposed revision of the Containment leak rate testing requirements as specified in 10 CFR Part 50, Appendix J, *Leakage Rate Testing of Containments of Light-Water Cooled Nuclear Power Plants*, as described in documents released to the NRC Public Document Room on January 10, 1992. It is our understanding that this proposed revision of Appendix J reflects the staff disposition of public comments that is in process of review by the Commissioners. The industry has maintained a continuing dialogue with the NRC through public forums such as interactions of the BWR NSSS Owners Group, the ANS 56.8 Committee, Containment Leak Rate Test Work Shops and, since 1991, as a generic issue through NUMARC/NRC meetings. This dialogue has positively contributed to a communication and understanding of methods and issues that can facilitate containment leak rate testing. The industry's review of the proposed Appendix J revision indicates that resolution of certain aspects of the revision could further reduce contamination, exposure and unnecessary use of resources without any reduction in the health and safety of the public.

## RECOMMENDED CHANGES TO THE PROPOSED APPENDIX J REVISION

NUMARC, in a letter to the NRC dated May 13, 1992, recommended that the following requirements of the proposed revision to Appendix J be addressed prior to Commission approval and issue for implementation:

### LOCAL LEAK RATE TESTING DURING NON A TYPE OUTAGES - INTEGRATED LEAK RATE TESTING (ILRT)

The NRC proposes to require as-found testing of all containment penetrations and valves during every outage even if the penetration or valve has no history of degradation or failure. Unnecessary increased exposure, contamination and cost result. The industry proposes to perform as-found testing on penetrations and valves during ILRT cycle outages based on established criteria acceptable to the industry and the NRC. During non-ILRT outages, the focus should be on valves and penetrations whose performance during as-found testing indicates leak testing is needed during the next test interval. It is estimated that this approach would avoid unnecessary testing of 70% of the valves and penetrations during outages in which Type B and C testing is required, yet test all valves and penetrations during the Type A test (ILRT) cycle.

### MINIMUM VS. MAXIMUM PATHWAY AS FOUND LEAKAGE

For all sets of in-series valves, the NRC proposes to require licensees to include the greater of the leakages of any two in-series valves in the calculation of the as-found aggregate leak rates (this methodology is commonly referred to as maximum pathway leakage rate basis). Since the as-found actual leakage rate of both in series valves is known, the smaller leakage rate

of the two valves is the proper leakage rate for calculation of total leakage rate (this methodology is commonly referred to as minimum pathway leakage rate basis). Although highly conservative, the industry accepts the maximum pathway leakage rate of 0.60La as an appropriate target for as-left leakage prior to restart from an outage.

## REPORTING OF AS-FOUND LEAKAGE GREATER THAN 0.6La

The NRC's criterion for reporting as found leakage for Type B and C testing is inconsistent with its approach in establishing criteria for reporting as found leakage for Type A testing and is not technically justified. Under technical specification and Appendix J criteria, failure reporting is not required for Type A ILRT unless leakage exceeds 1.0La (note the allowable as left leakage rate is established as 0.75La to allow for operating cycle changes). In the proposed NRC revision to Appendix J, Type B and C testing establishes as left allowable leakage as 0.60La but after an operating cycle requires reporting of as found leakage in excess of 0.60La. The NRC appears to add this requirement as an indication of the effectiveness of maintenance and not because a 0.60La leakage level is necessary to provide assurance for public health and safety. The 1.0La criterion is already very conservative and is being reconsidered by the NRC as an opportunity to alleviate unnecessary regulatory burdens that do not ensure public health and safety. The current area of consideration addresses isotopic release concentrations.

## RETENTION OF BN-TOP ILRT METHODOLOGY

During Type A ILRT of the containment and after stabilization, utilities have often been able to complete containment testing within 6 hours and have been able to verify test instrumentation adequacy within 4 hours of completing the 6 hour test period through the use of the previously accepted BN-TOP testing methodology. The NRC proposed revision eliminates this option by imposing no less than 8 hour and 4 hour increments respectively. The cost to the industry is critical path off-line increased hours. In addition, the requirement for a BN-TOP stabilization period of one hour between the containment test and the instrumentation verification test is unnecessary and could be omitted. This deletion would be consistent with the NRC currently proposed approach for mass point testing. Although it is recognized that BN-TOP testing may be allowed, it is recommended that this option be specifically allowed in the rule, accompanying Regulatory Guide or a revision of ANS 56.8.

## REGULATORY GUIDE ENDORSEMENT OF ANSI/ANS 56.8

The purpose of the Appendix J proposed revision is to clarify requirements, minimize the need for waivers and facilitate field interfaces and enforcement. In order to achieve this objective the rule is tied to the 1987 version of ANSI/ANS 56.8 standard that does not adequately provide implementation guidance.

Some portions of the existing ANSI/ANS 56.8 are contrary to the existing licensing basis of some plants. For example, one utility's FSAR specifies different testing/controls for test, vent, and drain (TVD) valves than does the current revision of ANSI/ANS 56.8. The proposed revision to Appendix J should be implemented when the changes to ANSI/ANS 56.8 have been developed and incorporated into a revision of the standard. The Maintenance Rule has been issued without a regulatory guide; but, has been issued with a clear milestone that additional guidance will be developed and finalized by June 1993. A similar approach is warranted relative to the implementation of the proposed revision to Appendix J. A schedule that includes a commitment for resolution of the ANSI/ANS 56.8 issues should be established. The NRC has indicated it will consider endorsing a revision the ANSI/ANS 56.8 when it is completed.

## ADDITIONAL FLEXIBILITY IN TEST PERIODICITY CONSISTENT WITH GL 89-14

The NRC requires Type B and C tests periodicity not to exceed 3.25 times the scheduled test interval although waivers are allowed on the merits of the request. This requirement was deleted for technical specification surveillances in accordance with GL 89-14. To promote consistency and since no basis was provided to support the need for different time intervals, it is recommended that Appendix J test intervals be treated the same as the surveillance test addressed in NRC GL 89-14.

## REQUIREMENTS FOR MAINTAINING CONTAINMENT TEST PRESSURE

The NRC proposes a requirement in Appendix J, Section III.A.5 that, "...the Type A test pressure must be within 4 percent of Pac at the start of the test, but must not exceed containment design pressure and must not fall more than 4 percent below Pac for the duration of the test, not including the verification test." The October 29, 1986 version of the rule, which is the current industry practice, requires that, "the Type A test pressure must be equal to or greater than Pac at the start of the test, but must not exceed containment design pressure and must not fall more than 1 psi below Pac for the duration of the test, not including the verification test." The new rule relaxes the acceptable Type A test pressure band for high pressure containment designs (greater than 25 psig) and tightens the band significantly for low pressure containment designs such as ice condenser PWRs and some BWRs. For example, the acceptable band for a 10 psig containment is ± 0.4 psi; whereas, the acceptable band for a 50 psig containment is ± 2.0 psi. A 0.5 to 1.5 psi pressure drop can normally be expected during the temperature stabilization period followed by another 0.3 to 1.0 psi pressure drop during the leak rate test. Since the starting test pressure following the temperature stabilization period is often difficult to predict, the ± 4 percent pressure band requirement is too restrictive for low pressure containment designs. It is recommended that criteria be established that establish the allowable pressure drop to be

within either a ± four percent band or 1 psig, whichever is greater.

INSTRUMENT TEST FAILURE NON-EFFECT ON TYPE A ILRT RESULTS

A clarification is needed of Section III.A.7 to specify that a failure that occurs during a verification test because of a testing deficiency does not constitute a failure of the Type A test. The purpose of the verification test is to confirm that the instrumentation and data acquisition systems can detect leakage. Although the test is not concluded successfully and retest is required, the containment leak rate criteria are not failed unless a valid test demonstrates unacceptable leakage.

INTERPRETATION OF ONE INCH NOMINAL PIPE SIZE ATTACHMENTS

Section IV.E. has been changed to disallow deferral of Type A testing for modifications that result in welds attaching penetrations whose outside diameter exceed one inch. The original criterion was greater than one inch nominal pipe size. Any one inch nominal pipe size penetration will exceed a one inch outside diameter. The change in wording from nominal to outside diameter will force more frequent application of the requirement for a standard integrity test without a valid technical basis for the change in requirement. It is recommended that the original criterion remain unchanged.

ADDITIONAL FLEXIBILITY ALLOWANCE FOR EXTENDED OUTAGE PERIODS AND REPORTING

In the proposed revision the NRC already has allowed test frequency deferral if containment integrity is not required as would be the case for a utility that is an extended outage period. In paragraph B.3(a) on page 44 at the end of the second sentence, the same qualification that is allowed in paragraph III.A.3(c) on page 38 should be added

In paragraph VI.A.2 on page 51, additional flexibility could be provided to utilities if the first two lines were changed to read as follows: "... reported to the Commission in a manner specified in Section 50.4 not later that 3 months after the failures occur if operating or 3 months after the outage in which they occur. As indicated above, as found leakage should not be considered a failure on the basis of 0.60La criteria.

INDUSTRY PLANNED CONTINUED INTERACTION WITH THE NRC

We look forward to continued interaction with the NRC on the issues I have just discussed. In addition, we will continue to work on implementation of any revisions to the rule. The industry expects that the above issues will be considered by the NRC Staff and Commission in the near future.

# CONTAINMENT PENETRATIONS - FLEXIBLE METALLIC BELLOWS TESTING, SAFETY, LIFE EXTENSION ISSUES

James A. Brown
NUTECH Engineers

Greg A. Tice
NUTECH Engineers

## Abstract

The performance and long-term operational integrity of containment systems and components is being challenged as many of the world's nuclear plants progress into the second half of their design lives. As time in service increases, so does the likelihood of component degradation and failure. By observing trends in containment degradation, potential weaknesses can be anticipated and corrected, minimizing interruptions in operations, increasing safety and improving the plant's life extension outlook. One such trend, affecting containment penetration flexible metallic bellows that are subject to cyclic loading, is beginning to appear in some BWR plants.

Although the overall performance of flexible metallic bellows penetrations has appeared to be acceptable for approximately 20 years, aging and degradation of these components has been recently identified. Corrosion and fatigue mechanisms have lead to cracking and subsequent leakage through the stainless steel bellows elements. Although periodic testing in accordance with 10CFR50, Appendix J has been performed, fabrication features of some expansion joint assemblies has made it difficult to collect reliable leakage rate data. In fact, recent observations suggest that it is not possible to perform valid local leak rate testing of two-ply bellows elements.

This paper presents a description of efforts made to characterize the nature and significance of the penetration degradation observed. Field pressure testing and laboratory examinations are discussed, as well as evaluations to determine leak areas and leakage rates. Crack growth from both corrosion and fatigue mechanisms are examined, and methods for predicting remaining useful life are discussed. The repair and replacement methods employed will be summarized as well as the testing performed to demonstrate replacement effectiveness.

## BACKGROUND

The GE Mark I containment systems at several BWR units employ circular flexible metallic bellows at specific penetrations in the drywell. They are designed to isolate drywell motions, resulting from thermal and pressure transients that occur during normal operation and postulated accident conditions, from piping components and the reactor building structures that support them. Depending on the application, expansion joints are designed to accommodate varying degrees of freedom and amounts of motion or displacement. The most commonly used configuration, the universal expansion joint, permits axial, lateral and angular displacements acting simultaneously. These terms describe the motions that one end of the bellows assembly may make relative to the other end and the main axis of the penetration. Other joint designs, such as those that limit axial and angular displacement but permit lateral motions, are also used.

The bellows assemblies discussed in this paper were fabricated using two plies of stainless steel sheet material, rolled and formed together into their final configuration. The small annulus between the inner and outer plies is connected to tubing fitted to permit periodic pressure testing for leakage detection. Initially, such pressure testing discovered very little, if any, leakage. After approximately 15 years of operation, however, increases in leakage rates have been observed.

Since then, several bellows elements have been replaced to eliminate known leakage paths and reduce the primary containment system's total integrated leak rate. The removed components were subjected to metallographic examinations as

part of root cause investigations. The flaws thereby identified have been attributed to trans-granular stress corrosion cracking (TGSCC).

Several methods, including testing, analysis and modelling have been used to evaluate the observed degradation. The value of tracking integrated leak rate test (ILRT) data and how this information can be used to assess "safety significance" has been demonstrated by practical application. In addition to metallographic testing, fracture mechanics techniques have been used to estimate crack growth per unit of time, the results of which are used for predictive purposes. Finite element modelling coupled with flow calculations have been used to predict leakage rates for a wide range of flaw sizes. Finally, by integrating the results of these various efforts, a long term inspection and replacement program can be developed to proactively address bellows degradation issues.

## COMPONENT DESCRIPTION

The Mark I primary containment drywell vessel is a stand-alone steel structure around which the reactor building, consisting primarily of reinforced concrete, is constructed. Penetrations of various sizes are built into the drywell vessel shell to permit electrical connections, process piping, instrumentation, personnel and equipment to communicate between reactor vessel system components inside and the balance of plant systems outside. A typical penetration consists of a reinforced opening in the vessel shell with an integrally welded nozzle or "sleeve". This penetration sleeve may or may not form part of the process pipe. Usually, larger diameter sleeves and those designed for the passage of high energy pipes are configured as free-ended nozzles, which are connected to the process pipe by a flexible metallic bellows assembly as shown in Figure 1. Penetration sleeves can vary in length from a few feet to ten feet or more.

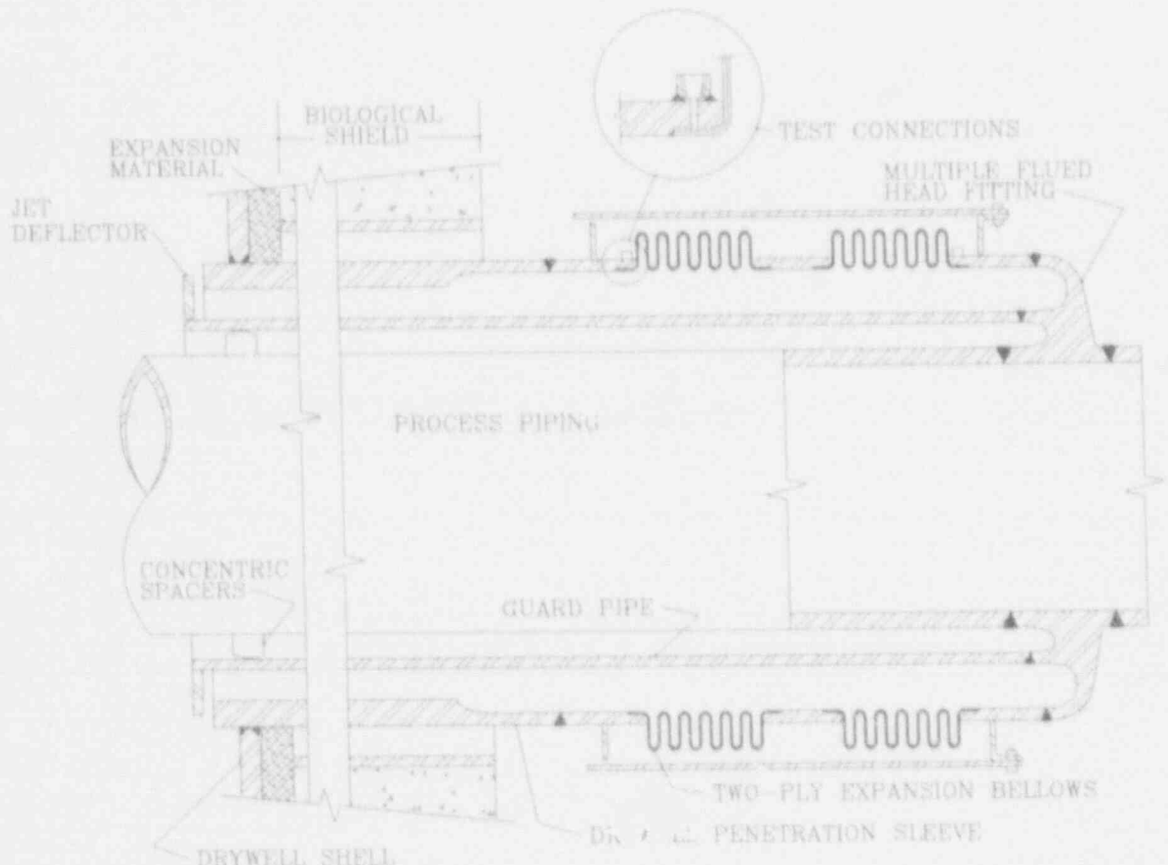


Figure 1. Drywell Penetration Configuration

Drywell penetration flexible metallic bellows are cylindrical in cross section and incorporate one or two thin-walled corrugated stainless steel elements. Most bellows assemblies are the "universal type" which incorporates two sets of corrugated elements with a short section of straight pipe between them (this is the type depicted in Figure 1). The corrugated elements themselves may be constructed using one or two layers or "plies", usually of an austenitic stainless steel material. Two ply bellows elements were intended to provide a means by which the assembly could be tested for leak tightness. Leak tightness could be demonstrated by the introduction of gas as a test medium between the plies which would then be monitored for pressure decay or make-up flow rate. It is this design feature that is of particular interest in this paper.

Flexible metallic bellows penetrations were typically manufactured as an assembly in the supplier's factory. The assembly would consist of the bellows elements themselves, two or three pipe spools pieces depending on the type specified, test taps (fittings) for connection with in-plant systems, and protective covers or guards intended to shield the bellows elements from mechanical damage. The various components are joined by welding and those joints forming part of the pressure boundary meet the ASME rules for metal containment. The materials used to fabricate the spool pieces were generally selected to match the materials to which they would be joined in the field. The protective covers were usually made from sheet metal formed into a cylindrical sleeve of sufficient inside diameter to permit the full range of bellows movements without coming into contact with them. The covers are held in place by mechanical fasteners ' angle clips welded to one of the end spool pieces, and prevented from contacting the bellows by "bumper" spacer bars welded to the other end spool piece.

The bellows elements themselves are fabricated from thin-gauge (approximately 0.030" - 0.050") stainless steel sheet metal. The sheet metal is first roll formed into a tube and the longitudinal joint autogenously welded in a special welding machine made for this purpose. These tube "blanks" are made long enough for subsequent axial collapse resulting from convolute forming, and of a diameter approximately equal to that of the finished elements. The tube blanks are then pre-formed by selective expansion (using hydrostatic pressure and/or mechanical force) in local circumferential zones that will subsequently become the convolutes. Final forming of each convolute is accomplished by rolling the pre-formed tube between rotating opposing dies whose spacing and degree of engagement can be varied until the desired convolute shape is achieved. Two-ply bellows are fabricated in the same fashion except that two tube blanks are fitted one inside the other. The space between the two plies is generally kept as small as practical to assure uniform inner and outer ply convolute shape. In some cases a wire mesh was "sandwiched" between the inner and outer plies in an attempt to assure that an annulus was mairtained throughout the entire bellows surface.

The ends of each bellows element assembly was formed into a straight "cuff" and trimmed square to the bellows axis. This cuff was fit into recesses machined into the I.D. of the pipe spool pieces, in effect forming a socket type connection. The end of the recess was typically beveled such that when the bellows element cuff was inserted a single bevel groove joint was formed. When this joint was welded, both plies would be welded to each other and to the spool pieces, forming both the containment pressure boundary and a testable annulus between the inner and outer plies. A test tap fitting was then seal welded to an opening in the outer ply which provided access to the annulus between plies. The outer ends of the pipe spool pieces were machined for standard V-groove preparations.

At the plant construction site, this assembly was fit and welded to either the flued head process pipe fitting or to the drywell nozzle. The process pipe with integral flued head fitting was then inserted into the drywell nozzle and aligned to be coaxial with the nozzle. The final closure weld between the bellows assembly and either the flued head fitting or the drywell nozzle was then completed. Tubing would be subsequently field routed and connected to the test taps. Although installation tolerances were provided, it was generally intended

that the bellows penetration assemblies be installed in the "neutral" position, such that it was not subjected to initial displacement due to misalignment.

## DESIGN CONSIDERATIONS

Flexible metallic bellows penetrations are used to accommodated the relative motion between process pipes and the primary containment vessel resulting from thermal expansion and pressure displacement. The GE primary containment vessel (drywell) is a "bulb shaped" steel structure consisting of spherical and cylindrical sections. The drywell is considered free to move under pressure and thermal loads except where it is fixed at the base where a support skirt bears both the drywell and reactor pressure vessel components. Internal pressure and thermal expansion result in radial and vertical movements of the drywell vessel shell. The drywell vessel is enclosed in reinforced concrete for biological shielding, protection from external (environmental) forces and lateral restraint from seismic loads. A gap between the steel shell and the concrete shielding was formed by the application of polyurethane foam batting to the vessel external surface before pouring the concrete to allow for unimpeded drywell expansion. A schematic of the drywell vessel geometry is depicted in Figure 2.

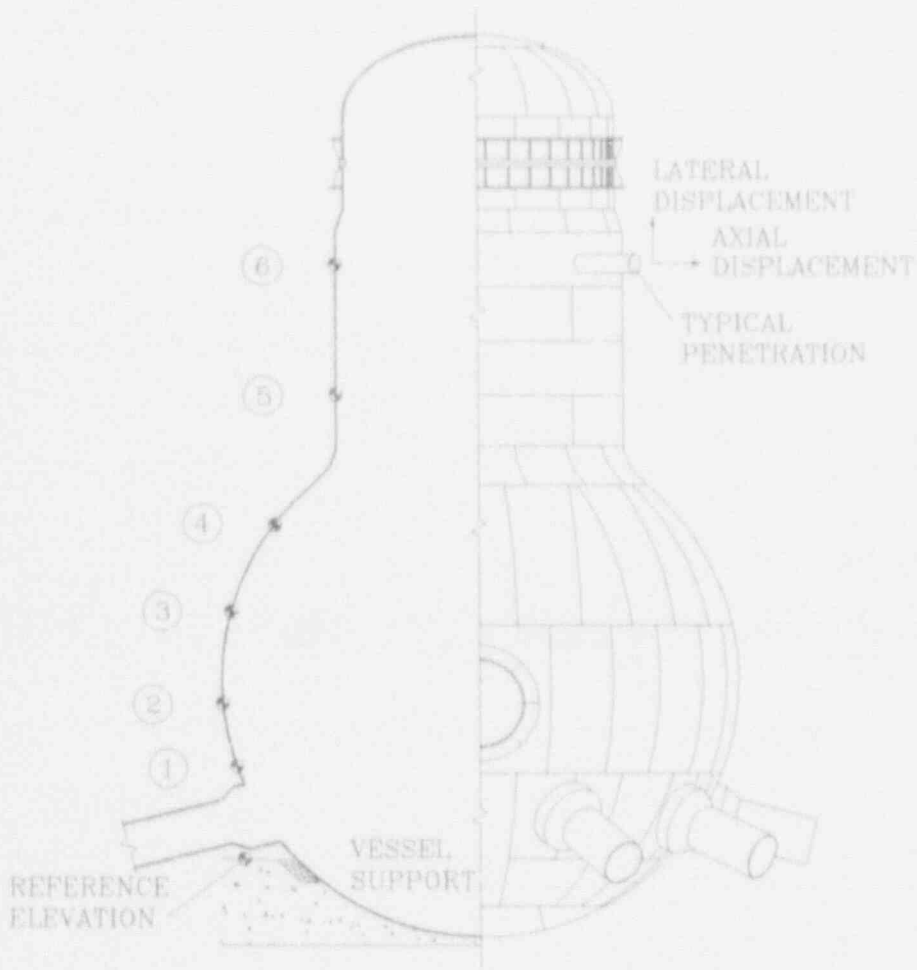


**Figure 2. Mark I Drywell Vessel Geometry**

Drywell movements result in bellows axial and lateral displacements. The bellows displacements are derived from penetration nozzle movements at particular drywell

elevations. Process pipe movements would also be expected to result in relative displacements. However, high energy lines and other process piping using bellows assemblies, are typically anchored at the flued head resulting in negligible movement attributable to the pipe. Drywell shell movements are calculated with respect to a fixed reference point (i.e. the vessel pedestal). Typical resulting drywell penetration displacements at various elevations are depicted in Table 1 (see Figure 2 for relative locations).

| Penetration No. | Elevation (ft.) (from Reference Elevation) | Axial Displacement (in.) | Lateral Displacement (in.) |
|---|---|---|---|
| 1 | 14'-0" | 0.82" | 0.25" |
| 2 | 21'-0" | 0.84" | 0.40" |
| 3 | 39'-0" | 0.84" | 0.78" |
| 4 | 48'-0" | 0.70" | 0.97" |
| 5 | 65'-0" | 0.57" | 1.20" |
| 6 | 81'-0" | 0.56" | 1.49" |

**Table 1. Typical Displacements Relative to Elevation**

The bellows assemblies are designed for normal operating conditions (NOC) and Loss-of-Coolant-Accident (LOCA) conditions. The NOC is based on the pressure, temperature and drywell movements that occur during normal operation of the plant. Cycling between cold shutdown and NOC occurs many times during the plant's service life. In addition, loads resulting from periodic pressure testing (ILRT) stress the bellows elements many times during their design life. LOCA design conditions, derived from a postulated double-ended rupture of a large-bore reactor coolant pipe, are considered a one-time event. Typical conditions for which bellows assemblies are designed are summarized in Table 2.

| Parameter | NOC | LOCA |
|---|---|---|
| Drywell Pressure (psig) | 2 | 62 |
| Drywell Temperature (°F) | 150 | 350 |
| Test Pressure (psig) | 48 | - |
| Axial Displacement (in.) | $x_{NOC}$ | $x_{LOCA}$ |
| Lateral Displacement (in.) | $y_{NOC}$ | $y_{LOCA}$ |

**Table 2. Typical Design Conditions**

As indicated earlier, process pipes routed through drywell penetrations incorporating flexible metallic bellows are typically high energy lines. Therefore, the potential for line break within the penetration must be considered. Guard pipes are positioned around the process pipes and welded to the flued head fitting to permit escaping process fluid to be vented back into the drywell should such a rupture occur. In some installations, jet deflectors are also attached to the ends of the guard pipes just inside the drywell to deflect jet streams from inside the drywell entering the penetrations.

Flexible metallic bellows are typically designed using the analysis and criteria established in the Expansion Joint Manufacturer's Association (EJMA) Standards. The design of a particular bellows assembly is affected by numerous variables including diameter, thickness, convolution pitch and height, number of plies, method of reinforcement, manufacturing technique, material and material heat

In typical installations of new bellows assemblies, initial LLRT values are zero or very small. Trending of LLRT data at some domestic BWR plants indicates that these leak rate values remain stable for a period of time, suggesting that the condition of the bellows elements has remained essentially unchanged. After a period of approximately 5 to 15 years, an increase in leakage rates has been observed at some of the drywell penetrations (see Figure 3). Initially, these leakage rates tend to increase linearly with time, indicating that whatever is causing the rates to change is progressive, and that future leakage rates can be projected. Predictability is a necessary attribute for planning the required corrective actions which usually have a significant impact on plant operating and maintenance schedules.

In a number of cases the recorded LLRT data shows a tendency for rates to flatten out over time (as shown in Figure 3). In some cases the reported leakage rates actually begin to reduce after reaching a maximum value. These results are counter-intuitive and were initially attributed to ongoing improvements in techniques and instrumentation which tended to correct over-estimation of actual leakage rates made in the past. A recent discovery at an operating domestic BWR generating plant suggests that certain features of two-ply bellows elements impose limits on the degree of leakage rate accuracy attainable.

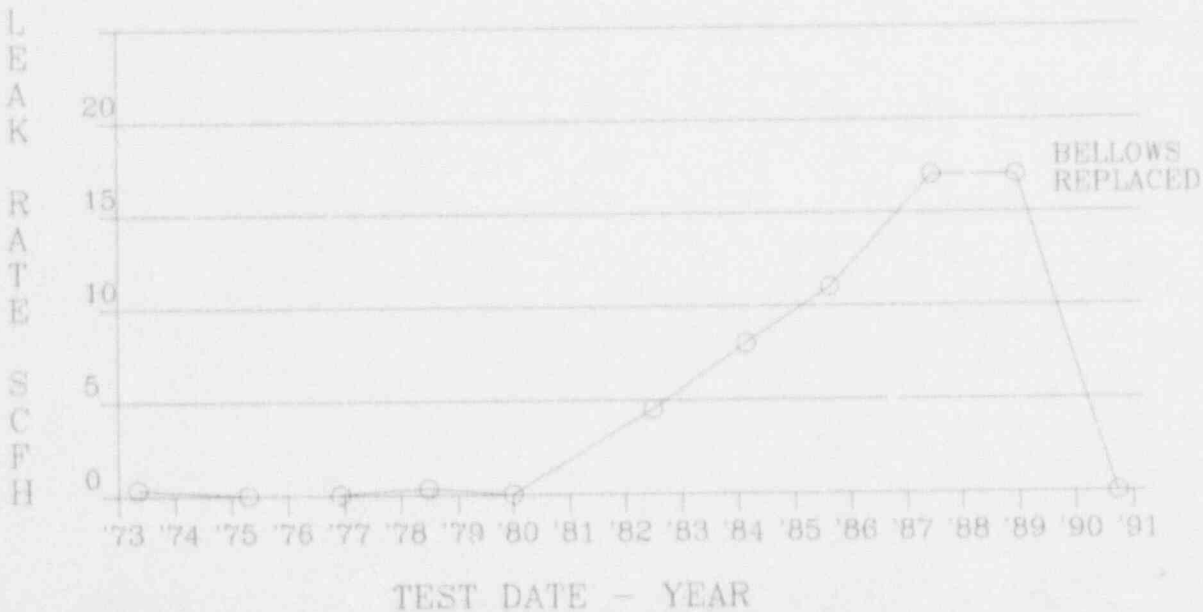


**Figure 3. LLRT Flow Rate vs. Time**

This recent case was initially discovered during performance of an Appendix J Type "A" test prior to start-up of the unit following a regularly scheduled refueling outage. During pressurization, a worker heard the hissing sound of gas escaping through an orifice. Since the sound was coming from the drywell vent penetration area, the bellows protective cover was removed to permit visual inspection of the bellows assembly. The leakage was readily identified as emanating from an apparent crack approximately one inch long in one of the bellows elements. Since the bellows appeared to be stable and the crack showed no evidence of growing, the penetration was monitored and the pressure test completed.

The most recent LLRT data for the affected penetration had been collected earlier during the refueling outage and indicated a leakage rate of approximately 6 standard cubic feet per hour (scfh). Since this particular penetration has no process pipe running through it, a flange had previously been installed on the

a proven Type B test can be implemented, the following procedure to test and evaluate bellows should be considered. Two-ply penetration bellows elements would be locally pressurized (between the plies) to determine if leakage exists. Those bellows that exhibit leakage greater than a small, minimum threshold value would then receive progressively rigorous inspections according to the following steps:

(1) If a bellows demonstrates a leakage rate above the minimum threshold, it would be locally pressurized with helium. The outer ply would be tested for the presence of helium as an indication of leakage through the outer ply. Since both the inner and outer plies are qualified primary containment boundaries, no further inspection is required if there is no leakage through the outer ply. If helium leakage is detected through the outer ply, inspection proceeds to step 2.

(2) If helium leakage is detected through the outer ply, then the inner ply would be tested for the presence of helium. If there is no leakage through the inner ply then no further inspection is required. If helium leakage is detected through the inner ply, inspection proceeds to step 3.

(3) If helium leakage is detected through both the inner and outer plies, then the bellows protective cover would be removed and the outer ply examined by PT and/or, after pressure was again introduced between the plies, a soap bubble "snoop" test performed. All observed flaw indications would be measured and mapped.

(4) All crack indications would then be evaluated to estimate current and projected leakage rates. This review would include a structural assessment of the bellows with regards to critical flaw size. (These considerations are described below in **SAFETY SIGNIFICANCE**.)

(5) Those bellows failing to meet the established acceptance criteria would be replaced.

These steps, the actions they require, and the options they present are further described below in **LIFE EXTENSION ISSUES**, Figure 6.

## SAFETY SIGNIFICANCE

Metallurgical examinations of several bellows elements have been performed over the past few years. Samples of failed bellows elements become available when the original components are replaced to restore containment boundary integrity. Various specimens have been examined using metallography, scanning electron microscopy (SEM), and energy-dispersive x-ray spectroscopy. In all cases, failure of the bellows was attributed to through-wall transgranular stress corrosion cracking (TGSCC). Crack propagation appears to be from the inner surface of the inner ply to the annulus between the plies. Once through the inner ply, cracking begins on the inner surface of the outer ply propagating to its outer surface.

Analysis of residues collected from the inner surface of bellows elements removed from service has revealed the presence of small amounts of fluoride, chloride and sulfide compounds. Inspection of the inner surface of the inner bellows also suggests that the penetrations have had small amounts of standing water in them at some time (or on several occasions). It has been suggested that the corrosion causing compounds may have originated in welding electrode coatings which were transported to the bellows elements and adjacent surfaces by the smoke liberated during welding. This material would then have been concentrated on the bellows elements by water from condensation, hydro-spray cleaning operations, or other sources.

The combined effect of contact with materials corrosive to stainless steel and

sleeve inside the drywell which is intended for mounting a blind flange to facilitate periodic testing of the containment isolation valve outside of the drywell. After the ILRT was completed, the blind flange was installed and the volume between it and the containment isolation valve was pressurized such that both plies of the bellows were again challenged from the inside, in effect setting up a "local Type A" test. This permitted determination of the leakage attributed to the bellows only, which resulted in a measured leakage rate of approximately 137 scfh. Although this rate met Appendix J acceptance criteria, the bellows elements were immediately replaced with components of similar design.

The large difference between the previously obtained "inter-ply" LLRT results and the "local Type A" test rate was confirmed by connecting leak rate testing instrumentation directly to the penetration's test port. In an effort to determine if the bellows configuration may have contributed to the disparity, a small (approximately 1/4" diameter) hole was drilled through the bellows elements at a point furthest away from the test port. Re-testing showed that the leakage rate increased by approximately 1 scfh. Drilling another hole in the bellows elements near the test port only increased inter-ply LLRT leakage by approximately 2 scfh.

As previously discussed, the annulus between the inner and outer plies of two-ply bellows elements is kept small during manufacture to aid in subsequent forming operations. Two-ply bellows elements that have been removed from service and sectioned along the bellows longitudinal axis reveal that the spacing between plies can be reduced by forming operations to virtually an interference fit (as shown in Figure 4). This extreme proximity inhibits the flow of test medium and severely limits inter-ply LLRT capability to accurately measure leakage rates. It is this limitation that has led to the conclusion that it is not possible to perform a valid Type B LLRT on this type of bellows assembly. It also explains why in some cases measured leakage rates reach maximums, beyond which little if any further increase occurs, regardless of changes in flaw geometry.

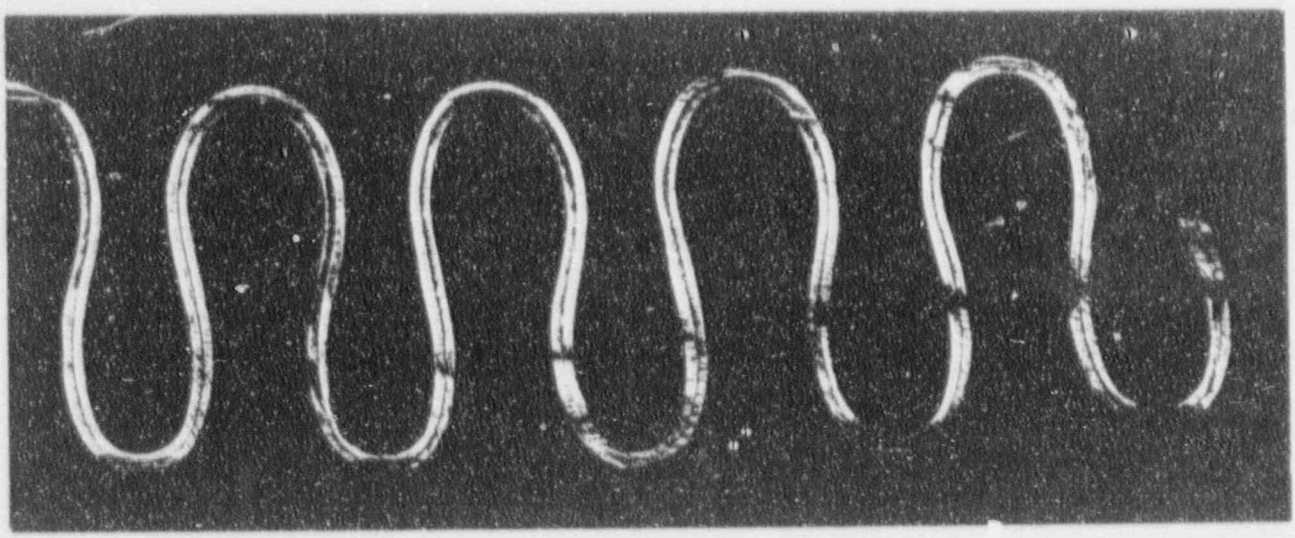

**Figure 4. Section of Two-Ply Bellows Elements**

Although flow rate of the test medium is apparently impeded by the two-ply bellows element design, it is nevertheless capable of challenging all surfaces exposed to it. In other words, inter-ply LLRT is still an effective leak *detection* method, but not a reliable leak rate measurement method. Thus, until

bellows elements subjected to plastic strain during manufacture and service could lead to the types of flaws observed. Normal cyclic displacement may also introduce fatigue as a crack growth mechanism, although the low frequency of operating deflections suggests that fatigue is likely a minor contributor to crack growth rates.

Since inter-ply LLRT cannot provide accurate leakage rate information, and not all penetrations can currently be isolated such that a "local Type A" test can be performed, method to estimate leakage rates through various known flaw sizes is needed. One method used to accomplish this is to approximate the geometry of crack-like orifices and then calculate gas flow rates through them. In an effort to account for the fact that bellows elements are subjected to internal pressures during testing that tend to expand the bellows radially and force tight cracks to open slightly, a finite element model is used to simulate such a system's response to pressure loads (as shown in Figure 5). The resulting crack geometries are used to describe the orifice for pneumatic flow calculations which are adjusted to reflect empirical data obtained on known flow rates through known flaws.

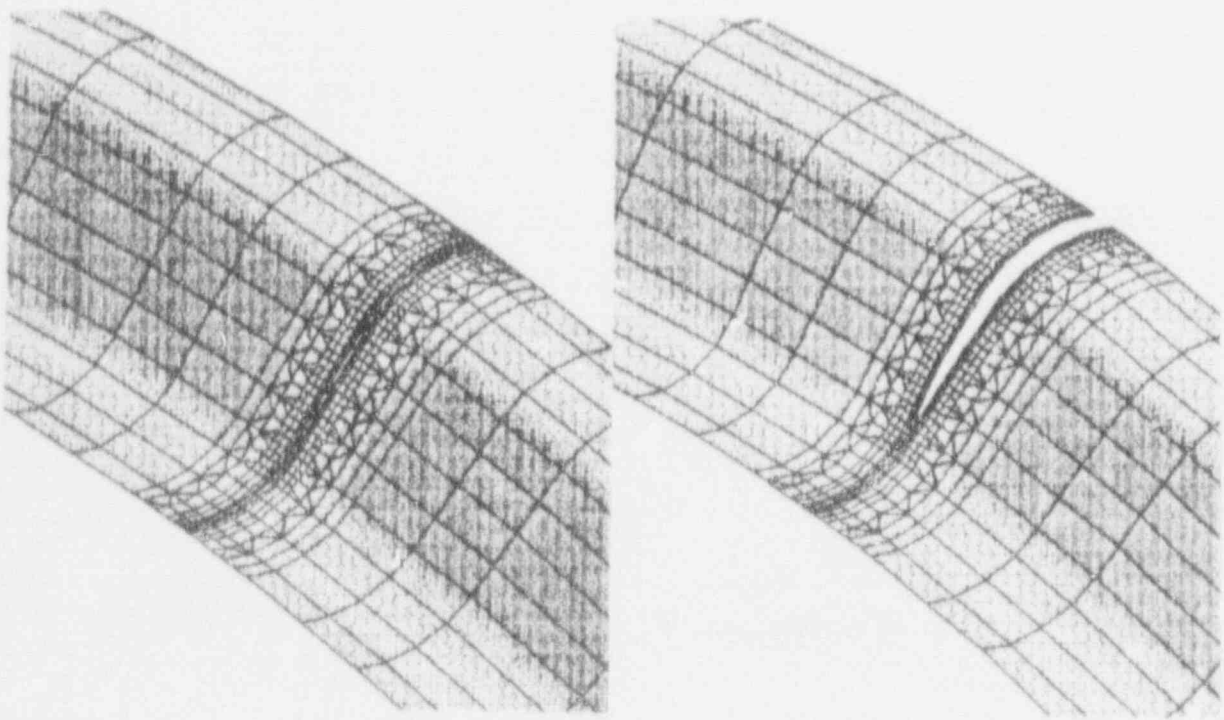

Undeflected Model

Deflected Model (Exaggerated)

**Figure 5. Cracked Bellows Finite Element Model**

In evaluating the service suitability of bellows with known flaws, it may also become necessary to consider what maximum size flaw or combination of flaws is acceptable. A fracture mechanics evaluation of critical flaw size during design basis accident conditions can establish limits on permissible flaw size(s) to assure that uncontrolled crack growth during accident conditions cannot occur. Since access for inspection to most bellows penetrations is limited to refueling outages, it is also necessary to estimate the rate at which flaws may grow over time. Both TGSCC and fatigue factors should be considered when estimating crack growth rates, and applied to observed flaw sizes for the amount of time that will elapse until the next inspection becomes possible. The resulting projected flaw

size is then compared to the critical flaw size to confirm that the bellows are structurally sound for the service period.

## LIFE EXTENSION ISSUES

When determining whether given bellows elements are suitable for continued service, or when evaluating appropriate corrective actions, a logical sequence of actions and decision points can be constructed as a guide. One example of such a process is depicted in the logic diagram shown in Figure 6. The application of such guidelines is necessary for assuring consistency and thoroughness when evaluating useful life and planning replacement activities.

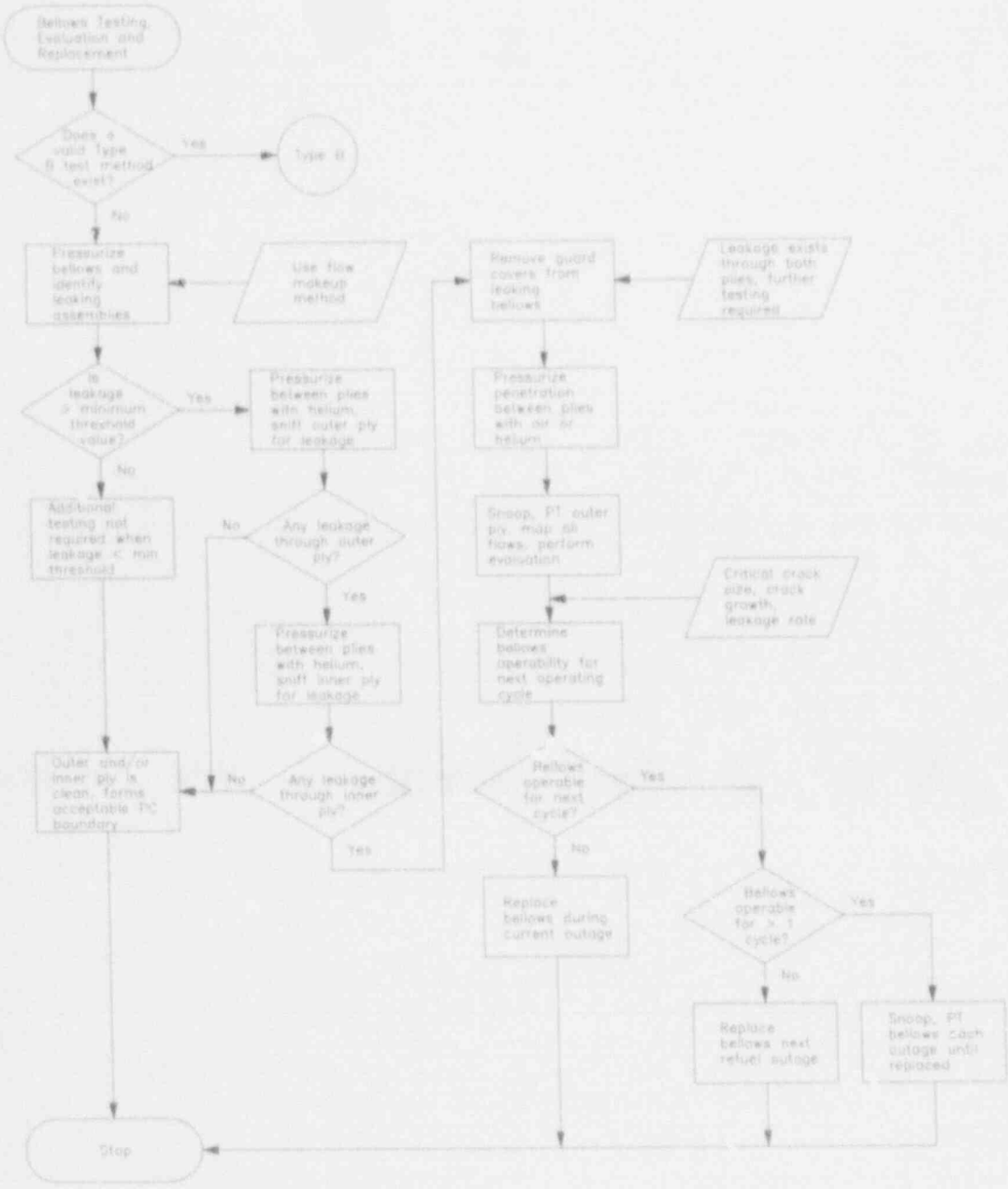


Figure 6. Corrective Action Decision Tree

The fundamental repair methodology for failed two-ply tandem type flexible metallic bellows is replacement. Since the original bellows elements were formed from single, seamless pieces of cylindrically shaped stainless steel sheet, the bellows elements usually cannot be replaced with identical units without necessitating disassembly of the process pipe and its supports. For this reason, the existing bellows elements of the expansion joint assembly are removed by mechanical means and the existing spool pieces are reused in the repaired assembly. The replacement design concept utilizes single-ply elements that are longitudinally split into two "clam shell" halves and assembled in-situ. Local leak rate testability can be restored by installing an additional single-ply bellows assembly just outside of the containment boundary bellows.

Variations of this type of replacement concept have been previously used in the petroleum and process industries. For primary containment boundary applications, two concentric single ply bellows, which may be made of stainless steel, nickel alloy or other suitable material, incorporate longitudinal field welded seams to form complete bellows elements. A typical example of this concept is shown in Figure 7. Circumferential field welds are then made to complete the pressure retaining boundaries. The inner bellows, which form part of the containment boundary, are subject to drywell normal operating and accident conditions on its inner surface and leak rate test environment on its outer surface. The outer bellows, which can be designed to act only as a test apparatus or as a redundant containment pressure boundary, is exposed to leak rate test environment on its inner surface and reactor building ambient conditions on its outer surface. Clearance between the inner and outer bellows elements is maintained by the utilization of a series of "standoff" rings, the height of which is determined such that no contact between the bellows can occur during all operating, accident and testing conditions. Maintaining this clearance also assures that future LLRT results are accurate since no test medium flow restrictions exist.

Although this corrective action concept results in replacement of the failed bellows elements, existing penetration assembly components are reused and the replaced components incorporate new longitudinal welds. For this reason, the replacement design should be qualified by prototype testing in accordance with Code Case N-315 of the American Society of Mechanical Engineers. This Code Case requires that the repair be qualified on a full scale facsimile bellows to simulate the production replacement. The facsimile is then subjected to fatigue testing (by displacement through a prescribed distance and number of cycles) and proof testing (by pneumatic or hydrostatic pressurization). Following testing, the repair welds are then examined by liquid penetrant (PT). The objective of prototype testing is to demonstrate that the replacement bellows have sufficient resilience to operate (maintain their pressure retaining integrity) for the remaining design life of the plant from the time of the replacement.

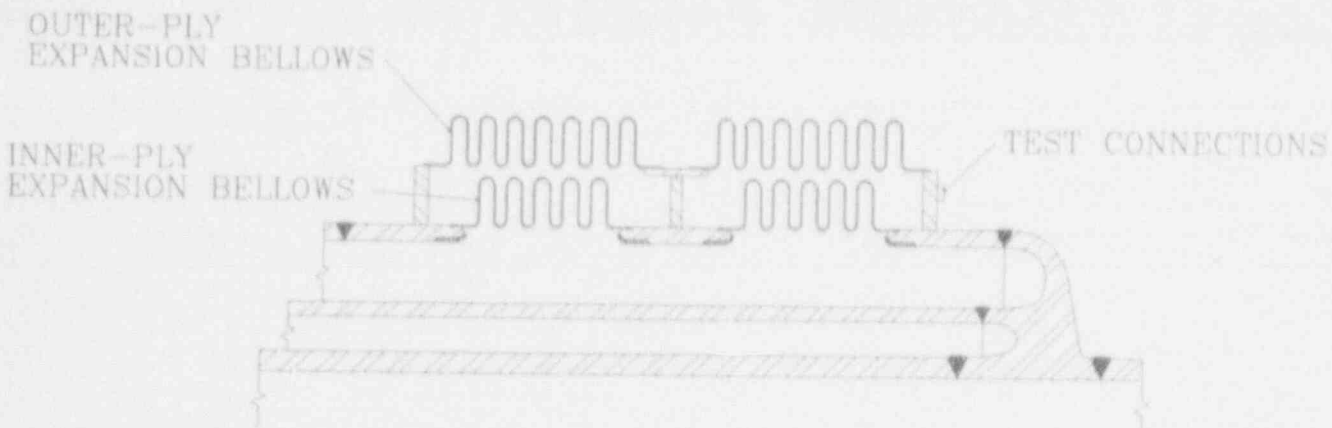


Figure 7. Bellows Replacement Configuration

SUMMARY

Primary containment flexible metallic bellows elements are designed to isolate drywell movements from penetrating components and have successfully performed this function while maintaining containment leakage integrity. Bellows long-term performance is now being challenged as many nuclear plants progress through the second half of their design life. In order to assure that bellows continue to perform their intended function, reliable leak rate testing is necessary, and when problems are found, effective corrective action is required.

Recent experience suggests that accurate determination of leakage rates through inter-ply pressurization of two-ply bellows elements may not be possible due to geometric constraints on test medium flow. Although Type A testing challenges the entire containment system boundary, it is important to know the contribution "testable" seals, valves and penetrations make to the integrated leak rate. Various methods can be used to obtain required LLRT data, however, replacement with a system fully capable of producing reliable test results may ultimately be the best solution. In our efforts to maintain the highest safety and reliability performance standards, we must endeavor to understand, and appreciate, the details.

Acknowledgement

The authors would like to express their appreciation to Messrs. Paul Berg, Scott Pape, Chris Johns and Dave DeGrush from NUTECH Engineers for their help in preparing this paper.

# AGING OF CONCRETE CONTAINMENT STRUCTURES IN NUCLEAR POWER PLANTS*

Dan J. Naus and C. Barry Oland
Oak Ridge National Laboratory (ORNL)
Oak Ridge, TN 37831-8056

Bruce Ellingwood and Yasuhiro Mori
The Johns Hopkins University
2400 N. Charles Street
Baltimore, Maryland 21218

E. Gunter Arndt
United States Nuclear Regulatory Commission (USNRC)
Washington, D.C. 20555

## Abstract

Concrete structures play a vital role in the safe operation of all light-water reactor plants in the U. S. Pertinent concrete structures are described in terms of their importance, design considerations, and materials of construction. Degradation factors which can potentially impact the ability of these structures to meet their functional and performance requirements are identified. Current inservice inspection requirements for concrete containments are summarized. A review of the performance history of the concrete components in nuclear power plants is provided. A summary is presented of the Structural Aging (SAG) Program being conducted at the Oak Ridge National Laboratory for the U. S. Nuclear Regulatory Commission. The SAG Program is addressing the aging management of safety-related concrete structures in nuclear power plants for the purpose of providing improved bases for their continued service. The program consists of a management task and three technical tasks: materials property data base, structural component assessment/repair technologies, and quantitative methodology for continued service conditions. Objectives and a summary of accomplishments under each of these tasks are presented.

## INTRODUCTION

History tells us that concrete is a durable material. However, a number of factors can compromise its performance, singly or in combination: (1) faulty design, (2) use of unsuitable materials, (3) improper workmanship, (4) exposure to aggressive environment, (5) excessive structural loads, and (6) accident conditions. Furthermore, aging of nuclear power plant concrete containment structures occurs with the passage of time and has the potential, if its effects are not controlled, to increase the risk to public health and safety. Many factors complicate the affect of aging on the residual life of the concrete containment structures in a plant. Uncertainties arise due to the following: (1) differences in design codes and standards for components of different vintage; (2) lack of past measurements and records; (3) limitations in the applicability of time-dependent models for quantifying the contribution of aging to overall structure, system, or

*Research sponsored by the Office of Nuclear Regulatory Research, U.S. Nuclear Regulatory Commission under Interagency Agreement 1886-8084-5B with the U.S. Department of Energy under Contract DE-AC05-84OR21400 with Martin Marietta Energy Systems, Inc.

component failure; and (4) inadequacy of detection, inspection, surveillance, and maintenance methods or programs [1].

Within the nuclear power industry, factors which affect the performance of the concrete structures due to aging or environmental stressors have become the subject of significant research in the last few years [2–4]. This interest is prompted by the need to quantify these effects in terms of potential loss of component integrity or function and to support current or future condition assessments in association with requests to continue the service of nuclear power plants. Since certain concrete structures play a vital role in the safe operation of nuclear power plants [5–8], guidelines and criteria for use in evaluating the remaining structural margins (residual life) of each structure are needed. Standardized review guidelines for near-term evaluation of operating license renewal applications may be required as early as the mid-1990's, when utilities are planning to submit initial requests.

## CATEGORY I CONCRETE STRUCTURES

### Design Considerations

Category I structures are those essential to the function of the safety-class systems and components, or that house, support, or protect safety-class systems or components, and whose failure could lead to loss of function of safety-class systems and components housed, supported, or protected. In addition, these structures may serve as barriers to the release of radioactive material and/or as biological shields. The basic laws that regulate the design (and construction) of nuclear power plants are contained in Part 50 of Title 10 of the *Code of Federal Regulations* (10CFR50) [9], which is clarified by Regulatory Guides, Standard Review Plans, NUREG reports, etc. "General Design Criteria" of Appendix A to 10CFR50 requires that structures, systems, and components important to safety shall be designed, fabricated, erected, and tested to quality standards commensurate with the importance of the safety functions to be performed. "General Design Criteria 2" requires that the structures important to safety be designed to withstand the effects of natural phenomena (e.g., earthquakes, tsunamis, hurricanes, floods, seiches, and tornados) without loss of capability to perform their safety function. "General Design Criteria 4" requires that structures important to safety be able to accommodate the effects of and to be compatible with the environmental conditions associated with normal operation, maintenance, testing, and postulated accidents including loss-of-cooling accidents. Furthermore, these structures must be appropriately protected against dynamic effects including the effects of missiles, pipe whip, and flooding that may result from equipment failures and from events and conditions outside the nuclear power facility. Section III, Division 2, Subsection CC, of the American Society of Mechanical Engineers Boiler and Pressure Vessel Code (ASME/ACI 359), first published in 1975, contains current rules for the design of concrete containments. Prior to 1975, concrete containments were designed and constructed to codes and standards developed by the American Concrete Institute such as ACI 318 [10]. Code requirements for nuclear safety-related concrete structures other than containments and reactor pressure vessels are contained in ACI 349 [11].

### Materials of Construction

Category I concrete structures are composed of several constituents which, in concert, perform more than one function, i.e., load-carrying capacity, radiation shielding, and leak tightness. Primarily, they include the following material systems: concrete, mild steel reinforcement, prestressing steel, and steel liner plate.

The concrete typically used in nuclear safety-related structures consists of Type II portland cement, fine aggregates, water, various admixtures for improving properties or performance of the concrete, and either normal-weight or heavyweight coarse aggregate. Type II portland

cement has been used because of its improved sulfate resistance and reduced heat of hydration relative to the general purpose or Type I portland cement. Coarse aggregate consists of gravel, crushed gravel, or crushed stone. For those concrete structures in nuclear power plants which provide primary (biological) radiation shielding, heavyweight or dense aggregate materials (e.g., barites, limonites, magnetites, ilmenites, etc.) may have been used to reduce the section thickness requirements needed for attenuation.* The hardened concrete typically provides the compressive load capacity for a structure. Design 28-day compressive strengths for the concrete materials utilized in nuclear power plant structures have typically ranged from 21 to 41 MPa depending on the application.

Most of the mild, or conventional, reinforcing steels used in nuclear power plant structures to provide primary tensile and shear load resistance/transfer consist of low-alloy carbon steels rolled or drawn into standard sizes and shapes. The surfaces of the reinforcing steel are either smooth (plain) or are provided with deformations (lugs or protrusions) to increase bond strength. The minimum yield strength of this material ranges from about 270 to 415 MPa, with the 415-MPa material being most common. Conventional reinforcing steel also encompasses welded wire fabric, deformed wire, bar and rod mats, and all accessory steel components used in positioning/placing the reinforcement, e.g., seats, ties, etc.

A post-tensioning system consists of prestressing tendons, which are installed and tensioned using jacks and other devices and then anchored to hardened concrete. A number of containment structures utilize steel prestressing tendons to provide primary resistance to tensile loadings. Three major categories of prestressing systems exist depending on the type of tendon utilized: wire, strand, or bar. These materials typically have minimum ultimate tensile strengths ranging from 1035 to 1860 MPa. The tendons are installed within preplaced ducts (conduits) in the containment structure and are post-tensioned from one or both ends after the concrete has achieved sufficient strength. After tensioning, the tendons are anchored by buttonheads, wedge anchors, or nuts, depending on the prestressing system utilized. Corrosion protection is provided by filling the ducts with corrosion-inhibiting grease (unbonded) or portland cement grout (bonded). With the exception of Robinson 2 (bar tendons) and Three Mile Island 2 (strand tendons), plants that have post-tensioned containments utilize unbonded tendons. A few plants have used bonded rock anchor tendons, e.g., Ginna and Bellefonte.

Leak tightness of reinforced and post-tensioned concrete containment structures is provided by a liner system. A typical liner system is composed of steel plate stock less than 13-mm thick, joined by welding, and anchored to the concrete by studs, structural steel shapes, or other steel products. The pressurized-water reactor (PWR) containments and the "dry well" portions of boiling-water reactor (BWR) containments are typically lined with carbon steel plate. The liner of the "wet well" of boiling-water reactor containments, as well as that of the light-water reactor (LWR) fuel pool structures, typically consists of stainless steel plates. Certain LWR facilities have used carbon steel plates clad with stainless steel for liner members. Although the liner's primary function is to provide a leaktight barrier, it also acts as part of the formwork during concrete placement and is used for supporting internal piping and equipment.

## Description of Category I Concrete Structures

A myriad of concrete structures are contained as a vital part of an LWR facility to provide support, foundation, shielding, and containment functions. Table 1 provides a general listing of safety-related concrete structures in LWR plants.

* Applications of heavyweight concretes primarily have been associated with research reactors.

Table 1. Representative LWR Safety-Related Concrete Structures*

| | |
|---|---|
| Primary Containment/Basemat | Intake Structure |
| BWR Reactor Building | Cooling Tower |
| PWR Shield Building | Spray Ponds |
| Containment Internal Structures | Utility or Piping Tunnels |
| Auxiliary Building | Part of Turbine Building (Category I Components) |
| Control Room/Control Building | Auxiliary Feedwater Pump House |
| Diesel Generator Building | Switchgear Room |
| Fuel Storage Facility | Unit Vent Stack |
| Tanks and Tank Foundation | Radwaste Building |

*Source: "Class I Structures License Renewal Industry Report," NUMARC 90-06, Nuclear Management and Resources Council, Washington, D.C., June 1990 (draft).

The names and configurations of these structures vary somewhat from plant to plant depending on the nuclear steam supply system vendor, architect-engineer firm and owner preference. Primary containment construction types utilized in the U.S. include: steel (PWR ice condensor, PWR large dry, BWR pre-MK, BWR MK I, BWR MKII, and BWR MK III), reinforced concrete (PWR ice condensor, PWR large dry, PWR subatmospheric, BWR MK I, BWR MK II, and BWR MK III), and post-tensioned concrete (PWR large dry and BWR MKII). As noted in Table 2, a reinforced or post-tensioned concrete material system has been selected as the primary construction type for over 60% of the LWR plant containments in the U. S. For the remainder of the plants which utilize steel primary containments, reinforced concrete is relied upon for fabrication of many of the safety-related structures (see Table 1). More detailed descriptions of the primary containments and other safety-related concrete structures are provided in Refs. 7, 8, 12, 13, and 14.

## Potential Degradation Factors

The longevity, or long-term performance, of Cat[illegible] concrete structures is primarily a function of the durability or propensity of these stru[illegible]s to withstand potential degradation effects. Over the life of a nuclear power plant, changes in the properties of the structure's constituent materials will in all likelihood occur as a result of aging and environmental stressor effects. These changes in properties, however, do not have to be detrimental to the point that the structure has deteriorated and is unable to meet its functional and performance requirements. In fact, it has been noted that when specifications covering concrete's production are correct and are followed, concrete will not deteriorate [15]. Concrete in many structures, however, can suffer undesirable degrees of change with time because of improper specifications, a violation of specification, or environmental stressor or aging factor effects. Table 3 summarizes primary mechanisms (factors) which can produce premature deterioration of reinforced and post-tensioned concrete structures. Reference 16 presents a good summary of potential degradation of reinforced and post-tensioned concrete structures in nuclear power plants in terms of locations, mechanisms, indications, potential problem areas, failure modes and examination methods/remedies. More detailed discussions of the potential degradation mechanisms are provided in Refs. 6–8, and 12.

Table 2. LWR Containment Distribution by Construction Type

| Plant Type | Containment Designation | Construction | | | Total |
|---|---|---|---|---|---|
| | | Steel | Reinforced Concrete | Post-Tensioned Concrete | |
| BWR | Pre - Mark | 1 | – | – | 1 |
| | Mark I | 22 | 2 | – | 24 |
| | Mark II | 1 | 5 | 2 | 8 |
| | Mark III | 2 | 2 | – | 4 |
| PWR | Large Dry | 9 | 11 | 42 | 62 |
| | Ice Condenser | 8 | 2 | – | 10 |
| | Sub-Atmospheric | – | 8 | – | 8 |

## INSERVICE INSPECTION REQUIREMENTS

Licensing and regulation of the nuclear industry in the U.S. is the responsibility of the USNRC under the provisions of the Atomic Energy Act of 1954, the Energy Reorganization Act of 1974, and the National Environmental Policy Act. Title 10, Part 50 of the U.S. Code of Federal Regulations (10CFR50) requires that safety-related nuclear systems and components, including containments, comply with specific editions and addenda of the American Society of Mechanical Engineers Boiler and Pressure Vessel Code (ASME Code). General Design Criteria in Appendix A of 10CFR50 specifically require containments to be designed to permit: (1) appropriate periodic inspection of all important areas, such as penetrations; (2) an appropriate surveillance program; and (3) periodic testing at containment design pressure of the leak tightness of penetrations which have resilient seals and expansion bellows. Appendix J, *Primary Reactor Containment Leakage Testing for Water-Cooled Power Reactors*, of 10CFR50, prescribes periodic leakage testing requirements for containments to assure that leakage does not exceed allowable leakage rate values as specified in the plant technical specifications, and that periodic surveillance of penetrations and isolation valves is performed. Section XI of the ASME Code provides rules for inservice inspection of nuclear power plant components. Before use is mandated in the U.S., specific editions and addenda of Section XI (also Section III) must be approved by the USNRC (paragraph 55a to 10CFR50).

### USNRC Regulatory Guides for Inservice Inspection

Regulatory Guides (RGs) are issued by the USNRC to provide guidance for practices acceptable to the USNRC for nuclear-related activities. Pertinent guides include RG 1.35, *Inservice Inspection of Ungrouted Tendons in Concrete Containments*, its companion RG 1.35.1, *Determining Prestressed Forces for Inspection of Prestressed Concrete Containments*, and RG 1.127, *Inspection of Water-Control Structures Associated with Nuclear Power Plants*. ASME Section XI Code Cases acceptable to the USNRC are contained in RG 1.147, *Inservice Code Case Acceptability for ASME Section XI, Division 1*.

Table 3. Degradation Factors That Can Impact Category I Concrete Structures

| Material System | Degradation Factor | Primary Manifestation |
|---|---|---|
| Concrete | Chemical attack | |
| | Efflorescence and leaching | Increased porosity |
| | Salt crystallization | Cracking |
| | Alkali-aggregate reactions[a] | Volume change/cracking |
| | Sulfate attack | Volume change/cracking |
| | Bases and acids | Increased porosity/ erosion |
| | Physical attack | |
| | Freeze/thaw cycling | Cracking/spalling |
| | Thermal exposure/ thermal cycling | Cracking/spalling |
| | Irradiation | Volume change/cracking |
| | Abrasion/erosion/cavitation | Section loss |
| | Fatigue/vibration | Cracking |
| Mild Steel reinforcement | Corrosion | Concrete cracking/ spalling |
| | Elevated temperature | Decreased yield strength |
| | Irradiation | Reduced ductility |
| | Fatigue | Bond loss |
| Prestressing | Corrosion (including microbiological) | Reduced section |
| | Elevated temperature | Reduced strength |
| | Irradiation | Reduced ductility |
| | Stress relaxation | Prestress force loss |
| Liner/Structural steel | Corrosion | Section loss |

[a]Includes reactions of cement aggregate and carbonate aggregate.

## ASME Code Requirements for Inservice Inspection

Section XI, Subsections IWE and IWL of the ASME Code address requirements for preservice examination, inservice inspection, leakage testing, repair and replacement for metallic and concrete containments, respectively. At present, neither Subsection IWE nor Subsection IWL has been endorsed by the USNRC.

Subsection IWE, although it was developed primarily for metallic containments, applies to steel liners and steel portions not backed by concrete for concrete containments and their integral attachments. Additional rules for preservice examination and inservice inspection, leakage testing, repair and replacement of containments and for other portions of a nuclear plant are contained in Subsection IWA, *General Requirements*. Subsection IWE requires periodic leakage tests as specified in Appendix J of 10CFR50 during which a general visual examination of the

entire containment boundary (e.g., liner of concrete containments) is required prior to each Type A containment integrated leak rate test (three tests required in each ten year inspection interval).

Subsection IWL includes rules for the preservice and inservice examination of concrete pressure-retaining shells and shell components and for unbonded post-tensioning tendon systems, tendons, and anchorages. Preservice examination requirements for concrete include a general visual examination of the entire exposed concrete surface including painted or coated areas. For unbonded post-tensioning systems, the preservice examination includes documentation of the construction records, e.g., tendon tensioning date, initial tendon seating force, location of any tendon system defects such as missing or cracked buttonheads, and the product designation for the corrosion inhibitor. A general visual inspection of all exposed portions of the concrete surface, including painted or coated areas, tendon anchorage assembly hardware, and bottom grease caps of all vertical tendons, is required at 1, 3, and 5 years following completion of the Initial Strength Test (ISIT) and every 5 years thereafter. With minor exceptions, rules for inservice examination of unbonded post-tensioning systems in Subsection IWL closely parallel the requirements of Regulatory Guides 1.35 and 1.35.1. For inspections at 1, 3, and 5 years after the ISIT, 4 % of the tendons in each population group (vertical, hoop, dome, and inverted U) of tendons is selected randomly for examination of four tendons from each group (sample size from any group need not exceed 10). Thereafter, if no abnormal degradation of the post-tensioning system is indicated, the sample size may be reduced to 2 % of the population of each group, or five tendons in each group, whichever is less, provided at least three tendons are inspected for each group. One tendon in each group should be kept unchanged after initial selection for use as a control (common) tendon during each inspection. For each tendon inspected, lift-off tests are performed to determine tendon force. One sample tendon from each group is detensioned, and a single wire or strand removed for examination and testing, e.g., corrosion, mechanical damage, tension tests, etc. In addition, samples of corrosion protection medium are analyzed for reserve alkalinity, water content, and concentrations of water soluble chlorides, nitrates, and sulfides.

Additional information on ASME Code rules for inservice inspection of both concrete and steel containments is provided in Ref. 17.

## PERFORMANCE HISTORY OF CATEGORY I CONCRETE STRUCTURES

In general, the performance of concrete materials and structures in nuclear power plants has been good. This to a large degree can be attributed to the effectiveness of the quality control/quality assurance programs in detecting potential problems (and subsequent remedial measures) prior to plant operation [18]. However, there have been several instances in nuclear power plants where the capability of concrete structures to meet future functional/ performance requirements has been challenged due to problems arising from either improper material selection, construction/design deficiencies, or environmental effects. Examples of some of the potentially more serious instances include anchorhead failures, voids under vertical tendon bearing plates, dome delaminations, and corrosion of steel tendons and rebars. Other problems such as the presence of voids or honeycomb in concrete, contaminated concrete, cold joints, cadweld (steel reinforcement connector) deficiencies, concrete cracking, higher than code-allowable concrete temperatures, materials out of specification, misplaced rebar, lower than predicted prestressing forces, post-tensioning system buttonhead deficiencies, water contaminated corrosion inhibitors, water intrusion through basemat cracks, low tensile strength of post-tensioning tendon wire material, leaching of concrete in tendon galleries, and leakage of corrosion inhibitor from tendon sheaths also have been identified [7, 12, 19, 20]. These documented problems, if not discovered, could potentially compromise integrity of the structures during an extreme event or exhibit synergistic effects with any environmental stressors or aging factors present.

## STRUCTURAL AGING PROGRAM

While the performance of safety-related concrete components in nuclear power plants has been reasonably good, there is a need for improved surveillance, inspection testing, and maintenance to enhance the technical bases for assurances of continued safe operation of nuclear power plants throughout any extended continued service period. Results of a study [12] conducted under the NRC Nuclear Plant Aging Research (NPAR) Program [21] were utilized to help formulate the Structural Aging (SAG) Program which was initiated in 1988. The SAG Program has the overall objective of preparing a handbook or report which will provide the NRC license reviewers and licensees with the following: (1) identification and evaluation of the structural degradation processes; (2) issues to be addressed under nuclear power plant continued-service reviews, as well as criteria, and their bases, for resolution of these issues; (3) identification and evaluation of relevant inservice inspection or structural assessment programs in use, or needed; and (4) methodologies required to perform current assessments and reliability-based life-predictions of safety-related concrete structures. To accomplish this objective, the SAG Program is addressing the sources of uncertainty identified earlier with respect to determination of the residual life of safety-related components or structures. Structural Aging Program activities are conducted under a management task and three major technical task areas: (1) materials property data base, (2) structural component assessment/ repair technologies, and (3) quantitative methodology for continued service determinations.

### Program Management

The overall objective of the program management task is to coordinate the technical tasks that address priority structural safety issues related to nuclear power plant continued-service applications. Primary management activities include: (1) program planning and resource allocation, (2) program monitoring and control, and (3) documentation and technology transfer. Under the first of these activities, a five-year plan was prepared [22], and 12 subcontracts related to meeting objectives of the technical task areas have been implemented. The program monitoring and control activity primarily addresses the preparation of management reports, annual technical progress reports (Ref. 23 presents the most recent information), and participation in NRC information meetings. The major emphasis under this task has been related to documentation and technology transfer actions. These actions have included: preparation of 42 technical reports and papers, 41 formal technical presentations, and participation in 11 national or international technical committees. Technology exchange at both the national and international levels has been very active with 89 domestic and 98 foreign organizations having been contacted.

### Materials Property Data Base

The objective of the materials property data base task is to develop a reference source which contains data and information on the time variation of material properties under the influence of pertinent environmental stressors and aging factors. This source will be used to assist in the prediction of potential long-term deterioration of critical structural components in nuclear power plants and to establish limits on hostile environmental exposure for these structures, i.e. establish component service life or improve the probability of a component surviving an extreme event. Primary activities under this task include the development of the Structural Materials Information Center, assemblage of materials property data, and formulation of material behavior models.

#### Structural Materials Information Center (SMIC)

Utilizing results of a review and assessment of materials property data bases [24] and a plan which had been prepared for development of the Structural Materials Information Center

(SMIC) [25], initial formatting of SMIC has been completed and results presented in a report [26]. Contained in the report are detailed descriptions of the *Structural Materials Handbook* and the *Structural Materials Electronic Data Base* which form the SMIC.

## Structural Materials Handbook

The *Structural Materials Handbook* is an expandable, hard-copy reference document that contains complete sets of data and information for each material in the SMIC. The handbook consists of four volumes that are provided in loose-leaf binders for ease of revision and updating. Volume 1 contains performance and analysis information useful for structural assessments and safety margins evaluations, for example, performance values for mechanical, thermal, physical, and other properties presented as tables, graphs, and mathematical equations. Volume 2 provides test results and data used to develop the performance values in Volume 1. Volume 3 contains material data sheets which provide general information, as well as material composition and constituent material properties, for each material system contained in the handbook. Volume 4 contains appendices describing the handbook organization, as well as updating and revision procedures.

Volumes 1, 2, and 3 of the handbook presently contain four chapters of materials property data and information, with the chapters consistent between volumes. Each material in the data base is assigned a unique seven-character material code which is used in the handbook and the electronic data base to organize materials with common characteristics. This code consists of a chapter index, a group index, a class index, and an identifier. The chapter index is used to represent the various material systems in the data base. The group index is used to arrange materials in each chapter into subsets of materials having distinguishing qualities such as common compositional traits. The class index is used to organize groups of materials with common compositional traits into subsets having a similar compositional makeup or chemistry. The identifier is used to differentiate structural materials having the same chapter, group, and class indices according to a specific concrete mix, American Society for Testing and Materials standard specification for metallic reinforcement, etc.
A wide variety of information and materials property data is collected and assembled for each material system included in the data base, for example, general description, composition, mechanical property data, etc. In setting up the data base, each material property has been identified by a unique four-digit property code [26] selected from an established set of material property categories, e.g., general information, constituent material and plastic concrete properties, mechanical properties, etc.

Associated with each entry of data (numerical results of tests) or values (results of evaluation of data) into the data base is an assessment of the quality of the entries presented in the form of a letter grade. Although the criteria for assessing the quality of data and values are somewhat subjective, five quality levels have been developed. These levels, presented, in order of descending quality, include recommended, selected, typical, provisional, and interim. The 11 criteria utilized to evaluate the quality of data and values are provided in Ref. 26.

## Structural Materials Electronic Data Base

The *Structural Materials Electronic Data Base* is an electronically accessible version of the *Structural Materials Handbook*. It has been developed on an IBM-compatible personal computer using a data base management system designed specifically for maintaining and displaying properties of engineering materials. To ensure that the handbook and electronic data base are compatible, each material included in the electronic data base is identified by the same common name and material code that has been used to represent the material in the handbook. Also, each electronic data base material record contains data and information taken directly from the handbook. Due to software limitations, the electronic data base is not as comprehensive as

the handbook, but it does provide an efficient means for searching the various data base files to locate materials with similar characteristics or properties.

The electronic data base management system includes two software programs: Mat.DB [27] and EnPlot [28]. Mat.DB is a menu-driven software program that employs window overlays to access data searching and editing features. It is capable of maintaining, searching, and displaying textual, tabular, and graphical information and data contained in electronic data base files. EnPlot is a software program that incorporates pop-up menus for creating and editing engineering graphs. It includes curve-fitting and scale-conversion features for preparing engineering graphs and utility features for generating output files. The graphs generated with EnPlot can be entered directly into the Mat.DB data base files. These graphs are compatible with Microsoft Word, the word processing software used to prepare the handbook. Both Mat.DB and EnPlot operate on an IBM PC, PC/XT, PC/AT, or compatible computer. System requirements include 640 K of memory, hard disk, graphics card, monitor, and DOS 3.0 or later.

Each material record in the electronic data base could include up to nine major categories of data and information: designations, specifications, composition, notes, forms, graphs, properties, classes, and rankings [26]. The user may search an entire data base file to locate materials with similar material properties. During the search each material may be screened for selected tabular data and certain property values based on comparison operators (for instance, =, >, <, >=, <=, and <>). The user may elect to perform property searches using either the International System of Units (SI) or customary units.

**Data Collection**

In parallel with efforts to develop the SMIC, activities are being conducted to establish materials property data for input into the SMIC. To date, two approaches have been utilized: (1) pursuing technology exchange with U. S. and foreign research establishments and (2) obtaining and testing of prototypical concrete materials.

**Technology Exchange**

Domestic and foreign organizations have been contacted in an effort to obtain concrete properties information for input into the data base. To date, 46 concrete, 12 metallic reinforcement, 1 prestressing steel, 1 structural steel, and 1 rubber material data bases have been developed and are contained in the SMIC. A description of the these data bases is provided in Ref. 23.

**Prototypical Sample Procurement**

Several U.S. utilities and concrete research organizations, as well as a national laboratory, have been contacted to pursue the possibilities of removing and testing concrete core samples from prototypical structures. These contacts have resulted in procurement of samples from the Shippingport Power Station (Battelle Pacific Northwest Laboratories), EBR-II (Argonne National Laboratory-West), Palisades and Midland Power Stations (Consumers Power Co.), Dresden and LaSalle Power Stations (Commonwealth Edison Co.), and Vallecitos Nuclear Center (General Electric). Five concrete material property data bases have been developed for the EBR-II materials. Furthermore, subcontracts have been implemented with Sargent & Lundy Engineers, Construction Technology Laboratories, Inc., and Taywood Engineering Ltd. to provide data on prototypical concrete material properties.

The purpose of the subcontract with Sargent & Lundy Engineers (Chicago, IL) is to locate, review, evaluate and provide baseline material property information regarding the concrete materials utilized in the construction of Commonwealth Edison Company's (CECO) nuclear power stations at Byron, Braidwood, Dresden, LaSalle, Quad Cities and Zion. Sargent & Lundy

Engineers also will assist in the obtaining and shipment of concrete core samples to ORNL for testing. The samples will be provided from CECO facilities when modifications are made that require the coring and removal of concrete materials. In addition to the core samples, information will be provided which identifies the plant from which the sample was obtained, the location in the plant, and any available background information (constituents, mix designs, environments, etc.). To date, background information has been provided pertaining to the construction specifications and reference concrete compressive strength data (90-day) for each of the six stations.

Two subcontracts have been implemented with Construction Technology Laboratories, Inc. (Skokie, Illinois), to provide concrete material property data. Under the first activity data have been provided for three of four series of tests from a study that has been ongoing since the early 1940s to investigate the long-term performance of cements in concrete. The overall program encompassed about 500 concrete mixes fabricated using a wide variety of cement and aggregate materials. Beam and cylindrical test specimens were either moist cured, air cured, air cured followed by soaking 48 hours in water before testing, cured outdoors at Skokie, Illinois, or cured outdoors at Dallas, Texas, until testing. Periodically, at ages from 1 day to 34-years, specimens were tested to determine values of compressive strength, modulus of elasticity, and modulus of rupture as a function of materials, environment, and time. Reference 29 presents summary descriptions of the overall program, material characteristics, mixture proportions, specimen geometries, curing conditions, test methods, and available data. Under the second activity which has just initiated, selected specimens remaining from one of the test series will be tested to provide compressive and flexural strength results. Also petrographic examinations will be conducted on several of the specimens. The results of these tests will extend the period for which results are available from 34 to 42 years.

A subcontract has been implemented with Taywood Engineering Ltd. (London, England) to provide data from archived test specimens that were cast in conjunction with fabrication of several of the United Kingdom nuclear power stations. Over 100 test specimens, generally 450-mm long by 150-mm diameter and having ages from 4 to 22 years, are available from the Wylfa, Heysham, Heysham II, Hartlepool, Torness and Sizewell "B" stations. The specimens have been stored in a sealed, stable moisture state at temperatures from 20° to 90° C with some having been under sustained loading. Available baseline data for the six concretes include compressive strength (up to 1 year), thermal expansion, thermal conductivity, and details on constituent materials and mixture proportions. Also, a limited number of cylinders for the Heysham and Heysham II concretes have been tested for elastic and creep recovery, and for compressive strength at ages to 4 years. Elastic modulus and creep results are available for the Wylfa concrete up to an age of 12.5 years. Twenty-nine specimens of the over 100 available have been selected for testing to provide information on the long-term performance of nuclear grade concretes. Variables being investigated include age of specimen, concrete mix design, loaded or unloaded while curing, and storage temperature. After being subjected to a series of nondestructive tests (density, ultrasonic pulse velocity, Schmidt hammer, surface hardness, and dynamic modulus of elasticity), the specimens are loaded to one-third their estimated compressive strength to determine the static modulus of elasticity, followed by determination of the compressive strength. These tests are being complemented by results from inspections of power station buildings to investigate the state of concrete and rebar in-situ. Also, the results from routine inspections of withdrawn tendons at power stations are being analyzed to determine the durability of nongrouted post-tensioning systems.

**Material Behavior Modeling**

The main activity under this subtask has been related to the work done at the National Institute of Standards and Technology (Gaithersburg, Maryland) to identify and evaluate models and

accelerated aging techniques and methodologies which can be used in making predictions of the remaining service life of concrete in nuclear power plants. The program consisted of two major tasks. The first task involved an evaluation of models which can be used to predict the remaining service life of concrete exposed to major environmental stressors and aging factors potentially encountered in nuclear power plant facilities. Degradation processes considered included corrosion of steel reinforcement, sulfate attack, alkali-aggregate reactions, frost attack, leaching, irradiation, salt crystallization and microbiological attack. Each of these processes was reviewed based on its mechanism, likelihood of occurrence, manifestations, and detectability. Models identified for each process were evaluated considering: (1) their basis (for example, theoretical, empirical, or some combination), (2) correctness of assumptions used in their derivation, (3) availability of data to perform an evaluation, (4) their applicability to the problem, and (5) degree of quantitativeness of their predictions.

The second task involved a review and evaluation of accelerated aging techniques and tests which can either provide data for service life models or which by themselves can be used to predict the service life or performance of reinforced concrete materials. In comparison to predicting the life of new concretes, few studies were identified on predicting the remaining service life of in-service concretes. Most of the reported studies dealt with corrosion of steel reinforcement, reflecting the magnitude and seriousness of this problem. Methods which are often used for predicting the service lives of construction materials include: (1) estimates based on experience, (2) deductions from performance of similar materials, (3) accelerated testing, (4) applications of reliability and stochastic concepts, and (5) mathematical modeling based on the chemistry and physics of degradation processes. The most promising approach for predicting the remaining service life of concrete involves the application of mathematical models of the degradation processes. Theoretical models need to be developed, however, rather than relying solely on empirical models. Advantages of this approach are that predictions are more reliable, far less data are needed, and the theoretical models would have wider applications, e.g., applicable to a broad range of environmental conditions. Deterministic and stochastic models should be combined to give realistic predictions of the service life of an engineering material. Purely stochastic models have limited application because of the lack of adequate data to determine the statistical parameters. Accelerated tests do not provide a direct method for making the life predictions, but can be useful in obtaining data required to support the use of analytical models. Results of this activity are presented in Ref. 30.

## Structural Component Assessment/Repair Technology

The objectives of this task are to: (1) develop a systematic methodology which can be used to make quantitative assessments of the presence, magnitude, and significance of any environmental stressors or aging factors which adversely impact the durability of safety-related concrete structures in nuclear power plants; and (2) provide recommended inservice inspection or sampling procedures which can be utilized to develop the data required both for evaluating the current condition of concrete structures as well as trending the performance of these components. Primary activities under this task include development of a structural aging assessment methodology for concrete structures in nuclear power plants, review and evaluation of inservice inspection and structural integrity assessment methods for detection and quantification of potential deterioration phenomena in concrete structures, and evaluation of remedial/preventative measures considerations for concrete structures.

### Structural Aging Assessment Methodology

Under a subcontract with Multiple Dynamics Corporation (Southfield, Mich.), a report has been published which identifies safety-related concrete structures in LWR plants as well as the degradation factors which can impact the performance of these structures [19]. Results of this study will assist in providing a logical basis for identifying the critical structural elements for

evaluation. Pertinent sections of the report are summarized below, for instance, concrete component description/classification system, degradation factor significance classification, and structural aging assessment methodology.

Typical safety-related concrete structures at LWR facilities are identified, described, and their design and construction requirements and primary materials of construction designated. The relative importance of the structure's subelements, safety significance of each Category I structure, and influences of environmental exposure are presented in terms of numerical rating systems. The importance of a subelement to a specific structure is related to its impact on the ability of the structure to meet its functional and performance requirements. The rating system established for structural subelement importance is based on a 1 to 10 scale, with 10 being highest. The safety significance of the subelement is assessed based on the importance of the safety function (developed in compliance with 10CFR regulations) the subelement performs, as well as the number of safety functions it must meet. Each subelement is ranked on a scale of 0 to 10, with 10 being highest, using ranking criteria that have been established. Since environmental effects are highly influential on the service life of concrete structures, an environmental exposure classification procedure was also developed. A rating system was established to incorporate environmental exposure conditions and is based on (1) historical environmental data, (2) exposure conditions for all surfaces of the structure, (3) accessibility of the structure's exposed surfaces for inspection, and (4) quantity/severity of the specific environmental conditions to which it is exposed. Seven environmental exposure categories, ranging from most severe (subterranean) to mildest (controlled interior), were identified and a rating system was developed by comparing each of the environments to one another and identifying their relative significance. The resulting environmental rating system is based on a 1 to 10 scale, with 10 being most aggressive.

Potential degradation or aging factors which could affect the performance of the Category I concrete structures during their lifetime were identified. The significance of a particular degradation factor is evaluated for a particular structure/subelement in terms of (1) its effect on overall structural integrity, (2) environmental conditions present, and (3) materials of construction. The effect of a degradation factor on structural integrity includes its rate of attack, inspectability/early identification, repairability, and ultimate impact on the structure. Because of the variability in likelihood of occurrence of degradation to concrete structures in U.S. LWR plants due to design differences, material utilization, geographical location, etc., the grading system for degradation factors is stated in terms of a possible range of values. Pertinent degradation factor grading values are selected from the ranges of possible values, based on site-specific characteristics. The resulting degradation factor grading values for the individually evaluated subelement (between 1 and 10) are then combined into a single degradation factor significance value by summing the degradation factor grading values and dividing by the number of degradation factors, for instance,

$$DFS = \left(\sum_{i=1}^{n} DFG_i\right) / n, \qquad (1)$$

where,

DFS = degradation factor significance value, rounded to nearest integer,
DFG = degradation factor grading value, and
n = number of degradation factors, up to a total of three.

The structural aging assessment methodology that has been developed is founded on several criteria: relation of subelements to overall importance of the parent safety-related structure, safety significance of the structure as a whole, influence of applied environment, and possibility of occurrence as well as end result of degradation. Determination of the relative ranks of the

Category I structures and their subelements is based on the weighted contributions of the four criteria discussed earlier: (1) structural importance of subelements, (2) safety significance, (3) environmental exposure, and (4) degradation factor significance. A subelement rank within each Category I structure is determined as follows:

$$SR = w_1(I) + w_2(SS) + w_3(DEG), \tag{2}$$

where

| | |
|---|---|
| SR | = subelement rank, |
| I | = subelement importance, |
| SS | = safety significance |
| DEG | = (EE + DFS)/2, rounded to nearest integer, |
| EE | = environmental exposure, |
| DFS | = degradation factor significance [Eq. (1)], and |
| $w_1, w_2, w_3$ | = weighting factors. |

Use of weighting factors (1 to 10, with 10 highest) permits certain components of Eq. (2) to be emphasized. Since the degradation factor significance (DFS) was considered to be heavily influenced by the environmental exposure (EE), these two criteria were combined, averaged, and rounded to the nearest whole integer. The cumulative rank for each Category I concrete structure is determined as follows:

$$CR = \sum_{i=1}^{N} SR_i / N, \tag{3}$$

where

CR = cumulative rank,
SR = subelement rank, and
N = number of subelements for the particular primary structure.

Application of Eq. (3) ensures that the cumulative rank of a Category I concrete structure is based on aging importance rather than total number of subelements. The methodology has been applied to a PWR with large dry metal containment, a BWR with reinforced concrete Mark II containment, and PWR with large dry prestressed concrete containment [19]. The highest ranking primary structure for each of these plants was found to be the shield building, containment vessel, and containment vessel, respectively.

**NDE/Sampling Inspection Technology**

Basic activities under this subtask have been related to an evaluation of nondestructive and sampling/analysis procedures which are available for performing inservice inspections of the critical concrete components in nuclear power plants. These activities have been conducted through subcontracts with Construction Technology Laboratories, Inc. (CTL) and the National Institute of Standards and Technology (NIST).

The overall objective of the subcontract with CTL was related to a review and assessment of inservice inspection techniques and methodologies for application to concrete structures in nuclear power plants. Both direct and indirect methods used to detect degradation of concrete materials have been reviewed. Direct techniques generally involve a visual inspection of the structure, removal/testing/analysis of material, or a combination. Periodic visual examinations of exposed concrete provides a rapid and effective means for identifying and defining areas of

distress, for example, cracking, spalling, and volume change. In areas exhibiting extensive deterioration, or when quantitative results are desired, core samples can be removed for strength testing and petrographic examination. The indirect techniques measure some property of concrete from which an estimate of concrete strength, elastic behavior, or extent of degradation can be made through correlations that have been developed. Several potential nondestructive techniques for evaluating concrete materials and structures include: (1) audio, (2) electric, (3) impulse radar, (4) infrared thermography, (5) magnetic, (6) microscopic refraction, (7) modal analysis, (8) nuclear, (9) radiography, (10) rebound hammer, (11) ultrasonic, and (12) pulse echo. In addition to core sampling, potential destructive testing techniques that can be used to evaluate concrete materials include (1) air permeability, (2) break-off, (3) chemical, (4) probe penetration, and (5) pullout. Contained in the final report for this activity are: (1) reviews in the form of capabilities, accuracies, and limitations, of available nondestructive and destructive techniques that may be utilized in the assessment of concrete components; (2) current in-service inspection methodologies that have been utilized in the assessment of concrete components in civil engineering structures, e. g., routine and periodic inspections, condition surveys, and examples of applications of several of the nondestructive testing techniques; (3) recommended testing methods for use in the detection of the occurrence of the effects of several of the potential degradation factors; and (4) relatively new techniques that potentially have application in the detection of degradation of concrete, e.g., magnetic (leakage flux, nuclear magnetic resonance), electrical (capacitance, polarization resistance, half-cell potential using impulse radar), ultraviolet radiation and finite-element analysis methods [31].

Under the subcontract with the NIST, correlation curves and other statistical data are being developed for selected nondestructive testing techniques. Monovariant linear regression analyses (Mandel's method [32]) are being performed on data obtained from publications on selected nondestructive testing techniques, i.e. break-off, pullout, rebound hammer, ultrasonic pulse velocity, and probe penetration. These methods were selected since they comprise an overwhelming majority of the nondestructive tests performed. For each of the nondestructive techniques investigated, the data identified were subdivided by coarse aggregate type and coarse aggregate content (by weight). This subdivision was based on results provided in the literature indicating that the techniques are influenced by aggregate characteristics, e.g. the pullout and break-off tests are dependent on the aggregate type and maximum aggregate size and the probe penetration and rebound hammer results are influenced by the aggregate hardness. Unfortunately insufficient data were available to further subdivide the data by maximum coarse aggregate size. Since all of the data used in the study were not the result of careful experimentation, a quality rating system was developed for application to each of the data sources. The rating system utilizes nine criteria, e.g., completeness of material description, type of input, completeness of data, completeness of resources, quality of resources, consistency of results, precision and scatter, uncertainty and bias, and statistical methods used. Each data source used was given a rating from A to D (A being highest), based on these criteria. Results developed under this activity will facilitate the evaluation of the in-situ concrete strength results based on the use of nondestructive techniques when only limited destructive information is available. Also, in the absence of destructive test results, correlations developed for the nondestructive test methods can be used as guidelines to estimate the in-situ strength of concrete based solely on nondestructive evaluation results.

**Remedial/Preventative Measures Considerations**

Activities under this subtask are related to an assessment of repair procedures for concrete material/structural systems and establishment of criteria for their utilization. Techniques which can be used to mitigate the effects of environmental stressors or aging factors are being identified. Current work under this subtask is through subcontracts with Wiss, Janney, Elstner (WJE) Associates (Northbrook, Illinois), Taywood Engineering Limited (TEL) (London, England), Howard University (Washington, D. C.), and CORRPRO Companies (Medina, Ohio).

The overall objective of the WJE subcontract is to identify, describe, and quantify the effectiveness of techniques and materials which are available for use in the repair of civil engineering concrete structures. A state-of-the-art manual on repair of deteriorated concrete structures is being prepared which identifies repair methodologies and materials for repair, and ranks repair procedures based on historical performance. Basic components of the manual will include discussions of: when a specific repair technique is applicable, e.g. specific crack sizes; how the techniques or materials are used, e.g. injection, grouting; how to evaluate and test a repair; how to maintain the repair after it has been installed; the expected life of the repair technique; methods for determining when a repair has failed; and methods for re-repair. An important activity under this subcontract has been the preparation of a questionnaire which has been sent to the utilities. The questionnaire requests information on repairs that have been undertaken of concrete structures, research investigations on repair materials, and studies on the long-term effectiveness of repair procedures that have been utilized. Responses to the questionnaire are just beginning to be provided so no trending or quantitative information is available at present.

A companion research effort with the same general overall objective as the WJE subcontract is being conducted by TEL. The distinction between the two efforts is that TEL is addressing the assessment of repair procedures from a European perspective. In the U. S. the primary repair activities have addressed roads and bridge structures, whereas in Europe substantial activities have taken place with respect to buildings and other engineered structures. Damage occurring from carbonation and chloride presence are important sources of concrete distress in Europe and several remedial programs have been developed to address the resulting corrosion problems. For carbonation, the emphasis has been placed on anti-carbonation surface treatments, protective properties of patch materials, and the durability/compatibility of these materials. For chloride attack, efforts are underway to provide an improved understanding of the corrosion mechanisms, the mechanism of incipient anode development, and the use of cathodic protection to overcome the problem. Taywood Engineering Limited is currently involved in a collaborative European (BRITE/EURATOM) project addressing repair of reinforced concrete structures. As well as managing the project, TEL has a number of specific technical tasks, the principal activity involving the development of standardized performance tests and criteria to provide guidance for selection of repair materials that will be durable. Other tasks involve the preparation of a state-of-the-art report summarizing repair activities used by member states of the Commission of European Communities and investigation of the effect of repair techniques on structural performance. A second BRITE/EURATOM project, completed in 1991, investigated methods that can be used to extend the lifetime of structures, either during the construction stage, by the incorporation of chemical admixtures or alternative cementing materials, or post-construction use of surface coatings and treatments. Results of TEL's participation in these programs will be used to provide an assessment of European repair practices. Specific topics being addressed include identification of the repair procedures that have been utilized, establishment of criteria used in the selection of a particular repair procedure, and an assessment of the effectiveness of the various techniques as determined through in-situ evaluations (test methods) or performance history. Results of this activity will be available shortly.

Under a subcontract with Howard University, a systematic methodology for repair, restoration, and rehabilitation of concrete structures in nuclear power plants is being developed. Also to be provided is an expandable manual and user-friendly computer program for use in the inspection of concrete structures in nuclear power plants. A similar computerized rating system has been developed for evaluating general civil works concrete structures, that is, BRAIN (Building Rating Analysis and Investigation System). The first of two planned phases for this program is in progress and is establishing the differences and similarities between existing repair prioritization systems that have been developed for bridge and building structures; determining the applicability of these systems to nuclear power plant concrete structures; and establishing an

approach for development of a repair, restoration, and rehabilitation methodology for nuclear power plant concrete structures. Input developed under the first phase of the study will be used in the second phase to develop a manual and user-friendly computer program. When completed, results of this work will complement the aging assessment methodology developed by Multiple Dynamics Corporation (described previously) and provide a link between the materials studies, nondestructive evaluations, repair technology assessments, and quantitative methodology for current and reliability-based future condition assessment activities.

The overall objective of the subcontract with CORRPRO Companies is to provide a state-of-the-art report addressing corrosion of reinforced concrete structures, where reinforcement includes both mild steel reinforcement and post-tensioning tendons. The report will contain a brief overview relative to the three primary mechanisms leading to corrosion of steel embedded in concrete: (1) chloride ions, (2) carbonation, and (3) stray electrical currents. However, the major emphasis of the report will be to discuss: (a) the potential for stray electrical current corrosion in reinforced concrete structures contained as a part of a nuclear power plant, i.e., equipment foundations, basemat, containment building, balance-of-plant structures, etc.; and (b) cathodic protection systems for use with reinforced concrete structures in nuclear power plants. Specific areas being covered relative to stray electrical current corrosion include: potential sources, methods for detection, factors that affect the rate of corrosion and threshold limits below which stray electrical currents may not be a problem, impact on structural performance, mitigation techniques and their effectiveness, and any synergistic effects (e.g., it has been indicated in at least one reference that stray currents accelerate alkali-aggregate reactions in reinforced concrete structures). With respect to cathodic protection systems, pros and cons for their use to mitigate corrosion of reinforced concrete structures are being addressed, as well as criteria for their application, their overall effectiveness, and any limitations on their use such as the potential to accelerate or induce corrosion. As this work has just initiated, no results are presently available.

## Quantitative Methodology for Continued-Service Determinations

The overall objective of this task is to develop a methodology which can be used for performing condition assessments and making reliability-based life predictions of critical safety-related concrete structures in nuclear power plants. The methodology will integrate information on degradation and damage accumulation, environmental factors, and load history into a decision tool that will provide a quantitative measure of structural reliability and performance under projected future service conditions based on an assessment of a new or existing structure. When completed, the methodology will take into account the stochastic nature of past and future loads due to operating conditions and the environment, randomness in those physical processes and environmental stressors that may lead to degradation in strength, and uncertainty in non-destructive evaluation techniques. Activities associated with this task include: (1) identification and appraisal of existing condition assessment methods and damage prediction models, (2) assembly of pertinent data for use in the predictive models, (3) development of reliability-based condition assessment methodologies for the analysis of current and future reliability, and (4) validation of condition assessment using laboratory or prototypical structures data. Results to date are discussed below and include development of the methodology for use in condition assessments and reliability-based life prediction of concrete structures in nuclear power plants. A more detailed discussion of the methodology is provided in Ref. 33.

### Reliability-Based Condition Assessment

The evaluation of safety-related concrete structures for continued service should provide quantitative evidence that their strength is sufficient to withstand future extreme events within the proposed service period with a level of reliability sufficient for public safety. Structural loads, engineering material properties, and strength degradation mechanisms are random in

nature. Thus, time-dependent reliability analysis can provide a framework for performing condition assessments of existing structures and for determining whether inservice inspection/maintenance is required to maintain reliability and performance at the desired level.

The strength of structural members and components can be described statistically by data gathered in research over the past decade to develop improved bases for structural design of new reinforced concrete structures [34,35]. Time dependent changes in concrete strength due to aging phenomena were not considered in developing these statistics, and they are not directly applicable to the evaluation of existing, possibly degraded, structures with a given service history [36]. Some of the environmental stressors that may affect the strength or deformations of reinforced concrete structures in nuclear power plants include sulfate or acid attack on the concrete, alkali-aggregate reactions within the concrete, freeze-thaw cycling, temperature and irradiation affects, corrosion of reinforcement, and detensioning of prestressing tendons due to relaxation, anchorage failure, or creep in the concrete.

The statistical descriptions of concrete structure strength must account for such aging effects. This can be done by modeling the structural resistance as a time-dependent function,

$$R(t) = R_0\, g(t) \tag{4}$$

in which $R_0$ is the initial resistance and g(t) is a time-dependent degradation function defining the fraction of initial strength remaining at time, t. Conceptually, a function g(t) can be associated with each environmental stressor [30,37], and most significant degradation mechanisms have been identified, at least qualitatively.

Structural loads occur randomly in time and are random in their intensity. If the load intensity varies slowly during the load event, its effect on the structure is essentially static. Moreover, the duration of significant load events usually is short, and such events occupy only a small fraction of the total life of a structure. With these assumptions, structural loads can be modeled as a sequence of pulses, the occurrence of which is described by a Poisson process with mean rate of occurrence $\lambda$, random intensity $S_i$ and duration $\tau$. A typical sample function of such a load process is illustrated in Figure 1. Many of the loads for which nuclear power plant structures are designed can be modeled by such processes [38]. A summary of the parameters describing several load processes is given in Table 4. Some of these parameters were determined through a consensus estimation survey [38].

Table 4. Load process parameters.

| | Mean* | C.O.V. | pdf | $\lambda$ ($yr^{-1}$) | $\tau$ |
|---|---|---|---|---|---|
| Dead Load | $1.00D_n$ | 0.07 | Normal | --- | 40 years |
| Live Load | $0.40L_n$ | 0.50 | Type I | 0.5 | 3 months |
| Acc. Pres. Load | $0.80P_a$ | 0.20 | Type I | $10^{-4}$ | 30 min. |
| Earthquake Load | $0.08E_{ss}$ | 0.85 | Type II | 0.11 | 30 sec. |

*$D_n$, $L_n$, $P_n$, and $P_a$ are nominal loads and $E_{ss}$ is structural action due to safe shutdown earthquake.

## Time-Dependent Reliability Analysis

The reliability analysis of a structure can be visualized by the sample functions of time-dependent strength and loads illustrated in Figure 1. We assume that g(t) is independent of the load history, and arises from deterioration mechanisms such as corrosion and sulfate attack.

The reliability function, L(t), is defined as the probability that the structure survives during interval of time (0,t). If n events occur within time interval (0,t), the reliability function for a structural component can be represented as:

$$L(t) = P\left[R(t_1) \rangle S_1 \cap R(t_2) \rangle S_2 \cap \cdots \cap R(t_n) \rangle S_n\right] \tag{5}$$

Taking into account the randomness in the number of loads and the times at which they occur as well as in the initial strength, the reliability function becomes [33,39],

$$L(t) = \int_0^\infty \exp\left[-\lambda\left[t - \int_0^t F_s(r \bullet g(t))dt\right]\right] f_{R_0}(r)dr \tag{6}$$

in which $f_{R_0}(r)$ = probability density function (pdf) of the initial strength $R_0$. The limit state probability or probability of failure during (0,t) is,

$$F(t) = 1 - L(t) \tag{7}$$

The hazard function, h(t), is defined as the probability of failure within time interval (t,t+dt), given that the component has survived up to time t. This conditional probability can be expressed as,

$$h(t) = -\frac{d}{dt} \ln L(t) \tag{8}$$

The reliability function can be determined from h(t) as,

$$L(t) = \exp\left[-\int_0^t h(\xi)d\xi\right]. \tag{9}$$

When structural failure occurs due to aging, h(t) increases with time. The common assumption in some time-dependent reliability studies that the failure rate is linear gives rise to a Rayleigh distribution for the limit state probability, F(t). As will be shown subsequently, this assumption may not be valid for concrete structures in nuclear plants.

The methods summarized above have been extended to structures subjected to combinations of structural load processes and to structural systems [39]. The reliability function has a similar appearance to that in Eq. 6, but the outer integral on resistance increases in dimension in accordance with the number of components in the system. The system reliability is evaluated by Monte Carlo simulation, using an adaptive importance sampling technique [40] to enhance the efficiency of the simulation.

## Illustration of Time-Dependent Reliability

The effect of degradation in component strength on component reliability function is illustrated using several simple parametric representations of time-dependent strength summarized in

Table 5. Additional data to define the time-dependent resistance are expected to become available later in the Structural Aging Program. The sensitivity study herein identifies some of the more important parameters for condition assessment purposes. Each reliability analysis is carried out for a period of 60 years, the sum of the initial service period of 40 years and a tentative 20-year period of continued service. The degradation is defined with reference to the residual strength at 40 years; e.g., g(40) = 0.8 means that 80 percent of the initial strength remains at 40 years.

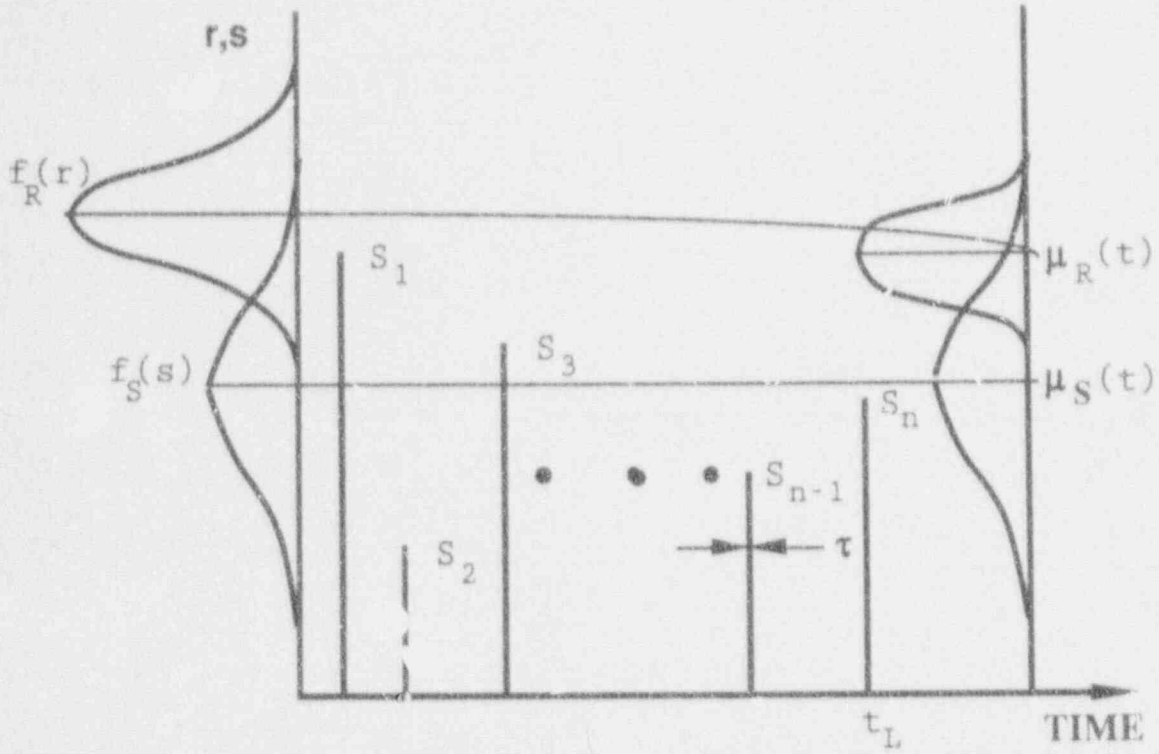


Figure 1. Schematic Representation of Load Process and Degradation of Resistance.

Table 5. Degradation model.

| Shape of the Degradation Function | Corresponding Degradation Mechanism |
|---|---|
| Linear: $g(t) = 1 - at$ | Corrosion |
| Parabolic: $g(t) = 1 - at^2$ | Sulfate Attack |
| Square Root: $g(t) = 1 - a\sqrt{t}$ | Diffusion Controlled Degradation |

Components were designed using three design requirements for concrete structures in nuclear plants [11,39]:

$$0.9\ R_n = 1.4\ D_n + 1.7\ L_n \quad (10)$$

$$0.9\ R_n = -\ 0.9\ D_n + 1.5\ P_a \quad (11)$$

$$0.9\ R_n = D_n + L_n + E_{ss}. \quad (12)$$

The initial strength is assumed to have lognormal distribution with a mean value of 1.15 $R_n$ (in which $R_n$ is nominal strength) and a coefficient of variation, $V_R$, of 0.15. These statistics are

typical for reinforced concrete elements in flexure and/or compression [34,35]. Each of the loads has different temporal characteristics, as summarized in Table 4.

The effect of the general characteristics of the degradation function on F(t) is presented in Figs. 2(a) and 2(b) for the load combination involving dead and live load. Up to 40 years, the failure probability associated with the square root model is the highest. However, after 40 years, the failure probability associated with the parabolic model increases rapidly when the degradation rate increases. Note from Fig. 2(b) the effect of neglecting strength degradation entirely in a time-dependent reliability assessment.

Hazard functions, h(t), associated with the reliability analyses presented in Fig. 2 are illustrated in Fig. 3. It may be observed that h(t) clearly is nonlinear for linear and parabolic degradation models, and its slope increases as g(40) decreases. Thus, the assumption of a linear failure rate may be unconservative for components whose strength is governed by such mechanisms.

Time-dependent reliabilities are presented in Fig. 4 for the load combinations involving dead load and accidental pressure and in Fig. 5 for the dead plus live plus earthquake effect combination, respectively; in the latter, $\lambda$ of 0.014 represents the mean rate of occurrence of L+E. The degradation models affect the failure probability under either D + P or D + L + E in a manner similar to that under D + L. However, the failure probability under D + P is smaller by four orders of magnitude than that under D + L because of the small mean occurrence rate of P. In an absolute sense, then, the failure probabilities for these load combinations are less sensitive to degradation mechanism than under D + L, because of the small mean load occurrence rate and, in the case of E, its large variability. In other words, given that a (rare) load event occurs, the intensity of the load may be large enough to cause failure of the component regardless of whether or not the component has degraded.

**Inservice Inspection/Maintenance Strategies**

Periodic in-service inspection followed by suitable maintenance may restore a degraded reinforced concrete structure to near-original condition. Such inspection/maintenance strategies should be designed so that the failure probability of the component is kept lower than an established target probability, $P_f$, during its service life. Since inspection and maintenance are costly, there are tradeoffs between the extent and accuracy of inspection, required reliability, and cost. An optimum inspection/maintenance program might be obtained from the following constrained optimization problem:

$$\text{Minimize } C_T \tag{13}$$

$$\text{Subject to } F(t) < P_f \tag{14}$$

in which $C_T$ is the total cost of inspection/maintenance plus expected losses if the component fails in service.

Time-dependent reliability analysis can be used in performing this minimum cost analysis. To illustrate this with a very simple example, consider two alternative strategies: (1) infrequent but thorough inspection/maintenance performed at 20, 40, and 60 years, with restoration of full strength; and (2) frequent but limited inspection/maintenance performed at 10, 20, 30, 40, and 50 years, with restoration of 97% of full strength. Degradation is assumed to occur linearly, with g(40) = 0.8. The failure probabilities associated with these strategies (as well as with doing nothing) are compared in Fig. 6 for the D + L combination. At the time of inspection/maintenance, F(t) changes slope. If, e.g., $P_f = 0.00025$ in 40 years, strategy (1) would

be unacceptable, while strategy (2) would be acceptable. Note that in this case, at least, frequent cursory inspection seems preferable to infrequent thorough inspection.

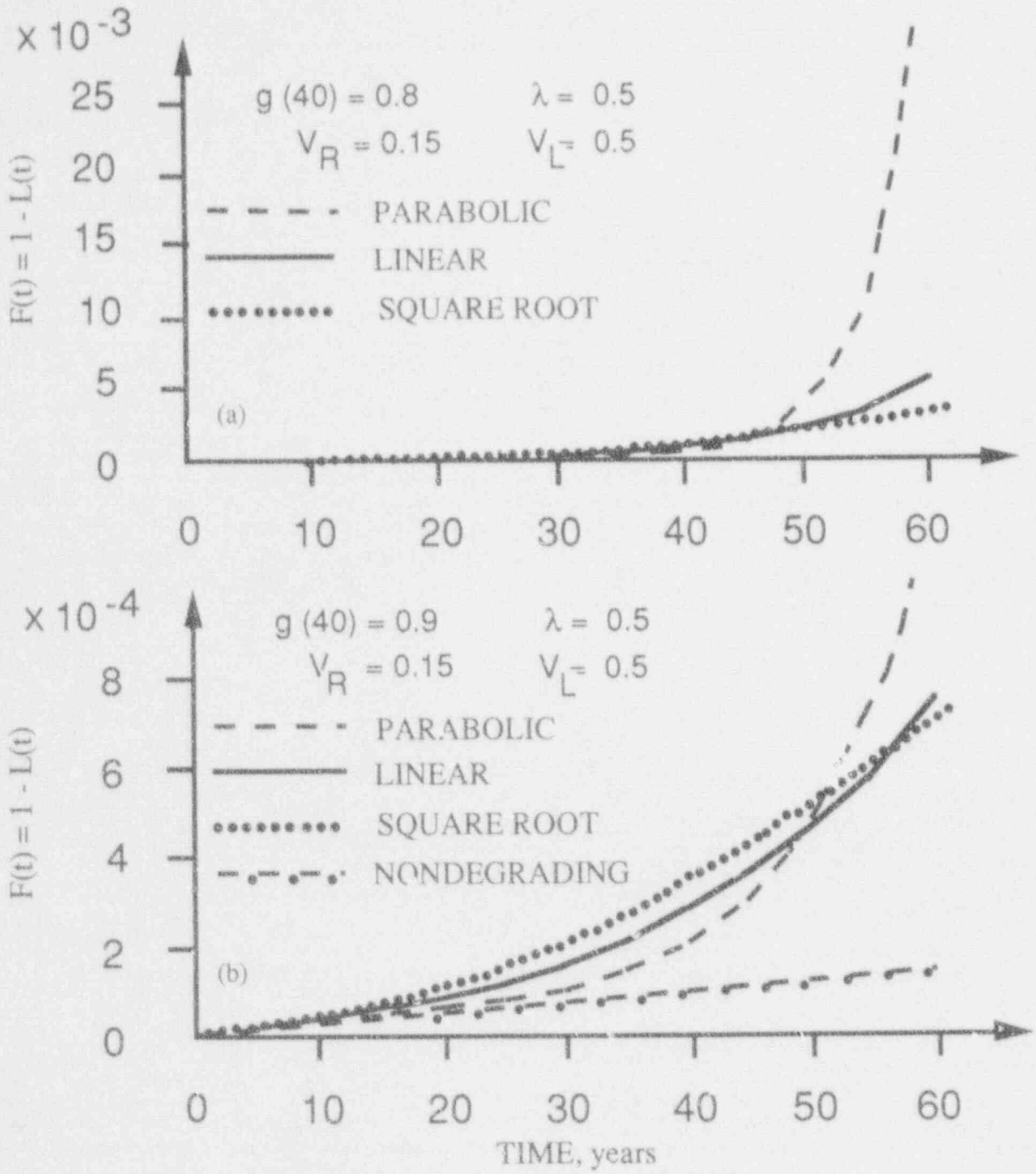


Figure 2. Dependence of Single Component Failure Probability on Degradation Model: D+ L.

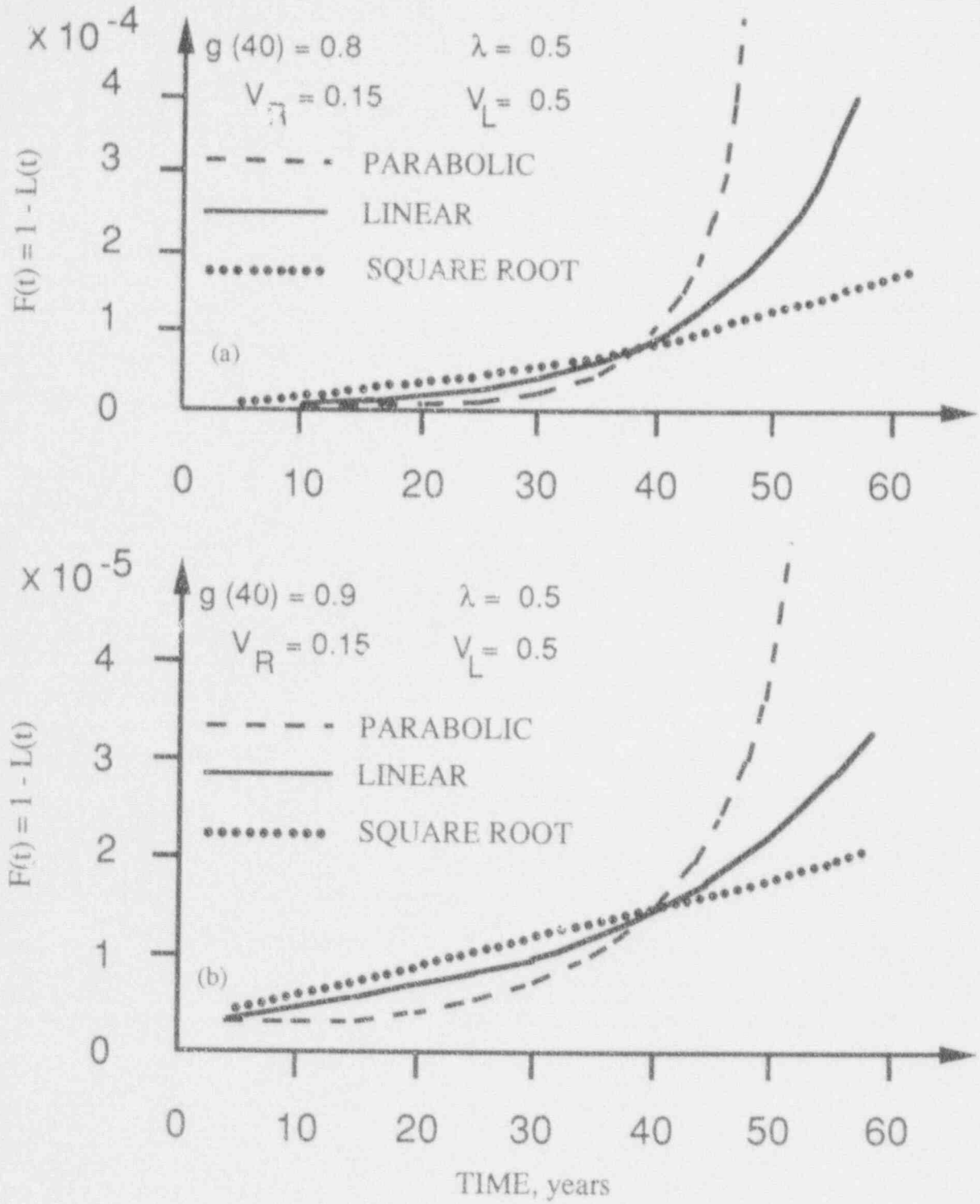


Figure 3. Hazard Function of Single Component.

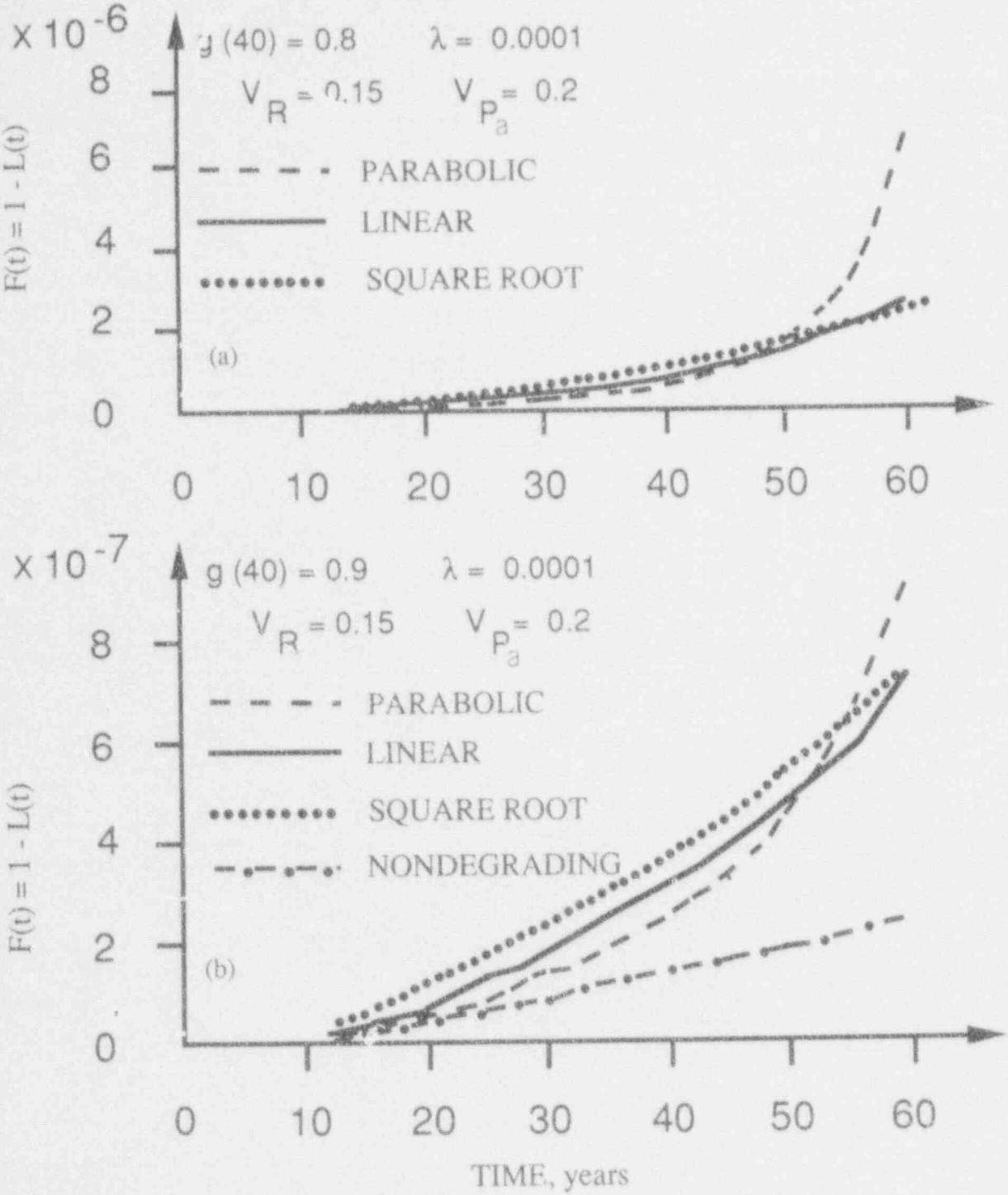


Figure 4. Dependence of Single Component Failure Probability on Degradation Model: D+P.

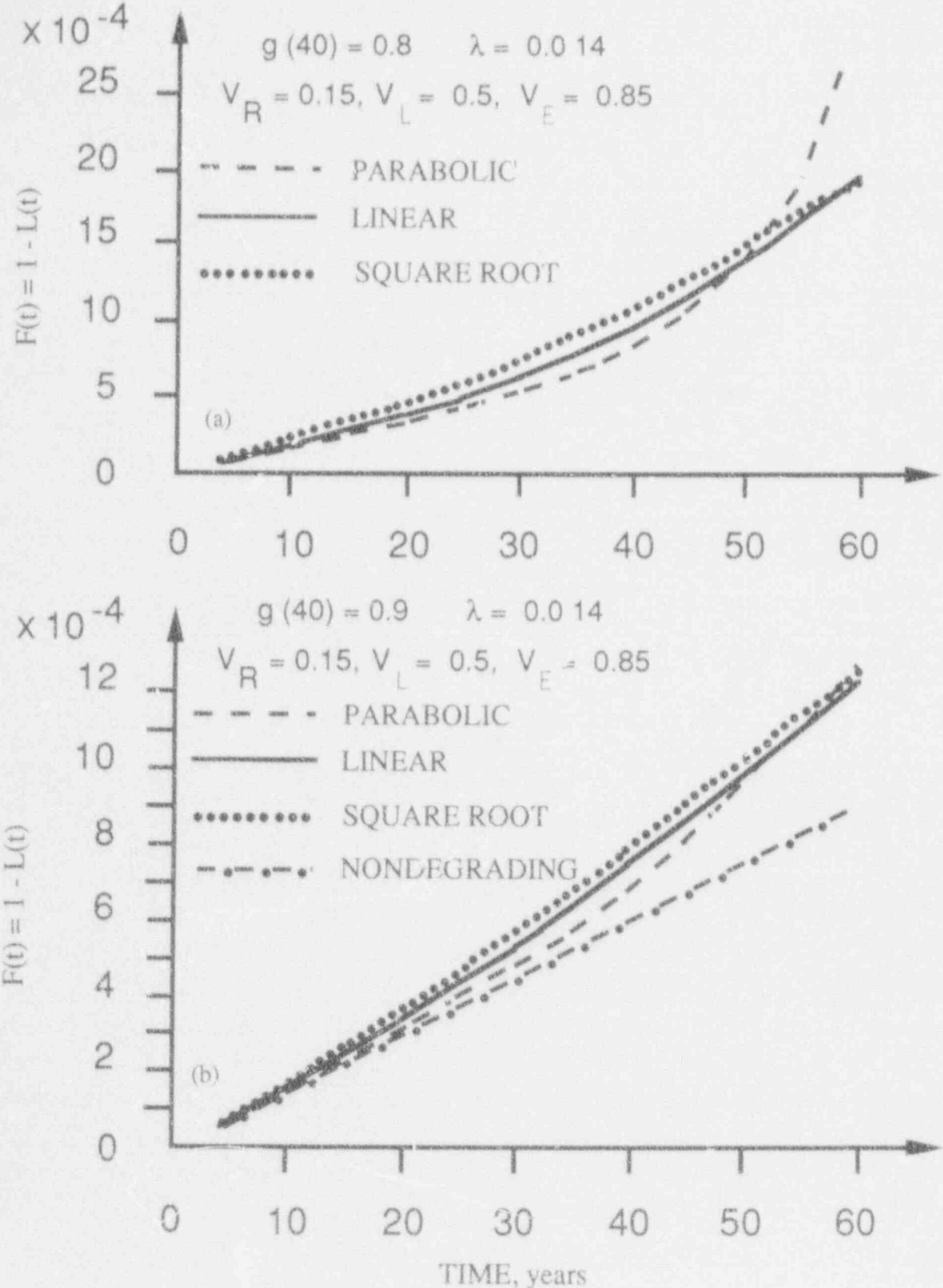


Figure 5. Dependence of Single Component Failure Probability on Degradation Model: D+L+E.

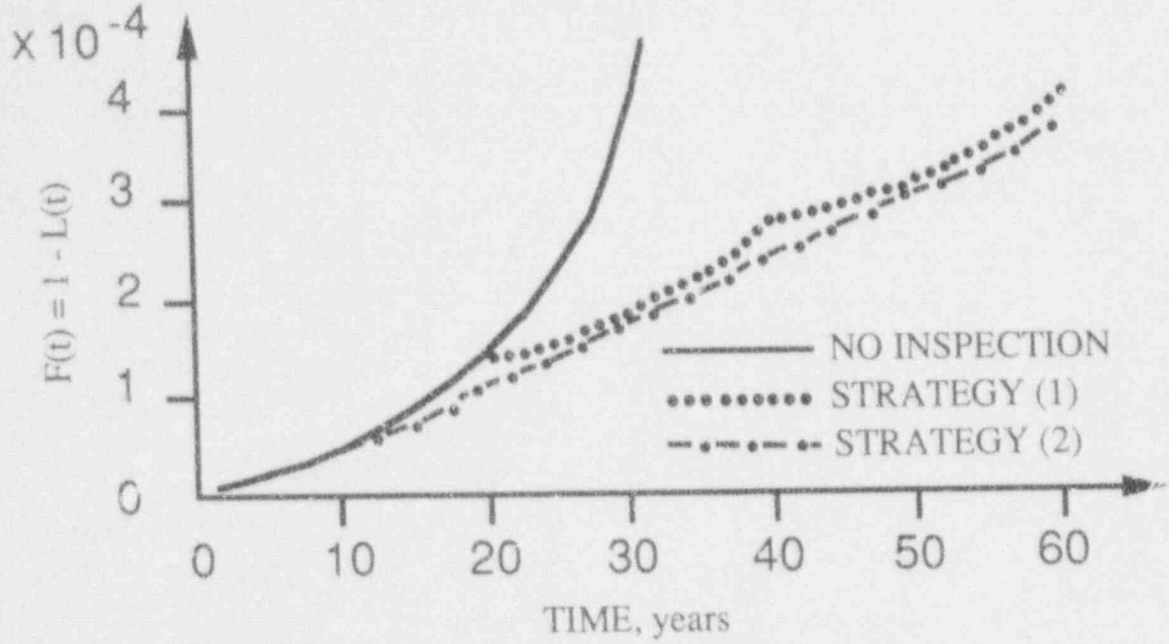


Figure 6. Failure Probability with Repair.

## APPLICATION OF STRUCTURAL AGING PROGRAM RESULTS

When completed, the results of this program will provide an improved basis for the USNRC staff to permit continued operation of a nuclear power plant. More specifically, potential regulatory applications of this research include: (1) improved predictions of long-term material and structural performance and available safety margins at future times, (2) establishment of limits on exposure to environmental stressors, (3) reduction in total reliance by licensing on inspection and surveillance through development of a methodology which will enable the integrity of structures to be assessed (either pre- or post-accident), and (4) improvements in damage inspection methodology through potential incorporation of results into national standards which could be referenced by standard review plans.

## References

1. "Regulatory Options for Nuclear Power Plant License Renewal," NUREG-1317, Division of Reactor and Plant Systems, Office of Nuclear Regulatory Research, U.S. Nuclear Regulatory Commission, Washington, D.C., June 1988.

2. "LWR Plant Life Extension," EPRI NP-5002, Electric Power Research Institute, Palo Alto, CA, January 1987.

3. "*BWR Pilot Plant Life Extension Study at the Monticello Plant*, EPRI NP-5181M, Electric Power Research Institute, Palo Alto, CA, May 1987.

4. PWR Pilot Plant Life Extension Study at Surry Unit 1: Phase 1," EPRI NP-5289P, Electric Power Research Institute, Palo Alto, CA, July 1987.

5. D. J. Naus, "Appendix B, Concrete Material Systems in Nuclear Safety-Related Structures – A Review of Factors Related to their Durability, Degradation Detection and Evaluation, and Remedial Measures for Areas of Distress," in *The Longevity of Nuclear Power Plant Systems*, by I. Spiewak and R. S. Livingston, EPRI NP-4208, Electric Power Research Institute, Palo Alto, CA, August 1985.

6. "Pressurized Water Reactor Containment Structures License Renewal Industry Report," Nuclear Management and Resources Council (NUMARC), Washington, D.C., August 16, 1989 (draft).

7. C. J. Hookham, "Life Assessment Procedures for Major LWR Components – Concrete Containments," NUREG/CR-5314, Idaho National Engineering Research Laboratory, Idaho Falls, April 1990 (draft).

8. "Class I Structures License Renewal Industry Report," NUMARC 90-06, Nuclear Management and Resources Council, Washington, D.C., June 1990 (draft).

9. 10 CFR Part 50, *Domestic Licensing of Production and Utilization Facilities*.

10. ACI Committee 318, "Building Code Requirements for Reinforced Concrete, ACI Standard 318-77, American Concrete Institute, Detroit, MI, 1977.

11. ACI Committee 349, Code Requirements for Nuclear Safety Related Concrete Structures, ACI Standard 349-85, American Concrete Institute, Detroit, MI, 1985.

12. D. J. Naus, "Concrete Component Aging and Its Significance Relative to Life Extension of Nuclear Power Plants," NUREG/CR-4652 (ORNL/TM-10059), Martin Marietta Energy Systems, Inc., Oak Ridge Natl. Lab., Oak Ridge, TN, September 1986.

13. D. J. Naus, C. B. Oland, and E. G. Arndt, "Management of the Aging of Critical Safety-Related Concrete Structures in Light-Water Reactor Plants," *Proc. United States Nuclear Regulatory Commission Eighteenth Water Reactor Safety Information Meeting*, Rockville, MD, October 22-24, 1990.

14. P. Lobner et al., "Overview and Comparison of U.S. Commercial Nuclear Power Plants," NUREG/CR-5640 (SAIC-89/1541), Science Applications International Corporation, San Diego, CA, September 1990.

15. B. Mather, "Concrete Need Not Deteriorate," J. Am. Concr. Inst. 1(9), 32-37, September 1979.

16. R. F. Sammataro, "Containment Inservice Inspection and Testing," Technical Seminars, Inc., Great Neck, NY, 1990.

17. R. F. Sammataro, "Updated ASME Code Rules for Inservice Inspection of Steel and Concrete Containments," *Proceedings - Fifth International Workshop on Containment Integrity*, Washington, D.C., May 12-14, 1992.

18. J. H. Willenbrock et al., "Final Summary Report: A Comparative Analysis of Structural Concrete Quality Assurance Practices of Nine Nuclear and Three Fossil Fuel Power Plant Construction Projects," COO/4120-3, Dept. Civil Eng., The Pennsylvania State Univ., University Park, December 1978.

19. C. J. Hookham, "Structural Aging Assessment Methodology for Concrete Structures in Nuclear Power Plants," ORNL/NRC/LTR-90/17 (Subcontract report from Multiple Dynamics Corp., Southfield, MI), Martin Marietta Energy Systems, Inc., Oak Ridge Natl. Lab., Oak Ridge, TN, September 1990.

20. H. Ashar and D. Jeng, "Effectiveness of Inservice Inspection Requirements of Prestressed Concrete Containments - U.S. Experience," Second International Conference on Containment Design and Operation, Canadian Nuclear Society, Toronto, October 14-17, 1990.

21. B. M. Morris and J. P. Vora, "Nuclear Plant Aging Research (NPAR) Program Plan," NUREG-1144 (Rev. 1), Division of Engineering, Office of Nuclear Regulatory Research, U.S. Nuclear Regulatory Commission, Washington, D.C., July 1985.

22. D. J. Naus, M. F. Marchbanks, C. B. Oland, and E. G. Arndt, "Structural Aging (SAG) Program Five-Year Plan: FY 1988-1992," ORNL/NRC/LTR-89/1, Martin Marietta Energy Systems, Inc., Oak Ridge Natl. Lab., Oak Ridge, TN, March 1989.

23. D. J. Naus and C. B. Oland, "Structural Aging Program Technical Progress Report for Period January 1, 1991, to December 31, 1991," ORNL/NRC/LTR-92/3, Martin Marietta Energy Systems, Inc., Oak Ridge Natl. Lab., Oak Ridge, TN, Febr[illegible] 1992.

24. M. F. Marchbanks, "A Review and Assessment of Materials Property Databases with Particular Reference to Concrete Material Systems," ORNL/NRC/LTR-89/3, Martin Marietta Energy Systems, Inc., Oak Ridge Natl. Lab., Oak Ridge, TN, March 1989.

25. C. B. Oland, and D. J. Naus, "Plan for Use in Development of the Structural Materials Information Center," ORNL/NRC/LTR-89/8, Martin Marietta Energy Systems, Inc., Oak Ridge Natl. Lab., Oak Ridge, TN, September 1989.

26. C. B. Oland, and D. J. Naus, "Structural Materials Information Center for Presentation Time Variation of Material Properties," ORNL/NRC/LTR-90/22, Martin Marietta Energy Systems, Inc., Oak Ridge Natl. Lab., Oak Ridge, TN, September 1990.

27. *Mat.DB*, Version 1.0, ASM International, ASM/Center for Materials Data, Materials Park, OH, 1990.

28. *EnPlot*, Version 2.0, ASM International, ASM/Center for Materials Data, Materials Park, OH, 1989.

29. M. G. Van Geem and D. J. Naus, *Summary of Test Results for Portland Cement Association Study on Long-Term Properties of Concrete*, ORNL/NRC/LTR-91/26, Martin Marietta Energy Systems, Inc., Oak Ridge Nat'l Lab., Oak Ridge, TN, January 1992.

30. J. R. Clifton, *Predicting the Remaining Life of In-Service Concrete*, NISTIR 4712, National Institute of Standards and Technology, U.S. Department of Commerce, Gaithersburg, MD, November 1991.

31. T. M. Refai and M. K. Lim, *Inservice Inspection and Structural Integrity Assessment Methods for Nuclear Power Plant Concrete Structures*, ORNL/NRC/LTR-90/29 (Subcontract Report 17X-SE611V from Construction Technology Laboratories, Inc., Skokie, Ill.), Martin Marietta Energy Systems, Inc., Oak Ridge Natl. Lab., Oak Ridge, TN, September 1991.

32. J. Mandel, "Fitting Straight Lines When Both Variables are Subject to Error," *J. of Quality Technology* **16**(1), 1- 14, January 1984.

33. B. Ellingwood and Y. Mori, "Condition Assessment and Reliability-Based Life Prediction of Concrete Structures in Nuclear Plants," ORNL/NRC/LTR-92/4 (Subcontract Report 19X-SD684V from The Johns Hopkins University, Baltimore, Maryland), Martin Marietta Energy Systems, Inc., Oak Ridge Natl. Lab., Oak Ridge, TN, January 1992.

34. J. G. MacGregor, S. A. Mirza, and B. Ellingwood, "Statistical Analysis of Resistance of Reinforced and Prestressed Concrete Members," *ACI Journal* 80(3): 167–176, 1983.

35. B. Ellingwood and H. Hwang, "Probabilistic Descriptions of Resistance of Safety-Related Structures in Nuclear Plants," *Nuclear Engineering and Design* 88(2): 169–178, 1985.

36. A. J. M. Siemes, A. Vrouwenvelder and A. van den Beukel, "Durability of Buildings: A Reliability Analysis," *Heron* 30(3): 1–48, 1985.

37. J. R. Clifton and L. I. Knab, "Service Life of Concrete," National Bureau of Standards, NUREG/CR-5466, U.S. Nuclear Regulatory Commission, Washington, D.C., 1989.

38. H. Hwang, B. Ellingwood, K. Shinozuka, and M. Reich, "Probability-Based Design Criteria For Nuclear Plant Structures," *Journal of Structural Engineering, ASCE* 113(5): 925–942, 1987.

39. B. Ellingwood and Y. Mori, "Reliability-Based Condition Assessment of Concrete Structures in Nuclear Power Plants," NRC Aging Research Information Conference, Rockville, MD, March 1992.

40. R. G. Melchers , "Search-Based Importance Sampling," *Structural Safety* 9(2): 117–128, 1990.

# UPDATED ASME CODE RULES FOR INSERVICE INSPECTION OF STEEL AND CONCRETE CONTAINMENTS

Robert F. Sammataro
General Dynamics Corporation

## Abstract

Rules for the inservice inspection of nuclear power plant components are contained in Section XI of the American Society of Mechanical Engineers Boiler and Pressure Vessel Code. These rules form a basis for the preservice examination, inservice inspection. modification, repair, replacement, and leakage testing for steel and concrete containments. The rules for steel containments in Subsection IWE, including metallic liners for concrete containments, were first published in 1981. These inservice inspection requirements were based upon visual examination of the containment welds. The rules for concrete containments in Subsection IWL were first published in 1988. These rules apply to concrete surfaces and to post-tensioning systems for post-tensioned containments. Experience has shown that steel containments and metallic liners of concrete containments are not susceptible to failure of the containment pressure boundary welds. Rather, base metal degradation through corrosion and other mechanisms has been found to be a significant and potentially limiting condition for acceptability of containments for continued service. A program was therefore initiated in 1989 to revise the ASME Code containment inservice inspection rules for steel containments to replace the requirements for weld-based inspections with requirements for containment surface examinations. These revised rules were published in December 1991. This paper describes the updated rules for inservice inspection of steel and concrete containments in Subsection IWE and Subsection IWL of Section XI. A history of the development of these rules and the experience base that fostered a change in the containment inspection philosophy is presented. These rules will require mandatory compliance by all nuclear utilities in the United States upon final approval of amendments to paragraph 55a of Title 10, Part 50 of the U.S. Code of Federal Regulations.

## INTRODUCTION

### The ASME Code

Since its first publication in 1914, the American Society of Mechanical Engineers Boiler and Pressure Vessel Code (ASME Code) has provided rules and requirements to assure the public health and safety. During the late 1800's and early 1900's, boiler explosions were commonplace with resulting loss of life and property. The first ASME Code, titled the *ASME Boiler Code,* resulted from the vision of Col. E.D. Meir, the newly elected president of the Society. He acted to promote uniformity and safety in the design, construction, installation, and operation of steam boilers and pressure vessels. His intent was for adoption of uniform rules by all of the states as a basis for their laws. This first ASME Code was developed by a committee of seven members including a consulting engineer, two professors of engineering, two boiler manufacturer's representatives, and one boiler insurance engineer.

From 1914 to today, the ASME Code has grown to keep in step with the increasing growth in steam power and, later, with nuclear power. Whereas the first ASME Code dealt only with "boilers," today's ASME Code contains rules for boilers, pressure vessels, piping, pumps, valves, component supports, and other design features for non-nuclear as well as for nuclear installations. Throughout it's growth, the concept of a voluntary committee responsible for the development and maintenance of the "Code," as envisioned by Col. Meir, has similarly grown. Today's ASME

Code is the responsibility of a tiered organization of voluntary committees administered by the ASME and composed of representatives from all interested parties such as owners, manufacturers, designers, analysts, regulators, jurisdictional authorities, inspectors, and educators.

The ASME Code is significant and unique for several reasons. First, it is accepted by federal, state and local jurisdictional authorities and carries the force of law through legislative acts. Second, it is a consensus Code that is developed and maintained by volunteers representing a cross-section of all interested parties and functioning at open and participative meetings. And, third, it requires the involvement of an independent third party inspection organization to assure adherence to design, construction, and quality assurance standards.

## ASME Code Requirements for Containments

When first published in 1921, Section III of the ASME Code contained rules for locomotive boilers. With the changing technology, and with the development of nuclear power in the 1950's and early 1960's, a new Section III of the ASME Code was issued in 1963 with rules for the design and construction of nuclear power plant components. These rules contained requirements for Class A, B, and C vessels and were applicable to steel nuclear containments. Prior to the publication of the Section III rules for nuclear pressure vessels, most steel containments in the United States were designed and constructed to the rules in Section VIII of the ASME Code for unfired pressure vessels.

Rules for Class MC (metal) containments in Section III were significantly revised and published in the 1971 Edition, Summer 1972 Addenda of the ASME Code. Section III, Division 2, first published in 1975, contains rules for the design and construction of Class CC (concrete) containments. Prior to that time, concrete containments were designed and constructed to the rules in various standards published by the American Concrete Institute for concrete pressure-retaining structures. These containments utilized a steel membrane or liner as the pressure-retaining barrier.

The need for rules for the care and maintenance of nuclear components and systems was addressed as early as 1967. At that time, the Advisory Committee on Reactor Safeguards (ACRS) of the U.S. Atomic Energy Commission, later the Nuclear Regulatory Commission, recommended that criteria be developed for nuclear inservice inspection. An American National Standards Institute (ANSI) committee was formed and resulted in publication of *Rules for Inservice Inspection of Nuclear Power Plant Components* in Section XI of the ASME Code in 1970. Later in 1970, the ANSI Committee became a Subgroup under the responsibility of the Section III Subcommittee for Nuclear Power. The Subgroup subsequently was elevated and retitled the Subcommittee for Nuclear Inservice Inspection with full and independent responsibility for the rules in Section XI.

## Class MC (Metal) Containments

Development of ASME Code inservice requirements for containments can be traced to the problems with the design of MARK I steel containments identified in 1975. These problems, related to modifications to the torus to address conditions not considered in the original design, established the need for major repairs by welding on inservice steel containments. A Working Group for Class MC containment inspection under the Section XI Subcommittee on Nuclear Inservice Inspection was formed in 1977. In 1978, the Working Group prepared the first draft of containment inservice rules. The prime objective was to provide rules suitable for MARK I containment torus modifications. In 1979, the Working Group was elevated to its present status as a Subgroup. Also in 1979, ASME Code Case N-236 was issued with rules for the repair and replacement of Class MC containment vessels. The Subgroup next prepared the rules in Section XI, Subsection IWE, *Rules for Inservice Inspection of Class MC Components of Nuclear Power Plants*, with initial publication in the 1980 Edition, Winter 1981 Addenda to Section XI of the ASME Code.

Experience has shown that steel containments and metallic liners of concrete containments are not susceptible to failure of the containment pressure boundary welds. Rather, base metal degradation through corrosion and other mechanisms has been found to be a significant and potentially limiting condition for acceptability of containments for continued service. A program was therefore initiated in 1989 to revise the ASME Code containment inservice inspection rules to replace the requirements for weld-based inspections with requirements for containment surface examinations. The ASME Section XI Subgroup on Containment established five objectives for revisions to the inservice inspection requirements for Class MC containments and steel liners for Class CC containments in August, 1989. These are:

(1) Incorporate visual examination requirements for containment surfaces in areas of potential degradation from corrosion;

(2) Reduce or delete current rules for visual examination of containment welds;

(3) Restate and clarify requirements for general visual examination prior to Type A tests as required by 10CFR50 and extend to reinforcing structure and other areas of the containment;

(4) Establish ultrasonic thickness measurement requirements for areas of potential containment degradation; and

(5) Establish surface and volumetric acceptance standards for containment flaw indications.

Except for surface and volumetric acceptance standards that are still in course of preparation, revisions to Subsection IWE to include these changes were incorporated in the 1991 Addenda to Section XI published in December 1991. These revisions are discussed in this paper.

### Class CC (Concrete) Containments

A Working Group for development of rules for inservice inspection of Class CC (concrete) containments was formed as a joint ASME/ACI Committee under Section III in 1976. This group was transferred to Section XI in 1983. It then became the Working Group for Concrete Pressure Components under the Subgroup on Containment in 1985. The rules for inservice requirements for Class CC containments were first published in the 1986 Edition, 1988 Addenda to Section XI. Members of the Working Group as of the publication of the Class CC rules in 1988 were individually awarded the first ASME Certificate of Acclamation for their efforts in May 1990.

## REGULATORY REQUIREMENTS

### U. S. Code of Federal Regulations

Licensing and regulation of the nuclear industry in the United States is the responsibility of the U.S. Nuclear Regulatory Commission (USNRC). This authority is granted under the provisions of the Atomic Energy Act of 1954, the Energy Reorganization Act of 1974, and the National Environmental Policy Act. These acts establish a national policy and framework for regulating civilian nuclear power activities to ensure that they are conducted in a manner that will protect public health and safety, preserve environmental quality, maintain national security, and comply with antitrust laws

Title 10, Part 50 of the U.S. Code of Federal Regulations (10CFR50) requires that safety-related nuclear systems and components, including containments, comply with specific editions and addenda of the ASME Code. 10CFR50.34 contains Three Mile Island (TMI) related requirements

for containment integrity. Specifically, 10CFR50.34(f)(3) requires that steel containments meet the design requirements for containment integrity in Section III of the ASME Code. 10CFR50.44(c)(3) requires that the containment be capable of handling prescribed hydrogen release without loss of containment structural integrity or safety function demonstrated by methods such as those defined in Section III.

10CFR50.55a, *Codes and Standards,* requires that "structures, systems and components shall be designed, fabricated, erected, constructed, tested and inspected to quality standards commensurate with the importance of the safety function to be performed" and that "systems and components of boiling and pressurized water-cooled nuclear power reactors must meet the requirements of the ASME Boiler and Pressure Vessel Code."

The General Design Criteria (GDC) in Appendix A of 10CFR50 prescribe additional requirements for containments. GDC 53, *Provisions for Containment Inspection and Testing,* requires that "The containment shall be designed to permit: (1) appropriate periodic inspection of all important areas, such as penetrations; (2) an appropriate surveillance program; and (3) periodic testing at containment design pressure of the leak tightness of penetrations which have resilient seals and expansion bellows."

10CFR50, Appendix J, *Primary Reactor Containment Leakage Testing for Water-Cooled Power Reactors,* prescribes periodic leakage testing requirements for containments. These include tests to verify the containment leak tight integrity, assure that leakage does not exceed allowable leakage rate values as specified in the technical specifications, and assure that periodic surveillance of penetrations and isolation valves is performed.

## Subsection IWE and Subsection IWL Approval

Specific editions and addenda of Section III and Section XI of the ASME Code must be approved by the USNRC in 10CFR50.55a before use is mandated in the United States. For Section XI, approval of the 1986 Edition of Section XI was announced in the Federal Register (FR) in May, 1988 (53 FR 16051). Approval of the 1989 Edition of Section XI is expected in early 1992 (56 FR 37961).

However, one significant exception, first established in 1983 in 48 FR 5532 , exempts Class MC containments from compliance with the inservice requirements in Section XI, Subsection IWE:

> *Subsection IWE, "Requirements for Class MC Components of Light-Water Cooled Power Plants," was added to Section XI by these Addenda. However, 10CFR50.55a presently only incorporated those portions of Section XI that address the ISI requirements for Class 1, 2, and 3 components and their supports. The regulation does not currently address the ISI of containments. Since this regulation is only intended to update current regulatory requirements to include the latest Code addenda, the requirements of Subsection IWE are not imposed upon licensees by this amendment. The applicability of Subsection IWE will be considered separately.*
>
> *48 FR 5532*
> *Published: 2/7/83*
> *Effective: 3/9/83*

The above exemption in 10CFR50 for Class MC containments from compliance with Section XI, Subsection IWE, remains as of the date of this report (May, 1992). Similarly, Subsection IWL for Class CC containments, first published in 1988, has not yet been approved by the USNRC. These delays are the result of several factors. Foremost is the intricacy of the regulatory process that requires preparation of value and impact statements, public review and comment, and approval by a number of USNRC organizations for all new requirements. Both the rules in

Subsection IWE and Subsection IWL are considered to be "new" requirements as no rules for containment inservice inspection have previously been approved.

An increased effort is underway in the USNRC, however, to approve the ASME Code rules in both Subsection IWE and Subsection IWL. This activity is in light of the increased concern for the safety of nuclear plants resulting from containment aging and degradation. It also reflects cooperation between both the ASME Code committees and the USNRC to develop containment inservice inspection rules that address current concerns for containment degradation. Current estimates anticipate that the USNRC will approve the Section XI rules for both steel and concrete containments and a phased implementation schedule for containment inservice inspection for all nuclear plants in the United States in 1992.

### USNRC Regulatory Guides

Regulatory Guides are issued by the USNRC to provide guidance for practices acceptable to the USNRC for nuclear-related activities. Three guides are of specific interest to containment inservice requirements. Regulatory Guide 1.35, *Inservice Inspection of Ungrouted Tendons in Concrete Containments*, and Regulatory Guide 1.35.1, *Determining Prestressed Forces for Inspection of Prestressed Concrete Containments*, are the basis for the requirements in Subsection IWL for tendons for post-tensioned containments. Regulatory Guide 1.147, *Inservice Code Case Acceptability for ASME Section XI, Division 1*, defines those ASME Section XI Code Cases that are acceptable to the USNRC.

## CONTAINMENT INSERVICE REQUIREMENTS

### Containment Inspection Philosophy

Section XI, Subsection IWE, for Class MC containments and Section XI, Subsection IWL, for Class CC containments define requirements for containment preservice examination, inservice inspection, leakage testing, repair, and replacement. Consistent with the inspection philosophy in other portions of Section XI, the condition of the containment, or baseline, is first documented through a preservice examination prior to initial commercial operation of the nuclear plant. For Class MC containments, this preservice examination uses the same inspection methods to be used for the inservice inspections and is extended to essentially 100% of the containment. For Class CC containments, the preservice examination of the concrete surfaces is, similarly, extended to essentially 100% of the concrete surface using the same methods to be used during the plant lifetime. However, preservice examination for the post-tensioning system for post-tensioned containments is based upon documentation of the plant construction records.

Inservice inspections for both Class MC and Class CC containments are based upon visual inspection of representative portions of the containment and, for post-tensioned containments, the post-tensioning system on a prescribed schedule throughout the plant lifetime. These examinations may, and should, be done for the as-painted or as-coated condition of the containment without removal of the paint or coating. Subsection IWL also incorporates provisions similar to and based upon those defined in USNRC Regulatory Guides 1.35 and 1.35.1 including those for physical tests of representative tendons from the post-tensioning system.

Subsection IWE was initially developed with the objective of assuring that the critical areas of the containment maintain their pressure-retaining and structural integrity throughout the plant lifetime. When first published in the 1980 Edition, Winter 1981 Addenda, of Section XI, Subsection IWE reflected the premise that welds in pressure vessels and piping were the areas of the greatest concern for potential failure. This philosophy, established in the 1970's as plants were being constructed, became the basis for the weld-based rules initially published in Section XI for the

inservice inspection of piping and pressure vessels including containment vessels in Subsection IWE.

As containments age, however, containment welds have not been found to be the limiting area for containment integrity. Instead, base metal degradation mechanisms such as corrosion, rather than weld defects, have been found to be the most significant area of concern. Consequently, the priorities for containment integrity have changed from weld-based examinations to examinations of the entire containment surface. These changes for Class MC containments were addressed in the 1991 Addenda to the 1988 Edition of Subsection IWE.

Subsection IWL has been developed with the objective of assuring that the critical areas of concrete containments maintain their pressure-retaining integrity throughout the plant lifetime. To meet this objective, the preservice condition of the finished concrete surface must be visually examined and documented to provide a reference baseline. Construction records provide baseline information for the post-tensioning system. This baseline is then used for comparison with the existing condition at each inservice inspection. Subsection IWL has been written for new plants with considerations for older plants. Compliance with Subsection IWL rules is to be invoked by the USNRC through the regulatory process in the United States. For older plants, implementation on a plant-by-plant basis with the opportunity for justifiable waivers for individual requirements when granted by the USNRC is anticipated.

The rules in Subsection IWL address only unbonded post-tensioning systems for Class CC containments. They reflect the requirements in USNRC Regulatory Guide 1.35. The format in Subsection IWL has been prepared to allow the addition of rules for prestressed concrete containment structures with grouted tendons. However, there are no activities to prepare such rules at the present time since no active nuclear plants in the United States utilize bonded or grouted tendon design.

Pressure tests for both Class MC and Class CC containments are limited to the periodic integrated leakage rate test (ILRT) prescribed in Appendix J to 10CFR50. For Class MC containments and the metallic liners for Class CC containments, the general visual examination of the containment prior to the Type A test required by Appendix J is incorporated as a specific Subsection IWE requirement with attendant acceptance criteria and documentation requirements.

The Pressure Vessel Research Council (PVRC) commissioned a study of the ASME Code rules in Section III and Section XI in 1988. The objective of this study was to prepare recommendations for simplification of the rules for the the design, construction, inservice inspection, repair, and replacement of nuclear systems and components. Several of these recommendations will result in changes to Section XI, including Subsections IWE and IWL, in the future. Revisions to address three of the initial recommendations from the PVRC Steering Committee have already been initiated. They include relocation of all preservice examination requirements in now in Section XI to Section III and elimination of the words "preservice" and "baseline." Also, extension of the present jurisdiction of Section III to the time of filing the N-3 Data Report by the Owner, and separation of Section XI into three distinct areas: Inservice Inspection (ISI), Inservice Testing (IST), and Repairs, Replacements, and Modifications (RRM). The final PVRC report containing several hundred recommendations is scheduled for publication in 1992.

## Scope

Subsection IWE contains rules for the preservice examination, inservice inspection, repair, replacement and leakage testing of Class MC steel containments and their integral attachments. It also applies to the steel liners and steel portions not backed by concrete for Class CC concrete containments and their integral attachments. Subsection IWL includes rules for the preservice examination and inservice inspection for concrete pressure-retaining shells and shell components

and for unbonded post-tensioning systems, tendons and anchorages. Rules for concrete and post-tensioning system repairs and replacements were first published in the 1991 Addenda to Subsection IWL. Rules for containments with grouted tendons are not anticipated at this time because of limited need. Rules for leakage testing of Class CC containments after repair or replacement have been approved for publication in the 1992 Addenda to Subsection IWL. Additional rules for the preservice examination, inservice inspection, leakage testing, repair, and replacement of containments and for other portions of a nuclear plant are contained in Section XI, Subsection IWA, *General Requirements*.

## Exemptions from Containment Inspection

Certain imbedded or inaccessible portions of containment vessels that are within the scope of Subsection IWE or Subsection IWL may be exempted from the preservice examination and inservice inspection requirements. For Class MC, the following components, or parts of components, are exempted:

(1) vessels, parts, and appurtenances that are outside the boundaries of the containment as defined in the Design Specifications;

(2) embedded or inaccessible portions of containment vessels, parts, and appurtenances that met the requirements of the original Construction Code; and

(3) portions of containment vessels, parts, and appurtenances that become embedded or inaccessible as a result of vessel repair or replacement provided certain provisions are met prior to becoming inaccessible.

For Class CC containments, inaccessible tendon end anchorages and portions of the concrete surface that are covered by the liner, foundation material, or backfill or are otherwise obstructed by adjacent structures, components, parts, or appurtenances are also exempt.

## Class MC (Metal) Containments

### Preservice Examination

Prior to the 1991 Addenda, rules in Subsection IWE for Class MC containments required that the preservice condition of containment welds as painted or coated and the preservice condition of other pressure-retaining components be visually examined and documented to provide a reference baseline. This baseline was then used for comparison with the existing condition at each inservice inspection. It was required, therefore, that the preservice baseline records for the containment welds be restored when the existing surface treatment of the containment was altered, repaired, or replaced. In the 1991 Addenda, the requirements were changed to address the examination of the containment surface, rather than the containment welds. The surface, of course, includes the welds.

Removal of paint or coatings is not required for visual preservice examination or inservice inspections for containments except for dissimilar metal welds such as those at nozzles and penetrations. Preservice and inservice nondestructive surface examinations of the base metal surface are required for containment dissimilar metal welds because of their increased sensitivity and importance.

Prior to initial plant startup, essentially 100% of the containment must be visually examined. Use of binoculars, telescopes, boroscopes, video cameras and other remote optical devices is allowed provided the visual acuity standards for each examination method are satisfied. Surface examination is also required for pressure-retaining dissimilar metal welds. Bolt torque or tension

tests are required for pressure-retaining bolting. Areas suspect as a result of visual examination must be cleaned by removal of paint or coatings to the base metal surface for surface examination. Exposed areas must be repaired, if required, and repainted or recoated after examination.

Components accepted for service as a result of a preservice examination shall either (1) have no indications from visual or surface examination that exceed the acceptance standards, or (2) be repaired or replaced to the extent necessary to meet the acceptance standards prior to placement of the component into service. Visual examinations that detect surface indications must be supplemented by either surface or volumetric methods. All indications in components accepted for service that meet the acceptance standards must be documented. The examination results are subject to review by the Authorized Nuclear Inservice Inspector (ANII) having jurisdiction at the plant site.

**Inservice Inspection Schedule**

Containment vessels, pressure-retaining bolting, and seals, gaskets, and moisture barriers must be inspected on a scheduled basis during the normal plant lifetime. The inspections may be performed to either Inspection Program A or Inspection Program B as shown in Figures 1 and 2, respectively. Each inspection interval may be increased or decreased, but not cumulatively, by as much as one year except that the first interval for Inspection Program A may not be decreased. For power units that are out of service for six months or more, the inspection interval may be extended for a period equal to the outage and the original pattern of intervals extended accordingly. The intervals continue to the end of the plant lifetime. In the United States, only Inspection Program B is in use. Therefore, each inspection interval is ordinarily ten years.

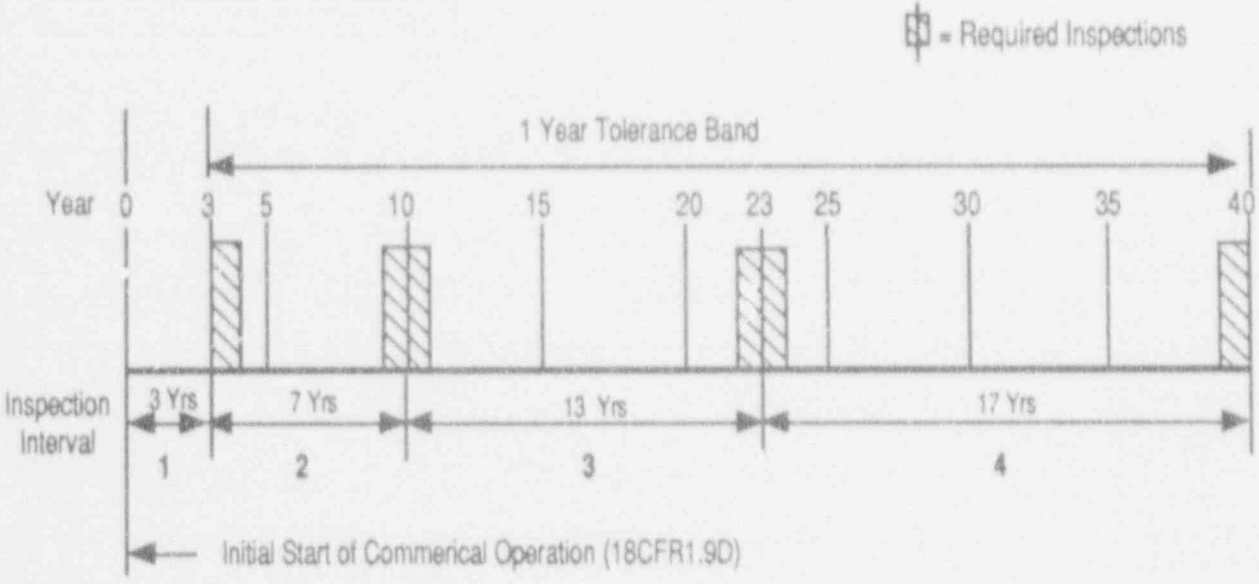


Figure 1. Inspection Program A

For Inspection Program B, unless deferral to the end of the inspection interval is specifically allowed, a minimum of 16% and a maximum of 34% of the scheduled inservice examinations must be completed in the first inspection period of three years of the inspection interval. A minimum of 50% and a maximum of 67% of the scheduled examinations must be completed by the second inspection period or by the seventh year of the inspection interval. All examinations must be completed by the end of the third inspection period or the end of the ten year inspection interval.

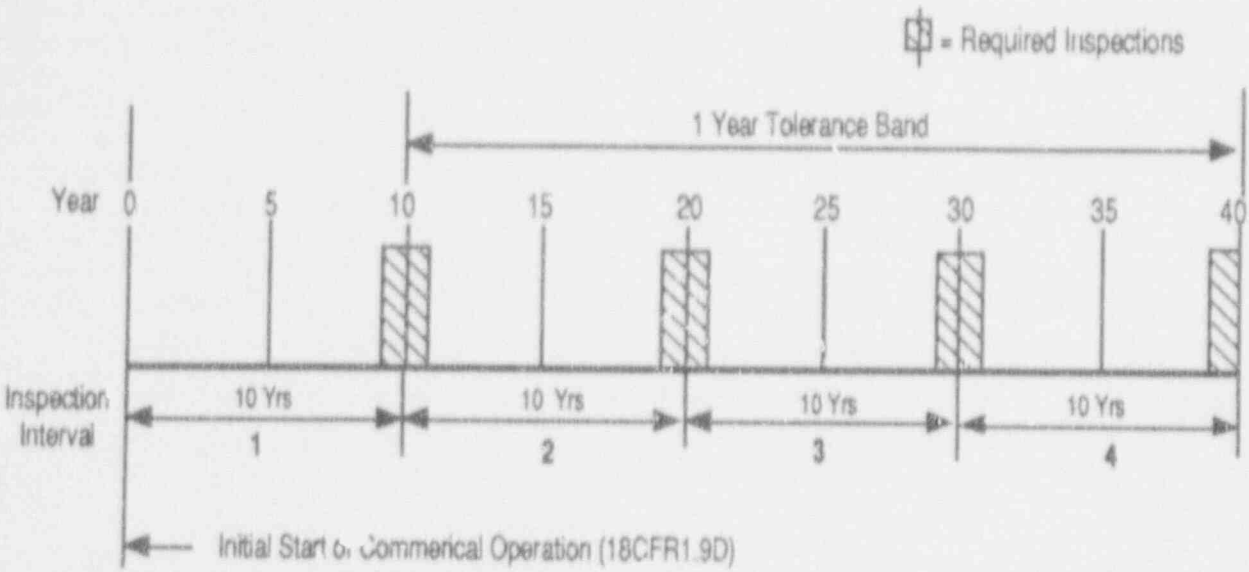


Figure 2. Inspection Program B

Examination of seals, gaskets, and moisture barriers and pressure tests may not be deferred to the end of the interval. Similarly, the general visual examination of containment surfaces required prior to each Type A integrated leak rate test and examination of containment surfaces requiring augmented examination may not be deferred to the end of the interval. Other examinations may be deferred to the end of the first three ten year inspection intervals. In light of the increased concern for age-related degradation, these examinations may not be deferred in the fourth and subsequent inservice inspection intervals.

**Inservice Inspection**

Inservice inspection requirements for Class MC containments in Subsection IWE are defined in tables of Examination Categories. Prior to the 1991 Addenda, the rules in Subsection IWE required periodic inservice inspection of the containment welds. In the 1991 Addenda, the rules were revised to address containment surfaces in lieu of containment welds. These changes are best reflected in a comparison of the Examination Categories for Subsection IWE before and after the change in containment inspection philosophy as shown in Table 1.

Revisions to replace the weld based inservice inspection requirements with surface based inservice inspection requirements are defined below. Requirements for the inservice inspection of pressure-retaining welds at containment penetrations (Examination Category E-B), seals, gaskets and moisture barriers (Examination Category E-D), pressure-retaining dissimilar metal welds (Examination Category E-F), bolting (Examination Category E-G), and pressure testing (Examination Category E-P) remain unchanged. The revisions are discussed below:

(1) Incorporate Visual Examination Requirements for Containment Surfaces in Areas of Potential Degradation from Corrosion

This revision in Examination Category E-C requires the periodic VT-1 visual examination of visible and accessible containment surfaces of Class MC containments and steel liners of Class CC containments in areas requiring augmented examination. These areas are those susceptible to corrosion or other degradation. They are to be identified on a case basis for each containment type or are to be identified as a result of the the general visual inspection now required by 10CFR50, Appendix J, prior to each Type A containment integrated leak

rate test. Typical areas to be included are those subject to accelerated corrosion with no or minimal corrosion allowance or areas where the absence or repeated loss of protective coatings has resulted in substantial corrosion and pitting. These include areas exposed to standing water, repeated wetting and drying, persistent leakage and those with geometries that permit water accumulation, condensation, and microbiological attack. Such areas include penetration sleeves, surfaces wetted during refueling, concrete-to-steel shell or liner interfaces, embedment zones, leak chase channels, drain areas and sump liners. All designated areas require visual VT-1 examination in each inspection interval. Deferral to the end of the interval is not permissible. Any indications of corrosion or degradation must be repaired or found acceptable by an Engineering Evaluation before the containment is returned to service.

Table 1. Subsection IWE Examination Categories for Class MC Containments

| | PARTS EXAMINED | |
|---|---|---|
| EXAMINATION CATEGORY[1] | WELD-BASED RULES (1981 - 1990) | SURFACE-BASED RULES (1991 AND LATER) |
| E-A | Pressure-Retaining Welds in Vessels | Containment Surfaces |
| E-A-1 | Nonpressure-Retaining Welds | Deleted |
| E-B | Pressure-Retaining Welds in Containment Penetrations | Pressure-Retaining Welds in Containment Penetrations |
| E-C | Pressure-Retaining Welds in Airlocks and Equipment Hatches | Containment Surfaces Requiring Augmented Examination |
| E-D | Seals, Gaskets, and Moisture Barriers | Seals, Gaskets, and Moisture Barriers |
| E-E | Integral Attachments | Deleted |
| E-F | Pressure-Retaining Dissimilar Metal Welds | Pressure-Retaining Dissimilar Metal Welds |
| E-G | Pressure-Retaining Bolting | Pressure-Retaining Bolting |
| E-P | All Pressure-Retaining Components (Pressure Tests) | All Pressure-Retaining Components (Pressure Tests) |

Note: (1) In addition to the Examination Categories shown, Examination Category E-Q for Base Metal Examinations was introduced in the 1990 Addenda. These requirements were restated in Examination Category E-C and Examination Category E-Q was deleted in the 1991 Addenda.

(2) Reduce or Delete Current Rules for Visual Examination of Containment Welds

These revisions replaced weld based inspections with requirements for visual VT-3 examinations of accessible surface areas as the primary basis for containment inspection in Examination Category E-A. This examination of all accessible containment surfaces is to be performed at the end of each inspection interval. Interim inspections at the end of each inspection period within the inspection interval are not required. All reportable conditions require repair or replacement or acceptance by an Engineering Evaluation. Areas of observed or potential base metal degradation must be identified and included in the base

metal examination areas susceptible to corrosion or degradation and inspected in accordance with Examination Category E-C, as discussed in (1) above and (3) below.

(3) Restate and Clarify Requirements for General Visual Examination Prior to Type A Tests as Required by 10CFR50 and Extend to Reinforcing Structure and Other Areas of the Containment

The rules in 10CFR50, Appendix J require a general visual examination of the entire containment surface prior to each Type A test. These tests are required three times in each ten year inspection interval for Inspection Program B and ordinarily coincide with plant refueling outages. Although presently required by 10CFR50, nuclear utility practice often results in an informal, undocumented examination with no prescribed inspection procedure, repair procedure, or documentation of results. A requirement for a General Visual Examination has been added to Examination Category E-A. The General Visual Examination is to be performed by, or under the direction of, a Registered Professional Engineer or other individual knowledgeable in the requirements for design, inservice inspection, and testing of Class MC and metallic liners of Class CC components. The examination may be performed either directly or remotely, by an examiner with visual acuity sufficient to detect evidence of degradation that may affect either the containment structural integrity or leak tightness. This examination elevates this existing Appendix J requirement to become the primary containment inspection with the attendant requirements for inservice inspection procedure preparation, repair program procedures and documentation, and documentation of inspection results. This revision is integral with the revisions stated in (1) and (2) above.

(4) Establish Ultrasonic Thickness Measurement Requirements for Areas of Potential Containment Degradation

Revisions to establish ultrasonic thickness measurements as a means to monitor containment shell or liner wall thinning are incorporated in Examination Category E-C. Periodic ultrasonic thickness measurements are required to determine and monitor the wall thickness in areas designated as surface areas requiring augmented examination. These areas are those susceptible to corrosion or degradation, as defined in (1) above, that are not accessible for visual examination from both sides. This includes areas such as containment liners backed by concrete and areas of steel containment shells adjacent to the sand pocket areas of BWR containments. When so designated, the area requires marking into one foot square grids. An initial ultrasonic scan to determine and mark the point of minimum thickness in each grid is then required. Periodic ultrasonic examinations are then performed for all marked locations in each inservice inspection interval to determine loss of wall thickness. Deferral of the ultrasonic thickness measurements to the end of the interval is not permissible. Areas that remain essentially unchanged for three consecutive inspection periods may then revert to the requirements of Examination Category E-A. Areas that exhibit reduced thickness from the prior measurement must be evaluated to determine acceptability for continued service. Containment vessel examinations that reveal material loss exceeding 10% of the nominal containment wall thickness, or material loss that is projected to exceed 10% of the nominal containment wall thickness prior to the next examination, must be documented. Areas that are suspect must be accepted by engineering evaluation or corrected by repair or replacement.

Table 2 summarizes the inservice inspection requirements for Class MC containments based upon the surface based examination rules first published in the 1991 Addenda to Subsection IWE.

Table 2. Class MC Inservice Inspection Examination Requirements

| EXAM CATEGORY | PARTS EXAMINED | EXAMINATION METHOD | EXTENT AND FREQUENCY OF EXAMINATION | |
|---|---|---|---|---|
| | | | 1ST INTERVAL | SUCCESSIVE INTERVALS |
| E-A | Containment Surfaces | | | |
| | Containment Boundary | General Visual | 100% Prior to Type A Test | 100% Prior to Type A Test |
| | Access. Surface Areas | Visual, VT-3 | 100% End of Interval | 100% End of Interval |
| E-B | Pressure-Retaining Welds (Penetrations) | Visual, VT-1 | 25% of Total Number of Welds | 25% of Total Number of Welds |
| E-C | Containment Surfaces Requiring Augmented Examination | | | |
| | Visible Surfaces | Visual, VT-1 | 100% of Identified Areas Each Period | 100% of Identified Areas Each Period |
| | Surfaces Accessible from One Side Only | Volumetric, UT Thickness | 100% of Identified Areas Each Period | 100% of Identified Areas Each Period |
| E-D | Seals, Gaskets, and Moisture Barriers | Visual, VT-3 | 100% of Each Item | 100% of Each Item |
| E-F | Pressure-Retaining Dissimilar Metal Welds | Surface, MT or PT | 50% of Total Number of Welds | 50% of Total Number of Welds |
| E-G | Pressure-Retaining Bolting | Visual, VT-1 | 100% of Each Bolted Connection | 100% of Each Bolted Connection |
| | | Bolt Torque or Tension Test | 100% of Bolts | 100% of Bolts |
| E-P | All Pressure-Retaining Components | | | |
| | Containment Boundary | 10CFR50, Appendix J | Each Repair, Modification, or Replacement | Each Repair, Modification, or Replacement |
| | Bellows, Airlocks, Seals, and Gaskets | 10CFR50, Appendix J | 10CFR50, Appendix J | 10CFR50, Appendix J |

## Acceptance Standards

Visual containment surface examinations may be made without removal of paint or coatings. The inspected area, when painted or coated, is to be examined for evidence of flaking, blistering, peeling, discoloration, and other signs of distress. For noncoated areas, the inspected areas are to be examined for evidence of cracking, discoloration, wear, pitting, excessive corrosion, arc strikes, gouges, surface discontinuities, dents, and other signs of surface irregularities.

Seals, gaskets, and moisture barriers examined in accordance with Examination Category E-D must be examined for wear, damage, erosion, tear, surface cracks, or other defects that may violate the leak-tight integrity. Defective items are to be be replaced. A proposed revision to Subsection IWE will not require disassembly of sealed or gasketed connections solely for the performance of this examination.

Bolting materials examined in accordance with Examination Category E-G must be examined in accordance with the material specification for defects which may cause the bolted connection to violate either the leak-tight or structural integrity. Defective items are to be replaced. In addition, either bolt torque or bolt tension must be within the limits specified for the original design. If no limits have been specified, acceptable bolt torque or bolt tension limits must be determined and utilized. Examination of bushings, threads, and ligaments in base material of flanges is required only when the connection is disassembled. Also, deferral of the examination to the end of the inspection interval is not allowed when the connection is otherwise disassembled or the bolting is removed.

Components accepted for continued service as a result of inservice inspections must either (1) have no indications from visual or surface examination that exceed the acceptance standards, (2) be repaired or replaced to the extent necessary to meet the acceptance standards, or (3) be found acceptable for continued service by an Engineering Evaluation. Results of inservice inspections are to be compared with recorded results of the preservice examination and prior inservice inspections to determine acceptability for continued service. Visual examinations that detect surface indications must be supplemented by either surface or volumetric methods. When an Engineering Evaluation is performed, it must demonstrate that the margins required by the Design Specifications are maintained. The Engineering Evaluation is subject to review by the regulatory and enforcement authorities having jurisdiction at the plant site.

### Containment Leakage Tests

Subsection IWE does not require containment leakage tests other than the periodic leakage tests specified in Appendix J of 10CFR50. This accommodation was made within Subsection IWE to reduce the potential fatigue effects of excessive pressure testing and to recognize that 10CFR50, Appendix J, provides an adequate basis for assuring continued containment leakage integrity. In accordance with 10CFR50, Appendix J, a general visual examination of the entire containment boundary is required as prescribed in Examination Category E-A prior to each Type A containment integrated leakage rate test.

Repair, modification or replacement of the pressure-retaining boundary of metal containments requires a Type A pneumatic leakage test as prescribed in 10CFR50, Appendix J. Type A tests are intended to measure the primary reactor containment overall integrated leakage rate after the containment has been completed and is ready for operation and at periodic intervals thereafter. Visual examination is required after repair, modification or replacement and may be limited to the area of the repair, modification or replacement including any connection made to the existing system. If the applicable leakage test requirements of 10CFR50, Appendix J, cannot be satisfied, corrective action must be taken and leakage testing must be repeated until the leakage requirement is satisfied prior to returning the component to service.

Leakage tests following minor repairs or modifications to the pressure-retaining boundary may be deferred until the next scheduled leakage test provided nondestructive examination is performed in accordance with an approved repair program. Such minor repairs or modifications are: (a) welds of attachments to the surface of the pressure-retaining boundary; (b) repair cavities, the depth of which does not penetrate the required design wall thickness by more than 10%; and (c) welds attaching penetrations that are NPS 1 or smaller.

### Repairs and Replacements

Specific requirements for repairs and replacements for nuclear components and systems, including Class MC containments and liners of Class CC containments, are provided in Section XI, Subsection IWA, *General Requirements*. Two repair techniques specifically for containments are the butterbead-temperbead and the half-bead weld repair methods. Both methods are intended for

repair welding in areas where factors such as water backing or adjacent structural members result in highly restrained welds. Both procedure qualification and welder performance qualification on full size mock-ups that simulate the field conditions are required.

### Code Cases

The butterbead-temperbead and the half-bead weld repair methods are the subject of ASME Code Case N-236-1, *Repair and Replacement for Class MC Vessels*. USNRC Regulatory Guide 1.147 approves use of this Code Case with some additional requirements.

ASME Code Case N-486, *Inservice Inspection, Repair and Replacement Requirements for Class MC and Metallic Liners of Class CC Components of Light-Water Cooled Plants*, was approved in April 1990. The Code Case is applicable from the 1974 Edition to the 1989 Edition of Section XI and prescribes the use of the 1989 Edition of Subsection IWE. The sole purpose for this Code Case was to provide a vehicle for USNRC endorsement of the Code Case in Regulatory Guide 1.147 in advance of the date when Subsection IWE is approved in 10CFR50.55a. This was intended to allow for use of Subsection IWE rules by plant Owners with USNRC endorsement, but on a non-mandatory basis, until full approval is established in 10CFR50. To date, this Code Case has not been addressed in the Regulatory Guide.

Two Code Cases provide rules for examination of containment surfaces by surface examination methods without removal of paint or coatings. These are Code Case N-458, *Magnetic Particle Examination of Coated Materials*, and Code Case N-485-1, *Eddy Current Examination of Ferritic Surfaces as an Alternative to Surface Examination*.

## Class CC (Concrete) Containments

### Preservice Examination

The preservice examination for Class CC containments must be performed following completion of the containment Structural Integrity Test (SIT) and prior to initial startup of the nuclear plant. The examination requires visual examination of all concrete surfaces of the containment and documentation of the as-built condition of the post-tensioning system. Information for the post-tensioning system may be extracted from the construction records. Table 3 defines the requirements for the preservice examinations.

When a concrete containment is repaired or modified during the service lifetime of a power unit, the preservice examination requirements must be met for the repaired or modified area to reestablish the preservice baseline. The preservice examination must be performed prior to the resumption of service when the power unit is not in service. The examination may be deferred to the next scheduled outage when the power unit is in service.

### Inservice Inspection Schedule

Periodic inspections of the concrete surfaces and of the post-tensioning system tendons, anchorages and other features are required throughout the lifetime of the nuclear plant. The inservice inspection schedule for plants with one power unit is defined in Figure 3. The inspections are required at 1, 3 and 5 years following the SIT required by Article CC-6000 of Section III, Division 2, and every 5 years thereafter. For the 1, 3 and 5 year inspections, the inspections must commence not more than 6 months prior to the specified dates and be completed not more than 6 months after such dates. If plant conditions are such that the inspections cannot be completed within the stated time interval, the remaining portions may be deferred to the next regularly scheduled plant outage. The ten year and subsequent inspections must commence not more than one year prior to and be completed not more than one year after the scheduled dates.

Table 3. Preservice Examination Requirements for Class CC Containments

| AREA EXAMINED | EXAMINATION METHOD | PRESERVICE CRITERIA OR DOCUMENTATION |
|---|---|---|
| Concrete Surface | Visual | No Evidence Of D ..age Or Degradation Sufficient To Warrant Evaluation Or Repair |
| Unbonded Post-Tensioning System | Documentation From Construction Records | (1) Tendon Tensioning Date<br>(2) Initial Tendon Seating Force<br>(3) Location Of All Missing Or Broken Wires Or Strands Unseated Wires, Missing Or Detached Buttonheads Or Missing Wedges<br>(4) Product Designation For Corrosion Protection Medium |

For sites with two power units, the inspection requirements for concrete containments may be modified if both containments are essentially similar in design and utilize the same prestressing system. The post-tensioning operations for the two containments must have been completed not more than two years apart and both containments must be similarly exposed to or protected from the outside environment. The inservice inspections for sites with two power units that meet these conditions are summarized in Table 4. In Table 4, inservice inspections defined as "Part" require only examination of tendon anchorage areas and examination of the corrosion protection medium and free water at the specified times. All examinations are required at the times specified as "All" in Table 4.

The 40 year period shown in Figure 3 is based upon the current licensed lifetime of nuclear plants in the United States. Consistent with changes in other Subsections of Section XI, the 40 year period is being deleted to recognize activities underway to extend the nuclear plant lifetime by amendments to the operating licenses granted by the USNRC.

## Inservice Inspection

All accessible concrete surfaces of the containment, including coated areas, require visual examination for evidence of conditions which may be indicative of damage or degradation. ACI 201.1R-68, *Guide for Making a Condition Survey of Concrete in Service,* is recommended as a guide for the inspections. The inspections and the evaluation of the findings must be performed by or under the direction of a Professional Engineer (the Responsible Engineer) experienced in evaluating the inservice condition of structural concrete. The inspections may be performed from floors, roofs, platforms, walkways, ladders, the ground surface and other permanent vantage points unless temporary close-in access to suspect areas of the concrete surface is required by the Responsible Engineer. Optical aids and artificial lighting may be used. As shown in Table 5, Examination Category L-A, Item No. L1.10 is assigned to the examination of the concrete surface.

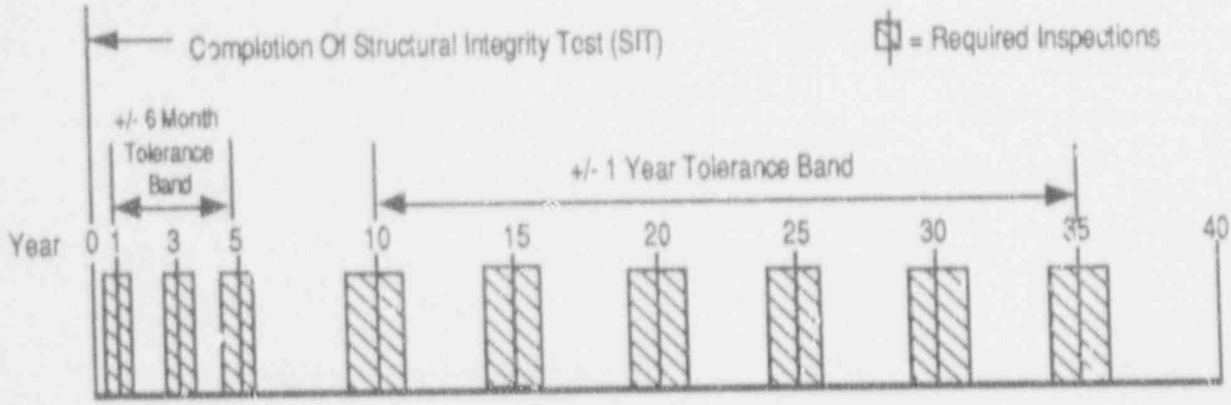


Figure 3. Class CC Inservice Inspection Schedule-One Power Unit

Several alternatives were considered during development of the rules for the inservice inspection of concrete in Subsection IWL. The Working Group initially favored the requirement that "suspect areas" of the concrete containment be predefined and that those areas be examined during each inspection period. Cracks 0.01 inches or greater were to be mapped and monitored. It was concluded, however, that such requirements would unnecessarily burden plant owners with repetitive examinations that would not necessarily reflect degradation of the structural integrity of the concrete. It was therefore decided that the responsibility for the concrete examination and the evaluation of the results that indicated damage or degradation would be left to the responsibility and judgment of the Responsible Engineer.

Table 4. Inservice Inspections for Sites with Two Power Units.

| CONTAINMENT | YEARS SINCE STRUCTURAL INTEGRITY TEST (SIT) | | | | | | | | |
|---|---|---|---|---|---|---|---|---|---|
| | 1 | 3 | 5 | 10 | 15 | 20 | 25 | 30 | 35 |
| FIRST UNIT | All | All | Part | All | Part | All | Part | All | Part |
| SECOND UNIT | All | Part | All | Part | All | Part | All | Part | All |

Examination Category L-B, Item Numbers L2.10 to L2.50, are assigned to the inservice inspection of unbonded post-tensioning systems as shown in Table 5. Separate requirements are contained in Subsection IWL for each inspection item.

Tendons examined during an inspection are to be selected on a random basis as shown in Table 6. The population from which the random sample is drawn consists of all tendons that have not been examined during earlier inspections. Tendon type is defined by geometry and position in the containment; e.g., hoop, vertical, dome, helical, and inverted U. The following apply:

(1) One tendon of each type must be selected from the first year inspection sample and designated as a common tendon. Each common tendon is examined during each

inspection. A common tendon is not to be detensioned unless it does not meet acceptance requirements. If a common tendon is detensioned, another common tendon of the same type must be selected from the first year inspection sample.

(2) If a containment with a stranded post-tensioning system is constructed with a predesignated number of detensionable tendons, one tendon of each type is to be selected from among those that are detensionable. The remaining tendons must be selected from among those that cannot be detensioned.

(3) Tendon anchorages that are not accessible for examination because of safety or radiological hazards or structural obstructions may be exempt from inspection. After tendons are randomly selected, any inaccessible tendons may be removed from the sample. Substitute tendons, located as close as possible to the exempted tendons, must be selected for all exempted tendons.

Table 5. Examination Categories for Concrete Containments

| AREA EXAMINED | EXAMINATION CATEGORY | ITEM NO. | PARTS EXAMINED |
|---|---|---|---|
| CONCRETE SURFACE | L-A | L1.10 | Concrete Surface |
| UNBONDED POST-TENSIONING SYSTEM | L-B | L2.10 | Tendon |
| | | L2.20 | Wire or Strand |
| | | L2.30 | Anchorage Hardware and Surrounding Concrete |
| | | L2.40 | Corrosion Protection Medium |
| | | L2.50 | Free Water |

The prestressing force in all inspection sample tendons must be measured by liftoff or an equivalent test. The equipment used to measure tendon force must be calibrated prior to the first tendon measurement following the final measurement of the inspection period. Accuracy of the calibration must be within 1.5% of the specified minimum ultimate strength of the tendon.

One sample tendon of each tendon type must be completely detensioned. A single wire or strand from the tendon is then to be visually examined over its entire length for evidence of corrosion or mechanical damage. Strand ends are to be examined for wedge slippage marks. In addition, tension tests are to be performed on at least three samples cut from each removed wire or strand, one at each end and one at mid-length. The yield strength, ultimate tensile strength, and elongation are to be recorded for each test.

Tendons that have been detensioned must be retensioned to at least the force predicted for the tendon at the time of the test. However, the retensioning force should not exceed 70% of the specified minimum ultimate tensile strength of the tendon based on the number of effective wires or strands in the tendon at the time of retensioning.

A visual examination is required on the tendon anchorage hardware, including bearing plates, anchorheads, wedges, buttonheads, shims, and the concrete extending outward a distance of two

feet from the edge of the bearing plate. Documentation is required for concrete cracks having widths greater than 0.01 inch, corrosion, broken or protruding wires, missing buttonheads, broken strands, and cracks in tendon anchorage hardware. Broken wires or strands, protruding wires and detached buttonheads following retensioning of tendons which have been detensioned must also be documented. The quantity of free water contained in the anchorage end cap as well as any which drains from the tendon during the examination process is also to be documented.

Table 3. Tendon Selection for inservice Inspection

| YEAR | % OF ALL TENDONS OF EACH TYPE | MINIMUM REQUIRED NO. OF EACH TYPE | MAXIMUM REQUIRED NO. OF EACH TYPE |
|---|---|---|---|
| 1 | 4% | 4 | 10 |
| 3 | 4% | 4 | 10 |
| 5 | 4% | 4 | 10 |
| 10 | 2% | 3 | 5 |
| 15 | 2% | 3 | 5 |
| 20 | 2% | 3 | 5 |
| 25 | 2% | 3 | 5 |
| 30 | 2% | 3 | 5 |
| 35 | 2% | 3 | 5 |

A visual VT-1 examination as defined in Subsection IWA, *General Requirements*, of Section XI is presently specified for the anchorage and adjacent concrete. The definition of the parameters for VT-1 examinations pertain only generally to the examination of steel surfaces. A revision scheduled for publication in the 1992 Addenda to Section XI establishes VT-1C and VT-3C visual examination to better define visual examination requirements for concrete and the requirements for the qualifications of personnel who conduct concrete examinations.

Samples of the corrosion protection medium, exclusive of any free water in the tendon, are to be taken from each end of each tendon examined. The samples are to be thoroughly mixed and analyzed for reserve alkalinity, water content and concentrations of water soluble chlorides, nitrates and sulfides. Specific requirements for the sample analysis are contained in Subsection IWL. The amount of corrosion protection medium removed at each anchorage must be measured and the total amount removed from each tendon (two anchorages) must be recorded. The total amount replaced in each tendon is to be recorded and the difference between the amount removed and the amount replaced is to be documented.

Samples of free water in tendons is to be taken where water is present in quantities sufficient for laboratory analysis. The samples require analysis to determine pH.

### Acceptance Standards

Concrete surfaces and post-tensioning system components are acceptable for continued service if the items examined in the inservice inspections meet specific acceptance criteria, are evaluated and found acceptable for continued plant operation, or are repaired to reestablish acceptability for continued service.

If an evaluation is performed, an Engineering Evaluation Report must be prepared by or on behalf of the nuclear plant owner. This report must define the source of the condition that does not meet the acceptance criteria, the basis for acceptability of the concrete containment without repair of the nonconforming condition, whether or not repair is required and, if required, the extent, method, and completion date for the repair and the extent, nature, and frequency of additional examinations. The Engineering Evaluation Report is subject to review by the regulatory and enforcement authorities having jurisdiction at the plant site.

Evaluation criteria and requirements for inservice inspection of the concrete surface are defined in Table 7. The condition of the concrete surface is acceptable if the Responsible Engineer determines that there is no evidence of damage of degradation sufficient to warrant further evaluation or repair.

Table 7 defines the evaluation criteria and requirements for the inservice inspection of post-tensioning systems. The acceptance criteria are discussed below:

Tendon forces are acceptable if the average of all measured tendon forces for each type of tendon is equal to or greater than the minimum required prestress specified at the anchorage for that type of tendon. In addition, the measured force in each individual tendon must be not less than 95% of the predicted force unless:

(1) the measured force in not more than one tendon is between 90% and 95% of the predicted force;

(2) the measured forces in two tendons located adjacent to the tendon in (a) above are not less than 95% of the predicted forces; and

(3) the measured forces in all the remaining sample tendons are not less than 95% of the predicted forces.

Tendon wires and strands are acceptable if the samples are free of physical damage, the location of severe corrosion is located and documented, and sample ultimate tensile strength and elongation are not less than minimum specified values. Concrete within two feet of the edge of the anchorage bearing plate is acceptable if cracks do not exceed 0.01 inches in width. The condition of tendon anchorage hardware is acceptable if there is no evidence of cracking in anchor heads, shims or bearing plates, if corrosion is not severe, and if broken or unseated wires, broken strands and detached buttonheads were documented and accepted during a previous inservice inspection.

The corrosion protection medium is acceptable when the reserve alkalinity, water content and soluble ion concentrations of all samples are within the limits specified in Subsection IWL.

The alkalinity of tendon free water is to be documented.

USNRC Regulatory Guide 1.35, *Inservice Inspection of Ungrouted Tendons in Prestressed Concrete Containment Structures*, contains guidance for the inservice inspection of post-tensioning systems for concrete containments. This Regulatory Guide describes a basis acceptable to the USNRC staff for developing an appropriate inservice inspection and surveillance program for ungrouted tendons in prestressed concrete containment structures of light-water cooled reactors. This guide formed the basis for many of the requirements in Subsection IWL for ungrouted tendons in post-tensioned containments. The Regulatory Guide, however, is more specific than the requirements in Subsection IWL in several areas for tendons but does not contain requirements for the inspection of concrete surfaces. Areas of difference between the Regulatory Guide and Subsection IWL are being reviewed by the Section XI Working Group on Concrete Pressure Components responsible for Subsection IWL.

Table 7. Inservice Inspection Requirements for Class CC Containments

| AREA EXAMINED | EXAMINATION METHOD | EVALUATION CRITERIA | INSERVICE CRITERIA OR DOCUMENTATION |
|---|---|---|---|
| Concrete Surface | Visual | Evidence Of Conditions Indicative Of Damage Or Degradation | No Evidence Of Damage Or Degradation Sufficient To Warrant Evaluation Or Repair |
| Tendon Force | Liftoff Or Equivalent Test | Prestress Force | (1) Average Measured Forces In All Tendons Equal To Or Greater than Required Prestress<br><br>(2) Individual Measured Force In Each Tendon Not Less Than 95% Of Predicted Force |
| Tendon Wire or Strand | (A) Visual<br><br>(B) Tension Test | (A) Corrosion, Mechanical Damage, And Wedge Slippage Marks<br><br>(B) Yield Strength, Ultimate Tensile Strength, And Elongation | (A) Severe Corrosion Located And Physical Damage<br><br>(B) Ultimate Tensile Strength and Elongation Not Less Than Minimum Specified Values |
| Tendon Anchorage Areas | (A) Visual, VT-1<br><br>(B) Free Water In End Cap | (A) Concrete Cracks; Corrosion, Broken Or Protruding Wires, Missing Buttonheads, Broken Strands, Cracks in Anchorage Hardware<br><br>(B) Volume Measurement | (A) Concrete Cracks Do Not Exceed 0.01 Inches Within 2 Feet Of Bearing Plates; No Cracks In Anchor Heads, Shims, Or Bearing Plates, No Severe Corrosion, Broken Or Unseated Wires, Strands, And Buttonheads Previously Documented and Accepted<br><br>(B) Volume Documentation |
| Corrosion Protection Medium | Sample Analysis | Reserve Alkalinity, Water Content, Water Soluble Chlorides, Nitrates, Sulfides | Reserve Alkalinity, Water Content, Soluble Ion Concentrations Within Specified Limits; Document Amount Removed and Replaced |
| Tendon Free Water | Alkalinity Analysis | pH | No Limits Specified |

### Leakage Tests

Requirements for leakage tests for Class CC containments will be published in the 1992 Addenda to Subsection IWL. The leakage test requirements in Subsection IWE for Class MC containments also apply to Class CC containments. No additional leakage tests are required in Subsection IWL for Class CC containments. The revision to Subsection IWL does, however, contain requirements for a containment pressure test at the design basis accident pressure following repair or replacement of a portion of the containment. This test is the same as the Type A test required by 10CFR50, Appendix J. The test is not required if the any of the following conditions exist:

(1) The Engineering Evaluation Report demonstrates that the structural integrity of the containment in the existing unrepaired condition has not been reduced below that required by the original design criteria;

(2) The repair or replacement affects only the cover concrete external to the outermost layer of structural reinforcing steel or post-tensioning tendons; or

(3) The repair or replacement involves only exchange of post-tensioning tendons, tendon anchorage hardware, shims, or corrosion protection medium.

### Repairs and Replacements

Procedures for repairs and replacements for Class CC containments were first published in the 1991 Addenda to Subsection IWL. These rules allow for repair or replacement of concrete, reinforcing steel, or post-tensioning system components by any appropriate method. However, the repairs or replacements must be performed in accordance with a documented Repair/Replacement Program that meets the requirements of Subsection IWA, *General Requirements*.

### Code Cases

ASME Code Case N-478, *Inservice Inspection for Class CC Concrete Components of Light-Water Cooled Power Plants*, was approved in July 1989. The Code Case is applicable from the 1974 Edition to the 1989 Edition of Section XI. The requirements are identical to the first publication of Subsection IWL in the 1986 Edition, 1988 Addenda of Section XI. As for Code Case N-486 for Subsection IWE, the sole purpose for Code Case N-478 was to provide a vehicle for USNRC endorsement of the Code Case in Regulatory Guide 1.147 in advance of the date when Subsection IWL is approved in 10CFR50.55a. To date, this Code Case is not addressed in the Regulatory Guides.

## AGING AND EXTENDED SERVICE LIFE

### Degradation Mechanisms

Numerous containment degradation mechanisms have emerged from studies and experience as containments in the United States grow older. Table 8 summarizes several of the potential degradation mechanisms, locations, indicators, problem areas, failure modes, and examination methods/remedies for steel and concrete in containment structures.

### Inservice Corrosion

Corrosion of shell plating and liners is potentially the most limiting degradation mechanism for containments. Significant corrosion in the containment for an early BWR MARK I nuclear plant was identified in 1986. This corrosion of more than 0.35 inches in the 1.154 inch thick

containment drywell shell occurred on the outside of the containment immediately above the concrete floor. This is an area packed with sand to form a cushion to allow drywell expansion during operation. As reported in USNRC Inspection and Enforcement Notice 86-99, *Degradation of Steel Containments*, in December 1986, the corrosion resulted from leakage over a long period of time from the bellows at the drywell to cavity seal. The leakage resulted in continual wetting of the sand in the sand cushion. Supplement 1 to this Regulatory Guide was issued in February 1991.

Table 8. Potential Degradation Mechanisms for Steel and Concrete Containments

| | STEEL | CONCRETE |
|---|---|---|
| Locations | Shell Plating; Penetrations; Hatches; Structural Reinforcing Structure; Structural & Nonstructural Attachments; Dome & Basemat Liner; Leak Chase Channels; Torus; Supports; Anchor Bars & Studs; Embedments. | Structural Concrete for Shells, Domes, Basemat, Supports and Related Areas. |
| Mechanisms | Electrochemical Corrosion; Fatigue; Chemical Attack; Microbiologically-Induced Corrosion; Stress Corrosion Cracking; Galvanic Corrosion; Radiation Embrittlement. | Chemical Attack; Acid Rain; Groundwater Chemistry; Alkali-Silica/ Alkali-Carbonate Aggregate Reactions; Freeze-Thaw Cycles; Shrinkage; Thermal Cycling> 50°; Radiation (Internal Heating); Dehydration; Vibration; Differential Settlement. |
| Indicators | Rust; Discoloration; Scale Buildup; Staining, Blistering & Bubbling Paint; Leakage from Drains; Clogged Drains; Buckling/Lift-Off of Liner; Spalling/ Pop-Out of Concrete. | Cracking; Discoloration; Spalling; Pop-Out; Loss of Strength; Aggregate Breakdown; Peeling, Discoloration or Delamination of Coatings. |
| Problem Areas | Areas of Water Accumulation; High Humidity Areas; Areas Exposed to Chemical or Borated Water Spills; Flashed , Caulked or Sealed Joints; Dissimilar Metal Welds; Penetrations; Condensation & Leak Paths; Sand Pockets; Locations with Stray Currents; Heat Trace Areas. | Areas of Water Accumulation; Areas Exposed to Chemical Spills; Areas Below Groundwater Level; Concrete-Steel Interfaces; Steel Encased Concrete Structures; "Hot" Penetration Sleeves. |
| Failure Modes | Leakage; Loss of Structural Integrity; Catastrophic Failure Under Severe Accident Loads. | Leakage; Loss of Structural Integrity. |
| Examination Methods/ Remedies | Leakage Testing; Visual Examination; UT Wall Thickness Trending; Coating Repair or Replacement; Surface NDE of Dissimilar Metal Welds; Replacement of Seals, Gaskets and Caulked Joints; Tap Liner for Hollow Spots; Open Drains. | Visual Examination; Crack Mapping and Repair; Coating Repair or Replacement; Replacement of Seals, Gaskets & Caulked Joints; Tapping of Liners for Hollow Spots; Groundwater Monitoring; Core Sampling & Testing; Spill Prevention/Cleanup; Open Drains |

Metallurgical examination of the samples removed from the drywell shell and chemical analyses of the sand and water obtained from the sand cushion region showed that the corrosion appeared to be the result of general wastage of the ASTM A212, Grade B, carbon steel plate from corrosion

caused by water containing aggressive anions. This containment was returned to service after significant testing, repairs, installation of a cathodic protection system, and completion of an Engineering Evaluation to demonstrate that the safety margins required by the design specifications were maintained. However, recent indications are that the corrosion has not been arrested and that it may become limiting to continued plant operation.

USNRC Information Notice 88-82, *Torus Shells with Corrosion and Degraded Coatings in BWR Containments*, October 1988, identified problems with corrosion of MARK I torus shells resulting from degraded coatings in BWR containments. Supplement 1 to this Regulatory Guide was issued in May 1989. Measurements of the shell plating revealed several areas in which the thickness was at or below the minimum specified wall thickness. Additional plants were found to have experienced degradation of the protective coating requiring cleaning and reapplication. These findings were significant since the measured corrosion rates of the torus shells were greater that the corrosion rates assumed as a part of the original design.

Severely degraded coatings and significant corrosion of a steel ice condenser containment vessel caused by boric acid and collected condensation in the annular space between the steel shell and the surrounding concrete shield was documented in USNRC Information Notice 89-79, *Degraded Coatings and Corrosion of Steel Containments*, in December 1989. Supplement 1 to this Regulatory Guide was issued in June 1990. This condition was discovered during the general visual examination required to be performed prior to the Type A containment integrated leak rate test required by 10CFR50, Appendix J. A similar degradation was subsequently found in a second, nearly identical plant at the same site. The probable cause of the degradation is attack by condensed boric acid coolant leaking from instrument line compression fittings. The corrosion measured an average depth of 0.1 inch with pits of up to 0.125 inches in an area no higher than 1-1/2 inches above the annulus floor. Additional corrosion up to 0.03 inches deep was found in areas below the floor where concrete was removed. This corrosion was due to a lack of sealant at the interface between the shell and the annulus floor.

## Microbiologically-Induced Corrosion

Microbiologically-Induced Corrosion (MIC) is a recently identified corrosion mechanism for carbon steel containments that can cause substantial pitting. Its mechanics are less well understood than the processes that result in more common forms of electrolytic, electrochemical, or galvanic corrosion. The MIC process can best be summarized as one in which bacteria, generally in an anaerobic zone adjacent to the base metal, develop by-products which enhance the corrosion process. These by-products can be either corrosive to the base metal or products which allow the electrochemical corrosion process to continue. By comparison, the electrochemical corrosion process should, in theory, either terminate or slow down in low oxygen conditions such as those found at the bottom of stagnant systems such as torus suppression pools.

The anaerobic zone in MIC may be caused by bacteria becoming captured under a a protective film of red rust due to the normal oxidation of the steel surface. The anaerobic zone is also caused by "sessile" or adhering bacteria generating protective biofilms after attaching themselves to the steel surface. Anaerobic bacteria will grow because bulk water biocides will not penetrate these protective coatings under stagnant or low flow conditions. Localized concentrated corrosion occurring in the anaerobic zones accounts for the existence of pits prevalent with the MIC process.

The most prevalent organism in the MIC anaerobic conditions are sulfate reducing bacteria which reduce sulfates to sulfides. The resulting sulfides are active and react with iron to produce and iron sulfide precipitate which is cathodic to the base metal. In the presence of this cathode, iron ions are drawn out of the anodic base metal. This iron sulfide is a transitory product which, upon breaking down, allows the iron to oxidize into the red and black rust that can be easily observed under a

microscope. In the presence of oxygen, the sulfides may be oxidized to form sulfuric acid which can aggressively attack the metal surface.

## Extended Service Life

Programs have been underway in the United States for several years to assess the extended service life potential of operating nuclear plants beyond the present 40 year licensed life. The two major pilot programs have been for the Surry 1 PWR nuclear plant operated by the Virginia Electric Power Company and the Monticello BWR nuclear plant operated by the Northern States Power Company. These programs have been funded primarily by the Electric Power Research Institute (EPRI) and the U.S. Department of Energy (DOE). The plant owners regulatory agencies, nuclear component manufacturers, engineering organizations, industry research organizations, government laboratories, and numerous others have been responsible for program administration. The American Society of Mechanical Engineers has taken a leadership role in coordinating the results of these studies with the objective of providing revisions to the ASME Code to allow continued, safe plant operation beyond 40 years.

Cost/benefit evaluations have shown that it is feasible to consider extended plant operation and that the time at which continued operation is no longer feasible is based primarily on economic rather than technical factors. Studies to define the most important plant components in terms of safety for continued operation have concluded that the containment is the most important component for BWR plants and second in importance only to the reactor pressure vessel for PWR plants.

## Containment Life Assessment and Projection

Results to date from the Surry and Monticello life extension studies indicate that the containment is not limiting in continued plant operation beyond the present 40 year nuclear plant licensed lifetime. With reasonable inspection and maintenance, service life of greater than 70 years for current containments appears to be technically and economically achievable. Present rules in Section XI of the ASME Code are not limiting in continued serviceability of containments beyond 40 years. However, long-term monitoring and trending of containment degradation parameters and evaluations for fatigue life based on actual plant cyclic loadings are needed. Also, improvements in inspection methods, accessibility for inspection, plant operation, preventive maintenance, and repair and replacement techniques for areas such as concrete and protective coatings need to be developed and implemented.

## SUMMARY

Containment leak-tight and structural integrity for operating nuclear plants in the United States has become increasingly important in light of renewed concerns for nuclear plant safety and the need to establish parameters for continued plant operation beyond the present 40 year licensed lifetime. A comprehensive basis exists for the design, construction, preservice examination, inservice inspection, periodic leakage testing, and repair for containments through the regulatory process for licensing and regulation administered by the United States Nuclear Regulatory Commission and the rules of Section III and Section XI of the American Society of Mechanical Engineers Boiler and Pressure Vessel Code.

Section XI of the ASME Code provides rules for the inservice inspection for both metal and concrete containments. Rules for metal containments in Subsection IWE were originally based on the philosophy that welds are the area of most significant concern. Recent experience has shown, however, that base metal corrosion and other degradation mechanisms can severely limit containment service life. The condition of containment base metal and liners is consequently more important to continued containment integrity. The rules in Subsection IWE have therefore been

updated to incorporate requirements for examination of the base metal together with a reduction of weld inspections to provide better assurance of continued containment safety.

Subsection IWE for Class MC (metal) containments was first published in the 1980 Edition, Winter 1981 Addenda, to Section XI Subsection IWL for Class CC (concrete) containments was first published in the 1986 Edition, 1988 Addenda. Neither Subsection IWE nor Subsection IWL has been endorsed in Title 10, Part 50 of the U.S. Code of Federal Regulations to date. Consequently, containment inservice inspection to the rules in the ASME Code is not mandated for nuclear plants in the United States at this time.

When mandated in 10CFR50 and implemented by nuclear plant owners, updated ASME Code inservice requirements for Class MC and Class CC containments together with the revisions to address current experience will provide a sound basis for improved leak-tight and structural integrity for steel and concrete containments.

# A REVIEW ON OPERATING EXPERIENCES OF CONTAINMENT ISOLATION SYSTEMS IN KOREA

Ingoo Kim and Hho-Jung Kim
Korea Institute of Nuclear Safety

## Abstract

Wide experiences in operating containment isolation systems have been accumulated in Korea since 1978. Hence, it becomes necessary to review the operating data in order to confirm the integrity of containments with about 50 reactor-years of experience and to establish the future direction to the containment test program. The objectives of the present work are to collect, consolidate and assess the operational data relevant to containment isolation systems, and then to find out types of isolation valve failures, dominant leakage paths and factors affecting integrated leakage rate test. Leakage is observed to be the most frequent type of isolation valve failure. The causes of the leakage are packing leakage, seat damage due to foreign material, and mis-adjustment of torque switches. The malfunction and deterioration are also observed to be a frequent failure modes. General trends of overall leakage show that more careful surveillance during pre-operational test can reduce the containment leakage. Dominant leakage paths are found to be through air locks and large-sized valves, such as butterfly valves of purge lines, so that weighted surveillance and inspection on these dominant leakage paths can considerably reduce the containment leakage. The atmosphere stabilization are found to be the most important to obtain the reliable result. In order to get well stabilized atmosphere, temperature and flow rate of compressed air should be kept constant and it is preferable not to operate fan cooler during pressurizing the containment for test.

## INTRODUCTION

Containment is the last barrier to mitigate the effect of a potential Loss of Coolant Accident (LOCA). Recently, the long-term operational integrity of containment systems is becoming increasingly important for ensuring the nuclear [illegible] safety. The operational integrity of containment mainly depends on the operability and leak-tightness of containment isolation systems. The performance of these systems must be assured by inspection, testing and maintenance; leak rate tests and stroke tests are performed periodically to examine the leak-tightness and the operability of containment isolation system, respectively. To ensure leak-tightness of the containment, three types of test are to be periodically performed; integrated leakage rate test (ILRT) termed Type A test, and local leakage rate test (LLRT) consisted of test for penetration termed Type B, and test for isolation valves termed Type C.

Currently, eight PWRs with large dry containment are in operation in Korea; Their design parameters relevant to containment systems are listed in Table 1. After Kori unit 1, as a first operating PWR in Korea, has been started in commercial operation since 1978, the wide experiences in operating containment isolation systems have been accumulated. Hence, it becomes necessary to review the operating data in order to confirm the integrity of containments with about 50 reactor-years of experience and to establish the future direction to

Table 1 Design Parameters of Containment Systems

| Plant | Kori 1 | Kori 2 | Kori 3,4 | YGN 3,4 | UCN 1,2 |
|---|---|---|---|---|---|
| Power (MWe) | 587 | 650 | 950 | 950 | 950 |
| Volume Size ($ft^3$) | $1.45X10^6$ | $1.44X10^6$ | $2.08X10^6$ | $2.08X10^6$ | $1.74X10^6$ |
| Test Pressure (psig) | 40.5 | 42 | 48 | 48 | 60 |
| La (W%/day) | 0.1 | 0.1 | 0.1 | 0.1 | 0.3 |
| Number of Isolation Valves | 125 (23) | 136 (30) | 123 (40) | 123 (40) | 176 (76) |

Note: La is the acceptance leakage rate and numbers in parentheses indicate number of valves of which diameters are 6 inch or larger.

the containment test program.

Operational data relevant to assessing the performance of containment isolation systems are at first collected and consolidated. Failure trends for isolation valves, dominant leakage paths in containment isolation systems and factors affecting ILRT are examined in the present study.

A simple data base program, which is named as TACIV (Trend Analysis of Containment Isolation Valves), has been developed for classifying the failures modes and analyzing the leakage trends of isolation valves. Sources of data base are the trouble reports and other report from surveillance programs such as LLRT and so on. The structure of TACIV is shown in Fig.1. Although a few features of TACIV program remains under development for improvement, it provides sufficient information to support our work.

## ASSESSMENTS AND FINDINGS

General findings with the assessment of operational experiences and test results are presented in the following paragraphs.

### Isolation Valve Failure

Typical causes for valve maintenance and repairs are shown in Fig.2, and the leakage is observed to be the most frequent type of isolation valve failure. It accounts for 61.8 % of all applicable failure. The causes of the leakage are packing leakage, seat damage due to foreign material, and mis-adjustment of torque switches. The malfunction, which is related to the operability, also observed to be a frequent failure mode. The seat/disc corrosion and wear classified as deterioration are failure causes which could not be negligible. This result on the

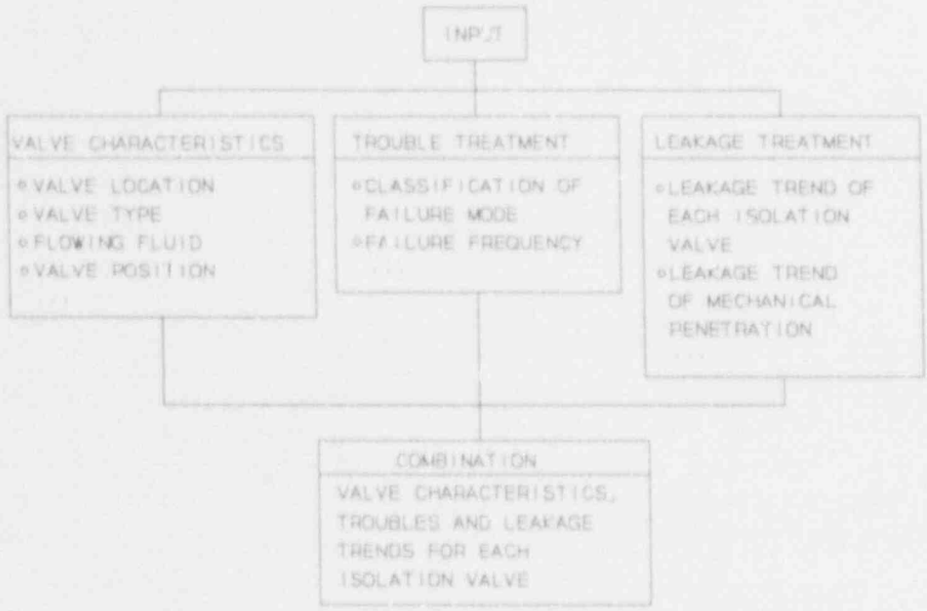


**Fig.1 Structure of TACIV Program**

valve failure mode is very similar to the result of Pelto and Counts [1].

## Local Leakage Rate Test

The total containment leakage trends of two typical plants are shown in Fig.3. 40,000 sccm is approximately equivalent to 0.25 La. It is found that the leakage appears significantly higher at the tests during the periods of first or second refueling, and thereafter leakage is reduced and converged to a certain value. Leakage trends of air locks and isolation valves (Type C) are also shown in Fig.3. The trend of Type C leakage is nearly same as that of total leakage, but leakage through air locks is not greatly changed per cycle. From the above fact, it can be seen that large leakage at initial operational stage is originated from Type C. The large leakage of Type C is due to the unfitness of seat/disc and mis-adjustment of torque switches. These troubles have been removed by the continued tests and repairs. Figure 3 shows that more careful surveillance during pre-operational test can reduce the containment leakage.

There were some excessive leakage rate through a isolation valve at the time of initial operating period. Excessive leakage rate means large leakage rate which can not be measured by instrument due to off-scale. In the past LLRTs had been performed with the measuring instruments of the range of 2 - 20,000 sccm. Any large leakage over the range of measurement system made difficulty in determining the overall leakage rate at the '*as is*' condition. Strictly speaking, it could not be judged whether LLRTs with such excessive leakages were success or not. In order to overcome the instrumental limit and to measure sufficiently large leakage, the pressure decay method has been used as an alternative.

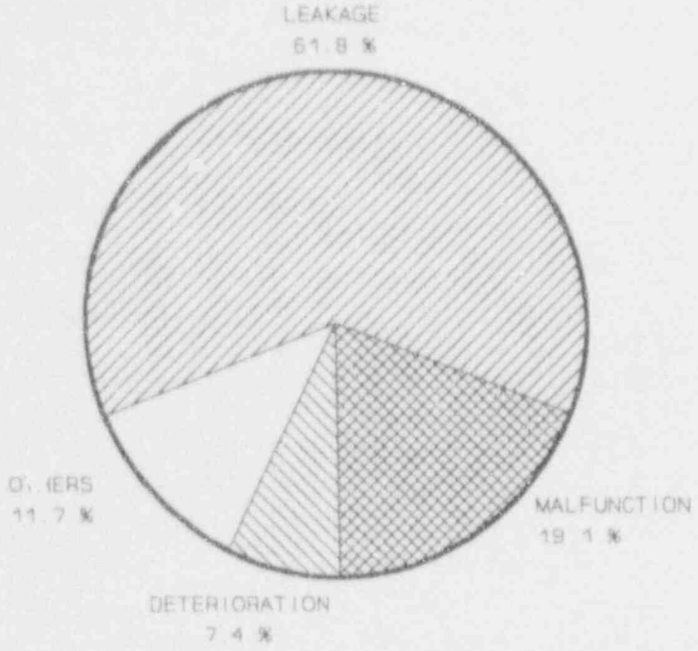


**Fig.2 Failure Modes of Isolation Valves**

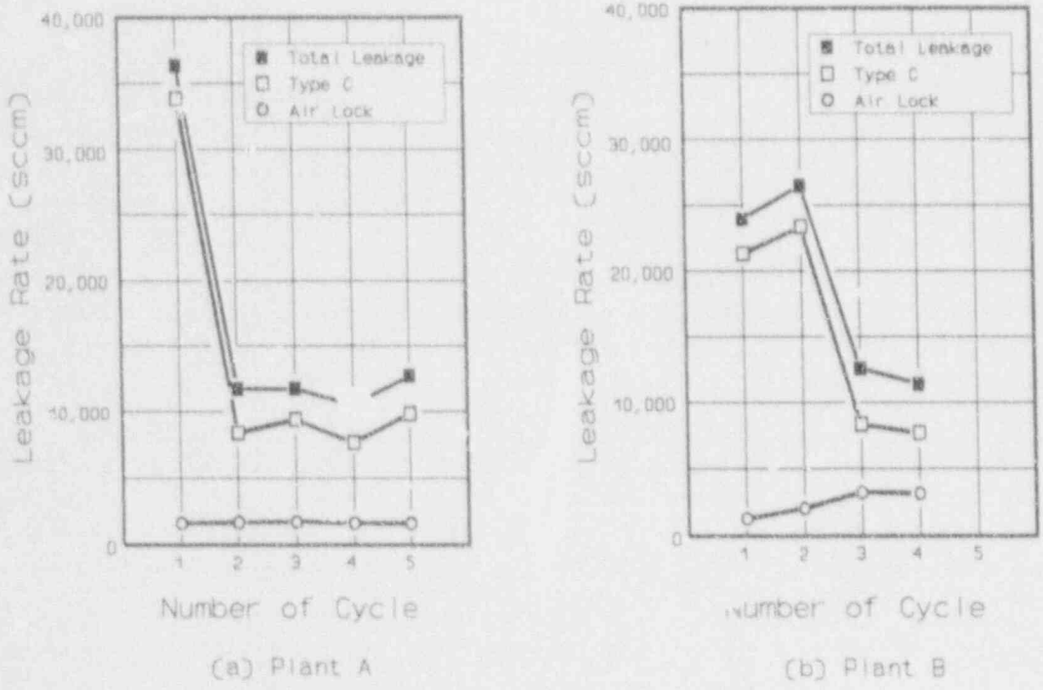


**Fig.3 Trends of Leakage Rates**

The leakage portions of Type B and Type C are shown in Fig.4, and it can be easily seen that the Type C leakage is the dominant contributor to containment leakage. There are a number of isolation valves of various diameters spanning from 0.25 to 48 inches. Because ASME IWV-3427[2] criteria is implemented, implicit classification based on the valve diameter exists; one group in which valve diameters are less than 6 inch and the other in which valve diameters are 6 inch or larger. The number of large-sized valves forms 18 - 32 % of total number of isolation valves; the number of large-sized valves appears to increase with the plant power (see Table 1). In Fig.4, the leakage of large-sized valves forms 38 - 54 % of total leakage while the leakage portion of the small ones does 36 - 43 %. Among the large-sized valves, butterfly valves of purge lines are found to be dominant leakage paths due to the largest pipe size and the relatively bad leak-tightness of butterfly valves. Considering the relatively small number of valves but large leakage of the latter group, weighted inspection on large-sized valves is thought as a effective way to reduce the Type C leakage.

The major items which belong to Type B test are air locks and electrical penetrations. Basically, the deteriorations of electrical penetrations have not been occurred, and the leakage through electrical penetrations is found to be negligible; as the minimum leakage not detectable to measurement system.

As mentioned earlier, The leakage of Type C test is larger than that of Type B. However, this does not imply that the leakage through air locks is not important. Because of larger leakage per path, air locks should be considered as dominant leakage paths.

In summary, dominant leakage paths are found to be air locks and large-sized valves such as butterfly valves of purge lines. If more attention is given to these dominant leakage paths,

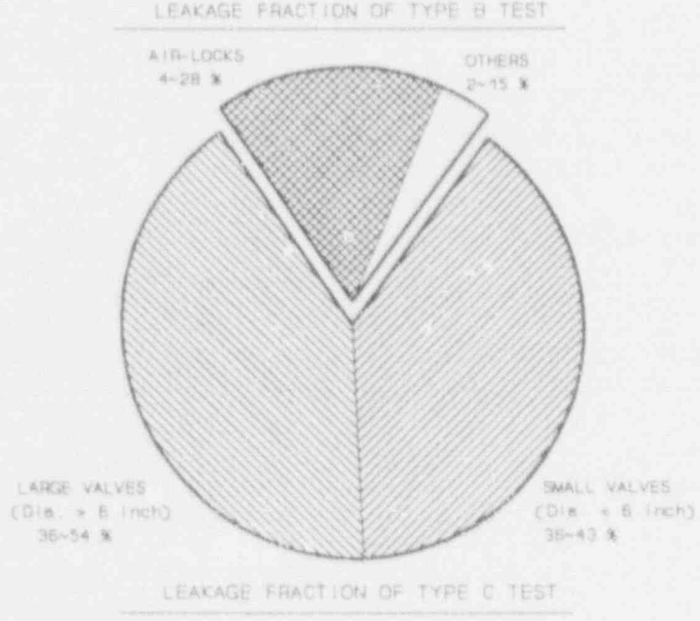


Fig.4 Leakage Rate Fractions of Type B and Type C

containment leakage can be considerably reduced.

**Integrated Leakage Rate Test**

The acceptance criteria in Appendix J to 10 CFR 50 [3] and the method of ANSI/ANS-56.8 [4] are applied for ILRT. Mass Point method with minimum test duration of eight hour has been adopted as a test method.

For the purpose of re-evaluating ILRTs, other statistical methods [5-7] are used in addition to Mass Point method of ANSI/ANS-56.8. Figure 5 shows two typical results of ILRTs analyzed different ways. At a glance, the result of case 1 test is very reliable regardless of analysis methods. However, as shown in Fig.5(b), there are some analysis results of ILRT indicating that the leakage rate data have low reliabilities. Mass Point method itself is well known as the most appropriate statistical method, however the ILRT methodology addressed in ANSI/ANS-56.8 seems to be insufficient to get the reliable leakage data at all time.

A number of works [8-10] has been carried out to improve the ILRT method. Those are mainly interested in the termination criteria or test duration time. The termination criterion is still open issue [11]. It is known that this criterion is most important to get the reliable result. On the other hand, it is also considered that the criterion on the entry condition to the test, that is atmosphere stabilization, is just as important as the termination criteria. However, it is interesting to note that the termination criteria may be closely related with the entry condition to the ILRT. In the present, the condition of the atmosphere stabilization is decided by average temperature history. According to ANSI/ANS-56.8, if average containment temperature does not deviate by more than 0.5 °F/hr from the average rate of volume weighted temperature averaged over the last four hours, containment atmosphere can be considered to be stabilized; at this time, ILRT can be started. But this criterion seems not to be practical. Many workers involved in ILRT implicitly thought that the criterion of 0.5 °F/hr determined with above-mentioned way is not insufficient to decide stabilization condition of containment atmosphere, since the 0.5 °F/hr deviation is not small to get the reliable leakage rate.

In order to investigate the effect of entry condition, a set of ILRT data is re-analyzed with different entry conditions based on the average rate of volume weighted temperature, $T_{ave}$ of 0.5, 0.1, 0.05 and 0.02 °F/hr. Figure 6 shows the effect of entry condition on the ILRT. If ILRT is started with $T_{ave} < 0.5$ °F/hr, then the leakage does not fall below the acceptance criteria even for the test duration of 16 hours (Case A in Fig.6). On the other hand, if ILRT is started with $T_{ave} < 0.02$ °F/hr, it takes about 7 hours for leakage to be within the acceptance criteria (Case D in Fig.6). From Fig.6, it is concluded that the leakage rate is mostly affected by the degree of atmosphere stabilization; as the test begins with more stabilized atmosphere, the time at which the leakage rate falls below the acceptance criteria is reduced.

Because it is not practical to wait for a long time in order to get the fully stabilized condition, it is necessary to find out more suitable criterion on the atmosphere stabilization. Although a criterion on the atmosphere stabilization is not considered in the present study, The ways of getting the stabilized atmosphere in a short time are examined.

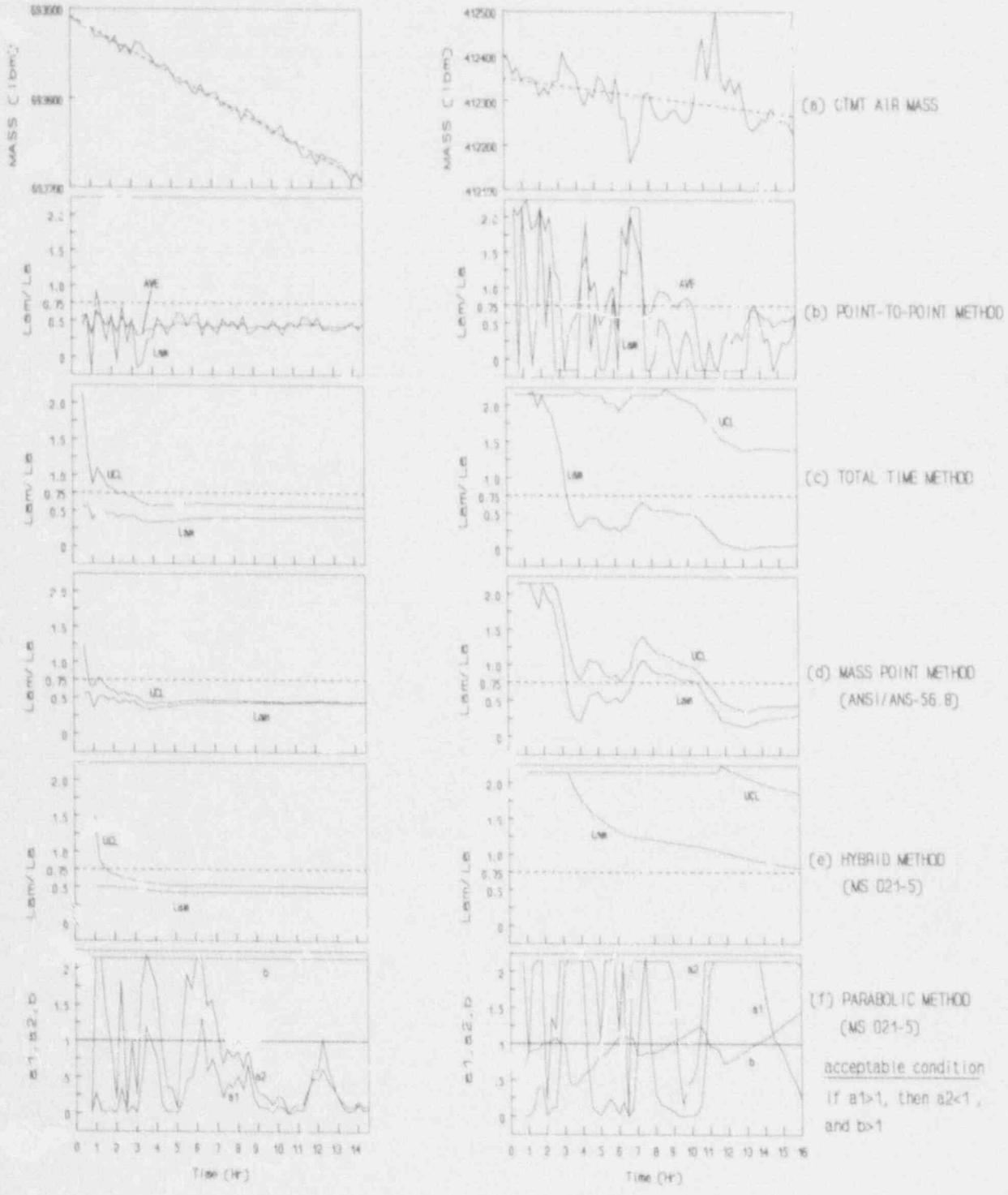


Fig.5 Results of Two Typical ILRTs

First of all, it is most important for the temperature and flowrate of compressed air into the containment for the pressurization to keep constant in the pressurized stage. Next, the effect of fan coolers is examined. Figure 7 shows the effect of fan coolers on the containment temperature. Without fan coolers, containment atmosphere is stabilized with natural circulation and heat transfer between atmosphere and containment structures, and the density stratification must exist at the end. (Fig.7(a)) With fan coolers, the effects of heat transfer through CCW (Component Cooling Water) heat exchanger and forced circulation are added. Because the temperature of CCW is lower than that of compressed air, the atmosphere temperature

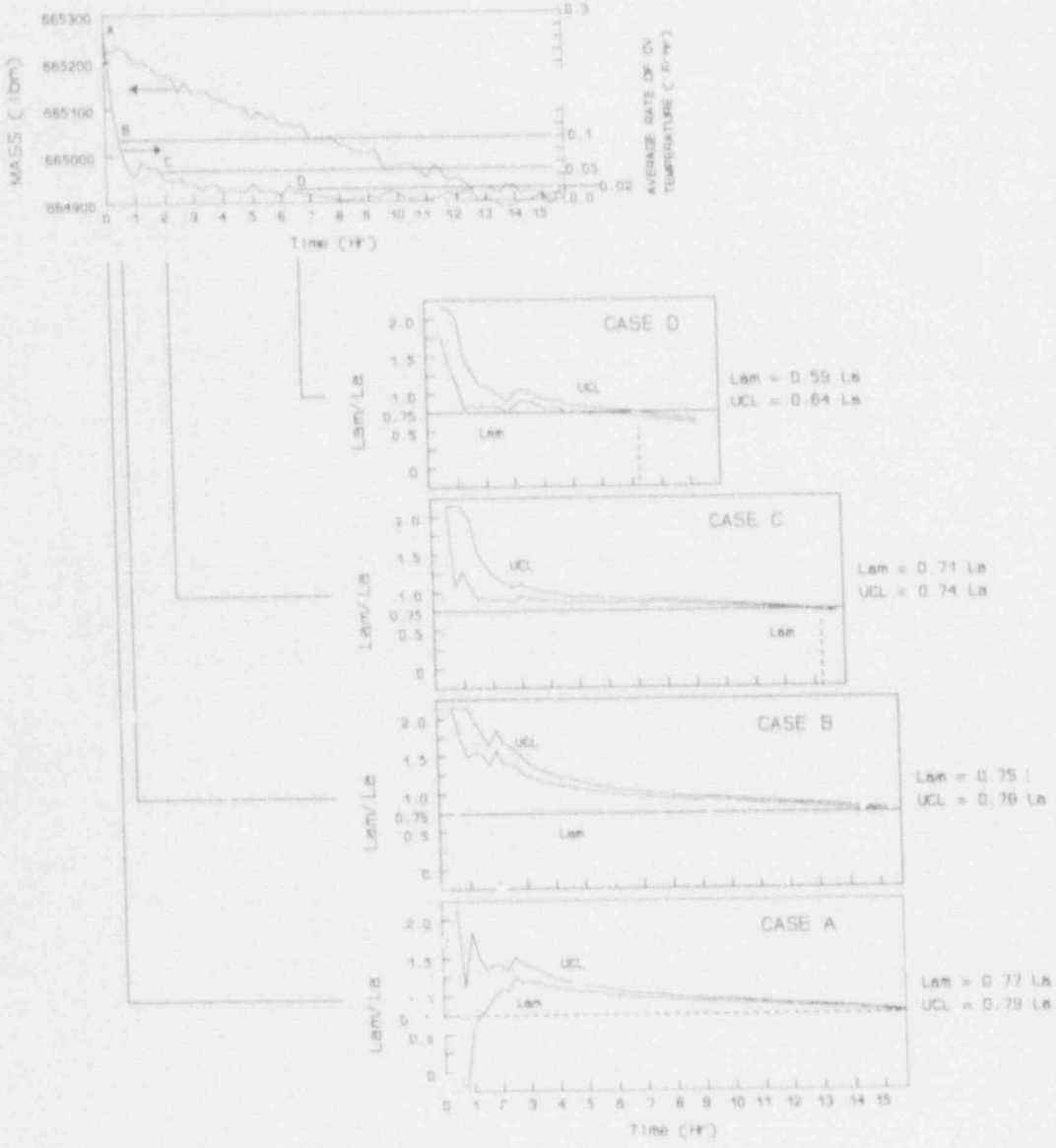


Fig.6 Effect of Entry Condition on ELRT

gradually decreases and it takes much time to reach a certain balanced condition. It is apparent that the containment atmosphere are well mixed with fan coolers. The differences among the temperature measured at various elevation are smaller than those without fan coolers. However, forced convection due to fan coolers inevitably disturbs the inherent density stratification so that temperature fluctuations appears due to the competition between forced and natural circulation. Considering small temperature fluctuations can affect the result, operation of fan coolers may have an adverse effect on the atmosphere stabilization.
In summary, the atmosphere stabilization is the most influencing factor to obtain the reliable result. In order to a have well stabilized atmosphere, temperature and flow rate of compressed air should be kept constant and it is preferrible not to operate fan coolers.

In addition, the instrumentation, in-leakage into the primary and secondary system and weather condition are observed as another influencing factors on ILRT.

Because La is a relatively small value, the results of ILRT can be seriously effected by the range and resolution of instrumentation. ANSI/ANS-56.8 requirements on the instrumentation seem sufficient to make the effect of measurement errors on ILRT to be negligible.

Besides the direct leakage through the containment walls, the in-leakage to the primary system and steam generators appears to be an important leakage source. Because inspection on the primary and secondary systems are performed at the pressurized condition of two systems, it is not easy to find the in-leakage path reversely to the pressurized systems. In order to minimize the effect of the leakage into the primary system, primary system is operated at solid state during ILRT.

The effect of weather on ILRTs is not direct but indirect. Bad weather condition such as rain and wind makes stabilization of containment atmosphere more difficult. As mentioned earlier, it is difficult to control the temperature and flow rate of compressed air to constant values

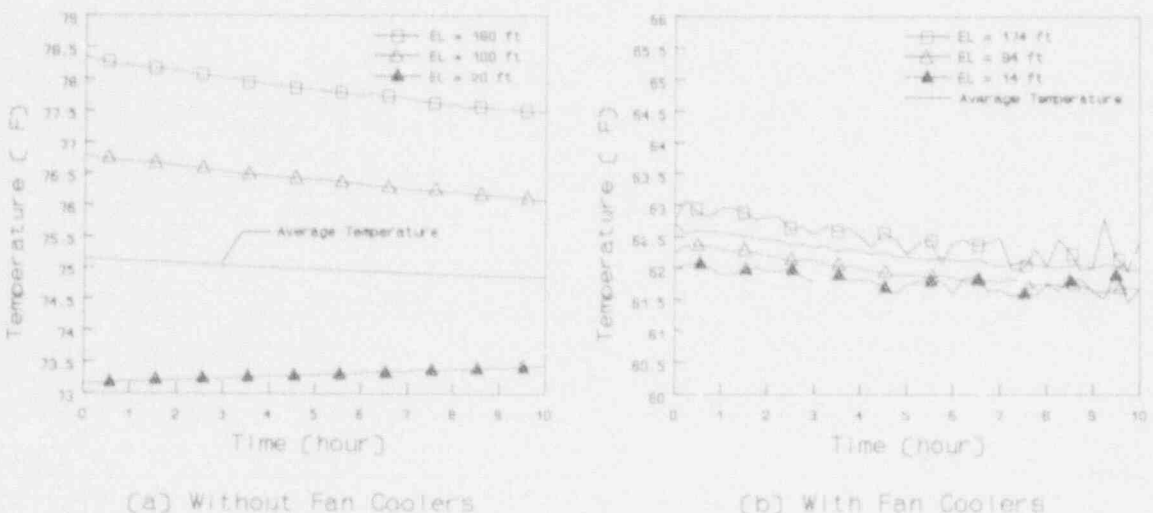


(a) Without Fan Coolers (b) With Fan Coolers

**Fig.7 Temperatures Measured at Various Elevations as a Function of Time**

since inlet air condition into the compressors is changed. Therefore it can be concluded that the effect of weather is small but not negligible.

## SUMMARY

The results of the present work are summarized as follows;

Leakage is observed to be the most frequent type of isolation valve failure. The causes of the leakage are packing leakage, seat damage due to foreign material, and mis-adjustment of torque switches. The malfunction and deterioration are observed to be frequent modes of isolation valve failure.

General trends of overall leakage show that the leakage appears significantly higher at the tests during the periods of first or second refueling, and thereafter leakage is reduced and converged to a certain value. This implies the fact that more careful surveillance during pre-operational test can reduce the containment leakage.

Dominant leakage paths are found to be through air locks and large-sized valves such as butterfly valves of purge lines, therefore weighted inspection on these dominant leakage paths can considerably reduce the containment leakage.

The atmosphere stabilization are found to be the most influencing factor to obtain the reliable result. For better atmosphere stabilization, temperature and flow rate of compressed air should be kept constant and it is preferable not to operate fan cooler.

The instrumentation, in-leakage into the primary and secondary system and weather are observed as another influencing factors on ILRT.

## References


1. P.J.Pelto and C.A.Counts, "Reliability Analysis of Containment Isolation Systems," NUREG/CP-0056, pp. 31-46.
2. "Inservice Testing of Valves in Nuclear Power Plant," ASME Subsection IWV.
3. "Primary Containment Leakage Testing for Water-cooled Power Reactors," 10CFR50 Appendix J.
4. "Containment System Leakage Testing Requirements," ANSI/ANS-56.8 , 1981.
5. "Leakage-rate Testing of Containment Structures for Nuclear Reactors," ANSI-N45.4 1972.
6. G.V.Cranston, "Testing Criteria for Integrated Leakage Testing of Primary Containment Structures for Nuclear Power Plants," BN-TOP-1, Bechtel Power Corporation, November 1, Revision 1, 1972.
7. "Draft Regulatory Guide MS-021-5 Containment System Leakage Rate," Draft dated May 1, 1985.
8. L.R.Young, "Methods for Determining Integrated Leakage Rate Test Duration - Case Study -," NUREG/CP-0076, pp. 185-204.
9. C.W.Rowley, "Criteria for Determining the Duration of Containment Integrated

Leakage Rate Tests," Trans. ANS, August 1-3, 1983.
10. W.T.Wagner and J.P.Langan, "The Influence of Data Collection Rate, Containment Size, and Data Smoothing on Containment Integrated Leak Rate Tests," NUREG/CP-0095, 1988.
11. Federal Register 45891, Vol.53, No.220, USNRC, November 1988.

Distribution:

J. F. Costello (20 Copies)
USNRC/RES
Mail Stop NL/S-217A
5650 Nicholson Lane
Rockville, MD 20852

Tony D'Angelo
USNRC/RES
NRR/DST/PSB
OWFN 8-D-1
Washington, DC 20555

H. L. Graves, III
USNRC/RES
Mail Stop NL/S-217A
5650 Nicholson Lane
Rockville, MD 20852

US Department of Energy
Office of Nuclear Energy
Attn: D. Giessing
W. Pasedag (2 copies)
Mail Stop B-107
NE-540
Washington, DC 20545

ABB-Combustion Engineering, Inc.
Attn: Lyle Gerdes
ABB-Combustion Engineering Nucl. Pwr.
P.O. Box 500, 1000 Prospect Hill Rd.
Windson, CT 06095-0500

ANATECH Research Corp.
Attn: Y. R. Rashid
P. O. Box 9165
LaJolla, CA 92038

Argonne National Laboratory
Attn: R. F. Kulak,
R. W. Seidensticker (2 copies)
9700 South Cass Avenue
Argonne, IL 60439

Babcock & Wilcox Co.
Attn: James R. Farr
20 S. van Buren Ave.
Barberton, OH 44203

Battelle Columbus Laboratories
Attn: Richard Denning
Peter Cybulskis (2 copies)
505 King Avenue
Columbus, OH 43201

Bechtel Power Corporation
Attn: Subir Sen
K. Y. Lee (2 copies)
15740 Shady Grove Rd.
Gaithersburg, MD 20877

Bechtel Power Corporation
Attn: Asadour H. Hadjian
Bertold Pfeifer (2 copies)
12400 E. Imperial Highway
Norwalk, CA 90650

Bechtel Savannah River, Inc.
Attn: T. E. Johnson
802 E. Martintown Road
North Augusta, SC 29841

Brookhaven National Laboratory
Attn: C. Hofmayer,T. Pratt
M. Reich (3 copies)
Building 130
Upton, NY 11973

Brookhaven National Laboratory
Attn: Ted Ginsberg
Building 820M
Upon, NY 11973

CBI NaCon, Inc.
Attn: Thomas J. Ahl
800 Jorie Boulevard
Oak Brook, IL 60521

City College of New York
Attn. C. Costantino
Dept. of Civil Engineering
140 Street and Convent Ave.
New York, NY 10031

Cornell University
Attn: Professor Richard N. White
School of Civil & Environ. Engr.
Hollister Hall
Ithaca, NY 14853

EBASCO Services, Inc.
Attn: Robert C. Iotti
Two World Trade Center
New York, NY 10048

EG&G Idaho
Attn: B. Barnes, T. L. Bridges
(2 copies)
Willow Creek Bldg. W-3
PO Box 1625
Idaho Falls, ID 83415

Electrical Power Research Institute
Attn: H. T. Tang, Y. K. Tang
Raf Sehgal, J. J. Taylor (4 copies)
3412 Hillview Avenue
PO Box 10412
Palo Alto, CA 94304

EQE Inc.
Attn: M. K. Ravindra
3300 Irvine Avenue
Suite 345
Newport Beach, CA 92660

General Electric Company
Attn: E. O. Swain, D. K. Henrie,
R. Gou, H. Townsend(4 copies)
175 Curtner Ave.
San Jose, CA 95125

Iowa State University
Attn: L. Greimann
Department of Civil Engineering
420 Town Engineering Bldg.
Ames, IA 50011

Los Alamos National Laboratories
Attn: C. Anderson, C. Farrar (2 copies)
PO Box 1663
Mail Stop N576
Los Alamos, NM 87545

Northern Illinois University
Attn: A. Marchertas
Mechanical Engineering Dept.
DeKalb, IL 60115

Oak Ridge National Laboratory
Attn: Steve Hodge
PO Box Y
Oak Ridge, TN 37830

Quadrex Corporation
Attn: Quazi A. Hossain
1700 Dell Ave.
Campbell, CA 95008

Sargent & Lundy Engineers
Attn: A. Walser
P. K. Agrawal (2 copies)
55 E Monroe St.
Chicago, IL 60603

Stevenson & Associates
Attn: John D. Stevenson
9217 Midwest Ave.
Cleveland, OH 44125

Tennessee Valley Authority
Attn: Nathaniel Foster
1101 Market Street, (LP4G-C)
Chattanooga TN 37408

Tennessee Valley Authority
Attn: D. Denton, W9A18
400 Commerce Ave.
Knoxville, TN 37902

United Engineers & Constructors, Inc.
Attn: Joseph J. Ucciferro
30 S. 17th St.
Philadelphia, PA 19101

University of California Santa Barbara
Attn: T. G. Theofanous
Dept. of Chemical & Nuclear Engineering
Santa Barbara, CA 93106

University of Illinois
Attn: Prof. Mete A. Sozen
1245 Newmark CE Lab
208 N. Romine, MC-250
Urbana, IL 61801

University of Illinois
Attn: C. Siess
Dept. of Civil Engineering
Urbana, IL 61801

University of Wisconsin
Attn: Prof. Michael Corradini
Nuclear Engineering Dept.
Madison, WI 53706

Westinghouse Electric Corp.
Nuclear and Advanced Technology Division
Attn: Richard S. Orr (MS 4-28)
P.O. Box 355
Pittsburg, PA 15230-0355

Westinghouse Electric Corp.
Attn: Vijay K. Sazawal
Waltz Mill Site
Box 158
Madison, PA 15663

Wilfred Baker Engineering
8700 Crownhill, Suite 310
San Antonio, TX 78209-1128

Universität Innsbruck
Attn: Prof. G. I. Schueller
Institut für Mechanik
Technikerstrasse 13
A-6020 Innsbruck
AUSTRIA

Brunswick Power Company
Attn: K. George Comeau
Point Lepreau Generating Station
Lepreau, New Brunswick E0G 2H0
CANADA

Ontario Hydro
Attn: W. J. Penn
Nuclear Studies & Safety Dept.
700 University Avenue
Toronto, Ontario
M5G 1X6
CANADA

University of Alberta
Dept. of Civil Engineering
Attn: Prof. D. W. Murray
Edmonton, Alberta
CANADA T6G 2G7

Commissariat a L'Energie Atomique
Centre d'Etudes Nucleaires de Saclay
Attn: M. Livolant, P. Jamet (2 copies)
F-91191 Gif-Sur-Yyette Cedex
FRANCE

Commissariat a l'Energie Atomique
Institut de Protection et de Surete Nucleaire
Attn: M. Barbe
Centre d'Etudes de Fontenay aus Roses,
BP No. 6
F-92665 Fontenay-aux-Roses
FRANCE

OECD Nuclear Energy Agency
Attn: K. Stadie, J. Royen (2 copies)
38, Boulevard Suchet
F-75016 Paris
FRANCE

Gesellschaft für Anlagen-und Reaktorsicherheit
Attn: H. Schulz, A. Höfler,
F. Schleifer (3 copies)
Schwertnergasse 1
D-5000 Köln 1
GERMANY

Kernforschungszentrum Karlsruhe GmbH
Institut für Reaktorsicherheit
Attn: R. Krieg
Postfach 3640
D-7500 Karlsruhe
GERMANY

Kraftwerk Union AG
Attn: M. Hintergraber
Hammerbacherstr. 12-14
D-8520 Erlangen
GERMANY

Technische Universität Muenchen
Lehrstuhl für Reaktordynamik
und Reaktorsicherheit
Attn: Prof. H. Karwat
D-8046 Garching
GERMANY

TUV Sudwest e.V.
Attn: Dr. Glock
Postfach 1380
D-7024 Filderstadt
GERMANY

University of Stuttgart
Staatliche Materialpruefungsanstalt (MPA)
Attn: Prof. K. F. Kussmaul
Pfaffenwaldring 32
D-7000 Stuttgart 80 (Vaihingen)
GERMANY

ENEA
Attn: Raffaele Di Sapia
via Le Regina Margherita, 125
I-00198 Roma
ITALY

ENEA
Dipartimento Reattori Innovativi
Attn: Paolo Corticelli
via Dell'Arcoveggio, 56/22 - 56/23
I-40129 Bologna
ITALY

ENEA-DISP
Attn: Giuseppe Pino, G. Petrangeli (2 copies)
Via Vitaliano Brancati 48
I-00144 Roma
ITALY

ISMES
Attn: A. Peano
Viale Giulio Cesare 29
I-24100 Bergamo
ITALY

Central Research Institute of
Electric Power Industry
Civil Engineering Laboratory
Attn: Yukio Aoyagi
1646 Abiko, Abiko-shi, Chiba-ken
JAPAN

Hitachi Works, Hitachi, Ltd.
Attn: O. Oyamada
Nuclear Equipment Design Dept.
3-1-1 Saiwaicho, Hitachi-Shi
Ibaraki-ken 317
JAPAN

Japan Atomic Energy Research Institute
Attn: Kunihisa Soda
Toshikuni Isozaki (2 copies)
Tokai-Mura, Naka-Gun
Ibaraki-Ken 319-11
JAPAN

Japan Atomic Energy Research Institute
Attn. Jun-ichi Shimokawa
Division of Technical Information
2-2, Uchisaiwai-cho 2-chome
Chiyoda, Tokyo 100
JAPAN

Kajima Corporation
Attn: T. Sugano, K. Umeda
H. Tsubota (3 copies)
KI Building
5-30, Akasada 6-chome
Minato-ku, Tokyo 107
JAPAN

Mitsubishi Heavy Industries, Ltd.
Attn: Kaoru Nagata
Manager, Nucl. Containment Vessel Design Sect.
Steel Structure Dept., Kobe Works
1-1, Wadasaki-cho, 1-chome, Hyogo-ku
Kobe 652, JAPAN

Nuclear Power Engineering Corporation
Attn: K. Takumi, A. Nonaka (2 copies)
Equipment and Components Department
Shuwa-Kamiyacho Building
4-3-13 Toranomon, Minato-ku
Tokyo 105, JAPAN

Obayashi Corporation
Attn: Toshikazu Takeda
Matsutaro Seki (2 copies)
Technical Research Institute
4-640, Shimokiyoto, Kiyose-shi
Tokyo 204, JAPAN

Shimizu Corporation
Attn: T. Kuroda, Y. Takeuchi (2 copies)
Nuclear Power Division
SEAVANS SOUTH, No. 2-3, Shibaura
1-chome, Minato-ku
Tokyo 105-7
JAPAN

University of Tokyo
Institute of Industrial Science
Attn: Prof. H. Shibata
7-22-1, Roppongi, Minatu-ku
Tokyo 106
JAPAN

I. V. Kurchatov Institute of Atomic Energy
Attn: Dr. Vladimir Asmolov
Head, Nuclear Safety Department
Moscow, 123182
RUSSIA

Central Nuclear de Almaraz
Attn: Sr. D. Jose Maria Zamarron
Subdirector Tecnico
Claudio Coello, 123
ES-28006 Madrid
SPAIN

Central Nuclear de Asco
Attn: Sr. D. Joaquin Sanchez Baptista
Servicio Licenciamiento
Tres Torres, 7
ES-08017 Barcelona
SPAIN

Nuclenor, S.A.
Attn: Sr. D. Federico del Pozo Obeso
Director General
Hernan Cortes, 26
ES-39003 Santander
SPAIN

Principia Espana, SA
Attn: Joaquin Marti
Orense, 36-2
ES-28020 Madrid
SPAIN

UNESA
Attn: Sr. D. Jose Puga Fernandez
Francisco Gervas, 3
ES-28020 Madrid
SPAIN

Unidad Electrica S.A.
Attn: Jose Puga
UNESA
ES-28020 Madrid
SPAIN

Universidad Politecnica
Attn: Agustin Alonso
Escuela Tecnica Superior
de Ingenieros Industriales
J. Gutierrez Abascal. 2
ES-28006 Madrid
SPAIN

Studsvik Energiteknik AB
Attn: Kjell O. Johansson
S-611 82 Nykoping
SWEDEN

Swedish State Power Board
Nuclear Reactor Safety
Attn: Hans Cederberg
Per-Eric Ahlstrom
Ralf Espefaelt (3 copies)
S-162 87 Vallingby
SWEDEN

Colenco Power Consulting Ltd.
Attn: J. Jemielewski (2 copies)
Mellingerstrasse 207
CH-5405 Baden
SWITZERLAND

Gahler & Partner AG
Attn: K. Gahler
Postfach 124
CH-5400 Ennetbaden
SWITZERLAND

Nordostschweiz, Kraftwerke AG
Attn: A. Huber
Parkstrasse 23
CH-5400 Baden
SWITZERLAND

Paul Scherrer Institut (PSI)
Attn: P Hoseman
CH-5232 Villigen-HSK
SWITZERLAND

Swiss Federal Institute of Technology
for Building Materials
Attn: Prof. F. H. Wittmann
ETH-Honggerberg
CH-8093 Zurich
SWITZERLAND

Swiss Federal Nuclear Safety Inspectorate
Federal Office of Energy
Attn: S. Chakraborty
CH-5232 Villigen-HSK
SWITZERLAND

DIANA Analysis
Attn: Ingeborg Huizing
P.O. Box 113
N-2600 AC Delft
THE NETHERLANDS

AEA Technology
Attn: Andrew Cruickshank
Editor, Atom
Harwell Didcot
Oxfordshire 0X11 0RA
UNITED KINGDOM

Atomic Energy Authority
Attn: D. W. Phillips
Safety and Reliability Directorate
Wigshaw Lane
Culcheth, Warrington WA3 4NE
UNITED KINGDOM

Atomic Energy Establishment
Attn: Peter Barr
Winfrith 215/A32
Dorchester, Dorset DT2 8DH
UNITED KINGDOM

HM Nuclear Installation Inspectorate
Attn: R. Bye, R. J. Stubbs (2 copies)
St. Peter's House
Stanley Precinct, Balliol Road
Bootle, Merseyside L20 3LZ
UNITED KINGDOM

INSPEC, Acquisitions Section
Attn: M. G. Merton
Michael Faraday House, Six Hills Way
Stevenage, Herts SG1 2AY
UNITED KINGDOM

Nuclear Electrip plc
Attn: J. Irving
Booths Hall, Chelford Road
Knutsford, Cheshire WA16 8QZ
UNITED KINGDOM

Taywood Engineering Ltd.
Attn: Carl C. Fleischer
Richard Crowder (2 copies)
Taywood House, 345 Ruislip Road
Southall, Middlesex UB1 2QX
UNITED KINGDOM

Sandia National Laboratories:
7141 S. A. Landenberger (5)
7151 G. C. Claycomb
6400 N. R. Ortiz
6403 W. A. von Riesemann
6404 D. A. Powers
6405 D. A. Dahlgren
6412 A. L. Camp
6413 F. T. Harper
6414 J. E. Kelly
6415 K. D. Bergeron
6418 S. L. Thompson
6449 M. P. Bohn
6422 M. D. Allen
6423 K. O. Reil
6429 K. E. Washington
6471 A. K. Moonka
6449 L. D. Lambert
6449 J. S. Ludwigsen
6449 D. W. Pace
6449 M. B. Parks (30)
6449 B. L. Spletzer
6449 R. A. Watson
8523-2 Central Technical Files

NRC FORM 335 (2-89) NRCM 1102, 3201, 3202

U.S. NUCLEAR REGULATORY COMMISSION

# BIBLIOGRAPHIC DATA SHEET

(See instructions on the reverse)

1. REPORT NUMBER (Assigned by NRC, Add Vol., Supp., Rev., and Addendum Numbers, If any.)

NUREG/CP - 0120
SAND92 - 0173

2. TITLE AND SUBTITLE

Proceedings of the Fifth Workshop on Containment Integrity

3. DATE REPORT PUBLISHED

MONTH: July | YEAR: 1992

4. FIN OR GRANT NUMBER

A1401

5. AUTHOR(S)

Edited by M. B. Parks, C. E. Hughey

6. TYPE OF REPORT

Conference Proceedings

7. PERIOD COVERED (Inclusive Dates)

NA

8. PERFORMING ORGANIZATION – NAME AND ADDRESS (If NRC, provide Division, Office or Region, U.S. Nuclear Regulatory Commission, and mailing address; if contractor, provide name and mailing address.)

Sandia National Laboratories
Albuquerque, NM 87185-5800

9. SPONSORING ORGANIZATION – NAME AND ADDRESS (If NRC, type "Same as above"; if contractor, provide NRC Division, Office or Region, U.S. Nuclear Regulatory Commission, and mailing address.)

Division of Engineering
U.S. Nuclear Regulatory Commission
Washington, DC 20555

10. SUPPLEMENTARY NOTES

11. ABSTRACT (200 words or less)

The Fifth Workshop on Containment Integrity was held in Washington, DC, on May 12-14, 1992. The purpose of these workshops is to provide an international forum for the exchange of information on performance of containments in nuclear power plants under severe accident loadings. Severe accident investigations of existing containment designs as well as future advanced containments were presented during the workshop. There were 145 participants at the workshop from 15 countries.

Ivan Selin, Chairman of the NRC, provided the opening address for the meeting.

A total of 39 papers were presented on the following topics: Containment Design Considerations for Severe Accident Conditions, Advanced Containment Design and Related Research, Containment Behavior Under Accident Conditions, Testing/Analysis of Containment Systems, and Containment Operational Experience (Leakage, Aging, and Operation). A copy of the final program, including last minute changes, is provided in these proceedings. Papers that were presented at the workshop make up the body of this report.

The workshop was hosted by Sandia National Laboratories under the sponsorship of the U.S. Nuclear Regulatory Commission. Principal organizers for the workshop were James F. Costello of the U.S. Nuclear Regulatory Commission and Walter A. von Riesemann and M. Brad Parks of Sandia National Laboratories.

12. KEY WORDS/DESCRIPTORS (List words or phrases that will assist researchers in locating the report.)

containment integrity, severe accident

13. AVAILABILITY STATEMENT

Unlimited

14. SECURITY CLASSIFICATION

(This Page)
Unclassified

(This Report)
Unclassified

15. NUMBER OF PAGES

16. PRICE

THIS DOCUMENT WAS PRINTED USING RECYCLED PAPER

UNITED STATES
NUCLEAR REGULATORY COMMISSION
WASHINGTON, D.C. 20555-0001

OFFICIAL BUSINESS
PENALTY FOR PRIVATE USE, $300

SPECIAL FOURTH-CLASS RATE
POSTAGE AND FEES PAID
USNRC
PERMIT NO. G-67